

Radiobiology for the Radiologist

EIGHTH EDITION

Eric J. Hall
Amato J. Giaccia



Wolters Kluwer

Eighth Edition

Radiobiology for the Radiologist

Eric J. Hall DPhil, DSc, FACP, FRCR, FASTRO

Higgins Professor Emeritus of Radiation Biophysics
Special Lecturer in Radiation Oncology
Special Research Scientist
Columbia University Medical Center, New York, New York

Amato J. Giaccia PhD

Jack, Lulu, and Sam Willson Professor of Cancer Biology
Professor of Radiation Oncology
Director, Radiation and Cancer Biology Division
Stanford University School of Medicine, Stanford, California



Philadelphia • Baltimore • New York • London
Buenos Aires • Hong Kong • Sydney • Tokyo

Senior Acquisitions Editor: Sharon Zinner

Editorial Coordinator: Lauren Pecarich

Marketing Manager: Dan Dressler

Production Project Manager: Bridgett Dougherty

Design Coordinator: Holly McLaughlin

Manufacturing Coordinator: Beth Welsh

Prepress Vendor: Absolute Service, Inc.

Copyright © 2019 Wolters Kluwer

All rights reserved. This book is protected by copyright. No part of this book may be reproduced or transmitted in any form or by any means, including as photocopies or scanned-in or other electronic copies, or utilized by any information storage and retrieval system without written permission from the copyright owner, except for brief quotations embodied in critical articles and reviews. Materials appearing in this book prepared by individuals as part of their official duties as U.S. government employees are not covered by the above-mentioned copyright. To request permission, please contact Wolters Kluwer at Two Commerce Square, 2001 Market Street, Philadelphia, PA 19103, via email at permissions@lww.com, or via our website at lww.com (products and services).

9 8 7 6 5 4 3 2 1

Printed in China

Library of Congress Cataloging-in-Publication Data

Names: Hall, Eric J., author. | Giaccia, Amato J., author.

Title: Radiobiology for the radiologist / Eric J. Hall, Amato J. Giaccia.

Description: Eighth edition. | Philadelphia : Wolters Kluwer, [2019] | Includes bibliographical references and index.

Identifiers: LCCN 2017057791 | ISBN 9781496335418

Subjects: | MESH: Radiation Effects | Radiobiology | Radiotherapy

Classification: LCC R895 | NLM WN 600 | DDC 616.07/57—dc23 LC record available at <https://lccn.loc.gov/2017057791>

This work is provided “as is,” and the publisher disclaims any and all warranties, express or implied, including any warranties as to accuracy, comprehensiveness, or currency of the content of this work.

This work is no substitute for individual patient assessment based upon healthcare professionals’ examination of each patient and consideration of, among other things, age, weight, gender, current or prior medical conditions, medication history, laboratory data, and other factors unique to the patient. The publisher does not provide medical advice or guidance and this work is merely a reference tool. Healthcare professionals, and not the publisher, are solely responsible for the use of this work including all medical judgments and for any resulting diagnosis and treatments.

Given continuous, rapid advances in medical science and health information, independent professional verification of medical diagnoses, indications, appropriate pharmaceutical selections and dosages, and treatment options should be made, and healthcare professionals should consult a variety of sources. When prescribing medication, healthcare professionals are advised to consult the product information sheet (the manufacturer’s package insert) accompanying each drug to verify, among other things, conditions of use, warnings, and side effects and identify any changes in dosage schedule or contraindications, particularly if the medication to be administered is new, infrequently used, or has a narrow therapeutic range. To the maximum extent permitted under applicable law, no responsibility is assumed by the publisher for any injury and/or damage to persons or property, as a matter of products liability, negligence law or otherwise, or from any reference to or use by any person of this work.

LWW.com

Preface to the First Edition

This book, like so many before it, grew out of a set of lecture notes. The lectures were given during the autumn months of 1969, 1970, and 1971 at the Columbia-Presbyterian Medical Center, New York City. The audience consisted primarily of radiology residents from Columbia, affiliated schools and hospitals, and various other institutions in and around the city.

To plan a course in radiobiology involves a choice between, on the one hand, dealing at length and in depth with those few areas of the subject in which one has personal expertise as an experimenter or, on the other hand, surveying the whole field of interest to the radiologist, necessarily in less depth. The former course is very much simpler for the lecturer and in many ways more satisfying; it is, however, of very little use to the aspiring radiologist who, if this course is followed, learns too much about too little and fails to get an overall picture of radiobiology. Consequently, I opted in the original lectures, and now in this book, to cover the whole field of radiobiology as it pertains to radiology. I have endeavored to avoid becoming evangelical over those areas of the subject which interest me, those to which I have devoted a great deal of my life. At the same time I have attempted to cover, with as much enthusiasm as I could muster and from as much knowledge as I could glean, those areas in which I had no particular expertise or personal experience.

This book, then, was conceived and written for the radiologist—specifically, the radiologist who, motivated ideally by an inquiring mind or more realistically by the need to pass an examination, elects to study the biological foundations of radiology. It may incidentally serve also as a text for graduate students in the life sciences or even as a review of radiobiology for active researchers whose viewpoint has been restricted to their own area of interest. If the book serves these functions, too, the author is doubly happy, but first and foremost, it is intended as a didactic text for the student of radiology.

Radiology is not a homogenous discipline. The diagnostician and therapist have divergent interests; indeed, it sometimes seems that they come together only when history and convenience dictate that they share a common course in physics or radiobiology. The bulk of this book will be of concern, and hopefully of interest, to all radiologists. The diagnostic radiologist is commended particularly to Chapters 11, 12, and 13 concerning radiation accidents, late effects, and the irradiation of the embryo and fetus. A few chapters, particularly

Chapters 8, 9, 15, and 16, are so specifically oriented towards radiotherapy that the diagnostician may omit them without loss of continuity.

A word concerning reference material is in order. The ideas contained in this book represent, in the author's estimate, the consensus of opinion as expressed in the scientific literature. For ease of reading, the text has not been broken up with a large number of direct references. Instead, a selection of general references has been included at the end of each chapter for the reader who wishes to pursue the subject further.

I wish to record the lasting debt that I owe my former colleagues at Oxford and my present colleagues at Columbia, for it is in the daily cut and thrust of debate and discussion that ideas are formulated and views tested.

Finally, I would like to thank the young men and women who have regularly attended my classes. Their inquiring minds have forced me to study hard and reflect carefully before facing them in a lecture room. As each group of students has grown in maturity and understanding, I have experienced a teacher's satisfaction and joy in the belief that their growth was due in some small measure to my efforts.

E. J. H.

New York

July 1972

Preface

The eighth edition is a significant revision of this textbook and includes new chapters that were not included in the seventh edition. We have retained the same format as the seventh edition, which divided the book into two parts. Section I contains 16 chapters and represents both a general introduction to radiation biology and a complete self-contained course in the subject, suitable for residents in diagnostic radiology and nuclear medicine. It follows the format of the syllabus in radiation biology prepared by the Radiological Society of North America (RSNA). Section II consists of 12 chapters of more in-depth material designed primarily for residents in radiation oncology.

Dickens's famous beginning to a Tale of Two Cities, "It was the best of times, it was the worst of times, it was the age of wisdom, it was the age of foolishness, it was the epoch of belief, it was the epoch of incredulity . . .," very much applies to the current world order. Although medical science and technology have made great advances in alleviating disease and suffering, irrational and unpredictable events occur quite frequently, instilling fear and apprehension about potential nuclear terrorism. The eighth edition contains a new chapter (Chapter 9) on "Medical Countermeasures to Radiation Exposure" that summarizes the current therapies available to prevent or mitigate radiation damage to normal tissues. This chapter nicely complements Chapter 14 on "Radiologic Terrorism."

Due to the strong request for including more information on molecular techniques, we have included a new Chapter 17 on "Molecular Techniques in Radiology." The techniques described in this chapter should be useful to both the novice as well as the skilled practitioner in molecular biology.

In this edition, we have eliminated the chapter on "Molecular Imaging." The basis for this decision was that the subject matter covered in this chapter does not involve any radiobiologic principles, and in any case, there are several textbooks devoted solely to the subject of molecular imaging. For these reasons, we have decided to remove this chapter from the eighth edition. Overall, we believe that this new edition represents a well-balanced compilation of both traditional and molecular radiation biology principles.

The ideas contained in this book represent, we believe, the consensus of opinion as expressed in the scientific literature. We have followed the precedent of previous editions, in that, the pages of text are unencumbered with flyspeck-

like numerals referring to footnotes or original publications, which are often too detailed to be of much interest to the general reader. On the other hand, there is an extensive and comprehensive bibliography at the end of each chapter for those readers who wish to pursue the subject further.

We commend this new edition to residents in radiology, nuclear medicine, and radiation oncology, for whom it was conceived and written. If it serves also as a text for graduate students in the life sciences or even as a review of basic science for active researchers or senior radiation oncologists, the authors will be doubly happy.

Eric J. Hall

Columbia University, New York

Amato J. Giaccia

Stanford University, California

October 2017

Acknowledgments

We would like to thank the many friends and colleagues who generously and willingly gave permission for diagrams and illustrations from their published work to be reproduced in this book.

Although the ultimate responsibility for the content of this book must be ours, we acknowledge with gratitude the help of several friends who read chapters relating to their own areas of expertise and made invaluable suggestions and additions. With each successive edition, this list grows longer and now includes Drs. Ged Adams, Philip Alderson, Sally Amundson, Joel Bedford, Roger Berry, Max Boone, Victor Bond, David Brenner, J. Martin Brown, Ed Bump, Denise Chan, Julie Choi, James Cox, Nicholas Denko, Bill Dewey, Mark Dewhirst, Frank Ellis, Peter Esser, Stan Field, Greg Freyer, Charles Geard, Eugene Gerner, Julian Gibbs, George Hahn, Simon Hall, Ester Hammond, Tom Hei, Robert Kallman, Richard Kolesnick, Norman Kleiman, Gerhard Kraft, Adam Krieg, Edward LaGory, Dennis Leeper, Howard Lieberman, Philip Lorio, Edmund Malaise, Gillies McKenna, Mortimer Mendelsohn, George Merriam, Noelle Metting, Jim Mitchell, Thomas L. Morgan, Anthony Nias, Ray Oliver, Stanley Order, Tej Pandita, Marianne Powell, Simon Powell, Julian Preston, Elaine Ron, Harald Rossi, Robert Rugh, Chang Song, Fiona Stewart, Herman Suit, Robert Sutherland, Roy Tishler, Len Tolmach, Liz Travis, Lou Wagner, John Ward, Barry Winston, Rod Withers, and Basil Worgul. The principal credit for this book must go to the successive classes of residents in radiology, radiation oncology, and nuclear medicine that we have taught over the years at Columbia and Stanford, as well as at American Society for Radiation Oncology (ASTRO) and RSNA refresher courses. Their perceptive minds and searching questions have kept us on our toes. Their impatience to learn what was needed of radiobiology and to get on with being doctors has continually prompted us to summarize and get to the point.

We are deeply indebted to the U.S. Department of Energy, the National Cancer Institute, and the National Aeronautical and Space Administration, which have generously supported our work and, indeed, much of the research performed by numerous investigators that is described in this book.

We owe an enormous debt of gratitude to Ms. Sharon Clarke, who not only typed and formatted the chapter revisions but also played a major role in editing and proofreading. Our publisher, Lauren Pecarich, guided our efforts at every

stage.

Finally, we thank our wives, Bernice Hall and Jeanne Giaccia, who have been most patient and have given us every encouragement with this work.

Contents

Preface to the First Edition

Preface

Acknowledgments

SECTION I For Students of Diagnostic Radiology, Nuclear Medicine, and Radiation Oncology

1 Physics and Chemistry of Radiation Absorption

TYPES OF IONIZING RADIATIONS

Electromagnetic Radiations

Particulate Radiations

ABSORPTION OF X-RAYS

DIRECT AND INDIRECT ACTION OF RADIATION

ABSORPTION OF NEUTRONS

ABSORPTION OF PROTONS AND HEAVIER IONS SUCH AS CARBON

SUMMARY OF PERTINENT CONCLUSIONS

BIBLIOGRAPHY

2 Molecular Mechanisms of DNA and Chromosome Damage and Repair

GENERAL OVERVIEW OF DNA STRAND BREAKS

MEASURING DNA STRAND BREAKS

DNA REPAIR PATHWAYS

Base Excision Repair

Nucleotide Excision Repair

DNA Double-Strand Break Repair

Nonhomologous End-Joining

Homologous Recombination Repair

Crosslink Repair

Mismatch Repair

RELATIONSHIP BETWEEN DNA DAMAGE AND CHROMOSOME ABERRATIONS

CHROMOSOMES AND CELL DIVISION

THE ROLE OF TELOMERES

RADIATION-INDUCED CHROMOSOME ABERRATIONS

EXAMPLES OF RADIATION-INDUCED ABERRATIONS

CHROMOSOME ABERRATIONS IN HUMAN LYMPHOCYTES

SUMMARY OF PERTINENT CONCLUSIONS

BIBLIOGRAPHY

3 Cell Survival Curves

REPRODUCTIVE INTEGRITY

THE *IN VITRO* SURVIVAL CURVE

THE SHAPE OF THE SURVIVAL CURVE

MECHANISMS OF CELL KILLING

DNA as the Target

The Bystander Effect

Apoptotic and Mitotic Death

Autophagic Cell Death

Senescence

SURVIVAL CURVES FOR VARIOUS MAMMALIAN CELLS IN CULTURE

SURVIVAL CURVE SHAPE AND MECHANISMS OF CELL DEATH

ONCOGENES AND RADIRESISTANCE

GENETIC CONTROL OF RADIOSensitivity

INTRINSIC RADIOSensitivity AND CANCER STEM CELLS

EFFECTIVE SURVIVAL CURVE FOR A MULTIFRACTION REGIMEN

CALCULATIONS OF TUMOR CELL KILL

Problem 1

Answer

Problem 2

Answer

Problem 3

Answer

Problem 4

Answer

THE RADIOSENSITIVITY OF MAMMALIAN CELLS COMPARED WITH MICROORGANISMS

SUMMARY OF PERTINENT CONCLUSIONS

BIBLIOGRAPHY

4 Radiosensitivity and Cell Age in the Mitotic Cycle

THE CELL CYCLE

SYNCHRONOUSLY DIVIDING CELL CULTURES

THE EFFECT OF X-RAYS ON SYNCHRONOUSLY DIVIDING CELL CULTURES

MOLECULAR CHECKPOINT GENES

THE EFFECT OF OXYGEN AT VARIOUS PHASES OF THE CELL CYCLE

THE AGE-RESPONSE FUNCTION FOR A TISSUE *IN VIVO*

VARIATION OF SENSITIVITY WITH CELL AGE FOR HIGH-LINEAR ENERGY TRANSFER RADIATIONS

MECHANISMS FOR THE AGE-RESPONSE FUNCTION

THE POSSIBLE IMPLICATIONS OF THE AGE-RESPONSE FUNCTION IN RADIOTHERAPY

SUMMARY OF PERTINENT CONCLUSIONS

BIBLIOGRAPHY

5 Fractionated Radiation and the Dose-Rate Effect

OPERATIONAL CLASSIFICATIONS OF RADIATION DAMAGE

Potentially Lethal Damage Repair

Sublethal Damage Repair

MECHANISM OF SUBLETHAL DAMAGE REPAIR

REPAIR AND RADIATION QUALITY

THE DOSE-RATE EFFECT

EXAMPLES OF THE DOSE-RATE EFFECT *IN VITRO* AND *IN VIVO*

THE INVERSE DOSE-RATE EFFECT

THE DOSE-RATE EFFECT SUMMARIZED

BRACHYTHERAPY OR ENDOCURIETHERAPY

Intracavitary Brachytherapy

Permanent Interstitial Implants

SUMMARY OF PERTINENT CONCLUSIONS

Potentially Lethal Damage Repair

Sublethal Damage Repair

Dose-Rate Effect

Brachytherapy

BIBLIOGRAPHY

6 Oxygen Effect and Reoxygenation

THE NATURE OF THE OXYGEN EFFECT

THE TIME AT WHICH OXYGEN ACTS AND THE MECHANISM OF THE OXYGEN EFFECT

THE CONCENTRATION OF OXYGEN REQUIRED

CHRONIC AND ACUTE HYPOXIA

Chronic Hypoxia

Acute Hypoxia

THE FIRST EXPERIMENTAL DEMONSTRATION OF HYPOXIC CELLS IN A TUMOR

PROPORTION OF HYPOXIC CELLS IN VARIOUS ANIMAL TUMORS
EVIDENCE FOR HYPOXIA IN HUMAN TUMORS
TECHNIQUES TO MEASURE TUMOR OXYGENATION

Oxygen Probe Measurements

Markers of Hypoxia

REOXYGENATION

TIME SEQUENCE OF REOXYGENATION

MECHANISM OF REOXYGENATION

THE IMPORTANCE OF REOXYGENATION IN RADIOTHERAPY

HYPOXIA AND CHEMORESISTANCE

HYPOXIA AND TUMOR PROGRESSION

SUMMARY OF PERTINENT CONCLUSIONS

BIBLIOGRAPHY

7 Linear Energy Transfer and Relative Biologic Effectiveness

THE DEPOSITION OF RADIANT ENERGY

LINEAR ENERGY TRANSFER

RELATIVE BIOLOGIC EFFECTIVENESS

RELATIVE BIOLOGIC EFFECTIVENESS AND FRACTIONATED DOSES

RELATIVE BIOLOGIC EFFECTIVENESS FOR DIFFERENT CELLS AND TISSUES

RELATIVE BIOLOGIC EFFECTIVENESS AS A FUNCTION OF LINEAR ENERGY TRANSFER

THE OPTIMAL LINEAR ENERGY TRANSFER

FACTORS THAT DETERMINE RELATIVE BIOLOGIC EFFECTIVENESS

THE OXYGEN EFFECT AND LINEAR ENERGY TRANSFER

RADIATION WEIGHTING FACTOR

SUMMARY OF PERTINENT CONCLUSIONS

BIBLIOGRAPHY

8 Acute Radiation Syndrome

ACUTE RADIATION SYNDROME

EARLY LETHAL EFFECTS

THE PRODROMAL RADIATION SYNDROME

THE CEREBROVASCULAR SYNDROME

THE GASTROINTESTINAL SYNDROME

THE HEMATOPOIETIC SYNDROME

THE FIRST AND MOST RECENT DEATHS FROM THE HEMATOPOIETIC SYNDROME

PULMONARY SYNDROME

CUTANEOUS RADIATION INJURY

SYMPTOMS ASSOCIATED WITH THE ACUTE RADIATION SYNDROME

TREATMENT OF RADIATION ACCIDENT VICTIMS EXPOSED TO DOSES CLOSE TO THE LD_{50/60}

TRIAGE

SURVIVORS OF SERIOUS RADIATION ACCIDENTS IN THE UNITED STATES

RADIATION EMERGENCY ASSISTANCE CENTER

SUMMARY OF PERTINENT CONCLUSIONS

BIBLIOGRAPHY

9 Medical Countermeasures to Radiation Exposure

INTRODUCTION AND DEFINITIONS

THE DISCOVERY OF RADIOPROTECTORS

MECHANISM OF ACTION

DEVELOPMENT OF MORE EFFECTIVE COMPOUNDS

AMIFOSTINE (WR-2721) AS A RADIOPROTECTOR IN RADIOTHERAPY

AMIFOSTINE AS A PROTECTOR AGAINST RADIATION-INDUCED CANCER

A NEW FAMILY OF AMINOTHIOL RADIOPROTECTORS

RADIATION MITIGATORS

RADIONUCLIDE ELIMINATORS

DIETARY SUPPLEMENTS AS COUNTERMEASURES TO RADIATION

SUMMARY OF PERTINENT CONCLUSIONS

BIBLIOGRAPHY

10 Radiation Carcinogenesis

TISSUE REACTIONS (DETERMINISTIC EFFECTS) AND STOCHASTIC EFFECTS

CARCINOGENESIS: THE HUMAN EXPERIENCE

THE LATENT PERIOD

ASSESSING THE RISK

COMMITTEES CONCERNED WITH RISK ESTIMATES AND RADIATION PROTECTION

RADIATION-INDUCED CANCER IN HUMAN POPULATIONS

Leukemia

Thyroid Cancer

Breast Cancer

Lung Cancer

Bone Cancer

Skin Cancer

QUANTITATIVE RISK ESTIMATES FOR RADIATION-INDUCED CANCER

DOSE AND DOSE-RATE EFFECTIVENESS FACTOR

SUMMARY OF RISK ESTIMATES

SECOND MALIGNANCIES IN RADIOTHERAPY PATIENTS

Second Cancers after Radiotherapy for Prostate Cancer

Radiation Therapy for Carcinoma of the Cervix

Second Cancers among Long-Term Survivors from Hodgkin Disease

DOSE-RESPONSE RELATIONSHIP FOR RADIATION
CARCINOGENESIS AT HIGH DOSES

CANCER RISKS IN NUCLEAR INDUSTRY WORKERS

EXTRAPOLATING CANCER RISKS FROM HIGH TO LOW DOSES

MORTALITY PATTERNS IN RADIOLOGISTS

CHILDHOOD CANCER AFTER RADIATION EXPOSURE IN UTERO

NONNEOPLASTIC DISEASE AND RADIATION

SUMMARY OF PERTINENT CONCLUSIONS

BIBLIOGRAPHY

11 Heritable Effects of Radiation

GERM CELL PRODUCTION AND RADIATION EFFECTS ON
FERTILITY

REVIEW OF BASIC GENETICS

MUTATIONS

Mendelian

Chromosomal Changes

Multifactorial

RADIATION-INDUCED HERITABLE EFFECTS IN FRUIT FLIES

RADIATION-INDUCED HERITABLE EFFECTS IN MICE

RADIATION-INDUCED HERITABLE EFFECTS IN HUMANS

INTERNATIONAL COMMISSION ON RADIOLOGICAL
PROTECTION ESTIMATES OF HEREDITARY RISKS

MUTATIONS IN THE CHILDREN OF THE A-BOMB SURVIVORS

CHANGING CONCERN FOR RISKS

EPIGENETICS

Imprinted Genes

SUMMARY OF PERTINENT CONCLUSIONS

BIBLIOGRAPHY

12 Effects of Radiation on the Embryo and Fetus

HISTORICAL PERSPECTIVE

OVERVIEW OF RADIATION EFFECTS ON THE EMBRYO AND FETUS

DATA FROM MICE AND RATS

Preimplantation

Organogenesis

The Fetal Period

EXPERIENCE IN HUMANS

Survivors of the A-Bomb Attacks on Hiroshima and Nagasaki Irradiated In Utero

Exposure to Medical Radiation

COMPARISON OF HUMAN AND ANIMAL DATA

CANCER IN CHILDHOOD AFTER IRRADIATION IN UTERO

OCCUPATIONAL EXPOSURE OF WOMEN

THE PREGNANT OR POTENTIALLY PREGNANT PATIENT

SUMMARY OF PERTINENT CONCLUSIONS

BIBLIOGRAPHY

13 Radiation Cataractogenesis

CATARACTS OF THE OCULAR LENS

LENS OPACIFICATION IN EXPERIMENTAL ANIMALS

RADIATION CATARACTS IN HUMANS

THE LATENT PERIOD

DOSE-RESPONSE RELATIONSHIP FOR CATARACTS IN HUMANS

SUMMARY OF PERTINENT CONCLUSIONS

BIBLIOGRAPHY

14 Radiologic Terrorism

POSSIBLE SCENARIOS FOR RADIOLOGIC TERRORISM

AVAILABILITY OF RADIOACTIVE MATERIAL

HEALTH EFFECTS OF RADIATION

**EXTERNAL EXPOSURE TO RADIATION AND CONTAMINATION
WITH RADIOACTIVE MATERIALS**

EXTERNAL CONTAMINATION

INTERNAL CONTAMINATION

**MEDICAL MANAGEMENT ISSUES IN THE EVENT OF
RADIOLOGIC TERRORISM**

FURTHER INFORMATION

SUMMARY OF PERTINENT CONCLUSIONS

BIBLIOGRAPHY

15 Doses and Risks in Diagnostic Radiology, Interventional Radiology and Cardiology, and Nuclear Medicine

DOSES FROM NATURAL BACKGROUND RADIATION

Cosmic Radiation

Natural Radioactivity in the Earth's Crust

Internal Exposure

Areas of High Natural Background

**COMPARISON OF RADIATION DOSES FROM NATURAL SOURCES
AND HUMAN ACTIVITIES**

DIAGNOSTIC RADIOLOGY

Dose

Effective Dose

Collective Effective Dose

INTERVENTIONAL RADIOLOGY AND CARDIOLOGY

Patient Doses and Effective Doses

Dose to Personnel

NUCLEAR MEDICINE

Historical Perspective

Effective Dose and Collective Effective Dose

Principles in Nuclear Medicine

Positron Emission Tomography

The Therapeutic Use of Radionuclides

MEDICAL IRRADIATION OF CHILDREN AND PREGNANT WOMEN

Irradiation of Children

Irradiation of Pregnant Women

DOSES TO THE EMBRYO AND FETUS

RECOMMENDATIONS ON BREASTFEEDING INTERRUPTIONS

SUMMARY

SUMMARY OF PERTINENT CONCLUSIONS

Computed Tomography

Effective Dose and Cancer

Interventional Procedures

Nuclear Medicine

Medical Radiation of Children and Pregnant Women

Summary

BIBLIOGRAPHY

16 Radiation Protection

DE MINIMIS DOSE AND NEGLIGIBLE INDIVIDUAL DOSE

RADIATION DETRIMENT

NATIONAL COUNCIL ON RADIATION PROTECTION AND MEASUREMENTS AND THE INTERNATIONAL COMMISSION ON RADIOLOGICAL PROTECTION COMPARED

THE HISTORY OF THE CURRENT DOSE LIMITS

DOSE RANGES

SUMMARY OF PERTINENT CONCLUSIONS

GLOSSARY OF TERMS

BIBLIOGRAPHY

THE ORIGINS OF RADIATION PROTECTION

ORGANIZATIONS

QUANTITIES AND UNITS

Dose

Radiation Weighting Factor

Equivalent Dose

Effective Dose

Committed Equivalent Dose

Committed Effective Dose

Collective Equivalent Dose

Collective Effective Dose

Collective Committed Effective Dose

Summary of Quantities and Units

TISSUE REACTIONS AND STOCHASTIC EFFECTS

PRINCIPLES OF RADIATION PROTECTION

BASIS FOR EXPOSURE LIMITS

LIMITS FOR OCCUPATIONAL EXPOSURE

Stochastic Effects

Tissue Reactions (Formerly Known as Deterministic Effects)

AS LOW AS REASONABLY ACHIEVABLE

PROTECTION OF THE EMBRYO/FETUS

EMERGENCY OCCUPATIONAL EXPOSURE

EXPOSURE OF PERSONS YOUNGER THAN 18 YEARS OF AGE

EXPOSURE OF MEMBERS OF THE PUBLIC (NONOCCUPATIONAL LIMITS)

EXPOSURE TO INDOOR RADON

SECTION II For Students of Radiation Oncology

17 Molecular Techniques in Radiobiology

HISTORICAL PERSPECTIVES

THE STRUCTURE OF DNA

RNA AND DNA

TRANSCRIPTION AND TRANSLATION

THE GENETIC CODE

AMINO ACIDS AND PROTEINS

RESTRICTION ENDONUCLEASES

VECTORS

Plasmids

Bacteriophage λ

Bacterial Artificial Chromosomes

Viruses

LIBRARIES

Genomic Library

cDNA Library

HOSTS

Escherichia Coli

Yeast

Mammalian Cells

DNA-MEDIATED GENE TRANSFER

AGAROSE GEL ELECTROPHORESIS

POLYMERASE CHAIN REACTION

Polymerase Chain Reaction-mediated Site-directed Mutagenesis

GENE-CLONING STRATEGIES

GENOMIC ANALYSES

Mapping

Contiguous Mapping

DNA Sequence Analyses

Polymorphisms or Mutations

Restriction Fragment Length Polymorphisms

Comparative Genome Hybridization

GENE KNOCKOUT STRATEGIES

Clustered Regularly Interspaced Short Palindromic Repeats and CRISPR Associated Protein

Homologous Recombination to Knockout Genes

Knockout Mice

GENE EXPRESSION ANALYSIS

Northern Blotting

RNA Interference

Reverse Transcription Polymerase Chain Reaction

Quantitative Real-Time Polymerase Chain Reaction

Genetic Reporters

Promoter Bashing

Chromatin Immunoprecipitation

Protein–DNA Interaction Arrays (Chromatin Immunoprecipitation-Chips)

Microarrays to Assay Gene Expression

RNA-Seq to Assay Gene Expression

Chromatin Immunoprecipitation-Seq

PROTEIN ANALYSIS

Western Blotting

Antibody Production

Immunoprecipitation

Far Western Blotting
Fluorescent Proteins
Two-Hybrid Screening
Split Luciferase Complementation Assay
Proteomics
Two-Dimensional Electrophoresis

DATABASES AND SEQUENCE ANALYSIS

SUMMARY OF PERTINENT CONCLUSIONS

GLOSSARY OF TERMS

BIBLIOGRAPHY

18 Cancer Biology

MECHANISMS OF CARCINOGENESIS

ONCOGENES

MECHANISMS OF ONCOGENE ACTIVATION

Retroviral Integration through Recombination

DNA Mutation of Regulatory Sites

Gene Amplification

Chromosome Translocation

MUTATION AND INACTIVATION OF TUMOR SUPPRESSOR GENES

The Retinoblastoma Paradigm

The Li–Fraumeni Paradigm

Familial Breast Cancer, BRCA1 and BRCA2

SOMATIC HOMOZYGOSITY

THE MULTISTEP NATURE OF CANCER

FUNCTION OF ONCOGENES AND TUMOR SUPPRESSOR GENES

Dysregulated Proliferation

Failure to Respond to Growth-Restrictive Signals

Failure to Commit Suicide (Apoptosis)

Escaping Senescence

Angiogenesis

Invasion and Metastasis

THE CONCEPT OF GATEKEEPERS AND CARETAKERS

MISMATCH REPAIR

HERITABLE SYNDROMES THAT AFFECT RADIOSENSITIVITY, GENOMIC INSTABILITY, AND CANCER

Ataxia-Telangiectasia

Seckel Syndrome

Mouse versus Human Severe Combined Immunodeficiency

Ataxia-Telangiectasia-Like Disorder

Nijmegen Breakage Syndrome

Fanconi Anemia

Homologues of RecQ—Bloom Syndrome, Werner Syndrome, and Rothmund–Thompson Syndrome

RADIATION-INDUCED SIGNAL TRANSDUCTION

Early Response Genes

The Ceramide Pathway

T CELL CHECKPOINT THERAPY

SUMMARY OF PERTINENT CONCLUSIONS

BIBLIOGRAPHY

Signal Transduction

Heritable Syndromes that Affect Radiosensitivity, Genomic Instability, and Cancer

Oncogenes and Tumor Suppressor Genes

Cancer Genetics

Multistep Nature of Cancer and Mismatch Repair

Genes and Ionizing Radiation

DOSE-RESPONSE RELATIONSHIPS

Therapeutic Ratio (Therapeutic Index)

TYPES OF CELL DEATH: HOW AND WHY CELLS DIE

ASSAYS FOR DOSE-RESPONSE RELATIONSHIPS

CLONOGENIC END POINTS

Clones Regrowing *In Situ*

Skin Colonies

Crypt Cells of the Mouse Jejunum

Testes Stem Cells

Kidney Tubules

Cells Transplanted to Another Site

Bone Marrow Stem Cells

Mammary and Thyroid Cells

SUMMARY OF DOSE-RESPONSE CURVES FOR CLONOGENIC ASSAYS IN NORMAL TISSUES

DOSE-RESPONSE RELATIONSHIPS FOR FUNCTIONAL END POINTS

Pig Skin

Rodent Skin

Early and Late Response of the Lung Based on Breathing Rate

Spinal Cord Myelopathy

Latency

Fractionation and Protraction

Volume Effects

Retreatment after Long Time Intervals

INFERRING THE RATIO α/β FROM MULTIFRACTION EXPERIMENTS IN NONCLONOGENIC SYSTEMS

SUMMARY OF PERTINENT CONCLUSIONS

BIBLIOGRAPHY

20 Clinical Response of Normal Tissues

CELLS AND TISSUES

EARLY (ACUTE) AND LATE EFFECTS

FUNCTIONAL SUBUNITS IN NORMAL TISSUES

THE VOLUME EFFECT IN RADIOTHERAPY: TISSUE ARCHITECTURE

RADIATION PATHOLOGY OF TISSUES

CASARETT'S CLASSIFICATION OF TISSUE RADIOSensitivity

MICHALOWSKI'S H- AND F-TYPE POPULATIONS

GROWTH FACTORS

SPECIFIC TISSUES AND ORGANS

Skin

Skin Appendages: A Special Case

Hematopoietic System

Blood Cell Counts after Total Body Irradiation

Partial Body Irradiation

Radiation and Chemotherapy Agents

Lymphoid Tissue and the Immune System

Digestive Tract

Oral Mucosa

Esophagus

Stomach

Small and Large Intestines

Lungs

Kidneys

Liver

Bladder Epithelium

Central and Peripheral Nervous Systems

Brain
Spinal Cord
Peripheral Nerves
Testes
Ovaries
Female Genitalia
Blood Vessels and the Vascular System
Heart
Bone and Cartilage

QUANTITATIVE ANALYSIS OF NORMAL TISSUE EFFECTS IN THE CLINIC

LATE EFFECTS OF NORMAL TISSUE AND SOMA

The SOMA Scoring System

APPLICATION OF STEM CELLS TO REGENERATE RADIATION-SENSITIVE ORGANS—SALIVARY GLAND REGENERATION

SUMMARY OF PERTINENT CONCLUSIONS

BIBLIOGRAPHY

21 Model Tumor Systems

TRANSPLANTABLE SOLID TUMOR SYSTEMS IN EXPERIMENTAL ANIMALS

APOPTOSIS IN TUMORS

TUMOR GROWTH MEASUREMENTS

TUMOR CURE (TCD₅₀) ASSAY

DILUTION ASSAY TECHNIQUE

LUNG COLONY ASSAY

IN VIVO/IN VITRO ASSAY

XENOGRAFTS OF HUMAN TUMORS

PATIENT-DERIVED XENOGRAFTS MODELS

AUTOCHTHONOUS AND TRANSGENIC TUMOR MODELS

SPHEROIDS: AN *IN VITRO* MODEL TUMOR SYSTEM

SPHEROIDS OF HUMAN TUMOR CELLS

ORGANOID MODELS OF HUMAN TUMORS

COMPARISON OF THE VARIOUS MODEL TUMOR SYSTEMS

SUMMARY OF PERTINENT CONCLUSIONS

BIBLIOGRAPHY

22 Cell, Tissue, and Tumor Kinetics

THE CELL CYCLE

CYCLINS AND KINASES

CHECKPOINT PATHWAYS

QUANTITATIVE ASSESSMENT OF THE CONSTITUENT PARTS OF
THE CELL CYCLE

THE PERCENT-LABELED MITOSES TECHNIQUE

EXPERIMENTAL MEASUREMENTS OF CELL CYCLE TIMES *IN
VIVO* AND *IN VITRO*

PULSED FLOW CYTOMETRY

THE GROWTH FRACTION

POTENTIAL DOUBLING TIME

CELL LOSS

DETERMINATIONS OF CELL LOSS IN EXPERIMENTAL ANIMAL
TUMORS

GROWTH KINETICS OF HUMAN TUMORS

SUMMARY OF PERTINENT CONCLUSIONS

BIBLIOGRAPHY

23 Time, Dose, and Fractionation in Radiotherapy

THE INTRODUCTION OF FRACTIONATION

THE FOUR Rs OF RADIOBIOLOGY

THE STRANDQUIST PLOT AND THE ELLIS NOMINAL STANDARD
DOSE SYSTEM

PROLIFERATION AS A FACTOR IN NORMAL TISSUES

**THE SHAPE OF THE DOSE-RESPONSE RELATIONSHIP FOR
EARLY- AND LATE-RESPONDING TISSUES**

**A POSSIBLE EXPLANATION FOR THE DIFFERENCE IN SHAPE OF
DOSE-RESPONSE RELATIONSHIPS FOR EARLY- AND LATE-
RESPONDING TISSUES**

**FRACTION SIZE AND OVERALL TREATMENT TIME: INFLUENCE
ON EARLY- AND LATE-RESPONDING TISSUES**

ACCELERATED REPOPULATION

THE IMPORTANCE OF OVERALL TREATMENT TIME

MULTIPLE FRACTIONS PER DAY

HYPOFRACTIONATION: RENEWED INTEREST

**USING THE LINEAR-QUADRATIC CONCEPT TO CALCULATE
EFFECTIVE DOSES IN RADIOTHERAPY**

Choice of α/β

Model Calculations

Allowance for Tumor Proliferation

Calculations Suggested by Fowler

Pragmatic Approach of Peters and Colleagues

SUMMARY OF PERTINENT CONCLUSIONS

BIBLIOGRAPHY

24 Retreatment after Radiotherapy: The Possibilities and the Perils

THE NATURE OF THE PROBLEM

EARLY- AND LATE-RESPONDING TISSUES

PRECLINICAL DATA

CLINICAL STUDIES

Spinal Cord

Brain

Head and Neck

Rectum

Bone Metastases

Breast

Lung

Recurrent Vaginal Metastases

SUMMARY OF PERTINENT CONCLUSIONS

Animal Studies

Clinical Studies

BIBLIOGRAPHY

Reviews

Preclinical (Animal Studies)

Clinical

25 Alternative Radiation Modalities

FAST NEUTRONS

Rationale

The Hammersmith Neutron Experience

The United States Neutron Experience

BORON NEUTRON CAPTURE THERAPY

Boron Compounds

Neutron Sources

Clinical Trials

PROTONS

Depth-Dose Patterns and the Bragg Peak

Advantages of Protons

CARBON ION RADIOTHERAPY

Depth-Dose Profiles

Radiobiologic Properties

Design of a Carbon Ion Beam for Clinical Use

Scattering and Fragmentation

Positron Emission Tomography Verification of Treatment Plans

Reasons for the Choice of Carbon Ions

SUMMARY OF PERTINENT CONCLUSIONS

Hadron Therapy

Neutrons

Boron Neutron Capture Therapy

Protons

Carbon Ion Radiotherapy

BIBLIOGRAPHY

26 The Biology and Exploitation of Tumor Hypoxia

HYPOXIA-INDUCIBLE FACTOR

Oxygen-Dependent Regulation of Hypoxia-Inducible Factor

Cancer Mutations that Activate Hypoxia-Inducible Factor

Important Roles of Hypoxia-Inducible Factor in Tumors

Tumor Angiogenesis

Tumor Metabolism

Tumor Metastasis

Hypoxia-Inducible Factor and Radiotherapy

UNFOLDED PROTEIN RESPONSE

RADIOSENSITIZING HYPOXIC CELLS

Hyperbaric Oxygen

Improving the Oxygen Supply to Tumors

Hypoxic Cell Radiosensitizers

Misonidazole

Etanidazole and Nimorazole

Overgaard's Meta-analysis of Clinical Trials Addressing the Problem of Hypoxia

Nicotinamide and Carbogen Breathing
HYPOXIC CYTOTOXINS

Tirapazamine

Clinical Trials with Tirapazamine and New Bioreductive Drugs

TARGETING TUMOR METABOLISM TO KILL HYPOXIC CELLS

Targeting Tumor Metabolism to Enhance the Efficacy of Radiotherapy

SUMMARY OF PERTINENT CONCLUSIONS

Hypoxia-Inducible Factor

The Unfolded Protein Response

Radiosensitizing Hypoxic Cells

Hypoxic Cytotoxins

BIBLIOGRAPHY

- 27 Chemotherapeutic Agents from the Perspective of the Radiation Biologist

BIOLOGIC BASIS OF CHEMOTHERAPY

CLASSES OF AGENTS AND THEIR MODE OF ACTION

Alkylating Agents

Procarbazine

Cis-Platinum

Antibiotics

Antimetabolites

5-Fluorouracil

Hydroxyurea

Nucleoside Analogues

Vinca Alkaloids

Taxanes

Hormone Targeted Therapies

Topoisomerase Inhibitors

Targeted Therapy

Cetuximab (Erbitux)

Bevacizumab (Avastin)

Poly Adenosine Diphosphate-Ribose Polymerase Inhibitors

Immune Checkpoint Therapies

DOSE-RESPONSE RELATIONSHIPS

SUBLETHAL AND POTENTIALLY LETHAL DAMAGE REPAIR

THE OXYGEN EFFECT AND CHEMOTHERAPEUTIC AGENTS

RESISTANCE TO CHEMOTHERAPY AND HYPOXIC CYTOTOXINS

DRUG RESISTANCE AND CANCER STEM CELLS

COMPARISON OF CHEMOTHERAPEUTIC AGENTS WITH RADIATION

ADJUNCT USE OF CHEMOTHERAPEUTIC AGENTS WITH RADIATION

ASSAYS FOR SENSITIVITY OF INDIVIDUAL TUMORS

SECOND MALIGNANCIES

SUMMARY OF PERTINENT CONCLUSIONS

BIBLIOGRAPHY

28 Hyperthermia

HISTORICAL

RESPONSE TO HEAT AT CYTOTOXIC TEMPERATURES

Dose Response

Sensitivity to Heat as a Function of Cell Age in the Mitotic Cycle

Hypoxia and Hyperthermia

Effect of pH and Nutrient Deficiency on Sensitivity to Heat

Response of Normal Tissues to Heat

Thermotolerance

Heat and Tumor Vasculature

METHODS OF HEATING AND THE IMPACT ON CLINICAL HYPERTERMIA

Methods of Heating in Experimental Systems

Methods of Heating in Patients

Thermal Ablation

RESPONSE TO HEAT AT NONCYTOTOXIC TEMPERATURES

Reoxygenation

Immunologic Effects of Hyperthermia

THERMAL ENHANCEMENT RATIO

HEAT AND THE THERAPEUTIC GAIN FACTOR

MEASURING THERMAL DOSE IN PATIENTS

PHASE III CLINICAL TRIALS TESTING BENEFITS OF HYPERTHERMIA FOR ENHANCING RADIATION THERAPY

CLINICAL TRIALS ASSESSING THE BENEFIT OF HYPERTHERMIA IN COMBINATION WITH CHEMOTHERAPEUTIC AGENTS

Development and Evaluation of “Thermosensitive” Liposomes for Improved Tumor Targeting of Chemotherapy

METHODS OF TUMOR HEATING

Magnetic Hyperthermia

CLINICAL THERMOMETRY

Invasive Thermometry Methods

Progress toward Clinically Achievable Noninvasive Thermometry

SUMMARY OF PERTINENT CONCLUSIONS

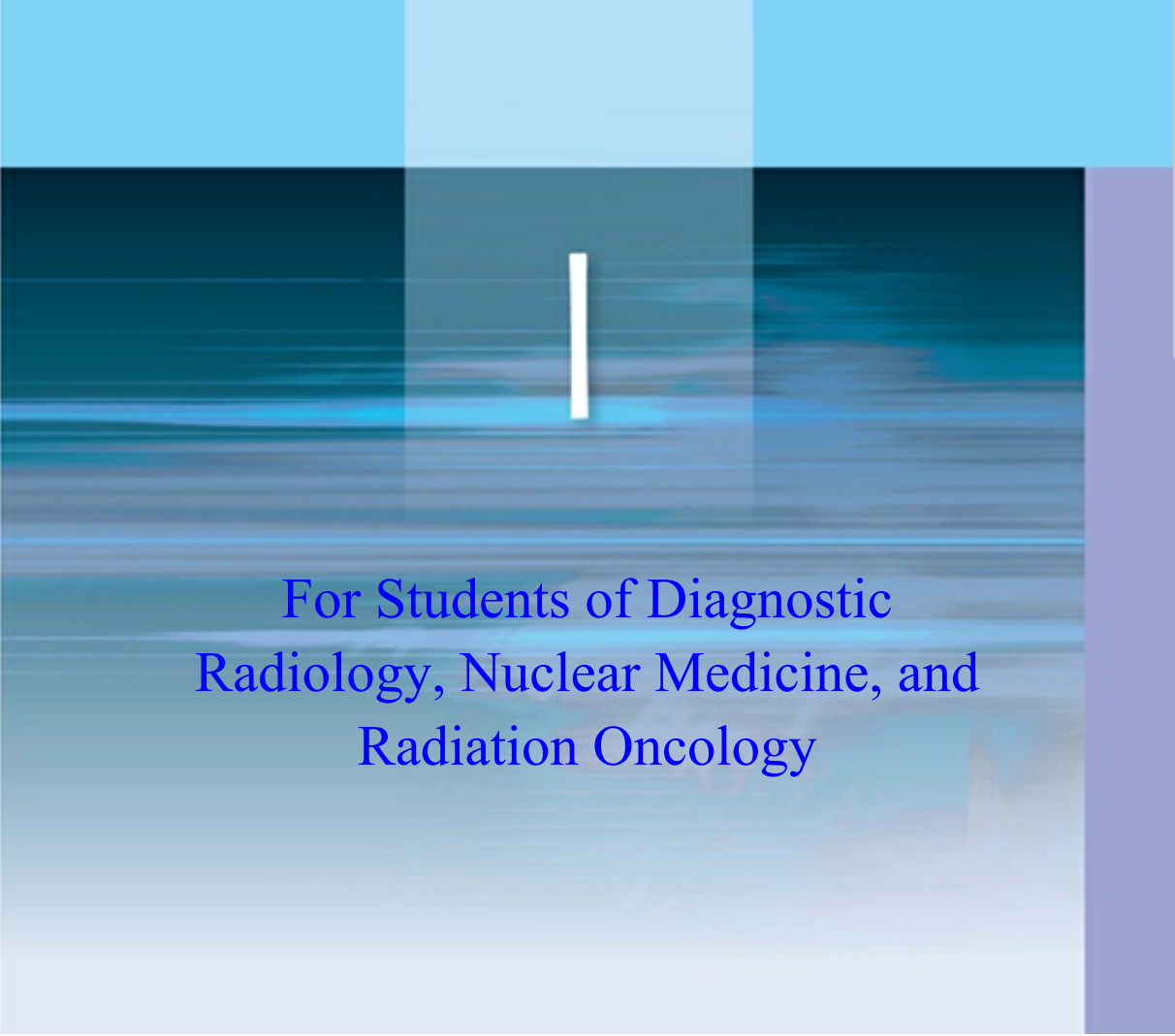
Hyperthermia at Cytotoxic Temperatures (42° to 45° C)

Hyperthermia at Modest Temperatures that Can Be Achieved in Human Tumors

BIBLIOGRAPHY

Glossary

Index



For Students of Diagnostic
Radiology, Nuclear Medicine, and
Radiation Oncology

chapter 1

Physics and Chemistry of Radiation Absorption

Types of Ionizing Radiations

Electromagnetic Radiations

Particulate Radiations

Absorption of X-rays

Direct and Indirect Action of Radiation

Absorption of Neutrons

Absorption of Protons and Heavier Ions Such as Carbon

Summary of Pertinent Conclusions

Bibliography

In 1895, the German physicist Wilhelm Conrad Röntgen discovered “a new kind of ray,” emitted by a gas discharge tube, that could blacken photographic film contained in light-tight containers. He called these rays “x-rays” in his first announcement in December 1895—the x representing the unknown. In demonstrating the properties of x-rays at a public lecture, Röntgen asked Rudolf Albert von Kölliker, a prominent Swiss professor of anatomy, to put his hand in the beam and so produced the first publicly taken radiograph (Fig. 1.1).



FIGURE 1.1 The first publicly taken radiograph of a living object, taken in January 1896, just a few months after the discovery of x-rays. (Courtesy of Röntgen Museum, Würzburg, Germany.)

The first medical use of x-rays was reported in the *Lancet* of January 23, 1896. In this report, x-rays were used to locate a piece of a knife in the backbone of a drunken sailor, who was paralyzed until the fragment was removed following its location. The new technology spread rapidly through Europe and the United States, and the field of diagnostic radiology was born. There is some debate about who first used x-rays therapeutically, but by 1896, Leopold Freund, an Austrian surgeon, demonstrated before the Vienna Medical Society the disappearance of a hairy mole following treatment with x-rays. Antoine Henri Becquerel discovered radioactivity emitted by uranium compounds in 1896, and 2 years later, Pierre and Marie Curie isolated the radioactive elements polonium and radium. Within a few years, radium was used for the treatment of cancer.

The first recorded biologic effect of radiation was due to Becquerel, who inadvertently left a radium container in his vest pocket. He subsequently described the skin erythema that appeared 2 weeks later and the ulceration that developed and that required several weeks to heal. It is said that Pierre Curie repeated this experience in 1901 by deliberately producing a radium “burn” on his own forearm (Fig. 1.2). From these early beginnings, at the turn of the century, the study of radiobiology began.



FIGURE 1.2 Based on Becquerel's earlier observation, Pierre Curie is said to have used a radium tube to produce a radiation ulcer on his arm. He charted its appearance and subsequent healing.

Radiobiology is the study of the action of ionizing radiations on living things. As such, it inevitably involves a certain amount of radiation physics. The purpose of this chapter is to present, in summary form and with a minimum of mathematics, a listing of the various types of ionizing radiations and a description of the physics and chemistry of the processes by which radiation is absorbed.

TYPES OF IONIZING RADIATIONS

The absorption of energy from radiation in biologic material may lead to *excitation* or to *ionization*. The raising of an electron in an atom or molecule to a higher energy level without actual ejection of the electron is called **excitation**. If the radiation has sufficient energy to eject one or more orbital electrons from the atom or molecule, the process is called **ionization**, and that radiation is said to be **ionizing radiation**. The important characteristic of ionizing radiation is the localized release of large amounts of energy. The energy dissipated per ionizing event is about 33 eV, which is more than enough to break a strong chemical bond; for example, the energy associated with a C=C bond is 4.9 eV. For convenience, it is usual to classify ionizing radiations as either **electromagnetic** or **particulate**.

Electromagnetic Radiations

Most experiments with biologic systems have involved x- or γ -rays, two forms of electromagnetic radiation. X- and γ -rays do not differ in nature or in properties; the designation of x- or γ -rays reflects the ways they are produced. X-rays are produced *extranuclearly*; γ -rays are produced *intranuclearly*. In practical terms, this means that x-rays are produced in an electrical device that accelerates

electrons to high energy and then stops them abruptly in a target usually made of tungsten or gold. Part of the kinetic energy (the energy of motion) of the electrons is converted to x-rays. On the other hand, γ -rays are emitted by radioactive isotopes; they represent excess energy that is given off as the unstable nucleus breaks up and decays in its efforts to reach a stable form. Natural background radiation from rocks in the earth also includes γ -rays. Everything that is stated about x-rays in this chapter applies equally well to γ -rays.

X-rays may be considered from two different standpoints. First, they may be thought of as waves of electrical and magnetic energy. The magnetic and electrical fields, in planes at right angles to each other, vary with time, so that the wave moves forward in much the same way as ripples move over the surface of a pond if a stone is dropped into the water. The wave moves with a velocity, c , which in a vacuum has a value of 3×10^{10} cm/s. The distance between successive peaks of the wave, λ , is known as the wavelength. The number of waves passing a fixed point per second is the frequency, v . The product of frequency times wavelength gives the velocity of the wave; that is, $\lambda v = c$.

A helpful, if trivial, analogy is to liken the wavelength to the length of a person's stride when walking; the number of strides per minute is the frequency. The product of the length of stride multiplied by the number of strides per minute gives the speed or velocity of the walker.

Like x-rays, radio waves, radar, radiant heat, and visible light are forms of electromagnetic radiation. They all have the same velocity, c , but they have different wavelengths and, therefore, different frequencies. To extend the previous analogy, different radiations may be likened to a group of people: Some are tall, some are short, but all walking together at the same speed. The tall walkers take long measured strides but make few strides per minute; to keep up, the short walkers compensate for the shortness of their strides by increasing the frequencies of their strides. A radio wave may have a distance between successive peaks (i.e., wavelength) of 300 m; for a wave of visible light, the corresponding distance is about 500 thousandths of a centimeter (5×10^{-5} cm). The wavelength for x-rays may be 100 millionths of a centimeter (10^{-8} cm). X- and γ -rays, then, occupy the short-wavelength end of the electromagnetic spectrum (Fig. 1.3).

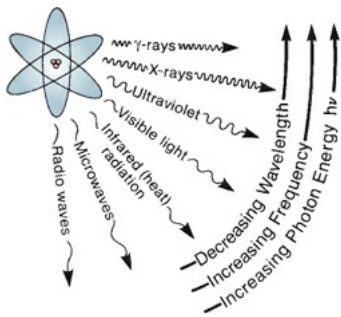


FIGURE 1.3 Illustration of the electromagnetic spectrum. X- and γ -rays have the same nature as visible light, radiant heat, and radio waves; however, they have shorter wavelengths and, consequently, a larger photon energy. As a result, x- and γ -rays can break chemical bonds and produce biologic effects.

Second, x-rays may be thought of as streams of photons, or “packets” of energy. Each energy packet contains an amount of energy equal to $h\nu$, where h is known as Planck’s constant and ν is the frequency. If a radiation has a long wavelength, it has a small frequency, and so, the energy per photon is small. Conversely, if a given radiation has a short wavelength, the frequency is large and the energy per photon is large. There is a simple numeric relationship between the photon energy (in kiloelectron volts*) and the wavelength (in angstroms†):

$$\lambda \text{\AA} = 12.4 / E \text{ (keV)}$$

For example, x-rays with wavelengths of 0.1 Å correspond to a photon energy of 124 keV.

The concept of x-rays being composed of photons is very important in radiobiology. If x-rays are absorbed in living material, energy is deposited in the tissues and cells. This energy is deposited unevenly in discrete packets. The energy in a beam of x-rays is quantized into large individual packets, each of which is big enough to break a chemical bond and initiate the chain of events that culminates in a biologic change. The critical difference between nonionizing and ionizing radiations is the size of the *individual* packets of energy, not the *total* energy involved. A simple calculation illustrates this point. It is shown in Chapter 8 that a total body dose of about 4 Gy‡ of x-rays given to a human is lethal in about half of the individuals exposed. This dose represents absorption of energy of only about 67 cal, assuming the person to be a “standard man” weighing 70 kg. The smallness of the amount of energy involved can be illustrated in many ways. Converted to heat, it would represent a temperature rise of 0.002° C, which would do no harm at all; the same amount of energy in the form of heat is absorbed in drinking one sip of warm coffee. Alternatively, the

energy inherent in a lethal dose of x-rays may be compared with mechanical energy or work. It would correspond to the work done in lifting a person about 16 in. from the ground (Fig. 1.4).

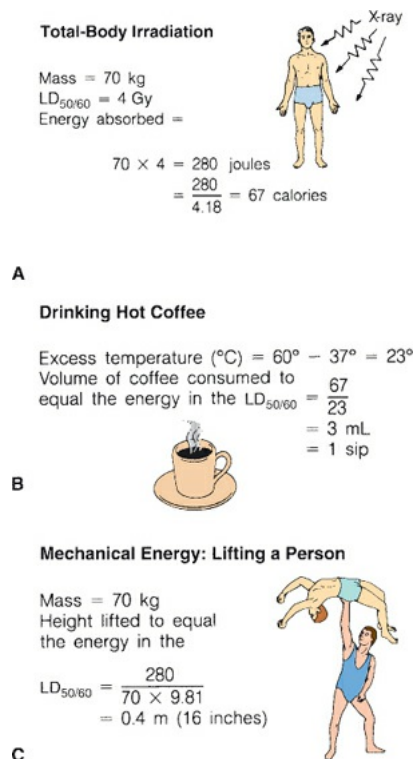


FIGURE 1.4 The biologic effect of radiation is determined not by the amount of the energy absorbed but by the photon size, or packet size, of the energy. **A:** The total amount of energy absorbed in a 70-kg human exposed to a lethal dose of 4 Gy is only 67 cal. **B:** This is equal to the energy absorbed in drinking one sip of warm coffee. **C:** It also equals the potential energy imparted by lifting a person about 16 in.

Energy in the form of heat or mechanical energy is absorbed uniformly and evenly, and much greater quantities of energy in these forms are required to produce damage in living things. The potency of x-rays, then, is a function not so much of the total energy absorbed as of the size of the individual energy packets. In their biologic effects, electromagnetic radiations are usually considered ionizing if they have a photon energy in excess of 124 eV, which corresponds to a wavelength shorter than about 10^{-6} cm.

Particulate Radiations

Other types of radiation that occur in nature and that are also used experimentally are electrons, protons, α -particles, neutrons, negative π -mesons, and heavy charged ions. Some also are used in radiation therapy and have a

potential in diagnostic radiology not yet explored.

Electrons are small, negatively charged particles that can be accelerated to high energy to a speed close to that of light by means of an electrical device, such as a betatron or linear accelerator. They are widely used for cancer therapy.

Protons are positively charged particles and are relatively massive, having a mass almost 2,000 times greater than that of an electron. Because of their mass, they require more complex and more expensive equipment, such as a cyclotron, to accelerate them to useful energies, but they are increasingly used for cancer treatment in specialized centers because of their favorable dose distribution (see [Chapter 25](#)).

In nature, the earth is showered with protons from the sun, which represent a component of natural background radiation. We are protected on earth to a large extent by the earth's atmosphere. In addition, the earth behaves like a giant magnet so that charged particles from solar events on the sun are deflected away from the equator by the earth's magnetic field; most miss the earth altogether, whereas others are funneled into the polar regions. This is the basis of the "aurora borealis," or northern lights caused by intense showers of charged particles that spiral down the lines of magnetic field into the poles, ionizing the air as they do so (see [Chapter 15](#)). Protons are a major hazard to astronauts on long-duration space missions.

α -Particles are nuclei of helium atoms and consist of two protons and two neutrons in close association. They have a net positive charge and, therefore, can be accelerated in large electrical devices similar to those used for protons.

α -Particles are also emitted during the decay of heavy, naturally occurring radionuclides, such as uranium and radium ([Fig. 1.5](#)). α -Particles are the major source of natural background radiation to the general public. Radon gas seeps out of the soil and builds up inside houses, where, together with its decay products, it is breathed in and irradiates the lining of the lung. It is estimated that 10,000 to 20,000 cases of lung cancer are caused each year by this means in the United States, mostly in smokers.

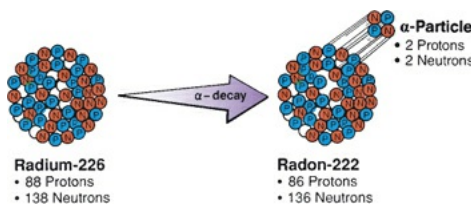


FIGURE 1.5 Illustration of the decay of a heavy radionuclide by the emission of an α -particle. An α -particle is a helium nucleus consisting of two protons and

two neutrons. The emission of an α -particle decreases the atomic number by 2 and the mass number by 4. Note that radium has changed to another chemical element, radon, as a consequence of the decay.

Neutrons are particles with a mass similar to that of protons, but they carry no electrical charge. Because they are electrically neutral, they cannot be accelerated in an electrical device. They are produced if a charged particle is accelerated to high energy and then made to impinge on a suitable target material. Neutrons are also emitted as a by-product if heavy radioactive atoms undergo fission; that is, a split to form two smaller atoms. Consequently, neutrons are present in large quantities in nuclear reactors and are emitted by some artificial heavy radionuclides. They are also an important component of space radiation and contribute significantly to the exposure of passengers and crews of high-flying jetliners.

Heavy charged particles are nuclei of elements, such as carbon, neon, argon, or even iron, that are positively charged because some or all of the planetary electrons have been stripped from them. To be useful for radiation therapy, they must be accelerated to energies of thousands of millions of volts and, therefore, can be produced in only a few specialized facilities, although the number of such centers is increasing.

Charged particles of enormous energy are encountered in space and represent a major hazard to astronauts on long missions, such as the proposed trip to Mars. During the lunar missions of the 1970s, astronauts “saw” light flashes while their eyes were closed in complete darkness, which turned out to be caused by high-energy iron ions crossing the retina.

ABSORPTION OF X-RAYS

Radiation may be classified as *directly* or *indirectly* ionizing. All of the charged particles previously discussed are **directly ionizing**; that is, provided the individual particles have sufficient kinetic energy, they can disrupt the atomic structure of the absorber through which they pass directly and produce chemical and biologic changes. Electromagnetic radiations (x- and γ -rays) are **indirectly ionizing**. They do not produce chemical and biologic damage themselves, but when they are absorbed in the material through which they pass, they give up their energy to produce fast-moving charged particles that in turn are able to produce damage.

The process by which x-ray photons are absorbed depends on the energy of the photons concerned and the chemical composition of the absorbing material.

At high energies, characteristic of a cobalt-60 unit or a linear accelerator used for radiotherapy, the **Compton process** dominates. In this process, the photon interacts with what is usually referred to as a “free” electron, an electron whose binding energy is negligibly small compared with the photon energy. Part of the energy of the photon is given to the electron as kinetic energy; the photon, with whatever energy remains, continues on its way, deflected from its original path (Fig. 1.6). In place of the incident photon, there is a fast electron and a photon of reduced energy, which may go on to take part in further interactions. In any given case, the photon may lose a little energy or a lot; in fact, the fraction lost may vary from 0% to 80%. In practice, if an x-ray beam is absorbed by the tissue, several photons will interact with several atoms, and on a statistical basis, all possible energy losses occur. The net result is the production of several fast electrons, many of which can ionize other atoms of the absorber, break vital chemical bonds, and initiate the change of events that ultimately is expressed as biologic damage.

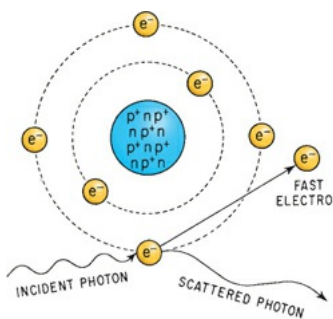


FIGURE 1.6 Absorption of an x-ray photon by the Compton process. The photon interacts with a loosely bound planetary electron of an atom of the absorbing material. Part of the photon energy is given to the electron as kinetic energy. The photon, deflected from its original direction, proceeds with longer wavelength (i.e., with reduced energy).

For photon energies, characteristic of diagnostic radiology, both Compton and photoelectric absorption processes occur, the former dominating at the higher end of the energy range and the latter being most important at lower energies. In the photoelectric process (Fig. 1.7), the x-ray photon interacts with a bound electron in, for example, the K, L, or M shell of an atom of the absorbing material. The photon gives up all of its energy to the electron; some is used to overcome the binding energy of the electron and release it from its orbit; the remainder is given to the electron as kinetic energy of motion. The kinetic energy (KE) of the ejected electron is, therefore, given by the expression

$$KE = h\nu - E_B$$

in which $h\nu$ is the energy of the incident photon and E_B is the binding energy of the electron in its orbit. The vacancy left in the atomic shell as a result of the ejection of an electron, then, must be filled by another electron falling in from an outer shell of the same atom or by a conduction electron from outside the atom. The movement of an electron from one shell to another represents a change of energy states. Because the electron is negatively charged, its movement from a loosely bound to a tightly bound shell represents a decrease of potential energy; this energy change is balanced by the emission of a photon of “characteristic” electromagnetic radiation. In soft tissue, this characteristic radiation has a low energy, typically 0.5 kV, and is of little biologic consequence.

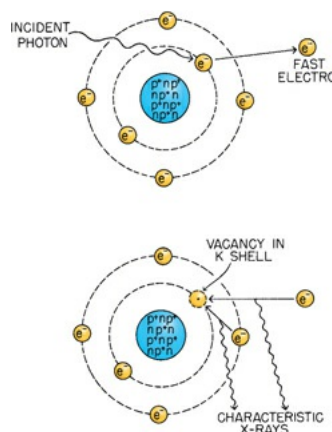


FIGURE 1.7 Absorption of a photon of x- or γ -rays by the photoelectric process. The interaction involves the photon and a tightly bound orbital electron of an atom of the absorber. The photon gives up its energy entirely; the electron is ejected with a kinetic energy equal to the energy of the incident photon less the binding energy that previously held the electron in orbit (**top**). The vacancy is filled either by an electron from an outer orbit or by a free electron from outside the atom (**bottom**). If an electron changes energy levels, the difference in energy is emitted as a photon of characteristic x-rays. For soft tissue, these x-rays are of very low energy.

The Compton and photoelectric absorption processes differ in several respects that are vital in the application of x-rays to diagnosis and therapy. The mass absorption coefficient for the Compton process is independent of the atomic number of the absorbing material. By contrast, the mass absorption coefficient for photoelectric absorption varies rapidly with atomic number (Z)** and is, in fact, about proportional to Z^3 .

For diagnostic radiology, photons are used in the energy range in which photoelectric absorption is as important as the Compton process. Because the mass absorption coefficient varies critically with Z , the x-rays are absorbed to a

greater extent by the bone because the bone contains elements with high atomic numbers, such as calcium. This differential absorption in materials of high Z is one reason for the familiar appearance of the radiograph. For radiotherapy, however, high-energy photons in the megavoltage range are preferred because the Compton process is overwhelmingly important. As a consequence, the absorbed dose is about the same in soft tissue, muscle, and bone so that differential absorption in bone, which posed a problem in the early days when lower energy photons were used for therapy, is avoided.

Although the differences among the various absorption processes are of practical importance in radiology, the consequences for radiobiology are minimal. Whether the absorption process is the photoelectric or the Compton process, much of the energy of the absorbed photon is converted to the kinetic energy of a fast electron.

DIRECT AND INDIRECT ACTION OF RADIATION

The biologic effects of radiation result principally from damage to deoxyribonucleic acid (DNA), which is the critical target, as described in [Chapter 2](#).

If any form of radiation— x - or γ -rays, charged or uncharged particles—is absorbed in biologic material, there is a possibility that it will interact directly with the critical targets in the cells. The atoms of the target itself may be ionized or excited, thus initiating the chain of events that leads to a biologic change. This is called **direct action** of radiation ([Fig. 1.8](#)); it is the dominant process if radiations with high **linear energy transfer (LET)**, such as neutrons or α -particles, are considered.

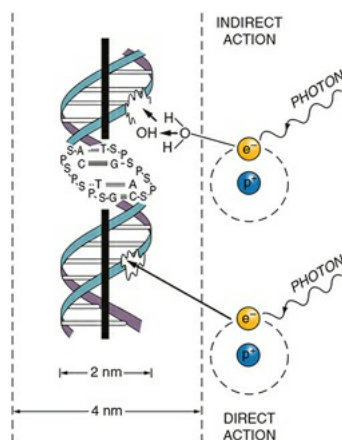


FIGURE 1.8 Direct and indirect actions of radiation. The structure of DNA is shown schematically. In direct action, a secondary electron resulting from absorption of an x-ray photon interacts with the DNA to produce an effect. In

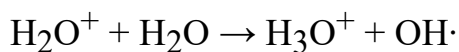
indirect action, the secondary electron interacts with, for example, a water molecule to produce a hydroxyl radical ($\text{OH}\cdot$), which in turn produces the damage to the DNA. The DNA helix has a diameter of about 20 Å (2 nm). It is estimated that free radicals produced in a cylinder with a diameter double that of the DNA helix can affect the DNA. Indirect action is dominant for sparsely ionizing radiation, such as x-rays. S, sugar; P, phosphorus; A, adenine; T, thymine; G, guanine; C, cytosine.

Alternatively, the radiation may interact with other atoms or molecules in the cell (particularly water) to produce free radicals that are able to diffuse far enough to reach and damage the critical targets. This is called **indirect action** of radiation. A **free radical** is an atom or molecule carrying an unpaired orbital electron in the outer shell. An orbital electron not only revolves around the nucleus of an atom but also spins around its own axis. The spin may be clockwise or counterclockwise. In an atom or molecule with an even number of electrons, spins are paired; that is, for every electron spinning clockwise, there is another one spinning counterclockwise. This state is associated with a high degree of chemical stability. In an atom or molecule with an odd number of electrons, there is one electron in the outer orbit for which there is no other electron with an opposing spin; this is an unpaired electron. This state is associated with a high degree of chemical reactivity.

For simplicity, we consider what happens if radiation interacts with a water molecule because 80% of a cell is composed of water. As a result of the interaction with a photon of x- or γ -rays or a charged particle, such as an electron or proton, the water molecule may become ionized. This may be expressed as



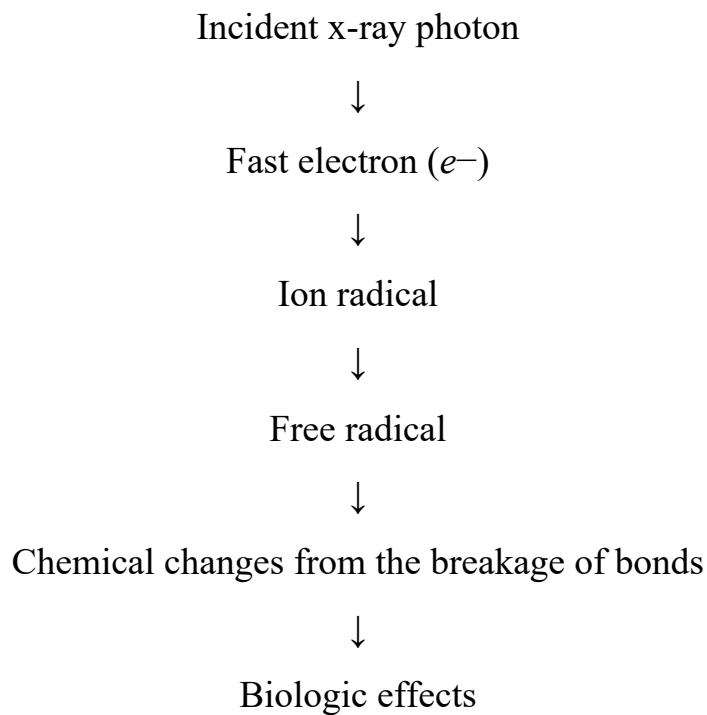
H_2O^+ is an ion radical. An **ion** is an atom or molecule that is electrically charged because it has lost an electron. A free radical contains an unpaired electron in the outer shell, making it highly reactive. H_2O^+ is charged and has an unpaired electron; consequently, it is both an ion and a free radical. The primary ion radicals have an extremely short lifetime, on the order of 10^{-10} second. They decay to form free radicals, which are not charged but still have an unpaired electron. In the case of water, the ion radical reacts with another water molecule to form the highly reactive hydroxyl radical ($\text{OH}\cdot$):



The hydroxyl radical possesses nine electrons; therefore, one of them is

unpaired. It is a highly reactive free radical and can diffuse a short distance to reach a critical target in a cell. For example, it is thought that free radicals can diffuse to DNA from within a cylinder with a diameter about twice that of the DNA double helix. It is estimated that about two-thirds of the x-ray damage to DNA in mammalian cells is caused by the hydroxyl radical. The best evidence for this estimate comes from experiments using free radical scavengers, which can reduce the biologic effect of sparsely ionizing radiations, such as x-rays, by a factor of close to 3. This is discussed further in [Chapter 9](#). Indirect action is illustrated in [Figure 1.8](#). This component of radiation damage is most easily modified by chemical means—either protectors or sensitizers—unlike direct action.

For the indirect action of x-rays, the chain of events, from the absorption of the incident photon to the final observed biologic change, may be described as follows:



There are vast differences in the time scale involved in these various events. The physics of the process, the initial ionization, may take only 10^{-15} second. The primary radicals produced by the ejection of an electron generally have a lifetime of 10^{-10} second. The OH· radical has a lifetime of about 10^{-9} second in cells, and the DNA radicals formed either by direct ionization or by reaction with OH· radicals have a lifetime of perhaps 10^{-5} second (in the presence of air). The period between the breakage of chemical bonds and the expression of the biologic effect may be hours, days, months, years, or generations, depending on

the consequences involved. If cell killing is the result, the biologic effect may be expressed hours to days later when the damaged cell attempts to divide. If the radiation damage is oncogenic, its expression as an overt cancer may be delayed for 40 years. If the damage is a mutation in a germ cell leading to hereditary changes, it may not be expressed for many generations.

ABSORPTION OF NEUTRONS

In contrast to x-rays, *neutrons* interact not with the planetary elections but with the nuclei of the atoms that make up the tissue resulting in recoil protons, or in the case of higher energy neutrons “spallation products,” that is, a high-energy neutron may hit a carbon atom which then breaks up into three α -particles, or may hit an oxygen atom to produce four α -particles.

ABSORPTION OF PROTONS AND HEAVIER IONS SUCH AS CARBON

When protons pass through matter, they are subject to three phenomena. First, Coulomb interactions with atomic electrons which results in ionization of atoms and setting loose electrons to go on and ionize further atoms. Second, Coulomb interactions with atomic nuclei which deflect protons. Third, nuclear interactions with atomic nuclei which usually results in a fragment of the nucleus, a proton or an α -particle, for example, being knockout of the nucleus leaving behind a heavy fragment that is heavily ionizing. Nuclear disintegration becomes more and more likely to happen as the proton energy increases. The absorption of carbon ions involves similar processes with the added complication that some of the carbon ions themselves may fragment and break apart.

For heavy particles, as for x-rays, the biologic effect may be a consequence of the direct or indirect action, but there is a shift in the balance between the two modes of action. For x-rays, indirect action is dominant, whereas for the neutrons or heavy ions, the direct action assumes greater importance, increasingly so as the density of ionization increases, that is, as the density of ionization increases, the probability of a direct interaction between the particle track and the target molecule increases.

It is important to note at this stage that the indirect effect involving free radicals is most easily modified by chemical means. Radioprotective compounds have been developed that work by scavenging free radicals. Such compounds, therefore, are quite effective for x- and γ -rays but of little use for neutrons, α -particles, or heavier ions.

SUMMARY OF PERTINENT CONCLUSIONS

X- and γ -rays are indirectly ionizing; the first step in their absorption is the production of fast recoil electrons.

Neutrons are also indirectly ionizing; the first step in their absorption is the production of fast recoil protons, α -particles, and heavier nuclear fragments.

Biologic effects of x-rays may be caused by direct action (the recoil electron directly ionizes the target molecule) or indirect action (the recoil electron interacts with water to produce an OH^- , which diffuses to the target molecule).

About two-thirds of the biologic damage by x-rays is caused by indirect action (i.e., involving free radicals), and this component of the biologic damage can be modified by chemical protectors.

Chemical protectors are less effective with high-LET radiations where most biologic damage is a result of the direct effect.

The physics of the absorption process is over in 10^{-15} second; the chemistry takes longer because the lifetime of the DNA radicals is about 10^{-5} second; the biology takes hours, days, or months for cell killing, years for carcinogenesis, and generations for heritable effects.

BIBLIOGRAPHY

Goodwin PN, Quimby EH, Morgan RH. *Physical Foundations of Radiology*. 4th ed. New York, NY: Harper & Row; 1970.

Johns HE, Cunningham JR. *The Physics of Radiology*. Springfield, IL: Charles C Thomas; 1969.

Rossi HH. Neutron and heavy particle dosimetry. In: Reed GW, ed. *Radiation Dosimetry: Proceedings of the International School of Physics*. New York, NY: Academic Press; 1964:98–107.

Smith VP, ed. *Radiation Particle Therapy*. Philadelphia, PA: American College of Radiology; 1976.

*The kiloelectron volt (keV) is a unit of energy. It is the energy possessed by an electron that has been accelerated through 1,000 volts (V). It corresponds to 1.6×10^{-9} ergs.

†The angstrom (\AA) is a unit of length equal to 10^{-8} cm.

‡Quantity of radiation is expressed in röntgen, rad, or gray. The röntgen (R) is the unit of

exposure and is related to the ability of x-rays to ionize air. The rad is the unit of absorbed dose and corresponds to energy absorption of 100 erg/g. In the case of x- and γ -rays, an exposure of 1 R results in an absorbed dose in water or soft tissue roughly equal to 1 rad. The *International Commission on Radiological Units and Measurements* (ICRU) recommended that the rad be replaced as a unit by the gray (Gy), which corresponds to an energy absorption of 1 J/kg. Consequently, 1 Gy = 100 rad.

**Z, the atomic number, is defined as the number of positive charges on the nucleus; it is, therefore, the number of protons in the nucleus.

chapter 2

Molecular Mechanisms of DNA and Chromosome Damage and Repair

General Overview of DNA Strand Breaks

Measuring DNA Strand Breaks

DNA Repair Pathways

Base Excision Repair

Nucleotide Excision Repair

DNA Double-Strand Break Repair

Nonhomologous End-Joining

Homologous Recombination Repair

Crosslink Repair

Mismatch Repair

Relationship between DNA Damage and Chromosome Aberrations

Chromosomes and Cell Division

The Role of Telomeres

Radiation-Induced Chromosome Aberrations

Examples of Radiation-Induced Aberrations

Chromosome Aberrations in Human Lymphocytes

Summary of Pertinent Conclusions

Bibliography

GENERAL OVERVIEW OF DNA STRAND BREAKS

There is strong evidence that DNA is the principal target for the biologic effects of radiation, including cell killing, carcinogenesis, and mutation. A consideration of the biologic effects of radiation, therefore, begins logically with a description of the breaks in DNA caused by charged-particle tracks and by the chemical

species produced.

Deoxyribonucleic acid (DNA) is a large molecule with a well-known double helical structure. It consists of two strands held together by hydrogen bonds between the bases. The “backbone” of each strand consists of alternating sugar and phosphate groups. The sugar involved is deoxyribose. Attached to this backbone are four bases, the sequence of which specifies the genetic code. Two of the bases are single-ring groups (pyrimidines); these are thymine and cytosine. Two of the bases are double-ring groups (purines); these are adenine and guanine. The structure of a single strand of DNA is illustrated in [Figure 2.1](#). The bases on opposite strands must be complementary; adenine pairs with thymine, and guanine pairs with cytosine. This is illustrated in the simplified model of DNA in [Figure 2.2A](#).

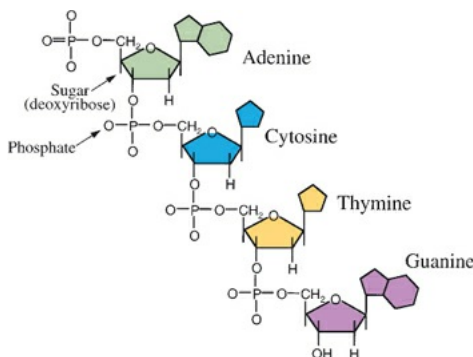


FIGURE 2.1 The structure of a single strand of DNA.

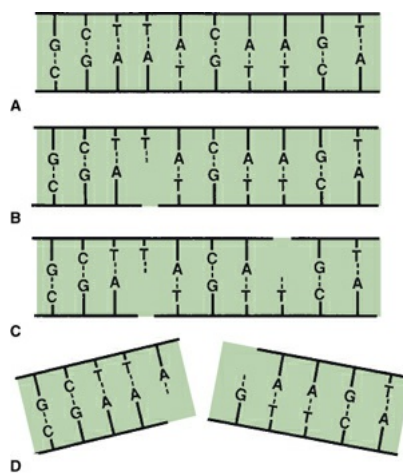


FIGURE 2.2 Diagrams of single- and double-strand DNA breaks caused by radiation. **A:** Two-dimensional representation of the normal DNA helix. The base pairs carrying the genetic code are complementary (i.e., adenine pairs with thymine, guanine pairs with cytosine). **B:** A break in one strand is of little significance because it is repaired readily using the opposite strand as a template. **C:** Breaks in both strands, if well separated, are repaired as independent breaks. **D:** If breaks occur in both strands and are directly opposite or separated by only

a few base pairs, this may lead to a double-strand break in which the chromatin snaps into two pieces. (Courtesy of Dr. John Ward.)

Radiation induces a large number of lesions in DNA, most of which are repaired successfully by the cell and are discussed in the following sections of this chapter. A dose of radiation that induces an average of one lethal event per cell leaves 37% of irradiated cells still viable; this is called the D₀ dose and is discussed further in [Chapter 3](#). For mammalian cells, the x-ray D₀ usually lies between 1 and 2 Gy. The number and type of DNA lesions per cell detected immediately after a dose of 1 Gy of x-rays is approximately:

Double-strand breaks (DSBs) 40

Single-strand breaks (SSBs) 1,000

Base damage >2,000

DNA-DNA crosslinks 30

If cells are irradiated with a modest dose of x-rays, many breaks of a single strand occur. These can be observed and scored as a function of dose if the DNA is denatured and the supporting structure is stripped away. In intact DNA, however, SSBs are of little biologic consequence as far as cell killing is concerned because they are repaired readily using the opposite strand as a template ([Fig. 2.2B](#)). If the repair is incorrect (misrepair), it may result in a mutation. If both strands of the DNA are broken and the breaks are well separated ([Fig. 2.2C](#)), repair again occurs readily because the two breaks are handled separately.

By contrast, if the breaks in the two strands are opposite one another or separated by only a few base pairs ([Fig. 2.2D](#)), this may lead to a **DSB (double-strand break)**, resulting in the cleavage of chromatin into two pieces. DSBs are believed to be the most important lesions produced in chromosomes by radiation; as described in the next section, the interaction of two DSBs may result in cell killing, carcinogenesis, or mutation. There are many kinds of DSBs,

varying in the distance between the breaks on the two DNA strands and the kinds of end groups formed. Their yield in irradiated cells is about 0.04 times that of SSBs, and they are induced linearly with dose, indicating that they are formed by single tracks of ionizing radiation.

Both free radicals and direct ionizations may be involved in the formation of the type of strand break illustrated in [Figure 2.2D](#). As described in [Chapter 1](#), the energy from ionizing radiations is not deposited uniformly in the absorbing medium but is located along the tracks of the charged particles set in motion—electrons in the case of x- or γ -rays and protons and α -particles in the case of neutrons. Radiation chemists speak in terms of “spurs,” “blobs,” and “short tracks.” There is, of course, a full spectrum of energy event sizes, and it is quite arbitrary to divide them into just three categories, but it turns out to be instructive. A spur contains up to 100 eV of energy and involves, on average, three ion pairs. In the case of x- or γ -rays, 95% of the energy deposition events are spurs, which have a diameter of about 4 nm, which is about twice the diameter of the DNA double helix ([Fig. 2.3](#)). Blobs are much less frequent for x- or γ -rays; they have a diameter of about 7 nm and contain on average about 12 ion pairs with an energy range of 100 to 500 eV (see [Fig. 2.3](#)). Because spurs and blobs have dimensions similar to the DNA double helix, multiple radical attacks occurs if they overlap the DNA helix. There is likely to be a wide variety of complex lesions, including base damage as well as DSBs. The term **locally multiply damaged site** was initially coined by John Ward to describe this phenomenon, but it has been replaced with the term *clustered lesion*. Given the size of a spur and the diffusion distance of hydroxyl free radicals, the clustered lesion could be spread out up to 20 base pairs. This is illustrated in [Figure 2.3](#), in which a DSB is accompanied by base damage and the loss of genetic information.

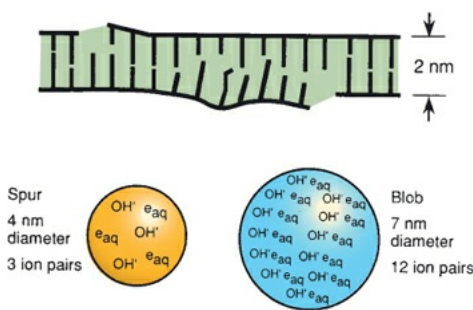


FIGURE 2.3 Illustration of a locally multiply damaged site. Energy from x-rays is not absorbed uniformly but tends to be localized along the tracks of charged particles. Radiation chemists speak in terms of spurs and blobs, which contain several ion pairs and have dimensions comparable to the DNA double helix. A

double-strand break is likely to be accompanied by extensive base damage. John Ward coined the term *locally multiply damaged site* to describe this phenomenon.

In the case of densely ionizing radiations, such as neutrons or α -particles, a greater proportion of blobs are produced. The damage produced, therefore, is qualitatively different from that produced by x- or γ -rays, and it is much more difficult for the cell to repair.

MEASURING DNA STRAND BREAKS

Over the years, various techniques have been used to measure DNA strand breaks, including sucrose gradient sedimentation, alkaline and neutral filter elution, nucleoid sedimentation, pulsed-field gel electrophoresis (PFGE), and single-cell gel electrophoresis (also known as the comet assay). Of these techniques, PFGE and single-cell gel electrophoresis are currently used to measure DNA strand breaks. In addition to these techniques, radiation-induced nuclear foci have become a popular approach to visualize DNA damage through the recruitment of DNA repair proteins to sites of DNA damage.

PFGE is the method most widely used to detect the induction and repair of DNA DSBs. It is based on the electrophoretic elution of DNA from agarose plugs within which irradiated cells have been embedded and lysed. PFGE allows separation of DNA fragments according to size in the megabase-pair range, with the assumption that DNA DSBs are induced randomly. The fraction of DNA released from the agarose plug is directly proportional to dose ([Fig. 2.4A](#)). The kinetics of DNA DSB rejoining exhibits a fast initial rate, which then decreases with repair time. The most widely accepted description of this kinetic behavior uses two first-order components (fast and slow) plus some fraction of residual DSBs. Studies have supported the finding that rejoining of incorrect DNA ends originates solely from slowly rejoining DSBs, and this subset of radiation-induced DSBs is what is manifested as chromosomal damage (i.e., chromosome translocations and exchanges).

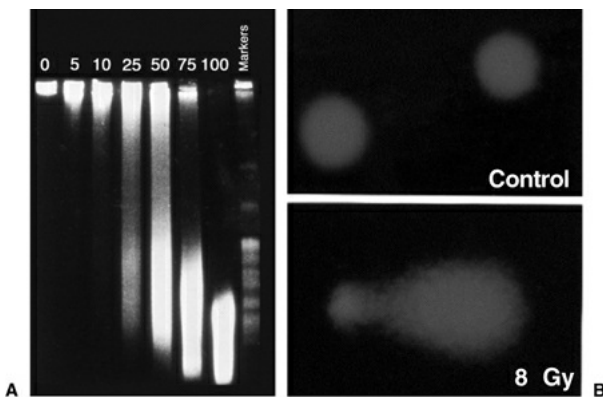


FIGURE 2.4 **A:** The effect of ionizing radiation on DNA strand break induction as measured by pulsed-field gel electrophoresis. As the dose of ionizing radiation increases from 5 to 100 Gy, the size of the DNA fragments as detected by ethidium bromide staining decreases. Thus, more DNA enters the gel with increasing dose of ionizing radiation. In these experiments, cells were embedded in agarose and irradiated on ice to eliminate the effects of repair. The *number* above each lane refers to the dose in Gy to which each group of cells was exposed. (Courtesy of Dr. Nicholas Denko.) **B:** Photomicrograph of control and 8-Gy irradiated cells as detected by the comet assay. Unirradiated cells possess a near-spherical appearance, whereas the fragmented DNA in irradiated cells gives the appearance of a comet when stained with ethidium bromide. (Courtesy of Drs. Ester Hammond and Mary Jo Dorie.)

Single-cell electrophoresis (comet assay) has the advantage of detecting differences in DNA damage and repair at the single-cell level. This is particularly advantageous for biopsy specimens from tumors in which a relatively small number of cells can be assayed to determine DNA damage and repair. Similar to PFGE (described earlier), cells are exposed to ionizing radiation, embedded in agarose, and lysed under neutral buffer conditions to quantify induction and repair of DNA DSBs. To assess DNA SSBs and alkaline-sensitive sites, lysis is performed with an alkaline buffer. If the cells are undamaged, the DNA remains compact and does not migrate. If the cell has incurred DNA DSBs, the amount of damage is directly proportional to the migration of DNA in the agarose. As a result of the lysis and electrophoresis conditions, the fragmented DNA that migrates takes the appearance of a comet's tail (Fig. 2.4B). This assay has high sensitivity and specificity for SSBs and alkaline sensitive sites and to a lesser degree DNA DSBs. By changing the lysis conditions from an alkaline to a neutral pH, the comet technique can be used to measure DNA DSB repair.

Both of these assays are cell based, where DNA in cells is much more

resistant to damage by radiation than would be expected from studies on free DNA. There are two reasons for this: (1) the presence in cells of low-molecular-weight scavengers that mop up some of the free radicals produced by ionizing radiation and (2) the physical protection afforded the DNA by packaging with proteins such as histones. Certain regions of DNA, particularly actively transcribing genes, appear to be more sensitive to radiation, and there is some evidence also of sequence-specific sensitivity.

DNA damage-induced nuclear foci (radiation-induced foci assay) in response to ionizing radiation represents complexes of signaling and repair proteins that localize to sites of DNA strand breaks in the nucleus of a cell. There are several advantages of assaying for foci formation over other techniques to measure DNA strand breaks, which include the ease of the protocol and that it can be carried out on both tissue sections and individual cell preparations. Technically, cells/tissues are incubated with a specific antibody raised to the signaling/repair protein of interest, and binding of the antibody is then detected with a secondary antibody, which carries a fluorescent tag. Fluorescence microscopy detects the location and intensity of the tag, which can then be quantified.

The most commonly assayed proteins for foci formation are γ H2AX and 53BP1 ([Fig. 2.5](#)). H2AX is a histone protein, which is rapidly phosphorylated in response to damage to form γ H2AX. Staining for the unmodified histone (H2AX) gives a pan nuclear stain or unchanging band on a western blot while γ H2AX is rapidly induced on a western blot in response to stress and can be seen to form discreet nuclear foci in damaged cells (see [Fig. 2.5](#)). 53BP1 also becomes phosphorylated in response to stress and forms nuclear foci at the sites of DNA DSBs. In this case, antibodies to either the phosphorylated or unmodified form can be used to detect DSBs as the protein relocates to the damaged chromatin (i.e., it is not already part of the chromatin as is the case for H2AX). DNA damage-induced increases in γ H2AX or phosphorylated 53BP1 can also be quantified by flow cytometry. Other proteins also form foci in response to damage such as ataxia-telangiectasia mutated (ATM), replication protein A (RPA), RAD51, and BRCA1 (discussed in subsequent sections).

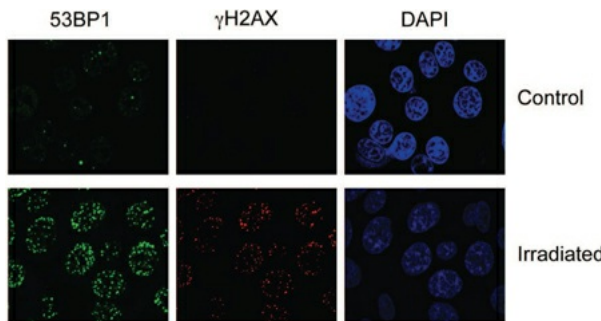


FIGURE 2.5 Photomicrograph of nuclear foci in control and 2-Gy irradiated cells as detected by staining with antibodies to 53BP1 (*green*) and γ H2AX (*red*). Cells were also stained with the nuclear stain 4',6-diamidino-2-phenylindole (DAPI) to show the location of nuclei. Without DNA strand breaks, there is little staining with γ H2AX and 53BP1 in foci. In contrast, staining for both proteins increases significantly after 2 Gy. (Courtesy of Dr. Ester Hammond.)

The γ H2AX or 53BP1 foci that form in a damaged cell correlate with the presence of DSBs. Thus, the decrease of foci over time reflects the kinetics of DSB repair (i.e., as the DSBs are repaired, the number of foci decreases). Recently, BRCA1 and RAD51, two proteins involved in the repair of DNA damage by homologous recombination, have been used as biomarkers in a small pilot study by Willers et al. to detect repair defects in breast cancer biopsies.

DNA REPAIR PATHWAYS

Mammalian cells have developed specialized pathways to sense, respond to, and repair base damage, SSBs, DSBs, sugar damage, and DNA–DNA crosslinks. Research from yeast to mammalian cells has demonstrated that the mechanisms used to repair ionizing radiation-induced base damage are different from the mechanisms used to repair DNA DSBs. In addition, different repair pathways are used to repair DNA damage, depending on the stage of the cell cycle.

Much of our knowledge of DNA repair is the result of studying how mutations in individual genes result in radiation hypersensitivity. Radiation-sensitive mutants identified from yeast and mammalian cells appear either to be directly involved in the repair process or to function as molecular checkpoint–controlling elements. The pathways involved in the repair of base damage, SSBs, DSBs, pyrimidine dimers, and DNA–DNA crosslinks are discussed in the next sections and represent a simplified representation of our current state of understanding. In [Chapter 18](#), the syndromes associated with mutations in genes involved in sensing DNA damage or repairing DNA damage are discussed in more detail.

Base Excision Repair

Base damage is repaired through the base excision repair (BER) pathway illustrated in [Figure 2.6](#). Bases on opposite strands of DNA must be complementary: adenine (A) pairs with thymine (T), and guanine (G) pairs with cytosine (C). U represents a putative single-base mutation that is first removed by a glycosylase/DNA lyase ([Fig. 2.6A](#)). Removal of the base is followed by the removal of the sugar residue by apurinic endonuclease 1 (APE1), replacement with the correct nucleotide by DNA polymerase β , and joined by DNA ligase III–*XRCC1*–mediated ligation. If more than one nucleotide is to be replaced (illustrated by the putative mutation UU in [Fig. 2.6B](#)), then the complex of replication factor C (RFC)/proliferating cell nuclear antigen (PCNA)/DNA polymerase δ/ϵ performs the repair synthesis, the overhanging flap structure is removed by the flap endonuclease 1 (FEN1), and DNA strands are sealed by ligase I (see [Fig. 2.6B](#)). Although ionizing radiation–induced base damage is efficiently repaired, defects in BER may lead to an increased mutation rate but usually do not result in cellular radiosensitivity. One exception to this is the mutation of the x-ray cross complementing factor 1 (*XRCC1*) gene, which confers about a 1.7-fold increase in radiation sensitivity. However, the radiation sensitivity of *XRCC1*-deficient cells may come from *XRCC1*'s potential involvement in other repair processes such as SSBs.

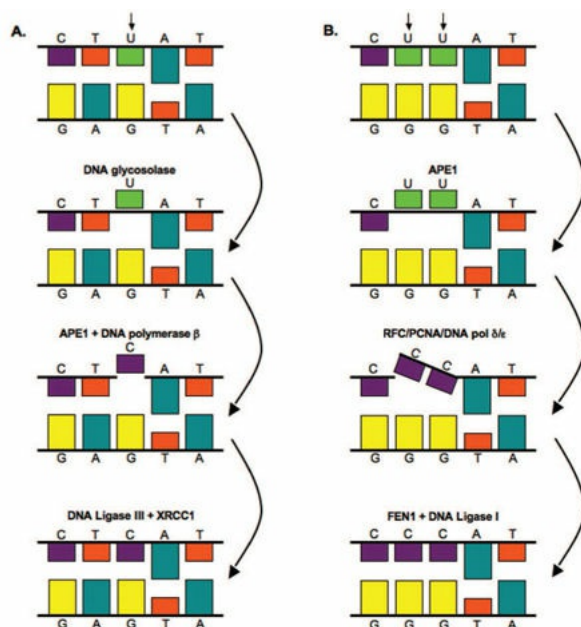


FIGURE 2.6 Base excision repair pathways. **A:** Base excision repair of a single nucleotide. Bases on opposite strands must be complementary; adenine (A) pairs with thymine (T), and guanine (G) pairs with cytosine (C). U represents a putative mutation that is first removed through a DNA glycosylase–mediated

incision step. **B:** Base excision repair of multiple nucleotides. In this case, the double UU represents a putative mutation that is first removed through APE1. See text for details.

Nucleotide Excision Repair

Nucleotide excision repair (NER) removes bulky adducts in the DNA such as pyrimidine dimers. The process of NER can be subdivided into two pathways: global genome repair (GGR or GG-NER) and transcription-coupled repair (TCR or TC-NER). The process of GG-NER is genome-wide (i.e., lesions can be removed from DNA that encodes or does not encode for genes). In contrast, TC-NER only removes lesions in the DNA strands of actively transcribed genes. When a DNA strand that is being actively transcribed becomes damaged, the RNA polymerase can block access to the site of damage and hence prevents DNA repair. TC-NER has evolved to prevent this blockade by RNA polymerase by effectively removing it from the site of damage to allow the repair proteins access. The mechanism of GG-NER and TC-NER differs only in the detection of the lesion; the remainder of the pathway used to repair the damage is the same for both. The essential steps in this pathway are (1) damage recognition; (2) DNA incisions that bracket the lesion, usually between 24 and 32 nucleotides in length; (3) removal of the region containing the adducts; (4) repair synthesis to fill in the gap region; and (5) DNA ligation ([Fig. 2.7](#)). Mutation in NER genes does not lead to ionizing radiation sensitivity. However, defective NER increases sensitivity to ultraviolet (UV)-induced DNA damage and anticancer agents such as alkylating agents that induce bulky adducts. Germline mutations in NER genes lead to human DNA repair deficiency disorders such as xeroderma pigmentosum in which patients are hypersensitive to UV light.

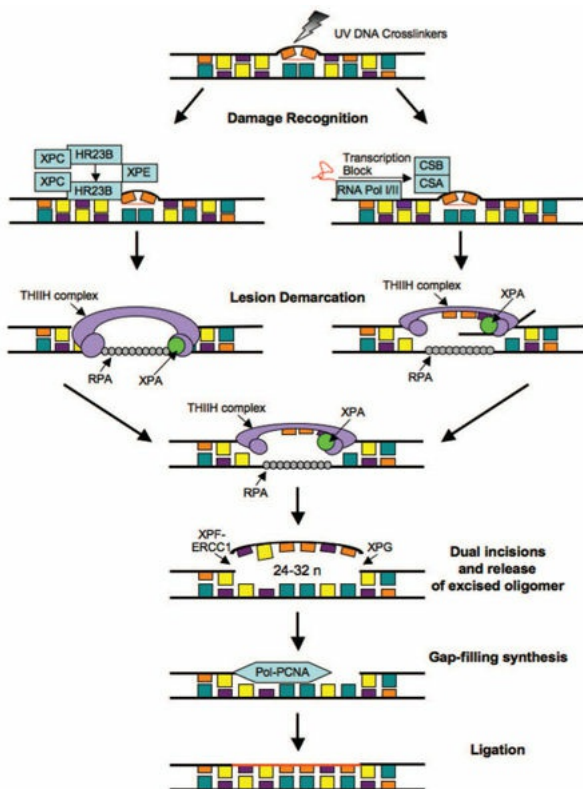


FIGURE 2.7 Nucleotide excision repair pathways. The two subpathways of NER, GG-NER/GGR and TC-NER/TCR, differ at the initial damage recognition step. GGR uses the XPC-XPE protein complexes, whereas in TCR, the NER proteins are recruited by the stalled RNA polymerase in cooperation with CSB and CSA. Following recognition, the lesion is demarcated by binding of the transcription factor IIH (TFIIEH) complex, XPA and RPA. The TFIIEH complex helicase function unwinds the DNA and generates an open stretch around the lesion, at which point the XPG and XPF-ERCC1 endonucleases make incisions at the 3' and 5' ends, respectively, releasing a 24–32 oligomer. The resulting gap is filled by the polymerases δ/ϵ aided by RFC and PCNA, and the strand is finally ligated. XPC, xeroderma pigmentosum, complementation group C; XPE, xeroderma pigmentosum, complementation group E; CSB, Cockayne syndrome B gene; CSA, Cockayne syndrome A gene; XPG, xeroderma pigmentosum, complementation group G; XPF, xeroderma pigmentosum, complementation group F; ERCC1, excision repair cross-complementation group 1 gene.

DNA Double-Strand Break Repair

In eukaryotic cells, the two predominant pathways for the repair of DNA DSBs are homologous recombination repair (HRR) and nonhomologous end-joining (NHEJ). Mechanistically, HRR requires an undamaged DNA strand to serve as a template for repair to proceed through strand invasion, and NHEJ repairs DNA

DSBs through the orchestration of end-to-end joining. In lower eukaryotes such as yeast, HRR is the predominant pathway used for repairing DNA DSBs. Homologous recombination is an error-free process because repair is performed by copying information from the undamaged homologous chromatid/chromosome. In mammalian cells, the choice of repair is biased by the phase of the cell cycle and by the abundance of repetitive DNA. HRR occurs primarily in the late S/G₂ phase of the cell cycle, when an undamaged sister chromatid is available to act as a template, whereas NHEJ occurs in the G₁ phase of the cell cycle, when no such template exists (Fig. 2.8). NHEJ is error prone and probably accounts for many of the premutagenic lesions induced in the DNA of human cells by ionizing radiation. However, it is important to keep in mind that NHEJ and HRR are not mutually exclusive, and both have been found to be active in the late S/G₂ phase of the cell cycle, indicating that other as-yet-unidentified factors, in addition to cell cycle phase, are important in determining what repair program is used.

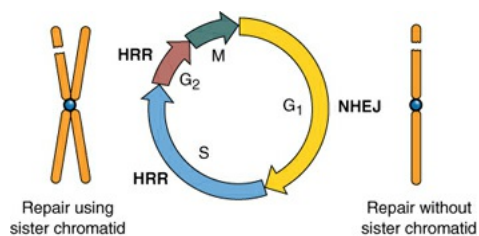


FIGURE 2.8 Illustration showing that nonhomologous recombination occurs in the G₁ phase of the cell cycle, at which stage, there is no sister chromatid to use as a template for repair. In contrast, homologous recombination occurs in the S and G₂ phases of the cell cycle, when there is a sister chromatid to use as a template in repair.

Furthermore, two additional repair pathways have been identified that can also be considered error prone. Single-strand annealing (SSA) is a specialized DNA end-joining process between interspersed repetitive DNA throughout the genome and requires RAD52 and DNA ligase I. Interestingly, although this type of repair uses a homology-based mechanism, loss of repeat sequences and associated intervening sequences is quite common. An alternative DNA end-joining (Alt-EJ) process has also been described that involves XRCC1, DNA ligase III, and PARP. Alt-EJ is still not well understood but is active in cells where classical NHEJ is lost. Similar to SSA, Alt-EJ is also error prone and can lead to insertions and deletions.

Nonhomologous End-Joining

The immediate response of a cell to a DNA DSB is the activation of a group of sensors that serve both to promote DNA repair and to prevent the cell from proceeding in the cell cycle until the break is faithfully repaired. These sensors, ATM and Rad3-related (ATR), are protein kinases that belong to the phosphatidylinositol-3-kinase–related kinase (PIKK) family and are recruited to the sites of DNA strand breaks induced by ionizing radiation. The competition for repair by HRR versus NHEJ is in part regulated by the protein 53BP1. Functionally, ATM promotes the processing of broken DNA ends to generate recombinogenic single-strand DNA by regulating the activity of the NBS/MRE11/Rad50 protein complex (Fig. 2.9), and this resection activity is diminished by 53BP1.

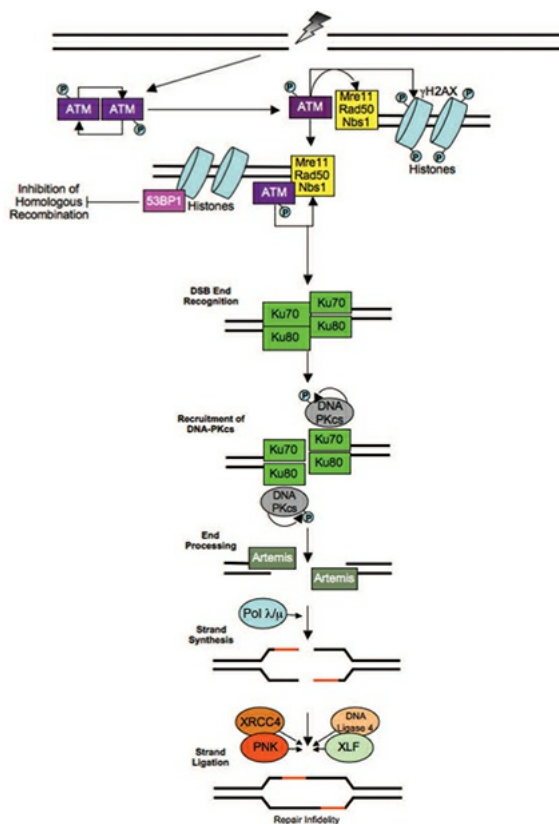


FIGURE 2.9 Nonhomologous end-joining. DNA strand breaks are recognized by the ATM and the MRN (Mre11-Rad50-Nbs1) complex, resulting in resection of the DNA ends. Homologous recombination is inhibited by the activity of 53BP1. The initial step of the core NHEJ pathway starts with the binding of the ends at the double-strand break by the Ku70/Ku80 heterodimer. This complex then recruits and activates the catalytic subunit of DNA-PK (DNA-PKcs), whose role is the juxtaposition of the two DNA ends. The DNA-PK complex then recruits the ligase complex (XRCC4/XLF-LIGIV/PNK) that promotes the final ligation step.

The ligation of DNA DSBs by NHEJ does not require sequence homology. However, the damaged ends of DNA DSBs cannot simply be ligated together; they must first be modified before they can be rejoined by a ligation reaction. NHEJ can be divided into five steps: (1) end recognition by Ku binding, (2) recruitment of DNA-dependent protein kinase catalytic subunit (DNA-PKcs), (3) end processing, (4) fill-in synthesis or end bridging, and (5) ligation (see Fig. 2.9).

End recognition occurs when the Ku heterodimer, composed of 70-kDa and 83-kDa subunits, and the DNA-PKcs bind to the ends of the DNA DSB. Although the Ku/DNA-PKcs complex is thought to bind ends first, it is still unknown what holds the two DNA DSB ends together before Ku binding. Although microhomology between one to four nucleotides can aid in end alignment, there is no absolute requirement for microhomology for NHEJ. In fact, Ku does not recruit only DNA-PKcs to the DNA ends but also an additional protein, Artemis. The Artemis protein possesses endonuclease activity and forms a physical complex with DNA-PKcs. The Ku/DNA-PKcs complex that is bound to the DNA ends can phosphorylate Artemis and activate its endonuclease activity to deal with 5' and 3' overhangs as well as hairpins. End processing is followed by fill-in synthesis of gaps formed by the Artemis endonuclease activity. This aspect of NHEJ may not necessarily be essential, for example, in the ligation of blunt ends or ends with compatible termini. At present, it is unclear what the signal is for a fill-in reaction to proceed after endonuclease processing. However, DNA polymerase μ or λ has been found to be associated with the Ku/DNA/XRCC4/DNA ligase IV complex and serves as the polymerase for the fill-in reaction. In the final step of NHEJ, ligation of nicked DNA ends that have been processed is mediated by a PNK/XRCC4/DNA ligase IV/XLF complex that is probably recruited by the Ku heterodimer. Polynucleotide kinase (PNK) is a protein that has both 3'-DNA phosphatase and 5'-DNA kinase activities and serves to remove end groups that are not ligatable to allow end-joining. XRCC4-like factor (XLF) is a protein that has a similar protein structure as x-ray repair complementing defective repair in Chinese hamster cells 4 (XRCC4) and stimulates the activity of DNA ligase IV. NHEJ is error prone and plays an important physiologic role in generating antibodies through V(D)J rejoining. The error-prone nature of NHEJ is essential for generating antibody diversity and often goes undetected in mammalian cells, as errors in the noncoding DNA that composes most of the human genome has little consequence. NHEJ is primarily found in the G₁ phase of the cell cycle, where there is no sister chromatid.

Homologous Recombination Repair

HRR provides the mammalian genome a high-fidelity mechanism of repairing DNA DSBs (Fig. 2.10). In particular, the increased activity of this recombination pathway in late S/G₂ suggests that its primary function is to repair and restore the functionality of replication forks with DNA DSBs. Compared to NHEJ, which requires no sequence homology to rejoin broken ends, HRR requires physical contact with an undamaged chromatid or chromosome (to serve as a template) for repair to occur.

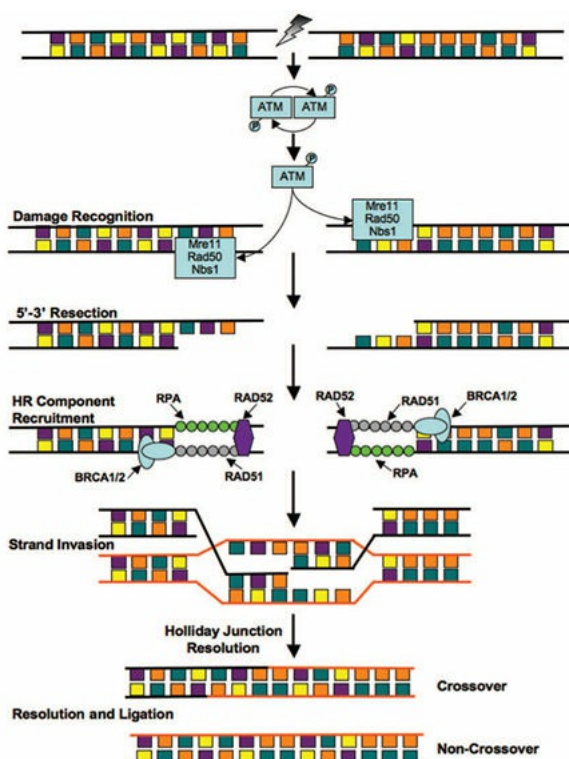


FIGURE 2.10 Homologous recombinational repair. The initial step in HRR is the recognition of the lesion and processing of the double-strand DNA ends into 3' DNA single-strand tails by the MRN (Mre11-Rad50-Nbs1) complex, which are then coated by RPA forming a nucleoprotein filament. Then, specific HRR proteins are recruited to the nucleoprotein filaments, such as RAD51, RAD52, and BRCA1/2. RAD51 is a key protein in homologous recombination as it mediates the invasion of the homologous strand of the sister chromatid, leading to formation of Holliday junctions. The Holliday junctions are finally resolved into two DNA duplexes. See text for details.

During recombination, evidence exists that ATM phosphorylates the breast cancer tumor suppressor protein BRCA1, which is then recruited to the site of the DSB that has been bound by the NBS/MRE11/Rad50 protein complex (see Fig. 2.10). MRE11 and perhaps other yet unidentified endonucleases resect the

DNA, resulting in a 3' single-strand DNA that serves as a binding site for Rad51. BRCA2, which is attracted to the DSB by BRCA1, facilitates the loading of Rad51 onto RPA-coated single-strand overhangs produced by endonuclease resection. Rad51 protein is a homologue of the *Escherichia coli* recombinase RecA and possesses the ability to form nucleofilaments and catalyze strand exchange with the complementary strand in the undamaged chromosome. Five additional paralogues of Rad51 also bind to the RPA-coated single-stranded region and recruit Rad52, which protects against exonucleolytic degradation. To facilitate repair, Rad54 uses its ATPase activity to unwind the double-stranded molecule. The two invading ends serve as primers for DNA synthesis, and the so-called Holliday junctions are resolved by MMS4 and MUS81 by noncrossing over. The Holliday junctions disengage and DNA strand pairing is followed by gap filling, or by crossing over of the Holliday junctions, which is followed by gap filling. The identities of the polymerase and ligase involved in these latter steps are unknown. Because inactivation of HRR genes results in radiosensitivity and genomic instability, these genes provide a critical link between HRR and chromosome stability. Dysregulated homologous recombination can also lead to cancer by loss of heterozygosity (LOH).

Crosslink Repair

Crosslinks can be divided into intrastrand crosslinks, which occur on one strand of DNA, and interstrand crosslinks, which occur between two strands of DNA. Crosslinks are particularly problematic during replication and can lead to cell cycle arrest and even cell death. DNA intrastrand crosslinks can lead to a block of DNA polymerase activity and to a single-strand DNA gap. This gap can be resolved by DNA polymerase switching to a template without the intrastrand crosslink or by translesion synthesis. In contrast to intrastrand crosslinks, interstrand crosslinks will result in a complete block to replication and prevent the unwinding of duplex DNA, leading to cell death if unrepaired.

Interstrand crosslinks are repaired by different protein complexes depending on the phase of the cell cycle. In G₁ phase, interstrand crosslinks are removed by NER. Both sides of the interstrand crosslink are cleaved by XPF on the 3' end and Fanconi-associated nuclease 1 (FAN1) on the 5' end. Excision of the interstrand crosslink is followed by translesion synthesis. However, only a small percentage of interstrand crosslinks are repaired in G₁ phase, and the unrepaired lesions will present a major problem for the cell in S phase. During S phase ([Fig. 2.11](#)), the interstrand crosslink is recognized by Fanconi anemia complementation group M (FANCM), which binds to the abnormal crosslinked

structure as well as binding to the Fanconi anemia (FA) core complex containing FANCA, FANCB, FANCC, FANCE, FANCF, FANCG, and FANCL. FANCM binding to the crosslink structure protects against collapse of the replication fork. FAN1 and XPF/MUS81 are also recruited to the crosslink site and excise the crosslink. Replication through the excised sites is mediated by translesion polymerases such as REV1/DNA polymerase ζ . After translesion synthesis, the replication fork is repaired by HRR and the crosslink removed by NER. Cells with mutations in NER and HRR pathways are modestly sensitive to crosslinking agents. In contrast, individuals afflicted with the syndrome FA are hypersensitive to crosslinking agents. Chromatin that contains actively transcribed genes is more susceptible to DNA–protein crosslinks, and the crosslinked proteins are usually nuclear matrix proteins.

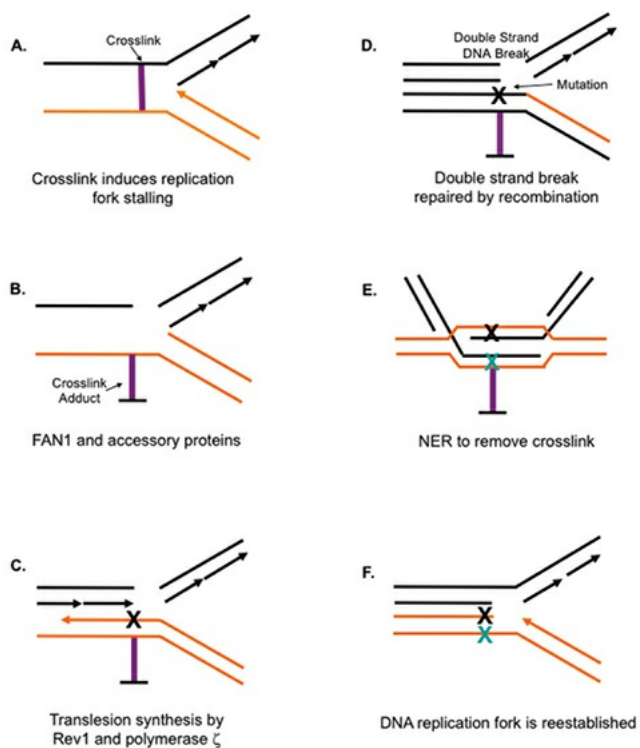


FIGURE 2.11 DNA–DNA interstrand crosslink repair in S phase. The initial signal for DNA–DNA crosslink repair is stalling of the replication fork (**A**). Fork stalling results in recruitment of FANCM and the FA core complex. Incision or unhooking of the crosslink is achieved by the action of FAN1 and accessory proteins. **B:** Translesion synthesis is achieved by polymerases such as Rev1 and polymerase ζ (**C**). The resulting DNA double-strand break is repaired by homologous recombination (**D**), and the crosslink is removed from the DNA by nucleotide excision repair (**E–F**). This schema for crosslink repair is still a work in progress.

Mismatch Repair

The mismatch repair (MMR) pathway removes base–base and small insertion mismatches that occur during replication. In addition, the MMR pathway removes base–base mismatches in homologous recombination intermediates. See [Figure 2.12](#) for schematic representation and an indication of the critical gene products. The process of MMR can be subdivided into four components: First, the mismatch must be identified by sensors that transduce the signal of a mismatched base pair; second, MMR factors are recruited; third, the newly synthesized strand harboring the mismatch is identified and the incorrect/altered nucleotides are excised; and in the fourth stage, resynthesis and ligation of the excised DNA tract is completed. MMR was first characterized in *E. coli* by the characterization of the *Mut* genes, of which homologues of these gene products have been identified and extensively characterized in both yeast and humans. Mutations in any of the mismatch *MSH*, *MLH*, and *PSM* families of repair genes lead to microsatellite instability (small base insertions or deletions) and cancer, especially hereditary nonpolyposis colon cancer (HNPCC).

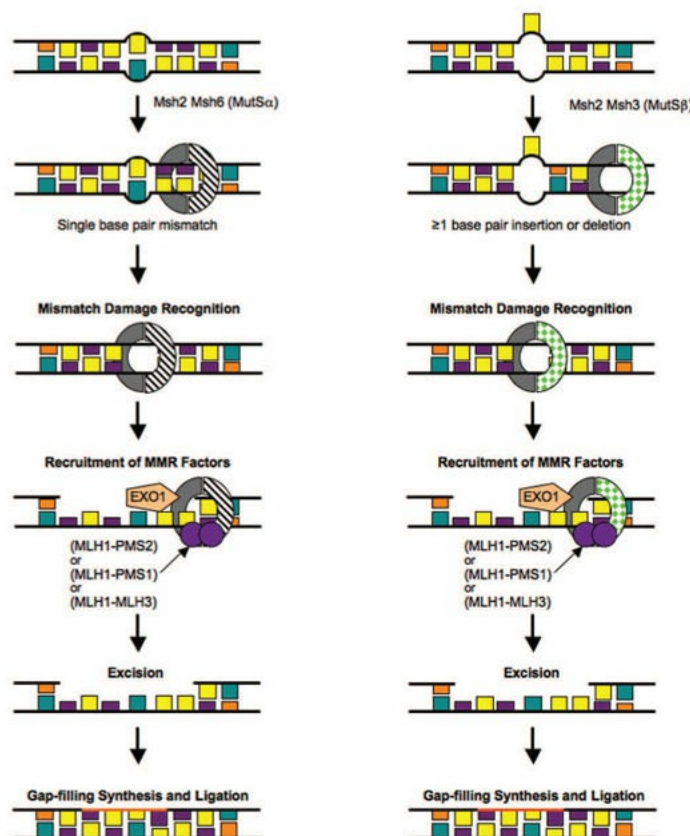


FIGURE 2.12 Mismatch repair. The initial step in the MMR pathway is the recognition of mismatched bases through either Msh2-Msh6 or Msh2-Msh3 complexes. These recognition complexes recruit MLH1-PMS2, MLH1-PMS1,

and MLH1-MLH3, alongside the exonuclease EXO1 that catalyzes the excision step that follows. A gap-filling step by polymerases δ/ϵ , RFC, and PCNA is followed by a final ligation step.

RELATIONSHIP BETWEEN DNA DAMAGE AND CHROMOSOME ABERRATIONS

Cell killing does not correlate with SSBs but relates better to DSBs. Agents such as hydrogen peroxide produce SSBs efficiently, but very few DSBs, and kill very few cells. Cells defective in DNA DSB repair exhibit hypersensitivity to killing by ionizing radiation and increased numbers of chromosome aberrations. On the basis of evidence such as this, it is concluded that DSBs are the most relevant lesions leading to most biologic insults from radiation, including cell killing. The reason for this is that DSBs can lead to chromosomal aberrations that present problems at cell division.

CHROMOSOMES AND CELL DIVISION

The backbone of DNA is made of molecules of sugar and phosphates, which serve as a framework to hold the bases that carry the genetic code. Attached to each sugar molecule is a base: thymine, adenine, guanine, or cytosine. This whole configuration is coiled tightly in a double helix.

Figure 2.13 is a highly schematized illustration of the way an organized folding of the long DNA helix might be achieved as a closely packed series of looped domains wound in a tight helix. The degree of packing also is illustrated by the relative dimensions of the DNA helix and the condensed metaphase chromosome.

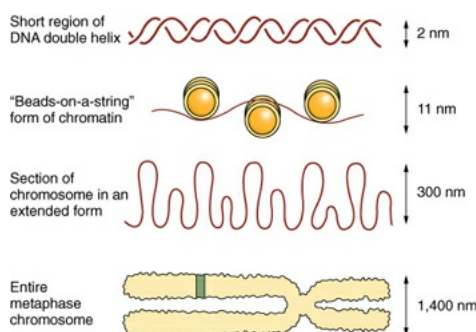


FIGURE 2.13 Illustration of the relative sizes of the DNA helix, the various stages of folding and packing of the DNA, and an entire chromosome condensed at metaphase.

The largest part of the life of any somatic cell is spent in interphase, during

which the nucleus, in a stained preparation, appears as a lacework of fine and lightly stained material in a translucent and colorless material surrounded by a membrane. In the interphase nucleus of most cells, one or more bodies of various sizes and shapes, called **nucleoli**, are seen. In most cells, little more than this can be identified with a conventional light microscope. In fact, a great deal is happening during this time: The quantity of DNA in the nucleus doubles as each chromosome lays down an exact replica of itself next to itself. When the chromosomes become visible at mitosis, they each present in duplicate. Even during interphase, there is good evidence that the chromosomes are not free to move about within the nucleus but are restricted to “domains.”

The various events that occur during **mitosis** are divided into several phases. The first phase of division is called **prophase**. The beginning of this phase is marked by a thickening of the chromatin and condensation into light coils. By the end of prophase, each chromosome has a lightly staining constriction known as a **centromere**; extending from the centromere are the arms of the chromosome. Prophase ends when the chromosomes reach maximal condensation and the nuclear membrane disappears, as do any nucleoli.

With the disappearance of the nuclear membrane, the nucleoplasm and the cytoplasm mix. **Metaphase** then follows, in which two events occur simultaneously. The chromosomes move to the center of the cell (i.e., to the cell’s equator), and the spindle forms. The spindle is composed of fibers that cross the cell, linking its poles. Once the chromosomes are stabilized at the equator of the cell, their centromeres divide, and metaphase is complete.

The phase that follows, **anaphase**, is characterized by a movement of the chromosomes on the spindle to the poles. The chromosomes appear to be pulled toward the poles of the cell by fibers attached to the centromeres. The arms, particularly the long arms, tend to trail behind.

Anaphase is followed by the last phase of mitosis, **telophase**. In this phase, the chromosomes, congregated at the poles of the cell, begin to uncoil. The nuclear membrane reappears, as do the nucleoli, and as the phase progresses, the chromosome coils unwind until the nucleus regains the appearance characteristic of interphase.

THE ROLE OF TELOMERES

Telomeres cap and protect the terminal ends of chromosomes. The name *telomere* literally means “end part.” Mammalian telomeres consist of long arrays of TTAGGG repeats that range in total length anywhere from 1.5 to 150

kilobases. Each time a normal somatic cell divides, telomeric DNA is lost from the lagging strand because DNA polymerase cannot synthesize new DNA in the absence of an RNA primer. Successive divisions lead to progressive shortening, and after 40 to 60 divisions, the telomeres in human cells are shortened dramatically, so that vital DNA sequences begin to be lost. At this point, the cell cannot divide further and undergoes senescence (irreversible arrest of proliferation). Telomere length has been described as the “molecular clock” or generational clock because it shortens with age in somatic tissue cells during adult life. Stem cells in self-renewing tissues, and cancer cells in particular, avoid this problem of aging by activating the enzyme telomerase. Telomerase is a reverse transcriptase that includes the complementary sequence to the TTAGGG repeats and so continually rebuilds the chromosome ends to offset the degradation that occurs with each division.

In tissue culture, immortalization of cells—that is, the process whereby cells pass through a “crisis” and continue to be able to divide beyond the normal limit—is associated with telomere stabilization and telomerase activity.

Virtually, all human tumor cell lines and approximately 90% of human cancer biopsy specimens exhibit telomerase activity. By contrast, normal human somatic tissues, other than stem cells, do not possess detectable levels of this enzyme. Both immortalization and carcinogenesis are associated with telomerase expression.

RADIATION-INDUCED CHROMOSOME ABERRATIONS

In the traditional study of chromosome aberrations, the effects of ionizing radiations are described in terms of their appearance when a preparation is made at the first metaphase after exposure to radiation. This is the time when the structure of the chromosomes can be discerned.

The study of radiation damage in mammalian cell chromosomes is hampered by the large number of mammalian chromosomes per cell and by their small size. Most mammalian cells currently available for experimental purposes have a diploid complement of 40 or more chromosomes. There are exceptions, such as the Chinese hamster, with 22 chromosomes, and various marsupials, such as the rat kangaroo and woolly opossum, which have chromosome complements of 12 and 14, respectively. Many plant cells, however, contain fewer and generally much larger chromosomes; consequently, much information on chromosomal radiation damage accrued from studies with plant cells.

If cells are irradiated with x-rays, DSBs are produced in the chromosomes. The broken ends appear to be “sticky” because of unpaired bases and can rejoin with any other sticky end. It would appear, however, that a broken end cannot join with a normal, unbroken chromosome. Once breaks are produced, different fragments may behave in various ways:

1. The breaks may restitute, that is, rejoin in their original configuration. In this case, of course, nothing amiss is visible at the next mitosis.
2. The breaks may fail to rejoin and give rise to an aberration, which is scored as a deletion at the next mitosis.
3. Broken ends may reassort and rejoin other broken ends to give rise to chromosomes that appear to be grossly distorted if viewed at the following mitosis.

The aberrations seen at metaphase are of two classes: *chromosome* aberrations and *chromatid* aberrations. **Chromosome aberrations** result if a cell is irradiated early in interphase, before the chromosome material has been duplicated. In this case, the radiation-induced break is in a single strand of chromatin; during the DNA synthetic phase that follows, this strand of chromatin lays down an identical strand next to itself and replicates the break that has been produced by the radiation. This leads to a chromosome aberration visible at the next mitosis because there is an identical break in the corresponding points of a pair of chromatin strands. If, on the other hand, the dose of radiation is given later in interphase, after the DNA material has doubled and the chromosomes consist of two strands of chromatin, then the aberrations produced are called **chromatid aberrations**. In regions removed from the centromere, chromatid arms may be fairly well separated, and it is reasonable to suppose that the radiation might break one chromatid without breaking its sister chromatid, or at least not in the same place. A break that occurs in a single chromatid arm after chromosome replication and leaves the opposite arm of the same chromosome undamaged leads to chromatid aberrations.

EXAMPLES OF RADIATION-INDUCED ABERRATIONS

Many types of chromosomal aberrations and rearrangements are possible, but an exhaustive analysis is beyond the scope of this book. Three types of aberrations that are *lethal* to the cell are described, followed by two common rearrangements that are consistent with cell viability but are frequently involved in carcinogenesis. The three lethal aberrations are the **dicentric**; the **ring**, which are chromosome aberrations; and the **anaphase bridge**, which is a chromatid

aberration. All three represent gross distortions and are clearly visible. Many other aberrations are possible but are not described here.

The formation of a **dicentric** is illustrated in diagrammatic form in [Figure 2.14A](#). This aberration involves an interchange between two separate chromosomes. If a break is produced in each chromosome early in interphase and the sticky ends are close to one another, they may rejoin as shown. This bizarre interchange is replicated during the DNA synthetic phase, and the result is a grossly distorted chromosome with two centromeres (hence, dicentric). There also are two fragments that have no centromere (acentric fragment), which will therefore be lost at a subsequent mitosis. The appearance at metaphase is shown in the bottom panel of [Figure 2.14A](#). An example of a dicentric and fragment in a metaphase human cell is shown in [Figure 2.15B](#); [Figure 2.15A](#) shows a normal metaphase for comparison.

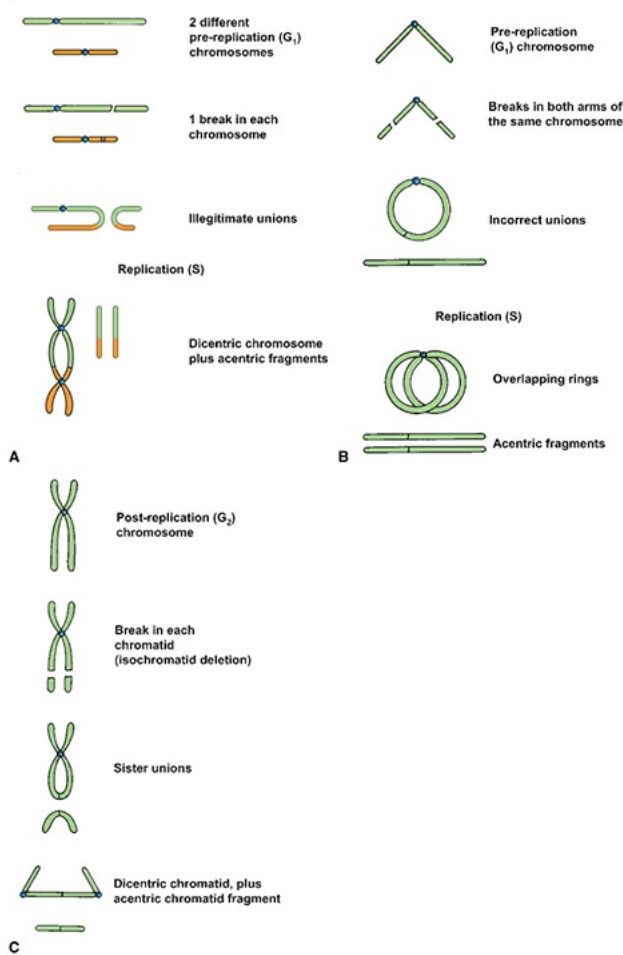


FIGURE 2.14 A: The steps in the formation of a dicentric by irradiation of prereplication (i.e., G_1) chromosomes. A break is produced in each of two separate chromosomes. The “sticky” ends may join incorrectly to form an interchange between the two chromosomes. Replication then occurs in the DNA

synthetic period. One chromosome has two centromeres: a dicentric. The acentric fragment will also replicate, and both will be lost at a subsequent mitosis because, lacking a centromere, they will not go to either pole at anaphase. **B:** The steps in the formation of a ring by irradiation of a prereplication (i.e., G₁) chromosome. A break occurs in each arm of the same chromosome. The sticky ends rejoin incorrectly to form a ring and an acentric fragment. Replication then occurs. **C:** The steps in the formation of an anaphase bridge by irradiation of a postreplication (i.e., G₂) chromosome. Breaks occur in each chromatid of the same chromosome. Incorrect rejoining of the sticky ends then occurs in a sister union. At the next anaphase, the acentric fragment will be lost, one centromere of the dicentric will go to each pole, and the chromatid will be stretched between the poles. Separation of the progeny cells is not possible; this aberration is likely to be lethal. (Courtesy of Dr. Charles Geard.)

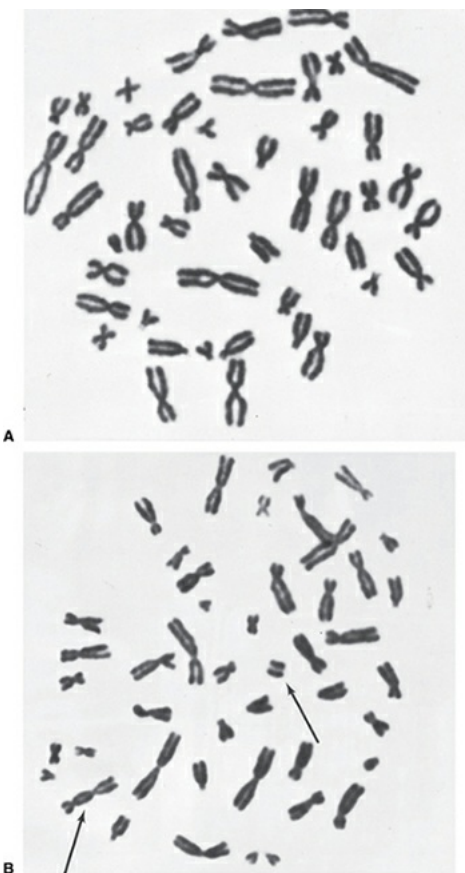




FIGURE 2.15 Radiation-induced chromosome aberrations in human leukocytes viewed at metaphase. **A:** Normal metaphase. **B:** Dicentric and fragment (arrows). **C:** Ring (arrow). (Courtesy of Drs. Brewen, Luippold, and Preston.)

The formation of a **ring** is illustrated in diagrammatic form in [Figure 2.14B](#). A break is induced by radiation in each arm of a single chromatid early in the cell cycle. The sticky ends may rejoin to form a ring and a fragment. Later in the cycle, during the DNA synthetic phase, the chromosome replicates. The ultimate appearance at metaphase is shown in the lower panel of [Figure 2.14B](#). The fragments have no centromere and probably will be lost at mitosis because they will not be pulled to either pole of the cell. An example of a ring chromosome in a human cell at metaphase is illustrated in [Figure 2.15C](#).

An **anaphase bridge** may be produced in various ways. As illustrated in [Figure 2.14C](#) and [Figure 2.16](#), it results from breaks that occur late in the cell cycle (in G₂) after the chromosomes have replicated. Breaks may occur in both chromatids of the same chromosome, and the sticky ends may rejoin incorrectly to form a sister union. At anaphase, when the two sets of chromosomes move to opposite poles, the section of chromatin between the two centromeres is stretched across the cell between the poles, hindering the separation into two new progeny cells, as illustrated in [Figure 2.14C](#) and [Figure 2.16B](#). The two fragments may join as shown, but because there is no centromere, the joined fragments will probably be lost at the first mitosis. This type of aberration occurs in human cells and is essentially always lethal. It is hard to demonstrate because preparations of human chromosomes usually are made by accumulating cells at metaphase, and the bridge is only evident at anaphase. [Figure 2.16](#) is an anaphase preparation of *Tradescantia paludosa*, a plant used extensively for cytogenetic studies because of the small number of large chromosomes. The anaphase bridge is seen clearly as the replicate sets of chromosomes move to opposite poles of the cell.

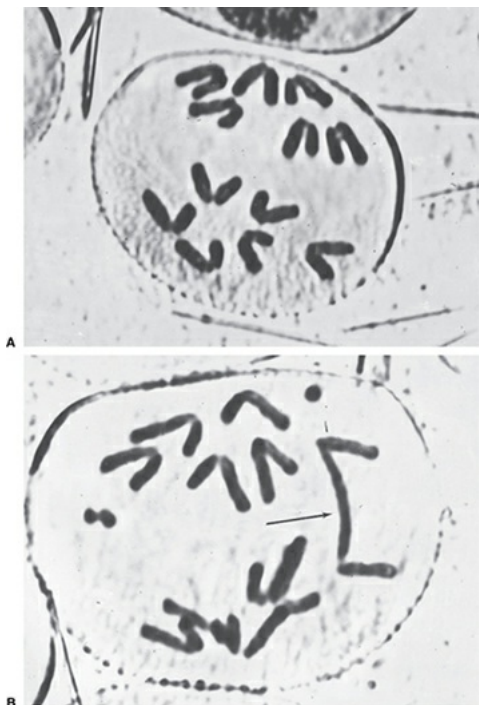


FIGURE 2.16 Anaphase chromosome preparation of *Tradescantia paludosa*. **A:** Normal anaphase. **B:** Bridge and fragment resulting from radiation (arrow). (Courtesy of Drs. Brewen, Luippold, and Preston.)

Gross chromosome changes of the types discussed previously inevitably lead to the reproductive death of the cell.

Two important types of chromosomal changes that are not lethal to the cell are symmetric translocations and small deletions. The formation of a **symmetric translocation** is illustrated in [Figure 2.17A](#). It involves a break in two prereplication (G_1) chromosomes, with the broken ends being exchanged between the two chromosomes as illustrated. An aberration of this type is difficult to see in a conventional preparation but is easy to observe with the technique of fluorescent *in situ* hybridization (FISH), or *chromosome painting*, as it commonly is called. Probes are available for every human chromosome that makes them fluorescent in a different color. Exchange of material between two different chromosomes then is readily observable ([Fig. 2.18](#)). Translocations are associated with several human malignancies caused by the activation of an oncogene; Burkitt lymphoma and certain types of leukemia are examples.

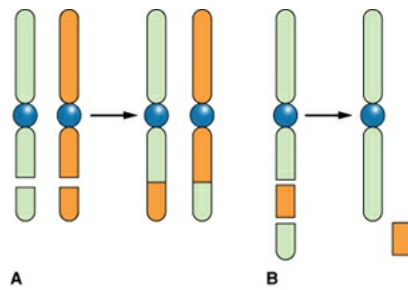


FIGURE 2.17 **A:** Formation of a symmetric translocation. Radiation produces breaks in two different prereplication chromosomes. The broken pieces are exchanged between the two chromosomes, and the “sticky” ends rejoin. This aberration is not necessarily lethal to the cell. There are examples in which an exchange aberration of this type leads to the activation of an oncogene. See Chapter 10 on radiation carcinogenesis. **B:** Diagram of a deletion. Radiation produces two breaks in the same arm of the same chromosome. What actually happens is illustrated more clearly in Figure 2.18.

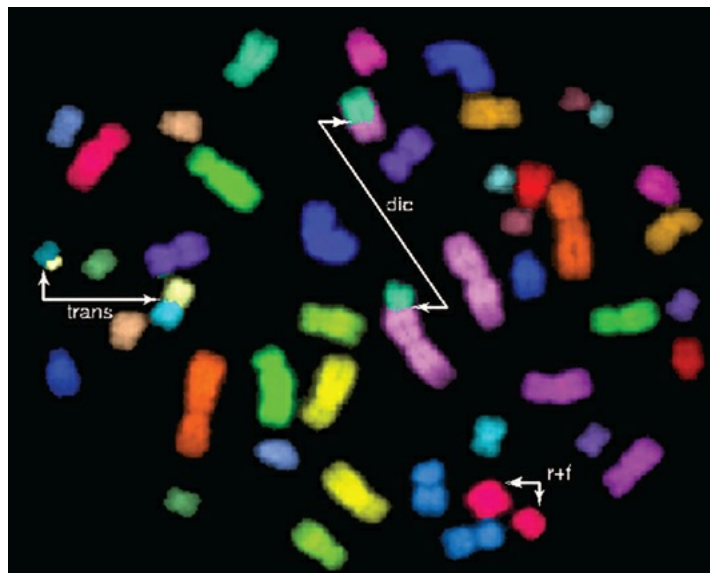


FIGURE 2.18 Fluorescence *in situ* hybridization of a metaphase spread from a cell that received 4 Gy. The hybridization was performed with a cocktail of DNA probes that specifically recognize each chromosome pair. Chromosome aberrations are demarcated by the *arrows*. (Courtesy of Dr. Michael Cornforth.)

The other type of nonlethal chromosomal change is a **small interstitial deletion**. This is illustrated in Figure 2.17B and may result from two breaks in the same arm of the same chromosome, leading to the loss of the genetic information between the two breaks. The actual sequence of events in the formation of a deletion is easier to understand from Figure 2.19, which shows an interphase chromosome. It is a simple matter to imagine how two breaks may isolate a loop of DNA—an acentric ring—which is lost at a subsequent mitosis.

Deletions may be associated with carcinogenesis if the lost genetic material includes a tumor suppressor gene. This is discussed further in [Chapter 10](#) on radiation carcinogenesis.

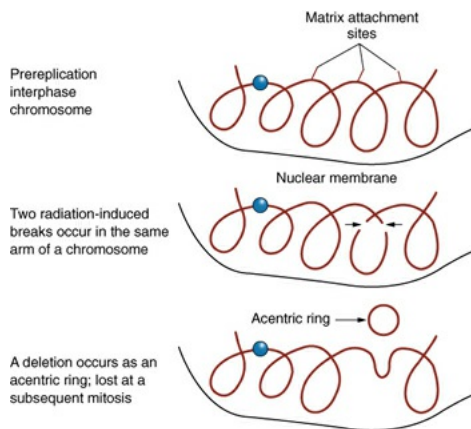


FIGURE 2.19 Formation of a deletion by ionizing radiation in an interphase chromosome. It is easy to imagine how two breaks may occur (by a single or two different charged particles) in such a way as to isolate a loop of DNA. The “sticky” ends rejoin, and the deletion is lost at a subsequent mitosis because it has no centromere. This loss of DNA may include the loss of a suppressor gene and lead to a malignant change. See [Chapter 10](#) on radiation carcinogenesis.

The interaction between breaks in different chromosomes is by no means random. There is great heterogeneity in the sites at which deletions and exchanges between different chromosomes occur; for example, chromosome 8 is particularly sensitive to exchanges. As mentioned previously, each chromosome is restricted to a domain, and most interactions occur at the edges of domains, which probably involves the nuclear matrix. Active chromosomes are therefore those with the biggest surface area to their domains.

CHROMOSOME ABERRATIONS IN HUMAN LYMPHOCYTES

Chromosomal aberrations in peripheral lymphocytes have been used widely as biomarkers of radiation exposure. In blood samples obtained for cytogenetic evaluation within a few days to a few weeks after total body irradiation, the frequency of asymmetric aberrations (dicentrics and rings) in the lymphocytes reflects the dose received. Lymphocytes in the blood sample are stimulated to divide with a mitogen such as phytohemagglutinin and are arrested at metaphase, and the incidence of rings and dicentrics is scored. The dose can be estimated by comparison with *in vitro* cultures exposed to known doses. [Figure 2.20](#) shows a dose-response curve for aberrations in human lymphocytes produced by γ -rays.

The data are fitted by a linear-quadratic relationship, as would be expected, because rings and dicentrics result from the interaction of two chromosome breaks, as previously described. The linear component is a consequence of the two breaks resulting from a single charged particle. If the two breaks result from different charged particles, the probability of an interaction is a quadratic function of dose. This also is illustrated for the formation of a dicentric in [Figure 2.20](#).

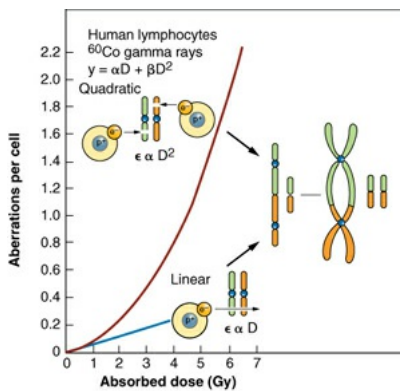


FIGURE 2.20 The frequency of chromosomal aberrations (dicentrics and rings) is a linear-quadratic function of dose because the aberrations are the consequence of the interaction of two separate breaks. At low doses, both breaks may be caused by the same electron; the probability of an exchange aberration is proportional to dose (D). At higher doses, the two breaks are more likely to be caused by separate electrons. The probability of an exchange aberration is proportional to the square of the dose (D^2).

If a sufficient number of metaphases are scored, cytogenetic evaluations in cultured lymphocytes readily can detect a recent total body exposure of as low as 0.25 Gy in the exposed person. Such studies are useful in distinguishing between “real” and “suspected” exposures, particularly in those instances involving “black film badges” or in potential accidents in which it is not certain whether individuals who were at risk for exposure actually received a dose of radiation.

Mature T lymphocytes have a finite life span of about 1,500 days and are eliminated slowly from the peripheral lymphocyte pool. Consequently, the yield of dicentrics observed in peripheral lymphocytes declines in the months and years after a radiation exposure.

During *in vivo* exposures to ionizing radiation, chromosome aberrations are induced not only in mature lymphocytes but also in lymphocyte progenitors in marrow, nodes, or other organs. The stem cells that sustain asymmetric aberrations (such as dicentrics) die in attempting a subsequent mitosis, but those

that sustain a symmetric nonlethal aberration (such as a translocation) survive and pass on the aberration to their progeny. Consequently, dicentrics are referred to as “unstable” aberrations because their number declines with time after irradiation. Symmetric translocations, by contrast, are referred to as “stable” aberrations because they persist for many years. Either type of aberration can be used to estimate dose soon after irradiation, but if many years have elapsed, scoring dicentrics underestimates the dose, and only stable aberrations such as translocations give an accurate picture. Until recently, translocations were much more difficult to observe than dicentrics, but now, the technique of FISH makes the scoring of such symmetric aberrations a relatively simple matter. The frequency of translocations assessed in this way correlates with total body dose in exposed individuals even after more than 50 years, as was shown in a study of the survivors of the atomic bomb attacks on Hiroshima and Nagasaki.

SUMMARY OF PERTINENT CONCLUSIONS

Ionizing radiation induces base damage, SSBs, DSBs, and DNA protein crosslinks.

The cell has evolved an intricate series of sensors and pathways to respond to each type of radiation-induced damage.

DNA DSBs, the most lethal form of ionizing radiation-induced damage, is repaired by nonhomologous recombination in the G₁ phase of the cell cycle and homologous recombination (mainly) in the S/G₂ phase of the cell cycle.

Defective nonhomologous recombination leads to chromosome aberrations, immune deficiency, and ionizing radiation sensitivity.

Defective homologous recombination leads to chromatid and chromosome aberrations, decreased proliferation, and ionizing radiation sensitivity.

There is good reason to believe that DSBs rather than SSBs lead to important biologic end points including cell death, carcinogenesis, and mutation.

Radiation-induced breakage and incorrect rejoining in prereplication (G₁) chromosomes may lead to chromosome aberrations.

Radiation-induced breakage and incorrect rejoining in postreplication (late S or G₂) chromosomes may lead to chromatid aberrations.

Lethal aberrations include dicentrics, rings, and anaphase bridges. Symmetric translocations and small deletions are nonlethal.

There is a good correlation between cells killed and cells with asymmetric exchange aberrations (i.e., dicentrics or rings).

The incidence of most radiation-induced aberrations is a linear-quadratic function of dose.

Scoring aberrations in lymphocytes from peripheral blood may be used to estimate total body doses in humans accidentally irradiated. The lowest single dose that can be detected readily is 0.25 Gy.

Dicentrics are “unstable” aberrations; they are lethal to the cell and are not passed on to progeny. Consequently, the incidence of dicentrics declines slowly with time after exposure.

Translocations are “stable” aberrations; they persist for many years because they are not lethal to the cell and are passed on to the progeny.

BIBLIOGRAPHY

- Alper T, Fowler JF, Morgan RL, et al. The characteristics of the “type C” survival curve. *Br J Radiol.* 1962;35:722–723.
- Andrews JR, Berry RJ. Fast neutron irradiation and the relationship of radiation dose and mammalian tumor cell reproductive capacity. *Radiat Res.* 1962;16:76–81.
- Bakkenist CJ, Kastan MB. Initiating cellular stress responses. *Cell.* 2004;118:9–17.
- Barendsen GW, Beusker TLJ, Vergroesen AJ, et al. Effects of different ionizing radiations on human cells in tissue culture: II. Biological experiments. *Radiat Res.* 1960;13:841–849.
- Bender M. Induced aberrations in human chromosomes. *Am J Pathol.* 1963;43:26a.
- Blackburn EH. Telomeres. *Annu Rev Biochem.* 1992;61:113–129.
- Bonner WM, Redon CE, Dickey JS, et al. γH2AX and cancer. *Nat Rev Cancer.* 2008;8:957–967.
- Bunting SF, Callén E, Wong N, et al. 53BP1 inhibits homologous recombination in Brca1-deficient cells by blocking resection of DNA breaks. *Cell.* 2010;141:243–254.
- Carrano AV. Chromosome aberrations and radiation-induced cell death: II. Predicted and observed cell survival. *Mutat Res.* 1973;17:355–366.

- Cornforth MN, Bedford JS. A quantitative comparison of potentially lethal damage repair and the rejoicing of interphase chromosome breaks in low passage normal human fibroblasts. *Radiat Res.* 1987;111:385–405.
- Cornforth MN, Bedford JS. X-ray-induced breakage and rejoicing of human interphase chromosomes. *Science*. 1983;222:1141–1143.
- Cremer C, Mükel C, Granzow M, et al. Nuclear architecture and the induction of chromosomal aberrations. *Mutat Res.* 1996;366(2):97–116.
- Cromie GA, Connelly JC, Leach DRF. Recombination at double-strand breaks and DNA ends: conserved mechanisms from phage to humans. *Mol Cell*. 2001;8:1163–1174.
- Elkind MM, Sutton H. Radiation response of mammalian cells grown in culture: I. Repair of X-ray damage in surviving Chinese hamster cells. *Radiat Res.* 1960;13:556–593.
- Evans HJ. Chromosome aberrations induced by ionizing radiation. *Int Rev Cytol*. 1962;13:221–321.
- Frankenberg D, Frankenberg-Schwager M, Harbich R. Split-dose recovery is due to the repair of DNA double-strand breaks. *Int J Radiat Biol Relat Stud Phys Chem Med*. 1984;46:541–553.
- Gasser SM, Laemmli UK. A glimpse at chromosomal order. *Trends Genet*. 1987;3:16–22.
- Geard CR. Effects of radiation on chromosomes. In: Pizzarello D, ed. *Radiation Biology*. Boca Raton, FL: CRC Press; 1982:83–110.
- Georgiev GP, Nedospasov SA, Bakayev VV. Supranucleosomal levels of chromatin organization. In: Busch H, ed. *The Cell Nucleus*. Vol 6. New York, NY: Academic Press; 1978:3–34.
- Gilson E, Laroche T, Gasser SM. Telomeres and the functional architecture of the nucleus. *Trends Cell Biol*. 1993;3:128–134.
- Grell RF. The chromosome. *J Tenn Acad Sci*. 1962;37:43–53.
- Hammond EM, Pires I, Giaccia AJ. DNA damage and repair. In: Leibel S, Phillips TL, Hoppe RT, et al, eds. *Textbook of Radiation Oncology*. Philadelphia, PA: Elsevier; 2010;31–39.
- Ishihara T, Sasaki MS, eds. *Radiation-Induced Chromosome Damage in Man*. New York, NY: Alan R Liss; 1983.

Jackson SP. Sensing and repairing DNA double-strand breaks. *Carcinogenesis*. 2002;23:687–696.

Jeggo PA, Hafezparast M, Thompson AF, et al. Localization of a DNA repair gene (XRCC5) involved in double-strand-break rejoining to human chromosome 2. *Proc Natl Acad Sci USA*. 1992;89:6423–6427.

Lea DEA. *Actions of Radiations on Living Cells*. 2nd ed. Cambridge, United Kingdom: Cambridge University Press; 1956.

Littlefield LG, Kleinerman RA, Sayer AM, et al. Chromosome aberrations in lymphocytes-biomonitor of radiation exposure. In: Gledhill BL, Francesco M, eds. *New Horizons in Biological Dosimetry*. New York, NY: Wiley Liss; 1991:387–397.

Littlefield LG, Lushbaugh CC. Cytogenetic dosimetry for radiation accidents: “The good, the bad, and the ugly.” In: Ricks RC, Fry SA, eds. *The Medical Basis for Radiation-Accident Preparedness*. New York, NY: Elsevier; 1990:461–478.

Mahaney BL, Meek K, Lees-Miller SP. Repair of ionizing radiation-induced DNA double strand breaks by non-homologous end-joining. *Biochem J*. 2009;417:639–650.

Marsden M, Laemmli UK. Metaphase chromosome structure: evidence for a radial loop model. *Cell*. 1979;17:849–858.

Moorhead PS, Nowell PC, Mellman WJ, et al. Chromosome preparation of leukocytes cultured from human peripheral blood. *Exp Cell Res*. 1960;20:613–616.

Muller HJ. The remaking of chromosomes. In: *Studies in Genetics: The Selected Papers of HJ Muller*. Bloomington, IN: Indiana University Press; 1962:384–408.

Muniandy PA, Liu J, Majumdar A, et al. DNA interstrand crosslink repair in mammalian cells: step by step. *Crit Rev Biochem Mol Biol*. 2010;45:23–49.

Munro TR. The relative radiosensitivity of the nucleus and cytoplasm of the Chinese hamster fibroblasts. *Radiat Res*. 1970;42:451–470.

Petrini JHJ, Bressan DA, Yao MS. The rad52 epistasis group in mammalian double strand break repair. *Semin Immunol*. 1997;9:181–188.

Puck TT, Markus PI. Action of x-rays on mammalian cells. *J Exp Med*. 1956;103:653–666.

- Revell SH. Relationship between chromosome damage and cell death. In: Ishihara T, Sasaki MS, eds. *Radiation-Induced Chromosome Damage in Man*. New York, NY: Alan R Liss; 1983:215–233.
- Ris H. Chromosome structure. In: McElroy WD, Glass B, eds. *Chemical Basis of Heredity*. Baltimore, MD: Johns Hopkins University Press; 1957:215–233.
- Sancar A, Lindsey-Boltz LA, Ünsal-Kaçmaz K, et al. Molecular mechanisms of mammalian DNA repair and the DNA damage checkpoints. *Annu Rev Biochem*. 2004;73:39–85.
- Schultz LB, Chehab NH, Malikzay A, et al. p53 binding protein 1 (53BP1) is an early participant in the cellular response to DNA double-strand breaks. *J Cell Biol*. 2000;151:1381–1390.
- Spear FG. On some biological effects of radiation. *Br J Radiol*. 1958;31:114–124.
- Thacker J, Zdzienicka MZ. The mammalian XRCC genes: their roles in DNA repair and genetic stability. *DNA Repair*. 2003;2:655–672.
- Thompson LH, Brookman KW, Jones NJ, et al. Molecular cloning of the human XRCCI gene, which corrects defective DNA strand break repair and sister chromatid exchange. *Mol Cell Biol*. 1990;20:6160–6271.
- Ward JF. DNA damage produced by ionizing radiation in mammalian cells: identities, mechanisms of formation and repairability. *Prog Nucleic Acid Res Mol Biol*. 1988;35:95–125.
- Ward JF. Some biochemical consequences of the spatial distribution of ionizing radiation produced free radicals. *Radiat Res*. 1981;86:185–195.
- Willers H, Taghian AG, Luo CM, et al. Utility of DNA repair protein foci for the detection of putative BRCA1 pathway defects in breast cancer biopsies. *Mol Cancer Res*. 2009;7:1304–1309.

chapter 3

Cell Survival Curves

[Reproductive Integrity](#)

[The *In Vitro* Survival Curve](#)

[The Shape of the Survival Curve](#)

[Mechanisms of Cell Killing](#)

[DNA as the Target](#)

[The Bystander Effect](#)

[Apoptotic and Mitotic Death](#)

[Autophagic Cell Death](#)

[Senescence](#)

[Survival Curves for Various Mammalian Cells in Culture](#)

[Survival Curve Shape and Mechanisms of Cell Death](#)

[Oncogenes and Radioresistance](#)

[Genetic Control of Radiosensitivity](#)

[Intrinsic Radiosensitivity and Cancer Stem Cells](#)

[Effective Survival Curve for a Multifraction Regimen](#)

[Calculations of Tumor Cell Kill](#)

[Problem 1 • Answer](#) [Problem 2 • Answer](#)

[Problem 3 • Answer](#) [Problem 4 • Answer](#)

[The Radiosensitivity of Mammalian Cells Compared with Microorganisms](#)

[Summary of Pertinent Conclusions](#)

[Bibliography](#)

REPRODUCTIVE INTEGRITY

A **cell survival curve** describes the relationship between the radiation dose and the proportion of cells that survive. What is meant by “survival”? Cell survival, or its converse, cell death, may mean different things in different contexts;

therefore, a precise definition is essential. For differentiated cells that do not proliferate, such as nerve, muscle, or secretory cells, death can be defined as the loss of a specific function. For proliferating cells, such as stem cells in the hematopoietic system or the intestinal epithelium, loss of the capacity for sustained proliferation—that is, loss of *reproductive integrity*—is an appropriate definition. This is sometimes called **reproductive death**. This is certainly the end point measured with cells cultured *in vitro*.

This definition reflects a narrow view of radiobiology. A cell may still be physically present and apparently intact, may be able to make proteins or synthesize DNA, and may even be able to struggle through one or two mitoses; but if it has lost the capacity to divide indefinitely and produce a large number of progeny, it is by definition dead; it has not survived. A survivor that has retained its reproductive integrity and is able to proliferate indefinitely to produce a large clone or colony is said to be *clonogenic*.

This definition is generally relevant to the radiobiology of whole animals and plants and their tissues. It has particular relevance to the radiotherapy of tumors. For a tumor to be eradicated, it is only necessary that cells be “killed” in the sense that they are rendered unable to divide and cause further growth and spread of the malignancy. Cells may die by different mechanisms, as is described here subsequently. For most cells, death while attempting to divide, that is, **mitotic death**, is the dominant mechanism following irradiation. For some cells, programmed cell death, or **apoptosis**, is important. Whatever the mechanism, the outcome is the same: The cell loses its ability to proliferate indefinitely, that is, its reproductive integrity.

In general, a dose of 100 Gy is necessary to destroy cell function in nonproliferating systems. By contrast, the mean lethal dose for loss of proliferative capacity is usually less than 2 Gy.

THE *IN VITRO* SURVIVAL CURVE

The capability of a single cell to grow into a large colony that can be seen easily with the naked eye is a convenient proof that it has retained its reproductive integrity. The loss of this ability as a function of radiation dose is described by the dose-survival curve.

With modern techniques of tissue culture, it is possible to take a specimen from a tumor or from many normal regenerative tissues, chop it into small pieces, and prepare a single-cell suspension by the use of the enzyme trypsin, which dissolves and loosens the cell membrane. If these cells are seeded into a

culture dish, covered with an appropriate complex growth medium, and maintained at 37° C under aseptic conditions, they attach to the surface, grow, and divide.

In practice, most fresh explants grow well for a few weeks but subsequently peter out and die. A few pass through a crisis and continue to grow for many years. Every few days, the culture must be “farmed”: The cells are removed from the surface with trypsin, most of the cells are discarded, and the culture flask is reseeded with a small number of cells, which quickly repopulate the culture flask. These are called **established cell lines**; they have been used extensively in experimental cellular radiobiology.

Survival curves are so basic to an understanding of much of radiobiology that it is worth going through the steps involved in a typical experiment using an established cell line in culture.

Cells from an actively growing stock culture are prepared into a suspension by the use of trypsin, which causes the cells to round up and detach from the surface of the culture vessel. The number of cells per unit volume of this suspension is counted in a hemocytometer or with an electronic counter. In this way, for example, 100 individual cells may be seeded into a dish; if this dish is incubated for 1 to 2 weeks, each single cell divides many times and forms a colony that is easily visible with the naked eye, especially if it is fixed and stained (Fig. 3.1). All cells making up each colony are the progeny of a single ancestor. For a nominal 100 cells seeded into the dish, the number of colonies counted may be expected to be in the range of 50 to 90. Ideally, it should be 100, but it seldom is for various reasons, including suboptimal growth medium, errors and uncertainties in counting the cell suspension, and the trauma of trypsinization and handling. The term **plating efficiency** indicates the percentage of cells seeded that grow into colonies. The plating efficiency is given by the formula

$$PE = \frac{\text{Number of colonies counted}}{\text{Number of cells seeded}} \times 100$$

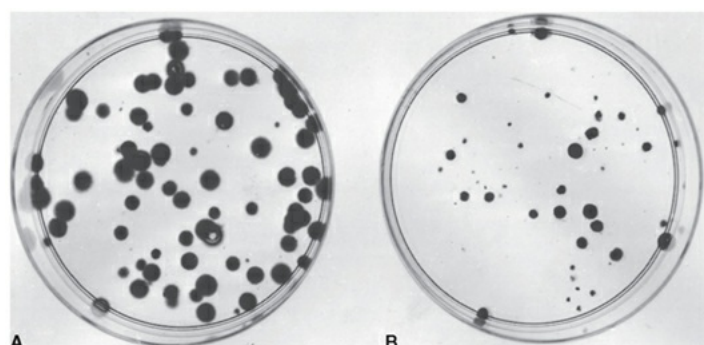


FIGURE 3.1 Colonies obtained with Chinese hamster cells cultured *in vitro*. **A:** In this unirradiated control dish, 100 cells were seeded and allowed to grow for 7 days before being stained. There are 70 colonies; therefore, the plating efficiency is 70/100 or 70%. **B:** Two thousand cells were seeded and then exposed to 8 Gy of x-rays. There are 32 colonies on the dish. Thus,

$$\text{Surviving fraction} = \text{Colonies counted} / [\text{Cells seeded} \times (\text{PE} / 100)]$$

$$= 32 / (2,000 \times 0.7)$$

$$= 0.023$$

There are 70 colonies on the control dish in [Figure 3.1A](#); therefore, the plating efficiency is 70%. If a parallel dish is seeded with cells, exposed to a dose of 8 Gy of x-rays, and incubated for 1 to 2 weeks before being fixed and stained, then the following may be observed: (1) Some of the seeded single cells are still single and have not divided, and in some instances, the cells show evidence of nuclear deterioration as they die an apoptotic death; (2) some cells have managed to complete one or two divisions to form a tiny abortive colony; and (3) some cells have grown into large colonies that differ little from the unirradiated controls, although they may vary more in size. These cells are said to have survived because they have retained their reproductive integrity.

In the example shown in [Figure 3.1B](#), 2,000 cells had been seeded into the dish exposed to 8 Gy. Because the plating efficiency is 70%, 1,400 of the 2,000 cells plated would have grown into colonies if the dish had not been irradiated. In fact, there are only 32 colonies on the dish; the fraction of cells surviving the dose of x-rays is thus

$$\frac{32}{1,400} = 0.023$$

In general, the surviving fraction is given by

$$\text{Surviving fraction} = \frac{\text{Colonies counted}}{\text{Cells seeded} \times (\text{PE}/100)}$$

This process is repeated so that estimates of survival are obtained for a range of doses. The number of cells seeded per dish is adjusted so that a countable number of colonies results: Too few reduce statistical significance; too many

cannot be counted accurately because they tend to merge into one another. The technique is illustrated in [Figure 3.2](#). This technique, and the survival curve that results, does not distinguish the mode of cell death, that is, whether the cells died mitotic or apoptotic deaths.

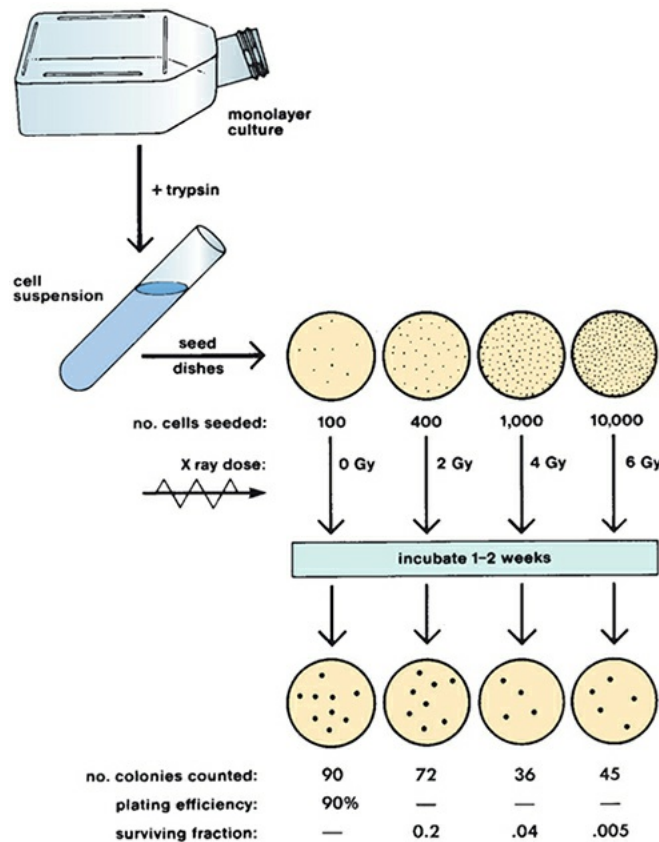


FIGURE 3.2 The cell culture technique used to generate a cell survival curve. Cells from a stock culture are prepared into a single-cell suspension by trypsinization, and the cell concentration is counted. Known numbers of cells are inoculated into petri dishes and irradiated. They are then allowed to grow until the surviving cells produce macroscopic colonies that can be counted readily. The number of cells per dish initially inoculated varies with the dose so that the number of colonies surviving is in the range that can be counted conveniently. Surviving fraction is the ratio of colonies produced to cells plated, with a correction necessary for plating efficiency (i.e., for the fact that not all cells plated grow into colonies, even in the absence of radiation).

THE SHAPE OF THE SURVIVAL CURVE

Survival curves for mammalian cells usually are presented in the form shown in [Figure 3.3](#), with dose plotted on a linear scale and surviving fraction on a logarithmic scale. Qualitatively, the shape of the survival curve can be described in relatively simple terms. At “low doses” for sparsely ionizing (low-linear

energy transfer [LET]) radiations, such as x-rays, the survival curve starts out straight on the log-linear plot with a finite initial slope; that is, the surviving fraction is an exponential function of dose. At higher doses, the curve bends. This bending or curving region extends over a dose range of a few grays. At very high doses, the survival curve often tends to straighten again; the surviving fraction returns to being an exponential function of dose. In general, this does not occur until doses in excess of those used as daily fractions in radiotherapy have been reached.

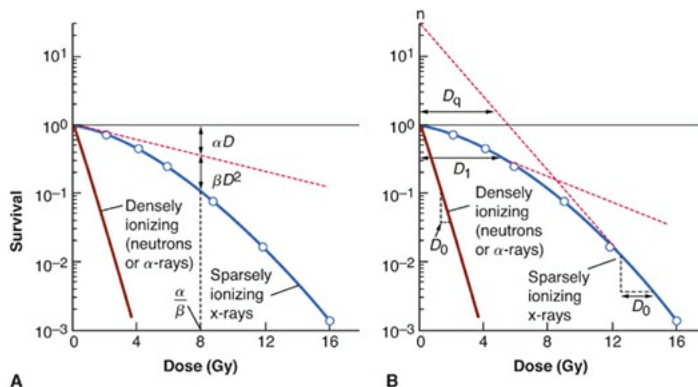


FIGURE 3.3 Shape of survival curve for mammalian cells exposed to radiation. The fraction of cells surviving is plotted on a logarithmic scale against dose on a linear scale. For α -particles or low-energy neutrons (said to be densely ionizing), the dose-response curve is a straight line from the origin (i.e., survival is an exponential function of dose). The survival curve can be described by just one parameter, the slope. For x- or γ -rays (said to be sparsely ionizing), the dose-response curve has an initial linear slope, followed by a shoulder; at higher doses, the curve tends to become straight again. **A:** The linear-quadratic model. The experimental data are fitted to a linear-quadratic function. There are two components of cell killing: One is proportional to dose (αD); the other is proportional to the square of the dose (βD^2). The dose at which the linear and quadratic components are equal is the ratio α/β . The linear-quadratic curve bends continuously but is a good fit to experimental data for the first few decades of survival. **B:** The multitarget model. The curve is described by the initial slope (D_1), the final slope (D_0), and a parameter that represents the width of the shoulder, either n or D_q .

By contrast, for densely ionizing (high-LET) radiations, such as α -particles or low-energy neutrons, the cell survival curve is a straight line from the origin; that is, survival approximates to an exponential function of dose (see Fig. 3.3).

Although it is a simple matter to qualitatively describe the shape of the cell survival curve, finding an explanation of the biologic observations in terms of

biophysical events is another matter. Many biophysical models and theories have been proposed to account for the shape of the mammalian cell survival curve. Almost all can be used to deduce a curve shape that is consistent with experimental data, but it is never possible to choose among different models or theories based on goodness of fit to experimental data. The biologic data are not sufficiently precise, nor are the predictive theoretic curves sufficiently different, for this to be possible.

Two descriptions of the shape of survival curves are discussed briefly with a minimum of mathematics (see Fig. 3.3). First, the **multitarget model** that was widely used for many years still has some merit (see Fig. 3.3B). In this model, the survival curve is described in terms of an *initial slope*, D_1 , resulting from single-event killing; a *final slope*, D_0 , resulting from multiple-event killing; and some quantity (either n or D_q) to represent the size or width of the shoulder of the curve. The quantities D_1 and D_0 are the reciprocals of the initial and final slopes. In each case, it is the dose required to reduce the fraction of surviving cells to 37% of its previous value (i.e., e^{-1}). As illustrated in Figure 3.3B, D_1 , the initial slope, is the dose required to reduce the fraction of surviving cells to 0.37 on the initial straight portion of the survival curve. The final slope, D_0 , is the dose required to reduce survival from 0.1 to 0.037 or from 0.01 to 0.0037, and so on. Because the surviving fraction is on a logarithmic scale and the survival curve becomes straight at higher doses, the dose required to reduce the cell population by a given factor (to 0.37 or e^{-1}) is the same at all survival levels. It is, on average, the dose required to deliver one inactivating event per cell.

The **extrapolation number**, n , is a measure of the width of the shoulder. If n is large (e.g., 10 or 12), the survival curve has a broad shoulder. If n is small (e.g., 1.5 to 2), the shoulder of the curve is narrow. Another measure of shoulder width is the **quasithreshold dose**, shown as D_q in Figure 3.3. This sounds like a term invented by a committee, which in a sense it is. An easy way to remember its meaning is to think of the hunchback of Notre Dame. When the priest was handed the badly deformed infant who was to grow up to be the hunchback, he cradled him in his arms and said, “We will call him Quasimodo—he is almost a person!” Similarly, the quasithreshold dose is almost a threshold dose. It is defined as the dose at which the straight portion of the survival curve, extrapolated backward, cuts the dose axis drawn through a survival fraction of unity. A threshold dose is the dose below which there is no effect. There is no

dose below which radiation produces no effect, so there can be no true threshold dose; D_q , the quasithreshold dose, is the closest thing.

At first sight, this might appear to be an awkward parameter, but in practice, it has certain merits that become apparent in subsequent discussion. The three parameters, n , D_0 , and D_q , are related by the expression

$$\log_e n = D_q / D_0$$

The linear-quadratic model has taken over as the model of choice to describe survival curves. It is a direct development of the relation used to describe exchange-type chromosome aberrations that are clearly the result of an interaction between two separate breaks. This is discussed in some detail in [Chapter 2](#).

The **linear-quadratic model**, illustrated in [Figure 3.3A](#), assumes that there are two components to cell killing by radiation: one that is proportional to dose and one that is proportional to the square of the dose. The notion of a component of cell inactivation that varies with the square of the dose introduces the concept of dual radiation action. This idea goes back to the early work with chromosomes in which many chromosome aberrations are clearly the result of two separate breaks. (Examples discussed in [Chapter 2](#) are dicentrics, rings, and anaphase bridges, all of which are likely to be lethal to the cell.)

By this model, the expression for the cell survival curve is

$$S = e^{-\alpha D - \beta D^2}$$

in which S is the fraction of cells surviving a dose D , and α and β are constants. The components of cell killing that are proportional to dose and to the square of the dose are equal if

$$\alpha D = \beta D^2$$

or

$$D = \alpha/\beta$$

This is an important point that bears repeating: The linear and quadratic contributions to cell killing are equal at a dose that is equal to the ratio of α to β .

A characteristic of the linear-quadratic formulation is that the resultant cell survival curve is continuously bending; there is no final straight portion. This does not coincide with what is observed experimentally if survival curves are determined down to seven or more decades of cell killing in which case the

dose-response relationship closely approximates to a straight line in a log-linear plot; that is, cell killing is an exponential function of dose. In the first decade or so of cell killing and up to any doses used as daily fractions in clinical radiotherapy, however, the linear-quadratic model is an adequate representation of the data. It has the distinct advantage of having only two adjustable parameters: α and β .

MECHANISMS OF CELL KILLING

DNA as the Target

Abundant evidence shows that the principal sensitive sites for radiation-induced cell lethality are located in the nucleus as opposed to the cytoplasm. Evidence for chromosomal DNA as the principal target for cell killing is circumstantial but overwhelming and may be summarized as follows:

1. Cells are killed by radioactive tritiated thymidine incorporated into the DNA. The radiation dose results from short-range β -particles and is therefore very localized.
2. Certain structural analogues of thymidine, particularly the halogenated pyrimidines, are incorporated selectively into DNA in place of thymidine if substituted in cell culture growth medium. This substitution dramatically increases the radiosensitivity of the mammalian cells to a degree that increases as a function of the amount of the incorporation. Substituted deoxyuridines, which are not incorporated into DNA, have no such effect on cellular radiosensitivity.
3. Factors that modify cell lethality, such as variation in the type of radiation, oxygen concentration, and dose rate, also affect the production of chromosome damage in a fashion qualitatively and quantitatively similar. This is at least *prima facie* evidence to indicate that damage to the chromosomes is implicated in cell lethality.
4. Early work showed a relationship between virus size and radiosensitivity; later work showed a better correlation with nucleic acid volume. The radiosensitivity of a wide range of plants has been correlated with the mean interphase chromosome volume, which is defined as the ratio of nuclear volume to chromosome number. The larger the mean chromosome volume, the greater the radiosensitivity.

However, although chromosomal DNA is the principal target for radiation-

induced lethality, sophisticated experiments with microbeams have shown clearly that low levels of mutations can be induced by α -particles which pass through the cytoplasm and never touch the nucleus.

The Bystander Effect

Generations of students in radiation biology have been taught that heritable biologic effects require direct damage to DNA; however, experiments in the last decade have demonstrated the existence of a **bystander effect**, defined as the induction of biologic effects in cells that are not directly traversed by a charged particle but are in proximity to cells that are. Interest in this effect was sparked by the 1992 report of Nagasawa and Little that following a low dose of α -particles, a larger proportion of cells showed biologic damage than was estimated to have been hit by an α -particle; specifically, 30% of the cells showed an increase in sister chromatid exchanges even though less than 1% were calculated to have undergone a nuclear traversal. The number of cells hit was arrived at by a calculation based on the fluence of α -particles and the cross-sectional area of the cell nucleus. The conclusion was thus of a statistical nature because it was not possible to know on an individual basis which cells were hit and which were not.

This observation has been extended by the use of sophisticated single-particle microbeams, which make it possible to deliver a known number of particles through the nucleus of specific cells, whereas biologic effects can be studied in unirradiated close neighbors. Most microbeam studies have used α -particles because it is easier to focus them accurately, but a bystander effect has also been shown for protons and soft x-rays. Using single-particle microbeams, a bystander effect has been demonstrated for chromosomal aberrations, cell killing, mutation, oncogenic transformation, and alteration of gene expression. The effect is most pronounced when the bystander cells are in gap-junction communication with the irradiated cells. For example, up to 30% of bystander cells can be killed in this situation. The bystander effect is much smaller when cell monolayers are sparsely seeded so that cells are separated by several hundred micrometers. In this situation, 5% to 10% of bystander cells are killed, the effect being due, presumably, to cytotoxic molecules released into the medium. The existence of the bystander effect indicates that the target for radiation damage is larger than the nucleus and, indeed, larger than the cell itself. Its importance is primarily at low doses, where not all cells are “hit,” and it may have important implications in risk estimation.

In addition to the experiments described previously involving sophisticated single-particle microbeams, there is a body of data involving the transfer of medium from irradiated cells that results in a biologic effect (cell killing) when added to unirradiated cells. These studies, which also evoke the term *bystander effect*, suggest that irradiated cells secrete a molecule into the medium that is capable of killing cells when that medium is transferred onto unirradiated cells. Most bystander experiments involving medium transfer have used low-LET x- or γ -rays.

Apoptotic and Mitotic Death

Apoptosis was first described by Kerr and colleagues as a particular set of changes at the microscopic level associated with cell death. The word *apoptosis* is derived from the Greek word meaning “falling off,” as in petals from flowers or leaves from trees. Apoptosis, or programmed cell death, is common in embryonic development in which some tissues become obsolete. It is the mechanism, for example, by which tadpoles lose their tails.

This form of cell death is characterized by a stereotyped sequence of morphologic events. One of the earliest steps a cell takes if it is committed to die in a tissue is to cease communicating with its neighbors. This is evident as the dying cell rounds up and detaches from its neighbors. Condensation of the chromatin at the nuclear membrane and fragmentation of the nucleus are then evident. The cell shrinks because of cytoplasmic condensation, resulting from crosslinking of proteins and loss of water. Eventually, the cell separates into several membrane-bound fragments of differing sizes termed *apoptotic bodies*, which may contain cytoplasm only or nuclear fragments. The morphologic hallmark of apoptosis is the condensation of the nuclear chromatin in either crescents around the periphery of the nucleus or a group of spheric fragments.

Double-strand breaks (DSBs) occur in the linker regions between nucleosomes, producing DNA fragments that are multiples of approximately 185 base pairs. These fragments result in the characteristic ladders seen in gels. In contrast, necrosis causes a diffuse “smear” of DNA in gels. Apoptosis occurs in normal tissues, as described previously, and also can be induced in some normal tissues and in some tumors by radiation.

As a mode of radiation-induced cell death, apoptosis is highly cell-type dependent. Hemopoietic and lymphoid cells are particularly prone to rapid radiation-induced cell death by the apoptotic pathway. In most tumor cells, mitotic cell death is at least as important as apoptosis, and in some cases, it is the

only mode of cell death. Several genes appear to be involved. First, apoptosis after radiation seems commonly to be a *p53*-dependent process; Bcl-2 is a suppressor of apoptosis.

The most common form of cell death from radiation is mitotic death: Cells die attempting to divide because of damaged chromosomes. Death may occur in the first or a subsequent division following irradiation. Many authors have reported a close quantitative relationship between cell killing and the induction of specific chromosomal aberrations. The results of one of the most elegant studies by Cornforth and Bedford are shown in [Figure 3.4](#). It should be noted that these experiments were carried out in a cell line where apoptosis is not observed. The log of the surviving fraction is plotted against the average number of putative “lethal” aberrations per cell, that is, asymmetric exchange-type aberrations such as rings and dicentrics. There is virtually a one-to-one correlation. In addition, there is an excellent correlation between the fraction of cells surviving and the fraction of cells without visible aberrations.

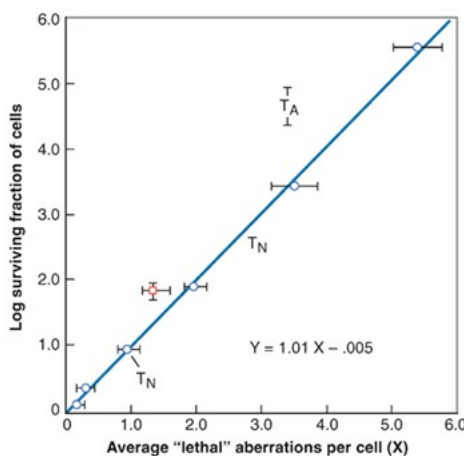


FIGURE 3.4 Relationship between the average number of “lethal” aberrations per cell (i.e., asymmetric exchange-type aberrations such as dicentrics and rings) and the log of the surviving fraction in AC 1522 normal human fibroblasts exposed to x-rays. There is virtually a one-to-one correlation. (From Cornforth MN, Bedford JS. A quantitative comparison of potentially lethal damage repair and the rejoicing of interphase chromosome breaks in low passage normal human fibroblasts. *Radiat Res.* 1987;111:385–405, with permission.)

Data such as these provide strong circumstantial evidence to support the notion that asymmetric exchange-type aberrations represent the principle mechanism for radiation-induced mitotic death in mammalian cells.

[Figure 3.5](#) illustrates, in a much oversimplified way, the relationship between chromosome aberrations and cell killing. As explained in [Chapter 2](#), cells, in

which there is an asymmetric exchange-type aberration (such as a dicentric or a ring), lose their reproductive integrity. Exchange-type aberrations require *two* chromosome breaks. At low doses, the two breaks may result from the passage of a single electron set in motion by the absorption of a photon of x- or γ -rays. The probability of an interaction between the two breaks to form a lethal exchange-type aberration is proportional to dose. Consequently, the survival curve is linear at low doses. At higher doses, the two chromosome breaks may result from two *separate* electrons. The probability of an interaction between the two breaks is then proportional to the square of the dose. If this quadratic component dominates, the survival curve bends over and becomes curved. Thus, the linear-quadratic relationship characteristic of the induction of chromosome aberrations is carried over to the cell survival curve.

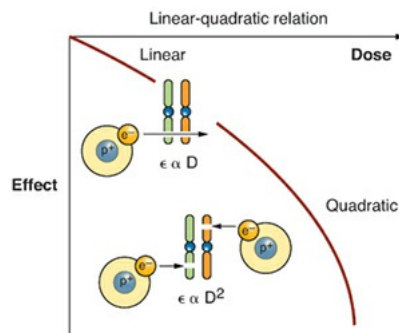


FIGURE 3.5 Relationship between chromosome aberrations and cell survival. Cells that suffer exchange-type chromosome aberrations (such as dicentrics) are unable to survive and continue to divide indefinitely. At low doses, the two chromosome breaks are the consequence of a single electron set in motion by the absorption of x- or γ -rays. The probability of an interaction between the breaks is proportional to dose; this is the linear portion of the survival curve. At higher doses, the two chromosome breaks may result also from two separate electrons. The probability of an interaction is then proportional to the square of the dose. The survival curve bends if the quadratic component dominates.

Autophagic Cell Death

Autophagy is literally defined as a self-digestive process that uses lysosomal degradation of long-lived proteins and organelles to restore or maintain cellular homeostasis. Autophagy is evolutionarily conserved and is considered a dynamic process that involves a unique series of steps, of which the sequestration of portions of the cytoplasm and organelles in a double-membrane vesicle, called an autophagosome, is a hallmark characteristic. These autophagosomes ultimately fuse with lysosomes, where protein and organelles are degraded and reprocessed. Autophagosomes then fuse with lysosomes, which acidify as they

mature to become autolysosomes in a step called autophagic flux. Autophagy is a multistep process that is genetically regulated by a unique set of genes termed *autophagy-related genes* (Atgs). These Atgs were first discovered in yeast, and approximately 30 Atg orthologs have been identified in mammals that include two ubiquitin-like conjugation systems: the Atg12-Atg5 and the Atg8 (LC-3)-phosphatidylethanolamine. These systems are required for the elongation of the autophagosomal membrane. However, the proteins and trafficking mechanisms involved in the autophagosomal maturation step are not completely understood.

Although autophagy was initially described as a protective mechanism for cells to survive and generate nutrients and energy, studies have been published to demonstrate that continuous exposure to a stress-inducing condition can also promote autophagic, or what has been termed programmed type II, cell death. Defective autophagy has been characterized in different diseases including infections, neurodegeneration, aging, Crohn disease, heart disease, and cancer. Although autophagy can be found in cells dying from stress, it is unclear whether it represents a drastic means for the cell to survive by digesting part of itself or whether it actually promotes cell death. Evidence for both possibilities exist in different cell types and will require further studies to clarify its role in irradiated cells.

The induction of apoptosis by anticancer agents, as described previously, including ionizing radiation, is directed at specifically eliminating cancer cells. However, defects in apoptosis observed in many solid tumor cells possess diminished apoptotic programs because of mutations in key regulatory proteins and develop resistance to killing by apoptosis when exposed to chemotherapy and radiotherapy. Previous studies have reported that the metabolic stress observed in human tumors leads cancer cells to acquire resistance to apoptosis and to stimulate autophagy to maintain energy demand and prevent necrosis. Furthermore, chemotherapeutic agents and radiotherapy have been reported to induce autophagy and autophagic cell death. Although the mechanism underlying this form of cell death is unclear, accumulation of autophagosomes in response to chemotherapy or radiotherapy suggests that this type of cell death is associated with an inhibition of the maturation and degradation process. The signals for the induction of autophagy by radiotherapy are still under investigation but may involve signaling from the endoplasmic reticulum, particularly, the protein kinase-like endoplasmic reticulum kinase (PERK), which is described in more detail in [Chapter 26](#). Induction of endoplasmic reticulum stress in cells that have lost their ability to die by apoptosis when exposed to radiation results in radiosensitization. This data suggests that the

combination of endoplasmic stress-inducing agents and ionizing radiation could enhance cell killing by inducing autophagic cell death. Thus, in the regulation of cancer, autophagy should be considered a new target for anticancer therapy.

Senescence

Cellular senescence has emerged as a programmed cellular stress response that represents a unique response to the accumulation of damage to a cell. Whether through the shortening of telomeres associated with a high number of cell divisions, activation of oncogenes, or DNA damage caused by oxidative stress, induction of senescence in primary cells leads to an irreversible cell cycle arrest that is almost invariably characterized by the activation of the p53 and retinoblastoma (Rb) proteins and is associated with chromatin modifications that result in the silencing of genes necessary to promote transition from the G1 to the S phase of the cell cycle. For these reasons, senescence has been classified as a tumor suppressor mechanism that prevents excessive cellular divisions in response to inappropriate growth signals or division of cells that have accumulated DNA damage. Because it is a genetically regulated process that involves the p53 and Rb proteins, it is understandable that loss of p53 and Rb control through gene mutation will result in loss of senescence in response to DNA damage. However, although tumor cells typically lose their ability to undergo senescence in response to DNA damage caused by mutations in the p53 and Rb pathways, normal cells do not lose this ability. The induction of senescence in normal tissue is important to consider because these cells are still metabolically active but reproductively inhibited. This is best exemplified by fibroblasts that, when irradiated in cell culture, stay attached to plates for weeks but never divide. However, they are able to secrete growth factors and mitogens that promote the growth of tumor cells. Therefore, senescence results in a permanent cell cycle arrest but will not eliminate the mitogenic or cytokine contribution of the arrested cell that could ultimately promote tumor regrowth.

SURVIVAL CURVES FOR VARIOUS MAMMALIAN CELLS IN CULTURE

Survival curves have been measured for many established cell lines grown in culture. These cell lines have been derived from the tissues of humans or other mammals such as small rodents. In some cases, the parent tissue has been neoplastic; in other cases, it has been normal. The first *in vitro* survival curve for mammalian cells irradiated with x-rays is shown in [Figure 3.6](#). All mammalian cells studied to date, normal or malignant, regardless of their species of origin,

exhibit x-ray survival curves similar to those in [Figure 3.6](#); there is an initial shoulder followed by a portion that tends to become straight on a log-linear plot. The size of the initial shoulder is extremely variable. For some cell lines, the survival curve appears to bend continuously so that the linear-quadratic relationship is a better fit and n has no meaning. The D_0 of the x-ray survival curves for most cells cultured *in vitro* falls in the range of 1 to 2 Gy. The exceptions are cells from patients with cancer-prone syndromes such as ataxiatelangiectasia (AT); these cells are much more sensitive to ionizing radiations, with a D_0 for x-rays of about 0.5 Gy. This *in vitro* sensitivity correlates with a hypersensitivity to radiotherapy found in these patients.

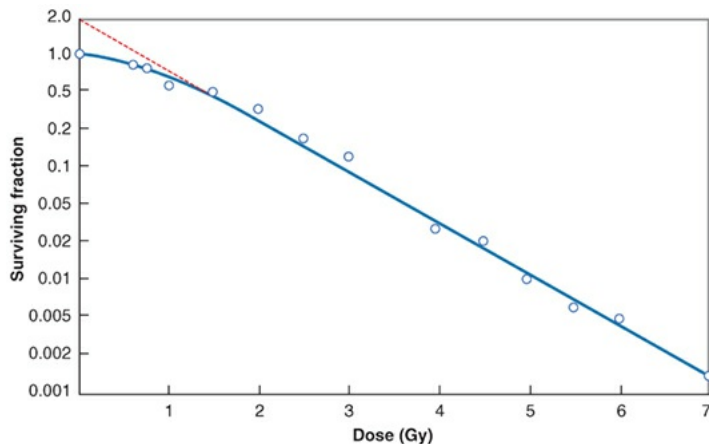


FIGURE 3.6 Survival curve for HeLa cells in culture exposed to x-rays. Characteristically, this cell line has a small initial shoulder. (From Puck TT, Marcus PI. Action of x-rays on mammalian cells. *J Exp Med.* 1956;103:653–666, with permission.)

The first *in vitro* survival curve was reported in 1956 and generated great excitement in the field of radiobiology. It was thought that at last, with a quantitative system available to relate absorbed dose with surviving fraction of cells, great strides would be made in understanding the effect of ionizing radiation on biologic materials. In particular, it was anticipated that significant contributions would be made toward understanding radiotherapeutic practice. This enthusiasm was not shared by everyone. Some researchers were skeptical that these *in vitro* techniques, which involved growing cells in petri dishes in very artificial conditions, would ever benefit clinical radiotherapy. The fears of these skeptics were eloquently voiced by Spear in the MacKenzie Davidson Memorial Lecture given to the British Institute of Radiology in 1957:

An isolated cell *in vitro* does not necessarily behave as it would have done if left *in vivo* in normal association with cells of other types. Its

reactions to various stimuli, including radiations, however interesting and important in themselves, may indeed be no more typical of its behavior in the parent tissue than Robinson Crusoe on his desert island was representative of social life in York in the mid-seventeenth century.

The appropriate answer to this charge was given by David Gould, then professor of radiology at the University of Colorado. He pointed out that the *in vitro* culture technique measured the reproductive integrity of cells and that there was no reason to suppose that Robinson Crusoe's reproductive integrity was any different on his desert island from what it would have been had he remained in York; all that Robinson Crusoe lacked was the opportunity. The opportunity to reproduce to the limit of their capability is afforded to cells cultured *in vitro* if they find themselves in the petri dish, with temperature and humidity controlled and with an abundant supply of nutrients.

At the time, it required a certain amount of faith and optimism to believe that survival curves determined with the *in vitro* technique could be applied to the complex *in vivo* situation. Such faith and optimism were completely vindicated, however, by subsequent events. When techniques became available to measure cell survival *in vivo*, the parameters of the dose-response relationships were shown to be similar to those *in vitro*.

In more recent years, extensive studies have been made of the radiosensitivity of cells of human origin, both normal and malignant, grown and irradiated in culture. In general, cells from a given normal tissue show a narrow range of radiosensitivities if many hundreds of people are studied (Fig. 3.7). By contrast, cells from human tumors show a very broad range of D_0 values; some cells, such as those from squamous carcinomas, tend to be more radioresistant, whereas sarcomas are somewhat more radiosensitive. Each tumor type, however, has a broad spectrum of radiosensitivities that tend to overlap. Tumor cells bracket the radiosensitivity of cells from normal tissues; that is, some are more sensitive, and others are more resistant.

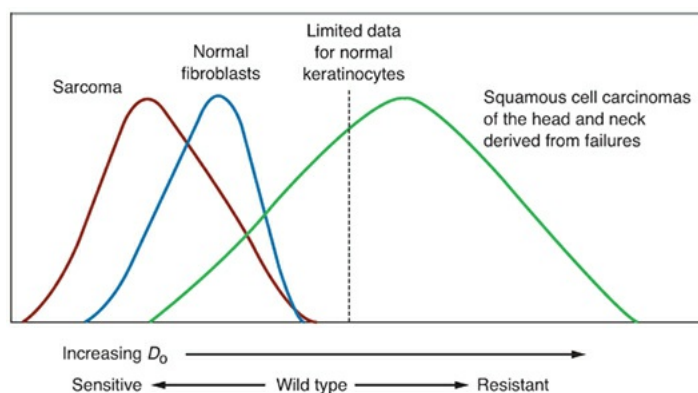


FIGURE 3.7 Summary of D_0 values for cells of human origin grown and irradiated *in vitro*. Cells from human tumors tend to have a wide range of radiosensitivities, which brackets the radiosensitivity of normal human fibroblasts. In general, squamous cell carcinoma cells are more resistant than sarcoma cells, but the spectra of radiosensitivities are broad and overlap. (Courtesy of Dr. Ralph Weichselbaum.)

SURVIVAL CURVE SHAPE AND MECHANISMS OF CELL DEATH

Mammalian cells cultured *in vitro* vary considerably in their sensitivity to killing by radiation. This is illustrated in **Figure 3.8A**, which includes survival curves for asynchronous cultures of mouse tumor cells (EMT6) as well as for six cell lines derived from human tumors.

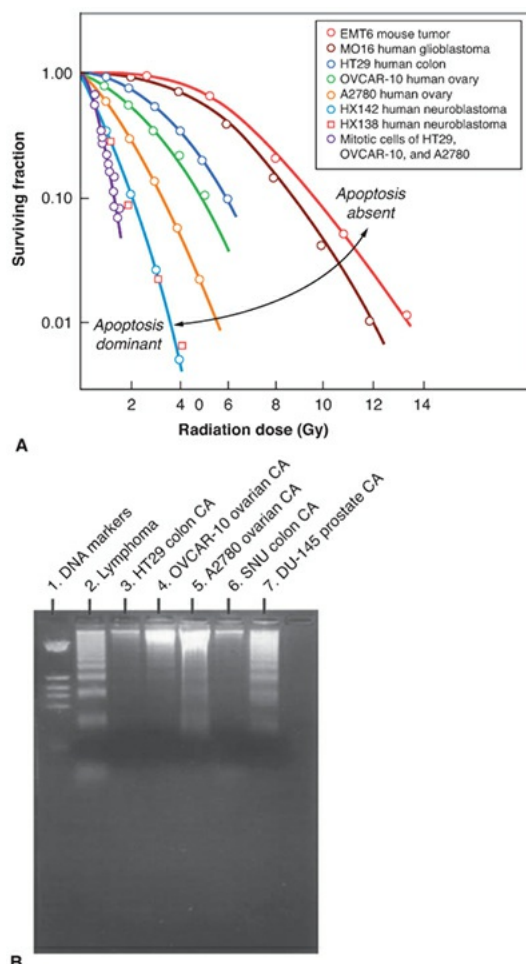


FIGURE 3.8 A: Compilation of survival curves for asynchronous cultures of several cell lines of human and rodent origin. Note the wide range of radiosensitivity (most notably the size of the shoulder) between mouse EMT6 cells (the most resistant) and two neuroblastoma cell lines of human origin (the

most sensitive). The cell survival curve for mitotic cells is very steep, and there is little difference in radiosensitivity for cell lines that are very different in asynchronous culture. (Data compiled by Dr. J. D. Chapman, Fox Chase Cancer Center, Philadelphia.) **B:** DNA purified from various cell lines (survival curves shown in [Fig. 3.8A](#)) 18 hours after irradiation with 10 Gy and electrophoresed for 90 minutes at 6 V/cm. Note the broad variation in the amount of “laddering”—which is characteristic of an apoptotic death. In this form of death, DSBs occur in the linker regions between nucleosomes, producing DNA fragments that are multiples of about 185 base pairs. Note that cell lines that show prominent laddering are radiosensitive. CA, carcinoma. (Gel prepared by Drs. S. Biade and J. D. Chapman, Fox Chase Cancer Center, Philadelphia.)

Asynchronous EMT6 cells are the most radioresistant, followed closely by glioblastoma cells of human origin; thereafter, radiosensitivity increases, with two neuroblastoma cell lines being the most sensitive. Although asynchronous cells show this wide range of sensitivities to radiation, it is a remarkable finding that mitotic cells from all of these cell lines have essentially the same radiosensitivity. The implication of this is that if the chromosomes are condensed during mitosis, all cell lines have the same radiosensitivity governed simply by DNA content, but in interphase, the radiosensitivity differs because of different conformations of the DNA. Another interesting observation comes from a comparison of the survival curves in [Figure 3.8A](#) with the DNA laddering in [Figure 3.8B](#).

Characteristic laddering is indicative of programmed cell death or apoptosis during which the DNA breaks up into discrete lengths as previously described. Comparing [Figure 3.8A](#) and [B](#), it is evident that there is a close and impressive correlation between radiosensitivity and the importance of apoptosis. The most radioresistant cell lines, which have broad shoulders to their survival curves, show no evidence of apoptosis; those most radiosensitive, for which survival is an exponential function of dose, show clear DNA laddering as an indication of apoptosis. The increased clarity of the laddering correlates with increasing radiosensitivity together with a smaller and smaller shoulder to the survival curve. Many of the established cell lines that have been cultured *in vitro* for many years, and with which many of the basic principles of radiation biology were demonstrated, show no apoptotic death and have an abrogated *p53* function. Continued culture *in vitro* appears often to select for cells with this characteristic.

Mitotic death results (principally) from exchange-type chromosomal

aberrations; the associated cell survival curve, therefore, is curved in a log-linear plot, with a broad initial shoulder. As is shown subsequently here, it is also characterized by a substantial dose-rate effect. Apoptotic death results from mechanisms that are not yet clearly understood, but the associated cell survival curve appears to be a straight line on a log-linear plot—that is, survival is an exponential function of dose. In addition, there appears to be little or no dose-rate effect, although data are sparse on this point.

Although there are some cell lines in which mitotic death dominates and others in which apoptosis is the rule, most cell lines fall somewhere in between, with contributions from both mitotic and apoptotic death following a radiation exposure, in varying proportions. It has been proposed that the dose-response relationship be described by the following relation:

$$S = e^{-(\alpha_M + \alpha_A)D - \beta_M D^2}$$

in which S is the fraction of cells surviving a dose D , α_M and α_A describe the contributions to cell killing from mitotic and apoptotic death that are linear functions of dose, and β_M describes the contribution to mitotic death that varies with the square of the dose.

ONCOGENES AND RADIRESISTANCE

Numerous reports have appeared in the literature that transfection of activated oncogenes into cells cultured *in vitro* increases their radioresistance, as defined by clonogenic survival. Reports include the transfection of activated *N-ras*, *raf*, or *ras* + *myc*, a combination that is particularly effective in transforming primary explants of rodent embryo cells to a malignant state. Results, however, are equivocal and variable. The change of radiosensitivity did not correlate with cell cycle distribution or DNA DSBs or their repair; the best correlation was with the length of the G₂ phase delay induced by radiation. It is by no means clear that oncogene expression is directly involved in the induction of radioresistance, and it is far less clear that oncogenes play any major role in radioresistance in human tumors.

GENETIC CONTROL OF RADIOSENSITIVITY

The molecular biology of repair processes in lower organisms, such as yeast and bacteria, has been studied extensively. In several instances, a dramatically radiosensitive mutant can result from a mutation in a single gene that functions as a repair or checkpoint gene. In mammalian cells, the situation is much more

complicated, and it would appear that a large number of genes may be involved in determining radiosensitivity. Many radiosensitive mutants have been isolated from cell lines maintained in the laboratory, especially rodent cell systems. In many but not all cases, their sensitivity to cell killing by radiation has been related to their greatly reduced ability to repair DNA DSBs. Examples of these genes are *Ku 80*, *Ku 70*, and *XRCC7*. The first of these two genes are involved in DNA-dependent kinase activity that binds to the free ends at the site of a DSB, so that if they are defective, repair of DSBs is prejudiced. The third gene codes for a protein that is defective in mice with the “severe combined immune deficiency syndrome” that are sensitive to radiation.

Some patients who show an abnormally severe normal tissue reaction to radiation therapy exhibit the traits of specific inherited syndromes. These are listed in [Table 3.1](#) and discussed in more detail in [Chapter 18](#). The most striking example is AT. Fibroblasts taken from patients with this syndrome are 2 or 3 times as radiosensitive as normal, and patients with AT receiving radiation therapy show considerable normal tissue damage unless the doses are reduced appropriately. They also have an elevated incidence of spontaneous cancer. Cells from AT heterozygotes are slightly more radiosensitive than normal, and there is some controversy whether AT heterozygotes are predisposed to cancer.

Table 3.1 Inherited Human Syndromes Associated with Sensitivity to X-rays

Ataxia-telangiectasia (AT)
Seckel syndrome
AT-like disorder
Nijmegen breakage syndrome
Fanconi anemia

Homologues of RecQ–Bloom syndrome, Werner syndrome, and Rothmund-Thompson syndrome

The gene associated with AT has been identified and sequenced and called the ataxia-telangiectasia mutated (ATM) gene. The ATM protein appears to be part of signal transduction pathways involved in many physiologic processes, although the exact mechanism by which the genetic defect in AT cells leads to radiosensitivity is not altogether clear.

INTRINSIC RADIOSENSITIVITY AND CANCER STEM CELLS

Assays of individual tumor radiosensitivity require cells to be grown from fresh explants of human tumor biopsies. These do not grow well as attached cells in regular clonogenic assays. Better results have been obtained with the Courtenay assay in which cells grow in a semisolid agar gel supplemented with growth factors. In addition, several nonclonogenic assays have been developed based on cell growth in a multiwell plate. Growth is assessed in terms of the ability of cells to reduce a compound that can be visualized by staining or is based on total DNA or RNA content of the well. These end points are surrogates for clonogenicity or reproductive integrity.

It has been well accepted that the radiosensitivity of cells changes as they undergo differentiation. If this is true, then cell death in tumors exposed to ionizing radiation in tumors should correlate with the elimination of tumor stem cells and survival of the more differentiated tumor cells that have lost their renewal capability. However, this has not what has been recently reported in the literature. In fact, cancer stem cells may be more resistant to radiation than their more differentiated counterparts. Mechanistically, cancer stem cells appear to have lower levels of reactive oxygen species because of increased levels of free radical scavengers. If this is the case, then the same increased levels of free radical scavengers that protect the cancer stem cells from the metabolic consequences of reactive oxygen species during their growth also protect them when exposed to ionizing radiation. The radiosensitivity of cancer stem cells can be increased if they are first treated with inhibitors of free radical scavengers before radiation exposure.

These rather provocative results will definitely require further investigation to determine whether all cancer stem cells possess high levels of free radical

scavengers both in experimental tumor systems as well as in human biopsies. If this is the case, then a potential means of radiosensitizing these stem cells through the targeting of free radical scavengers could be tested.

EFFECTIVE SURVIVAL CURVE FOR A MULTIFRACTION REGIMEN

Because multifraction regimens are used most often in clinical radiotherapy, it is frequently useful to think in terms of an effective survival curve.

If a radiation dose is delivered in a series of equal fractions, separated by sufficient time for repair of sublethal damage to occur between doses, the *effective dose-survival curve* becomes an exponential function of dose. The shoulder of the survival curve is repeated many times so that the effective survival curve is a straight line from the origin through a point on the single-dose survival curve corresponding to the daily dose fraction. This is illustrated in Figure 3.9. The effective survival curve is an exponential function of dose whether the single-dose survival curve has a constant terminal slope (as shown) or is continuously bending, as implied by the linear-quadratic relation. The D_0 of the effective survival curve (i.e., the reciprocal of the slope), defined to be the dose required to reduce the fraction of cells surviving to 37%, has a value close to 3 Gy for cells of human origin. This is an average value and can differ significantly for different tumor types.

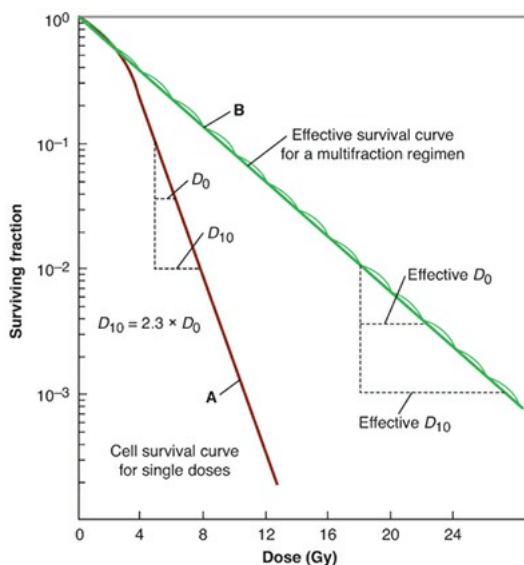


FIGURE 3.9 The concept of an “effective” survival curve for a multifraction regimen is illustrated. If the radiation dose is delivered in a series of equal fractions separated by time intervals sufficiently long for the repair of sublethal damage to be complete between fractions, the shoulder of the survival curve is

repeated many times. The effective dose-survival curve is an exponential function of dose, that is, a straight line from the origin through a point on the single-dose survival curve corresponding to the daily dose fraction (e.g., 2 Gy). The dose resulting in one decade of cell killing (D_{10}) is related to the D_0 by the expression $D_{10} = 2.3 \times D_0$.

For calculation purposes, it is often useful to use the D_{10} , the dose required to kill 90% of the population. From similar triangles in [Figure 3.9](#), it is evident that

$$\frac{D_{10}}{D_0} = \frac{\log_{10}}{\log_e} = \frac{2.3}{1}$$

or

$$D_{10} = 2.3 \times D_0$$

CALCULATIONS OF TUMOR CELL KILL

The concept outlined previously of an effective survival curve for a multifraction radiation treatment may be used to perform simple calculations of tumor cell kill after radiotherapy. Although such calculations are greatly oversimplified, they are nevertheless instructive. Four examples are given here.

Problem 1

A tumor consists of 10^8 clonogenic cells. The effective dose-response curve given in daily dose fractions of 2 Gy has no shoulder and a D_0 of 3 Gy. What total dose is required to give a 90% chance of tumor cure?

Answer

To give a 90% probability of tumor control in a tumor containing 10^8 cells requires a cellular depopulation of 10^{-9} . The dose resulting in one decade of cell killing (D_{10}) is given by

$$D_{10} = 2.3 \times D_0 = 2.3 \times 3 = 6.9 \text{ Gy}$$

The total dose for nine decades of cell killing, therefore, is $9 \times 6.9 = 62.1$ Gy.

Problem 2

Suppose that in the previous example, the clonogenic cells underwent three cell doublings during treatment. About what total dose would be required to achieve the same probability of tumor control?

Answer

Three cell doublings would increase the cell number by

$$2 \times 2 \times 2 = 8$$

Consequently, about one extra decade of cell killing would be required, corresponding to an additional dose of 6.9 Gy. The total dose is $62.1 + 6.9 = 69$ Gy.

Problem 3

During the course of radiotherapy, a tumor containing 10^9 cells receives 40 Gy. If the D_0 is 2.2 Gy, how many tumor cells will be left?

Answer

If the D_0 is 2.2 Gy, the D_{10} is given by

$$D_{10} = 2.3 \times D_0$$

$$= 2.3 \times 2.2 = 5 \text{ Gy}$$

Because the total dose is 40 Gy, the number of decades of cell killing is $40 / 5 = 8$. The number of cells remaining is $10^9 \times 10^{-8} = 10$.

Problem 4

If 10^7 cells were irradiated according to single-hit kinetics so that the average number of hits per cell is one, how many cells would survive?

Answer

A dose that gives an average of one hit per cell is the D_0 , that is, the dose that on the exponential region of the survival curve reduces the number of survivors to 37%. The number of surviving cells is therefore

$$10^7 \times \frac{37}{100} = 3.7 \times 10^6$$

THE RADIOSENSITIVITY OF MAMMALIAN CELLS

COMPARED WITH MICROORGANISMS

The final illustration in this chapter (Fig. 3.10) is a compilation from the literature of survival data for many types of cells. The steepest dose-response relationship (curve A) is an average curve for mammalian cells; it is evident that they are exquisitely radiosensitive compared with microorganisms. The bacterium *Escherichia coli* is more resistant, yeast is more resistant still, and the most resistant is *Micrococcus radiodurans*, which shows no significant cell killing even after a dose of 1,000 Gy. There are several important points to be made from this:

1. The dominant factor that accounts for this huge range of radiosensitivities is the DNA content. Mammalian cells are sensitive because they have a large DNA content, which represents a large target for radiation damage.
2. DNA content is not the whole story, however. *E. coli* and *E. coli* B/r have the same DNA content but differ in radiosensitivity because B/r has a mutant and more efficient DNA repair system. In higher organisms, mode of cell death—that is, apoptotic versus mitotic—also affects radiosensitivity.
3. Figure 3.10 explains why, if radiation is used as a method of sterilization, doses of the order of 20,000 Gy are necessary. Even if objects are socially clean, such huge doses are necessary to reduce the population of contaminating microorganisms because of their extreme radioresistance.

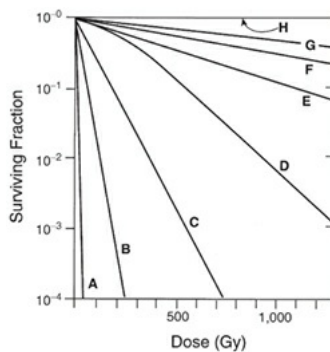


FIGURE 3.10 Survival curves for mammalian cells and for various microorganisms including *E. coli*, yeast, and *M. radiodurans*. It is evident that mammalian cells are exquisitely radiosensitive compared with microorganisms, principally because they have a much larger DNA content, which represents a bigger “target” for radiation damage. A, mammalian cells; B, *E. coli*; C, *E. coli* B/r; D, yeast; E, phage *Staphylococcus epidermidis*; F, *Bacillus megaterium*; G, potato virus; H, *M. radiodurans*.

SUMMARY OF PERTINENT CONCLUSIONS

Cells from tumors and many normal regenerative tissues grow and form colonies *in vitro*.

Fresh explants of normal tissues often grow well in culture for a few weeks before they peter out and die. A few pass through a “crisis” and become immortal; these are the established cell lines.

A cell is said to have retained its reproductive integrity if it is capable of sustained proliferation, that is, if it can grow into a macroscopic colony.

A survivor that has retained its reproductive integrity is said to be *clonogenic*.

The percentage of untreated cells seeded that grow into macroscopic colonies is known as the plating efficiency. Thus,

$$PE = \frac{\text{Number of colonies counted}}{\text{Number of cells seeded}} \times 100$$

The plating efficiency may be close to 100% for some established cell lines but 1% or less for fresh explants of human cells.

The fraction of cells surviving a given dose is determined by counting the number of macroscopic colonies as a fraction of the number of cells seeded. Allowance must be made for the plating efficiency. Thus,

$$SF = \frac{\text{Number of colonies counted}}{\text{Number of cells seeded} \times (PE / 100)}$$

A cell survival curve is the relationship between the fraction of cells retaining their reproductive integrity and the absorbed dose.

Conventionally, surviving fraction on a logarithmic scale is plotted on the ordinate against dose on the abscissa. The shape of the survival curve is important.

The cell survival curve for α -particles and low-energy neutrons (densely ionizing radiations) is a straight line on a log-linear plot; that is, survival approximates to an exponential function of dose.

The cell survival curve for x- or γ -rays (sparsely ionizing radiations) has an initial slope, followed by a bending region or shoulder, after which it tends to straighten again at higher doses.

Survival data are adequately fitted by many models and theories. The data are never sufficiently precise, nor are the models sufficiently different for experimental results to discriminate among models.

For the first one or two decades of survival and up to doses used in single fractions in radiotherapy, survival data are adequately represented by the

linear-quadratic relationship

$$S = e^{-\alpha D - \beta D^2}$$

in which S is the fraction of cells surviving a dose D and α and β are constants representing the linear and quadratic components of cell killing.

The initial slope of the cell survival curve is determined by α ; the quadratic component of cell killing (β) causes the curve to bend at higher doses.

The ratio α/β is the dose at which linear and quadratic components of cell killing are equal.

There is good evidence that the nucleus, specifically the DNA, is the principal target for radiation-induced cell lethality. Membrane damage also may be a factor.

Following exposure to radiation, cells may die attempting the next or a subsequent mitosis (mitotic death), or they may die programmed cell deaths (apoptotic death).

In cells that die a mitotic death, there is a one-to-one correlation between cell survival and the average number of putative “lethal” chromosomal aberrations per cell, that is, asymmetric exchange-type aberrations such as dicentrics and rings.

Cells that die an apoptotic death follow a stereotyped sequence of morphologic events, culminating in the breaking up of the DNA into fragments that are multiples of 185 base pairs; this leads to the characteristic DNA laddering seen in gels.

In some cell types (such as lymphoid cells), apoptotic death is dominant following irradiation. Survival is then an exponential function of dose; that is, the survival curve is straight and shoulderless on the usual log-linear plot. There is also no dose-rate effect.

In some cell types (such as Chinese hamster ovary [CHO] or V79 cells in culture), mitotic death is dominant following irradiation. Survival is then a linear-quadratic function of dose; that is, the survival curve has a shoulder on the usual log-linear plot. There is usually a large dose-rate effect.

Many cell populations die both mitotic and apoptotic deaths. There is, in general, a correlation between the importance of apoptosis and radiosensitivity. If apoptosis is dominant, cells are radiosensitive; if apoptosis is absent, cells are radioresistant.

In addition to mitotic and apoptotic cell death, cells exposed to ionizing radiation can die by autophagic cell death or enter senescence, which is a permanent type of growth arrest.

Cells cultured from different tumors in humans show a broad range of radiosensitivities that bracket the sensitivity of normal cells from different people.

There is some evidence in cells cultured *in vitro* that transfection of activated oncogenes in cells increases their radioresistance. It is not clear that oncogenes play a role in the radioresistance of human tumors *in vivo*.

Several genes that influence the radiosensitivity of mammalian cells have been identified.

If these genes are defective, the repair of DSBs is often prejudiced.

Several human syndromes have been found to be associated with radiosensitivity; AT is the best example.

There is often a link between sensitivity to killing by radiation and predisposition to cancer.

Cancer stem cells may be more radioresistant than their differentiated tumor cell counterparts because of increased levels of reactive oxygen-specific scavengers.

The effective survival curve for a multifraction regimen is an exponential function of dose: a straight line from the origin through a point on the single-dose survival curve corresponding to the daily dose fraction.

The average value of the effective D_0 for the multifraction survival curve for human cells is about 3 Gy.

The D_{10} , the dose resulting in one decade of cell killing, is related to the D_0 by the expression

$$D_{10} = 2.3 \times D_0$$

Calculations of tumor cell kill can be performed for fractionated clinical radiotherapy regimens using the concept of effective survival curve.

Mammalian cells are exquisitely radiosensitive compared with microorganisms such as bacteria and yeast, principally because of their larger DNA content, which represents a bigger “target” for radiation damage.

BIBLIOGRAPHY

- Alper T, Fowler JF, Morgan RL, et al. The characteristics of the “type C” survival curve. *Br J Radiol.* 1962;35:722–723.
- Andrews JR, Berry RJ. Fast neutron irradiation and the relationship of radiation dose and mammalian tumor cell reproductive capacity. *Radiat Res.* 1962;16:76–81.
- Barendsen GW, Beusker TL, Vergroesen AJ, et al. Effects of different radiations on human cells in tissue culture. II. Biological experiments. *Radiat Res.* 1960;13:841–849.
- Baumann M, Krause M, Hill R. Exploring the role of cancer stem cells in radioresistance. *Nat Rev Cancer.* 2008;8:545–554.
- Bender M. Induced aberrations in human chromosomes. *Am J Pathol.* 1963;43:26a.
- Carrano AV. Chromosome aberrations and radiation-induced cell death. II. Predicted and observed cell survival. *Mutat Res.* 1973;17:355–366.
- Cornforth MN, Bedford JS. A quantitative comparison of potentially lethal damage repair and the rejoining of interphase chromosome breaks in low passage normal human fibroblasts. *Radiat Res.* 1987;111:385–405.
- Cornforth MN, Bedford JS. X-ray-induced breakage and rejoining of human interphase chromosomes. *Science.* 1983;222:1141–1143.
- Diehn M, Cho RW, Clarke MF. Therapeutic implications of the cancer stem cell hypothesis. *Semin Radiat Oncol.* 2009;19(2):78–86.
- Elkind MM, Sutton H. Radiation response of mammalian cells grown in culture. I. Repair of x-ray damage in surviving Chinese hamster cells. *Radiat Res.* 1960;13:556–593.
- Evans HJ. Chromosome aberrations induced by ionizing radiation. *Int Rev Cytol.* 1962;13:221–321.
- Frankenberg D, Frankenberg-Schwager M, Harbich R. Split-dose recovery is due to the repair of DNA double strand breaks. *Int J Radiat Biol Relat Stud Phys Chem Med.* 1984;46:541–553.
- Gatti RA, Berkel I, Boder E, et al. Localization of an ataxia-telangiectasia gene to chromosome 11q22–23. *Nature.* 1988;336:577–580.
- Geard CR. Effects of radiation on chromosomes. In: Pizzarello D, ed. *Radiation*

- Biology*. Boca Raton, FL: CRC Press; 1982:83–110.
- Grell RF. The chromosome. *J Tenn Acad Sci*. 1962;37:43–53.
- Ishihara T, Sasaki MS, eds. *Radiation-Induced Chromosome Damage in Man*. New York, NY: Alan R Liss; 1983.
- Jackson SP, Jeggo PA. DNA double-strand break repair and V(D)J recombination: involvement of DNA-PK. *Trends Biochem Sci*. 1995;20:412–415.
- Jeggo PA, Holliday R. Azacytidine-induced reactivation of a DNA repair gene in Chinese hamster ovary cells. *Mol Cell Biol*. 1986;6:2944–2949.
- Jeggo PA, Kemp LM. X-ray-sensitive mutants of Chinese hamster ovary cell line. Isolation and cross-sensitivity to other DNA-damaging agents. *Mutat Res*. 1983;112:313–327.
- Kerr JF, Wyllie AH, Currie AR. Apoptosis: a basic biological phenomenon with wide-ranging implications in tissue kinetics. *Br J Cancer*. 1972;26:239–257.
- Kuerbitz SJ, Plunkett BS, Walsh WV, et al. Wild-type p53 is a cell cycle checkpoint determinant following irradiation. *Proc Natl Acad Sci USA*. 1992;89:7491–7495.
- Lea DE. *Actions of Radiations on Living Cells*. 2nd ed. Cambridge, United Kingdom: Cambridge University Press; 1956.
- Lowe SW, Schmitt EM, Smith SW, et al. p53 is required for radiation-induced apoptosis in mouse thymocytes. *Nature*. 1993;362:847–849.
- McKenna WG, Iliakis G, Muschel RJ. Mechanism of radioresistance in oncogene transfected cell lines. In: Dewey WC, Eddington M, Fry RJM, et al, eds. *Radiation Research: A Twentieth Century Perspective*. San Diego, CA: Academic Press; 1992:392–397.
- Moorhead PS, Nowell PC, Mellman WJ, et al. Chromosome preparation of leukocytes cultured from human peripheral blood. *Exp Cell Res*. 1960;20:613–616.
- Munro TR. The relative radiosensitivity of the nucleus and cytoplasm of the Chinese hamster fibroblasts. *Radiat Res*. 1970;42:451–470.
- Nagasawa H, Little JB. Induction of sister chromatid exchanges by extremely low doses of alpha-particles. *Cancer Res*. 1992;52:6394–6396.
- Prise KM, O’Sullivan JM. Radiation-induced bystander signaling in cancer

- therapy. *Nat Rev Cancer*. 2009;9(5):351–360.
- Puck TT, Marcus PI. Action of x-rays on mammalian cells. *J Exp Med*. 1956;103:653–666.
- Ris H. Chromosome structure. In: McElroy WD, Glass B, eds. *Chemical Basis of Heredity*. Baltimore, MD: Johns Hopkins University Press; 1957.
- Savitsky K, Bar-Shira A, Gilad S, et al. A single ataxia telangiectasia gene with a product similar to PI-3 kinase. *Science*. 1995;268:1749–1753.
- Schmitt CA. Cellular senescence and cancer treatment. *Biochim Biophys Acta*. 2007;1775:5–20.
- Spear FG. On some biological effects of radiation. *Br J Radiol*. 1958;31:114–124.
- Swift M. Ionizing radiation, breast cancer, and ataxia-telangiectasia. *J Natl Cancer Inst*. 1994;86:1571–1572.
- Taccioli GE, Gottlieb TM, Blunt T, et al. Ku80: product of the XRCC5 gene and its role in DNA repair and V(D)J recombination. *Science*. 1994;265:1442–1445.
- Turcotte S, Giaccia AJ. Targeting cancer cells through autophagy for anticancer therapy. *Curr Opin Cell Biol*. 2010;22:246–251.

chapter 4

Radiosensitivity and Cell Age in the Mitotic Cycle

The Cell Cycle

Synchronously Dividing Cell Cultures

The Effect of X-rays on Synchronously Dividing Cell Cultures

Molecular Checkpoint Genes

The Effect of Oxygen at Various Phases of the Cell Cycle

The Age-Response Function for a Tissue *In Vivo*

Variation of Sensitivity with Cell Age for High-Linear Energy Transfer Radiations

Mechanisms for the Age-Response Function

The Possible Implications of the Age-Response Function in Radiotherapy

Summary of Pertinent Conclusions

Bibliography

THE CELL CYCLE

Mammalian cells propagate and proliferate by mitosis. When a cell divides, two progeny cells are produced, each of which carries a chromosome complement identical to that of the parent cell. After an interval of time has elapsed, each of the progeny may undergo a further division. The time between successive divisions is known as the **mitotic cycle time** or, as it is commonly called, the **cell cycle time** (T_C).

If a population of dividing cells is observed with a conventional light microscope, the only event in the entire cell cycle that can be identified and distinguished is mitosis, or division itself. Just before the cell divides to form two progeny cells, the chromosomes (which are diffuse and scattered in the nucleus in the period between mitoses) condense into clearly distinguishable forms. In addition, in monolayer cultures of cells just before mitosis, the cells round up and become loosely attached to the surface of the culture vessel. This

whole process of mitosis—in preparation for which the cell rounds up, the chromosome material condenses and the cell divides into two and then stretches out again and attaches to the surface of the culture vessel—lasts only about 1 hour. The remainder of the cell cycle, the interphase, occupies all of the intermitotic period. No events of interest can be identified with a conventional microscope during this time.

Because cell division is a cyclic phenomenon repeated in each generation of the cells, it is usual to represent it as a circle, as shown in [Figure 4.1](#). The circumference of the circle represents the full mitotic cycle time for the cells (T_C); the period of mitosis is represented by M. The remainder of the cell cycle can be further subdivided by using some marker of DNA synthesis. The original technique was autoradiography, introduced by Howard and Pelc in 1953.

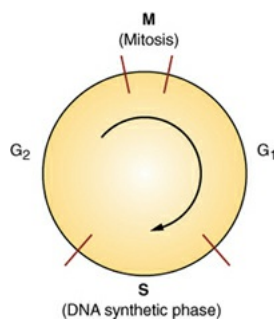


FIGURE 4.1 The stages of the mitotic cycle for actively growing mammalian cells. M, mitosis; S, DNA synthetic phase; G₁ and G₂, “gaps,” or periods of apparent inactivity between the major discernible events in the cycle.

The basis of the technique, illustrated in [Figure 4.2](#), is to feed the cells thymidine, a basic building block used for making DNA, which has been labeled with radioactive tritium ($^3\text{H-TdR}$). Cells that are actively synthesizing new DNA as part of the process of replicating their chromosome complements incorporate the radioactive thymidine. Then, the surplus radioactive thymidine is flushed from the system, the cells are fixed and stained so that they may be viewed easily, and the preparation of cells is coated with a very thin layer of nuclear (photographic) emulsion.

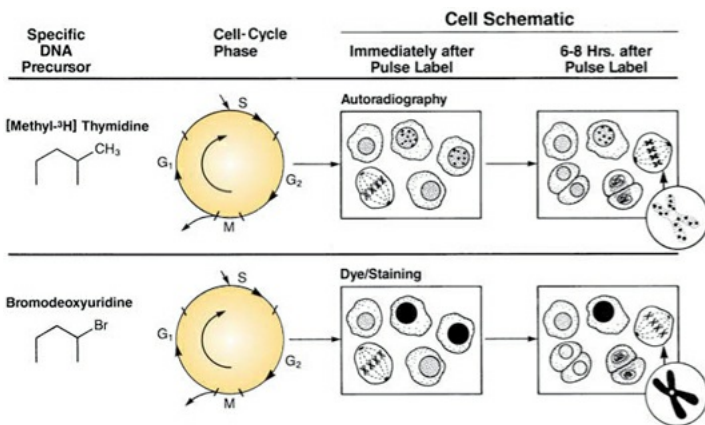


FIGURE 4.2 Cell-labeling techniques. **Top panels:** The principle of autoradiography, which may be applied to cells in culture growing as a monolayer on a glass microscope slide or to thin sections cut from a tumor or normal tissue. Cells in the DNA synthetic phase (S) take up tritiated thymidine. After the cells are fixed and stained so that they are visible by light microscopy, they are covered with a layer of nuclear (photographic) emulsion and left for several weeks in a cool refrigerator. As β -particles from the tritiated thymidine pass through the emulsion, they form latent images that appear as black grains when the emulsion is subsequently developed and fixed. If cells are stained and autoradiographed immediately after incorporation of the tritiated thymidine, cells that are labeled are in S phase (**top middle panel**). If staining and autoradiography are delayed for 6 to 8 hours after the pulse label, some cells may move from S to M, and labeled mitotic cells are observed (**top right panel**). The lengths of the various phases of the cycle can be determined in this way. **Bottom panels:** The principle of cell cycle analysis using 5-bromodeoxyuridine as the DNA precursor instead of radioactively labeled thymidine. The bromodeoxyuridine is incorporated into cells in S. It can be recognized by the use of a Giemsa stain (which is purple) or a monoclonal antibody to bromodeoxyuridine-substituted DNA. The antibody is tagged with a fluorescing dye (e.g., fluorescein), which shows up bright green under a fluorescence microscope. If cells are stained immediately after labeling with bromodeoxyuridine, those staining darkly are in S phase (**bottom middle panel**). If staining is delayed for 6 to 8 hours, cells incorporating bromodeoxyuridine may move from S to M, and a darkly staining mitotic cell is seen (**bottom right panel**). (Courtesy of Dr. Charles Geard.)

β -Particles from cells that have incorporated radioactive thymidine pass through the nuclear emulsion and produce a latent image. When the emulsion is subsequently developed and fixed, the area through which a β -particle has passed appears as a black spot. It is then a comparatively simple matter to view the

preparation of cells and to observe that some of the cells have black spots or “grains” over them, which indicates that they were actively synthesizing DNA at the time radioactive thymidine was made available. Other cells do not have any grains over their nuclei; this is interpreted to mean that the cells were not actively making DNA when the radioactive label was made available to them. Examples of labeled cells are shown in [Figure 4.3](#). If the cells are allowed to grow for some time after labeling with tritiated thymidine so that they move into mitosis before being fixed, stained, and autoradiographed, then a labeled mitotic cell may be observed (see [Fig. 4.3A](#)).

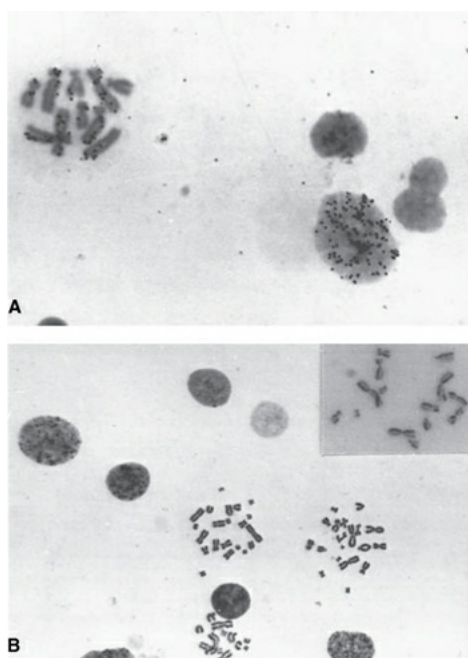


FIGURE 4.3 **A:** Autoradiograph of Chinese hamster cells in culture flash-labeled with tritiated thymidine. The black grains over some cells indicate that they were synthesizing DNA when they were labeled. Also shown is a labeled mitotic cell. This cell was in S phase when the culture was flash-labeled but moved to M phase before it was stained and autoradiographed. **B:** Color photomicrograph showing cells labeled and unlabeled with bromodeoxyuridine. Cells were grown in the presence of bromodeoxyuridine and then fixed and stained 20 hours later. Incorporated bromodeoxyuridine stains purple. The purple-stained interphase cell (**upper right**) was in S phase during the time the bromodeoxyuridine was available. Also shown is a first-generation mitotic cell (**upper left**), which had been in S phase at the time the bromodeoxyuridine was available and had moved to M phase by the time it was fixed and stained. It can be identified as first generation because both chromatids of each chromosome are stained uniformly. A second-generation mitotic cell (**lower right**) passed through two S phases during bromodeoxyuridine availability. One chromatid of

each chromosome is darker because both strands of the DNA double helix have incorporated bromodeoxyuridine. One chromatid is lighter because only one strand of the DNA has incorporated bromodeoxyuridine. (Courtesy of Dr. Charles Geard.)

The use of tritiated thymidine to identify cells in the DNA synthetic phase (S) has been replaced largely by the use of 5-bromodeoxyuridine, which differs from thymidine only by the substitution of a bromine atom for a methyl group. If this halogenated pyrimidine is fed to the cells, it is incorporated into DNA in place of thymidine, and its presence can be detected by using an appropriate stain (see [Fig. 4.3B](#)). Cells that have incorporated bromodeoxyuridine appear darkly stained a bright purple color. To identify cells that are in S phase and have incorporated bromodeoxyuridine even more readily, one can use a fluorochrome-tagged antibody against bromodeoxyuridine-substituted DNA, which fluoresces brightly under a fluorescence microscope. Examples of stained and unstained cells are shown in [Figure 4.3B](#). If time is allowed between labeling with bromodeoxyuridine and staining, then a cell may move from S to M phase, and a stained mitotic cell is observed (see [Fig. 4.3B](#)). If the cell is in the first mitosis after bromodeoxyuridine incorporation, both chromatids of each chromosome are equally stained, as shown in the [Figure 4.3B](#) (upper left), but by the second mitosis, one chromatid is stained darker than the other (lower right in [Fig. 4.3B](#))

The use of bromodeoxyuridine has two advantages over conventional autoradiography using tritiated thymidine. First, it does not involve radioactive material. Second, it greatly shortens the time to produce a result because if cells are coated with emulsion to produce an autoradiograph, they must be stored in a refrigerator for about a month to allow β -particles from the incorporated tritium to produce a latent image in the emulsion.

By using either of these techniques, it can be shown that cells synthesize DNA only during a discrete well-defined fraction of the cycle, the S phase. There is an interval between mitosis and DNA synthesis in which no label is incorporated. This first “gap” in activity was named G₁ by Howard and Pelc, and the nomenclature is used today. After DNA synthesis has been completed, there is a second gap before mitosis, G₂.

All proliferating mammalian cells, whether in culture or growing normally in a tissue, have a cycle of mitosis (M), followed by G₁, S, and G₂, after which mitosis occurs again. The relative lengths of these various constituent parts of the cell cycle vary according to the particular cells studied. If cells stop

progressing through the cycle (i.e., are arrested), they are said to be in G₀ (Fig. 4.4).

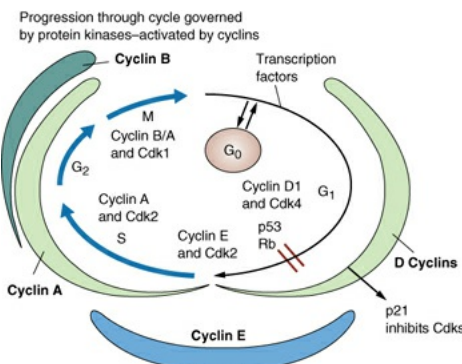


FIGURE 4.4 Update of the phases of the cell cycle, showing how they are regulated by the periodic activation of different members of the cyclin-dependent kinase (Cdk) family. Various Cdk–cyclin complexes are required to phosphorylate several protein substrates, which drive key events, including the initiation of DNA replication and the onset of mitosis.

The characteristics of two cell lines commonly used for *in vitro* culture are summarized in Table 4.1. HeLa cells have a total cell cycle time of about 24 hours, which is more than double that of the Chinese hamster cell, which has a cell cycle time of about 11 hours. Mitosis lasts only a relatively short time, about 1 hour, and is not very different for those two cell lines or for most others. The S phase is 8 hours for HeLa cells and 6 hours for hamster cells; in all cell lines studied in culture or growing *in vivo*, the S phase never exceeds about 15 hours. The G₂ period is very similar in HeLa and hamster cells; in fact, the difference in the total cell cycle time between these two cell lines is accounted for almost entirely by the difference in the length of the G₁ period.

Table 4.1 Phases of the Cell Cycle for Two Commonly Used Cell Lines Cultured *In Vitro*

	HAMSTER CELLS, h	HELA CELLS, h
T _C	11	24
T _M	1	1

T _S	6	8
T _{G1}	1	11
T _{G2}	3	4

This is an important point: The difference among mammalian cell cycle times in different circumstances, varying from about 10 hours for a hamster cell grown in culture to hundreds of hours for stem cells in some self-renewal tissues, is the result of a dramatic variation in the length of the G₁ period. The remaining components of the cell cycle (M, S, and G₂) vary comparatively little among different cells in different circumstances.

The description of the principal phases of the cell cycle (M, G₁, S, and G₂) dates from Howard and Pelc in 1953, as previously discussed. During a complete cell cycle, the cell must accurately replicate the DNA once during S phase and distribute an identical set of chromosomes equally to two progeny cells during M phase. In recent years, we have learned much more about the mechanisms by which the cycle is regulated in eukaryotic cells. Regulation occurs by the periodic activation of different members of the cyclin-dependent kinase (Cdk) family. In its active form, each Cdk is complexed with a particular cyclin. Different Cdk–cyclin complexes are required to phosphorylate several protein substrates that drive such cell cycle events as the initiation of DNA replication or the onset of mitosis. Cdk–cyclin complexes are also vital in preventing the initiation of a cell cycle event at the wrong time.

Extensive regulation of Cdk–cyclin activity by several transcriptional and posttranscriptional mechanisms ensures perfect timing and coordination of cell cycle events. The Cdk catalytic subunit by itself is inactive, requiring association with a cyclin subunit and phosphorylation of a key threonine residue to become fully active. The Cdk–cyclin complex is reversibly inactivated either by phosphorylation on a tyrosine residue located in the adenosine triphosphate–binding domain or by association with Cdk inhibitory proteins. After the completion of the cell cycle transition, the complex is inactivated irreversibly by

ubiquitin-mediated degradation of the cyclin subunit.

Entry into S phase is controlled by Cdks that are sequentially regulated by cyclins D, E, and A. D-type cyclins act as growth factor sensors, with their expression depending more on the extracellular cues than on the cell's position in the cycle. Mitogenic stimulation governs both their synthesis and complex formation with Cdk4 and Cdk6, and catalytic activity of the assembled complexes persists through the cycle as long as mitogenic stimulation continues. Cyclin E expression in proliferating cells is normally periodic and maximal at the G₁/S transition, and throughout this interval, it enters into active complexes with its catalytic partner, Cdk2. [Figure 4.4](#) illustrates this view of the cell cycle and its regulation. This is, in essence, an update of [Figure 4.1](#) and is discussed in more detail in [Chapter 18](#).

SYNCHRONOUSLY DIVIDING CELL CULTURES

In the discussion of survival curves in [Chapter 3](#), the assumption was implicit that the population of irradiated cells was asynchronous; that is, it consisted of cells distributed throughout all phases of the cell cycle. Study of the variation of radiosensitivity with the position or age of the cell in the cell cycle was made possible only by the development of techniques to produce synchronously dividing cell cultures—populations of cells in which all of the cells occupy the same phase of the cell cycle at a given time.

There are essentially two techniques that have been used to produce a synchronously dividing cell population. The first is the **mitotic harvest** technique, first described by Terasima and Tolmach. This technique can be used only for cultures that grow in monolayers attached to the surface of the growth vessel. It exploits the fact that if such cells are close to mitosis, they round up and become loosely attached to the surface. If at this stage the growth medium over the cells is subjected to gentle motion (by shaking), the mitotic cells become detached from the surface and float in the medium. If this medium is then removed from the culture vessel and plated out into new petri dishes, the population consists almost entirely of mitotic cells. Incubation of these cell cultures at 37° C then causes the cells to move together synchronously in step through their mitotic cycles. By delivering a dose of radiation at various times after the initial harvesting of mitotic cells, one can irradiate cells at various phases of the cell cycle.

An alternative method for synchronizing cells, which is applicable to cells in a tissue as well as cells grown in culture, involves the use of a drug. Several

different substances may be used. One of the most widely applicable drugs is hydroxyurea. If this drug is added to a population of dividing cells, it has two effects on the cell population. First, all cells that are synthesizing DNA (S phase) take up the drug and are killed. Second, the drug imposes a block at the end of the G₁ period; cells that occupy the G₂, M, and G₁ compartments when the drug is added progress through the cell cycle and accumulate at this block.

The dynamics of the action of hydroxyurea are illustrated in [Figure 4.5](#). The drug is left in position for a period equal to the combined lengths of G₂, M, and G₁ for that particular cell line. By the end of the treatment period, all of the viable cells left in the population are situated in a narrow “window” at the end of G₁, poised and ready to enter S phase. If the drug is then removed from the system, this synchronized cohort of cells proceeds through the cell cycle. For example, in hamster cells, 5 hours after the removal of the drug, the cohort of synchronized cells occupies a position late in the S phase. Some 9 hours after the removal of the drug, the cohort of cells is at or close to mitosis.

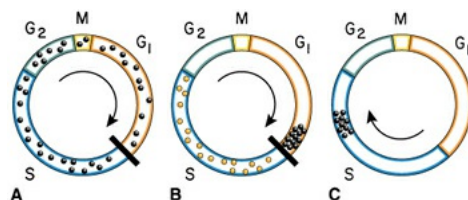


FIGURE 4.5 Mode of action of hydroxyurea as an agent to induce synchrony. **A:** This drug kills cells in S phase and imposes a “block” at the end of the G₁ phase. **B:** Cells in G₂, M, and G₁ accumulate at this block when the drug is added. **C:** If the block is removed, the synchronized cohort of cells moves on through the cycle.

Techniques involving one or another of a wide range of drugs have been used to produce synchronously dividing cell populations in culture, in organized tissues (in a limited number of cases), and even in the whole animal. [Figure 4.6](#) is a photomicrograph of a squash preparation of the root tip of a *Vicia faba* plant seedling 11 hours after synchrony was induced with hydroxyurea. A very large proportion of the cells are in mitosis.

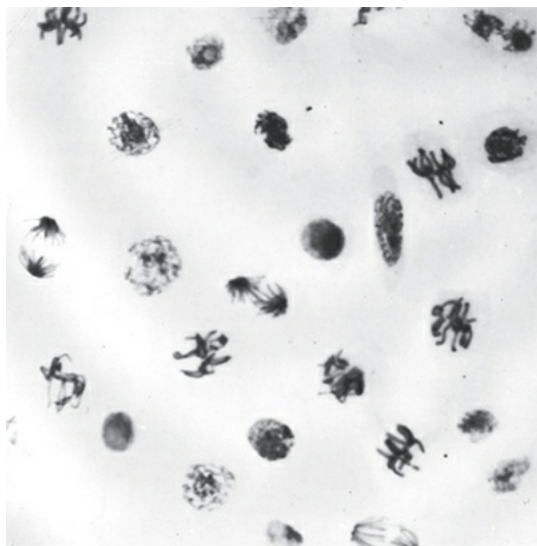


FIGURE 4.6 Photomicrograph of a squash preparation of the root tip of a *Vicia faba* seedling 11 hours after synchrony was induced with hydroxyurea. Note the large proportion of cells in mitosis. (From Hall EJ, Brown JM, Cavanagh J. Radiosensitivity and the oxygen effect measured at different phases of the mitotic cycle using synchronously dividing cells of the root meristem of *Vicia faba*. *Radiat Res.* 1968;35:622–634, with permission.)

THE EFFECT OF X-RAYS ON SYNCHRONOUSLY DIVIDING CELL CULTURES

Figure 4.7 shows results of an experiment in which mammalian cells, which were harvested at mitosis, were irradiated with a single dose of 6.6 Gy at various times afterward, corresponding to different phases of the cell cycle. The data (from Sinclair) were obtained using Chinese hamster cells in culture. As can be seen from the figure, 1 hour after the mitotic cells are seeded into the petri dishes, when the cells are in G₁, a dose of 6.6 Gy results in a surviving fraction of about 13%. The proportion of cells that survive the dose increases rapidly with time as the cells move into S phase; by the time the cells near the end of S phase, 42% of the cells survive this same dose. When the cells move out of S phase into G₂ phase and subsequently to a second mitosis, the proportion of surviving cells falls again. This pattern of response is characteristic for most lines of Chinese hamster cells and has been reported by several independent investigators.

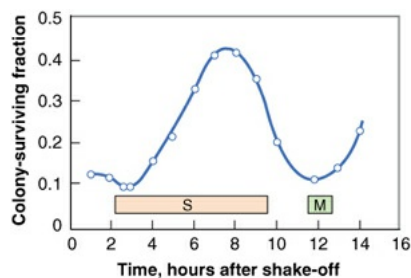


FIGURE 4.7 Fraction of Chinese hamster cells surviving a dose of 6.6 Gy of x-rays as a function of time. Time zero corresponds to the harvesting of mitotic cells. The surviving fraction increases to a maximum late in S phase. (Adapted from Sinclair WK, Morton RA. X-ray sensitivity during the cell generation cycle of cultured Chinese hamster cells. *Radiat Res.* 1966;29:450–474, with permission.)

Complete survival curves at several discrete points during the cell cycle were measured by Sinclair. The results are shown in Figure 4.8. Survival curves are shown for mitotic cells, for cells in G₁ and G₂, and for cells in early and late S phase. It is at once evident that the most sensitive cells are those in M and G₂, which are characterized by a survival curve that is steep and has no shoulder. At the other extreme, cells in the latter part of S phase exhibit a survival curve that is less steep, but the essential difference is that the survival curve has a very broad shoulder. The other phases of the cycle, such as G₁ and early S, are intermediate in sensitivity between the two extremes.

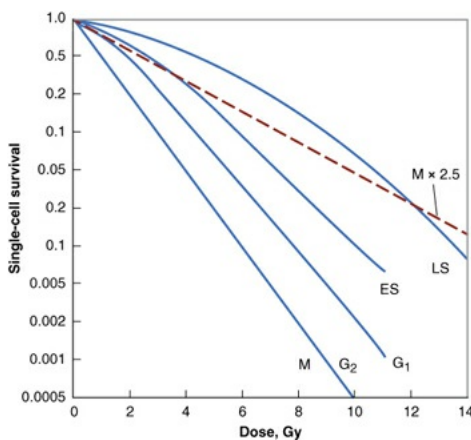


FIGURE 4.8 Cell survival curves for Chinese hamster cells at various stages of the cell cycle. The survival curve for cells in mitosis is steep and has no shoulder. The curve for cells late in S phase is shallower and has a large initial shoulder. G₁ and early S phases are intermediate in sensitivity. The *broken line* is a calculated curve expected to apply to mitotic cells under hypoxia. (Adapted from Sinclair WK. Cyclic x-ray responses in mammalian cells in vitro. *Radiat Res.* 1968;33:620–643, with permission.)

The broken line in [Figure 4.8](#) is the calculated survival curve that would be expected to apply for mitotic cells under conditions of hypoxia; that is, the slope is 2.5 times shallower than the solid line for mitotic cells, which applies to the aerated condition. This line is included in the figure to show that the range of sensitivity between the most sensitive cells (mitotic) and the most resistant cells (late S) is of the same order of magnitude as the oxygen effect (the oxygen effect is discussed in [Chapter 6](#)).

The experiments of Terasima and Tolmach with HeLa cells, in which a dose of 3 Gy was delivered to cultures at various intervals after mitotic harvesting of the cells, are shown in [Figure 4.9](#). From the beginning of S phase onward, the pattern of sensitivity is very similar to that of hamster cells; the cells become progressively more resistant as they proceed toward the latter part of S, and after the cells move from S into G₂, their sensitivity increases rapidly as they approach mitosis. The important difference between HeLa and hamster cells is the length of the G₁ phase. The G₁ of HeLa cells is appreciably long, and there appears to be a fine structure in the age-response function during this period. At the beginning of G₁, there is a peak of resistance, followed by a sensitive trough toward the end of G₁. This pattern cannot be distinguished in the hamster cell because G₁ is too short.

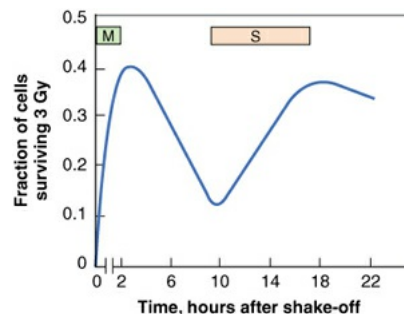


FIGURE 4.9 Fraction of HeLa cells surviving a dose of 3 Gy of x-rays administered at different times in the division cycle. Time zero represents mitosis. (Adapted from Terasima T, Tolmach LJ. Variations in several responses of HeLa cells to x-irradiation during the division cycle. *Biophys J.* 1963;3:11–33, with permission.)

[Figure 4.10](#) compares the age-response curves for cells with short G₁, represented by V79 hamster cells, and cells with a long G₁, represented by HeLa cells. If the time scales are adjusted so that S phase has a comparable length for both cell lines, it is evident that the general pattern of cyclic variation is very similar, the only important difference being the extra structure during G₁ in the

HeLa cells. In later experiments, other sublines of hamster cells were investigated for which G₁ had an appreciable length; an extra peak of resistance was noted for hamster cells that was similar to the one observed for HeLa cells.

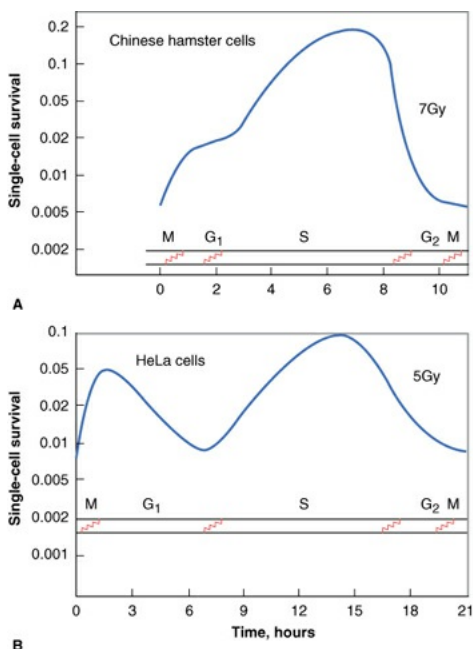


FIGURE 4.10 Age-response curves for cells with short G₁ phase, represented by hamster cells (**A**), and cells with long G₁ phase, represented by HeLa cells (**B**). The time scales have been adjusted so that S phase has a comparable length on the figure for both cell lines. (Adapted from Sinclair WK. Dependence of radiosensitivity upon cell age. In: *Proceedings of the Carmel Conference on Time and Dose Relationships in Radiation Biology as Applied to Radiotherapy*. Upton, NY: Brookhaven National Library; 1969:97–107, Report 50203 (C-57) with permission.)

The sensitivity of cells in different parts of G₂ is difficult to determine if synchrony is produced by mitotic selection because of synchrony decay during the passage of the starting population of mitotic cells through their first G₁ and S phases and because G₂ transit times are relatively short (about 1 to 2 hours). A modification of the technique, however, allows a much greater resolution for studying G₂ sensitivity. This is sometimes called “retroactive synchronization”: Cells first are irradiated, and then, as a function of time, cells arriving in mitosis are harvested by mitotic shake-off and plated for survival. In this way, it was shown that early G₂ cells are as radioresistant as late S cells and late G₂ cells are nearly as sensitive as mitotic cells; that is, a sharp transition in radiosensitivity occurs around the so-called x-ray transition point (now often called a “checkpoint”) for G₂ cell cycle delay.

The following is a summary of the main characteristics of the variation of radiosensitivity with cell age in the mitotic cycle:

1. Cells are most sensitive at or close to mitosis.
2. Resistance is usually greatest in the latter part of S phase. The increased resistance is thought to be caused by homologous recombination repair between sister chromatids that is more likely to occur after the DNA has replicated (see [Chapter 2](#)).
3. If G₁ phase has an appreciable length, a resistant period is evident early in G₁, followed by a sensitive period toward the end of G₁.
4. G₂ phase is usually sensitive, perhaps as sensitive as M phase.

Several cell lines other than HeLa and hamster have been investigated, some of which tend to agree with these results and some of which are contradictory. The summary points listed here are widely applicable, but exceptions to every one of these generalizations have been noted for one cell line or another.

MOLECULAR CHECKPOINT GENES

Cell cycle progression is controlled by a family of genes known as **molecular checkpoint genes**. It has been known for many years that mammalian cells exposed to radiation tend to experience a block in the G₂ phase of the cell cycle. For example, the inverse dose-rate effect has been reported for cells of human origin, whereby over a limited range of dose rates around 0.30 to 0.40 Gy per hour, cells become more sensitive to radiation-induced cell killing as the dose rate is reduced, resulting in their accumulation in G₂, which is a radiosensitive phase of the cell cycle. This is described in [Chapter 5](#). The mechanisms for this observation in human cells are not understood in detail, but the molecular genetics in yeast have been worked out, and the search is on for homologous pathways in mammalian cells.

In several strains of yeast, mutants have been isolated that are more sensitive than the wild type to both ionizing radiation and ultraviolet light by a factor between 10 and 100. The mutant gene has been cloned and sequenced and found to be a “G₂ molecular checkpoint gene.”

In the most general terms, the function of checkpoint genes is to ensure the correct order of cell cycle events, that is, to ensure that the initiation of later events depends on the completion of earlier events. The particular genes

involved in radiation effects halt cells in G₂ so that an inventory of chromosome damage can be taken, and repair is initiated and completed before the complex task of mitosis is attempted (Fig. 4.11). Mutant cells that lose this G₂ checkpoint gene function move directly into mitosis with damaged chromosomes and are, therefore, at a higher risk of dying—hence their greater sensitivity to radiation or, for that matter, to any DNA-damaging agent.

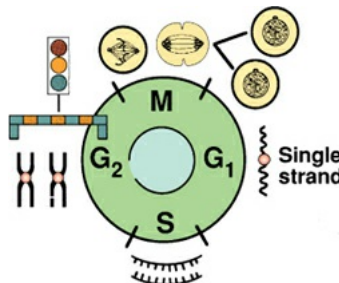


FIGURE 4.11 Diagram illustrating the site of action and function of the molecular checkpoint gene. Cells exposed to any DNA-damaging agent, including ionizing radiation, are arrested in G₂ phase. The function of the pause in cell cycle progression is to allow a check of chromosome integrity before the complex task of mitosis is attempted. Cells in which the checkpoint gene is inactivated are much more sensitive to killing by γ -rays or ultraviolet light. The mutant gene isolated from a sensitive strain of yeast functions as a checkpoint gene.

It has been proposed that a checkpoint control monitors spindle function during mitosis. If the spindle is disrupted by a microtubular poison, progression through mitosis is blocked. The checkpoint control is involved in this dependency of mitosis on spindle function. It is thought that the mechanism of action of G₂ checkpoint genes involves Cdk1 (p34 protein kinase), levels of which control passage through mitosis. It is likely that mammalian cells that lack checkpoint genes would be sensitive not only to radiation-induced cell killing but also to carcinogenesis. Cells with damaged chromosomes that survive mitosis are likely to give rise to errors in chromosome segregation at mitosis, and this is one of the hallmarks of cancer.

THE EFFECT OF OXYGEN AT VARIOUS PHASES OF THE CELL CYCLE

By combining the most sophisticated techniques of flow cytometry to separate cells in different phases of the cycle with the most sensitive assays for cell survival, it has been shown that the **oxygen enhancement ratio (OER)** varies

significantly through the cycle, at least if measured for fast-growing proliferating cells cultured *in vitro*. The OER was measured at 2.3 to 2.4 for G₂ phase cells, compared with 2.8 to 2.9 for S phase, with G₁ phase cells showing an intermediate value. This is discussed in more detail in [Chapter 6](#).

For any given phase of the cell cycle, oxygen was purely dose modifying; that is, the value of the OER was the same for all dose levels. For an asynchronous population of cells, however, the OER does vary slightly with dose or survival level. This is illustrated in [Figure 6.1](#). The OER appears to be smaller at high levels of survival, at which the survival curve is dominated by the killing of the most sensitive moieties of the population; the OER appears to be larger at higher doses and lower levels of survival, at which the response of the most resistant (S phase) cells, which also happen to exhibit the largest OER, dominates.

This is an interesting radiobiologic observation, but the small change of OER is of little or no clinical significance in radiation therapy.

THE AGE-RESPONSE FUNCTION FOR A TISSUE *IN VIVO*

Most studies of the variation in radiosensitivity with phase of the mitotic cycle have been done with mammalian cells cultured *in vitro* because of the ease with which they can be made to divide synchronously. The mitotic harvest technique is clearly only applicable to monolayer cultures, but techniques that involve a drug, such as hydroxyurea, to produce a synchronously dividing population can be applied to some organized tissues.

The epithelial lining of the mouse jejunum represents a classic self-renewal tissue. (The technique used to obtain a survival curve for the crypt cells is described in [Chapter 19](#).) The rapidly dividing crypt cells can be synchronized by giving each mouse five intraperitoneal injections of hydroxyurea every hour. The rationale for this regimen is that all S cells are killed by the drug, and cells in other phases of the cycle are accumulated at the G₁/S boundary for at least 4 hours (the overall time of the five injections).

[Figure 4.12](#), from Withers and his colleagues, shows the response of the jejunal crypt cells to a single dose of 11 Gy of γ -rays (uppermost curve) delivered at various times after the synchronizing action of the five injections of hydroxyurea. The number of crypt cells per circumference of the sectioned jejunum varies by a factor of 100, according to the phase in the cycle at which

the radiation is delivered, ranging from about 2 survivors per circumference for irradiation 2 hours after the last injection of hydroxyurea to about 200 survivors per circumference by 6 hours. The DNA synthetic activity of the synchronized jejunal mucosa was monitored by injecting groups of mice with tritiated thymidine at hourly intervals after the last injection of hydroxyurea and subsequently removing a sample of the jejunum and assaying the radioactive content. The bottom curve of Figure 4.12 shows the variation of thymidine uptake with time. The first wave of the thymidine uptake represents the period of DNA synthesis of the synchronized crypt cells. The peak coincides closely with the period of maximum resistance to x-rays (about 5 hours after the last injection of hydroxyurea).

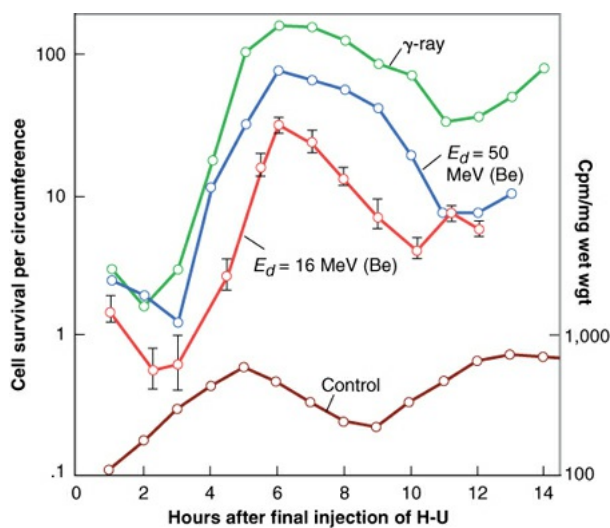


FIGURE 4.12 The upper three curves represent fluctuations in the survival of jejunal crypt cells exposed to γ -rays or neutrons as they pass through the cell cycle after synchronization with hydroxyurea (H-U). The doses were 11 Gy of γ -rays, 7 Gy of neutrons generated by 50 MeV $d^+ \rightarrow Be$, and 6 Gy of neutrons generated by 16 MeV $d^+ \rightarrow Be$. The lower curve represents the uptake of tritiated thymidine (expressed as counts per minute) per wet weight of jejunum as a function of time after the last injection of H-U. The first wave indicates crypt stem cells passing through S phase after synchronization at G₁ to S phase by H-U. (Adapted from Withers HR, Mason K, Reid BO, et al. Response of mouse intestine to neutrons and gamma rays in relation to dose fractionation and division cycle. *Cancer*. 1974;34:39–47, with permission.)

These data indicate clearly that the radiosensitivity of crypt cells in the mouse jejunum varies substantially with the phase of the cell cycle at which the radiation is delivered. Further, the pattern of response in this organized normal tissue, with a sensitive period between G₁ and S and maximum radioresistance

late in S, is very similar to that characteristic of many cell lines cultured *in vitro*.

VARIATION OF SENSITIVITY WITH CELL AGE FOR HIGH-LINEAR ENERGY TRANSFER RADIATIONS

Figure 4.12 compares the fluctuations in survival of jejunal crypt cells in the mouse after irradiation with γ -rays or neutrons. The variation in radiosensitivity as a function of cell age is qualitatively similar for neutrons and x-rays; that is, with both types of radiation, maximum sensitivity is noted at or close to mitosis, and maximum resistance is evident late in S phase. There is, however, a quantitative difference in that the range of radiosensitivity between the most resistant and the most sensitive phases of the cell cycle is much less for fast neutrons than for x-rays. As linear energy transfer (LET) increases, the variation in radiosensitivity through the cell cycle decreases so that at very high LET, the age-response function is almost flat—that is, radiosensitivity varies little with the phase of the cell cycle.

MECHANISMS FOR THE AGE-RESPONSE FUNCTION

The reasons for radiosensitivity changes through the cell cycle are not fully understood. The most likely correlation involves the mechanism of DNA repair. DNA double-strand break (DSB) repair occurs either by homologous recombination or by nonhomologous end-joining. In the early part of the cycle, before replication has occurred, DSBs must be repaired by nonhomologous end-joining because no template exists to guide gap filling. This process is error prone. On the other hand, in S phase after replication, DSBs can be repaired by homologous recombination because a template is available (i.e., an identical sister chromatid is available). This process is less likely to result in errors. Radiosensitivity correlates with error-prone nonhomologous end-joining of DSBs; radioresistance correlates with homologous recombination of DSBs, which is likely to be more faithful. For a description of homologous and nonhomologous repair, see [Chapter 2](#).

THE POSSIBLE IMPLICATIONS OF THE AGE-RESPONSE FUNCTION IN RADIOTHERAPY

If a single dose of radiation is delivered to a population of cells that are asynchronous—that is, distributed throughout the cell cycle—the effect is different on cells occupying different phases of the cell cycle at the time of the radiation exposure. A greater proportion of cells are killed in the sensitive

portions of the cell cycle, such as those at or close to mitosis; a smaller proportion of those in the DNA synthetic phase are killed. The overall effect is that a dose of radiation, to some extent, tends to synchronize the cell population, leaving most cells in a resistant phase of the cycle. Between dose fractions, movement of cells through the cycle into more sensitive phases may be an important factor in “sensitizing” a cycling population of tumor cells to later doses in fractionated regimen. This is considered sensitization resulting from reassortment. It results in a therapeutic gain because sensitization by this mechanism occurs only in rapidly dividing cells and not in late-responding normal tissues.

SUMMARY OF PERTINENT CONCLUSIONS

The cell cycle for mammalian cells can be divided into four phases: mitosis (M), followed by G₁, followed by the DNA synthetic phase (S), then G₂, and into mitosis again.

The phases of the cycle are regulated by the periodic activation of different members of the Cdk family.

The fastest cycling mammalian cells in culture, as well as crypt cells in the intestinal epithelium, have cycle times as short as 9 to 10 hours. Stem cells in resting mouse skin may have cycle times of more than 200 hours. Most of this difference results from the varying length of G₁, the most variable phase of the cycle. The M, S, and G₂ phases do not vary much.

In general, cells are most radiosensitive in the M and G₂ phases and most resistant in late S phase.

For cells with longer cell cycle times and significantly long G₁ phases, there is a second peak of resistance early in G₁.

Molecular checkpoint genes stop cells from cycling if exposed to x-rays or any other DNA-damaging agent, allowing the chromosomes to be checked for integrity before the complex task of mitosis is attempted.

The OER varies little with phase of the cell cycle but may be slightly lower for cells in G₁ than for cells in S.

The age-response function for crypt cells in the mouse jejunum is similar to that for cells in culture. This is the only tissue in which this has been studied.

The age-response function for neutrons is qualitatively similar to that for x-

rays, but the magnitude of changes through the cycle is smaller.

The patterns of radiosensitivity and radioresistance correlate with the mechanism of repair of DNA DSBs. Radiosensitivity correlates with nonhomologous end-joining, which dominates early in the cell cycle and is error prone. Radioresistance correlates with homologous recombinational repair, which occurs after replication (in S phase) and is more faithful.

Variations in sensitivity through the cell cycle may be important in radiation therapy because they lead to “sensitization resulting from reassortment” in a fractionated regimen.

BIBLIOGRAPHY

- Dewey WC, Highfield DP. G₂ block in Chinese hamster cells induced by x-irradiation, hyperthermia, cycloheximide, or actinomycin-D. *Radiat Res.* 1976;65:511–528.
- Dolbeare F, Beisker W, Pallavicini M, et al. Cytochemistry for bromodeoxyuridine/DNA analysis: stoichiometry and sensitivity. *Cytometry*. 1985;6:521–530.
- Dolbeare F, Gratzner H, Pallavicini M, et al. Flow cytometric measurement of total DNA content and incorporated bromodeoxyuridine. *Proc Natl Acad Sci USA*. 1983;80:5573–5577.
- Freyer JP, Jarrett K, Carpenter S, et al. Oxygen enhancement ratio as a function of dose and cell cycle phase for radiation-resistant and sensitive CHO cells. *Radiat Res.* 1991;127:297–307.
- Gray JW. Quantitative cytokinetics: cellular response to cell cycle specific agents. *Pharmacol Ther.* 1983;22:163–197.
- Gray JW, Dolbeare F, Pallavicini MG, et al. Cell cycle analysis using flow cytometry. *Int J Radiat Biol Relat Stud Phys Chem Med.* 1986;49:237–255.
- Griffith TD, Tolmach LJ. Lethal response of HeLa cells to x-irradiation in the latter part of the generation cycle. *Biophys J.* 1976;16:303–318.
- Hall EJ. Radiobiological measurements with 14 MeV neutrons. *Br J Radiol.* 1969;42:805–813.
- Hall EJ, Brown JM, Cavanagh J. Radiosensitivity and the oxygen effect measured at different phases of the mitotic cycle using synchronously dividing cells of the root meristem of *Vicia faba*. *Radiat Res.* 1968;35:622–

634.

- Hartwell LH, Weinert TA. Checkpoints: controls that ensure the order of cell cycle events. *Science*. 1989;246:629–634.
- Hoshino T, Nagashima T, Murovic J, et al. Cell kinetic studies of in situ human brain tumors with bromodeoxyuridine. *Cytometry*. 1985;6:627–632.
- Howard A, Pelc SR. Synthesis of deoxyribonucleic acid in normal and irradiated cells and its relation to chromosome breakage. *Heredity*. 1953;6(suppl):261–273.
- Hoyt MA, Totis L, Roberts BT. *S. cerevisiae* genes required for cell cycle arrest in response to loss of microtubule function. *Cell*. 1991;66:507–517.
- Legrys GA, Hall EJ. The oxygen effect and x-ray sensitivity in synchronously dividing cultures of Chinese hamster cells. *Radiat Res*. 1969;37:161–172.
- Li R, Murray AW. Feedback control of mitosis in budding yeast. *Cell*. 1991;66:519–531.
- Lieberman HB, Hopkins KM, Laverty M, et al. Molecular cloning and analysis of *Schizosaccharomyces pombe rad 9*, a gene involved in DNA repair and mutagenesis. *Mol Gen Genet*. 1992;232:367–376.
- Morstyn G, Hsu SM, Kinsella T, et al. Bromodeoxyuridine in tumors and chromosomes detected with a monoclonal antibody. *J Clin Invest*. 1983;72:1844–1850.
- Schneiderman MH, Dewey WC, Leeper DB, et al. Use of the mitotic selection procedure for cell cycle analysis. Comparison between the x-ray and G₂ markers. *Exp Cell Res*. 1972;74:430–438.
- Sinclair WK. Cyclic x-ray responses in mammalian cells in vitro. *Radiat Res*. 1968;33:620–643.
- Sinclair WK. Dependence of radiosensitivity upon cell age. In: *Proceedings of the Carmel Conference on Time and Dose Relationships in Radiation Biology as Applied to Radiotherapy*. Upton, NY: Brookhaven National Laboratory;1969:97–107. Report 50203 (C-57).
- Sinclair WK. Radiation survival in synchronous and asynchronous Chinese hamster cells in vitro. In: *Biophysical Aspects of Radiation Quality: Proceedings of the Second International Atomic Energy Agency Panel*. Vienna, Austria: International Atomic Energy Agency; 1968:39–54.

- Sinclair WK, Morton RA. X-ray sensitivity during the cell generation cycle of cultured Chinese hamster cells. *Radiat Res.* 1966;29:450–474.
- Steel G, Hanes S. The technique of labelled mitoses: analysis by automatic curve-fitting. *Cell Tissue Kinet.* 1971;4:93–105.
- Terasima T, Tolmach LJ. Variations in several responses of HeLa cells to x-irradiation during the division cycle. *Biophys J.* 1963;3:11–33.
- Terasima T, Tolmach LJ. X-ray sensitivity and DNA synthesis in synchronous populations of HeLa cells. *Science.* 1963;140:490–492.
- Withers HR, Mason K, Reid BO, et al. Response of mouse intestine to neutrons and gamma rays in relation to dose fractionation and division cycle. *Cancer.* 1974;34:39–47.

chapter 5

Fractionated Radiation and the Dose-Rate Effect

Operational Classifications of Radiation Damage

Potentially Lethal Damage Repair

Sublethal Damage Repair

Mechanism of Sublethal Damage Repair

Repair and Radiation Quality

The Dose-Rate Effect

Examples of the Dose-Rate Effect *In Vitro* and *In Vivo*

The Inverse Dose-Rate Effect

The Dose-Rate Effect Summarized

Brachytherapy or Endocurietherapy

Intracavitory Brachytherapy

Permanent Interstitial Implants

Summary of Pertinent Conclusions

Potentially Lethal Damage Repair

Sublethal Damage Repair

Dose-Rate Effect

Brachytherapy

Bibliography

OPERATIONAL CLASSIFICATIONS OF RADIATION DAMAGE

Radiation damage to mammalian cells can operationally be divided into three categories: (1) **lethal damage**, which is irreversible and irreparable and, by definition, leads irrevocably to cell death; (2) **potentially lethal damage (PLD)**,

the component of radiation damage that can be modified by postirradiation environmental conditions; and (3) **sublethal damage (SLD)**, which, under normal circumstances, can be repaired in hours unless additional SLD is added (e.g., from a second dose of radiation) with which it can interact to form lethal damage (SLD repair, therefore, is manifested by the increase in survival observed if a dose of radiation is split into two fractions separated by a time interval).

Potentially Lethal Damage Repair

Varying environmental conditions after exposure to x-rays can influence the proportion of cells that survive a given dose because of the expression or repair of PLD. This damage is potentially lethal because under ordinary circumstances, it causes cell death, but if survival is increased as a result of the manipulation of the postirradiation environment, PLD is considered to have been repaired. PLD is repaired if cells are incubated in a balanced salt solution instead of a full growth medium for several hours after irradiation. This is a drastic treatment, however, and does not mimic a physiologic condition that is ever likely to occur. Little and his colleagues chose to study PLD repair in density-inhibited stationary-phase cell cultures, which are considered a better *in vitro* model for tumor cells *in vivo* (Fig. 5.1). Cell survival was enhanced considerably if the cells were allowed to remain in the density-inhibited state for 6 or 12 hours after irradiation before being subcultured and assayed for colony-forming ability.

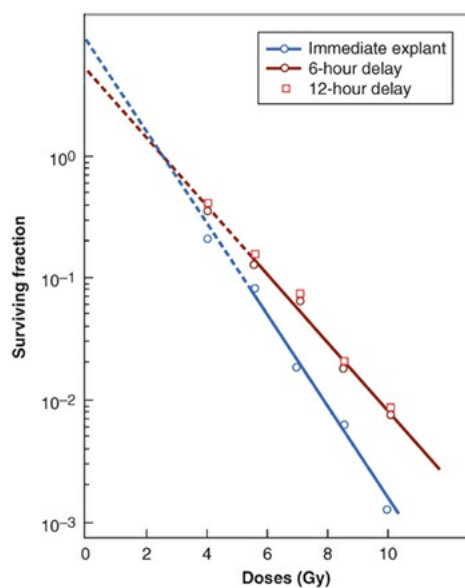


FIGURE 5.1 X-ray survival curves for density-inhibited stationary-phase cells, subcultured (trypsinized and plated) either immediately or 6 or 12 hours after irradiation. Cell survival is enhanced if cells are left in the stationary phase after

irradiation, allowing time for the repair of PLD. (Adapted from Little JB, Hahn GM, Frindel E, et al. Repair of potentially lethal radiation damage in vitro and in vivo. *Radiology*. 1973;106:689–694, with permission.)

The relevance of PLD to radiotherapy became much more obvious when it was shown that repair, comparable in magnitude and kinetics to that found *in vitro*, also occurred *in vivo* in experimental tumors. In this case, repair took the form of significantly enhanced cell survival if several hours were allowed to elapse between irradiation of the tumor *in situ* and removal of the cells from the host to assess their reproductive integrity (Fig. 5.2).

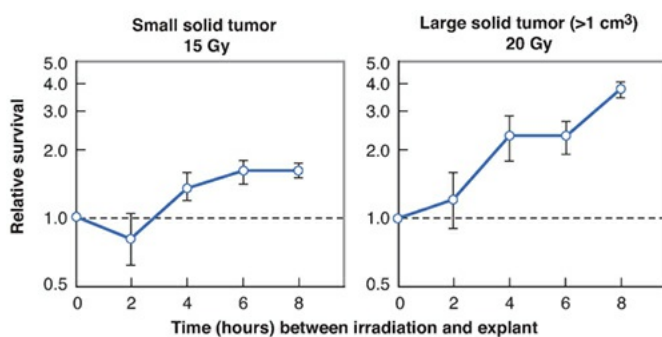


FIGURE 5.2 Repair of potentially lethal damage in mouse fibrosarcomas. The tumors were irradiated *in situ* and then removed and prepared into single cell suspensions. The number of survivors was determined by their ability to form colonies *in vitro*. The fraction of cells surviving a given dose increases if a time interval is allowed between irradiation and removal of the tumor because during this interval, PLD is repaired. (Adapted from Little JB, Hahn GM, Frindel E, et al. Repair of potentially lethal radiation damage in vitro and in vivo. *Radiology*. 1973;106:689–694, with permission.)

To summarize the available experimental data, there is a general agreement that PLD is repaired, and the fraction of cells surviving a given dose of x-rays is enhanced if postirradiation conditions are suboptimal for growth, so that cells do not have to attempt the complex process of mitosis while their chromosomes are damaged. If mitosis is delayed by suboptimal growth conditions, DNA damage can be repaired.

The importance of PLD repair to clinical radiotherapy is a matter of debate. That it occurs in transplantable animal tumors has been documented beyond question, and there is no reason to suppose that it does not occur in human tumors. It has been suggested that the radioresistance of certain types of human tumors is linked to their ability to repair PLD; that is, radiosensitive tumors repair PLD inefficiently, but radioresistant tumors have efficient mechanisms to repair PLD. This is an attractive hypothesis, but it has never been proven.

Sublethal Damage Repair

SLD repair is the operational term for the increase in cell survival that is observed if a given radiation dose is split into two fractions separated by a time interval.

Figure 5.3 shows data obtained in a split-dose experiment with cultured Chinese hamster cells. A single dose of 15.58 Gy of absorbed radiation leads to a surviving fraction of 0.005. If the dose is divided into two approximately equal fractions separated by 30 minutes, the surviving fraction is already appreciably higher than for a single dose. As the time interval is extended, the surviving fraction increases until a plateau is reached at about 2 hours, corresponding to a surviving fraction of 0.02. This represents about 4 times as many surviving cells as for the dose given in a single exposure. A further increase in the time interval between the dose fractions is not accompanied by any significant additional increment in survival. The increase in survival in a split-dose experiment results from the repair of sublethal radiation damage.

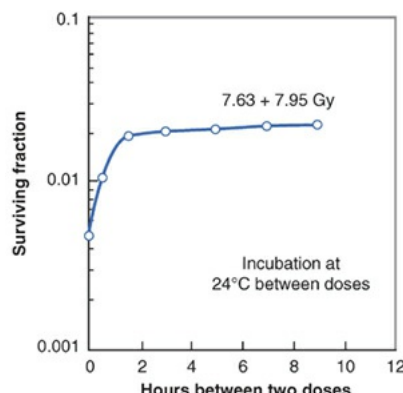


FIGURE 5.3 Survival of Chinese hamster cells exposed to two fractions of x-rays and incubated at room temperature for various time intervals between the two exposures. (Adapted from Elkind MM, Sutton-Gilbert H, Moses WB, et al. Radiation response of mammalian cells grown in culture. V. Temperature dependence of the repair of x-ray damage in surviving cells [aerobic and hypoxic]. *Radiat Res.* 1965;25:359–376, with permission.)

The data shown in Figure 5.3 were obtained with cultured mammalian cells maintained at room temperature (24° C) between the dose fractions to prevent the cells from moving through the cell cycle during this interval. This rather special experiment is described first because it illustrates repair of sublethal radiation damage uncomplicated by the movement of cells through the cell cycle.

Figure 5.4 shows the results of a parallel experiment in which cells were exposed to split doses and maintained at their normal growing temperature of

37° C . The pattern of repair seen in this case differs from that observed for cells kept at room temperature. In the first few hours, prompt repair of SLD is again evident, but at longer intervals between the two split doses, the surviving fraction of cells decreases, reaching a minimum with about a 5-hour separation.

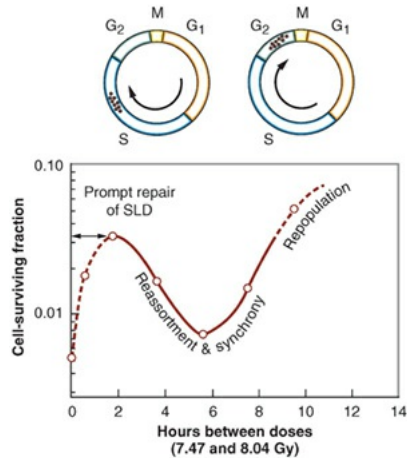


FIGURE 5.4 Survival of Chinese hamster cells exposed to two fractions of x-rays and incubated at 37° C for various time intervals between the two doses. The survivors of the first dose are predominantly in a resistant phase of the cycle (late S). If the interval between doses is about 6 hours, these resistant cells have moved to the G₂M phase, which is sensitive. (Adapted from Elkind MM, Sutton-Gilbert H, Moses WB, et al. Radiation response of mammalian cells in culture. V. Temperature dependence of the repair of x-ray damage in surviving cells [aerobic and hypoxic]. *Radiat Res.* 1965;25:359–376, with permission.)

An understanding of this phenomenon is based on the age-response function described in [Chapter 4](#). If an asynchronous population of cells is exposed to a large dose of radiation, more cells are killed in the sensitive than in the resistant phases of the cell cycle. The surviving population of cells, therefore, tends to be partly synchronized.

In Chinese hamster cells, most of the survivors from a first dose of radiation are located in the S phase of the cell cycle. If about 6 hours are allowed to elapse before a second dose of radiation is given, this cohort of cells progresses around the cell cycle and is in G₂/M, a sensitive period of the cell cycle at the time of the second dose. If the increase in radiosensitivity in moving from late S to the G₂/M period exceeds the effect of repair of SLD, the surviving fraction falls.

The pattern of repair shown in [Figure 5.4](#) is therefore a combination of three processes occurring simultaneously. First, there is the prompt repair of sublethal radiation damage. Second, there is progression of cells through the cell cycle during the interval between the split doses, which has been termed

reassortment. Third, there is an increase of surviving fraction resulting from cell division, or **repopulation**, if the interval between the split doses is from 10 to 12 hours because this exceeds the length of the cell cycle of these rapidly growing cells.

This simple experiment, performed *in vitro*, illustrates three of the “four Rs” of radiobiology: **repair**, **reassortment**, and **repopulation**. The fourth “R,” **reoxygenation**, is discussed in [Chapter 6](#). It should be emphasized that the dramatic dip in the split-dose curve at 6 hours caused by reassortment, and the increase in survival by 12 hours because of repopulation are seen only for rapidly growing cells. Hamster cells in culture have a cycle time of only 9 or 10 hours. The time sequence of these events would be longer in more slowly proliferating normal tissues *in vivo*.

Repair of sublethal radiation damage has been demonstrated in just about every biologic test system for which a quantitative end point is available. [Figure 5.5](#) illustrates the pattern for repair of sublethal radiation damage in two *in vivo* systems in mice, P388 lymphocytic leukemia and skin cells. In neither case, is there a dramatic dip in the curve at 6 hours resulting from movement of cells through the cycle because the cell cycle is long. In resting skin, for example, the cell cycle of stem cells may be as long as 10 days rather than 9 hours of the rapidly growing cells in [Figure 5.4](#). The mouse tumor data show more repair in small 1-day tumors than in large hypoxic 6-day tumors; this important point illustrates that repair is an active process requiring oxygen and nutrients.

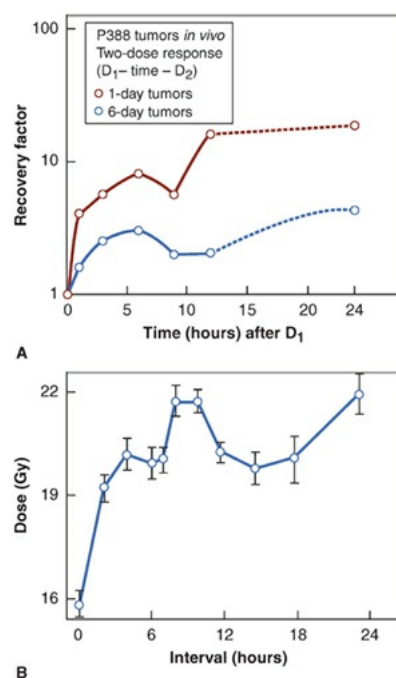


FIGURE 5.5 Repair of sublethal damage in two *in vivo* mammalian cell

systems. **A:** Split-dose experiments with P388 lymphocytic leukemia cells in the mouse. The recovery factor is the ratio of the surviving fraction resulting from two-dose fractionation to the survival from a single equivalent dose. One-day-old tumors are composed predominantly of oxygenated cells; the cells in 6-day-old tumors are hypoxic. (Adapted from Belli JA, Dicus GJ, Bonte FJ. Radiation response of mammalian tumor cells. I. Repair of sublethal damage in vivo. *J Natl Cancer Inst.* 1967;38:673–682, with permission.) **B:** Split-dose experiments with skin epithelial cells in the mouse. The total x-ray dose, given as two fractions, required to result in one surviving epithelial cell per square millimeter is plotted against the time interval between the two doses. (Adapted from Emery EW, Denekamp J, Ball MM, et al. Survival of mouse skin epithelial cells following single and divided doses of x-rays. *Radiat Res.* 1970;41:450–466, with permission.)

The various factors involved in the repair of SLD are summarized in [Figure 5.6](#). [Figure 5.6A](#) shows that if a dose is split into two fractions separated by a time interval, more cells survive than for the same total dose given in a single fraction because the shoulder of the curve must be repeated with each fraction. In general, there is a good correlation between the extent of repair of SLD and the size of the shoulder of the survival curve. This is not surprising because both are manifestations of the same basic phenomenon: the accumulation and repair of SLD. Some mammalian cells are characterized by a survival curve with a broad shoulder, and split-dose experiments then indicate a substantial amount of SLD repair. Other types of cells show a survival curve with a minimal shoulder, and this is reflected in more limited repair of SLD. In the terminology of the linear-quadratic (α/β) description of the survival curve, it is the quadratic component (β) that causes the curve to bend and that results in the sparing effect of a split dose. A large shoulder corresponds to a small α/β ratio.

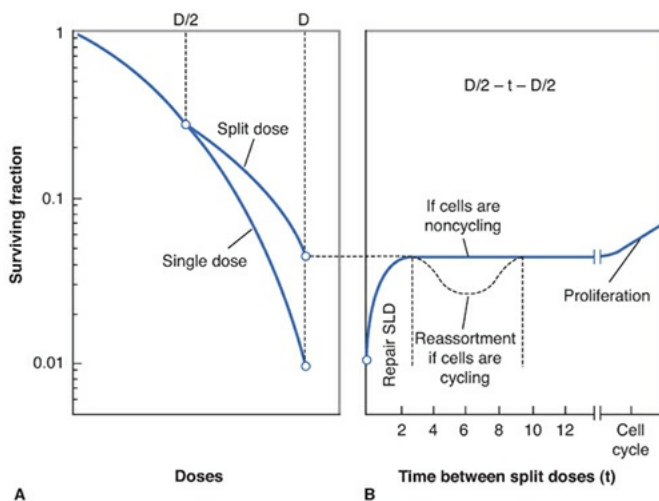


FIGURE 5.6 Summary of the repair of sublethal damage (SLD) as evidenced by a split-dose experiment. **A:** If the dose is delivered in two fractions separated by a time interval, there is an increase in cell survival because the shoulder of the curve must be expressed each time. **B:** The fraction of cells surviving a split dose increases as the time interval between the two dose fractions increases. As the time interval increases from 0 to 2 hours, the increase in survival results from the repair of SLD. In cells with a long cell cycle or that are out of cycle, there is no further increase in cell survival by separating the dose by more than 2 or 3 hours. In a rapidly dividing cell population, there is a dip in cell survival caused by reassortment. However, as shown in [Figure 5.4](#), if the time interval between the split doses exceeds the cell cycle, there is an increase in cell survival owing to proliferation or repopulation between the doses.

The time course of the increase in cell survival that results from the repair of SLD is charted in [Figure 5.6B](#). As the time interval between the two dose fractions is increased, there is a rapid increase in the fraction of cells surviving owing to the prompt repair of SLD. This repair is complete by 1 or 2 hours for cells in culture but may take longer for late-responding tissues *in vivo* (see [Chapter 23](#)). As the time interval between the two dose fractions is increased, there is a dip in the curve owing to the movement of surviving cells through the cell cycle, as explained in [Figure 5.4](#). This occurs only in a population of fast-cycling cells. In cells that are noncycling, there can be no dip. If the time interval between the two dose fractions exceeds the cell cycle, there is an increase in the number of cells surviving because of cell proliferation; that is, cells can double in number between the dose fractions.

MECHANISM OF SUBLETHAL DAMAGE REPAIR

In [Chapter 3](#), evidence was summarized of the correlation between cell killing and the production of asymmetric chromosomal aberrations, such as dicentrics and rings. This, in turn, is a consequence of an interaction between two (or more) double-strand breaks in the DNA. Based on this interpretation, the repair of SLD is simply the repair of double-strand breaks. If a dose is split into two parts separated by a time interval, some of the double-strand breaks produced by the first dose are rejoined and repaired before the second dose. The breaks in two chromosomes that must interact to form a lethal lesion such as a dicentric may be formed by (1) a single track breaking both chromosomes (i.e., single-track damage) or (2) separate tracks breaking the two chromosomes (i.e., multiple-track damage).

The component of cell killing that results from single-track damage is the same whether the dose is given in a single exposure or fractionated. The same is not true of multiple-track damage. If the dose is given in a single exposure (i.e., two fractions with $t = 0$ between them), all breaks produced by separate electrons can interact to form dicentrics. But if the two dose fractions ($D/2$) are separated by, for example, 3 hours, then breaks produced by the first dose may be repaired before the second dose is given. Consequently, there are fewer interactions between broken chromosomes to form dicentrics, and more cells survive. Based on this simple interpretation, the repair of SLD reflects the repair and rejoining of double-strand breaks before they can interact to form lethal lesions. This may not be the whole story, but it is a useful picture to keep in mind.

REPAIR AND RADIATION QUALITY

For a given biologic test system, the shoulder on the acute survival curve and, therefore, the amount of SLD repair indicated by a split-dose experiment vary with the type of radiation used. The effect of dose fractionation with x-rays and neutrons is compared in [Figure 5.7](#). For x-rays, dividing the total dose into two equal fractions, separated from 1 to 4 hours, results in a marked increase in cell survival because of the prompt repair of SLD. By contrast, dividing the dose into two fractions has little effect on cell survival if neutrons are used, indicating little repair of SLD.

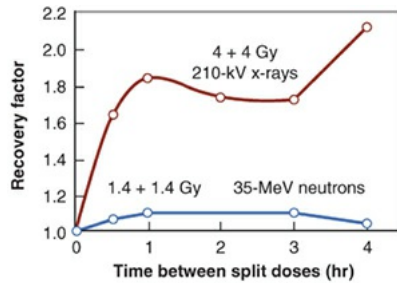


FIGURE 5.7 Split-dose experiments with Chinese hamster cells. For 210-kV x-rays, two 4-Gy doses, separated by a variable interval, were compared with a single dose of 8 Gy. For neutrons ($35\text{-MeV } d^+ \rightarrow Be$), two 1.4-Gy doses were compared with a single exposure of 2.8 Gy. The data are plotted in terms of the recovery factor, defined as the ratio of surviving fractions for a given dose delivered as two fractions compared with a single exposure. It is evident that repair of SLD during the interval between split doses is virtually nonexistent for neutrons but is a significant factor for x-rays. (Adapted from Hall EJ, Roizin-Towie L, Theus RB, et al. Radiobiological properties of high-energy cyclotron-produced neutrons used for radiotherapy. *Radiology*. 1975;117:173–178, with permission.)

permission.)

THE DOSE-RATE EFFECT

For x- or γ -rays, dose rate is one of the principal factors that determine the biologic consequences of a given absorbed dose. As the dose rate is lowered and the exposure time extended, the biologic effect of a given dose generally is reduced.

The classic dose-rate effect, which is very important in radiotherapy, results from the repair of SLD that occurs during a long radiation exposure. To illustrate this principle, [Figure 5.8](#) shows an idealized experiment in which each dose (D_2 , D_3 , D_4 , etc.) is delivered in several equal fractions of size D , with a time interval between fractions that is sufficient for repair of SLD. The shoulder of the survival curve is repeated with each fraction. The blue line, F , shows the overall survival curve that would be observed if only single points were determined, corresponding to equal dose increments. This survival curve has no shoulder. Because continuous low-dose-rate (LDR) irradiation may be considered to be an infinite number of infinitely small fractions, the survival curve under these conditions also would be expected to have no shoulder and to be shallower than for single acute exposures.

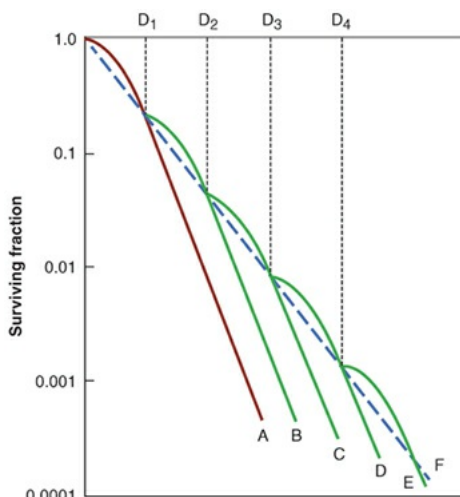


FIGURE 5.8 Idealized fractionation experiment. Curve A is the survival curve for single acute exposures of x-rays. Curve F is obtained if each dose is given as a series of small fractions of size D_1 with an interval between fractions sufficient for repair of SLD. Multiple small fractions approximate to a continuous exposure to an LDR. (Adapted from Elkind MM, Whitmore GF. *Radiobiology of Cultured Mammalian Cells*. New York, NY: Gordon and Breach; 1967, with permission.)

EXAMPLES OF THE DOSE-RATE EFFECT IN VITRO AND IN VIVO

Survival curves for HeLa cells cultured *in vitro* over a wide range of dose rates, from 7.3 Gy per minute to 0.535 cGy per minute, are summarized in Figure 5.9. As the dose rate is reduced, the survival curve becomes shallower and the shoulder tends to disappear (i.e., the survival curve becomes an exponential function of dose). The dose-rate effect caused by repair of SLD is most dramatic between 0.01 and 1 Gy per minute. Above and below this dose-rate range, the survival curve changes little, if at all, with dose rate.

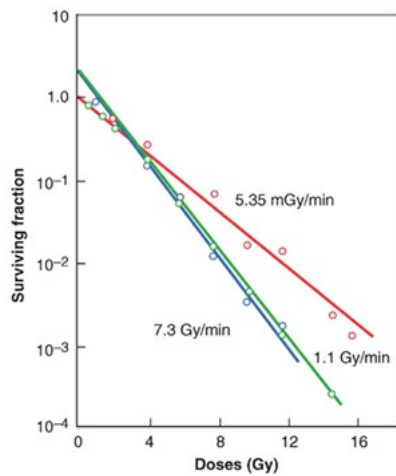


FIGURE 5.9 Survival curves for HeLa cells cultured *in vitro* and exposed to γ -rays at high and low dose rates.

The magnitude of the dose-rate effect from the repair of SLD varies enormously among different types of cells. HeLa cells are characterized by a survival curve for acute exposures that has a small initial shoulder, which goes hand in hand with a modest dose-rate effect. This is to be expected because both are expressions of the cell's capacity to accumulate and repair sublethal radiation damage. By contrast, Chinese hamster cells have a broad shoulder to their acute x-ray survival curve and show a correspondingly large dose-rate effect. This is evident in Figure 5.10; there is a clear-cut difference in biologic effect, at least at high doses, between dose rates of 1.07, 0.30, and 0.16 Gy per minute. The differences between HeLa and hamster cells in the size of the shoulder to the acute survival curve and the magnitude of the dose-rate effect reflect differences in the importance of apoptosis. In the case of HeLa cells, apoptosis is an important form of cell death following radiation, whereas for hamster cells, apoptotic death is rarely seen.

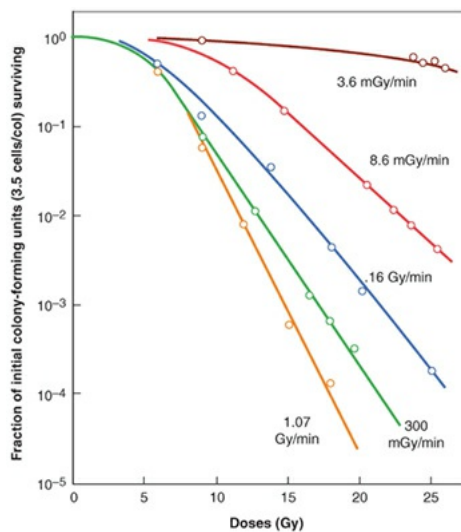


FIGURE 5.10 Dose–response curves for Chinese hamster cells (CHL-F line) grown *in vitro* and exposed to cobalt-60 γ -rays at various dose rates. At high doses, a substantial dose-rate effect is evident even when comparing dose rates of 1.07, 0.30, and 0.16 Gy per minute. The decrease in cell killing becomes even more dramatic as the dose rate is reduced further. (Adapted from Bedford JS, Mitchell JB. Dose-rate effects in synchronous mammalian cells in culture. *Radiat Res.* 1973;54:316–327, with permission.)

Figure 5.11 shows survival curves for 40 different cell lines of human origin, cultured *in vitro* and irradiated at high dose rates (HDR) and LDRs. At LDR, the survival curves “fan out” and show a greater variation in slope because, in addition to the variation of inherent radiosensitivity evident at an HDR, there is a range of repair times of SLD. Some cell lines repair SLD rapidly, some more slowly, and this is reflected in the different survival curves at LDR.

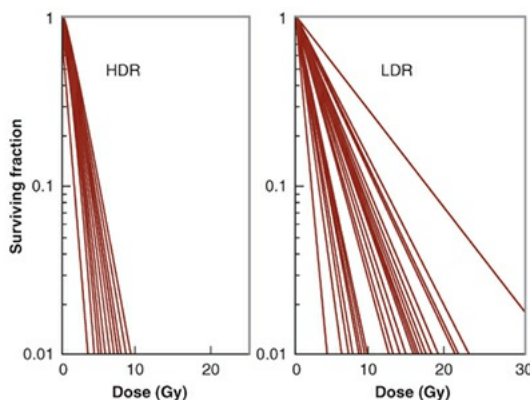


FIGURE 5.11 Dose survival curves at high dose rates (HDR) and low dose rates (LDR) for a large number of cell lines of human origin cultured *in vitro*. Note that the survival curves fan out at LDR because in addition to a range of inherent radiosensitivities (evident at HDR), there is also a range of repair times of SLD.

Survival curves for crypt cells in the mouse jejunum irradiated with γ -rays at various dose rates are shown in Figure 5.12. There is a dramatic dose-rate effect owing to the repair of sublethal radiation damage from an acute exposure at 2.74 Gy per minute to a protracted exposure at 0.92 cGy per minute. As the dose rate is lowered further, cell division begins to dominate the picture because the exposure time is longer than the cell cycle. At 0.54 cGy per minute, there is little reduction in the number of surviving crypts, even for very large doses, because cellular proliferation occurs during the long exposure and makes up for cell killing by the radiation.

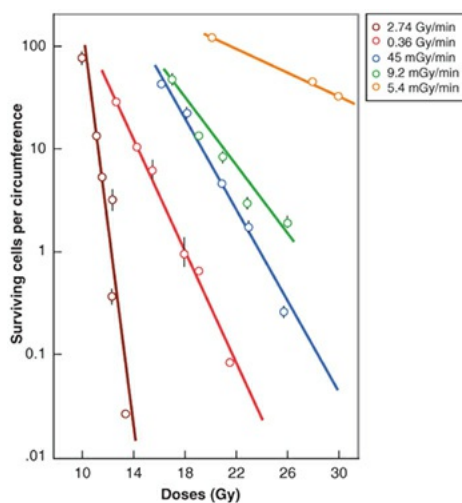


FIGURE 5.12 Response of mouse jejunal crypt cells irradiated with γ -rays from cesium-137 over a wide range of dose rates. The mice were given total body irradiation, and the proportion of surviving crypt cells was determined by the appearance of regenerating microcolonies in the crypts 3 days later. Note the large dose-rate effect. (Adapted from Fu KK, Phillips TL, Kane LJ, et al. Tumor and normal tissue response to irradiation *in vivo*: variation with decreasing dose rates. *Radiology*. 1975;114:709–716, with permission.)

THE INVERSE DOSE-RATE EFFECT

There is at least one example of an inverse dose-rate effect, in which decreasing the dose rate results in increased cell killing. This is illustrated in Figure 5.13. Decreasing the dose rate for this HeLa cell line from 1.54 to 0.37 Gy per hour increases the efficiency of cell killing, such that this LDR is almost as damaging as an acute exposure. The explanation is illustrated in Figure 5.14. At about 0.37 Gy per hour, cells tend to progress through the cycle and become arrested in G₂, a radiosensitive phase of the cycle. At higher dose rates, they are “frozen” in the phase of the cycle they are in at the start of the irradiation; at lower dose rates, they continue to cycle during irradiation.

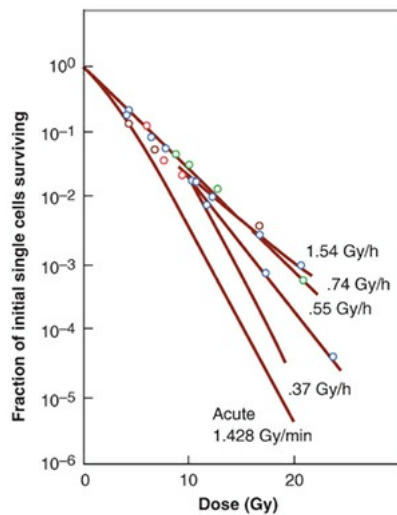


FIGURE 5.13 The inverse dose-rate effect. A range of dose rates can be found for HeLa cells such that lowering the dose rate leads to more cell killing. At 1.54 Gy per hour, cells are “frozen” in the various phases of the cycle and do not progress. As the dose rate is dropped to 0.37 Gy per hour, cells progress to a block in G₂, a radiosensitive phase of the cycle. (Adapted from Mitchell JB, Bedford JS, Bailey SM. Dose-rate effects on the cell cycle and survival of S3 HeLa and V79 cells. *Radiat Res.* 1979;79:520–536, with permission.)

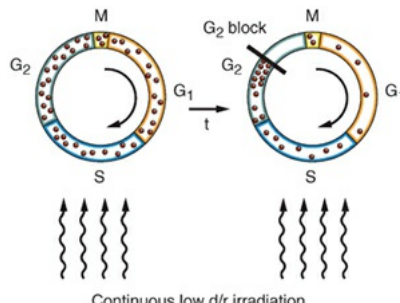


FIGURE 5.14 The inverse dose-rate effect. A range of dose rates can be found, at least for HeLa cells, that allows cells to progress through the cycle to a block in late G₂. Under continuous LDR irradiation, an asynchronous population becomes a population of radiosensitive G₂ cells. (Adapted from Hall EJ. The biological basis of endocurietherapy: the Henschke Memorial Lecture 1984. *Endocuriether Hypertherm Oncol.* 1985;1:141–151, with permission.)

THE DOSE-RATE EFFECT SUMMARIZED

Figure 5.15 summarizes the entire dose-rate effect. For acute exposures at HDRs, the survival curve has a significant initial shoulder. As the dose rate is lowered and the treatment time protracted, more and more SLD can be repaired during the exposure. Consequently, the survival curve becomes progressively more

shallow (D_0 increases) and the shoulder tends to disappear. A point is reached at which all SLD is repaired resulting in a limiting slope. In at least some cell lines, a further lowering of the dose rate allows cells to progress through the cycle and accumulate in G_2 . This is a radiosensitive phase and so the survival curve becomes steeper again. This is the inverse dose-rate effect. A further reduction in dose rate allows cells to pass through the G_2 block and divide. Proliferation then may occur during the radiation exposure if the dose rate is low enough and the exposure time is long compared with the length of the mitotic cycle. This may lead to a further reduction in biologic effect as the dose rate is progressively lowered because cell birth tends to offset cell death.

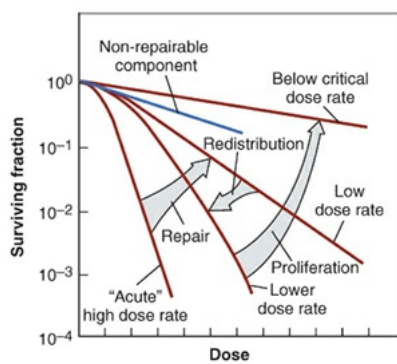


FIGURE 5.15 The dose-rate effect resulting from repair of sublethal damage, redistribution in the cycle, and cell proliferation. The dose-response curve for acute exposures is characterized by a broad initial shoulder. As the dose rate is reduced, the survival curve becomes progressively more shallow as more and more SLD is repaired, but cells are “frozen” in their positions in the cycle and do not progress. As the dose rate is lowered further and for a limited range of dose rates, the survival curve steepens again because cells can progress through the cycle to pile up at a block in G_2 , a radiosensitive phase, but still cannot divide. A further lowering of dose rate below this critical dose rate allows cells to escape the G_2 block and divide; cell proliferation then may occur during the protracted exposure, and survival curves become shallower as cell birth from mitosis offsets cell killing from the irradiation. (Based on the ideas of Dr. Joel Bedford.)

BRACHYTHERAPY OR ENDOCURIETHERAPY

Implanting radioactive sources directly into a tumor was a strategy first suggested by Alexander Graham Bell in 1901. Over the years, various groups in different countries coined various names for this type of therapy, using the prefix *brachy*, from the Greek word for “short range,” or *endo*, from the Greek word for “within.” There are two distinct forms of **brachytherapy**, also called

endocurietherapy: (1) *intracavitary* irradiation, using radioactive sources placed in body cavities in proximity to the tumor, and (2) *interstitial* brachytherapy, using radioactive wires or “seeds” implanted directly into the tumor volume.

Both intracavitary and interstitial techniques were developed to an advanced stage at an early date because the technology was readily available. Radium in sufficient quantities was extracted and purified in the early 1900s, whereas radioactive sources of sufficient activity for **teletherapy** (or external beam radiotherapy) sources of adequate dose rate only came as a spin-off of World War II nuclear technology.

Intracavitary Brachytherapy

Intracavitary brachytherapy at LDR is always temporary and usually takes 1 to 4 days (with a dose rate of about 50 cGy per hour). It can be used for several anatomic sites, but by far, the most common is the uterine cervix. There has been a continual evolution in the radionuclide used; in the early days, radium was used, but this went out of favor because of the safety concern of using an encapsulated source that can leak radioactivity. As an interim measure, cesium-137 was introduced, but today, most treatment centers use iridium-192; its shorter half-life and lower γ -ray energy make for ease of radiation protection, especially in conjunction with a remote afterloader.

To an increasing extent, LDR intracavitary brachytherapy is being replaced by HDR intracavitary therapy, delivered in 3 to 12 dose fractions. Replacing continuous LDR therapy with a few large-dose fractions gives up much of the radiobiologic advantage and the sparing of late-responding normal tissues, as described in [Chapter 23](#). It is only possible because the treatment of carcinoma of the cervix is a special case in which the dose-limiting normal tissues (e.g., bladder, rectum) receive a lower dose than the prescribed dose to the tumor (or to point A). For HDR treatments lasting a few minutes, it is possible to use retractors that result in even lower doses to the critical normal tissues than are possible with an insertion that lasts 24 hours or more. These physical advantages offset the radiobiologic disadvantages so that the general principle that administration of a few large fractions at an HDR gives poorer results than at an LDR does not apply to this special case.

Permanent Interstitial Implants

Encapsulated sources with relatively short half-lives can be left in place

permanently. There are two advantages for the patient: (1) An operation to remove the implant is not needed, and (2) the patient can go home with the implant in place. On the other hand, this does involve additional expense because the sources are not reused. The initial dose rate is high and falls off as the implanted sources decay. Iodine-125 has been used most widely to date for permanent implants. The total prescribed dose is usually about 160 Gy at the periphery of the implanted volume, with 80 Gy delivered in the first half-life of 60 days. The soft emission from iodine has a relative biologic effectiveness (explained in [Chapter 7](#)) of about 1.5; this corresponds to 80×1.5 or 120 Gy of high-energy γ -rays. This is a big dose, even at an LDR, and corresponds to a good level of cell kill. It is, however, spread over 60 days; consequently, the success of the implant in sterilizing the tumor depends critically on the cell cycle of the clonogenic cells. In a rapidly growing tumor, cell birth by mitosis compensates for cell killing by the radiation during the prolonged exposure time. This is much less of a problem with slowly growing tumors, such as carcinoma of the prostate, and it is in such sites that permanent implants with iodine-125 have found a place.

A major advantage of a radionuclide such as iodine-125 is the low energy of the photons emitted (about 30 keV). This makes little difference to the dose distribution in an implanted tumor but greatly simplifies radiation protection problems because medical and nursing staff are easily shielded. In addition, the dose falls off rapidly outside the treatment volume so that doses to parts of the patient's body remote from the implant are greatly reduced. Several other new radionuclides are under consideration as sources for brachytherapy that share with iodine-125 the properties of a relatively short half-life and a low-energy photon emission to reduce problems of radiation protection. By contrast, americium-241 emits a low-energy photon but has a long half-life of hundreds of years. [Table 5.1](#) summarizes some of the physical characteristics of the newly developed sources and contrasts them with the characteristics of radionuclides more commonly used for brachytherapy.

Table 5.1 Characteristics of Radionuclides for Intracavitary or Interstitial Brachytherapy

	PHOTON ENERGY, keV		

RADIOMAULIDE	AVERAGE	RANGE	HALF-LIFE	HVL, ^a LEAD	mm
<i>Conventional</i>					
Cesium-137	662	—	30 y	5.5	
Iridium-192	380	136–1060	74.2 d	2.5	
<i>New</i>					
Iodine-125	28	3–35	60.2 d	0.025	
Gold-198	412	—	2.7 d	2.5	
Americium-241	60	—	432 y	0.125	
Palladium-103	21	20–23	17 d	0.008	
Samarium-145	41	38–61	340 d	0.06	
Ytterbium-169	100	10–308	32 d	0.1	

^aHVL, half-value layer, the thickness required to reduce the incident radiation by 50.

Data computed by Dr. Ravinder Nath, Yale University.

SUMMARY OF PERTINENT CONCLUSIONS

Potentially Lethal Damage Repair

The component of radiation damage that can be modified by manipulation of the postirradiation conditions is known as PLD.

PLD repair can occur if cells are prevented from dividing for 6 hours or more after irradiation; this is manifested as an increase in survival. This repair can be demonstrated *in vitro* by keeping cells in saline or plateau phase for 6 hours after irradiation and *in vivo* by delayed removal and assay of animal tumors or cells of normal tissues.

PLD repair is significant for x-rays but does not occur after neutron irradiation.

It has been suggested that resistant human tumors (e.g., melanoma) owe their resistance to large amounts of PLD repair. This is still controversial.

Sublethal Damage Repair

SLD repair is an operational term that describes the increase in survival if a dose of radiation is split into two fractions separated in time.

The half-time of SLD repair in mammalian cells is about 1 hour, but it may be longer in late-responding normal tissues *in vivo*.

SLD repair occurs in tumors and normal tissues *in vivo* as well as in cells cultured *in vitro*.

The repair of SLD reflects the repair of DNA breaks before they can interact to form lethal chromosomal aberrations.

SLD repair is significant for x-rays but is almost nonexistent for neutrons.

Dose-Rate Effect

If the radiation dose rate is reduced from about 1 Gy per minute to 0.3 Gy per hour, there is a reduction in the cell killing from a given dose because SLD repair occurs during the protracted exposure.

As the dose rate is reduced, the slope of the survival curve becomes shallower (D_0 increases), and the shoulder tends to disappear.

In some cell lines, an inverse dose-rate effect is evident (i.e., reducing the dose rate increases the proportion of cells killed) owing to the accumulation of cells in G_2 , which is a sensitive phase of the cycle.

Brachytherapy

Implanting sources into or close to a tumor is known as brachytherapy (from the Greek word *brachy*, meaning “short”) or endocurietherapy (from the Greek word *endo*, meaning “within”).

Intracavitary radiotherapy involves placing radioactive sources into a body cavity close to a tumor. The most common example is the treatment of carcinoma of the uterine cervix.

Intracavitary brachytherapy at LDR may take 1 to 4 days with a dose-rate of about 50 cGy per hour. To an increasing extent, LDR intracavitary brachytherapy is being replaced by HDR intracavitary brachytherapy, delivered in 3 to 12 dose fractions.

Interstitial therapy involves implanting radioactive sources directly into the tumor and adjacent normal tissue for a period of 7 to 10 days. However, such techniques are little used nowadays.

Permanent implants can be used with radionuclides (such as iodine-125 or palladium-103) that have relatively short half-lives.

Several novel radionuclides are being considered as sources for brachytherapy. Most emit low-energy photons, which simplifies the problems of radiation protection.

BIBLIOGRAPHY

Ang KK, Thames HD Jr, van der Kogel AG, et al. Is the rate of repair of radiation-induced sublethal damage in rat spinal cord dependent on the size of dose per fraction? *Int J Radiat Oncol Biol Phys.* 1987;13:557–562.

Bedford JS, Hall EJ. Survival of HeLa cells cultured in vitro and exposed to protracted gamma-irradiation. *Int J Radiat Biol Relat Stud Phys Chem Med.* 1963;7:377–383.

Bedford JS, Mitchell JB. Dose-rate effects in synchronous mammalian cells in culture. *Radiat Res.* 1973;54:316–327.

Bell AG. The uses of radium. *Am Med.* 1903;6:261.

Belli JA, Bonte FJ, Rose MS. Radiation recovery response of mammalian tumour cells in vivo. *Nature.* 1966;211:662–663.

Belli JA, Dicus GJ, Bonte FJ. Radiation response of mammalian tumor cells. I. Repair of sublethal damage in vivo. *J Natl Cancer Inst.* 1967;38:673–682.

- Belli JA, Shelton M. Potentially lethal radiation damage: repair by mammalian cells in culture. *Science*. 1969;165:490–492.
- Berry RJ, Cohen AB. Some observations on the reproductive capacity of mammalian tumour cells exposed in vivo to gamma radiation at low dose-rates. *Br J Radiol*. 1962;35:489–491.
- Bryant PE. Survival after fractionated doses of radiation: modification by anoxia of the response of Chlamydomonas. *Nature*. 1968;219:75–77.
- Dale RG. The use of small fraction numbers in high dose-rate gynaecological afterloading: some radiobiological considerations. *Br J Radiol*. 1990;63:290–294.
- Denekamp J, Fowler JF. Further investigations of the response of irradiated mouse skin. *Int J Radiat Biol Relat Stud Phys Chem Med*. 1966;10:435–441.
- Elkind MM, Sutton H. Radiation response of mammalian cells grown in culture.
1. Repair of x-ray damage in surviving Chinese hamster cells. *Radiat Res*. 1960;13:556–593.
- Elkind MM, Sutton-Gilbert H, Moses WB, et al. Radiation response of mammalian cells grown in culture. V. Temperature dependence of the repair of x-ray damage in surviving cells (aerobic and hypoxic). *Radiat Res*. 1965;25:359–376.
- Elkind MM, Whitmore GF. *Radiobiology of Cultured Mammalian Cells*. New York, NY: Gordon and Breach; 1967.
- Emery EW, Denekamp J, Ball MM, et al. Survival of mouse skin epithelial cells following single and divided doses of x-rays. *Radiat Res*. 1970;41:450–466.
- Fu KK, Phillips TL, Kane LJ, et al. Tumor and normal tissue response to irradiation in vivo: variation with decreasing dose rates. *Radiology*. 1975;114:709–716.
- Hahn GM, Bagshaw MA, Evans RG, et al. Repair of potentially lethal lesions in x-irradiated, density-inhibited Chinese hamster cells: metabolic effects and hypoxia. *Radiat Res*. 1973;55:280–290.
- Hahn GM, Little JB. Plateau-phase cultures of mammalian cells: an in vitro model for human cancer. *Curr Top Radiat Res Q*. 1972;8:39–43.
- Hall EJ. Radiation dose-rate: a factor of importance in radiobiology and radiotherapy. *Br J Radiol*. 1972;45:81–97.

- Hall EJ. The biological basis of endocurietherapy: the Henschke Memorial Lecture 1984. *Endocuriether Hypertherm Oncol.* 1985;1:141–151.
- Hall EJ, Bedford JS. Dose rate: its effect on the survival of HeLa cells irradiated with gamma rays. *Radiat Res.* 1964;22:305–315.
- Hall EJ, Brenner DJ. The 1991 George Edelstyn Memorial Lecture: needles, wires and chips—advances in brachytherapy. *Clin Oncol (R Coll Radiol).* 1992;4:249–256.
- Hall EJ, Brenner DJ. The dose-rate effect revisited: radiobiological considerations of importance in radiotherapy. *Int J Radiat Oncol Biol Phys.* 1991;21:1403–1414.
- Hall EJ, Cavanagh J. The effect of hypoxia on recovery of sublethal radiation damage in Vicia seedlings. *Br J Radiol.* 1969;42:270–277.
- Hall EJ, Kraljevic U. Repair of potentially lethal radiation damage: comparison of neutron and x-ray RBE and implications for radiation therapy. *Radiology.* 1976;121:731–735.
- Hall EJ, Rossi HH, Roizin LA. Low-dose-rate irradiation of mammalian cells with radium and californium 252. *A comparison of effects on an actively proliferating cell population.* *Radiology.* 1971;99:445–451.
- Henschke UK, Hilaris BS, Mahan GD. Afterloading in interstitial and intracavitary radiation therapy. *Am J Roentgenol Radium Ther Nucl Med.* 1963;90:386–395.
- Hornsey S. The radiosensitivity of melanoma cells in culture. *Br J Radiol.* 1972;45:158.
- Hornsey S. The recovery process in organized tissue. *Radiat Res.* 1967;587–603.
- Howard A. The role of oxygen in the repair process. In: Bond VP, ed. *Proceedings of the Carmel Conference on Time and Dose Relationships in Radiation Biology as Applied to Radiotherapy.* Upton, NY: Brookhaven National Laboratory; 1969:70–81. Report 50203 (C-57).
- Joslin CAF. High-activity source afterloading in gynecological cancer and its future prospects. *Endocuriether Hypertherm Oncol.* 1989;5:69–81.
- Joslin CAF, Liversage WE, Ramsay NW. High dose-rate treatment moulds by afterloading techniques. *Br J Radiol.* 1969;42:108–112.
- Joslin CAF, Smith CW. The use of high activity cobalt 60 sources for intracavitary and surface mould therapy. *Proc R Soc Med.* 1970;63:1029–

1034.

Lajtha LG, Oliver R. Some radiobiological considerations in radiotherapy. *Br J Radiol.* 1961;34:252–257.

Lenhard RE Jr, Order SE, Spunberg JJ, et al. Isotopic immunoglobulin: a new systemic therapy for advanced Hodgkin's disease. *J Clin Oncol.* 1985;3:1296–1300.

Lieberman HB, Hopkins KM. A single nucleotide base-pair change is responsible for the radiosensitivity exhibited by *S pombe* cells containing the mutant allele RAD-192 [abstract]. In: Chapman JD, Devey WC, Whitmore GF, eds. *Radiation Research: A Twentieth Century Perspective*. Vol 1. San Diego, CA: Academic Press; 1991;1:333.

Lieberman HB, Hopkins KM, Laverty M, et al. Molecular cloning and analysis of *Schizosaccharomyces pombe* rad9, a gene involved in DNA repair and mutagenesis. *Mol Gen Genet.* 1992;232:367–376.

Little JB, Hahn GM, Frindel E, et al. Repair of potentially lethal radiation damage in vitro and in vivo. *Radiology.* 1973;106:689–694.

Mitchell JB, Bedford JS, Bailey SM. Dose-rate effects on the cell cycle and survival of S3 HeLa and V79 cells. *Radiat Res.* 1979;79:520–536.

Orton CG. What minimum number of fractions is required with high dose-rate remote afterloading? *Br J Radiol.* 1987;60:300–302.

Phillips RA, Tolmach LJ. Repair of potentially lethal damage in x-irradiated HeLa cells. *Radiat Res.* 1966;29:413–432.

Phillips TL, Ainsworth EJ. Altered split-dose recovery in mice irradiated under hypoxic conditions. *Radiat Res.* 1969;39:317–331.

Phillips TL, Hanks GE. Apparent absence of recovery in endogenous colony-forming cells after irradiation under hypoxic conditions. *Radiat Res.* 1968;33:517–532.

Shipley WU, Stanley JA, Courtenay VD, et al. Repair of radiation damage in Lewis lung carcinoma cells following in situ treatment with fast neutrons and gamma-rays. *Cancer Res.* 1975;35:932–938.

Stout R, Hunter RD. Clinical trials of changing dose rate in intracavitary low dose-rate therapy. In: Mould RF, ed. *Brachytherapy*. Amsterdam, The Netherlands: Nucletron; 1985.

- Suit H, Urano M. Repair of sublethal radiation injury in hypoxic cells of a C3H mouse mammary carcinoma. *Radiat Res.* 1969;37:423–434.
- Travis EJ, Thames HD, Watkins TL, et al. The kinetics of repair in mouse lung after fractionated irradiation. *Int J Radiat Biol Relat Stud Phys Chem Med.* 1987;52:903–919.
- Tubiana N, Malaise E. Growth rate and cell kinetics in human tumors: some prognostic and therapeutic implications. In: Symington T, Carter RL, eds. *Scientific Foundations of Oncology*. Chicago, IL: Year Book Medical; 1976:126–136.
- Turesson I, Thames HD. Repair capacity and kinetics of human skin during fractionated radiotherapy: erythema, desquamation, and telangiectasia after 3 and 5 year's follow-up. *Radiother Oncol.* 1989;15:169–188.
- Van't Hooft E. The selection HDR: philosophy and design. In: Mould RF. *Selectron Brachytherapy Journal*. Amsterdam, The Netherlands: Nucletron; 1985.
- Weichselbaum RR, Little JB, Nove J. Response of human osteosarcoma in vitro to irradiation: evidence for unusual cellular repair activity. *Int J Radiat Biol Relat Stud Phys Chem Med.* 1977;31:295–299.
- Weichselbaum RR, Nove J, Little JB. Deficient recovery from potentially lethal radiation damage in ataxia telangiectasia and xeroderma pigmentosum. *Nature.* 1978;271:261–262.
- Weichselbaum RR, Schmit A, Little JB. Cellular repair factors influencing radiocurability of human malignant tumours. *Br J Cancer.* 1982;45:10–16.
- Weichselbaum RR, Withers HR, Tomkinson K, et al. Potentially lethal damage repair (PLDR) in X-irradiated cultures of a normal human diploid fibroblast cell strain. *Int J Radiat Biol Relat Stud Phys Chem Med.* 1983;43:313–319.
- Wells RL, Bedford JS. Dose-rate effects in mammalian cells. IV. Repairable and nonrepairable damage in noncycling C3H 10T 1/2 cells. *Radiat Res.* 1983;94:105–134.
- Whitmore GF, Gulyas S. Studies on recovery processes in mouse L cells. *Natl Cancer Inst Monogr.* 1967;24:141–156.
- Winans LF, Dewey WC, Dettor CM. Repair of sublethal and potentially lethal x-ray damage in synchronous Chinese hamster cells. *Radiat Res.* 1972;52:333–351.

Withers HR. Capacity for repair in cells of normal and malignant tissues. In: Bond VP, ed. *Proceedings of the Carmel Conference on Time and Dose Relationships in Radiation Biology as Applied to Radiotherapy*. Upton, NY: Brookhaven National Laboratory; 1969:54–69. Report 50203 (C-57).

chapter 6

Oxygen Effect and Reoxygenation

The Nature of the Oxygen Effect

The Time at Which Oxygen Acts and the Mechanism of the Oxygen Effect

The Concentration of Oxygen Required

Chronic and Acute Hypoxia

Chronic Hypoxia

Acute Hypoxia

The First Experimental Demonstration of Hypoxic Cells in a Tumor

Proportion of Hypoxic Cells in Various Animal Tumors

Evidence for Hypoxia in Human Tumors

Techniques to Measure Tumor Oxygenation

Oxygen Probe Measurements

Markers of Hypoxia

Reoxygenation

Time Sequence of Reoxygenation

Mechanism of Reoxygenation

The Importance of Reoxygenation in Radiotherapy

Hypoxia and Chemoresistance

Hypoxia and Tumor Progression

Summary of Pertinent Conclusions

Bibliography

Several chemical and pharmacologic agents that modify the biologic effect of ionizing radiations have been discovered. None is simpler than oxygen, none produces such a dramatic effect, and, as it turns out, no other agent has such obvious practical implications.

The oxygen effect was observed as early as 1912 in Germany by

Swartz, who noted that the skin reaction produced on his forearm by a radium applicator was reduced if the applicator was pressed hard onto the skin. He attributed this to the interruption in blood flow. By 1921, it had been noted by Holthusen that *Ascaris* eggs were relatively resistant to radiation in the absence of oxygen, a result wrongly attributed to the absence of cell division under these conditions. The correlation between radiosensitivity and the presence of oxygen was made by Petry in 1923 from a study of the effects of radiation on vegetable seeds. All of these results were published in the German literature but were apparently little known in the English-speaking world.

In England in the 1930s, Mottram explored the question of oxygen in detail, basing his investigations on work of Crabtree and Cramer on the survival of tumor slices irradiated in the presence or absence of oxygen. He also discussed the importance of these findings to radiotherapy. Mottram began a series of experiments that culminated in a quantitative measurement of the oxygen effect by his colleagues Gray and Read, using as a biologic test system the growth inhibition of the primary root of the broad bean *Vicia faba*.

THE NATURE OF THE OXYGEN EFFECT

Survival curves for mammalian cells exposed to x-rays in the presence and absence of oxygen are illustrated in [Figure 6.1](#). The ratio of doses administered under hypoxic to aerated conditions needed to achieve the same biologic effect is called the **oxygen enhancement ratio (OER)**. For sparsely ionizing radiations, such as x- and γ -rays, the OER at high doses has a value of between 2.5 and 3.5. The OER has been determined for various chemical and biologic systems with different end points, and its value for x- and γ -rays always tends to fall in this range. There is some evidence that for rapidly growing cells cultured *in vitro*, the OER has a smaller value of about 2.5 at lower doses, on the order of the daily dose per fraction generally used in radiotherapy. This is believed to result from the variation of OER with the phase of the cell cycle: Cells in G₁ phase have a lower OER than those in S, and because G₁ cells are more radiosensitive, they dominate the low-dose region of the survival curve. For this reason, the OER of an asynchronous population is slightly smaller at low doses than at high doses. This result has been demonstrated for fast-growing cells cultured *in vitro*, for which precise survival measurements are possible, but would be difficult to show in a tissue. There is some evidence also that for cells in culture, the survival curve has a complex shape for doses less than 1 Gy. What effect, if any, this has

on the OER is not yet clear.

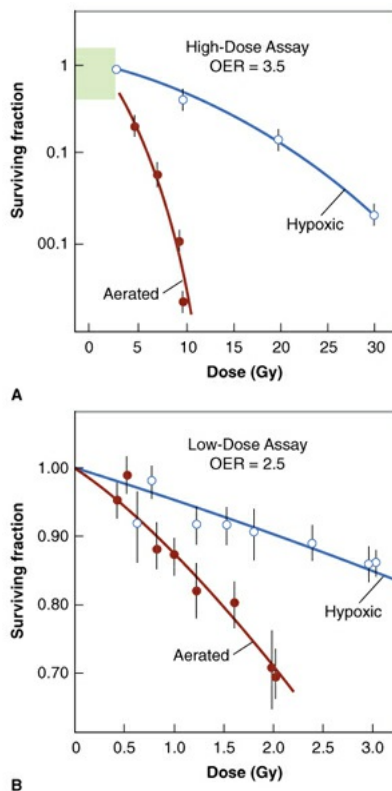


FIGURE 6.1 Cells are much more sensitive to x-rays in the presence of molecular oxygen than in its absence (i.e., under hypoxia). The ratio of doses under hypoxic to aerated conditions necessary to produce the same level of cell killing is called the *oxygen enhancement ratio* (OER). It has a value close to 3.5 at high doses (**A**) but may have a lower value of about 2.5 at x-ray doses less than about 2 to 3 Gy (**B**). (Adapted from Palcic B, Skarsgard LD. Reduced oxygen enhancement ratio at low doses of ionizing radiation. *Radiat Res.* 1984;100:328–339, with permission.)

Figure 6.2 illustrates the oxygen effect for other types of ionizing radiations. For a densely ionizing radiation, such as low-energy α -particles, the survival curve does not have an initial shoulder. In this case, survival estimates made in the presence or absence of oxygen fall along a common line; the OER is unity—in other words, there is no oxygen effect. For radiations of intermediate ionizing density, such as neutrons, the survival curves have a much reduced shoulder. In this case, the oxygen effect is apparent, but it is much smaller than is the case for x-rays. In the example shown in Figure 6.2, the OER for neutrons is about 1.6.

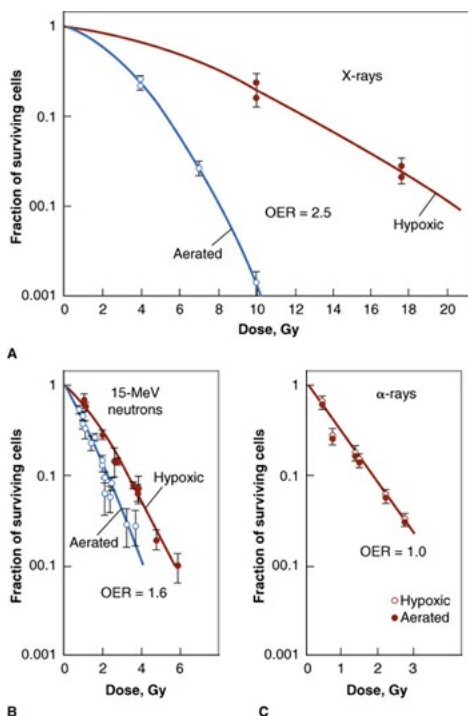


FIGURE 6.2 The oxygen enhancement ratio (OER) for various types of radiation. **A:** X-rays exhibit a larger OER of 2.5. **B:** Neutrons (15-MeV $d^+ \rightarrow T$) are between these extremes, with an OER of 1.6. **C:** The OER for low-energy α -particles is unity. (Adapted from Barendsen GW, Koot CJ, van Kersen GR, et al. The effect of oxygen on impairment of the proliferative capacity of human cells in culture by ionizing radiations of different LET. *Int J Radiat Biol Relat Stud Phys Chem Med.* 1966;10:317–327; and Broerse JJ, Barendsen GW, van Kersen GR. Survival of cultured human cells after irradiation with fast neutrons of different energies in hypoxic and oxygenated conditions. *Int J Radiat Biol Relat Stud Phys Chem Med.* 1968;13:559–572, with permission.)

In summary, the oxygen effect is large and important in the case of sparsely ionizing radiations, such as x-rays; is absent for densely ionizing radiations, such as α -particles; and has an intermediate value for fast neutrons.

THE TIME AT WHICH OXYGEN ACTS AND THE MECHANISM OF THE OXYGEN EFFECT

For the oxygen effect to be observed, oxygen must be present during the radiation exposure or, to be precise, *during or within microseconds after* the radiation exposure. Sophisticated experiments have been performed in which oxygen, contained in a chamber at high pressure, was allowed to “explode” onto a single layer of bacteria (and later mammalian cells) at various times before or after irradiation with a 2- μ electron pulse from a linear accelerator. It was found

that oxygen need not be present during the irradiation to sensitize but could be added *afterward*, provided the delay was not too long. Some sensitization occurred with oxygen added as late as 5 milliseconds after irradiation.

Experiments such as these shed some light on the mechanism of the oxygen effect. There is general agreement that oxygen acts at the level of the free radicals. The chain of events from the absorption of radiation to the final expression of biologic damage has been summarized as follows: The absorption of radiation leads to the production of fast-charged particles. The charged particles, in passing through the biologic material, produce several ion pairs. These ion pairs have very short life spans (about 10^{-10} second) and produce free radicals, which are highly reactive molecules because they have an unpaired valence electron. The free radicals are important because although their life spans are only about 10^{-5} second, that is appreciably longer than that of the ion pairs. To a large extent, it is these free radicals that break chemical bonds, produce chemical changes, and initiate the chain of events that result in the final expression of biologic damage; however, it has been observed that the extent of the damage depends on the presence or absence of oxygen.

If molecular oxygen is present, DNA reacts with the free radicals ($R\cdot$). The DNA radical can be chemically restored to its reduced form through reaction with a sulphydryl (SH) group. However, the formation of $RO_2\cdot$, an organic peroxide, represents a nonrestorable form of the target material; that is, the reaction results in a change in the chemical composition of the material exposed to the radiation. This reaction cannot take place in the absence of oxygen; since then, many of the ionized target molecules are able to repair themselves and recover the ability to function normally. In a sense, then, oxygen may be said to “fix” or make permanent the radiation lesion. This is known as the *oxygen fixation hypothesis*. The process is illustrated in [Figure 6.3](#).

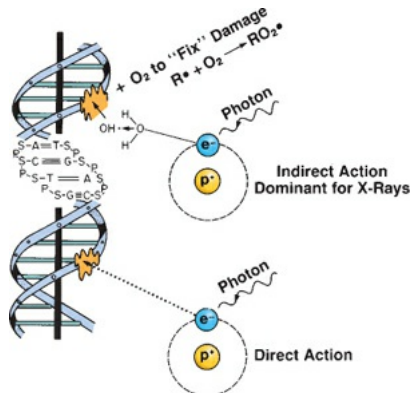


FIGURE 6.3 The oxygen fixation hypothesis. About two-thirds of the biologic

damage produced by x-rays is by indirect action mediated by free radicals. The damage produced by free radicals in DNA can be repaired under hypoxia but may be “fixed” (made permanent and irreparable) if molecular oxygen is available.

THE CONCENTRATION OF OXYGEN REQUIRED

A question of obvious importance is the concentration of oxygen required to potentiate the effect of radiation. Is the amount required small or large? Many investigations have been performed using bacteria, plants, yeast, and mammalian cells, and the similarities between them are striking.

The simple way to visualize the effect of oxygen is by considering the change of slope of the mammalian cell survival curve. [Figure 6.4](#) is a dramatic representation of what happens to the survival curve in the presence of various concentrations of oxygen. Curve A is characteristic of the response under conditions of equilibration with air. Curve B is a survival curve for irradiation in as low a level of hypoxia as usually can be obtained under experimental conditions (10 ppm of oxygen in the gas phase). The introduction of a very small quantity of oxygen, 100 ppm, is readily noticeable in a change in the slope of the survival curve. A concentration of 2,200 ppm, which is about 0.22% oxygen, moves the survival curve about halfway toward the fully aerated condition.

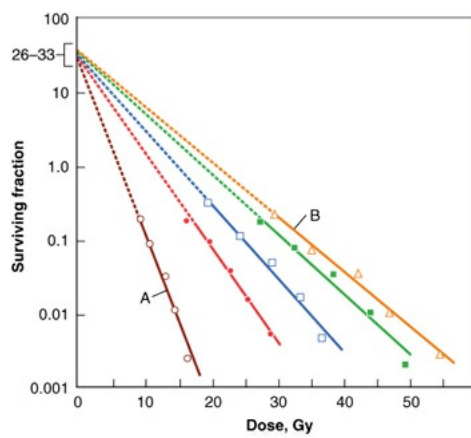


FIGURE 6.4 Survival curves for Chinese hamster cells exposed to x-rays in the presence of various oxygen concentrations. *Open circles*, air (A); *closed circles*, 2,200 ppm of oxygen or pO_2 of 1.7 mm Hg; *open squares*, 355 ppm of oxygen or pO_2 of 0.25 mm Hg; *closed squares*, 100 ppm of oxygen or pO_2 of 0.075 mm Hg; *open triangles*, 10 ppm of oxygen or pO_2 of 0.0075 mm Hg (B), which corresponded to the lowest level of hypoxia that could usually be obtained under experimental conditions. (Adapted from Elkind MM, Swain RW, Alescio T, et al. Oxygen, nitrogen, recovery and radiation therapy. In: Shalek R, ed. *Cellular*

Radiation Biology. Baltimore, MD: Williams & Wilkins; 1965:442–466, with permission.)

Other experiments have shown that, generally, by the time a concentration of oxygen corresponding to 2% has been reached, the survival curve is virtually indistinguishable from that obtained under conditions of normal aeration. Furthermore, increasing the amount of oxygen present from that characteristic of air to 100% oxygen does not further affect the slope of the curve. This has led to the more usual “textbook representation” of the variation of radiosensitivity with oxygen concentration as shown in Figure 6.5. The term used here to represent radiosensitivity is proportional to the reciprocal of the D_0 of the survival curve. It is arbitrarily assigned a value of unity for anoxic conditions. As the oxygen concentration increases, the biologic material becomes progressively more sensitive to radiation, until, in the presence of 100% oxygen, it is about 3 times as sensitive as under complete anoxia. Note that the rapid change of radiosensitivity occurs as the partial pressure of oxygen (pO_2) is increased from 0 to about 30 mm Hg (5% oxygen). A further increase in oxygen tension to an atmosphere of pure oxygen has little, if any, further effect. An oxygen concentration of 0.5% (or about 3 mm Hg) results in a radiosensitivity halfway between the characteristic of hypoxia and that of fully oxygenated conditions.

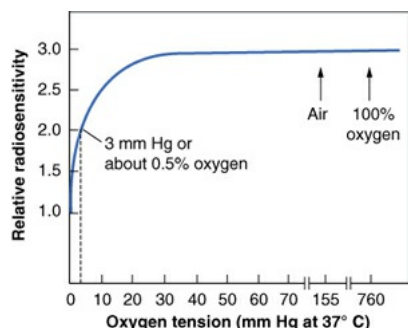


FIGURE 6.5 An idealized representation of the dependence of radiosensitivity on oxygen concentration. If the radiosensitivity under extremely anoxic conditions is arbitrarily assigned a value of unity, the relative radiosensitivity is about 3 under well-oxygenated conditions. Most of this change of sensitivity occurs as the oxygen tension increases from 0 to 30 mm Hg. A further increase of oxygen content to that characteristic of air or even pure oxygen at high pressure has little further effect. A relative radiosensitivity halfway between anoxia and full oxygenation occurs for a pO_2 of about 3 mm Hg, which corresponds to a concentration of about 0.5% oxygen. This illustration is idealized and does not represent any specific experimental data. Experiments have been performed with yeast, bacteria, and mammalian cells in culture; the

results conform to the general conclusions summarized here.

It is evident, then, that very small amounts of oxygen are necessary to produce the dramatic and important oxygen effect observed with x-rays. Although it is usually assumed that the oxygen tension of most normal tissues is similar to that of venous blood or lymph (20 to 40 mm Hg), in fact, oxygen probe measurements indicate that the oxygen tension may vary between different tissues over a wide range from 1 to 100 mm Hg. Many tissues are therefore borderline hypoxic and contain a small proportion of cells that are radiobiologically hypoxic. This is particularly true of, for example, the liver and skeletal muscles. Even mouse skin has a small proportion of hypoxic cells that show up as a change of slope if the survival curve is pushed to low survival levels.

CHRONIC AND ACUTE HYPOXIA

It is important to recognize that hypoxia in tumors can result from two quite different mechanisms. *Chronic* hypoxia results from the limited diffusion distance of oxygen through tissue that is respiring. The distance to which oxygen can diffuse is largely limited by the rapid rate at which it is metabolized by respiring tumor cells. Many tumor cells may remain hypoxic for long periods. In contrast to chronic hypoxia, *acute* hypoxia is the result of the temporary closing of a tumor blood vessel owing to the malformed vasculature of the tumor, which lacks smooth muscle and often has an incomplete endothelial lining and basement membrane. Tumor cells are exposed to a continuum of oxygen concentrations, ranging from the highest in cells surrounding the capillaries to almost anoxic conditions in cells more distant from the capillaries. This is significant because both chronic and acute hypoxia have been shown to drive malignant progression.

Chronic Hypoxia

As already mentioned, radiotherapists began to suspect that oxygen influences the radiosensitivity of tumors in the 1930s. It was, however, a paper by Thomlinson and Gray in 1955 that triggered the tremendous interest in oxygen as a factor in radiotherapy; they described the phenomenon of **chronic hypoxia** that they observed in their histologic study of fresh specimens of bronchial carcinoma. Cells of the stratified squamous epithelium, normal or malignant, generally remain in contact with one another; the vascular stroma on which their nutrition depends lies in contact with the epithelium, but capillaries do not penetrate between the cells. Tumors that arise in this type of tissue often grow in

solid cords that, seen in section, appear to be circular areas surrounded by stroma. The centers of large tumor areas are necrotic and are surrounded by intact tumor cells, which consequently appear as rings. [Figure 6.6A](#), reproduced from Thomlinson and Gray, shows a transverse section of a tumor cord and is typical of areas of a tumor in which necrosis is not far advanced. [Figure 6.6B](#) shows large areas of necrosis separated from stroma by a narrow band of tumor cells about $100\text{ }\mu\text{m}$ wide.

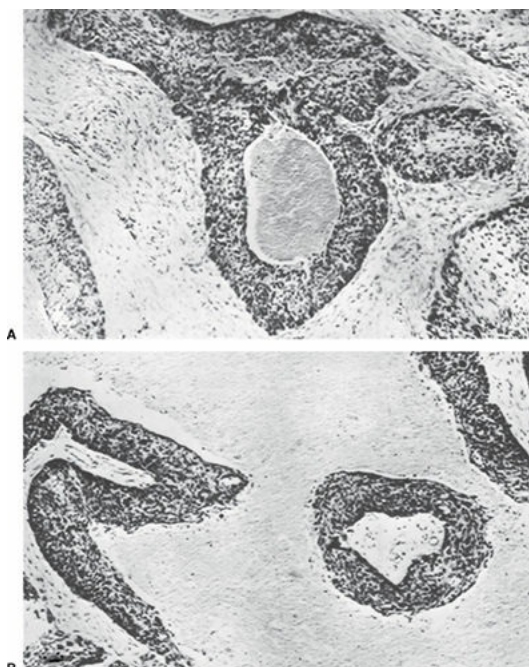


FIGURE 6.6 Transverse sections of tumor cords surrounded by stroma from human carcinoma of the bronchus. **A:** A typical tumor area in which necrosis is not far advanced. **B:** Large areas of necrosis separated from the stroma by a band of tumor cells about $100\text{ }\mu\text{m}$ wide. (From Thomlinson RH, Gray LH. The histological structure of some human lung cancers and the possible implications for radiotherapy. *Br J Cancer*. 1955;9:539–549, with permission.)

By viewing a large number of these samples of human bronchial carcinomas, Thomlinson and Gray recognized that as the tumor cord grows larger, the necrotic center also enlarges, so that the thickness of the sheath of viable tumor cells remains essentially constant. This is illustrated in [Figure 6.7](#).

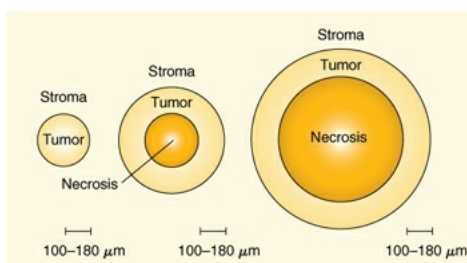


FIGURE 6.7 The conclusions reached by Thomlinson and Gray from a study of histologic sections of human bronchial carcinoma. No necrosis was seen in small tumor cords with a radius of less than about $160\text{ }\mu\text{m}$. No tumor cord with a radius exceeding $200\text{ }\mu\text{m}$ was without a necrotic center. As the diameter of the necrotic area increased, the thickness of the sheath of viable tumor cells remained essentially constant at 100 to $180\text{ }\mu\text{m}$.

The obvious conclusion was that tumor cells could proliferate and grow actively only if they were close to a supply of oxygen or nutrients from the stroma. Thomlinson and Gray then went on to calculate the distance to which oxygen could diffuse in respiring tissue and came up with a distance of about $150\text{ }\mu\text{m}$. This was close enough to the thickness of viable tumor cords on their histologic sections for them to conclude that oxygen depletion was the principal factor leading to the development of necrotic areas in tumors. Using more appropriate values of oxygen diffusion coefficients and consumption values, a better estimate of the distance that the oxygen can diffuse in respiring tissue is about $70\text{ }\mu\text{m}$. This, of course, varies from the arterial to the venous end of a capillary, as illustrated in [Figure 6.8](#).

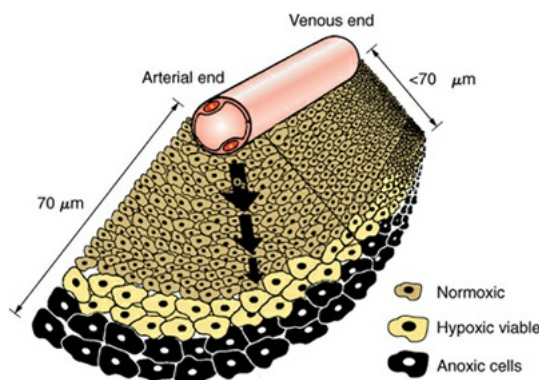


FIGURE 6.8 The diffusion of oxygen from a capillary through tumor tissue. The distance to which oxygen can diffuse is limited largely by the rapid rate at which it is metabolized by respiring tumor cells. For some distance from a capillary, tumor cells are well oxygenated. At greater distances, oxygen is depleted, and tumor cells become necrotic. Hypoxic tumor cells form a layer, perhaps one or two cells thick, in between. In this region, the oxygen concentration is high enough for the cells to be viable but low enough for them to be relatively protected from the effects of x-rays. These cells may limit the radiocurability of the tumor. The distance to which oxygen can diffuse is about $70\text{ }\mu\text{m}$ at the arterial end of a capillary and less at the venous end.

By histologic examination of sections, it is possible to distinguish only two classes of cells: (1) those that appear to be proliferating well and (2) those that

are dead or dying. Between these two extremes, and assuming a steadily decreasing oxygen concentration, one would expect a region in which cells would be at an oxygen tension high enough for cells to be clonogenic but low enough to render the cells protected from the effect of ionizing radiation. Cells in this region would be relatively protected from a treatment with x-rays because of their low oxygen tension and could provide a focus for the subsequent regrowth of the tumor ([Fig. 6.8](#)). Based on these ideas, it was postulated that the presence of a relatively small proportion of hypoxic cells in tumors could limit the success of radiotherapy in some clinical situations.

These ideas about the role of oxygen in cell killing dominated the thinking of radiobiologists and radiotherapists in the late 1950s and early 1960s. A great deal of thought and effort was directed toward solving this problem. The solutions proposed included the use of high-pressure oxygen chambers, the development of novel radiation modalities such as neutrons, negative π -mesons, and heavy-charged ions, and the development of hypoxic cell sensitizers.

Acute Hypoxia

Regions of **acute hypoxia** develop in tumors as a result of the temporary closing or blockage of a particular blood vessel. If this blockage were permanent, the cells downstream, of course, would eventually die and be of no further consequence. There is, however, good evidence that tumor blood vessels open and close in a random fashion, so that different regions of the tumor become hypoxic intermittently. In fact, acute hypoxia results from transient fluctuations in blood flow because of the malformed vasculature. At the moment when a dose of radiation is delivered, a proportion of tumor cells may be hypoxic, but if the radiation is delayed until a later time, a different group of cells may be hypoxic. The occurrence of *acute hypoxia* was postulated in the early 1980s by Martin Brown and was later demonstrated unequivocally in rodent tumors by Chaplin and his colleagues. [Figure 6.9](#), which illustrates how acute hypoxia is caused by fluctuating blood flow, also depicts the difference between acute and chronic hypoxia. In contrast to acutely hypoxic cells, chronically hypoxic cells are less likely to become reoxygenated and will die unless they are able to access a blood supply.

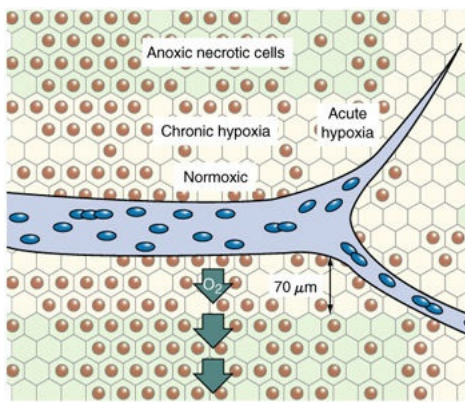


FIGURE 6.9 Diagram illustrating the difference between chronic and acute hypoxia. Chronic hypoxia results from the limited diffusion distance of oxygen in respiring tissue that is actively metabolizing oxygen. Cells that become hypoxic in this way remain hypoxic for long periods until they die and become necrotic. Acute hypoxia results from the temporary closing of tumor blood vessels. The cells are intermittently hypoxic because normoxia is restored each time the blood vessel opens up again. (Adapted from Brown JM. Tumor hypoxia, drug resistance, and metastases. *J Natl Cancer Inst.* 1990;82:338–339, with permission.)

THE FIRST EXPERIMENTAL DEMONSTRATION OF HYPOXIC CELLS IN A TUMOR

The dilution assay technique, described in Chapter 21, was used by Powers and Tolmach to investigate the radiation response of a solid subcutaneous lymphosarcoma in the mouse. Survival estimates were made for doses from 2 to 25 Gy. The results are shown in Figure 6.10, in which the dose on a linear scale is plotted against the fraction of surviving cells on a logarithmic scale.

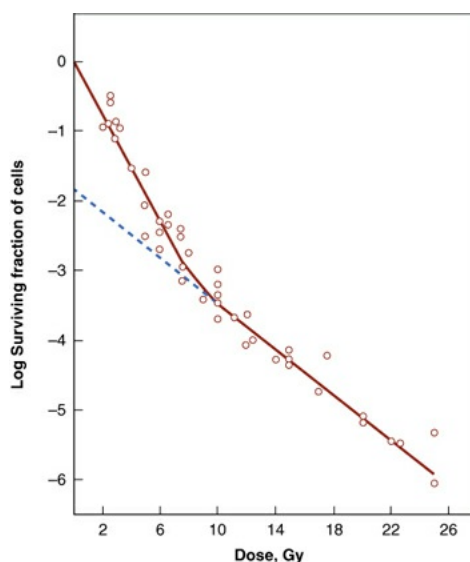


FIGURE 6.10 Fraction of surviving cells as a function of dose for a solid subcutaneous lymphosarcoma in the mouse irradiated *in vivo*. The first part of the curve has a slope D_0 of 1.1 Gy; the second component of the curve has a shallower slope D_0 of 2.6 Gy, indicating that these cells are hypoxic. (Adapted from Powers WE, Tolmach LJ. A multicomponent x-ray survival curve for mouse lymphosarcoma cells irradiated *in vivo*. *Nature*. 1963;197:710–711, with permission.)

The survival curve for this solid tumor clearly consists of two separate components. The first, up to a dose of about 9 Gy, has a D_0 of 1.1 Gy. The second has a shallower D_0 of 2.6 Gy. This biphasic survival curve has a final slope about 2.5 times shallower than the initial portion, which strongly suggests that the tumor consists of two separate groups of cells: one oxygenated and the other hypoxic. If the shallow component of the curve is extrapolated backward to cut the surviving fraction axis, it does so at a survival level of about 1%. From this, it may be inferred that about 1% of the clonogenic cells in the tumor were deficient in oxygen.

The response of this tumor to single doses of radiation of various sizes is explained readily on this basis. If 99% of the cells are well oxygenated and 1% are hypoxic, the response to lower doses is dominated by the killing of the well-oxygenated cells. For these doses, the hypoxic cells are depopulated to a negligibly small extent. Once a dose of about 9 Gy is exceeded, however, the oxygenated compartment of the tumor is depopulated severely, and the response of the tumor is characteristic of the response of hypoxic cells. This biphasic survival curve was the first unequivocal demonstration that a solid tumor could contain cells sufficiently hypoxic to be protected from cell killing by x-rays but still clonogenic and capable of providing a focus for tumor regrowth.

PROPORTION OF HYPOXIC CELLS IN VARIOUS ANIMAL TUMORS

Over the years, many investigators have determined the fraction of hypoxic cells in various tumors in experimental animals. The most satisfactory and most widely used method is to obtain paired survival curves (Fig. 6.11A). The steepest curve relates to a fully oxygenated population of cells; the uppermost curve, to a population made up entirely of hypoxic cells. The intermediate curves refer to mixed populations of oxygenated cells with varying proportions of hypoxic cells. At low doses, the survival curve for a mixed population closely follows that for the oxygenated population. At higher doses, the number of surviving oxygenated

cells is negligible compared with the number of anoxic cells, and consequently, the curve representing the mixed population is parallel to (i.e., has the same slope as) the curve for the hypoxic population. The fraction of hypoxic cells in the tumor determines the distance between the parallel terminal slopes of the dose-response curves, as shown in Figure 6.11A. This fraction is identical to the ratio of the surviving cells from the partially hypoxic tumor to those from the entirely hypoxic tumor.

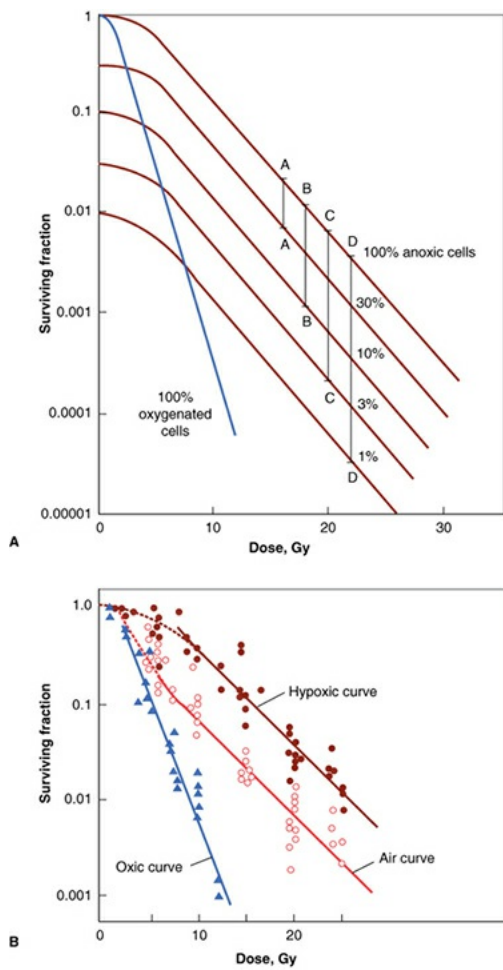


FIGURE 6.11 A: Theoretic survival curves for cell populations containing different fractions of hypoxic cells. The fraction of hypoxic cells in each population determines the distance between its survival curve and the curve for the completely hypoxic population. From the relative radiosensitivity at any dose level at which the survival curves are approximated by parallel lines, the fraction of hypoxic cells can be determined from the ratio of survival of the completely and partially hypoxic populations, as indicated by the vertical lines A-A, B-B, and so on. This illustration is based on the model proposed by Hewitt and Wilson. (Adapted from Van Putten LM, Kallman RF. Oxygenation status of a transplantable tumor during fractionated radiotherapy. *J Natl Cancer Inst.* 1968;40:441–451, with permission.) B: The proportion of hypoxic cells in a

mouse tumor. The biphasic curve labeled *Air curve* represents data for cells from tumors irradiated in mice breathing air, which are therefore a mixture of aerated and hypoxic cells. The hypoxic curve is for cells irradiated in mice asphyxiated by nitrogen breathing or for cells irradiated *in vitro* in nitrogen, so that they are all hypoxic. The oxic curve is for cells irradiated *in vitro* in air. The proportion of hypoxic cells is the ratio of the air to hypoxic curves or the vertical separation between the curves because the surviving fraction is on a logarithmic scale. (Courtesy of Dr. Sara Rockwell; based on data of Moulder and Rockwell and of Rockwell and Kallman.)

In practice, the procedure is as follows: Survival measurements are made at several dose levels under two different conditions:

1. The animal (e.g., a mouse) is asphyxiated several minutes before irradiation by breathing nitrogen. Under these conditions, all of the tumor cells are hypoxic, and the data points obtained define a line comparable to the upper curve in [Figure 6.11A](#).
2. The animal is alive and breathing air when irradiated so that the proportion of hypoxic cells in the tumor is at its normal level. The data points obtained define a lower line typical of a mixed population of hypoxic and oxygenated cells. The vertical separation between the two lines gives the proportion of hypoxic cells characteristic of that particular tumor.

An example of experimental data for a determination of the hypoxic fraction in a mouse tumor is shown in [Figure 6.11B](#). Hypoxic fractions can also be calculated from a comparison of the TCD₅₀ values (i.e., the doses at which 50% of the tumors are locally controlled) for clamped and unclamped tumors or from a comparison of growth delays from tumors irradiated under these two conditions. Any of these methods involves several assumptions, notably that cells made hypoxic artificially have the same sensitivity as those that have respiration to this condition in the tumor naturally and that the tumor is composed of two distinct populations, one aerated and the other hypoxic, with nothing falling in between. Consequently, measured values for hypoxic fractions can serve only as a guide and must not be taken too seriously.

Moulder and Rockwell published a survey of all published data on hypoxic fractions and reported that of 42 tumor types studied, 37 were found to contain hypoxic cells in at least one study. Hypoxic fractions range from 0% to 50%, with a tendency for many results to average about 15%. Comparable measurements cannot be made in human tumors, of course, to determine

precisely the proportion of hypoxic cells.

EVIDENCE FOR HYPOXIA IN HUMAN TUMORS

Over the last decade, various techniques have been used to determine the oxygenation of human tumors, including measuring the distance between tumor cells and vessels in histologic sections, determining the oxygen saturation of hemoglobin, and monitoring changes in tumor metabolism. These techniques have been replaced by newer methods, including oxygen probes, hypoxia markers, the comet assay, and noninvasive imaging. Although each of these techniques has strengths and weaknesses, together they convincingly demonstrate that hypoxia is a common feature of human solid tumors that can influence both the malignant progression and the response of tumors to therapy. In most studies, the assessment of hypoxia in human tumors has been based largely on oxygen probe measurements. This approach has been used to group patients based on their median pO_2 values but disregards a great deal of information that is obtained in the process, especially the heterogeneity of oxygen measurements in solid tumors. Although oxygen probes are considered the “gold standard” for measuring tumor pO_2 , newer noninvasive techniques will supplant them in the future.

TECHNIQUES TO MEASURE TUMOR OXYGENATION

Oxygen Probe Measurements

Oxygen probes—that is, electrodes implanted directly into tumors to measure oxygen concentration by a polarographic technique—have a long and checkered history. The widespread use of this technique did not come about until the development of the Eppendorf probe, which has a very fast response time and can be moved quickly through a tumor under computer control to obtain large numbers of oxygen measurements along multiple tracks through the tumor. The data from polarographic oxygen electrode studies indicate that hypoxia can be used to predict treatment outcomes for various tumor sites, including the cervix, prostate, and head and neck. Local control of tumors treated by radiotherapy correlates with oxygen probe measurements, indicating that oxygen measurements may have a predictive value in radiotherapy. Oxygen electrode studies of cervical cancers and sarcomas indicated that hypoxia was also predictive of tumor aggressiveness. A new fiber-optic probe has been introduced as an alternative oxygen sensor. A dye in the tip of the probe has a fluorescent lifetime that is inversely related to oxygen concentration.

Markers of Hypoxia

The idea of using hypoxia markers originated from the development of 2-nitroimidazoles, hypoxic radiosensitizers that bind irreversibly to macromolecules in hypoxic cells. These compounds are administered systemically but are only metabolized to form adducts under hypoxic conditions. Pimonidazole is an example of a hypoxia marker, which forms adducts in hypoxic tumor cells that can be detected by tumor biopsy and immunohistochemistry. The advantages of hypoxia markers over oxygen electrodes include (1) that they provide the relative oxygen concentrations on an individual cell basis, (2) that they make it possible to distinguish between viable and necrotic tissue, and (3) that they make it possible to distinguish between chronic and acute hypoxia.

Radioactively labeled 2-nitroimidazoles and other redox-sensitive compounds have been developed to monitor tissue hypoxia noninvasively. Although noninvasive imaging of hypoxia has a lower resolution than invasive approaches, it has the distinct advantage of monitoring changes in oxygenation of both the primary tumor and metastases. Various positron emission tomography (PET) and single photon emission computed tomography (SPECT) imaging agents are available, including F-18-MISO, F-18-EF5, Cu-60-ATSM, and I-123-IAZA. The use of these agents in combination with intensity-modulated radiation therapy (IMRT) theoretically allows the development of “physiologically targeted radiotherapy,” in which different portions of the tumor can receive different radiation doses based on differences in physiology such as oxygen tension. This is commonly referred to as “dose painting.”

Immunohistochemical staining for endogenous markers of tumor hypoxia, such as carbonic anhydrase IX (CA9) and hypoxia-inducible factor (HIF), has also been found to colocalize with 2-nitroimidazole binding, indicating that endogenous proteins are increased in hypoxic tumor regions. However, the expression of endogenous markers can be regulated by factors other than oxygen, complicating their use in quantifying tumor hypoxia.

[Figure 6.12](#) illustrates the way in which these various compounds can be harnessed to “visualize” hypoxic regions in tumors. [Figure 6.12](#) is a pretreatment frozen biopsy from a patient with carcinoma of the cervix. The blue staining shows the blood vessels. The green staining shows pimonidazole (i.e., cells that are hypoxic and will exhibit decreased sensitivity to ionizing radiation). The red staining shows cell nuclei that express the hypoxia-inducible factor 1 (HIF-1) (i.e., in regions where the oxygen tension is lower than normal but will not affect

the response of cells to ionizing radiation). Cells immediately surrounding the blood vessels are not visible because they are fully oxygenated and do not express HIF-1 or reduce the pimonidazole. As would be expected, there is a gradient in oxygen tension away from blood vessels, with therapeutically relevant hypoxic cells situated at some distance.

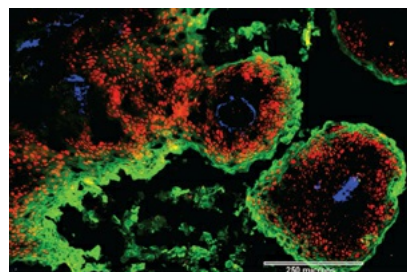


FIGURE 6.12 This image is from a pretreatment frozen biopsy from a patient with carcinoma of the cervix. Green staining shows pimonidazole binding (i.e., hypoxia), red nuclei express HIF-1 α (i.e., are in a region of decreasing oxygen tension), and blue staining shows blood vessels expressing CD31. (From Sobhanifar S, Aquino-Parsons C, Stanbridge EJ, et al. Reduced expression of hypoxia-inducible factor-1alpha in perinecrotic regions of solid tumors. *Cancer Res.* 2005;65:7259–7266. Courtesy of Dr. Peggy Olive.)

REOXYGENATION

Van Putten and Kallman determined the proportion of hypoxic cells in a transplantable sarcoma in the mouse. This tumor, which was of spontaneous origin, was transplanted from one generation of animals to the next by inoculating a known number of tumor cells subcutaneously. The tumor was allowed to grow for 2 weeks, by which time it had reached a size suitable for the experiment. The tumor was irradiated *in vivo* and then excised and made into a suspension of cells. The proportion of hypoxic cells was determined by the method described in [Figure 6.11](#).

The researchers found that for this mouse sarcoma, the proportion of hypoxic cells in the untreated tumor was about 14%. The vital contribution made by Van Putten and Kallman involved a determination of the proportion of hypoxic cells in this tumor after various fractionated radiation treatments. When groups of tumors were exposed to five daily doses of 1.9 Gy delivered Monday through Friday, the proportion of hypoxic cells was determined on the following Monday to be 18%. In another experiment, four daily fractions were given Monday through Thursday, and the proportion of hypoxic cells measured the following day, Friday, was found to be 14%.

These experiments have far-reaching implications in radiotherapy. The fact that the proportion of hypoxic cells in the tumor is about the same at the end of a fractionated radiotherapy regimen as in the untreated tumor demonstrates that during the course of the treatment, some hypoxic cells become oxygenated. If this were not the case, then the *proportion* of hypoxic cells would increase during the course of the fractionated treatment because the radiation depopulates the aerated cell compartment more than the hypoxic cell compartment. This phenomenon, by which hypoxic cells become oxygenated after a dose of radiation, is termed **reoxygenation**. The oxygen status of cells in a tumor is not static; it is dynamic and constantly changing.

The process of reoxygenation is illustrated in [Figure 6.13](#). A modest dose of x-rays to a mixed population of aerated and hypoxic cells results in significant killing of aerated cells but little killing of hypoxic cells. Consequently, the viable cell population immediately after irradiation is dominated by hypoxic cells. If sufficient time is allowed before the next radiation dose, the process of reoxygenation restores the proportion of hypoxic cells to about 15%. If this process is repeated many times, the tumor cell population is depleted, despite the intransigence to killing by x-rays of the cells deficient in oxygen. In other words, if reoxygenation is efficient between dose fractions, the presence of hypoxic cells does not have a significant effect on the outcome of a multifraction regimen.

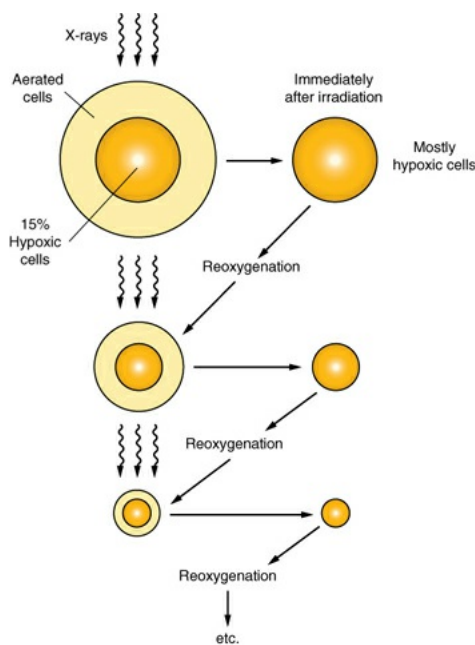


FIGURE 6.13 The process of reoxygenation. Tumors contain a mixture of aerated and hypoxic cells. A dose of x-rays kills a greater proportion of aerated cells than hypoxic cells because aerated cells are more radiosensitive. Therefore,

immediately after irradiation, most cells in the tumor are hypoxic. However, the preirradiation pattern tends to return because of reoxygenation. If the radiation is given in a series of fractions separated in time sufficient for reoxygenation to occur, the presence of hypoxic cells does not greatly influence the response of the tumor.

TIME SEQUENCE OF REOXYGENATION

In the particular tumor system used by Van Putten and Kallman, the proportion of hypoxic cells returned to its original pretreatment level by 24 hours after delivery of a fractionated dosage schedule. Kallman and Bleehen reported experiments in which the proportion of hypoxic cells in the same transplantable mouse sarcoma was determined at various times after delivery of a single dose of 10 Gy. Their results are shown in [Figure 6.14](#); the shape of the curve indicates that in this particular tumor, the process of reoxygenation is very rapid indeed.

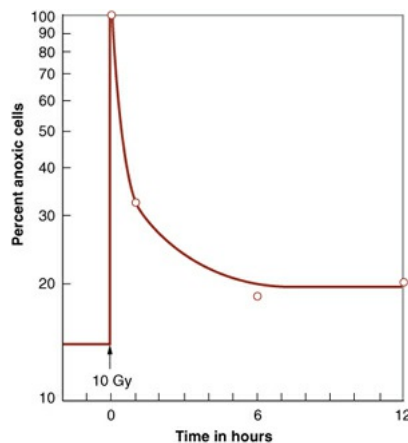


FIGURE 6.14 Percentage of hypoxic cells in a transplantable mouse sarcoma as a function of time after a dose of 10 Gy of x-rays. Immediately after irradiation, essentially 100% of the viable cells are hypoxic because such a dose kills a large proportion of the aerated cells. In this tumor, the process of reoxygenation is very rapid. By 6 hours after irradiation, the percentage of hypoxic cells has fallen to a value close to the preirradiation level. (Adapted from Kallman RF, Bleehen NM. Post-irradiation cyclic radiosensitivity changes in tumors and normal tissues. In: *Proceedings of the Symposium on Dose Rate in Mammalian Radiobiology*; April 28–May 1, 1968; Oak Ridge, TN, with permission.)

Similar results subsequently have been reported by several researchers using various tumor systems. The patterns of reoxygenation after irradiation observed in several different animal tumor systems are summarized in [Figure 6.15](#). Four of the five animal tumors show efficient and rapid reoxygenation, with the proportion of hypoxic cells returning to or even falling below the pretreatment

level in a day or two. The time sequence, however, is not the same for the five types of tumors. In particular, the mammary carcinoma investigated by Howes shows a minimum proportion of hypoxic cells that is very much lower than that characteristic of the unirradiated tumor. This point is reached 3 days after the delivery of a single large dose of radiation. The only one of the five tumors that does not show any significant rapid reoxygenation is the osteosarcoma studied by Van Putten, also illustrated in [Figure 6.15](#).

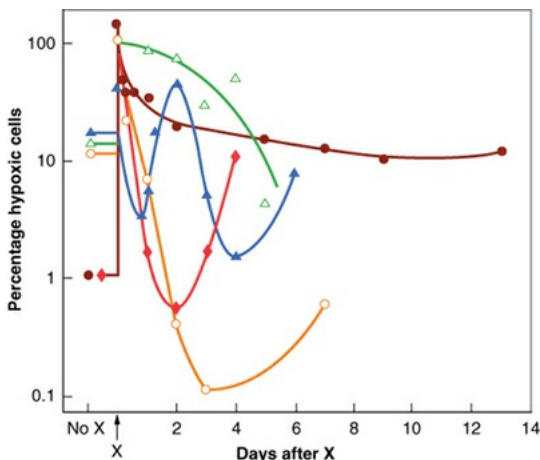


FIGURE 6.15 The proportion of hypoxic cells as a function of time after irradiation with a large dose of x-rays for five transplanted tumors in experimental animals. *Open circles* indicate mouse mammary carcinoma that reoxygenates rapidly and well (data from Howes). *Closed triangles* indicate rat sarcoma that shows two waves of reoxygenation (data from Thomlinson). *Open triangles* show mouse osteosarcoma that does not reoxygenate at all for several days and then only slowly (data from Van Putten). *Closed circles* indicate mouse fibrosarcoma that reoxygenates quickly but not as completely as the mammary carcinoma (data from Dorie and Kallman). *Closed diamonds* indicate mouse fibrosarcoma that reoxygenates quickly and well (data from Kummermehr, Preuss-Bayer, and Trott). The extent and rapidity of reoxygenation are extremely variable and impossible to predict. (Courtesy of Dr. Sara Rockwell.)

MECHANISM OF REOXYGENATION

In experimental animals, some tumors take several days to reoxygenate; in others, the process appears to be complete within 1 hour or so. In a few tumors, both fast and slow components to reoxygenation are evident. The differences of timescale reflect the different types of hypoxia that are being reversed, chronic versus acute. In the long term, a restructuring or a revascularization of the tumor occurs as the cells killed by the radiation are broken down and removed from the population. As the tumor shrinks in size, surviving cells that previously were

beyond the range of oxygen diffusion are closer to a blood supply and so reoxygenate. This slow component of reoxygenation, taking place over a period of days as the tumor shrinks, involves reoxygenation of cells that were *chronically* hypoxic. By contrast, the fast component of reoxygenation, which is complete within hours, is caused by the reoxygenation of acutely hypoxic cells; that is, those cells that were hypoxic at the time of irradiation because they were in regions in which a blood vessel was temporarily closed quickly reoxygenate when that vessel is reopened.

THE IMPORTANCE OF REOXYGENATION IN RADIOTHERAPY

The process of reoxygenation has important implications in practical radiotherapy. If human tumors do in fact reoxygenate as rapidly and efficiently as most of the animal tumors studied, then the use of a multifraction course of radiotherapy, extending over a long period, may well be all that is required to deal effectively with any hypoxic cells in human tumors.

The reoxygenation studies with mouse mammary carcinoma, included in [Figure 6.15](#), indicate that by 2 to 3 days after a dose of radiation, the proportion of hypoxic cells is actually lower than in untreated tumors. Consequently, it was predicted that several large doses of x-rays given at 48-hour intervals would virtually eliminate the problem of hypoxic cells in this tumor. Fowler and his colleagues indeed showed that for the eradication of this tumor, the preferred x-ray schedule was five large doses in 9 days. These results suggest that x-irradiation can be an extremely effective form of therapy but ideally requires a sharply optimal choice of fractionation pattern. Making this choice, however, demands a detailed knowledge of the time course of reoxygenation in the particular tumor to be irradiated. Unfortunately, however, this information is available for only a few animal tumors and is impossible to obtain at present for human tumors. Indeed, in humans, it is not known with certainty whether any or all tumors reoxygenate, although the evidence from radiotherapy clinics that many tumors are eradicated with doses on the order of 60 Gy given in 30 treatments argues strongly in favor of reoxygenation because the presence of a very small proportion of hypoxic cells would make “cures” unlikely at these dose levels. It is an attractive hypothesis that some of the human tumors that do not respond to conventional radiotherapy are those that do not reoxygenate quickly and efficiently.

HYPOXIA AND CHEMORESISTANCE

Hypoxia can also decrease the efficacy of some chemotherapeutic agents owing to fluctuating blood flow, drug diffusion distance, and decreased proliferation. In addition, some chemotherapeutic agents that induce DNA damage, such as doxorubicin and bleomycin, are less efficient at killing hypoxic tumor cells in part because of decreased free radical generation. Experimental animal studies have shown that 5-fluorouracil, methotrexate, and cisplatin are less effective at killing hypoxic cells than they are at killing normoxic tumor cells. Furthermore, hypoxic tumor regions are frequently associated with a low pH that can also diminish the activity of some chemotherapy agents. (For more about chemotherapy agents and hypoxia, see [Chapter 27](#).)

HYPOXIA AND TUMOR PROGRESSION

Evidence that low-oxygen conditions play an important role in malignant progression comes from studies of the correlation between tumor oxygenation and treatment outcome in patients as well as from laboratory studies in cells and animals. A clinical study in Germany in the 1990s showed a correlation between local control in advanced carcinoma of the cervix treated by radiotherapy and oxygen probe measurements. Specifically, patients in whom the probe measurements indicated pO₂ values greater than 10 mm Hg did better than those with pO₂ values less than 10 mm Hg. This suggested that the presence of hypoxic cells limited the success of radiotherapy. Later studies, however, indicated a similar improvement in outcome for patients with better oxygenated tumors if the treatment was by surgery rather than radiotherapy. This suggests that the correct interpretation is that hypoxia is a general indicator of tumor aggression in these patients rather than the initial view that hypoxia conferred radioresistance on some cells. A Canadian study supported the concept that hypoxia drove malignant progression of cervical carcinomas in node-negative patients, as most of the failures occurred in the poorly oxygenated tumors with distant tumor spread outside the pelvis.

Studies carried out in the United States on patients receiving radiotherapy for soft tissue sarcoma highlighted the correlation between tumor oxygenation and the frequency of distant metastases. Seventy percent of those patients with pO₂ values less than 10 mm Hg developed distant metastases versus 35% of those with pO₂ values greater than 10 mm Hg. This study is particularly compelling because the primary tumor was eradicated in all patients regardless of the level of oxygenation; only the incidence of metastases varied between high and low pO₂ values. These data were subsequently confirmed in a Danish study in which

28 patients with soft tissue sarcoma exhibited an increased risk of metastatic spread if they possessed low tumor pO₂ values. This argues strongly that the level of tumor oxygenation influences the aggressiveness of the tumor. This topic is discussed further in [Chapter 26](#).

SUMMARY OF PERTINENT CONCLUSIONS

The presence or absence of molecular oxygen dramatically influences the biologic effect of x-rays.

The OER is the ratio of doses under hypoxic to aerated conditions that produce the same biologic effect.

The OER for x-rays is about 3 at high doses and is possibly lower (about 2) at doses less than about 2 Gy.

The OER decreases as linear energy transfer increases. The OER approaches unity (i.e., no oxygen effect) for α -particles. For neutrons, the OER has an intermediate value of about 1.6.

To produce its effect, molecular oxygen must be present during the radiation exposure or at least during the lifetime of the free radicals generated by the radiation.

Oxygen “fixes” (i.e., makes permanent) the damage produced by free radicals. In the absence of oxygen, damage produced by the indirect action may be repaired.

Only a small quantity of oxygen is required for radiosensitization; 0.5% oxygen (pO₂ of about 3 mm Hg) results in a radiosensitivity halfway between hypoxia and full oxygenation.

There are two forms of hypoxia that are the consequence of different mechanisms: chronic hypoxia and acute hypoxia.

Chronic hypoxia results from the limited diffusion range of oxygen through respiring tissue.

Acute hypoxia is a result of the temporary closing of tumor blood vessels and is therefore transient.

In either case, there may be cells present during irradiation that are at a sufficiently low oxygen tension to be intransigent to killing by x-rays but high enough to be viable.

Most transplantable tumors in animals have been shown to contain hypoxic

cells that limit curability by single doses of x-rays. Hypoxic fractions vary from 0% to 50%, with a tendency to average about 15%.

There is strong evidence that human tumors contain hypoxic cells. This evidence includes histologic appearance, oxygen probe measurements, the binding of nitroimidazoles, PET and SPECT studies, and pretreatment hemoglobin levels.

Oxygen probes with fast response times, implanted in a tumor and moving quickly under computer control, may be used to obtain the oxygen profile of a tumor.

Hypoxia in tumors can be visualized by the use of hypoxia markers such as pimonidazole or HIFs.

Reoxygenation is the process by which cells that are hypoxic at the time of irradiation become oxygenated afterward.

The extent of reoxygenation and the rapidity with which it occurs vary widely for different experimental animal tumors.

If reoxygenation is rapid and complete, hypoxic cells have little influence on the outcome of a fractionated radiation schedule.

The “slow” component is caused by the reoxygenation of *chronically* hypoxic cells as the tumor shrinks. The “fast” component of reoxygenation is caused by the reoxygenation of acutely hypoxic cells as tumor blood vessels open and close.

Reoxygenation cannot be measured in human tumors, but presumably it occurs, at least in those tumors controlled by conventional fractionated radiotherapy.

There is clinical evidence that in addition to causing radioresistance, hypoxia may play an important role in malignant progression and in metastasis.

BIBLIOGRAPHY

Barendsen GW, Koot CJ, van Kersen GR, et al. The effect of oxygen on impairment of the proliferative capacity of human cells in culture by ionizing radiations of different LET. *Int J Radiat Biol Relat Stud Phys Chem Med.* 1966;10:317–327.

Brizel DM, Scully SP, Harrelson JM, et al. Tumor oxygenation predicts for the likelihood of distant metastases in human soft tissue sarcoma. *Cancer Res.*

1996;56:941–943.

Broerse JJ, Barendsen GW, van Kersen GR. Survival of cultured human cells after irradiation with fast neutrons of different energies in hypoxic and oxygenated conditions. *Int J Radiat Biol Relat Stud Phys Chem Med*. 1968;13:559–572.

Brown JM. Evidence for acutely hypoxic cells in mouse tumours, and a possible mechanism of reoxygenation. *Br J Radiol*. 1979;52:650–656.

Brown JM. Tumor hypoxia, drug resistance, and metastases. *J Natl Cancer Inst*. 1990;82:338–339.

Brown JM, Giaccia AJ. The unique physiology of solid tumors: opportunities (and problems) for cancer therapy. *Cancer Res*. 1998;58:1408–1416.

Chaplin DJ, Durand RE, Olive PL. Acute hypoxia in tumors: implications for modifiers of radiation effects. *Int J Radiat Oncol Biol Phys*. 1986;12:1279–1282.

Chaplin DJ, Olive PL, Durand RE. Intermittent blood flow in a murine tumor: radiobiological effects. *Cancer Res*. 1987;47:597–601.

Crabtree HG, Cramer W. Action of radium on cancer cells: some factors affecting susceptibility of cancer cells to radium. *Proc R Soc Lond B Biol Sci*. 1933;113:238–250.

Crabtree HG, Cramer W. The action of radium on cancer cells: I. Effects of hydrocyanic acid, iodoacetic acid, and sodium fluoride on the metabolism and transplantability of cancer cells. *Sci Rep Imp Cancer Res Fund*. 1934;11:75.

Denekamp J. Cytotoxicity and radiosensitization in mouse and man. *Br J Radiol*. 1978;51:636–637.

Denekamp J. Discussion in session on effects of radiation on mammalian cell populations. Paper presented at: Conference on Time and Dose Relationships in Radiation Biology as Applied to Radiotherapy; September 15–18, 1969; Carmel, CA.

Denekamp J, Fowler JF, Dische S. The proportion of hypoxic cells in a human tumor. *Int J Radiat Oncol Biol Phys*. 1977;2:1227–1228.

Deschner EE, Gray LH. Influence of oxygen tension on x-ray-induced chromosomal damage in Ehrlich ascites tumor cells irradiated in vitro and in vivo. *Radiat Res*. 1959;11:115–146.

Elkind MM, Swain RW, Alescio T, et al. Oxygen, nitrogen, recovery and radiation therapy. In: Shalek R, ed. *Cellular Radiation Biology*. Baltimore, MD: Williams & Wilkins; 1965:442–466.

Fowler JF. Review of the proceedings of session V: reoxygenation of tumour tissues. Paper presented at: Conference on Time and Dose Relationships in Radiation Biology as Applied to Radiotherapy; September 15–18, 1969; Carmel, CA.

Grau C, Overgaard J. Effect of etoposide, carmustine, vincristine, 5-fluorouracil, or methotrexate on radiobiologically oxic and hypoxic cells in a C3H mouse mammary carcinoma *in situ*. *Cancer Chemother Pharmacol*. 1992;30:277–280.

Gray LH, Conger AD, Ebert M, et al. The concentration of oxygen dissolved in tissues at the time of irradiation as a factor in radiotherapy. *Br J Radiol*. 1953;26:638–648.

Groebe K, Vaupel P. Evaluation of oxygen diffusion distances in human breast cancer xenografts using tumor-specific *in vivo* data: role of various mechanisms in the development of tumor hypoxia. *Int J Radiat Oncol Biol Phys*. 1988;15:691–697.

Hill RP, Bush RS, Yeung P. The effect of anaemia on the fraction of hypoxic cells in an experimental tumour. *Br J Radiol*. 1971;44:299–304.

Hockel M, Schlenger K, Aral B, et al. Association between tumor hypoxia and malignant progression in advanced cancer of the uterine cervix. *Cancer Res*. 1996;56:4509–4515.

Holthusen H. Beitrage zur Biologie der Strahlenwirkung. *Pflugers Arch*. 1921;187:1–24.

Howard-Flanders P, Alper T. The sensitivity of microorganisms to irradiation under controlled gas conditions. *Radiat Res*. 1957;7:518–540.

Howard-Flanders P, Moore D. The time interval after pulsed irradiation within which injury to bacteria can be modified by dissolved oxygen: I. A search for an effect of oxygen 0.02 second after pulsed irradiation. *Radiat Res*. 1958;9:422–437.

Howes AE. An estimation of changes in the proportions and absolute numbers of hypoxic cells after irradiation of transplanted C3H mouse mammary tumors. *Br J Radiol*. 1969;42:441–447.

- Kallman RF. The phenomenon of reoxygenation and its implication for fractionated radiotherapy. *Radiology*. 1972;105:135–142.
- Kallman RF, Bleehen NM. Post-irradiation cyclic radiosensitivity changes in tumors and normal tissues. In: *Proceedings of the Symposium on Dose Rate in Mammalian Radiobiology*; April 28–May 1, 1968; Oak Ridge, TN.
- Kallman RF, Jardine LJ, Johnson CW. Effects of different schedules of dose fractionation on the oxygenation status of a transplantable mouse sarcoma. *J Natl Cancer Inst*. 1970;44:369–377.
- Michael BD, Adams GE, Hewitt HB, et al. A posteffect of oxygen in irradiated bacteria: a submillisecond fast mixing study. *Radiat Res*. 1973;54:239–251.
- Milosevic M, Fyles A, Hedley D, et al. The human tumor microenvironment: invasive (needle) measurement of oxygen and interstitial fluid pressure. *Semin Radiat Oncol*. 2004;14:249–258.
- Mottram JC. Factor of importance in radiosensitivity of tumours. *Br J Radiol*. 1936;9:606–614.
- Mottram JC. On the action of beta and gamma rays of radium on the cell in different states of nuclear division. *Rep Cancer Labs (Middlesex Hospital, London)*. 1913:30–98.
- Moulder JE, Rockwell S. Hypoxic fractions of solid tumors: experimental techniques, methods of analysis, and a survey of existing data. *Int J Radiat Oncol Biol Phys*. 1984;10:695–712.
- Palcic B, Skarsgard LD. Reduced oxygen enhancement ratio at low doses of ionizing radiation. *Radiat Res*. 1984;100:328–339.
- Petry E. Zur Kenntnis der Bedingungen der biologischen Wirkung der Rontgenstrahlen. *Biochem Zeitschr*. 1923;135:353–383.
- Powers WE, Tolmach LJ. A multicomponent x-ray survival curve for mouse lymphosarcoma cells irradiated in vivo. *Nature*. 1963;197:710–711.
- Read J. Mode of addition of x-ray doses given with different oxygen concentrations. *Br J Radiol*. 1952;25:336–338.
- Read J. The effect of ionizing radiations on the broad bean root: I. The dependence of the alpha ray sensitivity on dissolved oxygen. *Br J Radiol*. 1952;25:651–661.
- Read J. The effect of ionizing radiations on the broad bean root: X. The

- dependence of the x-ray sensitivity of dissolved oxygen. *Br J Radiol.* 1952;25:89–99.
- Reinhold HS. The post-irradiation behaviour of transplantable solid tumors in relation to the regional oxygenation. In: Turano L, Ratti A, Biagini C, eds. *Progress in Radiology*. Vol 2. Amsterdam, The Netherlands: Excerpta Medica; 1967:1482–1486.
- Rockwell S, Moulder JE. Biological factors of importance in split-course radiotherapy. In: Paliwal BR, Herbert DE, Orton CG, eds. *Optimization of Cancer Radiotherapy*. New York, NY: American Institute of Physics; 1985:171–182.
- Secomb TW, Hsu R, Ong ET, et al. Analysis of the effects of oxygen supply and demand on hypoxic fraction in tumors. *Acta Oncol.* 1995;34:313–316.
- Sobhanifar S, Aquino-Parsons C, Stanbridge EJ, et al. Reduced expression of hypoxia-inducible factor-1alpha in perinecrotic regions of solid tumors. *Cancer Res.* 2005;65:7259–7266.
- Thomlinson RH. Changes of oxygenation in tumors in relation to irradiation. *Front Radiat Ther Oncol.* 1968;3:109–121.
- Thomlinson RH. Reoxygenation as a function of tumor size and histopathological type. Paper presented at: Conference on Time and Dose Relationships in Radiation Biology as Applied to Radiotherapy; September 15–18, 1969; Carmel, CA.
- Thomlinson RH, Gray LH. The histological structure of some human lung cancers and the possible implications for radiotherapy. *Br J Cancer.* 1955;9:539–549.
- Van Putten LM. Oxygenation and cell kinetics after irradiation in a transplantable osteosarcoma. *Eff Radiat Cell Prolif Differ.* 1968;1968:493–505.
- Van Putten LM. Tumour reoxygenation during fractionated radiotherapy: studies with a transplantable osteosarcoma. *Eur J Cancer.* 1968;4:172–182.
- Van Putten LM, Kallman RF. Oxygenation status of a transplantable tumor during fractionated radiation therapy. *J Natl Cancer Inst.* 1968;40:441–451.
- Wright EA, Howard-Flanders P. The influence of oxygen on the radiosensitivity of mammalian tissues. *Acta Radiol.* 1957;48:26–32.

chapter 7

Linear Energy Transfer and Relative Biologic Effectiveness

The Deposition of Radiant Energy

Linear Energy Transfer

Relative Biologic Effectiveness

Relative Biologic Effectiveness and Fractionated Doses

Relative Biologic Effectiveness for Different Cells and Tissues

Relative Biologic Effectiveness as a Function of Linear Energy Transfer

The Optimal Linear Energy Transfer

Factors that Determine Relative Biologic Effectiveness

The Oxygen Effect and Linear Energy Transfer

Radiation Weighting Factor

Summary of Pertinent Conclusions

Bibliography

THE DEPOSITION OF RADIANT ENERGY

If radiation is absorbed in biologic material, ionizations and excitations occur that are not distributed at random but tend to be localized along the tracks of individual charged particles in a pattern that depends on the type of radiation involved. For example, x-ray photons give rise to fast electrons, particles carrying unit electrical charge and having very small mass; neutrons, on the other hand, give rise to recoil protons, particles again carrying unit electrical charge but having mass nearly 2,000 times greater than that of the electron. α -Particles carry two electrical charges on a particle 4 times as heavy as a proton. The charge-to-mass ratio for α -particles therefore differs from that for electrons by a factor of about 8,000.

As a result, the spatial distribution of the ionizing events produced by different particles varies enormously. This is illustrated in Figure 7.1. The

background is an electron micrograph of a human liver cell. The white dots generated by a computer simulate ionizing events. The lowest track represents a low-energy electron, such as might be set in motion by diagnostic x-rays. The primary events are well separated in space, and for this reason, x-rays are said to be *sparsely ionizing*. The second track from the bottom represents an electron set in motion by cobalt-60 γ -rays, which is even more sparsely ionizing. For a given particle type, the density of ionization decreases as the energy goes up. The third track from the bottom represents a proton that might be set in motion by a fission spectrum neutron from a nuclear reactor; a dense column of ionization is produced, so the radiation is referred to as *densely ionizing*. The uppermost track refers to a 10-MeV proton, such as may be set in motion by the high-energy neutrons used for radiotherapy. The track is intermediate in ionization density.

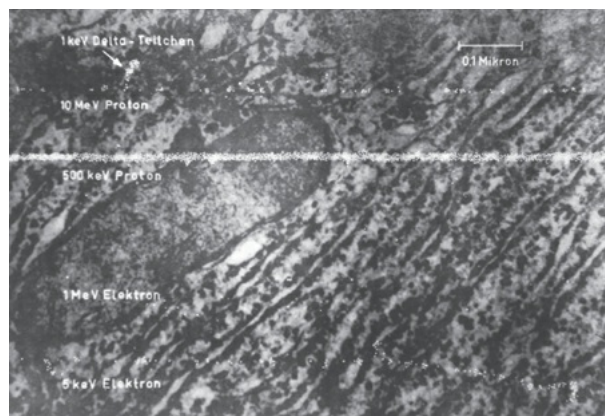


FIGURE 7.1 Variation of ionization density associated with different types of radiation. The background is an electron micrograph of a human cell. The white dots are a computer simulation representing ionizations. **Top to bottom:** A 10-MeV proton, typical of the recoil protons produced by high-energy neutrons used for radiotherapy. The track is intermediate in ionization density. Also shown is a secondary 1-keV δ -ray, an electron set in motion by the proton. A 500-keV proton, produced by lower energy neutrons (e.g., from fission spectrum) or by higher energy neutrons after multiple collisions. The ionizations form a dense column along the track of the particle. A 1-MeV electron, produced, for example, by cobalt-60 γ -rays. This particle is very sparsely ionizing. A 5-keV electron, typical of secondary electrons produced by x-rays of diagnostic quality. This particle is also sparsely ionizing but a little denser than the higher energy electron. (Courtesy of Dr. Albrecht Kellerer.)

LINEAR ENERGY TRANSFER

Linear energy transfer (LET) is the energy transferred per unit length of the track. The special unit usually used for this quantity is kiloelectron volt per

micrometer ($\text{keV}/\mu\text{m}$) of unit density material. In 1962, the International Commission on Radiological Units defined this quantity as follows:

The LET (L) of charged particles in medium is the quotient of dE/dl , where dE is the average energy locally imparted to the medium by a charged particle of specified energy in traversing a distance of dl .

That is,

$$L = dE/dl$$

LET is an average quantity because at the microscopic level, the energy per unit length of track varies over such a wide range. Indeed, the range is so large that some believe that the concept of LET has little meaning. This can be illustrated by the story of a Martian visitor to Earth who arrives knowing that the Earth is inhabited by living creatures with an average mass of 1 g. Not only is this information of very little use, but it also may be positively misleading, particularly if the first living creature that the Martian encounters is an elephant. An average quantity has little meaning if individual variation is great.

The situation for LET is further complicated by the fact that it is possible to calculate an average in many different ways. The most commonly used method is to calculate the **track average**, which is obtained by dividing the track into equal lengths, calculating the energy deposited in each length, and finding the mean. The **energy average** is obtained by dividing the track into equal energy increments and averaging the lengths of track over which these energy increments are deposited. These methods are illustrated in [Figure 7.2](#).

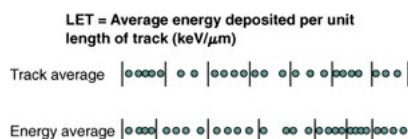


FIGURE 7.2 Linear energy transfer (LET) is the average energy deposited per unit length of track. The track average is calculated by dividing the track into equal lengths and averaging the energy deposited in each length. The energy average is calculated by dividing the track into equal energy intervals and averaging the lengths of the track that contain this amount of energy. The method of averaging makes little difference for x-rays or for monoenergetic charged particles, but the track average and energy average are different for neutrons.

In the case of either x-rays or monoenergetic charged particles, the two methods of averaging yield similar results. In the case of 14-MeV neutrons, by contrast, the track average LET is about $12 \text{ keV}/\mu\text{m}$ and the energy average LET

is about 100 keV/ μ m. The biologic properties of neutrons tend to correlate best with the energy average.

As a result of these considerations, LET is a quantity condemned by the purists as worse than useless because it can, in some circumstances, be very misleading. It is, however, useful as a simple and naive way to indicate the quality of different types of radiation. Typical LET values for various radiations are listed in [Table 7.1](#). Included are x- and γ -rays used for radiotherapy, protons, neutrons, and naturally occurring α -particles as well as high-energy heavy ions encountered by astronauts in space. Note that for a given type of charged particle, the higher the energy, the lower the LET and, therefore, the lower its biologic effectiveness. At first sight, this may be counterintuitive. For example, γ - and x-rays both give rise to fast secondary electrons; therefore, 1.1-MV cobalt-60 γ -rays have lower LETs than 250-kV x-rays and are less effective biologically by about 10%. By the same token, 150-MeV protons have lower LETs than 10-MeV protons and therefore are slightly less effective biologically.

Table 7.1 Typical Linear Energy Transfer Values

RADIATION	LINEAR ENERGY TRANSFER, KEV/ μ M
Cobalt-60 γ -rays	0.2
250-kV x-rays	2.0
10-MeV protons	4.7
150-MeV proton	0.5
Track average	—
	Energy average

14-MeV neutrons	12	—	100
2.5-MeV α -particles	—	166	—
2-GeV Fe ions (space radiation)	—	1,000	—

RELATIVE BIOLOGIC EFFECTIVENESS

The amount or quantity of radiation is expressed in terms of the **absorbed dose**, a physical quantity with the unit of gray (Gy). Absorbed dose is a measure of the energy absorbed per unit mass of tissue. Equal doses of different types of radiation do not, however, produce equal biologic effects. For example, 1 Gy of neutrons produces a greater biologic effect than 1 Gy of x-rays. The key to the difference lies in the pattern of energy deposition at the microscopic level.

In comparing different radiations, it is customary to use x-rays as the standard. The National Bureau of Standards in 1954 defined **relative biologic effectiveness (RBE)** as follows.

The RBE of some test radiation (r) compared with x-rays is defined by the ratio D_{250}/D_r , where D_{250} and D_r are, respectively, the doses of x-rays and the test radiation required for equal biologic effect.

To measure the RBE of some test radiation, one first chooses a biologic system in which the effect of radiations may be scored quantitatively. To illustrate the process involved, we discuss a specific example. Suppose we are measuring the RBE of fast neutrons compared with 250-kV x-rays, using the lethality of plant seedlings as a test system. Groups of plants are exposed to graded doses of x-rays; parallel groups are exposed to a range of neutron doses. At the end of the period of observation, it is possible to calculate the doses of x-rays and then of neutrons that result in the death of half of the plants in a group. This quantity is known as the LD₅₀, the mean lethal dose. Suppose that for x-rays, the LD₅₀ turns out to be 6 Gy, and that for neutrons, the corresponding quantity is 4 Gy. The RBE of neutrons compared with x-rays is then simply the ratio 6:4 or 1.5.

The study of RBE is relatively straightforward so long as a test system with a single, unequivocal end point is used. It becomes more complicated if, instead, a test system such as the response of mammalian cells in culture is chosen. [Figure 7.3A](#) shows survival curves obtained if mammalian cells in cultures are exposed to a range of doses of, on the one hand, fast neutrons and, on the other hand, 250-kV x-rays. The RBE may now be calculated from these survival curves as the ratio of doses that produce the same biologic effect. If the end point chosen for comparison is the dose required to produce a surviving fraction of 0.01, then the dose of neutrons necessary is 6.6 Gy; the corresponding dose of x-rays is 10 Gy. The RBE, then, is the quotient of 10/6.6 or about 1.5. If the comparison is made at a surviving fraction of 0.6, however, the neutron dose required is only 1 Gy and the corresponding x-ray dose is 3 Gy. The resultant RBE is 3:1 or 3.0. Because the x-ray and neutron survival curves have different shapes, the x-ray survival curve having an initial shoulder, and the neutron curve being an exponential function of dose, the resultant RBE depends on the level of biologic damage (and therefore the dose) chosen. The RBE generally increases as the dose is decreased, reaching a limiting value that is the ratio of the initial slopes of the x-ray and neutron survival curves.

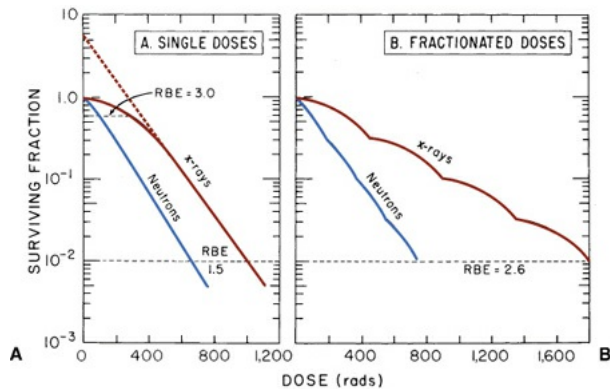


FIGURE 7.3 Typical survival curves for mammalian cells exposed to x-rays and fast neutrons. **A:** Single doses. The survival curve for x-rays has a large initial shoulder; for fast neutrons, the initial shoulder is smaller and the final slope is steeper. Because the survival curves have different shapes, the relative biologic effectiveness (RBE) does not have a unique value but varies with dose, getting larger as the size of the dose is reduced. **B:** Fractionated doses. The effect of giving doses of x-rays or fast neutrons in four equal fractions to produce the same level of survival as in **A**. The shoulder of the survival curves is re-expressed after each dose fraction; the fact that the shoulder is larger for x-rays than for neutrons results in an enlarged RBE for fractionated treatments.

RELATIVE BIOLOGIC EFFECTIVENESS AND

FRACTIONATED DOSES

Because the RBE of more densely ionizing radiations, such as neutrons, varies with the dose per fraction, the RBE for a fractionated regimen with neutrons is greater than for a single exposure because a fractionated schedule consists of several small doses and the RBE is large for small doses.

[Figure 7.3B](#) illustrates a hypothetical treatment with neutrons consisting of four fractions. For a surviving fraction of 0.01, the RBE for neutrons relative to x-rays is about 2.6. The RBE for the same radiations in [Figure 7.3A](#) at the same level of survival was about 1.5 because only single exposures were involved. This is a direct consequence of the larger shoulder that is characteristic of the x-ray curve, which must be repeated for each fraction. The width of the shoulder represents a part of the dose that is “wasted”; the larger the number of fractions, the greater the extent of the wastage. By contrast, the neutron survival curve has little or no shoulder, so there is correspondingly less wastage of dose from fractionation. The net result is that neutrons become progressively more efficient than x-rays as the dose per fraction is reduced and the number of fractions is increased. The same is true, of course, for exposure to continuous low-dose-rate irradiation. The neutron RBE is larger at a low dose rate than for an acute exposure because the effectiveness of neutrons decreases with dose rate to a much smaller extent than is the case for x- or γ -rays. Indeed, for low-energy neutrons, there is no loss of effectiveness.

RELATIVE BIOLOGIC EFFECTIVENESS FOR DIFFERENT CELLS AND TISSUES

Even for a given total dose or dose per fraction, the RBE varies greatly according to the tissue or cell line studied. Different cells or tissues are characterized by x-ray survival curves that have large but variable shoulder regions, whereas the shoulder region for neutrons is smaller and less variable. As a consequence, the RBE is different for each cell line. In general, cells characterized by an x-ray survival curve with a large shoulder, indicating that they can accumulate and repair a large amount of sublethal radiation damage, show larger RBEs for neutrons. Conversely, cells for which the x-ray survival curve has *little if any shoulder* exhibit smaller neutron RBE values.

RELATIVE BIOLOGIC EFFECTIVENESS AS A FUNCTION OF LINEAR ENERGY TRANSFER

Figure 7.4 illustrates the survival curves obtained for 250-kVp x-rays, 15-MeV neutrons, and 4-MeV α -particles. As the LET increases from about 2 keV/ μm for x-rays up to 150 keV/ μm for α -particles, the survival curve changes in two important respects. First, the survival curve becomes steeper. Second, the shoulder of the curve becomes progressively smaller as the LET increases. A more common way to represent these data is to plot the RBE as a function of LET (Fig. 7.5). As the LET increases, the RBE increases slowly at first and then more rapidly as the LET increases beyond 10 keV/ μm . Between 10 and 100 keV/ μm , the RBE increases rapidly with increasing LET and, in fact, reaches a maximum at about 100 keV/ μm . Beyond this value for the LET, the RBE again falls to lower values. This is an important effect and is explained in more detail in the next section.

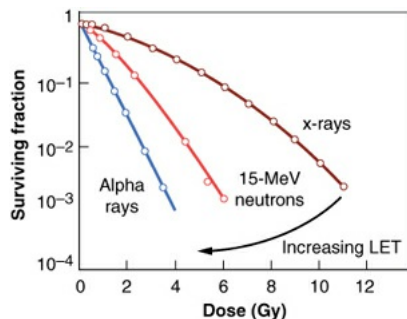


FIGURE 7.4 Survival curves for cultured cells of human origin exposed to 250-kVp x-rays, 15-MeV neutrons, and 4-MeV α -particles. As the linear energy transfer (LET) of the radiation increases, the slope of the survival curves gets steeper and the size of the initial shoulder gets smaller. (Adapted from Broerse JJ, Barendsen GW, van Kersen GR. Survival of cultured human cells after irradiation with fast neutrons of different energies in hypoxic and oxygenated conditions. *Int J Radiat Biol Relat Stud Phys Chem Med*. 1968;13:559–572, and Barendsen GW. Responses of cultured cells, tumors, and normal tissues to radiation of different linear energy transfer. *Curr Top Radiat Res Q*. 1968;4:293–356, with permission.)

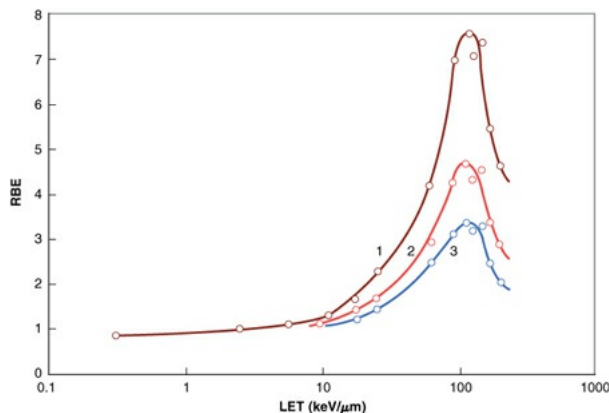


FIGURE 7.5 Variation of relative biologic effectiveness (RBE) with linear energy transfer (LET) for survival of mammalian cells of human origin. The RBE rises to a maximum at an LET of about $100 \text{ keV}/\mu\text{m}$ and subsequently falls for higher values of LET. Curves 1, 2, and 3 refer to cell survival levels of 0.8, 0.1, and 0.01, respectively, illustrating that the absolute value of the RBE is not unique but depends on the level of biologic damage and, therefore, on the dose level. (Adapted from Barendsen GW. Responses of cultured cells, tumors, and normal tissues to radiation of different linear energy transfer. *Curr Top Radiat Res Q.* 1968;4:293–356, with permission.)

The LET at which the RBE reaches a peak is much the same (about $100 \text{ keV}/\mu\text{m}$) for a wide range of mammalian cells, from mouse to human, and is the same for mutation as an end point as for cell killing.

THE OPTIMAL LINEAR ENERGY TRANSFER

It is of interest to ask why radiation with an LET of about $100 \text{ keV}/\mu\text{m}$ is optimal in terms of producing a biologic effect. At this density of ionization, the average separation between ionizing events just about coincides with the diameter of the DNA double helix (20 \AA or 2 nm). Radiation with this density of ionization has the highest probability of causing a double-strand break (DSB) by the passage of a single charged particle, and DSBs are the basis of most biologic effects, as discussed in Chapter 2. This is illustrated in Figure 7.6. In the case of x-rays, which are more sparsely ionizing, the probability of a single track causing a DSB is low, and in general, more than one track is required. As a consequence, x-rays have a low biologic effectiveness. At the other extreme, much more densely ionizing radiations (e.g., with an LET of $200 \text{ keV}/\mu\text{m}$) readily produce DSBs, but energy is “wasted” because the ionizing events are too close together. Because RBE is the ratio of doses producing equal biologic effect, this more densely ionizing radiation has a lower RBE than the optimal LET radiation. The more densely ionizing radiation is just as effective *per track* but less effective per unit dose.

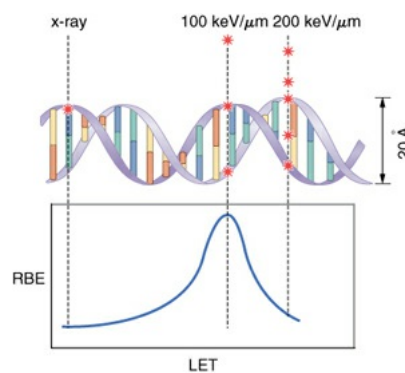


FIGURE 7.6 Diagram illustrating why radiation with a linear energy transfer (LET) of 100 keV/ μm has the greatest relative biologic effectiveness (RBE) for cell killing, mutagenesis, or oncogenic transformation. For this LET, the average separation between ionizing events coincides with the diameter of the DNA double helix (i.e., about 20 Å or 2 nm). Radiation of this quality is most likely to produce a DSB from one track for a given absorbed dose.

It is possible, therefore, to understand why RBE reaches a maximum value in terms of the production of DSBs because the interaction of two DSBs to form an exchange-type aberration is the basis of most biologic effects. In short, the most biologically effective LET is that at which there is a coincidence between the diameter of the DNA helix and the average separation of ionizing events. Radiations having this optimal LET include neutrons of a few hundred kiloelectron volts as well as low-energy protons and α -particles.

FACTORS THAT DETERMINE RELATIVE BIOLOGIC EFFECTIVENESS

The discussion of RBE began with a simple illustration of how this ratio may be determined for neutrons compared with x-rays using a simple biologic test system with a single, unequivocal end point, such as the LD₅₀ for plant seedlings. Under these circumstances, RBE is conceptually very simple. In the years immediately after World War II, it was commonplace to see references to the *RBE* for neutrons as if it were a single, unique quantity.

Now that more information is available from different biologic systems, many of which allow the researcher to investigate the relationship between biologic response and radiation dose rather than observing one end point at a single dose; it is apparent that RBE is a very complex quantity. RBE depends on the following:

- Radiation quality (LET)
- Radiation dose
- Number of dose fractions
- Dose rate
- Biologic system or end point

Radiation quality includes the type of radiation and its energy, whether electromagnetic or particulate, and whether charged or uncharged.

RBE depends on the dose level and the number of dose fractions (or, alternatively, the dose per fraction) because in general, the shape of the dose-response relationship varies for radiations that differ substantially in their LET.

RBE can vary with the dose rate because the slope of the dose-response curve for sparsely ionizing radiations, such as x - or γ -rays, varies critically with a changing dose rate. In contrast, the biologic response to densely ionizing radiations depends little on the rate at which the radiation is delivered.

The biologic system or end point that is chosen has a marked influence on the RBE values obtained. In general, RBE values are high for tissues that accumulate and repair a great deal of sublethal damage and low for those that do not.

THE OXYGEN EFFECT AND LINEAR ENERGY TRANSFER

An important relationship exists between LET and the **oxygen enhancement ratio (OER)**. [Figure 7.7](#) shows mammalian cell survival curves for various types of radiation that have very different LETs and that exhibit very different OERs. [Figure 7.7A](#) refers to x-rays, which are sparsely ionizing, have a low LET, and consequently exhibit a large OER of about 2.5. [Figure 7.7B](#) refers to neutrons, which are intermediate in ionizing density and characteristically show an OER of 1.6. [Figure 7.7D](#) refers to 2.5-MeV α -particles, which are densely ionizing and have a high LET; in this case, survival estimates, whether in the presence or absence of oxygen, fall along a common line, and so the OER is unity. [Figure 7.7C](#) contains data for 4-MeV α -particles, which are slightly less densely ionizing; in this case, the OER is about 1.3.

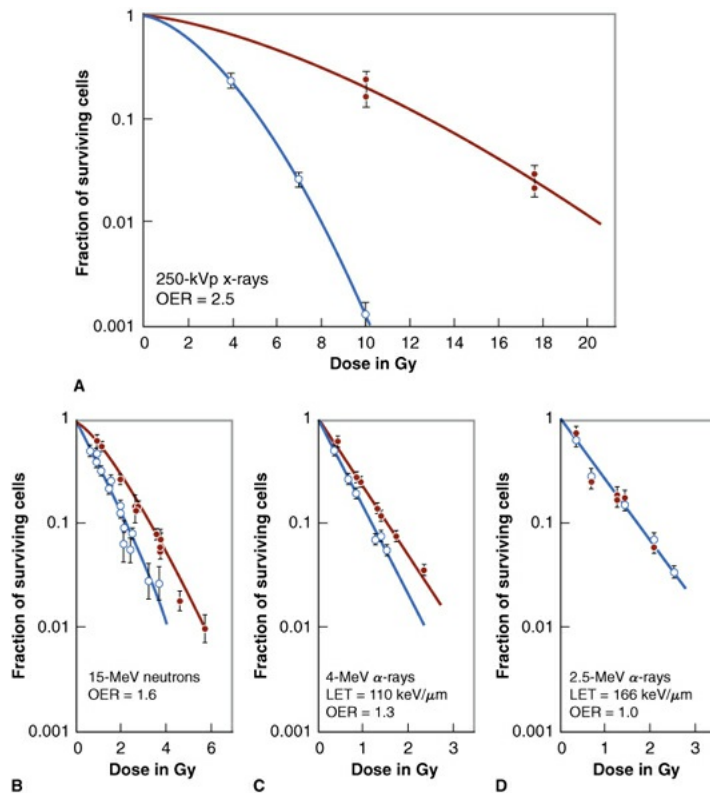


FIGURE 7.7 Survival curves for cultured cells of human origin determined for four different types of radiation. *Open circles* refer to aerated conditions, and *closed circles* to hypoxic conditions. **A:** For 250-kVp x-rays, oxygen enhancement ratio (OER) = 2.5. **B:** For 15-MeV $d^+ \rightarrow T$ neutrons, OER = 1.6. **C:** For 4-MeV α -particles, linear energy transfer (LET) = 110 keV/ μ m, OER = 1.3. **D:** For 2.5-MeV α -particles, LET = 166 keV/ μ m, OER = 1. (Adapted from Broerse JJ, Barendsen GW, van Kersen GR. Survival of cultured human cells after irradiation with fast neutrons of different energies in hypoxic and oxygenated conditions. *Int J Radiat Biol Relat Stud Phys Chem Med*. 1968;13:559–572, and Barendsen GW, Koot CJ, van Kersen GR, et al. The effect of oxygen on impairment of the proliferative capacity of human cells in culture by ionizing radiations of different LET. *Int J Radiat Biol Relat Stud Phys Chem Med*. 1966;10:317–327, with permission.)

Barendsen and his colleagues have used mammalian cells cultured *in vitro* to investigate the OER for a wide range of radiation types. Their results are summarized in Figure 7.8, in which OER is plotted as a function of LET. At low LET, corresponding to x- or γ -rays, the OER is between 2.5 and 3; as the LET increases, the OER falls slowly at first, until the LET exceeds about 60 keV/ μ m, after which the OER falls rapidly and reaches unity by the time the LET has reached about 200 keV/ μ m.

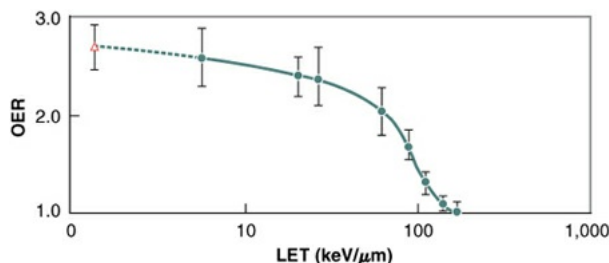


FIGURE 7.8 Oxygen enhancement ratio (OER) as a function of linear energy transfer (LET). Measurements were made with cultured cells of human origin. *Closed circles* refer to monoenergetic charged particles, and the *open triangle* to 250-kVp x-rays with an assumed track average LET of 1.3 keV/μm. (Adapted from Barendsen GW, Koot CJ, van Kersen GR, et al. The effect of oxygen on impairment of the proliferative capacity of human cells in culture by ionizing radiations of different LET. *Int J Radiat Biol Relat Stud Phys Chem Med*. 1966;10:317–327, with permission.)

Both OER and RBE are plotted as a function of LET in Figure 7.9. (The curves are taken from the more complete plots in Figs. 7.5 and 7.8.) Interestingly, the two curves are virtually mirror images of each other. The optimal RBE and the rapid fall of OER occur at about the same LET value (i.e., 100 keV/μm).

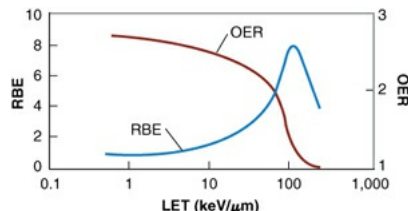


FIGURE 7.9 Variation of the oxygen enhancement ratio (OER) and the relative biologic effectiveness (RBE) as a function of the linear energy transfer (LET) of the radiation involved. The data were obtained using T1 kidney cells of human origin irradiated with various naturally occurring α -particles or with deuterons accelerated in the Hammersmith cyclotron. Note that the rapid increase in RBE and the rapid fall of the OER occur at about the same LET, 100 keV/μm. (Adapted from Barendsen GW. In: *Proceedings of the Conference on Particle Accelerators in Radiation Therapy*. LA-5180-C. Atomic Energy Commission, Technical Information Center; 1972:120–125, with permission.)

RADIATION WEIGHTING FACTOR

Radiations differ in their biologic effectiveness per unit of absorbed dose, as discussed previously. The complexities of RBE are too difficult to apply in specifying dose limits in everyday radiation protection; it is necessary to have a

simpler way to consider differences in biologic effectiveness of different radiations. The term **radiation weighting factor (W_R)** has been introduced for this purpose by International Commission on Radiological Protection (ICRP). The quantity produced by multiplying the absorbed dose by the weighting factor is called the **equivalent dose**. The unit of absorbed dose is the gray, and the unit of equivalent dose is the sievert (Sv). (In the old system of units, the unit of absorbed dose was the rad and the unit of equivalent dose was the rem.)

Radiation weighting factors are chosen by the ICRP based on a consideration of experimental RBE values, biased for biologic end points relevant to radiation protection, such as cancer and heritable effects, and also relevant to low doses and low dose rate. There is a considerable element of judgment involved. The radiation weighting factor is set at unity for all low-LET radiations (x-rays, γ -rays, and electrons), with a value of 20 for maximally effective neutrons and α -particles. Detailed values recommended by the ICRP are discussed in [Chapter 17](#). Using this system, an absorbed dose of 0.1 Gy of α -particles with a radiation weighting factor of 20 would result in an equivalent dose of 2 Sv.

SUMMARY OF PERTINENT CONCLUSIONS

X- and γ -rays are said to be sparsely ionizing because along the tracks of the electrons set in motion, primary ionizing events are well separated in space.

α -Particles and neutrons are densely ionizing because the tracks consist of dense columns of ionization.

LET is the energy transferred per unit length of track. Typical values are 0.2 keV/ μm for cobalt-60 γ -rays, 2 keV/ μm for 250-kV x-rays, 166 keV/ μm for 2.5-MeV α -particles, and 1,000 keV/ μm for heavy charged particles encountered in space.

RBE of some test radiation (r) is the ratio D_{250}/D_r , in which D_{250} and D_r are the doses of 250-kV x-rays and the test radiation, respectively, required to produce equal biologic effect.

RBE increases with LET to a maximum at about 100 keV/ μm , thereafter decreasing with higher LET.

For radiation with the optimal LET of 100 keV/ μm , the average separation between ionizing events is similar to the diameter of the DNA double helix (2 nm) so that DSBs can be most efficiently produced by a single track.

The RBE of high-LET radiations compared with that of low-LET radiations

increases as the dose per fraction decreases. This is a direct consequence of the fact that the dose-response curve for low-LET radiations has a broader shoulder than for high-LET radiations.

RBE varies according to the tissue or end point studied. In general, RBE values are high for cells or tissues that accumulate and repair a great deal of sublethal damage so that their dose-response curves for x-rays have a broad initial shoulder.

RBE depends on the following:

Radiation quality (LET)

Radiation dose

Number of dose fractions

Dose rate

Biologic system or end point

The OER has a value of about 3 for low-LET radiations, falls when the LET rises more than about 30 keV/ μ m, and reaches unity by an LET of about 200 keV/ μ m.

The radiation weighting factor (W_R) depends on LET and is specified by the ICRP as a representative RBE at low dose and low dose rate for biologic effects relevant to radiation protection, such as cancer induction and heritable effects. It is used in radiologic protection to reduce radiations of different biologic effectiveness to a common scale.

Equivalent dose is the product of absorbed dose and the radiation weighting factor. The unit of equivalent dose is the sievert (Sv). (In the old units, absorbed dose was expressed in rads and equivalent dose was expressed in rem.)

BIBLIOGRAPHY

Barendsen GW. Impairment of the proliferative capacity of human cells in culture by alpha-particles with differing linear-energy transfer. *Int J Radiat Biol Relat Stud Phys Chem Med.* 1964;8:453–466.

Barendsen GW. In: Proceedings of the Conference on Particle Accelerators in Radiation Therapy. LA-5180-C. Atomic Energy Commission, Technical Information Center; 1972:120–125.

Barendsen GW. Responses of cultured cells, tumors, and normal tissues to radiation of different linear energy transfer. *Curr Top Radiat Res Q*. 1968;4:293–356.

Barendsen GW, Beusker TLJ, Vergroesen AJ, et al. Effects of different ionizing radiations on human cells in tissue culture: II. Biological experiments. *Radiat Res*. 1960;13:841–849.

Barendsen GW, Koot CJ, van Kersen GR, et al. The effect of oxygen on impairment of the proliferative capacity of human cells in culture by ionizing radiations of different LET. *Int J Radiat Biol Relat Stud Phys Chem Med*. 1966;10:317–327.

Barendsen GW, Walter HM. Effects of different ionizing radiations on human cells in tissue culture: IV. Modification of radiation damage. *Radiat Res*. 1964;21:314–329.

Barendsen GW, Walter HM, Fowler JF, et al. Effects of different ionizing radiations on human cells in tissue culture: III. Experiments with cyclotron-accelerated alpha-particles and deuterons. *Radiat Res*. 1963;18:106–119.

Berry RJ, Bewley DK, Parnell CJ. Reproductive capacity of mammalian tumour cells irradiated in vivo with cyclotron-produced fast neutrons. *Br J Radiol*. 1965;38:613–617.

Bewley DK. Radiobiological research with fast neutrons and the implications for radiotherapy. *Radiology*. 1966;86:251–257.

Bewley DK, Field SB, Morgan RL, et al. The response of pig skin to fractionated treatments with fast neutrons and x-rays. *Br J Radiol*. 1967;40:765–770.

Broerse JJ, Barendsen GW. Relative biological effectiveness of fast neutrons for effects on normal tissues. *Curr Top Radiat Res Q*. 1973;8:305–350.

Broerse JJ, Barendsen GW, van Kersen GR. Survival of cultured human cells after irradiation with fast neutrons of different energies in hypoxic and oxygenated conditions. *Int J Radiat Biol Relat Stud Phys Chem Med*. 1968;13:559–572.

Field SB. The relative biological effectiveness of fast neutrons for mammalian tissues. *Radiology*. 1969;93:915–920.

Field SB, Jones T, Thomlinson RH. The relative effect of fast neutrons and x-rays on tumour and normal tissue in the rat: II. Fractionation recovery and

- reoxygenation. *Br J Radiol.* 1968;41:597–607.
- Fowler JF, Morgan RL. Pre-therapeutic experiments with the fast neutron beam from the Medical Research Council Cyclotron: VIII. General review. *Br J Radiol.* 1963;36:115–121.
- International Commission on Radiation Units and Measurements. *Radiation Quantities and Units*. Washington, DC: International Commission on Radiation Units and Measurements; 1980. Report 33.
- International Commission on Radiation Units and Measurements. *The Quality Factor in Radiation Protection*. Bethesda, MD: International Commission on Radiation Units and Measurements; 1986. Report 40.
- International Commission on Radiological Protection. *1990 Recommendations of the International Commission on Radiological Protection*. Oxford, United Kingdom: Pergamon Press; 1990. ICRP Publication 60.
- International Commission on Radiological Protection. *Recommendations of the International Commission on Radiological Protection*. New York, NY: Pergamon Press; 1977. ICRP Publication 26.
- International Commission on Radiological Protection. *The 2007 Recommendations of the International Commission on Radiological Protection*. New York, NY: Elsevier; 2007. ICRP Publication 103.
- International Commission on Radiological Protection, International Commission on Radiation Units and Measurements. Report of the RBE Committee to the ICRP and on radiation units and measurements. *Health Phys.* 1963;9:357–384.

chapter 8

Acute Radiation Syndrome

Acute Radiation Syndrome

Early Lethal Effects

The Prodromal Radiation Syndrome

The Cerebrovascular Syndrome

The Gastrointestinal Syndrome

The Hematopoietic Syndrome

The First and Most Recent Deaths from the Hematopoietic Syndrome

Pulmonary Syndrome

Cutaneous Radiation Injury

Symptoms Associated with the Acute Radiation Syndrome

Treatment of Radiation Accident Victims Exposed to Doses Close to the LD_{50/60}

Triage

Survivors of Serious Radiation Accidents in the United States

Radiation Emergency Assistance Center

Summary of Pertinent Conclusions

Bibliography

ACUTE RADIATION SYNDROME

The effect of ionizing radiation on the whole organism is discussed in this chapter. Data on the various forms of the **acute radiation syndrome (ARS)** have been drawn from many sources. Animal experiments provide the bulk of the data and result in a significant understanding of the mechanisms of death after exposure to total body irradiation. At the human level, data have been drawn from experiences in radiation therapy and studies of the Japanese survivors of Hiroshima and Nagasaki, the Marshallese accidentally exposed to fallout in 1954, and the victims of the limited number of accidents at nuclear installations, including Chernobyl and the Tokaimura accident in Japan. From

these various sources, the pattern of events that follows a total body exposure to a dose of ionizing radiation has been well documented. To date, worldwide, about 400 humans have suffered from the ARS.

EARLY LETHAL EFFECTS

Early radiation lethality generally is considered to be death occurring within a few weeks that can be attributed to a specific high-intensity exposure to radiation. Soon after irradiation, early symptoms appear, which last for a limited period; this is referred to as the **prodromal radiation syndrome**. These symptoms may clear up after a few days, to be followed by a latent period before the development of the eventual life-threatening syndrome. This is illustrated in [Figure 8.1](#). The eventual survival time and mode of death depend on the magnitude of the dose. In most mammals, three distinct modes of death can be identified, although in the circumstances of an actual accidental exposure, some overlap is frequently seen. At very high doses, in excess of about 100 Gy, death occurs 24 to 48 hours after exposure and appears to result from neurologic and cardiovascular breakdown; this mode of death is known as the **cerebrovascular syndrome**. At intermediate dose levels, approximately 5 to 12 Gy, death occurs in about 9 or 10 days and is associated with extensive bloody diarrhea and destruction of the gastrointestinal mucosa; this mode of death is known as the **gastrointestinal syndrome**. At lower dose levels, approximately 2.5 to 5 Gy, death occurs several weeks to 2 months after exposure and is caused by effects on the blood-forming organs; this mode of death has come to be known as **bone marrow death** or the **hematopoietic syndrome**.

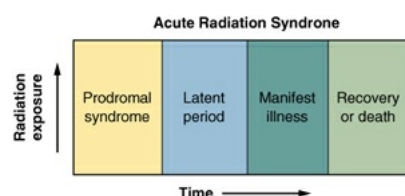


FIGURE 8.1 Illustrating the stages of the acute radiation syndrome. Following total body irradiation, the prodromal syndrome develops—the intensity and length depending on the dose. There follows a latent period when symptoms disappear, followed by the development of manifest illness described by the cerebrovascular, gastrointestinal, or hematopoietic syndrome, depending on the dose.

The exact cause of death in the cerebrovascular syndrome is by no means clear. In the case of both of the other modes of death—the gastrointestinal and the hematopoietic syndromes—the principal mechanisms that lead to the death

of the organism are understood. Death is caused by the depletion of the stem cells of a critical self-renewal tissue: the epithelium of the gut or the circulating blood cells, respectively. The difference in the dose level at which these two forms of death occur and the difference in the time scales involved reflect variations in the population kinetics of the two cell renewal systems involved and differences in the amount of the damage that can be tolerated in these different systems before death ensues.

THE PRODROMAL RADIATION SYNDROME

The various symptoms making up the human prodromal syndrome vary with respect to time of onset, maximum severity, and duration, depending on the size of the dose. With doses of a few tens of gray, all exposed individuals can be expected to show all phases of the syndrome within 5 to 15 minutes of exposure. Reaction might reach a maximum by about 30 minutes and persist for a few days, gradually diminishing in intensity until the prodromal symptoms merge with the universally fatal cerebrovascular syndrome or, after a lower dose, with the fatal gastrointestinal syndrome.

At lower doses, dose-response predictions are difficult to make because of the interplay of many different factors. A severe prodromal response usually indicates a poor clinical prognosis and portends at the least a prolonged period of acute hematologic aplasia accompanied by potentially fatal infection: anemia and hemorrhage.

The signs and symptoms of the human prodromal syndrome can be divided into two main groups: gastrointestinal and neuromuscular. The gastrointestinal symptoms are anorexia, nausea, vomiting, diarrhea, intestinal cramps, salivation, fluid loss, dehydration, and weight loss. The neuromuscular symptoms include easy fatigability, apathy or listlessness, sweating, fever, headache, and hypotension. At doses that would be fatal to 50% of the population, the principal symptoms of the prodromal reaction are anorexia, nausea, vomiting, and easy fatigability. Immediate diarrhea, fever, and hypotension frequently are associated with supralethal exposure ([Table 8.1](#)). One of the Soviet firefighters at the Chernobyl reactor accident vividly described the onset of these symptoms as he accumulated a dose of several grays working in a high-dose-rate area. The prodromal phase is followed by a latent stage before the final radiation syndrome develops. In the symptom-free *latent* stage, the patient may seem and feel relatively well for a period of hours or even weeks. The duration of the latent stage is inversely proportional to the dose and may last a few hours for high

exposures or as long as 2 or more weeks for lower exposures. Absence of a latent phase—that is, a progressive worsening from prodromal signs and symptoms directly into the manifest illness phase—is an indicator that the dose was probably very high.

Table 8.1 Symptoms of the Prodromal Syndrome

NEUROMUSCULAR	GASTROINTESTINAL
SIGNS AND SYMPTOMS TO BE EXPECTED AT ABOUT 50% LETHAL DOSE	
Easy fatigability	Anorexia
—	Nausea
—	Vomiting
ADDITIONAL SIGNS TO BE EXPECTED AFTER SUPRALETHAL DOSES	
Fever	Immediate diarrhea
Hypotension	

The diagnosis of the ARS can also be based on laboratory data. During the prodromal phase, evidence of hematopoietic damage can already be observed by a drop in the lymphocyte count after an exposure as low as 0.5 Gy. The circulating lymphocytes are one of the most radiosensitive cell lines, and a fall in the absolute lymphocyte count is the best and most useful laboratory test to determine the level of radiation exposure in the early phase of observation.

Among assays for biologic dosimetry, chromosomal aberration analysis from cultured circulating lymphocytes is the most widely accepted and reliable. The dose-response relationships are well established in many laboratories around the world. The lower limit of detection of a dose by using this cytogenetic method is approximately 0.2 Gy of γ - or x-rays.

THE CEREBROVASCULAR SYNDROME

A total body dose of about 100 Gy of γ -rays or its equivalent of neutrons results in death in 24 to 48 hours. At these doses, all organ systems are also seriously damaged; both the gastrointestinal and hematopoietic systems are, of course, severely damaged and would fail if the person lived long enough, but cerebrovascular damage brings death very quickly so that the consequences of the failure of the other systems do not have time to be expressed (i.e., death occurs before other symptoms have time to appear). The symptoms that are observed vary with the species of animal involved and also with level of radiation dose; they are summarized briefly as follows: There is the development of severe nausea and vomiting, usually within a matter of minutes. This is followed by manifestations of disorientation, loss of coordination of muscular movement, respiratory distress, diarrhea, convulsive seizures, coma, and finally death. Only a few instances of accidental human exposure have involved doses high enough to produce a cerebrovascular syndrome; two such cases are described briefly.

In 1964, a 38-year-old man working in a uranium-235 recovery plant was involved in an accidental nuclear excursion. He received a total body dose estimated to be about 88 Gy made up of 22 Gy of neutrons and 66 Gy of γ -rays. He recalled seeing a flash and was hurled backward and stunned; he did not lose consciousness, however, and was able to run from the scene of the accident to another building 200 yards away. Almost at once he complained of abdominal cramps and headache, vomited, and was incontinent of bloody diarrheal stools. The next day, the patient was comfortable but restless. On the second day, his condition deteriorated; he was restless, fatigued, apprehensive, and short of breath and had greatly impaired vision; his blood pressure could only be maintained with great difficulty. Six hours before his death, he became disoriented, and his blood pressure could not be maintained; he died 49 hours after the accident.

In a nuclear criticality accident at Los Alamos in 1958, one worker received a total body dose of mixed neutron and γ -radiation estimated to be between 39

and 49 Gy. Parts of his body may have received as much as 120 Gy. This person went into a state of shock immediately and was unconscious within a few minutes. After 8 hours, no lymphocytes were found in the circulating blood, and there was virtually a complete urinary shutdown despite the administration of large amounts of fluids. The patient died 35 hours after the accident.

The exact and immediate cause of death in what is known as the cerebrovascular syndrome is not fully understood. Although death is usually attributed to events taking place within the central nervous system, much higher doses are required to produce death if the head alone is irradiated rather than the entire body; this would suggest that effects on the rest of the body are by no means negligible. It has been suggested that the immediate cause of death is damage to the microvasculature, which results in an increase in the fluid content of the brain owing to leakage from small vessels, resulting in a buildup of pressure within the bony confines of the skull.

THE GASTROINTESTINAL SYNDROME

A total body exposure of more than 10 Gy of γ -rays or its equivalent of neutrons commonly leads in most mammals to symptoms characteristic of the gastrointestinal syndrome, culminating in death some days later (usually between 3 and 10 days). The characteristic symptoms are nausea, vomiting, and prolonged diarrhea. People with the gastrointestinal syndrome lose their appetite and appear sluggish and lethargic. Prolonged diarrhea, extending for several days, usually is regarded as a bad sign because it indicates that the dose received was more than 10 Gy, which is inevitably fatal. The person with this syndrome shows signs of dehydration, loss of weight, emaciation, and complete exhaustion; death usually occurs in a few days. There is no instance on record of a human having survived a dose in excess of 10 Gy.

The symptoms that appear and the death that follows are attributable principally to the depopulation of the epithelial lining of the gastrointestinal tract by the radiation. The normal lining of the intestine is a classic example of a self-renewing tissue; [Figure 8.2](#) shows the general characteristics of such a tissue. It is composed of a stem cell compartment, a differentiating compartment, and mature functioning cells.

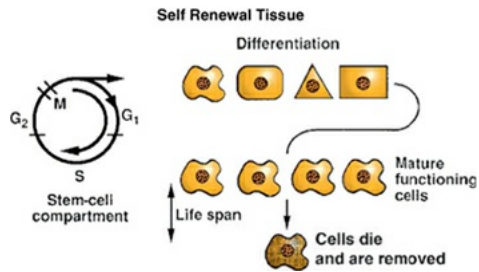


FIGURE 8.2 The classic self-renewal tissue. The stem cell compartment contains the dividing cells. Of the new cells produced, some maintain the pool, and some go on to differentiate and produce mature functioning cells. If the tissue is exposed to radiation, the “Achilles heel” is the stem cell compartment. Huge doses of radiation are needed to destroy differentiated cells and prevent them from functioning, but modest doses kill some or all of the stem cells in the sense that they lose their reproductive integrity. Irradiation does not produce an immediate effect on the tissue because it does not affect the functioning cells. The delay between the time of irradiation and the onset of the subsequent radiation syndrome is dictated by the normal life span of the mature functioning cells.

The structure of the intestinal epithelium is illustrated in [Figure 8.3](#). Dividing cells are confined to the crypts, which provide a continuous supply of new cells; these cells move up the villi, differentiate, and become the functioning cells. The cells at the top of the folds of villi are sloughed off slowly but continuously in the normal course of events, and the villi are continuously replaced by cells that originate from mitoses in the crypts. A single-cell-thick barrier separates the blood vessels in the villi from the contents of the intestine.

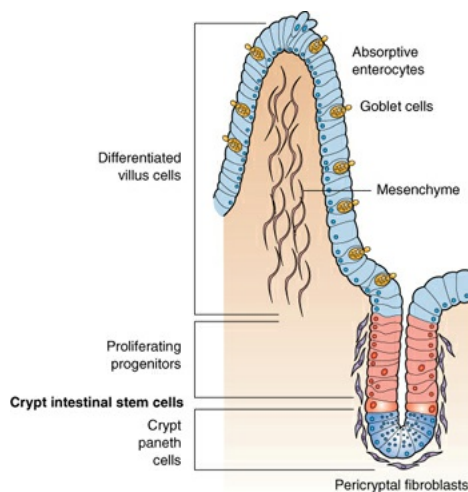


FIGURE 8.3 The gastrointestinal epithelium is an example of a classic self-renewal tissue. Stem cells in the crypts divide rapidly and provide cells that differentiate to form the lining of the villi. A single cell layer separates the blood

supply within the villus from the contents of the gastrointestinal (GI) tract. An exposure to radiation kills cells in the crypts, cutting off a supply of cells to cover the villi. As a consequence, the villi shrink and, eventually, the barrier between blood supply and the contents of the GI tract is compromised, leading to a loss of fluids and massive infections. (Courtesy of Dr. Jack Little.)

A dose of radiation of about 10 Gy sterilizes a large proportion of the dividing cells in the crypts; a dose of this order of magnitude does not seriously affect the differentiated and functioning cells. As the surface of the villi is sloughed off and rubbed away by normal use, there are no replacement cells produced in the crypt. Consequently, after a few days, the villi begin to shorten and shrink, and eventually, the surface lining of the intestine is completely denuded of villi. The rate of cell loss and shrinkage depends on the dose. It occurs faster at higher doses than at lower doses. At death, the villi are very clearly flat and almost completely free from cells.

The precise time schedule of these events and the time required before the intestine is denuded of cells entirely vary with the species. In small rodents, this condition is reached between 3 and 4 days after the dose of radiation is delivered. In humans, it does not occur until about 9 to 10 days after irradiation. All of the individuals who received a dose large enough for the gastrointestinal syndrome to result in death have already received far more than enough radiation to result in hematopoietic death. Death from a denuding of the gut occurs, however, before the full effect of the radiation on the blood-forming organs has been expressed because of differences in the population kinetics of the stem cell systems involved.

Before Chernobyl, there was probably only one example in the literature of a human suffering a gastrointestinal death as a result of radiation exposure. In 1946, a 32-year-old man was admitted to the hospital within 1 hour of a radiation accident in which he received a total body dose of neutrons and γ -rays. The dosimetry is very uncertain in this early accident, and various estimates of total body exposure range from 11 to 20 Gy. In addition, the man's hands received an enormous dose, possibly as much as 300 Gy. The patient vomited several times within the first few hours of the exposure. On admission, his temperature and pulse rate were slightly elevated; other than that, the results of his physical examinations were within normal limits. His general condition remained relatively good until the sixth day, at which time signs of severe paralytic ileus developed that could be relieved only by continuous gastric suction. On the seventh day, liquid stools that were guaiac-positive for occult blood were noted.

The patient developed signs of circulatory collapse and died on the ninth day after irradiation. At the time of death, jaundice and spontaneous hemorrhages were observed for the first time.

At autopsy, the small intestine showed the most striking change. The mucosal surface was edematous and erythematous, and the jejunum was covered by a membranous exudate. Microscopically, there was complete erosion of the epithelium of the jejunum and ileum as well as loss of the superficial layers of the submucosa. The duodenal epithelium was lost, except in the crypts; the colon epithelium was somewhat better preserved. The denuded surfaces were covered everywhere by a layer of exudate in which masses of bacteria were seen, and in the jejunum, the bacteria had invaded the intestinal wall. Blood cultures postmortem yielded *Escherichia coli*.

Several of the firefighters at Chernobyl, including those who received bone marrow transplants, died between a week and 10 days after exposure, suffering from symptoms characteristic of the gastrointestinal syndrome.

THE HEMATOPOIETIC SYNDROME

At doses of 2.5 to 5 Gy, death, if it occurs, is a result of radiation damage to the hematopoietic system. Mitotically active precursor cells are sterilized by the radiation, and the subsequent supply of mature red blood cells, white blood cells, and platelets is thereby diminished. The time of potential crisis at which circulating cells in the blood reaches a minimum value is delayed for some weeks. It is only when the mature circulating cells begin to die off and the supply of new cells from the depleted precursor population is inadequate to replace them that the full effect of the radiation becomes apparent.

The concept of the 50% lethal dose (LD₅₀) as an end point for scoring radiation death from this cause has been borrowed from the field of pharmacology. The LD₅₀ is defined as the dose of any agent or material that causes a mortality rate of 50% in an experimental group within a specified period.

Within a given population of humans or animals, there are many factors that influence the response of the individual to total body irradiation. For example, the very young and the old appear to be more radiosensitive than the young adult. The female, in general, appears to have a greater degree of tolerance to radiation than does the male. [Figure 8.4](#) shows a typical relationship between the dose of radiation and the percentage of monkeys killed by total body irradiation.

Up to a dose exceeding 2 Gy, no animals die, whereas a dose of about 8 Gy kills all the animals exposed. Between these two doses, there is a very rapid increase in the percentage of animals killed as the dose increases, and it is a simple matter by visual inspection of the graph or by a more sophisticated statistical analysis to arrive at a precise estimate of the LD₅₀ dose, which in this case is 5.3 Gy.

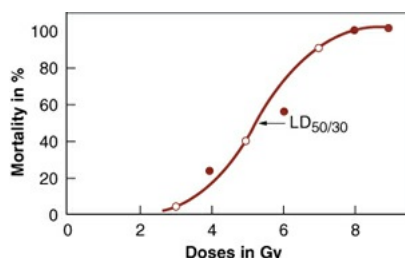


FIGURE 8.4 Mortality rate of rhesus monkeys at 30 days after a single total body exposure to x-rays. (Adapted from Henschke UK, Morton JL. Mortality of rhesus monkeys after single total body irradiation. *Am J Roentgenol Radium Ther Nucl Med*. 1957;77:899–909, with permission.)

Humans develop signs of hematologic damage and recover from it much more slowly than most other mammals. The peak incidence of human death from hematologic damage occurs at about 30 days after exposure, but deaths continue for up to 60 days. The LD₅₀ estimates for hematopoietic death for humans are therefore expressed as the LD_{50/60}, in contrast to the LD_{50/30} for mice, in which peak incidence of death occurs 10 to 15 days after exposure and is complete by 30 days.

A dose of radiation close to the LD₅₀ results in the prodromal syndrome already described, the chief symptoms of which are nausea and vomiting. A symptom-free interval, known as the *latent period*, follows. This is, in fact, a very inappropriate name because during this period, the most important consequences of the radiation exposure, leading to its lethal effects, are in progress. About 3 weeks after the radiation exposure, there is onset of chills, fatigue, petechial hemorrhages in the skin, and ulceration of the mouth; epilation (hair loss) also occurs at this time. These symptoms are a manifestation of the depression of blood elements: infections and fever from granulocyte depression and impairment of immune mechanisms, bleeding, and possibly anemia caused by hemorrhage resulting from platelet depression. Anemia from red blood cell depression usually does not occur. Death occurs at this stage unless the bone marrow has begun to regenerate in time. Infection is an important cause of death, but it may be controlled to a large extent by antibiotic therapy.

As a consequence of the reactor accident at Chernobyl, 203 operating

personnel, firemen, and emergency workers suffering from the early radiation syndrome were hospitalized, having received doses in excess of 1 Gy. Of these, 35 had severe bone marrow failure, and 13 of them died. The remainder recovered with conservative medical care.

Studies of total body irradiation have been performed on many species; a few LD₅₀ values are listed in [Table 8.2](#), ranging from mouse to human. Such studies were popular and important in the 1950s and 1960s, supported largely by the military. In more recent years, total body irradiation has been of interest from the point of view of bone marrow transplantation. This interest may stem from the treatment of radiation accidents, such as the Chernobyl disaster, or from the rescue of patients receiving cancer therapy with total body irradiation, radiolabeled antibodies, or cytotoxic drugs.

Table 8.2 The 50% Lethal Doses for Various Species from Mouse to Human and the Relation between Body Weight and the Number of Cells that Need to Be Transplanted for a Bone Marrow “Rescue”

SPECIES	AVERAGE BODY WEIGHT, kg	50% LETHAL TOTAL BODY IRRADIATION, Gy	RESCUE DOSE PER KILOGRAM $\times 10^{-8}$	RELATIVE HEMATOPOIETIC STEM CELL CONCENTRATION
Mouse	0.025	7	2	10
Rat	0.2	6.75	3	6.7
Rhesus monkey	2.8	5.25	7.5	7.3
Dog	12	3.7	17.5	1.1
Human	70	4	20	1

Data from Vriesendorp HM, van Bekkum DW. Susceptibility to total body irradiation. In: Broerse JJ, MacVittie T, eds. *Response to Total Body Irradiation in Different Species*. Amsterdam, The Netherlands: Martinus Nijhoff; 1984:43–57.

The best estimate of the LD_{50/60} for humans, based on the experiences at Hiroshima and Nagasaki, is about 3.5 Gy for young healthy adults without medical intervention. There does exist in the literature a surprising number of instances in which young men and women have received total body irradiation up to a dose of around 4 Gy and recovered under conservative care in a modern well-equipped hospital. The LD_{50/60} for those exposed at Chernobyl was closer to 7 Gy because, although general medical care was poor, antibiotics were available. It is now possible to increase the LD_{50/60} to an even higher dose by the use of hematopoietic growth factors, which has implications that will be discussed later.

THE FIRST AND MOST RECENT DEATHS FROM THE HEMATOPOIETIC SYNDROME

The most recent person to die of the ARS was Alexander Litvinenko, a former officer of the Russian Security Service who received political asylum in Great Britain and was assassinated by the administration of polonium-210 ([Fig. 8.5](#)). This radionuclide emits only α -particles that do not penetrate even a sheet of paper or the epidermis of human skin, so α -emitters can cause significant damage only if ingested. Litvinenko fell ill and was hospitalized on November 1, 2006, and died on November 23, just more than 3 weeks later. Scotland Yard initially investigated claims that he had been poisoned with thallium because the distinctive effects include hair loss and damage to peripheral nerves. Polonium-210 was identified only after his death. The administered activity was estimated to be about 2 GBq, which corresponds to about 10 mcg of polonium and is many times the mean lethal dose. This massive amount of polonium-210 could only be produced in a large state-controlled nuclear reactor. In retrospect, the symptoms were characteristic of the classic hematopoietic syndrome, hair loss, erythema, and death in about 3 weeks caused by loss of circulating blood elements.



FIGURE 8.5 Alexander Litvinenko, before and after radiation poisoning. Alexander Litvinenko was a former officer of the Russian Security Service who received political asylum in Great Britain. He was assassinated by the administration of a massive dose of polonium-210, presumably added to his food. He died 3 weeks later.

The first person to die of the ARS was a 26-year-old male involved in a criticality accident at Los Alamos in March 1945. He was exposed total body to a mixture of neutrons and γ -rays, the estimated equivalent dose being 6.35 Sv. His right hand received a much higher dose of 200 Gy, and his left hand received a dose of 30 Gy. His red blood count changed little up to the time of his death. The platelet count dropped before being restored by a transfusion and then fell again. There was the characteristic early initial rise in the granulocyte count, but it fell to eventually zero by the time of his death. The most important events can be listed as follows:

- Day 1: Nausea, anorexia, and vomiting
- Day 2: Greatly improved, except for numbness in his hand
- Day 3: Erythema on the front of the body
- Day 5: Rise of temperature
- Day 10: Nausea and cramps
- Day 12: Acute mucositis of mouth and tongue
- Day 17: Epilation of body hair
- Day 24: Died with white cell count close to zero

PULMONARY SYNDROME

In recent years, a few individuals exposed to 8 Gy or more, and who survived the hematopoietic syndrome as a result of intensive treatment with antibiotics, blood transfusions, and hematopoietic growth factors, died much later at 130 days after

irradiation with inflammatory pneumonitis. There was one example in Belarus in 1994 and two examples from the 1999 Tokaimura accident in Japan. This syndrome following total body irradiation was not seen in the Japanese exposed by the A-bombs because anyone exposed to 8 Gy died within 30 to 60 days from the hematopoietic syndrome and did not therefore live long enough for lung complications to show up. The pulmonary syndrome only assumes importance now that more sophisticated countermeasures have been developed to nuclear events. This is illustrated in [Figure 8.6](#). At the present time, it is not clear how high the LD_{50/60} for the hematopoietic syndrome may be raised as improvements in countermeasures are made.

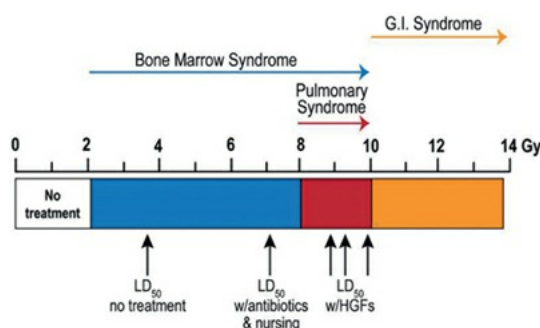


FIGURE 8.6 Illustrating how the pulmonary syndrome appeared in a few individuals exposed to a total body dose of 8 to 10 Gy but who survived the hematopoietic syndrome by intensive treatment with antibiotics, transfusions, and hematopoietic growth factors (HGFs). They died much later, about 130 days after irradiation, with inflammatory pneumonitis. G.I., gastrointestinal; LD₅₀, 50% lethal dose.

CUTANEOUS RADIATION INJURY

The hematopoietic, gastrointestinal tract, or pulmonary syndromes may be accompanied and complicated by **cutaneous radiation injury (CRI)**. Radiation injury to the skin can also occur in the absence of the ARS because nonpenetrating β -particles and low-energy photons may deposit excess dose only to the integument. Such an injury may become apparent within hours or may not be seen for weeks, depending on the dose. Findings and complaints can range from itching and tingling to epilation, erythema, edema, progressing to dry desquamation, wet desquamation, ulceration, and necrosis as the dose is increased. Chronic, possibly severe, skin infections and recurrent ulceration may complicate the process. The first person ever to die of the ARS in 1945, died a classic hematopoietic syndrome, having received a total body dose of about 6 Sv, but his hands received a much higher dose. Radiation damage to the skin and

microvasculature of his hands caused great suffering before he died on day 28 after exposure because of bone marrow failure.

Localized *radiation burns* to the skin differ from thermal and chemical burns primarily in the delay between exposure and effect and in their tendency to undergo recurrent breakdown, even after a scar has formed. The threshold local dose for epilation is approximately 3 Sv and that for erythema is about 6 Sv. With increasing dose of more than 10 Sv, the injury worsens progressively, involving dry desquamation, wet desquamation, bullae (blister) formation, ulceration, and finally necrosis. These may be debilitatingly painful like second-degree thermal burns and life threatening with concomitant infections.

SYMPTOMS ASSOCIATED WITH THE ACUTE RADIATION SYNDROME

The International Atomic Energy Agency and the World Health Organization jointly sponsored a report entitled *Diagnosis and Treatment of Radiation Injuries*. [Tables 8.3](#) and [8.4](#) have been adapted from that report, and the expected distribution of symptoms following whole body irradiation are summarized. [Table 8.3](#) refers to the prodromal syndrome in the period soon after irradiation, whereas [Table 8.4](#) refers to the later critical phase. These should not be taken too literally because the information is based on a limited number of exposed individuals over the years, but they are a useful guide. They cover the dose range from 1.0 Gy, which results in little effect, to more than 8 Gy, which is expected to result in 100% lethality. The nature of the symptoms, their severity, and the time of onset can be a useful predictor of the eventual outcome in the absence of physical dosimetry. For example, severe immediate diarrhea indicates that a supralethal dose has been received and that any treatment is likely to be ineffective and therefore useless.

Table 8.3 Latent Phase (Prodromal Syndrome) of Acute Radiation Syndrome

DEGREE OF ACUTE RADIATION SYNDROME AND APPROXIMATE DOSE OF ACUTE WHOLE BODY EXPOSURE (GY)				
				VERY

	MILD (1–2 Gy)	MODERATE (2–4 Gy)	SEVERE (4–6 Gy)	SEVERE (6–8 Gy)	LETHAL (>8 Gy)
Lymphocytes (G/L) (days 3–6)	0.8–1.5	0.5–0.8	0.3–0.5	0.1–0.3	0.0–0.1
Granulocytes (G/L)	>2.0	1.5–2.0	1.0–1.5	≤0.5	≤0.1
Diarrhea	None	None	Rare	Appears on days 6–9	Appears or days 4–5
Epilation	None	Moderate, beginning on day 15 or later	Moderate complete days 11–21	or Complete on earlier day 11	Complete earlier than day 10
Latency period (d)	21–35	18–28	8–18	7 or less	None
Medical response	Hospitalization not necessary	Hospitalization recommended	Hospitalization necessary	Hospitalization urgently necessary	Symptomatic treatment only

Adapted from International Atomic Energy Agency. *Diagnosis and Treatment of Radiation Injuries* Vienna, Austria: International Atomic Energy Agency; 1998.

Table 8.4 Critical Phase of Acute Radiation Syndrome

DEGREE OF ACUTE RADIATION SYNDROME	

	AND APPROXIMATE DOSE OF ACUTE WHOLE BODY EXPOSURE (GY)					
	MILD (1–2 Gy)	MODERATE (2–4 Gy)	SEVERE (4–6 Gy)	VERY SEVERE (6–8 Gy)	LETHAL (>8 Gy)	
Onset of symptoms	>30 d	18–28 d	8–18 d	<7 d	<3 d	
Lymphocytes (G/L)	0.8–1.5	0.5–0.8	0.3–0.5	0.1–0.3	0–0.1	
Platelets (G/L)	60–100 10%–25%	30–60 25%–35%	25–35 40%–80%	15–25 60%–80%	<20 80%–100% ^a	
Clinical manifestations	Fatigue, weakness	Fever, infections, bleeding, weakness, epilation	High fever, infections, bleeding, epilation	High fever, diarrhea, vomiting, dizziness and disorientation, hypotension	High fever, diarrhea, unconsciousness	
Lethality (%)	0 Onset 6–8 wk	0–50 Onset 4–8 wk	20–70 Onset 1–2 wk	50–100 1–2 wk	100	
Medical response	Prophylactic Special prophylactic treatment from days 14–	Special prophylactic treatment from days 1–	Special treatment from day 1; from days	Special treatment from day 1; isolation from	Symptomatic only	

	20; isolation 7–10; from days 10– isolation 20	the beginning from the beginning	
--	--	--	--

^aIn very severe cases, with a dose >50 Gy, death precedes cytopenia.

Adapted from International Atomic Energy Agency. *Diagnosis and Treatment of Radiation Injuries*. Vienna, Austria: International Atomic Energy Agency; 1998.

TREATMENT OF RADIATION ACCIDENT VICTIMS EXPOSED TO DOSES CLOSE TO THE LD_{50/60}

If the radiation exposure is known to be less than 4 to 5 Gy, most experts recommend that the patient be watched carefully but only treated in response to specific symptoms, such as antibiotics for an infection, fresh platelets for local hemorrhage, and so on. Petechial hemorrhages in skin were commonly observed in the Japanese irradiated in 1945 but are not reported so commonly among individuals exposed accidentally in nuclear power installations in the United States. Blood transfusions should not be given prophylactically because they delay the regeneration of the blood-forming organs.

If the dose is known to have exceeded about 5 Gy, then death from the hematopoietic syndrome 3 to 4 weeks later is a real possibility. In some countries, isolation and barrier nursing—that is, isolation of patients from others so that they do not come in contact with possible infections while their blood count is low—is recommended. It has been shown in animals that the LD₅₀ can be raised by a factor of about two by the use of antibiotics, and there is no reason to suppose that the same is not true in humans. Indeed, this is supported by the Chernobyl experience where the LD₅₀ was closer to 7 Gy than 4 Gy. The important things to avoid are infection, bleeding, and physical trauma during the period in which the circulating blood elements reach a nadir and to give the bone marrow a chance to regenerate.

The area of most discussion in the past was the use of bone marrow transplantation. This technique was used on four Yugoslav scientists who were exposed accidentally in the 1950s to doses initially estimated to be about 7 Gy. All of the grafts were rejected, but the exposed individuals survived anyway, probably because later estimates indicated that the dose received was much

lower, in the region of 4 Gy. In fact, many observers claim that the scientists survived in spite of the transplants rather than because of them. [Figure 8.7](#) shows the depression and recovery of blood elements in the Yugoslav scientists and also in victims of the famous Y-12 reactor accident at Oak Ridge, Tennessee, who received about 4 Gy.

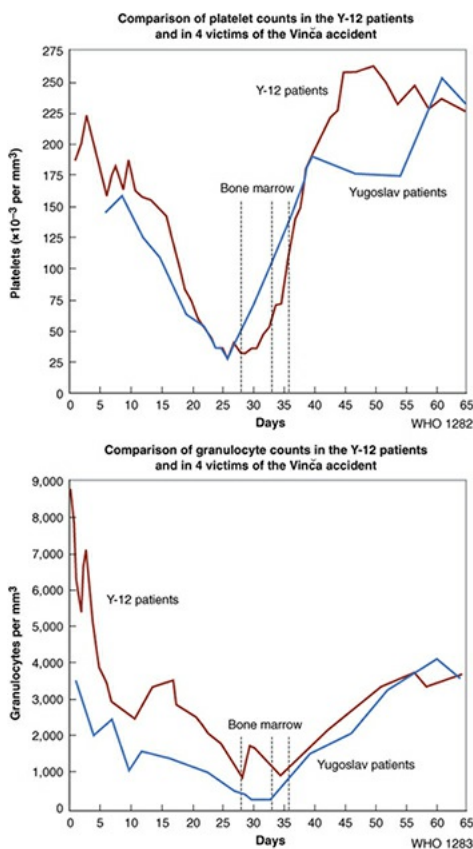


FIGURE 8.7 Depression and recovery of circulating blood elements in victims of the Y-12 reactor accident at Oak Ridge, Tennessee, and four accidentally exposed Yugoslav scientists. (Adapted from Andrews GA, Sitterson BW, Kretchmar AL, et al. *Diagnosis and Treatment of Acute Radiation Injury*. Geneva, Switzerland: World Health Organization; 1961:27–48.)

Of the Chernobyl accident victims, 13 received bone marrow transplants (some matched for immune compatibility and some are not). In addition, 6 received fetal liver transplants, but these patients all died early, some of gastrointestinal symptoms. Of the 13 who received bone marrow transplants, only 2 survived and 1 showed autologous bone marrow repopulation. There was, therefore, only one possible successful transplant that saved a life, and even that result has been questioned.

The situation was made difficult because the doses to which individuals had been exposed were not known with any precision. After doses close to the LD₅₀,

and certainly for higher doses, peripheral lymphocytes disappear before 24 hours, and then it is not possible to estimate total body doses by counting chromosome aberrations in stimulated lymphocytes taken from peripheral blood. Because the US transplant team did not arrive in Chernobyl for some time, biologic dosimetry was never possible for those exposed to higher doses. Consequently, some victims who received bone marrow transplants were already doomed to die of the gastrointestinal syndrome, having received doses in excess of 10 Gy.

In more recent years, bone marrow transplantation techniques have been greatly improved and, together with growth factors, have been used routinely to “rescue” patients given supralethal doses of radiation for the treatment of leukemia or in preparation for organ transplants. As already discussed, with intensive care, the LD_{50/60} can be raised to more than 8 Gy.

TRIAGE

Following an event in which several individuals are exposed to radiation, an immediate need is to know what doses are involved. If the exposed individuals are radiation workers wearing monitors, the solution is easy. However, in general, members of the public will not be monitored. The following are several possibilities:

1. *The average time to emesis decreases with increasing dose.* The original work was performed by Ricks and Lushbaugh at Oak Ridge Associated Universities and involved 502 patients who had undergone therapeutic or accidental radiation exposure between 1964 and 1975. Individual responses vary so widely that time to emesis can provide only rough guidance. For example, few individuals vomit if the acute radiation dose is less than 1 Gy, whereas most vomit if the dose is more than 2 Gy. Further, if no vomiting occurs during the first 4 hours after exposure, it is unlikely that severe clinical effects caused by radiation will follow later. On the other hand, Goans and colleagues has reported that if the time to emesis is less than 2 hours after exposure, the effective whole body dose is at least 3 Gy.
2. *The decline in the lymphocyte count allows an estimate to be made of the total body radiation exposure.* Goans and colleagues developed an algorithm to estimate an approximate dose based on the depletion rate from serial blood counts performed at various times after exposure because, of course, the preirradiation lymphocyte count is usually unknown.

Because the lymphocyte count falls more rapidly the higher the dose, the best estimate of dose and prognosis can be made at about 48 hours postexposure. Again, the estimate is only an approximation.

3. If a cytogenetic laboratory is available, the best method to assess radiation exposure is to measure the incidence of chromosomal aberrations in peripheral lymphocytes stimulated to divide *in vitro*. Doses of more than 0.2 Gy can be accurately assessed in this way. This technique is described in more detail in [Chapter 2](#). After high doses, of course, lymphocytes disappear quickly and so this technique has severe limitations.

SURVIVORS OF SERIOUS RADIATION ACCIDENTS IN THE UNITED STATES

Over the past 50 years, there have been several accidents in which small numbers of people employed in the nuclear program were exposed to total body or partial body irradiation. Most occurred in the early days of the nuclear program and involved criticality accidents. The number involved in the United States is about 70 workers in 13 separate accidents.

The long-term survivors have been studied exhaustively over the years. The medical history of these heavily irradiated people mirrors that of any aging population. The expected high incidences of shortened life span, early malignancies after a short latent period, and rapidly progressing lenticular opacities have not been observed. The numbers in any group are small, but the several malignancies, cataracts, and degenerative diseases that have been seen are no more than might be expected in a similar group of unirradiated people of the same age.

The survivors of the 1958 criticality accident at the Oak Ridge Y-12 plant are a case in point. Their blood cell counts are shown in [Figure 8.7](#). A group of eight workers, ranging in age from 25 to 56 years, received total body doses of 0.23 to 3.65 Gy; five of them received doses of more than 2 Gy. Nevertheless, as of 1999, more than 40 years after the accident, none had died of a classic “radiogenic” cancer. There were two cases of lung cancer in very heavy smokers, a meningioma, and prostate cancer in a 70-year-old man. In fact, the only medical finding likely to be radiation related is bilateral posterior capsular cataracts in two of these patients. Three of the workers who received the biggest doses are retired and in good health.

This highlights the problem of detecting an excess cancer incidence in any

small irradiated population. For example, if a group of workers receives a total body exposure of 3 Gy, the biggest dose possible without suffering early death from the hematopoietic syndrome, the excess cancer incidence would be expected to be about 30%. (The cancer risk estimates of the Biological Effects of Ionizing Radiation [BEIR] VII Committee based on the Japanese atomic bomb survivors amount to about 10% per sievert.) Thus, the biggest dose to which humans can be exposed and survive without medical intervention doubles the spontaneous cancer incidence. This is difficult to detect in a small group of people and is likely to be masked by other biologic factors. However, as countermeasures improve and individuals are able to survive larger doses of radiation, induced cancers become an increasingly important consideration.

RADIATION EMERGENCY ASSISTANCE CENTER

In the context of radiation accidents, it should be noted that the Medical Sciences Division of the Oak Ridge Institute for Science and Education operates a Radiation Emergency Assistance Center/Training Site (REAC/TS). This is operated on behalf of the U.S. Department of Energy.

REAC/TS provides 24-hour direct or consultative assistance with medical and health physics problems associated with radiation accidents in local, national, and international incidents. The resources of REAC/TS consist of expertise in cytogenetics for dose assessment, calculation of doses from internally deposited radionuclides, and laboratory facilities that include total body counting capabilities. The regular telephone number for information is (865) 576-3131, and the 24-hour emergency number is (865) 576-1005 (ask for REAC/TS). The REAC/TS website is <http://www.orau.gov/reacts>.

SUMMARY OF PERTINENT CONCLUSIONS

The prodromal syndrome varies in time of onset, severity, and duration.

At doses close to the dose that would be lethal to 50% of the population (LD₅₀), the principal symptoms of the prodromal syndrome are anorexia, nausea, vomiting, and easy fatigability.

Immediate diarrhea, fever, or hypotension indicates a supralethal exposure.

The cerebrovascular syndrome results from a total body exposure to about 100 Gy of γ -rays and in humans results in death in 24 to 48 hours. The cause of death may be changes in permeability of small blood vessels in the brain following damage to the microvasculature.

The gastrointestinal syndrome results from a total body exposure to about 10 Gy. Death occurs in about 7 to 10 days in humans because of depopulation of the epithelial lining of the gastrointestinal tract.

The hematopoietic syndrome results from total body exposure to 2.5 to 5 Gy. The radiation sterilizes some or all of the mitotically active precursor cells. Symptoms result from lack of circulating blood elements 3 or more weeks later.

A few individuals exposed to 8 Gy or more, and who survived the hematopoietic syndrome due to intense treatment with antibiotics, transfusions, and hematopoietic growth factors, died much later, about 130 days after irradiation, with inflammatory pneumonitis. This new pulmonary syndrome assumes importance because of the availability of effective countermeasures against the hematopoietic syndrome.

The hematopoietic, gastrointestinal, or pulmonary syndromes may be complicated by damage to the skin from high local doses.

The LD₅₀ for humans is estimated to be between 3 and 4 Gy for young adults without medical intervention. It may be less for the very young or the very old. The LD₅₀ may be raised to 7 Gy by the use of antibiotics, as was the case at Chernobyl. Intense countermeasures including antibiotics, infusions, and hematopoietic growth factors may increase the LD₅₀ for the hematopoietic syndrome to as much as 8 to 9 Gy.

Heavily irradiated survivors of accidents in the nuclear industry have been followed for many years; their medical history mirrors that of any aging population. An expected higher incidence of shortened life span, early malignancies after a short latency, and rapidly progressing cataracts has not been observed. That is not to say that heavily irradiated individuals are not at increased risk, but an excess cancer incidence can be observed only by a careful study of a large population.

The first recorded death with the ARS was a worker at Los Alamos in 1945. The most recent was the Russian agent, Litvinenko, who was “poisoned” with polonium-210 in 2006. Worldwide, about 400 individuals have suffered from the ARS.

BIBLIOGRAPHY

Andrews GA, Sitterson BW, Kretchmar AL, et al. *Diagnosis and Treatment of Acute Radiation Injury*. Geneva, Switzerland: World Health Organization;

1961:27–48.

Anno GH, Young RW, Bloom RM, et al. Dose response relationships for acute ionizing-radiation lethality. *Health Phys*. 2003;84:565–575.

Bacq ZM, Alexander P. *Fundamentals of Radiobiology*. 2nd ed. New York, NY: Pergamon Press; 1961.

Baranov AE, Selidovkin GD, Butturini A, et al. Hematopoietic recovery after 10-Gy acute total body radiation. *Blood*. 1994;83(2):596–599.

Bond VP, Fliedner TM, Archambeau JO. *Mammalian Radiation Lethality: A Disturbance in Cellular Kinetics*. New York, NY: Academic Press; 1965.

Fry SA, Littlefield G, Lushbaugh CC, et al. Follow-up of survivors of serious radiation accidents in the United States. In: Ricks R, Fry SA, eds. *The Medical Basis for Radiation-Accident Preparedness II*. New York, NY: Elsevier Science; 1990.

Goans RE, REAC/TS, and Medical Preparedness and Response Subgroup of Homeland Security Department Working Group on Radiological Dispersal Devices and Preparedness. December 9, 2003 update; p. 23. Available at: www1.va.gov/emshg/docs/Radiological_Medical_Countermeasures_Indexed-Final.pdf. Accessed January 12, 2006.

Hempelmann LH, Lisco H, Hoffman JG. The acute radiation syndrome: a study of nine cases and a review of the problem. *Ann Intern Med*. 1952;36:279–510.

Henschke UK, Morton JL. Mortality of rhesus monkeys after single total body irradiation. *Am J Roentgenol Radium Ther Nucl Med*. 1957;77:899–909.

International Atomic Energy Agency. *Diagnosis and Treatment of Radiation Injuries*. Vienna, Austria: International Atomic Energy Agency; 1998.

Karas JS, Stanbury JB. Fatal radiation syndrome from an accidental nuclear excursion. *N Engl J Med*. 1965;272:755–761.

Langham WH, ed. *Radiobiological Factors in Manned Space Flight: Report of the Space Radiation Study Panel of the Life Sciences Committee*. Washington, DC: National Academy of Sciences, National Research Council; 1967. Publication No. 1487.

Lushbaugh CC. Reflections on some recent progress in human radiobiology. In: Augenstein LC, Mason R, Zelle M, eds. *Advances in Radiation Biology*. New York, NY: Academic Press; 1969:277–314.

Shipman TL, Lushbaugh CC, Petersen D, et al. Acute radiation death resulting from an accidental nuclear critical excursion. *J Occup Med.* 1961;3(suppl):145–192.

United States Nuclear Regulatory Commission. *Review of the Tokai-mura Criticality Accident.* Washington, DC: United States Nuclear Regulatory Commission; 2000.

Vriesendorp HM, van Bekkum DW. Bone marrow transplantation in the canine. In: Shifrine M, Wilson FD , eds. *The Canine as a Biomedical Research Model: Immunological, Hematological, and Oncological Aspects.* Washington, DC: U.S. Department of Energy, Office of Health and Environmental Research; 1980.

Vriesendorp HM, van Bekkum DW. Role of total body irradiation in conditioning for bone marrow transplantation. In: Thierfelder S, Rodt H, Kolb HJ, eds. *Immunobiology of Bone Marrow Transplantation.* Berlin, Germany: Springer Verlag; 1980:349–364.

Vriesendorp HM, van Bekkum DW. Susceptibility to total body irradiation. In: Broerse JJ, MacVittie T, eds. *Response to Total Body Irradiation in Different Species.* Amsterdam, The Netherlands: Martinus Nijhoff; 1984:43–57.

Vriesendorp HM, Zurcher C. Late effects of total body irradiation in dogs treated with bone marrow transplantation. In: Fliedner TM, Grossner W, Patrick C, eds. *Proceedings of the Meeting of the European Late Effects Project Group of EURATOM.* Luxembourg: Commission of the European Communities; 1982. Report EUR 8078.

chapter 9

Medical Countermeasures to Radiation Exposure

Introduction and Definitions

The Discovery of Radioprotectors

Mechanism of Action

Development of More Effective Compounds

Amifostine (WR-2721) as a Radioprotector in Radiotherapy

Amifostine as a Protector against Radiation-Induced Cancer

A New Family of Aminothiol Radioprotectors

Radiation Mitigators

Radionuclide Eliminators

Dietary Supplements as Countermeasures to Radiation

Summary of Pertinent Conclusions

Bibliography

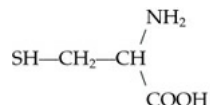
INTRODUCTION AND DEFINITIONS

World events in recent years have highlighted the threat of nuclear terrorism, as well as the possibility of accidents at nuclear installation, and so there is an urgent need to develop medical countermeasures for acute radiation exposures with the attendant bodily injuries. High doses of radiation to the whole or substantial parts of the body often result in life-threatening injuries, primarily to those radiosensitive self-renewing tissues but most markedly to the hematopoietic and gastrointestinal (GI) systems (see [Chapter 8](#)). Medical countermeasures for radiation fall into three broad classes. **Radioprotectors** are prophylactic agents administered prior to radiation exposure to reduce the level of cellular or molecular damage. **Radiation mitigators** are drugs administered shortly after irradiation, but prior to the manifestation of normal tissue toxicity, to reduce the severity of the radiation response. **Radiation therapeutics** or

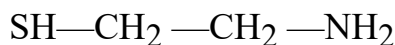
treatments are agents given after overt symptoms appear in order to stimulate repair or regeneration.

THE DISCOVERY OF RADIOPROTECTORS

The most important group of radioprotectors includes the sulphhydryl (SH) compounds. The simplest is **cysteine**, an SH compound containing a natural amino acid, the structure of which is



In 1948, Patt discovered that cysteine could protect mice from the effects of total body exposure to x-rays if the drug was injected or ingested in large amounts before the radiation exposure. At about the same time, Bacq and his colleagues in Europe independently discovered that **cysteamine** could also protect animals from total body irradiation. This compound has a structure represented by



Animals injected with cysteamine to concentrations of about 150 mg/kg require doses of x-rays 1.8 times larger than control animals to produce the same mortality rate. This factor of 1.8 is called the **dose reduction factor (DRF)**, defined as

$$DRF = \frac{\text{Dose of radiation in the presence of the drug}}{\text{Dose of radiation in the absence of the drug}}$$

to produce a given level of lethality.

MECHANISM OF ACTION

Many similar SH compounds have been tested and found to be effective as radioprotectors. The most efficient SH compounds tend to have certain structural features in common: a free SH group (or potential SH group) at one end of the molecule and a strong basic function, such as amine or guanidine, at the other end, separated by a straight chain of two or three carbon atoms. SH compounds are efficient radioprotectors against sparsely ionizing radiations such as x- or γ -rays.

The mechanisms most implicated in SH-mediated cytoprotection include:

1. Free-radical *scavenging* that protects against oxygen-based free radical generation by ionizing radiations or chemotherapy agents such as alkylating

agents

2. Hydrogen atom donation to facilitate direct chemical *repair* at sites of DNA damage

Chapter 1 includes a discussion of the chain of events between the absorption of a photon and the eventual biologic damage, which includes the production of free radicals, which are highly reactive species. If these free radicals are scavenged before they can interact with biologic molecules, the effect of the radiation is reduced. This process is illustrated in Figure 9.1.

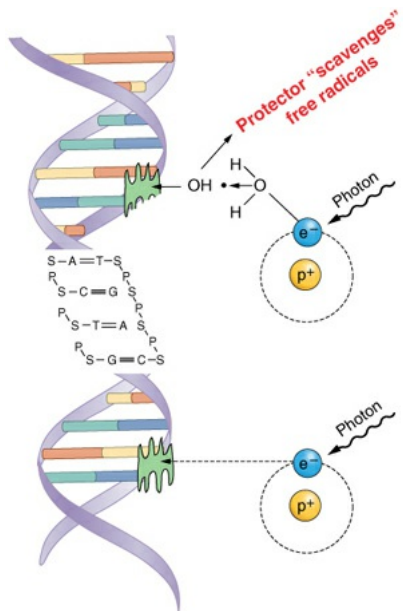


FIGURE 9.1 Radioprotectors containing a sulphydryl group exert their effect by scavenging free radicals and by reducing free radical damage to DNA. They are most effective for radiations characterized by low linear energy transfer (LET), becoming progressively less effective with increasing LET because the amount of local damage is so great.

The protective effect of SH compounds tends to parallel the oxygen effect, being maximal for sparsely ionizing radiations (e.g., x - or γ -rays) and minimal for densely ionizing radiations (e.g., low-energy α -particles). It might be predicted that with effective scavenging of all free radicals, the largest possible value of *DRF* for sparsely ionizing radiations would equal the oxygen enhancement ratio, with a value of 2.5 to 3.0, and this proved to be the case.

This simple description of the mechanism of action of SH radioprotectors is intellectually satisfying, but it is clearly not the whole story because radioprotectors of this class have more effect with densely ionizing radiations (such as neutrons) than would be expected based on this explanation alone.

Other factors must be involved that are not fully understood.

DEVELOPMENT OF MORE EFFECTIVE COMPOUNDS

The discovery in 1948 of a compound that offered protection against radiation excited the interest of the U.S. Army because the memory of Nagasaki and Hiroshima was vivid in the years immediately after World War II. However, although cysteine is a radioprotector, it is also toxic and induces nausea and vomiting at the dose levels required for radioprotection. A development program was initiated in 1959 by the U.S. Army in studies conducted at the Walter Reed Institute of Research to identify and synthesize drugs capable of conferring protection to individuals in a radiation environment but without the debilitating toxicity of cysteine or cysteamine. More than 4,000 compounds were synthesized and tested. At an early stage, the important discovery was made that the toxicity of the compound could be greatly reduced if the SH group was covered by a phosphate group. This is illustrated for cysteamine, otherwise known as mercaptoethylamine (MEA), in [Table 9.1](#). The 50% lethal dose of the compound in animals can be doubled, and the protective effect in terms of the *DRF* can be greatly enhanced if the SH group is covered by a phosphate. This tends to reduce systemic toxicity. Once in the cell, the phosphate group is stripped and the SH group begins scavenging for free radicals.

Table 9.1 Effect of Adding a Phosphate-Covering Function on the Free Sulphydryl of β -Mercaptoethylamine (MEA)

DRUG	FORMULA	MEAN 50% LETHAL DOSE (RANGE) IN MICE	DOSE REDUCTION FACTOR
MEA	$\text{NH}_2\text{—CH—CH}_2\text{—SH}$	343 (323–364)	1.6 at 200 mg/kg
MEA- PO_3	$\text{NH}_2\text{—CH}_2\text{—CH—SH}_2\text{PO}_3$	777 (700–864)	2.1 at 500 mg/kg

The structures of two typical compounds of more than 4,000 synthesized in the Walter Reed series are shown in [Table 9.2](#). The first compound, WR-638,

called *cystaphos*, was said to be carried routinely in the field pack of Soviet infantry in Europe during the Cold War for use in the event of a nuclear conflict.

Table 9.2 Two Radioprotectors in Practical Use

COMPOUND	STRUCTURE	USE
WR-638	$\text{NH}_2\text{CH}_2\text{CH}_2\text{SPO}_3\text{HNa}$	Carried in field pack by Russian army (cystaphos)
WR-2721	$\text{NH}_2(\text{CH}_2)_3\text{NHCH}_2\text{CH}_2\text{SPO}_3\text{H}_2$	Protector in radiotherapy and carried by US astronauts on lunar trips (amifostine)

Comparison of Gastrointestinal and Hematopoietic Dose Reduction Factors in Mice for these Radioprotectors (the Two Compounds Listed Previously)

DRUG COMPOUND	DOSE, mg/kg	DOSE REDUCTION FACTOR	
		7 (GASTROINTESTINAL)	30 (HEMATOPOIETIC)
WR-638	500	1.6	2.1
WR-2721	900	1.8	2.7

The second compound, WR-2721, now known as *amifostine*, is perhaps the most effective of those synthesized in the Walter Reed series. It gives good protection to the blood-forming organs, as can be seen by the *DRF* for 30-day death in mice, which approaches the theoretic maximum value of 3. It was probably the compound carried by US astronauts on their trips to the moon to be used if a solar event occurred. On these missions, when the space vehicle left

Earth's orbit and began coasting toward the moon, the astronauts were committed to a 14-day mission because they did not have sufficient fuel to turn around without first orbiting the moon and using its gravitational field. If there had been a major solar event in that period, the astronauts would have been exposed to a shower of high-energy protons, resulting in an estimated total body dose of several grays. The availability of a radioprotector with a *DRF* close to 3 would have been very important in such a circumstance. As it turned out, no major solar event occurred during any manned lunar mission; thus, the protectors were not used. The potential for this problem will be greatly magnified in future missions to Mars, which may take as long as 3 years.

Although radioprotectors were initially developed to offer some protection to combatants in a nuclear war, they turn out to be of very limited use in the context of nuclear terrorism. There are several reasons for this. First, radioprotectors that are free radical scavengers must be administered before exposure to radiation which is not always possible in a terrorism situation. Second, drugs such as amifostine cause nausea and vomiting at the doses necessary to provide protection; these side effects are performance decrementing. Third, amifostine has an extremely short time window of radioprotectiveness, generally less than 1 hour. Lastly, amifostine needs to be administered intravenously, which would be out of the question in a terrorist situation where hundreds or thousands of victims may be involved.

AMIFOSTINE (WR-2721) AS A RADIOPROTECTOR IN RADIOTHERAPY

Amifostine is a phosphorothioate that is nonreactive and does not readily permeate cells primarily because of its terminal phosphorothioic acid group. It is therefore a "prodrug." When dephosphorylated by the enzyme alkaline phosphatase, which is present in high concentrations in normal tissues and capillaries, it is converted to the active metabolite designated WR-1065. This metabolite readily enters normal cells by facilitated diffusion and scavenges free radicals generated by ionizing radiations or by drugs used in chemotherapy such as alkylating agents.

An agent that protects normal tissues and tumors equally would obviously be of no use in the treatment of cancer. The use of amifostine in radiotherapy is based on animal experiments that showed that amifostine concentrates much more rapidly in normal tissues than in tumors, which is thought to result from several factors, including the effects of tumor blood flow, the acidosis of tumors,

and the lower expression of alkaline phosphatase.

The only radioprotective drug approved by the U.S. Food and Drug Administration (FDA) for use in radiation therapy is amifostine (WR-2721), sold under the trade name Ethyol for use in the prevention of xerostomia in patients treated for head and neck cancer. The Radiotherapy Oncology Group (RTOG) conducted a phase III randomized clinical trial which demonstrated the efficacy of amifostine in reducing xerostomia in patients with head and neck cancer receiving radiotherapy without prejudice to early tumor control. The drug was administered daily, 30 minutes before each dose fraction in a multifraction regimen. Three months posttreatment, the incidence of xerostomia was significantly reduced in those patients treated with amifostine. There was no difference in locoregional tumor control between patients who received the radioprotector and those who did not. Giving the amifostine only 30 minutes before each treatment was designed to exploit the slower rate at which the drug penetrates tumors relative to normal tissues.

It might have been expected that radioprotectors would enjoy a wider use in radiation therapy, but in practice, clinical use continues to be plagued by issues relating to possible tumor protection and loss of therapeutic gain. As explained earlier, the use of such protectors is based on the observation from animal studies that amifostine quickly floods normal tissues but penetrates more slowly into tumors. Consequently, if the radiation dose is given within minutes after the administration of the radioprotector, there is a differential sparing of normal tissue compared with tumor cells. Because one can never be sure that the tumor is not protected to some extent, the use of radioprotectors is not “fail safe.” For this reason, radioprotectors are not widely used in radiotherapy, indeed, in practice they are used only for the reduction of xerostomia.

AMIFOSTINE AS A PROTECTOR AGAINST RADIATION-INDUCED CANCER

Although the emphasis for the development of amifostine was to protect against cell killing, this compound also protects against radiation-induced mutagenesis and oncogenic transformation in cells in culture and against carcinogenesis in mouse model systems. Furthermore, although a dose of about 400 mg/kg is required to demonstrate optimal cytoprotection—a dose that carries with it significant side effects—its antimutagenic effect persists following prolonged exposure to a dose as low as 25 mg/kg, which is nontoxic. Of even greater interest is the observation that the effect occurs even when cells are exposed to

amifostine up to 3 hours following irradiation. This has led to the speculation that the antioxidant properties of amifostine may not be the only mechanism by which it protects against cancer; it has been proposed that the polyamine-like properties of the phosphorothioates may result in a stabilization of DNA-damaged sites, facilitating a slower and more error-free repair of damage.

A NEW FAMILY OF AMINOTHIOL RADIOPROTECTORS

The three key elements in the design of the new generation of radioprotectors were (1) small size for efficient transmembrane diffusion; (2) positively charged amines in alkyl backbone for strong ionic interaction with DNA backbone; and (3) a perpendicular, alkyl side-chain with a terminal thiol that is projected away from the DNA backbone to enable scavenging of reactive oxygen species around DNA. The prototype aminothiol in this group is designated PrC-210 and has been tested in *in vitro* cellular systems and in limited small animal studies. Oral PrC-210 conferred 100% survival in rat and mouse models against an otherwise 100% lethal whole body radiation dose. In a head-to-head comparison of side effects with amifostine, there was no retching or emesis in ferrets treated with PrC-210 and no induced hypotension in arterial cannulated rats treated with PrC-210 compared with the debilitating side effects associated with comparable amounts of amifostine. The combination of oral administration and an absence of side effects make this new aminothiol an attractive possibility for radioprotection. However, tests in nonhuman primates and human subjects need to be conducted.

RADIATION MITIGATORS

There are a large number of radiation countermeasures for the acute radiation syndrome in various stages of development, but in this chapter, we restrict attention to the three drugs that are FDA approved for human use, plus seven promising compounds that, at the time of writing, have FDA Investigational New Drug (IND) status for the treatment of the acute radiation syndrome.

Granulocyte colony-stimulating factor (G-CSF) (filgrastim [Neupogen]), pegylated G-CSF (pegfilgrastim [Neulasta]), and granulocyte-macrophage colony-stimulating factor (GM-CSF) (sargramostim [Leukine]) belong to a class of agents known as “colony-stimulating factors.” They are FDA approved for the treatment of chemotherapy-induced neutropenia and have been used effectively. Some experience has been gained in using these cytokines in small numbers of

patients involved in accidental radiation exposures. The results are suggestive of an effect but not conclusive. Extensive experiments have been carried out with a range of animals including nonhuman primates. Figure 9.2 shows the result of an experiment in which the G-CSF (filgrastim [Neupogen]) was administered to nonhuman primates 24 hours after a total body dose of 7.5 Gy of 2-MV x-rays. Eighty percent of the animals that received G-CSF survived versus 40% of animals exposed to the same dose but received no G-CSF. In further experiments (results not shown), the drug was found to be totally ineffective if administration was delayed for 48 hours after irradiation. This would make the use of this compound logically difficult in the event of a radiation accident involving a large number of individuals. In 2015, filgrastim (Neupogen) was approved by the FDA for use in humans to increase survival in patients acutely exposed to myelosuppressive doses of radiation (hematopoietic syndrome of acute radiation syndrome). Pegfilgrastim (Neulasta) has also been shown to protect nonhuman primates from a lethal whole body dose of radiation.

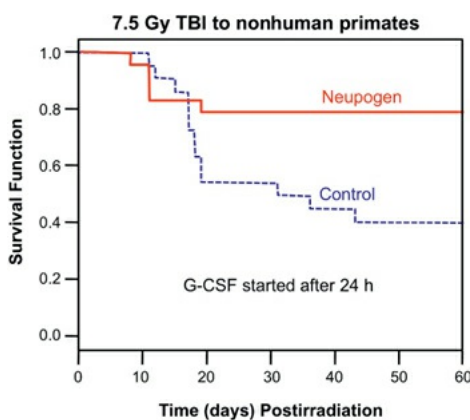


FIGURE 9.2 Showing the result of an experiment in which nonhuman primates were given the granulocyte colony-stimulating factor (G-CSF, filgrastim [Neupogen]) 24 hours after a total-body irradiation (TBI) of 7.5 Gy. Eighty percent of the animals survived compared with 40% in controls that did not receive the G-CSF. In other experiments (results not shown), the agent proved to be ineffective if administration was delayed to 48 hours postirradiation. (Adapted from Farese AM, Cohen MV, Katz BP, et al. Filgrastim improves survival in lethally irradiated nonhuman primates. *Radiat Res.* 2013;179:89–100; and Farese AM, Brown CR, Smith CP, et al. The ability of filgrastim to mitigate mortality following LD_{50/60} total-body irradiation is administration time-dependent. *Health Phys.* 2014;106[1]:39–47.)

The seven “promising” compounds granted IND status by the FDA include various compounds that purport to work by very different mechanisms: a steroid, an isoflavone, a truncated flagellin protein, a novel kinase inhibitor, recombinant

human interleukin (IL)-12, a dipropionate and, a growth factor. What they have in common is that all have been shown to enhance survival after total-body irradiation in mice, nonhuman primates, or both. Some appear to be more effective as radioprotectors than as mitigators. This list will change in future years as new radiation mitigators are still being discovered and tested.

Supportive care can be, in its own right, an extremely effective countermeasure. Supportive care includes the administration of cytokines, blood products, antibiotics, antiemetics, antidiarrheals, fluids, and electrolytes. It is interesting to note that the LD₅₀ observed at Hiroshima was about 3.5 Sv, whereas at Chernobyl, it almost doubled to 7 Sv largely due to better supportive care and especially to the availability of antibiotics to help exposed individuals survive the nadir in the white blood count.

RADIOMUCLIDE ELIMINATORS

In the event of an accident at a nuclear power facility, such as occurred at Chernobyl or at Fukushima, or a radiologic terrorist attack, there is the potential for members of the public to ingest radioactive materials that may have been released into the atmosphere. Radionuclide eliminators are drugs that disorporate or block absorption of internalized radionuclides. There are only just three compounds that have been identified and/or approved by the FDA:

1. Potassium iodide tablets flood the thyroid with nonradioactive iodine so that if radioactive iodine is ingested, it is less likely to be internalized in the thyroid. This is especially important for children or for any individuals living in areas with low iodine contents, as was the case at Chernobyl.
2. Prussian blue capsules, marketed as Radiogardase, contain insoluble ferric hexacyanoferrate. This compound is taken orally and traps ingested radioactive cesium in the intestine so that it can be eliminated in the stools rather than being absorbed into muscle.
3. Diethylenetriamine pentaacetic acid (DTPA) is a drug routinely used in cases of heavy metal poisoning. It is useful as a radiation countermeasure if transuranic elements, such as radioactive plutonium, americium, or curium, have been released into the atmosphere. DTPA comes in two forms: calcium (Ca-DTPA) and zinc (ZnDTPA). Both forms work by binding tightly to the radioactive plutonium, americium, or curium. These radioactive materials bound to the DTPA are then passed from the body in the urine.

Figure 9.3 is a photograph of the three radionuclide eliminators referred to

the aforementioned, ready for use in an emergency at the National Institute for Radiological Sciences in Chiba, Japan.



FIGURE 9.3 Photograph of a cabinet in the National Institute for Radiological Sciences in Chiba, Japan, containing an emergency supply of potassium iodide tablets, insoluble (Radiogardase), and DTPA, used in the event of internalized radionuclides.

DIETARY SUPPLEMENTS AS COUNTERMEASURES TO RADIATION

Long-term exposure to nonlethal doses of ionizing radiation is known to result in an excess incidence of cancer and other deleterious biologic effects. To the extent that the mechanism involved may include oxidative stress, dietary supplements involving antioxidants have a potential role to play. Several possibilities have shown promise in cellular and animal systems. One such example is the soybean-derived serine protease inhibitor known as the Bowman-Birk inhibitor (BBI), which has long been proposed as a cancer chemopreventive agent. Another possibility is a cocktail of common antioxidants, including L-selenomethionine, ascorbic acid, N-acetyl cysteine, alpha-lipoic acid, vitamin E succinate, and coenzyme Q10.

Following the destruction of the World Trade Center on September 11, 2001, and the rise of a nuclear terrorism threat, there has been a revived interest in the development of novel, effective, and nontoxic radioprotectors for potential use in homeland defense as well as in medical applications. In addition, National Aeronautics and Space Administration (NASA) is interested in countermeasures to the exposure to protons and high-energy heavy ions that astronauts experience during long-term missions in space.

SUMMARY OF PERTINENT CONCLUSIONS

Radioprotectors are agents administered prior to radiation exposure to reduce the level of radiation damage. **Radiation mitigators** are drugs administered shortly after irradiation but prior to the manifestation of normal tissue toxicity. **Radiation therapeutics** are agents given after overt symptoms appear in order to reduce the severity of the radiation response.

The radioprotectors, cysteine and cysteamine, were discovered early but are toxic. If the SH group is covered by a phosphate group, toxicity is reduced.

The mechanism of action is the scavenging of free radicals and restitution of free radical damage, although this is not the whole story.

The *DRF* is the ratio of radiation doses required to produce the same biologic effect in the absence and presence of the radioprotector.

The best available radioprotectors can attain *DRF* values of 2.5 to 3.0 for bone marrow death in mice irradiated with x-rays, but the effectiveness of radioprotectors decreases with increasing linear energy transfer.

During the Cold War, it is said that Soviet infantry in Europe carried the radioprotector cystaphos for use in a possible nuclear war. The radioprotector amifostine was carried to the moon by US astronauts to be used in the event of a solar flare.

More than 4,000 compounds were synthesized by the U.S. Army in studies conducted at the Walter Reed Institute of Research. Amifostine (WR-2721) appears to be the best for use in conjunction with radiotherapy.

Amifostine, sold under the trade name Ethyol, is the only radioprotective drug approved by the FDA for use in the prevention of xerostomia in patients treated for head and neck cancer.

An RTOG phase III trial demonstrated the efficacy of amifostine in reducing xerostomia in patients with head and neck cancer receiving radiation therapy without affecting locoregional control. The radioprotector was administered 30 minutes before radiation.

Amifostine is a “prodrug” that is unreactive and that penetrates poorly into cells until it is dephosphorylated by the enzyme alkaline phosphatase to the active metabolite WR-1065.

The rationale for the use of phosphorothioate radioprotectors in radiotherapy is that they flood normal tissues rapidly after administration but penetrate

tumors much more slowly. The strategy is to begin irradiation soon after administration of the drug to exploit a differential effect.

A dose of 400 mg/kg is required for optimal cytoprotection, which is toxic with many side effects, but its antimutagenic effect persists at a low nontoxic dose of 25 mg/kg. Furthermore, its antimutagenic effect still occurs if the drug is added 3 hours following irradiation.

A new family of aminothiol radioprotectors has been generated, of which PrC-210 is the prototype. This drug can be administered orally, protects against lethality from whole body irradiation in rodents, and appears to be free of the side effects of nausea and hypotension that are characteristic of amifostine.

Dietary supplements, including various antioxidants, have been suggested as countermeasures to the long-term biologic effects of radiation exposure.

Radiation mitigators are drugs added after radiation exposure, but before the symptoms of normal tissue toxicity appear, in an attempt to reduce the severity of the radiation response. Several colony-stimulating factors, such as filgrastim (Neupogen), are FDA approved to reduce chemotherapy-induced neutropenia, but filgrastim (Neupogen) is the only one so far approved by the FDA for use in humans exposed to radiation. A wide range of experimental compounds are under investigation to mitigate against the hematopoietic syndrome that follows total-body exposure to a large dose of radiation.

Radionuclide eliminators are drugs that disorporate or block absorption of internalized radionuclides released in a nuclear accident or radiologic terrorist event. Potassium iodide blocks the thyroid from taking up internalized radioactive iodine. Radiogardase traps cesium in the intestine so that it is eliminated in the stools. DTPA is used if transuranic elements, such as plutonium, americium, or curium, are ingested. The DTPA binds to the heavy radionuclide which is then passed from the body in the urine.

Following the destruction of the World Trade Center on September 11, 2001, and the rise of a nuclear terrorism threat, there has been a revived interest in the development of novel, effective, and nontoxic radioprotectors and radiation mitigators for potential use in homeland defense. In addition, NASA is interested in countermeasures to the radiation exposure that astronauts experience on long-term space missions.

BIBLIOGRAPHY

Brizel DM, Overgaard J. Does amifostine have a role in chemoradiation

- treatment? *Lancet Oncol.* 2003;4(6):378–381.
- Brizel DM, Sauer R, Wannenmacher M, et al. Randomized phase III trial of radiation ± amifostine in patients with head and neck cancer [abstract 1487]. *Proceedings of ASCO* 17. 1998.
- Bump EA, Malaker K, eds. *Radioprotectors: Chemical, Biological, and Clinical Perspectives*. Boca Raton, FL: CRC Press; 1998.
- Citrin D, Cotrim AP, Hyodo F, et al. Radioprotectors and mitigators of radiation-induced normal tissue injury. *Oncologist*. 2010;15:360–371.
- Copp RR, Peebles DD, Soref CM, et al. Radioprotective efficacy and toxicity of a new family of aminothiol analogs. *Int J Radiat Biol.* 2013;89(7):485–492.
- Farese AM, Brown CR, Smith CP, et al. The ability of filgrastim to mitigate mortality following LD50/60 total-body irradiation is administration time-dependent. *Health Phys.* 2014;106(1):39–47.
- Farese AM, Cohen MV, Katz BP, et al. Filgrastim improves survival in lethally irradiated nonhuman primates. *Radiat Res.* 2013;179:89–100.
- Grdina DJ, Kataoka Y, Basic I, et al. The radioprotector WR-2721 reduces neutron-induced mutations at the hypoxanthine-guanine phosphoribosyl transferase locus in mouse splenocytes when administered prior to or following irradiation. *Carcinogenesis*. 1992;13:811–814.
- Grdina DJ, Kataoka Y, Murley JS. Amifostine: mechanisms of action underlying cytoprotection and chemoprevention. *Drug Metabol Drug Interact.* 2000;16(4):237–279.
- Grdina DJ, Murley JS, Kataoka Y. Radioprotectants: current status and new directions. *Oncology*. 2002;63(suppl 2):2–10.
- Grdina DJ, Shigematsu N, Dale P, et al. Thiol and disulfide metabolites of the radiation protector and potential chemopreventive agent WR-2721 are linked to both its anti-cytotoxic and anti-mutagenic mechanisms of action. *Carcinogenesis*. 1995;16:767–774.
- Kennedy AR, Guan J, Ware JH. Countermeasures against space radiation induced oxidative stress in mice. *Radiat Environ Biophys.* 2007;46:201–203.
- Kennedy AR, Zhou Z, Donahue JJ, et al. Protection against adverse biologic effects induced by space radiation by the Bowman-Birk inhibitor and antioxidants. *Radiat Res.* 2006;166:327–332.

- Liu T, Liu Y, He S, et al. Use of radiation with or without WR-2721 in advanced rectal cancer. *Cancer*. 1992;69:2820–2825.
- Patt HM, Tyree B, Straube RL, et al. Cysteine protection against x-irradiation. *Science*. 1949;110:213–214.
- Peebles DD, Soref CM, Copp RR, et al. ROS-scavenger and radioprotective efficacy of the new PrC-210 aminothiol. *Radiat Res*. 2012;178:57–68.
- Rasey JS, Nelson NJ, Mahler P, et al. Radioprotection of normal tissues against gamma-rays and cyclotron neutrons with WR-2721: LD₅₀ studies and 35S-WR2721 biodistribution. *Radiat Res*. 1984;97:598–607.
- Saha S, Bhanja P, Kabarriti R, et al. Bone marrow stromal cell transplantation mitigates radiation-induced gastrointestinal syndrome in mice. *PLoS One*. 2011;6(9):e24072. doi:10.1371/journal.pone.0024072.
- Singh VK, Romaine PLP, Seed TM. Medical countermeasures for radiation exposure and related injuries: characterization of medicines, FDA-approval status and inclusion into the Strategic National Stockpile. *Health Phys*. 2015;108(6):607–630.
- Soref CM, Hacker TA, Fahl WE. A new orally active, aminothiol radioprotector-free of nausea and hypotension side effects at its highest radioprotective doses. *Int J Radiat Oncol Biol Phys*. 2012;82(5):e701–e707.
- Sweeney TR. *A Survey of Compounds from the Antiradiations Drug Development Program of the U.S. Army Medical Research and Development Command*. Washington, DC: Walter Reed Army Institute of Research; 1979.
- Utley JF, Marlowe C, Waddell WJ. Distribution of 35S-labeled WR-2721 in normal and malignant tissues of the mouse. *Radiat Res*. 1976;68:284–291.
- Yazlovitskaya EM. Radioprotectors and mitigators: current status. *J Bioequiv Bioavail*. 2013;5:e26. doi:10.4172/jbb.10000e26.
- Yuhas JM. Active versus passive absorption kinetics as the basis for selective protection of normal tissues by S-2-(3-aminopropylamino)-ethyl-phosphorothioic acid. *Cancer Res*. 1980;40:1519–1524.
- Yuhas JM, Storer JB. Differential chemoprotection of normal and malignant tissues. *J Natl Cancer Inst*. 1969;42:331–335.

chapter 10

Radiation Carcinogenesis

Tissue Reactions (Deterministic Effects) and Stochastic Effects

Carcinogenesis: The Human Experience

The Latent Period

Assessing the Risk

Committees Concerned with Risk Estimates and Radiation Protection

Radiation-Induced Cancer in Human Populations

Leukemia

Thyroid Cancer

Breast Cancer

Lung Cancer

Bone Cancer

Skin Cancer

Quantitative Risk Estimates for Radiation-Induced Cancer

Dose and Dose-Rate Effectiveness Factor

Summary of Risk Estimates

Second Malignancies in Radiotherapy Patients

Second Cancers after Radiotherapy for Prostate Cancer

Radiation Therapy for Carcinoma of the Cervix

Second Cancers among Long-Term Survivors from Hodgkin Disease

Dose-Response Relationship for Radiation Carcinogenesis at High Doses

Cancer Risks in Nuclear Industry Workers

Extrapolating Cancer Risks from High to Low Doses

Mortality Patterns in Radiologists

Childhood Cancer after Radiation Exposure In Utero

Nonneoplastic Disease and Radiation

Summary of Pertinent Conclusions

TISSUE REACTIONS (DETERMINISTIC EFFECTS) AND STOCHASTIC EFFECTS

Radiation clearly can produce two very different types of damage. **First**, there is damage due to cells being killed and removed from a tissue or organ, for example, lethality from total body irradiation. **Second**, effects due to cells that are not killed but are changed or mutated in some way, for example, cancer or heritable effects. These different effects have been given special names by the International Commission on Radiological Protection (ICRP). Damage due to cells being killed and removed from a tissue or organ was formerly called a **deterministic effect** but has been renamed a **tissue reaction**. An effect due to cells that are not killed but are changed or mutated is called a **stochastic effect**.

Most organs or tissues of the body are unaffected by the loss of a few cells; but if the number of cells lost is sufficiently large, there is observable harm, reflecting the loss of tissue function. The probability of such harm is zero at small radiation doses, but above some level of dose, called the *threshold dose*, the probability increases rapidly with dose to 100%. Above the threshold, the severity of harm also increases with dose. Tissue reactions, therefore, have a threshold in dose, and the severity of the effect is dose related. The dose-response relationship is said to be threshold-sigmoid and is illustrated in [Figure 10.1](#).

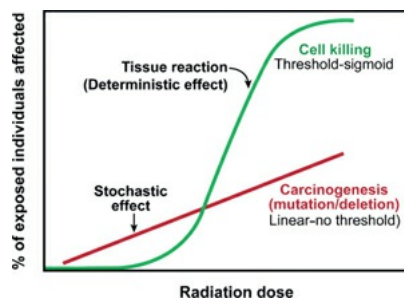


FIGURE 10.1 Illustrating the shapes of the dose-response relationships for tissue reactions versus stochastic effects. For tissue reactions, the shape is threshold-sigmoid, that is, there is a threshold in dose, after which the probability of the effect rises rapidly to 100%. For stochastic effects, the dose-response relationship is linear (or linear-quadratic), but there is no dose threshold.

The outcome is very different if the irradiated cell is viable but modified. Carcinogenesis and heritable effects fall into this category. If somatic cells are

exposed to radiation, the probability of cancer increases with dose, probably with no threshold, but the severity of the cancer is not dose related. A cancer induced by 1 Gy is no worse than one induced by 0.1 Gy, but of course, the probability of its induction is increased. This category of effect is called *stochastic*, a word that has been given a special meaning in radiation protection but, in general, just means “random.” If the radiation damage occurs in germ cells, mutations may occur that could cause deleterious effects in future generations. Again, there is probably no threshold and the severity of heritable effects is not dose related, although the probability of it occurring is. In this case, the dose–response relationship is linear, with no threshold (see [Fig. 10.1](#)).

The belief that stochastic effects have no dose threshold is based on the molecular mechanisms involved. For this reason, it is considered prudent and conservative to assume that no dose is too small to be effective, although this can never be proved.

The two types of effects are summarized as follows:

Tissue reactions (deterministic effect): severity increases with dose; practical threshold; probability of occurrence increases with dose (e.g., death from total body exposure)

Stochastic effect: severity independent of dose; no threshold; probability of occurrence increases with dose (e.g., cancer)

CARCINOGENESIS: THE HUMAN EXPERIENCE

Cancer induction is the most important somatic effect of low-dose ionizing radiation. In sharp contrast to the case for the heritable effects of radiation (see [Chapter 11](#)), risk estimates for leukemogenesis and carcinogenesis do not rely on animal data but can be based on experience in humans. There is a long history of a link between radiation exposure and an elevated incidence of cancer. [Figure 10.2](#) is a beautiful photograph of Marie Curie and her daughter Irene, who are both thought to have died of leukemia as a result of the radiation exposure they received while conducting their experiments with radioactivity. [Figure 10.3](#) is a photograph of the hand of a dentist in New York who held x-ray films in patients’ mouths for many years and who suffered malignant changes as a result. Quantitative data on cancer induction by radiation come from populations irradiated for medical purposes or exposed deliberately or inadvertently to nuclear weapons. Persons exposed therapeutically received comparatively high doses, and their susceptibility to the effects of radiation might have been influenced by the medical condition for which treatment was being given.

Populations exposed to γ -rays and neutrons from nuclear weapons represent a wider cross section in terms of age and health and also include persons exposed to lower doses. In both cases, dose rates were high and exposure times brief.



FIGURE 10.2 Marie Curie (seated) at work with her daughter Irene. Both are thought to have died of leukemia as a consequence of the radiation exposure they received during their experiments with radioactivity. (Courtesy of the Austrian Radium Institute and the International Atomic Energy Bulletin.)



FIGURE 10.3 Hand of a dentist who, for 35 years, held x-ray films in place in patients' mouths. The thumb has been partially amputated. Damaged skin on the fingers has been replaced by grafts. The lesion on the finger is a skin cancer subsequently removed. (Courtesy of Dr. Victor Bond, Brookhaven National Laboratory.)

There are a few groups of exposed persons to whom these generalizations do not apply. Examples include pitchblende and uranium miners who inhaled the radioactive gas radon and its progeny products over a prolonged period, patients injected with radium chloride or Thorotrast for medical purposes, and persons who ingested radionuclides while painting luminous dials on clocks and watches

with paint containing radium. Hundreds of thousands of nuclear workers have been exposed occupationally, and useful cancer risk estimates have become available in recent years. Miners exposed to radon in the uranium mines are an excellent source of data on lung cancer.

The early human experience of radiation-induced cancer may be summarized as follows:

1. Skin cancer and leukemia were common in early x-ray workers, principally physicists and engineers, who worked around accelerators before radiation safety standards were introduced.
2. Lung cancer was a frequent problem in pitchblende miners in Saxony, who dug out the ore from which radium was extracted. In the years following World War II, lung cancer also was noted in uranium miners in the central Colorado plateau. In both cases, the mines were poorly ventilated and there was a buildup of radon gas in the atmosphere of the mine; radon and its progeny were inhaled by the miners, depositing atoms of radioactive material in their lungs. The intense local α -radiation was responsible for inducing lung tumors. Bone tumors were observed in the radium dial painters. The painters were mostly young women who worked in factories in which the luminous dials on clocks and watches were painted with a special paint preparation containing radium. The workers dipped their brushes into the radium paint and used their tongues to shape the brushes into sharp points to paint the small dials on watches. As a result, some radium was ingested, which, because it is in the same group in the periodic table as calcium, was deposited in the tips of the growing bones. The intense α -radiation produced bone tumors. There is also history of bone tumors in people who, in the 1920s and 1930s, received injections of radium salts for the treatment of tuberculosis or ankylosing spondylitis.
3. An excess incidence of liver tumors was reported in patients in whom the contrast material Thorotrast was used. Thorotrast contains radioactive thorium, which, when deposited in the liver, produced a small incidence of liver tumors by α -radiation.

These early examples are interesting but largely anecdotal, although they did alert scientists to the danger of excessive radiation exposure. None of these examples involved situations that now constitute a public health hazard; these problems will never happen again, and the dosimetry in each instance is so uncertain that it is rarely possible to deduce any quantitative relationship between the dose of radiation involved and the tumor incidence.

More recent examples of the human experience with radiation-induced cancer and leukemia include the following:

1. The Japanese survivors of the atomic bomb attacks on Hiroshima and Nagasaki are the most important single group studied because of their large number, the care with which they have been followed, and the fact that people of all ages and both sexes received a wide range of doses. About 120,000 people have been followed carefully, of whom about 50,000 received doses in excess of 0.005 Sv. To date, about 22,000 cancers have been observed in the Life Span Study of which about 1,000 are attributable to the radiation exposure. The weapons used on the two cities were very different. The one used on Nagasaki was of a type that would be expected to emit γ -rays with few neutrons and had been previously tested, so dosimetry is based partly on measurements. The weapon used at Hiroshima was of a type never tested before or since so that dose estimates are based largely on computer simulations. The radiation from this weapon was a mixture of neutrons and γ -rays. The dosimetry relating to the atomic bombs has been revised several times over the years, leading to changes in the cancer risk estimates. The most recent estimates were published in the *Biologic Effects of Ionizing Radiation* (BEIR) VII report in 2006 and will be discussed later in this chapter.
2. In Britain, from 1935 through 1944, some 14,000 patients suffering from ankylosing spondylitis were given radiotherapy to various regions of their spine to relieve pain. A small risk of leukemia mortality has been reported in these patients. Although the spondylitic series provides one of the largest bodies of data on leukemia in humans after exposure to x- or γ -radiation, and the dosimetry is quite good, it is far from ideal because it lacks a proper control, consisting of patients with the same disease who did not receive x-ray therapy but whose treatment was otherwise the same. A possible contribution of carcinogenic drugs to the tumor incidence also has been suggested.
3. There is also documentation of an elevated incidence of leukemia in radiologists who joined learned societies before about 1922, before the introduction of radiation safety standards. This will be discussed later in the chapter.
4. Thyroid cancer has been observed in children who received radiotherapy for what was thought to be an enlarged thymus. The thyroid was included in the treatment field, and both malignant and benign thyroid tumors have been

observed. Breast cancer is also elevated in these patients.

5. Until the 1950s, it was common practice to use x-rays to epilate children suffering from *tinea capitis* (ringworm of the scalp). An increased incidence of thyroid cancer from this practice was first reported by Modan and his colleagues in Israel, who treated more than 20,000 immigrant children from North Africa in whom ringworm of the scalp reached epidemic proportions. There was also a significantly increased risk of brain tumors (mostly meningiomas), salivary gland tumors, skin cancer, and leukemia mortality. A comparable group of children in New York for whom x-rays were used for epilation before treatment for *tinea capitis* show quite different results. There were only two malignant thyroid tumors in addition to some benign tumors. There is, however, an incidence of skin cancer around the face and scalp in those areas also subject to sunlight. The skin tumors arose only in white children, and there were no tumors in black children in the New York series.
6. Patients with tuberculosis, who were fluoroscoped many times during artificial pneumothorax, have shown an elevated incidence of breast cancer. This was first reported in Nova Scotia, but the report was confirmed by a similar study in New England. The doses these patients received are uncertain but must have been about 0.8 to 0.9 Gy because some of the women developed skin changes in the chest wall on the side frequently fluoroscoped. Patients who received radiotherapy for postpartum mastitis were also shown to have an excess incidence of breast cancer.

THE LATENT PERIOD

The time interval between irradiation and the appearance of a malignancy is known as the **latent period**.

Leukemia has the shortest latent period. Excess cases began to appear in the survivors of Hiroshima and Nagasaki a few years after irradiation and reached a peak in 5 to 7 years; most cases occurred in the first 15 years. Solid tumors show a longer latency than the leukemias, on the order of anything from 10 to 60 years or more. For example, an excess incidence of solid tumors is still evident in Japanese survivors exposed to radiation from the atomic bombs in 1945. Indeed, for solid cancers, the excess risk is apparently more like a lifelong elevation of the natural age-specific cancer risk.

As the Japanese data have matured, the concept of a fixed time interval between irradiation and the appearance of the malignancy has been replaced by a

combination of “age at exposure” and “time since exposure.” Regardless of the age at the time of exposure, radiation-induced solid tumors tend to be expressed later in life, at the same time as spontaneous tumors of the same type. Breast cancer in women is the most striking example. This suggests that although radiation may initiate the carcinogenic process at a young age, additional steps are required later in life, some of which may well be hormone dependent.

ASSESSING THE RISK

To use the available human data to estimate risks as a function of dose, it is necessary to fit the data to a model. Several reasons for this are as follows:

1. Data obtained at relatively high doses must be extrapolated to the low doses of public health concern.
2. No large human population exposed to radiation has yet been studied for its full life span, and so estimates must be projected into the future. For example, in the year 2000, about half of the Japanese survivors irradiated in 1945 were still alive.
3. The best data pertain to the Japanese irradiated by the atomic bombs and risk estimates based on this must be transferred to other populations that have quite different characteristics, including their natural cancer incidence.

There are two types of models that are conceptually quite different: the absolute risk model and the relative risk model. The **absolute risk model** assumes that radiation induces a “crop” of cancers over and above the natural incidence unrelated to it. The **relative risk model** assumes that the effect of radiation is to increase the natural incidence *at all ages* subsequent to exposure by a given factor. Because the natural or spontaneous cancer incidence rises significantly in old age, the relative risk model predicts a large number of radiation-induced cancers in old age.

The model favored by recent BEIR committees, for the assessment of the cancer risks from the Japanese atomic bomb survivors is the **time-dependent relative risk model**. The excess incidence of cancer was assumed to be a function of dose, the square of the dose, age at exposure, and time since exposure. For some tumors, gender must be added as a variable—for example, in the case of breast cancer.

COMMITTEES CONCERNED WITH RISK ESTIMATES AND RADIATION PROTECTION

There are two series of reports that analyze available data and come up with risk estimates for radiation-induced cancer. The first is the United Nations Scientific Committee on the Effects of Atomic Radiation (UNSCEAR) reports. This committee reports to the General Assembly at regular intervals; the most recent report appeared in 2000. The second is the committee of the US National Academy of Sciences known as the BEIR. Reports appear periodically, the most recent comprehensive report (BEIR VII) appearing in 2006. To a large extent, these are “scholarly” committees, inasmuch as they are under no compulsion to draw conclusions if data are not available.

On the other hand, there are committees involved with radiation protection that cannot afford to be scholarly because they must make recommendations whether or not adequate data are available. First, there is the ICRP. This commission was originally set up and funded by the first International Congress of Radiology. Over the years, the funding base of this commission has broadened, and it has assumed the role of an independent, self-propagating committee. At a national level in the United States, there is the National Council on Radiation Protection and Measurements (NCRP). This is an independent body chartered by Congress and is funded from industry, government grants, and professional societies. The NCRP formulates policies for radiation protection in the United States often, but not always, following the lead of the ICRP. The recommendations of the NCRP carry no weight in law but are usually adopted eventually and enforced by the regulatory agencies in the United States, although there can often be a long lag period (see [Chapter 16](#) on radiation protection for more regarding these committees).

RADIATION-INDUCED CANCER IN HUMAN POPULATIONS

Under appropriate conditions, a malignancy can be induced in essentially all tissues of the body. Some of the most common are discussed in the following sections.

Leukemia

The incidence of chronic lymphocytic leukemia does not appear to be affected by radiation. Acute and chronic myeloid leukemia are the types chiefly responsible for the excess incidence observed in irradiated adults. Susceptibility to acute lymphatic or stem cell leukemia seems to be highest in childhood and to decrease sharply during maturation.

Two principal population groups provide data to determine risk estimates:

1. Survivors of the atomic bomb attacks on Hiroshima and Nagasaki
2. Patients treated for ankylosing spondylitis

Leukemia was the first malignancy to be linked with radiation exposure in the A-bomb survivors and has the highest relative risk of any malignancy. Leukemia risks increased with dose up to about 3 Sv, with evidence of upward curvature; that is, a linear-quadratic function of dose fits the data significantly better than a linear function. Because of this curvature, the risk per unit of dose at 1 Sv is about 3 times greater than at 0.1 Sv.

For those exposed younger than age about 30 years, nearly all of the excess deaths occurred before 1975, but for those exposed at older ages, the excess risk appeared to persist throughout the follow-up period. Because of these complications, simple models cannot adequately summarize leukemia risks.

Thyroid Cancer

The thyroid gland is an organ of high sensitivity for radiation carcinogenesis, at least in children; in adults, radiation is much less efficient in inducing thyroid cancer. The malignant tumors that have been produced, however, consistently have been of a histologically well-differentiated type, which develops slowly and often can be removed completely by surgery or treated successfully with radioactive iodine if metastasized; consequently, these tumors show a low mortality rate. It is estimated that about 5% of those with radiation-induced thyroid cancer die as a result.

The following are the principal population groups available for deriving risk estimates for thyroid cancer:

1. Survivors of the atomic bomb attacks on Hiroshima and Nagasaki
2. Residents of the Marshall Islands exposed to external radiation and ingested iodine-131 from fallout after the 1954 testing of a thermonuclear device, in whom there was a high incidence of nodule formation and some thyroid cancer (benign as well as malignant tumors)
3. Individuals who ingested radioactive iodine as a result of the Chernobyl accident. About 7,000 cases of thyroid cancer were observed, about half of which are thought to be due to radiation. The incidence is so high in Chernobyl because it is an area of low natural iodine levels. This experience shows how very sensitive children are and that adults are relatively resistant.

4. Children treated with x-rays for an enlarged thymus
5. Children treated for diseases of the tonsils and nasopharynx
6. Children epilated with x-rays for the treatment of tinea capitis
7. Children treated for cancer

[Figure 10.4](#) shows the relative risk for thyroid cancer after exposure to external radiation, taken from a pooled analysis of seven different studies, which dramatically illustrates the importance of age at exposure.

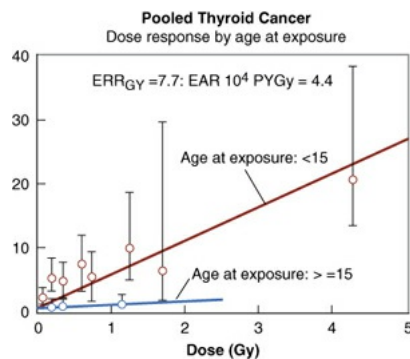


FIGURE 10.4 Relative risk of thyroid cancer after exposure to external radiation taken from a pooled analysis of seven studies. The data clearly show the importance of age at exposure. ERR, excess relative risk. (Figure prepared by Dr. Elaine Ron, based on the data from Ron E, Lubin JH, Shore RE, et al. Thyroid cancer after exposure to external radiation: a pooled analysis of seven studies. *Radiat Res.* 1995;141:259–277.)

Breast Cancer

Breast cancer may be induced with relatively high frequency by radiation. The cancer is of the type arising initially from duct cells but is commonly found to infiltrate breast tissue.

There are three principal exposed populations from which the risk of breast cancer incidence may be derived:

1. Japanese female survivors of the atomic bomb attacks on Hiroshima and Nagasaki
2. Female patients in a Nova Scotia sanatorium subjected to multiple fluoroscopies during artificial pneumothorax for pulmonary tuberculosis. There is doubt about the dosimetry, but the dose to breast tissue per fluoroscopy is estimated to have been 0.04 to 0.2 Gy. The number of examinations commonly exceeded 100, and in some instances, women received more than 500 fluoroscopies; three patients, in fact, developed

radiation dermatitis. This group of exposed women probably constitutes the most convincing evidence of the production of cancer by fractionated x-rays used for diagnosis. This Canadian study also showed the importance of age at the time of exposure. The study was later confirmed by the follow-up of patients discharged from two tuberculosis sanatoria in Massachusetts. These patients were examined fluoroscopically at an average of 102 times over a period of years and, subsequently, were found to be 80% more likely to develop breast cancer than a comparable unexposed population.

3. Females treated for postpartum mastitis and other benign conditions. Patients typically received 1 to 6 Gy and showed an excess incidence of breast cancer compared with the general female population of New York State. A legitimate objection to the use of these data for risk estimates is the uncertainty of whether postpartum mastitis predisposes to breast cancer.

The data for excess incidence of breast cancer in these populations are shown in [Figure 10.5](#). Several interesting points are immediately apparent. First, the data from the New York series of postpartum mastitis patients are so poor that they do not give any clue about the shape of the dose-response relationship. Second, there is a marked difference in the natural incidence of breast cancer in Japanese women in whom it is low, compared with American and Canadian women in whom it is high; nevertheless, in all cases, incidence rises with radiation dose. Third, the data for breast cancer are reasonably well fitted by a straight line.

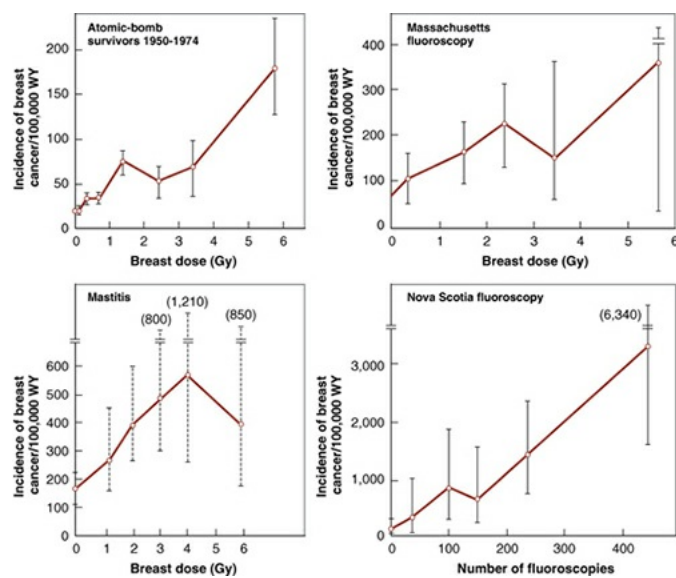


FIGURE 10.5 Incidence of breast cancer as a function of dose for four human populations that allow risk estimates to be made. The data are expressed in terms of the number of cases per 100,000 women-years (WY). Note that the natural

incidence of breast cancer is low in Japanese women and high in American and Canadian women. (Adapted from Boice JD Jr, Land CE, Shore RE, et al. Risk of breast cancer following low-dose radiation exposure. *Radiology*. 1979;131:589–597, with permission.)

Lung Cancer

Radiation is but one of a long list of carcinogens for lung cancer: Cigarette smoking, asbestos, chromium salts, mustard gas, hematite, and asphalt derivatives have also been implicated. Radiation risk estimates come from two principal sources:

1. Individuals exposed to external sources of radiation, including the Japanese survivors and those with ankylosing spondylitis. An excess was found even when smoking was taken into account.
2. Underground miners exposed to radon in the mine atmosphere. The naturally occurring deposits of radioactive materials in the rocks of the earth decay through a long series of steps until they reach a stable isotope of lead. One of these steps involves radon, which, unlike the other elements in the decay series, is a gas. In the closed environment of a mine, workers inhale radon gas and some radon atoms decay to the next solid member of the radioactive series, which consequently is deposited on the bronchial epithelium. Subsequent steps in the radioactive decay series take place in the lungs, causing intense α -irradiation of localized surrounding tissue.

There is a clear excess of lung cancer among workers in the uranium mines of the Colorado plateau in the United States, the uranium mines in Czechoslovakia, the nonuranium mines in Sweden, and the fluorspar mines in Newfoundland. It remains difficult to separate adequately the contributory effects of radon and cigarette smoking in causing the cancers because there are too few nonsmoking miners to form an adequate control group. In addition, the average duration of exposure usually spans from 15 to 20 years, during which standards of safety and ventilation have changed substantially. In any case, it is no easy matter to estimate the dose to the critical cells in the basal layer of the epithelium of the lung from knowledge of the radon concentration in the air that is breathed. There is also some evidence, summarized in the BEIR VI report, of an excess of lung cancer from domestic radon exposure. It is estimated that 10% of the 150,000 lung cancer deaths annually in the United States are caused by radon.

Bone Cancer

There is some evidence of bone cancer induced by external x-irradiation in children epilated for the treatment of tinea capitis and in patients treated for ankylosing spondylitis. The numbers are small and the risk estimates poor. The largest body of data comes from two populations, each of which ingested isotopes of radium that emit high-linear energy transfer (LET) α -particles and that follow the metabolic pathways of calcium in the body to become deposited in the bone. The populations include the following:

1. Young persons, mostly women, employed as dial painters, who ingested radium as a result of licking their brushes into a sharp point for application of luminous paint to watches and clocks. In this group, there have been bone sarcomas and carcinomas of epithelial cells lining the paranasal sinuses and nasopharynx. None of these tumors occurred at doses below 5 Gy; above this level, the incidence rose sharply, particularly the sarcomas. The radium in these paints consisted of the isotopes radium-226 and radium-228, with half-lives of about 1,600 years and 6 years, respectively.
2. Patients given injections of radium-224 for the treatment of tuberculosis or ankylosing spondylitis

There are three points that need to be emphasized. First, the dose is made up of α -particles, which have a short range and deposit their energy close to the site at which the isotope is deposited; α -particles are also more effective than x-rays by a factor of about 20. Second, osteosarcomas arise predominantly from endosteal cells, and the relevant dose for estimating the risk of sarcoma is the dose to these cells, which lie at a distance of up to $10\ \mu\text{m}$ from the bone surface rather than the mean dose throughout the bone. Radium-224 has a short half-life (3.6 days), and its radiation therefore is largely delivered while it is still present on the bone surface. This contrasts sharply with radium-226 and radium-228, which have long half-lives and, consequently, become distributed throughout the bone during their periods of radioactive decay. The dose to endosteal cells from radium-224 is about 9 times larger than the dose averaged throughout bone, whereas it is about two-thirds of the mean bone value from radium-226. Consequently, it is difficult to compare data from the two groups of people who were exposed to these very different isotopes of radium. Third, age at the time of exposure is an important factor in the development of bone cancer. For young persons, and possibly for those exposed in utero, the rapid deposition of bone-seeking radioisotopes during active bone growth might confer a higher risk of cancer than in adults. There is, in general, poor agreement among the risk

estimates derived from the various groups of persons showing an excess of bone cancer so that risk estimates must be very crude. Figure 10.6 shows the incidence of bone sarcoma in female dial painters as a function of activity of radium ingested. These data imply that a linear extrapolation from high to low doses would overestimate risks at low doses. It appears that sarcomas are induced only after large doses that are sufficient to cause tissue damage and, therefore, to stimulate cell proliferation.

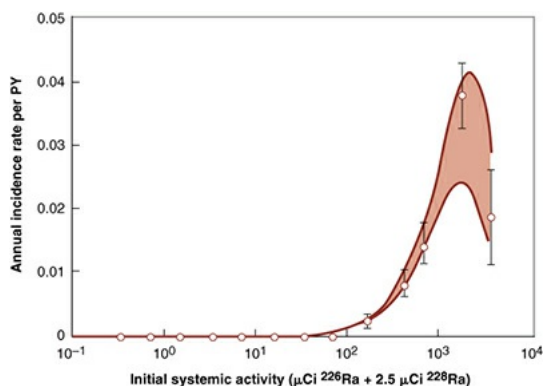


FIGURE 10.6 A semilogarithmic plot of bone sarcoma incidence rate as a function of systemic intake for female dial painters employed before 1950, showing a dose-squared exponential fit. The *shaded band* indicates the range covered by the fitted function if the coefficients are allowed to vary by ± 1 standard deviation. (Adapted from Rowland RE, Stehney AF, Lucas HF. Dose-response relationships for radium-induced bone sarcomas. *Health Phys.* 1983;44:15–31, with permission.)

Skin Cancer

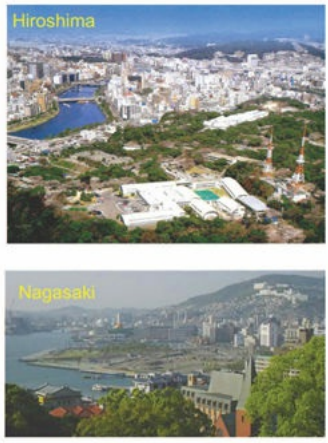
The first neoplasm attributed to x-rays was an epidermoid carcinoma on the hand of a radiologist, which was reported in 1902. In the years that followed, several hundred of such cases arose among physicians, dentists, physicists, and x-ray technicians, in an era in which safety standards were virtually nonexistent. In most cases, the onset of neoplasms followed chronic radiodermatitis and a long latent period. Squamous cell and basal cell carcinomas have been most frequently observed, and occasionally, a sarcoma of the subcutaneous tissues has been seen. Since the evolution of modern safety standards, epidermoid carcinoma has ceased to be an occupational disease of radiation workers.

Radiation-induced skin cancers are diagnosed readily and treated at an early stage of development, and there is a large difference between rates of incidence and mortality. There is a small excess incidence of skin cancer in the children epilated with x-rays for the treatment of tinea capitis.

QUANTITATIVE RISK ESTIMATES FOR RADIATION-INDUCED CANCER

Despite a diverse collection of data for cancer in humans from medical sources, both the BEIR and UNSCEAR reports elect to base their risk estimates almost entirely on the data from the survivors of the atomic bomb attacks on Hiroshima and Nagasaki. [Figure 10.7](#) summarizes the study groups available from the Radiation Effects Research Foundation (RERF).

RERF A-Bomb Cohorts	
Cohort	Size
Life Span Study	120,000 Allows an estimate of cancer incidence and mortality
In-Utero Cohort	3,600 Allows estimates of mental retardation, microcephaly, etc.
Children of exposed individuals	77,000 Allows estimate of heritable effects



The figure consists of two small photographs side-by-side. The top photograph, labeled 'Hiroshima', shows a wide view of the city with a river flowing through it. The bottom photograph, labeled 'Nagasaki', shows a more hilly and densely built urban area. Both images provide a visual context for the locations of the atomic bomb attacks.

FIGURE 10.7 There are three cohorts of A-bomb survivors available at the Radiation Effects Research Foundation (RERF) in Japan. The life span cohort includes 120,000 people that allow an estimate to be made of the cancer incidence and mortality that resulted from radiation exposure. The in utero cohort, consisting of 3,300 people who were irradiated in utero, allows an estimate to be made of mental retardation and microcephaly caused by radiation. The F1 generation (i.e., the children of exposed persons) allows a study of the heritable effects of radiation. (Reproduced with permission of RERF.)

1. The Life Span Study, comprising about 120,000 people, allows estimates to be made of the radiation-induced cancer incidence and cancer mortality. The sample includes 59% women, of whom 40% were younger than 20 years old at the time of the bombing.
2. The in utero cohort, comprising about 3,600 people who were exposed to radiation from the bombs while in utero, allows estimates to be made of the incidence of malformations, growth retardation, microcephaly, and mental retardation.
3. The children of the exposed persons, the so-called F1 generation, allows estimates to be made of heritable effects.

Figure 10.8 charts the incidence of radiation-associated deaths following the A-bomb attacks in 1945. Leukemia was the first malignancy to be linked with radiation exposure in bomb survivors and has the highest relative risk of any malignancy. Leukemia deaths reached a peak of 5 to 7 years after irradiation, subsequently falling rapidly. For those exposed younger than the age of about 30 years, nearly all of the excess deaths occurred within 30 years, but for those exposed at older ages, the excess risk appears to persist throughout the follow-up period. An excess of solid tumors did not appear at first, but once they did, excess deaths have continued up to the present time. There are about six solid cancers for each leukemia. Since about 1990, there is evidence for the induction of noncancer effects, particularly heart disease, stroke, digestive disorders, and respiratory disease, particularly at higher doses of around 1 Sv. For these noncancer end points, it is not possible to say with any certainty whether there is a threshold, nor is it clear what cellular or tissue mechanisms might underlie such a diverse set of disorders.

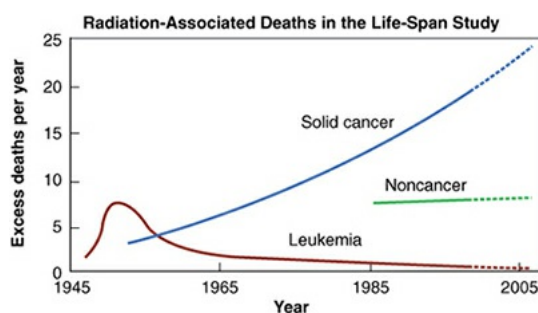


FIGURE 10.8 Illustrating the pattern of radiation-associated deaths in the Life Span Study in the A-bomb survivors. Leukemia appeared first, reaching a peak by 5 to 7 years after irradiation, before falling off later. Solid cancers did not appear in excess for several years but have continued to increase ever since. By about 1990, it was evident that there is also an excess of noncancer deaths, especially stroke and heart disease. (Courtesy of Dr. Mabuchi.)

Table 10.1 shows a summary of the data for cancer incidence in the atomic bomb survivors up to 1998. The raw data are shown principally to emphasize the relative poverty of the data; only a few hundred excess cancer cases caused by radiation are involved, compared with many thousands of naturally occurring malignancies—and these must be allocated to different dose groups and different sites.

Table 10.1 Solid Cancer 1958 through 1998

DOSE, Gy	SUBJECTS	MEAN DISTANCE, m	CASES	EXCESS
----------	----------	------------------	-------	--------

No in city	25,427	—	3,994	0
<0.005	35,545	3,969	5,603	3
0.005–	27,789	2,114	4,406	81
0.1–	5,527	1,608	968	75
0.2–	5,935	1,430	1,144	179
0.5–	3,173	1,260	688	206
1–	1,647	1,118	460	196
2–4	564	934	185	111
Total	105,427	—	17,448	853

Source: Preston DL, Ron E, Tokuoka S, et al. Solid cancer incidence in atomic bomb survivors: 1958–1998. *Radiat Res.* 2007;168:1–64.

Figure 10.9 shows the data for cancer incidence in the A-bomb survivors for the years 1958–1994. The relative risk is a linear function of dose up to about 2 Sv. Over the lower dose range from 0 to 0.5 Sv, there is a suggestion that the risks are slightly higher than the linear extrapolation from higher doses. There is some uncertainty in the control group (i.e., the zero-dose group) used for comparison. There are in fact two zero-dose groups; survivors beyond 3,000 m

and survivors within 3,000 m who, for one reason or another, were not exposed (e.g., they might have been out of the city at the time). The two groups have slightly different cancer rates, which is not surprising, because one is a rural and the other, an urban population.

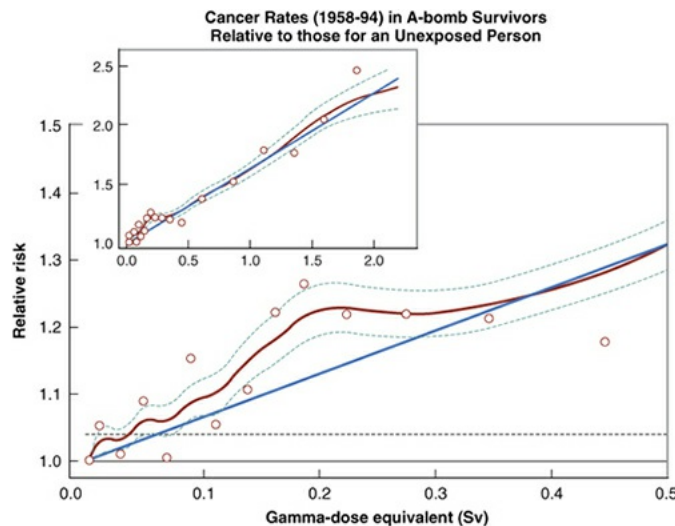


FIGURE 10.9 Estimated relative risks for cancer rates in the A-bomb survivors over the 1958–1994 follow-up period relative to unexposed persons. The *dashed curve* represents ± 1 standard error for the smoothed curve. The *inset* shows data over the whole dose range 0 to 2 Sv (0 to 200 rem), to which a straight line is fitted (i.e., relative risk is proportional to dose) with no threshold. The *main figure* is an expanded version of the low-dose region up to 0.5 Sv (500 rem). The *straight line* is taken from the inset data for the whole dose range. There is a suggestion that low-dose risks are above the line. (Adapted from Pierce DA, Preston DL. Radiation-related cancer risks at low doses among atomic bomb survivors. *Radiat Res.* 2000;154:178–186.)

DOSE AND DOSE-RATE EFFECTIVENESS FACTOR

The Japanese data relate only to high dose rates (HDRs) because they are based on the atomic bomb survivors. Both the UNSCEAR and BEIR committees considered that there is a dose-rate effect for low LET radiations; that is, fewer malignancies are induced if a given dose is spread out over a period of time at low dose rate (LDR) than if it is delivered in an acute exposure. The **dose and dose-rate effectiveness factor (DDREF)** is defined as the factor by which radiation cancer risks observed after large acute doses should be reduced when the radiation is delivered at LDR or in a series of small dose fractions. Animal data are equivocal on the subject with experiments suggesting a DDREF in the range of 2 to 10. For purposes of radiation protection, the ICRP recommends a DDREF of 2, which reflects their policy of being conservative. BEIR VII came

up with an even lower value of 1.5 based of the possible slight curvature of the dose-response relationship for solid cancers.

SUMMARY OF RISK ESTIMATES

The population averaged cancer risk estimates from the BEIR VII committee are summarized in [Table 10.2](#). As would be expected, the radiation-induced cancer incidence at 10.8% per sievert is approximately double the cancer mortality at 5.4% per sievert. It is also clear that the female cancer risks are significantly higher than the male cancer risks not only because of breast cancer but also because of lung and bladder cancers, which are affected by smoking. In Japan in 1945, smoking was common in males, but not in females.

Table 10.2 Population Average Cancer Risk Percentage per Sievert

	INCIDENCE	MORTALITY
Male	8.6	4.6
Female	12.8	6.2
Combined	10.8	5.4

Source: Calculated from the Biologic Effects of Ionizing Radiation (BEIR) VII report.

Muirhead CR, O'Hagan JA, Haylock RGE, et al. Mortality and cancer incidence following occupational radiation exposure: third analysis of the National Registry for Radiation Workers. *Br J Cancer*. 2009;100:206–212.

These estimates from the BEIR committee are for all solid cancers lumped together and for all age groups. The data from the A-bomb survivors also make it possible to calculate organ-specific risk estimates. These are summarized in [Figure 10.10](#). It appears that the bladder, breast, lung, thyroid, and colon are more radiosensitive than the average, whereas the stomach and liver are less sensitive. These data are of enormous importance because they can be used, for example, to calculate cancer risks from diagnostic or therapeutic procedures

where only a specific area of the body is irradiated.

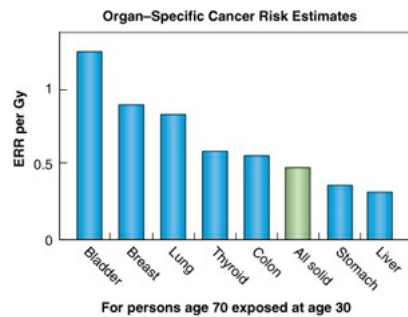


FIGURE 10.10 The study of the A-bomb survivors also makes it possible to calculate cancer risk estimates for some specific organs. In this figure, they are expressed in terms of the excess relative risk (ERR) per sievert. These figures are useful for estimating the possible risks from medical radiation where often only part of the body is exposed.

As the data from Japan have matured and more detailed information has become available, it is evident that the risk of radiation-induced cancer also varies considerably with age at the time of exposure. In most cases, those exposed at an early age are much more susceptible than those exposed at later times. The difference is most dramatic for thyroid cancer; children are very radiosensitive, whereas adults are quite resistant. It is also dramatic for breast cancer in females; females exposed before 15 years of age are most susceptible; women 50 years of age or older show little or no excess. [Figure 10.11](#) shows the variation of cancer incidence as a function of age for males and females as calculated by the BEIR VII committee from the A-bomb data. There are exceptions to this general rule. Susceptibility to radiation-induced leukemia is relatively constant throughout life, and susceptibility to respiratory cancers increases in middle age. The overall risk, however, drops dramatically with age; children and young adults are much more susceptible to radiation-induced cancer than the middle- and old-aged.

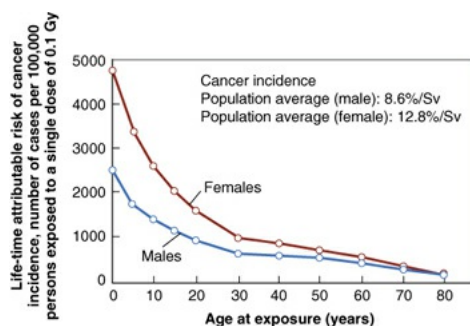


FIGURE 10.11 Illustrating how cancer incidence from radiation exposure falls dramatically with age. Children are 10 times more sensitive than older adults. It

is also clear that females are more radiosensitive than males. (Based on data from the BEIR VII report.)

An important question is the lowest dose at which there is epidemiologic evidence of a radiation-induced excess cancer incidence. There is a population of about 30,000 A-bomb survivors who lived in the outskirts of the two cities and were exposed to doses in the range of 5 to 100 mSv. This low-dose subpopulation has been studied for more than 70 years and shows a small but statistically significant increased cancer risk.

SECOND MALIGNANCIES IN RADIOTHERAPY PATIENTS

The risk of second malignancies after radiotherapy is a subject not without controversy. One of the reasons for the uncertainty is that patients undergoing radiotherapy are often at high risk of a second cancer because of their lifestyles, and this factor is more dominant than the radiation risk.

There are many single institution studies in the literature involving radiotherapy from various sites that conclude that there is no increase in second malignancies, although a more accurate assessment would have been that the studies had limited statistical power to detect a relatively small increased incidence of second malignancies induced by the treatment.

Whenever large studies have been performed, radiotherapy has been shown to be associated with a statistically significant, although small, enhancement in the risk of second malignancies, particularly in long-term survivors. The three requirements for a study to be credible are as follows:

1. A sufficiently large number of patients
2. A suitable comparison group; that is, patients with the same cancer treated by some means other than radiation
3. A sufficiently long follow-up for radiation-induced solid tumors to manifest

Only a few studies satisfy these criteria; these will be further discussed in details.

Second Cancers after Radiotherapy for Prostate Cancer

Brenner and colleagues described a study using data from the National Cancer Institute's Surveillance, Epidemiology, and End Results (SEER) program. The SEER program is a set of geographically defined, population-based tumor

registries, covering approximately 10% of the US population. The database contained information on 51,584 men with prostate cancer treated by radiotherapy and 70,539 men who underwent surgery. There was no evidence of a difference in the risk of leukemia for radiotherapy versus surgery patients, but the risk of a second solid tumor at any time postdiagnosis was significantly greater after radiotherapy than after surgery. The relative risk increased with time posttreatment and reached 34% after 10 years or more. The most dramatic increases in relative risk were for the bladder (77%) and the rectum (105%) for 10 years or more following diagnosis. The relative risks are shown in [Figure 10.12](#), together with the distribution of second cancers; note that even sites remote from the treatment area (e.g., lung) show an increased incidence. The absolute risk was about 1 in 70 by 10 years posttreatment. [Figure 10.13](#) shows the relative risk of sarcomas in the heavily irradiated tissues in or near the treatment field. It can be seen that the relative risk increases to more than 200% at 10 years or more compared with the surgical patients.

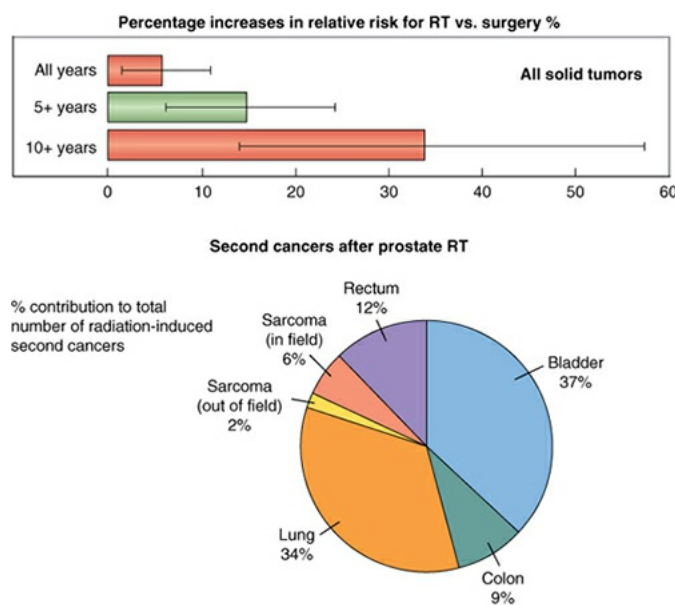


FIGURE 10.12 **Top panel:** Percentage increase in relative risk for all solid tumors (except prostate cancer) for patients who received radiotherapy (RT) for prostate cancer relative to the risk for patients who underwent surgery for prostate cancer. **Bottom panel:** Distribution of radiation-induced second cancer at 5+ years post-RT. (Illustration prepared by Dr. David Brenner based on the data from Brenner DJ, Curtis RE, Hall EJ, et al. Second malignancies in prostate carcinoma patients after radiotherapy compared with surgery. *Cancer*. 2000;88:398–406.)

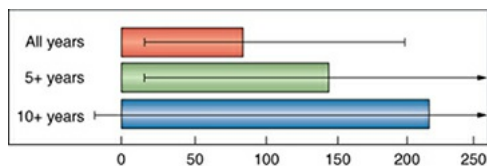


FIGURE 10.13 Percentage increase in relative risk for sarcomas in or near the treatment field for patients who received radiotherapy for prostate cancer relative to patients who underwent surgery. Although the number of tumors involved is much smaller than for all solid tumors (shown in Fig. 10.10), the relative risks are extremely high. (Adapted from Brenner DJ, Curtis RE, Hall EJ, et al. Second malignancies in prostate carcinoma patients after radiotherapy compared with surgery. *Cancer*. 2000;88:398–406, with permission.)

It is interesting to note that the increase in relative risk for carcinoma of the lung, which was exposed to a relatively low dose (about 0.5 Gy), is of the same order as that for carcinomas of the bladder, rectum, and colon, all of which were subject to much higher doses (typically more than 5 Gy). This pattern may reflect the fact that carcinomas, originating in actively dividing cells or cells under hormonal control, can be efficiently induced by relatively low doses of radiation as evidenced by the atomic bomb survivors, but the cancer risk at high doses decreases because of the effects of cell killing. In contrast to this pattern for radiation-induced carcinomas, radiation-induced sarcomas appear only in heavily irradiated sites, close to the treatment volume because large radiation doses are needed to produce sufficient tissue damage to stimulate cellular renewal in mostly dormant cells. The sarcoma data in this study appear to follow this pattern, with significant radiation-related risks being exhibited for sites in and close to the treatment volume, but no significant increases being shown for sites that are more distant.

Radiation Therapy for Carcinoma of the Cervix

In the largest study of its kind, Boice and colleagues studied the risk of second malignancies in a wide range of organs and tissues as a consequence of the treatment by radiation of carcinoma of the uterine cervix. This huge international study was a tour de force. The paper had 42 authors from 38 institutions representing both sides of the Atlantic. Such collaboration allowed the accumulation of data from 150,000 patients to be studied. This study is strengthened enormously by the fact that an ideal control group is available for comparison. This malignancy is equally well treated by radiation or surgery. The results can be summarized as follows:

1. Very high doses, on the order of several hundred gray, were found to

increase the risk of cancer of the bladder, rectum, vagina, and possibly bone, uterine corpus, and cecum as well as non-Hodgkin lymphoma. The risk ratios vary from a high of 4.0 for the bladder to a low of 1.3 for the bone. For all female genital cancers combined, a steep dose-response curve was observed, with a fivefold excess at doses of more than 150 Gy.

2. Doses of several grays increased the risk of stomach cancer and leukemia.
3. Perhaps surprisingly, radiation was found not to increase the overall risk of cancers of the small intestine, colon, ovary, vulva, connective tissue, or breast or of Hodgkin disease, multiple myeloma, or chronic lymphocytic leukemia.

The overall conclusion of this study was that excess cancers certainly were associated with radiotherapy, as opposed to surgery, and that the risks were highest among long-term survivors and concentrated among women irradiated at relatively young ages.

Second Cancers among Long-Term Survivors from Hodgkin Disease

Second cancer represents the leading cause of death in long-term survivors of Hodgkin disease, with exceptionally high risks of breast cancer among women treated at a young age. Several studies have been reported. Bhatia and colleagues reported that 17 out of 483 girls in whom Hodgkin disease was diagnosed before the age of 16 years subsequently developed breast cancer, with radiotherapy implicated in most cases. The ratio of observed to expected cases is 75.3. Another study (by Sankila and colleagues) involved 1,641 patients treated for Hodgkin disease as children in five Nordic countries and reported a relative risk that was 17 times higher than the general population based on 16 cases of breast cancer. Travis and colleagues evaluated 3,869 women in population-based registries participating in the SEER program. All these women received radiotherapy as an initial treatment for Hodgkin disease. Breast cancer developed in 55 patients, who represent a ratio of observed to expected cases of 2.24. The risk of breast cancer, however, was 60.57% in women treated before the age of 16 years, with most tumors appearing 10 or more years later. This agrees with previous studies that have shown the female breast to be very radiosensitive to carcinogenesis at young ages. The risk of breast cancer decreased with increasing age at the time of therapy and was only slightly elevated in women who were 30 years old or older when treated. In a later study, Travis and colleagues followed 3,817 female survivors of Hodgkin disease, diagnosed at

age 30 years or younger, over a long period of time. A radiation dose of 4 Gy or more delivered to the breast was associated with a 3.2-fold increase in risk. Risk increased eightfold with a dose of more than 40 Gy hormonal stimulation appears to be important for the development of radiation-induced breast cancer, as evidenced by the reduced risk in patients who received alkylating agents, as well as radiation, which caused ovarian damage.

A 2015 paper in *The New England Journal of Medicine* reported on a study of 3,905 persons followed for up to 40 years after treatment with radiation and chemotherapy for Hodgkin lymphoma. Patients had received treatment between 1965 and 2000 when they were 15 to 50 years of age. During the long follow-up, the standardized incidence ratio (SIR) for second solid cancers remained remarkably stable at about 4.5, resulting in strongly increasing excess rates of a second cancer when survivors reached ages at which background cancer rates were substantial. Even 40 years posttreatment, survivors were at increased risk for second cancers, with the cumulative incidence reaching 48.5%, compared with 19.0% in the general population. The risk of solid cancer after treatment for Hodgkin lymphoma was not lower among more recently treated patients than among those who were treated in earlier time periods despite changes in treatment protocols. However, the risk of hematopoietic second malignancies has clearly decreased among 5-year survivors who were treated in the most recent study period, which correlates with the declining use of alkylating agent-based chemotherapy. Breast cancer contributed most to the overall absolute excess risk, followed by lung cancer, gastrointestinal cancer, and non-Hodgkin lymphoma. Leukemia accounted for only 5.0% of the absolute excess risk of any cancer. As a result of increased knowledge of late effects, the treatment of Hodgkin lymphoma has evolved in recent years, with a trend toward the use of smaller radiation target volumes, lower radiation dose, and less toxic chemotherapy schemes. It is too soon to know if these changes will reduce the risk of a second cancer.

These studies clearly show that if an adequate cohort can be studied, there is a clear excess of second cancers induced by radiotherapy. The data confirm previous studies that show that in the young, the breast is especially sensitive to the carcinogenic effects of radiation. In addition, excess cancers develop with a latency of 10 years or more and persist for decades after exposure.

DOSE-RESPONSE RELATIONSHIP FOR RADIATION CARCINOGENESIS AT HIGH DOSES

In the 1960s, Gray proposed that the dose–response relationship for radiation-induced malignancies would be bell-shaped, as illustrated in [Figure 10.14](#); that is, the incidence would rise at low doses but fall at high doses. He explained this shape by the concurrent presence of two phenomena: (1) a “dose-related” *increase* in the proportion of normal cells that are transformed to a malignant state and (2) a dose-related *decrease* in the probability that transformed cells may survive the radiation exposure. Gray argued that whatever sequence of changes has taken place in the course of cell transformation, the changes must have been such as to leave the cell capable of indefinite proliferation; that is, with full reproductive integrity. The balance between transformation and cell killing leads to the overall shape, with cell killing becoming dominant at increasingly high doses. With [Figure 10.14](#), Gray was specifically attempting to explain the shape of the dose–response relationship for the induction of leukemia in mice exposed to total body irradiation, which is why the dose goes up only to 5 Gy, but it has been tacitly assumed ever since that this bell-shaped curve applies to radiation-induced carcinogenesis in general. However, several recent studies challenge the validity of this assumption by examining whether the linear dose response for radiation-induced cancer, evident in the A-bomb survivors at doses up to 2 Sv, extends to the higher dose ranges used for radiotherapy. Two studies involved the incidence of breast cancer in women treated for Hodgkin disease with a mantle field, which results in a large dose gradient across the breast (3 to 42 Gy). There was an increasing risk of breast cancer over this entire dose range. Some of the data from the Hodgkin patients, together with data from the A-bomb survivors, are shown in [Figure 10.15](#), taken from a paper by Sachs and Brenner. It clearly shows that the excess relative risk (ERR) for high-fractionated doses is larger than at the low doses received by the A-bomb survivors. It certainly does not fall as would be predicted by the Gray model in [Figure 10.14](#). Sachs and Brenner explained this difference by suggesting that cells initiated and transformed by radiation proliferate rapidly between daily dose fractions commonly used in radiotherapy.

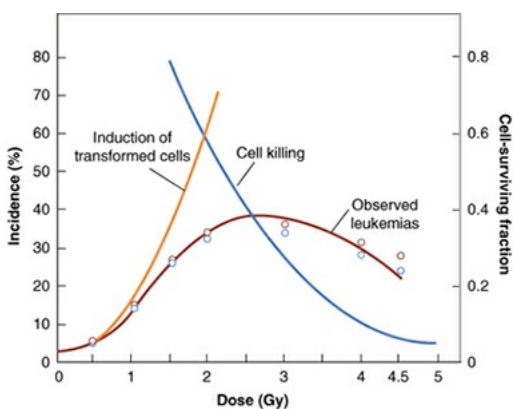


FIGURE 10.14 Illustrating the concept, introduced by Gray, that the incidence of radiation-induced leukemia in mice follows a “bell” shape because of the balance between the induction of transformed cells and cell killing. (Adapted from Gray LH. Radiation biology and cancer. In: *Cellular Radiation Biology: A Symposium Considering Radiation Effects in the Cell and Possible Implications for Cancer Therapy: A Collection of Papers*. Baltimore, MD: Lippincott Williams & Wilkins; 1965:8–25.)

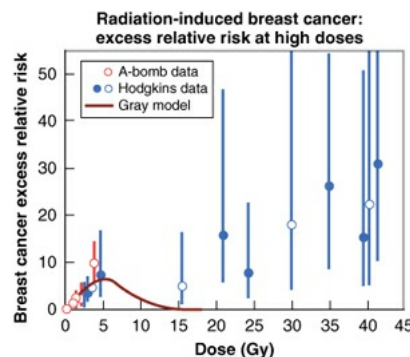


FIGURE 10.15 Excess relative risks for radiation-induced breast cancer. The low-dose data come from the A-bomb survivors, whereas the high-dose data are taken from patients treated for Hodgkin disease. The ERR does not fall at high doses as would be predicted by the Gray model, illustrated in Figure 10.12, but of course, the high doses were delivered in many small fractions over a period of time, not in a single exposure as in the Gray model. (Adapted from Sachs RK, Brenner DJ. Solid tumor risks after high doses of ionizing radiation. *Proc Natl Acad Sci U S A*. 2005;102:13040–13045, with permission).

Another study from St. Jude Children’s Research Hospital evaluated 1,612 patients with acute lymphoblastic leukemia whose primary treatment was chemotherapy but who also received prophylactic cranial irradiation because many chemotherapy agents do not effectively cross the blood–brain barrier (BBB). An excess of high-grade gliomas and meningiomas were evident during the first decade of follow-up, whereas an increased risk of low-grade brain tumors was observed at later follow-up intervals. The risk of brain tumors increased significantly with increasing radiation dose, as shown in Figure 10.16, but there is no sign of the cancer incidence falling at high doses. There is some indication of a plateau but no fall as would be predicted as cell killing takes over. As a consequence of these studies, prophylactic cranial radiotherapy (PCR) in children with leukemia has been largely replaced by intrathecal methotrexate.

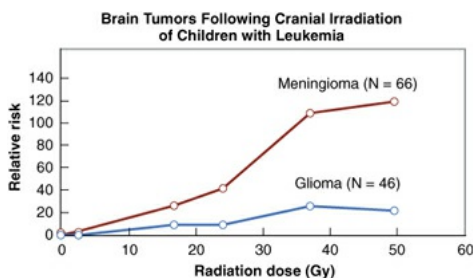


FIGURE 10.16 Illustrating the incidence of brain tumors, meningiomas, and glioma as a function of dose in children receiving total brain irradiation during the treatment of leukemia with chemotherapy. Note how the incidence tends to plateau. (Adapted from Neglia JP, Robison LL, Stovall M, et al. New primary neoplasms of the central nervous system in survivors of childhood cancer: a report from the Childhood Cancer Survivor Study. *J Natl Cancer Inst.* 2006;98:1528–1537, with permission.)

These examples are further evidences that the incidence of radiation-induced solid cancers does not fall at the high-fractionated doses typically used therapeutically and accords with the clinical observation that second cancers often occur in or near the treatment field in high-dose areas as well as in more remote locations.

CANCER RISKS IN NUCLEAR INDUSTRY WORKERS

The **International Nuclear Workers Study (INWORKS)** was done to strengthen the scientific basis for protecting people from low-dose protracted or intermittent radiation exposure in the workplace. It involved a retrospective cohort study of 308,297 workers from the nuclear industries in France, the United Kingdom, and the United States who have been monitored for external exposure to radiation with personal dosimeters and followed up for up to 60 years after exposure. This study is, to some extent, a reworking of the previously published 15-nation study but restricted to only 3 of the previous 15 countries and with a much longer follow-up. The first published part of the study involved the risk of death from leukemia and lymphoma. They showed a positive association between cumulative dose of ionizing radiation and death caused by leukemia (excluding chronic lymphocytic leukemia) among adults who were exposed to typically low doses (mean of 1.1 mGy per year) over many years (Fig. 10.17). The association was greatest for chronic myeloid leukemia, with a positive but imprecise dose-response relationship for deaths caused by acute myeloid leukemia, acute lymphoblastic leukemia, Hodgkin lymphoma, non-Hodgkin lymphoma, and multiple myeloma. It is interesting to note that the ERR (2.96 per Gy with confidence interval [CI], 1.17–5.21) is quite similar in both

size and precision to the linear dose–response relationship for male atomic bomb survivors exposed between the ages of 20 and 60 years (ERR 2.63, CI, 1.5–4.27) despite the fact that the A-bomb survivors received an acute dose, whereas the nuclear workers dose was accumulated over many years (mean of 27 years). This implies a small or nonexistent DDREF for radiation carcinogenesis.

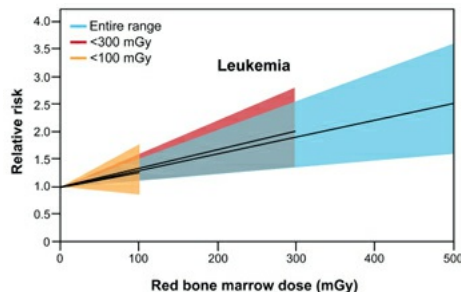


FIGURE 10.17 Relative risk of leukemia, excluding chronic lymphocytic leukemia, associated with 2-year lagged cumulative red bone marrow dose. The *lines* are the fitted linear dose–response model for different dose ranges, whereas the *shaded areas* represent the 90% CIs. (Adapted from Leuraud K, Richardson DB, Cardis E, et al. Ionising radiation and risk of death from leukaemia and lymphoma in radiation-monitored workers [INWORKS]: an international cohort study. *Lancet Haematol.* 2015;2:e276–e281.)

The second published part of the study involved the risk of mortality from all cancers excluding leukemia. The data are shown in Figure 10.18. The risk increased with cumulative dose by 48% per Gy (CI, 20%–79%). Similar associations were seen for mortality from all solid cancer, 47% per Gy (CI, 18–79%). The estimated association over the lower dose range of 0 to 100 mGy is similar in magnitude to that obtained over the entire dose range, although less precise, which indicates that the estimated risks are not driven by the highest dose categories. This excess relative risk for solid cancer is larger than, but statistically compatible with, the estimate from a mortality analysis of the Japanese male survivors of the atomic bombs who are exposed at ages 20 to 60 years (excess relative rate 0.32 per sievert with 95% CI, 0.01–0.50). Again, little indication of a DDREF.

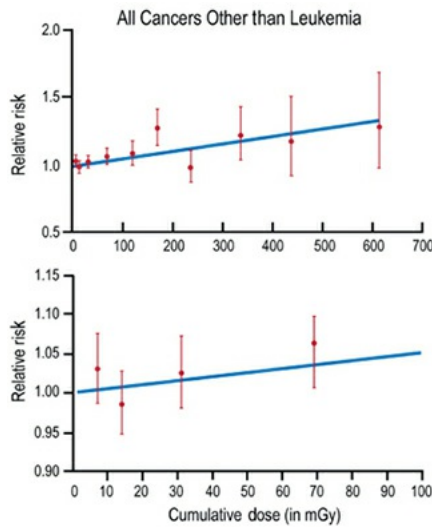


FIGURE 10.18 Relative rate of mortality due to all cancer other than leukemia as a function of dose. The **upper panel** shows the entire dose range; the **lower panel** shows the lower dose range data up to 100 mGy. (Adapted from Richardson DB, Cardis E, Daniels RD, et al. Risk of cancer from occupational exposure to ionizing radiation: retrospective cohort study of workers in France, the United Kingdom, and the United States [INWORKS]. *BMJ*. 2015;351:h5359.)

EXTRAPOLATING CANCER RISKS FROM HIGH TO LOW DOSES

The A-bomb data for the relative risk of cancer as a function of dose is well fitted by a straight line, that is, risk proportional to dose, with no obvious dose threshold (Fig. 10.9). However, the lower dose points have a large uncertainty and the epidemiologic data do not extend down to the low doses to which radiation workers are exposed. As a consequence, there has been a long-standing controversy of how best to extrapolate cancer risks from high doses to low doses. The problem is illustrated in Figure 10.19. The **linear no-threshold (LNT)** hypothesis assumes that risks at low doses can be linearly extrapolated from high doses, with no threshold in dose. Consequently, any dose greater than zero has a positive probability of producing an effect: This is illustrated as line B in Figure 10.19. This view is favored by the BEIR Committee of the US National Academy of Sciences, UNSCEAR, ICRP, and NCRP. These committees do not regard LNT as a scientific fact but describe it as a **prudent and conservative assumption** for radiation protection purposes. There are other possibilities. For example, line A in Figure 10.19 assumes that risks are higher at low doses than would be predicted from a linear extrapolation from high doses, as might be the consequence of nontargeted effects such as the bystander effect. By contrast,

some have suggested that there is a threshold in dose, below which there are no deleterious effects of radiation (line C in Fig. 10.19). Beyond this, it has been hypothesized that low levels of radiation are actually beneficial, activating repair mechanisms that protect against disease; this is known as **hormesis** and is illustrated as line D in Figure 10.19. The report of the French Academy of Sciences claims that “hormesis is seen in many laboratory studies, but not yet in humans.” Both BEIR and UNSCEAR reject hormesis in favor of LNT.

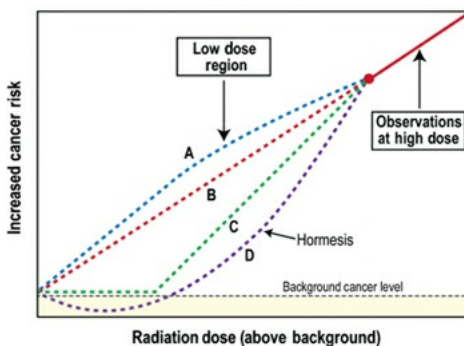


FIGURE 10.19 Illustrating the controversy of how to extrapolate cancer risks from high doses, for which there are epidemiologic data, to low doses characteristic of the radiation protection scenario. *Line B* illustrates the linear no-threshold hypothesis, favored by BEIR, UNSCEAR, ICRP, and NCRP. *Line A* assumes that risks are higher at low doses than would be predicted from a linear extrapolation. This might, for example, be a consequence of the bystander effect. *Line C* assumes that there is a threshold in dose, below which there are no deleterious biologic effects. *Line D* illustrates the hypothesis that low levels of radiation are beneficial, activating repair mechanisms that protect against disease; this is known as *hormesis*.

It is interesting to note that the new INWORKS data, described earlier, which quantify risks of leukemia and solid cancers in radiation workers studied over many years tend to support the LNT hypothesis because there is no sign of a dose threshold or any health benefit to workers exposed to low doses. Of course, the existence of a dose threshold can never be proved or disproved because it might occur at doses below which observations can be made.

MORTALITY PATTERNS IN RADIOLOGISTS

An extensive and interesting report was published by Sir Richard Doll and colleagues in 2003 that assessed 100 years of observations in terms of mortality from cancer and other causes in British radiologists entering the field from 1897 to 1997. Table 10.3 shows the trend in the standard mortality ratio (SMR) over the years. There was a clear excess of cancer in the early radiologists in the years

before the introduction of radiation safety standards. This is not surprising in that estimated annual doses to early radiologists were typically in the range of 1 Gy per year. What is surprising is that the SMR for the postwar period 1955–1979 is much smaller than unity due largely to a statistically significant lower rate of noncancer deaths. This attracted much interest, leading to speculation by some that low doses of radiation may be beneficial and may actually lead to a longer life.

Table 10.3 Standard Mortality Ratios for All Causes of Death in British Radiologists, 1897–1997

YEARS	STANDARD MORTALITY RATIO
1897–1920	1.75
1921–1935	1.24
1936–1954	1.12
1955–1979	0.71
All post 1920	1.04

Source: Berrington A, Darby SC, Weiss HA, et al. 100 years of observation on British radiologists: mortality from cancer and other causes 1897–1997. *Brit J Radiol.* 2001;74:507–519.

A weakness of the British study is that the data for the control group, labeled “all-male medical practitioners,” were in fact estimated indirectly from census data, with adjustments made to account for socioeconomic status. This weakness was remedied in a later paper by Carpenter and colleagues in which a subset of British radiologists, entering the field in the postwar years, were compared

directly with other physicians. When this was done, the SMR for either cancer mortality or overall mortality is indistinguishable from unity (Table 10.4).

Table 10.4 Second Analysis of Post–World War II British Radiologists

	BERRINGTON ET AL.	CARPENTER ET AL.
Employment years	1955–1979	1962–1979
Controls	Based on census data	Other physicians
SMR for cancer mortality	0.71 n.s.	0.99 n.s.
SMR for overall mortality	0.68 s.s.	1.03 n.s.

Abbreviations: SMR, standard mortality ratio; n.s., not statistically significant; s.s., statistically significant.

Source: Berrington A, Darby SC, Weiss HA, et al. 100 years of observation on British radiologists: mortality from cancer and other causes 1897–1997. *Br J Radiol.* 2001;74:507–519; and Carpenter LM, Swerdlow AJ, Fear NT. Mortality of doctors in different specialties: findings from a cohort of 20000 NHS hospital consultants. *Occup Environ Med.* 1997;54:388–395.

In summary, in the early days before the establishment of radiation safety standards, radiation risks to radiologists were large and easily demonstrable. In more recent years, when annual occupational doses are more than a hundredfold lower, there is no sign of an excess mortality in radiologists, compared with other medical specialties, although the numbers involved are small. At the same time, there is no good evidence that low doses of radiation may be beneficial or can prolong life.

CHILDHOOD CANCER AFTER RADIATION EXPOSURE IN UTERO

In several widely publicized British studies in the 1950s and 1960s, Stewart and her colleagues reported an excess of leukemia and childhood cancer in children irradiated in utero as a consequence of diagnostic x-ray examinations involving the pelvis of the mother. An association between leukemia and x-rays in utero was confirmed in the United States by MacMahon.

This has been a highly controversial topic. It is discussed in more detail in [Chapter 12](#). In a 1997 paper, Doll and Wakeford summarized all of the available data and came to the conclusion that radiation was the causative agent. They concluded that

Low-dose irradiation of the fetus in utero, particularly in the last trimester, causes an increased risk of childhood malignancies.

An obstetric x-ray examination, even though the dose is only about 10 mGy, increases the risk of childhood cancer by 40%.

The excess absolute risk is about 6% per gray.

The relative risk of 40% is very high because, of course, cancer is relatively rare in children. The absolute risk works out to be about 6% per gray, which is not very different from the cancer risk calculated for the atomic bomb survivors following adult exposure.

NONNEOPLASTIC DISEASE AND RADIATION

A link between exposure to high doses of ionizing radiation and damage to the heart and coronary arteries has been well established for many years based on patients irradiated for Hodgkin lymphoma and particularly patients with breast cancer from the era of cobalt-60 units, characterized by a large penumbra to the treatment field, which inevitably resulted in an appreciable dose to the heart. Darby and colleagues studied ischemic heart disease in more than 2,000 women treated for breast cancer in Sweden and Denmark between 1958 and 2001. The average mean dose to the heart was 4.9 Gy but varied widely, and the rate of coronary events increased linearly with dose to the heart by 7.4% per Gy. This, of course, is the ERR, and it is necessary to consider the baseline risk of cardiovascular disease before it is possible to obtain an estimate of the percentage of patients suffering from radiation-induced cardiovascular disease. Brenner and colleagues applied the ERR derived by Darby and colleagues to a group of patients treated for breast cancer after 2004 where the radiation doses to the heart were much lower and used three different baseline risks described as low, medium, or high. Estimates of the lifetime risks of major coronary events

for patients receiving “contemporary radiotherapy” fall in the range of 0.05% to 3.5%, with a typical value of 0.3%.

An association between radiation exposure and late occurring cardiovascular diseases emerged in the 1990s from a study of the A-bomb survivors (see Fig. 10.8). Statistically, significant associations were seen for the categories of heart disease and stroke for doses in excess of about 0.5 Sv. Shimizu and colleagues derived ERR estimates that are not very different from those derived from the radiotherapy studies. The biologic mechanism for these effects is not clear.

SUMMARY OF PERTINENT CONCLUSIONS

Radiation can produce two quite different forms of damage.

A tissue reaction (formerly called a deterministic effect) results from some cells being killed and removed from a tissue or organ. Such effects have a threshold in dose, and the severity of the effect is dose related. Radiation-induced lethality from total body irradiation is an example of a tissue reaction (deterministic effect).

A stochastic effect results when a cell is not killed by radiation but survives with a change or mutation. Radiation-induced carcinogenesis or heritable effects are examples of stochastic effects. In the case of stochastic effects, the severity of the effect is not dose related, although the probability of it occurring increases with dose with no threshold.

The human experience of radiation-induced carcinogenesis includes the survivors of the atomic bomb attacks on Hiroshima and Nagasaki, patients exposed to medical irradiation, and early workers exposed occupationally. Some examples include the following:

1. Leukemia and solid tumors in Japanese survivors of the atomic bomb
2. Leukemia in patients irradiated for ankylosing spondylitis
3. Thyroid cancer in children irradiated for benign conditions of the head and neck, such as enlarged thymus or tonsils, and children epilated for tinea capitis. Benign and malignant thyroid tumors were seen in children exposed to radioactive iodine at Chernobyl.
4. Breast cancer in patients treated with x-rays for postpartum mastitis and patients fluoroscoped repeatedly during the management of tuberculosis
5. Lung cancer in uranium miners

6. Bone cancer in dial painters who ingested radium and patients who had injections of radium for tuberculosis or ankylosing spondylitis

Latency refers to the time interval between irradiation and the appearance of the malignancy.

The shortest latency is for leukemia, with a peak of 5 to 7 years. For solid tumors, the latency may extend for 60 years or more.

Regardless of the age at exposure, radiation-induced malignancies tend to appear at the same age as spontaneous malignancies of the same type. Indeed, for solid cancers, the excess risk is apparently more like a lifelong elevation of the natural age-specific cancer risk.

To determine risk estimates for radiation-induced cancer from observed data (the Japanese atomic bomb survivors), a model must be assumed because of the following:

1. Data must be extrapolated from relatively high doses to the low doses of public health concern.
2. Data must be projected out to a full life span because large exposed populations, such as the A-bomb survivors, have not yet lived out their life spans.
3. Risks must be “transferred” from the Japanese population to, for example, a Western population with different natural cancer rates.

There are two principal risk models: The absolute risk model assumes that radiation produces a discrete “crop” of cancers, over and above the spontaneous level and unrelated to the spontaneous level. The relative risk model assumes that radiation increases the spontaneous incidence by a factor. Because the natural cancer incidence increases with age, this model predicts excess cancers appearing late in life after irradiation.

The assessment of radiation-induced cancer risks by both the BEIR and UNSCEAR committees is based on a time-related relative risk model. Excess cancer deaths were assumed to depend on dose, square of the dose, age at exposure, time since exposure, and, for some cancers, gender.

For solid tumors, the A-bomb data show that both the excess cancer incidence and mortality are a linear function of dose up to about 2 Sv.

Leukemia data were best fitted by a linear-quadratic function of dose (i.e., an upward curvature) so that the risk per unit of dose at 1 Sv is about 3 times

that at 0.1 Sv.

The Japanese atomic bomb data refer to acute exposure at an HDR. A DDREF is needed to convert risk estimates to the low dose and LDR encountered in radiation protection. From animal studies, this is anywhere from 2 to 10. The ICRP conservatively assumes a value of 2, whereas the BEIR VII committee assumes a value of 1.5.

The BEIR VII committee suggests a risk estimate of excess cancer incidence of 10.8% per sievert and excess cancer mortality of 5.4% per sievert, including a DDREF of 1.5. These figures represent a population average, with risks for females slightly higher than for males.

There is a marked reduction with age of the risk of both cancer incidence and cancer mortality. Children are so much more radiosensitive than adults.

The ICRP estimates that, on average, 13 to 15 years of life are lost for each radiation-induced cancer and that death occurs at age 68 to 70 years.

There is a clear excess of second cancers induced by radiation therapy, both in heavily irradiated tissue and in more remote organs. This is evident if a sufficiently large number of patients and an adequate control group are available for study and if there is a sufficiently long follow-up for solid tumors to manifest.

Large studies show a clear excess of second cancers after radiotherapy for prostate cancer, carcinoma of the cervix, and Hodgkin lymphoma. An excess has also been shown following radiation therapy for breast cancer, carcinoma of the testes, and various childhood malignancies.

The INWORKS involved 308,297 workers from the nuclear industries of France, the United Kingdom, and the United States, monitored for external radiation exposures and followed for up to 60 years. The first part involved death from leukemia and lymphoma. The ERR (2.63) is quite similar to that for the A-bomb survivors despite the fact the latter received an acute dose. This implies a DDREF close to unity. The second part of the study involved the risk of mortality from all cancers excluding leukemia. The ERR for solid cancers is larger than, but statistically compatible with, the estimate from a mortality analysis of A-bomb survivors of the same age. The risk over the 0 to 100 mGy range is similar in magnitude to that for the entire dose range, although less precise; again, little evidence of a DDREF.

Early radiologists who practiced prior to the 1920s showed an excess of

malignancies. No excess is evident in radiologists in recent years. The report that British radiologists live longer is not confirmed in later studies.

Irradiation in utero by diagnostic x-rays appears to increase the spontaneous incidence of leukemia and childhood cancers by a factor of about 1.4. This is a high relative risk because malignancies in children are rare, but the absolute risk is about 6% per gray—not very different from the risk estimate calculated for the A-bomb survivors following adult exposure.

From a study of both breast cancer patients receiving radiotherapy and the A-bomb survivors, it is evident that doses of more than about 0.5 Sv can result in an excess of cardiovascular diseases. It is estimated the lifetime risks of major coronary events for patients who receive radiotherapy for breast cancer (post-2004) range from 0.05% to 3.5%.

BIBLIOGRAPHY

- Andersson M, Carstensen B, Storm HH. Mortality and cancer incidence after cerebral arteriography with or without Thorotrust. *Radiat Res.* 1995;142:305–320.
- Arai T, Nakano T, Fukuhisa K, et al. Second cancer after radiation therapy for cancer of the uterine cervix. *Cancer.* 1991;67:398–405.
- Berrington A, Darby SC, Weiss HA, et al. 100 years of observation on British radiologists: mortality from cancer and other causes 1897–1997. *Br J Radiol.* 2001;74:507–519.
- Bhatia S, Robison LL, Oberlin O, et al. Breast cancer and other second neoplasms after childhood Hodgkin's disease. *N Engl J Med.* 1996;334:745–751.
- Boice JD Jr, Engholm G, Kleinman RA, et al. Radiation dose and second cancer risk in patients treated for cancer of the cervix. *Radiat Res.* 1988;116:3–55.
- Boice JD Jr, Hutchison GB. Leukemia in women following radiotherapy for cervical cancer: ten-year follow-up of an international study. *J Natl Cancer Inst.* 1980;65:115–129.
- Boice JD Jr, Land CE, Shore RE, et al. Risk of breast cancer following low-dose radiation exposure. *Radiology.* 1979;131:589–597.
- Boice JD Jr, Preston D, David FG, et al. Frequent chest X-ray fluoroscopy and breast cancer incidence among tuberculosis patients in Massachusetts. *Radiat Res.* 1991;125:214–222.

- Brenner DJ, Curtis RE, Hall EJ, et al. Second malignancies in prostate carcinoma patients after radiotherapy compared with surgery. *Cancer*. 2000;88:398–406.
- Brenner DJ, Doll R, Goodhead DT, et al. Cancer risks attributable to low doses of ionizing radiation: assessing what we really know. *Proc Natl Acad Sci U S A*. 2003;100:13761–13766.
- Brenner DJ, Hall EJ. Mortality patterns in British and US radiologists: what can we really conclude? *Br J Radiol*. 2003;76:1–2.
- Brenner DJ, Shuryak I, Jozsef G, et al. Risk and risk reduction of major coronary events associated with contemporary breast radiotherapy. *JAMA*. 2014;174:158–160.
- Cardis E, Vrijheid M, Blettner M, et al. Risk of cancer after low doses of ionising radiation: retrospective cohort study in 15 countries. *BMJ*. 2005;331:77.
- Carpenter LM, Swerdlow AJ, Fear NT. Mortality of doctors in different specialties: findings from a cohort of 20000 NHS hospital consultants. *Occup Environ Med*. 1997;54:388–395.
- Coleman CN. Secondary malignancy after treatment of Hodgkin's disease: an evolving picture. *J Clin Oncol*. 1986;4:821–824.
- Cześnin K, Wronkowski Z. Second malignancies of the irradiated area in patients treated for uterine cervix cancer. *Gynecol Oncol*. 1978;6:309–315.
- Darby SC, Ewertz M, McGale P, et al. Risk of ischemic heart disease in women after radiotherapy for breast cancer. *N Engl J Med*. 2013;368:987–998.
- Darby SC, Reeves G, Key T, et al. Mortality in a cohort of women given X-ray therapy for metropathia haemorrhagica. *Int J Cancer*. 1994;56:793–801.
- Delongchamp RR, Mabuchi K, Yoshimoto Y, et al. Cancer mortality among atomic bomb survivors exposed in utero or as young children, October 1950–May 1992. *Radiat Res*. 1997;147:385–395.
- Doll R, Wakeford R. Risk of childhood cancer from fetal irradiation. *Br J Radiol*. 1997;70:130–139.
- Fry SA. Studies of U.S. radium dial workers: an epidemiological classic. *Radiat Res*. 1998;150:S21–S29.
- Giles D, Hewitt D, Stewart A, et al. Malignant disease in childhood and

- diagnostic irradiation in utero. *Lancet*. 1956;271:447.
- Gray LH. Radiation biology and cancer. In: *Cellular Radiation Biology: A Symposium Considering Radiation Effects in the Cell and Possible Implications for Cancer Therapy: A Collection of Papers*. Baltimore, MD: Lippincott Williams & Wilkins; 1965:8–25.
- Hildreth NG, Shore RE, Hempelmann LH, et al. Risk of extrathyroid tumors following radiation treatments in infancy for thymic enlargement. *Radiat Res*. 1985;102:378–391.
- Howe GR, McLaughlin J. Breast cancer mortality between 1950 and 1987 after exposure to fractionated moderate-dose-rate ionizing radiation in the Canadian fluoroscopy cohort study and a comparison with breast cancer mortality in the atomic bomb survivors study. *Radiat Res*. 1996;145:694–707.
- International Commission on Radiation Units and Measurements. *Radiation Quantities and Units*. Washington, DC: International Commission on Radiation Units and Measurements; 1967. Report 33.
- International Commission on Radiological Protection. *Recommendations of the ICRP*. Oxford, United Kingdom: Pergamon Press; 1990. ICRP Publication 60.
- Kapp DS, Fischer D, Grady KJ, et al. Subsequent malignancies associated with carcinoma of the uterine cervix: including an analysis of the effect of patient and treatment parameters on incidence and sites of metachronous malignancies. *Int J Radiat Oncol Biol Phys*. 1982;8:197–205.
- Kleinerman RA, Boice JD Jr, Storm HH, et al. Second primary cancer after treatment for cervical cancer. An international cancer registries study. *Cancer*. 1995;76:442–452.
- Land CE. Studies of cancer and radiation dose among atomic bomb survivors. The example of breast cancer. *JAMA*. 1995;274:402–407.
- Land H, Parada LF, Weinberg RA. Tumorigenic conversion of primary embryo fibroblasts requires at least two cooperating oncogenes. *Nature*. 1983;304:596–602.
- Lee JY, Perez CA, Ettinger N, et al. The risk of second primaries subsequent to irradiation for cervix cancer. *Int J Radiat Oncol Biol Phys*. 1982;8:207–211.
- Leuraud K, Richardson DB, Cardis E, et al. Ionising radiation and risk of death

from leukaemia and lymphoma in radiation-monitored workers (INWORKS): an international cohort study. *Lancet Haematol.* 2015;2:e276–e281.

MacMahon B. Prenatal x-ray exposure and childhood cancer. *J Natl Cancer Inst.* 1962;28:1173–1191.

Matanoski GM. Risk of cancer associated with occupational exposure in radiologists and other radiation workers. In: Burchenal JH, Oettgen HF, eds. *Cancer—Achievements, Challenges and Prospects for the 1980s*. New York, NY: Grune and Stratton; 1981:241–254.

Matanoski GM, Sternberg A, Elliott EA. Does radiation exposure produce a protective effect among radiologists? *Health Phys.* 1987;52:637–643.

Modan B, Baidatz D, Mart H, et al. Radiation-induced head and neck tumours. *Lancet.* 1974;1:277–279.

Mole RH. Endosteal sensitivity to tumor induction by radiation in different species: a partial answer to an unsolved question? In: Mays C, Jee W, Lloyd R, et al, eds. *Delayed Effects of Bone-Seeking Radionuclides*. Salt Lake City, UT: University of Utah Press; 1969:249–258.

Muirhead CR, O'Hagan JA, Haylock RGE, et al. Mortality and cancer incidence following occupational radiation exposure: third analysis of the National Registry for Radiation Workers. *Br J Cancer.* 2009;100:206–212.

National Research Council. *Health Effects of Exposure of Low Levels of Ionizing Radiation: BEIR V*. Washington, DC: The National Academies Press; 1990.

National Research Council. *Health Effects of Exposure of Low Levels of Ionizing Radiation: BEIR VII*. Washington, DC: The National Academies Press; 2006.

National Research Council. *The Effects on Populations of Exposure to Low Levels of Ionizing Radiation*. Washington, DC: The National Academies Press; 1972.

National Research Council. *The Effects on Populations of Exposure to Low Levels of Ionizing Radiation: 1980*. Washington, DC: The National Academies Press; 1980.

Nekolla EA, Kellerer AM, Kuse-Isingschulte M, et al. Malignancies in patients treated with high doses of radium-224. *Radiat Res.* 1999;152:S3–S7.

Nyandoto P, Muhonen T, Joensuu H. Second cancers among long-term survivors

- from Hodgkin's disease. *Int J Radiat Oncol Biol Phys.* 1998;42:373–378.
- Pedersen-Bjergaard J, Larsen SO. Incidence of acute nonlymphocytic leukemia, preleukemia, and acute myeloproliferative syndrome up to 10 years after treatment of Hodgkin's disease. *N Engl J Med.* 1982;307:965–971.
- Pierce DA, Preston DL. Radiation-related cancer risks at low doses among atomic bomb survivors. *Radiat Res.* 2000;154:178–186.
- Pierce DA, Shimizu Y, Preston DL, et al. Studies of the mortality of atomic bomb survivors. Report 12, part I. Cancer: 1950–1990. *Radiat Res.* 1996;146:1–27.
- Preston DL, Kusumi S, Tomonaga M, et al. Cancer incidence in atomic bomb survivors. Part III. Leukemia, lymphoma and multiple myeloma, 1950–1987. *Radiat Res.* 1994;137:S68–S97.
- Preston DL, Pierce DA. The effect of changes in dosimetry on cancer mortality risk estimates in the atomic bomb survivors. *Radiat Res.* 1988;114:437–466.
- Richardson DB, Cardis E, Daniels RD, et al. Risk of cancer from occupational exposure to ionizing radiation: retrospective cohort study of workers in France, the United Kingdom, and the United States (INWORKS). *BMJ.* 2015;351:h5359.
- Ron E, Lubin JH, Shore RE, et al. Thyroid cancer after exposure to external radiation: a pooled analysis of seven studies. *Radiat Res.* 1995;141:259–277.
- Rotblat J, Lindop P. Long-term effects of a single whole-body exposure of mice to ionizing radiations: II. Causes of death. *Proc R Soc Lond B Biol Sci.* 1961;154:350–368.
- Rowland RE, Stehney AF, Lucas HF. Dose–response relationships for radium-induced bone sarcomas. *Health Phys.* 1983;44:15–31.
- Sachs RK, Brenner DJ. Solid tumor risks after high doses of ionizing radiation. *Proc Natl Acad Sci U S A.* 2005;102:13040–13045.
- Saenger EL, Thoma BE, Tompkins EA. Incidence of leukemia following treatment of hyperthyroidism. Preliminary report of the Cooperative Thyrotoxicosis Therapy Follow-Up Study. *JAMA.* 1968;205:855–862.
- Sankila R, Garwicz S, Olsen JH, et al. Risk of subsequent malignant neoplasms among 1,641 Hodgkin's disease patients diagnosed in childhood and adolescence: a population-based cohort study in the five Nordic countries. Association of the Nordic Cancer Registries and the Nordic Society of

- Pediatric Hematology and Oncology. *J Clin Oncol.* 1996;14:1442–1446.
- Schaapveld M, Aleman BM, van Eggermond AM, et al. Second cancer risks up to 40 years after treatment for Hodgkin's lymphoma. *N Engl J Med.* 2015;373:2499–2511.
- Shimizu Y, Kodama K, Nishi N, et al. Radiation exposure and circulatory disease risk: Hiroshima and Nagasaki atomic bomb survivor data, 1950–2003. *BMJ.* 2010;340:b5349.
- Shore RE, Hildreth N, Woodard E, et al. Breast cancer among women given X-ray therapy for acute postpartum mastitis. *J Natl Cancer Inst.* 1986;77:689–696.
- Shore RE, Woodard E, Hildreth N, et al. Thyroid tumors following thymus irradiation. *J Natl Cancer Inst.* 1985;74:1177–1184.
- Stewart A, Kneale GW. Changes in the cancer risk associated with obstetric radiography. *Lancet.* 1968;1:104–107.
- Stewart A, Webb J, Hewitt D. A survey of childhood malignancies. *Br Med J.* 1958;1:1495–1508.
- Thompson DE, Mabuchi K, Ron E, et al. Cancer incidence in atomic bomb survivors. Part II: Solid tumors, 1958–1987. *Radiat Res.* 1994; 137:S17–S67.
- Tokunaga M, Land CE, Tokuoka S, et al. Incidence of female breast cancer among atomic bomb survivors, 1950–1985. *Radiat Res.* 1994;138:209–223.
- Travis LB, Curtis RE, Boice JD Jr. Late effects of treatment for childhood Hodgkin's disease. *N Engl J Med.* 1996;335:352–353.
- Travis LB, Hill DA, Dores GM, et al. Breast cancer following radiotherapy and chemotherapy among young women with Hodgkin disease. *JAMA.* 2003;290:465–475.
- United Nations Scientific Committee on the Effects of Atomic Radiation. *Sources and Effects of Atomic Radiation: UNSCEAR 1994 Report to the General Assembly, with Scientific Annexes. E 94 IXII.* New York, NY: United Nations Scientific Committee on the Effects of Atomic Radiation; 1994.
- United Nations Scientific Committee on the Effects of Atomic Radiation. *Sources and Effects of Ionizing Radiation.* New York, NY: United Nations Scientific Committee on the Effects of Atomic Radiation; 1988.
- Upton AC. The dose-response relation in radiation-induced cancer. *Cancer Res.*

1961;21:717–729.

van Kaick G, Dalheimer A, Hornik S, et al. The German Thorotrast study: recent results and assessment of risks. *Radiat Res.* 1999;152:S64–S71.

van Leeuwen FE, Klokman WJ, Stovall M, et al. Roles of radiation dose, chemotherapy and hormonal factors in breast cancer following Hodgkin's disease. *J Natl Cancer Inst.* 2003;95:971–980.

Wall PL, Clausen KP. Carcinoma of urinary bladder in patients receiving cyclophosphamide. *N Engl J Med.* 1975;293:271–273.

Walter AW, Hancock ML, Pui CH, et al. Secondary brain tumors in children treated for acute lymphoblastic leukemia at St. Jude Children's Research Hospital. *J Clin Oncol.* 1998;16:3761–3767.

Weiss HA, Darby SC, Doll R. Cancer mortality following X-ray treatment for ankylosing spondylitis. *Int J Cancer.* 1994;59:327–338.

Yamamoto T, Kopecky KJ, Fujikura T, et al. Lung cancer incidence among Japanese A-bomb survivors, 1950–80. *J Radiat Res.* 1987;28:156–171.

chapter 11

Heritable Effects of Radiation

Germ Cell Production and Radiation Effects on Fertility

Review of Basic Genetics

Mutations

Mendelian

Chromosomal Changes

Multifactorial

Radiation-Induced Heritable Effects in Fruit Flies

Radiation-Induced Heritable Effects in Mice

Radiation-Induced Heritable Effects in Humans

International Commission on Radiological Protection Estimates of Hereditary Risks

Mutations in the Children of the A-Bomb Survivors

Changing Concerns for Risks

Epigenetics

Imprinted Genes

Summary of Pertinent Conclusions

Bibliography

GERM CELL PRODUCTION AND RADIATION EFFECTS ON FERTILITY

In the male mammal, spermatozoa arise from the germinal epithelium in the seminiferous tubules of the testes, and their production is continuous from puberty to death. The spermatogonial (stem) cells consist of several different populations that vary in their sensitivity to radiation. The postspermatogonial cells pass through several stages of development: primary spermatocytes, secondary spermatocytes, spermatids, and finally spermatozoa. The division of a spermatogonium to the development of mature sperm involves a period of 6

weeks in the mouse and 10 weeks in the human. The effect of radiation on fertility is not apparent immediately because the postspermatogonial cells are relatively resistant compared with the sensitive stem cells. After exposure to a moderate dose of radiation, the person remains fertile as long as mature sperm cells are available, but decreased fertility or even temporary sterility follows if these are used up. The period of sterility lasts until the spermatogonia are able to repopulate by division.

Radiation doses as low as 0.15 Gy result in oligospermia (diminished sperm count) after a latent period of about 6 weeks. Doses greater than 0.5 Gy result in azoospermia (absence of living spermatozoa) and therefore temporary sterility. The duration of azoospermia is dose dependent; recovery can begin within 1 year after doses of less than 1 Gy but requires 2 to 3.5 years after a dose of 2 Gy. The original single-dose data came from the irradiation of prisoners, which showed that a dose in excess of 6 Gy is needed to result in permanent sterility. In contrast to most organ systems where fractionation of dose results in sparing, fractionated courses cause more gonadal damage than a single dose. Studies of patients receiving radiation therapy indicate that permanent sterility can result from 2.5 to 3 Gy in a fractionated regime over 2 to 4 weeks. The induction of sterility by radiation in human males does not produce significant changes in hormone balance, libido, or physical capability.

Gonadal kinetics in women is opposite to those in men, as the germ cells are nonproliferative. All cells in the oogonial stages progress to the oocyte stage in the embryo. By 3 days after birth, in the mouse or human, all of the oocytes are in a resting phase and there is no cell division. Consequently, in the adult, there are no stem (oogonial) cells, but there are three types of follicles: immature, nearly mature, and mature. At birth, a woman has about 1 million oocytes, which are reduced to about 300,000 at puberty.

In women, radiation is highly effective at inducing permanent ovarian failure, but there is a marked age dependence in sensitivity. The dose required to induce permanent sterility varies from 12 Gy prepubertal to 2 Gy premenopausal. Pronounced hormonal changes, comparable to those associated with the natural menopause, accompany radiation-induced sterilization in females.

Overall, radiation sterility is very different between men and women, and these differences are compared and contrasted in [Table 11.1](#).

Table 11.1 Radiation Sterility—Comparing Male and Female

MALE	FEMALE
<p>Self-renewal system:</p> <p>Spermatogonia → spermatocytes → spermatids → spermatozoa</p>	<p>Gonadal kinetics opposite of males:</p> <p>By 3 d after birth, all cells progressed to oocyte stage; no further cell division</p>
<p>Latent period between irradiation and sterility</p>	<p>Neither latent period nor temporary sterility in females</p>
<p>Oligospermia and reduced fertility: 0.15 Gy</p>	—
<p>Azoospermia and temporary sterility: 0.5 Gy</p>	—
	<p>Recovery is dose dependent (1 y after 2 Gy). —</p>
<p>Permanent sterility:</p> <p>6 Gy, single dose</p> <p>2.5–3 Gy, fractionated, 2–4 wk</p>	<p>Radiation can induce permanent ovarian failure; marked age dependence</p> <p>Permanent sterility: 12 Gy, prepuberty 2 Gy, premenopausal</p>
<p>Induction of sterility does not affect hormone balance, libido, or physical capability.</p>	<p>Radiation sterility produces hormonal changes like those seen in natural menopause.</p>

REVIEW OF BASIC GENETICS

The study of the inheritance of observable characteristics includes molecular as well as morphologic and some behavioral traits. The **chromosomes** carry, in

code form, all of the information that specifies a particular human, with all of his or her individual characteristics. The chromosomes are long threadlike structures, the essential ingredient of which is DNA, which is itself a long complex molecule with a sugar-phosphate backbone. Attached to each sugar molecule is an organic base; these come in four varieties: thymine, adenine, guanine, and cytosine. This whole configuration is tightly coiled in a double helix, rather like a miniature spiral staircase, with chains of sugar molecules linked by phosphates forming the rails on either side, bridged at regular intervals by pairs of bases, which form the steps. The order or sequence of the bases contains the genetic information in code form.

A **gene** is a finite segment of DNA specified by an exact sequence of bases. Genes occur along chromosomes in linear order like beads on a string, and the position of a gene is referred to as its **locus**.

The human chromosome complement consists of 22 pairs of autosomes present in both sexes, plus a pair of sex chromosomes—the X and Y. Males have 22 pairs of autosomes plus an X and a Y. Females have 22 pairs of autosomes plus a pair of Xs. One chromosome of each pair is derived from each parent.

The human **genome** is composed of the DNA of chromosomes and, to a minute extent, the DNA of mitochondria. The 46 chromosomes contain about 6×10^9 base pairs of DNA, with each chromosomal arm including a single supercoiled molecule of DNA associated with chromosomal proteins. The total number of protein-encoding genes is in the range of 25,000 to 50,000 per haploid set of chromosomes. The study of individual genes hardly has begun, but it is apparent that some genes are smaller than this and at least one, whose mutation can cause Duchenne-type muscular dystrophy, has been reported to contain more than 103 kb of DNA. Because most protein products of genes are less than 300 kDa, the translated portions of genes are seldom larger than 10 kb, so a major part of the genome appears to be untranslated. Some of this DNA appears to be transcribed but not translated. Much of the untranslated DNA consists of **introns** that reside between translated **exons**. In addition, much of the DNA outside the exons is involved in gene regulation and RNA polymerase attachment.

Not only does this genome recombine in each generation, but it also may undergo **mutation**, a term used here to denote any change in chromosomes, their genes, and their DNA. Thus, alterations in chromosome number and structure would be included along with changes not visible microscopically. These latter changes include an array of changes in DNA, such as deletion, rearrangement, breakage in the sugar-phosphate backbone, and base alterations. Gene function

can be disturbed not only by loss or by modification of translated exons, but also through alteration of nonexonic sites that regulate transcription and translation. Mutation occurs in both germ cells and somatic cells, although it is much less apparent in the latter unless it occurs under conditions of clonal proliferation, as happens with cancer. On the other hand, many mutations in the germ line are lethal during embryonic development.

In humans, every normal cell has 46 chromosomes, 23 derived from the mother and 23 from the father. The two members of a pair of chromosomes normally have the same genes for given characteristics lined up in the same sequence. In this case, the two chromosomes are said to be **homologous**. The pair of chromosomes that determine sex is XX in the female and XY in the male; in the case of the male, therefore, the two chromosomes of this pair are **heterologous**; they do not contain parallel genes. If the two members of a pair of genes are alike, the person is said to be **homozygous** for that pair of genes; if they are different, the person is said to be **heterozygous**.

The fact that pairs of chromosomes contain corresponding sets of genes introduces the idea of dominant and recessive genes. A dominant gene, by definition, expresses itself if its corresponding gene is recessive, the recessive gene in this case being either ineffective or suppressed. A completely recessive gene is expressed only if both corresponding genes of a pair of chromosomes are recessive (i.e., the person must be homozygous for the recessive gene) or if the recessive gene is on the X chromosome in a male. Eye color is the simplest example. The gene for blue eyes is recessive; that for brown eyes is dominant. A child will have blue eyes only if he or she receives the gene for blue eyes from both parents. If both or only one of the genes that determine eye color is for brown eyes, then the child will have brown eyes because this gene is dominant. It should be pointed out that not all genes are completely dominant; some permit expression of the recessive counterpart to a varying extent, depending on the particular characteristics involved.

The Y sex chromosome in humans has genes that determine maleness but appears to have few other genes. The X chromosome, on the other hand, has many genes. If a mother carries a recessive mutant gene on the single X chromosome that she donates to her son, there is no matching gene from the father, and consequently, the recessive gene is expressed. If the offspring is a daughter, there may well be a dominant gene on the X chromosome supplied by the father, which would suppress the expression of the recessive mutant. The daughter, however, could transmit the mutant gene to her son in whom it would

be expressed. Characteristics that result from recessive genes on the X chromosome, so that they are expressed almost exclusively in male children, are said to be sex-linked. The most common examples are color blindness and hemophilia.

An elementary discussion of genetics, such as presented here, may give the impression that each characteristic of a person is determined by a single pair of genes. On the contrary, this is the exception rather than the rule because most characteristics are the result of an interplay in the expression of many genes.

MUTATIONS

Exposure of a population to radiation can cause adverse health effects in the descendants as a consequence of mutations induced in the germ cells. **Heritable diseases**, also known as **genetic diseases**,* may result when mutations occurring in the germ cells of parents are transmitted to progeny; in contrast, most cancers result from mutations in somatic cells. Because the human genome includes between 25,000 to 50,000 genes, the potential number of mutations, and thus heritable diseases, is staggering.

It is a commonly held view that radiation produces bizarre mutants and monsters, as illustrated in [Figure 11.1](#). This view is absolutely false. Radiation does not result in heritable effects that are new or unique but rather increases the frequencies of the same mutations that already occur spontaneously or naturally in that species.

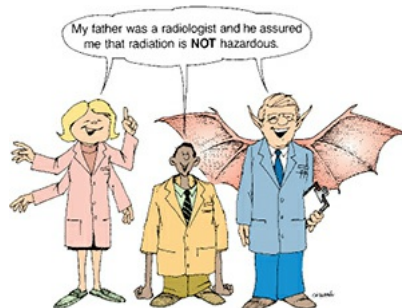


FIGURE 11.1 It is a commonly held view that radiation produces bizarre mutations or monsters that may be recognized readily. This is not true. Radiation increases the incidence of the same mutations that occur spontaneously in a given population. The study of radiation-induced heritable effects is difficult because the mutations produced by the radiation must be identified on a statistical basis in the presence of a high natural incidence of the same mutations.

Heritable diseases are classified into three principal categories: **mendelian**, **chromosomal**, and **multifactorial** ([Table 11.2](#)). The baseline frequencies of

these different classes of heritable diseases in the human population have been estimated by the United Nations Scientific Committee on the Effects of Atomic Radiation (UNSCEAR) 2001 committee and are summarized in [Table 11.3](#).

Table 11.2 Heritable Effects of Radiation

HERITABLE EFFECT	EXAMPLE
Gene mutations ^a	
Single dominant 736 (753)	Polydactyly, Huntington chorea
Recessive 521 (596)	Sickle cell anemia, Tay-Sachs disease, cystic fibrosis, retinoblastoma
Sex-linked 80 (60)	Color blindness, hemophilia
Chromosomal changes	
Too many or too few	Down syndrome (extra chromosome 21), mostly embryonic death
Chromosome aberrations, physical abnormalities	Embryonic death or mental retardation
Robertsonian translocation	Patau Syndrome or may be normal

Multifactorial	
Congenital abnormalities present at birth	Neural tube defects, cleft lip, cleft palate
Chronic diseases of adult onset	Diabetes, essential hypertension, coronary heart disease

^aThe numbers following types of gene mutations refer to several human diseases known to be caused by such a mutation. The numbers in parentheses refer to additional possible diseases.

Table 11.3 Baseline Frequencies of Genetic Diseases in Human Populations (from UNSCEAR 2001)

DISEASE CLASS	FREQUENCY PER MILLION ^a
Mendelian diseases	— 24,000
Autosomal dominant diseases	15,000 —
X-linked diseases	1,500 —
Autosomal recessive diseases	7,500 —
Chromosomal diseases	— 4,000
Multifactorial diseases	— 710,000

Chronic diseases	650,000	—
Congenital abnormalities	60,000	—
Total	—	738,000

^aFor mendelian and chromosomal diseases and for congenital abnormalities, the frequencies are per million live births; for chronic multifactorial diseases, the frequency is per million of the population.

From United Nations Scientific Committee on the Effects of Atomic Radiation. *Hereditary Effects of Radiation: UNSCEAR 2001 Report to the General Assembly, with Scientific Annex*. New York, NY: United Nations; 2001.

Mendelian

Mendelian diseases are those caused by mutations in single genes located on either the autosomes or the sex chromosomes. The mutation may be a change in the structure of DNA, which may involve either the base composition, the sequence, or both. An alteration so small that it involves the substitution, gain, or loss of a single base can be the cause of significant heritable changes. A striking example is sickle cell anemia, which results from the substitution of only one base. The important point with respect to mendelian diseases is that the relationship between mutation and disease is simple and predictable.

These diseases are subdivided into autosomal dominant, autosomal recessive, and X-linked conditions, depending on which chromosome the mutant genes are located on and the pattern of transmission. In the case of dominant diseases, one mutant gene received from either one of the parents is sufficient to cause disease, although the copy of the gene from the other parent is normal.

A **dominant** gene mutation is expressed in the first generation after its occurrence. More than 700 such conditions have been identified with certainty, and an additional 700 or more are less well established. Some examples are polydactyly, achondroplasia, and Huntington chorea. By contrast, **recessive** mutations, unless sex-linked, require that the gene be present in duplicate to produce the trait, which means that the mutant gene must be inherited from each

parent; consequently, many generations may pass before it is expressed. If one copy of the gene is mutant and the other is normal, the person is not affected. More than 500 recessive diseases are known and another 600 are suspected. Some examples are sickle cell anemia, cystic fibrosis, and Tay-Sachs disease.

X-linked recessive diseases are caused by mutations in genes located on the X chromosome. The Y chromosome contains far fewer genes than the X. Because males have only one X chromosome, all males having a mutation in the X chromosome show the effect of mutation; like dominant mutations, they are expressed soon after the mutation occurs. Because females have two X chromosomes, they need two mutant genes to show the effect of an X-linked recessive mutation. The best known examples of sex-linked disorders are hemophilia, color blindness, and a severe form of muscular dystrophy, but altogether, there are more than 80 well-established and another 60 probable conditions of this sort.

In the case of mendelian diseases, about 67% are caused predominantly by point mutations (base pair changes in the DNA), 22% by both point mutations and DNA deletions within genes (i.e., they are intragenic), and 13% by intragenic deletions and large multilocus deletions. In some genes, the mutational sites of mutations are distributed throughout the gene; in a large proportion, however, these are nonrandomly distributed—that is, restricted to specific sites along the gene (specificities). Likewise, the break points of deletions are also nonrandomly distributed, showing specificities.

Some dominant and some recessive mutant genes cause traits that are regarded by society as normal or acceptable, such as different eye colors or blood groups. The majority, however, cause diseases ranging from mild to severe in their impact on the person.

The three types of mendelian diseases are summarized as follows:

Autosomal dominant: The disease is caused by a mutation in a single gene on one chromosome.

Autosomal recessive: The disease is caused by a defective copy of the same gene from each parent.

Sex-linked: Males have one X chromosome, so one mutation can cause the disease; females have two Xs, so two mutant genes are needed to cause the disease.

Chromosomal Changes

Chromosomal diseases are caused by gross abnormalities either in the structure of the chromosomes or in the number of chromosomes (too many or too few). With a few important exceptions, gross chromosome changes that can be seen under the microscope are not compatible with viability in the fertilized egg. Down syndrome is the best known example: It results from an extra chromosome 21. It is estimated that at least 40% of the spontaneous abortions that occur from the 5th through the 28th week of gestation and about 6% of stillbirths are associated with chromosomal anomalies. This kind of chromosome error is not believed to be influenced strongly by radiation, particularly at low doses. Chromosome breakage is less frequent than aberrations among spontaneous instances of severe human anomalies, but radiation is much more effective at breaking chromosomes than in causing errors in chromosome distribution. Chromosomes that are broken may rejoin in various ways (see [Chapter 2](#)). A translocation, for example, involves the reciprocal exchange of parts between two or more chromosomes and is not necessarily harmful as long as both rearranged chromosomes are present and contain the full gene complement. Children of a person with a translocation often receive only one of the rearranged chromosomes, and their cells are therefore genetically unbalanced. The nature and extent of the abnormality may vary enormously, and the harm to the person ranges from rather mild to very severe. Chromosome imbalance, if it does not cause the death of the embryo, typically leads to physical abnormalities, usually accompanied by mental deficiency.

Robertsonian translocations are the most common type found in normal humans. These are fusions of two chromosomes, each having a spindle attachment at the end of the chromosome, to produce a single chromosome with the spindle attachment in the center. The children of a person with this type of translocation are usually normal because they inherit either the translocated pair or a pair of normal chromosomes. Radiation does not appear to be a major cause of robertsonian translocations but rather tends to induce those of the reciprocal-exchange type.

Multifactorial

The term *multifactorial* is a general designation assigned to a disease known to have a genetic component but whose transmission patterns cannot be described as simple mendelian. The common congenital abnormalities that are present at birth (e.g., neural tube defects, cleft lip with or without cleft palate) and many chronic diseases of adult onset, such as diabetes, essential hypertension, and coronary heart disease, are examples of multifactorial diseases. These diseases

result from several causes, both genetic and environmental, the nature of which can vary among persons, families, and populations. For these diseases, there is no simple relationship between mutation and disease, but the fact that genetic factors are involved is evident from observations of familial clustering; that is, these diseases run in families, but the recurrence risk to first-degree relatives is in the range of 5% to 10%, depending on the multifactorial disease, but never close to the 25% to 50% characteristic of mendelian diseases. The potential role of some of the environmental factors has been delineated for only a few of these diseases; for example, excess caloric intake rich in saturated fat is an environmental risk factor for coronary heart disease, as are environmental allergens for asthma. Mendelian and chromosomal diseases are rare and account for only a very small proportion of heritable diseases in the population; the major load is from multifactorial diseases.

Characteristics of multifactorial diseases include the following:

Known to have a genetic component

Transmission pattern not simple mendelian

Congenital abnormalities: cleft lip with or without cleft palate, neural tube defects

Adult onset: diabetes, essential hypertension, coronary heart disease

Interaction with environmental factors

RADIATION-INDUCED HERITABLE EFFECTS IN FRUIT FLIES

As early as 1927, Müller reported that exposure to x-rays could cause readily observable mutations in the fruit fly, *Drosophila melanogaster*. These included a change of eye color from red to white, the ebony mutant with its jet-black color, the “vestigial wing” mutant, and the easiest of all to observe, the recessive lethal mutation. The fact that mutants produced by radiation cannot be identified as different compared with those that occur spontaneously makes their study particularly difficult. Sample sizes must be sufficiently large to detect the small excess by radiation, which made *Drosophila* an attractive and economical biologic test system because huge numbers can be accommodated in a small space (compared, e.g., with mice). Indeed, it was heritable data from the fruit fly that led to the recommendation of a 5-R maximum permissible annual dose for radiation workers in the 1950s. The units have changed from roentgen (R) to rem to millisievert (mSv), and the justification has also changed, but the quantity

remains to this day. In the 1950s, heritable changes were considered the principal hazard of exposure to ionizing radiation. There were three reasons for this:

1. A low **doubling dose** (5 to 150 R) for mutations was estimated from fruit fly experiments. (The doubling dose is the dose required to double the spontaneous mutation rate.)
2. Based again in the fruit fly experiments, it was thought that heritable effects were cumulative; that is, a little radiation now, some next week, and some next year all added up and contributed to the genetic load carried by the human race.
3. In the 1950s, little was known of the carcinogenic potential of low doses of radiation. An excess incidence of leukemia was evident in the Japanese survivors of the A-bomb attacks, but the much larger number of solid cancers did not appear until many years later.

Over the past 50 years, the heritable risks of radiation have been progressively reduced, replaced by a concern over carcinogenesis as the data from the A-bomb survivors have matured.

RADIATION-INDUCED HERITABLE EFFECTS IN MICE

The most common way to estimate the heritable risks of radiation is to compare radiation-induced mutations with those that occur spontaneously and to express the results in terms of the doubling dose—the amount of radiation required to produce as many mutations as would occur spontaneously in a generation. The idea is based on the assumption that “if nature can do it, radiation can do it, too.” This is the **relative mutation risk**.

In the years following World War II, the husband-and-wife team of Russell and Russell, working at Oak Ridge National Laboratory, mounted an experiment of heroic proportions to determine specific locus mutation rates in the mouse under various irradiation conditions. This experiment often is referred to as the “megamouse project” because of the enormous number of animals involved. Before the study ended, 7 million mice had been used.

An inbred mouse strain was chosen in which seven specific locus mutations occur, six involving a change of coat color and one expressed as a stunted ear. [Figure 11.2](#) shows three coat-color variations: a piebald, a light honey, and a darker brown. These mutations occur spontaneously, and their incidence is increased by radiation.



FIGURE 11.2 In the megamouse project, seven specific locus mutations were used to study radiation-induced hereditary effects. This photo shows three of the mutations, which involve changes of coat color. (Courtesy of Dr. William L. Russell, Oak Ridge National Laboratory.)

These extensive studies included the irradiation of both male and female mice with a range of doses, dose rates, and fractionation patterns. Five major conclusions are pertinent to the radiologist:

1. The radiosensitivity of different mutations varies by a significant factor of about 35 so that it is only possible to speak in terms of average mutation rates. We now know that this is caused simply by a size difference among the various genes involved.
2. In the mouse, there is a substantial dose-rate effect so that spreading the radiation dose over a period results in fewer mutations for a given dose than in an acute exposure. This is in complete contrast to the data on *Drosophila*, where fractionated doses are cumulative. The big dose-rate effect discovered in the mouse was attributed to a repair process. The data are shown in Figure 11.3.

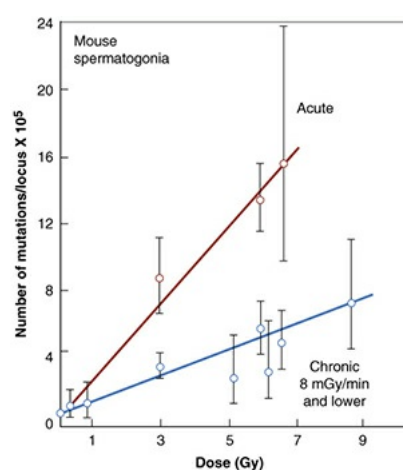


FIGURE 11.3 Mutations in mice as a function of dose, delivered at high and low dose rates. (Courtesy of Dr. William L. Russell, Oak Ridge National Laboratory.)

3. Essentially, all of the radiation-induced heritable data come from experiments with male mice. In the female, the oocytes are exquisitely radiosensitive and are readily killed by even low doses of radiation. For this reason, the mouse was an unfortunate choice as an experimental animal.
4. The heritable consequences of a given dose can be reduced greatly if a time interval is allowed between irradiation and conception, presumably caused by repair.

This information is already used in genetic counseling given to people who have received radiation. In the mouse, an interval between irradiation and insemination of 2 months in the male and rather longer in the female is sufficient to produce a maximum reduction in the effect of radiation. Although data are not available for humans, by analogy, a period of 6 months usually is recommended. Consequently, if people are exposed to significant doses of radiation, either accidentally or because of their occupation, it is recommended that 6 months be allowed to elapse between the exposure to the radiation and a planned conception to minimize the genetic consequence. This would be good advice to a person accidentally exposed to, say 0.1 Gy, to young patients with Hodgkin disease receiving radiotherapy, or even to patients subjected to diagnostic x-ray procedures involving the lumbar spine or the lower gastrointestinal tract in which a large exposure is used and the gonads must be included within the radiation field.

5. The estimate of the doubling dose favored by the Committee on the Biological Effects of Ionizing Radiation (BEIR V) and the UNSCEAR 1988 is 1 Gy, based on low-dose-rate exposure. This is a calculated rather than a measured quantity, based on the measured mutation rate per locus in the mouse adjusted for the estimated comparable number of loci in the human. It also allows for the fact that the human is usually exposed at low dose rate, whereas the mouse data reflect acute exposures.

RADIATION-INDUCED HERITABLE EFFECTS IN HUMANS

To estimate the risk of heritable effects in the human population caused by

exposure to radiation, two basic pieces of data are needed: first, the baseline spontaneous mutation rate, which is known for humans, and second, the doubling dose, which can only come from mouse experiments (1 Gy). Two correction factors must then be applied, which were derived by a task force of the International Commission on Radiological Protection (ICRP) in 2000. The first must allow for the fact that not all mutations lead to a disease. This so-called **mutation component** (MC) varies for different classes of heritable diseases; it is simple for autosomal recessive diseases and very complex for multifactorial diseases. For the first generation following radiation exposure, the MC is about 0.3 for autosomal dominant and X-linked diseases, close to zero for autosomal recessive diseases, and about 0.01 to 0.02 for chronic multifactorial diseases. The second correction factor must allow for the fact that the seven specific locus mutations used to assess the doubling dose in the megamouse project are not representative of the spectrum of inducible heritable diseases in humans. The success of experimental radiation mutagenesis studies in the mouse is mainly caused by the fortunate choice of genes that are nonessential for survival of the animal or the cell and also happen to be located in nonessential regions of the genome. Most human disease-causing genes are not of this type. Among the human autosomal and X-linked genes studied, only 15% to 30% may be responsive to induced mutations that are potentially recoverable in live births. For chronic multifactorial diseases, which involve several genes, the fraction recoverable in live births would be even lower.

The [UNSCEAR 2001](#) estimates of hereditary risks for the first generation and first two generations of an irradiated population are listed in [Table 11.4](#). The risk of autosomal dominant and X-linked diseases for the first generation after irradiation is about 750 to 1,500 cases per million progeny per gray of chronic low-linear energy transfer (LET) radiation (compared with the baseline of 16,500 cases per million). The risk of autosomal recessive diseases is essentially zero (compared with the baseline of 7,500 per million). The risk of chronic diseases is about 250 to 1,200 cases per million (compared with the baseline of 650,000 per million). The risk of multisystem developmental or congenital abnormalities may be about 2,000 cases per million. Note that the total risk per gray is only about 0.41% to 0.64% of the baseline risk of 738,000 per million live births—that is, a relatively small proportion.

Table 11.4 Current Estimates of Genetic Risks from Continuing Exposure to Low–Linear Energy Transfer, Low-Dose, or Chronic Irradiation (from UNSCEAR 2001) (Assumed Doubling Dose: 1 Gy)

DISEASE CLASS	BASED FREQUENCY PER 10 ⁶ LIVE BIRTHS	RISK PER Gy PER 10 ⁶ PROGENY	
		FIRST GENERATION	UP TO SECOND GENERATION
Mendelian			
Autosomal dominant and X-linked	16,500	750–1,500	1,300–2,500
Autosomal recessive	7,500	0	0
Chromosomal	4,000	<i>a</i>	<i>a</i>
Multifactorial			
Chronic	650,000	~250–1,200	~250–1,200
Congenital abnormalities	60,000	2,000	2,400–3,000
Total	738,000	~3,000–4,700	3,950–6,700
Total risk per Gy —		~0.41–0.64	~0.53–0.91

expressed as percent of baseline			
----------------------------------	--	--	--

^aAssumed to be subsumed in part under the risk of autosomal dominant and X-linked diseases and in part under congenital abnormalities.

From United Nations Scientific Committee on the Effects of Atomic Radiation. *Heredity Effects of Radiation: UNSCEAR 2001 Report to the General Assembly, with Scientific Annex*. New York, NY: United Nations; 2001.

INTERNATIONAL COMMISSION ON RADIOLOGICAL PROTECTION ESTIMATES OF HEREDITARY RISKS

The strategy of ICRP to estimate hereditary risks is based on the data for the first two generations calculated by [UNSCEAR 2001](#) shown in [Table 11.4](#). These data refer to a “reproductive” population and apply when the radiation doses received by all people in the population are genetically significant. However, when the *total* population of all ages is considered, the genetically significant dose will be markedly lower than the total dose received over a lifetime. Genetic damage sustained by germ cells of persons who are beyond the reproductive period or who are not procreating for any reason poses no heritable risks. Assuming an average life expectancy of 75 years, with mean reproductive age stopping at 30 years, the risk coefficients for a total population of all ages will be 30/75, that is, 40% of that for a reproductive population. This rounds out at 0.2% per sievert. For a *working* population, the relevant age range is only from 18 to 30 years because of the fact that no one is allowed to be a radiation worker before the age of 18 and the reproductive cycle is assumed to end at the age of 30; consequently, the risk coefficients will be 12/75, or 16% of that for a reproductive population, which rounds out at 0.1% per sievert. These figures are summarized in [Table 11.5](#).

Table 11.5 Heritable Effects—International Commission on Radiological Protection (2003)

- Total population 0.2%/Sv
- Working population 0.1%/Sv
- Based on:
 - Heritable risks for first two generations

- Life expectancy 75 years; reproductive age 30 years
- $\frac{30}{75}$
- Total population of reproductive population
- $\frac{30 - 18}{75}$
- Working population of reproductive population

MUTATIONS IN THE CHILDREN OF THE A-BOMB SURVIVORS

The survivors of the atomic bomb attacks on Hiroshima and Nagasaki constitute the largest irradiated human population studied carefully for heritable effects. Over the years, a cohort of 31,150 children born to parents receiving significant amounts of radiation (within 2 km of the bomb's hypocenter) and a somewhat larger control cohort (41,066) have been studied with respect to various indicators: first, in the early years, for congenital defects, gender of child, physical development, and survival; then, in the middle years, for cytogenetic abnormality; and, more recently, for the occurrence of malignant disease and for electrophoretic or functional defects in a battery of some 30 serum proteins or erythrocyte enzymes. None of these indicators was related significantly to parental radiation exposure, but the net regression was slightly positive.

For these various measures of heritable effects, the differences between the children of proximally and distally exposed survivors is in the direction expected if a heritable effect did result from the radiation, but in fact, none of the findings are statistically significant. Nevertheless, the differences between these groups of children were used to calculate doubling doses.

Only three of these indicators lend themselves to an estimate of doubling dose, and the results are shown in [Table 11.6](#), taken from a study in the early 1980s. The simple average of the three estimates is 1.56 Sv. In a more recent review paper, Neel estimated the doubling dose for the human to be about 2 Sv; this is subject to considerable uncertainties, with a lower limit of 1 Sv and an upper limit that is indeterminate. This, of course, refers to an acute radiation dose because it is based on the Japanese survivors.

Table 11.6 Doubling Dose (Gametic) in the Offspring of Survivors of the Atomic Bomb Attacks on Hiroshima and Nagasaki

GENETIC INDICATOR	DOUBLING DOSE, Sv
Untoward pregnancy outcome	0.69
Childhood mortality	1.47
Sex chromosome aneuploidy	2.52
Simple average	1.56

Adapted from Schull WJ, Otake M, Neel JV. Genetic effects of the atomic bomb: a reappraisal. *Science*. 1981;213:1220–1227, with permission.

A more recent study involved a subset of 11,951 of the first-generation offspring of survivors in Hiroshima and Nagasaki, conceived after the bombing, who were examined to assess the prevalence of common polygenic multifactorial diseases, including hypertension, hypercholesterolemia, diabetes mellitus, angina pectoris, myocardial infarction, or stroke. There was no evidence that maternal or paternal (or the sum of doses) was associated with an increased risk of any of the six multifactorial diseases.

The lack of a statistically significant excess of heritable effects in the children of the A-bomb survivors is consistent with the current thinking of ICRP and UNSCEAR that the risk of radiation-induced heritable effects is very small.

CHANGING CONCERNS FOR RISKS

In 1956, the ICRP reduced the dose limit for radiation workers to, effectively, what it is today—a maximum of 50 mSv per year. This was based entirely on heritable effects in the fruit fly, *Drosophila*. In the half century or so that has elapsed since that time, the level of concern involving genetic effects, or heritable effects as we call them, has declined steadily—first, because of the availability of mouse data and, more recently, with a reassessment of the importance of multifactorial diseases and doubt about the relevance of the specific locus mutations in mice. As a consequence, the percentage of radiation

detriment attributed to the genetic component in the view of ICRP has declined from 100% in 1955, to 25% in 1977, to 18% in 1991, and to only 4% in 2007. In the meantime, the level of concern involving radiation carcinogenesis has increased as more and more solid tumors have appeared in the Japanese A-bomb survivors. This trend is illustrated in [Figure 11.4](#). In the 1950s, genetic effects were considered to be the most important because solid tumors had not then appeared in large numbers in the A-bomb survivors. Over the years, concern has switched entirely so that at the present time, radiation carcinogenesis is considered to be by far the most important consequence of low doses of radiation. Meanwhile, radiation protection standards have changed little.

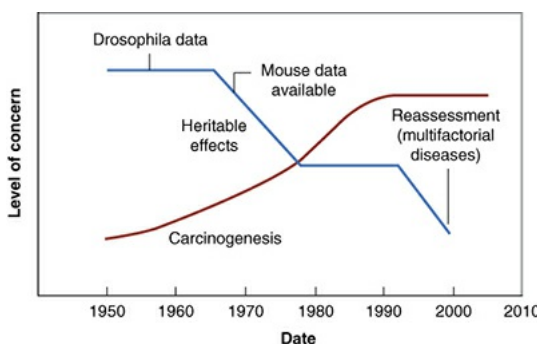


FIGURE 11.4 Illustrating how, over the past half a century, the concern regarding exposure to ionizing radiation has changed from heritable (genetic) effects to carcinogenesis. In 1950, based on mutations in the fruit fly *Drosophila*, heritable effects were considered to be the major risk of exposure to radiation. At that time, although an excess of leukemia had been observed in the A-bomb survivors, solid cancers had not shown up. Over the years, concern for heritable effects has declined, but the maturing of the A-bomb data has revealed a significant excess incidence of a whole spectrum of solid cancers.

EPIGENETICS

In this chapter so far, it has been tacitly assumed that a transgenerational heritable effect must, of necessity, involve a change in the DNA sequence. The emerging study of epigenetics implies that this is not necessarily the case.

The Greek prefix *epi-* in epigenetics implies features that are “on top of” or “in addition to” genetics; the term is now generally used to refer to changes in gene expression that takes place without a change in the DNA sequence. Epigenetic changes can result from various molecular modifications, but the most extensively studied and best understood are as follows:

1. DNA methylation, which takes place at the carbon-5 position of cytosine in CpG dinucleotides

2. Changes to chromatin packaging of DNA by posttranslational histone modifications

Both of these mechanisms can have a profound effect on gene expression, including the silencing of the gene. Other epigenetic mechanisms that are less well understood include regulation of gene expression by noncoding RNAs, including micro RNAs, and mechanisms that control the higher level organization of chromatin within the nucleus.

There is increasing evidence from animal studies that prenatal and early postnatal environmental factors can result in altered epigenetic programming and subsequent changes in the risk of developing disease later in life. Environmental factors studied to date include nutritional supplements, xenobiotic chemicals and, interestingly enough, exposure to ionizing radiation. The radiation studies showed that exposure of adult male or female mice led to transgenerational genome instability in the offspring, resulting from a significant loss of DNA methylation in somatic tissue. In addition, there is some evidence from animal studies that epigenetic alterations may be inherited transgenerationally, thereby affecting the health of future generations.

Imprinted Genes

Most autosomal genes are expressed from the alleles of both parents; however, about 1% of autosomal genes in humans are “imprinted” (i.e., expression is from only one parental allele with the other allele silenced). This leads to a nonmendelian germ line inherited form of gene regulation that involves heritable DNA methylation and histone modification. In addition, expression of the single functioning allele is parent-of-origin-dependent. Consequently, expression of an imprinted gene in the present generation depends on the environment that it experienced in the previous generation. Several human syndromes, and even some cancers, result from genetic and epigenetic modifications at imprinted loci.

An interesting example in the human involves children exposed prenatally to the Dutch famine at the end of World War II that now have an increased incidence of metabolic disorders, cardiovascular disease, and mental disorders in adulthood. They also show significant alterations in DNA methylation at both imprinted and nonimprinted loci, decades after birth.

The study of radiation on epigenetics is in its infancy, but it is a factor that may influence the perception of radiation-induced heritable effects in the future. Mutations in DNA are no longer the whole story.

SUMMARY OF PERTINENT CONCLUSIONS

In the male, doses as low as 0.15 Gy result in oligospermia (diminished sperm count) after a latent period of about 6 weeks. Doses greater than 0.5 Gy result in azoospermia (absence of living spermatozoa) and therefore temporary sterility. Recovery time depends on dose.

Permanent sterility in the male requires a single dose in excess of 6 Gy.

In the male, fractionated doses cause *more* gonadal damage than a single dose. Permanent sterility can result from a dose of 2.5 to 3 Gy in a fractionated regime over 2 to 4 weeks.

In the female, radiation is highly effective in inducing permanent ovarian failure, with a marked age dependence on the dose required.

The dose required for permanent sterility in the female varies from 12 Gy prepubertal to 2 Gy premenopausal.

The induction of sterility in males does not produce significant changes in hormone balance, libido, or physical capability, but in the female, it leads to pronounced hormonal changes comparable to natural menopause.

Exposure of a population can cause adverse health effects in the descendants because of mutations induced in germ cells. These used to be called “genetic” effects but are now more often called “heritable” effects.

Heritable diseases are classified into three principal categories: mendelian, chromosomal, and multifactorial.

Radiation does not produce new, unique mutations but increases the incidence of the same mutations that occur spontaneously.

Information on the heritable effects of radiation comes almost entirely from animal experiments.

The earlier mutation experiments were carried out with the fruit fly, *D. melanogaster*.

Relative mutation rates have been measured in the megamouse project by observing seven specific locus mutations. This leads to an estimate of the “doubling dose.”

The doubling dose is the dose required to double the spontaneous mutation incidence; put another way, it is the dose required to produce an incidence of mutations equal to the spontaneous rate. Based on the mouse data, the

doubling dose for low dose-rate exposure in the human is estimated to be 1 Gy.

Not more than 1% to 6% of spontaneous mutations in humans may be ascribed to background radiation.

To estimate the risk of radiation-induced heritable diseases in the human, two quantities are required: (1) the baseline mutation rate for a human, which is estimated to be 738,000 per million, and (2) the doubling dose from the mouse data, which is about 1 Gy.

Two correction factors are needed: (1) to allow that not all mutations lead to a disease—this is MC, which varies for different classes of heritable diseases, and (2) to allow for the fact that the seven specific locus mutations used in the mouse experiments are not representative of inducible heritable diseases in the human because they are all nonessential for the survival of the animal or cell.

The ICRP estimates that the heritable risk of radiation is about 0.2% per sievert for the general population and about 0.1% per sievert for a working population.

In terms of detriment, expressed in years of life lost or impaired, congenital anomalies (i.e., resulting from effects on the developing embryo and fetus) are much more important than heritable disorders.

First-generation children of the atomic bomb survivors have been studied for a variety of end points, including several common polygenic multifactorial diseases, but there is no evidence that the incidence of any of them is associated with paternal or maternal radiation dose.

Since the 1950s, concern for the heritable effects of radiation has declined continuously and has been replaced by carcinogenesis as the principal effect of low doses of radiation.

Epigenetics refers to changes in gene expression that take place without a change in the DNA sequence. The most studied mechanisms include DNA methylation and changes in chromatin packaging by posttranslational histone modification.

There is evidence from animal studies that prenatal and early postnatal environmental factors, including exposure to radiation, can alter epigenetic programming with subsequent changes in the risk of developing disease in later life.

BIBLIOGRAPHY

- Anway AD, Skinner MK. Epigenetic transgenerational actions of endocrine disruptors. *Endocrinology*. 2006;147:S43–S49.
- Bacq ZM, Alexander P. *Fundamentals of Radiobiology*. 2nd ed. New York, NY: Pergamon Press; 1961:436–450.
- Barker DJ. The origins of the developmental origins theory. *J Intern Med*. 2007;261:412–417.
- Gluckman PD, Hanson MA, Beedle AS. Early life events and their consequences for later disease: a life history and evolutionary perspective. *Am J Hum Biol*. 2007;19:1–19.
- Heijmans BT, Tobi EW, Stein AD, et al. Persistent epigenetic differences associated with prenatal exposure to famine in humans. *Proc Natl Acad Sci USA*. 2008;105:17046–17049.
- International Commission on Radiological Protection. Risk estimation for multifactorial diseases: ICRP Publication 83. *Ann ICRP*. 1999;29(3–4):1–2.
- International Commission on Radiological Protection, International Commission on Radiation Units and Measurements. Exposure of man to ionizing radiation arising from medical procedures: an enquiry into methods of evaluation: a report of the International Commission on Radiological Protection and International Commission on Radiological Units and Measurements. *Phys Med Biol*. 1957;2:107–151.
- Jirtle RJ. Epigenome: the program for human health and disease. *Epigenomics*. 2009;1:13–16.
- Jirtle RJ, Skinner MK. Environmental epigenetics and disease susceptibility. *Nat Rev Gen*. 2007;8:253–261.
- Koturbash I, Baker M, Loree J, et al. Epigenetic dysregulation underlies radiation-induced transgenerational genome instability in vivo. *Int J Radiat Oncol Biol Phys*. 2006;66:327–330.
- McKusick VAP. *Human Genetics*. Englewood Cliffs, NJ: Prentice Hall; 1969.
- Müller HJ. Advances in radiation mutagenesis through studies on Drosophila. In: Bugher JC, ed. *Progress in Nuclear Energy Series VI*. New York, NY: Pergamon Press; 1959:146–160.
- Müller HJ. Artificial transmutation of the gene. *Science*. 1927;66:84–87.

National Research Council. *Health Effects on Populations of Exposure to Low Levels of Ionizing Radiation: BEIR V*. Washington, DC: The National Academies Press; 1990.

National Research Council. *The Effects on Populations of Exposure to Low Levels of Ionizing Radiation*. Washington, DC: National Academy of Sciences, National Research Council; 1972.

National Research Council. *The Effects on Populations of Exposure to Low Levels of Ionizing Radiation: 1980*. Washington, DC: The National Academies Press; 1980.

Neel JV. Reappraisal of studies concerning the genetic effects of the radiation of humans, mice and *Drosophila*. *Environ Mol Mutagen*. 1998;31:4–10.

Neel JV, Schull WJ, Awa AA, et al. The children of parents exposed to atomic bombs: estimates of the genetic doubling dose of radiation for humans. *Am J Hum Genet*. 1990;46: 1053–1072.

Pochin EE. *Sizewell 13 Inquiry: The Biological Basis of the Assumption Made by NRPB in the Calculation of Health Effects and Proof of Evidence*. NRPB/P/2 (Rev). Chilton, Oxon, United Kingdom: National Radiological Protection Board; 1983.

Russell LB, Russell WL. The sensitivity of different stages in oogenesis to the radiation induction of dominant lethals and other changes in the mouse. In: Mitchell JS, Holmes BE, Smith CL, eds. *Progress in Radiobiology*. Edinburgh, United Kingdom: Oliver & Boyd; 1956:187–192.

Russell WL. Effect of the interval between irradiation and conception on mutation frequency in female mice. *Proc Natl Acad Sci USA*. 1965;54:1552–1557.

Russell WL. Genetic hazards of radiation. *Proc Am Phil Soc*. 1963;107:11–17.

Russell WL. Studies in mammalian radiation genetics. *Nucleonics*. 1965;23:53–56.

Russell WL. The effect of radiation dose rate and fractionation on mutation in mice. In: Sobels FH, ed. *Repair from Genetic Radiation Damage*. New York, NY: Pergamon Press; 1963:205–217.

Sankaranarayanan K. Ionizing radiation and genetic risks. IX. Estimates of the frequencies of mendelian diseases and spontaneous mutation rates in human populations: a 1998 perspective. *Mutat Res*. 1998;411:129–178.

Sankaranarayanan K. Ionizing radiation and genetic risks. X. The potential “disease phenotypes” of radiation-induced genetic damage in humans: perspectives from human molecular biology and radiation genetics. *Mutat Res.* 1999;429:45–83.

Sankaranarayanan K, Chakraborty R. Ionizing radiation and genetic risks. XI. The doubling dose estimates from the mid-1950s to the present and the conceptual change to the use of human data for spontaneous mutation rates and mouse data for induced rates for doubling dose calculations. *Mutat Res.* 2000;453:107–127.

Sankaranarayanan K, Chakraborty R. Ionizing radiation and genetic risks. XII. The concept of “potential recoverability correction factor” (PRCF) and its use for predicting the risk of radiation-inducible genetic diseases in human live births. *Mutat Res.* 2000;453:129–181.

Sankaranarayanan K, Chakraborty R. Ionizing radiation and genetic risks. XIII. Summary and synthesis of papers VI to XII and estimates of genetic risks in the year 2000. *Mutat Res.* 2000;453:183–197.

Schull WL, Otake M, Neel JV. Genetic effects of the atomic bomb: a reappraisal. *Science*. 1981;213:1220–1227.

Searle GH, Phillips RJS. Genetic effect of high-LET radiation in mice. *Space Radiol Biol Radiat Res.* 1967;7(suppl): 294–303.

Selby PB. Induced skeletal mutations. *Genetics*. 1979;92(suppl):127–133.

Selby PB. Radiation-induced dominant skeletal mutations in mice: mutation rate, characteristics, and usefulness in estimating genetic hazard to human from radiation. In: Okada S, Imamura M, Terasima T, et al, eds. *Radiation Research: Proceedings of the Sixth International Congress of Radiation Research*. Tokyo, Japan: Toppan Printing; 1979:537–544.

Selby PB. The doubling dose for radiation, or for any other mutagen, is actually several times larger than has been previously thought if it is based on specific-locus mutation frequencies in mice. *Environ Mol Mutagen.* 1996;27:61.

Selby PB, Selby PR. Gamma-ray-induced dominant mutations that cause skeletal abnormalities in mice: I. Plan, summary of results and discussion. *Mutat Res.* 1977;43:357–375.

Spencer WP, Stern C. Experiments to test the validity of the linear R-dose/mutation frequency relation in *Drosophila* at low dosage. *Genetics*.

1948;33:43–74.

Susser E, Neugebauer R, Hock HW, et al. Schizophrenia after prenatal famine. Further evidence. *Arch Gen Psychiatry*. 1996;53:25–31.

Tatsukawa Y, Cologne JB, Hsu WL, et al. Radiation risk of individual multifactorial diseases in offspring of the atomic-bomb survivors: a clinical health study. *J Radiol Prot*. 2013;33:281–293.

Tobi EW, Lumey LH, Talens RP, et al. DNA methylation differences after exposure to prenatal famine are common and timing- and sex-specific. *Hum Mol Genet*. 2009;18:4046–4053.

United Nations Scientific Committee on the Effects of Atomic Radiation. *Genetic Effect of Radiation*. New York, NY: United Nations; 1977.

United Nations Scientific Committee on the Effects of Atomic Radiation. *Heredity Effects of Radiation: UNSCEAR 2001 Report to the General Assembly, with Scientific Annex*. New York, NY: United Nations; 2001.

United Nations Scientific Committee on the Effects of Atomic Radiation. *Ionizing Radiation: Sources and Biological Effects*. New York, NY: United Nations; 1982.

United Nations Scientific Committee on the Effects of Atomic Radiation. *Sources, Effects and Risks of Ionizing Radiation*. New York, NY: United Nations; 1988.

United Nations Scientific Committee on the Effects of Atomic Radiation. *Sources and Effects of Ionizing Radiation: UNSCEAR 1993 Report to the General Assembly, with Scientific Annexes*. New York, NY: United Nations; 1993.

Waterland RA, Lin JR, Smith CA, et al. Post-weaning diet affects genomic imprinting at the insulin-like growth factor 2 (*Igf2*) locus. *Hum Mol Genet*. 2006;15:705–716.

*Such diseases were formerly called *genetic* diseases, but the term *heritable* is more descriptive, reflecting the transfer from one generation to the next, to distinguish them from cancer, which is also, in essence, genetic.

chapter 12

Effects of Radiation on the Embryo and Fetus

Historical Perspective

Overview of Radiation Effects on the Embryo and Fetus

Data from Mice and Rats

Preimplantation

Organogenesis

The Fetal Period

Experience in Humans

Survivors of the A-Bomb Attacks on Hiroshima and Nagasaki Irradiated In Utero

Exposure to Medical Radiation

Comparison of Human and Animal Data

Cancer in Childhood after Irradiation In Utero

Occupational Exposure of Women

The Pregnant or Potentially Pregnant Patient

Summary of Pertinent Conclusions

Bibliography

HISTORICAL PERSPECTIVE

In the early years of the 20th century, case reports began to appear in the medical literature that described mental retardation in children with small head size, as well as other gross malformations, born to mothers who had received pelvic radiotherapy before realizing that they were pregnant. As early as 1929, Goldstein and Murphy reviewed 38 such cases. Interestingly enough, they concluded that large doses were needed to produce such effects and did not consider diagnostic pelvic irradiation of the mother to be a hazard.

We now have a great deal of information concerning the effects of radiation

on the developing embryo and fetus from both animal experiments and the human experience.

OVERVIEW OF RADIATION EFFECTS ON THE EMBRYO AND FETUS

Among the somatic effects of radiation other than cancer, developmental effects on the unborn child are of greatest concern. The classic effects are listed as follows:

1. *Lethal effects* are induced by radiation before or immediately after implantation of the embryo into the uterine wall or are induced after increasingly higher doses during all stages of intrauterine development to be expressed either before birth (prenatal death) or at about the time of birth (neonatal death).
2. *Malformations* are characteristic of the period of major organogenesis in which the main body structures are formed and especially of the most active phase of cell multiplication in the relevant structures.
3. *Growth disturbances and growth retardation, without malformations* are induced at all stages of development but particularly in the latter part of pregnancy.

The principal factors of importance are the *dose* and the *stage of gestation at which it is delivered*. *Dose rate* is also of significance because many pathologic effects on the embryo are reduced significantly by reducing the dose rate.

It should be recognized that congenital anomalies arise in all animal species, even in the absence of any radiation beyond that received from natural sources. The incidence depends largely on the time at which the anomalies are scored. In humans, the average incidence of malformed infants at birth is about 6%. Some malformations disappear after birth, but more become evident later that are not scored at birth. The global incidence roughly doubles to 12% if grown children rather than infants are examined. Any assessment of the effectiveness of radiation in inducing damage in utero must be viewed against this natural level of inborn defects and its variable expression.

DATA FROM MICE AND RATS

Most experimental data on the effect of radiation on the developing embryo or fetus have been obtained with the mouse or rat, animals that reproduce in quantity with relatively short gestation periods. Russell and Russell divided the

total developmental period in utero into three stages: (1) **preimplantation**, which extends from fertilization to the time at which the embryo attaches to the wall of the uterus; (2) **organogenesis**, the period during which the major organs are developed; and (3) the **fetal period**, during which growth of the structures already formed takes place. There is a very large variability in the relative duration of these periods among animal species as well as in the total duration of intrauterine life. In addition, at any given stage of development, the state of differentiation or maturation of any one structure, with respect to all the others, varies considerably in different species.

In the mouse, preimplantation corresponds to days 0 through 5; organogenesis, days 5 through 13; and the fetal period, day 13 through full term, which is about 20 days. The effect of about 2 Gy of x-rays delivered at various times after conception is illustrated in [Figure 12.1](#). The lower scale contains Rugh's estimates of the equivalent ages for human embryos based solely on comparable stages of organ development. It is a nonlinear match because preimplantation, organogenesis, and the fetal period in the mouse are about equal in length, whereas the fetal period in the human is proportionately much longer.

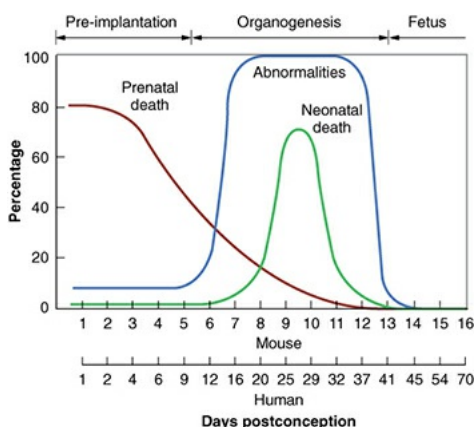


FIGURE 12.1 Incidence of abnormalities and of prenatal and neonatal death in mice given a dose of about 2 Gy of x-rays at various times after fertilization. The lower scale consists of Rugh's estimates of the equivalent stages for the human embryo. (Data from Russell LB, Russell WL. An analysis of the changing radiation response of the developing mouse embryo. *J Cell Physiol*. 1954;43[suppl 1]:103–149.)

[Figure 12.2](#) is taken from the work of Brent and Ghosh, who performed an extensive series of experiments with rats. It shows the various periods during gestation in which the principal effects of radiation are most evident. The horizontal scale refers to the times of the major events during gestation for the rat and gives an estimate of the comparable stages for the human. The following

discussion of the principal effects of radiation delivered during preimplantation, organogenesis, and the fetal stages represents a consensus view, combining conclusions from various experiments with either rats or mice.

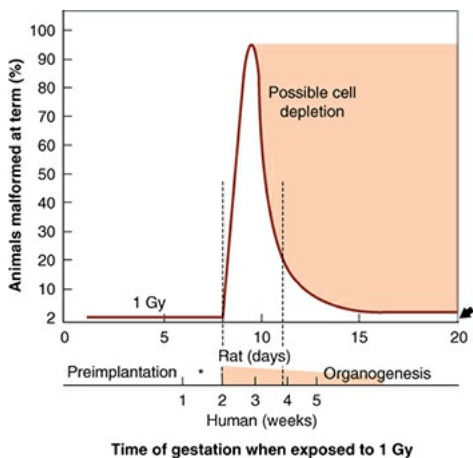


FIGURE 12.2 Relative incidence of congenital malformations in the rat after an x-ray exposure of about 1 Gy delivered at various stages during gestation. The control incidence in this species is about 2%, indicated by the *arrow* on the **right**. The incidence of malformation after irradiation before the eighth day is not detectably different from controls. A large incidence, approaching 100%, occurs if the radiation is delivered during early organogenesis, corresponding to the second through fourth week of a human pregnancy. The number of malformations produced falls off rapidly as organogenesis diminishes, although some organogenesis of the central nervous system continues to term. During the fetal stage, a dose of about 1 Gy causes an irreversible loss of cells that is expressed as growth retardation persisting to adulthood. (From Brent RL, Ghosson RO. Radiation exposure in pregnancy. *Curr Probl Radiol.* 1972;2:1–48, with permission.)

Preimplantation

Preimplantation is the most sensitive stage to the lethal effects of radiation. The high incidence of prenatal death may be expressed in a decrease in litter size. Growth retardation is not observed after irradiation at this stage; if the embryo survives, it grows normally in utero and afterward. Few, if any, abnormalities are produced by irradiation at this stage. The International Commission on Radiological Protection (ICRP) Publication 103 confirms embryonic susceptibility to the lethal effects of irradiation in the preimplantation period of embryonic development but suggests that at doses less than 100 mGy, such lethal effects will be very infrequent in the human.

Thus, the irradiated preimplanted embryo that survives grows normally, that

is, there is an “all-or-nothing” effect of radiation because if the number of cells in the conceptus is small and their nature is not yet specialized, the effect of damage to these cells is most likely to take the form of a failure to implant or an undetected death of the conceptus. This is illustrated in the remarkable pictures produced by Pedersen and reproduced in [Figure 12.3](#). If too many cells are killed by irradiation, the embryo dies and is resorbed. If only a few cells are killed, one or two cell divisions can make good the damage.

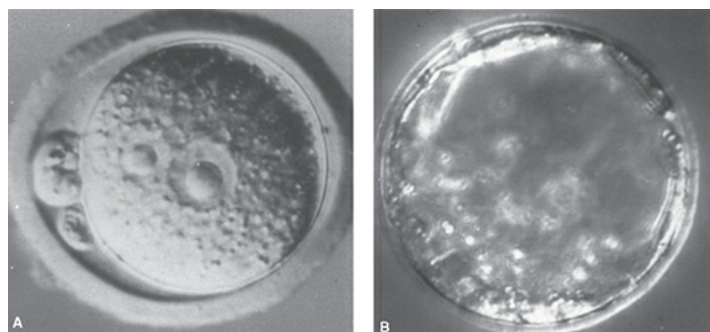


FIGURE 12.3 During preimplantation, the embryo consists of a limited number of cells. **A:** Newly fertilized mouse egg. **B:** By the third day, the mouse embryo consists of only 16 cells. About 5 days after conception in the mouse, which corresponds to about 9 or 10 days in the human, the embryo becomes embedded in the wall of the uterus, and at about this time, cells begin to differentiate to form specific tissues and organs. (Courtesy of Dr. Pedersen, University of California at San Francisco.)

Organogenesis

During organogenesis, the principal effect of radiation in small rodents is the production of various congenital anomalies of a structural nature. As seen in [Figure 12.1](#), a dose of about 2 Gy of x-rays to the mouse embryo during the period of maximum sensitivity can result in a 100% incidence of malformations at birth. A similar result is seen in [Figure 12.2](#) for rats exposed to about 1 Gy. During organogenesis, most of the embryonic cells are in their blastula or differentiating stage and are particularly sensitive. This corresponds to the period in the human at which the tranquilizer thalidomide produced such disastrous effects (i.e., at about 35 days after conception), and it is also the time of maximum risk of deleterious effects from the rubella virus.

Examples of gross anomalies resulting from irradiation during the period of organogenesis are shown in [Figures 12.4](#) and [12.5](#). It is characteristic of mice and rats that various structural malformations are seen. The production of a specific defect is associated with a definite time during this period of

organogenesis, usually the time of the first morphologic evidence of differentiation in the organ or portion of the organ involved. On the basis of animal experiments, there appears to be a dose threshold of about 100 mGy for the induction of malformations during organogenesis, so that for practical purposes, the risks of malformations in the human, for doses well below 100 mGy, would not be expected (ICRP Publication No. 103).



FIGURE 12.4 Litter from a female mouse irradiated with x-rays during organogenesis and sacrificed at 19 days. Several anomalies are demonstrated in this litter. There are four resorbed embryos (**bottom**) and five fetuses that would have been born alive (**top**). From **left** to **right**, the first shows exencephaly; the second, exencephaly and evisceration; the third is apparently normal; and the remaining two are anencephalics with stunting. (Photograph by Dr. Roberts Rugh.)

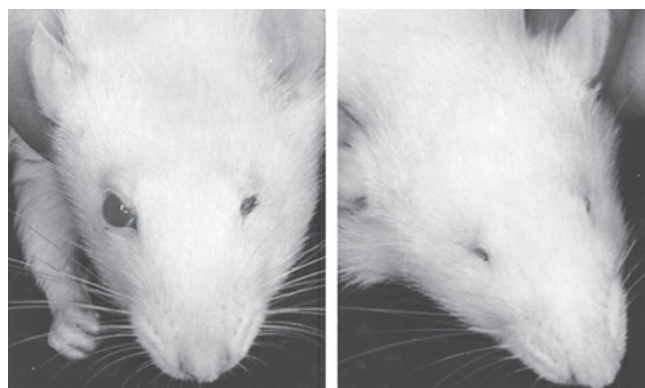


FIGURE 12.5 Two rats from the same litter exposed to a dose of about 1 Gy of x-rays 9.5 days after conception. The rat on the **left** has a normal right eye and microphthalmus of the left. The rat on the **right** shows anophthalmia of both eyes. (From Rugh R, Caveness WF, Duhamel L, et al. Structural and functional (electroencephalographic) changes in the post-natal mammalian brain resulting from x-irradiation of the embryo. *Mil Med*. 1963;128:392–408, with permission.)

Embryos exposed during early organogenesis also exhibit the greatest intrauterine growth retardation. This is expressed as a weight reduction at term and is a phenomenon resulting from cell depletion. Animals show a remarkable

ability to recover from the growth retardation produced by irradiation during organogenesis, and although they may be smaller than usual at birth, they may achieve a normal weight as adults. There is an association between growth retardation and teratogenesis: Irradiated embryos that show major congenital anomalies also suffer an overall reduction of growth. In animals, a dose of about 1 Gy of x-rays produces growth retardation if delivered at any stage of gestation (except during preimplantation); 0.25 Gy does not produce an observable effect, even at the most sensitive stage.

If death occurs because of irradiation in organogenesis, it is likely to be neonatal death—occurring at or about the time of birth. The transition from prenatal death from irradiation mainly during preimplantation to neonatal death resulting from irradiation mainly in organogenesis is very clear from [Figure 12.1](#). The neonatal deaths peak at 70% for mice receiving about 2 Gy on about the 10th day.

The Fetal Period

The remainder of pregnancy, the fetal period, extends from about day 13 onward in the mouse; this corresponds to about 6 weeks onward in the human. Various effects have been documented in the experimental animal after irradiation during the fetal stages, including effects on the hematopoietic system, liver, and kidney, all occurring, however, after relatively high radiation doses. The effects on the developing gonads have been documented particularly well, both morphologically and functionally. There appears at present to be little correspondence between the cellular and functional damage as a function of dose, but doses of a few tenths of a gray as a minimum are necessary to produce fertility changes in various animal species. The effects of radiation on humans were discussed in more detail in [Chapter 11](#).

Much higher doses of radiation are required to cause lethality during this period than at earlier stages of development, although the irradiated early fetus exhibits the largest degree of permanent growth retardation, in contrast to the embryo in early organogenesis, which exhibits the most temporary growth retardation, which is evident at term but from which the animal is able to recover later.

EXPERIENCE IN HUMANS

Information on the irradiation of human concepti comes from two major sources: studies of atomic bomb survivors in Japan and medical exposures, particularly

therapeutic irradiations, especially during the early 1900s, when hazards were not yet fully appreciated. These will be discussed in turn.

Survivors of the A-Bomb Attacks on Hiroshima and Nagasaki Irradiated In Utero

The growth to maturity of children exposed in utero at Hiroshima and Nagasaki has been studied carefully. There are difficulties associated with the dosimetry, but the conclusions have far-reaching implications.

Data on the children exposed in utero in Hiroshima and Nagasaki show too few individuals who were younger than 4 weeks of gestational age at the time the bomb was dropped. This deficiency presumably results from increased fetal loss or infant mortality rate. This stage of development is so early that damage to a single cell or group of cells is likely to impair the function of all the progeny cells and leads to death of the embryo. In accordance with this reasoning is the observation that no birth defects were found because of irradiation before 15 days of gestational age. This is in accordance with the experimental data for rats and mice in which exposure during preimplantation had an all-or-nothing effect: death of the embryo or normal development.

Exposure to radiation resulted in growth retardation ([Table 12.1](#)). Children exposed as embryos closer than 1,500 m to the hypocenter of the atomic explosion were shorter, weighed less, and had head diameters significantly smaller than children who were more than 3,000 m from the hypocenter and received negligibly small doses. It is of interest to note that there was no catchup growth because the smallness in head size was maintained into adulthood. The principal effects of irradiation in utero of the Japanese at Hiroshima and Nagasaki are small head size (microcephaly) and mental retardation. [Figure 12.6](#) is one of the few photographs available of young Japanese adults who had been exposed in utero to radiation from the atomic bomb and whose head circumference is evidently smaller than normal. The prevalence of small head diameter and mental retardation has been evaluated in persons exposed in utero to the A-bombs in Japan. The study involved about 1,600 exposed children of whom about 62 had small heads and 30 showed clinically severe mental retardation.

Table 12.1 Growth Retardation at Hiroshima from In Utero Irradiation^a:
Comparison of Those Exposed within 1,500 m^b of the Hypocenter with Those More than 3,000 m from the Hypocenter

Height	2.25 cm shorter
Weight	3 kg lighter
Head diameter	1.1 cm smaller

^a80% of 1,613 children exposed in utero followed to age 17 years.

^bAverage kerma, 0.25 Gy.

Data from Committee on the Biological Effects of Ionizing Radiations. *The Effects on Populations of Exposure to Low Levels of Ionizing Radiation*. Washington, DC: National Academy of Sciences; 1980.



FIGURE 12.6 One of the few photographs available of Japanese youths with reduced head circumference as a result of radiation exposure in utero from the atomic bombs. (From Committee for the Compilation of Materials on Damage Caused by the Atomic Bomb in Hiroshima and Nagasaki. *Hiroshima and Nagasaki: The Physical, Medical and Social Effects of the Atomic Bombings*. New York, NY: Basic Books; 1981, with permission.)

1. *Microcephaly*. A significant effect of radiation on the frequency of small heads is observed only in the periods 0 to 7 and 8 to 15 weeks postovulation. No significant excess was seen among persons exposed at 16 weeks or more. The proportion of exposed persons with microcephaly increases with dose, and there is little evidence for a threshold in dose (Fig. 12.7). As pointed out earlier, radiation-related small head size is related to a generalized growth retardation, including reduced height and weight.

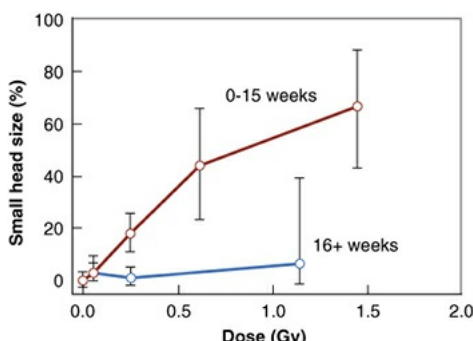


FIGURE 12.7 Proportion of exposed persons with small head sizes as a function of dose and gestational age. (Redrawn from the data of Otake M, Schull WJ. Radiation-related small head sizes among prenatally exposed A-bomb survivors. *Int J Radiat Biol.* 1993;63:255–270.)

2. *Mental retardation.* A child was deemed to be severely retarded if he or she was “unable to perform simple calculations, to make simple conversation, to care for himself or herself, or if he or she was completely unmanageable or has been institutionalized.” Most of these children were never enrolled in public schools, but among the few who were, the highest IQ was 68. In all, 30 children were judged to be severely mentally retarded; in 5 of these children, causes other than radiation were considered likely, including Down syndrome, neonatal jaundice, encephalitis, or birth trauma. Nevertheless, the remaining number represents an incidence far higher than normal. Severe mental retardation was not observed to be induced by radiation before 8 weeks after conception or after 25 weeks. The most sensitive period is 8 to 15 weeks after conception; for exposure during weeks 16 to 25, the risk is 4 times smaller. [Figure 12.8](#) shows the relation between the incidence of mental retardation and absorbed dose for this most sensitive period. The relationship appears to be linear, and the data are consistent with a probability of occurrence of mental retardation of 40% at a dose of 1 Gy. The data are clearly consistent with a threshold in dose because the incidence of severe mental retardation at the two lower doses in [Figure 12.8](#) is not statistically significant. A dose threshold is also consistent with the presumed deterministic nature of mental retardation that would require the killing of a minimum number of cells to be manifest. ICRP Publication 90 (2003) offers the view that the induction of severe mental retardation during this most sensitive period has a threshold of at least 0.3 Gy, with the absence of risk at lower doses.

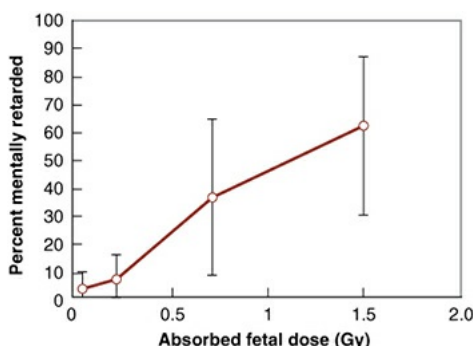


FIGURE 12.8 The frequency of mental retardation as a function of dose among those exposed in utero to atomic bomb radiation. The data are pooled from Hiroshima and Nagasaki for those exposed at 8 to 15 weeks gestational age. The vertical bars represent the 90% confidence intervals. There was no risk at 0 to 8 weeks after conception, and for exposure at later periods during gestation (16+ weeks), the excess is barely significant even at the higher doses. (Adapted from Otake M, Schull WJ. In utero exposure to A-bomb radiation and mental retardation: a reassessment. *Br J Radiol.* 1984;57:409–414, with permission.)

Microcephaly and mental retardation differ somewhat in the gestational ages at which they occur. Both occur in the 8- to 15-week period, but in the earlier period (0 to 7 weeks), microcephaly appears without mental retardation, whereas in the later period (16 to 25 weeks), mental retardation is observed in the absence of microcephaly. The highest risk of mental retardation occurs at a gestational age at which the relevant tissue, that is, the brain cortex, is being formed. It is thought to be associated with impaired proliferation, differentiation, and, most of all, migration of cells from their place of birth to their site of function. Cells killed before 8 weeks of gestation can cause small head size without mental retardation because the neurons that lead to the formation of the cerebrum are at a stage not yet sensitive to impairment by radiation. Glial cells that provide structural support for the brain are, however, susceptible to depletion. Magnetic resonance images of persons irradiated in utero at 8 to 15 weeks of gestation show evidence of massive impairment of cells to migrate from proliferative zones. A typical distribution of gray matter is often seen in patients with spontaneous mental retardation, but it is usually *unilateral*; that caused by radiation exposure is *bilateral*.

Although severe mental retardation requiring the children to be institutionalized has been known for many years in those exposed in utero at Hiroshima, later studies have shown mental impairment of less severity, indicated by IQ test scores. For irradiation during the sensitive period of 8 to 15 weeks after conception, the observed shift in intelligence test scores corresponds

to about 25 IQ points per Gy. ICRP regards these data as more difficult to interpret than the severe mental retardation data, and the possibility of a nonthreshold response cannot be ruled out. However, even in the absence of a true dose threshold, any effects on IQ following in utero doses less than about 0.1 Gy would be of no practical significance (ICRP Publication No. 103, 2003).

Exposure to Medical Radiation

A relationship between microcephaly and x-irradiation during intrauterine life has been recognized since Goldstein and Murphy first focused attention on the subject in 1929. The numbers are small and the doses are not known with any certainty, although most were in the therapeutic range. Microcephaly was reported as well as mental retardation and various defects, including spina bifida, bilateral clubfoot, ossification defects of the cranial bones, deformities of the upper extremities, hydrocephaly, alopecia of the scalp, divergent squint, and blindness at birth.

Dekaban surveyed the literature for instances of pelvic x-irradiation in pregnant women. Based on the available data, the following generalizations were proposed:

1. Large doses of radiation (2.5 Gy) delivered to the human embryo before 2 to 3 weeks of gestation are not likely to produce severe abnormalities in most children born, although a considerable number of the embryos may be resorbed or aborted.
2. Irradiation between 4 and 11 weeks of gestation would lead to severe abnormalities of many organs in most children.
3. Irradiation between 11 and 16 weeks of gestation may produce a few eye, skeletal, and genital organ abnormalities; stunted growth, microcephaly, and mental retardation are frequently present.
4. Irradiation of the fetus between 16 and 25 weeks of gestation may lead to a mild degree of microcephaly, mental retardation, and stunting of growth.
5. Irradiation after 30 weeks of gestation is not likely to produce gross structural abnormalities leading to a serious handicap in early life but could cause functional disabilities.

COMPARISON OF HUMAN AND ANIMAL DATA

Figure 12.9 is an attempt to summarize the data for the effects of radiation on the developing embryo and fetus, comparing the information from animals and

human A-bomb survivors.

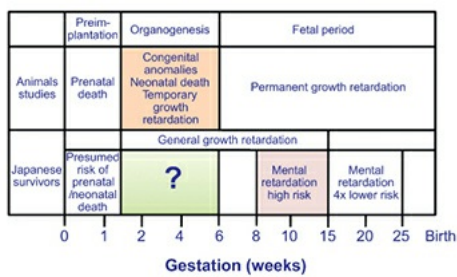


FIGURE 12.9 Chart illustrating the similarities and differences between data from small laboratory animals and data from the Japanese survivors of the atomic bomb attacks. The gestation weeks are for the human; the equivalent gestation periods have been matched for animal studies. Both sets of data indicate that irradiation early in gestation may result in the death of the embryo but that malformations do not occur. The animal data show a high incidence of a wide spectrum of malformations during organogenesis. The principal finding in the Japanese is microcephaly, which occurred up to 15 weeks, and mental retardation, which occurred most frequently following irradiation at 8 to 15 weeks of gestation and, to a lesser extent, at 16 to 25 weeks.

Exposure to radiation during preimplantation leads to a high incidence of embryonic death, but embryos that survive develop normally. This has been shown clearly in experiments with both rats and mice and is consistent with the data from Japan. In animals, irradiation during organogenesis leads to neonatal death, temporary growth retardation, and, above all, a wide range of malformations affecting many different limbs and organs. By contrast, the principal effect in the Japanese survivors of the atomic bomb attacks is microcephaly with or without mental retardation, and this begins in the eighth week, that is, after the period classically described as organogenesis. The wide array of congenital malformations found in rats and mice irradiated during organogenesis (and in humans in medical exposures) was not reported in the Japanese survivors. Much has been made of this difference. On the one hand, it has been suggested that the gross structural deformities in Japan simply were not recorded in the chaos that followed the dropping of the atomic bombs. On the other hand, it is argued that humans differ from rats and mice in that the period of susceptibility to a wide array of congenital malformations (i.e., during organogenesis) is short compared with the period during which mental retardation can be induced. Because the number of children involved is quite small, it might be expected that effects on the central nervous system, which is developing over a larger period, would dominate. The situation is different in

laboratory animals: Their susceptibility to radiation-induced small head size is of similar duration to that for the induction of other deformities. The data from patients exposed to therapeutic doses of medical radiation show a range of congenital malformations that more closely mirrors the animal results, although the numbers are small and the doses are high. To be on the safe side, it must be assumed that the entire period of gestation from about 10 days to 25 weeks is sensitive to the induction of malformations by radiation.

Table 12.2 summarizes the lowest doses at which effects on the embryo and fetus have been observed. This table summarizes the conclusions of the third report of the Committee on the Biological Effects of Ionizing Radiation (BEIR III). Readily measurable damage can be observed at doses less than 0.1 Gy delivered at sensitive stages of gestation. The principal abnormalities produced by radiation are almost certainly the consequence of damage to many cells (i.e., tissue reactions) and, therefore, would be consistent with a threshold in dose. There is also some indication of this in the data for mental retardation.

Table 12.2 Minimum Doses at Which Effects on the Embryo and Fetus Have Been Observed

ANIMAL DATA	
Oocyte killing (primates)	50% Lethal dose at 0.5 Gy
Central nervous system damage (mouse)	Threshold at 0.1 Gy
Brain damage and behavioral damage (rat)	Threshold at 60 mGy
HUMAN DATA	
Small head circumference	Air kerma, 0.1–0.19 Gy

Summary	Fetal dose, 0.06 Gy
Readily measurable damage caused by doses less than 0.1 Gy (acute exposure) delivered at sensitive stages	

Summarized from Committee on the Biological Effects of Ionizing Radiation. *The Effects on Populations of Exposure to Low Levels of Ionizing Radiation*. Washington, DC: National Academy of Sciences; 1980.

CANCER IN CHILDHOOD AFTER IRRADIATION IN UTERO

The *Oxford Survey of Childhood Cancers*, published by Stewart and Kneale in the 1950s, suggested an association between the risk of cancer, principally leukemia, up to 15 years of age and exposure in utero to diagnostic x-rays. This was a retrospective case-control study and is summarized in Table 12.3. Of 7,649 children who died of leukemia or childhood cancers, 1,141 had been x-rayed in utero. Of an equal number of controls who did not develop childhood cancer, only 774 had been irradiated prenatally. The irradiated children received one to five films, with a fetal dose per film of 4.6 to 2 mGy; however, the estimated doses are uncertain and probably varied over the period of the study. A subsequent study in New England by MacMahon also reported an association between prenatal x-rays and childhood leukemia.

Table 12.3 Childhood Cancer and Irradiation In Utero

Number of children with leukemia or cancer before age 10 years	7,649
Number x-rayed in utero	1,141
Number of matched controls	7,649

Number of controls irradiated in utero	774
Number of films	1–5
Fetal dose per film	4.6–2 mGy
Relative cancer risk estimate assuming radiation to be the causative agent	1.52

Based on Stewart A, Kneale GW. Radiation dose effects in relation to obstetric x-rays and childhood cancer. *Lancet*. 1970;1:1185–1188.

This subject has been the source of great controversy for many years. No one seriously doubts the *association* between in utero irradiation and childhood cancer; the debate is whether the radiation is *causative*. It has been suggested that, in the Oxford study discussed earlier, the maternal medical condition that prompted the x-ray examination is to blame for the observed cancer incidence rather than the irradiation itself. This is a phenomenon known as reverse causation. These uncertainties prompted studies in twins because the likelihood of medical irradiation bias would be reduced. A case-control study mounted by the National Cancer Institute involved 32,000 twins born in the 1930s and early 1940s, a period of time when pelvimetry for pregnant women was common practice. A total of 32 cancers were observed, 12 in boys and 20 in girls. Each of the cancer cases was matched for sex, year of birth, and race with two twin controls. The conclusion drawn from this study is that twins in whom leukemia or other childhood cancer developed were 2.4 times as likely to have been irradiated in utero. This study supports a causal explanation for the excess cancers seen in the earlier studies.

In a careful paper in 1997, Doll and Wakeford summarized all of the studies of in utero exposure and came to the following conclusions:

Low-dose irradiation of the fetus in utero causes an increased risk of childhood malignancies. Most of the data refer to exposure in the third trimester.

An obstetric x-ray examination results in a 40% increase in the risk of childhood cancer over the spontaneous level.

Radiation doses of around 10 mGy increase the risk.

The excess absolute risk is about 6% per Gy.

These risk estimates are highly uncertain except to say that they are not zero.

In a later (2003) paper, Wakeford and Little compared the risk of childhood cancer per unit dose of radiation received in utero for the obstetric x-ray examinations and the Japanese A-bomb survivors. They concluded that once all sources of uncertainty are taken into account, the risks are not inconsistent, which also supports a causal explanation for the cancers seen in the Oxford survey. Largely due to the earlier studies, ultrasound has virtually replaced x-ray pelvimetry as a diagnostic tool in obstetric care despite the fact that no comparable studies have been conducted to check its safety.

OCCUPATIONAL EXPOSURE OF WOMEN

The National Council on Radiological Protection and Measurements (NCRP) in its NCRP Report 116 recommends a monthly limit of 0.5 mSv to the embryo or fetus once pregnancy is declared. This recommendation is designed to limit the risk of mental retardation, congenital malformations, and carcinogenesis. NCRP no longer recommends specific controls for occupationally exposed women *until* a pregnancy is declared. Once a pregnancy is declared, the radiation worker should be interviewed by the radiation safety officer or the chair of the radiation safety committee to discuss the advisability of changing or curtailing duties to limit exposure.

THE PREGNANT OR POTENTIALLY PREGNANT PATIENT

Most practicing radiologists at some time in their careers are faced with a patient who has discovered in retrospect that she was pregnant at a time when extensive x-ray procedures were performed involving the pelvis or lower abdomen.

The only completely satisfactory solution to this problem is to ensure that the situation never occurs in the first place. Patients should always be asked if they are, or may be, pregnant, and in the case of procedures involving larger doses of radiation to the pelvis, a pregnancy test may be in order.

Despite the best laid plans and the most careful precautions, there still are occasional instances in which, because of clinical urgency or unusual accident, an early developing embryo is exposed to a substantial dose of radiation amounting to several tens of millisieverts or more. The first step in evaluating

whether or not damage may have been done to the embryo is to estimate the dose involved. It is sometimes useful to solicit the help of an experienced medical physicist to make measurements in a phantom after carefully reconstructing the setup that was used. No dose level can be regarded as completely safe. Congenital abnormalities occur in 5% to 10% of the human population anyway, so it is impossible in retrospect to attribute a given anomaly to a small dose of radiation received by an embryo or fetus. All that can be said is that radiation increases the probability of an anomaly and that this increase is a function of dose.

Doses less than about 100 mSv during preimplantation and organogenesis, and perhaps 200 mSv during the fetal period, pose a low risk of deleterious effects except the very small possibility of carcinogenesis, which is difficult to quantify. Much higher doses than this to the developing embryo or fetus may be justification for considering a therapeutic abortion. Not everyone would agree with this view, but if the dose involved is sufficiently large, it may be prudent to consider the relative merits of terminating the pregnancy in consultation with the referring physician as well as with the patient and her family.

There are several factors to consider in conjunction with the dose. These include the hazard of the pregnancy to the expectant mother, the probability of future pregnancies, the extent to which the prospective parents want the unborn infant, their mental outlook on the possibility of a deformed child, and the ethnic and religious background of the family. The exact dose level at which it is justifiable to terminate the pregnancy may be flexible within broad limits around the guideline figure, depending on a combination of these other circumstances.

There are special problems involved in the use of nuclear medicine procedures in pregnant or potentially pregnant females. This is particularly true in the case of radionuclides that are able to cross the placenta. This topic is discussed in [Chapter 15](#).

[Table 12.4](#) is a historical summary of events in our gradual understanding of radiation effects on the developing embryo and fetus.

Table 12.4 Major Events in Understanding Effects of Radiation on the Developing Embryo and Fetus

ANIMAL DATA	YEAR	OBSERVATIONS

Goldstein Murphy	and 1929	Various abnormalities, including mental retardation and small head diameter in children born to mothers who received pelvic radiation therapy during pregnancy
Job et al.	1935	Recognition that different periods of gestation differ in radiosensitivity
Russell	1950	Nature of developmental abnormality determined by gestational age at exposure
Russell and Russell	1952	Clinical implications of irradiation in pregnancy
Plummer	1952	Mental retardation and microcephaly observed in children of atomic bomb survivors
Stewart and Kneale	1952	Leukemia and childhood cancer in children irradiated in utero with diagnostic x-rays
Otake and Schull	1984	Mental retardation caused by irradiation at 8–15 wk of pregnancy in Japanese survivors

SUMMARY OF PERTINENT CONCLUSIONS

Doses that have little effect on adults can produce catastrophic effects on the developing embryo and fetus.

The effects depend on the stage of gestation, the dose, and the dose rate.

Gestation is divided into preimplantation, organogenesis, and the fetal period. In humans, these periods correspond to about 0 through 9 days, 10 days through 6 weeks, and 6 weeks through term, respectively.

The principal effects of radiation on the developing embryo and fetus, aside

from cancer, are embryonic, fetal, or neonatal death; congenital malformations; growth retardation; and functional impairment, such as mental retardation.

Irradiation during preimplantation leads to potential death of the embryo. At doses less than 100 mGy, such lethal effects will be infrequent in humans. Growth retardation or malformations are not seen in animals from irradiation at this time. The human data are consistent with this conclusion.

In animals, embryos exposed to radiation in early organogenesis exhibit the most severe intrauterine growth retardation, from which they can recover later (i.e., temporary growth retardation). Irradiation in the fetal period leads to the greatest degree of permanent growth retardation.

In animals, lethality from irradiation varies with stage of development. The embryonic 50% lethal dose is lowest during early preimplantation; at this stage, embryos killed by radiation suffer a prenatal death and are resorbed. In organogenesis, prenatal death is replaced by neonatal death—death at or about the time of birth. During the fetal stage, the 50% lethal dose approaches that of the adult.

In animals, the peak incidence of teratogenesis, or gross malformations, occurs if the fetus is irradiated in organogenesis. For practical purposes, the risk of malformations for doses well below 100 mGy would not be expected.

In contrast to what is observed in experimental animals, radiation-induced malformations of body structures other than the central nervous system are uncommon in the Japanese survivors irradiated in utero, although they have been reported in patients exposed to therapeutic doses of medical radiation.

In the Japanese survivors, irradiation in utero resulted in small head size (microcephaly) and mental retardation.

Mental retardation from irradiation occurred primarily at 8 to 15 weeks of gestational age, with a smaller excess at 16 to 25 weeks. It is thought to be caused by radiation effects on cell migration within the brain.

The incidence of severe mental retardation as a function of dose is apparently linear at 8 to 15 weeks, with a risk coefficient of 0.4 per Gy. The incidence is about 4 times lower at 16 to 25 weeks. The data are also consistent with a dose threshold of 0.3 Gy.

Small head circumference was more common than mental retardation.

Data on atomic bomb survivors indicate that microcephaly can result from

exposure at 0 to 7 and 8 to 15 weeks postovulation but not at later times. There is little evidence for a threshold in dose.

Various effects have been documented in experimental animals after irradiation during fetal stages, including effects on the hematopoietic system, liver, and kidney, all occurring, however, after quite high radiation doses.

There is an association between exposure to diagnostic x-rays in utero and the subsequent development of childhood malignancies, although there are particular uncertainties concerning the risk involved.

The original study of diagnostic x-ray exposure in utero and subsequent malignancies, principally leukemia, was done by Stewart and Kneale at Oxford University, but the same association was observed in the United States by MacMahon. If x-rays are the causative agent, these studies imply that radiation at low doses in utero increases the spontaneous cancer incidence in the first 10 to 15 years of life by 50%—that is, by a factor of 1.5.

It has been argued for years whether radiation is the causative agent or whether there are other factors involved.

A study of twins born in the 1930s and early 1940s also found an increase in childhood cancers in children who had been irradiated in utero which supports the causal nature of the childhood cancers in the earlier studies because in twins, most x-rays in those days were not ordered for medical reasons but simply to observe progress in the pregnancy.

Doll and Wakeford in 1997 summarized all of the evidence for and against the calculated risks and concluded that an obstetric x-ray examination, particularly in the third trimester, increased the risk of childhood cancer by 40%. The risk is increased by a dose of only 10 mGy. The excess absolute risk is about 6% per Gy, which is not very different from the risk estimates from the atomic bomb survivors for adult exposure.

Until a pregnancy is declared, no special limits apply to women other than those applicable to any radiation worker. Once a pregnancy is declared, the maximum permissible dose to the fetus is 0.5 mSv per month.

Once a pregnancy is declared, the duties of a radiation worker should be reviewed to ensure that this limit is not exceeded.

A sufficiently large dose to the embryo or fetus during the sensitive period of gestation (10 days to 25 weeks) may be justification for considering a therapeutic abortion to avoid the possibility of an anomalous child. Not

everyone would agree with this, and the decision to terminate a pregnancy should be flexible and must depend on many factors in addition to dose.

BIBLIOGRAPHY

- Adelstein SJ. Administered radionuclides in pregnancy. *Teratology*. 1999;59:236–239.
- Antypas C, Sandilos P, Kouvaris J, et al. Fetal dose evaluation during breast cancer radiotherapy. *Int J Radiat Oncol Biol Phys*. 1998;40:995–999.
- Balakier H, Pedersen RA. Allocation of cells to inner cell mass and trophectoderm lineages in preimplantation mouse embryos. *Dev Biol*. 1982;90:352–362.
- Bitell JF, Stiller CA. A new calculation of the carcinogenic risk of obstetric x-raying. *Stat Med*. 1988;7:857–864.
- Boice JD Jr, Miller RW. Childhood and adult cancer after intrauterine exposure to ionizing radiation. *Teratology*. 1999;59:227–233.
- Brent RL, Ghorson RO. Radiation exposure in pregnancy. *Curr Probl Radiol*. 1972;2:1–48.
- Committee for the Compilation of Materials on Damage Caused by the Atomic Bomb in Hiroshima and Nagasaki. *Hiroshima and Nagasaki: The Physical, Medical and Social Effects of the Atomic Bombings*. New York, NY: Basic Books; 1981.
- Committee on the Biological Effects of Ionizing Radiation. *Health Effects of Exposure to Low Levels of Ionizing Radiations*. Washington, DC: National Academy of Sciences; 1990.
- Committee on the Biological Effects of Ionizing Radiations. *The Effects on Populations of Exposure to Low Levels of Ionizing Radiation*. Washington, DC: National Academy of Sciences; 1980.
- Dekaban AS. Abnormalities in children exposed to x-radiation during various stages of gestation: tentative timetable of radiation to the human fetus. *J Nucl Med*. 1968;9:471–477.
- Delongchamp RR, Mabuchi K, Yoshimoto Y, et al. Cancer mortality among atomic bomb survivors exposed in utero or as young children, October 1950–May 1992. *Radiat Res*. 1997;147:385–395.
- Doll R, Wakeford R. Risk of childhood cancer from fetal irradiation. *Br J*

Radiol. 1997;70:130–139.

Goldstein L, Murphy DP. Microcephalic idiocy following radium therapy for uterine cancer during pregnancy. *Am J Obstet Gynecol.* 1929;18:189–195, 281–283.

Hammer-Jacobsen E. Therapeutic abortion on account of x-ray examination during pregnancy. *Dan Med Bull.* 1959;6:113–122.

Harvey EB, Boice JD, Honeyman M, et al. Prenatal x-ray exposure and childhood cancer in twins. *N Engl J Med.* 1985;312:541–545.

International Commission on Radiological Protection. The 2007 recommendations of the International Commission on Radiological Protection. ICRP Publication No. 107. *Ann ICRP.* 2007;37:1–332.

Little MP, Charles MW, Wakeford R. A review of the risks of leukemia in relation to parental pre-conception exposure to radiation. *Health Phys.* 1995;68:299–310.

MacMahon B. Prenatal x-ray exposure and childhood cancer. *J Natl Cancer Inst.* 1962;28:1173–1191.

Mayr NA, Wen BC, Saw CB. Radiation therapy during pregnancy. *Obstet Gynecol Clin North Am.* 1998;25:301–321.

Meinert R, Kaletsch U, Kaatsch P, et al. Associations between childhood cancer and ionizing radiation: results of a population-based case-control study in Germany. *Cancer Epidemiol Biomarkers Prev.* 1999;8:793–799.

Miller RW, Mulvihill JJ. Small head size after atomic irradiation. In: Sever JL, Brent RL, eds. *Teratogen Update: Environmentally Induced Birth Defect Risks.* New York, NY: Alan R. Liss; 1986:141–143.

Mole RH. Childhood cancer after prenatal exposure to diagnostic x-ray examinations in Britain. *Br J Cancer.* 1990;62:152–168.

Mole RH. The biology and radiobiology of *in utero* development in relation to radiological protection. *Br J Radiol.* 1993;66:1095–1102.

National Council on Radiation Protection and Measurements. *Limitation of Exposure to Ionizing Radiation.* Bethesda, MD: National Council on Radiation Protection and Measurements; 1993. NCRP report no. 116.

Otake M, Schull WJ. In utero exposure to A-bomb radiation and mental retardation: a reassessment. *Br J Radiol.* 1984;57:409–414.

- Otake M, Schull WJ. Radiation-related brain damage and growth retardation among the prenatally exposed atomic bomb survivors. *Int J Radiat Biol.* 1998;74:159–171.
- Otake M, Schull WJ. Radiation-related small head sizes among prenatally exposed A-bomb survivors. *Int J Radiat Biol.* 1993;63:255–270.
- Otake M, Schull WJ, Lee S. Threshold for radiation-related severe mental retardation in prenatally exposed A-bomb survivors: a re-analysis. *Int J Radiat Biol.* 1996;70:755–763.
- Rodvall Y, Pershagen G, Hrubec Z, et al. Prenatal x-ray exposure and childhood cancer in Swedish twins. *Int J Cancer.* 1990;46:362–365.
- Rugh R. The impact of ionizing radiations on the embryo and fetus. *Am J Roentgenol Radium Ther Nucl Med.* 1963;89:182–190.
- Rugh R, Caveness WF, Duhamel L, et al. Structural and functional (electroencephalographic) changes in the post-natal mammalian brain resulting from x-irradiation of the embryo. *Mil Med.* 1963;128:392–408.
- Russell LB, Montgomery CS. Radiation-sensitivity differences within cell-division cycles during mouse cleavage. *Int J Radiat Biol Relat Stud Phys Chem Med.* 1966;10:151–164.
- Russell LB, Russell WL. An analysis of the changing radiation response of the developing mouse embryo. *J Cell Physiol.* 1954;43(suppl 1):103–149.
- Russell WL. Effect of the interval between irradiation and conception on mutation frequency in female mice. *Proc Natl Acad Sci USA.* 1965;54:1552–1557.
- Schull WJ, Otake M. Cognitive function and prenatal exposure to ionizing radiation. *Teratology.* 1999;59:222–226.
- Seigel DG. Frequency of live births among survivors of Hiroshima and Nagasaki atomic bombings. *Radiat Res.* 1966;28:278–288.
- Stabin MG. Health concerns related to radiation exposure of the female nuclear medicine patient. *Environ Health Perspect.* 1997;105(suppl 6):1403–1409.
- Stewart A, Kneale GW. Radiation dose effects in relation to obstetric x-rays and childhood cancers. *Lancet.* 1970;1:1185–1188.
- Streffer C, Shore R, Konermann G, et al. Biological effects after prenatal irradiation (embryo and fetus). A report of the International Commission on

Radiological Protection. ICRP Publication No. 90. *Ann ICRP*. 2003;33:5–206.

United Nations Scientific Committee on the Effects of Atomic Radiation. *Sources and Effects of Ionizing Radiation*. New York, NY: United Nations Scientific Committee on the Effects of Atomic Radiation; 1986.

Wakeford R, Little MP. Risk coefficients for childhood cancer after intrauterine irradiation: a review. *Int J Radiat Biol*. 2003;79:293–309.

Cataracts of the Ocular Lens**Lens Opacification in Experimental Animals****Radiation Cataracts in Humans****The Latent Period****Dose–Response Relationship for Cataracts in Humans****Summary of Pertinent Conclusions****Bibliography**

CATARACTS OF THE OCULAR LENS

The word **cataract** is used to describe an opacity in the normally transparent lens of the eye. Its clinical presentation may vary from tiny flecks in the posterior portion of the lens to complete opacification, resulting in blindness. Cataracts are commonly associated with aging but can also be caused by metabolic disorders such as diabetes, arise after ocular inflammation, result from eye trauma, or develop after chronic systemic steroid use. There are three major forms of cataract depending on their anatomical location in the lens: cortical, involving the outer layers of the lens; nuclear, arising from the lens central region; and posterior subcapsular (psc), a discrete opacity beginning at the posterior lens pole. Only this last type of cataract is closely associated with exposure to ionizing radiation such as x or γ -rays, charged particles, or neutrons.

The lens has no blood supply. It is completely encased by a basement membrane termed the “lens capsule” (Fig. 13.1). There is a single layer of epithelial cells under the anterior, corneal-facing side of the capsule, which, for the most part, do not divide. Throughout life, however, a small population of epithelial cells just anterior of the lens equator divide and differentiate into lens fiber cells, which make up the majority of the lens mass. Fiber cells are elongated, terminally differentiated, and do not contain nuclei or mitochondria. Thus, they are dependent on the overlying epithelial cell layer for nutrient and

waste transport, energy production, and protection from insult. Epithelial cell division slows markedly during puberty; yet, the lens continues to grow throughout life, eventually tripling in weight. It is believed that radiation damage to the dividing and differentiating epithelial cell population is the initiating event that results in radiation cataract. Curiously, the aberrant lens fiber cells arising from abnormal epithelial cell division or differentiation are not removed from the lens but instead appear to migrate toward the lens posterior pole, where they accumulate and interfere with lens transparency.

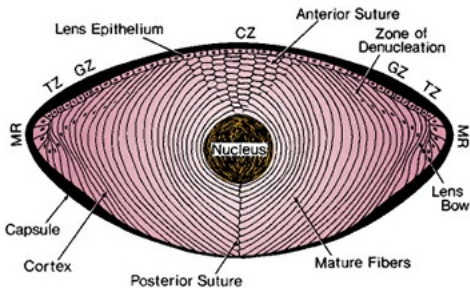


FIGURE 13.1 Diagram of a sagittal section of a human lens, illustrating the various cellular relationships. Epithelial cells in the germinative zone (GZ) divide, turn 90 degrees, and begin to differentiate into mature elongated lens fiber cells at the meridional rows (MR) near the lens equator. Epithelial cells in the central zone (CZ) do not normally divide. TZ, transitional zone. (From Merriam GR Jr, Worgul BV. Experimental radiation cataract—its clinical relevance. *Bull NY Acad Med*. 1983;59:372–392, with permission.)

LENS OPACIFICATION IN EXPERIMENTAL ANIMALS

Some species of animals, especially the mouse, are very sensitive to radiation as far as lens opacification is concerned. A large proportion of a mouse population naturally develops opacifications as they become older. A dose of a few tens of milligray (mGy) of x-rays or a fraction of 1 mGy of fast neutrons produces readily discernible changes in the lens. As the dose is increased, the *latent period* (i.e., the time that elapses before an opacity of given severity is evident) becomes shorter. Put another way, radiation advances in time, a process that occurs normally late in life.

Neutrons and other densely ionizing radiations are very effective at inducing cataracts, as evidenced by several physicists and engineers who developed cataracts as a result of working around high-energy accelerators in the early days before safety procedures were introduced. The relative biologic effectiveness (RBE) of fast neutrons is a strong function of dose, with a value of about 10 pertaining to high-dose levels on the order of several grays relative to x-rays but

rising to 50 or more for small doses of less than 10 mGy. Worgul and his associates have reported similar RBEs for lens damage in rat eyes exposed to accelerated heavy ions. The increase in RBE at low doses is caused largely by the sharply declining effectiveness of x-rays with decreasing dose rather than an increase in effect per unit dose of neutrons or charged particles.

RADIATION CATARACTS IN HUMANS

The year 1905 marked the first mention of a human radiation cataract in an x-ray laboratory worker. For more than a century, radiologists have known that the lens of the eye may be damaged by radiation. Following World War II, side-by-side publications in science reported lens opacities in cyclotron workers and A-bomb survivors. These studies stimulated much interest and research into this phenomenon. Later studies of patients treated with x or γ -rays, in which a proportion of the dose reached the anterior portion of the eye, provided critical insights into radiation cataract pathogenesis. [Figure 13.2](#) shows the typical initial presentation of a posterior opacity in an interventional radiologist who has been occupationally exposed to x-rays without use of eye protection for 22 years. Both retroillumination, that is, using light that is reflected by the retina back through the lens (panel A), and conventional slit lamp imaging, that is, where an optical section of the lens is directly visualized (panel B), depict the same centrally located posterior lens defect.



FIGURE 13.2 Clinical appearance of a typical radiation cataract in the posterior scapular region in an interventional cardiologist with 22 years of occupational radiation exposure. **A:** Retroillumination image (i.e., using the light that is reflected by the retina back through the lens). **B:** Conventional slit lamp imaging (i.e., where an optical section of the lens is directly visualized). In both cases, the position of the opacity is indicated by an arrow. (Courtesy of Dr. Norman Kleiman.)

Initial radiation-induced posterior lens changes include the formation of small opaque dots and vacuoles, often accompanied by a small central opacity at

the posterior pole. With time, the posterior changes expand in area and smaller dot and vacuolar opacities coalesce. With further time, dependent on dose, the central opacity can enlarge to several millimeters in diameter. At about the same time, granular opacities and vacuoles may appear in the anterior subcapsular region, usually in the pupillary area. Although this morphology is not unique to radiation exposure, its appearance in a person with a history of radiation exposure strongly suggests radiation as the causative agent. Similarly, an absence of this sequence of events would exclude radiation as a causative agent. In other words, although it is never possible to state unequivocally that a given cataract is radiation-induced, it is possible to say with some certainty that some cataracts, for example, those originating in the nuclear region, are not due to radiation exposure. Depending on dose, radiation cataracts may progress slowly or not at all, remaining confined to the psc region. If, however, they continue to progress and involve large areas of the lens cortex, they cannot be distinguished from other types of cataracts. Despite their small size, the location of these opacities, at the lens posterior visual axis, may result in a disproportionate effect on visual function and thus require cataract surgery to restore vision.

[Figure 13.3](#) shows the system of cataract classification devised in the 1950s by Merriam and Focht. The accumulation of an opaque plaque at the posterior pole is termed a *stage 1 cataract*; as the severity of this opacity increases and the anterior lens region becomes involved, the stage progressively increases, where grade 4 denotes a total opacity.

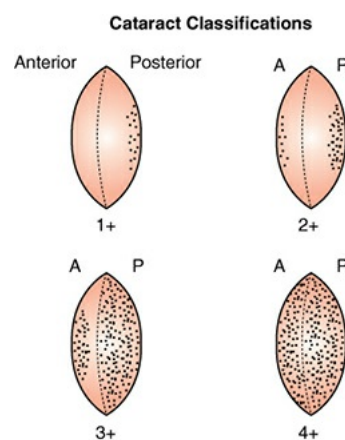


FIGURE 13.3 The system of cataract classification devised by Merriam and Focht, illustrating the stages assigned to progressive severities of cataracts. (Courtesy of Dr. Basil Worgul.)

The severity of the cataract can be assessed quantitatively and objectively by using the Scheimpflug imaging system. This device provides a distortion-free digitized image for densitometric analysis of the cataract. [Figure 13.4](#) shows

such a cross section of the lens from a Chernobyl “liquidator,” part of the some 600,000 workers who helped clean up the reactor site in the 2-year period immediately after the nuclear accident, many of whom received lens doses averaging 100 mSv. The degree of opacity, measured with the Scheimpflug system, is shown in the lower panel.

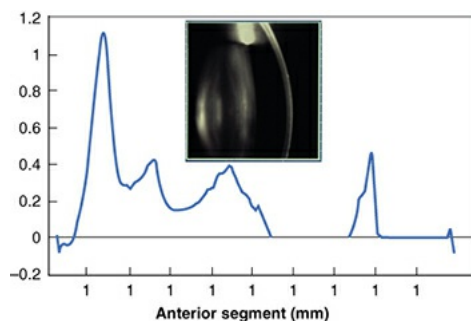


FIGURE 13.4 **Top:** Scheimpflug image of the lens of a Chernobyl “liquidator” who accumulated a substantial radiation dose while cleaning up after the nuclear accident. **Bottom:** Graphical representation of lens density measured with the Scheimpflug imaging system. The region of greatest opacification is under the posterior capsule at the far **left**. The corneal peak is depicted at the far **right**. (Courtesy of Dr. Basil Worgul.)

THE LATENT PERIOD

Time to onset of clinically relevant disabling opacities ultimately requiring cataract extraction surgery is variable, but in general, dose-related; the latency gets shorter with increasing dose. In radiotherapy patients who had received 2.5 to 6.5 Gy to the eye, the average latent period was about 8 years. At higher doses of between 6.51 and 11.5 Gy, the average latent period was reduced to about 4 years. By contrast, in A-bomb survivors who received a much smaller dose, the latency was 50 years. This and other evidence indicate that the latent period becomes shorter as dose is increased.

DOSE-RESPONSE RELATIONSHIP FOR CATARACTS IN HUMANS

Both the National Council on Radiation Protection and Measurements (NCRP) and the International Commission on Radiological Protection (ICRP) have categorized a radiation-induced cataract as a “tissue reaction” (formerly called a deterministic effect). That is, a cataract is characterized by the following:

A threshold in dose below which visually disabling cataracts do not form.

The severity of the effect increases with dose above the threshold.

Visually disabling cataracts may require damage to a population of cells rather than to a single cell.

In 2011, based on a review of recent epidemiology findings, the ICRP reduced the recommended threshold dose for radiation cataractogenesis to 0.5 Gy from the previous values of 2 Gy delivered in a single exposure, or a larger dose (5 to 8 Gy) for a prolonged or fractionated exposure. At the same time, occupational lens exposure limits were also lowered from 150 mSv per year to an average of 20 mSv per year over 5 years, with no single year exceeding 50 mSv. The NCRP reached similar conclusions in 2016 after a task force was established to review the most recent research. The NCRP now recommends an occupational exposure limit of 50 mGy per year.

The earlier radiation cataract threshold of 2 Gy, delivered in a single exposure, or 5 to 8 Gy for a prolonged or fractionated exposure was based on early work by Cogan, Merriam and Focht, and others, which involved the study of a limited number of individuals (mostly elderly patients receiving radiotherapy as a treatment for cancer) exposed to relatively large radiation doses and followed for a relatively short period of time. For example, Merriam and colleagues reviewed the case histories of 233 patients on radiotherapy who received radiation to the lens of the eye and for whom dose estimates were available. Of these patients, 128 developed cataracts, whereas 105 did not.

In 1990, Otake and Schull analyzed the cataract data in A-bomb survivors and concluded that the data were consistent with a threshold of about 1.5 Gy; however, their analysis was based on data collected in the 1960s (i.e., with a 20-year follow-up after the bombings) and principally involved persons irradiated as adults.

More recent studies of the A-bomb survivors, involving persons exposed at earlier ages and followed for much longer periods until they reached the age at which cataracts occur anyway, showed that the prevalence of cataracts requiring surgery (i.e., vision-impairing cataracts) increases significantly with radiation dose, with little sign of a threshold in dose, certainly not as large as 2 Gy. [Figure 13.5](#) shows the relationship between the odds ratio and radiation dose for visually disabling cataracts that needed to be removed surgically in the Japanese A-bomb survivors. The odds ratio at 1 Gy is 1.39, which is statistically significant.

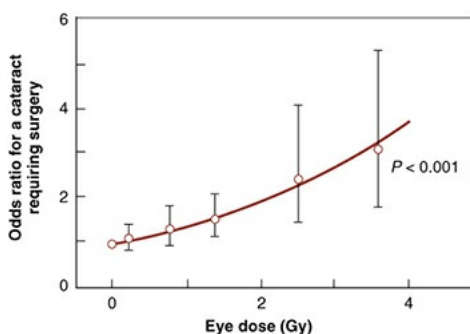


FIGURE 13.5 Odds ratio as a function of dose for the induction of a cataract requiring surgical lens removal in Japanese A-bomb survivors. (Redrawn from Neriishi K, Nakashima E, Minamoto A, et al. Postoperative cataract cases among atomic bomb survivors: radiation dose response and threshold. *Radiat Res.* 2007;168:404–408, with permission.)

These and other recent data call into question the classification of an ocular cataract as a tissue reaction or deterministic effect because vision-impairing cataracts appear following quite low doses of radiation in persons who are exposed at younger ages and followed for a sufficiently long period. This view is supported by the unexpected appearance of cataracts in astronauts, clean-up workers from Chernobyl, and radiation technologists, all of whom received doses well below the old threshold dose of 2 Gy.

SUMMARY OF PERTINENT CONCLUSIONS

A cataract is an opacification of the normally transparent lens of the eye.

The progeny of dividing cells in the pre-equatorial region of the lens epithelium differentiate into lens fiber cells. The failure of these cells to differentiate correctly leads to a radiation cataract.

Unique features of the lens include the absence of nuclei and mitochondria in lens fiber cells as well as no mechanism for the removal of dead or damaged cells.

The latent period between irradiation and the appearance of lens opacity is dose related. The latency is about 8 years after exposure to a dose in the range of 2.5 to 6.5 Gy.

It is never possible to state unequivocally that a given cataract is radiation-induced; however, the clinical presentation of a plaque-like opacity at the posterior lens pole in a person with a radiation history strongly suggests radiation as the causative agent. On the other hand, it is possible to say with some certainty that some cataracts—for example, nuclear cataracts—do not

have a radiation etiology.

Neutrons or heavy ions are very effective at producing cataracts. The RBE may be as high as 50 or more for small doses.

There is evidence of radiation-associated lens changes in a variety of human populations exposed to low doses of radiation, including the astronaut core, medical workers, A-bomb survivors, accidentally exposed individuals, and those undergoing diagnostic or radiotherapeutic procedures.

Both ICRP and NCRP classify a radiation-induced cataract as a tissue reaction (formerly called a deterministic effect) but with a much reduced threshold dose of only 0.5 Gy

Occupational exposure limits have been reduced from 150 mSv per year to 20 mSv per year averaged over 5 years, with no single year exceeding 50 mSv (ICRP) or 50 mGy per year (NCRP).

BIBLIOGRAPHY

Bateman JL, Bond VP. Lens opacification in mice exposed to fast neutrons. *Radiat Res.* 1967;7(suppl):239–249.

Cogan DG, Martin SF, Kimura SJ. Atom bomb cataracts. *Science* 1949;110(2868):654.

Cucinotta FA, Manuel FK, Jones J, et al. Space radiation and cataracts in astronauts. *Radiat Res.* 2001;156(5 pt 1):460–466.

Hall EJ, Brenner DJ, Worgul BV, et al. Genetic susceptibility to radiation. *Adv Space Res.* 2005;35:249–253.

International Commission on Radiological Protection. Early and late effects of radiation in normal tissues and organs: threshold doses for tissue reactions and other non-cancer effects of radiation in a radiation protection context. *Ann ICRP.* 2012;41:1–322.

International Commission on Radiological Protection. The 2007 recommendations of the International Commission on Radiological Protection. *Ann ICRP.* 2007;37:1–332.

Kleiman NJ. Radiation cataract. *Ann ICRP.* 2012;41(3–4):80–97.

Kleiman NJ, David J, Elliston CD, et al. *Mrad9* and *atm* haploinsufficiency enhance spontaneous and X-ray-induced cataractogenesis in mice. *Radiat Res.* 2007;168:567–573.

- Merriam GR Jr, Focht EF. A clinical study of radiation cataracts and the relationship to dose. *Am J Roentgenol Radium Ther Nucl Med.* 1957;77:759–785.
- Merriam GR Jr, Focht EF. Radiation dose to the lens in treatment of tumors of the eye and adjacent structures: possibilities of cataract formation. *Radiology.* 1958;71:357–369.
- Merriam GR Jr, Szechter A, Focht EF. The effects of ionizing radiations on the eye. *Front Radiat Ther Oncol.* 1972;6:346–385.
- Merriam GR Jr, Worgul BV. Experimental radiation cataract—its clinical relevance. *Bull NY Acad Med.* 1983;59:372–392.
- Nakashima E, Neriishi K, Minamoto A. A reanalysis of atomic-bomb cataract data, 2000–2002: a threshold analysis. *Health Phys.* 2006;90:154–160.
- Neriishi K, Nakashima E, Minamoto A, et al. Postoperative cataract cases among atomic bomb survivors: radiation dose response and threshold. *Radiat Res.* 2007;168:404–408.
- Otake M, Schull WJ. A review of forty-five years study of Hiroshima and Nagasaki atomic bomb survivors. Radiation cataract. *J Radiat Res.* 1991;32(suppl 32):283–293.
- Vañó E, González L, Beneytez F, et al. Lens injuries induced by occupational exposure to non-optimized interventional radiology laboratories. *Br J Radiol.* 1998;71:728–733.
- Worgul BV, Kundiyev YI, Sergiyenko NM, et al. Cataracts among Chernobyl clean-up workers: implications regarding permissible eye exposures. *Radiat Res.* 2007;167:233–243.
- Worgul BV, Merriam GR Jr, Medvedovsky C. Accelerated heavy particles and the lens II. Cytopathological changes. *Invest Ophthalmol Vis Sci.* 1986;27:108–114.

Possible Scenarios for Radiologic Terrorism

Availability of Radioactive Material

Health Effects of Radiation

External Exposure to Radiation and Contamination with Radioactive Materials

External Contamination

Internal Contamination

Medical Management Issues in the Event of Radiologic Terrorism

Further Information

Summary of Pertinent Conclusions

Bibliography

In the years following the 2001 attack on the World Trade Center in New York City and the resulting tension between the Western world and militant elements of Islam, there has been much talk of the possibility of an attack involving radiation and/or radioactive materials.

Several different scenarios are possible, varying widely in the probability that they may occur and result in very different consequences. The various possibilities and the consequences are discussed in more detail in the subsequent paragraphs.

POSSIBLE SCENARIOS FOR RADIOLOGIC TERRORISM

1. **The detonation of a nuclear weapon or improvised nuclear device in or close to a city.** This is considered “highly unlikely” but not impossible because several portable “suitcase bombs” are said to be missing, following the breakup of the former Soviet Union. These weapons might perhaps be comparable to the bombs used on Hiroshima and Nagasaki that ended World War II, or they could be much smaller.

The detonation of a nuclear device would lead to both prompt and delayed sources of damage. [Table 14.1](#) lists these sources of damage. The initial explosion gives rise to blast heat and radiation which is over in a matter of seconds and results in many casualties in the close vicinity. Potentially, the greatest source of fatalities comes from the radioactive fallout, which may be carried a distance of several miles and cause fatalities far from the initial explosion and some days later. The number of casualties from fallout may be greatly reduced if people in the path of the fallout are warned and can stay indoors.

TABLE 14.1 Improvised Nuclear Device: Prompt Versus Delayed Sources of Damage

PROMPT (<1 s) GREATEST SOURCE OF PHYSICAL DAMAGE AND TERROR	
Blast	
Thermal radiation	
Electromagnetic pulse	
Nuclear radiation	
DELAYED (>1 s to days)	
Primarily radioactive fallout	
Potentially the greatest source of fatalities	

Primary health hazard is external γ -radiation from fallout on horizontal surfaces (groundshine).

Dominated by Na-24 (15-h half-life) from soil, concrete, steel

Inhalation generally less important

Casualties potentially reducible

If such an event were to take place, the consequences would be catastrophic.

- Thousands of people would be killed by blast and heat.
- Hundreds to thousands would be killed or made ill by the acute radiation syndrome (ARS) because of exposure to γ -rays and neutrons as well as to fallout.
- A long-term risk of leukemia and solid cancers in those who survive the acute effects would result principally because of exposure to γ -rays and neutrons and also to fallout.

2. An attack on a nuclear power station. It is claimed (although, of course, never tested) that the containment vessel housing the nuclear reactor itself is so massively built that it would not be destroyed if a jetliner, full of fuel, were deliberately flown into it. What may be more vulnerable are the used fuel elements often stored in “swimming pool” facilities close to the reactor because, to date, no long-term storage facilities are in widespread use. An attack of this nature is usually considered unlikely, but if it occurred, the huge amount of radioactive material in the used fuel elements (with both long and short half-lives) would be spread over the surrounding countryside. The consequences might be the following:

- Individual doses are unlikely to be high enough to cause the ARS.
- There would be a long-term risk of leukemia and solid cancers in those exposed to external radiation or in those ingesting and/or inhaling radioactive material.

- There would certainly be chaos and enormous economic loss because cleanup would be a long and slow process.

Although a terrorist attack on a nuclear power station has not, to date, occurred, there have been several accidents at nuclear power station, notably at Chernobyl in 1986 and at Fukushima in 2010. These events are attributed largely to human error. The consequences are quite similar to the scenario imagined for a terrorist attack. In both cases, there was a massive release of radioactive material that contaminated a large area. In the case of Chernobyl, there were about 49 “immediate” deaths due to trauma, the ARS (see [Chapter 8](#)), and a helicopter crash. The United Nations (UN) has estimated that there may be about 4,000 premature deaths due to cancer, and there are still widespread psychological problems due to the disruption of life. In the case of Fukushima, there were thousands of deaths due to the earthquake and tsunami but no deaths due to the ARS. Workers were rotated on and off the site so that no one received a sufficiently high dose to cause an acute death, although some 20,000 received a measurable dose. No estimate has been published so far of the long-term cancer risk. The biggest problem to date has been a consequence of the forced evacuation of thousands of people from the contaminated area which has led indirectly to several deaths including suicides.

3. **The detonation of a “dirty bomb,” or to give its official description, a radiologic dispersal device (RDD).** This consists of a relatively small amount of radioactive material attached to a conventional explosive material, such as a plastic explosive or even a quantity of fertilizer ([Fig. 14.1](#)). The principle is that the conventional explosive material scatters the radioactive material over a wide area. Ideally, the radioactive material should be vaporized, but in practice, this is difficult to achieve except perhaps for cesium-137.

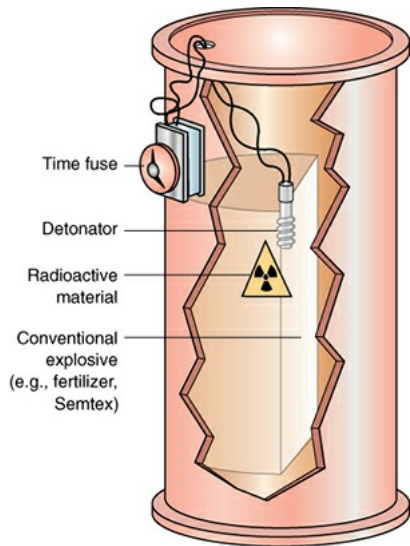


FIGURE 14.1 A radioactive dispersal device, commonly known as a “dirty bomb,” consists simply of a small amount of radioactive material attached to a conventional explosive material, such as Semtex or even fertilizer. When the explosive material is detonated, the radioactive material is scattered over a wide area.

The probability of a “dirty bomb” is considered to be “highly likely”; indeed, some wonder why such an event has not yet occurred. For example, in the year 2003, British intelligence found a diagram illustrating the principle of an RDD in Herat, Afghanistan, and concluded that Al Qaeda had succeeded in constructing a small dirty bomb, although the device was never found (Fig. 14.2). The consequences of a “dirty bomb” might be as follows:

- It is unlikely that any person will receive a dose of radiation sufficient to cause the ARS.
- The most likely scenarios would be a small number of persons contaminated with radioactive materials, either on their clothes and skin, or inhaled or ingested. The possibility of a minimal long-term risk of leukemia or solid cancers could not be ruled out.
- The certain consequence would be chaos, psychological terror, and widespread fear.

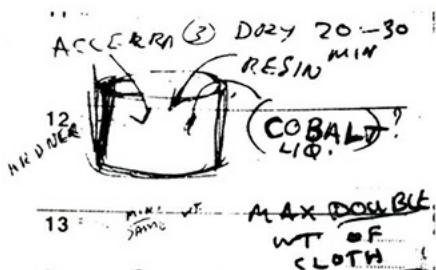


FIGURE 14.2 Diagram of a “dirty bomb” discovered in 2003 by British intelligence in Afghanistan. It was assumed that Al Qaeda had succeeded in constructing a small “dirty bomb,” but the device was never found.

4. Hidden radiation exposure device (RED). An alternative to the “dirty bomb” would be to place a γ -emitting source, such as cesium-137, in a locker or garbage can in a busy public place, such as Grand Central Station, and then make a public disclosure of its presence some days or weeks later. In the intervening period, thousands of people passing close by may have been exposed to a dose of radiation. Like the “dirty bomb,” the probability of an RED is considered to be “highly likely.” The consequences of an RED are as follows:

- Fear and psychological chaos
- Unlikely that any person would receive sufficient radiation to result in the ARS
- Very small long-term possibility of radiation-induced malignancies

AVAILABILITY OF RADIOACTIVE MATERIAL

As was previously discussed in scenario 1, the detonation of a nuclear weapon would involve a leftover “suitcase bomb” from the former Soviet Union or the production or theft of fissile material. All are possible but very unlikely. The attack on a nuclear power station, as discussed in scenario 2, would necessitate the hijacking of a commercial airliner. This is again possible but unlikely because of improved security. Scenarios 3 and 4 require the availability of only relatively small quantities of radioactive material. In both cases, the fear and psychological chaos are not directly related to the quantity of radioactivity or the magnitude of the radiation dose involved. If a Geiger counter ticks, that would be sufficient to cause chaos. Small amounts of radioactive material are readily available.

There are several examples. First, in 2004 in London, an Islamic terrorist cell had collected several thousand household smoke detectors, readily available from hardware stores (Fig. 14.3). Each contains a tiny amount (few thousand becquerels) of americium-241, which is an α -emitter, only dangerous if inhaled or ingested. Imagine the chaos if these were dispersed in a crowded public place.



FIGURE 14.3 An Islamic terrorist cell in London in 2004 had collected several thousand household smoke detectors, which can be readily purchased from hardware stores. Each contains a tiny amount of americium-241, which is an α -emitter. This could be combined with a conventional explosive to produce a “dirty bomb.” Imagine the chaos that would result if this radioactive material were dispersed in a busy public place.

Second, moisture density gauges, used in the laying of tarmacadam on road surfaces, contain small amounts of americium-241 and cesium-137 (Fig. 14.4). More than 23,000 are in regular use in the United States, and about 50 per year are lost or reported missing.



FIGURE 14.4 Moisture density gauges, used in the laying of tarmacadam road surfaces, contain small quantities of both americium-241 and cesium-137. About 22,000 are in use in the United States, and 50 or more are reported lost or missing each year. This material would be suitable to construct a “dirty bomb.” (Shutterstock/TFoxFoto)

Third, cesium-137 sources are widely used in hospitals and medical centers (Fig. 14.5). Cesium is a very suitable material for a “dirty bomb” because it has a relatively long half-life of about 30 years and, more importantly, it vaporizes

readily and can be widely spread by an explosive device. Large cesium sources such as blood or total body animal irradiators are now the subject of intense security and would be difficult to acquire illegally. On the other hand, the smaller sources used for the brachytherapy of cancer do get lost occasionally. In 1998, 19 small tubes of cesium-137, with total activity of about 22 GBq, were reported missing from a medical center in Greensboro, North Carolina.



Cesium tubes similar to the ones missing from Greensboro

FIGURE 14.5 Cesium-137 would be a very suitable material for a “dirty bomb” because it has a relatively long half-life (about 30 years) and can be widely disseminated because it vaporizes readily. For this reason, security of large cesium-137 irradiators in medical centers has been greatly improved in recent years. Nevertheless, small sources used in the brachytherapy of cancer do get lost from time to time. For example, 19 small cesium-137 sources with a total activity of about 22 GBq were reported missing from a medical center in North Carolina in 1998.

HEALTH EFFECTS OF RADIATION

The health consequences of radiation can be divided into two types: tissue reactions (formerly called deterministic effects) and stochastic effects, which have quite different characteristics.

Tissue reactions occur at relatively high doses and result from the killing of many cells in a tissue or organ. Above a tissue-specific dose threshold, the severity of the damage increases with increasing dose as more and more cells are killed. As long as the dose threshold is not exceeded, the effect will not be seen.

Some tissue reactions do not manifest until years later (e.g., cataract, fibrosis) and are therefore known as *late effects*. By contrast, those that manifest

in days to weeks are called *early effects*, or acute effects. A sufficiently large radiation dose over a short time can result in the ARS, which may result in death. This results from the killing of many cells in the bone marrow or lining of the intestines. Examples of this occurred at Hiroshima and Nagasaki and also following the reactor accident at Chernobyl. A dose of several grays is needed to result in these effects, which is possible following the detonation of a nuclear weapon or the meltdown of a nuclear reactor but would be unlikely to occur following a dirty bomb. Because a whole chapter is devoted to the ARS (see [Chapter 8](#)), no more will be said about it here.

Stochastic effects, of which carcinogenesis is the most important, are all-or-nothing effects (i.e., the severity of the effect does not alter with the magnitude of the dose, although the probability of the event occurring does increase with dose). For example, if one person is exposed to 0.1 Gy and another is exposed to 1 Gy, the person exposed to the higher dose would have a greater probability of having cancer, but if both contracted the same malignancy, it would not be more severe in the person who received the higher dose. Cancer is an all-or-nothing event. The other important characteristic of a stochastic effect is that there is believed to be no threshold in dose (i.e., even the smallest dose carries some level of risk, which, however, becomes vanishingly small at very low doses).

EXTERNAL EXPOSURE TO RADIATION AND CONTAMINATION WITH RADIOACTIVE MATERIALS

External exposure describes irradiation of a person by γ - or β -rays from a radioactive source, which never comes in contact with the body. This would be the type of exposure from a hidden RED and could also result from a dirty bomb (RDD) if a fragment of the exploded radioactive material came close to a person but did not actually touch his or her body.

By contrast, a dirty bomb, which scatters radioactive materials over a wide area, could result in people nearby becoming *contaminated*. Radioactive contamination may consist of radionuclides that emit α -, β -, or γ -radiation, or any combination of all three. The most important distinction between the three is their ability to penetrate tissues. α -Particles have a very short range and cannot even penetrate the outer layer of skin. Consequently, they cause harm only if they are internalized by inhalation, ingestion, or absorption through intact skin or through a wound. Examples of α -emitters include polonium-210 that was used to “poison” the Russian defector, Alexander Litvinenko. It was presumably added to his drink, and it is estimated that a huge activity must have been used because

he died a classic bone marrow death 3 to 4 weeks later, which would have required a total body dose of external radiation of at least 4 Gy. In contrast, β -particles can penetrate several centimeters into tissue, whereas γ -rays are so penetrating that they can pass right through the body.

EXTERNAL CONTAMINATION

External contamination refers to radioactive material on the surface of the body. Most external contamination (up to 90%), following an event like a dirty bomb, can be disposed of by removing the clothing, which should be placed in a plastic bag and labeled. A Geiger counter can then be used to survey the patient. The top priority to decontaminate is open wounds because they offer a fast direct route for internalizing radioactive materials and transportation to critical organs.

Next is the nose and mouth, followed by intact skin. Contaminated areas should be carefully washed with soap and water. The survey-scrub-rinse sequence of a wound or intact skin should be repeated until the readings on the survey meter drop to twice background or until further efforts do not result in a decrease in radiation levels. Too vigorous an effort should be avoided because damaging the skin could create a pathway for internal contamination.

INTERNAL CONTAMINATION

The possibility of significant internal contamination is a much more difficult problem. Contaminants gain entry into the body by several routes, such as through inhalation into the lungs, ingestion into the gastrointestinal (GI) tract, or percutaneous or transdermal absorption through intact skin and particularly through open wounds. Some radionuclides tend to remain in the body, often concentrating in a particular tissue or organ. Iodine in the thyroid and transuranics such as plutonium or americium in the bone are some examples. Others may be eliminated in urine, feces, or perspiration. Radionuclides within the body that are γ -emitters can be detected and measured with a whole body counter. Quantities of α -emitters can only be estimated by measuring amounts in excreted materials. Not much can be done to counter the effects of internal contamination, except in a few specific cases. One such case is radioactive iodine. If taken within 4 to 6 hours of contamination, stable iodine in the form of potassium iodine saturates binding sites in the thyroid and inhibits the incorporation of radioactive iodine. The Chernobyl experience has shown clearly that radioactive iodine can cause hypothyroidism and can also result in cancer. This is particularly important for children as well as for the developing embryo

or fetus. Radioactive iodine is unlikely to be released from an RDD but certain to be present with a nuclear weapon or a serious accident at a nuclear reactor because it is a fission product.

The only other countermeasure approved by the U.S. Food and Drug Administration (FDA) is the use of Prussian blue (ferric III hexacyanoferrate II) to block the uptake of cesium-137 from the intestine. This could be important because, as previously mentioned, cesium-137 would be well suited for an RDD.

MEDICAL MANAGEMENT ISSUES IN THE EVENT OF RADIOLOGIC TERRORISM

Many major medical centers have put together a “radiation casualty team” consisting of health providers, physicists, social workers, and administrators to cope with the possibility of a radiation accident or an act of radiologic terrorism. In most circumstances that can be imagined, there is likely to be a large number of people who are frightened and worried, a much smaller number that may actually be contaminated with radioactive material, and an even smaller number who need treatment for a significant radiation exposure.

The highest priority is to give critical care to those who have suffered life-threatening injuries ([Table 14.2](#)). This should not be delayed because of the possibility of radioactive contamination. Radiation exposure and contamination are secondary considerations. Once life-threatening injuries are taken care of, the next step is to use a sensitive Geiger counter to identify those persons who are contaminated with radioactive materials, which in most cases, will be in the form of dust particles on the body and/or clothing. Contaminated clothing should be removed and sealed in plastic bags; this is likely to account for 80% to 90% of the contamination. The next priority is to decontaminate any open wounds because this can be a conduit for radioactive material to be internalized. This can be achieved by gentle irrigation. Lastly comes the decontamination of intact skin. Overly aggressive methods should be avoided, and decontamination efforts should be stopped when radiation levels are less than about twice background. Urine samples should be collected to identify persons who have internalized radioactive material by inhalation or ingestion, but there are very limited treatments available as discussed previously.

Table 14.2 Patient Management Priorities

- Standard medical triage

- Attend first to critical injuries
- Decontaminate
- Remove clothing
- Survey with Geiger counter
- Open wounds
- Mouth and nose
- Intact skin
- Cease decontamination when further efforts do not reduce count and when count is less than twice background.

FURTHER INFORMATION

More detailed information on this topic is available from several sources, such as the following:

The U.S. Department of Health & Human Services (DHHS) established the Radiation Emergency Medical Management website (<http://www.remm.nlm.gov>) in 2007 to give guidance to healthcare workers on radiation health effects.

The Radiation Studies Branch of the Centers for Disease Control and Prevention has a website (<http://www.bt.cdc.gov/radiation/clinicians.asp>)

suitable for both professionals and the public, giving information on protective measures during a nuclear attack or a radiologic event. They also offer a handbook, which is available at <http://www.bt.cdc.gov/radiation/pocket.asp>.

The Department of Energy's Radiation Emergency Assistance Center Training Site (REAC/TS) in Oak Ridge, Tennessee, provides online guidance for medical management of radiation events.

The American College of Radiology (ACR) and the American Society for Therapeutic Radiology and Oncology (ASTRO) have prepared a primer entitled *Disaster Preparedness of Radiology Professional: Response to Radiological Terrorism*, which is available at <https://www.acr.org/Membership/Legal-Business-Practices/Disaster-Preparedness>.

The National Council on Radiation Protection and Measurements (NCRP) prepared NCRP Report No. 138 entitled *Management of Terrorist Events Involving Radioactive Material*, which aims to provide guidance to those responsible for responding to terrorist events.

SUMMARY OF PERTINENT CONCLUSIONS

The following are several possible scenarios for radiologic terrorism:

Detonation of a nuclear weapon

Risk

Exposure to γ -rays and neutrons

Fallout of fission products

Outcome

Large number of acute deaths

Long-term carcinogenesis

Likelihood

Remote

Attack on a nuclear power plant

Risk

Attack on reactor itself

Attack on stored used fuel elements

Release of fission products

Outcome

Unlikely to involve acute deaths

Long-term carcinogenesis

Likelihood

Extremely unlikely

Dirty bomb (RDD)

Risk

Release of radioactive material

Small number of contaminated people

Large number of slightly contaminated people

Psychological chaos, many frightened people

Outcome

Unlikely to involve acute deaths

Small risk of long-term carcinogenesis

Likelihood

Likely

Hidden RED

Risk

Large number of people exposed to small doses of radiation

Psychological chaos, many frightened people

Outcome

Unlikely to result in acute deaths

Small risk of long-term carcinogenesis

Likelihood

Likely

Availability of radioactive material

Small amounts readily available from smoke detectors, humidity gauges, and lost or stolen medical sources

Health effects of radiation

Tissue reactions occur at high doses, such as cataract, fibrosis, or the ARS. Stochastic effects, including carcinogenesis and heritable effects, are important even at lower doses and occur much later.

External exposure to radiation refers to irradiation from an outside source that never comes in contact with the body. External contamination refers to radioactive material on the skin or clothing. Internal contamination refers to radioactive materials that are inhaled, ingested, or internalized through open wounds.

Medical management issues in the event of radiologic terrorism

Standard medical triage; attend first to critical injuries

Decontaminate

Remove clothing; survey with Geiger counter

Decontaminate

Open wounds

Mouth and nose

Intact skin

Cease decontamination efforts when:

Further efforts do not reduce count

Count less than twice background

Collect urine sample to detect internal contamination

Potassium iodide (KI) tablets to stop uptake of radioactive iodine

Prussian blue to prevent absorption of cesium-137

BIBLIOGRAPHY

American Academy of Pediatrics. Policy statement on radiation disasters and children. *Pediatrics*. 2003;111:1455–1466. Available at: <http://aappolicy.aappublications.org/cgi/reprint/pediatrics;111/6/1455.pdf>.

American College of Radiology. Disaster preparedness for radiology

professionals: response to radiological terrorism. A primer for radiologists, radiation oncologists, and medical physicists. 2006. Available at: <http://www.acr.org/SecondaryMainMenuCategories/BusinessPracticeIssues/E> Accessed April 29, 2008.

American Red Cross. Terrorism: preparing for the unexpected. Available at: http://www.redcross.org/services/disaster/0,1082,0_589_,00.html. Accessed April 2, 2008.

Armed Forces Radiobiology Research Institute. *Medical Management of Radiological Casualties Handbook*. 2nd ed. Bethesda, MD: Armed Forces Radiobiology Research Institute; 2003. Available at: <http://www.afrrri.usuhs.mil/outreach/pdf/2edmmrchandbook.pdf>. Accessed April 22, 2008.

Barnett DJ, Parker CL, Blodgett DW, et al. Understanding radiologic and nuclear terrorism as public health threats: preparedness and response perspectives. *J Nucl Med*. 2006;47:1653–1661.

Centers for Disease Control and Prevention. Acute radiation syndrome: a fact sheet for physicians. Available at: <http://www.bt.cdc.gov/radiation/arsphysicianfactsheet.asp>. Accessed May 1, 2008.

Centers for Disease Control and Prevention. Cutaneous radiation injury: a fact sheet for physicians. Available at: <http://www.bt.cdc.gov/radiation/crisphysicianfactsheet.asp>. Accessed May 1, 2008.

Centers for Disease Control and Prevention. Emergency management pocket guide for clinicians. Available at: <http://www.bt.cdc.gov/radiation/pocket.asp>. Accessed May 1, 2008.

Centers for Disease Control and Prevention. Prenatal radiation exposure: a fact sheet for physicians. <http://www.bt.cdc.gov/radiation/prenatalphysician.asp>. Accessed May 1, 2008.

Centers for Disease Control and Prevention. Radiation emergencies. Available at: <http://www.bt.cdc.gov/radiation/>. Accessed December 24, 2008.

Centers for Disease Control and Prevention. Radiation emergency information for clinicians and hospitals. Available at: <http://www.bt.cdc.gov/radiation/clinicians.asp>. Accessed May 1, 2008.

Centers for Disease Control and Prevention. Radiological terrorism: just in time

training for hospital clinicians. Available at: <http://www.bt.cdc.gov/radiation/justintime.asp>. Accessed May 1, 2008.

Centers for Disease Control and Prevention. Use of radiation detection, measuring, and imaging instruments to assess internal contamination from inhaled radionuclides. Available at: <http://www.bt.cdc.gov/radiation/clinicians/evaluation/index.asp>. Accessed January 21, 2008.

Health Physics Society. Procedures for medical emergencies involving radiation. Available at: https://www.hps.org/hsc/documents/Dec_31_Reformatted_MRE_Chart.pdf. Accessed December 23, 2008.

Musolino SV, DeFranco J, Schlucock R. The ALARA principle in the context of a radiological or nuclear emergency. *Health Phys.* 2008;94:109–111.

Musolino SV, Harper FT. Emergency response guidance for the first 48 hours after the outdoor detonation of an explosive radiological dispersal device. *Health Phys.* 2006;90:377–385.

National Council on Radiation Protection and Measurements. *Management of Terrorist Events Involving Radioactive Material*. Bethesda, MD: National Council on Radiation Protection and Measurements; 2001. NCRP Report No. 138.

Radiation Emergency Assistance Center/Training Site. Guidance for hospital medical management. Available at: <http://www.orise.orau.gov/reacts/guide/guidesitemap.htm>. Accessed April 2, 2008.

Radiation Emergency Assistance Center/Training Site. Guidance for radiation accident management. Available at: <http://www.orise.orau.gov/reacts/guide/internal.htm>. Accessed May 1, 2008.

Radiation Emergency Assistance Center/Training Site. Procedure demonstrations. Available at: <http://www.orise.orau.gov/reacts/guide/procedures.htm>. Accessed January 27, 2009.

Smith JM, Ansari A, Harper FT. Hospital management of mass radiological casualties: reassessing exposures from contaminated victims of an exploded radiological dispersal device. *Health Phys.* 2005;89:513–520.

U.S. Department of Health & Human Services. Radiation event medical

management. Available at: <http://www.remm.nlm.gov>. Accessed April 2, 2008.

U.S. Department of Homeland Security. National response plan. Available at: http://www.dhs.gov/xpreprep/committees/editorial_0566.shtm. Accessed April 3, 2008.

Wrixon AD. New recommendations from the International Commission on Radiological Protection—a review. *Phys Med Biol*. 2008;53:R41–R60.

chapter 15

Doses and Risks in Diagnostic Radiology, Interventional Radiology and Cardiology, and Nuclear Medicine

Doses from Natural Background Radiation

- Cosmic Radiation
- Natural Radioactivity in the Earth's Crust
- Internal Exposure
- Areas of High Natural Background

Comparison of Radiation Doses from Natural Sources and Human Activities

Diagnostic Radiology

- Dose
- Effective Dose
- Collective Effective Dose

Interventional Radiology and Cardiology

- Patient Doses and Effective Doses
- Dose to Personnel

Nuclear Medicine

- Historical Perspective
- Effective Dose and Collective Effective Dose
- Principles in Nuclear Medicine
- Positron Emission Tomography
- The Therapeutic Use of Radionuclides

Medical Irradiation of Children and Pregnant Women

- Irradiation of Children
- Irradiation of Pregnant Women

Doses to the Embryo and Fetus

Recommendations on Breastfeeding Interruptions

Summary

Summary of Pertinent Conclusions

Computed Tomography

Effective Dose and Cancer

Interventional Procedures

Nuclear Medicine

Medical Radiation of Children and Pregnant Women

Summary

Bibliography

The purpose of this chapter is to review the doses involved and to estimate the associated risks in radiology, cardiology, and nuclear medicine. The bulk of radiation exposure is received by patients as part of their diagnosis or treatment, so there is a tangible medical benefit to balance against the risk, but medical radiation exposure is also conducted for medicolegal reasons and on volunteers (patients or healthy persons) for research purposes, and here, the risk–benefit equation is quite different. However, to put things in perspective, we first summarize the radiation doses from background sources that everyone receives naturally. This is usually regarded as an important benchmark because life on earth has evolved with this continuous background radiation.

DOSES FROM NATURAL BACKGROUND RADIATION

Natural sources of radiation include cosmic rays from outer space and from the sun, terrestrial radiation from natural radioactive materials in the ground, and radiation from radionuclides naturally present in the body, ingested from food, or inhaled. The sources of natural background radiation are illustrated in [Figure 15.1](#).

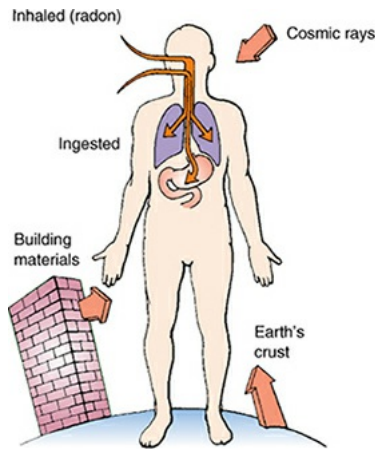


FIGURE 15.1 Three principal components of natural background radiation: (1) cosmic rays from solar flares in the sun or from outer space; (2) ingested radioactivity, principally potassium-40 in food, and inhaled radioactivity, principally radon; and (3) radiation from the earth's crust, which in practice means radiation emanating from building materials, because most people spend much of their lives indoors.

Enhanced natural sources are sources that are natural in origin but to which exposure is increased because of human activity (inadvertent or otherwise). Examples include air travel at high altitude, which increases cosmic ray levels, and movement of radionuclides on the ground in phosphate mining, which can increase the terrestrial component to persons living in houses built on waste landfills. Indoor radon exposure might be considered in some instances an enhanced natural source, inasmuch as it is not natural to live in an insulated house. In a sense, also, all operations associated with the nuclear fuel cycle, starting with mining, involve natural radionuclides, but these are more generally classified as a consequence of human activity.

Cosmic Radiation

Cosmic rays are made up of radiations originating from outside the solar system and from charged particles (largely protons) emanating from the surface of the sun. The intensity of cosmic rays arriving at the earth's surface varies with both latitude and altitude above sea level. The variation with latitude is a consequence of the magnetic properties of the earth: Cosmic rays are charged particles that tend to be deflected away from the equator and funneled into the poles. This is illustrated in [Figure 15.2](#). The *aurora borealis*, or northern lights, results from charged particles spiraling down the lines of magnetic field in the polar regions. Consequently, cosmic ray intensity is least in equatorial regions and rises toward the poles. There is an even larger variation in cosmic ray intensity with altitude

because at high elevations above sea level, there is less atmosphere to absorb the cosmic rays, so their intensity is greater. For example, the cosmic ray annual equivalent dose in the United States is about 0.26 mSv at sea level. This essentially doubles for each 2,000-m increase in altitude in the lower atmosphere, so that in Denver, Colorado, the annual effective dose* from cosmic radiation is about 0.5 mSv. The variation in dose from cosmic radiation across the United States is illustrated in [Figure 15.3](#). As would be expected, the highest doses are in the Rocky Mountains at high elevations.

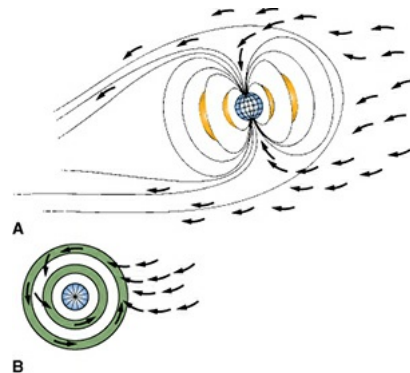


FIGURE 15.2 **A:** The earth behaves like a giant magnet. Showers of charged particles from solar events on the surface of the sun are deflected away from the equator by the earth's magnetic field; most miss the earth altogether; others are funneled into the polar regions. This explains why cosmic ray dose is low near the equator and high in the polar regions. It is also the basis of the aurora borealis, or northern lights, caused by intense showers of cosmic ray particles that spiral down the lines of magnetic field into the poles. **B:** Viewed from above the poles, the earth is ringed with lines of magnetic field that form regions of high radiation dose known as the *Van Allen belts*. Humans could not live for long in the dose rates characteristic of these belts. On lunar missions, spaceships pass quickly through the Van Allen belts; the space shuttle orbits well below them.

The annual outdoor effective dose (μSv) from cosmic radiation for Canada and the U.S.

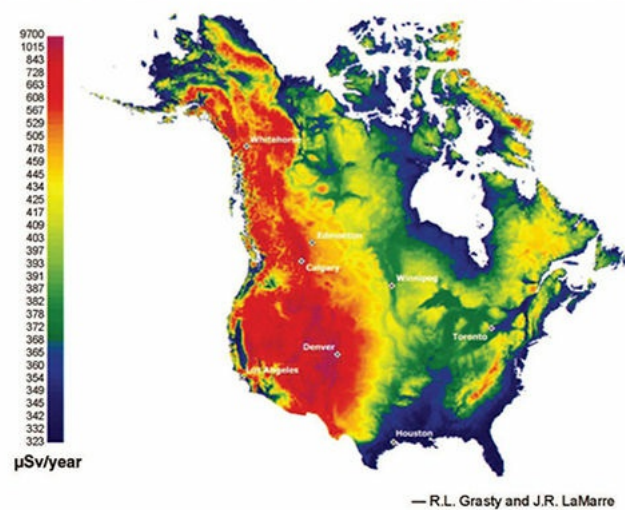


FIGURE 15.3 Color plot of the annual cosmic radiation doses (in microsievert) in North America. The variation with altitude is very clear, with the highest doses in the Rocky Mountains. (From Grasty RL, Lamarre JR. The annual effective dose from natural sources of ionizing radiation in Canada. *Radiat Prot Dosim*. 2004;108:215–226, with permission.)

Long flights at high altitudes involve some increased dose, too. For example, the extra dose from cosmic rays received by a passenger on a commercial flight flying from the United States to Europe is about 0.05 mSv. Flight crews on northerly routes accumulate larger doses than most radiology staff in hospitals; in fact, airline crews are already classified as radiation workers in Europe, but that is not yet the case in the United States.

Natural Radioactivity in the Earth's Crust

Naturally occurring radioactive materials are widely distributed throughout the earth's crust, and humans are exposed to the γ -rays from them. In the United States, there is a big variation between the Colorado plateau area, where the rocks and soil contain relatively more radioactive thorium and uranium (0.75 to 1.40 mGy per year), and the Atlantic seaboard, where radioactivity is low (0.15 to 0.35 mGy per year). This variation is illustrated in [Figure 15.4](#).

Terrestrial Gamma-Ray Exposure at 1m above ground

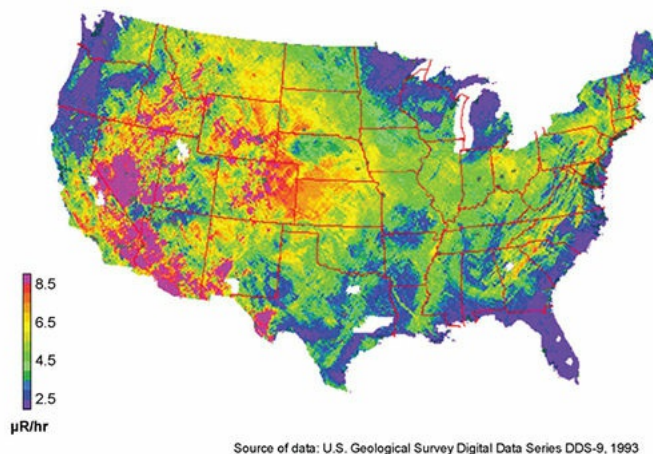


FIGURE 15.4 Terrestrial γ -ray exposure at 1 m aboveground for the United States, taken from the U.S. Geological Survey Digital Data Series for 1993. The units of exposure in the figure are in microroentgen per hour. Over the Colorado plateau, the equivalent dose would be about 0.75 mSv per year, compared with about 0.22 mSv per year over the Atlantic seaboard.

Internal Exposure

Small traces of radioactive materials are normally present in the human body, ingested from the tiny quantities present in food or inhaled as airborne particles. Radioactive thorium, radium, and lead can be detected in most persons, but the amounts are small and variable, and the figure usually quoted for the average dose rate resulting from these deposits is less than $10 \mu\text{Sv}$ per year. Only radioactive potassium-40 makes an appreciable contribution to human exposure from ingestion. The dose rate is about 0.2 mSv per year, which cannot be ignored as a source of mutations in humans.

The biggest source of natural background radiation is radon gas, which seeps into the basements of houses from rocks underground. Radon, a decay product in the uranium series, is a noble gas that does little harm itself because it is breathed in and breathed out again. However, in the confined space of an underground mine or the basement of a house, it decays with a 3-day half-life to form solid progeny that stick to dust or moisture particles and, if inhaled, become lodged on the surface of the bronchus or lung. Radon progeny emits α -particles that, it is believed, are responsible for lung cancer. Radon levels in houses vary enormously, but the average concentration in the United States is about 37 Bq per cubic meter in aboveground living areas and much more in basements. It is a sobering thought that in an average home, in every cubic meter of air, 37 atoms of radon decay each second, producing radioactive progeny. Only the bronchi

and lungs are irradiated by this source, but α -particles are highly effective and have a radiation weighting factor of 20 (radiation weighting factor is explained in [Chapters 7 and 16](#)). This translates into an annual average effective dose of about 2 mSv. There is no question that radon is by far the largest component of natural background radiation. The Environmental Protection Agency action level for radon is 148 Bq per cubic meter; remedial action is suggested for houses above this level. The Committee on the Biological Effects of Ionizing Radiation (BEIR) of the National Academy of Sciences (BEIR IV Report, 1998) estimates that radon may be responsible for between 15,400 and 21,800 lung cancer deaths per year in the United States (i.e., about 10% of the total lung cancer deaths).

Areas of High Natural Background

There are several inhabited areas of the world where background radiation is considerably higher than average because of radioactivity in rocks, soil, or in building materials from which houses are made. These areas are in Brazil, France, India, Niue Island (in the South Pacific), and Egypt.

In Brazil, some 30,000 people who live in coastal areas are exposed to dose rates of 5 mSv per year. About one-sixth of the population of France live in areas, largely in the Burgundy wine-growing district, in which the rocks are principally granite, and they receive 1.8 to 3.5 mSv per year from background radiation. Undoubtedly, the highest natural background radiation is in Kerala, India, where more than 100,000 people receive an average annual dose of about 13 mSv, reaching a high in certain locations on the coast of 70 mSv.

Many studies have been made of these human populations who have lived for many generations in areas of high natural background radiation. So far, no excess incidence of cancer or heritable anomalies has been observed that can reasonably be attributed to the radiation. Such studies, of course, are beset with difficulties. For example, the Kerala population has a very high incidence of congenital malformations, but with generations of in-breeding, it is impossible to attribute any effects to the higher background radiation.

COMPARISON OF RADIATION DOSES FROM NATURAL SOURCES AND HUMAN ACTIVITIES

In addition to natural background radiation, the human population is exposed to various sources of radiation resulting from human activities, as illustrated in [Figure 15.5](#), with by far the most important source being exposure to medical radiation. [Figure 15.6](#) compares the contribution of various sources of exposure

to the populations of the United States and the United Kingdom. The average effective dose to the individual in the US population (6.2 mSv) is more than double the comparable figure (2.7 mSv) for an individual in the United Kingdom. The difference is accounted for largely by the difference in the contribution from medical radiation which is more than 7 times larger in the United States than in the United Kingdom due to the big difference in health care systems between the two countries.

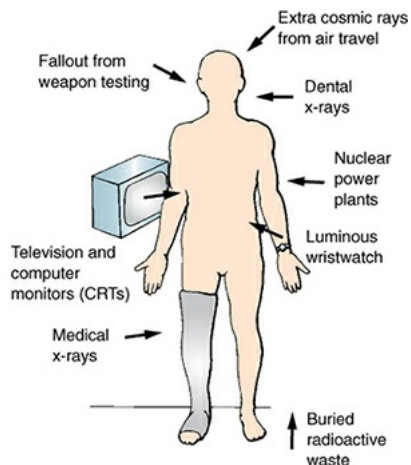


FIGURE 15.5 The various sources of radiation resulting from human activity to which the human population is exposed. In developed countries, the effective dose is dominated by medical radiation.

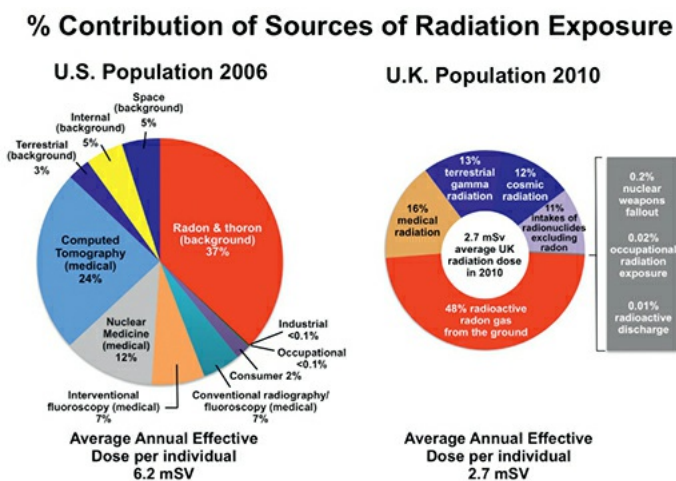


FIGURE 15.6 Percentage contribution of the various sources of exposure to the US population (in 2006) and the UK population (in 2010). The average annual effective dose per individual in the United States is more than double that in the United Kingdom (6.2 mSv compared with 2.7 mSv). There is not much difference in the contribution from natural background radiation between the two countries but the contribution from medical radiation is 7 times larger in the United States than in the United Kingdom (US data from National Council on

Radiation Protection and Measurements. *Ionizing Radiation Exposure of the Population of the United States*. Bethesda, MD: National Council on Radiation Protection and Measurements; 2009. Report 160; UK data from Public Health England. 2016.)

In both the United States and the United Kingdom, radon represents the largest source of natural background radiation, whereas medical radiation dominates the contribution from human activities.

It is important to realize that the populations exposed to these two major sources are not the same. The entire US population in age, gender, and health status is exposed to background radiation. By contrast, persons exposed to medical radiation are “patients” and, as such, are skewed to older ages and to those with health problems. The principal exceptions are x-rays used for screening purposes (e.g., mammography) and for trauma in children.

DIAGNOSTIC RADIOLOGY

The radiation doses involved in general radiology are seldom sufficiently large to result in *tissue reactions* (formerly known as *deterministic effects*). By definition, a tissue reaction has a practical threshold in dose, the severity of the effect increases with dose above the threshold, and it results from damage to many cells. One exception is the inadvertent exposure of the developing embryo or fetus, with a possible consequence of reduced head diameter (microcephaly) and mental retardation. The threshold for radiation-induced mental retardation is about 0.3 Gy (International Commission on Radiological Protection [ICRP], 2006), so few procedures are likely to cause this effect. Interventional radiology is, of course, a different story, and serious cases of skin damage are occasionally reported after long periods of fluoroscopy.

Apart from these important exceptions, the potential deleterious consequences of diagnostic radiology involve *stochastic effects*, that is, carcinogenesis and heritable effects. The characteristic of stochastic effects is that there is no threshold in dose; that is, there is no dose below which the effect does not occur, and the probability of carcinogenesis or heritable effects increases with dose. A stochastic effect may result from irradiation of one or a few cells, and the severity of the response is not dose related. As a consequence, *absorbed dose* to a limited portion of a person’s body does not provide by itself the overall perspective on risk associated with a given procedure.

Effective dose is a more relevant quantity; it takes into account the relative sensitivity of the tissues and organs irradiated as well as the dose involved. This

is important because some tissues and organs are more susceptible than others to radiation. (Effective dose is discussed in detail in [Chapter 16](#).) The technical definition of effective dose is the sum of the equivalent doses to each tissue and organ exposed multiplied by the appropriate tissue weighting factors (W_T). What this amounts to in simpler terms is that effective dose is the whole body dose of x-rays that would have to be delivered to produce the same stochastic risk as the partial body dose that actually was delivered. This quantity provides an easy assessment of overall risk and makes comparison of risks much simpler; for example, risk from a diagnostic examination is more readily compared with that from background radiation if effective dose is quoted. The unit of absorbed dose is the **gray**, whereas the unit of effective dose is the **sievert**. Most current reports in the literature use effective dose in discussing the potential health consequences of diagnostic radiology.

Last but not the least, the overall population impact of diagnostic radiology can be assessed in terms of the *collective effective dose*, the product of effective dose, and the number of persons exposed. In this case, the unit is the **person-sievert**. This quantity is a surrogate for “harm” resulting from a given event involving radiation exposure. For example, the collective effective dose from the Chernobyl accident multiplied by the risk coefficient (5% per sievert for fatal cancer) gives an estimate of the number of cancer cases resulting from the accident and is therefore a measure of the harm done. Later in this chapter, the consequences of the collective effective dose from diagnostic radiology will be discussed.

These three quantities—dose, effective dose, and collective effective dose—are discussed in turn. (In general, whenever the term *dose* is used alone, it refers to the absorbed dose.)

Dose

[Table 15.1](#) lists the organ doses involved in a few representative radiologic procedures to illustrate the fact the organ doses vary by orders of magnitude between different procedures.

Table 15.1 Illustrating the Wide Range of Organ Doses Resulting from Various Radiologic Procedures

EXAMINATION	RELEVANT ORGAN	RELEVANT DOSE (mGy)	ORGAN
Mammogram	Mammary gland	~0.1	breast
CT scan	Liver	~100	liver
Angiogram	Kidneys	~100	kidneys
Cardiac catheterization	Heart	~100	heart
Interventional procedure	Spine	~100	spine
Angiogram	Brain	~100	brain
Angiogram	Extremities	~100	extremities
Angiogram	Abdomen	~100	abdomen
Angiogram	Urinary tract	~100	urinary tract
Angiogram	Esophagus	~100	esophagus
Angiogram	Pancreas	~100	pancreas
Angiogram	Lungs	~100	lungs
Angiogram	Colon	~100	colon
Angiogram	Bladder	~100	bladder
Angiogram	Uterus	~100	uterus
Angiogram	Testes	~100	testes
Angiogram	Ovaries	~100	ovaries
Angiogram	Prostate	~100	prostate
Angiogram	Adrenal glands	~100	adrenal glands
Angiogram	Pituitary gland	~100	pituitary gland
Angiogram	Hypothalamus	~100	hypothalamus
Angiogram	Thalamus	~100	thalamus
Angiogram	Cerebellum	~100	cerebellum
Angiogram	Brain stem	~100	brain stem
Angiogram	Spinal cord	~100	spinal cord
Angiogram	Spine	~100	spine
Angiogram	Extremities	~100	extremities
Angiogram	Abdomen	~100	abdomen
Angiogram	Urinary tract	~100	urinary tract
Angiogram	Esophagus	~100	esophagus
Angiogram	Pancreas	~100	pancreas
Angiogram	Lungs	~100	lungs
Angiogram	Colon	~100	colon
Angiogram	Bladder	~100	bladder
Angiogram	Uterus	~100	uterus
Angiogram	Testes	~100	testes
Angiogram	Ovaries	~100	ovaries
Angiogram	Prostate	~100	prostate
Angiogram	Adrenal glands	~100	adrenal glands
Angiogram	Pituitary gland	~100	pituitary gland
Angiogram	Hypothalamus	~100	hypothalamus
Angiogram	Thalamus	~100	thalamus
Angiogram	Cerebellum	~100	cerebellum
Angiogram	Brain stem	~100	brain stem
Angiogram	Spinal cord	~100	spinal cord
Angiogram	Spine	~100	spine
Angiogram	Extremities	~100	extremities
Angiogram	Abdomen	~100	abdomen
Angiogram	Urinary tract	~100	urinary tract
Angiogram	Esophagus	~100	esophagus
Angiogram	Pancreas	~100	pancreas
Angiogram	Lungs	~100	lungs
Angiogram	Colon	~100	colon
Angiogram	Bladder	~100	bladder
Angiogram	Uterus	~100	uterus
Angiogram	Testes	~100	testes
Angiogram	Ovaries	~100	ovaries
Angiogram	Prostate	~100	prostate
Angiogram	Adrenal glands	~100	adrenal glands
Angiogram	Pituitary gland	~100	pituitary gland
Angiogram	Hypothalamus	~100	hypothalamus
Angiogram	Thalamus	~100	thalamus
Angiogram	Cerebellum	~100	cerebellum
Angiogram	Brain stem	~100	brain stem
Angiogram	Spinal cord	~100	spinal cord
Angiogram	Spine	~100	spine
Angiogram	Extremities	~100	extremities
Angiogram	Abdomen	~100	abdomen
Angiogram	Urinary tract	~100	urinary tract
Angiogram	Esophagus	~100	esophagus
Angiogram	Pancreas	~100	pancreas
Angiogram	Lungs	~100	lungs
Angiogram	Colon	~100	colon
Angiogram	Bladder	~100	bladder
Angiogram	Uterus	~100	uterus
Angiogram	Testes	~100	testes
Angiogram	Ovaries	~100	ovaries
Angiogram	Prostate	~100	prostate
Angiogram	Adrenal glands	~100	adrenal glands
Angiogram	Pituitary gland	~100	pituitary gland
Angiogram	Hypothalamus	~100	hypothalamus
Angiogram	Thalamus	~100	thalamus
Angiogram	Cerebellum	~100	cerebellum
Angiogram	Brain stem	~100	brain stem
Angiogram	Spinal cord	~100	spinal cord
Angiogram	Spine	~100	spine
Angiogram	Extremities	~100	extremities
Angiogram	Abdomen	~100	abdomen
Angiogram	Urinary tract	~100	urinary tract
Angiogram	Esophagus	~100	esophagus
Angiogram	Pancreas	~100	pancreas
Angiogram	Lungs	~100	lungs
Angiogram	Colon	~100	colon
Angiogram	Bladder	~100	bladder
Angiogram	Uterus	~100	uterus
Angiogram	Testes	~100	testes
Angiogram	Ovaries	~100	ovaries
Angiogram	Prostate	~100	prostate
Angiogram	Adrenal glands	~100	adrenal glands
Angiogram	Pituitary gland	~100	pituitary gland
Angiogram	Hypothalamus	~100	hypothalamus
Angiogram	Thalamus	~100	thalamus
Angiogram	Cerebellum	~100	cerebellum
Angiogram	Brain stem	~100	brain stem
Angiogram	Spinal cord	~100	spinal cord
Angiogram	Spine	~100	spine
Angiogram	Extremities	~100	extremities
Angiogram	Abdomen	~100	abdomen
Angiogram	Urinary tract	~100	urinary tract
Angiogram	Esophagus	~100	esophagus
Angiogram	Pancreas	~100	pancreas
Angiogram	Lungs	~100	lungs
Angiogram	Colon	~100	colon
Angiogram	Bladder	~100	bladder
Angiogram	Uterus	~100	uterus
Angiogram	Testes	~100	testes
Angiogram	Ovaries	~100	ovaries
Angiogram	Prostate	~100	prostate
Angiogram	Adrenal glands	~100	adrenal glands
Angiogram	Pituitary gland	~100	pituitary gland
Angiogram	Hypothalamus	~100	hypothalamus
Angiogram	Thalamus	~100	thalamus
Angiogram	Cerebellum	~100	cerebellum
Angiogram	Brain stem	~100	brain stem
Angiogram	Spinal cord	~100	spinal cord
Angiogram	Spine	~100	spine
Angiogram	Extremities	~100	extremities
Angiogram	Abdomen	~100	abdomen
Angiogram	Urinary tract	~100	urinary tract
Angiogram	Esophagus	~100	esophagus
Angiogram	Pancreas	~100	pancreas
Angiogram	Lungs	~100	lungs
Angiogram	Colon	~100	colon
Angiogram	Bladder	~100	bladder
Angiogram	Uterus	~100	uterus
Angiogram	Testes	~100	testes
Angiogram	Ovaries	~100	ovaries
Angiogram	Prostate	~100	prostate
Angiogram	Adrenal glands	~100	adrenal glands
Angiogram	Pituitary gland	~100	pituitary gland
Angiogram	Hypothalamus	~100	hypothalamus
Angiogram	Thalamus	~100	thalamus
Angiogram	Cerebellum	~100	cerebellum
Angiogram	Brain stem	~100	brain stem
Angiogram	Spinal cord	~100	spinal cord
Angiogram	Spine	~100	spine
Angiogram	Extremities	~100	extremities
Angiogram	Abdomen	~100	abdomen
Angiogram	Urinary tract	~100	urinary tract
Angiogram	Esophagus	~100	esophagus
Angiogram	Pancreas	~100	pancreas
Angiogram	Lungs	~100	lungs
Angiogram	Colon	~100	colon
Angiogram	Bladder	~100	bladder
Angiogram	Uterus	~100	uterus
Angiogram	Testes	~100	testes
Angiogram	Ovaries	~100	ovaries
Angiogram	Prostate	~100	prostate
Angiogram	Adrenal glands	~100	adrenal glands
Angiogram	Pituitary gland	~100	pituitary gland
Angiogram	Hypothalamus	~100	hypothalamus
Angiogram	Thalamus	~100	thalamus
Angiogram	Cerebellum	~100	cerebellum
Angiogram	Brain stem	~100	brain stem
Angiogram	Spinal cord	~100	spinal cord
Angiogram	Spine	~100	spine
Angiogram	Extremities	~100	extremities
Angiogram	Abdomen	~100	abdomen
Angiogram	Urinary tract	~100	urinary tract
Angiogram	Esophagus	~100	esophagus
Angiogram	Pancreas	~100	pancreas
Angiogram	Lungs	~100	lungs
Angiogram	Colon	~100	colon
Angiogram	Bladder	~100	bladder
Angiogram	Uterus	~100	uterus
Angiogram	Testes	~100	testes
Angiogram	Ovaries	~100	ovaries
Angiogram	Prostate	~100	prostate
Angiogram	Adrenal glands	~100	adrenal glands
Angiogram	Pituitary gland	~100	pituitary gland
Angiogram	Hypothalamus	~100	hypothalamus
Angiogram	Thalamus	~100	thalamus
Angiogram	Cerebellum	~100	cerebellum
Angiogram	Brain stem	~100	brain stem
Angiogram	Spinal cord	~100	spinal cord
Angiogram	Spine	~100	spine
Angiogram	Extremities	~100	extremities
Angiogram	Abdomen	~100	abdomen
Angiogram	Urinary tract	~100	urinary tract
Angiogram	Esophagus	~100	esophagus
Angiogram	Pancreas	~100	pancreas
Angiogram	Lungs	~100	lungs
Angiogram	Colon	~100	colon
Angiogram	Bladder	~100	bladder
Angiogram	Uterus	~100	uterus
Angiogram	Testes	~100	testes
Angiogram	Ovaries	~100	ovaries
Angiogram	Prostate	~100	prostate
Angiogram	Adrenal glands	~100	adrenal glands
Angiogram	Pituitary gland	~100	pituitary gland
Angiogram	Hypothalamus	~100	hypothalamus
Angiogram	Thalamus	~100	thalamus
Angiogram	Cerebellum	~100	cerebellum
Angiogram	Brain stem	~100	brain stem
Angiogram	Spinal cord	~100	spinal cord
Angiogram	Spine	~100	spine
Angiogram	Extremities	~100	extremities
Angiogram	Abdomen	~100	abdomen
Angiogram	Urinary tract	~100	urinary tract
Angiogram	Esophagus	~100	esophagus
Angiogram	Pancreas	~100	pancreas
Angiogram	Lungs	~100	lungs
Angiogram	Colon	~100	colon
Angiogram	Bladder	~100	bladder
Angiogram	Uterus	~100	uterus
Angiogram	Testes	~100	testes
Angiogram	Ovaries	~100	ovaries
Angiogram	Prostate	~100	prostate
Angiogram	Adrenal glands	~100	adrenal glands
Angiogram	Pituitary gland	~100	pituitary gland
Angiogram	Hypothalamus	~100	hypothalamus
Angiogram	Thalamus	~100	thalamus
Angiogram	Cerebellum	~100	cerebellum
Angiogram	Brain stem	~100	brain stem
Angiogram	Spinal cord	~100	spinal cord
Angiogram	Spine	~100	spine
Angiogram	Extremities	~100	extremities
Angiogram	Abdomen	~100	abdomen
Angiogram	Urinary tract	~100	urinary tract
Angiogram	Esophagus	~100	esophagus
Angiogram	Pancreas	~100	pancreas
Angiogram	Lungs	~100	lungs
Angiogram	Colon	~100	colon
Angiogram	Bladder	~100	bladder
Angiogram	Uterus	~100	uterus
Angiogram	Testes	~100	testes
Angiogram	Ovaries	~100	ovaries
Angiogram	Prostate	~100	prostate
Angiogram	Adrenal glands	~100	adrenal glands
Angiogram	Pituitary gland	~100	pituitary gland
Angiogram	Hypothalamus	~100	hypothalamus
Angiogram	Thalamus	~100	thalamus
Angiogram	Cerebellum	~100	cerebellum
Angiogram	Brain stem	~100	brain stem
Angiogram	Spinal cord	~100	spinal cord
Angiogram	Spine	~100	spine
Angiogram	Extremities	~100	extremities
Angiogram	Abdomen	~100	abdomen
Angiogram	Urinary tract	~100	urinary tract
Angiogram	Esophagus	~100	esophagus
Angiogram	Pancreas	~100	pancreas
Angiogram	Lungs	~100	lungs
Angiogram	Colon	~100	colon
Angiogram	Bladder	~100	bladder
Angiogram	Uterus	~100	uterus
Angiogram	Testes	~100	testes
Angiogram	Ovaries	~100	ovaries
Angiogram	Prostate	~100	prostate
Angiogram	Adrenal glands	~100	adrenal glands
Angiogram	Pituitary gland	~100	pituitary gland
Angiogram	Hypothalamus	~100	hypothalamus
Angiogram	Thalamus	~100	thalamus
Angiogram	Cerebellum	~100	cerebellum
Angiogram	Brain stem	~100	brain stem
Angiogram	Spinal cord	~100	spinal cord
Angiogram	Spine	~100	spine
Angiogram	Extremities	~100	extremities
Angiogram	Abdomen	~100	abdomen
Angiogram	Urinary tract	~100	urinary tract
Angiogram	Esophagus	~100	esophagus
Angiogram	Pancreas	~100	pancreas
Angiogram	Lungs	~100	lungs
Angiogram	Colon	~100	colon
Angiogram	Bladder	~100	bladder
Angiogram	Uterus	~100	uterus
Angiogram	Testes	~100	testes
Angiogram	Ovaries	~100	ovaries
Angiogram	Prostate	~100	prostate
Angiogram	Adrenal glands	~100	adrenal glands
Angiogram	Pituitary gland	~100	pituitary gland
Angiogram	Hypothalamus	~100	hypothalamus
Angiogram	Thalamus	~100	thalamus
Angiogram			

Dental x-ray	Brain	0.005
PA chest x-ray	Lung	0.01
Lateral chest x-ray	Lung	0.15
Screening mammogram	Breast	3
Adult abdominal CT	Stomach	11
Adult head CT	Brain	13
Child abdominal CT	Stomach	10–25
Child head CT	Brain	20–25
Adult ¹⁸ F-FDG PET	Bladder	18

Abbreviations: PA, posteroanterior; CT, computed tomography; ¹⁸F-FDG, [¹⁸F]-2-deoxy-2-fluoro-D-glucose; PET, positron emission tomography.

Courtesy of Dr. David Brenner.

The Nationwide Evaluation of X-ray Trends (NEXT) is a national program conducted to characterize the radiation doses patients receive and to document the state of the practice of diagnostic radiology. The program is a collaborative effort of the Conference of Radiation Control Program Directors, an association of state and local radiation control agencies and the U.S. Food and Drug

Administration, Center for Devices and Radiological Health. Every few years, the NEXT survey program selects a particular radiologic examination for study and captures radiation exposure data from a nationally representative sample of US clinical facilities. **Table 15.2** summarizes NEXT surveys that have been conducted in the past three decades.

Table 15.2 The Nationwide Evaluation of X-ray Trends Surveys

EXAMINATION	SURVEY YEARS
Chest radiography	1984, 1986, 1994, 2001
Mammography	1985, 1988, 1992
Abdomen and lumbosacral (LS) spine radiography	1987, 1989, 1995, 2002
Fluoroscopy (upper GI [1991, 1996, 2003], cardiac cath 1991, 1996, 2003, 2008 labs and mobile C-arms [1996], <i>coronary angiography</i> [2008])	
Computed tomography (CT)	1990, 2000, 2005
Dental radiography	1993, 1999, 2013
Pediatric chest	1998

Abbreviation: GI, gastrointestinal.

The 1992 NEXT report summarized mammography x-ray data. It was shown that over the years, the mean glandular dose per examination has fallen and is

now about 2 mGy while the image quality has improved. This is illustrated in [Figure 15.7](#).

The 1994 report summarized data for adult chest x-rays. The average entrance air kerma was 0.14 mGy at an average clinical kilovolt peak (kVp) of 101, with an average exposure time of 31 ms.

The 2002 report referred to abdomen and lumbosacral spine x-ray data, which are shown in [Table 15.3](#).

Table 15.3 Abdomen and Lumbosacral Spine

	LUMBOSACRAL SPINE	ABDOMEN
Number of Facilities	200	200
Entrance air kerma rate (mGy)	3.21	2.73
Clinical kVp	78	75
Exposure time (ms)	351	306
Phantom film optical density	1.41	1.83
Half value layer (mm Al)	3.2	3.1

From the NEXT 2002 Abdomen and LS Spine X-ray Data Survey.

Dental x-ray data were the subject of the 1999 survey. The average entrance air kerma was 1.6 mGy with an average clinical kVp of 71.

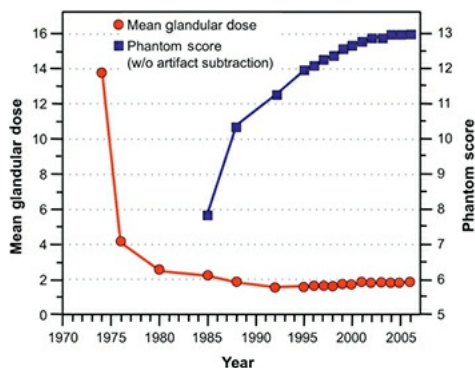


FIGURE 15.7 Graph showing how the mean glandular dose for mammography has fallen 1 dramatically over the years and is now about 1.4 mGy. Meanwhile, the image quality improved. Image quality is measured in terms of phantom score; a phantom contains fiber specks and spheres of different sizes, and the score indicates how many can be seen. (Adapted with permission from Nationwide Evaluation of X-ray Trends. Twenty-five years of NEXT. <http://www.crcpd.org/pubs/nexttrifolds/25yrsofnext%20trifold-rev2-4-03.pdf>. Accessed February 2003.)

Some of the largest doses in diagnostic radiology are associated with fluoroscopy. In this case, the dose rate is greatest at the skin, where the x-ray beam first enters the patient. Dose rates from fluoroscopy from the NEXT 1996 upper gastrointestinal (GI) fluoroscopy survey are shown in [Table 15.4](#).

Table 15.4 Fluoroscopy-Upper Gastrointestinal Exam and Special Topics

Number of Facilities	321	25	52
Type	Upper GI	Cardiac Cath Labs	Mobile C-arm Units
Entrance air kerma (mGy/min)	45	38	22
Clinical kVp	99	82	78
Tube current (mA)	2.3	5.1	3.0

Air kerma rate with contrast (mGy/min)	67	71	41
Maximum air kerma rate (mGy/min)	70	74	44

Abbreviation: GI, gastrointestinal.

From the NEXT 1996 X-ray Data Survey.

The number of computed tomography (CT) scanners in clinical use has risen steadily over the years and varies enormously between countries with very different health care systems. [Figure 15.8](#), taken from the United Nations Scientific Committee on the Effects of Atomic Radiation (UNSCEAR) review in 2008, shows Japan with 3 times as many CT scanners per million population as the United States and 12 times as many as the United Kingdom, the country where CT scan was developed. [Figure 15.9](#) shows the dramatic increase in the number of CT scans performed in the United States and in the United Kingdom in the past 35 years. By 2010, the number of CT scans performed in the United States reached 85 million, with about 10% of them in children. There was a pause in the rate of increase during the years when concerns were raised about the doses involved, but by 2015, the rate of use resumed an upward trend. The rate of increase in the United Kingdom is just as rapid, but, taking into account the relative population sizes of the two countries, the frequency of use of CT (in terms of the number of scans/person/year) is about 5 times lower in the United Kingdom than in the United States. For CT scanning, organs in the beam can receive doses in the range of 10 to 100 mGy but are usually in the range of 15 to 30 mGy for each single CT sequence. However, surveys emphasize the fact that doses can vary significantly between different manufacturers and for the same make scanner between different departments.

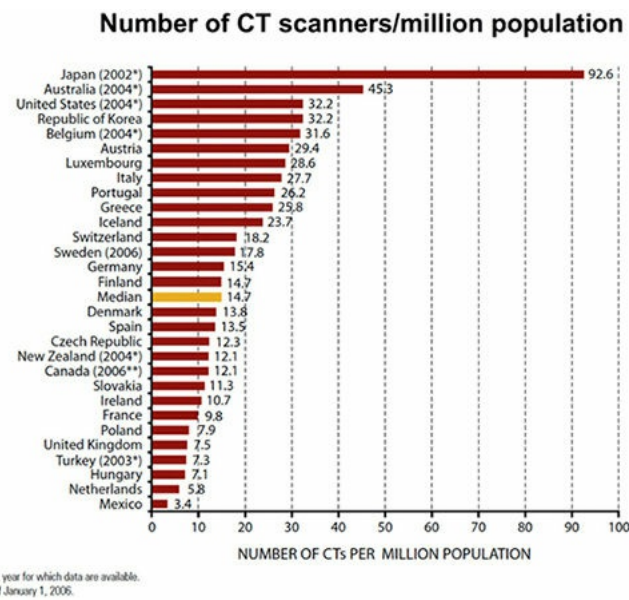


FIGURE 15.8 Number of computed tomography (CT) scanners per million population in various countries. (Based on United Nations Scientific Committee on the Effects of Atomic Radiation [UNSCEAR] 2008.)

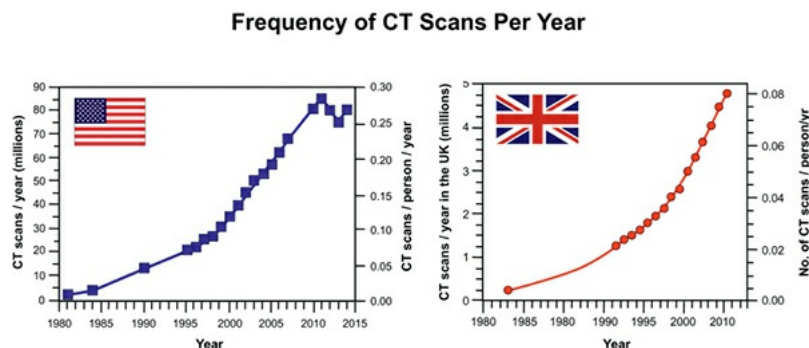


FIGURE 15.9 Estimated number of computed tomography (CT) scans performed annually in the United States and in the United Kingdom from 1980 until 2015. Note that although the rate of increase is similar in the United Kingdom to the United States, the number of scans per person is 5 times lower in the United Kingdom.

Effective Dose

Most recent surveys of diagnostic radiology quote effective dose because this is related to the risk of stochastic effects, such as the induction of cancer or heritable effects. Table 15.5 shows representative values (together with range of values) of effective doses from representative radiologic procedures reported in the literature and summarized by Mettler and colleagues in 2008.

Table 15.5 Adult Effective Doses for Various Diagnostic Radiology Procedures

EXAMINATION	AVERAGE EFFECTIVE DOSE (mSv)	VALUES REPORTED IN LITERATURE (mSv)
Skull	0.1	0.03–0.22
Cervical spine	0.2	0.07–0.3
Thoracic spine	1.0	0.6–1.4
Lumbar spine	1.5	0.5–1.8
Posteroanterior and lateral study of chest	0.1	0.05–0.24
Posteroanterior study of chest	0.02	0.007–0.050
Mammography	0.4	0.10–0.60
Abdomen	0.7	0.04–1.1
Pelvis	0.6	0.2–1.2
Hip	0.7	0.18–2.71

Shoulder	0.01	—
Knee	0.005	—
Other extremities	0.001	0.0002–0.1
Dual x-ray absorptiometry (without CT)	0.001	0.001–0.035
Dual x-ray absorptiometry (with CT)	0.04	0.003–0.06
Intravenous urography	3	0.7–3.7
Upper gastrointestinal series	6 ^a	1.5–12
Small-bowel series	5	3.0–7.8
Barium enema	8 ^a	2.0–18.0
Endoscopic retrograde cholangiopancreatography	4.0	—

Abbreviation: CT, computed tomography.

^aIncludes fluoroscopy.

From Mettler FA Jr, Huda W, Yoshizumi TT, et al. Effective doses in radiology and diagnostic nuclear medicine: a catalog. *Radiology*. 2008;248:254–263, with permission.

It is not difficult to understand why CT scans involve relatively larger

effective doses because larger volumes of tissue are exposed to higher doses than with plain x-rays. Table 15.6 shows representative values and ranges of values for effective doses from various CT procedures, again taken from the literature and summarized by Mettler and colleagues in 2008.

Table 15.6 Adult Effective Doses for Various Computed Tomography Procedures

EXAMINATION	AVERAGE EFFECTIVE DOSE (mSv)	VALUES REPORTED IN LITERATURE (mSv)
Head	2	0.9–4.0
Neck	3	—
Chest	7	4.0–18.0
Chest for pulmonary embolism	15	13–40
Abdomen	8	3.5–25
Pelvis	6	3.3–10
Three-phase liver study	15	—
Spine	6	1.5–10

Coronary angiography	16	5.0–32
Calcium scoring	3	1.0–12
Virtual colonoscopy	10	4.0–13.2

From Mettler FA Jr, Huda W, Yoshizumi TT, et al. Effective doses in radiology and diagnostic nuclear medicine: a catalog. *Radiology*. 2008;248:254–263, with permission.

Pediatric CT scans are a special case. If the same parameters (kilovolt and milliampere) are used for babies and small children as for adults, much larger doses and effective doses are received by the pediatric cases. This was common practice until 2001, when it was pointed out that children are at least 10 times as sensitive as adults to radiation-induced cancer. As a consequence, a major effort has been made by pediatric radiologists to tailor the appropriate parameters to the size of the person being scanned. This has led to a substantial dose reduction in children receiving CT scans. All major radiologic societies now support the “Image Gently” campaign to reduce doses in diagnostic radiology and to eliminate unnecessary procedures.

Collective Effective Dose

Next to be considered is the effect of diagnostic radiology on the population as a whole, rather than on the individual. The relevant quantity here is the *collective effective dose*, which is the product of the effective dose and the number of persons exposed. It can give a very rough indication of the harm or detriment to an exposed population in terms of the number of radiation-induced cancers or heritable effects that may be expected to be produced.

There are two values of the collective effective dose that are of particular interest in diagnostic radiology, that to patients and that to health care workers. **First**, to patients; in 2006, the collective effective dose to the population of the United States from medical radiation was 899,000 person-Sv (National Council on Radiation Protection and Measurements [NCRP] Report 160), which is a 700% increase from the corresponding figure from the 1980s (NCRP Report 100). Some of this increase is caused by the 30% rise in the population over

about 25 years, but mostly, it is a result of the burgeoning application of CT, nuclear medicine, and interventional radiology and cardiology. Half of this total is caused by CT. [Figure 15.10](#) shows the percentage contribution of the various CT categories to the total collective effective dose from all CT procedures; it is no surprise that abdominal scans are the biggest contributor (58%).

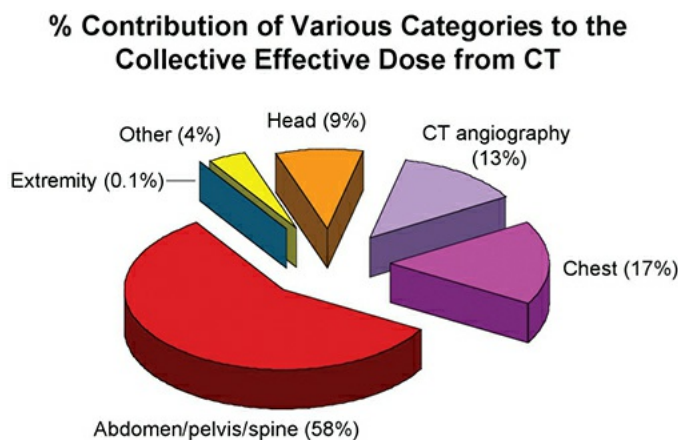


FIGURE 15.10 Percentage contribution of the various computed tomography (CT) categories to the total collective effective dose from CT. Note that abdominal and pelvic scans account for the largest contribution. (Data from National Council on Radiation Protection and Measurements. *Ionizing Radiation Exposure of the Population of the United States*. Bethesda, MD: National Council on Radiation Protection and Measurements; 2009. Report 160.)

It is interesting to calculate the *detriment* from this enormously large collective effective dose. Radiation detriment is a concept introduced by ICRP and used to quantify the harmful effects of radiation exposure to different parts of the body, taking into account the severity of the disease in terms of lethality, loss of quality of life, and years of life lost. Detriment includes a small component for heritable effects, a large component for fatal cancers, and an allowance for nonfatal cancers that, although they do not cause death, nevertheless affect quality of life. ICRP has suggested the detriment-adjusted risk coefficients for stochastic effects after exposure of the whole population to radiation at low dose rate to be 5.5% per sievert for cancer (fatal and nonlethal combined) and 0.2% per sievert for heritable effects, making a total of 5.7% per sievert. A collective effective dose of 899,000 person-Sv translates into 49,445 cases of cancer (fatal plus nonlethal), together with 1,798 cases of severe heritable effects resulting from 1 year's practice of radiology. This is almost certainly a gross overestimate because most radiologic procedures are performed late in life or during a terminal illness.

Second, occupational exposure. The total collective effective dose in the

United States in 2006 from occupational exposure to radiation was estimated to be 1,399 person-Sv. The two largest (and almost equal) contributors were medical and aviation workers, amounting to 77% of the total. However, the number of workers occupationally exposed in a medical setting is much greater than in the aviation industry so that the average effective dose to the person in aviation is 4 times larger than in medical.

INTERVENTIONAL RADIOLOGY AND CARDIOLOGY

Interventional radiology refers to any procedure in which the use or application of a medical device is fluoroscopically guided in the body and includes procedures that may be for diagnostic or therapeutic purposes. The past two decades have witnessed a major increase in such procedures in the United States. The collective effective dose has more than doubled in the past 10 years, making interventional radiology one of the fastest growing areas of medical radiation. These procedures include cardiac radiofrequency ablation, coronary artery angioplasty and stent placement, neuroembolization, and transjugular intrahepatic portosystemic shunt (TIPS) placement. Such procedures tend to be lengthy and involve fluoroscopy of a single area of the anatomy for a prolonged period—frequently for longer than 30 minutes and occasionally for over an hour. In addition, the need for multiple sequential treatment sessions can occur.

Procedures have evolved to include increasingly complex curative interventions that are associated with higher radiation exposures to both patients and health care workers. Angiography consists of inserting a catheter into a patient, guiding it along with the aid of fluoroscopy, and injecting contrast material into the vascular system. Stenosis, or blockage of one or more of these vessels, can lead to a myocardial infarction, but it can be visualized and treated with surgery or coronary angioplasty. Coronary angiography is a procedure that uses cineangiography in angulated projections, which can expose the operator to higher doses than when the x-ray equipment is used in the standard posteroanterior position.

Percutaneous transluminal coronary angioplasty is a therapeutic procedure to open blocked arteries by inflating a small balloon inside the artery, compressing and fracturing the obstruction, or using rotating blades to cut and remove the obstruction. It often requires the deployment of stents as well to maintain vessel patency. During conventional coronary angioplasty, prolonged fluoroscopy in severely angulated positions increases the dose to the operator and the patient. For coronary angioplasty, the overall potential radiation exposure to the

operators is medium to high. The usual arterial accesses are the femoral artery in the groin and the brachial artery in the shoulder. Large doses are also involved in the placement of TIPS. The clinical application of electrophysiology in cardiology is to study the electrical conduction pathways of the heart. In the cardiac catheterization laboratory, fluoroscopic control is used to position catheters in the heart to measure electrical activity and to map electrical conduction pathways. This technique is being used increasingly because abnormal conduction pathways, which may lead to life-threatening cardiac arrhythmias, can be controlled by ablation, now being performed using catheter-directed methods. Either a direct current or radiofrequency generator is used to produce a voltage of 20 or 30 V, which heats tissue to approximately 60° C for about 1 minute, destroying the abnormal electrical conduction pathways. These procedures usually require only posteroanterior fluoroscopy, although oblique or angulated views are also used. The successful treatment of some cardiac arrhythmias by radiofrequency ablation probably will increase the use of fluoroscopy for this type of therapy. Long fluoroscopic times and the occasional use of angulated views result in high-radiation exposures to workers during these procedures.

In addition, a large number of nonvascular interventional procedures using radiation are performed, such as the drainage of a blocked kidney or ablation of liver cancer.

Patient Doses and Effective Doses

Radiation doses received by patients from interventional radiology and cardiology are much higher than from general diagnostic radiology, so much so that there is a risk of tissue reactions (deterministic effects), such as early or late skin damage. During these procedures, typical fluoroscopic absorbed dose rates to the skin can range from 20 to more than 50 mGy per minute. There are reports in the literature of several dozen cases of skin damage following fluoroscopically guided interventional procedures. Also frequently reported are cases showing an acute phase involving erythema and deep ulceration, followed by a late phase involving telangiectasia, and/or hyperpigmentation. Less frequent and following more than 2 hours of fluoroscopy, erythema, desquamation, and later a moist ulcer with tissue necrosis have been reported, requiring a skin graft. [Table 15.7](#) is a compilation of the threshold dose levels and relative times at which effects in the skin are observed following a single acute radiation exposure.

Table 15.7 Potential Effects of Fluoroscopic Exposures on the Reaction of

the Skin

EFFECT	APPROXIMATE THRESHOLD DOSE, Gy	TIME OF ONSET
Early transient erythema	2	2–24 h
Main erythema reaction	6	~1.5 wk
Temporary epilation	3	~3 wk
Permanent epilation	7	~3 wk
Dry desquamation	14	~4 wk
Moist desquamation	18	~4 wk
Secondary ulceration	24	>6 wk
Late erythema	15	8–10 wk
Ischemic dermal necrosis	18	>10 wk
Dermal atrophy (first phase)	10	>12 wk

Dermal atrophy (second phase)	10	>52 wk
Telangiectasis	10	>52 wk
Delayed necrosis	12?	>52 wk (related to trauma)
Skin cancer	Not known	>15 y

Adapted from Wagner LK, Archer BR. *Minimizing Risks from Fluoroscopic X-rays*. 2nd ed. Houston, TX: Partners in Radiation Management; 1998, with permission, and modified by Hopewell (personal communication).

Serious injuries (tissue reactions) from fluoroscopically guided interventional procedures are rare relative to the number of procedures performed, but they still occur on an infrequent basis. Although early effects are of immediate concern, that is not to say that stochastic risks are absent. In 2006, the number of such procedures was estimated to be 16.7 million, with a corresponding collective effective dose of 128,394 person-Sv, slightly more than half of this coming from cardiac procedures. Table 15.8 shows typical effective doses from various interventional radiology procedures, collected by Mettler and colleagues in 2008. Long interventional procedures can result in effective doses of 5 to 70 mSv, with TIPS being perhaps the highest. Because the patients are, in general, older and suffering from life-threatening medical conditions, the possibility of radiation-induced cancer 10, 20, or 30 years down the road is largely academic. The immediate threat of deterministic effects, however, is very real and can affect quality of life in a serious way.

Table 15.8 Adult Effective Doses for Various Interventional Radiology Procedures

EXAMINATION	AVERAGE EFFECTIVE DOSE (mSv) ^a	VALUES REPORTED IN LITERATURE (mSv)

Head and/or neck angiography	5	0.8–19.6
Coronary angiography (diagnostic)	7	2.0–15.8
Coronary percutaneous transluminal angioplasty, stent placement, or radiofrequency ablation	15	6.9–57
Thoracic angiography of pulmonary artery or aorta	5	4.1–9.0
Abdominal angiography or aortography	12	4.0–48.0
Transjugular intrahepatic portosystemic shunt placement	70	20–180
Pelvic vein embolization	60	44–78

^aValues can vary markedly on the basis of the skill of the operator and the difficulty of the procedure.

From Mettler FA Jr, Huda W, Yoshizumi TT, et al. Effective doses in radiology and diagnostic nuclear medicine: a catalog. *Radiology*. 2008;248:254–263, with permission.

Dose to Personnel

Physicians involved in cardiology, angiography, and fluoroscopically guided interventional work routinely receive radiation doses higher than any other staff in a medical facility and comparable to doses received in the nuclear industry (Fig. 15.11 and Table 15.9). Frequently, doses received by interventional radiologists are close to the annual dose limits, and there is also evidence that ocular cataracts are not uncommon. This is principally because of prolonged

fluoroscopy.

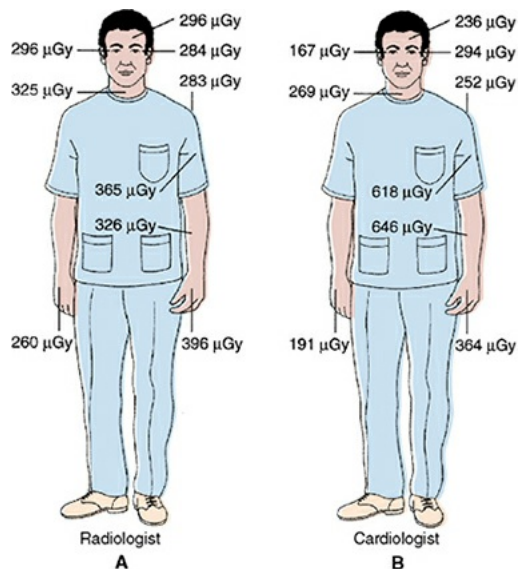


FIGURE 15.11 Graphic representation of the mean values of doses per procedure for a radiologist (A) and a cardiologist (B) engaged in an interventional procedure. The figures are the mean of measurements taken during more than 80 procedures. (Adapted from Vañó E, Gonzalez L, Guiberalde E, et al. Radiation exposure to medical staff in interventional and cardiac radiology. *Br J Radiol.* 1998;71:954–960, with permission.)

Table 15.9 Estimated Dose to Staff during Typical Cardiac Studies

CATEGORY OF STAFF	ONE CATHETERIZATION, mSv				ONE ANGIOPLASTY, mSv				ONE PACEMAKER mSv			
	WEIGHTED SURFACE DOSE, NO APRON		WEIGHTED SURFACE DOSE, NO APRON		WEIGHTED SURFACE DOSE, NO APRON		WEIGHTED SURFACE DOSE, NO APRON		WEIGHTED SURFACE DOSE, NO APRON		WEIGHTED SURFACE DOSE, NO APRON	
	HANDS	EYES										
Cardiologist	1.6	0.09	2.1	0.6	3.1	0.2	4.2	1.0	0.14	—	0.01	—
Cardiologist who stands back during cine	0.3	0.01	0.3	0.2	1.5	0.1	1.9	0.7	—	—	—	—

Technologist	0.08	<0.01	0.09	0.02	0.2	0.01	0.2	0.05	0.01	<0.01
Technologist who stands back during cine	0.04	<0.01	—	0.04	0.01	0.1	0.01	0.1	0.03	—
Nurse or 0.3 anesthetist	or 0.3	0.02	0.4	0.2	0.8	0.06	0.9	0.5	0.04	<0.01

Adapted from National Council on Radiation Protection and Measurements. *Implementation of the Principle of As Low As Reasonably Achievable (ALARA) for Medical and Dental Personnel*. Bethesda, MD: National Council on Radiation Protection and Measurements; 1990. Report 107, with permission.

NUCLEAR MEDICINE

Nuclear medicine is the medical specialty in which unsealed radionuclides, chemically manipulated to form radiopharmaceuticals, are used for diagnosis and therapy. Radiopharmaceuticals localize in various target tissues and organs, and although nuclear medicine images have less spatial and anatomic resolution than do radiographic or magnetic resonance images, they are better able to display physiology and metabolism.

Historical Perspective

The first person to suggest using radioactive isotopes to label compounds in biology and medicine was the Hungarian chemist Georg von Hevesy, whose work, beginning before World War II, earned him a Nobel Prize in 1943 (Fig. 15.12). The concept of using radioactive tracers in medicine could not be exploited until the means to produce artificial isotopes were readily available. The cyclotron was invented and developed by Ernest Lawrence in the 1930s, also leading to a Nobel Prize, and devices of this type have been used to produce short-lived isotopes and positron emitters (Fig. 15.13). Nuclear reactors were developed during World War II and are used to produce most medically used radioactive isotopes, all of which are electron or γ -ray emitters.



FIGURE 15.12 The great Hungarian chemist Georg von Hevesy (1885–1966), whose work, beginning before World War II, earned him a Nobel Prize in 1943. He was the first to conceive of using radioactive isotopes to label compounds for biology and medicine. (Courtesy of the University of California Lawrence Berkeley Laboratory.)

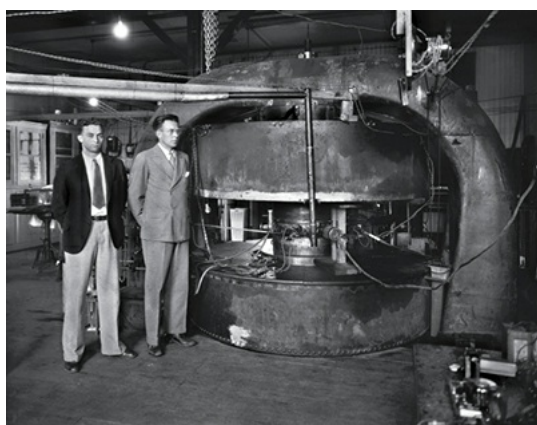


FIGURE 15.13 The concept of using radioactive isotopes as tracers in medicine was not fully explored until the invention of the cyclotron in 1931. Its inventor, Ernest O. Lawrence, is seen here (**right**) with his second cyclotron in 1934. Many short-lived isotopes that are positron emitters are made with a device of this sort. (Science History Images/Alamy Stock Photo.)

For the reasons mentioned earlier, nuclear medicine was a late starter compared with radiation therapy and x-ray diagnosis. Radiopharmaceuticals of adequate quality and consistency were not available until 1946, but since then, nuclear medicine has grown into a specialty in its own right and is now one of the most rapidly growing areas of radiation medicine largely because of nuclear cardiology. A broad array of pharmaceuticals, coupled with the development of sophisticated hardware, has made possible a widening diversity of applications.

Positron emission tomography (PET) scanning has opened up a whole new area of rapid growth that is discussed later in this chapter.

Most nuclear medicine procedures are diagnostic examinations. Therapeutic nuclear medicine procedures represent only 1% to 2% of all radionuclide use, involving principally the treatment of hyperthyroidism, thyroid cancer, and bone metastases. Because of the high doses involved in therapy, the quantity “effective dose” is not appropriate to use for these procedures, and the therapeutic use of radionuclides will be discussed separately later in this chapter.

Effective Dose and Collective Effective Dose

The NCRP estimated that, in 2006, there were 19.7 million nuclear medicine procedures performed in the United States, with more than three-quarters of these procedures being performed in patients older than 45 years. The resulting collective effective dose was 22,000 person-Sv, up about 600% from the 1980s. [Figure 15.14](#) shows the distribution of collective effective dose from nuclear medicine procedures, with nuclear cardiology accounting for 85% of the total. According to the 2008 UNSCEAR report, although the United States represents 5% of the world population, it receives 50% of the world’s nuclear medicine procedures—a staggering figure. These estimates from NCRP involve patients but do not include the many thousands of research procedures that use radionuclides because such data is hard to come by.

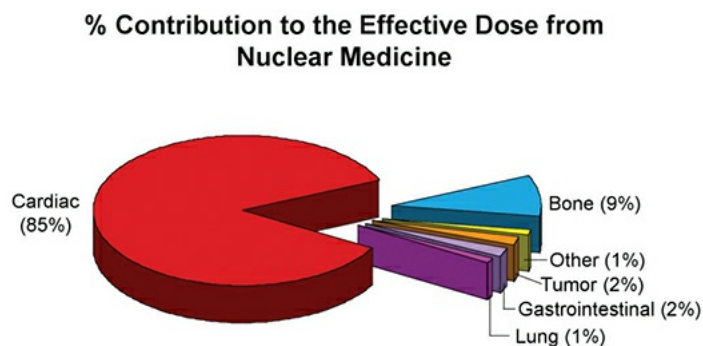


FIGURE 15.14 Percentage contributions of the various subcategories of nuclear medicine procedures to the total collective effective dose (220,500 person-Sv) from nuclear medicine. Cardiac procedures dominate the picture. (Data from National Council on Radiation Protection and Measurements. *Ionizing Radiation Exposure of the Population of the United States*. Bethesda, MD: National Council on Radiation Protection and Measurements; 2009. Report 160.)

[Table 15.10](#) shows representative effective doses from nuclear medicine procedures, collected from the literature by Mettler and colleagues in 2008. Some figures are as high as 40 mSv for a single procedure.

Table 15.10 Effective Doses for Adults from Various Nuclear Medicine Examinations

EXAMINATION	EFFECTIVE DOSE (mSv)	ADMINISTERED ACTIVITY (MBq)	EFFECTIVE DOSE (mSv/MBq) ^a
Brain (^{99m} Tc-HMPAO-exametazime)	6.9	740	0.0093
Brain (^{99m} Tc-ECD-Neurolite)	5.7	740	0.0077
Brain (¹⁸ F-FDG)	14.1	740	0.019
Thyroid scan (sodium iodine-123)	1.9	25	0.075 (15% uptake)
Thyroid scan (^{99m} Tc-pertechnetate)	4.8	370	0.013
Parathyroid scan (^{99m} Tc-sestamibi)	6.7	740	0.009
Cardiac stress-rest test (thallium-201 chloride)	40.7	185	0.22
Cardiac rest-stress test (^{99m} Tc-sestamibi 1-day)	9.4	1100	0.0085 (0.0079 stress, 0.0090)

protocol)				rest)
Cardiac rest-stress test (^{99m} Tc-sestamibi protocol)	12.8 2-day	1500	0.0085 stress, rest)	(0.0079 0.0090
Cardiac rest-stress test (Tc- tetrofosmin)	11.4	1500	0.0076	
Cardiac ventriculography (^{99m} Tc-labeled red blood cells)	7.8	1110	0.007	
Cardiac (¹⁸ F-FDG)	14.1	740	0.019	
Lung perfusion (^{99m} Tc-MAA)	2.0	185	0.011	
Lung ventilation (xenon-133)	0.5	740	0.00074	
Lung ventilation (^{99m} Tc-DTPA)	0.2	1300 (40 inhaled)	0.0049	actually 0.0049
Liver-spleen (^{99m} Tc-sulfur colloid)	2.1	222	0.0094	
Biliary tract (^{99m} Tc-	3.1	185	0.017	

disofenin)			
Gastrointestinal bleeding (^{99m} Tc-labeled red blood cells)	7.8	1110	0.007
Gastrointestinal emptying (^{99m} Tc-labeled solids)	0.4	14.8	0.024
Renal (^{99m} Tc-DTPA)	1.8	370	0.0049
Renal (^{99m} Tc-MAG3)	2.6	370	0.007
Renal (^{99m} Tc-DMSA)	3.3	370	0.0088
Renal (^{99m} Tc-glucoheptonate)	2.0	370	0.0054
Bone (^{99m} Tc-MDP)	6.3	1110	0.0057
Gallium-67 citrate	15	150	0.100
Pentreotide (¹¹¹ In)	12	222	0.054
White blood cells (^{99m} Tc)	8.1	740	0.011

White blood cells (^{111}In)	6.7	18.5	0.360
Tumor (^{11}F -FDG)	14.1	740	0.019

Abbreviations: $^{99\text{m}}\text{Tc}$, technetium-99m; HMPAO, hexamethylpropyleneamine oxime; ECD, ethyl cysteinate dimer; ^{18}F , fluorine-18; FDG, fluorodeoxyglucose; MAA, macroaggregated albumin; DTPA, diethylenetriaminepentaacetic acid; MAG3, mercaptoacetyltriglycine; DMSA, dimercaptosuccinic acid; MDP, methylene diphosphonate; ^{111}In , indium-111; ^{11}F , fluorine-11.

^aRecommended ranges vary, although most laboratories tend to use the upper end of suggested ranges.

From Mettler FA Jr, Huda W, Yoshizumi TT, et al. Effective doses in radiology and diagnostic nuclear medicine: a catalog. *Radiology*. 2008;248:254–263, with permission.

The dramatic increase in the use of nuclear medicine (and the concomitant rise in the collective effective dose) is driven largely by cardiology. Numerous reviews have appeared in recent years attempting to document this trend. One such review (Bedetti et al., 2008) drew attention to the fact that many cardiac patients undergo as many as 36 or more examinations, with a median effective dose of more than 60 mSv. Of course, most of these patients are elderly and have a life-threatening illness so that the risk of radiation-induced cancer 20 years down the road is largely academic. Fazel et al. (2009) performed a huge study of “nonelderly adults” and concluded that approximately 4 million Americans every year are subject to procedures that result in cumulative effective doses that exceed 20 mSv.

Principles in Nuclear Medicine

A wide range of radionuclides are used in diagnostic nuclear medicine that meets the necessary requirements for effective and efficient imaging. All are produced artificially, using four principal routes of manufacture: (1) cyclotron bombardment (producing, e.g., gallium-67, indium-111, thallium-201, cobalt-57, iodine-123, carbon-11, oxygen-15, nitrogen-13, and fluorine-18), (2) reactor irradiation (e.g., chromium-51, selenium-75, iron-59, cobalt-58, iodine-125, and iodine-131), (3) fission products (e.g., iodine-131, xenon-133, and strontium-90), and (4) generators that provide secondary decay products from longer lived

parent radionuclides. The most common example of the latter is the column generator incorporating molybdenum-99 for the provision of technetium-99m, which, because of its highly suitable physical characteristics for a wide range of applications, forms the basis for more than 80% of the radiopharmaceuticals used in nuclear medicine. Most technetium-99m generators use fission-produced molybdenum-99, although techniques of neutron irradiation could provide a viable alternative source of this important parent radionuclide. Other generators include those incorporating tin-113 (for the provision of indium-113m), rubidium-81 (for krypton-81m), and germanium-68 (for gallium-68).

The use of radiopharmaceuticals for diagnosis or therapy is based on the accumulation or concentration of the isotope in the organ of interest, referred to as the *target organ*. A radiopharmaceutical may have an affinity for a certain organ that is not necessarily the organ of interest, in which case this organ is termed a *critical organ*. Often, the dose to a critical organ limits the amount of radioisotope that may be administered. The risk to which the patient is subjected is clearly a function of the doses received in all organs and is expressed in terms of the *effective dose*. The risk must be balanced against the expected advantages and benefits rendered by the procedure.

In addition to conventional planar imaging, techniques have also been developed to allow emission tomography that, like x-ray CT, can demonstrate internal structures or functional information from cross-sectional slices of the patient. Two basic modalities have evolved. First, there is **single photon emission computed tomography (SPECT)**. This uses conventional γ -emitting radiopharmaceuticals and is often performed in combination with planar imaging. SPECT imaging requires a scanning system incorporating a circular array of detectors or, more often, a rotating γ -camera system with up to four detector heads. The second modality is the more specialized technique of PET. This is based on the simultaneous detection of the pairs of photons (511 keV) arising from positron annihilation and mostly uses the short-lived biologically active radionuclides oxygen-15, carbon-11, fluorine-18, and nitrogen-13. Dedicated PET scanners use a circular array of detectors, and PET scanning is now usually performed in conjunction with a CT scan so that the PET images, displaying information about metabolic and physiologic function, can be fused with the CT images that depict anatomy.

In general, there are three doses of interest after the administration of a given amount of a radiopharmaceutical:

1. *Effective dose*, because this determines the risk of stochastic effects (cancer

and heritable effects)

2. Dose to the target organ

3. Dose to the critical organ, because this may be many times larger than the total body dose, and it is known that certain tissues are particularly susceptible to radiation-induced cancer

Positron Emission Tomography

The important and unique feature of PET studies is that they document physiologic abnormalities, or changes in metabolism, rather than simply alterations in anatomy.

The principle of PET imaging is that the scanner locates the tracer by detecting the collinear pairs of 0.511-MeV photons emitted if a positron annihilates after uniting with an electron. A positron is a particle with the same mass and magnitude of charge as an electron except that the charge is positive. A positron cannot exist at rest if it has lost all its kinetic energy; it is electrostatically attracted to an electron with which it annihilates to produce two antiparallel 0.511-MeV photons. Radionuclides that emit positrons have excesses of protons in their nuclei and are produced by bombarding stable elements in a cyclotron. Positron emitters do not occur in nature.

Examples of radionuclides used for PET imaging include oxygen-15, nitrogen-13, carbon-11, and fluorine-18; these radionuclides have short half-lives of 2, 10, 20, and 110 minutes, respectively, so that the PET facility is frequently close to the cyclotron that produces the radionuclides. **Table 15.11** summarizes the most commonly used radiopharmaceuticals and the types of studies that are performed with them.

Table 15.11 Radiopharmaceuticals Used in Clinical Positron Emission Tomography Studies

RADIONUCLIDE COMPOUND	AND	TYPES OF STUDY PERFORMED
^{15}O		

Carbon dioxide	Cerebral blood flow
Oxygen	Quantification of myocardial oxygen consumption and oxygen extraction fraction, measurement of tumor necrosis
Water	Quantification of myocardial oxygen consumption and oxygen extraction fraction, tracer for myocardial blood perfusion
¹³ N	
Ammonia	Myocardial blood flow
¹¹ C	
Acetate	Oxidative metabolism
Carfentanil	Opiate receptors in the brain
Cocaine	Identification and characterization of drug binding sites in the brain
Deprenyl	Distribution of monoamine oxidase (MAO) type B, the isoenzyme that catabolizes dopamine
Leucine	Amino acid uptake and protein synthesis, providing an

	indicator of tumor viability
Methionine	Amino acid uptake and protein synthesis, providing an indicator of tumor viability
N-methylspiperone	Neurochemical effects of various substances on dopaminergic function
Raclopride	Function of dopaminergic synapses
¹¹ F	
Haloperidol	Binding sites of haloperidol, a widely used antipsychotic and anxiety-reducing drug
Fluorine ion	Clinical bone scanning
Fluorodeoxyglucose (FDG)	Neurology, cardiology, and oncology to study glucose metabolism
Fluorodopa	Metabolism, neurotransmission, and cell processes
Fluoroethylspiperone	Metabolism, neurotransmission, and cell processes
Fluorouracil	Delivery of chemotherapeutic agents in the treatment of cancer

^{82}Rb

82Rb

Myocardial perfusion

From UNSCEAR, 2008.

The most widely administered positron-emitting radionuclide is fluorine-18, which is used for the production of [^{18}F]-2-deoxy-2-fluoro-D-glucose, usually referred to as FDG. This material, used routinely in clinical care, highlights areas of metabolism and therefore can be used to detect the metastatic spread of cancer. [^{18}F]-FDG has also found a use in the early diagnosis of Alzheimer disease through the direct visualization of amyloid plaques in the brain. Better imaging agents are available for this purpose, but they are based on carbon-11 which, because of its 20-minute half-life, cannot be used as widely as [^{18}F]-FDG with its longer (2-hour) half-life. Other metabolic radiopharmaceuticals are rapidly finding a place in clinical practice—for example, [^{18}F]-fluorothymidine (FLT) to map areas of rapid cell proliferation within tumors, or compounds such as [^{18}F]-fluoromisonidazole (FMISO), [^{18}F]-fluoroazomycin arabinoside (FAZA), or 64-Cu-diacetyl-bis (N4-methylthiosemicarbazone) (64-Cu-ATSM) to highlight areas in tumors that are hypoxic. Many of the other positron-emitting radionuclides are used for the production of experimental compounds used in research studies. For example, oxygen-15 is used to label water for blood flow studies. In addition, there are more than a dozen radiopharmaceuticals labeled with carbon-11 that are used in brain research.

The doses delivered to patients or research subjects in PET studies are relatively low because of the short half-lives of the radionuclides, even though the administered amounts of radioactivity are high to allow rapid and detailed imaging. [Table 15.12](#) shows organ doses as well as effective doses for studies with [^{18}F]-FDG, for [^{15}O]-H₂O and for [13-N] ammonia.

Table 15.12 Organ Doses and Effective Doses in Adults for Positron Emission Tomography Compounds

ABSORBED DOSE PER UNIT ACTIVITY ADMINISTERED

Organ	$[^{18}\text{F}]\text{-FDG}$ $\text{mGy/MBq} \times 10^{-2}$	$[^{15}\text{O}]\text{-H}_2\text{O}$ $\text{mGy/MBq} \times 10^{-3}$	$[^{13}\text{N}]$ Ammonia $\text{mGy/MBq} \times 10^{-3}$
Brain	3.8	1.3	4.2
Heart	6.7	1.9	2.1
Kidneys	1.7	1.7	4.6
Ovaries	1.4	0.85	1.7
Red marrow	1.1	0.89	1.7
Spleen	1.1	1.6	2.5
Testes	1.1	0.74	1.8
Thyroid	1.0	1.5	1.7
Bladder	1.3	0.26	8.1
	$\text{mSv/MBq} \times 10^{-2}$	$\text{mSv/MBq} \times 10^{-3}$	$\text{mSv/MBq} \times 10^{-3}$

Effective dose	1.9	1.1	2.0
----------------	-----	-----	-----

Abbreviation: FDG, fluorodeoxyglucose.

Data from the Task Group on Absorbed Dose to Patients from Radiopharmaceuticals; Publication 17 (ICRP, 1971); Publication 53 (ICRP, 1987); and Publication 106 (ICRP, 2007).

PET technologists often have higher radiation exposures than other workers in nuclear medicine, and pharmacists at cyclotron facilities have even higher exposures, especially to their hands. This is a function of two factors: (1) the relatively high energy, and therefore penetrating nature, of the photons emitted by the radionuclides used (0.511 MeV), and (2) because of the short half-lives of the commonly used positron-emitting radionuclides, the large initial activities must be prepared so that a sufficient amount is left by the time the patient is imaged (this is especially true for oxygen-15, which has a half-life of only 2 minutes).

The Therapeutic Use of Radionuclides

The most common form of nuclear medicine therapy is the use of radioactive iodine-131 for the treatment of hyperthyroidism. A therapeutic treatment with iodine-131 involves an absorbed dose to the thyroid gland that varies with the person and is very nonuniform within the tissue itself but is on the order of many tens of grays. In addition, there is a total body dose of typically 70 to 150 mGy, which results from the isotope circulating in the blood. Because radiation is known to be a potent carcinogen, the risk of leukemia or of thyroid cancer following iodine-131 therapy has been appreciated from the outset, but quite large studies have failed to show an excess. Pregnancy is, of course, a contraindication to the treatment of hyperthyroidism with iodine-131. Treatment of fertile women should be preceded by the taking of a careful history and a pregnancy test. Treatment should be delayed, if possible, to eliminate the potential effects during pregnancy.

The second most common form of therapy with unsealed radionuclides is the treatment of thyroid cancer. Following complete surgical removal of the cancer and the thyroid gland, radioiodine may be given to destroy any residual iodine-accumulating cancer cells that had spread to lymph nodes, lungs, or bone. Such treatments involve large doses of iodine-131 that may result in a total body dose of 0.5 to 1.0 Gy, which is sufficient to cause severe depression of the bone marrow.

The therapy of bone metastases. Several cancers, including prostate and breast, have a predilection for diffuse spread throughout the skeleton. There are several radiopharmaceuticals (such as strontium-89 chloride) that will localize in the metastatic lesions to provide palliation (but not cure).

Polycythemia vera is a relatively rare disease that is characterized by overproduction of red and white blood cells by the bone marrow. Phosphate-32 is given intravenously, which localizes in the bone so that the γ -rays emitted result in a mild bone marrow suppression and reduction in the production of many blood elements.

Radioimmunotherapy uses radiolabeled antibodies directed against specific antigens. These agents can be used for the treatment of chemotherapy-resistant lymphomas. The antibodies are most commonly labeled with iodine-131 or yttrium-90 and injected intravenously in relatively large activities.

MEDICAL IRRADIATION OF CHILDREN AND PREGNANT WOMEN

Irradiation of Children

The hazards associated with medical radiation in children are basically the same as in adults—namely, cancer and heritable effects—except that the risks associated with a given absorbed dose of radiation are higher because of an increased sensitivity in younger persons. There is good evidence for this. The Japanese survivors of the atomic bomb attacks represent the most carefully studied human population exposed to radiation. There is a marked change in sensitivity to radiation-induced malignancies with increasing age, with young children being more radiosensitive than older adults by a factor of 10 to 15 ([Chapter 10](#)). Concern for possible heritable effects induced by radiation is likewise greater in children because they have their entire reproductive lives ahead of them.

In pediatric nuclear medicine, as in pediatric radiology, the general principle is that radiation exposures should be kept at the lowest practical level. In each case, the expected benefit should exceed the risk. Physicians and patients alike are much more cautious about nuclear medicine procedures in children than about diagnostic x-rays, even if the dose levels are similar.

[Table 15.13](#) compares the effective dose in children of various ages with adults for various diagnostic nuclear medicine procedures. In general, effective doses are larger in young children for the same procedure, even if the

administered activity is adjusted for body weight.

Table 15.13 Typical Effective Doses to Pediatric Patients from Diagnostic Nuclear Medicine Procedures

RADIOPHARMACEUTICAL MBq	ACTIVITY FOR ADULT PATIENT, MBq	ADULT 70 kg [1.0]	EFFECTIVE DOSE PER PROCEDURE BY PATIENT AGE ^a (mSv)				
			15-YEAR-OLD [0.9]	10-YEAR-OLD [0.69]	5-YEAR-OLD [0.44]	1-YEAR-OLD [0.27]	
99mTc-MAG3 (normal renal function)	100	0.7	0.8	0.7	0.6	6.0	
99mTc-MAG3 (abnormal renal function)	100	0.6	0.7	0.7	0.5	0.5	
99mTc-DTPA (normal renal function)	300	1.6	1.8	2.1	1.8	2.2	
99mTc-DTPA (abnormal renal function)	300	1.4	1.6	1.9	1.8	2.0	
99mTc-DMSA (normal renal function)	80	0.7	0.7	0.8	0.8	0.8	

^{99m}Tc -pertechnetate (no thyroid block)	80		1.0	1.2	1.3	1.4	1.4
^{99m}Tc -IDA (normal biliary function)	150		2.3	2.4	2.9	3.0	3.7
^{99m}Tc -HMPAO	500		4.7	5.0	5.9	5.7	6.5
^{99m}Tc -leukocytes	200		2.2	2.7	3.0	2.9	3.4
^{99m}Tc -erythrocytes	800		5.3	6.0	6.6	6.7	7.6
^{99m}Tc -phosphates	600		3.6	3.7	4.1	4.2	4.9
^{99m}Tc -MIBI (resting)	400		3.3	4.0	4.4	4.8	5.4
^{201}Tl -chloride	80	20	30	129	95	86	
^{125}I -iodide (55% thyroid uptake)	20		7.2	10.2	12.1	16.3	18.8
^{125}I -iodide (total thyroid block)	20		0.2	0.3	0.3	0.3	0.3
^{125}I -MIBG (no impurity)	400		5.6	6.5	9.1	8.8	10.1

⁶⁷ Ga-citrate	150	15	18.9	22.8	23.1	27.9
--------------------------	-----	----	------	------	------	------

Abbreviations: ^{99m}Tc, technetium-99m; MAG3, mercaptoacetyltriglycine; DTPA, diethylenetriaminepentaacetic acid; DMSA, dimercaptosuccinic acid; IDA; iminodiacetic acid; HMPAO, hexamethylpropyleneamine oxime; MIBI, methoxy-isobutyl-isonitrile; ²⁰¹Tl, thallium-201; ¹²⁵I, iodine-125; MIBG, metaiodobenzylguanidine; ⁶⁷Ga, gallium-67.

^aFigures in brackets are scaling factors for activity based on body weights shown. Doses are calculated using age-specific coefficients.

Based on UNSCEAR, 2000.

The implication of the review of carcinogenesis and heritable effects on humans ([Chapters 10 and 11](#)) is that any amount of radiation, no matter how small, has a deleterious effect. This conclusion is based on the assumption of a linear, nonthreshold, dose-effect model that has been adopted by most standard-setting bodies as the most conservative basis for risk estimates. This philosophy requires that the physicians have some reasonable indications that the potential gain for the patient from the use of a procedure in nuclear medicine exceeds the risks.

Irradiation of Pregnant Women

The risks involved in exposure to radiation of the embryo or fetus are discussed in detail in [Chapter 12](#). They may be summarized as follows:

1. For the first 10 days following conception (i.e., during preimplantation), the most significant effect of radiation may be to kill the embryo, leading to resorption.
2. Between 10 days and 8 weeks postconception (i.e., during organogenesis), the risks include congenital malformations and small head size as well as carcinogenesis.
3. Between 8 and 15 weeks, and to a lesser extent 15 to 25 weeks, the risks include mental retardation as well as small head size and carcinogenesis.
4. Beyond 25 weeks, the only risk of externally delivered diagnostic radiation is carcinogenesis, which is much reduced, compared with the risk during the first trimester.

Radiation-induced carcinogenesis is considered a stochastic effect; that is, there is no threshold and the risk increases with dose. One obstetric examination

involving a few films may increase the relative risk of leukemia and childhood cancer by about 40%; however, because malignancies are relatively rare in children, the absolute risk is small. The other serious effects, such as mental retardation and congenital malformations, are considered tissue reactions; that is, there is a dose threshold of about 0.3 Gy. It is against the background of these possible risks that the irradiation of the pregnant or potentially pregnant woman must be considered.

Some radiologists instruct their technologists to ask all female patients about possible pregnancy before these women have abdominal or pelvic radiographic examinations. This would appear to be prudent and expedient. Indeed, if time permits, a pregnancy test might be desirable. If a woman requires an emergency radiologic examination, however, there should be no hesitation to do the study. The health of the woman is of primary importance, and if serious injury or illness is suspected, this takes priority in determining the need for a study. The risk to a possible conceptus must be weighed against the risks of not performing the examination.

The NCRP in 1977 recommended for pregnant women that if, in the best judgment of the attending physician, a diagnostic examination or nuclear medicine procedure at that time is deemed advisable to the medical well-being of the patient, it should be carried out without delay, with special efforts being made, however, to minimize the dose received by the lower abdomen (uterus).

In the case of nonemergency examinations, it sometimes may be prudent to consider delaying the proposed procedure. The physician contemplating the delay of a study on a woman early in pregnancy should consider the consequences in view of the possibility that the diagnostic examination might become necessary later in the pregnancy, when the risks are much greater. For example, during the first 10 days postconception, the risk is the possible resorption of the embryo. If the study is delayed, however, but becomes essential during the 8th through the 15th week, the risks include small head size and carcinogenesis; in addition, this is the peak of sensitivity to mental retardation. Delay compounds the problem. Conversely, if the patient is already in this peak period of radiosensitivity when a procedure is contemplated, then a delay until after the 25th week would be an advantage because radiation risks during this period may be at their smallest.

DOSES TO THE EMBRYO AND FETUS

The effects of radionuclides on the developing embryo or fetus have not been

studied as extensively as the consequences of externally administered x-rays. The biologic effects may depend on many factors, including the chemical form of the isotope, the type and energy of the radiation emitted whether the compounds containing the radioactivity cross the placenta, and whether they tend to be concentrated in specific target organs.

The metabolism of the radiopharmaceutical may cause high concentrations of the radionuclide in organs of a conceptus if the material crosses the placenta. This may result in dysfunctioning fetal organs. The classic example of this effect involves the uptake of iodine-131 in the thyroid of the developing embryo and fetus. Up to about 12 weeks, the fetal thyroid does not take up iodine. After this time, iodine concentrates in the fetal thyroid in amounts considerably greater than those in the maternal thyroid (Table 15.14). Several cases from the 1950s through the 1980s have documented the induction of hypothyroidism and cretinism from doses of iodine-131 to the fetal thyroid.

Table 15.14 Thyroidal Radioiodine Dose to the Fetus

GESTATION PERIOD	FETAL/MATERNAL RATIO (THYROID GLAND)	DOSE TO FETAL THYROID, rad/ μ Ci ^a
10–12 wk	—	0.001 (precursors)
12–13 wk	1.2	0.7
Second trimester	1.8	6
Third trimester	7.5	—
Birth imminent	—	8

^aRad/ μ Ci of iodine-131 ingested by mother.

Courtesy of Dr. J. Keriakes, unpublished data.

Although pregnant women receive diagnostic x-rays occasionally, it is rare for them to be given radioactive isotopes. In general, physicians and patients alike are much more wary about nuclear medicine procedures than about diagnostic x-rays, even if dose levels may be similar. Never is this truer than in the case of pregnant or potentially pregnant women.

RECOMMENDATIONS ON BREASTFEEDING INTERRUPTIONS

Because many radiopharmaceuticals are secreted in breast milk, it is safest to assume that, unless there are data to the contrary, some radioactive compound will be found in breast milk when a radiopharmaceutical is administered to a lactating female. Consideration should be given to postponing the procedure. If the procedure is performed, the child should not be breastfed until the radiopharmaceutical is no longer secreted in an amount estimated to give an effective dose to the child of no more than 1 mSv. ICRP Publication 106 lists commonly used radiopharmaceuticals where no interruption in breastfeeding is necessary, and those where delays of 12 hours to 3 weeks are recommended.

SUMMARY

The three principal contributors to the collective effective dose from medical radiation are (1) CT scans, (2) nuclear medicine (including nuclear cardiology), and (3) interventional radiology and cardiology. This is illustrated in [Figure 15.15](#). The countless millions of conventional radiographs, including chest x-rays and mammography, account for no more than 10% of the total collective effective dose.

Contributions to the Effective Dose from Radiology

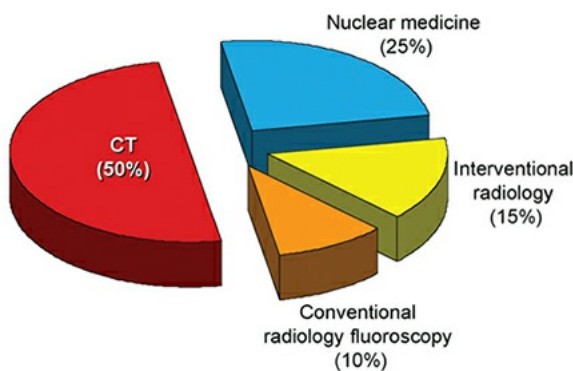


FIGURE 15.15 Contributions to the total collective effective dose from the medical uses of radiation (899,000 person-Sv). The biggest contributions come from computed tomography (CT), nuclear medicine, and interventional procedures, in that order. The millions of conventional procedures (mammograms, chest x-rays, etc.) account for only 10% of the total. (Data from National Council on Radiation Protection and Measurements. *Ionizing Radiation Exposure of the Population of the United States*. Bethesda, MD: National Council on Radiation Protection and Measurements; 2009. Report 160.)

SUMMARY OF PERTINENT CONCLUSIONS

Everyone is exposed to radiation from unperturbed natural sources, enhanced natural sources, and sources resulting from human activity, including medical x-rays.

Natural background radiation comes from cosmic rays, terrestrial radiation from the earth's crust, and inhaled or ingested radioactivity.

Cosmic ray levels vary with altitude and latitude.

Terrestrial radiation levels vary widely with locality.

Radon and its progeny result in irradiation of lung tissue with γ -particles; this is the largest source of natural radiation.

Medical radiation is by far the largest source of radiation resulting from human activities.

By the year 2006, the collective effective dose to the US population from medical radiation had increased by about 700% from the 1980s and now approximately equals that from natural background radiation.

The radiation doses involved in diagnostic radiology, except for interventional procedures, do not result in tissue reactions (deterministic effects); the risks are stochastic effects (i.e., carcinogenesis and heritable effects).

Computed Tomography

The use of CT has increased dramatically in the past 35 years.

By 2010, the number of CT scans in the United States reached 85 million per year, with about 10% of these in children. There was a small reduction in the number of scans performed for a few years, but by 2015, the number started to rise again. There is a wide variation in the number of scanners per million people between countries with different health care systems, with Japan

having by far the most.

CT scans involve relatively large effective doses because larger volumes of tissue are exposed to higher doses than with common x-rays. The effective dose varies from about 2 mSv for a head scan to about 15 mSv for chest or abdomen. Values vary significantly for different scanners and for the same make scanner in different departments.

Effective doses from CT scans are larger in small children than in adults, unless care is taken to adjust for kilovolt and milliamperes.

Effective Dose and Cancer

The cancer risk to a person is expressed in terms of the effective dose, the equivalent dose to the various organs and tissues exposed, multiplied by the appropriate W_T.

The collective effective dose is the product of the effective dose and the number of persons exposed. It gives an indication of the harm or “detriment” to an exposed population.

The collective effective dose to the US population in 2006 from medical radiation was estimated by NCRP to be 899,000 person-Sv, a 700% increase from the previous comprehensive survey conducted in the 1980s.

The “detriment” from medical radiation may be calculated from the collective effective dose and the risk estimate of 5.5% per sievert for cancer (fatal and nonfatal) and 0.2% per sievert for serious heritable effects.

Detriment includes an allowance for loss of quality of life as well as for death.

The use of medical radiation for 1 year in the United States may benefit more than half of the population but may result in about 50,000 cases of cancer (fatal plus nonfatal) and about 1,798 cases of serious heritable effects.

Interventional Procedures

The past two decades have witnessed a major increase in high-dose fluoroscopically guided interventional procedures in medicine. Interventional radiology and cardiology now represent one of the three fastest growing areas of radiation medicine (together with CT and nuclear medicine).

Radiation doses to patients from interventional radiology and cardiology are, in general, much higher than from general diagnostic radiology.

NCRP estimated that, in 2006, there were 16.7 million interventional procedures performed in the United States, with a corresponding collective effective dose of 128,394 person-Sv.

Long interventional procedures can result in effective doses to the individual of 5 to 70 mSv, with TIPS being one of the largest.

Because patients undergoing interventional procedures are, in general, older and/or with life-threatening illnesses, the possibility of radiation-induced malignancy 20 years down the road is largely academic. By contrast, doses are occasionally so high that tissue reactions can be an immediate problem.

There are reports in the literature of serious skin damage resulting from fluoroscopically guided interventional procedures, including erythema, deep ulceration, and occasionally necrosis requiring a skin graft. The number of such cases is very small compared with the number of procedures performed, but they do occur occasionally.

Doses to personnel involved in interventional procedures are among the highest recorded routinely in medical centers, and there is evidence that radiation-induced cataracts are not uncommon.

Nuclear Medicine

Nuclear medicine is the medical specialty in which unsealed radionuclides, chemically manipulated to form radiopharmaceuticals, are used for diagnosis and therapy.

Most nuclear medicine procedures are diagnostic examinations. Therapeutic procedures account for only about 1% to 2%.

NCRP estimated that, in 2006, there were 19.7 million nuclear medicine procedures performed in the United States, three-quarters of them in persons older than 45 years. This resulted in a collective effective dose of 22,000 person-Sv, an increase of about 600% from the 1980s, with cardiology accounting for much of this trend.

UNSCEAR estimated that, with 5% of the world population, the United States was responsible for 50% of the nuclear medicine procedures performed in the world.

Cardiac patients frequently undergo as many as 36 examinations, with a median effective dose of greater than 60 mSv.

In a 2009 survey, Fazel et al. concluded that every year, about 4 million

“nonelderly” adults are subject to nuclear cardiology procedures resulting in an effective dose in excess of 20 mSv.

In general, there are three doses of interest following a nuclear medicine procedure.

1. Dose to the target organ
2. Dose to the critical organ, which may be much higher
3. Effective dose, which determines the risk of stochastic effects (cancer and heritable effects)

PET displays physiologic and metabolic data that can be fused with the anatomic data from a CT scan.

The most commonly administered PET agent is [¹⁸F]-FDG that highlights areas of metabolism and can detect cancer metastases.

A PET image with [¹⁸F]-FDG results in an effective dose of about 11 mSv. However, this is usually accompanied by a CT scan, which increases the effective dose by an amount that depends on the site being imaged.

Other PET agents used in oncology can detect areas of rapid cellular proliferation in a tumor or areas of hypoxia. Still, other agents can be used to measure blood flow in cardiology.

The most common form of nuclear medicine therapy is the use of iodine-131 for the treatment of hyperthyroidism. The dose to the thyroid may be many tens of grays. In addition, there is a total body dose of 70 to 150 mGy, which is caused by the circulation of the radioactive iodine in the bloodstream. The second most common nuclear medicine therapy procedure is the treatment of thyroid cancer. Following surgical removal of the cancer and the thyroid gland, radioiodine may be used to destroy any residual iodine-accumulating cancer cells that had spread to lymph nodes, lung, or bone. The third most common therapy with radionuclides is the treatment of bony metastases. Radioimmunotherapy uses antibodies labeled with iodine-131 or yttrium-90 and injected against specific antigens to treat various malignancies.

Medical Radiation of Children and Pregnant Women

Children are more sensitive than adults to radiation-induced malignancies by a factor of 10 to 15. Physicians and patients alike are more cautious about nuclear medicine procedures in children than about diagnostic x-rays, even

when the radiation dose is comparable.

It is rare for radionuclides to be administered to a pregnant woman; great care should be exercised if in an emergency situation, this is deemed to be essential. Particular care is needed if the radionuclide involved is iodine because after the 12th week of gestation, the fetal thyroid avidly takes up iodine and can be seriously damaged.

Summary

The three principal contributors to the collective effective dose from medical radiation are (1) CT scans, (2) nuclear medicine (including nuclear cardiology), and (3) interventional radiology and cardiology. The millions of conventional radiographs, including chest x-rays and mammography, account for no more than 10% of the total collective effective dose.

BIBLIOGRAPHY

- Bahodar B. *Trends in Diagnostic Imaging to 2000*. London, United Kingdom: FT Pharmaceutical and Healthcare; 1996.
- Bakalyar D, Castellani M, Safian R. Radiation exposure to patients undergoing diagnostic and interventional cardiac catheterization procedures. *Cathet Cardiovasc Diagn*. 1997;42:121–125.
- Balter S, Hopewell JW, Miller DL, et al. Fluoroscopically guided interventional procedures: a review of radiation effects on the patient's skin and hair. *Radiology*. 2010;254(2):326–341.
- Bedetti G, Botto N, Andreassi MG, et al. Cumulative patient effective dose in cardiology. *Brit J Radiol*. 2008;81:699–705.
- Bell MR, Berger PB, Menke KK, et al. Balloon angioplasty of chronic total coronary artery occlusions: what does it cost in radiation exposure, time, and materials? *Cathet Cardiovasc Diagn*. 1992;25:10–15.
- Bergeron P, Carrier R, Roy D, et al. Radiation doses to patients in neurointerventional procedures. *AJNR Am J Neuroradiol*. 1994;15:1809–1812.
- Brenner DJ, Elliston CD, Hall EJ, et al. Estimated risks of radiation-induced fatal cancer from pediatric CT. *AJR Am J Roentgenol*. 2001;176:289–296.
- Broadhead DA, Chapple C-L, Faulkner K, et al. Doses received during interventional procedures. In: *Proceedings of the International Congress on*

Radiation Protection. Vienna, Austria: International Radiation Protection Association; 1996:38–440.

Committee on the Biological Effects of Ionizing Radiations. *Health Effects of Exposure to Low Levels of Ionizing Radiation: BEIR V*. Washington, DC: National Academy Press, National Research Council; 1990.

Committee on the Biological Effects on Ionizing Radiations. *Health Effects of Exposure to Radon : BEIR VI*. Washington, DC: National Academy Press, National Research Council; 1988.

Committee on the Biological Effects on Ionizing Radiations. *The Effects on Populations of Exposure to Low Levels of Ionizing Radiation: BEIR III*. Washington, DC: National Academy Press, National Research Council; 1980.

Conway BJ. *Nationwide Evaluation of X-ray Trends (NEXT): Summary of 1990 Computerized Tomography Survey and 1991 Fluoroscopy Survey*. Frankfort, KY: Conference of Radiation Control Program Directors; 1994.

Conway BJ, McCrohan JL, Antonsen RG, et al. Average radiation dose in standard CT examinations of the head: results of the 1990 NEXT survey. *Radiology*. 1992;184:135–140.

Cristy M, Eckerman K. *Specific Absorbed Fractions of Energy at Various Ages from Internal Photon Sources: Parts I–VII*. Oak Ridge, TN: Oak Ridge National Laboratory; 1987.

Duval JS, Carson JM, Holman PB, et al. Terrestrial Radioactivity and Gamma-ray Exposure in the United States and Canada. <https://pubs.usgs.gov/of/2005/1413/>. Accessed February 3, 2009. U.S. Geological Open-File Report 2005-1413.

Eckerman KF. Aspects of the dosimetry of radionuclides within the skeleton with particular emphasis on the active marrow. In: Schlafke-Stelson AT, Watson EE, eds. *Proceedings of the Fourth International Radiopharmaceutical Dosimetry Symposium*. Oak Ridge, TN: Oak Ridge Associated Universities; 1986:514–534.

Einstein AJ, Moser KW, Thompson RC, et al. Radiation dose to patients from cardiac diagnostic imaging. *Circulation*. 2007;116:1290–1305.

Fazel R, Krumholz HM, Wang Y, et al. Exposure to low-dose ionizing radiation from medical imaging procedures. *N Eng J Med*. 2009;361:849–857.

- Feygelman VM, Huda W, Peters K. Effective dose equivalents to patients undergoing cerebral angiography. *AJNR Am J Neuroradiol*. 1992;13:845–849.
- Grasty RL, Lamarre JR. The annual effective dose from natural sources of ionizing radiation in Canada. *Radiat Prot Dosimetry*. 2004;108:215–226.
- Hart D, Hillier MC, Wall BF. *Doses to Patients from Medical X-ray Examinations in the UK—2000 Review*. Chilton, United Kingdom: National Radiological Protection Board; 2000.
- Hart D, Wall BF. Estimation of effective dose from dose-area product measurements for barium meals and barium enemas. *Br J Radiol*. 1994;67:485–489.
- Hart D, Wall BF. Technical note: potentially higher patient radiation doses using digital equipment for barium studies. *Br J Radiol*. 1995;68:1112–1115.
- Huda W, Atherton JV, Ware DE, et al. An approach for the estimation of effective radiation dose at CT in pediatric patients. *Radiology*. 1997;203(2):417–422.
- Huda W, Morin RL. Patient doses in bone mineral densitometry. *Brit J Radiol*. 1996;69:422–425.
- International Commission on Radiological Protection. *1990 Recommendations of the International Commission on Radiological Protection*. Oxford, United Kingdom: Pergamon Press; 1991. Publication 60.
- International Commission on Radiological Protection. *Assessing Dose of the Representative Person for the Purpose of the Radiation Protection of the Public*. Bethesda, MD: International Commission on Radiological Protection; 2006. Report 101a.
- International Commission on Radiological Protection. *Gamma-Ray Spectrometry in the Environment*. Bethesda, MD: International Commission on Radiological Protection; 1971. Report 17.
- International Commission on Radiological Protection. *Gamma-Ray Spectrometry in the Environment*. Bethesda, MD: International Commission on Radiological Protection; 1994. Report 53.
- International Commission on Radiological Protection. *Radiation Dose to Patients from Radiopharmaceuticals*. Bethesda, MD: International Commission on Radiological Protection; 1987. Report 53.

International Commission on Radiological Protection. *Radiation Dose to Patients from Radiopharmaceuticals-Addendum 3 to ICRP Publication 53*. Bethesda, MD: International Commission on Radiological Protection; 2008. Report 106.

Jessen KA, Shrimpton PC, Gelejns J, et al. Dosimetry for optimisation of patient protection in computed tomography. *Appl Radiat Isot*. 1999;50(1):165–172.

Jones DG, Shrimpton PC. *Normalised Organ Doses for X-ray Computed Tomography Calculated Using Monte Carlo Techniques*. Chilton, United Kingdom: National Radiological Protection Board; 1993. Report NRPB-SR250.

Karppinen J, Parviainen T, Servoman A, et al. Radiation risk and exposure of radiologists and patients during coronary angiography and percutaneous transluminal coronary angioplasty (PCTA). *Radiat Prot Dosim*. 1995;57:481–485.

Knautz MA, Abele DC, Reynolds TL. Radiodermatitis after transjugular intrahepatic portosystemic shunt. *South Med J*. 1997;5:450–452.

Lichtenstein DA, Klapholz L, Vardy DA, et al. Chronic radiodermatitis following cardiac catheterization. *Arch Dermatol*. 1996;132:663–667.

Lindsay BD, Eichling JO, Ambos HD, et al. Radiation exposure to patients and medical personnel during radiofrequency catheter ablation for supraventricular tachycardia. *Am J Cardiol*. 1992;70:218–223.

Loevinger R, Budinger T, Watson E. *MIRD Primer for Absorbed Dose Calculations*. New York, NY: Society of Nuclear Medicine; 1991.

Mattson S, Johansson L, Leide Svegborn S, et al. *Radiation Dose to Patients from Radiopharmaceuticals*. Bethesda, MD: International Commission on Radiological Protection; 2007. Publication 106.

McCrohan JL, Patterson JF, Gagne RM, et al. Average radiation doses in a standard head examination for 250 CT systems. *Radiology*. 1987;163:263–268.

McParland BJ. A study of patient radiation doses in interventional radiological procedures. *Br J Radiol*. 1998;71:175–185.

Mejia AA, Nakamura T, Masatoshi I, et al. Estimation of absorbed doses in humans due to intravenous administration of fluorine-18-fluorodeoxyglucose in PET studies. *J Nucl Med*. 1991;32:699–706.

- Mettler FA Jr, Bhargavan M, Faulkner K, et al. Radiologic and nuclear medicine studies in the United States and worldwide: frequency, radiation dose, and comparison with other radiation sources —1950–2007. *Radiology*. 2009;253:520–531.
- Mettler FA Jr, Huda W, Yoshizumi TT, et al. Effective doses in radiology and diagnostic nuclear medicine: a catalog. *Radiology*. 2008;248:254–263.
- Mettler FA Jr, Wiest PW, Locken JA, et al. CT scanning: patterns of use and dose. *J Radiol Prot*. 2000;20(4):353–359.
- Nahass GT. Acute radiodermatitis after radiofrequency catheter ablation. *J Am Acad Dermatol*. 1997;36:881–884.
- Nahass GT, Cornelius L. Fluoroscopy-induced radiodermatitis after transjugular intrahepatic portosystemic shunt. *Am J Gastroenterol*. 1998;93:1546–1549.
- National Center for Devices and Radiological Health. Fluoroscopically guided procedures have potential for skin injury. *Radiological Health Bulletin*. 1994;28:1–2.
- National Council on Radiation Protection and Measurements. *Exposure of the U.S. Population from Diagnostic Medical Radiation*. Bethesda, MD: National Council on Radiation Protection and Measurements; 1989. Report 100.
- National Council on Radiation Protection and Measurements. *Exposure of the US Population from Occupational Radiation*. Bethesda, MD: National Council on Radiation Protection and Measurements; 1989. Report 101.
- National Council on Radiation Protection and Measurements. *Exposures of the Population of the United States to Ionizing Radiation*. Bethesda, MD: National Council on Radiation Protection and Measurements; 1987. Report 93.
- National Council on Radiation Protection and Measurements. *Implementation of the Principle of As Low As Reasonably Achievable (ALARA) for Medical and Dental Personnel*. Bethesda, MD: National Council on Radiation Protection and Measurements; 1990. Report 107.
- National Council on Radiation Protection and Measurements. *Ionizing Radiation Exposure of the Population of the United States*. Bethesda, MD: National Council on Radiation Protection and Measurements; 1987. Report 93.
- National Council on Radiation Protection and Measurements. *Ionizing Radiation*

Exposure of the Population of the United States. Bethesda, MD: National Council on Radiation Protection and Measurements; 2009. Report 160.

National Council on Radiation Protection and Measurements. *Sources and Magnitude of Occupational and Public Exposures from Nuclear Medicine Procedures.* Bethesda, MD: National Council on Radiation Protection; 1996. Report 124.

Paterson A, Frush DP, Donnelly LF. Helical CT of the body: are settings adjusted for pediatric patients? *AJR Am J Roentgenol.* 2001;176:297–301.

Pattee PL, Johns PC, Chambers RJ. Radiation risk to patients from percutaneous transluminal coronary angioplasty. *J Am Coll Cardiol.* 1993;22:1044–1051.

Public Health England. *Ionising Radiation Exposure of the UK Population: 2010 review.* www.gov.uk/government/collections/radiation-phe-crce-report-series. Report PHE-CRCE-026

Refetoff S, Harrison J, Karanfilski BT, et al. Continuing occurrence of thyroid carcinoma after irradiation to the neck in infancy and childhood. *N Engl J Med.* 1975;292:171–175.

Robinson AE, Hill EP, Harpen MD. Radiation dose reduction in pediatric CT. *Pediatr Radiol.* 1986;16(1):53–54.

Rosenstein M. *Handbook of Selected Tissue Doses for Projections Common in Diagnostic Radiology.* Rockville, MD: U.S. Department of Health and Human Services, Public Health Service, U.S. Food and Drug Administration; 1988. Publication no. 89–8031.

Rosenthal L, Beck TJ, Williams J, et al. Acute radiation dermatitis following radiofrequency catheter ablation of atrioventricular nodal reentrant tachycardia. *Pacing Clin Electrophysiol.* 1997;20:1834–1839.

Rowley KA. Patient exposure in cardiac catheterization and cinefluorography using the Eclair 16 mm camera at speeds up to 200 frames per second. *Br J Radiol.* 1974;47:169–178.

Shrimpton PC. *Protection of the Patient in X-ray Computed Tomography, in Documents of the NRPB.* Vol. 3. 4th ed. London, United Kingdom: Her Majesty's Stationery Office; 1992.

Shrimpton PC, Edyvean S. CT scanner dosimetry. *Br J Radiol.* 1998;71(841):1–3.

Shrimpton PC, Jessen KA, Geleijns J, et al. Reference doses in computed

- tomography. *Radiat Prot Dos.* 1998;80:55–59.
- Shrimpton PC, Wall BF, Hart D. Diagnostic medical exposures in the U.K. *Appl Radiat Isot.* 1999;50:261–269.
- Smith PG, Doll R. Mortality from cancer and all causes among British radiologists. *Br J Radiol.* 1981;54:187–194.
- Stern SH, Rosenstein M, Renaud L, et al. *Handbook of Selected Tissue Doses for Fluoroscopic and Cineangiographic Examination of the Coronary Arteries (in SI Units)*. Rockville, MD: U.S. Department of Health and Human Services, U.S. Food and Drug Administration, Center for Devices and Radiological Health; 1995.
- Stern SH, Spelic DC, Kaczmarek RV. *NEXT 2000 Protocol for Survey of Computed Tomography (CT)*. Frankfort, KY: Conference of Radiation Control Program Directors; 2000.
- Stewart A, Webb J, Hewitt D. A survey of childhood malignancies. *Br Med J.* 1958;1:1495–1508.
- Stone MS, Robson KJ, LeBoit PE. Subacute radiation dermatitis from fluoroscopy during coronary artery stenting: evidence for cytotoxic lymphocyte mediated apoptosis. *J Am Acad Dermatol.* 1998;38:333–336.
- United Nations Scientific Committee on the Effects of Atomic Radiation. *Annex C Medical Radiation Exposures*. New York, NY: United Nations Scientific Committee on the Effects of Atomic Radiation; 2000.
- United Nations Scientific Committee on the Effects of Atomic Radiation. *Sources and Effects of Ionizing Radiation*. New York, NY: United Nations Scientific Committee on the Effects of Atomic Radiation; 1986.
- United Nations Scientific Committee on the Effects of Atomic Radiation. *Sources and Effects of Ionizing Radiation*. New York, NY: United Nations Scientific Committee on the Effects of Atomic Radiation; 2000.
- United Nations Scientific Committee on the Effects of Atomic Radiation. *Sources and Effects of Ionizing Radiation*. New York, NY: United Nations Scientific Committee on the Effects of Atomic Radiation; 2008.
- Vaño E, Gonzalez L, Guibelalde E, et al. Radiation exposure to medical staff in interventional and cardiac radiology. *Br J Radiol.* 1998;71:954–960.
- Wagner HN. F-18 FDG in oncology: its time has come. *Appl Radiol.* 1997;26:29–31.

Wagner LK. *Radiation Bioeffects and Management Test and Syllabus*. Reston, VA: American College of Radiology; 1991.

Wagner LK, Archer BR. *Minimizing Risks from Fluoroscopic X-rays*. 2nd ed. Houston, TX: Partners in Radiation Management; 1998.

Wagner LK, Archer BR. *Radiation Protection Management for Fluoroscopy: A Manual for Physicians*. Houston, TX: RM Partnership; 1995.

Wagner LK, Eifel PJ, Geise RA. Effects of ionizing radiation. *J Vasc Interv Radiol*. 1995;6:988–989.

Wagner LK, Eifel PJ, Geise RA. Potential biological effects following high x-ray dose interventional procedures. *J Vasc Interv Radiol*. 1994;5:71–84.

Wagner LK, McNeese MD, Marx MV, et al. Severe skin reactions from interventional fluoroscopy: case report and review of the literature. *Radiology*. 1999;213:773–776.

Wall BF, Hart D. Revised radiation doses for typical X-ray examinations. Report on a recent review of doses from medical x-ray examinations in the UK by NRPB. *Br J Radiol*. 1997;70:437–439.

Ware DE, Huda W, Mergo PJ, et al. Radiation effective doses to patients undergoing abdominal CT examinations. *Radiology*. 1999;210:645–650.

Watson RM. Radiation exposure: clueless in the cath lab, or sayonara ALARA. *Cathet Cardiovasc Diagn*. 1997;42:126–127.

Whalen JP, Balter S. *Radiation Risks in Medical Imaging*. Chicago, IL: Yearbook Medical; 1984.

Williams J. The interdependence of staff and patient doses in interventional radiology. *Br J Radiol*. 1997;70:498–503.

*Readers unfamiliar with terms such as *effective dose* or any other quantities or units of dose should read the definitions in [Chapter 16](#).

chapter 16

Radiation Protection

The Origins of Radiation Protection

Organizations

Quantities and Units

Dose

Radiation Weighting Factor

Equivalent Dose

Effective Dose

Committed Equivalent Dose

Committed Effective Dose

Collective Equivalent Dose

Collective Effective Dose

Collective Committed Effective Dose

Summary of Quantities and Units

Tissue Reactions and Stochastic Effects

Principles of Radiation Protection

Basis for Exposure Limits

Limits for Occupational Exposure

Stochastic Effects

Tissue Reactions (Formerly Known as Deterministic Effects)

As Low as Reasonably Achievable

Protection of the Embryo/Fetus

Emergency Occupational Exposure

Exposure of Persons Younger than 18 Years of Age

Exposure of Members of the Public (Nonoccupational Limits)

Exposure to Indoor Radon

De Minimis Dose and Negligible Individual Dose

Radiation Detriment

National Council on Radiation Protection and Measurements and the International Commission on Radiological Protection Compared

The History of the Current Dose Limits

Dose Ranges

Summary of Pertinent Conclusions

Glossary of Terms

Bibliography

THE ORIGINS OF RADIATION PROTECTION

At the Second International Congress of Radiology (ICR) in Stockholm in 1928, member countries were invited to send representatives to prepare x-ray protection recommendations. The British recommendations were adopted because they were most complete; guidelines on radiation protection had been set up in that country as early as 1915.

The 1928 Congress set up the International X-Ray and Radium Protection Committee, which, after World War II, was remodeled into two commissions that survive to this day:

The International Commission on Radiological Protection (ICRP)

The International Commission on Radiation Units and Measurements (ICRU)

The US representative to the 1928 Congress was Dr. Lauriston Taylor who brought back to the United States the agreed radiation protection criteria and set up a national committee, the Advisory Committee on X-Ray and Radium Protection, under the auspices of the Bureau of Standards, which was perceived to be a “neutral territory” by the various radiologic societies of the day; this committee operated until World War II. In 1946, it was renamed the National Council on Radiation Protection and Measurements (NCRP), eventually receiving a charter from Congress as an independent body to provide advice and recommendations on matters pertaining to radiation protection in the United States. NCRP reports still form the basis of radiation protection policy in the United States today, although legal responsibility for the implementation of radiation safety is variously in the hands of the Nuclear Regulatory Commission (NRC), the Department of Energy (DOE), and state or city bureaus of radiation control.

ORGANIZATIONS

The organization of radiation protection and the interrelation of the various committees, whose reports are quoted, deserve a brief explanation.

First, there are the committees that summarize and analyze data and suggest risk estimates for radiation-induced cancer and heritable effects. At the international level, there is the United Nations Scientific Committee on the Effects of Atomic Radiation (UNSCEAR) which was set up in 1955. This committee has wide international representation, being composed of scientists from 21 member states. Comprehensive reports appeared at intervals over the years since 1958, with the latest report in 2013. The United States committee is appointed by the National Academy of Sciences and is now known as the Biological Effects of Ionizing Radiation (BEIR) Committee. The first report appeared in 1956, when it was known as the Biological Effects of Atomic Radiation (BEAR) Committee. Subsequent comprehensive reports appeared in 1972 (BEIR II), 1980 (BEIR III), 1990 (BEIR V), and 2006 (BEIR VII). BEIR VI, entitled *Health Effects of Exposure to Indoor Radon*, appeared in 1999.

These committees are “scholarly” committees in the sense that if information is not available on a particular topic, they do not feel compelled to make a recommendation. Because they do not serve an immediate pragmatic aim, they are not obliged to make a “best guess” estimate if data are uncertain.

Second, there are the committees that formulate the concepts for use in radiation protection and recommend maximum permissible levels. These committees serve more pragmatic aims and, therefore, must make best estimates even if good data are unavailable. At the international level, there is the ICRP, which, together with ICRU, was established in 1928 after a decision by the Second ICR, as mentioned earlier. In 1950, the ICRP was restructured and given its present name. The ICRP often takes the lead in formulating concepts in radiation protection and in recommending dose limits. As an international body, it has no jurisdiction over anyone and can do no more than recommend; it has established considerable credibility, however, and its views carry great weight. Its most recent comprehensive report is ICRP Publication No. 103, published in 2007. The United Kingdom, most of Europe, and Canada follow ICRP recommendations. In the United States, there is the NCRP (also mentioned earlier) chartered by Congress to be an “impartial” watchdog and consisting of 100 experts from the radiation sciences—who are, therefore, not impartial at all. The NCRP often, but not always, follows the lead of ICRP. Their most recent

comprehensive report on dose limits (NCRP Report No. 116, published in 1993) differs from ICRP in several important respects. The ICRP and NCRP suggest dose limits and safe practices, but, in fact, neither body has any jurisdiction to enforce their recommendations.

In the United States, the Environmental Protection Agency (EPA) has the responsibility for providing guidance to federal agencies; it is the EPA that sets, for example, the action level for radon. Each state can formulate its own regulations for x-rays and radiations produced by sources other than reactors. Under federal law, the use of by-product materials from reactors (i.e., most radioactive materials) in the United States is controlled by the NRC. Anyone who wants to use such radioactive materials must obtain a license from the NRC. Federal law also permits a state to reach an agreement with the NRC allowing that state to take over the regulation of radioactive materials within its borders. That state is then called an NRC Agreement State. [Figure 16.1](#) shows the agreement states as of 2014. In other states, this responsibility falls on the U.S. Department of Labor Occupational Safety and Health Administration (OSHA). The DOE is responsible for radiation safety regulations at all of its facilities operated by contractors. Up to the present, the various regulating bodies in the United States have accepted, endorsed, and used the reports issued by the NCRP, but they are not obliged to do so, and they are often slow to adopt the latest reports.

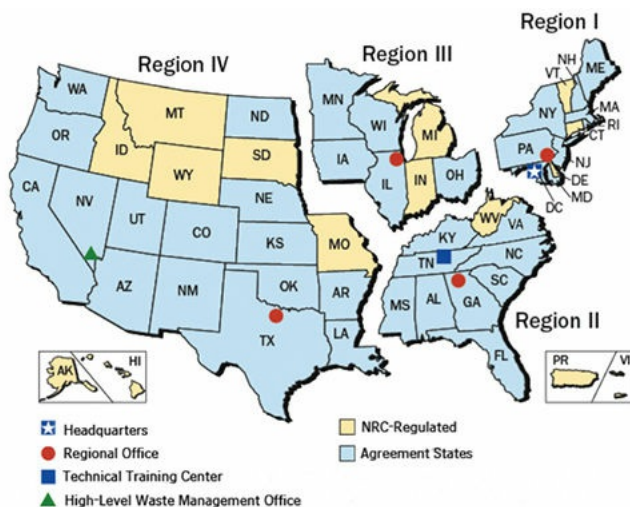


FIGURE 16.1 The Nuclear Regulatory Commission (NRC) formulates rules for radioactive by-product material from reactors in “agreement states.” The figure shows agreement states as of 2014.

QUANTITIES AND UNITS

Dose

The quantity used to measure the “amount” of ionizing radiation is the **absorbed dose**, usually termed simply as **dose**. This is defined as the energy absorbed per unit mass, and its unit is joules per kilogram, which is given a special name, the **gray (Gy)**, named after the British physicist who contributed to the development of ionization chamber theory. The unit used in the past was the radiation absorbed dose (rad), defined as an energy absorption of 100 erg/g. Consequently, 1 Gy equals 100 rad.

Radiation Weighting Factor

The probability of a stochastic effect, such as the induction of cancer or of heritable events, depends not only on the dose but also on the type and energy of the radiation; that is, some radiations are biologically more effective for a given dose than others. This is taken into account by weighting the absorbed dose by a factor related to the quality of the radiation. A radiation weighting factor (W_R) is a dimensionless multiplier used to place biologic effects (risks) from exposure to different types of radiation on a common scale. The W_R s are chosen by the ICRP as representative of relative biologic effectiveness (RBE) applicable to low doses and low dose rates (LDR) and for biologic end points relevant to stochastic late effects. They can be traced ultimately to experimentally determined RBE values, but a large judgmental factor is involved in their choice. The weighting factors recommended by the ICRP for photons, electrons, protons and α -particles, and heavy ions are shown in [Table 16.1](#). For neutrons, a continuous curve as a function of neutron energy is recommended ([Fig. 16.2](#)) with the most biologically effective neutrons having a W_R of 20.

Table 16.1 Radiation Weighting Factors^a

RADIATION TYPE	RADIATION WEIGHTING FACTORS
Photons	1
Electrons and muons	1

Protons and charged pions	2
α -Particles, fission fragments, heavy ions	20
Neutrons	A continuous curve as a function of neutron energy

^aAll values relate to the radiation incident on the body or, for internal sources, emitted from the source.

From International Commission on Radiological Protection. *The 2007 Recommendations of the International Commission on Radiological Protection*. New York, NY: Elsevier; 2007. ICRP publication 103.

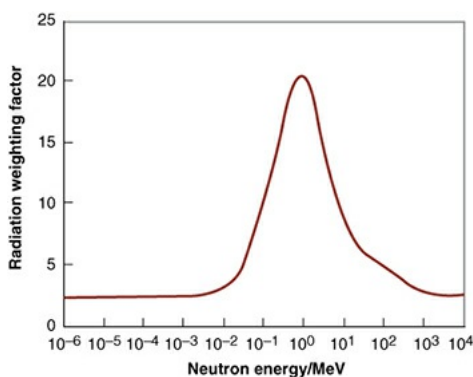


FIGURE 16.2 Radiation weighting factor for neutrons as a function of neutron energy. (From the ICRP 2007 recommendations.)

Equivalent Dose

In radiologic protection, the **equivalent dose** is the product of the absorbed dose averaged over the tissue or organ and the W_R selected for the type and energy of radiation involved. Thus,

$$\text{Equivalent dose} = \text{absorbed dose} \times W_R$$

If absorbed dose is measured in gray (Gy), the equivalent dose is measured in sievert (Sv), named after the Swedish physicist who designed early ionization chambers. Although 1 Gy of neutrons does not produce the same biologic effect as 1 Gy of x-rays, 1 Sv of either neutrons or x-rays does result in equal biologic effects. The ICRP has recommended a new name for this quantity: **radiation**

weighted dose. The commission is also considering a new (special) name for the unit of radiation weighted dose to avoid the use of “sievert” for both radiation weighted dose and effective dose, but no decision has been made as yet.

If a radiation field is made up of a mixture of radiations, the equivalent dose is the sum of the individual doses of the various types of radiations, each multiplied by the appropriate W_R . Thus, if a tissue or organ were exposed to 0.15 Gy of cobalt-60 γ -rays plus 0.02 Gy of 1-MeV neutrons, the equivalent dose would be:

$$(0.15 \times 1) + (0.02 \times 20) = 0.55 \text{ Sv}$$

Effective Dose

If the body is uniformly irradiated, the probability of the occurrence of stochastic effects (cancer and heritable effects) is assumed to be proportional to the equivalent dose, and the risk can be represented by a single value. In fact, truly uniform total body exposures are rare, particularly if irradiation is from radionuclides deposited in tissues and organs. Sometimes, equivalent doses to various tissues differ substantially, and it is well established that different tissues vary in their sensitivities to radiation-induced stochastic effects. For example, it is difficult to produce heritable effects by irradiation of the head or hands. On the other hand, the thyroid and breast appear to be particularly susceptible to radiation-induced cancer. To deal with this situation, the ICRP introduced the concept of the **tissue weighting factor (W_T)**, which represents the relative contribution of each tissue or organ to the total detriment resulting from uniform irradiation of the whole body. [Table 16.2](#) lists the W_T values recommended by the ICRP in 2007.

Table 16.2 Tissue Weighting Factors

ORGAN/TISSUE	NUMBER OF TISSUES	W_T	TOTAL CONTRIBUTION
Lung, stomach, colon, 6 bone marrow, breast, and remainder	6	0.12	0.72

Gonads	1	0.08	0.08
Thyroid, esophagus, 4 bladder, and liver		0.04	0.16
Bone surface, skin, 4 brain, and salivary glands		0.01	0.04

The specified remainder tissues (14 in total, 13 in each sex) are adrenals, extrathoracic tissue (ET), gall bladder, heart, kidneys, lymphatic nodes, muscle, oral mucosa, pancreas, prostate (m), small intestine (SI), spleen, thymus, uterus/cervix (f).

From International Commission on Radiological Protection. *The 2007 Recommendations of the International Commission on Radiological Protection*. New York, NY: Elsevier; 2007. ICRP publication 103.

The sum of all of the weighted equivalent doses in all the tissues or organs irradiated is called the **effective dose**, which is expressed by the formula

$$\text{Effective dose} = \sum \text{absorbed dose} \times W_R \times W_T$$

for all tissues or organs exposed. Effective dose is in principle, as well as in practice, a nonmeasurable quantity. The unit is the Sievert (Sv).

Committed Equivalent Dose

In the case of external irradiation, the absorbed dose is delivered at the time of exposure, but for irradiation from internally deposited radionuclides, the total absorbed dose is distributed over time as well as to different tissues in the body. The dose rate falls off depending on the physical and biologic half-lives of the radionuclide.

To take into account the varying time distributions of dose delivery, the ICRP defined the **committed equivalent dose** as the integral over 50 years of the equivalent dose in a given tissue after intake of a radionuclide. This time was chosen to correspond to the working life of a person. For radionuclides with effective half-lives of up to about 3 months, the committed equivalent dose is essentially equal to the annual equivalent dose in the year of intake, but for radionuclides with longer effective half-lives, it is greater because it reflects the

dose that will accrue over future years.

Committed Effective Dose

If the committed equivalent doses to individual organs or tissues resulting from the intake of a radionuclide are multiplied by the appropriate W_T and then summed, the result is the **committed effective dose**.

Collective Equivalent Dose

The quantities referred to previously all relate to the exposure of an individual. They become appropriate for application to the exposure of a group or population by the addition of the term *collective*. Thus, the **collective equivalent dose** is the product of the average equivalent dose to a population and the number of persons exposed. There appears to be some confusion about the accepted name of the unit for collective equivalent dose in the new SI system of units. Some use **man-sievert**, presumably agreeing with the judgment of Sir Winston Churchill that “man embraces woman.” The more liberated prefer the term **person-sievert**, which is used here.

Collective Effective Dose

The **collective effective dose** is likewise the product of the average effective dose to a population and the number of persons exposed. The unit is again the *person-sievert*. An example is in order here. If 100 persons receive an average effective dose of 0.3 Sv, the collective effective dose is 30 person-Sv.

Collective Committed Effective Dose

In the case of a population ingesting or inhaling radionuclides that deposit their dose over a prolonged period, the integral of the effective dose over the entire population out to a period of 50 years is called the **collective committed effective dose**.

These collective quantities can be thought of as representing the total consequences of exposure of a population or group and they can be thought of as surrogates for “harm.” For example, the annual collective effective dose to the US population from medical radiation is about 899,000 person-Sv. Such collective quantities are much beloved by the bureaucrats because they make it possible to compare different activities or accidents, inasmuch as each can be described by a single number. The danger is that the next step is to convert the collective dose into the number of cancers or heritable effects produced, which,

of course, assumes proportionality between dose and biologic effect, which is seldom true. The quantities certainly are used widely to give a rough guide to the probability of cancer and heritable effects in a population exposed to radiation, and in particular, they can be used to compare the approximate impact of different types of radiation accidents in terms of several health effects that might arise in that population.

Summary of Quantities and Units

Table 16.3 is a summary of the quantities and units that have been described here, showing how they build logically on one another. If on reading this section the reader gains the impression that the bureaucrats have taken over, it is because they have—at least in the field of radiation protection. An elaborate set of definitions has been produced based on the assumption of linearity between dose and risk. The whole business needs to be taken with a generous grain of salt because it is like a house of cards, based on somewhat shaky premises.

Table 16.3 Quantities and Units Used in Radiation Protection

QUANTITY	DEFINITION	UNIT
Absorbed dose	Energy per unit mass	Gray
<i>For individuals</i>		
Equivalent dose (radiation weighted dose)	Average dose \times radiation weighting factor	Sievert
Effective dose	Sum of equivalent doses to organs and tissues exposed, each multiplied by the appropriate tissue weighting factor	Sievert

Committed equivalent dose	Equivalent dose integrated over 50 y (relevant to incorporated radionuclides)	Sievert
Committed effective dose	Effective dose integrated over 50 y (relevant to Sievert incorporated radionuclides)	
<i>For populations</i>		
Collective effective dose	Product of the average effective dose and the Person-sievert number of individuals exposed	
Collective committed effective dose	Integration of the collective dose over 50 y (relevant to incorporated radionuclides)	Person-sievert

The concept of collective effective dose does allow a rough and quick estimate to be made of the potential health hazards to a population exposed to an accidental release of radioactivity from a nuclear reactor. For example, it is estimated that the collective effective dose from the Chernobyl accident, integrated over the world and all time, is about 600,000 person-Sv. Multiplying this quantity by the risk of a radiation-induced lethal cancer (5% per sievert) yields an estimate of 30,000 cancers produced by the accident.

It must be emphasized again that these concepts can be used only under conditions in which it is *reasonable to assume linearity between risk and dose*—that is, that risks are directly proportional to the summation of doses from different sources. Exposures that are within the administratively allowed dose limits may cause an increased incidence of stochastic effects, such as cancer and heritable effects, but are much below the thresholds for early deterministic effects. In the case of larger accidental releases in which doses to some people might be high enough to exceed these thresholds to the point of causing early death, collective effective dose is an inappropriate quantity.

TISSUE REACTIONS AND STOCHASTIC EFFECTS

Ionizing radiations clearly produce two very different types of damage. The first

type of damage is due to cells being killed and removed from an organ or tissue. The second type of effect is due to cells that are not killed by the radiation but are changed or mutated in some way. These different types of effects have been given special names by ICRP. Damage due to cells being killed by the radiation and removed from the tissue or organ has long been known as a deterministic effect but has recently been renamed as a **tissue reaction**. A small dose of radiation to a self-renewal system may result in the lethality of some of the dividing cells in the stem cell compartment, but lost cells can be quickly replaced by cell division and so the integrity of the tissue or organ is not compromised. Consequently, there is a dose threshold to the production of a tissue reaction. As the radiation dose is increased, the stem cell compartment may be severely depleted and if the dose is sufficiently large, it may be totally depleted resulting in a 100% chance of a tissue reaction. Consequently, the dose-response relationship for a tissue reaction has a threshold-sigmoid shape, as illustrated in [Figure 16.3](#). Other characteristics of a tissue reaction include the observed fact that the severity of the effect increases with dose above the threshold and the effect is clearly due to damage to many cells. Examples of tissue reactions include effects on fertility, lethality due to total body exposure, or failure of an organ such as the kidney due to radiation exposure.

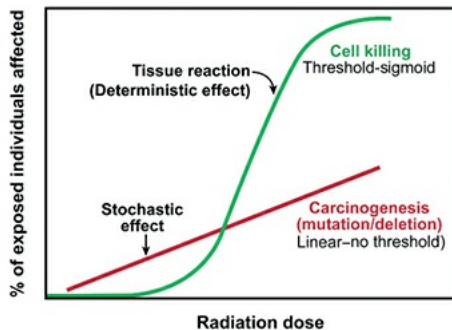


FIGURE 16.3 The basic differences in the shape of the dose-response relationship for stochastic as opposed to tissue reactions. Tissue reactions show a threshold in dose; the severity of the effect increases with dose above this threshold, and the proportion of individuals rises rapidly with dose to 100%. The dose-response relationship is, therefore, sigmoid after a threshold. Stochastic effects are all-or-nothing effects (e.g., cancer and heritable effects). The severity of the effect is not dose related, although the probability of it occurring is. The increase with dose may be linear or linear-quadratic. There is no threshold, that is, no dose below which the probability of an effect is zero. The dose-response relationship is, therefore, linear or linear-quadratic, with no threshold.

Effects due to cells that are not killed but are mutated in some way are

known as **stochastic effects**. The most important stochastic effect is cancer, and the other being heritable effects. A stochastic effect is an all or nothing effect, that is, the severity of the effect is not dose-dependent, although the probability of the effect occurring increases with dose. Because most cancers are monoclonal in origin, it is likely that the effect is due to damage to one or at most a few cells. For purposes of radiation protection, it is thought to be prudent and conservative to assume that there is no threshold in dose, that is, that any dose however small has some probability of producing an effect though that probability declines with declining dose. There is, of course, no way of knowing whether or not there is a dose threshold at doses below that at which experimental data are available. The difference in shape of the dose-response relationship for stochastic effects compared with tissue reactions is shown in [Figure 16.3](#).

PRINCIPLES OF RADIATION PROTECTION

NCRP in its 1993 recommendations established a framework for radiation protection composed of three main elements:

1. **Justification:** the need to justify an activity which involves radiation exposure on the basis that the expected benefits to society exceed the overall societal costs
2. **As low as reasonably achievable (ALARA):** the need to ensure that the total societal detriment from such justifiable activities or practices is maintained ALARA
3. **Limitation:** the need to apply individual dose limits to ensure that the procedures of justification and ALARA do not result in individuals or groups of individuals exceeding levels of acceptable risk

The objectives of radiation protection are

1. To prevent clinically significant radiation-induced tissue reactions by adhering to dose limits that are below the apparent or practical dose threshold
2. To limit the risk of stochastic effects (cancer and heritable effects) to a reasonable level in relation to societal needs, values, and benefits gained

The difference in shape of the dose-response relationships for tissue reactions compared with stochastic effects is illustrated in [Figure 16.3](#). The objectives of radiation protection can be achieved by reducing all exposure to

ALARA and by applying dose limits for controlling occupational and general public exposures. For radiation protection purposes, it is assumed that *the risk of stochastic effects is strictly proportional to dose without threshold throughout the range of dose and dose rates of importance in radiation protection*. Furthermore, the probability of response (risk) is assumed to accumulate linearly with dose. This is not true at higher doses characteristic of radiation accidents in which more complex (nonlinear) dose–risk relationships may apply.

Given these assumptions, any selected dose limit has an associated level of risk. Consequently, it is necessary to justify any use of radiation in terms of a benefit to a person or to society.

Justification of exposure is one of the basic principles of radiation protection. The concept was described in 1977 by the ICRP: A practice involving exposure to radiation should produce sufficient benefit to the exposed individual or to society to offset the radiation detriment it causes. This concept is sometimes difficult to put into practice in various situations in which individuals are exposed as follows:

1. In the case of patients, the diagnostic or therapeutic benefit should outweigh the risk of detriment.
2. In the case of occupational exposure, the radiation risk must be added to and compared with other risks in the workplace.
3. The most difficult situation is exposure for the sake of research, where volunteer subjects may fall into one of three categories: patients who may benefit, patients who may receive no benefit, and healthy volunteers. In cases in which the individual receives no benefit, the benefit to society must outweigh the risks.

BASIS FOR EXPOSURE LIMITS

Exposure limits have changed over the years in step with evolving information about the biologic effects of radiation and with changes in the social philosophy within which recommended exposure limits are developed.

In the 1930s, the concept of a **tolerance dose** was used, a dose to which workers could be exposed continuously without any evident deleterious acute effects such as erythema of the skin.

By the early 1950s, the emphasis had shifted to late effects. The **maximum permissible dose** was designed to ensure that the probability of the occurrence

of injuries was so low that the risk would be readily acceptable to the average person. At about that time, based on the results of genetic studies in *Drosophila* and mice, the occupational limit was reduced substantially and a limit for exposure of the public introduced. Subsequently, the heritable effects were found to be smaller, and cancer risks larger than were thought at the time.

By the 1980s, the NCRP was comparing the probability of radiation-induced cancer death in radiation workers with annual accidental mortality rates in “safe” industries. Exposure standards, therefore, are necessarily based partly on observed effects but with a great deal of judgment involved.

Earlier chapters described the deleterious effects of radiation in terms of heritable effects, carcinogenesis, and effects on the developing embryo and fetus. The risk estimates derived are summarized in [Table 16.4](#). By far, the largest risk estimate is 40% per sievert for severe mental retardation for the most sensitive period of gestation and above a threshold of at least 0.3 Gy. Next comes carcinogenesis as 5% per sievert, corresponding to exposure of the general population to low doses and dose rates. Last are heritable effects, lowered in 2004 by the ICRP to 0.2% per sievert for the general population.

Table 16.4 Deleterious Effects of Radiation that Highlight the Need for Protection

END POINT	RISK ESTIMATE
Severe mental retardation	
Exposure of embryo/fetus (8–15 wk)	40%/Sv
Carcinogenesis	
General population (low dose, low dose rate)	5%/Sv

Heritable effects	
General population	0.2%/Sv

Based on International Commission on Radiological Protection (ICRP), Biologic Effects of Ionizing Radiation (BEIR), and United Nations Scientific Committee on the Effects of Atomic Radiation (UNSCEAR).

LIMITS FOR OCCUPATIONAL EXPOSURE

The NCRP recommends the limits described in the following sections (and summarized in [Table 16.5](#)). These limits do not include natural background radiation or radiation for medical purposes.

Table 16.5 Summary of Recommended Dose Limits

	NCRP	ICRP
Occupational exposure		
Stochastic effects: effective dose limits		
Cumulative	$10 \text{ mSv} \times \text{age}$	20 mSv/y averaged over 5 y
Annual	50 mSv/y	50 mSv/y
Tissue reactions (deterministic effects): dose equivalent limits for tissues and organs (annual):		

Lens of eye	50 msV/y	20 mSv/y averaged over 5 y not more than 50 mSv in any year
Skin, hands, and feet	500 mSv/y	500 mSv/y
Embryo/fetus exposure		
Effective dose limit after pregnancy declared	0.5 mSv/mo	Total of 1 mSv to embryo/fetus
Public exposure (annual)		
Effective dose limit, continuous or frequent exposure	1 mSv/y	No distinction between frequent and infrequent —1 mSv/y
Effective dose limit, infrequent exposure	5 mSv/y	1 mSv/y
Dose equivalent limits; lens of the eye	15 mSv/y	15 mSv/y
Skin and extremities	50 mSv/y	50 mSv/y
Education and training exposure (annual)		
Effective dose limit	1 mSv/y	No statement

Dose equivalent limit for lens of eye	15 mSv/y	No statement
Skin and extremities	50 mSv/y	No statement
Negligible individual dose (annual):	0.01 mSv/y	No statement

Based on National Council on Radiation Protection and Measurements. *Limitation of Exposure to Ionizing Radiation*. Bethesda, MD: National Council on Radiation Protection and Measurements; 1993. NCRP report no. 116; and International Commission on Radiological Protection. *The 2007 Recommendations of the International Commission on Radiological Protection*. New York, NY: Elsevier; 2007. ICRP publication 103.

Stochastic Effects

1. No occupational exposure should be permitted until the age of 18 years.
2. The effective dose in any year should not exceed 50 mSv (5 rem).
3. The individual worker's lifetime effective dose should not exceed age in years \times 10 mSv.

These limits apply to the sum of the effective dose from external radiation and the committed effective dose from internal exposures.

Tissue Reactions (Formerly Known as Deterministic Effects)

1. 50 mGy per year for the lens of the eye
2. 500 mSv per year for localized areas of the skin and the hands and feet

These additional limits for tissue reactions are required because of the low sensitivity of the particular tissues involved to radiation-induced cancer. In the case of the lens of the eye, if a radiation other than x-rays is involved, an appropriate RBE should be used.

AS LOW AS REASONABLY ACHIEVABLE

The dose limits referred to previously are all upper limits and subject to the concept of ALARA. The recommendation that standard setting committees

would like to make for personnel protection is zero exposure. This is not feasible, however, if society is to realize the enormous benefits derived from the uses of radiations and radioactive materials.

Radiation is potentially harmful, and exposure to it should be monitored continually and controlled. No unnecessary exposure should be allowed. Equipment and facilities should be designed so that exposure of the personnel and the public is kept down to a minimum and not up to a limit. (The term ALARA is analogous to the term optimization favored by ICRP.) No exposure at all should be permitted without considering the benefits that may be derived from that exposure and the relative risks of alternative approaches.

Of course, the ultimate problem is determining what is “reasonable.” There is also the question: How much expense is justified to reduce the exposure of personnel by a given amount? As a rule of thumb in the nuclear power industry in the United States, ALARA has a cash value of about \$1,000 per 10 mSv. If the exposure of one person to 10 mSv can be avoided by the expenditure of this amount of money, it is considered reasonable. If the cost is more, it is considered unreasonable, and the exposure is allowed. However, the \$1,000 per 10 mSv figure applies specifically to low-dose levels. At higher dose levels at which the accumulation of an additional exposure may threaten a worker’s job by exceeding the lifetime dose limit and then the cash value of avoiding a 10-mSv exposure may be closer to \$10,000. This sort of choice seldom has to be made in a hospital setting except, for example, in the purchase of remote afterloading equipment for brachytherapy.

PROTECTION OF THE EMBRYO/FETUS

The NCRP recommends a monthly limit of 0.5 mSv to the embryo or fetus once a woman declares her pregnancy. In contrast to this, the ICRP recommends a limit of 2 mSv to the surface of the woman’s abdomen (lower trunk) for the remainder of her pregnancy. These recommendations are essentially similar and are designed to limit the risk of mental retardation, other congenital malformations, and carcinogenesis. The NCRP and ICRP no longer recommend specific controls for occupationally exposed women *until* the pregnancy is declared. There is a provision that a declared pregnancy can later be “undeclared” if the female worker so desires.

Internally deposited radionuclides pose special problems for protection of the embryo or fetus. Some remain in the body for long periods, and the doses delivered to fetal organs are not well known for all radionuclides. Consequently,

particular care should be taken to limit the intake of radionuclides by pregnant women so that the equivalent dose to the embryo or fetus would not exceed the recommended limit.

EMERGENCY OCCUPATIONAL EXPOSURE

Under normal conditions, only actions involving the saving of life justify acute exposures in excess of the annual effective dose limit. The use of volunteers for exposures during emergency actions is desirable. If possible, older workers with low lifetime accumulated effective doses should be chosen from among the volunteers. Exposure during emergency actions that do not involve the saving of life should be controlled, to the extent possible, at the occupational exposure limits. If this cannot be accomplished, the NCRP and ICRP recommendation of 0.5 Sv should be applied.

If, for lifesaving or equivalent purposes, the exposure may approach or exceed 0.5 Sv to a large portion of the body, the worker not only needs to understand the potential for acute effects but also should have an appreciation of the substantial increase in his or her lifetime risk of cancer. If the possibility of internal exposures also exists, this should also certainly be taken into account.

EXPOSURE OF PERSONS YOUNGER THAN 18 YEARS OF AGE

For educational and training purposes, it may be necessary and desirable to accept occasional exposure of persons younger than the age of 18 years, in which case an annual effective dose limit of 1 mSv should be maintained (NCRP).

EXPOSURE OF MEMBERS OF THE PUBLIC (NONOCCUPATIONAL LIMITS)

The limitation of radiation exposure for members of the public from human-made sources is inevitably arbitrary because it cannot be based on direct experience. Various risks of accident and death regularly faced by members of the public vary greatly; the numbers range from 10^{-4} to 10^{-6} per year. Depending on their nature, these risks seem to be accepted without much thought. At the same time, everyone is exposed to natural background radiation of about 1 mSv annually, excluding radon, which may result in a mortality risk of 10^{-4} to 10^{-5} annually.

Based on these considerations, the NCRP recommended limits for human-

made sources other than medical are as follows: For *continuous* or *frequent* exposure, the annual effective dose should not exceed 1 mSv. It is clear, however, that larger exposures to more limited groups of people are not especially hazardous, provided they do not occur often to the same groups. Consequently, a maximum permissible annual effective dose equivalent of 5 mSv is recommended as a limit for *infrequent* exposure. Medical exposures are excluded from these limitations because it is assumed that they confer personal benefit to the exposed person.

Because some organs and tissues are not necessarily protected against tissue reactions in the calculation of effective dose, the hands and feet as well as localized areas of the skin are subject to an annual dose limit of 50 mSv, whereas the dose limit to the lens of the eye is 15 mSv per year.

The fact that the terms *frequent* and *infrequent* in the public dose limits are not defined has caused some confusion. Nevertheless, the intention of the NCRP is laudable, namely, that exceptions to the 1 mSv per year for members of the public may be justified on the basis of significant benefit either to those exposed or to society as a whole. Here are three examples:

1. For workers who come into contact with a coworker who is a radionuclide therapy patient, the annual effective dose limit of 1 mSv may be exceeded under carefully controlled conditions for a small number of such workers who may receive up to 5 mSv annually.
2. For adult family members exposed to a patient who has received radionuclide therapy, the annual effective dose limit is 50 mSv. Thus, adult family members under this circumstance are considered separate from other members of the public and should receive appropriate training and individual monitoring.
3. Another example is the inadvertent irradiation of a stowaway in a cargo container irradiated with a pulsed fast neutron analysis system to assess the contents of the container. The NCRP has recommended that such systems be designed and operated in a manner such that the exposure of a stowaway would result in an effective dose of less than 1 mSv for that occurrence. However, an effective dose of up to 5 mSv would be permissible for such an occurrence if necessary to achieve national security objectives.

A more contentious issue is the exposure of members of the public to scattered radiation in a radiology department. For example, exposure of an individual member of the public to scattered radiation in the waiting room of a

radiology facility is infrequent for a given individual. On the other hand, a secretary or receptionist may be exposed frequently or continuously, so the desk area must be protected to a lower level, which can be an expensive proposition. It might be tempting to reclassify the office personnel as “radiation workers,” but to do so would offend all the basic principles of radiation protection.

EXPOSURE TO INDOOR RADON

Radon levels vary enormously with different localities, depending on the composition of the soil and the presence of cracks or fissures in the ground, which allow radon to escape to the surface. Many homes in the United States and Europe consequently contain an appreciable quantity of radon gas, which enters the living quarters through the basement. Insulating and sealing houses increased greatly because of the escalating cost of heating oil in the 1970s, and this has exacerbated the radon problem because a well-sealed house allows fewer exchanges of air with the outside and consequently results in a greater concentration of radon. Radon is a noble gas and is itself relatively nonhazardous because if breathed in, it is breathed out again without being absorbed. In a confined space such as a basement, however, the decay of radon leads to the accumulation of progeny that are solids, which stick to particles of dust or moisture and tend to be deposited on the bronchial epithelium. These progeny emit α -particles and cause intense local irradiation.

An extreme example is the famous case of Stanley Watras who went to work in a nuclear power station but set off the radiation monitors as he entered the plant due to the accumulation of radon progeny products deposited on his clothes. It turned out that he lived in a house with the highest concentration of radon ever measured.

Indoor radon currently is perceived to be an important problem involving radiation exposure of the public. In the United States and most European countries, the mean radon concentration in homes is in the range of 20 to 60 Bq/m^3 , with higher mean values of about 100 Bq/m^3 in Finland, Norway, and Sweden. Converting radon concentrations into dose to the bronchial epithelium involves many uncertainties because such conversion depends on the model used and the assumptions made. One widely used conversion factor equates an air concentration of 20 Bq/m^3 with an effective dose to the bronchial epithelium of 1 mSv per year.

The EPA has set the **action level** at about 148 Bq/m^3 , suggesting that

remedial action should be taken to reduce radon levels if they are higher than this. The action level is about 4 times the average radon concentration in homes, but it is estimated that about 1 in 12 homes in the United States—about 6 million in all—have radon concentrations above this action level. In the past, other countries, including Germany, Great Britain, and Canada, had much higher action levels, but these are all now under review.

The BEIR VI Committee of the National Academy of Sciences published a report on the health effects of radon in 1999. The committee's preferred central estimate was that about 1 in 10 to 1 in 7 of all lung cancer deaths—amounting to 15,400 to 21,800 per year in the United States—can be attributed to radon. There are considerable uncertainties involved, and the number could be as low as 3,000 or as high as 32,000 each year. Most of the radon-related lung cancers occur among smokers because of the synergism between smoking and radon. Among those who have never smoked, the committee's best estimate is that of the 11,000 lung cancer deaths each year, 1,200 to 2,900 were radon related. Of the deaths that can be attributed to radon, perhaps one-third could be avoided by reducing radon in homes in which it is above the “action level” of 148 Bq/m³ recommended by the EPA.

DE MINIMIS DOSE AND NEGLIGIBLE INDIVIDUAL DOSE

Collective dose to a population has little meaning without the concept of **de minimis** dose. The idea is to define some very low threshold below which it would make no sense to make any additional effort to reduce exposure levels further. For example, suppose there is a release of radioactivity from a reactor that dissipates into the atmosphere, blows around the world, and eventually exposes many hundreds of millions of people to very low doses. The doses may be so low that the biologic effects are negligible, but because the number of persons involved is so large, the product of the dose and the number of persons would dominate the collective dose. The term *de minimis* comes from the legal saying *De minimis non curat lex*, which roughly translates to “The law does not concern itself with trifles.”

Dr. Merril Eisenbud in an NCRP publication quotes this limerick of dubious origin.

There was a young lawyer named
Rex, who was very deficient in sex

When charged with exposure
He said with composure
De minimis non curat lex

The concept of *de minimis* dose has been espoused by the NCRP in the form of **negligible individual dose**, defined here to be the dose below which further efforts to reduce radiation exposure to the person are unwarranted. The NCRP considers an annual effective dose of 0.01 mSv to be a negligible individual dose. This dose is associated with a risk of death between 10^{-6} and 10^{-7} , which is considered trivial compared with the risk of fatality associated with ordinary and normal societal activities and, therefore, can be dismissed from consideration of additional radioprotective measures.

RADIATION DETERIMENT

Radiation detriment is a concept introduced by ICRP in order to quantify the harmful effects of radiation exposure to different parts of the body, taking into account the severity of the disease in terms of lethality, loss of quality of life, and years of life lost. Detriment includes a small component for heritable effects, a large component for lethal cancers, and an allowance for nonlethal cancers, which, although they do not cause death, nevertheless have an impact on quality of life. ICRP has suggested the detriment-adjusted risk coefficients for stochastic effects after exposure of the whole population to radiation at LDR to be 5.5% per sievert for cancer (lethal and nonlethal combined) and 0.2% per sievert for heritable effects, making a total of 5.7% per sievert.

Recent surveys indicate that the average annual dose to monitored radiation workers with measurable exposures is about 2 mSv. This results in a detriment of about 1 in 10,000, which is comparable to the death rate in what are considered to be “safe” industries such as trade and government service.

NATIONAL COUNCIL ON RADIATION PROTECTION AND MEASUREMENTS AND THE INTERNATIONAL COMMISSION ON RADIOLOGICAL PROTECTION COMPARED

At present, there are differences in the recommendations of the national and international bodies regarding the maximum permissible effective dose for occupational exposure (stochastic effects). The differences are highlighted in

Table 16.5. Both bodies recommend a maximum of 50 mSv in any 1 year, but the NCRP adds a lifetime cumulative limit of the person's age \times 10 mSv, whereas the ICRP adds a limit of 20 mSv per year averaged over defined periods of 5 years.

The practical consequence of this difference is that a radiation worker starting at, for example, age 18 years can accumulate a larger dose under the NCRP recommendations in the early years up to an age in the mid-30s but later in life could accumulate a larger dose under the ICRP recommendations. Under NCRP recommendations, a new radiation worker could receive 50 mSv in each of several consecutive years until the limit of age \times 10 mSv kicks in. Under ICRP rules, the average cannot exceed 20 mSv per year over a 5-year period, so one or two 50-mSv years would have to be followed by several years at very low exposure levels. If individuals were exposed throughout their working lives to the maximum permissible dose, the excess risk of stochastic effects (cancer and heritable effects) would be about the same under NCRP or ICRP recommendations. Under the NCRP, a person occupationally exposed from 18 to 65 years of age could receive a total dose of 650 mSv. Under the ICRP, the same person could receive 940 mSv, but less would be received in the early years and more at later ages, by which time individuals are less sensitive to radiation carcinogenesis.

The NCRP scheme is less restrictive for a few workers in the nuclear power industry who tend to receive large effective doses in their early years working on nuclear reactors. Later in life, these individuals tend to occupy supervisory or administrative positions and receive little, if any radiation. To cope with those who do not, the NCRP has added the extra recommendation that this limit, age \times 10 mSv, can be relaxed *in individual cases after counseling*, if implementation of the recommendation would mean loss of a job.

It should be emphasized that few persons exposed occupationally in a medical setting receive doses anywhere near the recommended limits, with the exception perhaps of some interventional radiologists.

THE HISTORY OF THE CURRENT DOSE LIMITS

In 1956, the ICRP reduced the dose limit for radiation workers from 0.3 R per week to 0.1 R per week. This corresponds to 5 R per year, which is still the maximum permissible dose allowed in 1 year to radiation workers today, except that the unit has changed and it is now called 50 mSv. This dose limit suggested by ICRP was based entirely on genetic effects in the fruit fly, *Drosophila*.

In the half century or so that has elapsed since then, concern for genetic effects, or heritable effects as we now call them, has declined steadily, first because of the availability of mouse data and, more recently, because of doubts about the relevance of specific locus mutations in mice. In the meantime, concern for radiation-induced carcinogenesis has increased as more and more solid cancers appeared in the A-bomb survivors. In the 1950s, heritable effects were considered to be the most important consequence of low doses of ionizing radiation.

To cope with these changing perceptions, and what was considered to be an alarming increase in cancer among the A-bomb survivors, ICRP in 1991 introduced a second limit. As well as the 50 mSv limit in any 1 year, they required that the average over 5 years should not exceed 20 mSv per year. NCRP in 1993 coped with the perceived increase in cancer risk by adding a cumulative limit of age \times 10 mSv to the existing annual limit of 50 mSv. Although these differ in detail, with NCRP allowing workers more doses in earlier years and less later on, the respective limits recommended by the two organizations are quite similar, the NCRP being a little more restrictive with respect to overall lifetime risks. Both organizations aimed to make the risks to radiation workers comparable to other “safe” industries, and both sets of recommendations would result in a radiation-induced cancer mortality risk of about 3%.

However, although the NCRP Report No. 116 was published in 1993 and included the cumulative limit of age \times 10 mSv, the Council only makes “recommendations” because the legal responsibility for the implementation of radiation safety is in the hands of the NRC, the DOE, and state or city bureaus of radiation control. In fact, the US NRC has never adopted the cumulative limit, and to this day, the annual limit is a total effective dose equivalent of 50 mSv. Consequently, if a radiation worker starts at age 18 years and works at the dose limit until retiring at age 65 years, he or she would face a radiation-induced cancer incidence of 19% and a cancer mortality of 10.8% ([Table 16.6](#)). This is in marked contrast to the corresponding figures that would be applicable if the ICRP or NCRP limitations were followed, when the radiation-induced cancer incidence would be 6% and mortality would be 3%. These estimates are based on data published in the BEIR VII report. It is not widely appreciated that radiation workers in the United States are allowed such significantly higher cancer risks than other industrialized countries that, by and large, adopt and enforce the recommendations of ICRP.

Table 16.6 Cancer Risks for a Radiation Worker Receiving the Maximum

Permissible Dose from Age 18 to 65 years

RULE	TOTAL DOSE	CANCER INCIDENCE	CANCER MORTALITY
NRC 50 mSv/y	2.35 Sv	19.0	10.8
NCRP 10 mSv × age	0.65 Sv	6.1	3.3

DOSE RANGES

Doses to which individuals are exposed vary enormously by several orders of magnitude. Figure 16.4 attempts to put this into perspective by comparing the ranges of doses used in medicine with doses received occupationally and from natural sources.

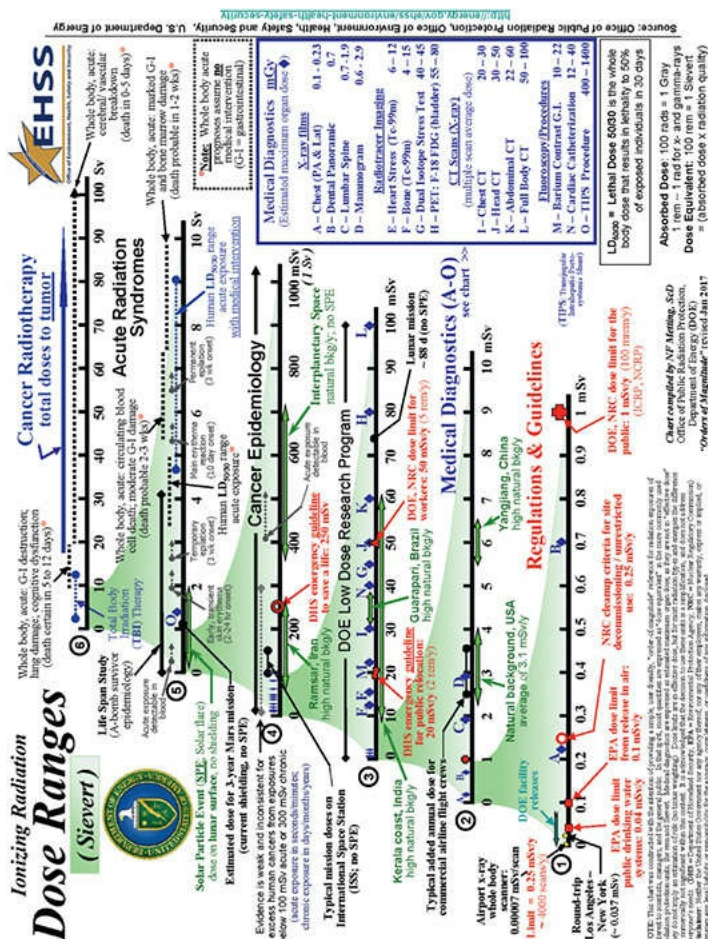


FIGURE 16.4 This chart compiled by Dr. Noelle Metting, Office of Science of the U.S. Department of Energy, puts into perspective the different dose ranges relevant to radiation therapy, diagnostic radiology, and background radiation.

SUMMARY OF PERTINENT CONCLUSIONS

The objectives of radiation protection are to **prevent** clinically significant tissue reactions by keeping doses below the practical threshold and to **limit** the risk of stochastic effects (cancer and heritable effects) to a reasonable level in relation to societal needs, values, and benefits gained.

Justification is one of the basic principles of radiation protection; a practice involving exposure to radiation should produce sufficient benefit to the exposed individual or to society to offset the radiation detriment it causes.

W_R are approximate values of the RBE applicable to low doses and relevant to carcinogenesis and heritable effects. Values of W_R are chosen by the ICRP based on experimental RBE values with a large judgmental factor.

Equivalent dose is the product of absorbed dose and W_R . The unit is sievert for an absorbed dose in gray (Gy). ICRP has recommended a new name for this quantity—radiation weighted dose—and is considering a new name for the unit.

W_T reflect the susceptibility of different organs or tissues to carcinogenesis or heritable effects.

Effective dose is the sum of the weighted equivalent doses for all irradiated tissues and organs multiplied by the appropriate W_T .

Committed equivalent dose is the integral over 50 years of the equivalent dose after the intake of a radionuclide.

Committed effective dose is the integral over 50 years of the effective dose in the case of an incorporated radionuclide.

Collective effective dose is a quantity for a population and is the sum of effective doses to all members of that population. The unit is person-sievert.

Collective committed effective doses applies to a population ingesting or inhaling radionuclides and is the integral over 50 years of the effective dose over the entire population.

All radiation exposures are governed by the ALARA principle.

No occupational exposure should be permitted before 18 years of age.

The effective dose in any 1 year should not exceed 50 mSv (NCRP).

The individual worker's cumulative lifetime effective dose should not exceed age in years \times 10 mSv (NCRP). However, to date, the NRC has not adopted this cumulative limit.

To limit tissue reactions, the dose limit to the lens of the eye is 50 mGy per year, and the dose limit to localized areas of the skin, hands, and feet is 500 mSv per year.

Once a pregnancy is declared, the NCRP recommends a monthly limit of 0.5 mSv to the embryo or fetus.

Specific controls for occupationally exposed women are no longer recommended until a pregnancy is declared.

Internally deposited radionuclides pose a special problem for protection of the embryo or fetus; particular care should be taken to limit intake.

Emergency occupational exposures normally justify doses in excess of the recommended limits only if life-saving actions are involved. Volunteers from among older workers with low lifetime accumulated effective doses should be chosen in emergencies in which the exposure may be up to 0.5 Sv. If the exposure may exceed 0.5 Sv, the worker should be counseled about the short- and long-term possible consequences.

For educational or training purposes, it may sometimes be desirable to accept radiation exposures of persons younger than 18 years of age, in which case the annual effective dose limit of 1 mSv should be maintained.

The annual effective dose limit for members of the public is 1 mSv, except for infrequent exposures in which the limit may be 5 mSv. Medical x-rays are excluded from these limitations because they are assumed to confer personal benefit.

For tissue reactions (deterministic effects), the dose limit for members of the general public is 50 mSv to the hands and feet and to localized areas of the skin and 15 mSv to the lens of the eye.

Indoor radon is perceived to be the most important problem involving radiation exposure of the general public to naturally occurring radiation. Remedial action in homes is recommended by the EPA if the radon concentration exceeds 148 Bq/m³.

Negligible individual dose is the dose below which further expenditure to improve radiation protection is unwarranted. The negligible individual dose is an annual effective dose of 0.01 mSv, which carries a risk of between 10^{-6} and 10^{-7} of carcinogenesis or heritable effects.

ICRP introduced the concept of “detriment” to quantify the harmful effects of radiation exposure in different parts of the body, taking account of the severity of the disease in terms of lethality, loss of quality of life, and years of life lost.

A uniform whole body equivalent dose of 1 Sv to an adult radiation worker is assumed to result in a total detriment of about 5.7% per Sv. This is made up of a risk of fatal and nonfatal cancer together with a small contribution from severe heritable effects.

The average annual equivalent dose to monitored radiation workers is about 2 mSv. This involves a total detriment of about one in 10,000, which is comparable to the annual risk of a fatal accident in a “safe” industry such as trade or government service.

The NCRP and ICRP differ in two important recommendations:

1. The effective dose limit for occupational exposure (stochastic effects). The NCRP recommends a lifetime cumulative limit of age \times 10 mSv, with a limit in any year of 50 mSv. The ICRP recommends a limit of 20 mSv per year averaged over defined periods of 5 years, with a limit in any year of 50 mSv.
2. The dose limit to the developing embryo or fetus once a pregnancy is declared. The NCRP recommends a monthly limit of 0.5 mSv to the embryo or fetus. The ICRP recommends a limit of 2 mSv to the surface of the woman’s abdomen for the remainder of pregnancy.

GLOSSARY OF TERMS

absorbed dose: The energy imparted to matter by ionizing radiation per unit mass of irradiated material at the place of interest. The unit is gray (Gy), defined as an energy absorption of 1 J/kg.

ALARA (as low as reasonably achievable): Economic and social factors being taken into account. This is identical to the principle of optimization of protection used by the ICRP.

annual limit on intake: The activity of a radionuclide taken into the body

during a year that would provide a committed equivalent dose to a person, represented by a reference “man,” equal to the occupational dose limit set by recommending and regulating bodies. The annual limit normally is expressed in.

becquerel (Bq): The special name for the unit of activity. 3.7×10^{-10} Bq = 1 Ci.

collective committed effective dose: Applies to a population ingesting or inhaling radionuclides that deposit their dose over a prolonged period of time and is the integral of the effective dose over the entire population out to a period of 50 years.

collective effective dose: Applies to a group of persons and is the sum of the products of the effective dose and the number of persons receiving that effective dose.

collective equivalent dose: Applies to a group of persons and is the sum of the products of the equivalent dose and the number of persons receiving that equivalent dose.

committed effective dose: The sum of the committed organ or tissue equivalent doses resulting from an intake multiplied by the appropriate tissue weighting factors.

committed equivalent dose: The equivalent dose averaged throughout a specified tissue in the 50 years after intake of a radionuclide into the body.

deterministic effects: See *tissue reactions*.

effective dose: The sum over specified tissues of the products of the equivalent dose in a tissue and the appropriate W_T for that tissue.

equivalent dose: A quantity used for radiation protection purposes that takes into account the different probability of effects that occur with the same absorbed dose delivered by radiations of different quality. It is defined as the product of the averaged absorbed dose in a specified organ or tissue and the W_R . The unit of equivalent dose is the sievert (Sv). The ICRP is now recommending that this be called the *radiation weighted dose*.

genetically significant dose (GSD): The dose to the gonads weighted for the age and sex distribution in those members of the population expected to have offspring. The genetically significant dose is measured in sievert.

gray (Gy): The special name for the SI unit of absorbed dose, kerma, and specific energy imparted. 1 Gy = 1 J/kg.

negligible individual dose: A level of effective dose that can be dismissed as insignificant and below which further efforts to improve radiation protection are not justified. The recommended negligible individual dose is 0.01 mSv per year.

nonstochastic effects: Previous term for deterministic effects now tissue reactions.

organ or tissue weighting factor (W_T): See *tissue weighting factor*.

rad: The old unit for absorbed dose, kerma, and specific energy imparted. One rad is 0.01 J absorbed per kilogram of any material (also defined as 100 erg/g). The term is being replaced by the gray: 1 rad = 0.01 Gy.

radiation weighted dose: New name recommended by ICRP for equivalent dose.

radiation weighting factor (W_R): A factor used for radiation protection purposes that accounts for differences in biologic effectiveness between different radiations. The W_R is independent of the W_T .

relative biologic effectiveness (RBE): A ratio of the absorbed dose of a reference radiation to the absorbed dose of a test radiation to produce the same level of biologic effect, other conditions being equal. It is the quantity that is measured experimentally.

rem: The old unit of equivalent dose or effective dose. It is the product of the absorbed dose in rad and modifying factors and is being replaced by the sievert.

sievert (Sv): The unit of equivalent dose or effective dose in the SI system. It is the product of absorbed dose in gray and modifying factors. 1 Sv = 100 rem.

stochastic effects: Effects for which the probability of their occurring, rather than their severity, is a function of radiation dose without threshold. More generally, stochastic means random in nature.

tissue reactions: New ICRP term for what used to be called a deterministic effect. Refers to damage due to cells being killed and removed from a tissue or organ as a result of radiation exposure. Characteristics include a threshold in dose; the severity of the effect increases with dose above the threshold and is thought to be caused by damage to many cells. Examples include fibrosis, effects on fertility, and lethality due to total body exposure. Ocular cataracts used to be classified as such, but there are now some doubts.

tissue weighting factor (W_T): A factor that indicates the ratio of the risk of stochastic effects attributable to irradiation of a given organ or tissue to the total

risk if the whole body is uniformly irradiated. Organs that have a large W_T are those that are susceptible to radiation-induced carcinogenesis (such as the breast or thyroid) or to hereditary effects (the gonads).

working level: The amount of potential α -particle energy in a cubic meter of air that results in the emission of 2.08×10^{-5} J of energy.

working level month: A cumulative exposure, equivalent to exposure to one working level for a working month (170 hours), that is, $2 \times 10^{-5} \text{ J} \cdot \text{m}^{-3} \times 170 = 3.5 \times 10^{-3} \text{ J} \cdot \text{h} \cdot \text{m}^{-3}$.

BIBLIOGRAPHY

Burkhart RL, Gross RE, Jans RG, et al, eds. *Recommendations for Evaluation of Radiation Exposure from Diagnostic Radiology Examinations*. Health and Human Services. Springfield, VA: U.S. Food and Drug Administration, National Technical Information Service; 1985. Publication no. 85-8247.

Committee on the Biological Effects on Ionizing Radiations. *Health Effects of Exposure to Radon : BEIR VI*. Washington, DC: National Academy Press, National Research Council; 1988.

International Commission on Radiation Units and Measurements. *Determination of Dose Equivalents Resulting from External Radiation Sources*. Bethesda, MD: International Commission on Radiation Units and Measurements; 1985. ICRU report 39.

International Commission on Radiation Units and Measurements. *The Quality Factor in Radiation Protection: Report of a Joint Task Group of the ICRP and the ICRU to the ICRP and ICRU*. Bethesda, MD: International Commission on Radiation Units and Measurements; 1986. ICRU report 40.

International Commission on Radiological Protection. *Biological Effects after Prenatal Irradiation (Embryo and Fetus)*. Oxford, United Kingdom: Elsevier Science; 2004. ICRP publication 90.

International Commission on Radiological Protection. *Developing a Unified Index of Harm*. New York, NY: Pergamon Press; 1985. ICRP publication 45.

International Commission on Radiological Protection. *Recommendations of the ICRP*. New York, NY: Pergamon Press; 1977. ICRP publication 26.

International Commission on Radiological Protection. *1990 Recommendations of the International Commission on Radiological Protection*. New York, NY:

- Pergamon Press; 1991. ICRP publication 60.
- International Commission on Radiological Protection. *Relative Biological Effectiveness (RBE), Quality Factor (Q), and Radiation Weighting Factor (W_R)*. Oxford, United Kingdom: Elsevier Science; 2004. ICRP publication 92.
- International Commission on Radiological Protection. *The 2007 Recommendations of the International Commission on Radiological Protection*. New York, NY: Elsevier; 2007. ICRP publication 103.
- Kato H, Schull WJ. Studies of the mortality of A-bomb survivors. 7. Mortality, 1950–1978: part I. Cancer mortality. *Radiat Res.* 1982;90:395–432.
- National Council on Radiation Protection and Measurements. *Basic Radiation Protection Criteria*. Bethesda, MD: National Council on Radiation Protection and Measurements; 1971. NCRP report no. 39.
- National Council on Radiation Protection and Measurements. *Comparative Carcinogenicity of Ionizing Radiation and Chemicals*. Bethesda, MD: National Council on Radiation Protection and Measurements; 1989. NCRP report no. 96.
- National Council on Radiation Protection and Measurements. *Evaluation of Occupational and Environmental Exposures to Radon and Radon Daughters in the United States*. Bethesda, MD: National Council on Radiation Protection and Measurements; 1984. NCRP report no. 78.
- National Council on Radiation Protection and Measurements. *Implementation of the Principle of As Low As Reasonably Achievable (ALARA) for Medical and Dental Personnel*. Bethesda, MD: National Council on Radiation Protection and Measurements; 1990. NCRP report no. 107.
- National Council on Radiation Protection and Measurements. *Limitation of Exposure to Ionizing Radiation*. Bethesda, MD: National Council on Radiation Protection and Measurements; 1993. NCRP report no. 116.
- National Council on Radiation Protection and Measurements. *Radiation Protection in Educational Institutions*. Bethesda, MD: National Council on Radiation Protection and Measurements; 1966. NCRP report no. 32.
- National Council on Radiation Protection and Measurements. *Recommendations on Limits for Exposure to Ionizing Radiation*. Bethesda, MD: National Council on Radiation Protection and Measurements; 1987. NCRP report no. 91.

National Council on Radiation Protection and Measurements. *Review of NCRP Radiation Dose Limit for Embryo and Fetus in Occupationally Exposed Women*. Bethesda, MD: National Council on Radiation Protection and Measurements; 1977. NCRP report no. 53.

National Research Council. *Health Effects of Exposure to Low Levels of Ionizing Radiation: BEIR V*. Washington, DC: The National Academies Press; 1990.

National Research Council. *The Effects on Populations of Exposure to Low Levels of Ionizing Radiation: 1980*. Washington, DC: The National Academies Press; 1980.

National Safety Council. *Accident Facts 1976*. Chicago, IL: National Safety Council; 1977.

National Safety Council. *Accident Facts 1989*. Chicago, IL: National Safety Council; 1990.

United Nations Scientific Committee on the Effects of Atomic Radiation. *Biological Effects of Pre-Natal Irradiation. Presented before the 35th Session of UNSCEAR*. New York, NY: United Nations Scientific Committee on the Effects of Atomic Radiation; 1986.

United Nations Scientific Committee on the Effects of Atomic Radiation. *Ionizing Radiation: Sources and Biological Effects. Report to the General Assembly, with Annexes*. New York, NY: United Nations Scientific Committee on the Effects of Atomic Radiation; 1982. Publication no. E.82.IX8.

United Nations Scientific Committee on the Effects of Atomic Radiation. *Sources and Effects of Ionizing Radiation. Report to the General Assembly, with Annexes*. New York, NY: United Nations Scientific Committee on the Effects of Atomic Radiation; 1977. Publication no. E.77.IXI.



For Students of Radiation Oncology

chapter 17

Molecular Techniques in Radiobiology

Historical Perspectives

The Structure of DNA

RNA and DNA

Transcription and Translation

The Genetic Code

Amino Acids and Proteins

Restriction Endonucleases

Vectors

Plasmids

Bacteriophage λ

Bacterial Artificial Chromosomes

Viruses

Libraries

Genomic Library

cDNA Library

Hosts

Escherichia Coli

Yeast

Mammalian Cells

DNA-mediated Gene Transfer

Agarose Gel Electrophoresis

Polymerase Chain Reaction

Polymerase Chain Reaction-mediated Site-directed Mutagenesis

Gene-Cloning Strategies

Genomic Analyses

Mapping

DNA Sequence Analyses

Polymorphisms or Mutations

Comparative Genome Hybridization

Gene Knockout Strategies

Clustered Regularly Interspaced Short Palindromic Repeats and CRISPR Associated Protein

Homologous Recombination to Knockout Genes

Knockout Mice

Gene Expression Analysis

Northern Blotting

RNA Interference

Reverse Transcription Polymerase Chain Reaction

Quantitative Real-Time Polymerase Chain Reaction

Genetic Reporters

Promoter Bashing

Chromatin Immunoprecipitation

Protein–DNA Interaction Arrays (Chromatin Immunoprecipitation-Chips)

Microarrays to Assay Gene Expression

RNA-Seq to Assay Gene Expression

Chromatin Immunoprecipitation-Seq

Protein Analysis

Western Blotting

Antibody Production

Immunoprecipitation

Far Western Blotting

Fluorescent Proteins

Two-Hybrid Screening

Split Luciferase Complementation Assay

Proteomics

Two-Dimensional Electrophoresis

Databases and Sequence Analysis

Summary of Pertinent Conclusions

Glossary of Terms

Bibliography

HISTORICAL PERSPECTIVES

Recombinant DNA technology has revolutionized research in biology. It allows questions to be asked that were unthinkable just a few years ago. It is also a technology that is moving so fast that anything written in a book is likely to be out of date before it appears in print. This technology is invading every field of biologic research, and radiobiology is no exception. To keep abreast of developments in the field, it is essential to know what recombinant DNA technology is and how it works. A detailed description is beyond the scope of this book; for a more extensive account, the interested reader is referred to several excellent volumes that have appeared in recent years and are listed in the “Bibliography.” The goal here is to provide an overview of core recombinant techniques and core technologies that are commonly used today in radiobiologic research.

The birth of molecular biology could be ascribed to the one-page publication in *Nature* in 1953 by James Watson and Francis Crick describing the structure of **DNA**. In short order, this work led the way to breaking the **genetic code** and understanding the process of **transcription** of DNA to **messenger RNA (mRNA)** and the **translation** of mRNA into proteins. At about the same time, in the late 1940s and early 1950s, Linus Pauling realized that three-dimensional structures were built by **amino acids** and folded into proteins. The whole concept emerged that the sequence of bases, which coded for a protein, ultimately determined function.

These remarkable discoveries were followed by a period of limited progress focusing mainly on simple systems such as viruses, bacteriophages, and bacteria, until new tools and techniques to work with DNA were perfected.

Recombinant DNA technology got its start with the first successful cloning experiment by Stanley Cohen, in which he joined two DNA fragments together (a **plasmid** containing a tetracycline resistance **gene** with a kanamycin resistance gene), introduced this recombinant molecule into *Escherichia coli* and demonstrated that the *E. coli* with the plasmid now had dual **antibiotic resistance**.

This simple experiment was only possible because of the simultaneous development of several techniques for cutting DNA with restriction enzymes, joining the fragments together with **ligases**, and using *E. coli* as a host to take up foreign DNA packaged as plasmid vectors. This critical demonstration was quickly followed by the development of methods to sort pieces of DNA and

RNA by size using gel electrophoresis. The stage was set for an explosion of new techniques.

What follows is a brief and simplified description of these techniques and technologies that followed.

THE STRUCTURE OF DNA

The structure of DNA arrived at by Crick and Watson is elegant in its simplicity. The molecule is composed of two antiparallel helices, looking rather like a gently twisted ladder. The rails of the ladder, which run in opposite directions, contain units of deoxyribose sugar alternating with a phosphate. Each rung is composed of a pair of nucleotides, a **base pair**, held together by hydrogen bonds (Fig. 17.1). There is a complementary relationship between the bases: Adenine always pairs with thymine, and cytosine always pairs with guanine (**complementary nucleotides**). Thus, the **nucleotide** sequence of one strand of the DNA helix determines the sequence of the other.

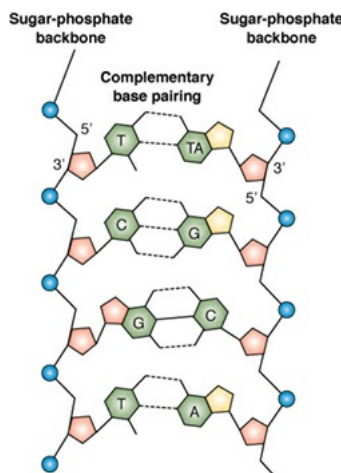


FIGURE 17.1 The DNA double helix is held together by hydrogen bonds between base pairs. These are shown as dotted lines in the figure.

This structure explains how a DNA molecule replicates during cell division so that each progeny cell receives an identical set of instructions. The hydrogen bonds between the base pairs break, allowing the DNA ladder to unzip (Fig. 17.2). Each half then constitutes a **template** for the reconstruction of the other half. Two identical DNA molecules result, one for each progeny cell.

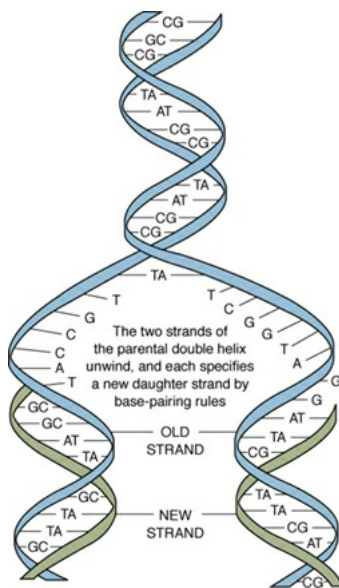


FIGURE 17.2 The complementary nature of DNA is at the heart of its capacity for self-replication. The two strands of the parental DNA unwind, and the hydrogen bonds break. Each strand then becomes a template to specify a new progeny strand obeying the base-pairing rules.

RNA AND DNA

Unlike DNA, which is located primarily in the nucleus, **RNA** is found throughout the cell. Within the nucleus, RNA is concentrated in the *nucleoli*, dense granules attached to chromosomes. The sugar molecule in RNA is a *ribose* (hence its name, *ribonucleic acid*), whereas in DNA, the sugar molecule is a *deoxyribose* (hence its name, *deoxyribonucleic acid*). In both DNA and RNA, the bases are made up of two *purines* and two *pyrimidines*. The two purines, *adenine* and *guanine*, as well as the pyrimidine, *cytosine*, are common to both DNA and RNA. However, although *thymine* is found only in DNA, the structurally similar pyrimidine *uracil* appears in RNA (Fig. 17.3).

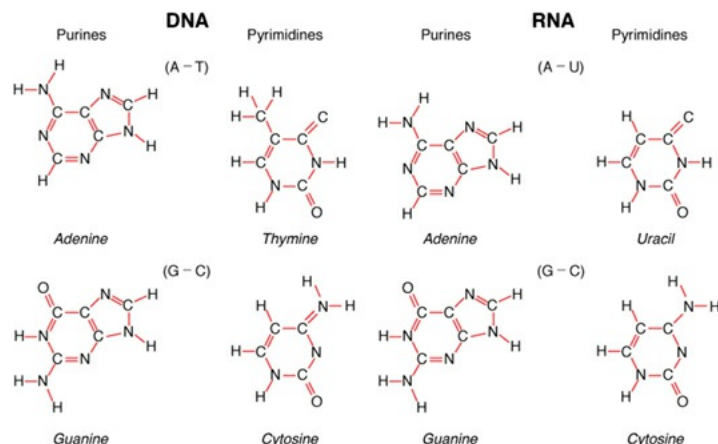


FIGURE 17.3 Illustrating the pairing of complementary bases in DNA and

RNA. **Left:** DNA contains the purines adenine (A) and guanine (G) as well as the pyrimidine's thymine (T) and cytosine (C). A purine always pairs with a pyrimidine; specifically, A pairs with T, and G pairs with C. **Right:** RNA contains uracil (U) instead of thymine. In this case, A pairs with U, and G pairs with C.

TRANSCRIPTION AND TRANSLATION

The flow of genetic information from DNA to protein requires a series of steps. In the first step, the DNA code is *transcribed* in the nucleus into mRNA by **RNA polymerase** (Fig. 17.4). It is at once obvious from a comparison of a mature cytoplasmic mRNA transcript with its parental DNA that the mRNA sequence is not contiguous with the DNA sequence. Some blocks of DNA sequence are represented in the mRNA; others are not. DNA is transcribed into pre-mRNA. During the process of splicing, large regions called *introns* are removed and the remaining *exons* are joined together into what is termed an **open reading frame**. Only the **exons** of the DNA are translated. Almost all genes from higher eukaryotes contain introns; genes may have only a few or as many as 100 introns. Typically, introns make up the bulk of the gene. For example, in the gene involved with muscular dystrophy, the mRNA consists of 14,000 bases, whereas the gene spans more than 2 million base pairs. The mRNA transcript associates with a ribosome, at which, with the help of ribosomal RNA and **transfer RNA (tRNA)**, the mRNA message is translated into a protein.

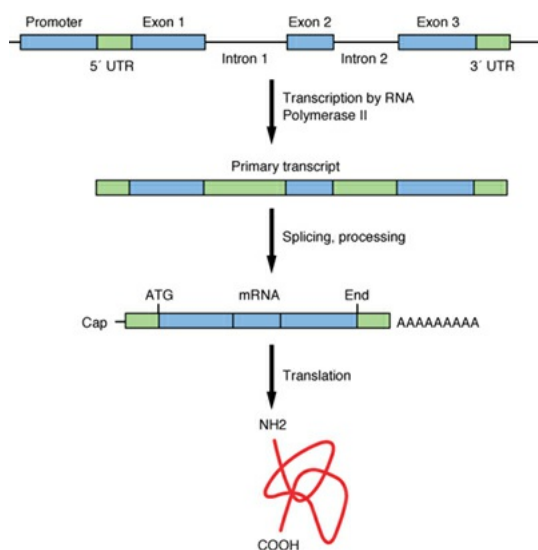


FIGURE 17.4 Transcription and translation. The “information” in DNA is linear, consisting of combinations of the four nucleotides: adenine, guanine, cytosine, and thymine. The information is transcribed into messenger RNA (mRNA), which in turn is a complementary version of the DNA code. The

mRNA message is spliced in the nucleus to remove introns and is then transported to the cytoplasm for translation into protein. Triplet RNA codons specify each of the 20 amino acids. The sequence of amino acids determines the protein, which ultimately has three-dimensional form.

THE GENETIC CODE

The genetic code was cracked by 1966. Triplet mRNA sequences specify each of the amino acids. Because there are four bases, the number of possibilities for a three-letter code is $4 \times 4 \times 4$, or 64. There are only 20 amino acids, however; consequently, more than one triplet can code for the same amino acid—that is, there is redundancy in the code. Because nearly all proteins begin with the amino acid methionine, the **initiation codon** (AUG) represents the “start” signal for protein synthesis. Three codons for which there are no naturally occurring tRNAs—UAA, UAG, and UGA—are “stop” signals that terminate translation (**termination codons**). Only methionine and tryptophan are specified by a unique codon; all other amino acids are specified by two or more different codons. As a consequence of this redundancy, a single-base change in RNA does not necessarily change the amino acid coded for.

Given the position of the bases in a codon, it is possible from [Table 17.1](#) to find the corresponding amino acid. For example, 5' CAU 3' specifies histidine, whereas AUG specifies methionine. Glycine is specified by any of four codons: GGU, GGC, GGA, or GGG.

Table 17.1 Codes for the Amino Acids

FIRST POSITION (5' END)	SECOND POSITION				THIRD POSITION (3' END)
	U	C	A	G	
U	Phe	Ser	Tyr	Cys	U
	Phe	Ser	Tyr	Cys	C

	Leu	Ser	Stop	Stop	A
	Leu	Ser	Stop	Trp	G
A	Ile	Thr	Asn	Ser	U
	Ile	Thr	Asn	Ser	C
	Ile	Thr	Lys	Arg	A
	Met	Thr	Lys	Arg	G
G	Val	Ala	Asp	Gly	U
	Val	Ala	Asp	Gly	C
	Val	Ala	Glu	Gly	A
	Val	Ala	Glu	Gly	G
C	Leu	Pro	His	Arg	U
	Leu	Pro	His	Arg	C

	Leu	Pro	Gln	Arg	A
	Leu	Pro	Gln	Arg	G

AMINO ACIDS AND PROTEINS

Most of proteins are composed of a mixture of the same 20 amino acids. Each polypeptide chain is characterized by a unique sequence of its amino acids. Chain lengths vary from 5 to more than 4,000 amino acids. Most proteins contain only one polypeptide chain, but others are formed through the aggregation of separately synthesized chains that have different sequences. Although most proteins are enzymes (i.e., they act as catalysts, inducing chemical changes in other substances but themselves remaining apparently unchanged), many have structural roles as well. The essential fabric of both nuclear and plasma membranes is formed of proteins.

Once a polypeptide chain is synthesized from a string of amino acids, it tends to fold up into a three-dimensional form, the shape of which is governed by the weak chemical interactions between the side groups of the amino acids. Each three-dimensional shape is unique to the amino acid sequence. The shape of a protein is the key to its function.

RESTRICTION ENDONUCLEASES

Restriction enzymes are endonucleases found in bacteria that have the property of recognizing a specific DNA sequence and cleaving at or near that site. These enzymes can be grouped into three categories: types I, II, and III. The restriction enzymes commonly used are of type II, meaning that they have endonuclease activity only (i.e., they cut the DNA without modification) at a predictable site within or adjacent to the recognition sequence. Types I and III have properties that make them impractical for use in molecular biology.

More than a thousand type II enzymes have been isolated, and more than 70 are commercially available. A few examples are shown in [Table 17.2](#). They are named according to the following system:

1. The first letter comes from the genus of the organism from which the enzyme was isolated.
2. The second and third letters follow the organism's species name.

3. If there is a fourth letter, it refers to a particular strain of the organism.
4. The roman numerals, as often as not, refer to the order in which enzymes were discovered, although the original intent was that it would indicate the order in which enzymes of the same organism and strain are eluted from a chromatography column.

Table 17.2 Examples of Type II Restriction Enzymes

ENZYME	ELEMENT TERMINOLOGY	OF MEANING
<i>Hind</i> III	<i>H</i>	Genus <i>Haemophilus</i>
	<i>in</i>	Species <i>influenzae</i>
	d	Strain Rd
	III	Third endonuclease isolated
<i>Eco</i> RI	<i>E</i>	Genus <i>Escherichia</i>
	<i>co</i>	Species <i>coli</i>
	R	Strain RY13
	I	First endonuclease isolated

<i>BamHI</i>	<i>B</i>	Genus <i>Bacillus</i>
	<i>am</i>	Species <i>amyloliquefaciens</i>
	H	Strain H
	I	First endonuclease isolated

Restriction endonucleases scan the DNA molecule, stopping if they recognize a particular nucleotide sequence. The recognition sites are short, four to eight nucleotides, and usually read the same in both directions, forward and backward, which is termed a *palindromic sequence*. Some endonucleases, such as *PvuII*, for example, produce blunt-ended fragments because they cut cleanly through the DNA, cleaving both complementary strands at the same nucleotide position, most often near the middle of the recognition sequence. Other endonucleases cleave the two strands of DNA at positions two to four nucleotides apart, creating exposed ends of single-stranded sequences. The commonly used enzymes *EcoRI*, *BamHI*, and *HindIII*, for example, leave 5' overhangs of four nucleotides, which represent “sticky” ends, very useful for making recombinant molecules. Table 17.3 shows the recognition sequence and point of cutting of a dozen commonly used restriction enzymes. This specificity is the same, regardless of whether the DNA is from a **bacterium**, a plant, or a human cell.

Table 17.3 Specificities of Some Typical Restriction Endonucleases

ENZYME	ORGANISM	RECOGNITION SEQUENCE ^a	RECOGNITION SEQUENCE ^a
<i>EcoRI</i>	<i>Escherichia coli</i>	GAATTC	Sticky
<i>BamHI</i>	<i>Bacillus</i>	GGATCC	Sticky

	<i>amyloliquefaciens</i>		
<i>BglfII</i>	<i>Bacillus globigii</i>	AGATCT	Sticky
<i>PvuI</i>	<i>Proteus vulgaris</i>	CGATCG	Sticky
<i>PvuII</i>	<i>Proteus vulgaris</i>	CAGCTG	Blunt
<i>HindIII</i>	<i>Haemophilus influenzae</i> R ₁	AAGCTT	Sticky
<i>HintI</i>	<i>Haemophilus influenzae</i> R ₁	GANTC	Sticky
<i>Sau3A</i>	<i>Staphylococcus aureus</i>	GATC	Sticky
<i>AluI</i>	<i>Arthrobacter luteus</i>	AGCT	Blunt
<i>TaqI</i>	<i>Thermus aquaticus</i>	TCGA	Sticky
<i>HaeIII</i>	<i>Haemophilus aegyptius</i>	GGCC	Blunt
<i>NotI</i>	<i>Nocardia otitidiscauli</i> varum	GCGGCCGC	Sticky

^aThe sequence shown is that of one strand given in the 5' to 3' direction. Only one strand is

represented.

Most restriction recognition sites have symmetry in that the sequence on one strand is the same as on the other. For example, *Eco*RI recognizes the sequence 5' GAATTC 3'; the complementary strand is also 5' GAATTC 3'. *Eco*RI cuts the DNA between the G and A on each strand, leaving a 5' single-strand sequence of AATT on each strand. The strands are complementary. Therefore, all DNA fragments generated with *Eco*RI are complementary and can "base-pair" with each other. This is illustrated in [Figure 17.5](#).

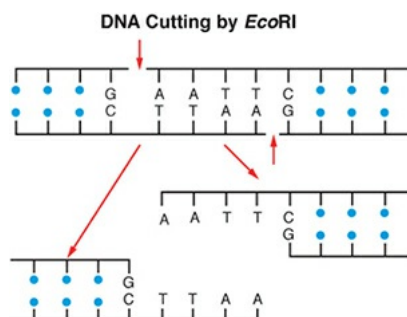


FIGURE 17.5 Illustration of how some endonucleases cleave each strand of the DNA off-center in the recognition site, creating fragments with exposed ends of short, single-stranded sequences. These "sticky" ends are extremely useful in making recombinant molecules because they rejoin only with complementary sequences.

VECTORS

A **vector** is a self-replicating DNA molecule that has the ability to carry another foreign DNA molecule into a host cell. In the context of this chapter, the object of the exercise is usually to insert a fragment of human DNA (perhaps containing a gene of interest [GOI]) into a bacterium so that it can be replicated and grown into quantities suitable for study.

Over the years, there have been many types of vectors, including plasmids, bacteriophages (especially **bacteriophage λ**), **bacterial artificial chromosomes** (BACs), and viruses. However, the two major vectors that are used today are plasmids and viruses.

Plasmids

The simplest bacterial vectors are plasmids, which are circular DNA molecules that can exist and replicate inside a bacterium, independent of the host chromosome. A piece of foreign DNA can be inserted into a plasmid, which in

turn is introduced into a bacterium. As the bacterium grows and replicates, so does the foreign DNA. The plasmid also contains a gene for resistance to an **antibiotic** (e.g., **ampicillin**), and if the bacteria are subsequently grown in a culture medium containing the antibiotic, only those bacteria that have taken up the plasmid survive and replicate. This is illustrated in Figure 17.6.

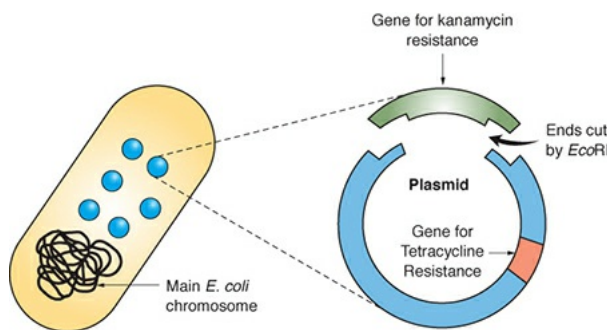


FIGURE 17.6 A plasmid is the simplest bacterial vector—a means of carrying foreign DNA sequences into bacteria such as *Escherichia coli*. A plasmid is a circular DNA molecule, capable of autonomous replication, that typically carries one or more genes encoding an antibiotic resistance. Foreign DNA (e.g., from a human cell) also can be incorporated into the plasmid. If inserted into a bacterium, the plasmid replicates along with the main chromosome.

It is a relatively simple matter, subsequently, to harvest the recombinant plasmids. There are two limitations to this technique. First, plasmids are useful only for relatively small DNA inserts up to about 10,000 base pairs (bp). Second, the plasmids do not transfect into bacteria with high efficiency.

Bacteriophage λ

Bacteriophages are bacterial viruses. The bacteriophage most commonly used as a cloning vector is bacteriophage λ . It has two advantages compared with other vectors. As a bacteriophage particle, bacteriophage λ can infect its host at a much higher efficiency than a plasmid, and it can accommodate a larger range of DNA fragments, from a few to up to 24,000 bp, depending on the specific vector used. Many vectors have been derived from bacteriophage λ . Some have been modified to clone small DNAs, usually **complementary DNAs (cDNAs)** derived from mRNA, and some have been modified to clone large genomic DNA molecules. If bacteriophage λ is used to clone large DNA molecules, the central portion of the bacteriophage DNA is deleted. This is to allow the foreign DNA to be accommodated within the bacteriophage particle, which has an upper limit of 55,000 bp. Once the bacteriophage DNA is ligated with the DNA to be cloned, the total DNA is mixed with extracts containing empty bacteriophage particles.

The ligated DNA is taken up into the bacteriophage, which is then used to infect *E. coli* and form **plaques**.

To insert itself into the *E. coli* chromosome, the phage DNA circularizes by the base pairing of the complementary single-strand tails that exist at its two ends—the cos sites. The resulting circular λ DNA then recombines into the *E. coli* chromosome.

If part of the wild-type DNA of the bacteriophage is removed, room can be made for a piece of human DNA to be inserted, again with a gene that confers resistance to an antibiotic to allow selection. The bacteriophage can then be used to infect bacteria that multiply their own DNA as well as the integrated piece of human DNA (Fig. 17.7).

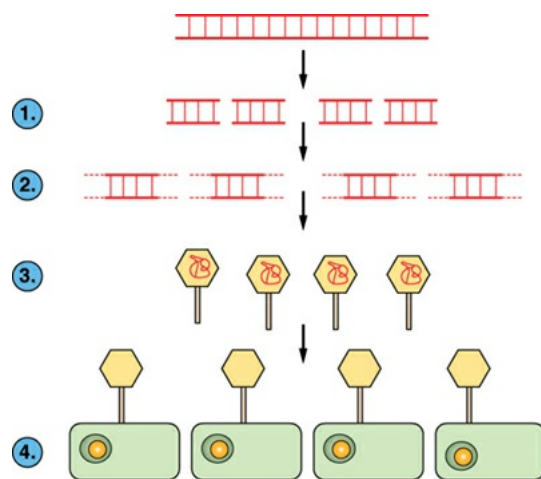


FIGURE 17.7 A bacteriophage is a virus that infects bacteria. It represents a much more efficient means of inserting foreign DNA into a bacterium than using a plasmid. If part of the wild-type DNA is removed, room can be made for a piece of “foreign” DNA, for example, from a human cell, as well as a gene that confers resistance to an antibiotic to allow selection. The DNA of the bacteriophage replicates along with that of the bacterium.

Bacterial Artificial Chromosomes

Sequencing large genomes requires a cloning vector capable of carrying very large fragments of DNA. BACs are vectors based on a type of plasmid with sequences encoding self-replication while maintaining a low copy number. BACs can accommodate approximately 300 kilobases (kb) of DNA, whereas plasmids are limited to approximately 10-kb insertions. BACs transform *E. coli* via electroporation more efficiently than comparable but larger constructs, compensating for the reduced amount of inserted DNA that can be accommodated. Because of the defined genetic backgrounds of their bacterial

hosts, BACs are also less prone to recombination events (a common problem with large DNA vectors). BACs were the primary vector used during the genome-sequencing projects, mainly because a BAC carrying a GOI is easily acquired.

Viruses

Viruses are highly efficient vectors for introducing foreign genes into mammalian cells. Viral infection of mammalian cells has proved to be an effective and efficient method for delivering and stably expressing a GOI. The three main types of viruses used for gene transfer are retroviruses, adenoviruses, and adeno-associated viruses (AAV). **Retroviruses** are a type of RNA virus. Unlike all other RNA viruses, the RNA **genome** of retroviruses is transcribed into DNA, which is then stably integrated into the host genome. Retroviruses can infect virtually every type of mammalian cell, making them very versatile. One well-known type of retrovirus used for gene transfer is lentivirus. They possess high rates of infectivity and can infect both dividing and nondividing cells. In contrast to retroviruses, adenoviruses are a type of DNA virus, and they can infect both proliferative and quiescent cells. Adenoviruses can be easily purified in high titers and the two major strains (Ad2, Ad5) used to make recombinant viruses can accept 37 kb of foreign DNA. Adenovirus **gene expression** is stable, but the genome remains epichromosomal. AAV are the third major vector family used. They get their name from being identified as contaminants of adenovirus isolates. AAV are relatively small viruses, which can package 5 kb of foreign DNA. In addition to their use in laboratory research, AAV has also been approved for the introduction of foreign DNA into humans for gene therapy.

LIBRARIES

Genomic Library

A **genomic library** is a compilation of DNA fragments that make up the entire genome. Making a genomic library is frequently the starting point of a gene isolation experiment. DNA is extracted from a tissue sample or from cultured cells, and a partial **digest** is made using *Eco*RI, for example. This enzyme has a six-nucleotide recognition sequence, so if the digest is complete, it cuts the DNA into pieces about 4,000 bp long. (The probability of cleaving a six base pair sequence is $[\frac{1}{4}]^6$, or once every 4,096 bases.) By reducing the enzyme concentration and incubation time, a partial digest is obtained so that the *Eco*RI enzyme cuts at only about one in five restriction sites, resulting in fragments of

about 40,000 bp.

The genomic DNA fragments are then ligated into a suitable vector based on the size of the DNA-plasmid (up to 10 kb), bacteriophage λ (up to 25 kb), BAC (up to 300 kb), and **yeast artificial chromosome** (up to 200 kb). The assembled particles are used to infect *E. coli* cells or yeast, which are spread on plates and incubated in growth medium containing the appropriate selection so that only bacteria or yeast that have taken up the vector grow into colonies. Each **colony** contains millions of copies of a single genomic DNA insert. However, the larger the fragment of DNA, the more prone to rearrangement in the host bacteria or yeast. Therefore, multiple clones overlapping the same genomic region need to be generated to ensure fidelity in assigning chromosome position or DNA sequence alignment. The most common use of genomic libraries was for “shotgun” DNA sequencing. By using this sequence as a **probe**, overlapping clones can be identified and then sequenced to ultimately develop a “**contig**,” which represents a contiguous DNA sequence for a portion of a chromosome.

cDNA Library

Sometimes, there is a need to focus only on DNA that will be transcribed into mRNAs. cDNA is DNA that is complementary to the mRNA and therefore includes only the expressed genes of a particular cell. For eukaryotic cells, the mRNA is usually much shorter than the total size of the gene because the coding sequences in the genome are split into exons separated by noncoding regions of DNA called introns.

cDNA libraries are made in either plasmids or bacteriophage λ . Often, these vectors have been modified such that the cDNA can be transcribed into mRNA and then translated into protein. Depending on the type of vector, the **library** can be screened by oligonucleotide probes or by an **antibody** that recognizes the protein of the GOI. This type of **cDNA library** is called an **expression library**.

HOSTS

Recombinant DNA molecules can be constructed and manipulated to some extent in the test tube, but amplification and expression ideally require a host.

Escherichia Coli

E. coli is the most widely used organism in molecular biology because it is relatively simple and well understood. It contains a single chromosome consisting of about 5 million base pairs.

In addition to their main chromosomes, many bacteria, including *E. coli*, possess large numbers of tiny circular DNA molecules that may contain only a few thousand base pairs. They are called *episomes*, a subset of which are known as plasmids as previously described. Plasmids are autonomously replicating “minichromosomes.” They were first identified as genetic elements separate from the main chromosome and carrying genes that conveyed resistance to antibiotics. Foreign DNA can be introduced readily into *E. coli* in the form of plasmids.

Because the DNA of all organisms is made of identical subunits, *E. coli* accepts foreign DNA from any organism. The DNA of bacteria, *Drosophila*, plants, and humans consists of the same four nucleotides: adenine, cytosine, guanine, and thymine. A foreign gene inside *E. coli* is replicated in essentially the same way as its own DNA.

Yeast

Yeast are simple eukaryotes that have many characteristics in common with mammalian cells but can be grown almost as quickly and inexpensively as bacteria.

The study of yeast has frequently provided insights into similar phenomena and functions in mammalian cells that are much more difficult to address. Yeast have been of particular value in radiobiology because the availability of a wide array of mutants that are sensitive to ultraviolet or ionizing radiations has made the study of the genes responsible for radiosensitivity and radioresistance much simpler than if studies were conducted only in mammalian cells. Complementation of many yeast mutants with mammalian genes has proved to be a powerful screening method to identify mammalian genes that affect radiosensitivity.

Yeast have also proved to be good systems for studying cell-cycle control. Because it appears that the cell-cycle machinery of all eukaryotes is very similar, it makes sense to concentrate on the simplest and most easily manipulated system. The availability of temperature-sensitive yeast mutants is of particular value. The yeast *Saccharomyces cerevisiae* (budding yeast, baker’s yeast, or brewer’s yeast) and *Schizosaccharomyces pombe* (fission yeast) have been used widely. They grow rapidly and have been well characterized genetically.

An approach has been developed for analyzing large numbers of uniquely tagged yeast deletion strains by **hybridization** to high-density oligonucleotide arrays. Deletion strains are generated using a polymerase chain reaction targeting

strategy, and each deletion strain is specifically labeled with two 20-base tag sequences. Each molecular tag is important, as it serves as a “bar code,” allowing approximately 4,500 deletion strains to be pooled and analyzed simultaneously by hybridization to an array. The abundance of a given strain is reflective of its hybridization to its corresponding complementary sequence on a high-density oligonucleotide array. The yeast deletion strains and oligonucleotide arrays containing complementary sequences for each deletion mutant are commercially available.

Mammalian Cells

The limited number of cell systems used in radiation and chemical **transformation** studies can be separated broadly into two categories. The first category includes short-term explants of cells derived from rodent or human embryos with a limited life span. These include:

- Hamster embryo cells
- Rat embryo cells
- Human skin fibroblasts
- Human foreskin cells
- Human embryo cells

These cell assay systems can be used to assess the expression or activity of foreign genes transfected into them, or they may be used in studies of oncogenic transformation induced by radiation or chemicals.

In practice, the bulk of the experimental work has been performed with hamster or rat embryo cells. One advantage of such systems is that they consist of diploid cells so that parallel cytogenetic experiments can be performed. Cell survival and cell transformation can be scored simultaneously in the same dishes.

The experimental methodology is illustrated in [Figure 17.8](#). Cells are seeded at low density into dishes or flasks and treated with radiation or chemicals. They are allowed to grow for 8 to 10 days, and the resultant colonies are fixed and stained. Transformed colonies are identifiable by dense multilayered cells, random cellular arrangement, and haphazard cell-to-cell orientation accentuated at the colony edge. Normal counterparts are flat, with an organized cell-to-cell orientation and no piling up of cells. An example of the contrast between a normal and a transformed colony is shown in [Figure 17.9](#).

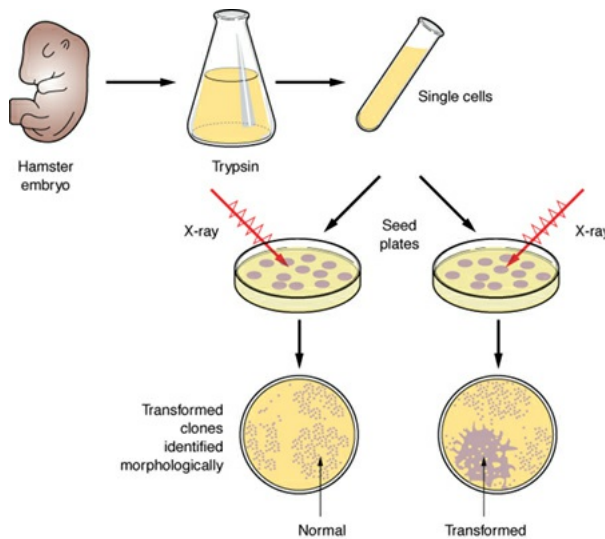


FIGURE 17.8 Protocol for the assay of oncogenic transformation in hamster embryo cells by radiation. Midterm hamster embryos are removed, minced, enzymatically dissociated, and seeded as single cells on feeder layers. They are then treated with either radiation or chemicals, and the resultant colonies (normal and transformed) are scored after 8 to 10 days of incubation.

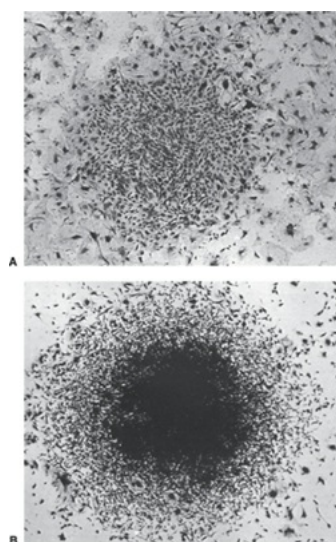


FIGURE 17.9 **A:** A normal untransformed colony of hamster embryo cells. The cells are orderly and show contact inhibition. **B:** A colony of radiation-transformed hamster embryo cells. Note the densely stained, piled up cells and the crisscross pattern at the periphery of the colony.

The second category of experimental systems includes established cell lines that have an unlimited life span. The karyotype of these cells shows various chromosomal rearrangements and heteroploidy. The two most widely used established cell lines for transformation studies are the BALB/C-3T3 cell line and the C₃H 10T1/2 cell line. Both originated from mouse embryos, are transformable by various oncogenic agents, and have been used extensively in

transformation studies. The advantage of these established cell lines lies in the fact that they are “immortal” so that a particular passage can be used over a long period of time and maintained in banks of frozen cells. The transformation assay is a focal assay. Cells are treated with radiation or chemicals and then allowed to grow for 6 weeks. The “normal” cells stop growing after confluence is reached, and transformed foci can be identified against a background of the contact-inhibited normal cells because they are densely stained, tend to pile up, and show a crisscross random pattern at the edge of the focus. Transformed cells, identified by their characteristic morphology, grow in soft agar, which indicates that they have lost anchorage dependence, and produce fibrosarcomas if injected into suitably prepared animals. This is illustrated in [Figure 17.10](#).

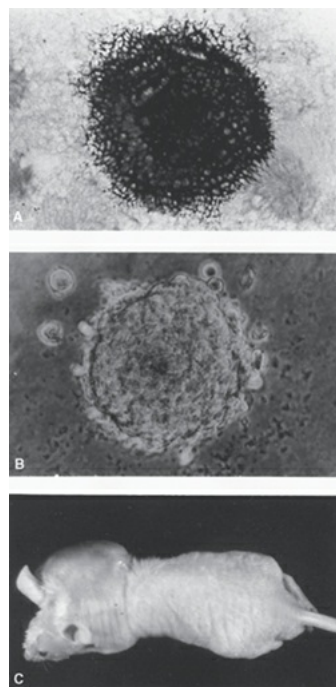


FIGURE 17.10 **A:** A type III transformed focus of C₃H 10T1/2 cells induced by the hypoxic cell sensitizer etanidazole (SR 2508). Note the multilayered growth and the crisscrossing of cells at the periphery of the clone over a contact-inhibited background of nontransformed cells. **B:** Cells from the focus shown in A were plucked, expanded in culture, and plated into semisolid medium; they formed colonies, indicating that they had lost anchorage dependence. This is an indication of malignancy. **C:** The ultimate test of malignancy is whether cells from a type III transformed clone injected into a suitably prepared animal produce a tumor (a fibrosarcoma) that eventually kills the animal.

The *in vitro* assay systems based on mammalian cells have two quite different uses in radiobiology. First, they may be used to accumulate data and information that are essentially pragmatic in nature; for example, they may be

used to compare the oncogenic potential of various chemical and physical agents. As such, they occupy a useful intermediate position between the bacterial mutagenesis assays, which are quick and inexpensive but score mutagenesis rather than carcinogenesis, and animal studies, which may be more relevant to humans but are quite cumbersome and inordinately expensive. Second, the assay systems can be used to study the mechanisms of carcinogenesis. In this context, transformation assays have played a vital role in unfolding the **oncogene** story because transfecting DNA from human tumors into established rodent cell lines used for transformation, and observing the induction of transformed foci is one way to detect the expression of an oncogene (see [Chapter 18](#) for more details).

DNA-MEDIATED GENE TRANSFER

Gene transfer is now a routine tool for studying gene structure and function. Because gene transfer into mammalian cells is an inefficient process, an abundant source of starting cells is necessary to generate a workable number of transfected cells—that is, cells containing a transferred gene.

Mammalian cells do not take up foreign DNA naturally; indeed, they try to protect themselves from invading DNA. Consequently, one of several techniques must be used to bypass natural barriers:

1. **Microinjection:** This is the most direct but the most technically demanding procedure to accomplish. DNA can be injected directly into the nucleus of a cell through a fine glass needle.
2. **Calcium phosphate precipitation:** Cells take up DNA relatively efficiently in the form of a precipitate with calcium phosphate. The efficiency varies markedly from one cell line to another. For example, NIH 3T3 cells are particularly receptive to foreign DNA introduced by this technique. High-molecular-weight DNA is mixed with insoluble calcium phosphate as a carrier and layered onto cells in petri dishes. Typically, a plasmid containing a **selectable marker**, such as G418 resistance, is copipetted and cotransfected into cells. In this way, cells that take up DNA can be selected. Of the cells that take up DNA, only a small percentage ultimately integrate the DNA into their genomes (are stably transfected). For example, if a fragment of DNA containing an activated oncogene is transfected into NIH 3T3 cells, morphologic transformation of the cell occurs, leading to loss of contact inhibition, and acquires the ability to grow as tumors if injected into immune-suppressed animals.
3. **Cationic lipids:** Cationic lipids offer some of the highest **transfection**

efficiencies and expression levels to a wide variety of cells, both in suspension and attached. The protocol is very simple in that you mix lipid and DNA, vortex gently, centrifuge, and allow to sit at room temperature for 10 to 30 minutes before adding to cells. Although cationic lipids produce high transfection efficiencies, some cells are sensitive to these lipids.

4. **Electroporation:** This technique is useful for cells that are resistant to transfection by calcium phosphate precipitation. Cells in solution are subjected to a brief electrical pulse that causes holes to open transiently in the membrane, allowing foreign DNA to enter.

AGAROSE GEL ELECTROPHORESIS

The purpose of **agarose gel electrophoresis** is to separate pieces of DNA of different size. This technique is based on the fact that DNA is negatively charged. Under the influence of an electrical field, DNA molecules move from negative to positive poles and are sorted by size in the gel. In a given time, small fragments migrate through the gel farther than large fragments.

The technique, illustrated in [Figure 17.11](#), is as follows: Molten agarose is poured into a tray in which a plastic comb is suspended near one end to form wells in the gel after it has solidified like gelatin. The concentration of the agarose is varied according to the size of the DNA fragment to be separated: high concentration for small fragments, lower concentration for larger fragments. The solidified gel is immersed in a tray containing an electrolyte to conduct electricity. The DNA samples, mixed with sucrose and a visible dye, are pipetted into the wells, and the electrical field is connected. **Electrophoresis** is monitored by observing the movement of the dye in the electrical field. After separation is complete, the gel is soaked in **ethidium bromide**, which intercalates into DNA and fluoresces under ultraviolet light to make the position of the DNA visible. The smaller DNA fragments migrate farther on the gel than the larger fragments, as illustrated in [Figure 17.12](#). In fact, the distance migrated is directly related to DNA size. (Illustrations of several examples appear elsewhere in this chapter.)

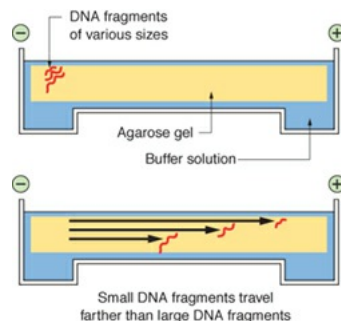


FIGURE 17.11 Illustration of agarose gel electrophoresis. DNA is negatively charged so that under the influence of an electrical field, it migrates toward the anode. During electrophoresis, DNA fragments sort by size, small molecules moving farther than larger molecules. Because smaller molecules move farther than larger molecules in a given time, polyacrylamide gel electrophoresis often is employed to separate smaller DNA fragments with greater resolution than with agarose.

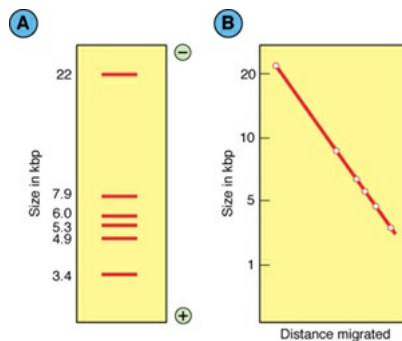


FIGURE 17.12 **A:** Illustration of the separation of λ DNA after digestion with *Eco*RI. Agarose gels separate DNA fragments that can be quite large. By varying the percentage of agarose, the resolution of different-sized fragments can be maximized. **B:** Regardless of change in agarose concentration, the distance migrated is directly proportional to DNA size.

POLYMERASE CHAIN REACTION

The **polymerase chain reaction (PCR)** technique uses enzymatic amplification to increase the number of copies of a DNA fragment. The principle is based on **primer extension by DNA polymerases**, which was discovered in the 1960s. First, primers that are complementary to the 5' end of the double-stranded DNA sequence to be amplified are synthesized. The two primers are mixed in excess with a sample of DNA that includes the fragments to be amplified, together with a heat-stable DNA polymerase. The four deoxyribonucleotide triphosphates are also included in excess; one or more of them may be radioactively labeled. The choice of the heat-stable DNA polymerase depends on the size of the DNA to be amplified, **Taq polymerase** is inexpensive and effective up to 500 bp but has a high error rate. Vent polymerase is considered a workhorse and is used to **amplify** DNA in the 1- to 5-kb range. At the high end of **polymerases** is Phusion, very high processivity and low error rate but very expensive. Heat stable polymerases such as Phusion are used to amplify DNA in the 20-kb range. The PCR technique is illustrated in [Figure 17.13](#).

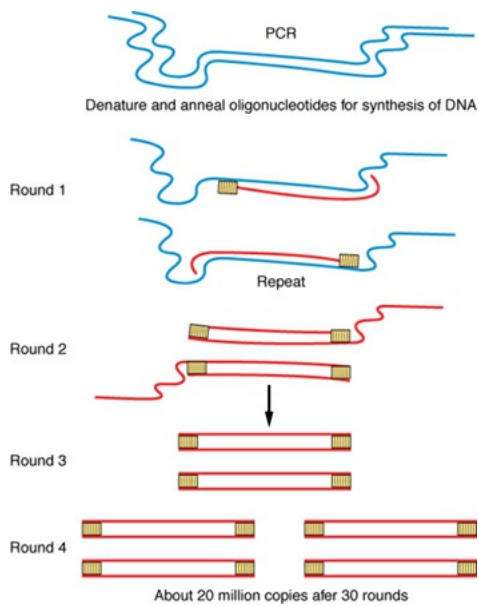


FIGURE 17.13 The polymerase chain reaction (PCR) for the amplification of DNA fragments. The number of DNA molecules is doubled in each cycle, which takes about 7 minutes so that in a matter of several hours, millions of copies of a DNA fragment can be made. (Courtesy of Dr. Greg Freyer.)

The amount of the sequence is doubled in each cycle, which takes about 7 minutes. During each cycle, the sample is heated to about 94° C to denature the DNA strands, then cooled to about 50° C to allow the primers to **anneal** to the template DNA, and then heated to 72° C, the optimal temperature for *Taq* polymerase activity. In a matter of a few hours, a million copies of the DNA fragment can be obtained in an essentially automated device. PCR has found many applications in both basic research and clinical settings. For example, it has been used to detect malignant cells in patients with leukemias that are characterized by consistent translocation breakpoints. Primers that span the breakpoint are added to a bone marrow sample and subjected to multiple cycles of PCR. Even one cell in a million with the translocation can be detected.

Polymerase Chain Reaction-mediated Site-directed Mutagenesis

PCR-mediated site-directed mutagenesis is a technique used to create mutations such as nucleotide replacements, insertions, or deletions at a desired location in the gene or its flanking sequences to investigate the relationship between gene sequence and gene function. The starting material is usually a double-stranded DNA vector with the gene or nucleotide of interest acting as the template for PCR. In this technique, two complementary oligonucleotides containing the **mutation** of interest are used as the primers for PCR. The mutant strand of DNA

is synthesized by denaturing the DNA template, annealing mutagenic primers to the DNA template, and extending the primers using a high-fidelity DNA polymerase to reduce the chance of unwanted random errors being introduced during replication. Bacteria modify DNA by methylation to prevent it from being digested by restriction endonucleases. This modification of DNA is then used to eliminate the starting DNA from the PCR-amplified DNA by digestion with a methylation-specific endonuclease (*Dpn I*), leaving only the mutated DNA. This DNA is then used to transform competent bacterial cells so that it can be used for further study.

GENE-CLONING STRATEGIES

Gene-cloning strategies in the past have revolved around choosing a source of DNA, either genomic or cDNA, constructing a library (a collection of DNA fragments in an appropriate vector), and screening the library to locate the GOI. This labor-intensive approach has now been supplanted with both public repositories of mammalian genes established by the National Institutes of Health (NIH) and commercial repositories. Even if you cannot find your GOI, PCR would be a rapid means of obtaining your gene.

GENOMIC ANALYSES

The complete sequencing of the human genome as well as the genomes of other organisms has led to the interdisciplinary field of genomics. During the last decade, DNA sequence information has made the task of investigating DNA much easier. This revolution has been brought about by two major approaches to sequencing: (1) hierarchical shotgun sequencing of cloned DNA fragments as described earlier and (2) whole genome shotgun sequencing in which DNA sequences of random, uncloned DNA fragments are obtained and aligned using computer algorithms. Although sequencing DNA fragments is straightforward, there is a great deal of effort in filling in the gaps between sequences (Fig. 17.14).

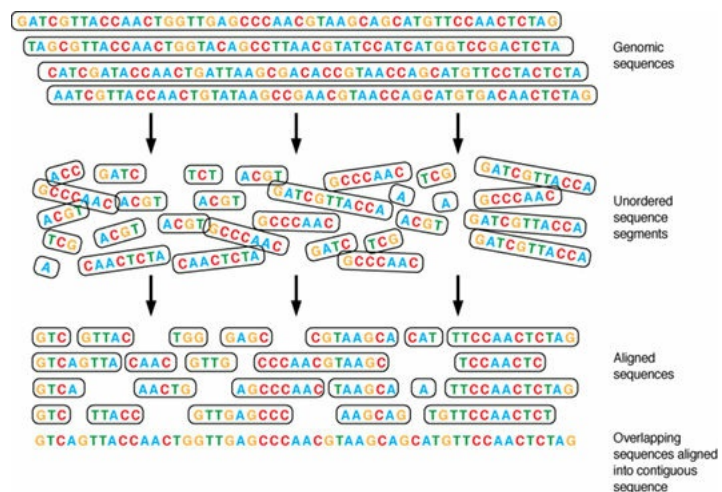


FIGURE 17.14 Illustration of the technique of “shotgun sequencing” to obtain contiguous sequences spanning the complete length of chromosomes. In this technique, which was successfully used to generate an almost complete sequence of the human genome, random fragments of DNA are generated in an unordered fashion and sequenced in a random fashion. Hence, the term shotgun sequencing as the sequence analysis is random as a shotgun blast covers a large target in a random fashion. Once the sequences of the random fragments are obtained, computer algorithms are used to align the random sequences. Then, overlapping sequences are aligned into a contiguous sequence.

Although it is extremely useful to have “a complete genomic DNA sequence” for humans, there is significant heterogeneity between individuals. Recognition of the importance of this heterogeneity between individuals stimulated the development of the Hap Map project, whose goal is to identify genome differences between individuals that can result in disease or even cancer. In fact, the differences between cancer genomes and cancer-free individuals stimulated “The Cancer Genome Atlas” (TCGA) project by the National Cancer Institute (NCI) and National Human Genome Research Institute (NHGRI). The initial thoughts were to sequence the genomes of cancers grouped by histologic type. Because genomic sequencing has become more cost effective, the ability to sequence the genomes of every cancer patient could become feasible in the future. Sequence analysis of a cancer genome has brought forth the concept of “personalized medicine” where the goal is to match a therapy with a genomic alteration. For example, a patient with breast cancer is found to have a mutation in the BRCA1 gene. This patient would be a candidate for poly adenosine diphosphate-ribose polymerase (PARP) inhibitors or a platinum drug that will kill BRCA1 mutated cells defective in homologous recombination. Unfortunately, most of the mutations identified in cancer genomes are “inactionable,” meaning that there is not a specific therapy targeting the

mutation. Furthermore, most of the mutations identified do not necessarily have a clear impact on radiosensitivity or radioresistance. One example where genomic analysis has been informative in regard to radiation resistance is deletion/inactivation of the Keap1 gene. Keap1 inhibits Nrf2, which promotes resistance to oxidative stress. Genome deletion of Keap1 increases the cancer cell's resistance to oxidative stress and decreases the efficacy of low-linear energy transfer (LET) radiation. Therefore, for patients with the loss of Keap1, the use of high-LET radiotherapy is potentially warranted.

Deletions or mutations of DNA repair genes detected by genomic analysis should theoretically increase the radiosensitivity of tumors. However, there have been few studies investigating the effect of DNA repair mutations on local control by radiotherapy. Such a study would seem an additional approach to “precision radiotherapy.”

Mapping

Contiguous Mapping

Mapping refers to the determination of the physical location of a gene or genetic marker on a chromosome. Contiguous mapping refers to the alignment of sequence data from large, adjacent regions of the genome to produce a continuous nucleotide sequence of a region of a chromosome. The basic idea is to orient physical markers, such as **restriction fragment length polymorphisms**, on adjacent fragments so that they can be lined up and the nucleotide sequence can be made continuous. If, for example, restriction fragments from a DNA library are sequenced, relating these sequences to known physical markers eventually can produce the nucleotide sequence of the entire genome. This is the goal of the Human Genome Project, but the task is so massive that it cannot be accomplished without the development of automated sequencing technology and sophisticated computer strategies to store and handle the data.

DNA Sequence Analyses

DNA sequencing is the process of identifying the exact sequence of nucleotides in a given DNA sample, whether it is a particular gene or an entire genome. DNA sequencing is achieved by the dideoxynucleotide chain termination method (the Sanger method), which exploits the fact that DNA is composed of deoxynucleotides. Primers are used to amplify a given target of the single-stranded DNA to be sequenced. Dideoxynucleotides lack a hydroxyl (OH) group

at the 3' position. Thus, when a dideoxynucleotide is added, the chain is terminated. Using conditions similar to PCR, multiple rounds of primer extension incorporate deoxynucleotides and labeled dideoxynucleotides on the sequenced strand. In manual sequencing, four separate reactions are run in which only one radiolabeled dideoxynucleotide is added to the reaction. Each of the four dideoxynucleotides is electrophoresed on a gel and visualized by autoradiography. A more recent (and commonly used) innovation is automated sequencing, in which a single reaction is run with a mixture of all four dideoxynucleotides, each carrying a different-colored fluorescent label. The products are electrophoresed in one lane, separating the replication products based on size. A laser scans the bottom of the gel, detecting the four fluorescent tags of the dideoxynucleotide from which the original strand sequence of nucleotides can be determined. The sequencing method described earlier is known as Sanger sequencing. The latest revolution in sequencing is known as “next generation sequencing” (NGS) or deep sequencing. Although different platforms for NGS have been used, they all involve sequencing of millions of small fragments of DNA in parallel. The sequence information is then stitched together using bioinformatic programs run on very powerful computers. The reason NGS is also known as deep sequencing is because the same genomic DNA from the normal or tissue material is sequenced multiple times to provide accurate sequence readouts. NGS can be used to sequence the entire human genome ($\sim 3 \times 10^9$ billion bases) or complete exome sequencing for all coding genes (~25,000 genes).

Polymorphisms or Mutations

Restriction Fragment Length Polymorphisms

Relatively small differences in similar DNA sequences (**alleles**), **DNA polymorphisms**, as they are called, may result from point mutations, deletions or insertions, or varying numbers of copies of a DNA fragment (so-called tandem repeats). A Southern blot analysis can be used to detect **DNA polymorphisms** by using a probe that hybridizes to a polymorphic region of the DNA molecule. Other techniques such as polymerase chain reaction–restriction fragment length polymorphism (PCR-RFLP) can also be used to determine genetic variations that result in single nucleotide polymorphisms (SNPs).

If a particular restriction enzyme is used to cut human DNA, a polymorphic locus yields restriction fragments of different sizes. These are called restriction fragment length polymorphisms. Deletions, insertions, or tandem repeats

involving more than about 30 nucleotides can be detected as recognizable shifts in the Southern blot hybridization pattern or PCR products. Even a **point mutation** can be detected if the resultant change in sequence removes or adds a new recognition site at which a restriction endonuclease cuts. Using different restriction enzymes will generate a unique pattern of DNA fragments that act as a fingerprint for normal cells and tumor cells.

Comparative Genome Hybridization

Genomic DNA is harvested from a tumor or cancer cell line and digested with *Dpn*II (a restriction endonuclease that cleaves DNA approximately every 256 bp), creating a random pool of DNA fragments. DNA is amplified with random primers and nucleotides labeled with the fluorescent dye Cy5 (red). As a control, DNA from a normal cell line is also digested and then amplified with the fluorescent dye Cy3 (green). The two samples are mixed and hybridized to a DNA microarray composed of cDNAs. The **microarray** is scanned and the ratio of Cy5 to Cy3 (red to green) fluorescence calculated for each cDNA spot to generate a baseline fluorescent ratio. Individual spots with a Cy5:Cy3 ratio significantly higher than background correspond to regions of the genome that are amplified (**gene amplification**) in that specific cancer cell, whereas those with lower than baseline correspond to chromosomal deletions (also called loss of heterozygosity). Spots corresponding to contiguous chromosomal regions should show similar alterations in enrichment and define a common locus. The genes residing in the altered loci are identified from the human genome database to generate a list of potential tumor suppressors or oncogenes (Fig. 17.15).

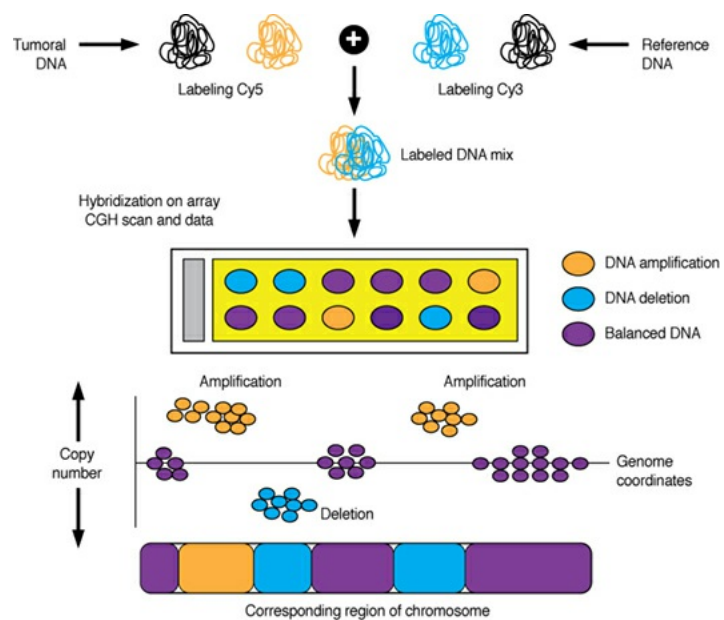


FIGURE 17.15 Illustration of the technique of comparative genomic

hybridization (CGH). Tumor and reference (normal) DNAs are fragmented and amplified with random primers and nucleotides labeled with Cy5 and Cy3. The two samples are mixed hybridized to a DNA microarray of cloned fragments containing cDNAs. The microarray is scanned, and the ratio of Cy5 to Cy3 fluorescence is calculated for each spot on the microarray. Spots with higher Cy5 to Cy3 compared to baseline represent amplifications, and spots with lower Cy5 to Cy3 represent deletions. The genes residing in these regions are then identified in a human database to generate potential oncogenes or tumor suppressors. (Modified from Helixio, with permission.)

Comparative genomic hybridization (CGH) has also been combined with SNP technology, which is commercially available through Agilent Sure Print Human Genomic CGH and SNP microarrays. In this technique, a similar protocol as described previously for CGH is used except that the Cy5 and Cy3 labeled DNAs from tumor and normal reference material are hybridized to the Agilent CGH and SNP oligonucleotide arrays. The combination of techniques is useful in showing copy number gain and loss both at the chromosome level as well as the gene level.

GENE KNOCKOUT STRATEGIES

Clustered Regularly Interspaced Short Palindromic Repeats and CRISPR Associated Protein

Clustered regularly interspaced short palindromic repeats (**CRISPR**) and CRISPR associated (Cas) genes have evolved to allow cells to respond and eliminate invading genetic material. In lower eukaryotes such as bacteria, viral infection activates the CRISPR pathway and a byproduct of CRISPR activation is short DNA sequences from the viral genome integrated into the bacterial genome, which serve as a physical reminder of the past viral infection. A new infection by a similar virus activates complementary CRISPR RNA (crRNA) to identify a homologous sequence. The Cas nuclease introduces a double-strand break at the “foreign” DNA sequence. In fact, to achieve specificity in DNA recognition and cleavage, the Cas nuclease forms a complex with a crRNA and a trans-activating crRNA (tracrRNA) which has complementarity to the crRNA. The **Cas9** nuclease cuts both DNA strands, generating double-strand breaks which are defined by 20-nucleotide “target” sequences within the crRNA (Fig. 17.16).

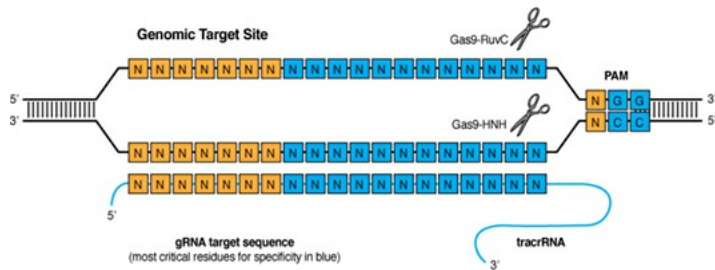


FIGURE 17.16 Illustration of clustered regularly interspaced short palindromic repeats (CRISPR) and CRISPR associated protein (Cas9) targeting. In lower eukaryotes, short interspersed sequences (approximately 20 base pairs) from viral infections or plasmids serve as a reminder of a previous infection. This is probably the same for mammalian cells as well. The system is relatively straightforward to use in gene editing because it requires a Cas nuclease (Cas9) and a guide RNA (gRNA) to the target sequence of choice. The gRNA contains a tracrRNA that is necessary for nuclease activity. Cas9-RuvC cleaves the DNA strand not complementary to the guide RNA. Cas9-HNH cleaves the DNA strand complementary to the guide RNA. Specificity of DNA binding is due to the gRNA and a three-nucleotide NGG sequence called the protospacer adjacent motif (PAM) sequence. Today, plasmids are commercially available that contain all in one Cas9-CRISPR components with codon-optimized Cas9 protein and a guide RNA. Furthermore, unique CRISPR sites have been developed to reduce the problem of off-target cutting for several genomes, including human. (Modified from Sigma-Aldrich, with permission.)

The power of CRISPR lies in the use of only three components—Cas9, crRNA, and trRNA. Nowadays, a ready-to-use CRISPR system is composed of two plasmids—one containing the Cas9 nickase and a second plasmid expressing a guide RNA (gRNA) under the control of the U6 promoter. Alternatively, CRISPR lentiviral vectors also are available which incorporates both gRNAs and the Cas9 genes. These are the basic workhorse components, but mutant forms of Cas9 have been developed to increase precision of cutting or targeting.

Homologous Recombination to Knockout Genes

Homologous recombination is the cellular process that allows the eukaryotic cell to repair damage to one chromosome with the DNA from the homologous sister chromosome acting as a template (see [Chapter 2](#)). This process also occurs during meiosis, where the DNA from the parental chromosomes is shuffled before segregation to gametes. Homologous recombination can be used to selectively delete or alter the endogenous gene in a cell line. A simplified version

of this process is illustrated in [Figure 17.17](#). Cloned DNA from a GOI is modified to delete a key functional domain from the middle of the sequence and replace it with a cDNA for neomycin resistance (*neoR*). A cDNA (*tk*) conferring sensitivity to another drug (ganciclovir) is ligated to the end of the GOI-*neo* construct. The linearized construct is then transfected into cells, and the cells are treated with both neomycin and ganciclovir. If the construct is randomly inserted into the cell's genome (a common event), both *neoR* and *tk* are inserted and expressed. These cells are resistant to neomycin but will be killed by ganciclovir. If homologous recombination occurs (a rare event), the GOI sequences flanking the *neoR* cassette will be recognized by the cellular recombination machinery and replace the original region of GOI with the *neoR* cassette but will not incorporate the *tk* gene. These cells will then be neomycin resistant and survive ganciclovir. The same process is repeated with a different antibiotic resistance marker to delete the other copy of the GOI. PCR or **Southern blotting** is then used to verify loss of the native gene and insertion of the *neoR* gene. A similar process can be used to swap native parts of a GOI with mutant forms.

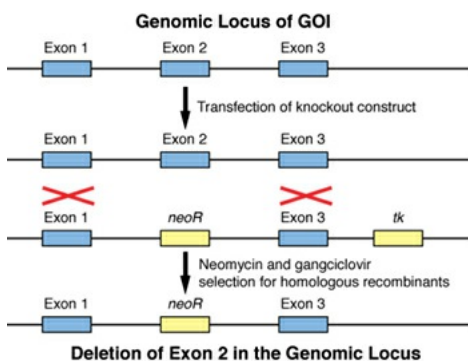


FIGURE 17.17 Use of homologous recombination to delete function in a gene of interest (GOI). Exon 2 of GOI is known to be responsible for GOI's biologic activity. A knockout construct is cloned from a genomic fragment spanning GOI by replacing exon 2 with the neomycin antibiotic resistance gene (*neoR*). The gene for thymidylate kinase (*tk*) at the 5' end of the construct is cloned. Cells are transfected with the knockout construct and treated with neomycin and ganciclovir to select for homologous recombinants and against random integrants. The surviving colonies are screened by PCR or Southern blotting to verify deletion of exon 2.

Knockout Mice

Using homologous recombination, one copy of a GOI is deleted in mouse embryonic stem (ES) cells. The neomycin- and ganciclovir-resistant ES cells are injected into early mouse embryos. The resultant chimeric mice that are

heterozygous for GOI in their gametes are bred to generate male and female GOI heterozygous mice. The heterozygotes are subsequently bred, and of their offspring, one in four should be homozygous knockouts for GOI. PCR or Southern blotting is used to confirm homozygous GOI deletion. More sophisticated methods use specialized recombination systems to delete a GOI in a tissue-specific and/or temporally regulated manner.

GENE EXPRESSION ANALYSIS

Northern Blotting

The name Northern blot was coined to describe the technique for separating RNA by gel electrophoresis and is analogous to the Southern blot technique used to study DNA. Both abundance and turnover of specific RNAs can be detected by Northern blot. Total cellular RNA is harvested from tissue or cells and then denatured to prevent hydrogen bonding between base pairs. Denatured RNA is in a linear, unfolded conformation, which allows fragments to be separated by gel electrophoresis according to size. This is then transferred to a membrane, made of either nitrocellulose or nylon, which can then be hybridized by a specific DNA probe. This technique is rarely used today because of the advent of reverse transcription (RT) PCR described in the following text.

RNA Interference

The expression of a given gene can be reduced through RNA interference (RNAi). In mammalian cells, gene silencing by RNAi is initiated in one of two ways, either **short-interfering RNAs (siRNAs)** or **short-hairpin RNA (shRNA)** expression vectors (Fig. 17.18). siRNAs utilize the fact that double-stranded RNA induces a potent antiviral response. Once introduced into a cell, siRNAs of 21 to 25 nucleotides in length interact with the RNA-induced silencing complex (RISC), composed of several proteins. The siRNA directs RISC to its **complementary RNA** target sequence, resulting in cleavage and subsequent silencing of the target RNA. Similar expression vectors can be used to introduce shRNAs, which are then cleaved into double-stranded RNAs by Dicer, a cytoplasmic nuclease. These RNAs of 21 to 25 nucleotides can then interact with RISC, leading to silencing of target RNA sequences. In general, siRNAs are useful for transient gene silencing, whereas shRNAs are more useful for long-term gene inactivation due to their inherent low rate of degradation.

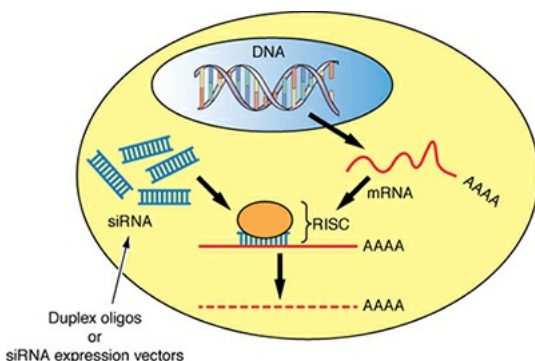


FIGURE 17.18 Short double-stranded RNA molecules (short-interfering RNAs [siRNA]) are transfected into a cell as chemically synthesized oligo duplexes or hairpin expression vectors. Cellular RNA degradation machinery incorporates the siRNA to form the RNA-induced silencing complex (RISC). The sequences incorporated cause the RISC complex to selectively recognize the complementary sequences on target messenger RNAs (mRNAs). RISC cleaves the mRNA, leading to degradation and a functional loss of protein expression. (Adapted from Brummelkamp TR, Bernards R. New tools for functional mammalian cancer genetics. *Nature Rev Cancer.* 2003;3:781–789.)

Reverse Transcription Polymerase Chain Reaction

Although the Northern blot is the classical method to assay gene expression, it requires a rather large amount of RNA (5 to 10 mcg), particularly if the RNA to assay is in low abundance. To circumvent this limitation, RNA can be amplified using RT followed by amplification of the resulting cDNA with conventional PCR techniques. Several retroviruses express DNA polymerases that can reverse transcribe viral RNA into DNA prior to genomic insertion. RNA purified from cells is annealed with random primers and incubated with a **reverse transcriptase** (Moloney Murine Leukemia Virus RT or a commercial variant is most common) and deoxynucleotides. The cDNA is amplified by PCR with primers specific for the GOI and separated by electrophoresis for imaging. It is important to use linear PCR conditions and to also amplify a control RNA (actin, glyceraldehyde 3-phosphate dehydrogenase [GAPDH]) for normalization, relative quantities can be determined and used to assay changes in gene expression. However, because this technique is subject to variation from primer efficiencies and PCR amplification, it is often referred to as semiquantitative RT-PCR.

Quantitative Real-Time Polymerase Chain Reaction

The need to verify gene expression data from microarray studies led to the

widespread use of **quantitative real-time PCR** (qRT-PCR). Originally developed for preimplantation diagnosis in fertility clinics, qRT-PCR makes it possible to accurately quantify RNA from very small amounts of a starting sample. Amplification and measurement take place in the same reaction vessel, enabling high-throughput analysis. The qRT-PCR thermocyclers have extremely large dynamic ranges (greater than five orders of magnitude), allowing for quantitation of both high- and low-abundance RNAs from the same sample. RNA from cells or tissue is reverse transcribed into cDNA and then amplified with specific primers in the presence of a fluorescent oligo specific for a GOI (TaqMan, minor groove binder [MGB] probes, etc.) or a fluorescent intercalating dye (SYBR Green). At each PCR cycle, the change in fluorescence is recorded. After normalizing amplification of a GOI against that of a control RNA, it is then possible to calculate the differences in gene expression among samples.

Genetic Reporters

Genetic reporters are extremely useful tools for monitoring a broad range of cellular processes. Reporters can be used to assay the cellular microenvironment, to study protein–protein interactions, to study RNA processing, or to study regulation of gene transcription. Reporters are often plasmids that contain a sequence of DNA derived from a promoter or other transcriptional regulatory sequence, such as an enhancer or repressor, that is ligated to a gene that is not normally expressed in the mammalian cell. These reporter genes encode proteins that are easily detected by changes in enzymatic activity, by resistance to antibiotics, or by expression of a membrane protein. Common reporter genes are those that code for β -galactosidase, chloramphenicol acetyltransferase, firefly luciferase, *Renilla* luciferase, and a host of fluorescent proteins from aquatic organisms (**green fluorescent protein [GFP]**, red fluorescent protein [RFP], etc.). There are many different types of promoter sequences that can be used to regulate the expression of a reporter gene: Some promoters are constitutively expressed (from housekeeping genes or viral genes), whereas others are artificial creations of a particular transcriptional regulatory sequence (i.e., the p53 tumor-suppressor binding sequence) and a basal promoter element. For example, to investigate the regulation of p53 in irradiated cells using a reporter gene, a promoter consisting of the p53 binding site and a basal regulatory element would be more appropriate than a large promoter that contains other radiation-responsive regulatory factors in addition to p53.

Promoter Bashing

A very common use of biologic reporters is the “promoter bash,” where a promoter is dissected to determine which region is responsible for an interesting activity (e.g., as induction during ionizing radiation or hypoxia). Using conventional techniques, the promoter is cloned upstream of a bioluminescent reporter gene, such as the gene coding for firefly luciferase, and transfected into cells with a control plasmid constitutively expressing *Renilla* luciferase. This approach makes use of the differing substrate dependencies of luciferase enzymes from fireflies (*Photinus pyralis*) and jellyfish (*Renilla reniformis*). Using two distinct reagents, light emitted by the firefly construct that reflects promoter activity in response to ionizing radiation can be normalized with the signal from the *Renilla* construct that reflects promoter expression in unstressed cells to correct for transfection efficiency. By systematically deleting parts of the **flanking region** of the promoter, one can isolate the DNA sequence that regulates promoter activity (Fig. 17.19).

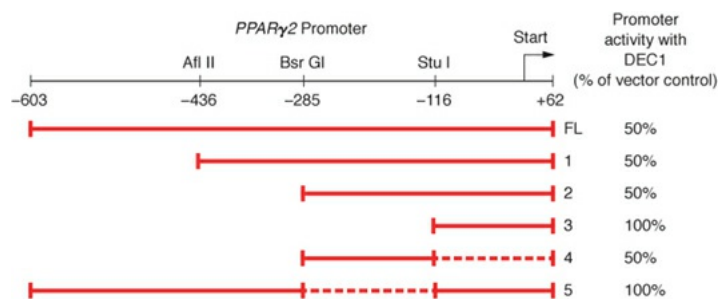


FIGURE 17.19 Example of a promoter-bashing experiment. *PPAR γ 2* expression has been shown to be repressed by the transcription repressor DEC1. 665 (the span from -603 to +62) base pairs of the *PPAR γ 2* promoter are cloned upstream of a firefly luciferase reporter (FL) and transfected into NIH3T3 mouse fibroblasts with either a *DEC1* expression construct or an empty vector. The activity of the FL construct is repressed to approximately 50% by DEC1. The FL construct was progressively truncated with restriction enzymes (constructs 1 to 3), demonstrating that deletion of a fragment spanning -285 through -116 (construct 3) removes the ability of DEC1 to repress transcription. Luciferase driven by the -285 through -116 fragment in isolation (construct 4) is still repressed by DEC1, confirming the location of a repressed region. This is confirmed by deletion of the region from the full-length promoter (construct 5), which is no longer repressed by DEC1. (From Yun Z, Maecker HL, Johnson RS, et al. Inhibition of *PPAR gamma* 2 gene expression by the HIF-1-regulated gene *DEC1/Stra13*: a mechanism for regulation of adipogenesis by hypoxia. *Dev Cell.* 2002;2:331–341.)

Chromatin Immunoprecipitation

Methods to study transcriptional regulation in mammalian cells are generally limited to biochemical assays (cell-free transcription, electrophoretic mobility shift assays, etc.) or cellular assays (transiently transfected reporter assays). Although both approaches are useful, they are limited in that they can only approximate the interactions that occur in the cell, primarily because neither can completely duplicate the chromatin environment *as it exists in the cell*. On the other hand, *in vivo* footprinting can demonstrate that something is bound to native chromatin but cannot identify the specific protein involved. **Chromatin immunoprecipitation** (ChIP) is a revolutionary advance that determines transcription factor interactions with a target promoter in the native chromatin environment (Fig. 17.20). Cells, tissues, or tumors are fixed with formaldehyde and sonicated to shear DNA into short fragments (typically 1 kb or less). Promoters and other regulatory regions are then immunoprecipitated with an antibody against a protein thought to bind to that region. DNA can then be identified and quantified by PCR or microarray analysis. Using this technique, it is possible to correlate the DNA-binding activity of a given transcription factor with corresponding changes in the surrounding chromatin environment and gene expression in cells exposed to different hormones, cellular stresses, and differentiation programs.

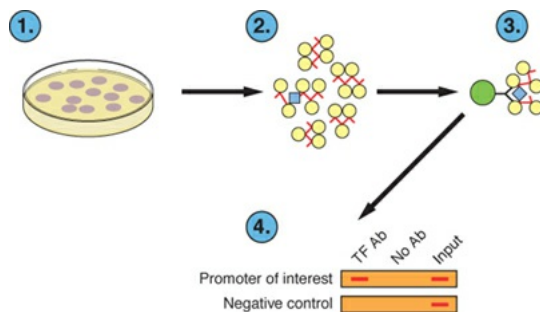


FIGURE 17.20 Illustration showing key steps in chromatin immunoprecipitation. 1. Fix cells with formaldehyde. 2. Sonicate chromatin into 500- to 1,000-bp fragments. 3. Immunoprecipitate transcription factor (TF) with a specific antibody. 4. De-crosslink DNA, use polymerase chain reaction (PCR) to verify specific interaction with target promoter and visualize specific amplification by agarose electrophoresis.

Protein–DNA Interaction Arrays (Chromatin Immunoprecipitation-Chips)

Surveying all of the interactions of the transcription apparatus with the human genome is a daunting task. ChIP-chips combine the power of the ChIP assay with microarray technology to investigate these interactions (the “Chips” are

chips of glass slides on which the ChIP is placed). Immunoprecipitated chromatin is ligated to universal primers and amplified by PCR to generate a pool of DNA associated with a given transcription factor. DNA is fluorescently labeled, mixed with amplified and labeled unprecipitated DNA (input), and hybridized to a microarray of regulatory DNA. Higher relative fluorescence from the immunoprecipitated DNA on a spot compared with input indicates an interaction of the protein with that regulatory sequence. This technique has been used primarily to map transcription factor binding and histone modification across the entire yeast genome. The vastly larger size of the human genome has made it necessary to focus on more specific regions using arrays of either cloned promoter fragments or CpG islands (sequences of DNA that cluster around promoters and other regulatory regions). Production of high-density tiled microarrays spanning all promoters in the human genome will soon make possible the correlation of transcription factor binding, chromatin structure, and gene expression.

Microarrays to Assay Gene Expression

With the sequencing of the human genome, studying global changes in gene expression became possible in principle. Efforts were being made to study the expression of as many genes as possible without resorting to individual Northern blots for each identified gene. In this way, the microarray was born. Expression arrays work like an inverse Northern blot: Cellular RNA is reverse transcribed, amplified with modified nucleotides that allow fluorescent detection, and hybridized to an array of sequences corresponding to the genes in an organism (Fig. 17.21). The arrays used for detection fall into two types: spotted and oligo arrays.

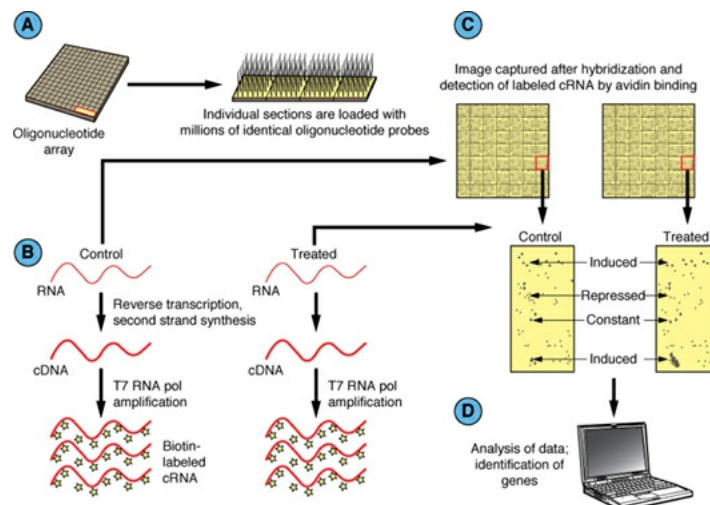


FIGURE 17.21 Oligonucleotide microarray analysis. **A:** Silicon wafers are

divided into thousands of sectors, each contains millions of identical 20- to 50-bp oligonucleotides corresponding to a different unique gene sequence. **B:** RNA from cell samples is reverse transcribed to complementary DNA (cDNA). Complementary RNA (cRNA) is amplified from the cDNA using T7 RNA polymerase and biotinylated nucleotides. **C:** The labeled cRNA is hybridized to the arrays, bound with fluorescently labeled avidin, and detected by microscopy. **D:** Differences in intensity between experimental and control samples are quantified and analyzed with computer software.

Spotted arrays consist of a glass microscope slide spotted with a grid of cDNAs for specific genes. RNA from two different samples are amplified with two different colored fluorescent dyes and scanned after hybridization. The ratio of fluorescence for each spot is calculated to generate a baseline ratio. Spots that differ from the baseline by a statistically determined amount correspond to genes whose expression differs between the two samples. Facilities to print spotted arrays can be found at most universities.

An alternative method is to use oligo arrays, like those offered by Affymetrix. Using photolithography, thousands of short DNA oligos corresponding to genes are printed in multiple places on an area about the size of a postage stamp. RNA is amplified with biotinylated nucleotides and hybridized. The hybridized RNA is then bound with fluorescently labeled avidin and visualized. Because of the large number of sequences printed with a high degree of redundancy, different samples can be compared with each other in separate hybridizations, removing the need to hybridize two samples on one slide.

With either type of array, the experiment needs to be repeated several times before the result can be relied upon. It is also necessary to verify selected expression differences using independent means, such as **Northern blotting**, RT-PCR, or qRT-PCR.

RNA-Seq to Assay Gene Expression

The advantages of gene arrays is that they are high throughput and relatively inexpensive. However, their weaknesses are (1) a heavy dependence on knowing genome sequence, (2) potentially high background for some sequences, and (3) a limited dynamic range to quantitatively assess gene expression. As an alternative to microarrays, sequencing-based approaches were developed, and although they were not subject to the same limitations as microarrays, they proved to be too expensive for widespread commercial use due to the need of traditional Sanger sequencing.

With the advent of NGS for DNA, it was not long before the same deep sequencing was applied to RNA. For RNA-Seq, either total or poly A purified RNA is made into a library of cDNA fragments with adaptors at one or both ends of the molecule. These molecules can then be directly sequenced or first amplified and then sequenced to obtain short sequence reads (30 to 300 bp) from one end (single end sequencing) or both ends (paired-end sequencing). After sequencing, the reads can be aligned with a known reference genome or generate a de novo reference transcriptome (Fig. 17.22). Two key advantages of RNA-Seq are you can get very precise information on transcript structure as well as transcript number.

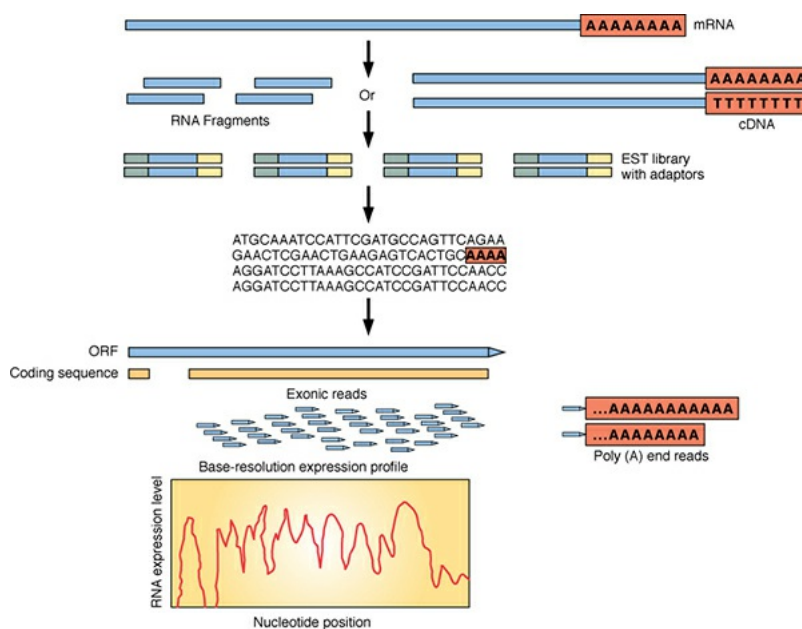


FIGURE 17.22 Illustration of the protocol for RNA-Seq. In this technique, RNAs are made into a complementary DNA (cDNA) library. To each of the cDNA fragments, sequencing adaptors (green and yellow) are added, and a short partial sequence of each cDNA is derived through sequencing. The sequenced fragments can then be subclassified into junction reads between exons, exon reads, and poly A reads. With these three classifications and the sequence, one can then quantitatively access expression changes. mRNA, messenger RNA; EST, expressed sequence tag; ORF, open reading frame. (Modified from Wang et al., *Nat Rev Genet.* 2009;10:57–63, with permission.)

Chromatin Immunoprecipitation-Seq

In a manner similar to RNA-Seq, ChIP-Seq combines ChIP with deep sequencing to identify the sequence specific binding sites of chromatin-associated proteins and transcriptional regulatory proteins. The two combined approaches have been discussed earlier. This approach has distinct advantages

over ChIP-Chips in that a single sequencing run can identify genome-wide protein–DNA interactions with high resolution and much lower cost than large sets of so-called “tiling arrays.”

PROTEIN ANALYSIS

Western Blotting

The term *Western blot* is used for proteins, analogous to Southern blot for DNA and Northern blot for RNA. Western blot analysis is a method to detect the presence and abundance of a specific protein within a mixture of proteins. This is achieved by first separating the mixture of proteins based on both charge and size through **polyacrylamide gel electrophoresis** (PAGE). A membrane (nitrocellulose or vinyl) is then placed on top of the gel, and the proteins are transferred by electrophoresis toward the membrane. The membrane is incubated with a primary antibody, which specifically recognizes the protein of interest (POI). Following a brief wash period to eliminate any excess primary antibody, the membrane is incubated with a secondary antibody, which specifically recognizes the primary antibody. The secondary antibody is conjugated to an enzyme to allow subsequent detection.

Antibody Production

Antibodies specific to a gene product of interest can be produced, provided there is a source of purified protein. This purified protein (**antigen**) is then injected into an animal (e.g., mouse, rat, rabbit, goat, sheep, or chicken) with an adjuvant to stimulate the immune response to the purified protein. **Monoclonal antibodies** are made by injecting either mouse or rats with the POI. The antibody-producing cells of the spleen (**B lymphocytes**) are then fused to a specific tumor cell line to create a hybridoma. The hybridoma is then screened for antibody production and specificity. For **polyclonal antibodies**, an animal is injected with the POI and adjuvant and then bled. The antibodies can then be purified out of the blood.

Immunoprecipitation

Immunoprecipitation is used to detect specific protein–protein interactions. An antibody against a specific protein is incubated with a sample that contains the target and allowed to form an immune complex. This complex is then captured and immobilized by the addition of proteins A and G agarose, which are used for the isolation and purification of the antibody and protein complex. Proteins A

and G are derived from streptococcal groups A and G, respectively, and bind immunoglobulin G (IgG) antibodies with high affinity. Unbound proteins are washed away, and the bound immune complex are eluted and analyzed by Western blot.

Far Western Blotting

The Far Western blot is another useful method for probing protein–protein interactions. In this variation of the Western blot (or immunoblot), instead of using an antibody to detect a specific protein, purified recombinant protein is used to probe a membrane of electrophoresed cellular protein. The recombinant protein (sometimes called the “bait”) binds to specific cellular proteins on the membrane and is detected by autoradiography or with a specific antibody. Various protein chemistry approaches can then be used to identify the interacting proteins on the membrane.

Fluorescent Proteins

Several aquatic organisms express fluorescent proteins that make excellent reporters. The two most commonly used fluorescent proteins are GFP from the jellyfish *Aequorea coerulescens* and RFP from *Discosoma* reef coral. Because of their widely different spectral properties, they make excellent reagents for two-color labeling of cells. A common practice is to fuse GFP to a POI and RFP to another POI to simultaneously monitor intracellular protein activity either in cells in culture or in mice (see Fig. 17.22). GFP has also been engineered to fluoresce in the cyan (cyan fluorescent protein [CFP]) and yellow (yellow fluorescent protein [YFP]) spectra. The emission spectrum of CFP overlaps with the excitation spectrum of YFP. By fusing CFP to a POI and YFP to another protein, it is possible to observe interactions by exciting CFP with light and observing YFP fluorescence. This method, called fluorescence resonance energy transfer (FRET), is a useful way to observe the dynamic interactions of proteins in the cell. Fluorescence recovery after photobleaching (FRAP) can be used to determine intracellular dynamics of proteins. A GFP fusion protein is bleached with laser light in a specific region of a cell. Observing the rate of fluorescence recovery to the bleached spot with a microscope can reveal the mechanisms governing cellular trafficking of the labeled protein.

Two-Hybrid Screening

The two-hybrid screen, most frequently performed in the model organism *Saccharomyces cerevisiae* (budding yeast), is a powerful method for identifying

factors that interact with a given protein. The cDNA for a POI is cloned into an expression vector as a fusion with the DNA-binding domain of a transcription factor (GAL4-DBD) (Fig. 17.23). This construct is referred to as the “bait.” A cDNA library is cloned into an expression vector as a fusion with the activation domain of a transcription factor. This library is referred to as the “prey.” The bait is transformed into a line of yeast that expresses a selection reporter (HIS3, an enzyme required for histidine biosynthesis). When the bait fusion is expressed, it binds to the HIS3 reporter with the GAL4-DBD, but cannot activate transcription and the yeast cannot grow on media lacking the amino acid histidine. If one of the “prey” constructs expresses a protein that interacts with the POI, it brings with it a transcription activation domain, HIS3 expression occurs, and a yeast colony grows on the selective media. The “prey” plasmid is recovered from the yeast colony and sequenced to identify the POI-interacting protein. The two-hybrid screen has been widely used to identify proteins that are involved in DNA repair complexes and radiation-induced signal transduction.

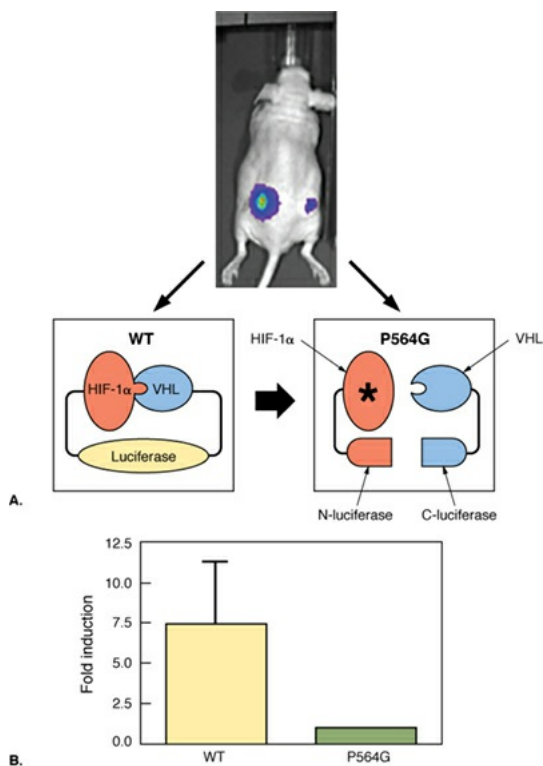


FIGURE 17.23 Illustration of the power of the Split luciferase technique to detect protein–protein interactions. **A:** Detection of Hypoxia-inducible factor 1-alpha (HIF-1 α) binding to Von Hippel-Lindau (VHL) in tumor cells. The premise of this technique is that by attaching the amino fragment of luciferase to HIF-1 α and the carboxyl fragment of luciferase to Von Hippel-Lindau (VHL), an interaction between HIF-1 α and VHL can be detected by changes in luciferase activity. The changes in luciferase activity act as a surrogate for changes in

binding activity between the two proteins. This change in luciferase can be compared to a control, which contains a point mutation in proline 564 (P564G) that virtually eliminates binding. In **A**, the difference between the wild-type and the mutant HIF-1 α and VHL interaction are seen in tumor cells implanted into an immunodeficient mouse. **B:** Quantitation of the differences in binding activity of HIF-1 α and VHL as a function of fold-changes in luciferase activity.

Split Luciferase Complementation Assay

A somewhat different approach to study protein–protein interactions involves splitting a reporter gene such as luciferase into amino (N–) and carboxyl (C–) fragments, which by themselves have no luciferase activity. These N– and C– fragments are then ligated to proteins that are known to interact or unknown to interact. If the proteins interact, they will then bring the luciferase fragments to come in close enough proximity to produce a functional luciferase molecule (see Fig. 17.23). This approach is quite robust, and the level of luciferase activity reflects the protein–protein interactions. The advantage of this approach over the two-hybrid screening is that it can be performed in mammalian cells both in cell culture as well as in tumors *in vivo*. In addition, the effect of the cellular microenvironment can be studied in how it affects protein–protein interaction.

Proteomics

Just as the field of genomics seeks to catalog genes and transcriptional regulation, the field of proteomics seeks to catalog all of the proteins in the cell and their interactions with each other. This is a tremendous endeavor. Although the genes in a genome are static, each gene can have different transcripts and splice variants, each of which may be translated into a distinct protein. Each protein may also be modified in multiple ways after translation, essentially creating a different protein with each modification. A given cell could contain several hundred thousand different proteins at a given instant. This phenomenal complexity has fed the innovation of several protein chemistry and detection technologies, including two-dimensional polyacrylamide gel electrophoresis/matrix-assisted laser desorption/ionization–time of flight (2-D PAGE/MALDI-TOF), microfluidic separation, and protein microarrays. Proteomics is currently being heralded as the future of personalized medicine, where a tissue or blood sample can be used to direct the course of therapy or determine prognosis (Fig. 17.24).

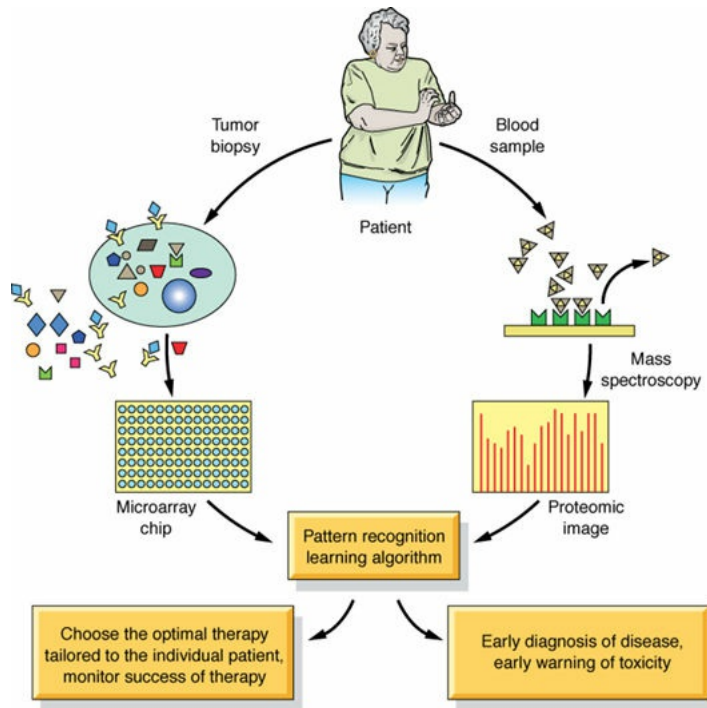


FIGURE 17.24 Proteomics has two major uses for cancer therapy. First, it can be used to detect specific secreted proteins or fragments in the serum of cancer patients that reflect a disease state or response to therapy. Second, it can be used to determine the protein profile of tumor cells to aid in directing therapy. Proteomic microarrays are still in their early days and are in large part arrayed antibodies that detect protein binding. (Adapted from Petricoin E, Zoon K, Kohn E, et al. Clinical proteomics: translating benchside promise into bedside reality. *Nat Rev Drug Discov.* 2002;1:683–695.)

Two-Dimensional Electrophoresis

2-D PAGE is a workhorse technique for molecular biologists studying posttranslational modification of proteins. Every protein has a distinct electrochemical charge that is a result of its unique amino acid composition. Using an electrophoresis technique known as isoelectric focusing (IEF), proteins can be separated by charge in tube gels or paper strips. The IEF tubes or strips are then laid across the top of a sodium dodecyl sulfate (SDS)-PAGE gel and separated by size. The gel is then stained to visualize proteins, which appear as slightly elongated spots. The identity (and modification) of the proteins in the spots can then be determined using **Western blotting** or mass spectrometry. High-throughput methods to automate this process are still in development.

DATABASES AND SEQUENCE ANALYSIS

Before completion of the large-scale genome-sequencing projects, when

individual research groups cloned and sequenced a gene, they needed to know if the same or if homologous sequences had already been identified in other model organisms. This led to the development of databases, like GenBank, a database at the National Center for Biotechnology Information (www.ncbi.nlm.nih.gov) for the deposition of individually cloned genomic, cDNA and protein sequences. At the same time, sequence analysis programs were developed to identify regions of similarity among different nucleotide or protein sequences. Related programs, called search engines, were developed to find similar sequences from the ever-growing list of identified genes contained in the databases. One of the most commonly used programs for finding related sequences from the genome databases is Basic Local Alignment Search Tool (BLAST), found on the National Center for Biotechnology Information website. These approaches expanded in scope to include the genomes of organisms and the annotated coding sequences and their identified functions. It is now possible to take virtually any sequence and search for the identity of the corresponding gene in humans, mice, and an ever-expanding collection of model and agricultural organisms. Similar search engines can identify putative transcription factor binding sites from a gene promoter region or cluster proteins by related enzymatic functions or predict protein structure. Another very useful site is the Cancer Genome Atlas and Genomic Data Commons sites. These sites provide a data repository, data analysis tools, and useful publications.

SUMMARY OF PERTINENT CONCLUSIONS

Restriction endonucleases are enzymes that cleave DNA after recognizing a specific sequence. Those most useful for constructing recombinant molecules leave a “sticky” end, that is, a single-strand overhang of two to four nucleotides that can pair with a complementary strand.

A vector is an autonomously replicating DNA molecule into which foreign DNA fragments are inserted and then propagated in a host cell. Vectors include plasmids, bacteriophage, BACs, and viruses.

A library is a collection of cells, usually bacteria or yeast, containing recombinant vectors, carrying DNA inserts from a different species. The inserts may be constructed by using restriction enzyme-digested genomic DNA or cDNA.

A host is used to grow (i.e., to multiply) or to express a DNA fragment containing a GOI.

In agarose gel electrophoresis, DNA or RNA molecules can be separated

according to size by causing them to move through a matrix composed of purified agar under the influence of an electrical field.

PCR is a procedure that enzymatically amplifies the number of copies of a DNA sequence, up to several thousand base pairs, through repeated replication by DNA polymerase. (A DNA polymerase is an enzyme that catalyzes the addition of nucleotides to a growing DNA molecule.) PCR has been adapted to analyze RNA expression through the use of RT-PCR. Use of a specialized thermocycler enables qRT-PCR, a very sensitive PCR technique that enables high-throughput nucleic acid analysis and quantitation.

CGH is a more modern refinement that starts by identifying regions of chromosomal duplication or deletion. The genes in the abnormal region can then be analyzed by expression or functional studies to identify candidate genes in the region.

RNA transcription can be measured by Northern blotting, RT-PCR methods, hybridization to microarrays, or RNA-Seq.

The microarray is a useful platform for studying gene expression changes (RNA), gene aneuploidy (CGH), and protein-DNA interactions (ChIP-Chips). The primary advantage of the microarray is the sheer number of sequences that can be analyzed at one time. The major disadvantage is a heavy reliance on knowing genome sequence.

The completion of whole genome-sequencing projects for humans, mice, fruit flies, nematodes, and yeast has made gene mapping largely obsolete. Virtually any genomic sequence can now be accessed from international databases.

Once a gene is cloned, it can be sequenced by one of several methods, the most common of which is the chain termination method. Use of fluorescently labeled dyes on the dideoxynucleotides enables automated laser scanners to acquire sequence from a single lane.

The amino acid sequences within a protein can be determined from the corresponding DNA sequence using the known genetic triplet code.

A newly acquired sequence can be compared with the international database to seek homologies with known genes or proteins.

Structural variations in DNA caused by point mutations, deletions, or insertions can result in restriction fragments of different lengths, which can often be detected by Southern blotting. These are known as restriction

fragment length polymorphisms, which can be used as genetic markers to map genes to specific chromosomal locations and identify aberrant genes causing disease.

A mutation involving only a single base-pair difference between two short single-stranded DNA molecules can be detected by the technique of single-stranded conformation polymorphism.

A useful approach to studying a GOI is to introduce it into a cell or organism (typically a mouse), overexpress it, and observe the biologic effect.

Another useful approach for studying the function of an identified gene is to “knockout” expression of a gene. This can be done by using either homologous recombination or RNAi.

CRISPR-Cas9 is a powerful new tool in genome editing, which requires three components—a Cas9 nuclease with its CRISPR RNA and tRNA. Commercial versions have combined all of these components into a synthetic guide RNA.

RNA-Seq exploits deep sequencing to obtain information on both transcript structure as well as transcript number.

Genetic reporters are useful tools for studying biologic phenomena like transcriptional regulation, protein dynamics, and intracellular location. Reporters have easily assayable activities (light emission, fluorescence, or colorimetric substrates), providing flexibility to suit a given experimental system.

The ChIP assay can be used to study promoter function in intact cells, either to identify transcription factor interactions with promoters or to dissect mechanisms of regulation. DNA purified by ChIP can be analyzed individually by PCR or by hybridization to promoter microarrays.

The field of proteomics seeks to define the quantities and interactions of the vast number of proteins in a given cell at a given instant in time. Proteomics uses established technology like 2-D electrophoresis, Western blotting, immunoprecipitation, and mass spectroscopy but uses more advanced high-throughput technology to expedite the process.

Protein–protein interactions can be identified by coimmunoprecipitation or two-hybrid analysis. Fluorescent protein fusion proteins are useful tools for further study of intracellular interactions and dynamics.

GLOSSARY OF TERMS

agarose gel electrophoresis: Electrophoresis in which a matrix composed of purified agarose is used to separate larger DNA and RNA molecules (ranging from 100 to 20,000 nucleotides).

alleles: Alternate forms of a gene or DNA sequence on the two homologous chromosomes of a pair.

amino acids: The 20 basic building blocks of proteins.

ampicillin: An antibiotic that prevents bacterial growth.

amplify: To increase the number of copies of a DNA sequence by inserting into a cell *in vivo* or *in vitro* by the polymerase chain reaction.

anneal: To pair complementary DNA or RNA sequences, via hydrogen bonding, to form a double-stranded polynucleotide.

antibiotic: A compound such as ampicillin that inhibits the growth of or kills microorganisms.

antibiotic resistance: The ability of a microorganism to disable an antibiotic or prevent transport of the antibiotic into the cell.

antibody: An immunoglobulin protein produced by B lymphocytes that binds to a specific antigen.

antigen: Any foreign substance that elicits an immune response by stimulating the production of antibodies.

bacterial artificial chromosome: A vector used to clone DNA fragments of up to 300,000 bp, which contains the minimum chromosomal sequences needed to replicate at a low copy number in bacteria.

bacteriophage: A virus that infects bacteria. Altered forms are used as vectors for cloning DNA.

bacterium: A single-celled prokaryotic organism.

base pair: A pair of complementary nitrogenous bases in a DNA molecule: adenine–thymine or guanine–cytosine. It is also a measure of the length of DNA sequences.

B lymphocyte: A white blood cell responsible for production of antibodies in the humoral immune response.

Cas9: CRISPR associated genes.

cDNA library: A library composed of complementary copies of cellular mRNAs (i.e., the exons without the introns).

cellular oncogene (proto-oncogene): A normal gene that if mutated or improperly expressed contributes to the development of cancer.

centromere: The central portion of the chromosome to which the spindle fibers attach during mitotic and meiotic division.

chromatin immunoprecipitation: The selective purification of transcription factors bound to DNA that provides information on transcriptional regulation inside cells.

codon: A group of three nucleotides that specifies the addition of one of the 20 amino acids during translation of mRNA into a polypeptide.

colony: A group of identical cells derived from a single ancestor cell.

complementary DNA (cDNA): DNA synthesized from an RNA template using reverse transcriptase.

complementary nucleotides: Members of the pairs adenine–thymine, adenine–uracil, and guanine–cytosine that have the ability to hydrogen-bond to each other.

complementary RNA (cRNA): RNA synthesized from a cDNA template using T7 RNA polymerase for the purpose of microarray hybridization.

contig: A collection of DNA sequences that overlap at portions of their ends.

CRISPR: Clustered regularly interspaced short palindromic repeats.

digest: To cut DNA molecules with one or more restriction endonucleases.

DNA (deoxyribonucleic acid): An organic acid composed of four nitrogenous bases (adenine, thymine, cytosine, and guanine) linked via sugar and phosphate units. DNA is the genetic material of most organisms and usually exists as a double-stranded molecule in which two antiparallel strands are held together by hydrogen bonds between adenine–thymine and cytosine–guanine base pairs.

DNA fingerprint: A unique pattern of DNA fragments identified by Southern hybridization or by polymerase chain reaction.

DNA polymerase: An enzyme that synthesizes a double-stranded DNA molecule using a primer and DNA as a template.

DNA polymorphism: Two or more alternate forms of a chromosomal locus that differ in nucleotide sequence or have variable numbers of repeated nucleotide

units.

DNA sequencing: Procedures for determining the nucleotide sequence of a DNA fragment.

electrophoresis: The technique of separating charged molecules in a matrix to which an electrical field is applied.

electroporation: Process in which high-voltage pulses of electricity are used to open pores in the cell membrane, through which foreign DNA can pass.

***Escherichia coli*:** A bacterium that is found in the human colon and is widely used as a host for molecular cloning experiments.

ethidium bromide: A fluorescent dye that is used to stain DNA and RNA and that intercalates between nucleotides and fluoresces if exposed to ultraviolet light.

exon: That portion of a gene expressed in mature mRNA.

expression library: A library of cDNAs whose encoded proteins are expressed by specialized vectors.

flanking region: The DNA sequences extending on either side of a specific locus or gene.

gene: A locus on a chromosome that encodes a specific protein or several related proteins.

gene amplification: The presence of multiple copies of a gene. This is one mechanism by which proto-oncogenes are activated to result in neoplasia.

gene expression: The process of producing a protein from its DNA- and mRNA-coding sequences.

genetic code: The three-letter code that translates a nucleic acid sequence into a protein sequence.

genome: The genetic complement contained in the chromosomes of a given organism.

genomic library: A library composed of fragments of genomic DNA.

green fluorescent protein (GFP): A naturally fluorescent protein that can be used as a bioluminescent marker in cell culture studies and in mice.

hybridization: The hydrogen bonding of complementary DNA or RNA sequences to form a duplex molecule.

immunoprecipitation: Detection of cellular proteins or protein complexes by the binding to antibodies immobilized on beads.

initiation codon: The mRNA sequence AUG, which codes for methionine and initiates translation.

library: A collection of cells (usually bacteria or yeast) that have been transformed with recombinant vectors carrying DNA inserts from a single species.

ligase: An enzyme that catalyzes a reaction that links two DNA molecules by the formation of a phosphodiester bond.

ligation: The process of joining two or more DNA fragments.

messenger RNA (mRNA): The class of RNA molecules that copies the genetic information from DNA in the nucleus and carries it to ribosomes in the cytoplasm.

microarray: A slide coated with thousands of oligonucleotides or cDNAs that is hybridized with labeled cRNA from cells to monitor expression changes.

microinjection: Introducing DNA into a cell using a fine microcapillary pipette.

Monoclonal antibodies: Immunoglobulin molecules of single-epitope specificity.

mutation: An alteration in DNA structure or sequence of a gene.

Northern blotting: A procedure in which RNA fragments are transferred from an agarose gel to a nitrocellulose filter, where the RNA is then hybridized to a radioactive probe.

nucleotide: A building block of DNA and RNA.

oncogene: A gene that contributes to cancer formation when mutated or inappropriately expressed.

open reading frame: A long DNA sequence, uninterrupted by a stop codon, that encodes part or all of a protein.

plaque: A clear spot on a lawn of bacteria or cultured cells where cells have been lysed by viral infection and replication.

plasmid: A circular DNA molecule that is capable of autonomous replication and may typically carry one or more genes encoding antibiotic resistance.

point mutation: A change in a single base pair in a gene.

polyacrylamide gel electrophoresis: Electrophoresis through a matrix composed of synthetic polymer, used to separate small DNA or RNA molecules (up to 1,000 nucleotides) or proteins.

polyclonal antibodies: A mixture of immunoglobulin molecules secreted against a specific antigen, each recognizing a different epitope.

polymerase: An enzyme that catalyzes the addition of multiple subunits to a substrate molecule.

polymerase chain reaction (PCR): A procedure that enzymatically amplifies a DNA sequence through repeated replication by DNA polymerase.

primer: A short DNA or RNA fragment annealed to single-stranded DNA.

probe: A single-stranded DNA (or RNA) that has been radioactively labeled and is used to identify complementary sequences.

quantitative real-time PCR: A very sensitive PCR technique to quantify changes in DNA or RNA accurately in a high-throughput manner.

recombinant DNA: The process of cutting and recombining DNA fragments.

restriction endonuclease: An enzyme that cleaves DNA after recognizing a specific sequence.

restriction fragment length polymorphism: Differences in nucleotide sequence between alleles that result in restriction fragments of varying lengths.

retrovirus: A type of virus whose genome consists of RNA and which utilizes the enzyme reverse transcriptase to copy its genome into a DNA intermediate, which integrates into the chromosome of a host cell.

reverse transcriptase: An enzyme that synthesizes a complementary DNA strand from an RNA template.

RNA (ribonucleic acid): An organic acid composed of repeating nucleotide units of adenine, guanine, cytosine, and uracil and whose ribose components are linked by phosphodiester bonds.

RNA polymerase: An enzyme that transcribes RNA from a DNA template.

Saccharomyces cerevisiae: Brewer's yeast.

selectable marker: A gene whose expression makes it possible to identify cells that have been transformed or transfected with a vector containing the marker gene. It is usually a gene for resistance to an antibiotic.

short-hairpin RNA (shRNA): A complementary hairpin expressed from a vector that causes target cellular RNA to be degraded.

short-interfering RNA (siRNA): A short inhibitory double-stranded RNA molecule that causes target cellular RNA to be degraded.

Southern blotting: A procedure in which DNA restriction fragments are transferred from an agarose gel to a nitrocellulose filter, where the denatured DNA is then hybridized to a radioactive probe.

sticky end: A single-stranded nucleotide sequence produced if a restriction endonuclease cleaves off-center in its recognition sequence.

Taq polymerase: A heat-stable DNA polymerase used in the polymerase chain reaction.

template: An RNA or single-stranded DNA molecule on which a complementary nucleotide strand is synthesized.

termination (stop) codon: Any of three mRNA sequences (UGA, UAG, UAA) that do not code for an amino acid and thus signal the end of protein synthesis.

transcription: The process of creating a complementary RNA copy of DNA.

transfection: The uptake and expression of foreign DNA by cultured eukaryotic cells.

transfer RNA (tRNA): Small RNA molecules that transfer amino acids to the ribosomes during protein synthesis.

transformation: In higher eukaryotes, the conversion of cultured cells to a malignant phenotype. In prokaryotes, the natural or induced uptake and expression of a foreign DNA sequence.

translation: The process of converting the genetic information of an mRNA on ribosomes into a polypeptide.

two-dimensional gel electrophoresis: Separation of cellular proteins in one dimension based on changes in protein charge followed by separation based on size using 2-D PAGE.

vector: An autonomously replicating DNA molecule into which foreign DNA fragments are inserted and then propagated in a host cell.

Western blotting: The detection of proteins and modifications of proteins immobilized on membranes by probing with specific antibodies.

yeast artificial chromosome: A vector used to clone DNA fragments of up to

400,000 bp, which contains the minimum chromosomal sequences needed to replicate in yeast.

BIBLIOGRAPHY

- Aguirre AJ, Brennan C, Bailey G, et al. High-resolution characterization of the pancreatic adenocarcinoma genome. *Proc Natl Acad Sci USA*. 2004;101(24):9067–9072.
- Altschul SF, Gish W, Miller W, et al. Basic local alignment search tool. *J Mol Biol*. 1990;215(3):403–410.
- Arya M, Shergill I, Williamson M, et al. Basic principles of real-time quantitative PCR. *Expert Rev Mol Diagn*. 2005;5(2):209–219.
- Berns K, Hijmans EM, Mullenders J, et al. A large-scale RNAi screen in human cells identifies new components of the p53 pathway. *Nature*. 2004;428:431–437.
- Brummelkamp TR, Bernards R. New tools for functional mammalian cancer genetics. *Nature Rev Cancer*. 2003;3:781–789.
- Capecchi MR. Altering the genome by homologous recombination. *Science*. 1989;244(4910):1288–1292.
- Chalfie M, Tu Y, Euskirchen G, et al. Green fluorescent protein as a marker for gene expression. *Science*. 1994;263(5148):802–805.
- Chien C, Bartel P, Sternglanz R, et al. The two-hybrid system: a method to identify and clone genes for proteins that interact with a protein of interest. *Proc Natl Acad Sci USA*. 1991;88(21):9578–9582.
- Copeland NG, Jenkins NA, Court DL. Recombineering: a powerful new tool for mouse functional genomics. *Nat Rev Genet*. 2001;2:769–779.
- Cullum R, Alder O, Hoodless PA. The next generation: using new sequencing technologies to analyse gene regulation. *Respirology*. 2011;16:210–222.
- Das PM, Ramachandran K, vanWert J. Chromatin immunoprecipitation assay. *Biotechniques*. 2004;37:961–969.
- Eckel-Passow JE, Hoering A, Therneau TM. Experimental design and analysis of antibody microarrays: applying methods from cDNA arrays. *Cancer Res*. 2005;65:2985–2989.
- Elbashir SM, Harborth J, Lendeckel W, et al. Duplexes of 21-nucleotide RNAs mediate RNA interference in cultured mammalian cells. *Nature*.

- 2001;411(6836):494–498.
- Fire A, Xu S, Montgomery MK, et al. Potent and specific genetic interference by double-stranded RNA in *Caenorhabditis elegans*. *Nature*. 1998;391(6669):806–811.
- Fukumura D, Xavier R, Sugiura T, et al. Tumor induction of *VEGF* promoter activity in stromal cells. *Cell*. 1998;94(6):715–725.
- Fukumura D, Xu L, Chen Y, et al. Hypoxia and acidosis independently up-regulate vascular endothelial growth factor transcription in brain tumors in vivo. *Cancer Res*. 2001;61(16):6020–6024.
- Gordon JW, Ruddle FH. Integration and stable germ line transmission of genes injected into mouse pronuclei. *Science*. 1981;214:1244–1246.
- Gordon JW, Scangos GA, Plotkin DJ, et al. Genetic transformation of mouse embryos by microinjection of purified DNA. *Proc Natl Acad Sci USA*. 1980;77:7380–7384.
- Hardiman G. Microarray platforms—comparisons and contrasts. *Pharmacogenomics*. 2004;5(5):487–502.
- Johnson DS, Mortazavi A, Myers RM, et al. Genome-wide mapping of in vivo protein-DNA interactions. *Science*. 2007;316:1497–1502.
- Joyner AL, Skarnes WC, Rossant J. Production of a mutation in mouse En-2 gene by homologous recombination in embryonic stem cells. *Nature*. 1989;338:153–156.
- Kuo M, Allis C. In vivo cross-linking and immunoprecipitation for studying dynamic protein: DNA associations in a chromatin environment. *Methods*. 1999;19(3):425–433.
- Lander ES, Linton LM, Birren B, et al; for International Human Genome Sequencing Consortium. Initial sequencing and analysis of the human genome. *Nature*. 2001;409(6822):860–921.
- Mali P, Yang L, Esvelt KM, et al. RNA-guided human genome engineering via Cas9. *Science*. 2013;339:823–826.
- Micklos DA, Freyer GA. *DNA Science: A First Course in Recombinant DNA Technology*. Burlington, NC: Cold Spring Harbor Laboratory Press; 1990.
- Murray JM, Carr AM, Lehmann AR, et al. Cloning and characterisation of the *rad9* DNA repair gene from *Schizosaccharomyces pombe*. *Nucleic Acids*

Res. 1991;19:3525–3531.

- Olive KP, Tuveson DA, Ruhe ZC, et al. Mutant *p53* gain of function in two mouse models of Li-Fraumeni syndrome. *Cell*. 2004;119:847–860.
- Palapattu GS, Bao S, Kumar TR, et al. Transgenic mouse models for tumor suppressor genes. *Cancer Detect Prev*. 1998;22:75–86.
- Palmiter RD, Brinster RL, Hammer RE, et al. Dramatic growth of mice that develop from eggs microinjected with metallothionein-growth hormone fusion genes. *Nature*. 1982;300:611–615.
- Palmiter RD, Chen HY, Brinster RL. Differential regulation of metallothionein-thymidine kinase fusion genes in transgenic mice and their offspring. *Cell*. 1982;29:701–710.
- Petricoin E, Zoon K, Kohn E, et al. Clinical proteomics: translating benchside promise into bedside reality. *Nat Rev Drug Discov*. 2002;1:683–695.
- Sambrook J, Fritsch EF, Maniatis T. *Molecular Cloning: A Laboratory Manual*. 2nd ed. New York, NY: Cold Spring Harbor Laboratory Press; 1989.
- van Duin M, deWit J, Odijk H, et al. Molecular characterization of the human excision repair gene *ERCC-I*: cDNA cloning and amino acid homology with the yeast DNA repair gene *RAD10*. *Cell*. 1986;44:913–923.
- Venter JC, Adams MD, Myers EW, et al. The sequence of the human genome. *Science*. 2001;291(5507):1304–1351.
- Vijg J, van Steeg H. Transgenic assays for mutations and cancer: current status and future perspectives. *Mutat Res*. 1998;400:337–354.
- Watson JD, Gilman M, Witkowski J, et al. *Recombinant DNA*. 2nd ed. New York, NY: Scientific American Books; 1992.
- Yu JY, DeRuiter SL, Turner DL. RNA interference by expression of short-interfering RNAs and hairpin RNAs in mammalian cells. *Proc Natl Acad Sci USA*. 2002;99(9):6047–6052.
- Yun Z, Maecker HL, Johnson RS, et al. Inhibition of *PPAR gamma 2* gene expression by the HIF-1-regulated gene *DEC1/Stra13*: a mechanism for regulation of adipogenesis by hypoxia. *Dev Cell*. 2002;2:331–341.
- Zimmer A, Gruss P. Production of chimaeric mice containing embryonic stem (ES) cells carrying a homoeobox Hox 1.1 allele mutated by homologous recombination. *Nature*. 1989;338:150–153.

chapter 18

Cancer Biology

Mechanisms of Carcinogenesis

Oncogenes

Mechanisms of Oncogene Activation

- Retroviral Integration through Recombination
- DNA Mutation of Regulatory Sites
- Gene Amplification
- Chromosome Translocation

Mutation and Inactivation of Tumor Suppressor Genes

- The Retinoblastoma Paradigm
- The Li–Fraumeni Paradigm
- Familial Breast Cancer, BRCA1 and BRCA2

Somatic Homozygosity

The Multistep Nature of Cancer

Function of Oncogenes and Tumor Suppressor Genes

- Dysregulated Proliferation
- Failure to Respond to Growth-Restrictive Signals
- Failure to Commit Suicide (Apoptosis)
- Escaping Senescence
- Angiogenesis
- Invasion and Metastasis

The Concept of Gatekeepers and Caretakers

Mismatch Repair

Heritable Syndromes that Affect Radiosensitivity, Genomic Instability, and Cancer

- Ataxia-Telangiectasia
- Seckel Syndrome
- Mouse versus Human Severe Combined Immunodeficiency
- Ataxia-Telangiectasia–Like Disorder

Nijmegen Breakage Syndrome

Fanconi Anemia

Homologues of RecQ—Bloom Syndrome, Werner Syndrome, and Rothmund–Thompson Syndrome

Radiation-Induced Signal Transduction

Early Response Genes

The Ceramide Pathway

T Cell Checkpoint Therapy

Summary of Pertinent Conclusions

Bibliography

Signal Transduction

Heritable Syndromes that Affect Radiosensitivity, Genomic Instability, and Cancer

Oncogenes and Tumor Suppressor Genes

Cancer Genetics

Multistep Nature of Cancer and Mismatch Repair

Genes and Ionizing Radiation

issue homeostasis depends on the regulated cell division and self-elimination (programmed cell death) of each of its constituent members except its stem cells. In fact, a tumor arises because of uncontrolled cell division and failure for self-elimination. One can consider cancer as a Darwinian-like process whereby the fittest cells reproduce to become the dominant population of a tumor. Alterations in three groups of genes are responsible for the dysregulated control mechanisms that are the hallmarks of cancer cells:

- **Proto-oncogenes** are components of signaling networks that act as positive growth regulators in response to mitogens, cytokines, and cell-to-cell contact. A gain-of-function mutation in only one copy of a proto-oncogene results in a dominantly acting oncogene that often fails to respond to extracellular signals.

Tumor suppressor genes are also components of the same signaling networks as proto-oncogenes except that they act as negative growth regulators. They modulate proliferation and survival by antagonizing the biochemical functions of proto-oncogenes or responding to unchecked growth signals. In contrast to oncogenes, inactivation of both copies of tumor suppressor genes

is required for loss of function in most cases.

DNA stability genes form a class of genes involved in both monitoring and maintaining the integrity of DNA. Loss of these genes results in defective sensing of DNA lesions as well as improper repair of the damaged template.

The malignant progression from normal tissue to tumor to metastasis occurs in various “steps” over a period of time. These steps, which are the result of mutations, deletions, or gene changes in the three groups of genes described previously, may occur spontaneously because of random errors or result from exposure to agents as diverse as chemical mutagens, ionizing radiations, ultraviolet light, and viruses and provide a growth or survival advantage that allows the cells to become the clonal origin of the tumor. To summarize, tumor evolution results from the accumulation of gene mutations that arise in a single cell that has suffered a disruption in its regulatory mechanisms for proliferation, self-elimination, immortalization, and genetic stability. This is illustrated in Figure 18.1.

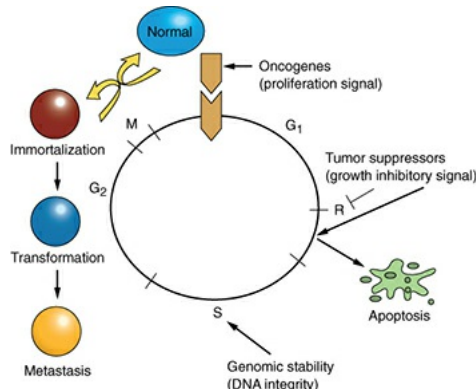


FIGURE 18.1 The process of malignant transformation results from mutations in three groups of genes: gain-of-function mutations that activate oncogenes, loss-of-function mutations that inactivate tumor suppressor genes, and loss of activity of DNA stability (e.g., repair) genes that increases the probability for genomic instability. This figure depicts how the stimulatory effects of oncogenes on the cell cycle are opposed by the inhibitory effects of tumor suppressor genes on the cell cycle that can lead to apoptosis. R indicates the restriction point that is regulated by the *p53* and *pRb* tumor suppressor genes. The consequences of oncogene activation and tumor suppressor gene and DNA integrity gene inactivation are immortalization, transformation, and metastasis.

MECHANISMS OF CARCINOGENESIS

A single genetic alteration that leads to the activation of an oncogene or loss of a tumor suppressor gene does not, by itself, lead to the formation of a solid tumor.

Instead, carcinogenesis appears to be a multistep process with multiple genetic alterations occurring over an extended period of time; at least, that is how it appears. Sometimes, these genetic alterations are carried in the germ line, like, for example, in the cancer-predisposing syndrome retinoblastoma; however, heritable mutations are rare. Most alterations that lead to cancer are acquired in the form of somatic mutations: chromosomal translocations, deletions, inversions, amplifications, or simple point mutations.

Initially, it was thought that cancer was the result of dysregulated growth signals by oncogenes, a concept supported by increased proliferation in many types of cancer. In the last decade, the finding that many cancers possess diminished apoptotic (programmed cell death) programs or loss of cell cycle control has led to the concept that mutations in proto-oncogenes and tumor suppressor genes that inhibit apoptosis provide a selective growth advantage to a premalignant cell that allows it to clonally expand. Mutations in DNA stability genes increase the rate of acquiring genetic mutations that will result in a malignant tumor. Thus, although tumor cells are considered clonal in origin, most tumors contain heterogeneous populations of cells that differ in their ability to repopulate the tumor or form metastases. In fact, only a small percentage of tumor cells possess the ability to form a tumor, leading to the concept that tumors possess “stem cells” and that elimination of these stem cells is essential for controlling tumor growth.

ONCOGENES

The first demonstration that a tumor was initiated by a cellular component found in tumor cells but not in normal cells was shown by Rous in the early 1900s. His landmark studies demonstrated that cell-free extracts derived from chicken sarcomas could cause a new sarcoma if injected into healthy chickens. In the 1970s, with the advent of molecular biology, several groups identified the etiologic agent for sarcoma formation in chickens as an RNA virus, designated as the Rous sarcoma virus (RSV), which belongs to a group of viruses designated as **retroviruses**—viruses whose genomes are composed of RNA. Thus, oncogenes were first discovered from a study of retroviruses that cause cancers in animals. Although the virus had been identified, it still remained to be elucidated how this retrovirus causes a sarcoma because another virus belonging to this same group of RNA viruses, avian leukosis virus (ALV), does not transform cells in culture or induce sarcomas. Analysis of the genomes of ALV and RSV revealed that RSV contains approximately 1,500 more base pairs (bp) of DNA than ALV. It was hypothesized, therefore, that these extra base pairs of

DNA in the RSV genome are responsible for the tumorigenic activity. This hypothesis was supported by the observation that deletion mutants of RSV that are missing this 1,500-bp region lose their transformation potential but can still replicate and produce viral progeny normally. This finding led to the conclusion that the transforming activity and replicative activity of RSV are encoded by genetically distinct regions of the virus, and that only a small portion of the RSV genome is needed for transformation.

From these early studies, several important conclusions could be derived:

1. Cancer can be caused by a genetically transmissible agent—in the case of chicken sarcoma, by a retrovirus containing a unique piece of genetic information that was later designated as the *src* gene;
2. Only a certain region of a retrovirus is needed for transformation; and
3. The region of the viral genome necessary for transformation is not involved in the normal replicative life cycle.

Huebner and Todaro later proposed that cancer-causing viral genes such as *src* are normally inactive but can be activated when they recombine with a retroviral genome. Once they do so, they pass from being a benign proto-oncogene (i.e., c-*src*) to a malignant form (v-*src*) capable of causing cancer when introduced into the appropriate host cell. Although we now know that viruses represent only one of several mechanisms that cause the dysregulated expression of a proto-oncogene, these studies helped to define oncogenes as mutant forms of normal cellular genes that are altered in expression and/or function by various agents, including radiation, chemicals, and viruses. Consequently, very different agents are involved in tumor formation. This is illustrated in [Figure 18.2](#).

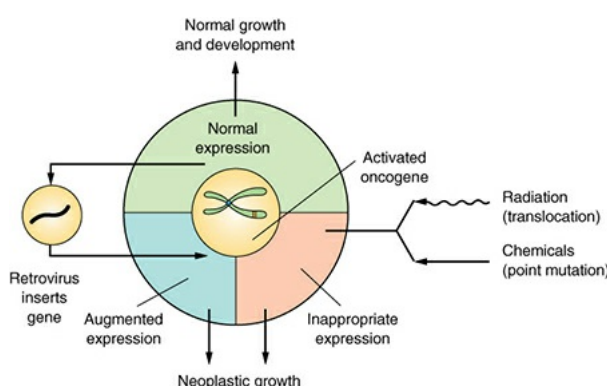


FIGURE 18.2 How the concept of oncogenes provides a ready answer for how agents as diverse as viruses, radiations, and chemicals all can induce tumors that are essentially indistinguishable one from another. The retrovirus inserts a gene;

a chemical may activate an endogenous oncogene by a point mutation; radiation may do the same by causing, for example, a translocation. (Adapted from Bishop JM. Cellular oncogene retroviruses. *Ann Rev Biochem.* 1983;52:301–354, with permission.)

MECHANISMS OF ONCOGENE ACTIVATION

Although many mechanisms are involved in oncogene activation, transcriptional dysregulation by overexpression or abnormal expression of the messenger RNA (mRNA) of a proto-oncogene is a common theme. At least four mechanisms exist for oncogene activation in human neoplasms (Fig. 18.3).

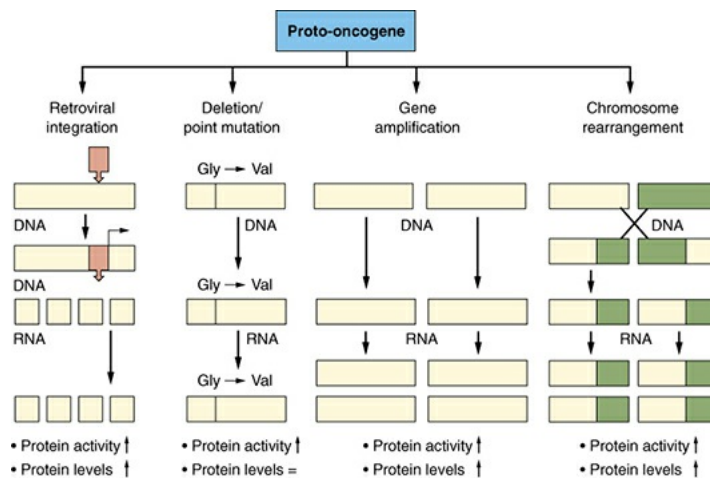


FIGURE 18.3 Four basic mechanisms of how a proto-oncogene can become an activated oncogene. Retroviral integration in proximity to a proto-oncogene results in transcriptional control of the proto-oncogene by the viral promoter, resulting in increased proto-oncogene protein and activity. Deletion or point mutations in the proto-oncogene result in increased activity of the proto-oncogene without necessarily changing transcription or protein levels of the proto-oncogene. Increased copy number of a proto-oncogene by gene amplification results in increased transcription, protein levels, and activity of the proto-oncogene. Chromosome translocation results in an altered proto-oncogene product that can have increased transcription, protein levels, and activity. All of these alterations in a proto-oncogene that occur at the DNA level manifest themselves at the protein level as increased activity and, in some cases, increased protein levels.

Retroviral Integration through Recombination

Retroviral integration of proto-oncogene sequences in retroviral genomes occurs through two possible recombination mechanisms. First, mRNAs from a proto-

oncogene recombine with viral genomic RNAs. During the recombination process, the proto-oncogene mRNA becomes dysregulated as it comes under the control of the viral promoter, termed **long terminal repeat (LTR)**. However, the probability of RNA recombination events between proto-oncogene mRNA and viral mRNA generating an oncogenic retrovirus is quite low and undermines the importance of this mechanism.

A second more probable mechanism is as follows: First, a retroviral genome integrates in proximity to a proto-oncogene, where the proto-oncogene is under the transcriptional control of the retrovirus LTR promoter. Then the viral and proto-oncogene sequences become closely associated through a DNA recombination event that permits the production of mRNAs that contain both viral and proto-oncogene sequences. In this scenario, the proto-oncogene becomes transcriptionally dysregulated because it is under the control of the viral promoter LTR. In addition, it can acquire mutations in its coding sequence. Although the proto-oncogene can become mutated during the recombination process, the key point is that its dysregulated expression by the viral LTR increases its expression and promotes cell growth.

DNA Mutation of Regulatory Sites

The union of the technique for gene transfer with mouse transformation assays facilitated the isolation of human oncogenes that were activated by DNA mutation. Transfection of human DNA into immortalized but untransformed mouse cells was first used to isolate the *H-ras* oncogene from bladder carcinoma cells. The key to this approach is that only transformed cells possess the ability to grow in soft agar ([Fig. 18.4](#)). The implicit assumption is that a specific gene (or more) is responsible for causing the bladder carcinoma and that it will act in a dominant fashion to induce a tumor. Indeed, multiple groups were successful in isolating the *H-ras* oncogene by this approach.

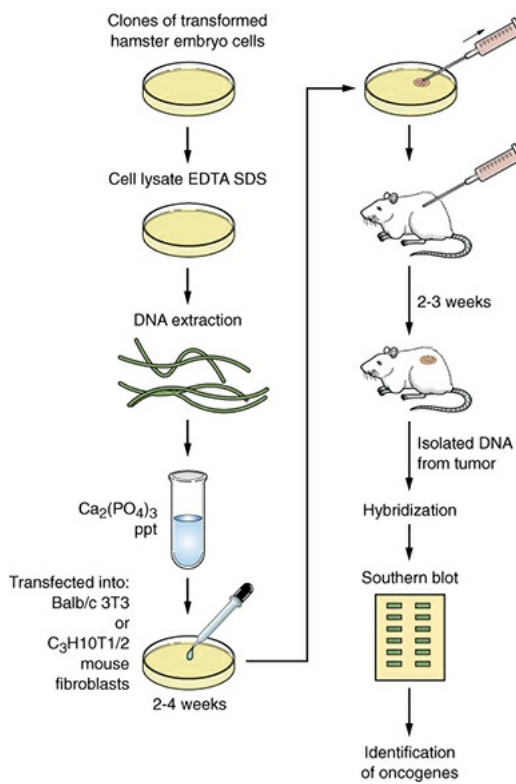


FIGURE 18.4 Schematic diagram of a typical DNA transfection protocol in which oncogenes can be isolated from cells transformed *in vitro* by either radiation or chemical carcinogens. DNA sequences are then characterized using Southern blot hybridization.

Several steps are needed for the molecular cloning of an oncogene from transformed rodent cells using the rodent fibroblast transformation assay. These are the following:

1. The human DNA containing the transforming oncogene is transfected into mouse cells.
2. The DNA from the transformed mouse cells is serially transfected to reduce the amount of human DNA that is not associated with the transforming oncogene.
3. After several rounds of transfection, the DNA is isolated from a soft agar colony and digested with restriction enzymes to make a genomic DNA library.
4. The library is then screened with a human-specific repetitive probe that does not cross-react with the mouse's DNA, thereby identifying human sequences in a mouse background.
5. Clones that possess human repetitive sequences are then isolated and digested with restriction enzymes to identify a similar-length fragment that

is common to all transformants.

6. Finally, the DNA from the clones is transfected into mouse cells to confirm its oncogenic potential. If the oncogene is present in this genomic clone, then a significant percentage of the transfected mouse cells should be transformed when compared with transfecting genomic DNA from untransformed cells.

Perhaps the prototypical example of oncogene activation by DNA mutation is the *H-ras* oncogene. The *H-ras* oncogene was isolated by the approach recently described, and its DNA sequence was compared with its normal cellular counterpart. At first comparison, there did not seem to be any difference between oncogenic and proto-oncogenic forms. However, because *H-ras* is a relatively small oncogene, it was possible to sequence the entire gene to rigorously search for small mutations. It did not take long to find the difference between the two forms of the gene. The transforming oncogenic *H-ras* gene possesses a single bp mutation that changes the 12th amino acid from glycine to valine. This single DNA mutation is responsible for changing *H-ras* from a benign proto-oncogene into a malignant oncogene. We now know that mutations in codons 13 and 61 will also produce oncogenic *H-ras* genes that are constitutively locked in an active state.

Gene Amplification

Oncogene amplification occurs through breakage-fusion-bridge cycles in anaphase during mitosis. In contrast to the other mechanisms discussed that involve transcriptional dysregulation as a key mechanism of oncogene activation, gene amplification represents an alternative means of increasing proto-oncogene expression by increasing the number of DNA copies of the proto-oncogene. Gene amplification can result in an increased number of copies of extrachromosomal molecules called **double minutes** or can result in intrachromosomal amplified regions called **homogeneously staining regions (HSR)**, both of which are detectable by fluorescence *in situ* hybridization or Giemsa banding of chromosomes. The *N-myc* oncogene is a classic example of an oncogene amplified in leukemia, neuroblastoma, and breast cancer.

Chromosome Translocation

It had long been known that tumors possessed abnormal karyotypes. However, the chromosome content of many solid tumors is unstable, making it difficult to determine which cytogenetic alterations are causative for tumorigenesis and

which are the consequence of the neoplastic process. The first real breakthrough in identifying tumor-specific chromosome alterations occurred in the late 1950s when Dr. Peter Nowell found a consistent shortened version of chromosome 22 in individuals afflicted with chronic myelogenous leukemia (CML). Because many patients with CML possess an abnormal chromosome 22 in their leukemic cells, this was a strong indication that a specific chromosome alteration is involved in the pathogenesis of this malignancy. With the advent of more sophisticated cytogenetic and molecular techniques, it was discovered that this shortened version of chromosome 22 is caused by a symmetric translocation with chromosome 9. It was hypothesized, therefore, that the translocation between chromosomes 9 and 22 gives rise to CML. Further molecular analysis revealed that the *bcr* gene on chromosome 9 translocates in front of the *abl* gene on chromosome 22, producing a fusion transcript with abnormal expression (Fig. 18.5).

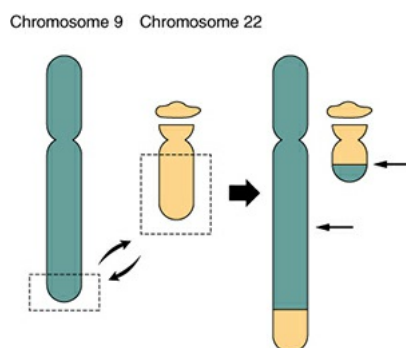


FIGURE 18.5 A symmetric translocation between chromosomes 9 and 22 brings together the *bcl* and *abl* genes to form a fusion gene associated with over 90% of cases of CML.

With the recent advent of molecular cytogenetics—that is, fluorescent *in situ* hybridization (FISH)—many translocation partners have been identified. In fact, a common strategy has been to use proto-oncogenes, which chromosomally map near translocation breakpoints, as markers to identify potential translocation partners. Although numerous translocation breakpoints have been identified in hematopoietic neoplasms, few consistent translocations have been found in solid tissue tumors. The reason for this is still unclear but may be attributed to the fact that hematopoietic cancers require fewer alterations for neoplasia than solid tumors. Table 18.1 provides examples of the chromosomal changes that result in oncogene activation and the associated human malignancies. Interestingly, there are no known examples of oncogenes activated by retroviruses in human malignancies.

Table 18.1 Examples of Chromosomal Changes Leading to Oncogene Activation and Their Associated Murine or Human Malignancies^a

ONCOGENE	CHROMOSOMAL CHANGE	CANCER
<i>int-1</i>	Proviral insertion	Murine breast carcinoma
<i>int-2</i>	Proviral insertion	Murine breast carcinoma
<i>pim-1</i>	Proviral insertion	Murine T-cell lymphoma
N- <i>ras</i>	Point mutation (1)	Melanoma
K- <i>ras</i>	Point mutation (12)	Pancreas carcinoma
H- <i>ras</i>	Point mutation (11)	Colon carcinoma
<i>neu</i>	Point mutation (17)	Neuroblastoma
N- <i>myc</i>	Gene amplification (8)	Neuroblastoma
L- <i>myc</i>	Gene amplification (8)	Lung carcinoma
<i>neu</i>	Gene amplification (17)	Breast carcinoma

<i>EGFR</i>	Gene amplification (7)	Squamous cell carcinoma
<i>bcr-abl</i>	Translocation (9–22)	Chronic myelogenous leukemia
<i>c-myc</i>	Translocation (8–14)	Burkitt lymphoma
<i>c-myc</i>	Translocation (2–8)	Burkitt lymphoma
<i>c-myc</i>	Translocation (8–22)	Burkitt lymphoma
<i>bcl-2</i>	Translocation (14–18)	Diffuse large B-cell lymphoma

^aHuman oncogenes activated by retroviruses have not yet been found in human malignancies, only murine cancers.

MUTATION AND INACTIVATION OF TUMOR SUPPRESSOR GENES

The Retinoblastoma Paradigm

Oncogenes result from a mutation, deletion, or alteration in the expression of one copy of a gene. Thus, oncogenes are dominant genes because a mutation in only one copy will cause their activation even though the other copy of the gene is unchanged. This concept led to speculation that another class of genes, termed “antioncogenes,” suppresses the effect of oncogenes on transformation and tumor formation. The existence of tumor suppressor genes was supported by cell fusion studies between tumor cells and normal cells and by the family history studies of people afflicted with inherited cancer-prone disorders such as retinoblastoma or Li–Fraumeni syndrome. Although one mutated version of an oncogene is sufficient to drive malignant progression, one functional copy of a

tumor suppressor gene is often insufficient to suppress transformation, suggesting that both copies of a tumor suppressor gene must be inactivated to inhibit tumor growth (Fig. 18.6). Insight into the mechanism of tumor suppressor gene inactivation came from Knudson's epidemiologic studies of families in which retinoblastoma appeared to be inherited in an autosomal dominant manner. Patients with familial retinoblastoma develop bilateral or multifocal disease at an earlier age than patients with sporadic retinoblastoma. Based on these observations, Knudson proposed that in the inherited form of retinoblastoma, patients possess a germ line mutation of the retinoblastoma (*Rb*) gene in all the cells of their body, but inactivation of one *Rb* allele does not give rise to retinoblastoma. Thus, the disease appeared to be autosomal dominant because individuals are born with one mutated allele. However, a second mutation in a retinal cell is required to develop retinoblastoma. In the sporadic form of the disease, an individual has to acquire two *Rb* mutations in the same retinal cell to develop retinoblastoma. The "two-hit hypothesis" by Knudson provided a genetic basis to understand the differences in inherited and sporadic mutations in the onset of tumors and to advance the concept that both alleles of a tumor suppressor gene need to be inactivated to promote tumor development. Thus, tumor suppressor genes are recessive genes that require the inactivation of both functional gene copies before malignancies develop, whereas loss of one functional copy results only in increased cancer susceptibility. In addition, it is often the case that the same tumor suppressor gene involved in hereditary cancer syndromes, such as retinoblastoma, is also inactivated in other forms of cancer. The *Rb* gene itself has now been implicated in several other human cancers, which indicates that it may play a generalized role in tumor growth suppression in various tissues. For example, patients who are cured of familial retinoblastoma are at increased risk for osteosarcoma, small cell lung cancer, and breast cancer; although the loss of the *Rb* gene alone is sufficient for retinoblastoma, further changes are required for the development of these other tumors.

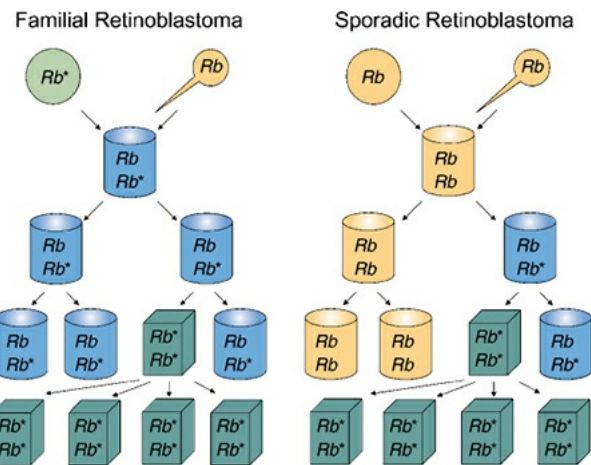


FIGURE 18.6 *Rb* mutations in familial and sporadic retinoblastoma. In familial retinoblastoma, one normal allele (*Rb*) and one mutated allele (*Rb**) are inherited from either parent, resulting in a heterozygous individual containing *Rb/Rb** retinal cells. Subsequent mutation in any retinal cell inactivates the remaining normal *Rb* allele, leading to loss of growth control and expansion of the homozygous mutant *Rb*/Rb** retinal cells that leads to retinoblastoma. In sporadic retinoblastoma, two normal *Rb* alleles are inherited from each parent. First, a mutation inactivates one copy, resulting in heterozygous *Rb/Rb** retinal cells. A subsequent mutation within the same retinal cell inactivates the remaining copy of normal *Rb*, leading to loss of growth control and expansion of homozygous *Rb*/Rb** retinal cells that leads to retinoblastoma. (Illustrating the concepts proposed by Knudson AG Jr. Mutation and cancer: statistical study of retinoblastoma. *Proc Natl Acad Sci USA*. 1971;68:820–823.)

The Li–Fraumeni Paradigm

The Li–Fraumeni syndrome (LFS) is a rare autosomal, dominantly inherited disease that predisposes individuals to develop osteosarcomas, soft-tissue sarcomas, rhabdomyosarcomas, leukemias, brain tumors, and carcinomas of the lung and breast (Fig. 18.7). Initial attempts to identify the genetic mutations that underlie LFS were unsuccessful because of the rarity of the syndrome and the high mortality of the patients. The major insight into the underlying cause of LFS came when it was found that mice that overexpress a mutant version of the *p53* tumor suppressor gene in the presence of the wild-type *p53* gene develop a spectrum of tumors similar to that seen in patients with LFS. Sequencing of *p53* in affected family members revealed germ line missense mutations in the *p53* tumor suppressor gene located on chromosome 17p13 that resulted in its inactivation, and tumors derived from affected individuals had lost the remaining wild-type allele of *p53*. Similar to retinoblastoma, loss or inactivation of both

wild-type copies of *p53* is needed for tumor formation. However, functional loss of one germ line inherited copy of mutant *p53* accelerates the onset of spontaneous tumor formation. Therefore, patients with LFS follow a similar paradigm as patients with retinoblastoma in developing spontaneous tumors, but unlike retinoblastoma in which germ line mutations mainly give rise to retinal tumors, loss of *p53* results in a wide spectrum of tumors. In addition to germ line mutations of *p53* in giving rise to Li-Fraumeni, heterozygous germ line mutations in checkpoint kinase 2 (Chk2) have also been reported. Germ line mutations in Chk2 predispose individuals to sarcoma and breast and brain tumors. Therefore, germ line mutations in either *p53* or Chk2 can predispose individuals to LFS. **Table 18.2** provides examples of other cancer predisposition genes and their associated syndromes.

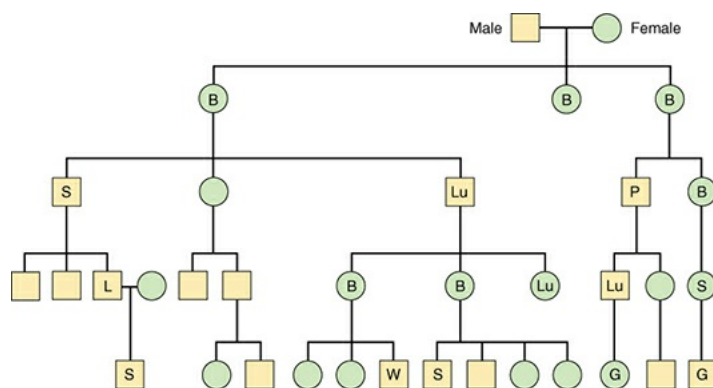


FIGURE 18.7 Pedigree analysis of familial cancer history of Li-Fraumeni syndrome. B, breast cancer; G, glioblastoma; L, leukemia; Lu, lung cancer; P, pancreatic cancer; S, sarcoma; W, Wilms tumor. (Adapted from Li FP, Fraumeni JF. Prospective study of a family cancer syndrome. *JAMA*. 1982;247:2692–2694, with permission.)

Table 18.2 Examples of Cancer Predisposition Genes and Their Associated Syndromes

TUMOR GENE	SUPPRESSOR GENE	SYNDROME	TUMOR
<i>Rb</i>		Retinoblastoma	Retinoblastoma
<i>WT1</i>		Familial Wilms tumor	Wilms tumor

<i>NFI</i>	Neurofibromatosis type 1	Neurofibroma, sarcoma
<i>NF2</i>	Neurofibromatosis type 2	Schwannoma, meningioma
<i>APC</i>	Familial adenomatous polyposis	Tumor of colon, stomach, and intestine
<i>p53</i>	Li–Fraumeni syndrome	Breast, lung, brain tumors, sarcoma
<i>VHL</i>	von Hippel-Lindau disease	Tumor of kidney, adrenal
<i>E-CAD</i>	Familial gastric cancer	Tumor of stomach, breast
<i>PTCH</i>	Gorlin syndrome	Basal cell carcinoma
<i>PTEN</i>	Cowden syndrome	Hamartoma
<i>MEN1</i>	Multiple endocrine neoplasia	Tumor of pituitary, pancreas, and parathyroid

Familial Breast Cancer, BRCA1 and BRCA2

The breast cancer susceptibility genes (BRCA1 and BRCA2) are found mutated in 5% and 10% of all breast cancer cases and are also associated with familial ovarian and prostate cancers. Familial breast cancer can be distinguished from sporadic breast cancer by its earlier age of onset, an increased frequency of

bilateral tumors, and a higher incidence of cancer, in general, within an affected family. Histopathologically and anatomically, familial and sporadic cases of breast cancer are indistinguishable. Although BRCA1 and BRCA2 mutations account for the most inherited forms of breast cancer, they are rarely found in sporadic cases of breast cancer. BRCA1 and BRCA2 have been implicated in DNA damage, repair, cell cycle progression, transcription, ubiquitination, apoptosis, and in the determination of stem-cell fate. The most well-studied roles of BRCA1 and BRCA2 are in homologous recombination (see [Chapter 2](#)). Phenotypically, cells deficient in BRCA1 or BRCA2 exhibit elevated levels of genomic instability, which is consistent with their roles in homologous recombination. This conclusion is also supported by the finding that mice lacking BRCA1 have the same phenotype as those null for the essential homologous recombination protein RAD51. Functionally, BRCA1 acts as a sensor of DNA damage and replication stress and mediates homologous recombination through BRCA2. In response to DNA damage-induced ionizing radiation, BRCA1 is phosphorylated at numerous sites by ataxia-telangiectasia mutated (ATM), ataxia-telangiectasia and Rad3-related (ATR), and Chk2 that direct it to associate with other repair proteins in nucleotide excision repair (NER), including xeroderma pigmentosum, complementation group C (XPC), and DNA damage-binding protein 2 (DDB2), in mismatch repair (MMR) MutS homolog 2 (MSH2), MSH6, and in DNA damage signaling ATM, and the MRN complex (MRE11, Rad50, and NBS1). In contrast to BRCA1, BRCA2 appears to play a more direct role in homologous recombination by binding to RAD51 and aiding in the formation of RAD51 foci at the sites of DNA breaks. Cells from patients deficient in BRCA1 or BRCA2 are defective in homologous recombination and rely on error-prone nonhomologous end-joining (NHEJ) to repair their DNA double-strand breaks (DSBs). The resulting accumulation of mutations in BRCA1 and BRCA2 deficient cells promotes tumor formation.

SOMATIC HOMOZYGOSITY

How are recessive tumor suppressor genes lost? Cytogenetic studies are used to identify chromosomal changes in peripheral blood lymphocytes or fibroblasts from patients with cancer, especially those with a family history of cancer, to identify chromosomal rearrangements or deletions. At the subchromosomal level, a genomewide linkage analysis is used to determine that a certain chromosome region is tightly linked with cancer predisposition. Both copies of a suppressor gene in the sporadic form of retinoblastoma and other solid tumors may result from two independent allelic mutations, but in practice, it occurs

more often by the process of **somatic homozygosity**. The steps appear to be as follows: One chromosome of a pair is lost, a deletion occurs in the remaining chromosome, and the chromosome with the deletion replicates. Instead of having each of the two alleles contributed by different parents, the cell has both alleles from the same parent, with loss of a vital piece containing the tumor suppressor gene (Fig. 18.8). This process has been documented for chromosome 13 in the case of retinoblastoma, chromosome 11 in Wilms tumor, chromosome 3 for small cell lung cancer, and chromosome 5 for colon cancer. Most interesting of all, perhaps, is the case of astrocytomas in which somatic homozygosity is observed for chromosome 10 in grades II and III astrocytoma and for both chromosomes 10 and 17 for grade IV glioblastoma.

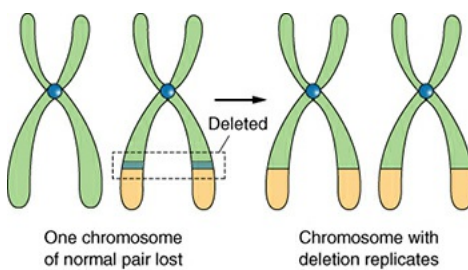


FIGURE 18.8 The process of somatic homozygosity. In a normal cell, there are two copies of each chromosome, one inherited from each parent. For a given suppressor gene to be inactivated, the copy must be lost from both chromosomes. This could, of course, occur by independent deletions from the two chromosomes; but in practice, it is more common for a single deletion to occur in one chromosome, whereas the second chromosome is lost completely. The remaining chromosome, with the deletion, then replicates. The cell is thus homozygous, rather than heterozygous, for that chromosome.

THE MULTISTEP NATURE OF CANCER

Perhaps, the most pervasive dogma in cancer research is that carcinogenesis is a multistage process. The implication is that there are several distinct events that may be separated in time. This idea is almost 70 years old and is exemplified by the skin cancer experiments in mice that introduced the concepts of initiation, promotion, and progression as stages in tumor development.

Genetic analysis of cells from solid tumors also suggests alterations, mutations, or deletions in multiple signaling genes, either oncogenes or suppressor genes; 6 to 12 mutations have been suggested for the formation of a carcinoma. In the case of colorectal cancer, a model has been proposed that correlates a series of chromosomal and molecular events with the changes in the histopathology of normal epithelium during the multistage formation of

colorectal cancer and metastatic carcinoma. This concept is illustrated in [Figure 18.9](#).

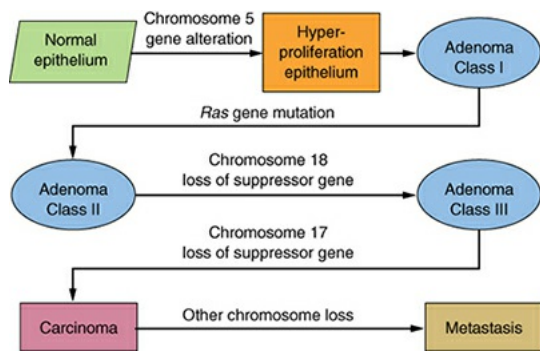


FIGURE 18.9 Cancer has long been thought to be a multistep process and has been described with operational terms such as initiation, promotion, and progression. In at least one human malignancy, namely, colon cancer, the molecular events during the progress of the disease have been identified. (Based on the work of Vogelstein and Kinzler.)

A more general model of the series of events in carcinogenesis is shown in [Figure 18.10](#). The first event, from whatever cause (including ionizing radiation), causes a mutation in a gene in one of the families responsible for the stability of the genome. This leads to a mutator phenotype, so that with many cells dividing, multiple mutations are likely in cancer-associated genes, both oncogenes and tumor suppressor genes. This in turn leads to progression of the cancer and ultimately its invasive and metastatic properties.

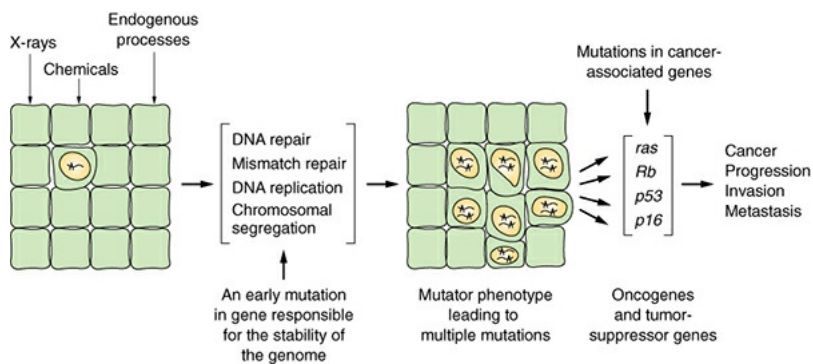


FIGURE 18.10 Illustrating the multistep nature of carcinogenesis and the concept of the mutator phenotype. The first step in carcinogenesis by radiation or any other agent may be a mutation in one of the gene families responsible for the stability of the genome. This may be a DNA repair gene, an MMR gene, or a gene in a family as yet unidentified. This leads to the mutator phenotype, with multiple mutations possible in both oncogenes and tumor suppressor genes. This then leads to a series of steps that result in an invasive metastatic cancer. Not all the same mutations need to be present in every case.

Therefore, it is not surprising that restoration of one copy of a tumor suppressor gene is sometimes not sufficient to restore tumor suppressor activity because solid tumors accumulate mutations that can make them refractory to the restoration of a single tumor suppressor gene. Although tumor suppressor genes are functionally quite different from oncogenes, they modulate similar cellular functions as oncogenes.

FUNCTION OF ONCOGENES AND TUMOR SUPPRESSOR GENES

The myriad of genetic and epigenetic changes that drive tumor evolution is a systems biology problem in which cells can be thought of as circuits, where an alteration of the circuit can lead to increased output, decreased output, complete loss of output, or no change. Therefore, cancer biologists attempt to determine how a specific gene, when mutated, alters normal tissue function. To understand how oncogenes and tumor suppressor genes lead to neoplasia, we need to understand how each of these circuits impacts normal cellular physiology. What cellular functions are disrupted by oncogene activation and tumor suppressor gene inactivation, and how do these disrupted functions affect the differentiation, growth, and death of cells? What follows is a description of the general categories of cell functions that are perturbed by deregulation of these two classes of genes during malignant progression.

Dysregulated Proliferation

The loss of proliferative control of cancer cells is evident to all who study cancer. In fact, the earliest concept suggested by tumor biologists was that cancer was a disease of uncontrolled proliferation. Untransformed cells respond to extracellular growth signals known as mitogens through a transmembrane receptor that signals to intracellular circuits that increase growth. Thus, the growth factor, the receptor, and the intracellular circuits can all lead to self-sufficiency when dysregulated. Typically, one cell secretes a mitogenic signal to stimulate the proliferation of another cell type. For example, an epithelial cell can secrete a signal to stimulate fibroblasts to proliferate. In contrast to untransformed cells, transformed cells have become autonomous in regulating their growth by responding to the mitogenic signals they themselves produce. In this manner, they use an autocrine circuit to escape the need for other cell types. For example, mesenchymal cells are responsive to transformation by *v-sis* because they possess receptors for platelet-derived growth factor (PDGF), and breast epithelial cells are responsive to *int-2* because they possess receptors for

fibroblast growth factor (FGF).

If overexpression of growth factors can lead to uncontrolled proliferation, then continuous activation or overexpression of growth factor receptors will do the same. Several well-known oncogenes, such as *v-erb-2* (*HER-2/neu*) and *v-fms*, encode growth factor receptors. These receptors are mutated at their amino terminal residues so that they no longer require their respective growth factor (ligand) to signal induction of their kinase activity. Growth factor receptors can structurally be divided into extracellular ligand-binding domains (LBDs), transmembrane-spanning domains (TMS), and intracellular kinase domains. Although mutations have been found in all three domains, mutations in the LBDs are a common alteration that results in constitutive kinase activity that transduces the signal for the cell to proliferate. In addition to structural alterations in the receptor, some tumors overexpress growth factor receptors that make them hyperresponsive to physiologic levels of growth factor stimulation. In contrast to mitogenic-responsive growth factor receptors, a second class of receptors that transmit signals from the extracellular matrix (ECM) can also regulate proliferation. Integrin receptors are the prototypical example of this class of regulators that transmit signals from different components of the ECM to signal proliferation or quiescence.

There are numerous intracellular circuits that transduce the signal from the cell surface to the nucleus of the cell. The *src*, *ras*, and *abl* proteins are all members of this group. Most members of this group are tyrosine kinases or serine/threonine kinases. *Src* and *abl* are tyrosine kinases located on the cytoplasmic side of the cell membrane. H-*ras*, K-*ras*, and N-*ras* are a family of guanosine triphosphate (GTP)-binding proteins also located on the cytoplasmic side of the cell membrane and are the most frequently mutated oncogene family in human cancers. The Ras/Raf/extracellular signal-regulated kinases (ERK), Ras/Ral guanine nucleotide dissociation stimulator (RalGDS)/Ral, and Ras/phosphoinositide 3-kinase (PI(3)K)/Akt/target of rapamycin (TOR) pathways play critical roles in transducing signals from growth factor receptors at the cell surface to the nucleus in untransformed cells. Oncogenic forms of *ras* bypass the normal growth regulatory signals of a cell by being locked in an “on” state, obviating the need for external signals from growth factors to activate them (Fig. 18.11).

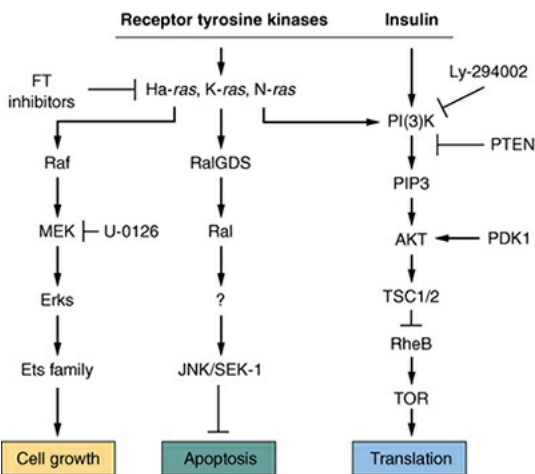


FIGURE 18.11 The *Ras* family (H-*Ras*, K-*Ras*, and N-*Ras*) are proteins that act as guanosine diphosphate/guanosine triphosphate-regulated binary switches that reside at the inner surface of the plasma membrane and act to relay extracellular ligand-stimulated signals to cytoplasmic signaling cascades. However, oncogenic forms of *Ras* lose their responsiveness to growth receptor tyrosine kinases and constitutively activate cascades of serine threonine kinases that control cell proliferation, inhibit apoptosis, and increase protein translation. These pathways are depicted in a linear fashion but are more complex and are regulated by positive and negative feedback loops. This illustration depicts three direct effectors of *Ras* that have been shown to mediate these events. *Ras* stimulates proliferation by activating the Raf/MEK/ERK pathway that phosphorylates and activates the Ets transcription factor that leads to increased levels of cyclin D₁, mRNA, and protein. Increased levels of cyclin D₁ result in increased Rb phosphorylation and transition of cells from G₁ to S phase of the cell cycle. A second direct effector of *Ras*, RalGDS, is a guanine nucleotide exchange factor that activates Ral A and B GTPases and promotes tumor cell survival through the Jun kinase/stress kinase (JNK/SEK) pathway. The third major pathway that *Ras* directly regulates is the PI(3)K pathway. This pathway has long been known to be important in regulating cell growth through insulin signaling. Like Raf and RalGDS, oncogenic forms of *Ras* increase PI(3)K activity that leads to increased phosphorylation of the lipid kinase PIP3, which in turn inhibits the negative regulation of TOR by tuberous sclerosis 1 and 2 (TSC1/2) and RheB. Increased TOR leads to increased translational initiation of mRNAs that possess a structured 5' region known as a “cap.” This is an oversimplified illustration because there are at least three other signaling pathways that lie downstream of *Ras*. The *Ras* pathway can be disrupted using pharmacologic inhibitors of farnesyltransferases (FT), PI(3)K (Ly-294002), or MEK (U-0126). (Adapted from Dr. Marianne Powell, with permission.)

Failure to Respond to Growth-Restrictive Signals

Signal transduction cascades often initiate at the cell membrane and end in the nucleus. Normally, various cells in the body are at rest in a nonproliferative state (G_0). The oncogenic activation of nuclear oncogenes stimulates the cell into the synthetic phase (S phase), where it duplicates its genetic material before cell division. Nuclear control proteins that regulate entry into S phase include transcription factors, such as *c-myc*, *c-rel*, *c-jun*, and *c-fos*, and cell cycle regulatory proteins such as E2F and cyclin D₁ (PRAD1). These nuclear proto-oncogenes can work as transcription factors by binding to DNA in a sequence-specific manner and forming complexes with themselves or other proteins that will increase mRNA transcription of genes such as cyclin D that promotes cell division.

To understand how tumor cells evade antiproliferative signals, one must appreciate how the cell cycle is regulated—in particular, the G_1 phase. It is during a cell's transit through the G_1 phase that it makes the decision to continue to the S phase and duplicate its genetic material or enter into a reversible state of quiescence (reversible growth arrest) or enter a permanent state of senescence (irreversible growth arrest). The *Rb* family of proteins is the most critical determinant of the fate of a G_1 phase cell. When *Rb* protein is in a hypophosphorylated state, *Rb* protein blocks progression into S phase by sequestering E2F transcription factors that regulate the expression of genes that are essential for the transition from G_1 to S phase. As previously discussed, the ECM can signal cell proliferation through integrin receptors. In addition, it can also produce antiproliferative signals through the secreted protein TGF- β . At the molecular level, TGF- β inhibits *Rb* protein phosphorylation and prevents the release and activation of the E2F family of transcription factors. It does this through the induction of inhibitors such as p21 and p15^{INK4B} that inhibit the activity of the kinases that are essential to phosphorylate *Rb* protein. Thus, loss of *Rb* or failure to induce p21 and p15^{INK4B} will aid cells in escaping antiproliferative signals.

In addition to extracellular antiproliferation signals, endogenous proteins that downregulate signal-amplifying kinases are also important in keeping signal transduction cascades in check. For example, the NF1 protein is a GTPase-activating protein that facilitates the hydrolysis of GTP by *ras*. When *ras* protein is complexed with guanosine diphosphate (GDP), it is inactive; when it is bound to GTP, it is active. Individuals afflicted with neurofibromatosis lack NF1

protein and have lower levels of GTPase activity and more *ras* protein complexed with GTP, resulting in a more active *ras* protein. Therefore, lack of NF1 protein activity will result in enhanced activity of *ras* protein similar to what is found in *ras*-transformed cells as already described. The NF1 protein and the *ras* protein are excellent examples of how a tumor suppressor gene and an oncogene work in unison to control a signal transduction pathway.

A second example of an endogenous protein that down-regulates signal-amplifying kinases is the phosphatase and tensin homolog (PTEN) lipid phosphatase. PTEN catalyzes the dephosphorylation of phosphatidyl inositol (3,4,5)-triphosphate (PIP3), a critical regulator of the Akt kinase. Next to p53, PTEN is the next most inactivated tumor suppressor gene.

Failure to Commit Suicide (Apoptosis)

Two major pathways that mediate cell death emanate either from the cell membrane or from the mitochondrion (Fig. 18.12). The signals transmitted by each pathway results in the activation of intracellular cysteine proteases, termed **caspases**, that cleave a diverse and ever-increasing number of substrates, including themselves, at aspartic acid residues. Caspases can broadly be divided into initiator caspases and effector caspases. The binding of ligands such as Fas to specific death receptors on the cell surface induces receptor activity and the recruitment of the initiator procaspase 8. The recruitment of procaspase 8 proteins near to each other results in active caspase 8 and effector caspases, such as caspases 3, 6, and 7, which are responsible for the ultrastructural changes in the cell. In response to mitochondrial-dependent cell death, activation of initiator caspases (e.g., caspase 9) is achieved by proteolytic cleavage of their inactive pro-forms through their recruitment and interaction with specific adapter proteins. The adapter proteins are in turn regulated by the mitochondria through the release of cytochrome *c*. The release of cytochrome *c* from the mitochondria is controlled by the Bcl-2 protein family, which is composed of proapoptotic regulators such as Bax, Bak, Bid, and Bim and antiapoptotic family members Bcl-2, Bcl-xL, and Mcl-1. The Bcl-2 oncogene is the prototypical example of a membrane-associated oncogene whose overexpression protects the cell from death-inducing stimuli by various agents.

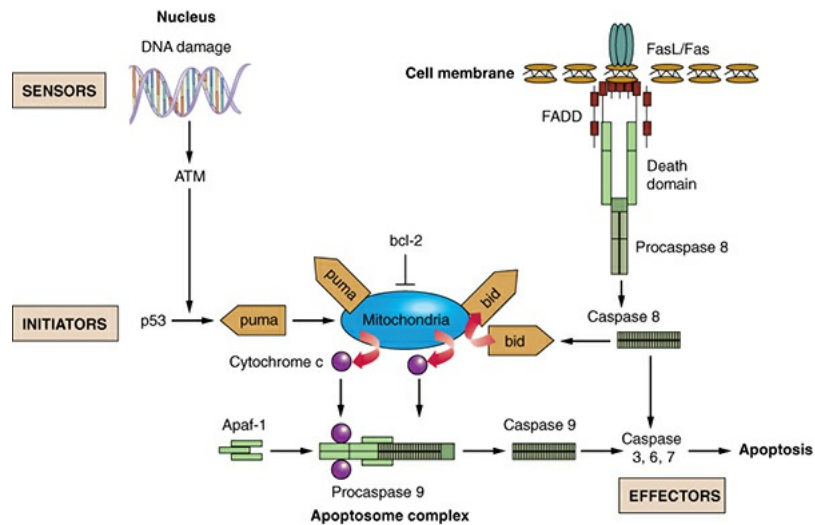


FIGURE 18.12 Two major pathways that mediate cell death. Pathways initiate at either the cell membrane with a death receptor or in the nucleus with the detection of DNA-damaging stresses. Each pathway can be divided into sensors (e.g., Fas ligand-binding to Fas receptor), initiators (e.g., caspases 8 and 9), and effectors (e.g., caspases 3, 6, and 7). See text for further details.

How does Bcl-2 protect cells from undergoing apoptosis? Both proapoptotic and antiapoptotic Bcl-2 family members can form dimers with themselves (homodimers) or with other family members (heterodimers). This ability to form dimers with a pro-death-promoting family member has been proposed as one mechanism of how Bcl-2 prevents apoptotic cell death that is signaled by the release of cytochrome *c* from the mitochondria. In the cytoplasm, cytochrome *c* forms a complex with the adapter protein Apaf-1, and together they recruit the inactive form of the initiator caspase, procaspase 9. In this complex, caspase 9 becomes activated and in turn activates effector caspases such as caspases 3, 6, and 7 through proteolytic cleavage. Cell lines deficient in caspases 3 and 9 exhibit substantially reduced levels of apoptosis during development and in response to exogenous stress-inducing stimuli (Fig. 18.13).

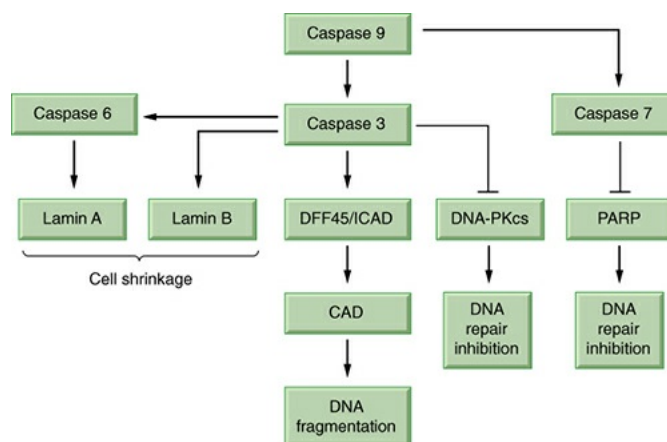


FIGURE 18.13 Examples of caspase substrates that are responsible for the cellular ultrastructural changes that result in classic apoptotic morphology. Caspases degrade Lamin and structural components of the cytoskeleton, fragment DNA, and inhibit DNA repair processes by degrading DNA repair proteins. ICAD, inhibitor of caspase-activated DNase; DNA-PK, DNA-directed protein kinase; PARP, poly-ADP ribose polymerase.

The *p53* tumor suppressor gene is an important modulator of oncogene-induced apoptosis. Levels of *p53* are kept low in unstressed cells through the binding of a specific E3-like ubiquitin ligase, murine double minute 2 (Mdm2). Binding of Mdm2 to the N-terminus of *p53* results in the complex being shuttled to the cytoplasm, where it is quickly degraded by the proteosome. However, in response to various stresses, including ionizing radiation, serum starvation, and hypoxia, *p53* protein levels increase both through protein stabilization and increased protein synthesis. Stabilization of *p53* in response to stress is thought to occur through several mechanisms, including prevention of Mdm2 binding and phosphorylation of *p53*. Once stabilized, *p53* is a powerful proapoptotic molecule capable of transcriptionally activating gene expression by sequence-specific DNA binding to regulatory sequences. Transcriptional targets of *p53* that induce apoptosis include *bax*, *puma*, *noxa*, and *perp* and provide a link between the tumor suppressor activity of *p53* and apoptosis. This list of *p53*-regulated apoptotic genes is always growing and very dependent on the cell type and stress. Many of the mutations in the *p53* gene found in human tumors are found within the DNA-binding domain (DBD), highlighting the importance of this region to the role of *p53* as a tumor suppressor and its ability to induce apoptosis. However, recent reports in the literature indicate a new role for *p53* in the cytoplasm and specifically at the mitochondria, where it may function directly to release cytochrome *c* to initiate the caspase cascade and apoptosis, bypassing the need for its transcriptional activity.

Seemingly paradoxical to its role in proliferation and oncogenic transformation is the fact that overexpression of the *myc* oncogene primes cells for apoptotic cell death under growth-restrictive conditions generated by nutrient deprivation or low oxygen conditions (Fig. 18.14). It is this paradox that has set forth the hypothesis that *myc* dysregulation results in a cellular state where increased proliferation or apoptotic death are both equally possible, depending on the cellular microenvironment and the activity of certain crucial genetic determinants such as the *p53* tumor suppressor gene. Evidence has accumulated that oncogenes such as *myc* and the adenovirus *E1A* gene increase *p53* protein stabilization and sensitize cells to killing by growth-restrictive conditions. Loss

of *p53* through mutation or functional inactivation severely attenuates the sensitivity of these same oncogene-expressing cells to stress-induced apoptosis. Analysis of cells deficient in *p19^{ARF}* (a cell cycle inhibitor protein) indicates that *myc* signals to *p53* through *p19^{ARF}*. Loss of *p19^{ARF}* attenuates the sensitivity of *myc*-expressing cells to apoptosis even in the presence of wild-type *p53*, suggesting that *myc* needs to signal *p19^{ARF}* to activate *p53*-dependent apoptosis. Furthermore, genetic analysis of tumor cells indicates that they possess either *p53* mutations or *p19^{ARF}* mutations but rarely both. Implicit in this observation is that *myc* dysregulation favors proliferation and that a growth-restrictive state induced by DNA damage, lack of nutrients, or oxygen starvation is needed to substantially tip the cellular balance to favor apoptotic cell death. Therefore, increased sensitivity to growth-restrictive conditions that induce apoptotic cell death will result in a selective pressure for the loss or inactivation of *p19^{ARF}*, *p53*, or other components of this stress-induced pathway. In addition to inactivating *p53*, overexpression of antiapoptotic proteins such as Bcl-2 can accelerate tumor expansion. *Myc* and Bcl-2 cooperate in lymphomagenesis *in vivo*, suggesting that overcoming apoptosis is an important step in stimulating tumor growth by the *myc* oncogene. In contrast to the death inducing changes in cellular architecture and macromolecules found during apoptosis, the process of autophagy engulfs intracellular organelles in double-membrane vacuoles called *autophagosomes*. These autophagosomes fuse with lysosomes, which leads to dysregulation of their contents. Autophagy removes organelles that are not functioning properly to allow them to be replaced with newer versions, thereby maintaining cellular homeostasis. Because autophagy is stimulated by hypoxia, growth factor depletion and even some chemotherapeutic agents, the concept of autophagic cell death was introduced into the literature as continuous organelle turnover, which could ultimately lead to cell death. A critical evaluation of the data indicates that autophagy promotes cell viability, not cell death in untransformed cells. However, under certain conditions in tumor cells, autophagy can play a role in the promotion of cell death. Therefore, the consequence of autophagy activation are both context and cell-type dependent.

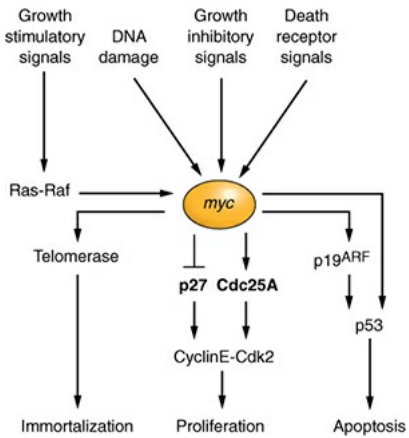


FIGURE 18.14 The *myc* oncogene can stimulate cell proliferation and primes the cell for apoptotic cell death. Depending on the cellular context, *myc* can stimulate proliferation through the activation of cyclin E–cdk2, which phosphorylates *pRb* and drives cells into S phase in response to mitogenic signals, and *myc* can prime cells for apoptosis by increasing the levels of *p53* through ARF (*p19*). Also, *myc* can promote the inactivation of the cyclin–cdk inhibitor *p27* as well as increase Cdc25A phosphatase activity. Also, *myc* can induce immortalization through regulating telomerase activity. Therefore, *myc* is the prototypical example of how one oncogene can affect cell proliferation, cell death, and immortalization.

Escaping Senescence

Just like Janus, the mythologic Roman god who had two faces, oncogenes that stimulate transformation, such as *ras*, can also drive cells into senescence. The observations that led to this discovery were based on the ability of the *ras* oncogene alone to transform and immortalize primary rodent fibroblasts only if they lacked the *p53* tumor suppressor gene or the cell cycle inhibitor *p16* that regulates the *Rb* pathway. The loss of *p53* and *p16* is also important for human cell immortalization. In addition, senescent cells have elevated levels of *p53* or *p16*, suggesting that senescence is ultimately an irreversible cell cycle arrest. In primary cells, such as fibroblasts, the activation of the constitutive growth signal by the *ras* oncogene will induce the activity of *p16* and *p53* that will counter this signal and result in the induction of cellular senescence. Therefore, for a cell to develop independence of extracellular mitogenic growth signals, it must develop mutations in pathways that send a continuous proliferation signal as well as in pathways that attempt to restrict this signal. Cell immortalization can be viewed as a competing process that requires both the activation of dominant activating oncogenes to induce proliferation and the loss of recessive tumor suppressor genes that induce a cell cycle arrest in response to this constitutive activating

signal.

Although cellular senescence can be delayed by mutations in the *p53* and *Rb* pathways, cells will ultimately encounter another junction in their road to transformation, namely, crisis (Fig. 18.15). The term **crisis** is highly appropriate, as this roadblock to cell immortalization results in chromosomal rearrangements and cell death. Less than 1 in 10 million cells that enter crisis survives and gains the ability to replicate indefinitely. One clue to what drives cells to the crisis stage comes from the end-to-end fusions of chromosomes. From this, it is apparent that crisis results from the progressive shortening of the protective caps (telomeres) on the ends of chromosomes.

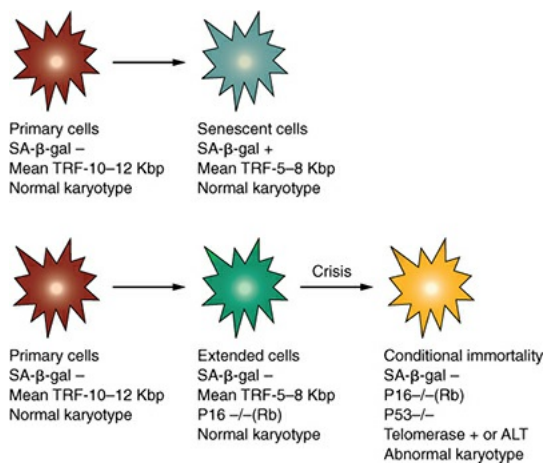


FIGURE 18.15 *In vitro* senescence has been classically defined in fibroblasts that go through a defined number of generations before they stop proliferating. This permanent arrest has been termed *senescence*. It is characterized biochemically by increased SA- β -galactosidase activity in the lysosomes and shortened telomeres (telomere restriction fragments [TRF]). Primary cells on the way to immortalization must overcome the crisis of shortened telomeres by reactivating telomerase and losing the *p53* and *pRb* (*p16* loss) control over the cell cycle and apoptosis to survive.

Mammalian telomeres consist of long arrays of the repeat sequence TTAGGG that range in length anywhere from 1.5 to 150 kb. Each time a normal somatic cell divides, the terminal end of the telomere is lost; successive divisions lead to progressive shortening, and after 40 to 60 divisions, vital DNA sequences are lost. At this point, the cell cannot divide further and undergoes senescence. Telomere length has been described as the “molecular clock” because it shortens with age in somatic tissue cells during adult life. Stem cells in self-renewing tissues, and cancer cells in particular, avoid this process of aging by activating the enzyme telomerase. Telomerase is a reverse transcriptase that polymerizes TTAGGG repeats to offset the degradation of chromosome ends that occurs with

successive cell divisions; in this way, the cell becomes immortal. Telomere shortening inhibits tumor expansion when the *p53* tumor suppressor gene is intact. Although it has not been proven, telomeres seem to engage the *p53* pathway by inducing a damage response signaled through the ATM pathway (see [Chapter 2](#)). Studies have shown that telomere shortening leads to senescence and tumor suppression in cells with an intact *p53* pathway. Surprisingly, telomere shortening accelerates tumorigenesis in cells that were deficient in *p53* activity. The ability of shortened telomeres to accelerate tumorigenesis in *p53*-deficient cells results from increased chromosomal instability and rearrangements and gene amplification.

Angiogenesis

Angiogenesis—the recruitment of new blood vessels to regions of chronically low blood supply—is essential for the progression of solid tumors to malignancy. Increasing evidence supports the hypothesis that tumor angiogenesis is controlled by an “angiogenic switch,” a physiologic mechanism involving a dynamic balance of angiogenic factors that include both inhibitors and inducers. Numerous angiogenic factors have been identified, including specific endothelial cell growth factors (e.g., vascular endothelial growth factor, or VEGF), cytokines and inflammatory agents (e.g., tumor necrosis factor α , or TNF- α , and interleukin-8, or IL-8), fragments of circulatory system proteins (e.g., angiotatin and endostatin), and ECM components (e.g., thrombospondins, or TSPs). Presumably, this diversity of angiogenic factors reflects a strict requirement for controlling angiogenesis under normal physiologic conditions and in response to oncogenic events by modulating the expression of both angiogenic inducers and inhibitors.

Although the list of proangiogenic growth factors is expanding, VEGF was the first growth factor isolated that could stimulate endothelial proliferation and migration. In tumors, VEGF can be regulated by oncogenic stimuli such as *ras* and *raf*, hypoxia, and dysregulated growth factor receptor signaling. Both tumor cells and host stromal cells produce VEGF. However, the target for VEGF lies on the cell surface of endothelial cells. These cells possess several specific transmembrane receptor tyrosine kinases that bind VEGF, which in turn initiate endothelial migration and proliferation. Regarding neoangiogenesis, VEGF receptor II is the most important for stimulating new blood vessel formation. Studies have shown that blocking the binding of VEGF to its receptor inhibits tumor angiogenesis and tumor growth. These findings have led to the development of new antibody approaches for antiangiogenesis therapy for

clinical use.

Tumors such as renal cell carcinomas that possess mutations in the von Hippel-Lindau gene (*VHL*) exhibit high aerobic expression of proangiogenic genes such as VEGF, whereas reintroduction of wild-type *VHL* substantially reduces VEGF levels to those found in untransformed cells. The mechanism underlying this observation is that *VHL* inhibits hypoxia-inducible factor (HIF) levels under aerobic conditions by targeting HIF for ubiquitin-mediated degradation. Cells that have lost *VHL* are impaired in their ability to degrade HIF and have constitutive elevated levels of HIF and HIF target genes such as *VEGF* under aerobic conditions (see [Chapter 26](#) for further explanation).

Thrombospondin 1 (TSP-1) is a secreted adhesive glycoprotein that has been shown to have antiangiogenic activity by preventing angiogenic factors such as VEGF from binding to their target receptors. Compelling evidence of an antiangiogenic function for TSP-1 is provided by studies showing that activation of the angiogenic switch in Li–Fraumeni fibroblasts lacking functional *p53* is associated with diminished TSP-1 expression. Furthermore, introduction of functional *p53* into carcinoma cells generates an antiangiogenic activity involving induction of TSP-1 expression. Reports that endogenous TSP-1 expression can be induced by *p53*, repressed by oncogenic signals such as *c-jun* overexpression, and silenced by DNA methylation, indicate that down-regulation of TSP-1 contributes to oncogenesis. As both *p53* and *c-jun* are inducible by hypoxia, the regulation of TSP-1 expression by these proteins suggests that it is also a hypoxia-responsive angiogenic inhibitor.

In summary, TSP-1 and VEGF are genetically controlled by both tumor suppressor gene and proto-oncogene activity, providing molecular mechanisms that could contribute to the switch to the angiogenic phenotype when these controls are dysregulated during oncogenesis.

Invasion and Metastasis

Many years ago, Paget realized that cancer spreads in defined patterns and is influenced by both lymph and blood flow patterns as well as the tissue being invaded. He proposed that a metastatic cell is analogous to a vegetable seed, in that, without the right soil conditions, it would never grow. Malignant tumor cells become locally invasive and escape their tissue confines by invading the substratum beneath them, before they can colonize to distant tissues ([Fig. 18.16](#)). Local invasion necessitates the breakdown of epithelial integrity that is influenced by cell–cell and cell–matrix interactions through the loss of adhesion

molecules such as E-cadherin (*E-CAD*). Decreased expression or impaired function of *E-CAD* leads to dysregulated intercellular adhesion and increases the invasive growth and spread of the primary tumor, whereas overexpression reduces the invasive and metastatic growth of transformed cells. In gastric carcinomas and lobular breast carcinomas, *E-CAD* has been found to be mutated and functionally inactivated. Thus, loss of *E-CAD* can permit local invasion of tumor cells and may be a common step in invasion. In addition to *E-CAD*, cell adhesion molecules such as neural cell adhesion molecule (NCAM) also appear to play an important role in invasion. Their expression is decreased in invasive cells and when overexpressed can decrease invasion and metastasis. One final group of proteins that contribute to the invasive capability of tumor cells are integrins, which relay signals from the ECM to epithelial cells. In this case, the cell surface repertoire of integrins changes when tumor cells become invasive. Loss of E-CAD has become linked to a developmental program termed *epithelial to mesenchymal transition (EMT)*. There are several similarities between an invasive phenotype and EMT. Both use the loss of E-CAD to escape the anti-invasive regulation of cell to cell adhesion and acquire the ability to migrate. During EMT, cells down-regulate their expression of E-CAD and increase their expression of N-CAD as they change their phenotypic appearance from an epithelial cell to a mesenchymal cell. Along with this change in phenotype, cells switch their affinity from cell to cell adhesion to cell to matrix adhesion.

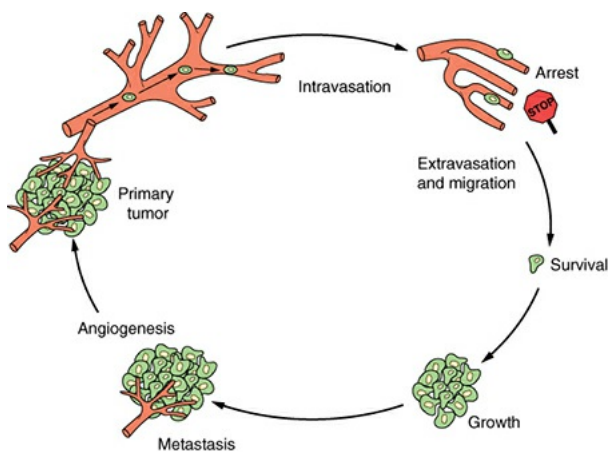


FIGURE 18.16 Critical steps in the metastatic process. Tumor cells acquire the ability to disrupt the ECM of the basement membrane, allowing them to intravasate into local blood or lymph vessels. To form metastases at remote locations, they must migrate and extravasate through the host tissue, blood, or lymph supply and survive and proliferate in the new soil. All of these processes are depicted in this figure. (Adapted from Le Q, Denko NC, Giaccia AJ. Hypoxic gene expression and metastasis. *Cancer Metastasis Rev.* 2004;23:293–

310, with permission.)

Mechanistically, oncogenic pathways such as Ras and Wnt play a major role in promotion of EMT, in part by increasing the expression of a group of transcription factors that include snail, slug, twist, and zeb1/2. A major consequence of the activation of these transcription factors is repression of E-CAD and induction of EMT. The elevation expression of snal, slug, twist, and zeb1/2 is often correlated with a poor prognosis and is associated with a highly invasive tumor.

The genetic circuits that regulate metastasis remain mainly undiscovered and elusive. Some broad concepts about metastasis have been proposed, such as the need for proteases to degrade the ECM. However, which proteases and how they are regulated differently in tumor cells compared with untransformed cells are unknown. An important question is whether or not tumor cells must acquire additional mutations to invade and metastasize. In returning to Paget's concept of the seed and the soil, only a small percentage of tumor cells are able to metastasize. Some die rapidly by apoptosis, some remain in the circulation, and a small number invade and colonize other tissues. One noteworthy point is that loss of apoptosis in response to detachment from neighboring cells and the ECM (anoikis) is essential for metastatic spread. Metastasis represents a major challenge in the treatment of cancer, especially as the ability to control local tumor growth is increasing through the combination of surgery and radiotherapy. Metastasis research represents the most critical frontier in cancer research.

THE CONCEPT OF GATEKEEPERS AND CARETAKERS

It appears that most tumor suppressor genes can be broadly divided into two classes that have been called "gatekeepers" and "caretakers." Gatekeepers are genes that directly regulate the growth of tumors by inhibiting cell division or promoting cell death. The function of these genes, therefore, is rate limiting for tumor growth; both alleles (maternal and paternal) must be lost or inactivated for a tumor to develop. Predisposed individuals inherit one damaged copy of such a gene and so require only one additional mutation for tumor initiation. The identity of gatekeepers varies with each tissue, such that inactivation of a given gene predisposes to specific forms of cancer; inherited mutations in adenomatous polyposis coli (APC) predispose to colon cancer, for example, mutations in VHL predispose to kidney cancers, and so on. Because these gatekeeper genes are rate limiting for tumor initiation, they tend to be mutated in many cancers. They can

arise both through somatic or germ line mutations.

By contrast, inactivation of caretaker genes does not directly promote the growth of tumors, but leads, instead, to genomic instability that only indirectly promotes growth by causing an increase in mutation rate. This increase in genetic instability can greatly accelerate the development of cancers, especially those that require numerous mutations for their full development. Colon cancer is a good example. The targets of the accelerated mutation rate that occurs in cells with defective caretakers are the gatekeeper tumor suppressor genes, oncogenes, or both. [Table 18.3](#) provides examples of cancer predisposition syndromes caused by mutations in DNA repair and stability genes. The evidence is highly suggestive that mutations in these predisposition genes increase the rate of acquiring cancer after exposure to DNA-damaging agents such as ionizing radiation.

Table 18.3 DNA Repair and Stability Genes and Their Associated Syndromes

SUPPRESSOR	SYNDROME	TUMOR
<i>ATM</i>	Ataxia-telangiectasia	Leukemia, lymphoma
<i>XP</i>	Xeroderma pigmentosum	Skin
<i>BRCA1</i>	Hereditary breast cancer 1	Breast
<i>BRCA2</i>	Hereditary breast cancer 2	Breast, ovary
<i>FANC</i>	Fanconi anemia	Leukemia

<i>NBS</i>	Nijmegen breakage syndrome	Lymphoma
<i>hMSH2</i>	Hereditary nonpolyposis colorectal Colon cancer	
<i>hMLH1</i>	Hereditary nonpolyposis colorectal Colon cancer	
<i>hMSH6</i>	Hereditary nonpolyposis colorectal Colon cancer	
<i>hPMS1</i>	Hereditary nonpolyposis colorectal Colon cancer	
<i>hPMS2</i>	Hereditary nonpolyposis colorectal Colon cancer	

Evidence for this comes from a review by Swift of 161 families affected by ataxia-telangiectasia (AT). In this prospective study, new cases of cancers were observed in blood relatives of persons with AT (of whom about half may be heterozygotic), in those who are definite heterozygotes (obligates), and in spouses who were assumed to be normal but who lived in the same environment. This extensive study also divided blood relatives of AT homozygotes into those with and those without a “radiation history.” A radiation history was interpreted loosely as fluoroscopy of the chest, back, or abdomen, therapeutic irradiation, or occupational exposure. [Table 18.4](#) shows the results of the survey: 53% of blood relatives with cancer had a radiation history, compared with 19% of those without cancer.

Table 18.4 Breast Cancer and Radiation in 161 Families with Ataxia-Telangiectasia

	BLOOD RELATIVES WITH CANCER	BLOOD RELATIVES WITHOUT CANCER
Number	19	57
With radiation history ^a	radiation 10/19 = 53%	11/57 = 19%

^aRadiation history includes fluoroscopy of chest, back, or abdomen; therapeutic radiation; and occupational exposure.

From Swift M, Morrell D, Massey RB, et al. *N Engl J Med.* 1991;325:1831–1836, with permission.

From these data, the study purported to show that AT heterozygotes are very sensitive to radiation-induced cancer; a control study of this kind does not provide proof of this, but the possibility certainly exists. It is a challenging and sobering thought to diagnostic radiologists that a proportion of the women routinely screened by mammography may be exquisitely sensitive to radiation-induced carcinogenesis because of repair deficiencies associated with being heterozygotic for AT.

MISMATCH REPAIR

Interest in MMR genes heightened with the discovery that they were responsible for the mutator phenotype associated with a predisposition for hereditary nonpolyposis colon cancer (HNPCC) and possibly other familial cancers. The initial clue to this novel molecular mechanism was the discovery of deletions of long monotonic (dA-dT) runs in a subset of human colon cancers. Soon after, insertions or deletions at mononucleotide, dinucleotide, and trinucleotide repeat sequences were discovered in subsets of colon tumors as well as in various colon cancers from individuals with HNPCC. This phenotype also has been detected in several other types of human malignancies, especially those associated with type 2 Lynch syndrome. These various investigations culminated in the identification and cloning of the human *hMSH2* gene, which maps to a locus linked to HNPCC on chromosome 2p21–22, and whose homologues in *Saccharomyces cerevisiae* and *Escherichia coli* are involved in the process of DNA MMR.

The primary function of MMR genes in *E. coli* is to scan the genome as it replicates and to spot errors of mismatch as the DNA is replicated, that is, as the new DNA strand is laid down using the stable methylated strand as a template. A growing number of human genes have been associated with HNPCC by means of linkage analysis and studies of mutational mapping. [Table 18.5](#) lists human MMR genes associated with HNPCC. The MMR process in yeast and bacteria involves a large number of proteins, and so it is likely that additional causes of HNPCC remain to be uncovered.

Table 18.5 Human Mismatch Repair Genes

GENE	CHROMOSOMAL LOCATION	GERM LINE MUTATIONS IN HEREDITARY NONPOLYPOSIS COLON CANCER CASES (REPORTED FAMILY STUDIES), %
<i>hMSH2</i>	2p21–22 (2p16?)	60
<i>hMLH1</i>	3p21	30
<i>hPMS1</i>	2q31–33	4
<i>hPMS2</i>	7p21	4
<i>GTBP</i>	2p16 (2p21–22?)	0

Cells with defective or nonfunctioning MMR genes can be identified by two quite different techniques:

1. By using a selectable reporter system that inserts an exogenous long repeat sequence into the cells in question and measures the mutation rate in it.
2. By measuring the mutation rate in one or more of the many endogenous

repeat sequences that already exist in every human cell—the so-called microsatellite instability assay. Microsatellite instability appears to be a factor of some importance in various human tumors.

Both techniques have strengths and weaknesses and are far from perfect.

HERITABLE SYNDROMES THAT AFFECT RADIOSENSITIVITY, GENOMIC INSTABILITY, AND CANCER

The DNA damage response in mammalian cells is composed of multiprotein complexes that sense, signal, and respond to DNA strand breaks. Disruption of the function of these multiprotein complexes by mutation of a single gene leads to cancer-prone syndromes that are characterized by hypersensitivity to DNA damage and genomic instability. Syndromes that exhibit hypersensitivity to ionizing radiation are discussed here.

Ataxia-Telangiectasia

AT is a rare autosomal recessive disease in which afflicted individuals present with progressive cerebellar ataxia caused by increased loss of Purkinje cells in the cerebellum as well as oculocutaneous telangiectasia. Patients with AT are immune deficient and have a high incidence of cancer, especially of the reticular endothelial system. Patients with AT exhibit a hypersensitive skin reaction to ionizing radiation and DNA breaking agents but not to ultraviolet light. Both lymphocytes and fibroblasts derived from these individuals are also hypersensitive to killing by ionizing radiation.

The genetic defect responsible for the AT phenotype is the result of mutations in the *ATM* gene. The *ATM* gene encodes for a kinase that phosphorylates a serine or threonine that is followed by a glutamine motif (S/T-Q) in target proteins (Fig. 18.17). ATM is involved in the rapid response of cells to DNA DSBs (it signals to the DNA repair machinery) as well as the activation of cell cycle checkpoints. However, it is important to recognize that although the ATM kinase is activated by DNA damage and chromatin alterations throughout the cell cycle, it uses different downstream effectors to mediate a checkpoint response in each of the different phases of the cell cycle. For example, the activation of a G₁ checkpoint is in large part mediated by ATM signaling to p53, which results in the transcriptional induction of the p21 cell cycle inhibitor. Perhaps the most distinctive hallmark of AT cells is their failure to arrest in S phase in response to DNA damage. This phenomenon has been termed

radioresistant DNA synthesis, and at least two pathways regulated by ATM control the passage of cells through S phase.

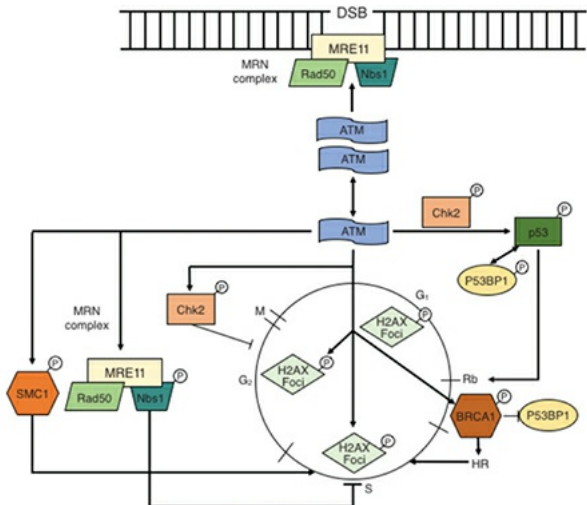


FIGURE 18.17 Activation of the ataxia-telangiectasia mutated (ATM) pathway by an ionizing radiation-induced DNA double-strand break (DSB). The model proposed by Kastan and Bakkenist indicates that ATM exists as a dimer and undergoes rapid autophosphorylation in response to DNA strand breaks and chromatin conformation changes. This results in dissociation of the dimer into a monomer and the phosphorylation of numerous substrates involved in DNA repair (H2AX, SMC1, BRCA1, and P53BP1) and cell cycle control (p53 and Chk2). Recent studies have shown that the MRN complex can function upstream of ATM by sensing and localizing to DNA breaks and can also be a target of ATM. BRAC1 inhibits P53BP1 to allow homologous recombination repair in S phase. Phosphorylation of H2AX at sites of DNA DSBs can occur throughout the cell cycle. SMC1 is involved in regulating the DNA damage response in S phase. Chk2 phosphorylates p53 in G₁ phase and is also involved in the G₂ checkpoint.

Much is known about the way in which ATM and its family members control cell cycle checkpoints, but the mechanism by which loss of ATM leads to increased radiosensitivity is still under investigation. It may involve both direct mechanisms, such as direct phosphorylation of the cohesin family member structural maintenance of chromosomes (SMC) or Nijmegen breakage syndrome (NBS) protein, and indirect mechanisms, such as dysregulated homologous recombination. Lymphoid cells in ATM homozygotes often exhibit increased chromosomal instability, and the lymphomas that develop demonstrate the importance of DNA repair and chromosome maintenance in tumor suppression.

Seckel Syndrome

In mammalian cells, ATM belongs to the phosphatidylinositol 3-kinase-related kinase (PIKK) family and shares homology with two other family members—ATR and DNA-dependent protein kinase catalytic subunit (DNA-PKcs)—that are also activated by DNA strand breaks. At the molecular level, ATR and DNA-PKcs like ATM regulate DNA repair and cell cycle regulatory proteins. Interestingly, although ATM is not an essential gene, ATR is essential. Some individuals afflicted with Seckel syndrome—a rare autosomal recessive disorder characterized by microcephaly and abnormal development—can possess an alteration in the ATR gene that reduces its absolute quantity but does not eliminate its activity. Patients with Seckel syndrome do not appear to be radiosensitive because they possess some ATR activity.

Mouse versus Human Severe Combined Immunodeficiency

DNA-PKcs is an essential component of nonhomologous recombination and is the defect in murine severe combined immunodeficiency (SCID) syndrome. However, human patients with SCID do not possess DNA-PKcs mutations, but instead possess mutations in Artemis, a target of DNA-PKcs. Artemis-deficient human SCID cells are radiosensitive, and fibroblasts from afflicted individuals exhibit increased chromosomal instability.

Ataxia-Telangiectasia-Like Disorder

Ataxia-telangiectasia-like disorder (ATLD) is an autosomal recessive disease caused by mutations in the gene MRE11 that forms a complex with Rad50 and NBS in irradiated cells. Cells derived from patients with ATLD are radiosensitive but repair their DNA DSBs similar to wild-type levels, leaving the mechanism for their radiosensitivity in question. ATLD1 cells are also defective in their checkpoint response following DNA damage.

Nijmegen Breakage Syndrome

NBS is a direct phosphorylation target of ATM and forms a complex with Rad50 and MRE11 (MRN complex). This complex possesses nuclease activity that is necessary for DNA DSB repair. The relationship between NBS and ATM is complex because ATM phosphorylates NBS in response to DNA damage, but NBS may also be required for activation of some ATM checkpoint responses. Thus, the mechanism of AT, ATLD1, and NBS sensitivity to ionizing radiation probably involves the same pathway.

Fanconi Anemia

Eight different proteins give rise to the autosomal recessive disorder Fanconi anemia (FA), which is characterized by spontaneous chromosomal instability, sensitivity to interstrand DNA crosslinks and, in some cases, sensitivity to ionizing radiation. The Fanconi anemia, complementation group D2 (*FANCD2*) gene is thought to be a key player in the FA pathway because it is the only *FANC* gene conserved through evolution, and most of the other *FANC* proteins form a complex that results in the monoubiquitination of *FANCD2* that results in its localization to foci that contain the breast cancer tumor suppressor genes *BRCA1* and *BRCA2* (also known as *FANCI*). The identification of *BRCA2* as an FA gene, together with its localization in foci with *FANCD2*, suggests an important role for *FANC* genes in homologous recombination. In addition, *FANCD2* has been implicated in the DNA damage checkpoint response and is phosphorylated by the ATM kinase on serine 222. The roles of *FANCD2* in the radiation response and crosslink response are separable because inhibition of phosphorylation on serine 222 inhibits the FA-mediated radiation response, and inhibition of ubiquitination of lysine 561 results in hypersensitivity to crosslinking agents.

Clinical reports have suggested that tumors derived from patients with FA are hypersensitive to radiotherapy. However, fibroblasts derived from individuals that possess mutated forms of each of the eight different FA proteins were not always found to exhibit radiosensitivity and never to the same level as AT cells. Therefore, the clinical response of patients with FA to radiotherapy does not always correlate with intrinsic radiosensitivity of fibroblasts derived from the same patients, suggesting that additional genetic alterations in tumor cells from patients with FA may be responsible for the enhanced radiosensitivity that has been observed.

Homologues of RecQ—Bloom Syndrome, Werner Syndrome, and Rothmund–Thompson Syndrome

RecQ was first identified in *E. coli*. and five human homologues of RecQ have been described, three of which are found mutated in cancer-prone syndromes. RecQ genes encode for DNA helicases that unwind DNA 3' to 5' in an adenosine triphosphate (ATP)-dependent manner and also have 3' to 5' exonuclease activity. The main function of RecQ helicases is to monitor the DNA replication fork for damage, acting as intermediaries between replication and recombination. RecQ helicases are found at DNA replication forks and protect them from stalling. In fact, RecQ expression is the highest in S phase of the cell cycle. Cells with reduced RecQ activity are hypersensitive to agents that inhibit DNA

synthesis such as hydroxyurea and aphidicolin. Even in the absence of DNA synthesis inhibitors, cells with reduced RecQ activity accumulate abnormal DNA structures as they traverse through S phase. The most well-studied human RecQ helicases are Bloom syndrome (BLM), Werner syndrome (WS), and Rothmund–Thompson syndrome (RTS). Loss of the BLM helicase results in BLM, which is associated with a high incidence of lymphomas, leukemias, gastrointestinal (GI) tract tumors, and breast tumors. Individuals with BLM exhibit sensitivity to sunlight, dwarfism, immunodeficiency, male sterility, and elevated levels of sister chromatid exchange (SCE). Similar to patients with BLM, individuals with WS also show an increased risk of cancers, and age at an accelerated rate (premature aging). This puts patients with WS at risk for age-related diseases such as cancer, diabetes, osteoporosis, and atherosclerotic cardiovascular disease. Mechanistically, the increase in cancer and potentially their premature aging are linked to their high levels of genomic instability; in particular, the cells of these patients have high levels of chromosomal deletions and translocations. RTS results from a loss of RecQ4 helicase. These afflicted individuals display growth deficiency, photosensitivity, early greying and hair loss, juvenile cataracts, skeletal dysplasias, a predisposition to malignancy, especially osteogenic sarcomas, and chromosomal instability.

RADIATION-INDUCED SIGNAL TRANSDUCTION

Ionizing radiation can regulate the expression of early response genes such as *c-fos*, *c-jun*, and *c-myc*, genes that control lipid signaling such as acid sphingomyelinase, and the PIKK family that includes ATM and DNA-PK.

Early Response Genes

The activation of early response genes by ionizing radiation suggests that radiation in some way mimics the mitogenic activation of quiescent cells. Evidence for the importance of such effects is that the overexpression of proto-oncogenes such as *c-ras* and *c-raf*, whose products are intermediates in the pathways of mitogenic signal transduction, is associated with radiation resistance. The induction of these pathways results in gene activation through elements such as activator protein 1 (AP-1), serum response element (SRE), and cAMP response element-binding protein (CREB).

The role of these early response genes is not clear at the present time, but the stimulation of signal transduction pathways and activation of transcription factors may enhance secondarily the response of the cell to radiation in terms of repair and cell cycle arrest. In addition, the activation of these early response

genes, in turn, could provide a mechanism for secondary stimulation of various late response genes such as TNF- α , PDGF, FGF, and IL-1. Activation of these genes may allow the cell to adapt to acute changes in the microenvironment and may be responsible for some of the chronic responses of the cell to ionizing radiation, including apoptosis.

The Ceramide Pathway

Exposure of cells to DNA damage induces the production of ceramide through two major pathways. In one pathway that is activated by ionizing radiation and DNA-damaging agents, ceramide is generated from sphingomyelin hydrolysis by the enzyme acid sphingomyelinase (Fig. 18.18). This results in the catalysis of up to one-half of total cellular sphingomyelin, most of which would be presumably associated with the plasma membrane. Ceramide can also be generated by ceramide synthase, which is inhibited by the ATM kinase. Therefore, in response to ionizing radiation, individuals who have lost ATM have elevated levels of ceramide synthase and increased apoptosis of certain cell types (e.g., crypt cells). It is important to note that ionizing radiation can activate both nuclear and membrane–cytoplasmic signal transduction pathways that can lead to either cell cycle arrest or, alternatively, apoptosis.

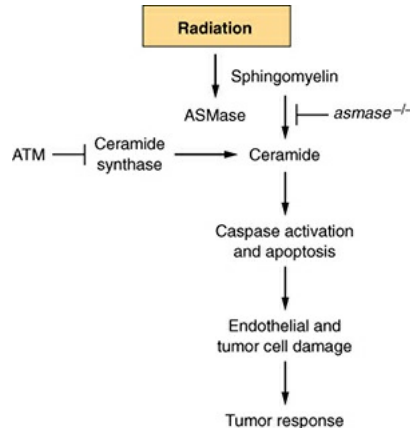


FIGURE 18.18 The acid sphingomyelinase (ASMase) pathway for the generation of ceramide. When cells are irradiated, ASMase activity increases and converts sphingomyelin to ceramide. The intracellular production of ceramide acts as a potent activator of the caspase cascade to induce apoptosis in endothelial cells as well as tumor cells. Cells deficient in acid sphingomyelinase ($asmase^{-/-}$) can only generate ceramide from ceramide synthase, which is negatively regulated by ATM. (Figure provided courtesy of Dr. Richard Kolesnick, Memorial Sloan Kettering Cancer Center.)

In summary, although there is little doubt that the lethal effects of ionizing

radiation result from extensive DNA damage leading to chromosomal aberrations, radiation can also stimulate signal transduction pathways that can lead to cell cycle arrest or cell death by apoptosis, depending on the dose of radiation and genetic background of the cell.

T CELL CHECKPOINT THERAPY

T cell checkpoint therapeutics have rapidly reached a prominent role in the treatment of metastatic cancer. However, on close examination of the statistics, the response to monotherapy for anti-cytotoxic T-lymphocyte-associated protein 4 (anti-CTLA-4), anti-programmed cell death protein 1 (anti-PD-1) or anti-programmed death-ligand 1 (anti-PD-L1) are in the range of 10% to 30%, clearly leaving room for improvement. Therefore, current investigations are focused on understanding what limits the response to these checkpoint immunotherapies and the discovery of therapeutics that can enhance cytotoxic T cell antitumor response. Recently identified mechanisms of resistance to T cell activity include increased levels of immunosuppressive Tregs, elevated levels of indoleamine 2,3-dioxygenase 1 (IDO1), which inhibits T cell responses by decreasing tryptophan levels, or active engagement of inhibitory receptors such as T cell immunoglobulin and mucin domain 3 (TIM3). In addition to these mechanisms, resistance to checkpoint immunotherapy can also be due to a suppressive immune microenvironment that promotes T cell exclusion. Studies show that a strong predictor to anti-PD-1 or PD-L1 therapy is the presence of pretreatment CD8⁺ T cells within the tumor. Thus, tumor resistance to checkpoint immunotherapy can be achieved by T cell exclusion.

One proposed mechanism to stimulate T cell infiltration into the tumor is to treat with cytotoxic chemotherapy or radiotherapy ([Fig. 18.19](#)). The potentially powerful combination of immunotherapy and radiotherapy was stimulated by a case report, which showed a remarkable systemic response of metastatic renal cancer to anti-CTLA therapy after palliative radiotherapy. However, more recent clinical studies have not generated strong support for the concept of combining radiotherapy and immunotherapy to generate increased systemic antitumor responses. Although the combination of radiotherapy and immunotherapy do not increase systemic responses in tumors which exhibit T cell immune exclusion, the possibility remains that the combination is more efficacious in tumors which already have T cell infiltrates. Finally, a major question that needs to be addressed is to what extent does genotoxic radiotherapy or chemotherapy cause the release of autologous neoantigens to stimulate the immune system.

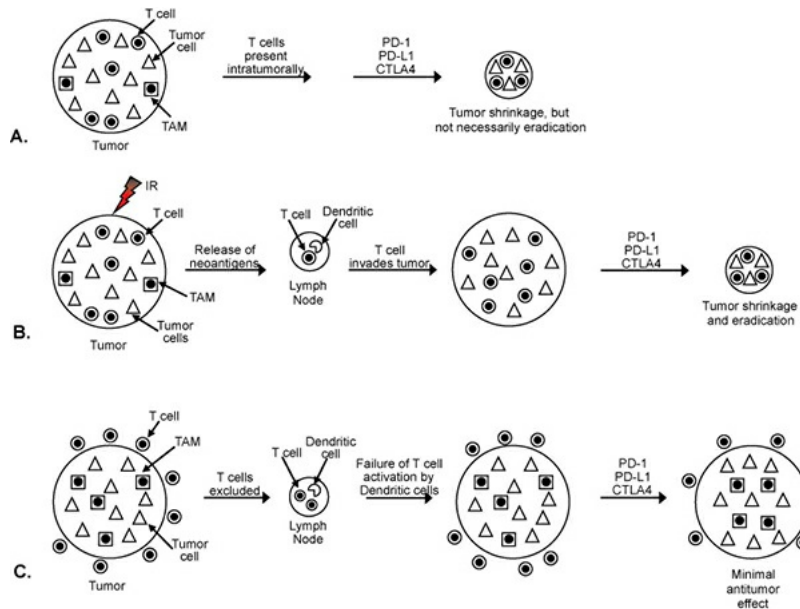


FIGURE 18.19 Three different scenarios to explain how T cell checkpoint therapy and radiotherapy can be effective or ineffective. **A:** T cells are found within the tumor but not very active in killing tumor cells. The addition of a T cell checkpoint inhibitor such as anti-CTLA-4, anti-PD-1, or anti-PD-L1 reduces inhibitory signals that prevent T cells from being effective in killing tumor cells. In about 20% to 30% of treated patients, T cell checkpoint therapy will result in a robust antitumor response. **B:** If tumors are irradiated before the addition of T cell checkpoint therapies, there is a proposed increase in neoantigens that can stimulate the activation of T cells in the lymph node through interaction with dendritic cells. These active T cells can then invade the tumor, which was irradiated can increase tumor shrinkage and potentially lead to tumor eradication. **C:** In many tumors, T cells are excluded from entering the tumor either by failure to be activated by dendritic cells in the lymph nodes or by an immune-suppressive microenvironment containing tumor-activated macrophages (TAMs). These tumors will be unresponsive to T cell checkpoint therapies and fail to be completely eliminated by radiotherapy.

SUMMARY OF PERTINENT CONCLUSIONS

Cancer is thought to be a clonal disorder.

The control of cell proliferation is the consequence of signals that may be positive or negative.

Gain-of-function mutations can activate oncogenes, which are positive growth regulators; tumor suppressor genes are a negative growth regulator.

Oncogenes are genes found in either a mutant or an abnormally expressed form

in many human cancers.

Oncogenes can be activated by retroviral integration, point mutation, a chromosomal rearrangement such as a translocation, or gene amplification.

Some human leukemias and lymphomas appear to be caused by specific chromosomal translocations that lead to oncogene activation in several different ways.

Knudson postulated that all types of retinoblastoma involve two separate mutations. In sporadic retinoblastoma, both mutations occur somatically in the same retinal cell; therefore, this condition is rare. In the heritable form, one of the two mutations is inherited from a parent and is present in all retinal cells so that the second mutation would occur somatically in any of these cells; hence, the incidence is close to 100%.

There are many tumor suppressor genes whose location and function are known; the two most intensively studied are *p53* and *Rb*.

Because oncogenes are gain-of-function mutations, only one copy needs to be activated; that is, they act in a dominant fashion. Tumor suppressor genes involve loss-of-function mutations so that both copies must be lost; that is, they act in a recessive fashion.

Somatic homozygosity is the process by which one chromosome of a pair is lost, a deletion occurs in the remaining chromosome, and the chromosome with the deletion replicates.

Carcinogenesis appears to be a multistep process with multiple genetic alterations occurring. An attractive model of carcinogenesis includes the idea that an early step causes a mutation in a gene in one of the families responsible for the stability of the genome. This leads to a mutator phenotype so that multiple further changes are likely in the progression of the cancer.

Telomeres cap the ends of chromosomes; they are long arrays of TTAGGG repeats. Each time a normal somatic cell divides, the terminal end of the telomere is lost; after 40 to 60 divisions, the cell undergoes senescence. Stem cells and cancer cells activate telomerase, which maintains telomere length, so the cell becomes immortal.

AT is an autosomal recessive disorder that is caused by a defect in the ATM kinase. AT cells fail to activate checkpoints in response to DNA damage, exhibit increased genomic instability at the chromosome level, and have an increased risk of lymphomas. AT cells and individuals are hypersensitive to

ionizing radiation.

The *ATR* gene expression (AT and Rad3 related) is decreased in patients with Seckel syndrome. Although it belongs to the same PIKK family as ATM, it is an essential gene at the cellular level. It has an important role in responding to DNA breaks in S phase.

RecQ genes encode helicases that play a critical role in protecting replication forks. Decreased expression of RecQ genes results in aberrant DNA replication and genomic instability.

There are at least three human syndromes involved in RecQ deficiency: BLM, WS, and RTS. A common feature of all these syndromes is increased chromosomal instability. These disorders do not result in hypersensitivity to ionizing radiation. However, BLM cells are sensitive to alkylating agents and mitomycin C.

NBS is a rare disorder that results in increased cancer incidence. Cells defective in NBS lack an S phase checkpoint and are radiosensitive.

Patients with ATLD are clinically similar to patients with AT except that their defect lies in the *MRE11* gene. Cells from these patients are also sensitive to ionizing radiation.

Patients with FA are characterized by their hypersensitivity to crosslinking agents. Although fibroblasts derived from these patients are not sensitive to ionizing radiation, tumors arising in these patients are hypersensitive. The reasons for this are currently unknown.

T cell checkpoint therapeutics are currently being tested in many different cancers alone or in combination with other anti-cancer agents. While great enthusiasm exists for T cell checkpoint therapeutics with radiotherapy, clinical trial data needs to demonstrate how effective this combination will be. Some of the mechanisms of resistance to T cell checkpoint therapeutics are known and one of the most important is T cell exclusion from the tumor.

BIBLIOGRAPHY

Signal Transduction

Aguilera TA, Giaccia AJ. Molecular pathways: oncologic pathways and their role in T-cell exclusion and immune evasion—a new role for the AXL receptor tyrosine kinase. *Clin Cancer Res.* 2017;23(12):2928–2933. doi:10.1158/1078-0432.CCR-17-0189.

- Amundson SA, Myers TG, Fornace AJ Jr. Roles of p53 in growth arrest and apoptosis: putting on the brakes after genotoxic stress. *Oncogene*. 1998;17:3287–3299.
- Bakkenist CJ, Kastan MB. Initiating cellular stress responses. *Cell*. 2004;14:9–17.
- Bell DW, Varley JM, Szydlo TE, et al. Heterozygous germ line hCHK2 mutations in Li-Fraumeni syndrome. *Science*. 1999;286:2528–2531.
- Datta R, Rubin E, Sukhatme V, et al. Ionizing radiation activates transcription of the EGR1 gene via CArG elements. *Proc Natl Acad Sci USA*. 1992;89:10149–10153.
- Dent P, Yacoub A, Contessa J, et al. Stress and radiation-induced activation of multiple intracellular signaling pathways. *Radiat Res*. 2003;159:283–300.
- Folkman J. Role of angiogenesis in tumor growth and metastasis. *Semin Oncol*. 2002;29:15–18.
- Fornace AJ, Fuks Z, Weichselbaum RR, et al. Radiation therapy. In: Mendelsohn J, Howley PM, Israel MA, et al, eds. *The Molecular Basis of Cancer*. Philadelphia, PA: Saunders; 1998.
- Hunter T. Signaling—2000 and beyond. *Cell*. 2000;100:113–127.
- Jones HA, Hahn SM, Bernhard E, et al. Ras inhibitors and radiation therapy. *Semin Radiat Oncol*. 2001;11:328–337.
- Kalluri R, Weinberg RA. The basics of epithelial-mesenchymal transition. *J Clin Invest*. 2009;119:1420–1428.
- Malumbres M, Pellicer A. Ras pathways to cell cycle control and cell transformation. *Front Biosci*. 1998;3:d887–d912.
- McCormick F. Signalling networks that cause cancer. *Trends Cell Biol*. 1999;9:M53–M56.
- Reynolds CP, Maurer BJ, Kolesnick RN. Ceramide synthesis and metabolism as a target for cancer therapy. *Cancer Lett*. 2004;206:169–180.
- Sebolt-Leopold JS, Herrera R. Targeting the mitogen-activated protein kinase cascade to treat cancer. *Nat Rev Cancer*. 2004;4:937–947.
- Stevenson MA, Pollock SS, Coleman CN, et al. X-irradiation phorbol esters, and H₂O₂ stimulate mitogen-activated protein kinase activity in NIH-3T3 cells through the formation of reactive oxygen intermediates. *Cancer Res*.

- 1994;54:12–15.
- Vogelstein B, Lane D, Levine AJ. Surfing the p53 network. *Nature*. 2000;408:307–310.
- Vojtek AB, Der CJ. Increasing complexity of the Ras signaling pathway. *J Biol Chem*. 1998;273:19925–19928.
- Xia Z, Dickens M, Raingeaud J, et al. Opposing effects of ERK and JNK-p38 map kinase on apoptosis. *Science*. 1995;270:1326–1331.
- ## Heritable Syndromes that Affect Radiosensitivity, Genomic Instability, and Cancer
- Bachrati CZ, Hickson ID. RecQ helicases: guardian angels of the DNA replication fork. *Chromosoma*. 2008;117:219–233.
- Carney JP, Maser RS, Olivares H, et al. The hMre11/hRad50 protein complex and Nijmegen breakage syndrome: linkage of double-strand break repair to the cellular DNA damage response. *Cell*. 1998;93:477–486.
- D’Andrea AD, Grompe M. The Fanconi anaemia/BRCA pathway. *Nat Rev Cancer*. 2003;3:23–34.
- Ellis NA, German J. Molecular genetics of Bloom’s syndrome. *Hum Mol Genet*. 1996;5:1457–1463.
- Gray MD, Shen JC, Kamath-Loeb AS, et al. The Werner syndrome protein is a DNA helicase. *Nat Genet*. 1997;17:100–103.
- Gurtan AM, D’Andrea AD. Dedicated to the core: understanding the Fanconi anemia complex. *DNA Repair (Amst)*. 2006;5:1119–1125.
- Hartman AR, Ford JM. BRCA1 and p53: compensatory roles in DNA repair. *J Mol Med (Berl)*. 2003;81:700–707.
- Huang S, Li B, Gray MD, et al. The premature ageing syndrome protein, WRN, is a 3’→5’ exonuclease. *Nat Genet*. 1998;20:114–116.
- Kitao S, Shimamoto A, Goto M, et al. Mutations in RECQL4 cause a subset of cases of Rothmund-Thomson syndrome. *Nat Genet*. 1999;22:82–84.
- Li GM. Mechanisms and functions of DNA mismatch repair. *Cell Res*. 2008;18:85–98.
- Malkin D, Li FP, Strong LC, et al. Germ line p53 mutations in a familial syndrome of breast cancer, sarcomas, and other neoplasms. *Science*.

- 1990;250:1233–1238.
- Moynahan ME, Chiu JW, Koller BH, et al. Brca1 controls homology-directed DNA repair. *Mol Cell*. 1999;4:511–518.
- Savitsky K, Bar-Shira A, Gilad S, et al. A single ataxia telangiectasia gene with a product similar to PI-3 kinase. *Science*. 1995;268:1749–1753.
- Srivastava S, Zou ZQ, Pirolo K, et al. Germ-line transmission of a mutated p53 gene in a cancer-prone family with Li-Fraumeni syndrome. *Nature*. 1990;348:747–749.
- Stewart GS, Maser RS, Stankovic T, et al. The DNA double-strand break repair gene hMRE11 is mutated in individuals with an ataxia-telangiectasia-like disorder. *Cell*. 1999;99:577–587.
- Taniguchi T, Garcia-Higuera I, Andreassen PR, et al. S-phase-specific interaction of the Fanconi anemia protein, FANCD2, with BRCA1 and RAD51. *Blood*. 2002;100:2414–2420.
- Zhang J, Powell SN. The role of the BRCA1 tumor suppressor in DNA double-strand break repair. *Mol Cancer Res*. 2005;3:531–539.
- ## Oncogenes and Tumor Suppressor Genes
- Adams JM, Harris AW, Pinkert CA, et al. The c-myc oncogene driven by immunoglobulin enhancers induces lymphoid malignancy in transgenic mice. *Nature*. 1985;318:533–538.
- Barbacid M. RAS genes. *Ann Rev Biochem*. 1987;56:779–827.
- Bishop JM. Cellular oncogene retroviruses. *Ann Rev Biochem*. 1983;52:301–354.
- Bishop JM, Varmus HE. Functions and origins of retroviral transforming genes. In: Weiss R, Teich N, Varmus H, et al, eds. *RNA Tumor Viruses: Molecular Biology of Tumor Viruses*. 2nd ed. Cold Spring Harbor, NY: Cold Spring Harbor Laboratory; 1984:990–1108.
- Bos J, Fearon E, Hamilton S, et al. Prevalence of RAS gene mutations in human colorectal cancers. *Nature*. 1987;327:293–297.
- Cavenee WK, Dryja T, Phillips R, et al. Expression of recessive alleles by chromosomal mechanisms in retinoblastoma. *Nature*. 1983;305:779–784.
- Cavenee WK, Hansen MF, Nordenskjold M, et al. Genetic origin of mutations predisposing to retinoblastoma. *Science*. 1985;228:501–503.

- Cole M. The *myc* oncogene: its role in transformation and differentiation. *Annu Rev Genet.* 1986;20:361–384.
- Der C, Krontiris T, Cooper G. Transforming genes of human bladder and lung carcinoma cell lines are homologous to the *ras* gene of Harvey and Kirsten sarcoma viruses. *Proc Natl Acad Sci USA.* 1982;79:3637–3640.
- El-Deiry W, Tokino T, Velculescu V, et al. WAF1, a potential mediator of p53 tumor suppression. *Cell.* 1993;75:817–825.
- Fernandez-Sarabia M, Bischoff J. Bcl-2 associates with the *ras*-related protein R-ras p23. *Nature.* 1993;366:274–275.
- Fidler IJ. Critical determinants of metastasis. *Semin Cancer Biol.* 2002;12:89–96.
- Grignani F, Ferrucci P, Testa U, et al. The acute promyelocytic leukemia-specific PML-RAR alpha fusion protein inhibits differentiation and promotes survival of myeloid precursor cells. *Cell.* 1993;74:423–431.
- Harley C, Futcher A, Greider C. Telomeres shorten during aging of human fibroblasts. *Nature.* 1990;345:458–460.
- Harris C, Hollstein M. Clinical implications of the p53 tumor-suppressor gene. *N Engl J Med.* 1993;329:1318–1327.
- Hartwell LH, Kastan MB. Cell cycle control and cancer. *Science.* 1994;266:1821–1828.
- Huebner RJ, Todaro GJ. Oncogenes of RNA tumor viruses as determinants of cancer. *Proc Natl Acad Sci USA.* 1969;64:1087–1094.
- Jiang W, Kahn S, Guillem J, et al. Rapid detection of *ras* oncogenes in human tumors: applications to colon, esophageal, and gastric cancer. *Oncogene.* 1989;4:923–928.
- Kastan M, Zhan Q, El-Deiry W, et al. A mammalian cell cycle checkpoint pathway utilizing p53 and GADD45 is defective in ataxia-telangiectasia. *Cell.* 1992;71:587–597.
- Kelly K, Cochran B, Stiles C, et al. Cell-specific regulation of the c-*myc* gene by lymphocyte mitogens and platelet-derived growth factor. *Cell.* 1983;35:603–610.
- Knudson AG Jr. Antioncogenes and human cancer. *Proc Natl Acad Sci USA.* 1993;90:10914–10921.

- Knudson AG Jr. Mutation and cancer: statistical study of retinoblastoma. *Proc Natl Acad Sci USA*. 1971;68:820–823.
- Land H, Parada L, Weinberg R. Tumorigenic conversion of primary embryo fibroblasts requires at least two cooperating oncogenes. *Nature*. 1983;304:596–602.
- Lengauer C, Kinzler KW, Vogelstein B. Genetic instabilities in human cancers. *Nature*. 1998;396:643–649.
- Lynch D, Watson M, Alderson M, et al. The mouse Fas-ligand gene is mutated in gld mice and is part of a TNF family gene cluster. *Immunity*. 1994;1:131–136.
- Nagata S, Golstein P. The Fas death factor. *Science*. 1995;267:1449–1456.
- Nowell PC. Tumor progression: a brief historical perspective. *Semin Cancer Biol*. 2002;12:261–266.
- Prives C, Hall PA. The p53 pathway. *J Pathol*. 1999;187:112–126.
- Rous P. A sarcoma of fowl transmissible by an agent separable from the tumor cells. *J Exp Med*. 1911;13:397.
- Rowley J. Molecular cytogenetics: Rosetta stone for understanding cancer—twenty-ninth G.H.A. Clowes memorial award lecture. *Cancer Res*. 1990;50:3816–3825.
- Sabbatini P, Lin J, Levine A, et al. Essential role for p53-mediated transcription in E1A-induced apoptosis. *Genes Dev*. 1995;9:2184–2192.
- Schwab M, Varmus H, Bishop J, et al. Chromosome localization in normal human cells and neuroblastomas of a gene related to c-myc. *Nature*. 1984;308:288–291.
- Shay JW, Roninson IB. Hallmarks of senescence in carcinogenesis and cancer therapy. *Oncogene*. 2004;23:2919–2933.
- Sherr CJ, McCormick F. The RB and p53 pathways in cancer. *Cancer Cell*. 2002;2:103–112.
- Sklar M, Thompson E, Welsh M, et al. Depletion of c-myc with specific antisense sequences reverses the transformed phenotype in ras oncogene-transformed NIH 3T3 cells. *Mol Cell Biol*. 1991;11:3699–3710.
- Spector D, Varmus H, Bishop J. Nucleotide sequences related to the transforming gene of avian sarcoma virus are present in the DNA of

- uninfected vertebrates. *Proc Natl Acad Sci USA*. 1978;75:4102–4106.
- Stanbridge EJ. Suppression of malignancy in human cells. *Nature*. 1976;260:17–20.
- Stewart T, Pattengale P, Leder P. Spontaneous mammary adenocarcinomas in transgenic mice that carry and express *MTV/myc* fusion genes. *Cell*. 1984;38:627–637.
- Tabin CJ, Bradley SM, Bargmann CI, et al. Mechanism of activation of a human oncogene. *Nature*. 1982;300:143–159.
- Temin HM, Rubin H. Characteristics of an assay for Rous sarcoma virus and Rous sarcoma cells in tissue culture. *Virology*. 1958;6:669–688.
- Vogelstein B, Kinzler KW. Cancer genes and the pathways they control. *Nat Med*. 2004;10:789–799.
- Weiss R, Teich N, Varmus H, et al. *RNA Tumor Viruses*. Cold Spring Harbor, NY: Cold Spring Harbor Laboratories; 1982.

Cancer Genetics

- Donis-Keller H, Dou S, Chi D, et al. Mutations in the RET proto-oncogene are associated with MEN 2A and FMTC. *Hum Mol Genet*. 1993;2:851–856.
- Evans DGR, Farndon PA, Burnell LD, et al. The incidence of Gorlin syndrome in 173 consecutive cases of medulloblastoma. *Br J Cancer*. 1991;64:959–961.
- Garber JE, Goldstein AM, Kantor AF. Follow-up study of twenty-four families with Li–Fraumeni syndrome. *Cancer Res*. 1991;51:6094–6097.
- Gorlin RJ, Goltz RW. Nevoid basal cell carcinoma syndrome. *Medicine*. 1987;66:98–113.
- Gruis NA, van der Velden PA, Sandkuijl LA, et al. Homozygotes for CDKN2 (p16) germline mutation in Dutch familial melanoma kindreds. *Nat Genet*. 1995;10:351–353.
- Kim WY, Kaelin WG. Role of VHL gene mutation in human cancer. *J Clin Oncol*. 2004;22:4991–5004.
- Knudson AG Jr. Mutation and cancer: statistical study of retinoblastoma. *Proc Natl Acad Sci USA*. 1971;68:820–823.
- Knudson AG Jr, Strong LC. Mutation and cancer: a model for Wilms' tumor of

- the kidney. *J Natl Cancer Inst.* 1972;48:313–324.
- Li FP. Familial cancer syndromes and clusters. *Curr Probl Cancer.* 1990;14:77–113.
- Li FP, Fraumeni JF Jr. Familial breast cancer, soft-tissue sarcomas, and other neoplasms. *Ann Intern Med.* 1975;83:833–834.
- Li FP, Fraumeni JF Jr. Prospective study of a family cancer syndrome. *JAMA.* 1982;247:2692–2694.
- Li FP, Garber JG, Friend SH, et al. Recommendations on predictive testing for germ line p53 mutations among cancer-prone individuals. *J Natl Cancer Inst.* 1992;84:1156–1160.
- Malkin D, Jolly KW, Barbier N, et al. Germline mutations of the p53 tumor-suppressor gene in children and young adults with second malignant neoplasms. *N Engl J Med.* 1992;326:1309–1315.
- McGlynn KA, Rosvold EA, Lustbader ED, et al. Susceptibility to hepatocellular carcinoma is associated with genetic variation in the enzymatic detoxification of aflatoxin B1. *Proc Natl Acad Sci USA.* 1995;92:2384–2387.
- Miller RW, Fraumeni JF Jr, Manning MD. Association of Wilms' tumor with aniridia, hemihypertrophy, and other congenital malformations. *N Engl J Med.* 1964;270:922–927.
- Parry DM, Eldridge R, Kaiser-Kupfer MI, et al. Neurofibromatosis 2 (NF2): clinical characteristics of 63 affected individuals and clinical evidence for heterogeneity. *Am J Med Genet.* 1994;52:450–461.
- Pelletier J, Bruening W, Li FP, et al. WTI mutations contribute to abnormal genital system development and hereditary Wilms' tumor. *Nature.* 1991;353:431–434.
- Seizinger BR, Rouleau GA, Ozelius LJ, et al. Genetic linkage of von Recklinghausen neurofibromatosis to the nerve growth factor receptor gene. *Cell.* 1987;49:589–594.
- Sparkes RS, Murphree AL, Lingua RW, et al. Gene for hereditary retinoblastoma assigned to human chromosome 13 by linkage to esterase D. *Science.* 1983;219:971–973.
- Strong LC, Williams WR, Trainsky MA. The Li-Fraumeni syndrome: from clinical epidemiology to molecular genetics. *Am J Epidemiol.* 1992;135:190–199.

van Heyningen V, Hastie ND. Wilms' tumor: reconciling genetics and biology. *Trends Genet.* 1992;8:16–21.

Multistep Nature of Cancer and Mismatch Repair

- Aaltonen L, Peltomäki P, Leach F, et al. Clues to the pathogenesis of familial colorectal cancer. *Science.* 1993;260:812–816.
- Armitage P, Doll R. The age distribution of cancer and a multistage theory of carcinogenesis. *Br J Cancer.* 1954;8:1–12.
- Bronner C, Baker S, Morrison P, et al. Mutation in the DNA mismatch repair gene homologue hMLH1 is associated with hereditary nonpolyposis colon cancer. *Nature.* 1994;368:258–261.
- Eshleman JR, Lang EZ, Bowerfind GK, et al. Increased mutation rate at the *hprt* locus accompanies microsatellite instability in colon cancer. *Oncogene.* 1995;10:33–37.
- Fearon ER, Vogelstein B. A genetic model for colorectal tumorigenesis. *Cell.* 1990;61:759–767.
- Fishel R, Lescoe MK, Rao M, et al. The human mutator gene homolog MSH2 and its association with hereditary nonpolyposis colon cancer. *Cell.* 1993;75:1027–1038.
- Hanahan D, Weinberg RA. The hallmarks of cancer. *Cell.* 2000;100:57–70.
- Ionov Y, Peinado M, Malkhosyan S, et al. Ubiquitous somatic mutations in simple repeated sequences reveal a new mechanism for colonic carcinogenesis. *Nature.* 1993;263:558–561.
- Le Q, Denko NC, Giaccia AJ. Hypoxic gene expression and metastasis. *Cancer Metastasis Rev.* 2004;23:293–310.
- Leach F, Nicolaides N, Papadopoulos N, et al. Mutations of a *mutS* homolog in hereditary nonpolyposis colorectal cancer. *Cell.* 1993;75:1215–1225.
- Lindblom A, Tannergård P, Werelius B, et al. Genetic mapping of a second locus predisposing to hereditary nonpolyposis colon cancer. *Nat Genet.* 1993;5:279–282.
- Luo J, Kahn S, O'Driscoll K, et al. The regulatory domain of protein kinase C beta 1 contains phosphatidylserine- and phorbol ester-dependent calcium binding activity. *J Biol Chem.* 1993;268:3715–3719.
- Lynch H, Smyrk T, Watson P, et al. Genetics, natural history, tumor spectrum,

- and pathology of hereditary nonpolyposis colorectal cancer: an updated review. *Gastroenterology*. 1993;104:1535–1549.
- Maity A, McKenna W, Muschel R. The molecular basis for cell cycle delays following ionizing radiation: a review. *Radiother Oncol*. 1994;31:1–13.
- Marx J. New link found between p53 and DNA repair. *Science*. 1994;266:1321–1322.
- McCann J, Dietrich F, Rafferty C, et al. A critical review of the genotoxic potential of electric and magnetic fields. *Mutat Res*. 1993;297:61–95.
- Nicolaides N, Papadopoulos N, Liu B, et al. Mutations of two PMS homologues in hereditary nonpolyposis colon cancer. *Nature*. 1994;371:75–80.
- Paget S. The distribution of secondary growths in cancer of the breast. *Lancet*. 1989;1:571–573.
- Papadopoulos N, Nicolaides NC, Wei Y-F, et al. Mutation of a mutL homologue in hereditary colon cancer. *Science*. 1994;263:1625–1629.
- Peltomäki P, Aaltonen L, Sistonen P, et al. Genetic mapping of a locus predisposing to human colorectal cancer. *Science*. 1993;260:810–812.
- Ridley AJ, Schwartz MA, Burridge K, et al. Cell migration: integrating signals from front to back. *Science*. 2003;302:1704–1709.
- ## Genes and Ionizing Radiation
- Amundson SA, Bittner M, Fornace AJ Jr. Functional genomics as a window on radiation stress signaling. *Oncogene*. 2003;22:5828–5833.
- Burns TF, El-Deiry WS. Microarray analysis of p53 target gene expression patterns in the spleen and thymus in response to ionizing radiation. *Cancer Biol Ther*. 2003;2:431–443.
- Chaudhry MA, Chodosh LA, McKenna WG, et al. Gene expression profile of human cells irradiated in G₁ and G₂ phases of cell cycle. *Cancer Lett*. 2003;195:221–233.
- Datta R, Hass R, Gunji H, et al. Down-regulation of cell cycle control genes by ionizing radiation. *Cell Growth Differ*. 1992;3:637–644.
- Nakanishi C, Toi M. Nuclear factor-kappaB inhibitors as sensitizers to anticancer drugs. *Nat Rev Cancer*. 2005;5:297–309.
- Swift M, Morrell D, Massey RB, et al. Incidence of cancer in 161 families

- affected by ataxia-telangiectasia. *N Engl J Med.* 1991;325:1831–1836.
- Woloschak G, Chang-Liu C. Differential modulation of specific gene expression following high-low-LET radiations. *Radiat Res.* 1990;124:183–187.
- Woloschak G, Chang-Liu C. Effects of low-dose radiation on gene expression in Syrian hamster embryo cells: comparison of JANUS neutrons and gamma rays. In: Sugahara T, Sagan L, Aoyama T, eds. *Low Dose Irradiation and Biological Defense Mechanisms*. Amsterdam, The Netherlands: Excerpta Medica, Elsevier Science; 1992:239–242.
- Woloschak G, Chang-Liu C, Jones P, et al. Modulation of gene expression in Syrian hamster embryo cells following ionizing radiation. *Cancer Res.* 1990;50:339–344.

chapter 19

Dose–Response Relationships for Model Normal Tissues

Dose–Response Relationships

Therapeutic Ratio (Therapeutic Index)

Types of Cell Death: How and Why Cells Die

Assays for Dose–Response Relationships

Clonogenic End Points

Clones Regrowing *In Situ*

Cells Transplanted to Another Site

Summary of Dose–Response Curves for Clonogenic Assays in Normal Tissues

Dose–Response Relationships for Functional End Points

Pig Skin

Rodent Skin

Early and Late Response of the Lung Based on Breathing Rate

Spinal Cord Myelopathy

Inferring the Ratio α/β from Multifraction Experiments in Nonclonogenic Systems

Summary of Pertinent Conclusions

Bibliography

DOSE–RESPONSE RELATIONSHIPS

Radiation biology applied to clinical radiotherapy is concerned with the relationship between a given absorbed dose of radiation and the consequent biologic response; of particular interest are factors that modify this relationship. With increasing radiation dose, radiation effects may increase in severity (i.e., grade), in frequency (i.e., incidence), or both. In most cases, it is the relationship between dose and incidence that is important. Such dose–response curves have a sigmoid (S) shape, with the incidence tending to zero as dose tends to zero and

the incidence tending to 100% at very large doses. This applies to both tumor control and normal tissue complications.

A simple example is shown in [Figure 19.1](#). Tumor control probability (TCP) is plotted as a function of total dose, and the incidence of normal tissue complications is also plotted as a function of dose. What is illustrated is a favorable situation where the tumor is more radiosensitive than the normal tissue. In the case of tumor control, the shape can be explained solely from the random nature of cell killing (or clonogen survival) after irradiation and the need to kill every single cell to achieve a cure.

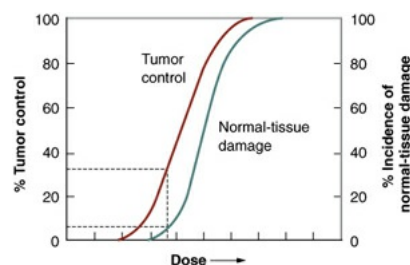


FIGURE 19.1 The dose–response relationship is sigmoid in shape for both tumor control and normal tissue damage. That for normal tissue damage may be steeper than for tumor control. The therapeutic ratio (or index) is the percentage of tumor control that can be achieved for a given level of normal tissue damage. In this hypothetical example, about 30% tumor control can be achieved for a 5% incidence of normal tissue damage.

For most normal tissue end points, the biologic interpretation of the S shape of the relationship is not obvious. Some researchers have evoked a hypothetical *tissue rescue unit* (TRU), arguing that tissue breakdown occurs when the number of TRUs falls below a critical level; however, this explanation is questionable.

Therapeutic Ratio (Therapeutic Index)

The ratio of the tumor response for a fixed level of normal tissue damage has been called either the *therapeutic ratio* or the *therapeutic index*. In the hypothetical example in [Figure 19.1](#), there is a favorable therapeutic ratio because a 30% probability of tumor control is possible for a 5% incidence of complications.

The time factor is the one parameter that has been most often manipulated to increase this ratio; hyperfractionation, for example, produces a greater sparing of late-responding normal tissue than tumor control. Another strategy often quoted, although seldom achieved in practice, is to add a drug or radiosensitizer that potentiates the tumor control without potentiating the radiation damage to

normal tissue. In practice, it does not need to be as clear-cut as this; it would suffice for the drug to increase tumor control to a greater extent than it increases normal tissue damage. This would result in a therapeutic gain. This is illustrated in [Figure 19.2](#). The addition of the drug moves the tumor control curve to the left farther than the normal tissue damage curve; that is, the drug has greater cytotoxic effect on the tumor than on the normal tissue. Consequently, with the combined modalities, an improved TCP is possible for the same probability of normal tissue injury.

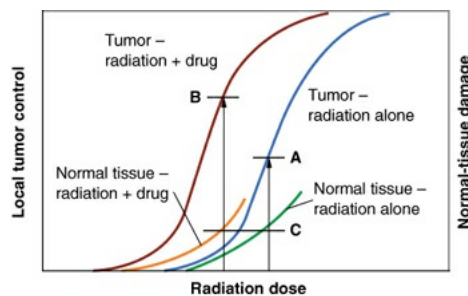


FIGURE 19.2 Illustrating how the addition of a drug, a chemotherapy agent, or a radiosensitizer may improve the therapeutic ratio (therapeutic index). With radiation alone, a given level (*A*) of tumor control is possible for a maximum tolerable level of normal tissue damage (*C*). The addition of the drug moves the dose-response curve for both tumor and normal tissue to the left. If the addition of the drug has a greater effect on tumor control than on normal tissue morbidity (i.e., it moves the curve further to the left), then a higher local tumor control (*B*) is possible for the same level of normal tissue injury (*C*).

TYPES OF CELL DEATH: HOW AND WHY CELLS DIE

Mammalian cells exposed to ionizing radiation can die through various mechanisms: mitotic-linked cell death, necrotic cell death, apoptotic cell death, autophagic cell death, and bystander induced cell death. The underlying mechanisms and importance of each of these forms of cell death have been described in [Chapters 3, 4, and 18](#) in detail. Regarding normal tissues that are exposed to ionizing radiation, mitotic-linked cell death and apoptotic cell death have been studied the most and are responsible for most cell killing by ionizing radiation. Other forms of cell death may also contribute to cell killing, but their mechanism and importance are still under investigation. One additional point to consider is that ionizing radiation also induces a form of senescence or permanent growth arrest in which cells are still metabolically active but reproductively inhibited. This is best exemplified by fibroblasts that, when irradiated in cell culture, stay attached to plates for weeks but never divide.

However, they are able to secrete growth factors and mitogens that promote the growth of tumor cells. Senescence has been largely studied in cell culture in the laboratory and only recently has evidence been accumulating that it occurs in tissues. Senescence is discussed in more detail in [Chapter 18](#).

Most cell lines cultured *in vitro* die a mitotic death after irradiation; that is, they die attempting to divide. This does not necessarily occur at the first postirradiation mitosis; the cell may struggle through one, two, or more mitoses before the damaged chromosomes cause it to die, attempting the complex task of cell division. Time-lapse films of irradiated cells cultured *in vitro* clearly show this process of mitotic death, which is the dominant cause of death if reproductive integrity is assessed *in vitro* as described in [Chapter 3](#).

The long-standing concept that ionizing radiation kills cells through direct exposure requires amendment. The demonstration that cells not exposed to ionizing radiation can be killed by being close to irradiated cells has coined the term “bystander induced cell death.” Therefore, the possibility exists that ionizing radiation can influence cell killing outside the field of radiation. This has been experimentally shown for tumors and is known as the abscopal effect. Such effects for normal tissues probably also exist in lymphopenia found after radiotherapy to nonlymphoid organs, and most probably represent an immune response.

ASSAYS FOR DOSE-RESPONSE RELATIONSHIPS

Most experimental techniques are available to obtain dose-response relationships for the cells of normal tissues. First, there are a limited number of clonogenic assays—techniques in which the end point observed depends directly on the reproductive integrity of individual cells. These systems are directly analogous to cell survival *in vitro*. The techniques developed by Withers and his colleagues are based on their observation of a clone of cells regenerating *in situ* in irradiated tissue. Skin colonies, regenerating crypts in the jejunum, testes stem cells, and kidney tubules are described briefly later in this chapter. It is also possible to obtain dose-response curves for the cells of the epithelial lining of the colon or stomach, but the method used is essentially the same as for the jejunum. Kember described a system for scoring regenerating clones in cartilage at about the same time as Withers’s skin colony system, but it has not been used widely and is not discussed here.

The assay system for the stem cells in the bone marrow or cells of the thyroid and mammary gland depends on the observation of the growth of clones of cells

taken from a donor animal and transplanted into a different tissue in a recipient animal. In Till and McCulloch's bone marrow assay, colonies of bone marrow cells are counted in the spleens of recipient animals. Dose-response curves for mammary and thyroid cells have been obtained by Gould and Clifton by observing colonies growing from cells transplanted into the fat pads of recipient animals.

Second, dose-response relationships that are repeatable and quantitative, but that depend on functional end points, can be obtained. These include skin reactions in rodents or pigs (e.g., erythema and desquamation), pneumonitis or fibrosis in mouse lungs reflected in an increased breathing rate, myelopathy of the hind limbs from damage to the spinal cord, and deformities to the feet of mice. The end points observed tend to reflect the minimum number of functional cells remaining in a tissue or organ rather than the fraction of cells retaining their reproductive integrity.

Finally, one can *infer* a dose-response curve, for a tissue, which cannot be observed directly by assuming the form of the dose-response curve (linear quadratic) and performing a series of multifraction experiments. This procedure, first suggested by Douglas and Fowler, has been used widely to infer values for α and β in the dose-response relationships for normal tissues in which the parameters cannot be measured directly.

This chapter includes assays for both early- and late-responding tissues. The skin, intestinal epithelium, and bone marrow cells, for example, are rapidly dividing self-renewal tissues and respond early to the effects of radiation. The spinal cord, lung, and kidney, by contrast, are late-responding tissues. This reflects the current philosophy that the radiation response of *all* tissues results from the depletion of the critical parenchymal cells and that the difference in time at which early- and late-responding tissues express radiation damage is a function simply of different cell turnover rates. Many older papers in the literature ascribe the response of late-responding tissues to vascular damage rather than to depletion of parenchymal cells, but this thesis is becoming increasingly difficult to accept.

The various types of normal tissue assay systems are described briefly.

CLONOGENIC END POINTS

Clones Regrowing *In Situ*

Skin Colonies

Withers developed an ingenious technique, shown in [Figure 19.3](#), to determine the survival curve for mouse skin cells. The hair was plucked from an area on the back of the mouse, and a superficial x-ray machine was used to irradiate an annulus of skin to a massive dose of 30 Gy. This produced a “moat” of dead cells, in the center of which was an isolated island of intact skin that had been protected during the first exposure to low voltage x-rays by a small metal sphere. This small area of intact skin was then given a test dose (D) and subsequently observed for regrowth of skin. If one or more stem cells survived in this small area, nodules of regrowing skin could be seen some days later. If no cells survived in this small area, the skin would heal much later by infiltration of cells crossing the moat. [Figure 19.4](#) shows nodules regrowing in mouse skin. To obtain a survival curve, it was necessary to repeat this operation with several different areas of skin. A range of ball bearings was used to shield a small area of skin in the middle of the “moat.” The resulting survival data are shown in [Figure 19.5](#) in which the dose (D) to the control area is plotted against the number of surviving cells per square centimeter of skin.

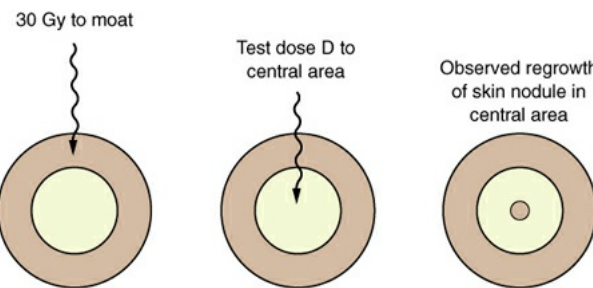


FIGURE 19.3 Technique used to isolate an area of skin for experimental irradiation. A superficial (30 kV) x-ray machine is used to irradiate an annulus of skin to a massive dose of about 30 Gy. An isolated island of intact skin in the center of this “moat” is protected from the radiation by a metal sphere. The intact skin is then given a test dose (D) and observed for nodules of regrowing skin. (Adapted from Withers HR. The dose–survival relationship for irradiation of epithelial cells of mouse skin. *Br J Radiol.* 1967;40:187–194, with permission.)

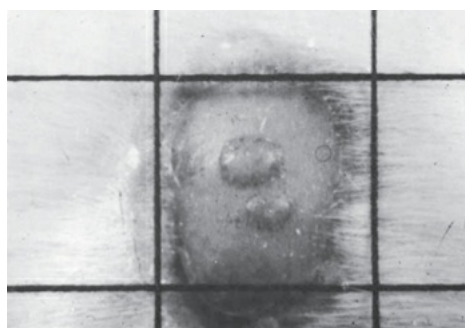


FIGURE 19.4 Photograph of nodules of mouse skin regrowing from a single

surviving cell in the treated area. (Courtesy of Dr. H. R. Withers.)

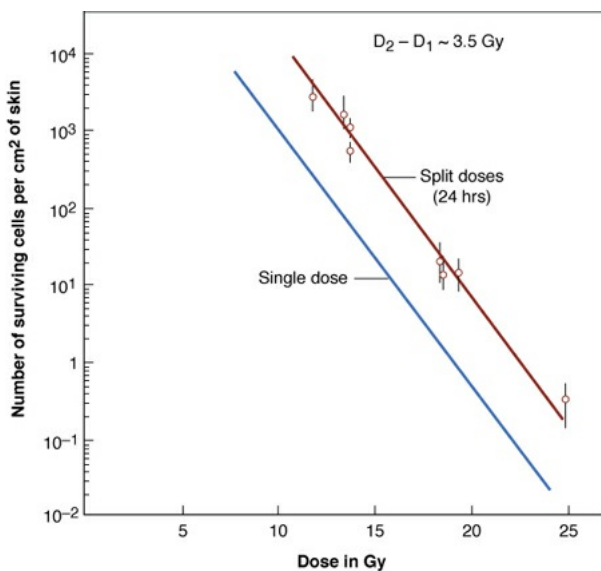


FIGURE 19.5 Single- and two-dose survival curves for epithelial cells of mouse skin exposed to 29 kVp x-rays. The 37% dose slope (D_0) is 1.35 Gy. The ordinate is not the surviving fraction, as in the survival curves for cells cultured *in vitro*, but is the number of surviving cells per square centimeter of skin. In the two-dose survival curve, the interval between dose fractions was always 24 hours. The curves are parallel, their horizontal separation being equal to about 3.5 Gy; this corresponds to D_q . From a knowledge of D_q and the slope of the survival curve, D_0 , the extrapolation number, n , may be calculated. (Adapted from Withers HR. Recovery and repopulation *in vivo* by mouse skin epithelial cells during fractionated irradiation. *Radiat Res.* 1967;32:227–239; and Withers HR. The dose–survival relationship for irradiation of epithelial cells of mouse skin. *Br J Radiol.* 1967;40:187–194, with permission.)

There are practical limits to the range in which the dose–response relationship can be determined. At one extreme, it is not possible to irradiate too large an area on the back of the mouse to produce the moat of sterilized skin. At the other extreme, the smallest area that can be used is determined by the fact that even 30 kV radiation scatters laterally to some extent. As can be seen in Figure 19.5, the technique results in a single-dose survival curve that extends from about 8 to 25 Gy. Over this range, with dose plotted on a linear scale and number of surviving cells per square centimeter plotted on a logarithmic scale, the survival curve is straight and has a D_0 of 1.35 Gy. This D_0 value is very similar to that obtained with mammalian cells cultured *in vitro*.

The extrapolation number cannot be obtained directly with this technique; the ordinate is the number of surviving cells per square centimeter of skin, and

this cannot be converted to the surviving fraction because it is not known with any accuracy how many skin stem cells there are per unit area. It is, however, possible to make an indirect estimate of the extrapolation number by obtaining the survival curve for doses given in two fractions separated by 24 hours. The survival curve obtained in this way is also shown in [Figure 19.5](#). It is parallel to that obtained for single doses but is displaced from it toward higher doses. As explained in [Chapter 3](#), this lateral displacement in a direction parallel to the dose axis is a measure of D_q , the *quasithreshold dose*. The D_q for mouse skin is about 3.5 Gy, which is very similar to the value for human skin estimated from split-dose experiments.

Crypt Cells of the Mouse Jejunum

A technique perfected by Withers and Elkind makes it possible to obtain the survival characteristics of the crypt cells of the mouse jejunum. The lining of the jejunum is a classic example of a self-renewal system. The cells in the crypts divide rapidly and provide a continuous supply of cells that move up the villi, differentiate, and become the functioning cells. The cells at the top of the folds of the villi are slowly but continuously sloughed off in the normal course of events and are replaced continuously by cells that originate from mitoses in the crypts.

[Figure 19.6](#) is a cartoon depicting the different cellular compartments of the crypts and villi of the jejunum. One model proposed by Potten defines the +4 position as critical for defining the stem cell population. In this model, stem cells defined as LGR5+ or BMI1+ differentiate from the +4 position of the crypt upward to the villi into enterocytes, goblet cells, and endocrine cells. Paneth cells differentiate downward from the +4 position. It takes approximately 4 days of transit time for the stem cells to regenerate the epithelial lining of the small intestine and 5 days for the large intestine. Although other models for epithelial regeneration in the intestines also exist, the key point is the existence of epithelial stem cells in the crypts that can regenerate the gastrointestinal tract, especially after exposure to radiotherapy.

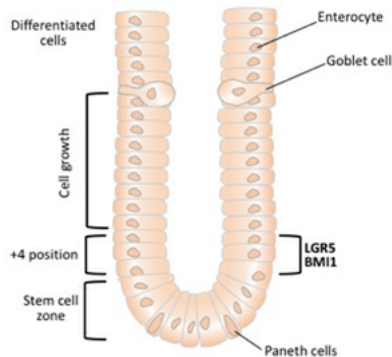


FIGURE 19.6 The jejunum is organized in different cellular compartments in the crypts and in the villi. The crypts contain the stem cell zone at position +4. These cells are thought to be critical for epithelial regeneration of the villi and differentiate upward from position +4. In the villi, these cells can differentiate further into enterocytes, the epithelial lining of the villi, goblet cells which secrete factors such as mucins to coat the epithelial lining. In addition, specialized endocrine cells called enteroendocrine cells serve as sensors to respond to foreign pathogens or secrete hormones useful in the process of digestion. In contrast to the upward differentiation of these three cell types, Paneth cells differentiate downward from the +4 position and possess granules, which contain antimicrobial factors to stimulate an immune response. Exposure of cells in the jejunum or the small intestine to ionizing radiation will initially result in loss of villi. Regeneration of the villi occurs through stem cell transit from position +4 and differentiation of stem cells.

To obtain a survival curve for the jejunal crypt cells, groups of animals are exposed to graded total body doses of radiation. After 3.5 days, each animal is sacrificed and sections are made of the jejunum (Fig. 19.7A). At this time, crypts are just beginning to regenerate, and it is relatively simple to identify them. Figure 19.7B shows several regenerating crypts at a higher magnification. These pictures also show the shortened villi and the greatly reduced density of cells lining the surface. The score of radiation damage is the *number of regenerating crypts per circumference* of the sectioned jejunum. This quantity is plotted as a function of dose and yields a survival curve as shown in Figure 19.8. The single-dose survival curve has a D_0 (for γ -rays) of about 1.3 Gy. Also shown in Figure 19.8 are survival curves for radiation delivered in multiple fractions, from 2 to 20. The separation between the single- and two-dose survival curves gives a measure of D_q , which has the very large value of between 4 and 4.5 Gy.

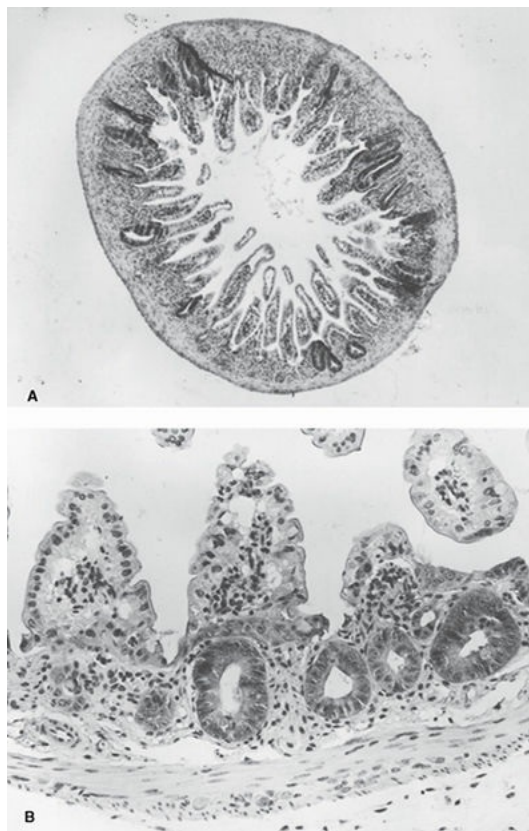


FIGURE 19.7 **A:** Section of mouse jejunum taken 3 days after a total body dose in excess of 10 Gy. Note the shortened villi and the regenerating crypts. **B:** Regenerating crypts shown at a higher magnification. (From Withers HR. Regeneration of intestinal mucosa after irradiation. *Cancer*. 1971;28:75–81, with permission.)

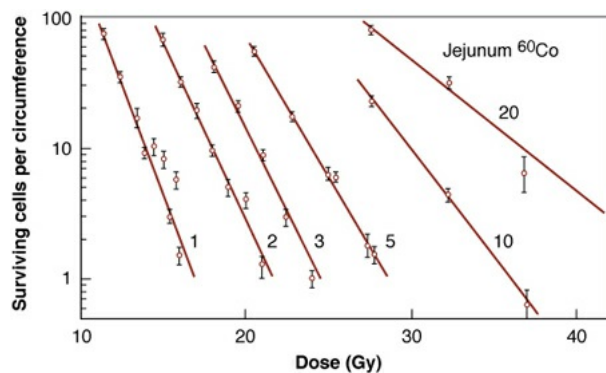


FIGURE 19.8 Survival curves for crypt cells in the mouse jejunum exposed to single or multiple doses of γ -rays (1 to 20 fractions). The score of radiation damage is the number of surviving cells per circumference (i.e., the number of regenerating crypts per circumference of the sectioned jejunum) counted from sections such as those shown in Figure 19.7. This quantity is plotted on a logarithmic scale against radiation dose on a linear scale. The D_0 for the single-dose survival curve is about 1.3 Gy. The shoulder of the survival curve is very

large. The separation between the single-dose survival and two-dose survival curves indicates that the D_q is 4 to 4.5 Gy. (Adapted from Withers HR, Mason K, Reid BO, et al. Response of mouse intestine to neutrons and gamma rays in relation to dose fractionation and division cycle. *Cancer*. 1974;34:39–47, with permission.)

This technique has two limitations. First, the quantity plotted on the ordinate is the number of surviving crypts per circumference, not the surviving fraction. Second, experiments can be done only at doses of about 10 Gy or more, at which there is a sufficient level of biologic damage for individual regenerating crypts to be identified. The doses can be delivered, however, in several smaller fractions, as long as the total results in sufficient biologic damage to be scored. The shape of the entire survival curve, then, can be reconstructed from the multifraction data if it is assumed that in a fractionated regimen each dose produces the same amount of cell killing and if an estimate is made of the number of clonogens at risk per crypt. This has been done by Withers and his colleagues; the resultant survival curve is shown in [Figure 19.9](#).

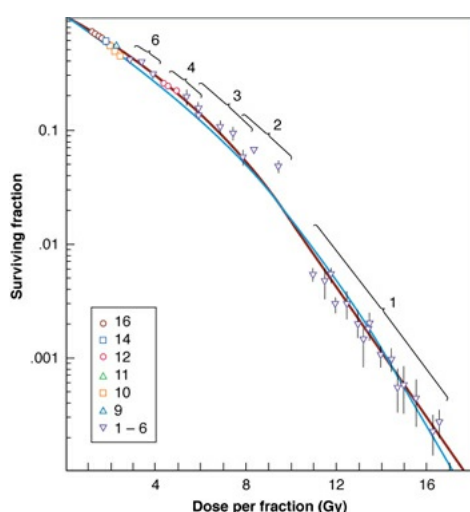


FIGURE 19.9 Effective single-dose survival curve reconstructed from multifraction experiments for clonogenic cells of the jejunal crypts of mice. The numbers on the curve refer to the number of fractions used to reconstruct that part of the curve. The initial and final slopes are about 3.57 and 1.43 Gy, respectively. The quasithreshold dose is 4.3 Gy. The data are equally well fitted by the LQ formulation. (Adapted from Thames HD, Withers HR, Mason K, et al. Dose-survival characteristics of mouse jejunal crypt cells. *Int J Radiat Oncol Biol Phys*. 1981;7:1591–1597, with permission.)

Testes Stem Cells

A technique to measure the radiation response of testicular cells capable of

sustaining spermatogenesis (i.e., the stem cells) was devised by Withers and his colleagues. About 6 weeks after irradiation, mouse testes are sectioned and examined histologically. Sections of normal and irradiated testes are shown in [Figure 19.10](#). The proportion of tubules containing spermatogenic epithelium is counted and plotted as a function of dose in [Figure 19.11](#). As in many *in vivo* assays, relatively high single doses of 8 to 16 Gy are necessary so that the level of damage is sufficient to be scored. In this dose range, D_0 is about 1.68 Gy. If the split-dose technique is used, the D_q is about 2.7 Gy. It is possible to estimate the effect of small doses and reconstruct a complete survival curve by giving large doses in multiple small fractions and assuming that the response to each fraction is the same. The result of this reconstruction is shown in [Figure 19.12](#).

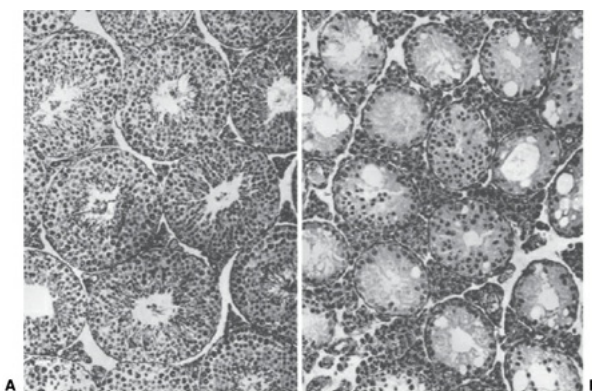


FIGURE 19.10 **A:** Histology of normal testis. **B:** Histology of testis 35 days after a dose of 9 Gy of γ -radiation. Some tubules are completely devoid of spermatogenic epithelium and some are not. (Sertoli's cells persist in the tubules sterilized of spermatogenic cells.) Foci of spermatogenesis can be derived from single surviving stem cells (magnification $\times 200$). (From Withers HR, Hunter N, Barkley HT Jr, et al. Radiation survival and regeneration characteristics of spermatogenic stem cells of mouse testis. *Radiat Res.* 1974;57:88–103, with permission.)

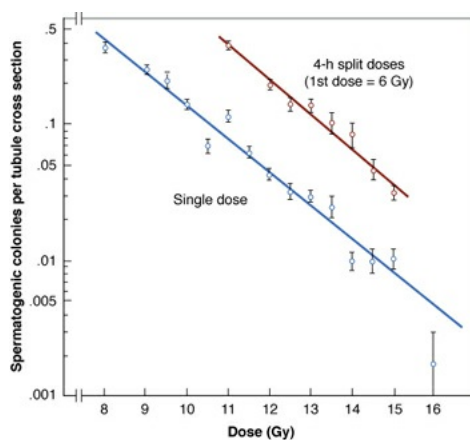


FIGURE 19.11 Single- and split-dose survival curves for spermatogenic stem

cells of the mouse testis. The D_0 is about 1.68 Gy. The D_q , assessed from the horizontal separation of the single- and split-dose curves, is about 2.7 Gy. (Adapted from Withers HR, Hunter N, Barkley HT Jr, et al. Radiation survival and regeneration characteristics of spermatogenic stem cells of mouse testis. *Radiat Res.* 1974;57:88–103, with permission.)

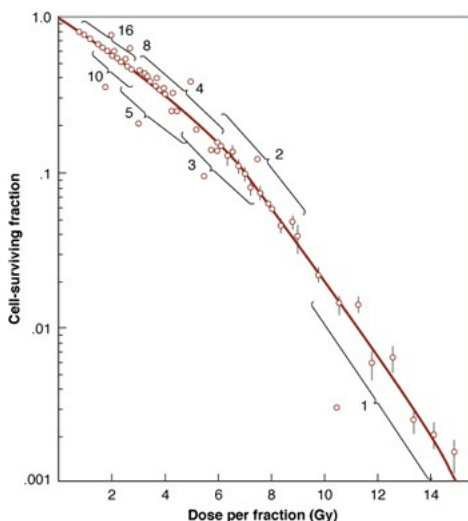


FIGURE 19.12 Survival curve for testis stem cells reconstructed from multifraction experiments, assuming that each fraction produces the same biologic effect. The *numbers on the curve* refer to the number of fractions used to reconstruct that portion of the curve. The D_0 is about 1.6 Gy, and the D_q is about 3.92 Gy. (Adapted from Thames HD, Withers HR. Test of equal effect per fraction and estimation of initial clonogen number in microcolony assays of survival after fractionated irradiation. *Br J Radiol.* 1980;53:1071–1077, with permission.)

Kidney Tubules

A technique using kidney tubules, again developed by Withers and his colleagues, is the first clonal assay for a late-responding tissue. One kidney per mouse is irradiated with a small field and removed for histologic examination, 60 weeks later. [Figure 19.13](#) shows sections of normal and irradiated kidneys. For ease of scoring, only those tubules touching the renal capsule are scored, and a tubule is considered fully regenerated only if it is lined with well-differentiated cuboidal or columnar cells with a large amount of eosinophilic cytoplasm. By 60 weeks, tubules either have no surviving epithelial cells or are lined completely with epithelium that has regenerated from a small number of surviving cells, usually one. The number of tubules regenerating in several arbitrary sections counted is plotted as a function of radiation dose. The result is shown in [Figure 19.14](#); D_0 is about 1.53 Gy.

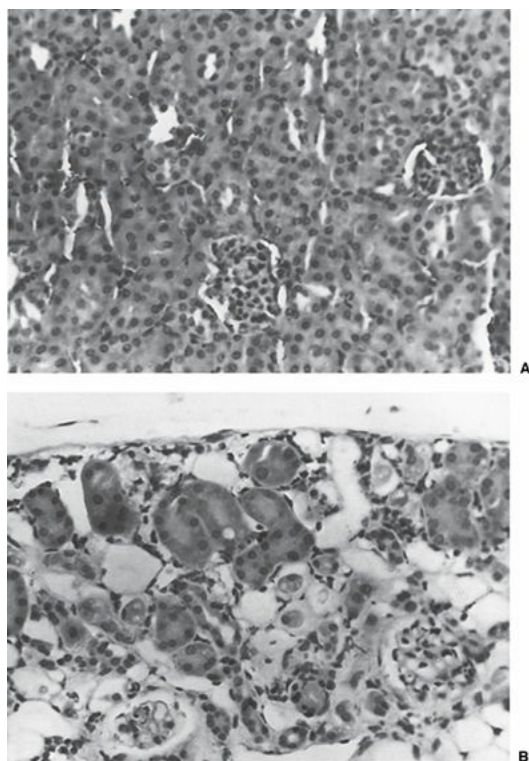


FIGURE 19.13 Photomicrographs of mouse kidney. **A:** Normal, showing proximal tubules in contact with the capsule (hematoxylin–eosin stain, magnification $\times 400$). **B:** Sixty weeks after irradiation with 13 Gy. Note normal proximal tubules and glomeruli amid ghosts of deepithelialized tubules. One epithelialized tubule is in contact with the capsule (hematoxylin–eosin stain, magnification $\times 200$). (From Withers HR, Mason K, Thames HD. Late radiation response of kidney assayed by tubule cell survival. *Br J Radiol.* 1986;59:587–595, with permission.)

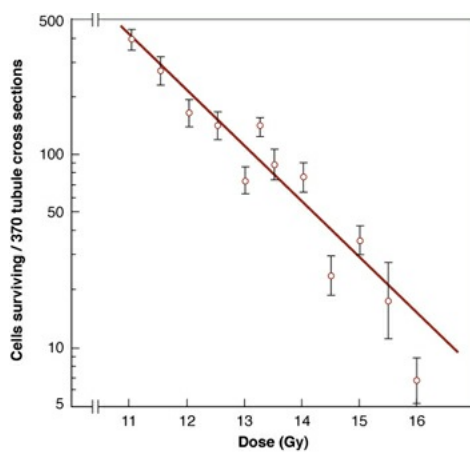


FIGURE 19.14 Dose-survival curve for tubule-regenerating cells. The D_0 is 1.53 Gy. (Adapted from Withers HR, Mason K, Thames HD Jr. Late radiation response of kidney assayed by tubule cell survival. *Br J Radiol.* 1986;59:587–595.)

The radiosensitivity of the cells of this late-responding tissue is not very different from that of early-responding tissues such as the skin or intestinal epithelium. The *rate* of response, however, is quite different. The time required for depletion of the epithelium after a single dose of 14 Gy is about 3 days in the jejunum, 12 to 24 days in the skin, and 30 days in the seminiferous tubules of the testes, but 300 days in the kidney tubules. These results argue strongly that radiation injury in the kidney results from depletion of parenchymal cells and that the slow expression of injury merely reflects the slow turnover of this cell population. Vascular injury is unlikely to be the mechanism underlying the destruction of renal tubules.

Cells Transplanted to Another Site

Bone Marrow Stem Cells

Till and McCulloch developed a system to determine a survival curve for colony-forming bone marrow cells (Fig. 19.15). Recipient animals first are irradiated supralethally with a dose of 9 to 10 Gy, which sterilizes their spleens. Nucleated isologous bone marrow cells taken from another animal are then injected intravenously into the recipient animals. Some of these cells lodge in the spleen, where they form nodules or colonies 10 to 11 days later because the spleen cells of the recipient animals have been sterilized previously by the large dose of radiation. At this time, the spleens are removed and the colonies counted. Figure 19.16 is a photograph of a spleen showing the colonies to be counted.

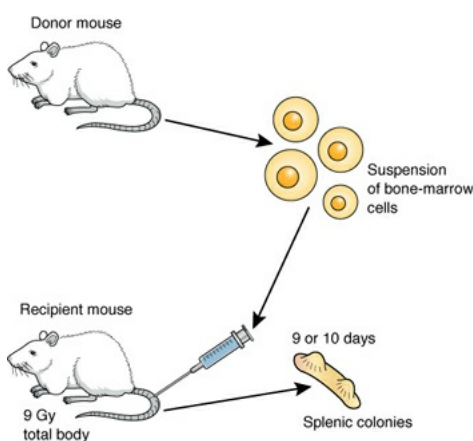


FIGURE 19.15 Till and McCulloch's technique. From the donor mouse, a cell suspension is made of nucleated isologous bone marrow. A known number of cells are injected into recipient mice previously irradiated with a 9-Gy total body dose. The spleen is removed from each recipient mouse 9 or 10 days later, and the number of nodules is counted. (Adapted from Till JE, McCulloch EA. In: Cameron IL, Padilla GM, Zimmerman AM, eds. *Developmental Aspects of the*

Cell Cycle. New York, NY: Academic Press; 1971:297–313, with permission.)



FIGURE 19.16 Photograph of a mouse's spleen. The mouse was irradiated supralethally to sterilize all the cells of the spleen. The nodules of regrowth originate from intravenously injected bone marrow cells from another animal. (Courtesy of Dr. A. Carsten, Brookhaven National Laboratory.)

About 10^4 cells must be injected into a recipient animal to produce one spleen colony because most of the cells in the nucleated isologous bone marrow are fully differentiated cells and would never be capable of forming a colony. To obtain a surviving fraction bone marrow cells, a donor animal is irradiated to some test dose, and the suspension of cells from the bone marrow is inoculated into groups of recipient animals that previously had been irradiated supralethally. By counting the colonies in the spleens of the recipient animals, and with a knowledge of the number of cells required to produce a colony in an unirradiated animal (plating efficiency), the surviving fraction may be calculated as follows:

Surviving fraction for a dose D =

$$\frac{\text{colonies counted}}{\text{cells inoculated} \times \text{plating efficiency}}$$

This procedure is repeated for a range of doses, and a survival curve is obtained (Fig. 19.17). These bone marrow stem cells are very sensitive with a D_0 of about 0.95 Gy and little or no shoulder to the survival curve.

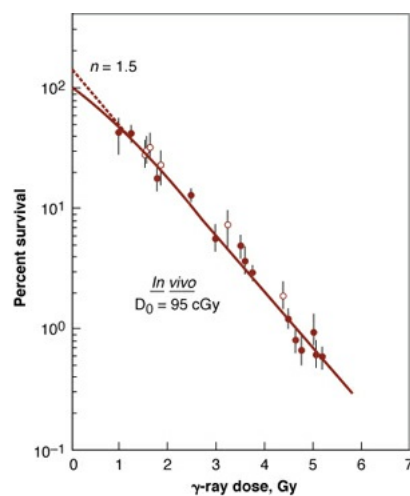


FIGURE 19.17 γ -Ray survival curve for the colony-forming ability of mouse bone marrow cells. The cells are irradiated *in vivo* in the donor animal and grow

into colonies in the spleens of supralethally irradiated recipient animals. (Adapted from McCulloch EA, Till JE. The sensitivity of cells from normal mouse bone marrow to gamma radiation in vitro and in vivo. *Radiat Res.* 1962;16:822–832, with permission.)

Mammary and Thyroid Cells

Clifton and Gould and their colleagues developed very useful clonogen transplant assays for epithelial cells of the mammary and thyroid glands. They have been used largely for cell survival studies, which are described later, but the initial motivation for their development was to study carcinogenesis in a quantitative system. Most *in vitro* transformation assays involve fibroblasts, and the bulk of human cancers arise in epithelial cells—hence, the importance and interest in these two systems.

The techniques for these two systems are much the same. To generate a survival curve for mammary or thyroid gland cells in the rat, cells may be irradiated *in vivo* before the gland is removed from donor animals and treated with enzymes to obtain a monodispersed cell suspension. Known numbers of cells are injected into the inguinal or interscapular white fat pads of recipient animals.

Under appropriate host conditions and grafted cell numbers, the injection of mammary cells gives rise to mammary structures that are morphologically and functionally normal. One such mammary structure may develop from a single cell. By 3.5 weeks after the injection of mammary cells, positive growth is indicated by alveolar units. An example of a milk-filled alveolar unit is shown as an inset in [Figure 19.18](#). If thyroid cells are injected, thyroid follicular units develop ([Fig. 19.19](#)).

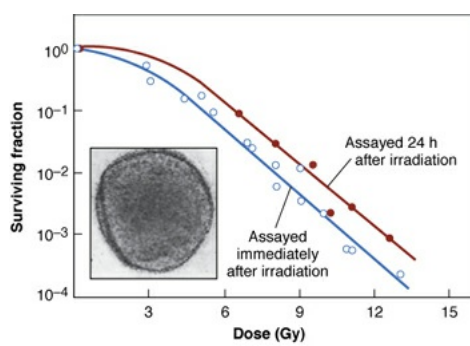


FIGURE 19.18 Dose–response relationship for rat mammary cells assayed by transplantation into the fat pads of recipient animals. (Adapted from Gould MN, Clifton KH. Evidence for a unique *in situ* component of the repair of radiation damage. *Radiat Res.* 1979;77:149–155, with permission.) **Inset:** A milk-filled

spherical alveolar unit developed from a transplanted cell. (From Gould MN, Biel WF, Clifton KH. Morphological and quantitative studies of gland formation from inocula of monodispersed rat mammary cells. *Exp Cell Res.* 1977;107:405–416, with permission.)

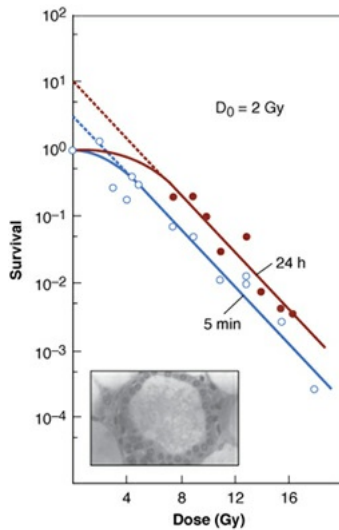


FIGURE 19.19 Dose–response relationship for rat thyroid cells assayed by transplantation into the fat pads of recipient animals. (Adapted from Mulcahy RT, Gould MN, Clifton KH. The survival of thyroid cells: *in vivo* irradiation and *in situ* repair. *Radiat Res.* 1980;84:523–528, with permission.) **Inset:** A single thyroid follicle that developed 4 weeks after the inoculation of thyroid cells into the fat pads of recipient animals. (From Clifton KH, Gould MN, Potten CS, et al, eds. *Cell Clones*. New York, NY: Churchill Livingstone; 1985:128–138, with permission.)

With either type of cell, a larger number must be injected to produce a growing unit, if the cells are irradiated first to a given dose. In practice, some fancy statistics are involved, a discussion of which is beyond the scope of this chapter; in essence, the ratio of the number of irradiated to unirradiated cells required to produce one growing unit (thyroid follicular unit or alveolar unit) is a measure of the cell-surviving fraction corresponding to the dose. This procedure must be repeated for a range of graded doses to generate a survival curve. The resultant survival curve for mammary cells is shown in Figure 19.18. The characteristics of the curve are unremarkable: D_0 is about 1.27 Gy, and the extrapolation number is about 5, quite typical of rodent cells cultured *in vitro*. The corresponding survival curve for thyroid cells is shown in Figure 19.19. D_0 is a little larger than for mammary glands assayed in a similar way, implying that the cells are a little more resistant. Figures 19.18 and 19.19 also show data for cells left *in situ* for 24 hours after irradiation, before being removed and assayed.

If this is done, the shoulder of the survival curve is larger because of the repair of potentially lethal damage. This is discussed in more detail in [Chapter 5](#).

An interesting use of these clonogen transplant assays is that the physiologic states of either donor or recipient animals can be manipulated hormonally. For the mammary cell assay, cells may be taken from inactive, slowly dividing glands of virgin rats, from rapidly dividing glands of rats in midpregnancy, or from milk-producing glands of lactating rats. For the thyroid cell assay, the physiologic states of both donor and recipient can be manipulated by control of the diet or by partial thyroidectomy.

SUMMARY OF DOSE-RESPONSE CURVES FOR CLONOGENIC ASSAYS IN NORMAL TISSUES

The survival curves for all of the clonogenic assays in normal tissues are plotted together in [Figure 19.20](#). There is a substantial range of radiosensitivities, with shoulder width being the principal variable. *In vitro* curves for cells from patients with ataxia-telangiectasia (AT) also are shown because these are probably the most radiosensitive mammalian cells.

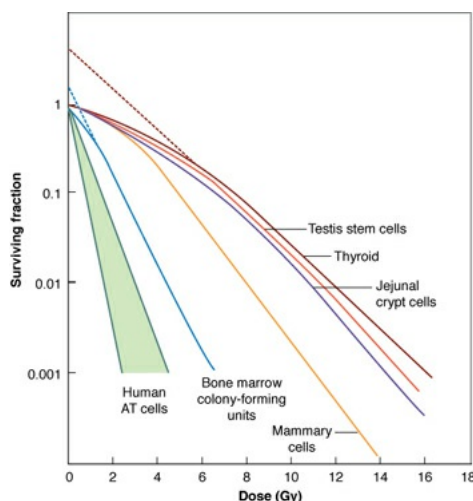


FIGURE 19.20 Summary of survival curves for clonogenic assays of cells from normal tissues. The human ataxia-telangiectasia (AT) cells are included because they are the most sensitive mammalian cells. The bone marrow colony-forming units, together with the mammary and thyroid cells, represent systems in which cells are irradiated and assayed by transplantation into a different tissue in recipient animals. The jejunal crypt and testis stem cells are examples of systems in which cells are assayed for regrowth *in situ* after irradiation.

DOSE-RESPONSE RELATIONSHIPS FOR

FUNCTIONAL END POINTS

Pig Skin

Pig skin has been used widely in radiobiologic studies because it has many features in common with human skin such as color, hair follicles, sweat glands, and a layer of subcutaneous fat. In view of these structural similarities, it is not surprising that the response of pig skin to radiation closely resembles that of human skin, both qualitatively and quantitatively.

Fowler and his colleagues pioneered the use of pig skin as a radiobiologic test system. Several small rectangular fields on the pig's flank were irradiated with graded doses of x-rays, and the reactions were scored daily using the arbitrary scale shown in [Table 19.1](#). After a single dose of radiation, the reaction becomes apparent after about 15 days and develops as shown in [Figure 19.21](#).

Table 19.1 Radiation Reactions in Pig Skin

ARBITRARY SCORE	REACTION
0	No visible reaction
1	Faint erythema
2	Erythema
3	Marked erythema
4	Moist desquamation of less than half the irradiated area
5	Moist desquamation of more than half the irradiated area

From Fowler JF, Morgan RL, Silvester JA, et al. Experiments with fractionated x-ray treatment of the skin of pigs. *Br J Radiol.* 1963;36:188–196, with permission.

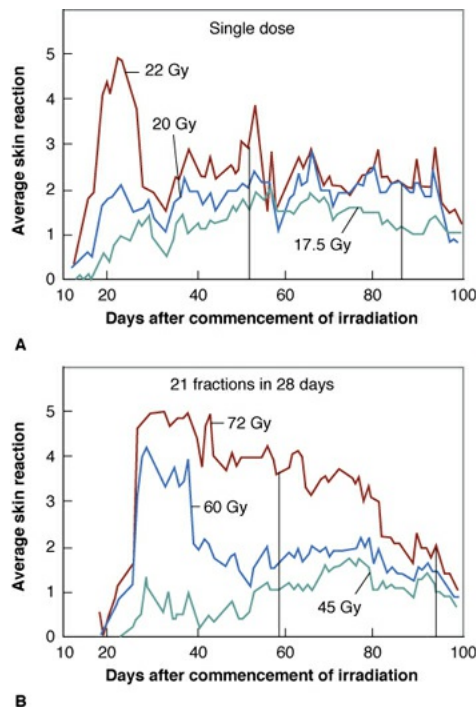


FIGURE 19.21 Development of skin reactions in the pig after graded doses of x-rays, delivered as a single exposure (A) or as multiple fractions spaced over time (B). (Adapted from Fowler JF, Morgan RL, Silvester JA, et al. Experiments with fractionated x-ray treatment of the skin of pigs. *Br J Radiol.* 1963;36:188–196, with permission.)

Two phases of the reaction can be distinguished. First, an early wave of erythema occurred (at 10 to 40 days), which was variable from one animal to another. This represents the uncomfortable “acute” reaction sometimes seen in patients on radiotherapy at about the end of a course of treatment. Second, a more gradual increase to a second broad wave of moderately severe reactions took place (at 50 to 100 days), representing a more permanent kind of damage. This second wave shows the tolerance of skin to a more serious type of long-term damage and is a more repeatable and consistent index of radiation damage. It was subsequently found to correlate well with longer term damage (up to 2 years) and with subcutaneous damage.

The “score” of radiation damage is taken to be the average skin reaction occurring between certain time limits that encompass the medium-term reactions. After a single dose, this might be a 35-day period between 50 and 85 days after irradiation. For a protracted fractionated regimen, this period of reaction may come later, between days 65 and 100. The average skin reaction in

the chosen time period then is plotted as a function of dose; examples of dose-response curves obtained this way are shown in [Figure 19.22](#) for single and fractionated doses.

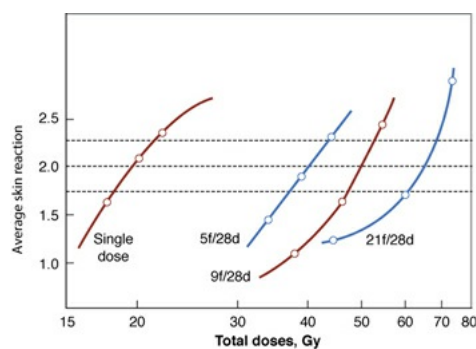


FIGURE 19.22 Average skin reaction as a function of total dose for medium-term skin reactions in pigs exposed to a single dose of x-rays or to fractionated doses given over 28 days. (Adapted from Fowler JF, Morgan RL, Silvester JA, et al. Experiments with fractionated x-ray treatment of the skin of pigs. *Br J Radiol.* 1963;36:188–196, with permission.)

Late effects also have been studied in pig skin by measuring the contraction that results from fibrosis a year or more after irradiation. A square is tattooed on the skin of the animal in the irradiated field, and the dimensions of this square are recorded as a function of dose as the contraction occurs. This is a primitive but effective measure of late effects.

Many of the important early studies on the fractionation effects of x-rays and the comparison of x-rays with fast neutrons were performed with this biologic system. One overwhelming advantage is that data obtained this way can be extrapolated to the human with a high degree of confidence. The disadvantage is that the animals are large and awkward to work with, and their maintenance involves a considerable expense.

Rodent Skin

Because of the inconvenience and expense of using pigs, the skin of the mouse leg and foot is commonly used instead. One hind leg of each animal is irradiated; the other serves as a control. The skin response is observed each day after irradiation and is scored according to the arbitrary scale shown in [Table 19.2](#). Various doses are used. The progressive development of the reaction after 10 doses of 6 Gy each is illustrated in [Figure 19.23](#); each point represents the mean of several animals. Reactions appear by about the 10th day, peak by 20 to 25 days, and then subside. The second wave of the reaction, noted for pig skin, is not seen in mice but is observed in rats. A dose-response curve is obtained by

averaging the skin reaction over a period of time and plotting this average as a function of dose.

Table 19.2 Radiation Reactions in Mouse Leg Skin

ARBITRARY SCORE ^a	OBSERVATIONS
0.5	50/50; doubtful if any difference from normal or not
1-	Because 1 covers a wide range of reddening, even before reaching the severity or additional factors requiring 1+, it is necessary to have 1- for “definite reddening (i.e., definitely not normal), but only a very slight degree”
1	Definite abnormality; definite reddening, top or bottom of leg; “clean” appearance means not greater than 1
1+	Severe reddening or reddening with definite white marks in creases under foot; query breakdown; query puffiness
1.5	Some breakdown of skin (usually seen on bottom of foot first); scaly or crusty appearance; definite puffiness, plus (query) breakdown; very marked white marks in creases plus puffiness or severe redness
1.5+	Query possibly moist desquamation in small areas
2	Breakdown of large areas of skin or toes stuck together; possibly moist in places but not all moist

2.5	Breakdown of large areas of skin with definite moist exudates
3	Breakdown of most of the skin with moist exudates
3.5	Complete necrosis of limb (rarely seen so far)

^a+ and – are equivalent to 0.25.

From Fowler JF, Kragt K, Ellis RE, et al. The effect of divided doses of 15 MeV electrons on the skin response of mice. *Int J Radiat Biol.* 1965;9:241–252, with permission.

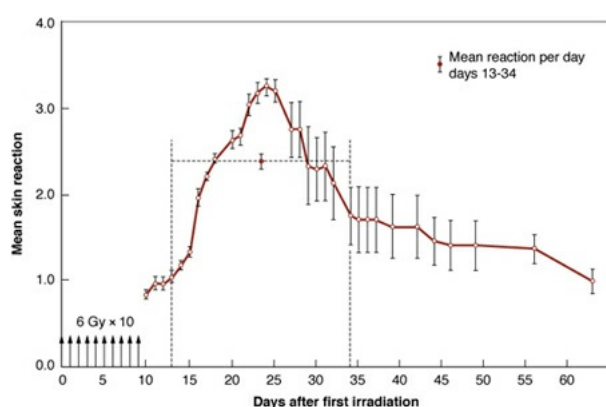


FIGURE 19.23 Daily skin reaction scores for mice receiving 60 Gy in 10 equal fractions to the right hind leg. Each *point* represents the mean score of six animals; the *vertical lines* represent the standard errors of the mean. (Adapted from Brown JM, Goffinet DR, Cleaver JE, et al. Preferential radiosensitization of mouse sarcoma relative to normal skin by chronic intra-arterial infusion of halogenated pyrimidine analogs. *J Natl Cancer Inst.* 1971;47:75–89, with permission.)

Early and Late Response of the Lung Based on Breathing Rate

Travis and her colleagues developed a noninvasive assay of breathing frequency to assess both early and late damage in mouse lungs. Breathing frequency increases progressively with dose after a threshold of about 11 Gy (Fig. 19.24). The increased breathing frequency in rodent lungs at 16 and 36 weeks is associated with the early response (i.e., pneumonitis); by 52 weeks, the elevated breathing frequency is associated with the late response (i.e., fibrosis). This is a

simple but highly quantitative and reproducible system.

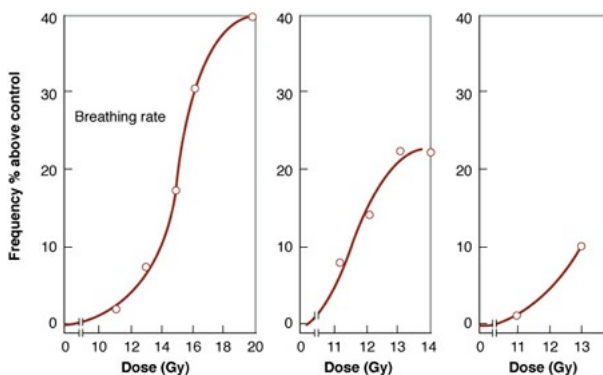


FIGURE 19.24 Breathing frequency in mice as a function of dose measured (left to right) 16, 36, and 52 weeks after irradiation with x-rays. Breathing frequency is expressed as a percentage increase above the age-related control value. (Adapted from Travis EL, Down JD, Holmes SJ, et al. Radiation pneumonitis and fibrosis in mouse lung assayed by respiratory frequency and histology. *Radiat Res.* 1980;84:133–143, with permission.)

Spinal Cord Myelopathy

A dose–response relationship can be determined for late damage caused by local irradiation of the spinal cords of rats. Several investigators have worked with this system, notably van der Kogel. After latent periods of 4 to 12 months, symptoms of myelopathy develop, the first signs of which are palpable muscle atrophy, followed some time later by impaired use of the hind legs. Figure 19.25 shows the steep dose–response relationship for hind limb paralysis following the irradiation of a section of the spinal cord in rats. These data also show the dramatic sparing that results from fractionation; this is discussed further in another section of this chapter.

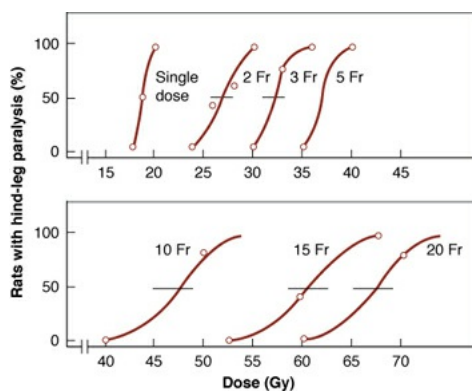


FIGURE 19.25 Dose–response curves for the induction of hind leg paralysis in rats following irradiation of a section of the spinal cord (L2–L5). Note how the dose necessary to produce paralysis increases rapidly with increasing numbers of

fractions. (Adapted from van der Kogel AJ. *Late Effects of Radiation on the Spinal Cord*. Rijswik, The Netherlands, the Radiobiological Institute of the Organization for Health Research TNO; 1979:1–160, with permission.)

The various syndromes of radiation-induced injury in rodent brain and spinal cord are very similar to those described in humans. Lesions observed within approximately the first 6 months after irradiation are limited primarily to the white matter and range between early diffuse or focal demyelination and extensive necrosis. Different pathogenic pathways toward the development of white matter necrosis have been proposed, with the glial and vascular tissue components as the major targets. The most common type of late delayed injury peaks at 1 to 2 years postirradiation and almost certainly has a vascular basis. Another type of late injury that has been described more recently in various species, including humans, is slowly progressive glial atrophy. This lesion is not associated with necrosis but occurs diffusely and at lower doses. With improvements in diagnostic procedures such as magnetic resonance imaging, glial atrophy may become a more frequently recognized adverse effect of brain tumor therapy.

Latency

Over a dose range of about 25 to 60 Gy, delivered in single doses, the general tendency is a decreasing latency with increases in dose of approximately 2 days per gray. There is a considerable variation with animal strain as well as with the region of the cord irradiated. In terms of mechanisms, demyelination or slowly progressive atrophy is probably a consequence of interference with the slow continuous turnover of oligodendrocytes by killing of glial progenitor cells. Vascular injury may accelerate, precipitate, or even initiate the white matter changes leading to necrosis. This is an area of some controversy.

Fractionation and Protraction

The effect of dose fractionation and protraction on tolerance to radiation has been investigated extensively in the rat spinal cord and to a lesser extent in the mouse, monkey, and guinea pig. Because these systems turn over slowly, there is little influence of overall treatment time up to any conventional clinical regimen of 6 to 8 weeks. On the other hand, dose per fraction is very important (see Fig. 19.25), with the dose to produce paralysis increasing dramatically with number of fractions. The effect of a large number of very small fractions has also been investigated. Figure 19.26 shows the relation between total dose and dose per fraction to produce paralysis in 50% of rats from irradiation of a short length of cervical spine. The smooth curve is an isoeffect curve calculated for the very low

α/β value of 1.5 Gy. The experimental data suggest that the linear-quadratic (LQ) model overestimates the tolerance for small doses per fraction of less than 2 Gy. However, this may be a result of incomplete repair because in these experiments, the interfraction interval was only 4 hours. There is good reason to believe that repair of sublethal damage takes place slowly in this normal tissue and, indeed, repair may be biphasic, with “fast” and “slow” components. For this reason, if multiple doses per day are used to the spinal cord, the interfraction interval should be at least 6 to 8 hours.

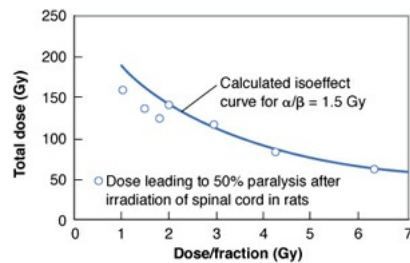


FIGURE 19.26 The data points show total dose, as a function of dose per fraction, to produce paralysis in 50% of rats after irradiation of the spinal cord. The curve is an isoeffect relationship based on the LQ equation with an α/β value of 1.5 Gy. The experimental data suggest that the LQ model overestimates tolerance for dose-per-fraction values less than 2 Gy. This may be a result of incomplete repair because the interfraction interval was only 4 hours. (Adapted from van der Kogel AJ. Central nervous system radiation injury in small animal models. In: Gutin PH, Leibel SA, Sheline GE, eds. *Radiation Injury to the Nervous System*. New York, NY: Raven Press; 1991:91–112, with permission.)

Volume Effects

The total volume of irradiated tissue usually is assumed to have an influence on the development of tissue injury. The spinal cord is perhaps the clearest case in which the functional subunits (FSUs) are arranged in linear fashion, like links in a chain. Figure 19.27 shows the relationship between tolerance dose and the length of cord irradiated in the rat. For short lengths of cord, below 1 cm, tolerance in terms of white matter necrosis shows a marked dependence on the length of cord irradiated. Late vascular injury shows less dependence on cord length. Beyond a few centimeters, the tolerance is virtually independent of the length of cord irradiated. This would be predicted from the linear arrangement of the FSUs. A chain is broken whether one, two, three, or more links are removed.

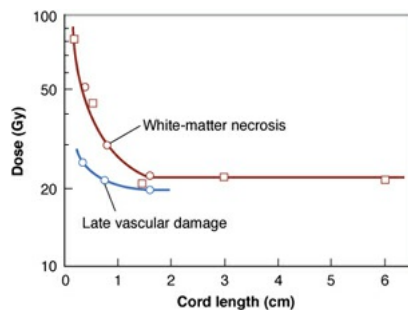


FIGURE 19.27 The dependence of spinal cord tolerance on the length of cord irradiated in the rat. For short lengths of cord, shorter than about 1 cm, tolerance for white matter necrosis shows a marked dependence on the length of cord irradiated. Late vascular injury shows less dependence on cord length. Beyond a few centimeters, the tolerance dose is virtually independent of the length of cord irradiated. (Adapted from van der Kogel AJ. Central nervous system radiation injury in small animal models. In: Gutin PH, Leibel SA, Sheline GE, eds. *Radiation Injury to the Nervous System*. New York, NY: Raven Press; 1991:91–112, with permission.)

Retreatment after Long Time Intervals

The spinal cord does recover to some extent after long time periods following irradiation. The extent of the recovery depends, of course, on the first treatment—that is, what fraction of tolerance was involved. Experiments with rats indicate that after an initial treatment to 50% tolerance, the retreatment tolerance approaches 90% of the tolerance of the untreated control group by about a year after the initial irradiation. If the initial treatment represented a larger fraction of tolerance, the retreatment that can be tolerated is reduced.

INFERRING THE RATIO α/β FROM MULTIFRACTION EXPERIMENTS IN NONCLONOGENIC SYSTEMS

The parameters of the dose–response curve for any normal tissue system for which a functional end point can be observed may be inferred by performing a multifraction experiment. Take, for example, an experiment in which mouse foot skin reaction is scored. Doses that result in the same skin reaction (e.g., moist desquamation of more than 50% of the area irradiated) if delivered as a single exposure in a multifraction regimen (e.g., 5, 10, or 20 fractions) must be determined experimentally. Several assumptions must be made as follows:

1. The dose–response relationship is represented adequately by the LQ formulation:

$$S = e^{-\alpha D - \beta D^2}$$

in which S is the fraction of cells surviving a dose, D , and α and β are constants.

2. Each dose in a fractionated regimen produces the same biologic effect.
3. Full repair of sublethal damage takes place between dose fractions, but no cell proliferation occurs.

Suppose the total dose, D , is divided into n equal fractions of d . The previous equation, then, can be rewritten as

$$S = (e^{-\alpha d - \beta d^2})^n$$

or

$$-\log_e S / nd = \alpha + \beta d$$

If the reciprocal of the total dose ($1/nd$) is plotted against the dose per fraction (d), a straight line results, as shown in Figure 19.28. The intercept on the ordinate gives $\alpha/\log_e S$; the slope gives $\beta/\log_e S$. In general, the value of $\log_e S$ is not known unless other cell survival studies are available, but the ratio of the intercept to the slope provides an estimate of α/β .

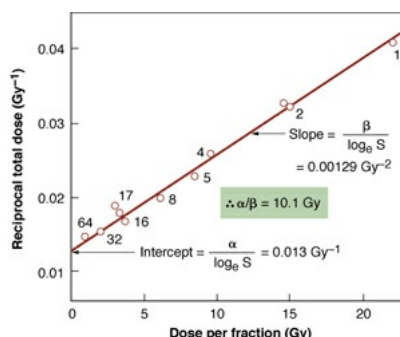


FIGURE 19.28 Reciprocal of the total dose required to produce a given level of injury (acute skin reaction in mice) as a function of dose per fraction in multiple equal doses. The overall time of these experiments was sufficiently short so that proliferation could be neglected. Numbers of fractions are shown by each point. From the values of the “intercept” and “slope” of the best-fit line, the values of α and β and the ratio α/β for the dose-response curve for organ function can be determined. (Adapted from Douglas BG, Fowler JF. The effect of multiple small doses of X rays on skin reactions in the mouse and a basic interpretation. *Radiat Res.* 1976;66:401–426, with permission.)

Multifraction experiments have been performed and estimates of α/β made

for essentially all of the normal tissue end points described in this chapter. One of the important conclusions arrived at is that the value of α/β tends to be larger for early-responding tissues, about 10 Gy, than for late-responding tissues, about 2 Gy. Because α/β is the dose at which cell killing by linear and by quadratic components of radiation damage are equal ([Chapter 3](#)), the implication is that dose–response relationships for late-responding tissues are “curvier” than for early-responding tissues. The importance of this conclusion becomes evident in the discussion of fractionation in radiotherapy in [Chapter 23](#).

SUMMARY OF PERTINENT CONCLUSIONS

The relationship between dose and incidence is sigmoid for both tumor control and normal tissue damage.

The ratio of tumor response to normal tissue damage is called the therapeutic ratio or therapeutic index.

The therapeutic index can be manipulated by dose fractionation or by the use of drugs that preferentially increase tumor response.

After irradiation, most cells die a mitotic death; that is, they die in attempting the next or a later mitosis. In some tissues, cells die by apoptosis, which is a programmed cell death.

Systems involving clonogenic end points (i.e., cell survival) for cells of normal tissues include some in which cells regrow *in situ* and some in which cells are transplanted to another site.

In situ regrowth techniques include skin colonies, crypts in the jejunum, testes stem cells, and kidney tubules. Single-dose experiments can yield the slope (D_0) of the dose–response curve over a range of high doses. Multifraction experiments allow the whole dose–response curve to be reconstructed.

Systems in which cell survival is assessed by transplantation into another site include bone marrow stem cells, thyroid cells, and mammary cells.

A dose–response curve for bone marrow stem cells can be obtained by allowing cells from the donor animal to lodge and grow in the spleens of recipient animals. These are very sensitive cells with a D_0 close to 1 Gy, with little or no shoulder.

Dose–response curves for mammary and thyroid cells can be obtained by transplanting them into fat pads of recipient animals.

The radiosensitivity of cells from normal tissues varies widely. The width of the shoulder of the curve is the principal variable. Jejunal crypt cells have a very large shoulder; bone marrow stem cells have little, if any, shoulder. Most other cell types studied in clonogenic assays fall in between.

Dose-response curves for functional end points, distinct from cell survival, can be obtained as follows:

1. Pig skin and rodent skin—by measuring skin reactions
2. Early and late response of the lung—by measuring breathing rate
3. Spinal cord—by observing myelopathy:
 - a. Paralysis develops after a latency of months to years.
 - b. Early lesions are limited to white matter; late delayed injury may have a vascular basis.
 - c. Spinal cord damage is very sensitive to fractionation— α/β of about 1.5 Gy.
 - d. Sublethal damage repair probably has “fast” and “slow” components.
 - e. If multiple fractions per day are used, the interfraction interval should be at least 6 to 8 hours.
 - f. FSUs are arranged serially like links in a chain.
 - g. For short lengths of cord, tolerance dose varies markedly with cord length irradiated; for cord lengths greater than a few centimeters, tolerance dose is virtually independent of cord length.

The shape of the dose-response relationship for functional end points, obtained from multifraction experiments, is more pertinent to radiotherapy than clonogenic assays.

The ratio α/β (the dose at which the linear and quadratic components of radiation damage are equal) may be inferred from multifraction experiments in systems scoring nonclonogenic end points.

BIBLIOGRAPHY

Andrews JR. *The Radiobiology of Human Cancer Radiotherapy*. Philadelphia, PA: Saunders; 1968.

Ang KK, Thames HD Jr, van der Kogel AJ, et al. Is the rate of repair of radiation-induced sublethal damage in rat spinal cord dependent on the size

- of the dose per fraction? *Int J Radiat Oncol Biol Phys.* 1987;13:557–562.
- Ang KK, van der Kogel AJ, van der Schueren E. Lack of evidence for increased tolerance of rat spinal cord with decreasing fraction doses below 2 Gy. *Int J Radiat Oncol Biol Phys.* 1985;11:105–110.
- Ang KK, van der Kogel AJ, van der Schueren E. The effect of small radiation doses on the rat spinal cord: the concept of partial tolerance. *Int J Radiat Oncol Biol Phys.* 1983;9:1487–1491.
- Barendsen GW, Broerse JJ. Experimental radiotherapy of a rat rhabdomyosarcoma with 15 MeV neutrons and 300 kV x-rays: I. Effects of single exposures. *Eur J Cancer.* 1969;5:373–391.
- Bradley WG, Fewings JD, Cumming WJ, et al. Delayed myeloradiculopathy produced by spinal x-irradiation in the rat. *J Neurol Sci.* 1977;31:63–82.
- Brown JM, Goffinet DR, Cleaver JE, et al. Preferential radiosensitization of mouse sarcoma relative to normal skin by chronic intra-arterial infusion of halogenated pyrimidine analogs. *J Natl Cancer Inst.* 1971;47:75–89.
- Clifton KH, Briggs RC, Stone HB. Quantitative radiosensitivity studies of solid carcinomas in vivo: methodology and effect of anoxia. *J Natl Cancer Inst.* 1966;36:965–974.
- Clifton KH, Gould MN, Potten CS, et al, eds. *Cell Clones.* New York, NY: Churchill Livingstone; 1985:128–138.
- DeMott RK, Mulcahy RT, Clifton KH. The survival of thyroid cells following irradiation: a directly generated single-dose survival curve. *Radiat Res.* 1979;77:395–403.
- Douglas BG, Fowler JF. The effect of multiple small doses of X rays on skin reactions in the mouse and a basic interpretation. *Radiat Res.* 1976;66:401–426.
- Field SB, Thomlinson RH, Jones T. The relative effects of fast neutrons and x rays on tumour and normal tissue in the rat. I. Single doses. *Br J Radiol.* 1967;40:834–842.
- Fowler JF, Denekamp J, Page AL, et al. Fractionation with x rays and neutrons in mice: response of skin and C3H mammary tumours. *Br J Radiol.* 1972;45:237–249.
- Fowler JF, Kragt K, Ellis RE, et al. The effect of divided doses of 15 MeV electrons on the skin response of mice. *Int J Radiat Biol.* 1965;9:241–252.

- Fowler JF, Morgan RL, Silvester JA, et al. Experiments with fractionated x-ray treatment of the skin of pigs. *Br J Radiol.* 1963;36:188–196.
- Goffinet DR, Marsa GW, Brown JM. The effects of single and multifraction radiation courses on the mouse spinal cord. *Radiology.* 1976;119:709–713.
- Gould MN, Biel WF, Clifton KH. Morphological and quantitative studies of gland formation from inocula of monodispersed rat mammary cells. *Exp Cell Res.* 1977;107:405–416.
- Gould MN, Clifton KH. Evidence for a unique in situ component of the repair of radiation damage. *Radiat Res.* 1979;77:149–155.
- Gould MN, Clifton KH. The survival of mammary cells following irradiation in vivo: a directly generated single-dose survival curve. *Radiat Res.* 1977;72:343–352.
- Hermens AF, Barendsen GW. Cellular proliferation patterns in an experimental rhabdomyosarcoma in the rat. *Eur J Cancer.* 1967;3:361–369.
- Hermens AF, Barendsen GW. Changes of cell proliferation characteristics in a rat rhabdomyosarcoma before and after x-irradiation. *Eur J Cancer.* 1969;5:173–189.
- Hewitt HB. Studies on the quantitative transplantation of mouse sarcoma. *Br J Cancer.* 1953;7:367–383.
- Hewitt HB, Chan DP, Blake ER. Survival curves for clonogenic cells of a murine keratinizing squamous carcinoma irradiated in vivo or under hypoxic conditions. *Int J Radiat Biol Relat Stud Phys Chem Med.* 1967;12:535–549.
- Hewitt HB, Wilson CW. A survival curve for mammalian leukaemia cells irradiated in vivo (implications for the treatment of mouse leukaemia by whole-body irradiation). *Br J Cancer.* 1959;13:69–75.
- Hewitt HB, Wilson CW. Survival curves for tumor cells irradiated in vivo. *Ann N Y Acad Sci.* 1961;95:818–827.
- Hill RP, Bush RS. A lung-colony assay to determine the radiosensitivity of the cells of a solid tumour. *Int J Radiat Biol Relat Stud Phys Chem Med.* 1969;15:435–444.
- Hopewell JW. Late radiation damage to the central nervous system: a radiobiological interpretation. *Neuropathol Appl Neurobiol.* 1979;5:329–343.
- Hopewell JW, Morris AD, Dixon-Brown A. The influence of field size on the

- late tolerance of the rat spinal cord to single doses of x rays. *Br J Radiol.* 1987;60:1099–1108.
- Kember NF. An in vivo cell survival system based on the recovery of rat growth cartilage from radiation injury. *Nature.* 1965;207:501–503.
- Kerr JFR, Searle J. Apoptosis: its nature and kinetic role. In: Meyn RE, Withers HR, eds. *Radiation Biology in Cancer Research*. New York, NY: Raven Press; 1980:367–384.
- McCulloch EA, Till JE. The sensitivity of cells from normal mouse bone marrow to gamma radiation in vitro and in vivo. *Radiat Res.* 1962;16:822–832.
- McNally NJ. A comparison of the effects of radiation on tumour growth delay and cell survival. The effect of oxygen. *Br J Radiol.* 1973;46:450–455.
- McNally NJ. Recovery from sub-lethal damage by hypoxic tumour cells in vivo. *Br J Radiol.* 1972;45:116–120.
- Mulcahy RT, Gould MN, Clifton KH. The survival of thyroid cells: in vivo irradiation and in situ repair. *Radiat Res.* 1980;84:523–528.
- Peters LJ, Brock WA, Travis EL. Radiation biology at clinically relevant doses. In: DeVita VT, Hellman S, Rosenberg SA, eds. *Important Advances in Oncology*. Philadelphia, PA: J.B. Lippincott; 1990:65–83.
- Potten CS. Regeneration in epithelial proliferative units as exemplified by small intestinal crypts. *Ciba Found Symp.* 1991;160:54–71.
- Reinhold HS. Quantitative evaluation of the radiosensitivity of cells of a transplantable rhabdomyosarcoma in the rat. *Eur J Cancer.* 1966;2:33–42.
- Rockwell SC, Kallman RF. Cellular radiosensitivity and tumor radiation response in the EMT6 tumor cell system. *Radiat Res.* 1973;53:281–294.
- Rockwell SC, Kallman RF, Fajardo LF. Characteristics of a serially transplanted mouse mammary tumor and its tissue-culture-adapted derivative. *J Natl Cancer Inst.* 1972;49:735–749.
- Scalliet P, Landuyt W, van der Schueren E. Repair kinetics as a determining factor for late tolerance of central nervous system to low dose rate irradiation. *Radiother Oncol.* 1989;14:345–353.
- Stephen LC, Ang KK, Schultheiss TE, et al. Apoptosis in irradiated murine tumors. *Radiat Res.* 1991;127:308–316.
- Suit HD, Maeda M. Hyperbaric oxygen and radiobiology of the C3H mouse

- mammary carcinoma. *J Natl Cancer Inst.* 1967;39:639–652.
- Suit HD, Wette R. Radiation dose fractionation and tumor control probability. *Radiat Res.* 1966;29:267–281.
- Suit HD, Wette R, Lindberg R. Analysis of tumor-recurrence times. *Radiology.* 1967;88:311–321.
- Sutherland RM, Durand RE. Radiation response of multicell spheroids—an in vitro tumour model. *Curr Top Radiat Res Q.* 1976;11:87–139.
- Sutherland RM, McCredie JA, Inch WR. Growth of multicell spheroids in tissue culture as a model of nodular carcinomas. *J Natl Cancer Inst.* 1971;46:113–120.
- Tannock IF. The relation between cell proliferation and the vascular system in a transplanted mouse mammary tumour. *Br J Cancer.* 1968;22:258–273.
- Taylor AB, Anderson JH. Scanning electron microscope observations of mammalian intestinal villi, intervillus floor, and crypt tubules. *Micron.* 1972;3:430–453.
- Thames HD, Withers HR. Test of equal effect per fraction and estimation of initial clonogen number in microcolony assays of survival after fractionated irradiation. *Br J Radiol.* 1980;53:1071–1077.
- Thames HD, Withers HR, Mason KA, et al. Dose-survival characteristics of mouse jejunal crypt cells. *Int J Radiat Oncol Biol Phys.* 1981;7:1591–1597.
- Till JE, McCulloch EA. In: Cameron IL, Padilla GM, Zimmerman AM, eds. *Developmental Aspects of the Cell Cycle.* New York, NY: Academic Press; 1971:297–313.
- Travis EL, Down JD, Holmes SJ, et al. Radiation pneumonitis and fibrosis in mouse lung assayed by respiratory frequency and histology. *Radiat Res.* 1980;84:133–143.
- Travis EL, Vojnovic B, Davies EE, et al. A plethysmographic method for measuring function in locally irradiated mouse lung. *Br J Radiol.* 1979;52:67–74.
- van der Kogel AJ. Central nervous system radiation injury in small animal models. In: Gutin PH, Leibel SA, Sheline GE, eds. *Radiation Injury to the Nervous System.* New York, NY: Raven Press; 1991:91–112.
- van der Kogel AJ. Effect of volume and localization on rat spinal cord tolerance.

- In: Fielden EM, Fowler JF, Hendry JH, Scott D, eds. *Radiation Research: Proceedings of the 8th International Congress of Radiation Research*. New York, NY: Taylor & Francis; 1987:352.
- van der Kogel AJ. *Late Effects of Radiation on the Spinal Cord*. Rijswik, The Netherlands: Radiobiological Institute of the Organization for Health Research TNO; 1979.
- van der Kogel AJ. Radiation-induced damage in the central nervous system: an interpretation of target cell responses. *Br J Cancer Suppl*. 1986;7:207–217.
- van der Kogel AJ. Radiation tolerance of the rat spinal cord: time-dose relationships. *Radiology*. 1977;122:505–509.
- van der Schueren E, Landuyt W, Ang KK, et al. From 2 Gy to 1 Gy per fraction: sparing effect in rat spinal cord? *Int J Radiat Oncol Biol Phys*. 1988;14:297–300.
- Wara WM, Phillips TL, Margolis LW, et al. Radiation pneumonitis: a new approach to the derivation of time-dose factors. *Cancer*. 1973;32:547–552.
- White A, Hornsey S. Radiation damage to the rat spinal cord: the effect of single and fractionated doses of x rays. *Br J Radiol*. 1978;51:515–523.
- Williams GT. Programmed cell death: apoptosis and oncogenesis. *Cell*. 1991;65:1097–1098.
- Withers HR. Recovery and repopulation in vivo by mouse skin epithelial cells during fractionated irradiation. *Radiat Res*. 1967;32:227–239.
- Withers HR. Regeneration of intestinal mucosa after irradiation. *Cancer*. 1971;28:75–81.
- Withers HR. The dose-survival relationship for irradiation of epithelial cells of mouse skin. *Br J Radiol*. 1967;40:187–194.
- Withers HR, Elkind MM. Microcolony survival assay for cells of mouse intestinal mucosa exposed to radiation. *Int J Radiat Biol Relat Stud Phys Chem Med*. 1970;17:261–267.
- Withers HR, Hunter N, Barkley HT Jr, et al. Radiation survival and regeneration characteristics of spermatogenic stem cells of mouse testis. *Radiat Res*. 1974;57:88–103.
- Withers HR, Mason K, Reid BO, et al. Response of mouse intestine to neutrons and gamma rays in relation to dose fractionation and division cycle. *Cancer*.

1974;34:39–47.

Withers HR, Mason K, Thames HD. Late radiation response of kidney assayed by tubule-cell survival. *Br J Radiol.* 1986;59:587–595.

chapter 20

Clinical Response of Normal Tissues

Cells and Tissues

Early (Acute) and Late Effects

Functional Subunits in Normal Tissues

The Volume Effect in Radiotherapy: Tissue Architecture

Radiation Pathology of Tissues

Casarett's Classification of Tissue Radiosensitivity

Michalowski's H- and F-Type Populations

Growth Factors

Specific Tissues and Organs

Skin

Hematopoietic System

Lymphoid Tissue and the Immune System

Digestive Tract

Lungs

Kidneys

Liver

Bladder Epithelium

Central and Peripheral Nervous Systems

Testes

Ovaries

Female Genitalia

Blood Vessels and the Vascular System

Heart

Bone and Cartilage

Quantitative Analysis of Normal Tissue Effects in the Clinic

Late Effects of Normal Tissue and SOMA

The SOMA Scoring System

Application of Stem Cells to Regenerate Radiation-Sensitive Organs—Salivary Gland Regeneration

Summary of Pertinent Conclusions

Bibliography

CELLS AND TISSUES

Most of the effects of radiation therapy on normal tissues can be attributed to cell killing, but there are some that cannot. Examples include the following:

Nausea or vomiting that may occur a few hours after irradiation of the abdomen

Fatigue felt by patients receiving irradiation to a large volume, especially within the abdomen

Somnolence that may develop several hours after cranial irradiation

Acute edema or erythema that results from radiation-induced acute inflammation and associated vascular leakage

It is thought that these effects are mediated by radiation-induced inflammatory cytokines. These effects aside, most effects of radiation on normal tissues result from the depletion of a cell population by cell killing.

The cells of normal tissues are not independent but form a complete integrated structure. There is a delicate balance between cell birth and cell death to maintain tissue organization and the number of cells. The response to damage is governed by (1) the inherent cellular radiosensitivity, (2) the kinetics of the tissue, and (3) the way cells are organized in that tissue. If the fate of individual cells is studied, as described in [Chapter 3](#), there is a continuous monotonic relationship between the magnitude of the dose and the fraction of cells that are “killed” in the sense that they lose their reproductive integrity—the ability to divide indefinitely. By contrast, no effects are seen in tissues after small doses, although effects of increasing severity become apparent if the dose rises above a threshold level. The reason is, of course, that killing small number of cells in a tissue matters very little; visible damage is evident only if a large enough proportion of the cells are killed and removed from the tissue. The threshold dose below which no effect is seen and the delay between irradiation and the time at which the damage becomes observable vary greatly among different

tissues.

Cell death after irradiation occurs mostly as cells attempt to divide. In tissues with a rapid turnover rate, damage becomes evident quickly—in a matter of hours in the intestinal epithelium and bone marrow and in a matter of days in the skin and mucosa. In tissues in which cells divide rarely, radiation damage to cells may remain latent for a long period and be expressed very slowly. Radiation damage to cells that are already on the path to differentiation (and would not have divided many times anyway) is of little consequence. By contrast, radiation damage to stem cells has serious repercussions because they are programmed to divide many times to maintain a large population, and if they lose their reproductive integrity, both they and their potential descendants are lost from the population. Thus, cells on the road to differentiation appear to be more **radioresistant** than stem cells. In fact, the fraction of cells surviving a given dose may be identical at the single-cell level, so strictly speaking, it is their **radioresponse** that is different, not their **radiosensitivity**. This explains the so-called law of Bergonié and Tribondeau (1906), who noted that tissues appear to be more “radiosensitive” if their cells are less differentiated, have a greater proliferative capacity, and divide more rapidly.

EARLY (ACUTE) AND LATE EFFECTS

Radiation effects are commonly divided into two categories, **early** and **late**, which show quite different patterns of response to fractionation; their dose-response relations are characterized by different α/β ratios, as described in more detail in [Chapter 23](#). **Late effects** are much more sensitive to changes in fractionation than early effects. **Early, or acute, effects** result from the death of a large number of cells and occur within a few days or weeks of irradiation in tissues with a rapid rate of turnover. Examples include effects in the epidermal layer of the skin, gastrointestinal epithelium, and hematopoietic system, in which the response is determined by a hierarchical cell lineage composed of stem cells and their differentiating offspring ([Fig. 20.1A](#)). The time of onset of early reactions correlates with the relatively short life span of the mature functional cells; the identity of the target cells is usually obvious.

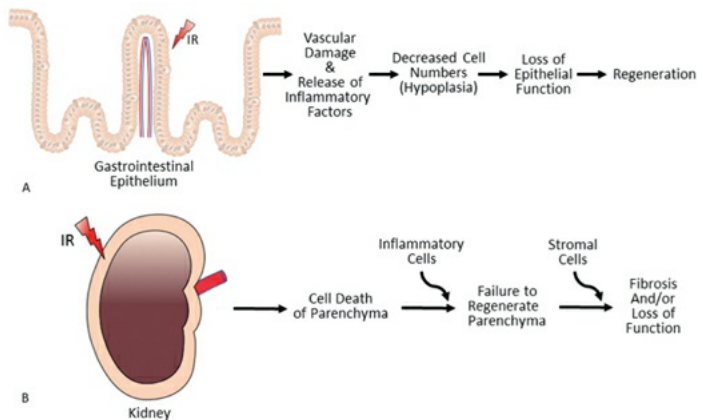


FIGURE 20.1 A: The proposed series of events that can be clarified as early (acute) effects in the gastrointestinal epithelium after exposure to ionizing radiation. The initial events are vascular damage and release of inflammatory cytokines. These events will result in hypoplasia or decreased cell numbers, leading to loss of epithelial function. However, in most cases, epithelial function will be restored through tissue regeneration. As discussed in [Chapter 19](#), regeneration in the gastrointestinal epithelium occurs through stem cell transit and differentiation upward. **B:** The proposed series of events that can be clarified as late effects in the irradiated kidney. In the irradiated kidney, cell death of the parenchyma stimulates an inflammatory response. In this case, chronic inflammation results in failure of the parenchyma to regenerate, ultimately leading to fibrosis and loss of function. IR, ionizing radiation.

Late effects appear after a delay of months or years and occur predominantly in slowly proliferating tissues, such as tissues of the lung, kidney, heart, liver, and central nervous system. The difference between the two types of lesions lies in their **progression**: Acute damage is repaired rapidly because of the rapid proliferation of stem cells and may be completely reversible. By contrast, late damage may improve but is never completely repaired. A late effect may result from a combination of vascular damage and loss of parenchymal cells (see [Fig. 20.1B](#)). Clearly, vascular damage is not the dominant factor in every case because if it were, the dose–effect relationship would be the same for all tissues, and that is not the case. It may be true for some tissues, however, including the spinal cord. If intensive fractionation protocols deplete the stem cell population below levels needed for tissue restoration, an early reaction in a rapidly proliferating tissue may persist as a chronic injury. This has been termed a **consequential late effect**, that is, a late effect consequent to, or evolving out of, a persistent severe early effect. The earlier damage is most often attributable to an overlying acutely responding epithelial surface—for example, fibrosis or necrosis of skin consequent to desquamation and acute ulceration.

FUNCTIONAL SUBUNITS IN NORMAL TISSUES

The fraction of cells surviving determines the success or failure of a treatment regimen as far as the tumor is concerned because a single surviving cell may be the focus for the regrowth of the tumor. For normal tissues, however, this is not the whole story. The tolerance of normal tissues for radiation depends on the ability of the clonogenic cells to maintain a sufficient number of mature cells suitably structured to maintain organ function. The **relationship** between the survival of clonogenic cells and organ function or failure depends also on the structural organization of the tissue. Many tissues may be thought of as consisting of **functional subunits (FSUs)**.

In some tissues, the FSUs are discrete, anatomically delineated structures whose relationship to tissue function is clear. Obvious examples are the nephron in the kidney, the lobule in the liver, and perhaps the acinus in the lung. In other tissues, the FSUs have no clear anatomic demarcation. Examples include the skin, the mucosa, and the spinal cord. The response to radiation of these two types of tissue—with structurally defined or structurally undefined FSUs—is quite different.

The survival of **structurally defined FSUs** depends on the survival of one or more clonogenic cells within them, and tissue survival in turn depends on the number and radiosensitivity of these clonogens. Although such tissues are composed of a large number of FSUs, each is a small self-contained entity independent of its neighbors. Surviving clonogens cannot migrate from one to the other. Because each FSU is both small and autonomous, low doses deplete the clonogens in it. Each kidney, for example, is composed of a large number of relatively small FSUs, each of which is a self-contained structural entity independent of its neighbors. Consequently, survival of a nephron after irradiation depends on the survival of at least one clonogen within it and therefore on the initial number of renal tubule cells per nephron and their radiosensitivity. Because this FSU is relatively small, it is completely depleted of clonogens by low doses, which accounts for the low tolerance to radiation of the kidney. Other organs that resemble the kidney in having structurally defined FSUs not repopulated from adjacent FSUs may be those with a branching treelike system of ducts and vasculature that ultimately terminate in “end structures” or lobules of parenchymal cells. These can be visualized as independent structurally defined FSUs. Examples of organs with this tissue architecture include the lung, liver, and exocrine organs. At least some of these also have low tolerance to radiation.

By contrast, the clonogenic cells that can repopulate the **structurally undefined FSUs** after depletion by radiation are not confined to one particular FSU. Rather, clonogenic cells can migrate from one FSU to another and allow repopulation of a depleted FSU. For example, reepithelialization of a denuded area of skin can occur either from surviving clonogens within the denuded area or by migration from adjacent areas.

A concept proposed to link the survival of clonogenic cells and functional survival is the **tissue rescue unit**, defined as the minimum number of FSUs required to maintain tissue function. This model assumes that the number of tissue rescue units in a tissue is proportional to the number of clonogenic cells, that FSUs contain a constant number of clonogens, and that FSUs can be repopulated from a single surviving clonogen.

Some tissues defy classification by this system. The crypts of the jejunum, for example, are structurally well-defined subunits, but surviving crypt cells can and do migrate from one crypt to another to repopulate depleted neighbors.

THE VOLUME EFFECT IN RADIOTHERAPY: TISSUE ARCHITECTURE

It is generally observed in clinical radiotherapy that the total dose that can be tolerated depends on the volume of tissue irradiated. **Tolerance dose** has been defined as the dose that produces an acceptable probability of a treatment complication. This definition includes objective criteria, such as the radiobiology involved, and subjective factors that may be socioeconomic, medicolegal, or psychological.

The spatial arrangement of the FSUs in the tissue is critical. In the case of tissues in which the FSUs are arranged in a series, like the links of a chain, the integrity of each is critical to organ function, and elimination of any one FSU results in a measurable probability of a complication. The spinal cord is the clearest example in which specific functions are controlled by specific segments arranged linearly, or serially. Because impulses must pass along the cord, death of critical cells in any one segment results in complete failure of the organ. Radiation damage to such tissues is expected to show a binary response, with a threshold dose below which there is normal function and above which there is loss of function (e.g., radiation-induced myelopathy). This is illustrated in [Figure 20.2](#). As the field size increases to include a greater number of FSUs—1, 4, or 16 in this example—the curve relating probability of a complication to dose rises much more steeply with dose and moves to lower doses. This explains the

important volume effect found in, for example, the spinal cord in which FSUs are arranged in series and loss of any one may result in myelopathy.

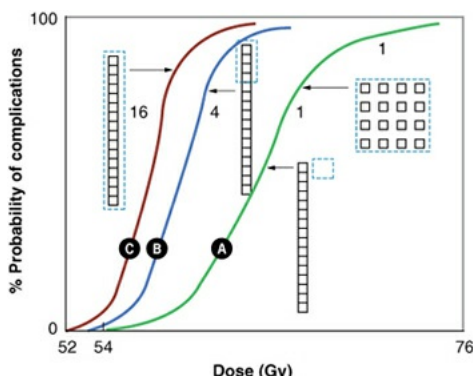


FIGURE 20.2 Relationship between dose and probability of complications for different types of normal tissues. *Curve A* relates to a normal tissue in which the functional subunits are not arranged serially regardless of whether one or all subunits are exposed (i.e., regardless of field size). It also applies to a normal tissue in which functional subunits are arranged serially if only one subunit is exposed (i.e., if the field is small). Note that the curve is relatively shallow (i.e., the probability of a complication rises relatively slowly with dose). *Curves B* and *C* refer to a tissue with serially arranged functional subunits; the complication curve gets steeper and moves to lower doses as the treatment field size increases. For example, *curves B* and *C*, respectively, relate to 4 or 16 functional subunits exposed. (Note that the position of the curves in relation to the abscissae is arbitrary, resulting from two assumptions: that there is an effective D_0 of 4 Gy for a survival curve for cells exposed to multiple doses of 2 Gy and that 58 Gy in 2-Gy fractions sterilizes 10% of the functional subunits.) (Adapted from Withers HR, Taylor JM, Maciejewski B. Treatment volume and tissue tolerance. *Int J Radiat Oncol Biol Phys.* 1988;14:751–759, with permission.)

Clinical tolerance also depends strongly on the volume irradiated in the kidney and lung; both of these organs are very sensitive to irradiation of their entire volume, but small volumes can be treated to much higher doses. This is because there is considerable functional reserve capacity, with only about 30% of the organ required to maintain adequate function under normal physiologic conditions. The large reserve capacity and increased tolerance to partial-volume irradiation are caused by the parallel organization of functional nephrons and alveolar subunits. Inactivation of a small number of FSUs does not lead to loss of organ function. Functional damage will not occur until a critical number of FSUs are inactivated by irradiation. This implies that there should also be a threshold volume of irradiation below which no functional damage will develop,

even after high-dose irradiation. Above this threshold, damage is usually exhibited as a graded response—increasing severity of functional impairment with increasing dose—rather than a binary, all-or-nothing response.

Skin and mucosa have no well-defined FSUs but respond in a way similar to tissues where the FSUs are in parallel. They do not show a volume effect at lower levels of injury at which healing can occur from surviving clonogens scattered throughout the treatment volume. This seemingly should be true for the skin or mucosa in which a volume effect would not be expected on radiobiologic grounds; however, this is never quite true in practice because if a larger area of skin or mucosa is ulcerated, the prolonged healing time plus the increased potential for infection are more debilitating than similarly severe ulceration in a smaller area. In other words, although the severity of a skin reaction is relatively independent of the area irradiated because healing occurs by regeneration of surviving clonogens scattered throughout the treated area, the tolerability is not. Therefore, there is a volume effect in clinical practice, but it is not based on an increased probability of injury as it is in tissues in which FSUs are arranged serially.

RADIATION PATHOLOGY OF TISSUES

As previously stated, the response of a tissue or organ to radiation depends primarily on three factors: (1) the inherent sensitivity of the individual cells, (2) the kinetics of the tissue as a whole of which the cells are a part, and (3) the way the cells are organized in that tissue. These factors combine to account for the substantial variation in response to radiation characteristic of different tissues.

In the case of tissues composed of highly differentiated cells performing specialized functions, cell survival curves (see [Chapter 3](#)) are largely irrelevant because these cells have no mitotic future. Little information is available at the cellular level concerning the effects of radiation on differentiated cells. All that can be said is that, in general, the amount of radiation needed to destroy the functioning ability of a differentiated cell is far greater than that necessary to stop the mitotic activity of a dividing cell.

A closed static population, composed entirely of mature differentiated cells, is therefore very resistant to radiation. In the case of self-renewing tissues, the Achilles heel is the dividing cell: Loss of reproductive ability in an appreciable fraction of these cells occurs after a moderate dose of a few grays. Whether the tissue or organ as a whole appears to be affected to a small or large extent—and is consequently labeled as sensitive or resistant—depends on the extent to which

the tissue involved can continue to function adequately with a reduced number of cells.

Another factor that is evident from even this most elementary consideration of population kinetics is that the time interval between the delivery of the radiation insult and its expression in tissue damage is very variable for different populations. This time interval is determined by the normal life span of the mature functional cells and the time it takes for a cell “born” in the stem cell compartment to mature to a functional state. For example, mature erythrocytes in circulating blood have a relatively long life span and are separated from the primitive stem cell compartment by several transit compartments, so that time is required for a cell to pass through the various stages of differentiation and maturation. Consequently, a considerable time interval elapses between the depopulation of the stem cell compartment and the final expression of this injury in terms of a reduced peripheral blood cell count. By contrast, in the case of the intestinal epithelium, the mature functional cells on the surface of the villi have a short life span, and the time interval between the “birth” of a new cell in the stem compartment of the crypt and its appearance as a mature functional cell is very short, on the order of a few days. As would be expected, therefore, radiation damage is expressed correspondingly quickly in this tissue. Two systems are typically used to classify tissue radiosensitivity in terms of population kinetics and tissue architecture: Casarett’s classification and Michalowski’s classification.

CASARETT’S CLASSIFICATION OF TISSUE RADIOSENSITIVITY

The limitation of our knowledge of cellular population kinetics is remedied to some extent by a wealth of information on the relative sensitivities of various tissues based on histopathologic observations. It must be emphasized that these data are based on entirely different end points than those with which previous chapters have been concerned. To score a cell as “dead” by observing a fixed and stained section of tissue through a microscope is quite different from the experimental test of cell death in terms of loss of reproductive capacity, which has been used previously. Nevertheless, the study of radiation pathology provides data that are highly relevant to clinical radiotherapy.

Casarett has suggested a classification of mammalian cell radiosensitivity based on histologic observation of early cell death. He divided parenchymal cells into four major categories, numbered I through IV ([Table 20.1](#)). The supporting

structures, such as the connective tissue and the endothelial cells of small blood vessels, are regarded as intermediate in sensitivity between groups II and III of the parenchymal cells.

Table 20.1 Categories of Mammalian Cell Sensitivity

CELL TYPE	PROPERTIES	EXAMPLES	SENSITIVITY ^a
I. Vegetative intermitotic cells	Divide regularly; no differentiation	Erythroblasts Intestinal crypt cells Germinal cells of epidermis	High
II. Differentiating intermitotic cells	Divide regularly; some differentiation between divisions		
<i>Connective tissue cells^b</i>			
III. Reverting postmitotic cells	Do not divide regularly; variably differentiated	Liver	
IV. Fixed postmitotic cells	Do not divide; highly differentiated	Nerve cells Muscle cells	Low

^aSensitivity decreases for each successive group.

^bIntermediate in sensitivity between groups II and III.

Based on Rubin P, Casarett GW. *Clinical Radiation Pathology*. Vol 1. Philadelphia, PA: W.B. Saunders; 1968, with permission.

One of the most sensitive cells to radiation, in fact, defies all the “laws” and systems of classification; it is the small lymphocyte. This cell, it is believed, never divides at all, or at least only in exceptional circumstances. Small lymphocytes disappear from circulating blood after very small doses of radiation, and it is believed that they suffer an interphase death (by the process of apoptosis). Most sensitive cells die a mitotic death after irradiation; most cells that never divide require very large doses to kill them. The small lymphocyte breaks both of these rules, inasmuch as it does not usually divide, dies of interphase death, and yet is one of the most sensitive mammalian cells.

Group I of Casarett’s classification, the most sensitive group, consists of vegetative intermitotic cells and includes the stem cells of the classic self-renewing systems, such as the basal layers of the epidermis and the intestine, the erythroblasts (precursors of red blood cells), intestinal crypt cells, and the primitive cells of the spermatogenic series. The stem cells divide regularly and provide a steady and abundant supply of progeny, some of which differentiate and mature into functioning cells. A reservoir of primitive dividing stem cells is maintained and, in some cases, can be triggered to divide more rapidly in response to a need. The primitive dividing stem cells are vulnerable to radiation; a moderate dose causes a proportion of them to “die” in attempting the next or a subsequent mitosis. The time of crisis for the organism as a whole occurs if the supply of functioning cells is inadequate: a shortage of circulating red and white blood cells in the case of the blood and a shortage of mature covering dermal cells in the case of the skin. The time interval between irradiation and the crisis is about equal to the life span of the mature functioning cells. As the functioning cells die off at the end of their natural life span, there are none to take their place if a dose of radiation previously has depopulated the stem cell compartment. Depending on the size of the dose, the organ or tissue may not survive the critical time at which the number of functioning cells reaches a minimum value.

Group II consists of cells that divide regularly but that also mature and differentiate between divisions. Cells in this category are relatively short-lived as individuals and are produced by division of vegetative intermitotic cells. These cells usually complete a limited number of divisions and differentiate to some extent between successive mitoses. This group includes cells of the hematopoietic series in the intermediate stages of differentiation and likewise the more differentiated spermatogonia and spermatocytes.

Group III, the reverting postmitotic cells, is relatively resistant and as individuals have relatively long lives. Ordinarily, the cells in this category do not

undergo mitosis, but they are capable of dividing with the appropriate stimulus, which is usually damage or loss of many of their own kind. The liver cells are a good example of this category. In the adult, there is normally little or no cell division, but if a large part of the liver is removed by surgery, the remaining cells are triggered to divide and make good the loss. Other examples in this category include the cells of the kidney and pancreas and of various glands, such as the adrenal, thyroid, and pituitary.

Group IV consists of the fixed postmitotic cells. The cells in this group are generally considered the most resistant to radiation. They are highly differentiated and appear to have lost the ability to divide. Some have a long life span, such as the neurons. Others have a short life span, such as the granulocytes, which have to be continually replaced by the division of more primitive cells. The superficial epithelial cells of the gut also fall into this category. In the normal course of events, they are sloughed off the tops of the villi and replaced by cells dividing in the crypts.

MICHALOWSKI'S H- AND F-TYPE POPULATIONS

Michałowski classified tissues as following either a “hierarchical” model or a “flexible” model. Within tissues, three distinct categories of cells can be identified. First are the **stem cells**, which are capable of unlimited proliferation and escape senescence because of telomere shortening by the enzyme telomerase. Examples include the crypt cells in the intestinal mucosa. The cells produced by stem cell proliferation both maintain the stem cell pool and provide candidates for differentiation. Second, at the other extreme, are **functional cells**, which are fully differentiated; they are usually incapable of further division and die after a finite life span, although the life span varies enormously among different cell types. Examples include circulatory granulocytes and the cells that make up the villi of the intestinal mucosa. Between these two extremes are **maturing partially differentiated cells**; these are descendants of the stem cells, still multiplying as they complete the process of differentiation. In the bone marrow, for example, the erythroblasts and granuloblasts represent intermediate compartments. Many tissues represent this **hierarchical** model (**H-type** populations), including the hematopoietic bone marrow, intestinal epithelium, and epidermis.

Other tissues, such as liver, thyroid, and dermis, are composed of cells that rarely divide under normal conditions but can be triggered to divide by damage to the tissue or organ. These **flexible tissues (F-type** populations) have no

compartments and no strict hierarchy. After damage to the tissue, all cells, including those that are functional, enter the cell cycle. The time interval before damage becomes evident is a function of dose. If the dose is small, the expression of damage is delayed because cells divide infrequently. Consequently, the damage may be hidden for a long time.

Many tissues are hybrids of these two extreme models, with most cells able to make a few divisions and a minority of the population behaving as stem cells.

GROWTH FACTORS

Radiation induces interleukin-1 as well as interleukin-6. Interleukin-1 acts as a radioprotectant of hematopoietic cells by increasing both the shoulder and the D_0 of the survival curve. **Basic fibroblast growth factor** induces endothelial cell growth, inhibits radiation-induced apoptosis, and therefore protects against microvascular damage. This growth factor is produced in response to stress (heat, hypoxia, chemicals, radiation) and tends to reduce late effects. Microvascular protection is more effective in branching midsize capillaries (in which higher concentrations of basic fibroblast growth factor are seen) than in nonbranching capillaries. To the extent that radiation-induced late effects are mediated by damage to blood vessels, radiation tolerance is high in organs with large blood vessels (corresponding to high levels of growth factors) and lower near nonbranching capillaries.

Platelet-derived growth factor β increases damage to vascular tissue. **Transforming growth factor β (TGF- β)** induces a strong inflammatory response—for example, in pneumonitis. It stimulates the growth of connective tissue and tends to inhibit epithelial cell growth. Consequently, fibrosis and vascular changes associated with late radiation effects are linked with this factor. TGF- β may downregulate interleukin-1 and **tumor necrosis factor (TNF)** and increase damage to hematopoietic tissue.

TNF is a cytotoxic agent that mediates the inflammatory response produced by monocytes and tumor cells by binding to cell-surface receptors that initiate signal transduction pathways. TNF induces proliferation of fibroblasts, inflammatory cells, and endothelial cells and so is associated with complications. In clinical trials, the administration of TNF causes fatigue, anorexia, weight loss, and transient leukopenia. TNF protects hematopoietic cells and sensitizes tumor cells to radiation. Serum concentrations of TNF correlate with severity of pneumonitis, hepatic dysfunction, renal insufficiency, and demyelination. TNF may contribute to the pathophysiology of radiation-induced central nervous

system symptoms. The expression of TNF following radiation is believed to be regulated at the transcriptional level and involves the protein kinase C-dependent pathway.

SPECIFIC TISSUES AND ORGANS

Table 20.2 is a compilation of tissue and organ sensitivities. Important examples will be discussed in turn.

Table 20.2 A Compilation of Tissue and Organ Sensitivities

	INJURY	TD _{5/5} , Gy	TD _{50/5} , Gy	FIELD SIZE
<i>Class I organs</i>				
Bone marrow	Aplasia, pancytopenia	2.5	4.5	Whole segment
Liver	Acute and chronic hepatitis	30 50	40 55	Whole 1/3
Intestine	Obstruction, perforation, fistula	40 50	55 60	Whole 1/3 or 1/2
Stomach	Perforation, ulcer, hemorrhage	50 60	65 70	Whole 1/3
Brain	Infarction, necrosis	45 60	60 75	Whole 1/3

Spinal cord	Infarction, necrosis	47 50	— 70	20 cm 5 or 10 cm
Heart	Pericarditis and pancarditis	40 60	50 70	Whole 1/3
Lung	Acute and chronic pneumonitis	17.5 45	24.5 65	Whole 1/3
Kidney	Acute and chronic nephrosclerosis	23 50	28 45	Whole 1/3 or 1/2
<i>Class II organs</i>				
Oral cavity and pharynx	Ulceration, mucositis	60	75	50 cm ²
Skin	Acute and chronic dermatitis, telangiectasia	55	65	100 cm ²
Esophagus	Esophagitis, ulceration	55 60	50 70	Whole 1/3
Rectum	Ulcer, stenosis, fistula	60	80	No volume effect
Salivary glands	Xerostomia	32	46	1/3 or 1/2

Bladder	Contracture	65	80	2/3	
		80	85	1/3	
Ureters	Stricture	70	100	5–10 cm length	
Testes	Sterilization	1	2	Whole	
Ovaries	Sterilization	2–3	6–12	Whole (age dependent)	
Growing child bone	cartilage, Growth dwarfing	arrest,	10	30	Whole
Mature cartilage, adult bone	Necrosis, sclerosis	fracture,	60 60	100 100	Whole 10 cm^2
Eye					
Retina	Blindness	45	65	Whole	
Cornea		50	6	Whole	
Lens	Cataract	10	18	Whole	
Endocrine					

Thyroid	Hypothyroidism	45	150	Whole
Adrenal	Hypoadrenalinism	60	—	Whole
Pituitary	Hypopituitarism	45	200	Whole
Peripheral nerves	Neuritis	60	100	—
Ear				
Middle	Serous otitis	30	40	No volume effect
Vestibular	Meniere syndrome	60	70	—
<i>Class III organs</i>				
Muscle				
Child	Atrophy	20	40	Whole
Adult	Fibrosis	60	80	Whole
Lymph nodes and Atrophy, sclerosis		50	70	Whole node

lymphatics				
Large arteries and Sclerosis veins		80	100	10 cm ²
Uterus	Necrosis, perforation	100	200	Whole
Vagina	Ulcer, fistula	90	100	Whole
Breast				
Child	No development	10	15	Whole
Adult	Atrophy, necrosis	50	100	Whole

Based on a combination of Rubin P, Casarett GW. *Clinical Radiation Pathology*. Vol. 1. Philadelphia, PA: W.B. Saunders; 1968; and Emami B, Lyman J, Broun A, et al. Tolerance of normal tissue to therapeutic irradiation. *Int J Radiat Oncol Biol Phys*. 1991;21:109–122, with permission. Table compiled by Dr. Richard Miller. The figures in this table are a guide only.

Skin

The skin is composed of the outer layer, the epidermis, which is the site of early radiation reactions, and the deeper layer, the dermis, which is the site of late radiation reactions ([Fig. 20.3](#)).

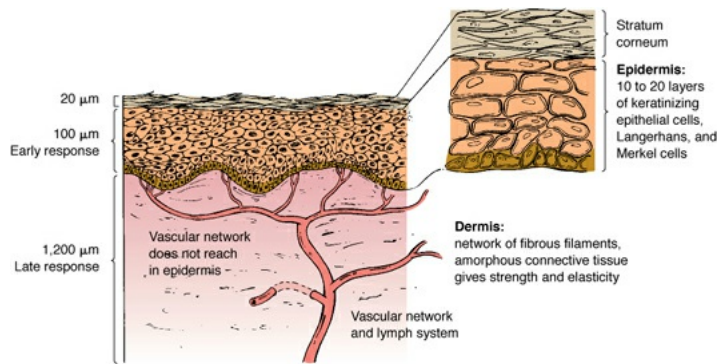


FIGURE 20.3 The skin from the perspective of a radiation biologist. The epidermis has a thickness of about $100\text{ }\mu\text{m}$, although it varies with body site (30 to $300\text{ }\mu\text{m}$). It consists of 10 to 20 layers of keratinizing epithelial cells. This is a self-renewing tissue. The stem cell compartment forms part of the basal layer and has an unlimited capacity for proliferation. Cells produced in the basal layer migrate to the surface, differentiating as they do so, but retaining some proliferative potential. Cells in the surface layer are fully differentiated and keratinized and gradually are sloughed off and lost. The transit time for an epidermal cell to pass from the basal layer to the surface is 12 to 48 days, depending on skin thickness. The dermis is about $1,200\text{ }\mu\text{m}$ thick (1,000 to 3,000 μm) and consists of a dense network of fibrous filaments and connective tissue. The vascular network, capillaries, and lymph system are in the dermis. The vascular network does not extend into the epidermis. Two distinct waves of reactions are observed in the skin following irradiation. An early, or acute, reaction is observed about 10 days after a single dose and results from damage to the epidermis. Late reactions occur months later, mediated through damage to the dermis, principally to the vasculature. In clinical radiation therapy, late damage is now the dose-limiting reaction because the buildup associated with megavoltage beams spares the epidermis.

The epidermis (30 to $300\text{ }\mu\text{m}$ thick) is derived from a basal layer of actively proliferating cells, which is covered by several layers of nondividing differentiating cells to the surface, at which the most superficial keratinized cells are desquamated. It takes about 14 days from the time a newly formed cell leaves the basal layer to the time it is desquamated from the surface. The target cells for radiation damage are the dividing stem cells in the basal layer.

The dermis is a dense connective tissue (1 to 3 mm thick) within which scattered fibroblasts produce most of the dermal proteins. The vasculature of the dermis plays a major role in the radiation response. The target cells are thus the fibroblasts and the vascular endothelial cells.

A few hours after doses greater than 5 Gy, there is an early erythema similar to sunburn, which is caused by vasodilation, edema, and loss of plasma constituents from capillaries. Reactions resulting from stem cell death take longer to develop. When orthovoltage (250-kV) x-rays were the modality commonly used, skin was frequently dose limiting because the full dose is deposited in the superficial layers. In this case, an erythema develops in the second to third week of a fractionated regimen, followed by dry or moist desquamation resulting from depletion of the basal cell population. At lower doses, islets of skin may regrow from surviving stem cells (see the model scoring system in mouse skin developed and described by Withers, described in [Chapter 19](#)); at higher doses, at which there are no surviving stem cells within the area treated, moist desquamation is complete, and healing must occur by migration of cells from outside the treated area.

With megavoltage x-ray equipment presently being used, the maximum dose (D_{max}) occurs at a depth from several millimeters to several centimeters below the skin surface, depending on the energy. Consequently, **epidermal** reactions usually are limited to dry desquamation and increased pigmentation. Conventional doses of 60 Gy or more are tolerated by the skin readily if they are spread out over 6 to 8 weeks because a substantial amount of stem cell proliferation can occur during this time. For skin, as for oral mucosa, the total dose tolerated depends more on overall time than on fraction size. Because for high-energy x-rays, D_{max} occurs at a depth below the surface, late damage may occur in the dermis in the absence of early reactions in the epidermis. The clinical appearance of radiation fibrosis results from atrophy, leading to contraction of the irradiated area. Telangiectasia developing more than a year after irradiation reflects late-developing vascular injury.

Skin Appendages: A Special Case

Within a few days after irradiation, the death of germinal cells results in hair dysplasia (i.e., short, thin hair). The proportion of dysplastic hair is dose dependent. Epilation occurs during the third week, and regrowth may occur after 1 to 3 months. Sebaceous glands are as sensitive as hair, but sweat glands are less radiosensitive. Regenerated skin may be dry and hairless. An objective measure of skin damage may be obtained by a determination of electrical conductivity, which is influenced by sweat production.

Hematopoietic System

Hematopoietic tissues are located primarily in the bone marrow, with 60%

located in the pelvis and vertebrae and the remainder in the ribs, skull, sternum, scapula, and proximal sections of the femur and humerus. A tiny fraction of stem cells are found in the circulation. In the normal healthy adult, the liver and spleen have no hematopoietic activity, but they can become active in some circumstances—for example, after partial body irradiation. The pluripotent stem cells go through a period of multiplication and maturation, followed by differentiation without division, before they become mature circulating blood elements of the various types.

The stem cells are particularly radiosensitive. The survival curve has little or no shoulder and a D_0 of slightly less than 1 Gy (see [Chapter 19](#)). There is little sparing from either fractionating the dose or lowering the dose rate. The transit time from stem cell to fully functioning cell, however, differs for the various circulatory blood elements, and these differences account for the complex changes in blood count seen after irradiation.

Blood Cell Counts after Total Body Irradiation

A dose as low as 0.3 Gy leads to a reduction in the number of lymphocytes because they are among the most sensitive cells in the body. After larger doses, the number of all blood cells is altered; lymphopenia is followed by granulopenia, then thrombopenia, and finally anemia.

Following a total body dose of 4 to 6 Gy, there is a temporary increase in the number of granulocytes because of the mobilization of the reserve pool, followed by a rapid fall by the end of the first week. The number then remains almost constant before falling again to a minimum value at 18 to 20 days after irradiation. After 1 week of aplasia, regeneration is rapid and takes place more or less simultaneously in platelets, reticulocytes, and granulocytes. After higher doses, the cell minimum is reached earlier and the period of aplasia lasts longer, increasing the possibility of hemorrhage and/or infection, which could prove fatal. At lower doses, around 1 Gy, the depression in granulocyte count is less marked and regeneration less rapid. The general pattern of the blood counts after a modest dose of radiation is illustrated in [Figure 20.4](#).

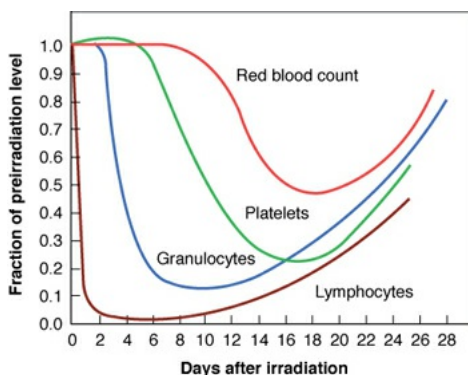


FIGURE 20.4 The pattern of depletion and recovery of the principal circulating elements of the blood following an intermediate dose of total body radiation. The curves are purely illustrative: The time at which the nadir occurs is a combination of the radiosensitivity of the stem cells and the lifetime of the mature functional cells.

The survival of stem cells determines the subsequent performance of the bone marrow after total body irradiation because in the first few hours, there is a sudden decrease in the number of pluripotent stem cells and progenitor cells. If the number of stem cells falls below a critical level, production of functional cells essentially stops until partial regeneration of the stem cell compartment occurs and differentiation is allowed to resume. Administration of hematopoietic growth factors can shorten the period of aplasia markedly and accelerate regeneration of all blood cells.

Partial Body Irradiation

In the irradiated volume, the effects of partial body irradiation are analogous to those following total body irradiation. In the unirradiated marrow, the stem cells start dividing within a few hours, and a compensatory hyperplasia attempts to maintain the total production of blood elements. There may also be an extension of hemopoiesis into the long bones, spleen, and liver, which are not normally hemopoietic in the adult human.

With fractionated radiation therapy, the pool of stem cells in the unirradiated volume falls progressively as differentiation is accelerated in an attempt to maintain the circulating blood count. Doses greater than about 30 Gy may cause permanent aplasia in the irradiated volume; hyperplasia and extension of the active bone marrow in the unirradiated volume may persist indefinitely.

Irradiation always reduces the number of stem cells in the bone marrow, and the return to normal may take a long time. This explains why patients remain sensitive to a new insult for months or even years following irradiation.

Radiation and Chemotherapy Agents

Some cytotoxic drugs act essentially on only those cells in cycle, and they have little effect on hematopoietic stem cells because 90% of them are out of cycle unless the marrow is regenerating following a previous insult. This explains why these drugs show extra toxicity if administered shortly after radiotherapy. The marrow of patients irradiated to a large volume is always more sensitive to cytotoxic drugs, partly because the pool of stem cells is reduced and partly because a greater proportion of stem cells are dividing actively.

The addition of chemotherapy may also have different effects on acute and late reactions. Although many chemotherapeutic agents are dose limited by their toxicity to rapidly proliferating tissues, such as gut mucosa and bone marrow, others (bleomycin, doxorubicin, and *cis*-platinum) have specific toxicities to slow turnover tissues, such as lung, heart, or kidney. The additive toxicities may therefore also differ for acute and late reactions of tissues included in the irradiated volume. (For more on chemotherapy, see [Chapter 27](#).)

Lymphoid Tissue and the Immune System

The immune system is composed of macrophages and lymphocytes. Macrophages are derived from the same progenitors as granulocytes. These give rise to monocytes, which are transformed into macrophages. This cell line is less radiosensitive than lymphocytes, which are derived, however, from the same pluripotent stem cells.

The B line gives rise to B lymphocytes and plasmocytes, which are responsible for humeral immunologic responses and have life spans of 7 weeks and 2 to 3 days, respectively. Cells of the T line pass through the thymus, where they mature to become T lymphocytes. These cells have a life span of about 5 months and are responsible for cellular immunity and for secreting lymphokines. There are also other types of lymphocytes, such as natural killer cells, which can recognize a cell undergoing stress with the need for antibodies or MHC I. They provide a rapid immune response.

Total body irradiation leads to a rapid fall in the number of circulating B and T lymphocytes, with the number returning to normal in a few weeks, depending on the dose. The lymphoid tissues (e.g., nodes, spleen) are very radiosensitive and are depleted of cells by quite small radiation doses. Lymphocytes are very radiosensitive largely because of apoptosis. B cells are more radiosensitive than T cells, and overall, their radiosensitivity, as measured by a clonogenic assay, is similar to that of hematopoietic stem cells.

The effect of irradiation on immune function is complex, depending on the volume irradiated and the number of surviving cells, as well as their capacity to migrate and become lodged in the microenvironment. Total body irradiation is used to inhibit the immune system in preparing patients for an organ transplant, such as a kidney or bone marrow transplant. A total body dose of 3.5 to 4.5 Gy inhibits the immune response against a new antigen, although it is much less effective against an antigen to which the individual is already sensitized. The graft-versus-host reaction after bone marrow transplantation is relatively radioresistant. Partial body irradiation, characteristic of ordinary radiation therapy, has only a limited effect on the immune response, and whether it influences metastatic dissemination is controversial. Total lymphoid irradiation to a dose of 30 to 40 Gy is used for the treatment of lymphomas and leads to a long-lasting T-cell lymphopenia. It can be used to treat autoimmune diseases and also to prepare patients for organ transplants.

Digestive Tract

Oral Mucosa

The cellular organization of the mucosa is similar to that of the skin in that cells multiply in the basal layer and then migrate toward the surface as they differentiate. The life span of the differentiated cells, however, is much shorter than in the epidermis, so there is a more rapid reaction to radiation. The intensity of early mucous membrane reactions is a major factor limiting daily and weekly dose accumulation in the treatment of cancer of the head and neck (see [Table 20.2](#)). For example, a schedule of 70 Gy delivered in 2-Gy fractions over 7 weeks leads to spotted-confluent mucositis in most patients, which approaches maximum tolerance if the schedule is accelerated to 5.5 weeks by, for example, the use of a concomitant boost technique.

The oral cavity contains various tissue types as well as the mucous membrane. The tongue consists of muscle bundles as well as mucosa with taste buds. The muscles undergo mild progressive fibrosis and fiber atrophy after irradiation. The tonsils are lymphatic tissues and function as sites of antigen process and recognition. Following radiation exposure to a maximum tolerance dose, desquamation of the oral cavity occurs by about day 12, with recovery in 2 to 3 weeks. Desquamation occurs first in the soft palate, followed by the hypopharynx, vallecula, floor of the mouth, cheeks, epiglottis, base of tongue, vocal chords, and dorsum of tongue.

The sequence of events that occurs during radiation therapy for head and

neck cancer is so important for the comfort and welfare of the patient that it is worth spelling out in detail. The order of events reflects the different kinetics of the cell populations involved:

First week: Asymptomatic to slight focal hyperemia and edema caused by dilatation of capillaries in sensitive patients. Sensitivity may be associated with alcohol or tobacco use, chemotherapy, infection (oral candidiasis, herpes simplex virus), or immunosuppression (HIV).

Second week: Increasing pain and loss of desire to eat. Sense of taste is altered; bitter and acid flavors are most changed, with less change with salty and sweet tastes. Erythema and edema increase, and early desquamative mucositis occurs. Basal cell division has been affected; this layer is being denuded, and vasculoconnective tissue damage becomes apparent. Mucositis is patchy.

Third week: Mucositis and swelling with depletion of gland secretions leading to difficulty in swallowing. Mucositis plaques are confluent.

Fourth week: Progression of signs. Confluent mucositis sloughs, resulting in denuded lamina propria. Mucosa becomes covered by fibrin and polymorphonuclear leukocytes.

Fifth week: Maximum radiation damage apparent by this time. Extreme sensitivity to touch, temperature, and grainy food. Recovery of epithelial layer may begin during therapy. Posttherapy, the basal cells migrate into the area and proliferate. In 2 to 4 weeks, complete resolution is observed. The serous acinar cells of the parotid and submaxillary salivary glands undergo interphase death, and hence salivary dysfunction appears after irradiation, with no threshold dose and little sparing by fractionation. Xerostomia is the main clinical effect that can interfere with nutrition, deteriorate oral hygiene, and predispose a patient to dental problems. TD_{5/5} (the tolerance dose for 5% complication in 5 years) is 32 Gy, and TD_{50/5} (the tolerance dose for 50% complication in 5 years) is 46 Gy. Impairment of taste acuity occurs during the third week of a multifraction radiotherapy regime.

Esophagus

The mucosa consists of rapidly dividing cells. After radiation, the esophagus displays an acute mucosal response of esophagitis and increased thickness of the squamous layer. Symptoms appear that include substernal burning with pain on swallowing at about 10 to 12 days after the start of therapy, with a return to

normal within a week of the end of therapy. Late effects are related to the muscle layer; they include necrosis and a thickening of the epithelium. This leads to symptoms of difficulty on swallowing and possibly ulcerations after high doses. The tolerance dose is 57.5 Gy in 10 fractions (acute effects limit).

Stomach

Irradiation of the stomach often causes nausea and vomiting immediately afterward. The precursor cells of the gastric glands give rise to mucin-secreting surface columnar cells with short life spans (about 3 or 4 days) and to acid-secreting parietal and pepsinogen-secreting chief cells that have long life spans (hundreds of days). The precursor cells are radiosensitive, and their death leads to early depletion of the surface columnar cell epithelium. Delayed gastric emptying and epithelial denudement are the two main early radiation effects. Peptic ulceration is seen in patients receiving more than 40 Gy to the upper abdomen.

Dyspepsia may be evident in 6 months to 4 years and gastritis in 1 to 12 months. Acute ulceration may occur shortly after the completion of treatment but rarely leads to perforation. At about 5 months, late ulceration and submucosal fibrosis leading to antral fibrosis may occur. Tolerance doses range from 40 to 50 Gy.

Small and Large Intestines

As with the skin and oral mucosa, both early and late complications are observed in the gastrointestinal tract. Acute mucositis frequently occurs, with symptoms such as diarrhea or gastritis, depending on the treatment field. If the dose is limited to 50 to 54 Gy in 2-Gy fractions, acute reactions are seldom dose limiting, and if they do occur, interruption of treatment for a few days usually alleviates the problem. Much more serious are the long-term late sequelae, which may develop either from persistent severe early reactions (consequential late effects) or independently of acute damage in the submucosal, muscular, or serosal layers.

In the small intestine, stem cells are located toward the bottom of the crypts of Lieberkühn. Atrophy of the villus occurs about 2 to 4 days postirradiation. Epithelial denudation is responsible for the acute gut reactions. A regenerative response appears rapidly, and within 2 to 4 days, microcolonies and macrocolonies are detectable. The surviving crypts have at least the same radiosensitivity to reirradiation as the unirradiated crypts, and very little dose is “remembered.”

Late bowel reactions involve all tissue layers and are caused by atrophy of the mucosa caused by vascular injury, with subsequent breakdown resulting from mechanical irritation and bacterial infection, which leads to an acute inflammatory response. In addition, overgrowth of the fibromuscular tissue with stenosis and serosal breakdown and adhesion formation may occur, which may be predisposed to by previous surgery and is related to inflammatory mediators. Fibrosis and ischemia are typical late effects. Tolerance dose is about 50 Gy for the small intestine and slightly higher for the large intestine. Rectal tolerance is about 70 Gy.

Lungs

The lung is an intermediate- to late-responding tissue. Two waves of damage can be identified: acute pneumonitis at 2 to 6 months after treatment, and fibrosis, which may develop slowly over a period of several months to years. The only symptom of early acute pneumonopathy may be an opacity on a chest x-ray, although it may be accompanied by functional signs, including cough, dyspnea, and respiratory difficulties. Progressive pulmonary fibrosis develops in most patients, including those who previously were asymptomatic, beginning about a year after irradiation.

Difficulties in respiratory function increase in severity with time and are generally irreversible. Their severity depends on three factors: volume irradiated, dose, and fraction size. The lung is particularly sensitive to fractionation, with an α/β estimated to be about 3 Gy. The most likely target cells are the pulmonary endothelial cells and the type II pneumocytes (cells of the alveolar wall). Type II cells are associated with the production of surfactant during the first few days after irradiation.

The lung is among the most sensitive of late-responding organs. The FSU in the lung is the pulmonary lobule, consisting of the terminal bronchioli and respiratory parenchyma that it serves. The FSUs are arranged in parallel, with a large number of bronchi and alveoli working together; consequently, volume as well as dose are important. Because of this organization of the FSUs, the lung is only dose limiting if large volumes are irradiated and if the remaining lung is not capable of providing adequate function.

Pulmonary damage also may occur following the use of chemotherapy agents, notably bleomycin, cyclophosphamide, and mustine. Combining radiation with these drugs reduces lung tolerance.

Kidneys

Together with the lung, the kidney is among the more radiosensitive late-responding critical organs (see [Table 20.2](#)). Irradiation of both kidneys to a modest dose of about 30 Gy in 2-Gy fractions results in nephropathy with arterial hypertension and anemia. Radiation damage develops slowly and may not become evident for years. Parts of one or even both kidneys can receive much higher doses. In contrast to most organs or tissues, increasing treatment time does not allow higher doses to be tolerated. FSUs are arranged in parallel, with each containing only about 1,000 stem cells. Damage to tubules, therefore, may result from sterilization of all the cells in a tubule.

Liver

In terms of radiosensitivity, the liver ranks immediately below the kidney and lung. It shares with these organs the fact that its FSUs are arranged in parallel, so that much larger doses are tolerated if only part of the organ is exposed. Taking a broader view, the liver is composed of both serial and parallel components. The liver parenchyma functions as a parallel FSU tissue, whereas the liver hilum where the bile duct, hepatic artery, and portal vein are centrally located functions as a serial FSU tissue. Damage to small volumes of the liver parenchyma can be tolerated, but damage to the bile duct will lead to dysfunctionality.

Liver tolerance is dose limiting only if the whole organ is irradiated, as in, for example, total body irradiation prior to bone marrow transplantation. The life span of a hepatocyte is about 1 year, so that, under normal conditions, the cell renewal rate in the liver is very slow. Even large doses apparently are tolerated for a few months, but then hepatic function deteriorates progressively. Fatal hepatitis may result from a fractionated protocol of only 35 Gy if the whole organ is irradiated.

Bladder Epithelium

The bladder epithelium consists of a basal layer formed of small diploid cells, covered by several layers of larger transitional cells and at the surface by a layer of very large polyploid cells with a thick membrane designed to resist the irritation caused by urine. Cell renewal rate is low, the superficial cells having a life span of several months. Because of this long life span, accelerated proliferation following irradiation does not begin for months. Senescence of the differentiated functional cells then reveals latent damage in the basal layer.

Frequency of urination increases in parallel with bladder damage and loss of surface cells. The absence of these surface cells explains the irritation by urine of the deeper cellular layers, leading to stimulation of cellular proliferation. Subsequent late effects are related to fibrosis and reduction in bladder capacity.

Central and Peripheral Nervous Systems

The nervous system is less sensitive to radiation than other late-responding organs and tissues such as the kidney or lung. Although tolerance doses are frequently quoted at the 5% complication level (i.e., TD₅), wide margins of safety in dose usually are included because damage to these tissues results in severe consequences, including paralysis.

Brain

Three main categories of cells are involved: neurons, vascular endothelial cells, and glial cells. Neurons are nonproliferating end cells in adults; glial cells have a slow rate of turnover, with a small precursor (stem cell) compartment of only about 1%. Endothelial cells also have a slow turnover but can proliferate rapidly after injury. The most important injuries to the brain by radiation are all late syndromes, developing months to years after exposure. Some reactions occur within the first 6 months, including transient demyelination (somnolence syndrome) or the much more serious leukoencephalopathy. Typical radiation necrosis may become evident as early as 6 months but may be delayed as long as 2 to 3 years. Histopathologic changes that occur within the first year are most likely to involve white matter, whereas for times beyond 6 to 12 months, the gray matter usually shows changes accompanied by vascular lesions such as telangiectasia and focal hemorrhages. A mixture of histologic characteristics is likely to be associated with radionecrosis, which manifests from 1 to 2 years postirradiation, accompanied by cognitive defects.

Spinal Cord

Radiation-induced changes in the spinal cord are similar to those seen in the brain as far as latency, tolerance dose, and histology are concerned. Lhermitte's sign is a demyelinating injury that develops early, by several months after treatment, persists for a few months to a year, but is usually reversible. It may occur at doses as low as 35 Gy, well below the tolerance dose for permanent radiation myelopathy, and its appearance does not predict later more serious problems.

Late damage includes two principal syndromes. The first, occurring from

about 6 to 18 months, involves demyelination and necrosis of the white matter; the second is mostly a vasculopathy and has a latency of 1 to 4 years.

For the spinal cord, the TD_{5/5} is about 50 Gy for a 10-cm length irradiated and 55 Gy for a 5-cm length. By 70 Gy, the incidence of myelopathy would be about 50%.

The tolerance dose to the spine shows little dependence on overall treatment time, at least for protocols of conventional length up to 10 weeks. By contrast, tolerance depends critically on dose per fraction. Lower doses per fraction reduce the risk of late effects, but if two doses per day are used, the time between fractions must be at least 6 hours (and preferably more) because the repair of sublethal damage is slow in this tissue. There is evidence of two components of repair, one with a halftime less than 1 hour and one with a halftime close to 4 hours. The spinal cord is the clearest example of a tissue in which FSUs are arranged in series. The probability of a myelopathy depends critically on the length irradiated for very small lengths, but once the length of the field exceeds a few centimeters, the treatment volume has little effect.

Caution must be exercised in combining radiation with chemotherapy agents because neurotoxic agents such as methotrexate, cis-platinum, vinblastine, and AraC reduce the tolerance to radiation delivered simultaneously or sequentially.

As far as retreatment is concerned, animal data suggest that by about 2 years, most of the damage from a prior exposure has been repaired; the extent of the repair depends very much on the level of the initial injury.

Peripheral Nerves

Radiation injury of peripheral nerves is probably more common than effects on the spinal cord. It is often said that peripheral nerves are more radioresistant than the cord or brain, but there are few quantitative data to support this. A dose of 60 Gy in a conventional regimen of 2-Gy fractions may lead to a 5% probability of injury, with the probability rising steeply thereafter with increasing dose.

Testes

The seminiferous tubules are composed of two types of cells: Sertoli cells, which secrete a hormone that controls the secretion of follicle-stimulating hormone by the hypophysis, and the germinal cells, the hierarchy of which is strictly defined. The stem cells, the type A spermatogonia, have a long cell cycle and divide infrequently. The process of differentiation proceeds through several types of spermatogonia to the spermatocytes, which are the cells in which meiosis occurs.

Each spermatocyte gives rise to four spermatids, which finally result in spermatozoa. In humans, the transit time from stem cell to spermatozoa is about 74 days. There is considerable cell loss along the way, so that the amplification factor is much less than might be calculated from the number of divisions that occur.

Leydig cells, which secrete testosterone, also are found in the testis, and their function is regulated by pituitary gonadotropins, prolactin, and luteinizing hormone. This is important in the use of neoadjuvant hormone therapy during the treatment of prostatic cancer.

In humans, a dose as low as 0.1 Gy leads to a temporary reduction in the number of spermatozoa, and 0.15 Gy leads to temporary sterility. Azoospermia lasting for several years occurs after 2 Gy, and permanent azoospermia occurs after about 6 to 8 Gy in 2-Gy fractions. On the other hand, even much larger doses have little effect on the Leydig cells in the adult, so that although irradiation of the testes may lead to sterility, it has little or no effect on the libido.

The stem cells appear to be more radiosensitive than the differentiating spermatogonia, which explains why the duration of azoospermia increases as the dose is increased. Fractionated or continuous low dose-rate irradiation is more effective than a single acute exposure because a large proportion of the stem cells are in a radioresistant phase of the cell cycle. If irradiation is protracted, it affects stem cells as they move through the cell cycle into more radiosensitive phases. This accounts for the long-lasting azoospermia seen after relatively low daily doses of scattered radiation reaching the testes during irradiation of the pelvis and also the occurrence of testicular dysfunction seen after years of occupational exposure to ionizing radiation.

Several cytotoxic drugs have substantial effects on spermatogenesis. For example, the alkylating agents included in MOPP (mechlorethamine [Mustargen], vincristine [Oncovin], procarbazine, and prednisone), the combination of chemotherapy agents used at one time for the treatment of Hodgkin lymphoma, led to sterility in almost all patients. Of course, the drug treatment was prolonged and simulated low dose-rate irradiation, killing stem cells as they came into cycle.

Ovaries

The effects of radiation on the ovaries are quite different from those on the testes because after the fetal stage, the oocytes no longer divide. They are all present at birth, and their number diminishes steadily with age, reaching zero by the time

of menopause. Oocytes are extremely radiosensitive to cell killing; like lymphocytes, they die in interphase death, with a D_0 of only 0.12 Gy. There is little effect of fractionation. Mature follicles and those in the process of maturation are damaged equally by radiation so that sterilization is immediate (i.e., there is no latent period, as in the male). Because hormonal secretion is associated with follicular maturation, sterilization by radiation leads to a loss of libido and all of the changes associated with menopause.

Female Genitalia

The skin of the vulva reacts like skin elsewhere but because of moisture and friction, a tolerance dose of 50 to 70 Gy in conventional fractions is considered on the high side.

Acute effects of irradiation of the vagina include erythema, moist desquamation, and confluent mucositis, leading to the loss of vaginal epithelium that may persist for 3 to 6 months. Gross abnormalities in the vagina may include pale color, a thin atrophic mucosa, inflammation, and tissue necrosis with ulceration leading to a fistula. Tolerance doses, however, are high: 90 Gy before ulceration and 100 Gy for the development of a fistula. From intracavitary treatments, doses to the cervix and uterus may reach as high as 200 Gy. Effects seen include atrophy of the endometrial glands and stroma as well as ulceration.

Blood Vessels and the Vascular System

The effects of radiation on blood vessels are particularly important because late damage to many different tissues and organs is mediated to some extent by effects on the vasculature. Blood vessels have a complex structure. A monolayer of endothelial cells lines the interior surface, resting on connective tissue, the thickness of which depends on the type of vessel. Under normal circumstances, the rate or proliferation of endothelial cells is low, so that following exposure to radiation, cell loss occurs over a period as cells enter mitosis. Regions of constriction appear because of the abnormal proliferation of surviving cells. Denudation of the surface of blood vessels leads to the formation of thromboses and capillary necroses. In the smooth muscle cells that make up the wall of blood vessels, the proportion of cells cycling is very low, so that it takes several years for the number of cells to diminish significantly following irradiation. The loss of muscular fibers plays an important role in the development of late damage that may become evident several years later. Muscle cells are replaced by collagen fibers, vessel walls lose their elasticity, and blood flow is diminished.

Arterial damage may occur after doses of 50 to 70 Gy delivered in conventional fractionation patterns, but capillaries are damaged by doses above about 40 Gy. In general, veins are less sensitive to radiation than arteries.

Heart

In its tolerance to radiation, the heart is intermediate between the kidney or lung and the central nervous system. The most common radiation-induced heart injury is acute pericarditis, which seldom occurs during the first year posttherapy. It varies in severity from transient pericarditis, which runs a benign course, to dense sclerosis with cardiac constriction. Anterior chest pain with shortness of breath and low-grade fever may be observed. The threshold dose may be as low as 20 Gy if more than 50% of the heart is irradiated but higher for partial exposure. A dose of 45 to 50 Gy in conventional fractions produces an 11% incidence. The α/β ratio for the heart is low (about 1 Gy), so that fractionation results in a substantial sparing effect.

Radiation-induced cardiomyopathy results from dense and diffuse fibrosis; it is a slowly evolving lesion that develops over a period of many years and leads to impaired function. Reduced cardiac function is seen in some patients with Hodgkin disease who receive a dose of about 30 Gy to most of the heart. Protection of part of the heart greatly reduces the incidence of symptoms.

The chemotherapy agent doxorubicin (Adriamycin) increases the severity of radiation-induced complications. In addition, Adriamycin may reveal latent radiation damage many years after radiation therapy.

Bone and Cartilage

In children, growing cartilage is particularly radiosensitive. Doses as low as 10 Gy can slow growth because of the death of chondroblasts. Above about 20 Gy, the deficit in growth is irreversible. The effects of radiation on bone growth are more serious for higher doses and for younger ages. Sequelae are particularly serious in children younger than 2 years of age, and radiation can affect stature adversely up to the time of puberty.

In the adult, osteonecrosis of the lower maxilla may be a serious complication following radiation therapy for cancer of the buccal cavity. The TD_{5/5} is 50 to 60 Gy; the TD_{50/5} is about 70 Gy for large irradiated volumes. Fractures of the humeral and femoral head are observed if the dose, in conventional fractions, is high. The TD_{5/5} is 52 Gy and the TD_{50/5} is 65 Gy. Fractures of the ribs and clavicle are sometimes seen in patients receiving

radiotherapy for breast cancer but are generally not serious complications.

QUANTITATIVE ANALYSIS OF NORMAL TISSUE EFFECTS IN THE CLINIC

Over the past several decades, with the development of more sophisticated three-dimensional treatment planning systems, numerous studies in the literature have reported associations between dosimetric parameters and normal tissue outcomes. The Quantitative Analysis of Normal Tissue Effects in the Clinic (QUANTEC) article, which appeared in the *International Journal of Radiation Oncology, Biology, and Physics* in 2010, summarized the available data in a clinically useful format. **Table 20.3** is the summary table from that publication. The authors concede that the data are far from ideal and that there are many limitations. First and foremost is the fact that the information is extracted largely from publications. Beyond that, there is the problem of evolving fractionation schemes, combined modality therapy, host factors, and so on. For all of these reasons, care must be taken when applying the QUANTEC data in the clinic. It is intended to be an update of the data published by Emami and colleagues in 1991, which is widely used despite the fact that it has often been criticized.

Table 20.3 QUANTEC Summary Table: Approximate Dose/Volume/Outcome Data for Several Organs Following Conventional Fractionation (Unless Otherwise Noted)^a

ORGAN	VOLUME SEGMENTED	IRRADIATION TYPE (PARTIAL ORGAN UNLESS OTHERWISE STATED) ^b	END POINT	DOSE (GY), DOSE/VOLUME PARAMETERS ^b	OR RATE (%)	NOTES ON DOSE/VOLUME PARAMETERS
Brain	Whole organ	3D-CRT	Symptomatic necrosis	D _{max}	<60	<3
	Whole organ	3D-CRT	Symptomatic necrosis	D _{max}	72	5
	Whole organ	3D-CRT	Symptomatic	D _{max}	90	10

			necrosis				
	Whole organ	SRS fraction)	(single Symptomatic necrosis	V12	<5–10 cc	<20	Rapid rise when V12 >5–10 cc
Brain stem	Whole organ	Whole organ	Permanent cranial neuropathy or necrosis	D _{max}	<54	<5	
	Whole organ	3D-CRT	Permanent cranial neuropathy or necrosis	D1–10 cc ^e	≤59	<5	
	Whole organ	3D-CRT	Permanent cranial neuropathy or necrosis	D _{max}	<64	<5	Point dose <<1 cc
	Whole organ	SRS fraction)	Permanent cranial neuropathy or necrosis	D _{max}	<12.5	<5	For patients with acoustic tumors
Optic nerve/chiasm	Whole organ	3D-CRT	Optic neuropathy	D _{max}	<55	<3	Given the small size, 3D-CRT is often whole organ ⁱ
	Whole organ	3D-CRT	Optic neuropathy	D _{max}	= 55–60	3–7	
	Whole organ	3D-CRT	Optic neuropathy	D _{max}	>60	>7–20	
	Whole organ	SRS fraction)	Optic neuropathy	D _{max}	<12	<10	
Spinal cord	Partial organ	3D-CRT	Myelopathy	D _{max}	50	0.2	Including full cord cross section

	Partial organ	3D-CRT	Myelopathy	D_{max}	60	6	
	Partial organ	3D-CRT	Myelopathy	D_{max}	69	50	
	Partial organ	SRS (single fraction)	Myelopathy	D_{max}	13	1	Partial cord cross section irradiated
	Partial organ	SRS (hypofraction)	Myelopathy	D_{max}	20	1	3 fractions, partial cord cross section irradiated
Cochlea	Whole organ	3D-CRT	Sensory neural hearing loss	Mean dose	≤ 45	<30%	Mean dose to cochlear, hearing at 4 kHz
	Whole organ	SRS (single fraction)	Sensory neural hearing loss	Prescription dose	≤ 14	<25%	Serviceable hearing
Parotid	Bilateral whole parotid glands	3D-CRT	Long-term salivary function reduced to <25% of pre-RT level	Mean dose	<25	<20%	For combined parotid glands ^f
	Unilateral whole parotid gland	3D-CRT	Long-term parotid salivary function reduced to <25% of pre-RT level	Mean dose	<20	<20%	For single parotid gland At least one parotid gland spared to less than 20 Gy ^f
	Bilateral whole parotid glands	3D-CRT	Long-term parotid salivary function reduced to <25% of pre-RT level	Mean dose	<39	<50%	For combined parotid glands (per figure 3 in paper) ^f

Pharynx	Pharyngeal constrictors	Whole organ	Symptomatic dysphagia and aspiration	Mean dose	<50	<20	Based on Section B4 of paper
Larynx	Whole organ	3D-CRT	Vocal dysfunction	D _{max}	<66	<20	With chemotherapy, based on single study (see Section A4.2 in paper)
	Whole organ	3D-CRT	Aspiration	Mean dose	<50	<30	With chemotherapy, based on single study (see Fig. 1 of paper)
	Whole organ	3D-CRT	Edema	Mean dose	<44	<20	Without chemotherapy, based on single study in patients without larynx cancer ^g
	Whole organ	3D-CRT	Edema	V50	<27%	<20	
Lung	Whole organ	3D-CRT	Symptomatic pneumonitis	V20	≤30%	<20	For combined lung; gradual dose response
	Whole organ	3D-CRT	Symptomatic pneumonitis	Mean dose	7	5	Excludes purposeful whole lung irradiation
	Whole organ	3D-CRT	Symptomatic pneumonitis	Mean dose	13	10	

	Whole organ	3D-CRT	Symptomatic pneumonitis	Mean dose	20	20	
	Whole organ	3D-CRT	Symptomatic pneumonitis	Mean dose	24	30	
	Whole organ	3D-CRT	Symptomatic pneumonitis	Mean dose	27	40	
Esophagus	Whole organ	3D-CRT	Grade ≥ 3 acute esophagitis	Mean dose	<34	5–20	Based on RTOG and several studies
	Whole organ	3D-CRT	Grade ≥ 2 acute esophagitis	V35	<50%	<30	Various alternate threshold doses have been implicated.
	Whole organ	3D-CRT	Grade ≥ 2 acute esophagitis	V50	<40%	<30	
	Whole organ	3D-CRT	Grade ≥ 2 acute esophagitis	V70	<20%	<30	Appears to be a dose/volume response
Heart	Pericardium	3D-CRT	Pericarditis	Mean dose	<26	<15	Based on single study
	Pericardium	3D-CRT	Pericarditis	V30	<46%	<15	Overly safe risk estimates based on model predictions
	Whole organ	3D-CRT	Long-term cardiac mortality	V25	<10%	<1	

Liver	Whole GTV	liver– organ	3D-CRT or whole organ	Classical RILD ^h	Mean dose	<30–32	<5	Excluding patients with preexisting liver disease or hepatocellular carcinoma because tolerance doses are lower in these patients
	Whole GTV	liver– organ	3D-CRT	Classical RILD	Mean dose	<42	<50	
	Whole GTV	liver– organ	3D-CRT or whole organ	Classical RILD	Mean dose	<28	<5	In patients with Child-Pugh A preexisting liver disease or hepatocellular carcinoma,
	Whole GTV	liver– organ	3D-CRT	Classical RILD	Mean dose	<36	<50	excluding hepatitis B reactivation as an end point
	Whole GTV	liver– organ	SBRT (hypofraction)	Classical RILD	Mean dose	<13	<5	3 fractions, for primary liver cancer
						<18	<5	6 fractions, for primary liver cancer
	Whole GTV	liver– organ	SBRT (hypofraction)	Classical RILD	Mean dose	<15	<5	3 fractions, for liver metastases
						<20	<5	6 fractions, for liver metastases
	>700 cc of normal liver	liver– organ	SBRT (hypofraction)	Classical RILD	Mean dose	<15	<5	Critical volume based in 3–5 fractions

Kidney	Bilateral whole kidney ^c	Bilateral organ or 3D-CRT	Clinically relevant renal dysfunction	Mean dose	<15–18	<5	
	Bilateral whole kidney ^c	Bilateral organ	Clinically relevant renal dysfunction	Mean dose	<28	<50	
	Bilateral whole kidney	3D-CRT	Clinically relevant renal dysfunction	V12	<55%	<5	For combined kidney
				V20	<32%		
				V23	<30%		
				V28	<20%		
Stomach	Whole organ	Whole organ	Ulceration	D100 ^e	<45	<7	
Small bowel	Individual small bowel loops	3D-CRT	Grade ≥3 acute toxicity ^d	V15	<120 cc	<10	Volume based on segmentation of the individual loops of bowel, not the entire potential space within the peritoneal cavity
	Entire potential space within peritoneal cavity	3D-CRT	Grade ≥3 acute toxicity ^d	V45	<195 cc	<10	Volume based on the entire potential space within the peritoneal cavity
Rectum	Whole organ	3D-CRT	Grade ≥2 late rectal toxicity	V50	<50%	<15	

		3D-CRT	Grade ≥3 late rectal toxicity		<10		
	Whole organ	3D-CRT	Grade ≥2 late V60 rectal toxicity	<35%	<15		
		3D-CRT	Grade ≥3 late rectal toxicity		<10	Prostate cancer treatment	
	Whole organ	3D-CRT	Grade ≥2 late V65 rectal toxicity	<25%	<15		
		3D-CRT	Grade ≥3 late rectal toxicity		<10		
	Whole organ	3D-CRT	Grade ≥2 late V70 rectal toxicity	<20%	<15		
		3D-CRT	Grade ≥3 late rectal toxicity		<10		
	Whole organ	3D-CRT	Grade ≥2 late V75 rectal toxicity	<15%	<15		
		3D-CRT	Grade ≥3 late rectal toxicity		<10		
Bladder	Whole organ	3D-CRT	Grade ≥3 late D _{max} RTOG	<65	<6	Bladder cancer treatment	
						Variations in	

							bladder size/shape/location during RT hamper ability to generate accurate data
	Whole organ	3D-CRT	Grade RTOG	≥ 3 late	V65	$\leq 50\%$	
					V70	$\leq 35\%$	Prostate cancer treatment
					V75	$\leq 25\%$	Based on current RTOG 0415 recommendation
					V80	$\leq 15\%$	
Penile bulb	Whole organ	3D-CRT	Severe dysfunction	erectile Mean dose to 95% of gland	<50	<35	
	Whole organ	3D-CRT	Severe dysfunction	erectile D90 ^e	<50	<35	
	Whole organ	3D-CRT	Severe dysfunction	erectile D60–70	<70	<55	

^aAll data are estimated from the literature summarized in the QUANTEC reviews (unless otherwise noted). Clinically, these data should be applied with caution. Clinicians are strongly advised to use the individual QUANTEC articles to check the applicability of these limits to the clinical situation at hand. They largely do not reflect modern IMRT.

^bAll at standard fractionation (i.e., 1.8–2.0 Gy per daily fraction) unless otherwise noted.

^cNon-TBI

^dWith combined chemotherapy

^eDx, minimum dose received by the “hottest” \times % (or \times cc’s) of the organ

^fSevere xerostomia is related to additional factors including the doses to the submandibular glands.

^gEstimated by Dr. Eisbruch

^hClassic RT-induced liver disease (RILD) involves anicteric hepatomegaly and ascites, typically occurring between 2 weeks to 3 months after therapy. Classic RILD also involves elevated alkaline phosphatase (more than twice the upper limit of normal or baseline value).

ⁱFor optic nerve, the cases of neuropathy in the 55–60 Gy range received ~59 Gy (see optic nerve paper for details). Excludes patients with pituitary tumors where the tolerance may be reduced.

LATE EFFECTS OF NORMAL TISSUE AND SOMA

The two large organizations that initiate and coordinate multicenter clinical trials in Europe and North America, namely, the European Organisation for Research and Treatment of Cancer (EORTC) and the Radiation Therapy Oncology Group (RTOG), formed working groups to update their system for assessing late injury to normal tissues. This led to the **Late Effects of Normal Tissue (LENT)** conference in 1992. This conference led to the introduction of the **SOMA** classification for late toxicity. SOMA is an acronym for subjective, objective, management criteria with analytic laboratory and imaging procedures. These scales, specific for each organ, form a scaffold for understanding the expression of later injury because they are the substance of LENT expression. The SOMA scales have been formulated for all anatomic sites listed in [Table 20.4](#). An example for the central nervous system is given in [Table 20.5](#).

Table 20.4 Anatomic Sites for which There Are Late Effects of Normal Tissue and SOMA Scales

Central nervous system
Brain
Spinal cord
Male hypothalamic/pituitary/gonadal axis

Female hypothalamic/pituitary/gonadal axis

Head and neck

Eye

Ear

Mucosa

Mandible

Teeth

Larynx

Thyroid and hypothalamic/pituitary/thyroid axis

Breast

Heart

Blood vessels

Lung

Gastrointestinal system

Esophagus

Stomach

Small intestine and colon

Rectum

Major digestive glands

Liver

Genitourinary system

Kidney

Ureter

Bladder/urethra

Testes

Male sexual dysfunction

Gynecologic system

Vulva

Vagina

Uterus/reproductive organs

Female sexual dysfunction

Bone, muscle, and skin

Muscle/soft tissue

Peripheral nerves

Growing bone

Mature bone (excluding mandible)

Bone marrow
Skin/subcutaneous tissue

Based on Rubin P, Constine LS, Fajardo LF, et al. Late Effects of Normal Tissues Consensus Conference. San Francisco, California, August 26–28, 1992. *Int J Radiat Oncol Biol Phys.* 1995;31:1035–1367.

Table 20.5 Central Nervous System SOMA

SUBJECTIVE	OBJECTIVE	MANAGEMENT	ANALYTIC
Headache	Neurologic deficit	Anticonvulsives	MRI
Somnolence	Cognitive function	Steroids	CT
Intellectual deficit	Mood and personality changes	Sedation	MRS PET
Functional competence	Seizures		Magnetic mapping
Memory			Serum Cerebrospinal fluid

Abbreviations: MRI, magnetic resonance imaging; CT, computed tomography; MRS, magnetic resonance spectroscopy; PET, positron emission tomography.

Based on Rubin P, Constine LS, Fajardo LF, et al. Late Effects of Normal Tissues Consensus Conference. San Francisco, California, August 26–28, 1992. *Int J Radiat Oncol Biol Phys.* 1995;31:1035–1367.

The SOMA Scoring System

The SOMA scales have been designed to allow the acquisition of data by several different methods, which it is hoped are not inevitably dependent one upon the other:

Subjective—in which the injury, if any, will be recorded from the subject's point of view, that is, as perceived by the patient. This information can be elicited during interviews or derived by asking the patient to complete a carefully designed questionnaire or diary.

Objective—in which the morbidity is assessed as objectively as possible by the clinician during a clinical examination. In this case, the clinician may be able to detect signs of tissue dysfunction that are still below the threshold that will give the patient symptoms but are an indication of how close to tissue tolerance the treatment is or that may be early indicators of more serious problems that are developing and will be expressed later.

Management—which indicates the active steps that may be taken in an attempt to ameliorate the symptoms.

Analytic—involving tools by which tissue function can be assessed even more objectively or with more biologic insight than by simple clinical examination. It is recognized that the tools available for such analysis may differ widely from one center to another and may evolve as the clinical trials progress. The invasiveness and cost of any tool used to quantify the late effects must be reasonable and proportional to the severity of the symptoms and the possible therapeutic consequences. The scales list the techniques that could yield valuable data, but it is not envisaged that all such tests would be feasible or even desirable in all studies.

The grading categories in the LENT and SOMA scoring system are shown in **Table 20.6**. There is no grade 0 because that would indicate no effect, and no grade 5 because that would indicate totality, or loss of an organ or function.

Table 20.6 Late Effects of Normal Tissue and SOMA Scoring System and Grading Categories

GRADE 1	GRADE 2	GRADE 3	GRADE 4

Subjective: ascending order of severity of symptoms perceived by patient (e.g., pain)			
Occasional and minimal	Intermittent and tolerable	Persistent intense	and Refractory and excruciating
Objective: signs that can be assessed by clinician (e.g., neurologic deficit)			
Barely detectable	Easily detectable	Focal motor signs, Hemiplegia, vision disturbances, hemisensory deficit, etc.	etc.
Management: active steps taken to ameliorate symptoms (e.g., pain)			
Occasional nonnarcotic	Regular nonnarcotic	Regular narcotic	Surgical intervention
Analytic: findings that are quantifiable (e.g., CT and MRI, special laboratory tests)			

Abbreviations: CT, computed tomography; MRI, magnetic resonance imaging.

Based on Rubin P, Constine LS, Fajardo LF, et al. Late Effects of Normal Tissues Consensus Conference. San Francisco, California, August 26–28, 1992. *Int J Radiat Oncol Biol Phys.* 1995;31:1035–1367.

APPLICATION OF STEM CELLS TO REGENERATE

RADIATION-SENSITIVE GLAND REGENERATION

ORGANS—SALIVARY

No matter how much effort is put into sparing normal tissue toxicity, invariably certain tissues cannot be spared and are subject to radiation-induced damages. In the treatment of head and neck cancer, a major complication of normal tissues is loss of salivary gland function, resulting in xerostomia. Salivary glands can be considered a radiation-sensitive tissue that differs from other radiation-sensitive tissues in not being rapidly proliferating and is well differentiated. Furthermore, the contralateral gland does not compensate for loss of function of the irradiated gland. The clinical response of the salivary gland differs in different individuals with doses as low as 10 Gy, leading to a marked reduction in salivary excretion. The variation in radiosensitivity of salivary glands is not well understood but seems to involve apoptotic cell death.

Over the years, different approaches have been used to prevent or restore salivary gland function, including radioprotectors, *in situ* manipulation of ductal cells, and implantation of an artificial salivary gland. All of these past approaches have met with failure or have failed to be clinically adopted. These past failures and the advent of stem cell biology has brought forth the possibility of using autologous stem cell transfer as a means of regenerating salivary glands after the completion of radiotherapy. Experimentally, salivary stem cells have been isolated, cultured *in vitro*, and reinjected into mice after irradiation. These reinjected stem cells were shown to repopulate the salivary glands and increased the salivary production of these mice. Therefore, the proof of concept experiment in rodents has demonstrated the feasibility of such an approach. Although this is an exciting result, there is still work that needs to be addressed to apply this to head and neck cancer patients. First, the *in vitro* culture of salivary stem cells needs to take place at least for several months, and the spontaneous differentiation of these cells in cell culture must be prevented. Second and probably more problematic is overcoming radiation-induced fibrosis in the area of the exposed gland. Both of these problems are not insurmountable as better culture methods are being developed to prevent stem cell differentiation *in vitro*, and small molecule inhibitors of fibrosis are making their way into clinical trials. Thus, the first application of stem cell biology to regenerate irradiated salivary glands and restore their function will most likely occur within the next decade.

SUMMARY OF PERTINENT CONCLUSIONS

Most effects of radiation on normal tissues are caused by cell killing, but some, such as nausea, vomiting, or fatigue experienced by patients following irradiation of large volumes including the abdomen, may be mediated by radiation-induced inflammatory cytokines.

Apparent radioresponsiveness of a tissue depends on inherent sensitivity of cells, kinetics of the tissue or cell population, and the way cells are organized in that tissue.

Sensitivity of actively dividing cells is expressed by their survival curve for reproductive integrity.

The radiation dose needed to destroy the functioning ability of a differentiated cell is far greater than that necessary to stop the mitotic activity of a dividing cell.

The shape of the dose-response relationship for functional end points, obtained from multifraction experiments, is more pertinent to radiotherapy than clonogenic assays.

The time interval between irradiation and its expression in tissue damage depends on the life span of mature functional cells and the time it takes for a cell born in the stem compartment to mature.

Hyperthermia damage is expressed early compared with radiation damage (see [Chapter 28](#)).

Both early and late effects may develop in one organ system because of injury to different target cell populations or tissue elements.

The α/β ratio (the dose at which the linear and quadratic components of radiation damage are equal) may be inferred from multifraction experiments in systems scoring nonclonogenic end points.

Tolerance doses for late effects are more sensitive to changes in dose per fraction (low α/β value) compared with tolerance doses for early effects.

Spatial arrangement of FSUs is critical to the tolerance of some normal tissues.

In some tissues (e.g., spinal cord), the FSUs are arranged serially (like links in a chain), and the integrity of each is critical to organ function.

Tissues with a serial organization (e.g., spinal cord) have little or no functional reserve, and the risk of developing a complication is less dependent on volume irradiated than for tissues with a parallel organization. The risk of complication is strongly influenced by high-dose regions and hot spots.

A tissue with intrinsically high tolerance may fail as a result of the inactivation of a small segment (as in the spinal cord); a tissue with an intrinsically low tolerance (kidney and lung) may lose a substantial number of its functional units without impact on clinical tolerance.

Casarett's classification of tissue radiosensitivity is based on histopathologic observations.

In terms of radiosensitivity based on histologic observation of cell death, parenchymal cells fall into four categories, from most sensitive to most resistant:

1. Stem cells of classic self-renewal tissues, which divide regularly
2. Differentiating intermitotic cells, which divide regularly but in which there is some differentiation between divisions and which are variably differentiated
3. Reverting postmitotic cells, which do not divide regularly but can divide under the appropriate stimulus
4. Fixed postmitotic cells, which are highly differentiated and appear to have lost the ability to divide

Connective tissue and blood vessels are intermediate in radiosensitivity between groups II and III.

Michalowski's classification divides tissues into H- and F-type populations, which respond differently to radiation.

Many tissues are a hybrid of H- and F-type.

The response of a tissue is influenced greatly by a host of growth factors, including interleukin-1 and 6, basic fibroblast growth factor, platelet-derived growth factor β , TGF- β , and TNF.

Early radiation response in the skin is caused by damage to the epidermis; the late response reflects damage to the dermis.

The hematopoietic system is very sensitive to radiation, especially the stem cells. The complex changes seen in peripheral blood count after irradiation reflect differences in transit time from stem cell to functioning cell for the various circulatory blood elements.

The effect of irradiation on the immune function is complex, depending on the volume irradiated and the number of surviving cells. A total body dose of 3.5

to 4.5 Gy inhibits the immune response against a new antigen.

The cellular organization of the lining of the gastrointestinal tract is similar to that of the skin, but the life span of the differentiated cells is shorter. Both early and late sequelae can occur.

Oral mucosa: Damage to the oral mucosa during radiotherapy for head and neck cancer is very important for both the comfort and welfare of the patient. Xerostomia can interfere with nutrition and dental health.

Esophagus: Early and late effects can occur and lead to difficulty in swallowing. Tolerance is 57.5 Gy in 10 fractions (acute effects limit).

Stomach: Irradiation of the stomach often leads to nausea and vomiting. Tolerance doses range from 40 to 50 Gy.

Small and large intestines: Both early and late complications can occur. Tolerance dose is about 50 Gy for the small intestine, slightly higher for the large intestine, and 70 Gy for the rectum.

The lung is an intermediate- to late-responding tissue. Two waves of damage can be identified: an acute pneumonitis and a later fibrosis. The lung is among the most sensitive late-responding organs. Pulmonary damage also may occur following chemotherapy.

Together with the lung, the kidney is among the more radiosensitive late-responding critical organs. FSUs are in parallel, with only about 1,000 stem cells in each. A dose of about 30 Gy in 2-Gy fractions to both kidneys results in nephropathy.

In terms of radiosensitivity, the liver ranks immediately below the kidney and lung. FSUs are in parallel so that much larger doses are tolerated if only part of the organ is exposed. Fatal hepatitis may result from 35 Gy (conventional fractionation) to the whole organ.

Cell renewal is low in the bladder epithelium, so proliferation following irradiation is delayed. Frequency of urination increases in parallel with loss of surface cells. Absence of surface cells explains irritation by urine.

The nervous system is less sensitive to radiation than other late-responding organs, such as the kidney or lung.

Brain: Histopathologic changes that occur in the first year are most likely to involve white matter; at later times, gray matter usually shows changes accompanied by vascular lesions. Radionecrosis may occur accompanied by

cognitive defects.

Spinal cord: Early demyelinating injuries may develop after doses as low as 35 Gy but are usually reversible. For late damage, the TD_{5/5} is about 50 Gy for a 10-cm length of cord. By 70 Gy in conventional fractions, the incidence of myelopathy would be 50%. FSUs are in series, but once the field exceeds a few centimeters, the treatment volume has little effect. Tolerance dose shows little dependence on overall time but depends critically on dose per fraction (α/β is low). If two doses per day are used, the interfractionation interval must be more than 6 hours because there is a slow component of repair.

In the testes, a dose of 0.1 to 0.15 Gy leads to temporary sterility. A dose of 6 to 8 Gy in 2-Gy fractions leads to permanent sterility. Such doses have little effect on libido. The stem cells are more radiosensitive than the differentiated cells, so continuous or fractionated radiation is more effective than a single acute dose.

Sterilization by radiation to the ovaries is immediate (no latent period, as in the male) and leads to all the changes associated with menopause.

Among the female genitalia, tolerance doses for the vagina are high: 90 Gy before ulceration and 100 Gy for the development of a fistula. For intracavitary treatment, doses to the cervix and uterus may reach 200 Gy.

Late damage to many different tissues and organs is mediated to some extent by effects on the vasculature. Arterial damage may occur after fractionated doses of 50 to 70 Gy, but capillaries are damaged by doses above about 40 Gy.

In its tolerance to radiation, the heart is intermediate between the kidney or lung and the central nervous system. The most common radiation-induced heart injury is acute pericarditis, which seldom occurs in the first year posttherapy. A dose of 40 to 50 Gy in conventional fractions induces about an 11% incidence. The α/β ratio is low (1 Gy) so that fractionation results in a substantial sparing. Protection of part of the heart reduces symptoms.

Growing cartilage is particularly radiosensitive in children: 10 Gy can slow growth, and deficits in growth are irreversible above about 20 Gy. In the adult, osteoporosis of the lower mandible may be a serious complication following radiotherapy for cancer of the buccal cavity. Fractures of the humeral or femoral head may occur; the TD_{50/5} is about 65 Gy.

Over the past several decades, with the development of more sophisticated three-dimensional treatment planning systems, numerous studies in the literature have reported associations between dosimetric parameters and normal tissue outcomes. QUANTEC summarized the available data in a clinically useful format. It is intended to be an update of the data published by Emami and colleagues in 1991, which is widely used despite the fact that it has often been criticized.

The RTOG and EORTC introduced the SOMA classification for LENT: SOMA is an acronym for subjective, objective, management criteria with analytic laboratory and imaging procedures.

BIBLIOGRAPHY

Al-Barwari SE, Potten CS. A cell kinetic model to explain the time of appearance of skin reaction after x-rays or ultraviolet light irradiation. *Cell Tissue Kinet.* 1979;12:281–289.

Bergonie J, Tribondeau L. Interpretation of some results of radiotherapy and an attempt at determining a logical technique of treatment. Fletcher GH, trans. *Radiat Res.* 1959;11:587–588. Originally published, in French, in: *C R Seances Acad Sci III.* 1906;143:983.

Blackett N, Aguado M. The enhancement of haemopoietic stem cell recovery in irradiated mice by prior treatment with cyclophosphamide. *Cell Tissue Kinet.* 1979;12:291–298.

Botnik LE, Hannon ECM, Hellman S. Late effects of cytotoxic agents on the normal tissue of mice. *Front Radiat Ther Oncol.* 1979;13:36–47.

Clifton KF. Thyroid and mammary radiobiology: radiogenic damage to glandular tissues. *Br J Cancer Suppl.* 1986;7:237–250.

Coppes RP, van der Goot A, Lombaert IM. Stem cell therapy to reduce radiation-induced normal tissue damage. *Semin Radiat Oncol.* 2009;19:112–121.

Croizat H, Frindel E, Tubiana M. Long term radiation effects on the bone marrow stem cells of C3H mice. *Int J Radiat Biol Relat Stud Phys Chem Med.* 1979;36:91–99.

Croizat H, Frindel E, Tubiana M. The effect of partial body irradiation on haemopoietic stem cell migration. *Cell Tissue Kinet.* 1980;13:319–325.

Denekamp J. Cell kinetics and radiation biology. *Int J Radiat Biol Relat Stud*

Phys Chem Med. 1986;49:357–380.

Emami B, Lyman J, Brown A, et al. Tolerance of normal tissue to therapeutic irradiation. *Int J Radiat Oncol Biol Phys.* 1991;21:109–122.

Fajardo LF. *Pathology of Radiation Injury.* New York, NY: Masson; 1982.

Frindel E, Croizat H, Vassort F. Stimulating factors liberated by treated bone marrow: in vitro effect on CFU kinetics. *Exp Hematol.* 1976;4:56–61.

Frindel E, Hahn C, Robaglia D, et al. Responses of bone marrow and tumor cells to acute and protracted irradiation. *Cancer Res.* 1972;32:2096–2103.

Hegazy MAH, Fowler JF. Cell population kinetics and desquamation skin reactions in plucked and unplucked mouse skin. II. Irradiated skin. *Cell Tissue Kinet.* 1973;6:587–602.

Hendry JH, Thames HD. The tissue-rescuing unit. *Br J Radiol.* 1986;59:628–630.

Hopewell JW. Mechanisms of the action of radiation on skin and underlying tissues. *Br J Radiol Suppl.* 1986;19:39–47.

Hopewell JW, Campling D, Calvo W, et al. Vascular irradiation damage: its cellular basis and likely consequences. *Br J Cancer Suppl.* 1986;7:181–191.

Hopewell JW, Morris AD, Dixon-Brown A. The influence of field size on the late tolerance of the rat spinal cord to single doses of X rays. *Br J Radiol.* 1987;60:1099–1108.

Job G, Pfreundschuh M, Bauer M, et al. The influence of radiation therapy on T-lymphocyte subpopulations defined by monoclonal antibodies. *Int J Radiat Oncol Biol Phys.* 1984;10:2077–2081.

Joiner MC, Denekamp J. The effect of small radiation doses on mouse skin. *Br J Cancer Suppl.* 1986;7:63–66.

Kaanders JHAM, van Daal WAAJ, Hoogenraad WJ, et al. Accelerated fractionation radiotherapy for laryngeal cancer, acute, and late toxicity. *Int J Radiat Oncol Biol Phys.* 1992;24:497–503.

Kotzin BL, Kansas GS, Engleman EG, et al. Changes in T-cell subsets in patients with rheumatoid arthritis treated with total lymphoid irradiation. *Clin Immunol Immunopathol.* 1983;27:250–260.

Le Bourgeois JP, Meignan M, Parmentier C, et al. Renal consequences of irradiation of the spleen in lymphoma patients. *Br J Radiol.* 1979;52:56–60.

- Marks LB, Yorke ED, Jackson A, et al. Use of normal tissue complication probability models in the clinic. *Int J Radiat Oncol Biol Phys.* 2010;76(suppl 3):S10–S19.
- Meistrich ML. Relationship between spermatogonial stem cell survival and testis function after cytotoxic therapy. *Br J Cancer Suppl.* 1986;7:89–101.
- Michalowski A. A critical appraisal of clonogenic survival assays in the evaluation of radiation damage to normal tissues. *Radiother Oncol.* 1984;1:241–246.
- Michalowski A. Effects of radiation on normal tissues: hypothetical mechanisms and limitations of in situ assays of clonogenicity. *Radiat Environ Biophys.* 1981;19:157–172.
- Parmentier C, Morardet N, Tubiana M. Late effects on human bone marrow after extended field radiotherapy. *Int J Radiat Oncol Biol Phys.* 1983;9:1303–1311.
- Potten CS, Hendry JH, eds. *Cytotoxic Insult to Tissue: Effects on Cell Lineages.* Edinburgh, United Kingdom: Churchill Livingstone; 1983.
- Rubin P. The Franz Buschke lecture: late effects of chemotherapy and radiation therapy: a new hypothesis. *Int J Radiat Oncol Biol Phys.* 1984;10:5–34.
- Rubin P, Casarett GW. *Clinical Radiation Pathology.* Vol 1. Philadelphia, PA: W.B. Saunders; 1968.
- Rubin P, Constine LS, Fajardo LF, et al. Late Effects of Normal Tissues Consensus Conference. San Francisco, California, August 26-28, 1992. *Int J Radiat Oncol Biol Phys.* 1995;31:1035–1367.
- Schofield R. Assessment of cytotoxic injury to bone marrow. *Br J Cancer Suppl.* 1986;7:115–125.
- Schultz-Hector S. Heart. In: Scherer E, Streffer C, Trott K-R, eds. *Radiopathology of Organs and Tissues.* Berlin, Germany: Springer; 1981:347–368.
- Stewart FA. Mechanism of bladder damage and repair after treatment with radiation and cytostatic drugs. *Br J Cancer Suppl.* 1986;7:280–291.
- Travis EL. The tissue rescuing unit. In: Fielden EM, Fowler JF, Hendry JH, et al, eds. *Proceedings of the Eighth International Congress of Radiation Research.* London, United Kingdom: Taylor & Francis; 1987:795–800.

- Travis EL, Down JD. Repair in mouse lung after split doses of X rays. *Radiat Res.* 1981;87:166–174.
- Travis EL, Liao Z-X, Tucker SL. Spatial heterogeneity of the volume effect for radiation pneumonitis in mouse lung. *Int J Radiat Oncol Biol Phys.* 1997;38:1045–1054.
- Travis EL, Tucker SL. The relationship between functional assays of radiation response in the lung and target cell depletion. *Br J Cancer Suppl.* 1986;7:304–319.
- Trott KR. Chronic damage after radiation therapy: challenge to radiation biology. *Int J Radiat Oncol Biol Phys.* 1984;10:907–913.
- Tubiana M. L.H. Gray Medal lecture: cell kinetics and radiation oncology. *Int J Radiat Oncol Biol Phys.* 1982;8:1471–1489.
- Turesson I, Notter G. Dose-response and dose-latency relationships for human skin after various fractionation schedules. *Br J Cancer Suppl.* 1986;7:67–72.
- Turesson I, Thames HD. Repair capacity and kinetics of human skin during fractionated radiotherapy: erythema, desquamation, and telangiectasia after 3 and 5 years' follow-up. *Radiother Oncol.* 1989;15:169–188.
- van der Kogel AJ. Central nervous system radiation injury in small animal models. In: Gutin PH, Leibel SA, Sheline GE, eds. *Radiation Injury to the Nervous System*. New York, NY: Raven Press; 1991:91–112.
- van der Kogel AJ. Mechanisms of late radiation injury in the spinal cord. In: Meyn RE, Withers HR, eds. *Radiation Biology in Cancer Research*. New York, NY: Raven Press; 1980:461–470.
- van der Kogel AJ. Radiation-induced damage in the central nervous system: an interpretation of target cell responses. *Br J Cancer Suppl.* 1986;7:207–217.
- van der Kogel AJ, Ang KK. Complications related to radiotherapy. In: Peckham M, Pinedo H, Veronesi U, eds. *Oxford Textbook of Oncology*. Vol 2. Oxford, United Kingdom: Oxford University Press; 1995:2295–2306.
- van der Kogel AJ, Sissingh HA, Zoetelief J. Effect of X rays and neutrons on repair and regeneration in the rat spinal cord. *Int J Radiat Oncol Biol Phys.* 1982;8:2095–2097.
- Vassort F, Wintherholer M, Frindel E, et al. Kinetic parameters of bone marrow stem cells using in vivo suicide by tritiated thymidine or by hydroxyurea. *Blood.* 1973;41:789–796.

Wheldon TE, Michalowski AS. Alternative models for the proliferative structure of normal tissues and their response to irradiation. *Br J Cancer Suppl.* 1986;7:382–385.

Withers HR, Taylor JM, Maciejewski B. Treatment volume and tissue tolerance. *Int J Radiat Oncol Biol Phys.* 1988;14:751–759.

Withers HR, Thames HD, Peters LJ, et al. Keynote address: normal tissue radioresistance in clinical radiotherapy. In: Fletcher GH, Nervi C, Withers HR, eds. *Biological Bases and Clinical Implications of Tumor Radioresistance*. New York, NY: Masson; 1983:139–152.

chapter 21

Model Tumor Systems

Transplantable Solid Tumor Systems in Experimental Animals

Apoptosis in Tumors

Tumor Growth Measurements

Tumor Cure (TCD₅₀) Assay

Dilution Assay Technique

Lung Colony Assay

***In Vivo/In Vitro* Assay**

Xenografts of Human Tumors

Patient-Derived Xenografts Models

Autochthonous and Transgenic Tumor Models

Spheroids: An *In Vitro* Model Tumor System

Spheroids of Human Tumor Cells

Organoid Models of Human Tumors

Comparison of the Various Model Tumor Systems

Summary of Pertinent Conclusions

Bibliography

TRANSPLANTABLE SOLID TUMOR SYSTEMS IN EXPERIMENTAL ANIMALS

A wide range of experimental tumors of various histologic types have been developed for radiobiologic studies. To produce a large number of virtually identical tumors, propagation by transplantation from one generation of animals to the next is used, which makes it mandatory that the animals be isogenic. In practice, pure inbred strains of rats or mice are used and are maintained by brother-sister mating, which also serves the function of reducing the variability among animals to a minimum.

The tumor from a donor animal is removed aseptically and, if possible, prepared into a single-cell suspension; this is accomplished by separating the cells with an enzyme such as trypsin and then forcing them through a fine wire mesh. To effect a transplant, 10^4 to 10^6 cells are inoculated subcutaneously into each of a large group of recipient animals of the same strain. The site of transplantation varies widely; the flank or back is commonly used, but sometimes, a special tumor requires a particular site, such as the brain. Some tumors cannot be handled in this way and must be propagated by transplanting a small piece of tumor rather than a known number of single cells; this is obviously less quantitative. Within days or weeks, depending on the type of tumor and the strain of animals, palpable tumors appear in the recipient animals that are uniform in size, histologic type, and so on. Hundreds to thousands of animals can be used, which makes it possible to design highly quantitative studies of tumor response to different radiations, fractionation regimens, sensitizers, and combinations of radiation and chemotherapeutic agents.

There are five commonly used techniques to assay the response of solid tumors to a treatment regimen:

1. Tumor growth measurements
2. Tumor cure (TCD₅₀) assay
3. Tumor cell survival determined *in vivo* by the dilution assay technique
4. Tumor cell survival assayed by the lung colony assays
5. Tumor cell survival using *in vivo* treatment followed by *in vitro* assay

Each of these methods is discussed briefly in this chapter. These assays take into account both intrinsic cell sensitivity to ionizing radiation as well as the influence of the microenvironment. Before we discuss the techniques used to assess tumor response to radiation, we should briefly revisit how the type of cell death and the tumor microenvironment can affect tumor response to therapy, in particular the role of apoptotic cell death.

APOPTOSIS IN TUMORS

It is generally thought that irradiated cells die in attempting the next or a subsequent mitosis. However, this is not the only form of cell death. Programmed cell death, or *apoptosis*, also occurs in both normal tissues and tumors, spontaneously, because of irradiation, and can be triggered by changes in the tumor microenvironment.

In [Chapter 22](#), it is pointed out that tumors grow much more slowly than would be predicted from the cell cycle time of the individual cells and the fraction of cells actively dividing. One of the reasons for this “cell loss,” as it is called, is random cell death resulting from apoptosis.

Studies with transplanted mouse tumors, as well as human tumors growing as xenografts in nude mice, have shown that the importance of apoptosis as a mechanism of cell death after x-irradiation varies substantially. Apoptosis was most important in lymphomas, essentially absent in sarcomas, and intermediate and very variable in carcinomas. In a mouse lymphoma, for example, 50% to 60% of the cells may show signs of dying an apoptotic death by 3 hours after irradiation, whereas in a sarcoma, there may be so few apoptotic cells that the process is of little significance. If a tumor responds rapidly to a relatively low dose of radiation, it generally means that apoptosis is involved because the process peaks at 3 to 5 hours after irradiation.

Susceptibility to the induction of apoptosis also may be an important factor determining radiosensitivity because programmed cell death appears to be a prominent early effect in radiosensitive mouse tumors and essentially absent in radioresistant tumors. In particular, the transformation of mouse cells of different histologic origins with oncogenes in cell culture makes them particularly sensitive to DNA damage-induced apoptosis. The concern with using cell lines that are highly susceptible to apoptosis is that cell culture will act as a selective pressure over time to select for variants of these cells that have lost their apoptotic sensitivity, thus changing their *in vivo* sensitivity to radiation and cytotoxic drugs used in cancer therapy.

Changes in the microenvironment can also influence the sensitivity of tumor cells to therapy ([Fig. 21.1](#)). Studies have shown that changes in tumor oxygenation, pH, and growth factors can induce apoptotic cell death in a subset of tumor cells that represent a therapeutically sensitive population. Therefore, cells that are sensitive to apoptosis will be more susceptible to killing by the environmentally restrictive conditions in experimental tumors and will be better able to be controlled by radiotherapy and chemotherapy. Cells with diminished apoptotic potential, which represent most tumor cell lines maintained in culture, will have lost this rapid response to radiotherapy but can still die by a mitotic cell death. Cells with diminished apoptotic sensitivity caused by genetic mutations in critical apoptotic pathways, such as the *p53* tumor suppressor gene or the *Bcl-2* oncogene (see [Chapter 18](#)), are probably more reflective of human solid tumors that are treated clinically.

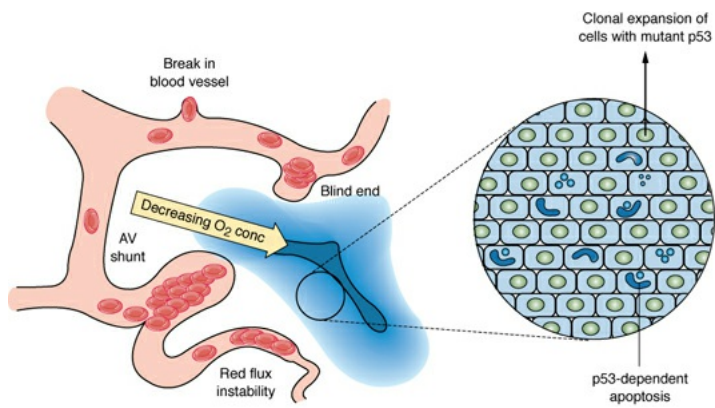


FIGURE 21.1 Regions of hypoxia form within solid tumors as a result of the inefficient and disorganized vasculature. Hypoxic regions represent a gradient of oxygen concentrations, the highest being nearest the vessels and the lowest being the farthest away. In the most hypoxic regions, *p53* is stabilized and induces apoptosis. A selection pressure therefore exists to lose *p53* and allows the clonal expansion of cells. These cells are also resistant to chemotherapy and radiotherapy, both of which require an efficient blood supply. (From Hammond EM, Giaccia AJ. Hypoxia-inducible factor-1 and *p53*: friends, acquaintances, or strangers? *Clin Cancer Res*. 2006;12:5007–5009, with permission.)

TUMOR GROWTH MEASUREMENTS

Tumor growth measurement is possibly the simplest end point to use and involves the daily measurement of each tumor to arrive at a mean diameter. For tumor growth experiments, a large number of transplanted tumors are prepared as previously described. When they have grown to a specified size (e.g., a diameter of 8 to 10 mm in rats or 2 to 4 mm in mice), they are treated according to the plan of the particular experiment. Figure 21.2 illustrates the variation of tumor size with time for unirradiated controls and tumors given a single dose of x-rays. The untreated tumors grow rapidly at a relatively uniform rate; the radiation treatment causes a temporary shrinkage of the tumor, followed by regrowth.

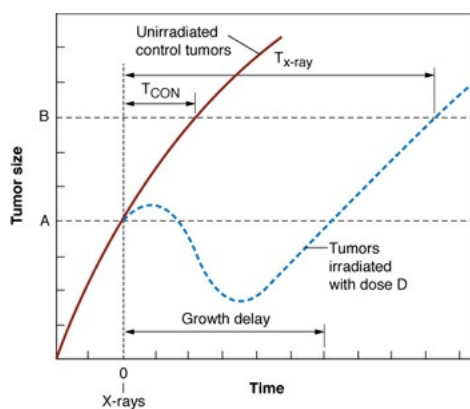


FIGURE 21.2 The pattern of response of a tumor to a dose of x-rays. The size of the tumor, either the mean diameter or the volume, is plotted as a function of time after irradiation. Two different indices of tumor responses have been used by different investigators. Growth delay represents the time after irradiation that it takes for the tumor to regrow to the size at the time of irradiation. Alternatively, the index of radiation damage may be the time taken for the tumor to grow from a specified size A at the time of irradiation to some specified larger size B . Typically, this may be from 9 to 25 mm in diameter for rat tumors. This quantity is shown as T_{CON} for unirradiated control animals and $T_{x\text{-ray}}$ for tumors irradiated with a dose (D) of x-rays. Either index of tumor response may be plotted as a function of radiation dose.

Two different methods have been used to score the tumor response. Barendsen and his colleagues have used growth delay, illustrated in [Figure 21.2](#), as the time taken after irradiation for the tumor to regrow to the size it was at the time of irradiation. Clearly, this index of response is only suitable for tumors that shrink significantly after irradiation. For tumors that do not shrink so obviously, a more convenient index of growth delay is the time taken for the irradiated tumor to grow to some specified size after exposure, compared with controls. Either index of growth delay increases as a function of radiation dose. [Figure 21.3A](#) shows growth curves for a rat rhabdomyosarcoma irradiated with various doses of x-rays or fast neutrons. In [Figure 21.3B](#), growth delay is expressed as a function of radiation dose.

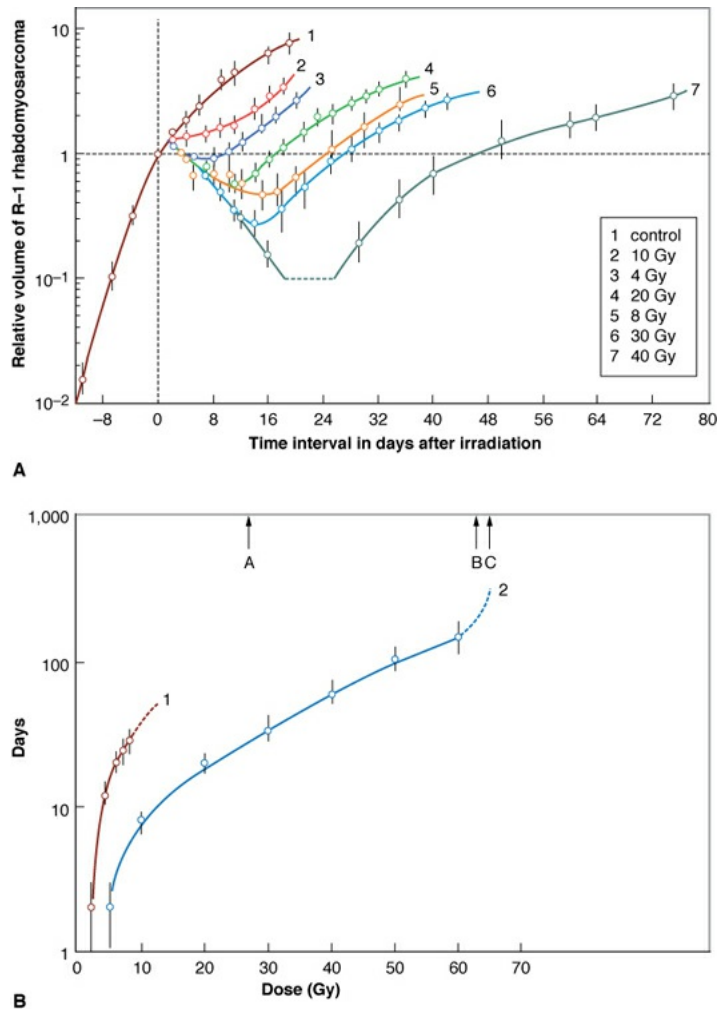


FIGURE 21.3 **A:** Volume changes of rhabdomyosarcomas in rats after irradiation. *Curve 1* represents the growth of the unirradiated control tumors. *Curves 2, 4, 6, and 7* refer to tumors irradiated with 10 to 40 Gy of 300-kV x-rays. *Curves 3 and 5* refer to tumors irradiated with 4 and 8 Gy of 15-MeV $d^+ \rightarrow T$ fast neutrons. **B:** Growth delay of rhabdomyosarcomas in rats as a function of dose of x-rays (*curve 2*) or fast neutrons (*curve 1*). *A* and *C* indicate the doses of neutrons and x-rays, respectively, required to “cure” 90% of the tumors, calculated based on the cell survival curves. *B* indicates the observed TCD₉₀ for x-rays. Note the good agreement between calculated and observed values of the TCD₉₀ for x-rays. (Adapted from Barendsen GW, Broerse JJ. Experimental radiotherapy of a rat rhabdomyosarcoma with 15 MeV neutrons and 300 kV x-rays: I. Effects of single exposures. *Eur J Cancer*. 1969;5:373–391, with permission.)

TUMOR CURE (TCD₅₀) ASSAY

Tumor control provides data of most obvious relevance to radiotherapy. In

experiments of this kind, a large number of animals with tumors of uniform size are divided into separate groups, and the tumors are irradiated locally with graded doses. The tumors subsequently are observed regularly for recurrence or local control. The proportion of tumors that are locally controlled can be plotted as a function of dose, and data of this kind are amenable to a sophisticated statistical analysis to determine TCD₅₀, the dose at which 50% of the tumors are locally controlled. This quantity is highly repeatable from one experiment to another in an inbred strain of animals.

Suit and his colleagues, over a period of more than 30 years, have made an extensive study of the response to radiation of a mammary carcinoma in C₃H mice. Data from a typical experiment are presented in Figure 21.4. Tumors were propagated by transplanting 4×10^4 cells into the outer portion of the mouse ear, and irradiations were performed when the tumors had grown to a volume of about 4 mm³. A brass circular clamp was fitted across the base of the ear and maintained for at least a minute before the initiation of the irradiation so that the tumors were uniformly hypoxic. Single-dose, 2-dose, and 10-dose experiments were performed, with a 24-hour interval between dose fractions. Tumor control results are shown in Figure 21.4. The TCD₅₀ for a single treatment is 45.75 Gy, rising to 51.1 Gy for 2 fractions and to 84 Gy if the radiation is delivered in 10 equal fractions. This indicates that a marked and extensive repair of sublethal damage has taken place during a multifraction regimen.

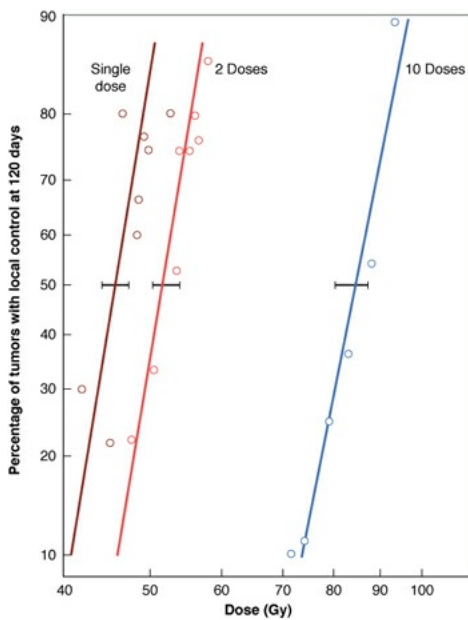


FIGURE 21.4 Percentage of mouse mammary tumors locally controlled as a function of x-ray dose for single exposures and for two different fractionation patterns. The tumors were isotransplants derived from a spontaneous mammary

carcinoma in a C₃H mouse. The transplantation was made into the outer portion of the ear with 4×10^4 viable cells. The tumors were treated when they reached a diameter of 2 mm (i.e., a volume of about 4 mm³). (Adapted from Suit HD, Wette R. Radiation dose fractionation and tumor control probability. *Radiat Res.* 1966;29:267–281, with permission.)

DILUTION ASSAY TECHNIQUE

The dilution assay technique was devised by Hewitt and Wilson, who used it to produce the first *in vivo* survival curve in 1959. They used a lymphocytic leukemia of spontaneous origin in mice. A single-cell suspension can be prepared from the infiltrated liver of an animal with advanced disease and the tumor transplanted by injecting known numbers of cells into the peritoneal cavities of recipient mice, which subsequently develop leukemias. The leukemia can be transmitted, on average, by the injection of only two cells; this quantity—the number of cells required to transmit the tumor to 50% of the animals—is known as TD₅₀. The dilution assay technique became the basis for obtaining an *in vivo* cell survival curve.

The procedure used, illustrated in [Figure 21.5](#), is as follows. An animal containing the tumor may be irradiated to a given dose of radiation, for example, 10 Gy. A single-cell suspension is then prepared from the infiltrated liver, the cells are counted and diluted, and various numbers of these cells are injected intraperitoneally into groups of recipient animals. It is then a matter of observation and calculation to determine how many irradiated cells are required to produce a tumor in half of the animals inoculated with that given number of cells. Suppose, for instance, that it takes 20 irradiated cells, on average, to transmit the tumor; because it is known that only 2 clonogenic cells are needed to transmit the tumor, it is a simple matter to decide that in the irradiated population of cells, 2 of 20, or 10%, were clonogenic and survived the dose of 10 Gy. That is,

$$\text{Surviving fraction} = \text{TD}_{50} \text{ controls} / \text{TD}_{50} \text{ irradiated}$$

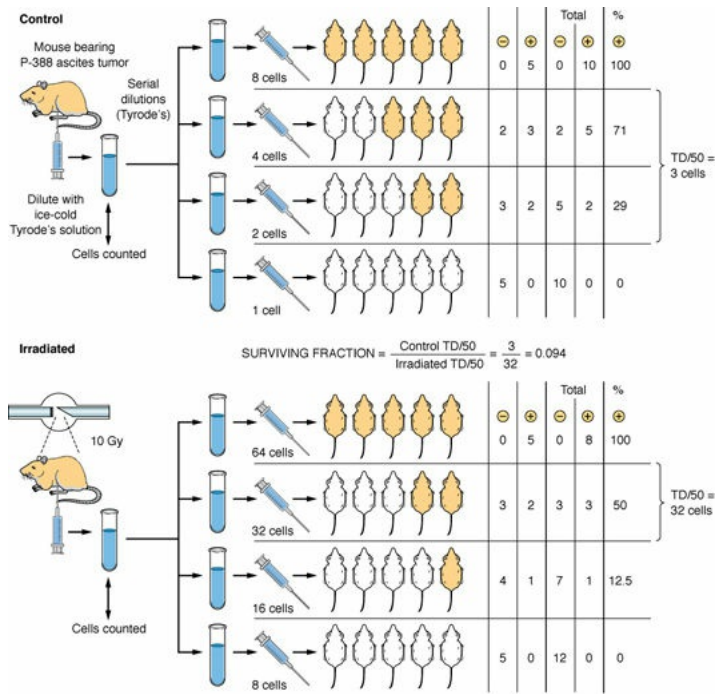


FIGURE 21.5 Schematic representation to show the general features of the dilution assay technique. Various numbers of tumor cells from the donor animal are injected into groups of recipients, and a determination is made of the number of cells required for a tumor to take in half of the animals of the group (TD₅₀). The ratio of this quantity for control and irradiated donors is the surviving fraction. (Adapted from Andrews JR, Berry RJ. Fast neutron irradiation and the relationship of radiation dose and mammalian tumor cell reproductive capacity. *Radiat Res.* 1962;16:76–81, with permission.)

If this process is repeated for several doses of radiation and the corresponding surviving fractions are determined by this assay technique, a survival curve for cells irradiated and assayed *in vivo* can be constructed.

This technique is a true *in vivo* system, but it involves a leukemia as opposed to a solid tumor. The cells, after reinoculation into the mouse, grow in the peritoneal cavity in much the same way that the cells grow in a petri dish in the *in vitro* technique; the mice are in fact being used as small portable incubators.

Since these pioneering efforts, the dilution assay technique has been applied by many different workers to measure survival curves for several leukemias and solid tumors if the tumors can be removed and prepared into a single-cell suspension; some collected results are shown in Figure 21.6. The survival curves obtained have a D₀ of about 4 Gy because the cells in the peritoneal cavity of the mouse are so numerous and so closely packed that they are deficient in oxygen. This technique, therefore, produces a “hypoxic” survival curve. To obtain a

survival curve characteristic of aerated conditions, it is necessary either to remove the cells from the donor animal and irradiate them in a petri dish in which they are in contact with air or to inject hydrogen peroxide into the peritoneal cavity of the mouse before irradiation so that oxygen is available to the tumor cells during the irradiation. If this is done, D_0 is about 1.3 to 1.6 Gy.

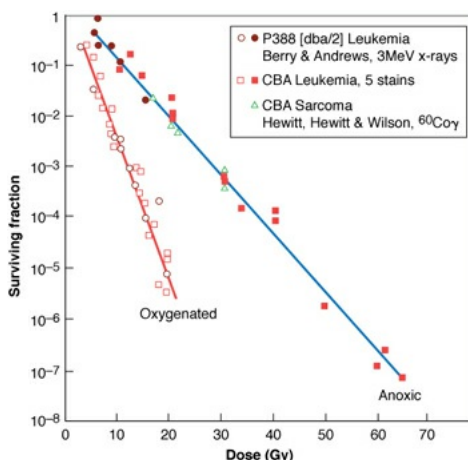


FIGURE 21.6 Dose-response curves *in vivo*, using the dilution assay technique, for various murine tumors under oxygenated and hypoxic conditions. (Adapted from Berry RJ. On the shape of x-ray dose-response curves for the reproductive survival of mammalian cells. *Br J Radiol.* 1964;37:948–951, with permission.)

LUNG COLONY ASSAY

Hill and Bush have devised a technique to assay the clonogenicity of the cells of a solid tumor irradiated *in situ* by injecting them into the recipient animals and counting the number of lung colonies produced. The general principles of the method are illustrated in Figure 21.7. The tumor used in these studies was the KHT sarcoma, which is a transplantable tumor that arose originally in a C₃H mouse and which has been propagated serially through many generations. Tumors are irradiated *in situ*, after which they are removed and made into a preparation of single cells by a combined trypsinization and mechanical procedure. A known number of cells then are mixed with a large number of heavily irradiated tumor cells and injected intravenously into recipient mice. About 3 weeks later, these mice are sacrificed, and the colonies formed in the lungs are readily countable. The number of lung colonies is a measure of the number of surviving clonogenic cells in the injected suspension.

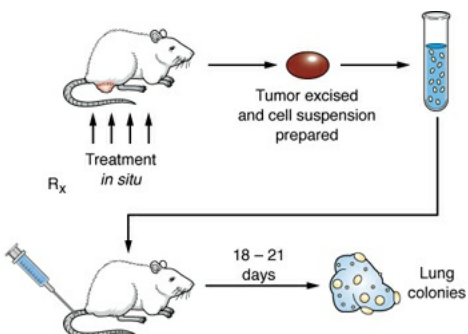


FIGURE 21.7 The lung colony assay system. The tumor is irradiated *in situ*, after which it is excised and made into a single-cell suspension. A known number of cells are then injected intravenously into the recipient animals. About 3 weeks later, the recipient animals are sacrificed and the colonies that have formed in the lungs are counted. The number of lung colonies is a measure of the number of surviving clonogenic cells in the injected suspension. (Adapted from Hill RP, Bush RS. The effect of continuous or fractionated irradiation on a murine sarcoma. *Br J Radiol.* 1973;46:167–174, with permission.)

The lung colony technique is not confined to the KHT sarcoma but has been used with other tumor cells. For example, the demonstration of the absence of repair of potentially lethal damage after neutron irradiation involved the use of the Lewis lung carcinoma, and the fraction of surviving cells was assayed by counting lung colonies.

IN VIVO/IN VITRO ASSAY

A limited number of cell lines have been adapted so that they grow either as a transplantable tumor in an animal or as clones in a petri dish. These cells can be readily transferred from *in vivo* to *in vitro* and back. In one generation, they may grow as a solid tumor in an animal, and in the next, as a monolayer in a petri dish. The three most commonly used systems are a rhabdomyosarcoma in the rat (Hermens and Barendsen), a fibrosarcoma in the mouse (McNally), and the EMT6 mammary tumor in the mouse (Rockwell and Kallman).

The steps involved in this method are illustrated in Figure 21.8. This method combines many of the advantages of the *in vitro* and *in vivo* techniques. The tumors are treated *in vivo* in a natural environment so that the cellular response is modified by the various factors that are important in determining gross tumor response. After treatment, each tumor is removed and prepared into a single-cell suspension, and the cell concentration is counted in a hemocytometer or electronic cell counter. Known numbers of cells can then be transferred to petri dishes containing fresh growth medium, and the proportion of clonogenic cells

can be determined by counting colonies 10 days later. The speed, accuracy, and relative economy of the *in vitro* system replace the expense and inconvenience of the recipient animals in the dilution assay technique.

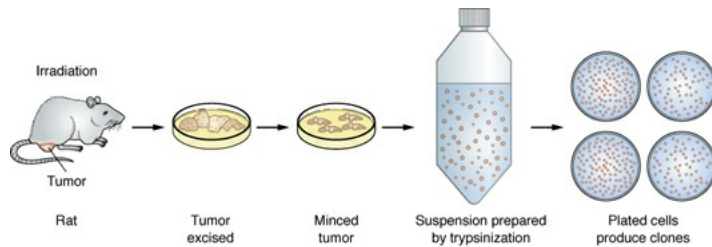


FIGURE 21.8 The principle of the *in vivo/in vitro* assay system using the rhabdomyosarcoma in the rat. The solid tumor in the animal can be removed and the tumor cells assayed for colony formation in petri dishes. This cell line can be transferred back and forth between the animal and the petri dish. (Adapted from a drawing courtesy of Drs. G. W. Barendsen and J. J. Broerse.)

XENOGRAFTS OF HUMAN TUMORS

A **xenograft** is a transplant from one species to another. In the cancer field, this usually refers to a human tumor transplanted into a laboratory animal. If the recipient animal has a normal immune system, a xenograft should not grow, but there are two main ways in which growth has been achieved. First, animal strains have been developed that are congenitally immune deficient. Best known are nude mice, which, in addition to being hairless, also lack a thymus. Many human tumors grow under the skin of nude mice. More recently, there have been nude rats and severe combined immune-deficient (SCID) mice, which suffer from the severe combined immunodeficiency syndrome and are deficient in both B cell and T cell immunity. Second, it is possible to severely immunosuppress mice by the use of radiation or drugs or a combination of both to the point at which they accept human tumor grafts. It is important to recognize that neither type of host completely fails to reject the human tumor cells: Rejection processes are still present, and these complicate the interpretation of *in situ* tumor therapeutic studies.

Despite the limitations, various human tumor cells have been grown as xenografts in immune-deficient animals. Steel has estimated that more than 300 individual human tumors have been investigated in this way. Breast and ovarian tumors generally have been difficult to graft, with grafting of melanomas and tumors of the colon and bronchus being relatively successful.

Xenografts retain human karyotypes through serial passages and maintain some of the response characteristics of the individual source human tumors; to

this extent, they have great advantages over mouse tumors. There are, however, certain drawbacks. First, there is a tendency for the tumor to be rejected so that observing tumor control as an end point can be misleading. Growth delay and cell survival studies, on the other hand, are probably less affected. Second, human tumor cells do undergo kinetic changes and cell selection if transplanted into mice. For example, xenografts commonly have doubling times about one-fifth of the values observed in humans so that increased responsiveness should be expected to proliferation-dependent chemotherapeutic agents. Third, although the histologic characteristics of the human source tumors are usually well maintained by xenografts, the stromal tissue is of mouse origin. Consequently, xenografts of human tumor cells are not much more valid than murine tumors for any studies in which the vascular supply plays an important role. For example, the fraction of hypoxic cells in xenografts is much the same as in mouse tumors.

Steel and colleagues reviewed the field in 1983 and concluded that xenografts generally maintain the chemotherapeutic response characteristics of the class of tumors from which they are derived. There is good evidence, too, for individuality of response among xenografts. For example, in studying melanomas, one was responsive clinically, but another was not, and the cell survival curve after therapy with melphalan was twice as steep in the xenograft of the cells from the responsive tumor.

[Figure 21.9](#) summarizes the correlation between growth delay in the xenograft and clinical remission of the donor patient. In the figure, the growth delay in xenografts for maximum-tolerated treatment with the single chemotherapeutic agents that are in common clinical use against the disease is plotted against the clinical complete response rate for that category of tumor. The correlation between these parameters is good. Testicular tumors are the most responsive in xenografts or in the clinic; small-cell lung cancer and breast tumors occupy an intermediate position; and the other three tumor types are unresponsive, either clinically or experimentally. This consistency of agreement between patient and xenograft responses to chemotherapeutic agents is encouraging for various human tumor types tested. Similarly, studies of radiation response indicate that measurements of growth delay in xenografts rank tumors in the same order as clinical responsiveness: Response is greater in testicular teratoma than in pancreatic carcinoma, which is greater than in bladder carcinoma, for example.

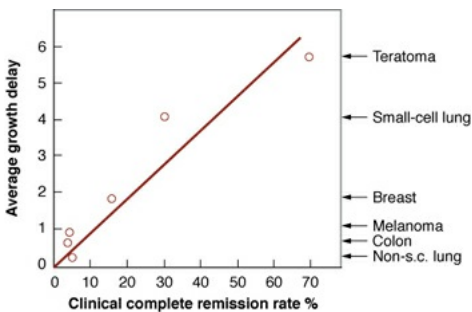


FIGURE 21.9 Correlation between response of human tumor xenografts and clinical complete remission rates to chemotherapy. The ordinate is the growth delay observed in 3 to 10 xenograft lines treated with the clinically used drugs that proved most effective in the xenografts. (Adapted from Steel GG. How well do xenografts maintain the therapeutic response characteristics of the source tumor in the donor patient? In: Kallman RF, ed. *Rodent Tumor Models in Experimental Cancer Therapy*. New York, NY: Pergamon; 1987, with permission.)

PATIENT-DERIVED XENOGRAFTS MODELS

Autochthonous and transgenic tumor models represent an advance in studying spontaneous tumors or genetic drivers of tumorigenesis; they do not necessarily reflect the heterogeneity of tumor responses to therapies used on found in human tumors. One recent advance to access the heterogeneity of human tumors is the development of patient-derived xenografts (PDXs). At one time, the use of PDXs was technically challenging, but the use of immune-deficient mouse strains such as NRG mice (non-obese diabetic-Rag1^{null} IL2rg^{null}), which were derived through a targeted knockout mutation in recombination activating gene 1 (Rag1^{null}) and a complete null allele of the IL-2 receptor common gamma chain (IL2rg^{null}). The Rag1^{null} mutation results in B and T cell–deficient mice, and IL2rg^{null} mutation prevents cytokine signaling through multiple receptors, leading to a deficiency in functional NK cells. The advantage of these mice is that they can be “humanized” by introducing human CD34⁺ hematopoietic stem cells. Using these mice, the growth of PDXs has been dramatically increased over the years and is rapidly being integrated into preclinical testing.

Just like xenografts, autochthonous, and transgenic models, PDXs have their advantages and disadvantages. In addition to the advantage of reflecting the heterogeneity of human tumors, PDXs are not cultured *in vitro* and therefore are not exposed to the selective growth conditions of cell culture. These tumor specimens, at least initially, possess stroma and cancer stem cell components of

the human tumor. The disadvantages are that the often long lag periods from implantation to growth, variability in tumor take rates and the requirement for a severely immunocompromised host. This latter point is highly significant and prevents the testing of immune modifying therapies with radiotherapy. More rigorous analysis will be required to determine if there is greater predictive value in testing PDXs versus more standard preclinical models.

AUTOCHTHONOUS AND TRANSGENIC TUMOR MODELS

Various inbred strains of mice have high incidences of spontaneous tumors that are the result of viral exposure or carcinogen treatment. For example, C₃H mice develop spontaneous mammary tumors as they can transmit the mouse mammary tumor virus (MMTV) in their milk and C57BL6 mice are highly susceptible to developing lymphomas when exposed to ionizing radiation. The advantages of using these autochthonous tumors in mice are that they are primary tumors that develop reproducibility in a certain organ, are influenced by the host stroma and immune systems and are able to metastasize through the hosts vasculature or lymphatic systems. Although these autochthonous tumors have these advantages, they have significant disadvantages that include variation in the number of primary tumors and the time for tumor development. The disadvantages far outweigh the advantages of using these tumors to study radiation response because a single experiment could take over a year to perform. To date, few studies using these types of animal models have been experimentally performed to study the effects of ionizing radiation on tumor growth and expansion.

Transgenic animals that possess specific mutations in a given oncogene or tumor suppressor gene have been proposed as better models to study the effects of ionizing radiation than autochthonous mice. Transgenic animal models have the advantage that the effect of a single or few genetic alterations on the response of tumors to radiation could be examined in an immune-competent mouse in a reproducible manner.

However, transgenic mice also suffer similar limitations regarding the timing of tumor development and variation in the number of primary tumors. An additional limitation of using transgenic mice is that no one transgenic mouse is a good model for human cancer. Even those mouse models that relate well to their human tumor counterparts fail to fully recapitulate the systemic spread in the mouse that is found in humans, a finding that is less of a concern in experiments examining the effect of dose on tumor control. A more significant

problem for radiation experiments lies in targeting the dose to spare normal tissue effects. This is not so inconsequential a problem and requires more sophisticated technology, which are now commercially available but expensive.

SPHEROIDS: AN *IN VITRO* MODEL TUMOR SYSTEM

Mammalian cells in culture may be grown either as a monolayer attached to a glass or plastic surface or in suspension, in which case they are prevented from settling out and attaching to the surface of the culture vessel by continual gentle stirring. Most cells in suspension, or in “spinner culture,” as it is often called, remain as single cells; at each mitosis, the progeny cells separate, and although the cell concentration increases with time, it continues to consist of individual separate cells.

Some cells, however, notably several rodent tumor cell lines such as Chinese hamster V79 lung cells, mouse EMT6 mammary cells, radiation-induced fibrosarcoma (RIF) cells, and rat 9L brain tumor cells do not behave in this way but instead grow as spheroids. At each successive division, the progeny cells stick together, and the result is a large spheric clump of cells that grows bigger with time. A photograph of a large spheroid consisting of about 8×10^4 cells is shown in [Figure 21.10](#). Five days after the seeding of single cells into suspension culture, the spheroids have a diameter of about 200 μm ; by 15 days, the diameter may exceed 800 μm . Oxygen and nutrients must diffuse into the spheroids from the surrounding tissue culture medium. In the center of a spheroid, there is a deficiency of oxygen and nutrients and a buildup of waste products because of diffusion limitations. Eventually, central necrosis appears and the mean cell cycle lengthens. Mature spheroids contain a heterogeneous population of cells resulting from many of the same factors as in a tumor *in vivo*.

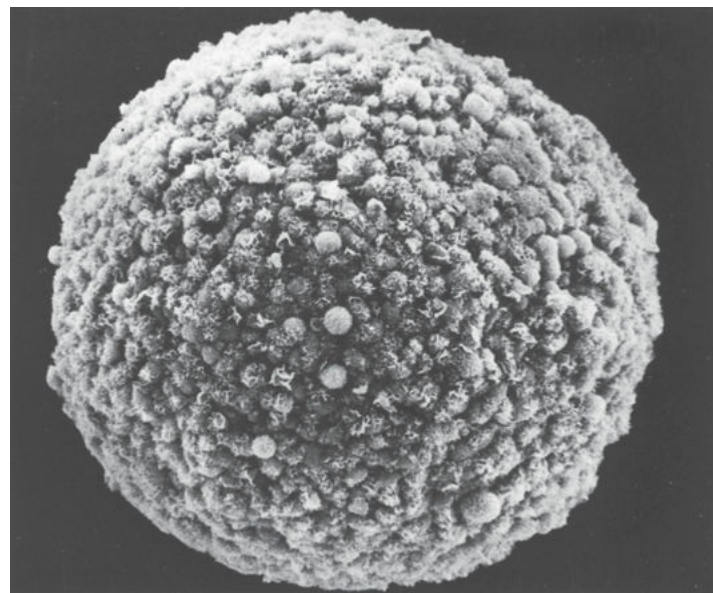


FIGURE 21.10 Photograph of an 800- μm spheroid containing about 8×10^4 cells. (Courtesy of Dr. R. M. Sutherland.)

The spheroid system is simpler, more reproducible, less expensive, and easier to manipulate than animal tumors, and yet, the cells can be studied in an environment that includes the complexities of cell-to-cell contact and nutritional stress from diffusion limitations that are characteristic of a growing tumor. Spheroids are irradiated intact and then separated into single cells by the use of trypsin and gentle agitation before being plated out into petri dishes to be assayed for the reproductive integrity of individual cells.

Mature spheroids consist of three populations of cells with varying radiosensitivity. Starting from the outside and working toward the center, they are asynchronous, aerobic cycling cells, aerated noncycling G₁-like cells, and noncycling G₁-like hypoxic cells. Very large spheroids may contain about 20% hypoxic cells, similar to many animal tumors. By gently trypsinizing the spheroids for varying periods, the spheroid can be peeled like an onion, and these three cell populations are separated out. Using more sophisticated methods, such as centrifugal elutriation and flow cytometry, it is possible to separate many more cell subpopulations based on location in the spheroid, cell cycle, or other parameters. [Figure 21.11](#) is a cross section through a large spheroid, showing clearly the development of a central necrotic area, which occurs when the spheroid's size is such that oxygen and other nutrients cannot diffuse into the center.

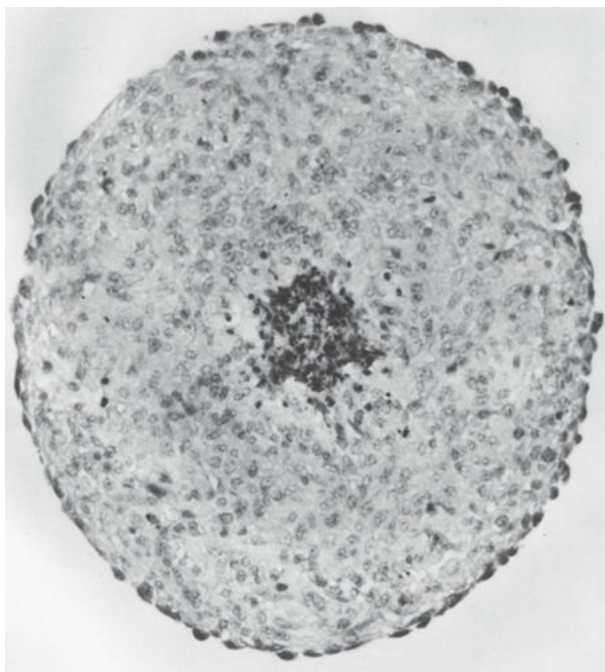


FIGURE 21.11 Photomicrograph of a spheroid cross section. Note the area of central necrosis. The spheroid was grown for 15 days and was $520\text{ }\mu\text{m}$ in diameter; the viable rim had an average thickness of about $200\text{ }\mu\text{m}$. (Courtesy of Dr. R. M. Sutherland.)

The spheroid system has been applied to several problems in radiobiology and in the study of pharmacologic agents, such as radiosensitizers or chemotherapeutic agents. A major problem in the application of these drugs to human tumors is the presence of resistant cells that are resting or noncycling, often located away from blood vessels. Drugs are required to diffuse in effective concentration to these cells through layers of growing, actively dividing cells, which may inactivate the drug through their metabolism. The spheroid system mimics many of these tumor characteristics and provides a rapid, useful, and economic method for screening sensitizers and chemotherapeutic agents because it is intermediate in complexity between single-cell *in vitro* culture and tumors in experimental animals.

SPHEROIDS OF HUMAN TUMOR CELLS

Many types of human tumor cells can be cultured as spheroids, with a wide spectrum of morphologic appearances and growth rates. In general, cells from disaggregated surgical specimens form spheroids if cultured in liquid suspension above a nonadhesive surface, which can be a thin layer of agar or agarose gel or the bottom of a culture dish not prepared for cell culture.

Only if the spheroid is formed and grown to a certain size can it be

transferred to a spinner culture vessel and grown in the same way as spheroids of established rodent cell lines. Human tumors successfully grown as spheroids include thyroid cancer, renal cancer, squamous carcinoma, colon carcinoma, neuroblastoma, human lung cancer, glioma, lymphoid tumors, melanoma, and osteosarcoma. There appears to be no general pattern. One glioma line might form and grow as spheroids; another might not. The same applies to other tumor types. Thus, it seems that the capacity to form and grow as spheroids is not a general property of tumor cells. Many nontumor cells also form spheroids, but only the spheroids of lymphoid origin continue to grow to any size.

Morphologic studies of spheroids of human tumor cells show that they maintain many characteristics of the original tumor specimens taken from the patient and of the cells if grown as a xenograft in nude mice. Radiobiologic studies show that in addition to maintaining histologic characteristics of individual tumors, spheroids of human cells preserve characteristic radiosensitivity because dose-response curves for spheroids are virtually identical to those for cells growing as xenografts in nude mice.

ORGANOID MODELS OF HUMAN TUMORS

Although spheroids represent a three-dimensional (3D) model of a tumor derived from a single cell to study the effects of radiation and radiation modifying therapies, they essentially represent a mass of cells and bear little resemblance to the tumor they were derived. Using a modification of the PDX model described earlier, resected tumor tissue can also be grown as “organoid” cultures in tissue culture by embedding the resected tissue within an extracellular matrix gel and providing defined growth factor mixtures. Depending on the growth conditions, the organoids can be composed solely of epithelial cells or both epithelial and stromal components. The power of this approach is that the tumor architecture can be recapitulated *in vitro* and that these structures can be generated repeatedly as they are derived from stem cells or tumor initiating cells.

Tumor-derived organoids represent an advance over spheroids and represent a new and exciting approach to testing radiation-induced modifiers. The advantages of tumor-derived organoids are their limitless life spans, biologic reproducibility, and relatively low cost. The disadvantages of organoids is that they need to be derived from a surgical biopsy and, depending on culture conditions, can be devoid of stromal and infiltrating immune cells. However, stromal endothelial and immune cells could be supplied at the time of encapsulation in extracellular gel.

COMPARISON OF THE VARIOUS MODEL TUMOR SYSTEMS

In all transplantable systems described, the tumor is treated *in situ*, with all of the realism and complexities of the *in vivo* milieu, such as cell-to-cell contact and the presence of hypoxic cells, factors that cannot be fully simulated in a petri dish. The tumor cure (TCD₅₀) and growth delay systems share the additional advantage that they are left *in situ* undisturbed after treatment. In the other techniques, the tumor must be removed, minced, and prepared into a single-cell suspension by the use of an enzyme, such as trypsin, before survival is assessed. Although this step does not appear to affect the assessment of the effects of radiation, it can result in artifacts in the case of other agents, such as chemotherapeutic drugs or hyperthermia, in which the cell membrane may be involved in the cellular response. The procedure of breaking up the tumor and partially dissolving the cell membrane with a digestive enzyme may influence results. For this reason, in the testing and evaluation of a new drug, one tumor system involving the determination of growth delay or TCD₅₀ is always included. These systems are very expensive because they require a large number of animals for the amount of information produced. The determination of TCD₅₀ is perhaps ideal for producing data relevant to clinical radiotherapy. It is certainly the most expensive; to produce a single TCD₅₀ value for one of the lines in [Figure 21.4](#), six to eight groups of up to 10 animals must be kept and observed for weeks. The same information can be obtained in 10 days with one or two mice and six petri dishes using the *in vivo/in vitro* technique.

The dilution assay technique allows clonogenic cell survival to be assessed over a large range of doses and for tumors that cannot be grown in culture. It, too, is relatively expensive because a whole group of recipient animals must be used and kept for weeks to obtain the same information obtained from one petri dish. Unquestionably, the most rapid and efficient technique is the *in vivo/in vitro* technique, which combines the realism of irradiation *in vivo* with the speed and efficiency of *in vitro* plating to assess clonogenic survival. The concomitant disadvantage is that any tumor that can be switched from petri dish to animal in alternate passages is so undifferentiated and anaplastic that it bears little resemblance to a spontaneous tumor in the human.

To some extent, the same criticism can be levied at all transplantable tumor systems. They are not only highly quantitative, but they are also very artificial. Having been cultured *in vitro* for many generations, they tend to be highly

undifferentiated, and they grow as encapsulated tumors in a muscle or beneath the skin rather than in the tissue of origin. In addition, some have produced misleading results because they are highly antigenic, which, in general, human tumors are not (Fig. 21.12).



FIGURE 21.12 Transplantable tumors in small laboratory animals not only have provided invaluable quantitative data, but they have also “led us up the garden path” on several occasions. Transplantable tumors tend to be fast growing, undifferentiated, and highly antigenic and are grown as encapsulated tumors in muscle or beneath the skin, not in their sites of origin. For all of these reasons, they are highly artificial, and care must be used in interpreting results.

Xenografts of human tumors so far have been used on a much more limited scale. Because they are grown in the absence of an immune response, it could be argued that they are the epitome of artificiality. They do, however, allow a comparison to be made of the intrinsic sensitivity to radiation or chemotherapeutic agents of fresh explants of human tumors. As *in vitro* culture techniques improve and better growth media are developed, xenografts may be less necessary.

PDXs of human tumors have been growing in use and are even now commercially available. Although they are grown in the absence of an immune system, they better reflect the heterogeneity of human tumors in a mouse model. Transgenic and autochthonous mouse models can model some aspects of cancer derived by known genetic drivers but suffer from variable growth rates.

A final point of consideration should be on the technical delivery of ionizing radiation to autochthonous or transgenic tumors. Compared to subcutaneously transplanted tumors in the flank of the animal that can be easily irradiated to spare normal tissue toxicity, spontaneous tumors are not superficial, and a more complex radiation protocol would have to be used to target the radiation to the

organ of interest and spare normal tissue toxicity. Such devices have started to become commercially available, and in some cases, include imaging capability as well. Thus, a new era in the postgenome era could emerge with the advent of transgenic mouse models, sophisticated technology to target radiotherapy to the tumor, and state-of-the-art imaging to quantify changes in tumor volume. The limitation to these studies will stem from cost.

Spheroids represent a most important intermediate model between monolayers of cells in culture and tumors *in vivo*. Several important radiobiologic principles have been established using spheroids of rodent cells, in which the various populations of cells, aerated versus hypoxic or cycling versus noncycling, can be separated out. Human cell spheroids have only been used on a limited scale, but it is clear that these cells retain many of the characteristics of the tumor from which they were taken. Spheroids are much less expensive than xenografts in immunosuppressed animals and perform much the same function. Human organoid cultures represent a cost-effective happy medium between PDXs and spheroids (Fig. 21.13). They possess similar architecture as the tumors they were derived from and can be cultured in conditions to allow the growth of stromal and immune cells. The use of human organoids in radiation biology research should significantly take off in the future as the culture conditions for tumors of different histologic origin become more defined.

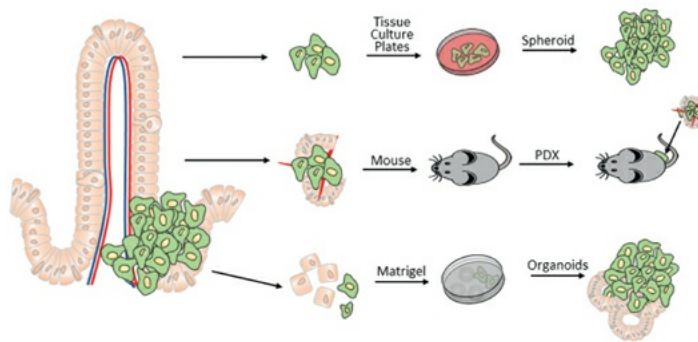


FIGURE 21.13 The choices of study the effect of therapy are based on ease of the assay, cost, and reliability. In this example of a colorectal tumor, tumor cells can be isolated from a colorectal tumor and can be used to generate a spheroid from *in vitro* cultured cells. These *in vitro* cultured cells can then be used to grow tumors when injected into immune-deficient mice. However, two more modern techniques will ultimately be more routinely used to investigate the effects of therapies on tumor biopsies. The first technique involves the direct implantation of tumor biopsies into a severely immune-compromised mouse. The advantage of this approach is that in many cases, the human stroma is still intact, and there has not been a selection bias from *in vitro* culture conditions.

These models reflect the heterogeneity of human tumors better than transplanted, transgenic, or autochthonous tumors. However, PDXs exhibit significant variability in their growth rates. A faster and more cost-effective approach to study the therapeutic effects of therapy is the use of organoids, which are derived from a tumor biopsy and, if embedded, in the appropriate gel matrix will grow in cell culture and possess the same architecture as the tumor from which it was derived.

SUMMARY OF PERTINENT CONCLUSIONS

A wide range of tumors of different histologic types can be grown in laboratory animals and propagated by transplantation.

Transplanted tumor systems can be highly quantitative, but, in general, the more quantitative the system, the more artificial it is because the tumors are highly undifferentiated and encapsulated.

The five assays in common use are tumor growth delay measurements, tumor cure (TCD_{50}) assay, tumor cell survival determined by the dilution assay technique, the production of lung colonies, and *in vivo* treatment followed by *in vitro* assay.

In all five assays, the cells can be irradiated *in situ* with all the realism and complexity of *in vivo* conditions.

If tumor cure (TCD_{50}) or growth delay is scored, the tumor is left undisturbed after treatment. This avoids artifacts involved in disaggregating the tumor, especially in the study of some chemicals or hyperthermia, in which cell membrane effects are important.

The dilution assay technique, the lung colony assay, and the *in vivo/in vitro* assay all measure the cell-surviving fraction; that is, they are clonogenic assays. They require fewer animals and are therefore more efficient than the scoring of tumor cure or growth delay. All three assays require, however, that a single-cell suspension be prepared from the tumor, and this may result in artifacts.

Transplantable tumors in small laboratory animals have been used to establish many radiobiologic principles, but they are highly artificial and must be used with care. They have “led us up the garden path” on several occasions.

Many human tumor cells can be grown as xenografts in immune-deficient animals.

Although the histologic characteristics of the human source tumor are maintained, the stroma is of mouse origin.

Xenografts of human tumor cells are not much better than mouse tumors for studies in which the vascular supply is important.

Human tumor cells undergo kinetic changes and selection if transplanted into immune-deficient mice.

Xenografts generally maintain the chemotherapeutic response characteristics of the class of tumors from which they are derived. There is evidence, too, of individuality of response.

Patient-derived biopsies (PDXs), which are immediately implanted into immune-deficient mice after excision, better reflect the heterogeneity of human tumors in mouse models.

Spheroids of established rodent cells can be grown in suspension culture (i.e., “spinner culture”). Oxygen and nutrients must diffuse into the spheroid from the surrounding culture medium. Oxygen deficiency and a buildup of waste products result, just as in a tumor.

Mature spheroids contain a heterogeneous population of cells, much like a tumor, but are more quantitative and more economical to work with.

Starting from the outside and working toward the center, spheroids consist of asynchronous aerated cells, noncycling G₁-like aerated cells, noncycling G₁-like hypoxic cells, and necrotic cells.

Spheroids are intermediate in complexity between monolayer cell cultures *in vitro* and transplantable tumors in experimental animals.

Organoids represent an advance over spheroids and reflect human tumor architecture in an *in vitro* model system.

Many types of human tumor cells grow as spheroids and maintain many characteristics of the original tumor from the patient or of the same cells grown as xenografts.

Programmed cell death, or apoptosis, occurs after irradiation in many animal tumors as well as in human xenografts in nude mice.

Apoptosis is most important in lymphomas, essentially absent in sarcomas, and intermediate and variable in carcinomas.

Cells may show signs of dying an apoptotic death by 3 hours after irradiation.

BIBLIOGRAPHY

- Acker H, Carlsson J, Durand R, et al, eds. *Spheroids in Cancer Research*. Berlin, Germany: Springer-Verlag; 1984.
- Andrews JR, Berry RJ. Fast neutron irradiation and the relationship of radiation dose and mammalian tumor cell reproductive capacity. *Radiat Res*. 1962;16:76–81.
- Barendsen GW, Broerse JJ. Experimental radiotherapy of a rat rhabdomyosarcoma with 15 MeV neutrons and 300 kV x-rays: I. Effects of single exposures. *Eur J Cancer*. 1969;5:373–391.
- Berry RJ. On the shape of x-ray dose-response curves for the reproductive survival of mammalian cells. *Br J Radiol*. 1964;37:948–951.
- Clifton KH, Briggs RC, Stone HB. Quantitative radiosensitivity studies of solid carcinomas in vivo: methodology and effect of anoxia. *J Natl Cancer Inst*. 1966;36:965–974.
- Dertinger H, Guichard M, Malaise EP. Relationship between intercellular communication and radiosensitivity of human tumor xenografts. *Eur J Cancer Clin Oncol*. 1984;20:561–566.
- Fowler JF. Biological foundations of radiotherapy. In: Turano L, Ratti A, Biagini C, eds. *Progress in Radiology*. Vol. 1. Amsterdam, Netherlands: Excerpta Medica; 1967:731–737.
- Hammond EM, Giaccia AJ. Hypoxia-inducible factor-1 and p53: friends, acquaintances, or strangers? *Clin Cancer Res*. 2006;12:5007–5009.
- Hermens AF, Barendsen GW. Cellular proliferation patterns in an experimental rhabdomyosarcoma in the rat. *Eur J Cancer*. 1967;3:361–369.
- Hermens AF, Barendsen GW. Changes of cell proliferation characteristics in a rat rhabdomyosarcoma before and after x-irradiation. *Eur J Cancer*. 1969;5:173–189.
- Hewitt HB. Studies of the quantitative transplantation of mouse sarcoma. *Br J Cancer*. 1953;7(3):367–383.
- Hewitt HB, Chan DP, Blake ER. Survival curves for clonogenic cells of a murine keratinizing squamous carcinoma irradiated in vivo or under hypoxic conditions. *Int J Radiat Biol Relat Stud Phys Chem Med*. 1967;12:535–549.
- Hewitt HB, Wilson CW. A survival curve for mammalian leukaemia cells

- irradiated in vivo (implications for the treatment of mouse leukaemia by whole-body irradiation). *Br J Cancer*. 1959;13:69–75.
- Hewitt HB, Wilson CW. Survival curves for tumor cells irradiated in vivo. *Ann NY Acad Sci*. 1961;95:818–827.
- Hill RP, Bush RS. A lung-colony assay to determine the radiosensitivity of the cells of a solid tumor. *Int J Radiat Biol Relat Stud Phys Chem Med*. 1969;15:435–444.
- Hill RP, Bush RS, Yeung P. The effect of anemia on the fraction of hypoxic cells in an experimental tumour. *Br J Radiol*. 1971;44:299–304.
- Izumchenko E, Meir J, Bedi A, et al. Patient-derived xenografts as tools in pharmaceutical development. *Clin Pharmacol Ther*. 2016;99:612–621.
- Kerr JFR, Searle J. Apoptosis: its nature and kinetic role. In: Meyn RE, Withers HR, eds. *Radiation Biology in Cancer Research*. New York, NY: Raven Press; 1980:367–384.
- McNally NJ. Recovery from sub-lethal damage by hypoxic tumour cells in vivo. *Br J Radiol*. 1972;45:116–120.
- Pourreau-Schneider N, Malaise EP. Relationship between surviving fractions using the colony methods, the LD₅₀, and the growth delay after irradiation of human melanoma cells grown as multicellular spheroids. *Radiat Res*. 1981;85:321–332.
- Reinhold HS. Quantitative evaluation of the radiosensitivity of cells of a transplantable rhabdomyosarcoma in the rat. *Eur J Cancer*. 1966;2:33–42.
- Rockwell SC, Kallman RF. Cellular radiosensitivity and tumor radiation response in the EMT6 tumor cell system. *Radiat Res*. 1973;53:281–294.
- Rockwell SC, Kallman RF, Fajardo LF. Characteristics of a serially transplanted mouse mammary tumor and its tissue-culture-adapted derivative. *J Natl Cancer Inst*. 1972;49:735–749.
- Sparrow S. *Immunodeficient Animals for Cancer Research*. London, United Kingdom: Macmillan; 1980.
- Steel GG. How well do xenografts maintain the therapeutic response characteristics of the source tumor in the donor patient? In: Kallman RF, ed. *Rodent Tumor Models in Experimental Cancer Therapy*. New York, NY: Pergamon; 1987.

- Steel GG, Courtenay VC, Peckham MJ. The response to chemotherapy of a variety of human tumour xenografts. *Br J Cancer*. 1983;47:1–13.
- Stephens LC, Ang KK, Schultheiss TE, et al. Apoptosis in irradiated murine tumors. *Radiat Res*. 1991;127:308–316.
- Suit HD, Maeda M. Hyperbaric oxygen and radiobiology of the C₃H mouse mammary carcinoma. *J Natl Cancer Inst*. 1967;39:639–652.
- Suit HD, Wette R. Radiation dose fractionation and tumor control probability. *Radiat Res*. 1966;29:267–281.
- Suit HD, Wette R, Lindberg R. Analysis of tumor-recurrence times. *Radiology*. 1967;88:311–321.
- Sutherland RM, Durand RE. Radiation response of multicell spheroids—an in vitro tumour model. *Curr Top Radiat Res Q*. 1976;11:87–139.
- Sutherland RM, McCredie JA, Inch WR. Growth of multicell spheroids in tissue culture as a model of nodular carcinomas. *J Natl Cancer Inst*. 1971;46:113–120.
- Sutherland RM, Sordat B, Bamat J, et al. Oxygenation and differentiation in multicellular spheroids of human colon carcinoma. *Cancer Res*. 1986;46:5320–5329.
- Tannock IF. The relation between cell proliferation and the vascular system in a transplanted mouse mammary tumour. *Br J Cancer*. 1968;22:258–273.
- Thomlinson RH, Craddock EA. The gross response of an experimental tumour to single doses of x-rays. *Br J Cancer*. 1967;21:108–123.
- Weeber F, Ooft SN, Dijkstra KK, et al. Tumor organoids as a pre-clinical cancer model for drug discovery. *Cell Chem Biol*. 2017;24:1092–1100.
- Williams GT. Programmed cell death: apoptosis and oncogenesis. *Cell*. 1991;65:1097–1098.
- Wong J, Armour E, Kazanzides P, et al. High-resolution, small animal radiation research platform with x-ray tomographic guidance capabilities. *Int J Radiat Oncol Biol Phys*. 2008;71:1591–1599.
- Yuhas JM, Blake S, Weichselbaum RR. Quantitation of the response of human tumor spheroids to daily radiation exposures. *Int J Radiat Oncol Biol Phys*. 1984;10:2323–2327.
- Yuhas JM, Tarleton AE, Molzen KB. Multicellular tumor spheroid formation by

breast cancer cells isolated from different sites. *Cancer Res.* 1978;38:2486–2491.

Zhou H, Rodriguez M, van den Haak F, et al. Development of a micro-computed tomography-based image-guided conformal radiotherapy system for small animals. *Int J Radiat Oncol Biol Phys.* 2010;78:297–305.

The Cell Cycle

Cyclins and Kinases

Checkpoint Pathways

Quantitative Assessment of the Constituent Parts of the Cell Cycle

The Percent-Labeled Mitoses Technique

Experimental Measurements of Cell Cycle Times *In Vivo* and *In Vitro*

Pulsed Flow Cytometry

The Growth Fraction

Potential Doubling Time

Cell Loss

Determinations of Cell Loss in Experimental Animal Tumors

Growth Kinetics of Human Tumors

Summary of Pertinent Conclusions

Bibliography

THE CELL CYCLE

The ability of cells to produce exact, accurate copies of themselves is essential to the continuance of life; it is accomplished through highly organized processes, well conserved through evolution. Lack of fidelity in cellular reproduction as manifested by DNA and chromosome alterations is a hallmark of cancer.

The only event in the cell cycle that can be identified with a simple light microscope is the condensation of the chromosomes during mitosis (M); this was observed in the late 19th century. Using autoradiography, Howard and Pelc in the early 1950s divided the cell cycle by showing that DNA was synthesized only during a discrete time interval, which they called the S phase. Between mitosis and the S phase was the “first gap in activity” (G₁), and between S phase and the next mitosis was the “second gap in activity” (G₂). If the cells stop

progressing through the cycle—that is, if they are arrested—they are said to be in G₀. The cell cycle was discussed in detail in [Chapter 4](#).

Howard and Pelc also showed that it was in these gaps that radiation affects cell cycle progression because in their early studies, it was obvious that cells arrest cell cycle progression after low-dose radiation damage not in S or M but in either G₁ or G₂. It was subsequently recognized that these arrests also were related to the process of malignancy because primary cells would arrest in both G₁ and G₂, but tumor cells often would show only the G₂ arrest point. Breakthroughs in understanding these events and the nature of the cell cycle itself came with the discovery of the cyclins, the cyclin-dependent kinases, and the cyclin–kinase inhibitors and with the elaboration by Hartwell and Weinert of the concept of cell cycle checkpoints. The current concept of the cell cycle and its regulation is illustrated in [Figure 22.1](#).

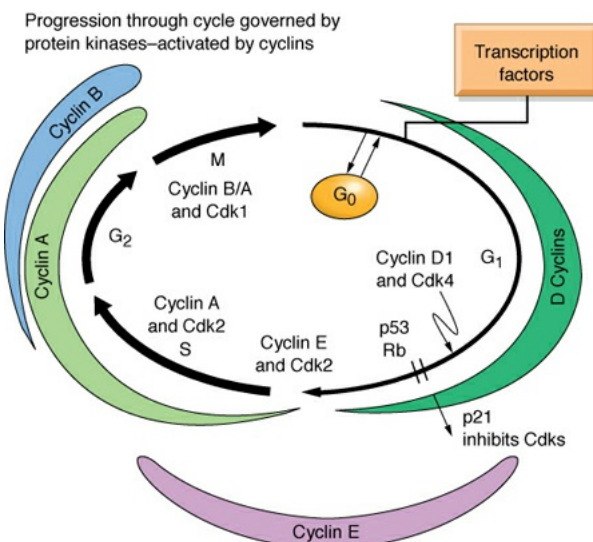


FIGURE 22.1 The current concept of the cell cycle and its regulation by protein kinases, activated by cyclins.

CYCLINS AND KINASES

Regulation of the complex processes that occur as a cell passes through the cycle is a result of a series of changes in the activity of intracellular enzymes known as **cyclin-dependent kinases (Cdks)**. The active forms of these enzymes exist in protein complexes with a cell cycle phase-specific protein known as a cyclin. Transitions from one phase to the next in the cycle occur only if the enzymatic activity of a given kinase activates the proteins required for progression.

In mammals, cyclins A through H have been described. Each cyclin protein is synthesized at a discrete phase of the cycle: cyclin D and E in G₁, cyclin A in

S and G₂, and cyclin B in G₂ and M. Cyclin levels oscillate with phase of the cycle.

Seven Cdks have been described. Cdk levels are constant throughout the cell cycle, but their activity is regulated by cyclin-dependent activating kinases, the protein level of cyclin regulatory subunits, and association with Cdk inhibitors.

Molecular events in G₁ prepare the cell for DNA synthesis. There is a stage in G₁, known as the G₁ restriction point, after which cells are committed to enter the S phase and no longer respond to growth conditions. Prior to this point, cells may take several routes: They may progress, differentiate, senesce, or die, depending on external signals. Key players in the G₁ restriction point include the protein of the retinoblastoma (Rb) gene, D-type cyclins, and Cdk4 and Cdk6 as well as Cdk inhibitors (see [Fig. 22.1](#)).

If extracellular signals stimulate a cell to enter the cycle from quiescence, D-type cyclins are stimulated and continue through G₁ and form a complex with Cdk4 or Cdk6. The activated cyclin–Cdk4 or cyclin–Cdk6 complex then phosphorylates the Rb protein, which releases it from E2F and its growth-suppressive function. E2F that is released from the Rb protein binds to the promoter of the cyclin E gene, resulting in increased cyclin E messenger ribonucleic acid (mRNA) and protein. There is more cyclin E available to bind Cdk2 and phosphorylate Rb, resulting in a positive feedback loop that is now refractory to mitogenic signals. Although numerous studies have documented the importance of all three D-type cyclins; two E-type cyclins; and Cdk2, Cdk4, and Cdk6, gene knockout studies in mice have indicated that all of these cyclins and their dependent kinases are not essential for normal cell cycle progression. However, the ability of cells to be transformed by oncogenes is dependent on G₁ cyclins and their dependent kinases. The current thinking is that untransformed cells require a lower level of G₁ cyclins to proliferate and differentiate, whereas transformation requires a quantitatively different level of G₁ cyclins. Thus, if increased G₁ cyclin activity is needed for transformation, then loss or diminished G₁ cyclin activity could act to suppress tumor formation.

Once a cell has committed to entering S, it must begin the incredibly difficult task of accurately copying more than 3 billion bases of the genome; this feat is completed in a matter of a few hours. DNA polymerases are the enzymes involved in this copying process, which must be completed with high fidelity, aided by repair and misrepair genes that remove and replace mismatched DNA bases. Cyclin A is maximally expressed in S phase and enhances transition of the

cell through this phase of the cycle.

After the cell has copied its entire genome, the next important task is to segregate the two copies of the DNA equally into the progeny cells. There is a gap (G_2), however, between the end of all detectable DNA synthesis and the beginning of cell division at which the process of condensing and segregating the chromosomes begins. Events during this period are controlled by Cdk activity analogous to that occurring at the G_1/S transition, but this time, it is a complex of cyclins B and A with Cdk1.

Although the cell is progressing through this complicated process of DNA replication and division, it must respond constantly to extracellular signals concerning nutrient status, cell-to-cell contact, and so forth that arrive at the nucleus through one or another signal transduction pathway.

CHECKPOINT PATHWAYS

Events in the cell cycle must take place in a specific order, and it is the function of several checkpoint genes to ensure that the initiation of late events is delayed until earlier events are complete.

There are three principal places in the cell cycle at which checkpoints function:

1. G_1/S checkpoint
2. S phase checkpoint
3. G_2/M checkpoint

If DNA is damaged, normal cells stop progressing through the cycle and are arrested at one of these checkpoints, depending on their position in the cell cycle at the time at which the damage occurs ([Fig. 22.2](#)).

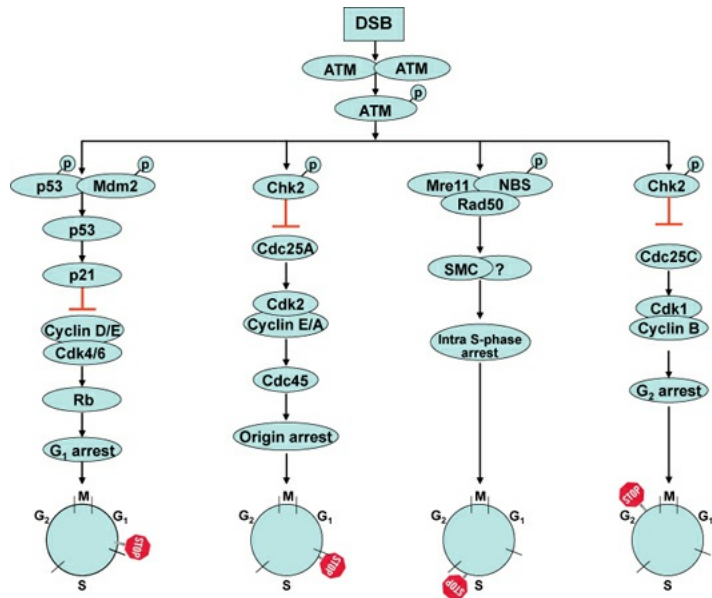


FIGURE 22.2 Diagram depicting the critical role of ataxia-telangiectasia mutated (ATM) and its downstream effectors in regulating the cell cycle. In response to DNA damage, ATM becomes activated and phosphorylates different key targets that will inhibit cell cycle progression in different phases of the cell cycle. In G₁ phase, ATM phosphorylates *p53* and Mdm2, resulting in increased *p53* transcriptional activation of the inhibitor p21, which inhibits the cyclin D/E–Cdk4/6 complex. In late G₁/early S phase, ATM phosphorylates Chk2 that in turn phosphorylates Cdc25A, a phosphatase that inhibits cyclin E/A–Cdk2 activity. In S phase, ATM is induced by DNA double-strand breaks (DSBs) that are not located at replication forks, phosphorylates Nijmegen breakage syndrome (NBS) and structural maintenance of chromosomes (SMC) proteins, and transiently inhibits DNA synthesis. In G₂ phase, ATM phosphorylates Chk1 that in turn phosphorylates Cdc25C, a phosphatase that inhibits cyclin B–Cdk1 activity. This diagram is included to reinforce the importance of ATM in inhibiting cell cycle progression in response to DNA damage. These interactions are dynamic and simplified and are, in reality, a great deal more complex with many additional accessory proteins. Rb, retinoblastoma.

Cells with damaged DNA in G₁ avoid replicating that damage by arresting at the G₁/S interface, or if they have already passed the restriction point governed by phosphorylation of Rb, they will transiently arrest in the S phase. Avoiding the replication of damaged DNA and allowing time for repair prevent cell death and the accumulation of heritable mutations. The tumor suppressor gene *p53* is critical in the pathway that leads to G₁ arrest (see Fig. 22.2). DNA damage initiates a chain of events: First, ataxia-telangiectasia mutated (ATM) autophosphorylates and releases an active monomer that can directly

phosphorylate *p53* and murine double minute 2 (Mdm2), the ubiquitin ligase that targets *p53* for degradation. In addition, the checkpoint kinases (Chk)—also targets of ATM—can also phosphorylate *p53* and Mdm2. Phosphorylation of both *p53* and Mdm2 results in increased levels of *p53* protein. Activated *p53* enhances p21^{WAF1/CIP1} gene expression, which results in a sustained inhibition of G₁ cyclin/Cdk5. G₁ cyclin inhibition prevents phosphorylation of Rb and progression from G₁ into S. Mutations in *p53* (which are present in so many human tumors) clearly compromise this checkpoint function. A second more rapid but transient checkpoint is also induced by DNA damage through Chk1 phosphorylation of the Cdc25A phosphatase and the inhibition of cyclin E–Cdk2 and cyclin A–Cdk2 complexes. This later checkpoint works independently of *p53* (see Fig. 22.2).

Control of the S phase checkpoint is in part mediated by the Cdc25A phosphatase inhibiting Cdk2 activity and the loading of Cdc45 onto chromatin. Failure to load Cdc45 onto chromatin prevents the recruitment of DNA polymerase α and replicon initiation (see Fig. 22.2). A second mechanism for S phase arrest is signaled by phosphorylation of Nijmegen breakage syndrome (NBS) by ATM. The importance of the S phase checkpoint is in protecting replication forks from trying to replicate through DNA strand breaks.

The arrest of cells in G₂ following DNA damage is observed readily in mammalian cells and was studied by radiation biologists for decades before checkpoints were understood at the molecular level. The arrest occurs after the levels of cyclin A increase in quantity but before cyclin B increases. The function of this checkpoint in normal cells is to prevent cells with damaged chromosomes from attempting the complex process of mitosis; they are arrested in G₂ to allow DNA repair to be completed. It follows, therefore, that cells lacking the G₂ checkpoint are radiosensitive because they cannot repair all of their damaged chromosomes before entering mitosis. At the molecular level, multiple kinase signaling pathways have been implicated in regulating this checkpoint (see Fig. 22.2). For example, ATM and Chk target the Cdc25C phosphatase and prevent cyclin B/A–Cdk1 activation. In addition, other regulatory proteins have been implicated in G₂ arrest, such as polo-like kinases, Brca1, and p53bp1. It appears that the G₂ checkpoint is the most regulated of all checkpoints and probably the most important in preventing the inappropriate entry of damaged cells into mitosis. Consequently, targeting the inhibition of key components of the G₂ checkpoint could increase radiosensitization.

The hallmark of cancer is a lack of the ability to respond to signals that normally would cause the cell to stop progressing through the cycle and dividing. Checkpoint proteins provide an important mechanism by which a cell can temporarily halt its transit through the cell cycle and attempt to restore chromosome integrity.

QUANTITATIVE ASSESSMENT OF THE CONSTITUENT PARTS OF THE CELL CYCLE

Two relatively simple measurements can be made on a population of cells. First, it is possible to count the proportion of cells that are seen to be in mitosis; this quantity is called the **mitotic index (MI)**. If it is assumed that all of the cells in the population are dividing and that all of the cells have the same mitotic cycle, then

$$MI = \lambda T_M / T_C$$

where T_M is the length of mitosis (i.e., the time taken for cells to complete division) and T_C is the total length of the mitotic cycle, or cell cycle.

The symbol λ is a correction factor to allow for the fact that cells cannot be distributed uniformly in time around the cycle because they double during mitosis (Fig. 22.3). The simplest assumption is that cells are distributed around the cycle exponentially in time, in which case λ has a value of 0.693. In any event, λ is a relatively small and unimportant correction factor.

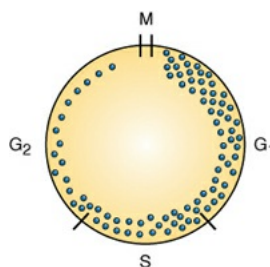


FIGURE 22.3 Diagram illustrating the fact that cells cannot be distributed uniformly in time around the cell cycle because they double in number during mitosis. The simplest assumption is that they are distributed as an exponential function of time.

The second relatively simple measurement requires that the cell population be fed for a brief time with a quantity of tritiated thymidine or 5-bromodeoxyuridine. In the jargon of cell kinetics, it is said to be **flash-labeled**. The cell population, whether on a petri dish or in a thin section cut from tissue, is then fixed, stained, and viewed through a microscope. A count is made of the

proportion of labeled cells. This quantity is called the **labeling index (LI)**.

Given the assumption that all the cells are dividing with the same cell cycle, then

$$LI = \lambda T_S / T_C$$

where T_S is the duration of the DNA synthetic period and T_C is the total cell cycle time.

In practice, these two quantities—the mitotic index and the labeling index—can be determined from a single specimen by counting the proportion of cells in mitosis and the proportion of cells that are labeled. This is a very important consideration in human studies in which it is usually not practical to obtain a large number of serial specimens of tumor or normal tissue material. Although these measurements yield ratios of the duration of mitosis and DNA synthesis as fractions of the T_C , they do not give the absolute duration of any part of the cycle.

THE PERCENT-LABELED MITOSES TECHNIQUE

A complete analysis of the cell cycle to obtain the length of each phase is only possible by labeling a cohort of cells in one phase of the cycle and observing the progress of this labeled cohort through a “window” in some other readily observable phase of the cycle. In practice, the easiest phase to label is S and the easiest to observe is M.

As stated previously, the labeling can be achieved by using either tritiated thymidine, identifiable by autoradiography, or bromodeoxyuridine, identifiable by a specific stain or antibody. The basis of the technique, therefore, is to feed the population of cells a label that is taken up in S and then to observe the appearance of that label in mitotic cells as they move around the cycle from S to M. To avoid confusion, the technique involving tritiated thymidine is described in detail partly because it is the original and classic technique and partly because pictures of autoradiographs show up well in black and white. The technique works equally well if bromodeoxyuridine is used. Bromodeoxyuridine-containing DNA can be stained and shows up well in color under a microscope but does not reproduce well in black and white.

The **percent-labeled mitoses technique** is laborious and time-consuming and requires a large number of serial samples. It is readily applicable *in vitro*, for which it is not difficult to obtain a large number of parallel replicate samples. It

may also be applied *in vivo* for determining the cell cycle parameters of normal tissue or tumors, provided a large number of sections from matched animals or tumors can be obtained at accurately timed intervals. The cell population first must be flash-labeled with tritiated thymidine. Theoretically, the labeled DNA precursor should be available to the cells for a negligibly short time; in practice, an exposure time of about 20 minutes is usually used. In *in vitro*, the thymidine is added to the growth medium; at the end of the flash-labeling period, it is simple to remove the radioactive medium and to add fresh medium. In *in vivo*, the tritiated thymidine is injected intraperitoneally; it clearly cannot be removed after 20 minutes, so the exposure time is terminated by the injection of a massive dose of “cold” (i.e., nonradioactive) thymidine.

During the period in which tritiated thymidine is available, cells in S phase take up the radioactive label. After the label is removed, cells progress through their cell cycles. At regular intervals, usually of 1 hour, a specimen of the cell population must be removed, fixed, and stained, and an autoradiograph is then prepared. This is continued for a total time longer than the cell cycle of the population under study. For each sample, the percentage of mitotic cells that carry a radioactive label must then be counted; this is the **percentage of labeled mitoses**. A photomicrograph of a cell preparation is shown in [Figure 22.4](#). This is a particularly laborious process because only 1% or 2% of the cells are in mitosis in any case, and only a fraction of these will be labeled.

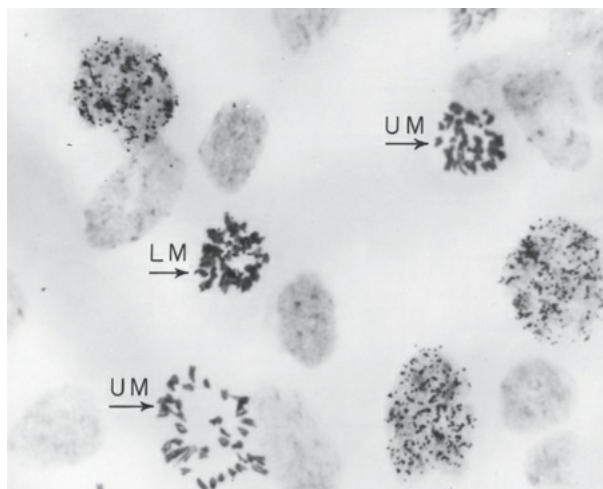


FIGURE 22.4 Photomicrograph of a preparation of mouse corneal cells. The cell preparation was flash-labeled some hours before with tritiated thymidine, which was taken up by cells in S phase. By the time the autoradiograph was made, the cell marked LM had moved around the cycle into mitosis; this is an example of a labeled mitotic figure. Other cells in mitosis are unlabeled (UM). (Courtesy of Dr. M. Fry.)

The basis for this type of experiment, if applied to an idealized population of cells that all have identical cell cycles, is illustrated in [Figure 22.5](#), a plot of the percentage of labeled mitoses as a function of time. The cells that are in S while the radioactive thymidine is available take up the label. This labeled cohort of cells then moves through the cell cycle (as indicated by the circles at the top of [Fig. 22.5](#)) after the pool of radioactive thymidine has been removed. Early samples contain no labeled mitotic figures, and the first labeled mitotic figure appears as the leading edge of the cohort of labeled cells reaches M. This point in time is labeled *b* on the time axis of [Figure 22.5](#); the position of the labeled cohort is indicated above on the circle, which is also marked *b*.

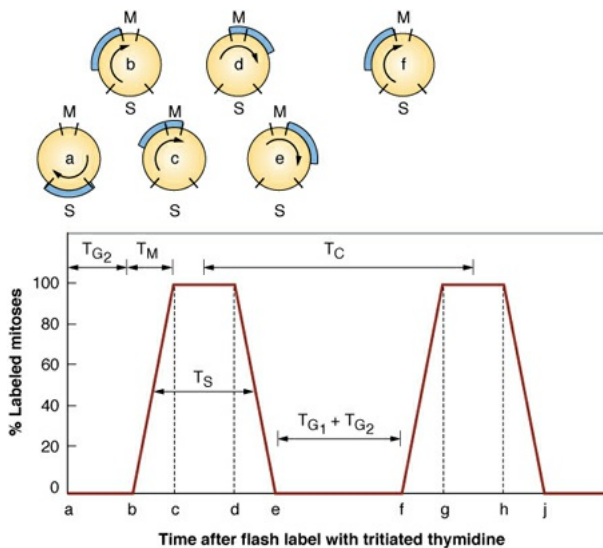


FIGURE 22.5 Percent-labeled mitoses curve for an idealized cell population in which all of the cells have identical mitotic cycle times. The cell population is flash-labeled with tritiated thymidine, which labels all cells in S. The proportion of labeled mitotic cells is counted as a function of time after labeling. The circles at the top of the figure indicate the position of the labeled cohort of cells as it progresses through the cycle. The length of the various phases (e.g., T_{G2} , T_M) of the cycle (T_C) may be determined as indicated.

The percentage of labeled mitotic figures increases rapidly as the leading edge of the labeled cohort of cells passes through the M phase; when it reaches the end of the M phase, all mitotic figures are labeled (position *c* in [Fig. 22.5](#)). For the next few hours, all mitotic figures continue to be labeled until the trailing edge of the labeled cohort of cells reaches the beginning of mitosis (position *d*), after which the percentage of labeled mitoses rapidly falls and reaches zero when the trailing edge reaches the end of mitosis (position *e*). There is then a long interval during which no labeled mitotic figures are seen until the labeled cohort of cells goes around the entire cycle and comes up to mitosis again, after which

the whole pattern of events is repeated.

All of the parameters of the cell cycle may be calculated from [Figure 22.5](#). The time interval before the appearance of the first labeled mitosis, the length ab , is in fact the length of G_2 or T_{G2} . The time it takes for the percent-labeled mitoses curve to rise from 0% to 100% (bc) corresponds to the time necessary for the leading edge of the labeled cohort of cells to proceed through mitosis and is therefore equal to the length of mitosis, T_M . The duration of DNA synthesis (T_S) is the time taken for the cohort of labeled cells to pass the beginning of mitosis (bd). Likewise, it is the time required for the labeled cohort to pass the end of mitosis (ce). In practice, T_S usually is taken to be the width of the curve at the 50% level, as marked in [Figure 22.5](#).

The T_C is the distance between corresponding points on the first and second wave (bf , cg , dh , or ej) or the distance between the centers of the two peaks as marked on the figure. The remaining quantity, T_{G1} , usually is calculated by subtracting the sum of all the other phases of the cycle from the T_C , or

$$T_{G1} = T_C (T_S + T_{G2} + T_M)$$

Experimental data are never as clear-cut as the idealized picture in [Figure 22.5](#). Points such as b and e , at which the curve begins to rise and reaches zero, are poorly defined. A more typical experimental result is illustrated in [Figure 22.6](#). The only points that can be defined with any certainty are the peaks of the curves and the 50% levels, and these may be used to give a rough estimate of the lengths of the various phases of the cycle. The S period (T_S) is given approximately by the width of the first peak, from the 50% level on the ascending portion of the wave to the corresponding point on the descending curve. The T_C , is readily obtained as the time between successive peaks. In a separate experiment, the mitotic index may be counted, which is equal to $\lambda T_M / T_C$; because T_C is known, T_M may be calculated. The time from flash-labeling to the point at which the curve passes the 50% level in [Figure 22.6](#) is $T_{G2} + 0.5 T_M$; because T_M already is known, T_{G2} may be calculated. The remaining quantity, T_{G1} , is deduced by subtraction because the T_C and all other phases are known.

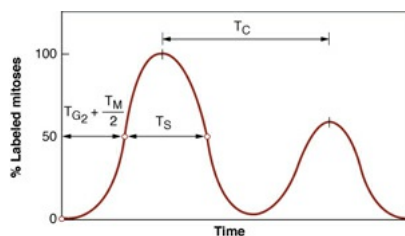


FIGURE 22.6 Typical percent-labeled mitoses curve obtained in practice for the cells of a tissue or tumor. It differs from the idealized curve in Figure 22.5 in that the only points that can be identified with precision are the peaks of the curve and the 50% levels. The first peak is not perfectly symmetric, and the second peak is lower than the first because the cells of a population have a range of cell cycle times.

A careful examination of an actual set of experimental data makes it plain that the first wave in the percent-labeled mitoses curve is not symmetric; the downswing is shallower than the upswing. This observation, coupled with the fact that the second peak is much smaller than the first, indicates that the population is made up of cells with a wide range of cycle times. In many instances, particularly if the population of cells involved is an *in vivo* specimen of a tumor or normal tissue, the spread of cell cycle times is so great that a second peak is barely discernible.

In practice, therefore, the constituent parts of the cycle are not simply read off the percent-labeled mitoses curve. Instead, a complex computer program is used to try various distributions of cell cycle times and to calculate the curve that best fits the experimental data. In this way, an estimate is obtained of the mean cell cycle time and of the range of cell cycle times in the population.

EXPERIMENTAL MEASUREMENTS OF CELL CYCLE TIMES *IN VIVO* AND *IN VITRO*

A vast number of cell cycle measurements have been made. Only a few representative results are reviewed here to highlight the most important points.

Figure 22.7 shows the percent-labeled mitoses data for two transplantable rat tumors with very different growth rates. The tumor represented in the upper panel (Fig. 22.7A) has a gross doubling time of about 20 hours, which can be judged easily from the separation of the first and second waves of labeled mitotic cells.

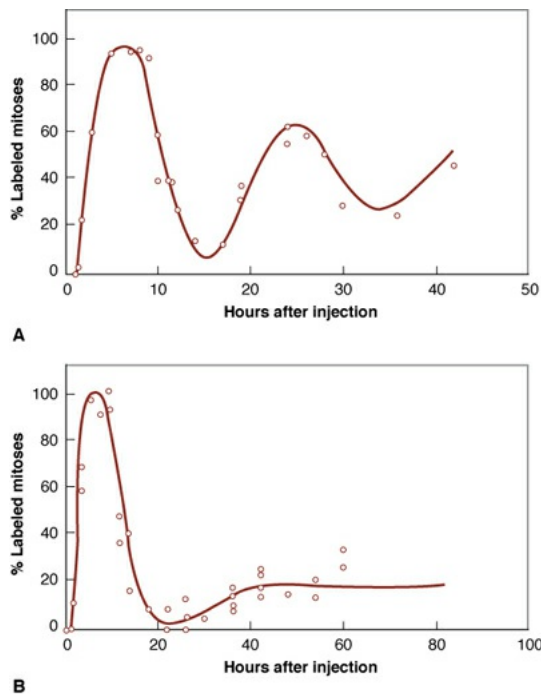


FIGURE 22.7 Percent-labeled mitoses curve for two transplantable rat sarcomas with widely different growth rates. The tumor in the **upper panel (A)** has a gross doubling time of 22 hours, compared with 192.5 hours for the tumor in the **lower panel (B)**. (Adapted from Steel GG, Adams K, Barrett JC. Analysis of the cell population kinetics of transplanted tumours of widely-differing growth rate. *Br J Cancer*. 1966;20:784–800, with permission.)

For the tumor illustrated in the lower panel (Fig. 22.7B), there is no discernible second peak in the percent-labeled mitoses curve because of the large range of cell cycle times among the cells of the population. To obtain an estimate of the average cell cycle in this case, it is necessary to pool information from the percent-labeled mitoses curve and from the knowledge of the labeling index. The width of the first wave of the percent-labeled mitoses curve indicates that the length of the DNA synthetic phase (T_S) is about 10 hours. To obtain the average cell cycle time (T_C), it is essential in this situation to know the labeling index. For this tumor, the labeling index is about 3.6%. The average cell cycle time (T_C) can then be calculated from the following equation:

$$LI = \lambda T_S / T_C$$

Therefore,

$$T_C = (0.693 \times 10) / (3.6 / 100) = 192.5 \text{ hours}$$

The absence of a second peak is a clue to the fact that there is a wide range of cell cycle times for the cells of this population, so 192.5 hours is very much an

average value.

A computer analysis makes it possible to estimate the distribution of cell cycle times in a population. For example, [Figure 22.8](#) shows the percent-labeled mitoses curve for a transplantable mouse tumor (see [Fig. 22.7B](#)), together with an analysis of cell cycle times based on a mathematical model ([Fig. 22.8A](#)). There is a wide range of cell cycle times, from less than 10 to more than 40 hours, with a modal value of about 19 hours. This range of cycle times explains the damped labeled mitoses curve and the fact that the first peak is not symmetric.

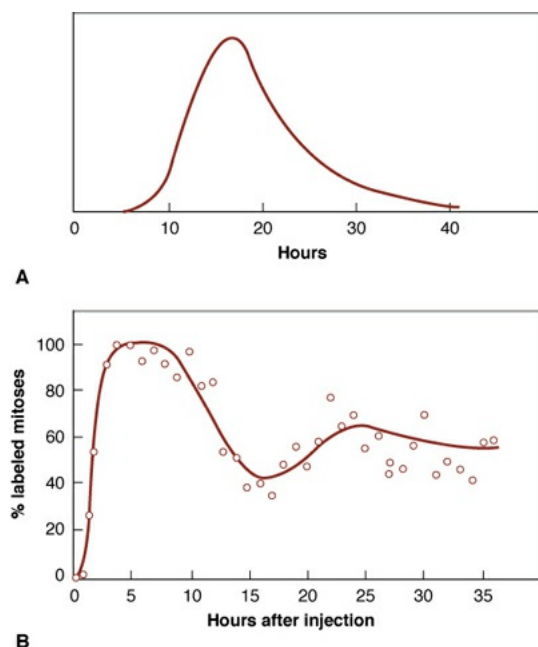


FIGURE 22.8 **A:** The distribution of cell cycle times consistent with the damped labeled mitoses curve, obtained by computer analysis of the data and a mathematical model. (Adapted from Steel GG. The growth kinetics of tumors in relation to their therapeutic response. *Laryngoscope*. 1975;85:359–370, with permission.) **B:** Percent-labeled mitoses curve for an EMT6 mouse tumor. (Data from Dr. Sara Rockwell.)

[Table 22.1](#) is a summary of the cell cycle parameters for cell lines in culture and some of the tissues and tumors for which percent-labeled mitoses curves have been shown in this chapter. The top row of [Table 22.1](#) shows the data for Chinese hamster cells in culture. These cells are characterized by a short cell cycle of only 10 hours and a minimal G₁ period. The second row of the table gives the comparable figures for HeLa cells. From a comparison of these two *in vitro* cell lines, a very important point emerges. The cell cycles of the two cell lines differ by a factor of more than 2, nearly all of which results from a

difference in the length of G₁. The other phases of the cycle are very similar in the two cell lines.

Also included in **Table 22.1** are data for the cells of the normal cheek pouch epithelium in the hamster and a chemically induced carcinoma in the pouch. These are representative of several studies in which cells from a solid tumor have been compared with their normal tissue counterparts. In general, it is usually found that the malignant cells have the shorter cycle time.

In reviewing the data summarized in **Table 22.1**, it is at once evident that although the length of the cell cycle varies enormously between populations, particularly *in vivo*, the lengths of G₂, mitosis, and S are remarkably constant. The vast bulk of the cell cycle variation is accounted for by differences in the length of the G₁ phase.

Table 22.1 The Constituent Parts of the Cell Cycle (in Hours) for Some Cells in Culture and Tumors in Experimental Animals

AUTHORS	CELL OR TISSUE	T _C	T _S	T _M	T _{G2}	T _{G1}
Bedford	Hamster cells <i>in vitro</i>	10	6	1	1	2
	HeLa cells <i>in vitro</i>	23	8	1	3	11
Steel	Mammary tumors in the rat					
	BICR/M1	19	8	~1	2	8
	BICR/A2	63	10	~1	2	50
Quastler and Mouse intestinal crypt		18.75	7.5	0.5	0.5–1.0	9.5

Sherman						
Brown Berry	and Hamster cheek pouch epithelium	120–152	8.6	1.0	1.9	108–140
	Chemically induced carcinoma in pouch	10.7	5.9	0.4	1.6	2.8

PULSED FLOW CYTOMETRY

During the past several decades, classic autoradiography largely has been replaced by pulsed flow cytometry (Fig. 22.9). The conventional techniques of autoradiography give precise, meaningful answers, but they are laborious and slow. Techniques based on flow cytometry provide data that are available within a few days. Detailed cell kinetic data can be obtained by such techniques, including an analysis of the distribution of cells in the various phases of the cycle (Fig. 22.10).

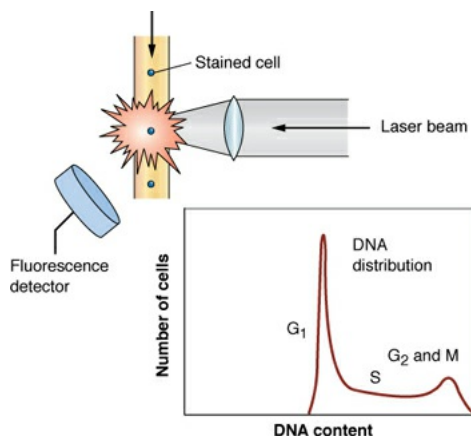


FIGURE 22.9 The principles of DNA distribution analysis of flow cytometry. Suspensions of fluorescent-stained single cells flow one at a time through a light beam, with its wavelength adjusted to excite the fluorescent dye. The fluorescence stimulated in each cell is recorded as a measure of that cell's DNA content. Thousands of cells can be measured each second, and the results accumulated to form a DNA distribution like that shown for asynchronously growing Chinese hamster ovary cells. (Adapted from Gray JW, Dolbeare F, Pallavicini MG, et al. Cell cycle analysis using flow cytometry. *Int J Radiat Biol.* 1986;49:237–255, with permission.)

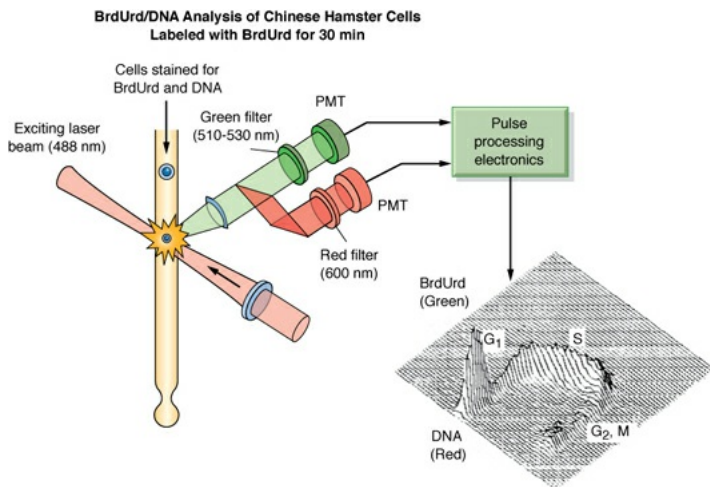


FIGURE 22.10 The flow cytometric analysis of cellular bromodeoxyuridine (BrdUrd) and DNA content for cells stained with fluorescein (linked to BrdUrd) and propidium iodide (linked to DNA). The cells are processed one at a time through a blue (488-nm) laser beam that excites cellular BrdUrd content, and red fluorescence is recorded as a measure of cellular DNA content. The BrdUrd (green fluorescence) axis in the bivariate is logarithmic, with every seven channels representing a doubling of fluorescence intensity. (Adapted from Gray JW, Dolbeare F, Pallavicini MG, et al. Cell cycle analysis using flow cytometry. *Int J Radiat Biol.* 1986;49:237–255, with permission.)

THE GROWTH FRACTION

Central to an appreciation of the pattern of growth of solid tumors is the realization that at any given moment, not all of the tumor cells that are viable and capable of continued growth are actually proceeding through the cell cycle. The population consists of proliferating (P) cells and quiescent (Q) cells. The growth fraction (GF), a term introduced by Mendelsohn, is defined as the ratio of the number of er of cells ($P + Q$), or

$$GF = P / (P + Q)$$

There are various ways to estimate growth fraction. One method consists of injecting tritiated thymidine into an animal with a tumor and then several cell generations later, preparing an autoradiograph from sections of the tumor. The growth fraction is given by the expression

$$GF = \frac{\text{fraction of cells labeled}}{\text{fraction of mitoses labeled}}$$

This method assumes that there are two distinct subpopulations, one growing with a uniform cell cycle, the other not growing at all.

Continuous labeling is an alternative way to provide an approximate measure

of the proportion of proliferating cells. Tritiated thymidine is infused continuously for a time equal to the cell cycle minus the length of the S phase. The fraction of labeled cells then approximates to the growth fraction.

Table 22.2 is a summary of growth fractions measured for various solid tumors in experimental animals, which frequently fall between 30% and 50%, even though the tumors vary widely in degree of differentiation, arise in different species, and are of varied histologic types. As a tumor outgrows its blood supply, areas of necrosis often develop that are accompanied by hypoxic cells, the proportion of which for many solid tumors is about 15%. This accounts for part, but not all, of the quiescent cell population.

Table 22.2 Growth Fraction for Some Tumors in Experimental Animals

TUMOR	AUTHOR	GROWTH FRACTION, %
Primary mammary carcinoma in the mouse (G ₃ H)	Mendelsohn	35–77
Transplantable sarcoma in the rat (RIB ₅)	Denekamp	55
Transplantable sarcoma in the rat (SSO)	Denekamp	47
Transplantable sarcoma in the rat (SSB ₁)	Denekamp	39
Mammary carcinoma in the mouse (C ₃ H)	Denekamp	30
Chemistry-induced carcinoma in the hamster Brown cheek pouch		29

POTENTIAL DOUBLING TIME

The potential doubling time (T_{pot}) of a tumor is defined as the cell doubling time without any cell loss. The T_{pot} is determined by the GF and the cell cycle time (T_C):

$$T_{\text{pot}} = \frac{T_C}{GF}$$

Using thymidine analogues and flow cytometry, the T_{pot} can be estimated from the duration of the S phase (T_S) and the fraction of cells within that phase (LI)

$$T_{\text{pot}} = \frac{\lambda T_S}{LI}$$

where λ is a correction factor for the nonrectangular age distribution of growing cell populations and usually has a value between 0.67 and 1. Using this method, the T_{pot} for various human tumors from different sites was found to vary between 4 days and 34 days. The differences in T_{pot} are mainly attributable to the variation in LI between tumors, whereas T_S appears to be relatively similar between tumors with an average value of about 12 hours. At one time, it was thought that T_{pot} might correlate with the repopulation rate of clonogenic cells, and thus predict outcome after radiotherapy, but this did not prove to be the case in clinical trials.

CELL LOSS

The overall growth of a tumor is the result of a balance achieved between cell production from division and various types of cell loss. In most cases, tumors grow much more slowly than would be predicted from a knowledge of the cycle time of the individual cells and the growth fraction. The difference is a result of cell loss. The extent of the cell loss from a tumor is estimated by comparing the rate of production of new cells with the observed growth rate of the tumor. The discrepancy provides a measure of the rate of cell loss. If T_{pot} is the potential tumor doubling time ($T_{\text{pot}} = \lambda T_S / LI$; where T_S is the length of the DNA synthetic period, LI is the labeling index, and λ is a correction factor between 0.67 and 1), and T_d is the actual tumor doubling time, obtained from simple direct measurements on the diameter of the tumor mass, the **cell-loss factor** (ϕ) has been defined by Steel to be

$$\phi = 1 - T_{\text{pot}} / T_d$$

The cell-loss factor represents the *ratio of the rate of cell loss to the rate of new cell production*. It expresses the loss of growth potential by the tumor. A cell-loss factor of 100%, for instance, indicates a steady state of neither growth nor regression.

Cells in tumors can be lost in several ways:

1. Death from inadequate nutrition: As the tumor outgrows its vascular system, rapid cell proliferation near capillaries pushes other cells into regions remote from blood supply, in which there is an inadequate concentration of oxygen and other nutrients. These cells die, giving rise to a progressively enlarging necrotic zone.
2. Apoptosis, or programmed cell death: This form of cell death is manifested by the occurrence of isolated degenerate nuclei remote from regions of overt necrosis.
3. Death from immunologic attack
4. Metastasis, including all processes by which tumor cells are lost to other parts of the body, such as spread through the bloodstream and lymphatic system
5. Exfoliation, which would not apply to most model tumors in experimental animals but which could be an important mechanism of cell loss from, for example, carcinoma of the gastrointestinal tract in which the epithelium is renewed at a considerable rate

There are limited data on the relative importance of these different processes in different tumor types, but it is clear that death from inadequate nutrition—by entry into necrotic areas—is often a major factor. It reflects the latent inability of the vascular system to keep up with the rate of cell production. There is still a great deal to be learned about the occurrence of cell loss from tumors, the mechanisms by which it occurs, and the factors by which it can be controlled. It is clear, however, that any understanding of the growth rate of tumors at the cellular level must include a consideration of this often dominant factor.

DETERMINATIONS OF CELL LOSS IN EXPERIMENTAL ANIMAL TUMORS

The cell-loss factor has been estimated in a considerable number of tumors in experimental animals. Some of the results are listed in [Table 22.3](#). Values for the cell-loss factor vary from 0% to more than 90%. In reviewing the literature on

this subject, Denekamp pointed out that sarcomas tended to have low cell-loss factors, but carcinomas tended to have high cell-loss factors. All the sarcomas investigated had cell-loss factors less than 55%; most carcinomas had cell-loss factors in excess of 70%. Therefore, cell loss appears to be a dominant factor in the growth of carcinomas and of considerably less importance for sarcomas. This pattern correlates with the importance of apoptosis as a mode of cell death. Apoptosis is quite common in carcinomas and rare in sarcomas. If this is found to be a general phenomenon, it might be attributed to the origin of carcinomas from continuously renewing epithelial tissues in which the cell-loss factor is 100%.

Table 22.3 Cell-Loss Factor (ϕ) for Some Tumors in Experimental Animals

TUMOR	AUTHOR	ϕ , %
Mouse sarcoma	Frindel	
3-d-old tumor		0
7-d-old tumor		10
20-d-old tumor		55
Rat carcinoma	Steel	9
Rat sarcoma	Steel	0
Mouse carcinoma	Mendelsohn	69

Hamster carcinoma	Brown	75
Rat sarcoma	Hermens	26
Hamster carcinoma	Reiskin	81–93
Mouse carcinoma	Tannock	70–92

This difference between sarcomas and carcinomas may also account for their differing responses to radiation. In carcinomas in which the production of new cells is temporarily stopped or reduced by a dose of radiation, cells continue to be removed from the tumor because of the high cell-loss factor, and the tumor shrinks. In sarcomas, however, even if a large proportion of the cells are sterilized by a dose of radiation, they do not disappear from the tumor mass as quickly.

It would be simple, then, to explain why two tumors, one a carcinoma and one a sarcoma, containing the same number of cells and exposed to the same radiation dose, would appear to behave quite differently. The carcinoma might shrink dramatically soon after the radiation dose, whereas the sarcoma would not appear as affected by the radiation. In the long term, the “cure” rates of both tumors may well be identical, but in the short term, the carcinoma would be said to have “responded” to the radiation, whereas the sarcoma might be said to be unresponsive or resistant to radiation.

GROWTH KINETICS OF HUMAN TUMORS

Perhaps the most basic question of tumor growth kinetics is “How fast do tumors grow?” The common observation of a tumor being undetectable for a considerable period of time but then proceeding to kill the patient within a relatively short time after detection should not be interpreted in terms of a period of dormancy followed by rapid growth. On the contrary, when the tumor consists of only a small number of cells, it may grow exponentially. As it gets larger, the growth rate slows as the supply of oxygen and nutrients are outgrown. The shape of the growth curve is best fitted by a Gompertz function. The mathematical formulation is complex and beyond the scope of this book, but the overall shape

of the growth curve is simple enough and is illustrated in Figure 22.11. The growth rate slows as the tumor gets larger.

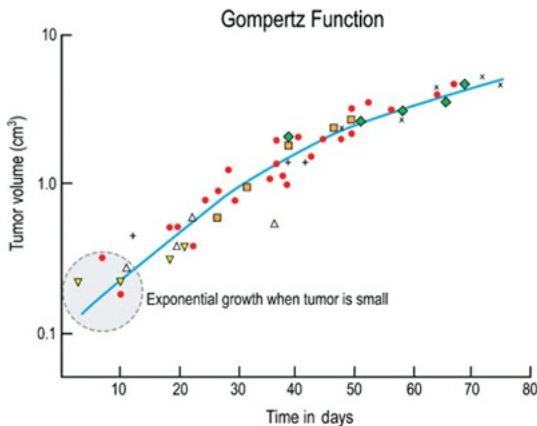


FIGURE 22.11 Illustrating a typical growth curve for an animal tumor, which is best fitted by a **Gompertz** function. When a tumor is composed of only a few cells, it may grow exponentially, but when it gets larger, the growth rate slows as the supply of oxygen and nutrients are outgrown.

The first quantitative study of the growth rate of human tumors was done by Collins and his colleagues in 1956. They observed the growth of pulmonary metastases from serial chest radiographs. It is now possible to gather information from the literature on the doubling time of more than 1,000 human tumors. Most of the data were obtained either by measurements from radiographs or by direct measurements of skin tumors or metastases in soft tissue. The doubling time of human tumors varies widely from patient to patient and is, on the average, very long; Tubiana and Malaise have estimated that the median value is about 2 months.

Tumors of the same histologic type arising in different patients differ widely in growth rate. By contrast, metastases arising in the same patient tend to have similar rates of growth. The latter observation is the basis for using patients with multiple skin or pulmonary metastases to test and compare new treatment modalities, such as high-linear energy transfer radiations or hyperthermia. There is certainly a correlation between histologic type and growth rate. Tubiana and Malaise have collected values for the doubling time in 389 patients with pulmonary metastases classified into five histologic categories. They can be arranged in order of doubling time as follows: embryonic tumors, 27 days; malignant lymphomas, 29 days; mesenchymal sarcomas, 41 days; squamous cell carcinomas, 58 days; and adenocarcinomas, 82 days. In addition, the degree of differentiation seems to be related to the doubling time, with poorly differentiated cancers generally progressing more rapidly.

In addition to growth rate measurements, studies of cell population kinetics also have been performed on a limited number of human tumors. Studies of this kind raise practical and ethical problems. The ethical problems stem from the fact that *in vivo* experiments require an injection of tritiated thymidine or bromodeoxyuridine, which limits such studies to patients who have short life expectancies and in whom the injection of the label does not raise any problems of possible genetic consequences. The practical problems arise because the percent-labeled mitoses technique, which is the most satisfactory way to obtain the duration of the various phases of the cell cycle, requires a large number of sequential samples to be taken for several days after the injection of the label.

In mice or rats, the multiple samples are obtained from a large number of identical animals bearing transplanted tumors of the same size and type by sacrificing one or more animals each time. In humans, each spontaneous tumor is unique, so the multiple samples must be obtained by repeated biopsies at frequent intervals from the same tumor. This heroic procedure is uncomfortable and inconvenient for the patient and is only practical with large superficial skin tumors, which may not be truly representative of human tumors in general. Nevertheless, a surprisingly large number of human tumors have been studied in this way. The percent-labeled mitoses curves obtained are similar to those for laboratory animals, although the second wave of labeled mitoses is rarely distinct and is usually altogether absent.

Tubiana and Malaise surveyed the field and reported 40 cases in which the cell cycle of solid tumors in humans had been evaluated with the percent-labeled mitoses technique. The cell cycles observed were between 15 and 125 hours in 90% of the cases, with a modal value of 48 hours ([Table 22.4](#)). The duration of S (T_S) was less variable than the T_C , with 90% of the values falling between 9.5 and 24 hours and a modal value of about 16 hours. As a first approximation, it can be assumed that T_S has a duration of about 16 hours and that the mean duration of the cell cycle is about 3 times the duration of T_S .

Table 22.4 Individual Values for the Duration of the Cell Cycle (T_C) in Human Solid Tumors of Various Histologic Types

AUTHORS	T_C , h
Frindel et al. (1968)	97, 51.5, 27.5, 48, 49.8

Bennington (1969)	15.5, 14.9
Young and de Vita (1970)	42, 82, 74
Shirakawa et al. (1970)	120, 144
Weinstein and Frost (1970)	217
Terz et al. (1971)	44.5, 31, 14, 25.5, 26
Peckham and Steel (1973)	59
Estevez et al. (1972)	37, 30, 48, 30, 38, 96, 48
Terz and Curutchet (1974) ^a	18, 19, 19.2, 120
Malaise et al. (unpublished data) ^a	24, 33, 48, 42
Muggia et al. (1972)	64
Bresciani et al. (1974)	82, 50, 67, 53, 58

^aMeasured by the mean grain count halving time. From Tubiana M, Malaise EP. Growth

rate and cell kinetics in human tumors: some prognostic and therapeutic implications. In: Symington T, Carter RL, eds. *Scientific Foundations of Oncology*. Chicago, IL: Year Book Medical; 1976:126–136, with permission.

Although the percent-labeled mitoses technique has been used on relatively few human tumors, the labeling index has been measured in many more after *in vitro* incubation of a fresh piece of excised tumor with tritiated thymidine. The rationale underlying this technique is that cells already synthesizing DNA *in vivo* are able to continue synthesis of DNA *in vitro*, but no new cells enter synthesis under the incubation conditions that normally are used.

The growth fraction, too, has been measured in only a limited number of human tumors by the method of continuous labeling. If a population of cells is labeled continuously during a period corresponding to the duration of the cell cycle less the duration of the DNA synthetic phase (i.e., $T_C - T_S$), all the actively proliferating cells should be labeled. This method of continuous labeling can be performed only with a small number of patients who are in no way representative. An alternative procedure is to estimate the growth fraction by assuming that the proportion of cells in cycle is about equal to 3 times the labeling index, an assumption based on the notion that the cell cycle is 3 times the length of the S phase. The growth fraction calculated in this way correlates well with the tumor doubling time: It is 0.9 in malignant lymphomas and embryonic tumors and less than 0.06 in adenocarcinomas. The relation between the growth rate and growth fraction appears to be much closer in human tumors than in animal tumors.

Of the various parameters that characterize tumor kinetics, the cell-loss factor is, in general, the most difficult to evaluate. The cell-loss factor for human tumors generally has been calculated by comparing the *observed tumor volume-doubling time* with the *potential doubling time*, which is the time required for the population of cells to double, assuming that all the cells produced are retained in the tumor. Tubiana and Malaise calculated a mean value of the cell-loss factor for five histologic groups of human tumors, assuming the duration of S to be 16 hours. Their results suggest that, in general, the mean cell-loss factor exceeds 50%. Furthermore, it appeared to be higher if the tumor was growing quickly and if its growth fraction was high. In humans, the smallest cell-loss factors seem to be associated with those histologic types of tumors that have the slowest rate of growth. The cell-loss factor, therefore, tends to reduce the spread of growth rates that results from the differences in growth fraction of the various types of tumors.

Steel has estimated independently the extent of cell loss in human tumors by comparing the potential doubling time with observed tumor growth rates. The relevant data on the volume doubling time for six groups of human tumors are given in [Table 22.5](#). They consist mostly of measurements of primary and secondary tumors of the lung. There are differences between individual series, which indeed may reflect significant differences in the growth rates of the various types of tumors, but if the results are all pooled, they yield an average median doubling time of 66 days, with 80% of the values falling in the range between 18 and 200 days. Taking the median values for the labeling index, doubling time, and S phase as suggested by Steel, the median cell-loss factor in all human tumors studied is 77%. It thus would appear that for human tumors, cell loss is generally the most important factor determining the pattern of tumor growth.

Table 22.5 Volume Doubling Times of Human Tumors

AUTHORS	SITE	VOLUME DOUBLING TIME, d	RANGE, d
Breur	Lung metastases	40	4–745
Collins et al.	Lung metastases	40	11–164
Collins	Lung metastases from colon or rectum	96	34–210
Garland	Primary bronchial carcinomas	105	27–480
Schwartz	Primary bronchial carcinomas	62	17–200
Spratt	Primary skeletal sarcomas	75	21–366

Based on the data from Steel GG. Cell loss from experimental tumors. *Cell Tissue Kinet.* 1968;1:193–207.

The high rate of cell loss in human tumors largely accounts for the great disparity between the cell cycle time of the individual dividing cells and the overall doubling time of the tumor. Although the tumor doubling time is characteristically 40 to 100 days, the cell cycle time is relatively short, 1 to 5 days. This has important implications, which often are overlooked, in the use of cycle-specific chemotherapeutic agents or radiosensitizing drugs for which it is the cell cycle time that is relevant.

Because Bergonié and Tribondeau established a relation between the rate of cell proliferation and the response to irradiation in normal tissues, it might be supposed that this would be the same for tumors. It is of interest to note that the histologic groups of human tumors that have the most rapid mean growth rates and the highest growth fractions and cell turnover rates are indeed those that are the most radiosensitive. There is also a correlation between, on the one hand, the growth rate and the labeling index or the cell loss and, on the other hand, the reaction to chemotherapy. This is not surprising because most drugs act essentially on cells in S phase. It is remarkable, however, that the only human tumors in which it is possible to achieve cures by chemotherapy are the histologic types with high labeling indexes. Furthermore, a high level of cell loss appears to favor the response to chemotherapy, and in humans, this occurs especially in tumors with high labeling indexes.

SUMMARY OF PERTINENT CONCLUSIONS

The division of the cell cycle into its constituent phases, M, G₁, S, and G₂, was accomplished in the 1950s.

The arrest of cells at various positions in the cycle by the action of “checkpoint genes” is an important response to DNA damage. The two principal checkpoints are the G₁/S and the G₂/M boundary, but there is also a checkpoint in S. G₂/M is the most important checkpoint following radiation damage; cells pause at G₂/M to repair radiation-induced damage before attempting the complex process of mitosis.

Progression through the cell cycle is governed by protein kinases, activated by cyclins. Each cyclin protein is synthesized at a discrete phase of the cycle: cyclin D and E in G₁, cyclin A in S and G₂, and cyclin B in G₂ and M.

Transitions in the cycle occur only if a given kinase activates the proteins required for progression.

Most of the difference in cell cycle between fast- and slow-growing cells is a result of differences in G₁, which varies from less than 1 hour to more than a week.

The mitotic index (MI) is the fraction of cells in mitosis:

$$MI = \lambda T_M / T_C$$

The labeling index (LI) is the fraction of cells that take up tritiated thymidine (i.e., the fraction of cells in S):

$$LI = \lambda T_S / T_C$$

The percent-labeled mitoses technique allows an estimate to be made of the lengths of the constituent phases of the cell cycle. The basis of the technique is to label cells with tritiated thymidine or bromodeoxyuridine in S phase and time their arrival in mitosis.

Flow cytometry allows a rapid analysis of the distribution of cells in the cycle. Cells are stained with a DNA-specific dye and sorted based on DNA content.

The bromodeoxyuridine–DNA assay in flow cytometry allows cells to be stained simultaneously with two dyes that fluoresce at different wavelengths: One binds in proportion to DNA content to indicate the phase of the cell cycle, and the other binds in proportion to bromodeoxyuridine incorporation to show if cells are synthesizing DNA.

The growth fraction is the fraction of cells in active cell cycle (i.e., the fraction of proliferative cells).

In animal tumors, the growth fraction frequently ranges from 30% to 50%.

The cell-loss factor (ϕ) is the fraction of cells produced by cell division lost from the tumor.

In animal tumors, ϕ varies from 0% to more than 90%, tending to be small in small tumors and to increase with tumor size.

The cell-loss factor ϕ tends to be large for carcinomas and small for sarcomas.

The shape of a tumor growth-curve is best fitted by a Gompertz function. Growth may be exponential when the tumor is small but slows as the tumor gets larger and outgrows the supply of oxygen and nutrients.

The observed volume doubling time of a tumor is the gross time for it to double overall in size as measured, for example, in serial radiographs.

Tumors grow much more slowly than would be predicted from the cycle time of individual cells. One reason is the growth fraction, but the principal reason is the cell-loss factor.

The overall pattern of tumor growth may be summarized as follows: A minority of cells (the growth fraction) are proliferating rapidly; most are quiescent. Most new cells produced by mitosis are lost from the tumor.

In general, the cell cycle time of malignant cells is appreciably shorter than that of their normal tissue counterparts.

In general, irradiation causes an elongation of the cell cycle time in tumor cells and a shortening of the cell cycle in normal tissues.

In 90% of human tumors, the cell cycle time has a modal value of 48 hours (a range of 15 to 125 hours).

In human tumors, T_S has a modal value of about 16 hours (a range of 9.5 to 24 hours).

As a first approximation, the mean duration of the cell cycle in human tumors is about 3 times the duration of the S phase.

Growth fraction is more variable in human tumors than in rodent tumors and correlates better with gross volume doubling time.

Cell-loss factor for human tumors has been estimated by Tubiana and Malaise to have an average value for a range of tumors in excess of 50%. Steel's estimate for a median value for all human tumors studied is 77%.

BIBLIOGRAPHY

Abraham RT. Cell cycle checkpoint signaling through the ATM and ATR kinases. *Genes Dev.* 2001;15:2177–2196.

Bakkenist CJ, Kastan MB. DNA damage activates ATM through intermolecular autophosphorylation and dimer dissociation. *Nature.* 2003;421:499–506.

Bartek J, Lukas J. Chk1 and Chk2 kinases in checkpoint control and cancer. *Cancer Cell.* 2003;3:421–429.

Begg AC, Haustermans K, Hart AA, et al. The value of pretreatment cell kinetic parameters as predictors for radiotherapy outcome in head and neck cancer: a

- multicenter analysis. *Radiother Oncol.* 1999;50:13–23.
- Begg AC, Hofland I, van Glabekke M, et al. Predictive value of potential doubling time for radiotherapy of head and neck tumor patients: results from the EORTC Cooperative Trial 22851. *Semin Radiat Oncol.* 1992;2:22–25.
- Begg AC, McNally NJ, Shrieve DC, et al. A method to measure the duration of DNA synthesis and the potential doubling time from a single sample. *Cytometry.* 1985;6:620–626.
- Begg AC, Moonen L, Hofland I, et al. Human tumour cell kinetics using a monoclonal antibody against iododeoxyuridine: intratumour sampling variations. *Radiother Oncol.* 1988;11:337–347.
- Bergonié J, Tribondeau L. Interpretation of some results of radiotherapy in an attempt at determining a logical technique of treatment. *Radiat Res.* 1959;11:587–588.
- Bresciani F. A comparison of the generative cycle in normal, hyperplastic and neoplastic mammary gland of the C3H mouse. In: *Cellular Radiation Biology*. Baltimore, MD: Williams & Wilkins; 1965:547–557.
- Breur K. Growth rate and radiosensitivity of human tumours. I. Growth rate of human tumours. *Eur J Cancer.* 1966;2:157–171.
- Brown JM. The effect of acute x-irradiation on the cell proliferation kinetics of induced carcinomas and their normal counterpart. *Radiat Res.* 1970;43:627–653.
- Brown JM, Berry RJ. Effects of x-irradiation on the cell population kinetics in a model tumor and normal tissue system: implication for the treatment of human malignancies. *Br J Radiol.* 1969;42:372–377.
- Collins VP, Loeffler RK, Tivey J. Observation on growth rates of human tumors. *Am J Roentgenol Radium Ther Nucl Med.* 1956;6:988–1000.
- Denekamp J. The cellular proliferation kinetics of animal tumors. *Cancer Res.* 1970;30:393–400.
- Denekamp J. The relationship between the ‘cell loss factor’ and the immediate response to radiation in animal tumours. *Eur J Cancer.* 1972;8:335–340.
- Dolbeare F, Beisker W, Pallavicini MG, et al. Cytochemistry for bromodeoxyuridine/DNA analysis: stoichiometry and sensitivity. *Cytometry.* 1985;6:521–530.

- Dolbeare F, Gratzner H, Pallavicini MG, et al. Flow cytometric measurement of total DNA content and incorporated bromodeoxyuridine. *Proc Natl Acad Sci USA*. 1983;80:5573–5577.
- el-Deiry WS, Kern SE, Pietenpol JA, et al. Definition of a consensus binding site for p53. *Nat Genet*. 1992;1:45–49.
- Elkind M, Han A, Volz K. Radiation response of mammalian cells grown in culture: IV. Dose dependence of division delay and post irradiation growth of surviving and nonsurviving Chinese hamster cells. *J Natl Cancer Inst*. 1964;30:705–711.
- Fornace AJ Jr, Nebert DW, Hollander MC, et al. Mammalian genes coordinately regulated by growth arrest signals and DNA-damaging agents. *Mol Cell Biol*. 1989;9:4196–4203.
- Frankfurt OS. Mitotic cycle and cell differentiation in squamous cell carcinomas. *Int J Cancer*. 1967;2:304–310.
- Frindel E, Malaise EP, Alpen E, et al. Kinetics of cell proliferation of an experimental tumor. *Cancer Res*. 1967;27:1122–1131.
- Frindel E, Malaise EP, Tubiana M. Cell proliferation kinetics in five human solid tumors. *Cancer*. 1968;22:611–620.
- Frindel E, Valleron AJ, Vassort F, et al. Proliferation kinetics of an experimental ascites tumor of the mouse. *Cell Tissue Kinet*. 1969;2:51–65.
- Gray JW. Cell-cycle analysis of perturbed cell populations: computer simulation of sequential DNA distributions. *Cell Tissue Kinet*. 1976;9:499–516.
- Gray JW, Carver JH, George YS, et al. Rapid cell cycle analysis by measurement of the radioactivity per cell in a narrow window in S phase (RCSi). *Cell Tissue Kinet*. 1977;10:97–109.
- Gray JW, Dolbeare F, Pallavicini MG, et al. Cell cycle analysis using flow cytometry. *Int J Radiat Biol*. 1986;49:237–255.
- Hartwell LH, Weinert TA. Checkpoints: controls that ensure the order of cell cycle events. *Science*. 1989;246:629–634.
- Hermens AF, Barendsen CW. Cellular proliferation patterns in an experimental rhabdomyosarcoma in the rat. *Eur J Cancer*. 1967;3:361–369.
- Hoshino T, Nagashima T, Murovic J, et al. Cell kinetic studies of in situ human brain tumors with bromodeoxyuridine. *Cytometry*. 1985;6:627–632.

- Howard A, Pelc SR. Synthesis of deoxyribonucleic acid in normal and irradiated cells and its relation to chromosome breakage. *Heredity*. 1952;6(suppl):261.
- Kastan MB, Bartek J. Cell-cycle checkpoints and cancer. *Nature*. 2004;432:316–323.
- Kastan MB, Onyekwere O, Sidransky D, et al. Participation of p53 protein in the cellular response to DNA damage. *Cancer Res*. 1991;51:6304–6311.
- Kastan MB, Zhan Q, el-Deiry WS, et al. A mammalian cell cycle checkpoint pathway utilizing p53 and GADD45 is defective in ataxia-telangiectasia. *Cell*. 1992;71:587–597.
- Kitagawa R, Bakkenist CJ, McKinnon PJ, et al. Phosphorylation of SMC1 is a critical downstream event in the ATM-NBS1-BRCA1 pathway. *Genes Dev*. 2004;18:1423–1438.
- Kuerbitz SJ, Plunkett BS, Walsh WV, et al. Wild-type p53 in a cell cycle checkpoint determinant following irradiation. *Proc Natl Acad Sci USA*. 1992;89:7491–7495.
- Lee JH, Paull TT. ATM activation by DNA double-strand breaks through the Mre11-Rad50-Nbs1 complex. *Science*. 2005;308:551–554.
- Lesher S. Compensatory reactions in intestinal crypt cells after 300 Roentgens of cobalt-60 gamma irradiation. *Radiat Res*. 1967;32:510–519.
- McKenna WG, Iliakis G, Weiss MC, et al. Increased G₂ delay in radiation-resistant cells obtained by transformation of primary rat embryo cells with the oncogens H-ras and v-myc. *Radiat Res*. 1991;125:283–287.
- Mendelsohn ML. Autoradiographic analysis of cell proliferation in spontaneous breast cancer of the C3H mouse. III. The growth fraction. *J Natl Cancer Inst*. 1962;28:1015–1029.
- Mendelsohn ML. Principles, relative merits, and limitations of current cytokinetic methods. In: Drewinko B, Humphrey RM, eds. *Growth Kinetics and Biochemical Regulation of Normal and Malignant Cells*. Baltimore, MD: Williams & Wilkins; 1977:101–112.
- Mendelsohn ML. The growth fraction: a new concept applied to tumors. *Science*. 1960;132:1496.
- Morstyn G, Hsu SM, Kinsella T, et al. Bromodeoxyuridine in tumors and chromosomes detected with a monoclonal antibody. *J Clin Invest*. 1983;72:1844–1850.

- Muschel RJ, Zhang HB, Iliakis G, et al. Cyclin B expression in HeLa cells during the G₂ block induced by ionizing radiation. *Cancer Res.* 1991;51:5113–5117.
- Muschel RJ, Zhang HB, Iliakis G, et al. Effects of ionizing radiation on cyclin expression in HeLa cells. *Radiat Res.* 1992;132:153–157.
- Norbury C, Nurse P. Animal cell cycles and their control. *Annu Rev Biochem.* 1992;61:441–470.
- Palekar SK, Sirsat SM. Replication time & pattern of transplanted fibrosarcoma in the mouse. *Indian J Exp Biol.* 1967;5:173–175.
- Pines J, Hunter T. Isolation of a human cyclin cDNA: evidence for cyclin mRNA and protein regulation in the cell cycle and for interaction with p34cdc2. *Cell.* 1989;58:833–846.
- Post J, Hoffman J. The replication time and pattern of carcinogen-induced hepatoma cells. *J Cell Biol.* 1964;22:341–350.
- Quastler H, Sherman FG. Cell population kinetics in the intestinal epithelium of the mouse. *Exp Cell Res.* 1959;17:420–438.
- Rashad AL, Evans CA. Radioautographic study of epidermal cell proliferation and migration in normal and neoplastic tissues of rabbits. *J Natl Cancer Inst.* 1968;41:845–853.
- Refsum SB, Berdal P. Cell loss in malignant tumors in man. *Eur J Cancer.* 1967;3:235–236.
- Reiskin AB, Berry RJ. Cell proliferation and carcinogenesis in the hamster cheek pouch. *Cancer Res.* 1968;28:898–905.
- Reiskin AB, Mendelsohn ML. A comparison of the cell cycle in induced carcinomas and their normal counterpart. *Cancer Res.* 1964;24:1131–1136.
- Sherr CJ, Roberts JM. Living with or without cyclins and cyclin-dependent kinases. *Genes Dev.* 2004;18:2699–2711.
- Shiloh Y. ATM and related protein kinases: safeguarding genome integrity. *Nat Rev Cancer.* 2003;3:155–168.
- Simpson-Herren L, Blow JG, Brown PH. The mitotic cycle of sarcoma 180. *Cancer Res.* 1968;28:724–726.
- Steel GG. Autoradiographic analysis of the cell cycle: Howard and Pelc to the present day. *Int J Radiat Biol Relat Stud Phys Chem Med.* 1986;49:227–235.

- Steel GG. Cell loss as a factor in the growth rate of human tumours. *Eur J Cancer*. 1967;3:381–387.
- Steel GG. Cell loss from experimental tumors. *Cell Tissue Kinet*. 1968;1:193–207.
- Steel GG. *The Growth Kinetics of Tumours*. Oxford, United Kingdom: Oxford University Press; 1977.
- Steel GG. The growth kinetics of tumors in relation to their therapeutic response. *Laryngoscope*. 1975;85:359–370.
- Steel GG. The kinetics of cell proliferation in tumors. In: Bond VP, ed. *Proceedings of the Carmel Conference on Time and Dose Relationships in Radiation Biology as Applied to Radiotherapy*. Upton, NY; 1969:130–149. BNL report 50203 (C-57).
- Steel GG, Adams K, Barrett JC. Analysis of the cell population kinetics of transplanted tumours of widely-differing growth rate. *Br J Cancer*. 1966;20:784–800.
- Steel GG, Hanes S. The technique labeled mitoses: analysis by automatic curve-fitting. *Cell Tissue Kinet*. 1971;4:93–105.
- Terry NH, White RA, Meistrich ML, et al. Evaluation of flow cytometric methods for determining population potential doubling times using cultured cells. *Cytometry*. 1991;12:234–241.
- Tubiana M, Malaise EP. Growth rate and cell kinetics in human tumors: some prognostic and therapeutic implications. In: Symington T, Carter RL, eds. *Scientific Foundations of Oncology*. Chicago, IL: Year Book Medical; 1976:126–136.

chapter 23

Time, Dose, and Fractionation in Radiotherapy

The Introduction of Fractionation

The Four Rs of Radiobiology

The Strandquist Plot and the Ellis Nominal Standard Dose System

Proliferation as a Factor in Normal Tissues

The Shape of the Dose–Response Relationship for Early- and Late-Responding Tissues

A Possible Explanation for the Difference in Shape of Dose–Response Relationships for Early- and Late-Responding Tissues

Fraction Size and Overall Treatment Time: Influence on Early- and Late-Responding Tissues

Accelerated Repopulation

The Importance of Overall Treatment Time

Multiple Fractions per Day

Hypofractionation: Renewed Interest

Using the Linear-Quadratic Concept to Calculate Effective Doses in Radiotherapy

Choice of α/β

Model Calculations

Allowance for Tumor Proliferation

Summary of Pertinent Conclusions

Bibliography

THE INTRODUCTION OF FRACTIONATION

The multifraction regimens commonly used in conventional radiation therapy are a consequence largely of radiobiologic experiments performed in France in the 1920s and in the 1930s. It was found that a ram could not be sterilized by exposing its testes to a single dose of radiation without extensive skin damage to the scrotum, whereas if the radiation was spread out over a period of weeks in a

series of daily fractions, sterilization was possible without producing unacceptable skin damage (Fig. 23.1). It was postulated that the testes were a model of a growing tumor, whereas the skin of the scrotum represented a dose-limiting normal tissue. The reasoning may be flawed, but the conclusion proved to be valid: Fractionation of the radiation dose produces, in most cases, better tumor control for a given level of normal tissue toxicity than a single large dose.



FIGURE 23.1 Conventional multifraction radiotherapy was based on experiments performed in Paris in the 1920s and in the 1930s. Rams could not be sterilized with a single dose of x-rays without extensive skin damage, whereas if the radiation were delivered in daily fractions over a period of time, sterilization was possible without skin damage. The testes were regarded as a model of a growing tumor and skin as dose-limiting normal tissue.

THE FOUR Rs OF RADIobiOLOGY

Now, more than 80 years later, we can account for the efficacy of fractionation based on more relevant radiobiologic experiments. We can appeal to the “four Rs” of radiobiology to be as follows:

- Repair of sublethal damage
- Reassortment of cells within the cell cycle
- Repopulation
- Reoxygenation

The basis of fractionation in radiotherapy can be understood in simple terms. Dividing a dose into several fractions spares normal tissues because of repair of sublethal damage between dose fractions and repopulation of cells if the overall time is sufficiently long. At the same time, dividing a dose into several fractions increases damage to the tumor because of reoxygenation and reassortment of cells into radiosensitive phases of the cycle between dose fractions.

The advantages of prolongation of treatment are to spare early reactions and

to allow adequate reoxygenation in tumors. Excessive prolongation, however, allows surviving tumor cells to proliferate during treatment.

THE STRANDQUIST PLOT AND THE ELLIS NOMINAL STANDARD DOSE SYSTEM

Early attempts to understand and account for fractionation gave rise to the well-known Strandquist plot, in which total dose was plotted as a function of the overall treatment time (Fig. 23.2). Because all treatments were given as three or five fractions per week, overall time in this plot contains, by implication, the number of fractions as well. It commonly was found in these plots that the slope of the isoeffect curve for skin was about 0.33; that is, the total dose for an isoeffect was proportional to $T^{0.33}$.

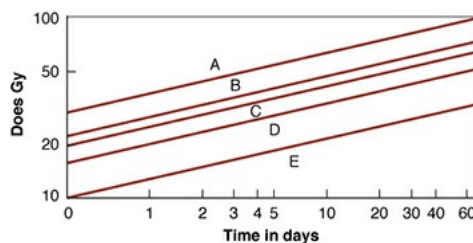


FIGURE 23.2 Isoeffect curves relating the total dose to the overall treatment time for skin necrosis (A), cure of skin carcinoma (B), moist desquamation of skin (C), dry desquamation of skin (D), and skin erythema (E). (Adapted from Strandquist M. A study of the cumulative effect of fractionated x-ray treatment based on the experience mined at the Radium Hemmant with the treatment of 280 cases of carcinoma of the skin and lip. *Acta Radiol*. 1944;55[suppl]:1–300, with permission.)

The most important contribution in this area, made by Ellis and his colleagues with the introduction of the **nominal standard dose (NSD)** system, was the recognition of the importance of separating overall time from the number of fractions. According to this hypothesis, total dose for the tolerance of connective tissue is related to the number of fractions (N) and the overall time (T) by the relation

$$\text{Total dose} = (\text{NSD})T^{0.11}N^{0.24}$$

The NSD system has been discussed extensively. It does enable predictions to be made of equivalent dose regimens, provided that the range of time and number of fractions are not too great and do not exceed the range over which the data are available. For example, in changing a treatment protocol from five to four fractions per week, the formula can be used to calculate the size of dose

fractions needed to result in the same normal tissue tolerance with the two different protocols. Of course, because the system is based ultimately on skin reaction data, it does not, in any way, predict *late effects*. An obvious weakness of the NSD system is that time is allowed for in terms of a single power function, in which the nominal single dose is proportional to $T^{0.11}$. In fact, biologic experiments with small animals have shown that this relationship is far from accurate. Proliferation does not affect the total dose required to produce a given biologic reaction at all until some time after the start of irradiation, but then, the dependence in time is much greater than allowed for by the Ellis formula. For these and other reasons, the NSD system is seldom used nowadays.

PROLIFERATION AS A FACTOR IN NORMAL TISSUES

Experimental evidence indicates that the total dose required to produce a given biologic effect is not a power function of time, as postulated by the Ellis NSD system, but turns out to be more complex. The extra dose required to counter proliferation and result in a given level of skin damage in mice does not increase at all until about 12 days into a fractionated regimen, but then, it increases very rapidly as a function of time. The shape of the curve is roughly sigmoidal (Fig. 23.3). If similar data were available for humans, the effects of proliferation would not be seen until a longer period into a fractionation regimen because of the slower response of the human skin and the longer cell cycle of the individual cells. Figure 23.3 is not meant to be quantitative but to indicate that the shape of the curve relating extra dose to proliferation is sigmoidal. This illustrates immediately that the method of allowing for overall time in the NSD system is incorrect or, at best, is a very crude approximation.

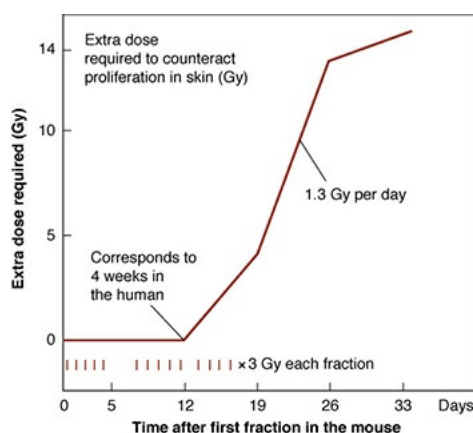


FIGURE 23.3 The extra dose required to counteract proliferation in the skin of mice as a function of time after starting daily irradiation with 3 Gy per fraction. A delay followed by a rapid rise is typical of time factors in proliferating normal

tissues. In mouse skin, the delay is about 2 weeks; in humans, it is about 4 weeks. (Adapted from Fowler JF. Fractionated radiation therapy after Strandquist. *Acta Radiol*. 1984;23:209–216, with permission; and data from Denekamp J. Changes in the rate of repopulation during multifraction irradiation of mouse skin. *Br J Radiol*. 1973;46:381, with permission.)

A further consideration is that all normal tissues are not the same. In particular, there is a clear distinction between tissues that are *early responding*, such as the skin, mucosa, and intestinal epithelium, and those that are *late responding*, such as the spinal cord. [Figure 23.4](#) shows the extra dose required to produce a given level of damage for a fractionated protracted regimen in the case of representative tissues from the early- and late-responding groups. This diagram compares mouse skin, representative of early-responding tissues, and rat spinal cord, representative of late-responding tissues. It is recognized that these may not be ideal examples, but suitable data for more relevant systems are simply not available; comparable quantitative data certainly are not available for humans. The point made by this figure is that the time after the start of a fractionated regimen at which extra dose is required to compensate for cellular proliferation is quite different for late- versus early-responding tissues. The other point made, of course, is that these are data from rodents and that in the case of humans, the time scales (although they are not known with any precision) are likely to be very much longer. In particular, the time at which extra dose is required to compensate for proliferation in late-responding tissues in humans is far beyond the overall time of any normal radiotherapy regimen.

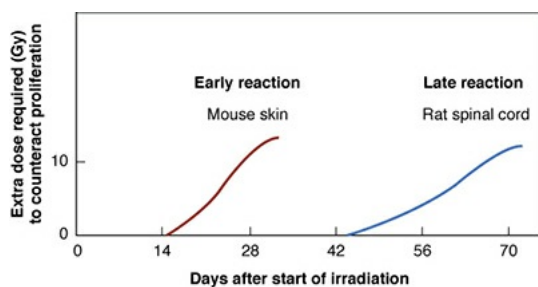


FIGURE 23.4 The extra dose required to counteract proliferation only as a function of time after starting daily irradiation in rodents. The *left curve* represents a typical early reaction; the *right curve* represents a typical late reaction. The delays are much longer in humans. (Adapted from Fowler JF. The second Klaas Breur memorial lecture. La Ronde—radiation sciences and medical radiology. *Radiother Oncol*. 1983;1:1–22, with permission.)

[Figure 23.5](#) is an attempt to convert the experimental laboratory data contained in [Figure 23.4](#) into a general principle that can be applied to clinical

practice. Early-responding tissues are triggered to proliferate within a few weeks of the start of a fractionated regimen so that the “extra dose to counter proliferation” increases with time, certainly during conventional radiotherapeutic protocols. By contrast, conventional radiotherapy extending to 6 or 8 weeks is never long enough to allow the triggering of proliferation in late-responding tissues. These considerations lead to the following important axiom:

Prolonging overall time within the normal radiotherapy range has little sparing effect on late reactions, but a large sparing effect on early reactions.

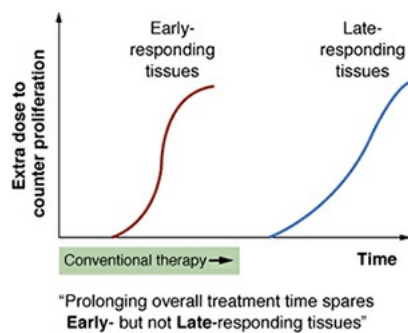


FIGURE 23.5 Highly speculative illustration attempting to extrapolate the experimental data for early- and late-responding tissue in rats and mice to principles that can be applied in clinical radiotherapy. The extra dose required to counter proliferation in early-responding tissues begins to increase after a few weeks into a fractionated regimen, certainly during the time course of conventional therapy. By contrast, conventional protocols are never sufficiently long to include the proliferation of late-responding tissues.

This has far-reaching consequences in radiotherapy. Early reactions, such as reactions of the skin or of the mucosa, can be dealt with easily by the simple expedient of prolonging the overall time. Although such a strategy overcomes the problem of the early reactions, it has no effect whatsoever on the late reactions.

THE SHAPE OF THE DOSE-RESPONSE RELATIONSHIP FOR EARLY- AND LATE-RESPONDING TISSUES

Clinical and laboratory data suggest that there is a consistent difference between early- and late-responding tissues in their responses to changing fractionation patterns. If fewer and larger dose fractions are given, late reactions are more severe, even though early reactions are matched by an appropriate adjustment in

total dose. This dissociation can be interpreted as differences in repair capacity or shoulder shape of the underlying dose–response curves. The dose–response relationship for late-responding tissues is more curved than that for early-responding tissues. In terms of the linear-quadratic relationship between effect and dose, this translates into a larger α/β ratio for early effects than for late effects. The difference in the shapes of the dose–response relationships is illustrated in [Figure 23.6](#). The α/β ratio is the dose at which cell killing by the linear (α) and the quadratic (β) components are equal (see [Fig. 23.14](#)).

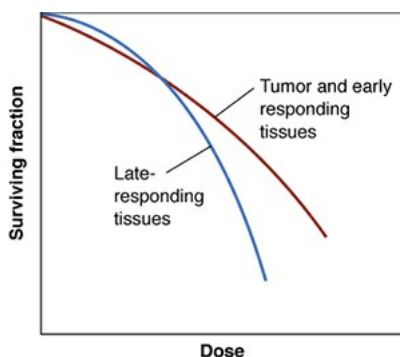


FIGURE 23.6 The dose–response relationship for late-responding tissues is more curved than for early-responding tissues. In the linear-quadratic formulation, this translates into a larger α/β ratio for early effects than for late effects. The α/β ratio is the dose at which the linear (α) and the quadratic (β) components of cell killing are equal, that is, $\alpha D = \beta D^2$ or $D = \alpha/\beta$. (Based on the concepts of Withers.)

For early effects, α/β is large; as a consequence, α dominates at low doses so that the dose–response curve has a marked initial slope and does not bend until higher doses. The linear and quadratic components of cell killing are not equal until about 10 Gy. For late effects, α/β is small so that the β term has an influence at low doses. The dose–response curve bends at lower doses to appear more curved; the linear and quadratic components of cell killing are equal by about 2 Gy.

Dose–response curves for organ function must be distinguished clearly from those for clonogenic cell survival. The distinction is not a trivial one. Organ function obviously is related more to the proportion of functional cells remaining in an irradiated organ at a particular time than to the proportion of clonogenic (stem) cells. The dose-effect curves for clonogenic cells tend to be straight, with relatively small shoulders, whereas dose-effect relations for organ function tend to be more curved, with larger shoulders. It is, of course, the dose–response curves for organ function that are more relevant to the tolerance of normal

tissues.

There are three pieces of information from clinical experience and animal studies that represent circumstantial evidence for the conclusion that the shape of the dose-response relationship differs for early- and late-responding tissues. First, if a fractionation scheme is changed in clinical practice from many small doses to a few large fractions and the total dose is titrated to produce equal early effects, the treatment protocol involving a few large fractions results in *more severe late effects*. There is an abundance of clinical evidence for the truth of this statement.

Second, clinical trials of hyperfractionation, in which two doses are delivered per day for 6 or 7 weeks, appear to result in greatly reduced late effects if the total dose is titrated to produce equal or possibly slightly more severe acute effects. Tumor control is the same or slightly improved. This important clinical observation has been made in several centers and, again, is compatible with the same difference in shape of dose-response curves between early- and late-responding tissues. Late-responding tissues are more sensitive to changes in fractionation patterns than are early-responding tissues.

Third, in experiments with small laboratory animals, the isoeffect curves (i.e., dose vs. number of fractions to produce an equal biologic effect) are *steeper* for a range of late effects than for various acute effects. The data are shown in [Figure 23.7](#), in which early effects are represented by, for example, skin desquamation or jejunal crypt colonies, and late effects are represented by, for example, lung or spinal cord injury.

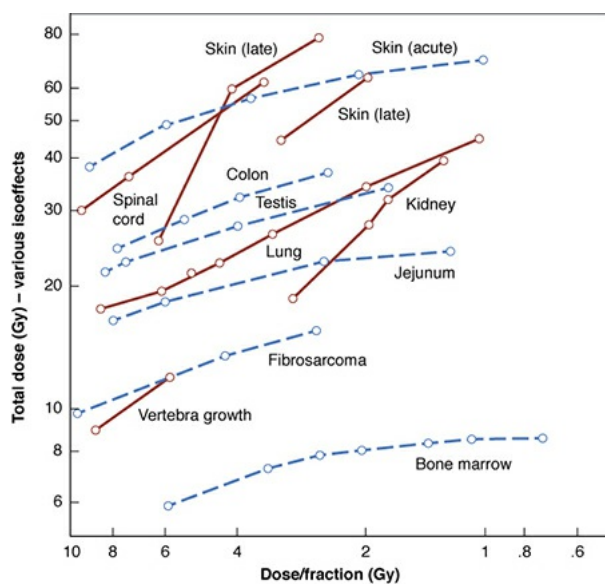


FIGURE 23.7 Isoeffect curves in which the total dose necessary for a certain effect in various tissues in laboratory animals is plotted as a function of dose per

fraction. Late effects are plotted with *red lines*, acute effects with *blue lines*. The data were selected to exclude an influence on the total dose of regeneration during the multifraction experiments. The main point of the data is that the isodoses for late effects increase more rapidly with a decrease in dose per fraction than is the case for acute effects. (Adapted from Withers HR. Biologic basis for altered fractionation schemes. *Cancer*. 1985;55:2086–2095, with permission.)

Table 23.1 is a summary of the values of α/β for several early- and late-responding tissues. The important result is that for early-responding tissues, α/β (i.e., the dose at which single- and multiple-event cell killing is about equal) occurs at the dose of about 10 Gy. By contrast, α/β for late-responding tissues is about 2 Gy. The values of α/β shown in **Table 23.1** come from experiments in which the reciprocal of the total dose is plotted against the quadratic relationship in biologic systems in which it is possible to observe equal effects from various fractionation regimens, even though single cell dose-survival curves cannot be generated (see [Fig. 19.28](#)).

Table 23.1 Ratio of Linear to Quadratic Terms from Multifraction Experiments

REACTIONS	α/β , Gy
Early	
Skin	9–12
Jejunum	6–10
Colon	10–11
Testis	12–13

Callus	9–10
Late	
Spinal cord	1.7–4.9
Kidney	1.0–2.4
Lung	2.0–6.3
Bladder	3.1–7

The parameters derived from curves reconstructed from multifraction experiments are specifically relevant to the end point measured in each experiment, whether it is a proportion of clonogenic cells or a stated reduction in organ function. The dose–response curve constructed from multifraction experimental data by making simple assumptions is a functional dose–response curve, deduced from data in which repair after each fractional dose is basically the quantity being measured. It is just such functional dose–response curves that are required to elucidate the relationship between tolerance dose in radiotherapy and size of dose per fraction, with overall time considered separately.

A POSSIBLE EXPLANATION FOR THE DIFFERENCE IN SHAPE OF DOSE–RESPONSE RELATIONSHIPS FOR EARLY- AND LATE-RESPONDING TISSUES

The radiosensitivity of a population of cells varies with the distribution of cells through the cycle. In general, cells are most resistant in late S phase; slowly growing cells with a long cycle, however, may have a second resistant phase in the early G₁ phase, which may be termed G₀ if the cells are out of cycle. Thus, two quite different cell populations may be radioresistant.

1. A population proliferating so fast that S phase occupies a major portion of the cycle
2. A population proliferating so slowly that many cells are in early G₁ or not proliferating at all so that many resting cells are in G₀

It is thought that many late-responding normal tissues are resistant, owing to the presence of many resting cells. This type of resistance applies particularly to small doses per fraction and disappears at larger doses per fraction.

If resistance results from the presence of many cells in S phase in a rapidly proliferating population, redistribution occurs through all the phases of the cell cycle, which can be considered as a “self-sensitizing” activity. The fast proliferation itself is a form of resistance because the new cells produced by division offset those killed by the dose fractions. This applies to *acutely responding tissues* and also to *tumors*. Proliferation occurring during a protracted, fractionated regimen helps to spare normal tissues but, of course, is a potential danger as far as the tumor is concerned. This is discussed later in this chapter.

FRACTION SIZE AND OVERALL TREATMENT TIME: INFLUENCE ON EARLY- AND LATE-RESPONDING TISSUES

The difference in shape of the dose–response relationship for early- and late-responding tissues leads to an important axiom:

Fraction size is the dominant factor in determining late effects; overall treatment time has little influence. By contrast, fraction size and overall treatment time both determine the response of acutely responding tissues.

It is remarkable that neither clinical radiation oncologists nor experimental radiobiologists came to recognize this simple fact before it was described by Withers in the 1980s.

ACCELERATED REPOPULATION

Treatment with any cytotoxic agent, including radiation, can trigger surviving cells (clonogens) in a tumor to divide faster than before. This is known as **accelerated repopulation**.

Figure 23.8 illustrates this phenomenon in a transplanted rat tumor. Figure 23.8A shows the overall growth curve for this tumor, together with the shrinkage

and regrowth that occurs after a single dose of 20 Gy of x-rays. Figure 23.8B shows the proliferation of individual surviving cells (i.e., clonogenic cells), which, after treatment, are dividing with a cycle time of 12 hours. The important point to note is that during the time that the tumor is overtly shrinking and regressing, the surviving clonogens are dividing and increasing in number more rapidly than before treatment.

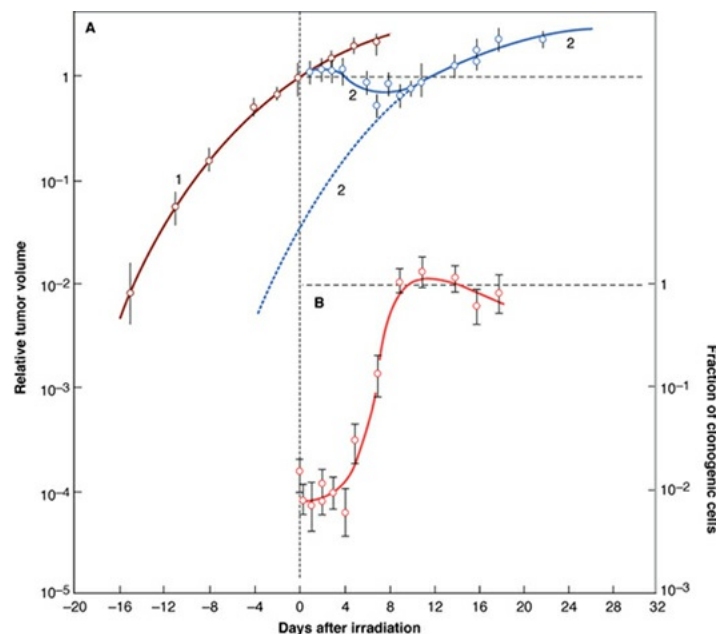


FIGURE 23.8 Accelerated repopulation. Growth curves of a rat rhabdomyosarcoma showing the shrinkage, growth delay, and subsequent recurrence following treatment with a single dose of 20 Gy of x-rays. **A:** *Curve 1:* Growth curve of unirradiated control tumors. *Curve 2:* Growth curve of tumors irradiated at time $t = 0$, showing tumor shrinkage and recurrence. **B:** Variation of the fraction of clonogenic cells as a function of time after irradiation, obtained by removing cells from the tumor and assaying for colony formation *in vitro*. The surviving clonogenic cells are dividing rapidly with a cell cycle of about 12 hours. (Adapted from Hermens AF, Barendsen GW. Changes of cell proliferation characteristics in a rat rhabdomyosarcoma before and after x-irradiation. *Eur J Cancer*. 1969;5:173–189, with permission.)

There is evidence for a similar phenomenon in human tumors. Withers and his colleagues surveyed the literature on radiotherapy for head and neck cancer and estimated the dose to achieve local control in 50% of cases as a function of the overall duration of fractionated treatment. The results are summarized in Figure 23.9. The analysis suggests that clonogen repopulation in this rapidly growing human cancer accelerates at about 28 days after the initiation of radiotherapy in a fractionated regimen. A dose increment of about 0.6 Gy per

day is required to compensate for this repopulation. Such a dose increment is consistent with a 4-day clonogen doubling rate, compared with a median of about 60 days for unperturbed growth.

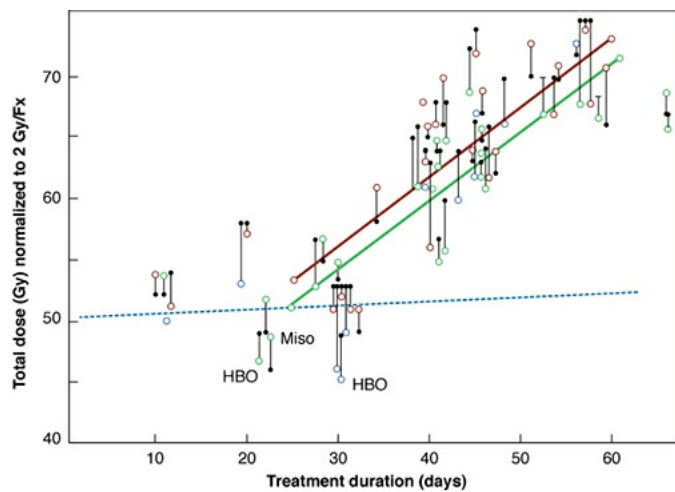


FIGURE 23.9 Doses to achieve local control in 50% of cases (TCD_{50}) as a function of overall treatment time for squamous cell tumors of the head and neck. The data points include many published results from the literature, including hyperbaric oxygen (HBO) trials and the trial of misonidazole (Miso). In those cases involving hypofractionation, the total dose was corrected to be relevant to a treatment schedule of 2 Gy per day. The *dashed line* shows the rate of increase in TCD_{50} predicted from a 2-month clonogen doubling rate. (Adapted from Withers HR, Taylor JM, Maciejewski B. The hazard of accelerated tumor clonogen repopulation during radiotherapy. *Acta Oncol*. 1988;27:131–146, with permission.)

The conclusion to be drawn from this is that radiotherapy, at least for head and neck cancer and probably for other fast-growing tumors, should be completed as soon after it has begun, as is practicable. It may be better to delay initiation of treatment than to introduce delays during treatment. If overall treatment time is too long, the effectiveness of later dose fractions is compromised because the surviving clonogens in the tumor have been triggered into rapid repopulation.

The experimental data referred to here all relate to radiotherapy. It might be anticipated, however, that similar considerations would apply to chemotherapy or to a combination of radiotherapy and chemotherapy. There is evidence in some human malignancies that radiotherapy produces poorer results if preceded by a course of chemotherapy. It may be that accelerated repopulation triggered by the chemotherapy is the explanation.

THE IMPORTANCE OF OVERALL TREATMENT TIME

The importance of overall treatment time is illustrated dramatically by the retrospective analysis by Overgaard of three consecutive trials of the Danish cooperative group. All three trials involved a total dose of 66 to 68 Gy. The first trial was of a split course regimen that extended over a total of 9.5 weeks. The 3-year local control was 32%. The second trial involved five fractions per week over a treatment time of 6.5 weeks, with a 3-year local control of 52%. The third trial included six fractions per week, reducing the overall treatment time to 5.5 weeks and improving the 3-year local control to 62%. There was no change in late effects, but as would be expected, the acute reactions became brisker as the overall time was shortened. The protocols and results of these three trials are illustrated in [Figure 23.10](#). These most interesting data must be viewed with some caution because the three treatment arms were not in a single randomized study but come from different trials over a period of years, the initial purpose of which was to investigate the usefulness of hypoxic cell radiosensitizers. They indicate strongly, nevertheless, that in the case of relatively rapidly growing tumors, such as head and neck cancer, overall treatment time can be a dominant factor in determining outcome ([Table 23.2](#)).

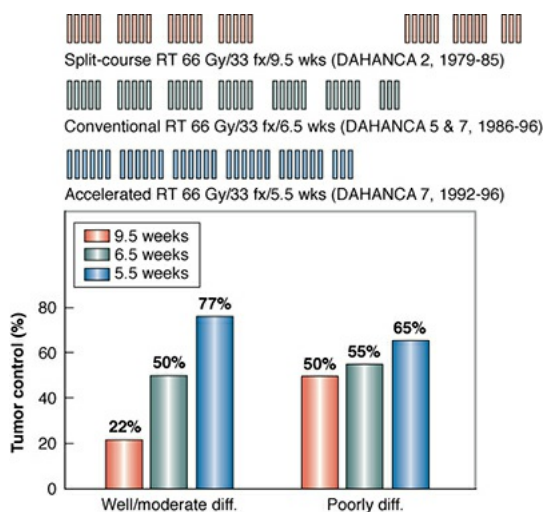


FIGURE 23.10 Top: Overview of the fractionation schedules used in the three Danish head and neck trials. Bottom: Relationship among histopathologic grading, overall treatment time, and local tumor control from the three trials. Only the well-differentiated and moderately differentiated tumors were significantly influenced by overall treatment time. (Adapted from Overgaard J, Sand Hansen H, Overgaard M, et al. Importance of overall treatment time for the outcome of radiotherapy in head and neck carcinoma: experience from the Danish Head and Neck Cancer Study. In: Kogelnik HD, Sedlmayer F, eds.

Proceedings of ICRO/ÖGRO 6, 6th International Meeting on “Progress in Radio-Oncology,” Salzburg, Austria. Bologna, Italy: Monduzzi Editore S.p.A; 1998:743–752, with permission.)

Table 23.2 Importance of Overall Treatment Time

TOTAL DOSE, Gy	DOSE, Gy	COMMENT	OVERALL TIME, wk	3-y LOCAL CONTROL
66–68	2	Split course	9.5	32%
66–68	2	5 fr/wk	6.5	52%
66–68	2	6 fr/wk	5.5	62%

Note: Danish Head and Neck Cancer (DAHANCA) trials show improved locoregional control with shorter overall time—no increase in late effects. fr/wk, fractions per week.

One of the major lessons to be learned from fractionation studies is that local control is lost if overall treatment time is prolonged. Since it first was proposed independently in the 1980s by Withers and by Fowler, it is now well documented for head and neck cancer that local control is reduced by about 1.4% (range of 0.4% to 2.5%) for each day that the overall treatment time is prolonged. This does not differ much from the other way of expressing the same problem—namely, that (after the first 4 weeks of a fractionated schedule) the first 0.6 Gy of each day’s dose fraction is required to overcome proliferation from the previous day. An equally solid estimate can be made from data for carcinoma of the cervix, in which a mean of 0.5% local control (range of 0.3% to 1.1%) is lost for each day that the overall time is prolonged.

Such rapid proliferation does not occur for carcinoma of the breast or prostate, so overall treatment time is not so critical. Although the potential tumor doubling time (T_{pot}) has not proved useful as a predictive assay for individual patients, mean T_{pot} values for groups of patients are in accord with the importance, or otherwise, of overall treatment time. For example, the T_{pot} for

prostate cancer is about 40 days and for noninflammatory breast cancer is about 14 days; in both cases, overall treatment time has not been found to be critical. This can be contrasted with head and neck cancer in which the mean T_{pot} can be as short as 4 days, and, as we have seen, overall treatment time is an important factor governing tumor control.

MULTIPLE FRACTIONS PER DAY

During the 1980s and 1990s, much research was carried out and thousands of patients enrolled in clinical trials to investigate treatment protocols consisting of multiple treatment fractions per day.

Hyperfractionation was based on the premise that because fractionation separates early and late effects, then hyperfractionation with double the number of fractions should be even better. However, in order not to increase the overall time, it was necessary to give two treatments each day separated by 6 hours to allow repair of sublethal damage. A large controlled clinical trial of hyperfractionation was conducted in the 1990s by the European Cooperative Group (European Organization for Research and Treatment of Cancer [EORTC] 22791) in the treatment of head and neck cancer. A hyperfractionated schedule of 80.5 Gy delivered in 70 fractions (1.15 Gy twice per day) over a period of 7 weeks was compared with a conventional regimen of 70 Gy delivered in 35 fractions of 2 Gy over 7 weeks. Local tumor control at 5 years was increased from 40% with the conventional regimen to 59% with hyperfractionation, and this was reflected in improved survival. There was no increase reported in late effects or complications. It was concluded that hyperfractionation confers an unequivocal advantage in the treatment of oropharyngeal cancer.

Accelerated treatment was based on the idea that giving the same dose in half the time by the strategy of delivering two fractions each day should increase tumor control without affecting the incidence of late effects because they are not dependent on overall time. Again, the European Cooperative Group performed large trials, and although the tumor control was improved, there was an unexpected increase in late effects involving complications that sometimes proved to be lethal.

Continuous hyperfractionated accelerated radiation therapy (CHART) was an ambitious project carried out at Mount Vernon Hospital in the United Kingdom. The protocol involved 36 fractions over 12 consecutive days, with 3 fractions per day separated by 6 hours.

The results of CHART can be summarized as follows:

Good local tumor control owing to short overall time

Acute reactions that are brisk but peak after treatment is completed

Most late effects acceptable because of small dose per fraction

Exception: spinal cord, with several myelopathies occurring at 50 Gy because the time between fractions (6 hours) was too short

The huge effort expended in these studies provided much new information, and some of the protocols resulted in impressive gains in tumor control. However, multiple fractions per day have never become mainstream in radiotherapy practice because of the logistics involved.

HYPOFRACTIONATION: RENEWED INTEREST

During the 1970s and the 1980s, the trend in radiotherapy, particularly in the United States, was to increase the number of fractions more and more to reduce the severity of late effects by exploiting the difference in shape of the dose-response relationship between early- and late-responding tissues, as described in detail previously. However, a dramatic recent trend in fractionation is the exact opposite, namely, a renewed interest in dose fractions much larger than 2 Gy for curative radiotherapy. Three lines of research all point in this direction.

First, evidence has accumulated to show that in the special case of prostate cancer, the α/β ratio is low, in the region of 1.5 to 2.5—more similar to late-responding normal tissues than to tumors. This essentially removes the basic rationale for a multifraction regimen of 35 or more fractions. The implication is that an external-beam regimen consisting of a smaller number of larger dose fractions, or alternatively high dose rate (HDR) brachytherapy delivered in a limited number of fractions, should result in good local tumor control without increased normal tissue damage. This argument, based on radiobiologic principles, has been confirmed in a number of clinical trials which show that hypofractionation gives results as good as conventional fractionation patterns, at least in low-risk prostate patients.

Second, stereotactic radiosurgery (SRS) and stereotactic body radiotherapy (SBRT) delivered in one or a few fractions have shown impressive results in some sites including the lung and the brain. These terms are defined in [Table 23.3](#). Such treatments are made possible because of technologic advances that enable the delivery of a very large dose of radiation to a tumor with reduced

margins and a high dose gradient outside the target area. As a consequence, the volume of normal tissue exposed to large radiation doses is greatly reduced. This technique can only be successful for relatively small tumors. [Figure 23.11](#) shows the local control of lung tumors by a single dose of stereotactic ablative radiotherapy (SABR) as a function of tumor volume. For small volumes the local control rates are very high but fall dramatically as the tumor volume increases. The most probable reason for the poorer control rates with larger tumors is the presence of hypoxic cells. It has been argued that this is the ideal situation in which to add a hypoxic cell sensitizer because drug toxicity is not a problem with just one, or a few, fractions.

Table 23.3 Defining the Terms

- | |
|--|
| ■ SRS: stereotactic radiosurgery; a single fraction to the brain |
| ■ SBRT: stereotactic body radiotherapy |
| ■ SABR: stereotactic ablative radiotherapy |
| ■ SBRT and SABR are essentially the same and refer to tumors outside the brain treated with one to five fractions |
| ■ These techniques are possible because of technologic advances that allow a large dose to be given to the tumor with reduced margins and steep gradients outside the target volume (i.e., little normal tissue irradiated). |
| ■ Only works for relatively small tumors |

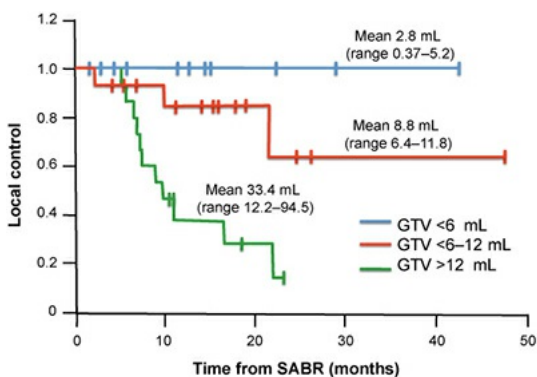


FIGURE 23.11 Local control of lung tumors as a function of tumor volume, treated by a single dose fraction (mostly 25 to 30 Gy). It is likely that the poor control of the larger tumors is due to the presence of hypoxic cells. (Redrawn from Brown JM, Diehn M, Loo BW. Stereotactic ablative radiotherapy should be combined with a hypoxic cell radiosensitizer. *Int J Radiat Oncol Biol Phys*. 2010;78:323–327.)

The question arises whether the impressive results of SRS and SBRT can be explained by the five Rs of conventional radiobiology or whether there is “new biology” involved. The proposed new biology may include, first, endothelial cell damage causing tumor cells to die from hypoxia rather than from the radiation or, second, that big doses of radiation may result in enhanced tumor immunity. This question was addressed by Brown and colleagues in a much quoted paper in 2013. Figure 23.12 shows the tumor control probability (TCP) as a function of the biologically effective dose for single fraction treatments with SBRT, three to eight fraction treatments with SBRT, or multifraction treatments with the standard three-dimensional conformal radiotherapy (3D-CRT). It appears that the TCP is a simple function of the BED regardless of the fractionation regime. High TCPs are associated with large BEDs, which are a result of a small number of large dose fractions. This result suggests that no new biology is required to explain the success of SRS or SBRT. It is simply a function of the large BEDs that result from one or a few large dose fractions.

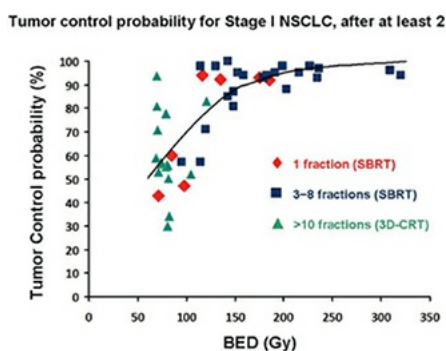


FIGURE 23.12 Weighted mean tumor control probabilities as a function of the

biologically effective dose (BED). Showing that the efficacy of a single dose fraction of stereotactic body radiotherapy (SBRT), a few fractions of SBRT and conventional three-dimensional conformal radiation therapy (3D-CRT) produce the same TCP for the same BED. NSCLC, nonsmall cell lung cancer. (Redrawn from Brown JM, Brenner DJ, Carlson DJ. Dose escalation, not “new biology,” can account for the efficacy of stereotactic body radiation therapy with non-small cell lung cancer. *Int J Radiat Oncol Biol Phys.* 2013;85:1159–1160.)

Third, the development of carbon ion beams has led to trials involving treatment with a small number of large dose fractions, even in some cases with a single fraction. It is not clear at present whether the apparent success of this strategy is caused by the superior dose distribution or the relatively high linear energy transfer (LET) of the radiation.

All of this means that hypofractionation—that is, a smaller number of larger dose fractions—emerges as an interesting alternative. Disasters from the past involving unacceptable late normal tissue damage limit enthusiasm for this strategy in many quarters. All of these ideas outlined earlier need to be approached cautiously, and the perceived benefits proven by careful clinical trials. Treatment regimens involving fewer fractions would clearly be more convenient for patients and result in significant economies in health care systems. However, it would be folly to espouse such strategies at the expense of either local tumor control or increased toxicity to normal tissues.

USING THE LINEAR-QUADRATIC CONCEPT TO CALCULATE EFFECTIVE DOSES IN RADIOTHERAPY

It is often useful in practice to have a simple way to compare different fractionation regimens and to assign them a numeric score. For many years, the NSD system developed by Ellis were used widely. They proved useful for assessing modest changes in fractionation but fell into dispute when extrapolated beyond the data range on which they were based.

The linear-quadratic model is now more widely used and has received greater acceptance. This section was suggested by Dr. Jack Fowler; the format is based on tutorials he has given at the American Society for Therapeutic Radiology and Oncology (ASTRO) and at the European Society for Therapeutic Radiology and Oncology (ESTRO) in the 1990s.

Use of the linear-quadratic model, with appropriate values for the parameters α and β , emphasizes the difference between early- and late-responding tissues

and the fact that it is never possible to match two different fractionation regimens to be equivalent for both. Calculations of this sort, although a useful guide for residents in training or for research purposes, are not to be considered a substitute for clinical judgment and experience. They are presented only as examples.

Figure 23.13 illustrates the familiar way in which biologic effect as a function of dose varies with the number of fractions in which the radiation is delivered—always assuming that the fractions are spaced sufficiently to allow full repair of sublethal radiation damage. For a multifraction regimen, the shoulder of the curve has to be repeated many times and, as a result, the effective dose–response relationship is a straight line from the origin through the point on the single dose–survival curve for that dose fraction (typically 2 Gy). This is discussed in Chapter 3. For the linear portion of the curve, α represents the loge of the cells killed per Gy. As the curve bends, the quadratic component of cell killing is represented by β , which is the loge of the cells killed per gray squared. This is illustrated in Figure 23.14. The ratio α/β has the dimensions of dose and is the dose at which the linear and quadratic components of cell killing are equal.

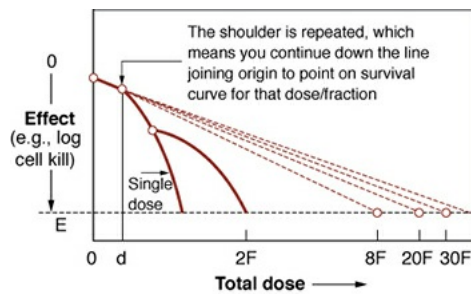


FIGURE 23.13 Graph illustrating that if the dose–response relationship is linear-quadratic in form for graded single doses, the effective dose–response curve for a multifraction regimen approaches an exponential function of dose for many doses. The effective dose–response relationship is a straight line from the origin through the point on the single-dose survival curve corresponding to the daily dose fraction (typically 2 Gy). (Based on the concepts of Fowler, 1989, and Barendsen, 1982.)

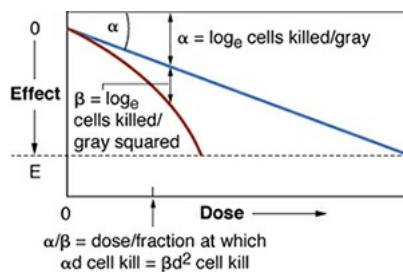


FIGURE 23.14 Graph illustrating the linear-quadratic nature of the radiation

cell survival curve, $S = e^{-\alpha D - \beta D^2}$, in which S is the fraction of cells surviving a dose D , α is the number of logs of cell kill per Gy from the linear portion of the curve, and β is the number of logs of cell kill per Gy² from the quadratic component. The linear and quadratic components of cell kill are equal at a dose $D = \alpha/\beta$.

For a single acute dose D , the biologic effect is given by

$$E = \alpha D + \beta D^2$$

For n well-separated fractions of dose d , the biologic effect is given by

$$E = n(\alpha d + \beta d^2)$$

As suggested by Barendsen, this equation may be rewritten as

$$\begin{aligned} E &= (nd)(\alpha + \beta d) \\ &= (\alpha)(nd) \left(1 + \frac{d}{\alpha/\beta}\right) \end{aligned}$$

but nd equals D , the total dose, so

$$E = \alpha(\text{total dose}) \text{ (relative effectiveness)}$$

in which the quantity $1 + [d/(\alpha/\beta)]$ is called *relative effectiveness*. If this equation is divided through by α , we have

$$\begin{aligned} \frac{E}{\alpha} &= (\text{total dose}) \times (\text{relative effectiveness}) \\ &= (nd) \times \left(1 + \frac{d}{\alpha/\beta}\right) \end{aligned}$$

The quantity E/α is the **biologically effective dose (BED)** and is the quantity by which different fractionation regimens are intercompared. In words, the final equation is

$$\begin{aligned} \text{BED} &= (\text{total dose}) \times (\text{relative effectiveness}) \\ \frac{E}{\alpha} &= (nd) \times \left(1 + \frac{d}{\alpha/\beta}\right) \end{aligned}$$

The quantity BED was first suggested by Barendsen but was popularized by Fowler.

Choice of α/β

For calculating the examples that follow, α/β is assumed to be 3 Gy for late-responding tissues and 10 Gy for early-responding tissues. The reader, of course, may substitute other values that seem more appropriate. It should be noted that parts of schedules can be added—that is, (partial effect)₁ and (partial effect)₂—as in the concomitant boost. It also should be noted that although it is permissible to compare BEDs for late effects (in Gy₃) of one schedule with

another and permissible to compare BEDs for early effects (in Gy₁₀) of one schedule with another, it is clearly not permissible or meaningful to compare early with late effects.

Model Calculations

1. Conventional treatment: 30 fractions of 2 Gy given one fraction per day, 5 days per week, for an overall treatment time of 6 weeks (this is written as 30F × 2 Gy/6 weeks)

$$\begin{aligned}\text{Early effects: } \frac{E}{\alpha} &= (nd) \left(1 + \frac{d}{\alpha/\beta}\right) \\ &= 60 \left(1 + \frac{2}{10}\right) \\ &= 72 \text{ Gy}_{10} \\ \text{Late effects: } \frac{E}{\alpha} &= 60 \left(1 + \frac{2}{3}\right) \\ &= 100 \text{ Gy}_3\end{aligned}$$

Comment: The subscripts to the BED are a reminder that this figure is not in gray and specify the particular values of α/β used in the calculation.

2. Hyperfractionation: 70 fractions of 1.15 Gy given twice daily, 6 hours apart, 5 days per week, for an overall treatment time of 7 weeks, that is, 70F × 1.15 Gy twice daily/7 weeks

$$\begin{aligned}\text{Early effects: } \frac{E}{\alpha} &= (nd) \left(1 + \frac{d}{\alpha/\beta}\right) \\ &= 80.5 \left(1 + \frac{1.15}{10}\right) \\ &= 89.8 \text{ Gy}_{10} \\ \text{Late effects: } \frac{E}{\alpha} &= 80.5 \left(1 + \frac{1.15}{3}\right) \\ &= 111.4 \text{ Gy}_3\end{aligned}$$

Comment: This treatment is much “hotter,” that is, more effective than the conventional 60 Gy for both early and late effects.

3. A one-fraction-a-day control schedule frequently used to compare with hyperfractionation: 35 fractions of 2 Gy given once a day for 5 days a week, for an overall treatment time of 7 weeks, that is, 35F × 2 Gy/ 7 weeks

$$\begin{aligned}\text{Early effects: } \frac{E}{\alpha} &= (nd) \left(1 + \frac{d}{\alpha/\beta}\right) \\ &= 70 \left(1 + \frac{2}{10}\right) \\ &= 84 \text{ Gy}_{10} \\ \text{Late effects: } \frac{E}{\alpha} &= 70 \left(1 + \frac{2}{3}\right) \\ &= 116.7 \text{ Gy}_3\end{aligned}$$

Comment: This “control” schedule is not as effective as the hyperfractionation because it is less effective by 7% for early effects, which

includes tumor control (84 vs. 89.8 Gy₁₀), but hotter for late effects by 5% (116.7 vs. 111.4 Gy₃).

4. Concomitant boost: 30 fractions of 1.8 Gy given once a day, 5 days a week, and at the same time (concomitant), a boost to a smaller field of 12 fractions of 1.5 Gy once a day; overall treatment time 6 weeks, that is, [(30F × 1.8 Gy) + (12F × 1.5 Gy)]/6 weeks (this protocol is much favored at the University of Texas MD Anderson Hospital and Tumor Institute; by giving the boost concomitantly, a prolongation of overall time is avoided)

$$\begin{aligned}\text{Early effects: } \frac{E}{\alpha} &= (nd) \left(1 + \frac{d}{\alpha/\beta}\right) \\ &= 54 \left(1 + \frac{1.8}{10}\right) + 18 \left(1 + \frac{1.5}{10}\right) \\ &= 84.4 \text{ Gy}_{10} \\ \text{Late effects: } \frac{E}{\alpha} &= 54 \left(1 + \frac{1.8}{3}\right) + 18 \left(1 + \frac{1.5}{3}\right) \\ &= 113.4 \text{ Gy}_3\end{aligned}$$

Comment: The Gy₁₀ and Gy₃ values should be compared with the comparable figures for the previous schedules given. The concomitant boost is hotter than the conventional schedule for both early and late effects. Compared with hyperfractionation, however, this concomitant boost is almost the same for late effects but less effective for early effects, including tumor control.

5. CHART: 36 fractions of 1.5 Gy given three fractions a day, 6 hours apart, for 12 consecutive days, with an overall treatment time of 12 days, that is, 36F × 1.5 Gy (3F/day)/12 days.

$$\begin{aligned}\text{Early effects: } \frac{E}{\alpha} &= (nd) \left(1 + \frac{d}{\alpha/\beta}\right) \\ &= 54 \left(1 + \frac{1.5}{10}\right) \\ &= 62.1 \text{ Gy}_{10} \\ \text{Late effects: } \frac{E}{\alpha} &= 54 \left(1 + \frac{1.5}{3}\right) \\ &= 81.0 \text{ Gy}_3\end{aligned}$$

Comment: Direct comparison of CHART with the previous examples in terms of Gy₁₀ and Gy₃ is meaningless because CHART has an overall time of only 12 days compared with 6 or 7 weeks for the other schedules.

Allowance for Tumor Proliferation

Calculations Suggested by Fowler

The correction proposed here for tumor proliferation is a crude approximation and should not be taken too seriously. It assumes, among other things, that the

rate of cellular proliferation remains constant throughout the overall treatment time.

The number of clonogens (N) at time t is related to the initial number of clonogens (N_0) by the expression

$$N = N_0 e^{\lambda t}$$

in which λ is a constant related to the potential doubling time of the tumor, T_{pot} , by the expression

$$\lambda = \frac{\log_e 2}{T_{\text{pot}}} = \frac{0.693}{T_{\text{pot}}}$$

The decrease in the number of clonogens because of cell killing by the fractionated radiation regimen is balanced to some extent by cell division of the surviving clonogens. The biologic effect in equation 2 now becomes

$$E = n(\alpha d + \beta d^2) - 0.693 \frac{t}{T_{\text{pot}}}$$

The BED E/α becomes

$$\frac{E}{\alpha} = (nd) \left(1 + \frac{d}{\alpha/\beta}\right) - \frac{0.693}{\alpha} \frac{t}{T_{\text{pot}}}$$

or, in words,

$$\begin{aligned} \text{BED} &= (\text{total dose}) \times (\text{relative effectiveness}) \\ &\quad - \frac{\log_e 2}{\alpha} (\text{no. of cell doublings}) \end{aligned}$$

The time t is the time in days available for proliferation. Rapid proliferation in tumors appears not to start up until about 21 to 28 days after treatment begins in head and neck tumors. Therefore, $t = T - 21$ or $t = T - 28$ is a suitable value, where T is overall time. The start-up time is called T_K for “kick-off” time, and $t = T - T_K$.

It is now necessary to assume a value for α , the initial slope of the cell survival curve, as well as for T_{pot} , the potential doubling time of the tumor. A reasonable value for α is $0.3 \pm 0.1/\text{Gy}$. T_{pot} may have a value of 2 to 25 days, with a median value of about 5 days.

For typical 6-week (39-day) schedules referred to earlier, proliferation may reduce the BED by

$$\frac{E}{\alpha} = \frac{0.693}{0.3} \times \frac{(39-21)}{5} = 8.3 \text{ Gy}_{10}$$

Note that because we are concerned with tumor proliferation, the reduction in BED is in Gy_{10} ; that is, an early-effect α/β value is used. By the same token,

proliferation during a 7-week protocol (i.e., 46 days) would decrease the BED by:

$$\frac{E}{\alpha} = \frac{0.693}{0.3} \times \frac{(46-21)}{5} = 11.6 \text{ Gy}_{10}$$

CHART calls for three fractions per day over 12 days and so rapid proliferation has not started in head and neck tumors by the time the treatment is completed in this very short schedule; that is, T_K is greater than T , so t must be set at zero.

Table 23.4 summarizes the effect of tumor proliferation on the BEDs characteristic of the various treatment regimens discussed earlier.

Table 23.4 Effect of Tumor Proliferation on Biologically Effective Doses Characteristic of Various Treatment Regimens

PROTOCOL	E/ α (i.e., Gy ₁₀)	EARLY, Tumor, CORRECTION, Gy ₁₀	CORRECTED FOR TIME, Gy ₁₀
Conventional protocol: 72 30F \times 2 Gy/6 wk (39 d)		-8.3	63.7
Hyperfractionation: 70F \times 89.8 1.15 Gy/7 wk (46 d)		-11.6	78.2
Concomitant boost: (30F 84.4 \times 1.8 Gy) + (12F \times 1.5 Gy)/6 wk (39 d)		-8.3	76.1
CHART: 36F \times 1.5 Gy/12 d	62.1	0	62.1

This correction for time assumes $T_p = 5$ days, $T_K = 21$ days, and $\alpha = 0.3$ In per gray.

Based on the assumptions made, hyperfractionation results in the largest BED and, therefore, may be expected to result in the best tumor control, followed closely by the concomitant boost schedule. CHART is a less effective schedule based on a T_{pot} of 5 days. It is necessary to assume a very fast growing tumor, with a T_{pot} of 3 days or less, for CHART to become the most effective schedule.

It must be emphasized again that calculations of this sort should be used only as a guide for residents in training because they do not, in any way, replace clinical judgment. It is useful, however, to have a yardstick by which new fractionation schemes may be judged.

Pragmatic Approach of Peters and Colleagues

Changing dose per fraction often results in a change in overall treatment time. This may be an important issue with the advent of intensity-modulated radiation therapy (IMRT), especially in the case of head and neck cancer, which may be rapidly growing. For example, with conventional treatment planning, a shrinking field technique may be used, with typically 50 Gy being given to known sites of disease and potential routes of regional spread, followed by a boost of 10 to 20 Gy using a one- or two-phase cone down, with all treatments being given in 2-Gy fractions. However, owing to the complexity of IMRT, a single plan can be utilized with differential dose per fraction to areas of different risk on the same day, in place of the shrinking field technique. This shortens the overall treatment time and raises the question “What total dose given in 35 fractions over 7 weeks is equivalent to 50 Gy in 25 fractions over 5 weeks, or 60 Gy in 30 fractions over 6 weeks?” Given that the α/β ratio for squamous cell carcinoma of the head and neck is usually considered high, the correction factor for overall treatment time becomes more important than the correction factor for fraction size. Some groups, notably Lester Peters and colleagues at the Peter McCallum Cancer Institute in Melbourne, Australia, have taken the pragmatic approach that between 5 and 7 weeks after the start of a fractionated regimen, the dose equivalent of regeneration with protraction of treatment is about 0.5 Gy per day, rounded down to 3 Gy per week. Thus, the equivalent of 50 Gy in 5 weeks is 56 Gy in 7 weeks at 1.6 Gy per fraction, whereas the equivalent of 60 Gy in 6 weeks is 63 Gy in 7 weeks at 1.8 Gy per fraction.

Obviously, there is considerable room for debate concerning the actual numeric values chosen, but in the case of rapidly growing squamous cell tumors of the head and neck, it would be wrong to simply ignore the time factor because it is more important than the correction for fraction size. For other tumor types,

the dose equivalent of regeneration is almost certainly different and, in most cases, less. For some tumors, such as low to intermediate prostate cancer, it may be negligible. There is a general lack of data regarding accelerated tumor cell regeneration, regarding both its magnitude and regarding the length of the lag time before it sets in.

SUMMARY OF PERTINENT CONCLUSIONS

The “four Rs” of radiobiology are the following:

Repair of sublethal damage

Reassortment of cells within the cell cycle

Repopulation

Reoxygenation

Some have added a fifth R, namely Resistance (intrinsic).

The basis of conventional fractionation may be explained as follows: Dividing a dose into several fractions spares normal tissues because of the repair of sublethal damage between dose fractions and cellular repopulation. At the same time, fractionation increases tumor damage because of reoxygenation and reassortment.

The Strandquist plot is the relation between total dose and overall treatment time. In this context, “time” includes the number of fractions. On a double log plot, the slope of the line for skin is often close to 0.33.

The Ellis NSD system made the important contribution of separating the effects of number of fractions and overall time. The time correction was a power function ($T^{0.11}$) that is far from accurate. The system is seldom used now.

The extra dose required to counteract proliferation in a normal tissue irradiated in a fractionated regimen is a sigmoidal function of time. No extra dose is required until some weeks into a fractionated schedule.

The delay before an extra dose is required to counteract the effects of proliferation is much longer for late-responding tissues and is beyond the overall time for conventional radiotherapy schedules.

Prolonging overall time within the normal radiotherapy range has little sparing effect on late reactions but a large sparing effect on early reactions.

The dose-response relationship for late effects is more curved than for early effects. The α/β ratio is about 10 Gy for early effects and about 3 Gy for late-responding tissues. Consequently, late-responding tissues are more sensitive to changes in fractionation pattern.

Fraction size is the dominant factor in determining late effects; overall treatment time has little influence. By contrast, fraction size and overall treatment time both determine the response of acutely responding tissues.

Accelerated repopulation refers to the triggering of surviving cells (clonogens) to divide more rapidly as a tumor shrinks after irradiation or treatment with a cytotoxic drug.

Accelerated repopulation starts in head and neck cancer in humans about 4 weeks after initiation of fractionated radiotherapy. About 0.6 Gy per day is needed to compensate for this repopulation.

This phenomenon mandates that treatment be completed as soon as practical once it has started; it may be better to delay the start than to introduce interruptions during treatment.

Overall treatment time is a very important factor for fast-growing tumors. In head and neck cancer, local tumor control is decreased by about 1.4% (range of 0.4% to 2.5%) for each day that the overall treatment time is prolonged. The corresponding figure for carcinoma of the cervix is about 0.5% (range of 0.3% to 1.1%) per day. Such rapid proliferation is not seen in breast or prostate cancer.

Multiple fractions per day: In the 1980s and 1990s, thousands of patients were enrolled in clinical trials to investigate treatment protocols that involved more than one treatment fraction per day. Hyperfractionation sought to improve treatment outcome by doubling the number of fractions in the same overall time by giving two fractions per day. Clinical trials showed a distinct advantage. Accelerated treatment sought to shorten overall treatment time by giving two doses per day on the premise that overall time would not affect late effects. Clinical trials showed an improvement in tumor response but an unexpected increase in late effects, some of which proved to be lethal. CHART involved 36 small dose fractions over 12 consecutive days in three treatment fractions per day. Good local control was seen with most late effects at an acceptable level except for the spinal cord, where several myelopathies were observed because the 6-hour period between fractions was not sufficient to allow repair of sublethal damage in this tissue.

Multiple fractions per day have never become mainstream in radiotherapy practice because of the logistical problems.

There is renewed interest in hypofractionation—that is, a smaller number of high dose fractions. There are several circumstances where this may be exploited: (1) for prostate cancer for which the α/β ratio is closer to that for late-responding tissues, which removes the benefit of fractionation; (2) for SRS and SBRT where technologic advances allow a high tumor dose with less dose to a smaller volume of normal tissue; and (3) for carbon ion beams, where the dose distribution is improved and, in addition, the radiation has a relatively high LET.

The linear-quadratic concept may be used to calculate the biologic effectiveness of various radiotherapy protocols involving different numbers of dose fractions. The useful formula is

$$\begin{aligned} \text{BED} &= (\text{total dose}) \times (\text{relative effectiveness}) \\ \frac{E}{\alpha} &= (nd) \times \left(1 + \frac{d}{\alpha/\beta}\right) \end{aligned}$$

An approximate allowance can be made for tumor cell proliferation when comparing protocols involving different overall treatment times. There are two approaches considered:

1. Fowler has suggested corrections based on the T_{pot} value for different tumors.
2. Peters and colleagues have suggested a pragmatic approach in the case of fast-growing squamous cell carcinomas of the head and neck, where corrections for overall time may be more important than number of fractions. They assume that between 5 and 7 weeks after the start of a fractionated regimen, the dose equivalent of regeneration with protraction of treatment is about 0.5 Gy per day, rounded down to 3 Gy per week. The correction will be different for other tumors and probably negligible for prostate cancer.

BIBLIOGRAPHY

Bentzen SM. High-tech in radiation oncology: should there be a ceiling? *Int J Radiat Oncol Biol Phys.* 2004;58:320–330.

Bentzen SM, Saunders MI, Dische S. Repair halftimes estimated from observations of treatment-related morbidity after CHART or conventional radiotherapy in head and neck cancer. *Radiother Oncol.* 1999;53:219–226.

- Bentzen SM, Saunders MI, Dische S, et al. Radiotherapy-related early morbidity in head and neck cancer: quantitative clinical radiobiology as deduced from the CHART trial. *Radiother Oncol.* 2001;60:123–135.
- Brenner DJ. Hypofractionation for prostate cancer radiotherapy—what are the issues? *Int J Radiat Oncol Biol Phys.* 2003;57:912–914.
- Brenner DJ. Toward optimal external-beam fractionation for prostate cancer. *Int J Radiat Oncol Biol Phys.* 2000;48:315–316.
- Brenner DJ, Hall EJ. Fractionation and protraction for radiotherapy of prostate carcinoma. *Int J Radiat Oncol Biol Phys.* 1999;43:1095–1101.
- Brown JM, Brenner DJ, Carlson DJ. Dose escalation, not “new biology,” can account for the efficacy of stereotactic body radiation therapy with non-small cell lung cancer. *Int J Radiat Oncol Biol Phys.* 2013;85:1159–1160.
- Brown JM, Diehn M, Loo BW Jr. Stereotactic ablative radiotherapy should be combined with a hypoxic cell radiosensitizer. *Int J Radiat Oncol Biol Phys.* 2010;78:323–327.
- Denekamp J. Changes in the rate of repopulation during multifraction irradiation of mouse skin. *Br J Radiol.* 1973;46:381–387.
- Dische S, Saunders M, Barrett A, et al. A randomised multicentre trial of CHART versus conventional radiotherapy in head and neck cancer. *Radiother Oncol.* 1997;44:123–136.
- Douglas BG, Fowler JF. The effect of multiple small doses of x rays on skin reactions in the mouse and a basic interpretation. *Radiat Res.* 1976;66:401–426.
- Ellis F. Dose, time, and fractionation: a clinical hypothesis. *Clin Radiol.* 1969;20:1–7.
- Ellis F. Nominal standard dose and the ret. *Br J Radiol.* 1971;44:101–108.
- Fowler JF. Dose-response curves for organ function or cell survival. *Br J Radiol.* 1983;56:497–500.
- Fowler JF. Fractionated radiation therapy after Strandqvist. *Acta Radiol Oncol.* 1984;23:209–216.
- Fowler JF. Potential for increasing the differential response between tumors and normal tissues: can proliferation rate be used? *Int J Radiat Oncol Biol Phys.* 1986;12:641–645.

- Fowler JF. The eighteenth Douglas Lea lecture. 40 Years of radiobiology: its impact on radiotherapy. *Phys Med Biol.* 1984;29:97–113.
- Fowler JF. The linear-quadratic formula and progress in fractionated radiotherapy. *Br J Radiol.* 1989;62:679–694.
- Fowler JF. The second Klaas Breur memorial lecture. La Ronde—radiation sciences and medical radiology. *Radiother Oncol.* 1983;1:1–22.
- Fowler JF. The first James Kirk memorial lecture. What next in fractionated radiotherapy? *Br J Cancer.* 1984;49(suppl 6):285S–300S.
- Fowler JF, Chappell R, Ritter M. Is alpha/beta for prostate tumors really low? *Int J Radiat Oncol Biol Phys.* 2001;50:1021–1031.
- Fowler JF, Lindstrom MJ. Loss of local control with prolongation in radiotherapy. *Int J Radiat Oncol Biol Phys.* 1992;23:457–467.
- Hansen O, Overgaard J, Hansen HS, et al. Importance of overall treatment time for the outcome of radiotherapy of advanced head and neck carcinoma: dependency on tumor differentiation. *Radiother Oncol.* 1997;43:47–51.
- Hendry JH, Bentzen SM, Dale RG, et al. A modelled comparison of the effects of using different ways to compensate for missed treatment days in radiotherapy. *Clin Oncol (R Coll Radiol).* 1996;8:297–307.
- Hermens AF, Barendsen GW. Changes of cell proliferation characteristics in a rat rhabdomyosarcoma before and after x-irradiation. *Eur J Cancer.* 1969;5:173–189.
- Horiot JC, Bontemps P, van den Bogaert W, et al. Accelerated fractionation (AF) compared to conventional fractionation (CF) improves loco-regional control in the radiotherapy of advanced head and neck cancers: results of the EORTC 22851 randomized trial. *Radiother Oncol.* 1997;44:111–121.
- Horiot JC, Le Fur R, N'Guyen T, et al. Hyperfractionation versus conventional fractionation in oropharyngeal carcinoma: final analysis of a randomized trial of the EORTC cooperative group of radiotherapy. *Radiother Oncol.* 1992;25:231–241.
- Overgaard J. Advances in clinical applications of radiobiology: phase III studies of radiosensitizers and novel fractionation schedules. In: Johnson JT, Didolkar MS, eds. *Head and Neck Cancer.* Vol. 3. Amsterdam, The Netherlands: Elsevier Science Publishers. 1993;863–869.
- Overgaard J, Hjelm-Hansen M, Johansen LV, et al. Comparison of conventional

and split-course radiotherapy as primary treatment in carcinoma of the larynx. *Acta Oncol.* 1988;27:147–152.

Overgaard J, Sand Hansen H, Andersen AP, et al. Misonidazole combined with split-course radiotherapy in the treatment of invasive carcinoma of larynx and pharynx: report from the DAHANCA 2 study. *Int J Radiat Oncol Biol Phys.* 1989;16:1065–1068.

Overgaard J, Sand Hansen H, Overgaard M, et al. A randomized double-bind phase III study of nimorazole as a hypoxic radiosensitizer of primary radiotherapy in supraglottic larynx and pharynx carcinoma. Results of the Danish Head and Neck Cancer Study (DAHANCA) Protocol 5–85. *Radiother Oncol.* 1998;46:135–146.

Overgaard J, Sand Hansen H, Overgaard M, et al. Importance of overall treatment time for the outcome of radiotherapy in head and neck carcinoma: experience from the Danish Head and Neck Cancer Study. In: Kogelnik HD, Sedlmayer F, eds. *Proceedings of ICRO/ÖGRO 6, 6th International Meeting on “Progress in Radio-Oncology,” Salzburg, Austria.* Bologna, Italy: Monduzzi Editore S.p.A; 1998:743–752.

Overgaard J, Sand Hansen H, Sapru W, et al. Conventional radiotherapy as the primary treatment of squamous cell carcinoma of the head and neck: a randomized multicenter study of 5 versus 6 fractions per week—preliminary report from the DAHANCA 6 and 7 trial. *Radiother Oncol.* 1996;40(suppl 1):S31.

Parsons JT, Bova FJ, Million RR. A re-evaluation of split-course technique for squamous cell carcinoma of the head and neck. *Int J Radiat Oncol Biol Phys.* 1980;6:1645–1652.

Peters LJ, Ang KK. The role of altered fractionation in head and neck cancers. *Semin Radiat Oncol.* 1992;2:180–194.

Peters LJ, Ang KK, Thames HD Jr. Accelerated fractionation in the radiation treatment of head and neck cancer. A critical comparison of different strategies. *Acta Oncol.* 1988;27:185–194.

Peters LJ, Withers HR, Thames HD Jr. Radiobiological bases for multiple daily fractionation. In: Kaercher KH, Kogelnik HD, Reinartz G, eds. *International Meeting on Progress in Radio-oncology.* New York, NY: Raven Press; 1982;11:317–323.

Saunders MI, Dische S. Continuous hyperfractionated accelerated radiotherapy

in non-small-cell carcinoma of the bronchus. In: McNally NJ, ed. *The Scientific Basis of Modern Radiotherapy*. London, United Kingdom: British Institute of Radiology; 1989:47–51. BIR report 19.

Saunders MI, Dische S, Barrett A, et al. Randomised multicentre trials of CHART vs conventional radiotherapy in head and neck cancer and non-small-cell lung cancer: an interim report. *Br J Cancer*. 1996;73:1455–1462.

Saunders MI, Dische S, Hong A, et al. Continuous hyperfractionated accelerated radiotherapy in locally advanced carcinoma of the head and neck region. *Int J Radiat Oncol Biol Phys*. 1989;17:1287–1293.

Strandquist M. A study of the cumulative effect of fractionated x-ray treatment based on the experience mined at the Radium Hemmant with the treatment of 280 cases of carcinoma of the skin and lip. *Acta Radiol*. 1944;55(suppl):1–300.

Thames HD Jr, Peters LJ, Withers HR, et al. Accelerated fractionation vs hyperfractionation: rationales for several treatments per day. *Int J Radiat Oncol Biol Phys*. 1983;127–138.

Thames HD Jr, Withers HR. Test of equal effect per fraction and estimation of initial clonogen number in microcolony assays of survival after fractionated irradiation. *Br J Radiol*. 1980;53:1071–1077.

Thames HD Jr, Withers HR, Peters LJ, et al. Changes in early and late radiation responses with altered dose fractionation: implications for dose-survival relationships. *Int J Radiat Oncol Biol Phys*. 1982;8:219–226.

Withers HR. Biologic basis for altered fractionation schemes. *Cancer*. 1985;55:2086–2095.

Withers HR. Cell cycle redistribution as a factor in multifraction irradiation. *Radiology*. 1975;114:199–202.

Withers HR. Response of tissues to multiple small dose fractions. *Radiat Res*. 1977;71:24–33.

Withers HR, Peters LJ, Kogelnik HD. The pathobiology of late effects of irradiation. In: Meyn RE, Withers HR, eds. *Radiation Biology in Cancer Research*. New York, NY: Raven Press; 1980:439–448.

Withers HR, Peters LJ, Taylor JM, et al. Late normal tissue sequelae from radiation therapy for carcinoma of the tonsil: patterns of fractionation study of radiobiology. *Int J Radiat Oncol Biol Phys*. 1995;33:563–568.

Withers HR, Taylor JM, Maciejewski B. The hazard of accelerated tumor clonogen repopulation during radiotherapy. *Acta Oncol*. 1988;27:131–146.

Withers HR, Thames HD Jr, Flow BL, et al. The relationship of acute to late skin injury in 2 and 5 fraction/week gamma-ray therapy. *Int J Radiat Oncol Biol Phys*. 1978;4:595–601.

Withers HR, Thames HD, Peters LJ, et al. Normal tissue radioresistance in clinical radiotherapy. In: Fletcher GH, Nervi C, Withers HR, eds. *Biological Bases and Clinical Implications of Tumor Radioresistance*. New York, NY: Masson; 1983:139–152.

chapter 24

Retreatment after Radiotherapy: The Possibilities and the Perils

The Nature of the Problem

Early- and Late-Responding Tissues

Preclinical Data

Clinical Studies

Spinal Cord

Brain

Head and Neck

Rectum

Bone Metastases

Breast

Lung

Recurrent Vaginal Metastases

Summary of Pertinent Conclusions

Animal Studies

Clinical Studies

Bibliography

Reviews

Preclinical (Animal Studies)

Clinical

THE NATURE OF THE PROBLEM

Of patients presenting at major cancer centers in the Western world, about 1 in 10 present with a second cancer. The following are the three major reasons for this:

1. **Continued lifestyle**—For example, factors associated with the first

malignancy may continue to have an effect; smoking that caused a lung cancer may result later in a head and neck cancer, or alcohol that caused esophageal cancer may also result in a cancer of the tongue.

2. **Genetic predisposition**—Some syndromes, such as Li–Fraumeni syndrome, predispose to multiple primary tumors. This involves a very small proportion of the population, but it is incredibly important to the persons affected.
3. **Treatment-related**—Radiotherapy and/or chemotherapy can induce second malignancies. In the case of radiotherapy, most second cancers not only occur within or close to the treatment field but also occur in remote locations, especially in radiogenic organs such as the lung. This is of particular importance in young children because they are 10 to 15 times as sensitive to radiation-induced malignancies as middle-aged adults are. For a second cancer to be considered as treatment-related, the latency must be appropriate, namely, short for a leukemia and long for a solid tumor.

An obvious first question is, what is the scale or magnitude of the problem of retreatment? This can be illustrated by a 2013 paper from the Peter McCallum Cancer Center in Australia. They studied the records of more than 48,000 radiotherapy patients over a 12-year period and found that, overall, about 1 in 5 patients, or 20.4%, needed to be retreated. Patients treated with radical intent had a retreatment rate of 13% compared with 45% for those treated initially with palliative intent. Interestingly enough, the rate of retreatment was much lower than the average in the most common cancers, which included breast, prostate, colorectal, and head and neck cancer, although being higher than average in the rare malignancies.

For any of the previously mentioned reasons, it may be necessary to consider treatment to a tumor located in any area of the body that had previously been irradiated. Decisions regarding the safety of such retreatment are complex. For example, surgery may be compromised if the tissues involved had been previously irradiated to a high dose. The discussion here, however, focuses principally on the safety of reirradiation of an area of normal tissue previously exposed to radiation. Information on this subject is far from complete, but certain general principles emerge from experimental and clinical experience. One thing is clear, namely, that if the radiation tolerance of a given organ or tissue has been exceeded by the initial treatment, to the extent that function is lost or is in the process of being lost, then subsequent retreatment cannot be contemplated with safety. By contrast, if the initial treatment is below the tolerance of the organ or

tissue exposed, then some retreatment at a later date is safe, varying very much with the organ or tissue involved and depending on several other factors.

When considering retreatment with radiation, whether it is intended to be either curative or palliative, several factors must be taken into account:

1. The dose and volume treated during the initial radiotherapy and the extent to which the retreatment fields overlap with the initial fields
2. Whether chemotherapy was added to the initial radiotherapy
3. The time interval that has elapsed since the initial radiotherapy
4. The tissues and organs involved because they differ markedly in their ability to recover
5. Highly conformal techniques, such as stereotactic radiosurgery, stereotactic body radiotherapy (SBRT), or brachytherapy, are most appropriate.
6. Whether there are alternative options to radiation that could be considered

EARLY- AND LATE-RESPONDING TISSUES

Early-responding tissues are usually self-renewing tissues and are characterized by a rapidly proliferating stem cell compartment that provides cells to differentiate and become the mature functioning cells. If some stem cells survive within the irradiated volume, or if undamaged stem cells can migrate into the irradiated volume from outside, the tissue architecture may be partially or completely restored. Consequently, rapidly proliferating tissues generally recover well from the initial radiotherapy and will tolerate reirradiation to almost full doses, provided sufficient time is allowed.

By contrast, most late-responding tissues are much less able to tolerate retreatment because they do not have the ability to recover from the initial damage inasmuch as they do not have a rapidly proliferating stem cell compartment. Some slowly proliferating tissues are capable of partial proliferative and functional recovery, although this takes months and some residual damage remains.

For the aforementioned reasons, it has been suggested that proton beam therapy might be the ideal choice for retreatment situations because prior radiotherapy effectively makes subsequent radiotherapy very challenging. The limiting factor in retreatment is usually the potential toxicity to nearby late-responding normal tissues, and the hallmark of proton treatment plans is their ability to maximize the tumor dose and minimize the dose to normal tissue.

Historically, the limited access to proton beam therapy has resulted in a form of “rationing” relative to the indications for which it is used. As more facilities become available, retreatment, where toxicity to normal tissues is so critical, may be an excellent choice for proton therapy.

PRECLINICAL DATA

Experiments with rodents show that radiation-induced skin damage can recover well, with restoration of almost full radiation tolerance. As would be expected, recovery occurs quickly after low doses but more slowly as the initial dose is increased. Using hind limb deformation as an endpoint, representing late subcutaneous fibrosis, much poorer retreatment tolerance was observed than for the early skin reaction. Preclinical data also show that retreatment with reduced doses is possible in both lung and spinal cord after an interval of 3 to 6 months. There is a plethora of data for the spinal cord in animals ranging from rodents to rhesus monkeys. The experiments with monkeys demonstrated a large capacity for the spinal cord to recover from occult radiation injury induced by a commonly prescribed elective dose (44 Gy in 2 Gy fractions) in that only 4 of 45 monkeys developed myeloparesis following a retreatment with 57.2 to 66 Gy given 1 to 3 years after the initial therapy.

Other slowly proliferating organs, such as the kidney or bladder, do not appear to be capable of recovery from late functional damage even after lower subtolerance doses.

CLINICAL STUDIES

Clinical radiation oncologists are, quite rightly, reluctant to transfer quantitative reirradiation data from animals (especially rodents) to humans, although the general principles and lessons, particularly the big difference between different organs and tissues, are probably applicable.

Unfortunately, the clinical data available are sketchy to say the least. In most cases, the number of patients is small, collected over a long period, with changing radiotherapy techniques (dose, fractionation pattern, etc.), and with no detailed outcome of a matched control group of patients who had received the same initial therapy but not the retreatment.

Clinical review papers are beginning to express data in terms of the biologically effective dose (BED), calculated on the basis of the linear-quadratic model, using an α/β ratio of 10 for early-responding tissues and 3 for late-responding tissues. This is a good first step, but unconventional fractionation

patterns are often used for retreatment schedules, particularly in a palliative setting, it would be necessary to convert the BED values obtained to an equivalent BED calculated for a 2 Gy per fraction schedule if different experiences are to be compared. Unfortunately, such complete data are seldom available.

Spinal Cord

The spinal cord is a major dose-limiting organ in the treatment of primary tumors of the spinal cord or of neoplastic disease in the direct vicinity of the cord. When initial radiation therapy is delivered in conventional 2 Gy per day fractions, the consensus is that the incidence of myelopathy is less than 1% for total doses of 50 to 55 Gy and up to 5% for total doses of 55 to 60 Gy. The published clinical data on reirradiation suggest that there is a substantial recovery, provided the initial treatment did not exceed about 90% of the acceptable BED and that there was a time interval of a year or more between the initial and subsequent treatments. The data suggest an important threshold of a cumulative BED of 130% to 135% of the acceptable BED in a single course of therapy (calculated with an appropriate α/β ratio of about 3). The reader is referred to the appropriate review papers (Grosu et al., Nieder et al.) for more details, but the overall conclusion is that it is not possible to suggest more detailed recommendations concerning the optimal total dose and fraction size to result in the maximal palliative effects accompanied by minimal side effects.

There are two later reports of the use of SBRT for the salvage therapy of patients with prior radiation of spinal metastases ([Nelson et al., 2009](#); [Sahgal et al., 2009](#)). The development of this highly conformal treatment makes it possible to give a dose of approximately 24 Gy in about three fractions, without unacceptable toxicity. The authors conclude that SBRT is both safe and effective in the palliative/retreatment setting.

In summary, the clinical data, although minimal, do not contradict the more detailed data available from primate studies, which suggest that retreatment is a real possibility in this site.

Brain

There are no animal data available on the reirradiation tolerance of the brain. It might be thought that information derived from studies of the spinal cord could be transferred to the brain, but the available clinical studies indicate that this is not the case, at least, in regard to the influence of the time interval between

initial treatment and reirradiation.

The most recent overview of currently available clinical data on reirradiation of the brain comes from studies of the treatment of recurrent glioma ([Mayer & Sminia, 2008](#)). For conventional radiotherapy techniques, radiation-induced normal brain tissue necrosis was found when the cumulative BED (i.e., the sum of the BEDs from both the initial treatment and reirradiation) exceeded 100 Gy. In most cases, the initial treatment consisted of a standard regimen of 60 Gy in 2 Gy fractions. The BED was calculated using the linear-quadratic formalism, employing an α/β ratio of 2 Gy and normalized to 2 Gy fractions because the literature contains several reirradiation schemes with regard to total dose and fraction size. There was no correlation between the time interval between the initial and reirradiation course and the incidence of radionecrosis. When more conformal techniques were employed, such as fractionated stereotactic radiosurgery, higher retreatment doses were possible without increasing the probability of normal brain tissue necrosis.

The Radiation Therapy Oncology Group Protocol 90–95 studied 156 patients with recurrent previously irradiated primary brain tumors and brain metastases, retreated with single fraction radiosurgery. They found that the maximum tolerated doses were 24 Gy, 18 Gy, and 15 Gy for tumors less than or equal to 20 mm, 21 to 30 mm, and 31 to 40 mm in diameter, respectively. Unacceptable central nervous system toxicity was more likely in patients with larger tumors, whereas local tumor control was most dependent on the type of recurrent tumor and the treatment unit used (linac vs. Gamma Knife).

Head and Neck

Despite significant improvements in outcome for head and neck squamous cell carcinoma treated aggressively by modern techniques, the major pattern of failure continues to be locoregional recurrence. There is no consensus on the best way to handle this problem, and as a result, there is a wide variation in the approaches used. There have been several reviews in recent years (Chopra et al., De Crevoisier et al., Kasperts et al., Lee et al., Salama et al., Wong et al.). Radical reirradiation with doses of 50 to 60 Gy, either definitive or postoperative, does improve locoregional control and possibly improves survival, whereas lower doses are ineffective. However, reirradiation with such potentially curative doses within a few years of a similar initial treatment is associated with severe toxicity and functional sequelae as well as a small but nonnegligible incidence of treatment-related deaths. The most recent review by

Sulman et al. reported on the use of intensity-modulated radiation therapy (IMRT) to retreat recurrent head and neck cancer and came to the same general conclusion except that the treatment-related morbidity, although significant, may have been less than in previously published reports using conventional techniques. In this case, the median time interval between initial radiation and retreatment was almost 4 years, and the median lifetime dose was 116.1 Gy.

Rectum

The addition of preoperative or postoperative chemotherapy and/or radiotherapy to radical surgery for rectal carcinoma has reduced the incidence of local recurrence to approximately 10% to 15%, but this group of patients presents a substantial problem.

Mohiuddin et al. published a review of 103 patients who underwent reirradiation with concurrent 5-fluorouracil-based chemotherapy.

Overall survival was poor, and there was a substantial incidence of both early and late complications. Such a wide range of doses were used, both for the initial treatment and the reirradiation, that it is difficult to draw any firm conclusions. Nevertheless, this remains an option for a particularly difficult group of patients.

Bone Metastases

Bone metastases are a frequent cause of morbidity in patients with malignant disease, occurring most often in patients with breast, lung, prostate, thyroid, and renal cancers and those with multiple myeloma. Pain is the most common symptom, which can be treated successfully in most patients by external beam radiotherapy. An increasing number of patients outlive the duration of the benefits of initial palliative radiotherapy for symptomatic bone metastases, requiring reirradiation of previously treated sites.

Chow et al. summarized the studies to date, which include several retrospective and prospective trials. The available data support the reirradiation of sites of metastatic bone pain after initial irradiation, particularly when this follows an initial period of response. In other words, patients who respond to the first treatment usually respond to subsequent treatments. There is limited evidence that a small proportion of initial nonresponders would respond to reirradiation. There is no agreement over the optimal treatment schedule to be used, with reports in the literature varying from a single fraction of 4 or 8 Gy, to fractionated regimens of up to 35 Gy in four fractions. The exact mechanism by which radiation relieves bone pain is not understood. Pain relief appears to be

independent of the reduction in tumor size or cell kill, as evidenced by the rapidity of onset of pain relief and the apparent absence of a dose response. Because most patients requiring treatment for painful bone metastases have a limited life expectancy, a short treatment course, with minimum inconvenience to the patient, would seem to be warranted, unless a multifraction course is clearly superior. With this in mind, Chow et al. have set up an international phase III randomized trial comparing single with multiple fractions for reirradiation of painful bone metastases.

Breast

Reirradiation after recurrence of breast cancer is a major problem. Harms et al. reviewed more than 250 cases, where the reirradiation was performed either with electron beams, which have a limited depth of penetration, or with continuous low dose rate (CLDR) or pulsed dose rate (PDR) brachytherapy. With both of these techniques, high doses can be applied to the chest wall, whereas deeper seated organs (lung, heart) can be spared to a large extent.

After retreatment using electron beams, complete remissions were obtained in 41% to 74% of the patients. The brachytherapy was judged to be superior, with complete remissions in 79% to 82% of the patients, an advantage that the authors (rightly or wrongly) attributed to the protracted irradiation schedule of the CLDR/PDR, which resulted in an improved therapeutic ratio. Severe grade IV complications occurred in less than 10% of the reirradiated patients.

This is an area where the use of hyperthermia has had some modest success. Although rather dated now, Vernon et al. reported on an international collaborative group, which combined the results of five randomized controlled trials conducted in the United Kingdom, Europe, and Canada, in which external beam radiation therapy alone was compared with radiation plus hyperthermia. The greatest advantage for the combined treatment was seen in patients with recurrent lesions in previously treated areas, in whom reirradiation was limited to lower doses. In these patients, the complete response rate was almost doubled.

Lung

Local recurrence of lung cancer after initial external beam radiotherapy poses substantial problems for the subsequent management of the patient. Okamoto et al. is often quoted in this context, but this paper describes a very small series of only 34 patients, with a wide range of doses used for the initial treatment (30 to 80 Gy) and an even wider range of retreatment doses (10 to 70 Gy). The authors

concluded that such reirradiation resulted in a symptomatic benefit in most patients but at a cost of substantial toxicity. Most patients succumbed to their disease before the serious late effect of lung fibrosis could be expressed.

Proton therapy, characterized by a well-defined localized high-dose region, would seem to be the logical way to approach reirradiation of recurrent lung cancer. Early experience from MD Anderson Cancer Center indicates that amazingly high doses can be tolerated, but no data have been published to date. When protons are not available, a highly conformal technique such as SBRT may give improved results.

Recurrent Vaginal Metastases

Radiotherapy has been an accepted form of treatment for decades, but when there is recurrent or persistent disease after a full course of radiation, the best option is radical surgery, which can result in a 5-year survival rate in excess of 60% (Rubin et al.). When this is not possible, reirradiation has been used in the past as an alternate, but both local control and survival rates were poor, although there was a significant rate of complications (Jones et al.).

A report from China concluded that reirradiation for late recurrence in the vagina after previous radiotherapy for cervical cancer is valuable in selected cases. Early detection, so that tumor volume is small, appears to be very important, although brachytherapy was performed in most cases (Xiang et al.).

SUMMARY OF PERTINENT CONCLUSIONS

Of patients presenting at major cancer centers in the Western world, 10% present with a second cancer.

If the radiation tolerance of a given organ or tissue was exceeded by the initial treatment to the extent that function is lost, or is in process of being lost, then retreatment cannot be contemplated safely.

If the normal tissue tolerance was not exceeded by the initial treatment, some reirradiation at a later date is safe, varying very much with the tissue or organ involved and depending on other factors.

In general, early-responding tissues recover and tolerate retreatment better than late-responding tissues, but there are exceptions.

Animal Studies

Radiation-induced skin damage recovers well, with restoration of almost full

radiation tolerance. Recovery is slower after larger doses.

Poorer retreatment tolerance for fibrosis.

Retreatment with reduced doses is possible in both lung and spinal cord. There are much data for spinal cord in both rodents and monkeys.

Kidney and bladder are not capable of recovery from late functional damage.

Clinical Studies

Most clinical studies involve small numbers of patients, variable doses, and various time intervals between the initial treatment and reirradiation.

Reirradiation is possible in various sites with reduced doses and with a high price in terms of morbidity.

Most data are for head and neck. Reirradiation with 50 to 60 Gy within a few years of the initial treatment improves local control and possibly survival but with severe toxicity and functional sequelae.

Studies using IMRT or, better still, protons to reduce the volume of normal tissue exposed, as well as hyperfractionation to spare normal tissues, may be called for in the future, but no data are available at the present time.

BIBLIOGRAPHY

Reviews

Stewart FA. Re-treatment after full-course radiotherapy: is it a viable option? *Acta Oncol.* 1999;38:855–862.

Stewart FA, van der Kogel AJ. Retreatment tolerance of normal tissues. *Semin Radiat Oncol.* 1994;4:103–111.

Preclinical (Animal Studies)

Ang KK, Price RE, Stephens LC, et al. The tolerance of primate spinal cord to re-irradiation. *Int J Radiat Oncol Biol Phys.* 1993;25:459–464.

Brown JM, Probert JC. Early and late radiation changes following a second course of irradiation. *Radiology.* 1975;115:711–716.

Foote RL, Stafford SL, Petersen IA, et al. The clinical case for proton beam therapy. *Radiat Oncol.* 2012;7:174–184.

Hendry JH, Feng-Tong Y. Response of bone marrow to low LET irradiation. In:

- Hendry JH, Lord BI, eds. *Radiation Toxicology: Bone Marrow and Leukemia*. London, United Kingdom: Taylor & Francis; 1995:82–104.
- Ruifrok AC, Kleiboer BJ, van der Kogel AJ. Reirradiation tolerance of the immature rat spinal cord. *Radiother Oncol*. 1992;23:249–256.
- Simmonds RH, Hopewell JW, Robbins ME. Residual radiation-induced injury in dermal tissue: implications for retreatment. *Br J Radiol*. 1989;62:915–920.
- Stewart FA, Luts A, Lebesque JV. The lack of long-term recovery and reirradiation tolerance in the mouse kidney. *Int J Radiat Biol*. 1989;56:449–462.
- Stewart FA, Oussoren Y, Luts A. Long-term recovery and re-irradiation tolerance of mouse bladder. *Int J Radiat Oncol Biol Phys*. 1990;18:1399–1406.
- Stewart FA, Oussoren Y, Van Tinteren H, et al. Loss of reirradiation tolerance in the kidney with increasing time after single or fractionated partial tolerance doses. *Int J Radiat Biol*. 1994;66:169–179.
- Terry NH, Tucker SL, Travis EL. Residual radiation damage in murine lung assessed by pneumonitis. *Int J Radiat Oncol Biol Phys*. 1988;14:929–938.
- Terry NH, Tucker SL, Travis EL. Time course of loss of residual radiation damage in murine skin assessed by retreatment. *Int J Radiat Biol*. 1989;55:271–283.
- van der Kogel AJ, Sissingh HA, Zoetelief J. Effect of X rays and neutrons on repair and regeneration in the rat spinal cord. *Int J Radiat Oncol Biol Phys*. 1982;8:2095–2097.
- White A, Hornsey S. Time dependent repair of radiation damage in the rat spinal cord after X-rays and neutrons. *Eur J Cancer*. 1980;16:957–962.

Clinical

- Anderson PR, Coia LR. Fractionation and outcomes with palliative radiation therapy. *Semin Radiat Oncol*. 2000;10:191–199.
- Ang KK, Jiang GL, Feng Y, et al. Extent and kinetics of recovery of occult spinal cord injury. *Int J Radiat Oncol Biol Phys*. 2001;50:1013–1020.
- Chopra S, Gupta T, Agarwal JP, et al. Re-irradiation in the management of isolated neck recurrences: current status and recommendations. *Radiother Oncol*. 2006;81:1–8.

- Chow E, Hoskin P, Wu J, et al. A phase III international randomised trial comparing single with multiple fractions for re-irradiation of painful bone metastases: National Cancer Institute of Canada Clinical Trials Group (NCIC CTG) SC 20. *Clin Oncol (R Coll Radiol)*. 2006;18:125–128.
- De Crevoisier R, Bourhis J, Domenge C, et al. Full-dose reirradiation for unresectable head and neck carcinoma: experience at the Gustave-Roussy Institute in a series of 169 patients. *J Clin Oncol*. 1998;16:3556–3562.
- Flynn CJ, Yip D, Ko YJ, et al. Clinical benefit of reirradiation: a case report. *J Palliat Med*. 2008;11(1):112–116.
- Grosu AL, Andratschke N, Nieder C, et al. Retreatment of the spinal cord with palliative radiotherapy. *Int J Radiat Oncol Biol Phys*. 2002;52:1288–1292.
- Harms W, Krempien R, Grehn C, et al. Reirradiation of chest wall local recurrences from breast cancer [in German]. *Zentralbl Gynakol*. 2004;126:19–23.
- Hayashi S, Hoshi H, Iida T. Reirradiation with local-field radiotherapy for painful bone metastases. *Radiat Med*. 2002;20:231–236.
- Jeba J, George R. The role of reirradiation versus chemotherapy in recurrent head and neck cancer. *Indian J Palliat Care*. 2006;12:56–64.
- Jeremic B, Shibamoto Y, Igrutinovic I. Single 4 Gy re-irradiation for painful bone metastasis following single fraction radiotherapy. *Radiother Oncol*. 1999;52:123–127.
- Jeremic B, Shibamoto Y, Igrutinovic I, et al. Second single 4 Gy reirradiation for painful bone metastasis. *J Pain Symptom Manage*. 2002;23:26–30.
- Jones TK Jr, Levitt SH, King ER. Retreatment of persistent and recurrent carcinoma of the cervix with irradiation. *Radiology*. 1970;95:167–174.
- Kasperts N, Slotman B, Leemans CR, et al. A review on re-irradiation for recurrent and second primary head and neck cancers. *Oral Oncol*. 2005;41:225–243.
- Khor R, Bressel M, Tai KH, et al. Patterns of retreatment with radiotherapy in a large academic centre. *J Med Imaging Radiat Oncol*. 2013;57:610–616.
- Kramer GW, Gans S, Ullmann E, et al. Hypofractionated external beam radiotherapy as retreatment for symptomatic non-small-cell lung carcinoma: an effective treatment? *Int J Radiat Oncol Biol Phys*. 2004;58:1388–1393.

- Lee AW, Foo W, Law SC, et al. Total biological effect on late reactive tissues following reirradiation for recurrent nasopharyngeal carcinoma. *Int J Radiat Oncol Biol Phys.* 2000;46:865–872.
- Lee N, Chan K, Bekelman JE, et al. Salvage re-irradiation for recurrent head and neck cancer. *Int J Radiat Oncol Biol Phys.* 2007;68:731–740.
- Maciejewski B, Zajusz A, Pilecki B, et al. Acute mucositis in the stimulated oral mucosa of patients during radiotherapy for head and neck cancer. *Radiother Oncol.* 1991;22:7–11.
- Marcus RB, Million RR. The incidence of myelitis after irradiation of the cervical spinal cord. *Int J Radiat Oncol Biol Phys.* 1990;19:3–8.
- Mayer R, Sminia P. Reirradiation tolerance of the human brain. *Int J Radiat Oncol Biol Phys.* 2008;70:1350–1360.
- Milano MT, Constine LS, Okunieff P. Normal tissue tolerance dose metrics for radiation therapy of major organs. *Semin Radiat Oncol.* 2007;17:131–140.
- Milker-Zabel S, Zabel A, Thilmann C, et al. Clinical results of retreatment of vertebral bone metastases by stereotactic conformal radiotherapy and intensity-modulated radiotherapy. *Int J Radiat Oncol Biol Phys.* 2003;55:162–167.
- Mithal N, Needham P, Hoskin PJ. Retreatment with radiotherapy for painful bone metastases. *Int J Radiat Oncol Biol Phys.* 1994;29:1011–1014.
- Mohiuddin M, Marks G, Marks J. Long-term results of reirradiation for patients with recurrent rectal carcinoma. *Cancer.* 2002;95:1144–1150.
- Moriya Y. Treatment strategy for locally recurrent rectal cancer. *Jpn J Clin Oncol.* 2006;36(3):127–131.
- Morris DE. Clinical experience with retreatment for palliation. *Semin Radiat Oncol.* 2000;10:210–221.
- Nelson JW, Yoo DS, Sampson JH, et al. Stereotactic body radiotherapy for lesions of the spine and paraspinal regions. *Int J Radiat Oncol Biol Phys.* 2009;73:1369–1375.
- Nieder C, Grosu AL, Andratschke NH, et al. Proposal of human spinal cord reirradiation dose based on collection of data from 40 patients. *Int J Radiat Oncol Biol Phys.* 2005;61:851–855.
- Nieder C, Milas L, Ang KK. Tissue tolerance to reirradiation. *Semin Radiat*

Oncol. 2000;10:200–209.

- Nieder C, Nestle U, Niewald M, et al. Hyperfractionate reirradiation for malignant glioma. In: Wiegel T, Hinkelbein W, Brock M, et al, eds. Controversies in neuro-oncology. *Front Radiat Ther Oncol.* 1999;33:150–157.
- Okamoto Y, Murakami M, Yoden E, et al. Reirradiation for locally recurrent lung cancer previously treated with radiation therapy. *Int J Radiat Oncol Biol Phys.* 2002;52:390–396.
- Rades D, Stalpers LJ, Veninga T, et al. Spinal reirradiation after short-course RT for metastatic spinal cord compression. *Int J Radiat Oncol Biol Phys.* 2005;63:872–875.
- Rubin SC, Hoskins WJ, Lewis JL Jr. Radical hysterectomy for recurrent cervical cancer following radiation therapy. *Gynecol Oncol.* 1987;27:316–324.
- Ruifrok A, Kleiboer BJ, van der Kogel AJ. Fractionation sensitivity of the rat cervical spinal cord during radiation retreatment. *Radiother Oncol.* 1992;25:295–300.
- Sahgal A, Ames C, Chou D, et al. Stereotactic body radiotherapy is effective salvage therapy for patients with prior radiation of spinal metastases. *Int J Radiat Oncol Biol.* 2009;74:723–731.
- Salama JK, Vokes EE, Chmura SJ, et al. Long-term outcome of concurrent chemotherapy and reirradiation for recurrent and second primary head-and-neck squamous cell carcinoma. *Int J Radiat Oncol Biol Phys.* 2006;64:382–391.
- Schiff D, Shaw EG, Cascino TL. Outcome after spinal reirradiation for malignant epidural spinal cord compression. *Ann Neurol.* 1995;37:583–589.
- Shaw E, Scott C, Souhami L, et al. Single dose radiosurgical treatment of recurrent previously irradiated primary brain tumors and brain metastases: final report of RTOG Protocol 90-05. *Int J Radiat Oncol Biol Phys.* 2000;47:291–298.
- Spanos W, Perez C, Marcus S. Effect of rest interval on tumor and normal tissue response: a report of phase III study of accelerated split course palliative radiation for advanced pelvis malignancies (RTOG 85-02). *Int J Radiat Oncol Biol Phys.* 1993;25:399–403.
- Sulman EP, Schwartz DL, Le TT, et al. IMRT reirradiation of head and neck

cancer—disease control and morbidity outcomes. *Int J Radiat Oncol Biol Phys.* 2009;73(2):399–409.

Valentini V, Morganti AG, Gambacorta MA, et al. Preoperative hyperfractionated chemoradiation for locally recurrent rectal cancer in patients previously irradiated to the pelvis: a multicentric phase II study. *Int J Radiat Oncol Biol Phys.* 2006;64:1129–1139.

Vernon CC, Hand JW, Field SB, et al. Radiotherapy with or without hyperthermia in the treatment of superficial localized breast cancer: results from five randomized controlled trials. *Int J Radiat Biol Phys.* 1996;35:731–744.

Winkler C, Dornfeld S, Dörr W, et al. Reirradiation after radiotherapy of primary brain tumors. In: Wiegel T, Hinkelbein W, Brock M, et al, eds. Controversies in neuro-oncology. *Front Radiat Ther Oncol.* 1999;33:276–283.

Wong SJ, Machtay M, Li Y. Locally recurrent, previously irradiated head and neck cancer: concurrent re-irradiation and chemotherapy, or chemotherapy alone? *J Clin Oncol.* 2006;24:2653–2658.

Xiang EW, Shu-mo C, Ya-qin D, et al. Treatment of late recurrent vaginal malignancy after initial radiotherapy for carcinoma of the cervix: an analysis of 73 cases. *Gynecol Oncol.* 1998;69:125–129.

chapter 25

Alternative Radiation Modalities

Fast Neutrons

Rationale

The Hammersmith Neutron Experience

The United States Neutron Experience

Boron Neutron Capture Therapy

Boron Compounds

Neutron Sources

Clinical Trials

Protons

Depth-Dose Patterns and the Bragg Peak

Advantages of Protons

Carbon Ion Radiotherapy

Depth-Dose Profiles

Radiobiologic Properties

Design of a Carbon Ion Beam for Clinical Use

Scattering and Fragmentation

Positron Emission Tomography Verification of Treatment Plans

Reasons for the Choice of Carbon Ions

Summary of Pertinent Conclusions

Hadron Therapy

Neutrons

Boron Neutron Capture Therapy

Protons

Carbon Ion Radiotherapy

Bibliography

The early recognition that x-rays could produce local tumor control in

some patients and not in others led to the notion that other forms of ionizing radiations might be superior. Particle therapy using beams of neutrons, energetic protons, or heavier positive ions is sometimes referred to as **hadron therapy**, that is, therapy with particles that are made of quarks.

T

Neutrons were first introduced in a speculative way, not based on any particular hypothesis. The later use of neutrons and the introduction of protons, negative π -mesons, and heavy ions were all based clearly on a putative advantage, either of physical dose distribution or of radiobiologic properties. In the case of neutrons, they give up their energy to produce recoil protons, α -particles, and heavier nuclear fragments. Consequently, their biologic properties differ from those of x-rays: reduced oxygen enhancement ratio (OER), little or no repair of sublethal damage, and less variation of sensitivity through the cell cycle.

The use of neutrons following World War II was based squarely on the premise that hypoxic cells limit the curability of human tumors by x-ray therapy, so the lower OER characteristic of neutrons might confer an advantage. An alternative rationale for neutrons, proposed at a later date, was that their relative biologic effectiveness (RBE) is larger for slow-growing tumors, possibly giving them an advantage in a limited number of specific human tumors.

Protons have radiobiologic properties similar to those of x-rays, and their introduction into radiotherapy was based entirely on the superiority of the physical dose distribution possible with charged particles. Negative π -mesons and heavy ions were introduced with the hope of combining the radiobiologic advantages attributed to neutrons with the dose distribution advantage characteristic of protons.

Neutrons have been shown to be superior to x-rays in a limited number of situations, specifically for the treatment of prostatic cancer, salivary gland tumors, and possibly soft tissue sarcomas. Several controlled clinical trials have been performed for various cancer sites, but a small gain was apparent only in these few circumstances. On the other hand, neutrons resulted in unacceptable late normal tissue damage in many cases and possibly a higher incidence of radiation-induced second cancers.

For almost 50 years, protons generated in facilities originally intended for physics research have found a small but important niche for the treatment of uveal melanoma and tumors such as chordomas, which are located close to the spinal cord and therefore benefit greatly from the localized dose distribution. The

wider use of protons for broad beam radiotherapy is being tested now that numerous custom-built hospital-based facilities are available in Europe, Japan, and the United States. It is hard to imagine that protons are not superior to x-rays because of the better dose distributions that can be obtained; however, to date, no controlled phase III clinical trials have been performed.

Negative π -mesons and heavy ions have been used to treat hundreds of patients, but prospective randomized trials have never been completed to prove their superiority over conventional x-rays. Negative π -mesons have completely disappeared from the scene, but high-energy carbon ions are enjoying a renaissance in Europe and Japan, and there are plans for similar units in the United States.

The casual reader may be content with this brief overview of alternative radiation modalities and may not wish to proceed further in this chapter. Interest in neutrons for radiotherapy largely has waned, but protons and carbon ions are very much in vogue. In this chapter, neutrons, protons, and carbon ions are considered in turn.

FAST NEUTRONS

Rationale

Neutrons were first used for cancer therapy at the Lawrence Berkeley Laboratory in California in the 1930s ([Fig. 25.1](#)). This first clinical trial of neutrons was not based on any radiobiologic rationale but was prompted largely by the availability of a new and unique beam. It is said that it received some impetus when the mother of the Lawrence brothers (E. O. Lawrence was the inventor of the cyclotron and the director of what was to become the Lawrence Berkeley Laboratory) contracted cancer, which was judged by her physician to be incurable by conventional means. She was treated with neutrons and lived for many years, although from a retrospective review of the case, it is probable that she did not have cancer in the first place. This early effort at Berkeley was hampered because the complexities of the relationship between the RBE and the dose for high-linear energy transfer (LET) radiations were not understood at the time. Consequently, several patients were overdosed seriously before the trial was terminated by the entry of the United States into World War II. In reviewing their experience many years later, Dr. Robert Stone, the radiotherapist in charge of the study, concluded in his famous Janeway Lecture of 1948 that “neutron therapy as administered by us resulted in such bad late sequelae in proportion to a few good results that it should not be continued.”



FIGURE 25.1 The first patient treated with neutrons in the 1930s at the Lawrence Berkeley Laboratory of the University of California. On the left is Dr. Robert Stone, the radiotherapist, and in the center is Dr. John Lawrence, the physician brother of the inventor of the cyclotron, E. O. Lawrence. (Courtesy of the University of California.)

The Hammersmith Neutron Experience

The renewed interest in neutrons in the years following World War II originated at the Hammersmith Hospital in London, where neutrons were generated by the Medical Research Council's 60-in. cyclotron. In this machine, 16-MeV deuterons incident on a beryllium target produced neutrons with a modal value of 6 MeV. The Hammersmith cyclotron was suggested and conceived by Gray based on the notion that a lowered OER would be advantageous to radiotherapy. The machine suffered from the limitations of poor depth doses (equivalent to 250-kVp x-rays) and a fixed horizontal beam.

A prospective randomized clinical trial to compare neutrons with x-rays was started in 1971. Advanced tumors of the head and neck were chosen because the poor depth-dose characteristics made neutrons suitable only for treating relatively superficial lesions. The trial involved patients with tumors of the salivary glands, buccal cavity, hypopharynx, and larynx. The neutron treatments delivered in only 12 fractions were clearly superior as judged by local control of the primary tumor, but the gain was achieved at the expense of a higher complication rate.

The United States Neutron Experience

Because of the limitations associated with low-energy cyclotrons, interest at several centers in the United States turned to the use of large cyclotrons that accelerate deuterons to energies of 22 to 50 MeV. Several such machines had been built for high-energy physics research and were converted for part-time

neutron therapy. In addition, neutrons were produced at the Fermilab in Batavia, Illinois, by bombarding a beryllium target with 67-MeV protons.

All of these machines had adequate dose rates and quite good depth doses. Unfortunately, they had other disadvantages: All had fixed horizontal beams, and all were located in physics installations rather than in large, busy hospitals so that the availability of a sufficient number of patients was a problem. Several controlled clinical trials were performed for various tumor sites, and they showed no advantage for neutrons over x-rays. Neutrons, however, appeared to be superior for salivary gland tumors, soft tissue sarcomas, and prostate cancer, but the downside was a significant increase in late normal tissue damage. It appears that high-LET radiation loses the differential sparing effect between tumors and late-responding normal tissues that is characteristic of x-rays.

Enthusiasm for neutron therapy waned just at a time when technology became available that allowed machines to be built that are suitable for clinical use. A new generation of hospital-based cyclotrons using the $p^+ \rightarrow Be$ reaction had adequate dose rates, good percentage depth doses, and a full isocentric mount, similar to a conventional linac. A few centers operated such machines for a while, but neutrons have never become mainstream in radiotherapy because of the unacceptable normal tissue complications.

BORON NEUTRON CAPTURE THERAPY

The basic idea behind boron neutron capture therapy (BNCT) is elegant in its simplicity. It has appealed to physicians, and particularly to physicists, for the best part of half a century. The idea is to deliver to the cancer patient a boron-containing drug that is taken up only in tumor cells and then to expose the patient to a beam of low-energy (thermal) neutrons that themselves produce little radiobiologic effect but that interact with the boron to produce short-range, densely ionizing α -particles. Thus, the tumor is intensely irradiated, but the normal tissues are spared. There are two problems inherent in this idea that have so far proved intractable:

1. How does one find a “magic” drug that can distinguish malignant cells from normal cells? (The skeptic might add that searching for such a drug has been the holy grail of cancer research and that if one were found, the obvious strategy would be to attach an alkylating agent or an α -emitting radionuclide to it; combining its use with neutrons would be a distant third.)
2. The low-energy neutrons necessary for BNCT are poorly penetrating in

tissue and consequently result in percentage depth doses that are extremely poor by today's standards.

Several nuclides have high propensities for absorbing low-energy or thermal neutrons; that is, they have a high neutron capture cross section. Boron is the most attractive of these because it is readily available in a nonradioactive form; its chemistry is such that it can be incorporated into various compounds; and if it interacts with low-energy neutrons, it emits short-range, high-LET α -particles.

Boron Compounds

For BNCT to be successful, the compounds used should have high specificity for malignant cells, with concomitantly low concentrations in adjacent normal tissues and in blood. In the early days, the compounds used were not specially synthesized for BNCT but were already available. In the brain, which is the site for which BNCT largely has been used, some selectivity is obtained because compounds do not penetrate normal brain tissue to the same degree as brain tumors in which the blood-brain barrier is absent or severely compromised.

Critical to the success of BNCT is the requirement that boron compounds be developed that target tumor versus normal cells selectively, achieve a sufficient concentration within the tumor, and produce tumor to normal tissue ratios of 3 or 4 to 1. This, of course, is a tall order.

Two classes of compounds have been proposed:

1. Low-molecular-weight agents that simulate chemical precursors required for tumor cell proliferation have the ability to traverse the cell membrane and be retained intracellularly. Two boron compounds have been identified and used clinically, known as sodium brocapate and boronophenylalanine. Both have been used to treat brain tumors, and the latter also has been listed for cutaneous melanoma.
2. High-molecular-weight agents such as monoclonal antibodies and bispecific antibodies that contain boron have been developed. These are highly specific, but very small amounts reach brain tumors following systemic administration. Boron-containing conjugates of epidermal growth factor, the receptor for which is overexpressed on some tumors (including glioblastoma), also have been developed.

If the blood-brain barrier is disrupted temporarily, these high-molecular-weight compounds may have some utility, or direct intracerebral delivery may be required. They have not yet proved effective in clinical use.

Neutron Sources

During fission within the core of a nuclear reactor, neutrons are “born” that have a wide range of energies. Neutron beams can be extracted from the reactor by the application of suitable techniques and the use of appropriate moderators. Thermal neutrons, or room-temperature neutrons (0.025 eV), react best with boron to produce densely ionizing α -particles. Unfortunately, thermal neutrons are attenuated rapidly by tissue; the half-value layer is only about 1.5 cm. Consequently, it is not possible to treat to depths of more than a few centimeters without heavily irradiating surface normal tissues. Nevertheless, most clinical trials have used neutrons of this energy.

Current interest in the United States focuses on the use of epithermal neutron beams (1 to 10,000 eV), which have a somewhat greater depth of penetration. These can be obtained by using moderators or filters to slow the fast neutrons into the epithermal range and filtering out the residual thermal neutrons. These epithermal neutrons do not interact themselves with the boron but are degraded to become thermal neutrons in the tissue by collisions with hydrogen atoms. Even so, the peak in dose occurs at a depth of only 2 to 3 cm, with a rapid falloff beyond this depth. Thus, the very high surface doses are avoided, but the depth doses are still poor.

Clinical Trials

Several clinical trials have been performed over the years, beginning in the 1950s and 1960s. Results are tantalizing but never definitive. Several patients have been treated with BNCT in the United States, but the results are largely anecdotal. The concept of BNCT is as attractive as ever, but it continues to be difficult to convert to a practical treatment modality even for shallow tumors.

PROTONS

Dr. Robert Wilson first proposed protons for radiotherapy as early as 1946 based on their superior physical dose distribution; their radiobiologic properties are unremarkable. The RBE of protons is indistinguishable from that of 250-kV x-rays, which means that they are about 10% more effective than megavoltage x-rays generated by a linear accelerator. The OER for protons also is indistinguishable from that for x-rays, namely, about 2.5 to 3. These biologic properties are consistent with the physical characteristics of high-energy proton beams; they are sparsely ionizing, except for a very short region at the end of the particles’ range, just before they stop. In the entrance plateau, the average LET is

about $0.5 \text{ keV}/\mu\text{m}$, rising to a maximum of $100 \text{ keV}/\mu\text{m}$ over a few microns as the particles come to rest. This high-LET component is restricted, however, to such a tiny length of track and represents such a small proportion of the energy deposited that, for high-energy protons, it does not have any significant effect.

To treat cancer in humans with charged particles, high-energy accelerators are necessary. Protons have been used for many years to treat choroidal melanoma of the eye as an attractive alternative to enucleation. Because the eye is small, an energy of 60 to 70 MeV is adequate. However, to treat deep-seated solid tumors, an energy of about 200 MeV, corresponding to a range in tissue of about 26 cm, is essential. This requires a large and expensive cyclotron or synchrotron, and so it is not surprising that the number of centers where charged particle therapy is available has been limited.

Depth-Dose Patterns and the Bragg Peak

The dose deposited by a beam of monoenergetic protons increases slowly with depth but reaches a sharp maximum near the end of the particles' range in the **Bragg peak**. The beam has sharp edges, with little side scatter, and the dose falls to zero after the Bragg peak at the end of the particles' range. The possibility of precisely confining the high-dose region to the tumor volume and minimizing the dose to surrounding normal tissue is obviously attractive to the radiotherapist. Protons come closest to realizing this dream at relatively modest cost.

Figure 25.2 shows the depth-dose curve for the 187-MeV proton beam from the synchrocyclotron at Uppsala, Sweden. The sharply defined Bragg peak occurs at a depth in tissue that depends on the initial energy of the particles.

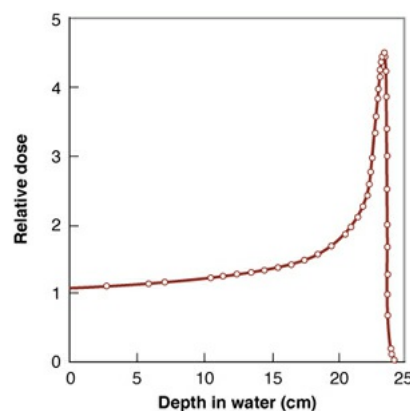


FIGURE 25.2 Depth-dose curve for 187-MeV protons from the Uppsala synchrocyclotron. The dose reaches a sharp peak at a depth of about 23 cm. (Adapted from Larsson B. Pre-therapeutic physical experiments with high

energy protons. *Br J Radiol.* 1961;34:143–151, with permission.)

The early medical use of ion beams (helium ions at Berkeley and protons at Harvard) involved treatment of the pituitary, first in patients with advanced breast cancer and later in patients with diabetic retinopathy, Cushing disease, and acromegaly. These ion beams were used for these applications to exploit their well-defined depth-dose pattern, which made it possible to give a huge dose to the pituitary without causing unacceptable damage to nearby structures. These treatments were performed for many years at both Berkeley and Harvard.

The way the Bragg peak can be spread out to encompass a tumor of realistic size is illustrated in [Figure 25.3](#). In this figure, curve A shows the narrow Bragg peak of the primary beam of the 160-MeV proton beam at the Harvard cyclotron. Beams of lower intensity and shorter range, shown in curves B, C, D, and E, are readily obtainable either by passing the beam through a rotating wheel with plastic sectors of varying thickness or by varying the energy of the beam. The composite curve, S, which is the sum of all the individual Bragg peaks of the beams of varying range, results in a uniform dose of more than 2.8 cm. The spread-out Bragg peak (SOBP), of course, can be made narrower or broader than this, as necessary.

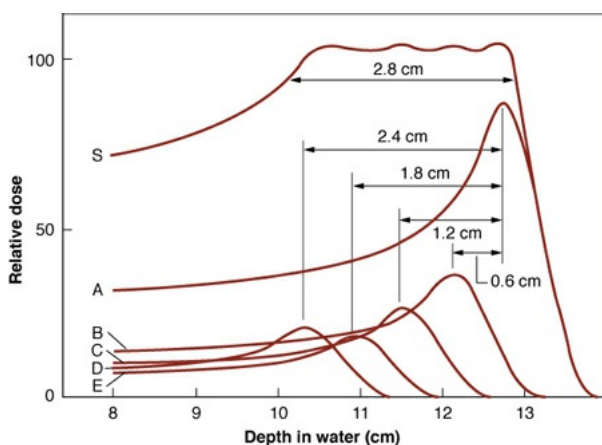


FIGURE 25.3 The way the Bragg peak for a proton beam can be spread out. *Curve A* is the depth-dose distribution for the primary beam of 160-MeV protons at the Harvard cyclotron, which has a half-width of only 0.6 cm. Beams of lower intensity and shorter range, as illustrated by *curves B, C, D, and E*, can be added to give a composite *curve S*, which results in a uniform dose of more than 2.8 cm. The broadening of the peak is achieved by passing the beam through a rotating wheel with sectors of varying thickness. (Adapted from Koehler AM, Preston WM. Protons in radiation therapy. Comparative dose distributions for protons, photons, and electrons. *Radiology*. 1972;104:191–195, with permission.)

Many researchers consider protons to be the treatment of choice for choroidal melanoma. [Figure 25.4](#) shows the dose distribution that is achieved at the Harvard cyclotron, which allows very high doses to be delivered to small tumors without unacceptable damage to nearby normal tissues. Protons have found a small but important place in the treatment of ocular tumors and some specialized tumors close to the spinal cord.

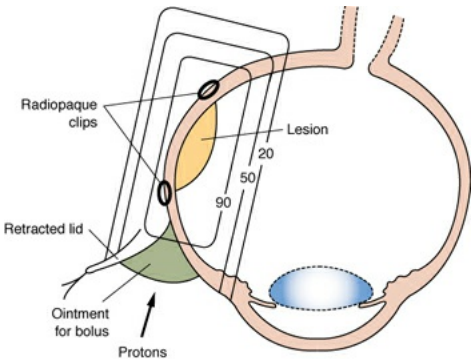


FIGURE 25.4 Dose distribution used for the treatment of choroidal melanoma at the Harvard cyclotron. Note the sharp edges to the beam and the rapid falloff of dose outside the treatment volume. (Courtesy of Dr. Herman Suit.)

Broad beam radiotherapy, with the Bragg peak spread out to cover a large tumor, has been in progress at Uppsala since 1957, and a comparable US effort began at Harvard in 1961 and at Loma Linda University in 1990. Most of the proton machines used in the past were built initially for physics research and were located in physics laboratories. There is much current interest in the development of hospital-based proton facilities producing beams sufficiently penetrating to make possible the treatment of any cancer sites in the human; such facilities would include a gantry with an isocentric mount and would feed several treatment rooms. The first machine of this kind was built at Loma Linda University in California, where a 250-MeV cyclotron produces a proton beam that can be directed into any one of four treatment rooms. The layout of the facility is shown in [Figure 25.5](#). The intention is to treat a broad spectrum of human cancers, not just the limited sites for which the dose distributions possible with protons already have proved their worth.

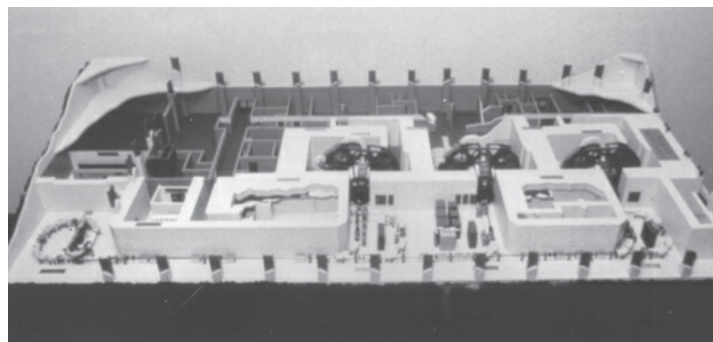


FIGURE 25.5 Model of the proton facility at Loma Linda. Protons are accelerated to energies up to 250 MeV in a synchrotron. The protons then can be directed into any one of four treatment rooms. This arrangement minimizes “idle” time because while one patient is being treated in one room, the next two patients can be set up in adjoining treatment rooms. This sort of facility sets the scene for the future: a large radiation therapy facility with multiple treatment rooms in the context of a cancer center. (Courtesy of Drs. James Slater and John Archambeau, Loma Linda University, Loma Linda, California.)

An even more impressive facility has been completed at the Massachusetts General Hospital in Boston. Although they formerly used a fixed horizontal beam from a cyclotron in the Harvard Physics Department, they now have a new facility constructed within the hospital. Similar facilities have been constructed at the MD Anderson Hospital in Houston, Texas, and at the University of Florida, whereas others are in the planning or construction stage at numerous locations in the United States, Europe, and Japan. Such facilities set the scene for the future. [Figure 25.6](#) shows a typical dose distribution that can be obtained with intensity-modulated proton therapy compared with intensity-modulated photon therapy. It is striking that with protons, the dose can be confined to the target volume, with much less irradiation of normal structures. With photons, a large fraction of the lungs are exposed to low doses of radiation.

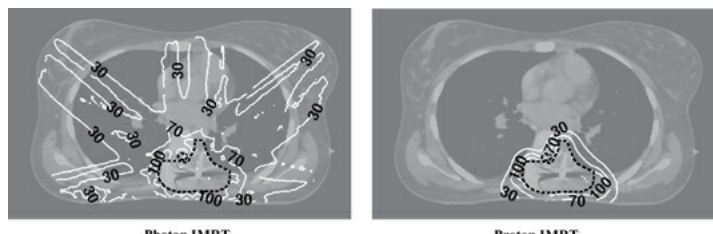


FIGURE 25.6 Treatment planning comparison of a seven-field intensity-modulated photon treatment plan (**left**) with an intensity-modulated proton (three scanned pencil beams) plan (**right**) for a patient with an epithelioid sarcoma involving the paravertebral tissues adjacent to the fifth through seventh vertebrae. The 30%, 70%, and 100% isodose lines are shown. The *dashed line*

outlines the target volume. Although dose to the target volume is similar, note the significantly higher integral dose to the lungs and heart with the intensity-modulated photon plan, which may be associated with an increase in acute and late normal tissue toxicity. Treatment comparison plans were prepared by Alexei V. Trofimov, PhD, at the Northeast Proton Therapy Center using the KonRad radiation treatment planning system originally designed at Deutsches Krebsforschungszentrum, Heidelberg, Germany. For further illustrations and discussion, see Weber DC, Trofimov AV, DeLaney TF, et al. A treatment planning comparison of intensity-modulated photon and proton therapy for paraspinal sarcomas. *Int J Radiat Oncol Biol Phys.* 2004;58:1596–1606. (Courtesy of Dr. Thomas DeLaney, Massachusetts General Hospital, Boston.)

Advantages of Protons

The basic principles of physics and biology imply that the dosimetric advantage of protons should translate into a clinical gain. These principles are as follows:

1. For the same dose to the target volume, protons deliver a lower absorbed dose to normal tissues than do high-energy x-rays.
2. There is no clinical advantage to be gained by irradiating normal tissues that do not harbor malignant cells.
3. There is little difference in the radiobiologic properties of protons used for therapy and high-energy x-rays; this includes repair, OER, and response through the cell cycle. The only relevant difference, therefore, is the dose distribution. The clinical proton facilities in the United States have agreed to use an RBE of 1.1 for protons in an SOBP relative to high-energy x-rays.
4. Ionizing radiations damage normal tissues as well as tumors, with the severity of the damage increasing with dose.

The consequence of these principles is that, for the same tumor dose, protons will deliver a lower dose to a smaller volume of normal tissue than high-energy x-rays. It is difficult to imagine that this can be other than a marked advantage, and the clinical results lean in that direction. Nevertheless, a comparison of clinical results between protons, intensity-modulated radiation therapy, and conventional conformal radiotherapy is somewhat controversial because of the lack of phase III clinical trials. This is unlikely to change any time soon because many consider it unethical to contemplate a trial in which patients are randomized to a less conformal technology when protons are available. The more complex issue of cost versus benefit is even more difficult to address; in

other words, protons may be better, but are they worth the cost?

CARBON ION RADIOTHERAPY

Interest in heavy ion radiotherapy centered initially at Berkeley, California, where in the 1970s, a large body of radiobiologic data was accumulated with positive ions from helium to argon, and a limited number of patients were treated with several different heavy ions, particularly neon. These heavier particles are characterized by a lower OER than x-rays, which may partly overcome the relative resistance of tumors that contain hypoxic cells. However, other radiobiologic properties of high-LET radiation, including the lack of repair of sublethal damage, resulted in unacceptable normal tissue late effects. The Berkeley facility closed some years ago, and interest in ion therapy has been rekindled largely in Europe and Japan, where several centers are using high-energy carbon ions for radiotherapy. Already more than 5,000 patients have received treatment.

Depth-Dose Profiles

Figure 25.7 shows the depth-dose profiles for carbon-12 (^{12}C) ions of two different energies compared with that for cobalt-60 (^{60}Co) γ -rays. In the case of carbon ions, dose is almost constant until close to the end of the range, when there is a sharp increase in dose in the Bragg peak. The depth at which the peak occurs depends on the energy. The peak is much too narrow to cover any tumor of realistic dimensions, and so the Bragg peak must be “spread out” to the required dimension by varying the energy of the beam. For carbon ions produced by a synchrotron, this can be achieved by varying the energy from pulse to pulse. Any required field size can be achieved from the narrow pencil beam that emerges from the synchrotron by “scanning” the beam, that is, deflecting the beam with magnetic fields so that, voxel by voxel, it conforms to the desired shape and size.

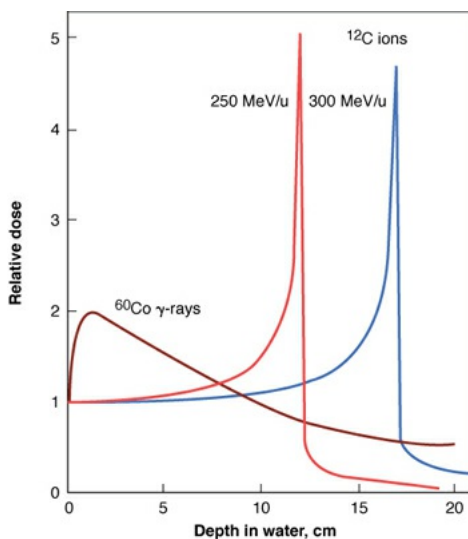


FIGURE 25.7 Comparison of the depth-dose profiles of carbon ions of two different energies with that of cobalt-60 γ -rays. (Adapted from Kraft G. Tumor therapy with heavy charged particles. *Prog Part Nucl Phys.* 2000;45:S473–S544.)

Radiobiologic Properties

Heavy ions, including carbon ions differ from both protons and high-energy x-rays in their radiobiologic properties on account of their higher LET. The rapid change of RBE with depth toward the end of the range of a carbon ion beam is illustrated in Figure 25.8. In principle, this is good news because the effectiveness of the dose is increased toward the end of the track which is located in the tumor volume, whereas the LET is low in the plateau region before the Bragg peak which corresponds to the normal tissue through which the beam must pass to reach the tumor.

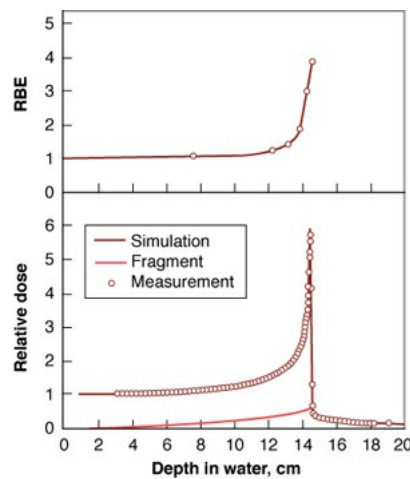


FIGURE 25.8 Top: Measured relative biologic effectiveness as a function of distance from the Bragg peak for 270-MeV/u carbon ions. Note the rapid

increase in RBE close to the peak. (Data taken from Blakely EA, Tobias CA, Ngo FQH, et al. Physical and cellular radiobiological properties of heavy ions in relation to cancer therapy applications. In: Pirruccello MD, Tobias CA, eds. *Biological and Medical Research with Accelerated Heavy Ions at the Bevalac, 1977–1980*. Berkeley, CA: Lawrence Berkeley Laboratory; 1980:73–86.) **Bottom:** Measured depth-dose profile for 270-MeV/u carbon ions, including the contribution from nuclear fragments in the “tail” beyond the Bragg peak. (Adapted from Kraft G. Tumor therapy with heavy charged particles. *Prog Part Nucl Phys*. 2000;45:S473–S544.)

Figure 25.9 shows survival curves for cells irradiated with photons compared with cells irradiated with high-energy carbon ions (corresponding to ions in the incident plateau) and with low-energy carbon ions (corresponding to ions at the end of their range in the Bragg peak). For high-energy carbon ions, the survival curve has a broad shoulder similar to that for x-rays, indicating the repair of sublethal damage and other radiobiologic properties characteristic of low-LET radiation. Only in the Bragg peak at the end of the range of the carbon ion beam, which is located in the tumor is a typical high-LET response seen; the survival curve is steep and has no shoulder, indicating the absence of repair.

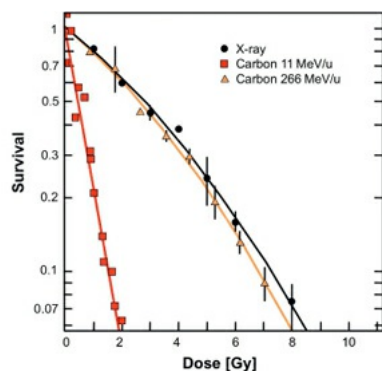


FIGURE 25.9 Survival curves for Chinese hamster ovary hamster cells irradiated with graded doses of x-rays, or with high-energy (266 MeV/u) carbon ions corresponding to the incident plateau of the depth-dose curve, or with low-energy carbon ions (11 MeV/u) corresponding to the Bragg peak. (Redrawn from the data of Weyrather WK, Ritter S, Scholz M, et al. RBE for carbon track-segment irradiation in cell lines of differing repair capacity. *Int J Radiat Biol*. 1999;75:1357–1364.)

Figure 25.10 shows the results of an experiment which simulates the treatment of a brain tumor 5 cm in diameter in the center of a head about 17 cm thick. Multiple plates covered with Chinese hamster ovary (CHO) cells were immersed in a tank of tissue culture medium and exposed with parallel opposed

beams of either protons or carbon ions. The SOBPs for either ion are about 5 cm wide and are designed to overlap from the two parallel opposed beams. It is evident that when the level of cell survival in the entrance plateau (corresponding to normal tissue) is the same for protons and carbon ions, the carbon ion treatment is far more effective at killing cells in the central tumor region covered by the SOBPs.

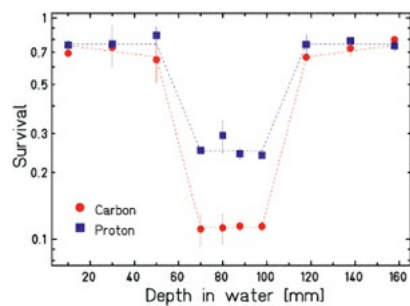


FIGURE 25.10 Measurement of cell survival of Chinese hamster ovary cells in a typical two-port irradiation with either protons or carbon ions. Cells were grown as a monolayer on multiple polyethylene slices immersed in a tank of tissue culture medium. The tank was 17 cm wide to simulate a human head, whereas the SOBP of the protons or carbon ions was 5 cm wide to simulate a centrally located brain tumor. The SOBPs of the parallel opposed fields were made to overlap. When cell survival in the entrance plateaus (corresponding to normal tissue) is matched for protons and carbon ions, there is a significantly greater level of cell killing in the SOBP region (corresponding to the tumor) for carbon ions than for protons. (Redrawn from the data of Elsässer T, Weyrather WK, Friedrich T, et al. Quantification of the relative biological effectiveness for ion beam radiotherapy: direct experimental comparison of proton and carbon ion beams and a novel approach for treatment planning. *Int J Radiat Oncol Biol Phys.* 2010;78:1177–1183.)

Design of a Carbon Ion Beam for Clinical Use

Factors to be considered in the design of a carbon ion beam for clinical use include the absorbed dose (in gray [Gy]), the RBE, and the effective dose, which is the product of the absorbed dose and the RBE. To achieve a uniform effective dose across the SOBP, the absorbed dose is decreased as the RBE rises. This is illustrated in Figure 25.11. In this example, the estimated peak RBE is 3.0, with an uncertainty band of 2.5 to 3.5. Estimation of the clinical RBE is not simple or straightforward. Experimentally determined RBE values are based on *in vitro* or *in vivo* laboratory systems, and it is impossible to know the extent to which they apply to human tumor or normal tissue.

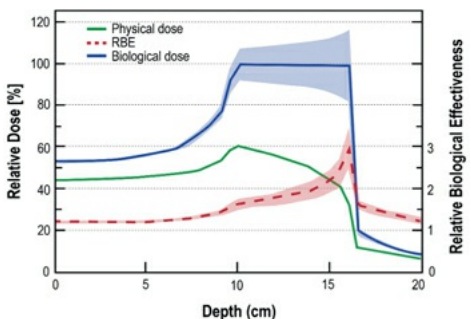


FIGURE 25.11 Design of a 290-MeV carbon ion beam with a 6-cm spread-out Bragg peak. For an assumed maximum relative biologic effectiveness (RBE) of 3.0, the impact of an error in selecting the RBE were the true RBE in the range of 2.5 to 3.5 is represented by the uncertainty bands around the effective dose, or what is labeled *Biological dose* in the figure. Effective dose is the product of absorbed dose and RBE. (From Suit H, DeLaney T, Goldberg S, et al. Proton vs carbon ion beams in the definitive radiation treatment of cancer patients. *Radiother Oncol.* 2010;95:3–22.)

Given the favorable depth-dose distribution and the high cell-killing effectiveness of carbon ions, short-course hypofractionated radiotherapy is currently being investigated in Europe and Japan, using only one or two large-dose fractions. Time will tell if this proves to be a successful strategy.

Scattering and Fragmentation

Compared with protons, carbon ions have less lateral scattering, leading to sharper beam edges, but there is a “tail” of lighter fragments beyond the Bragg peak. This is illustrated in the lower panel of Figure 25.8. Carbon ions, therefore, do not share the proton advantage that dose stops sharply at the end of the range of the primary particle.

Positron Emission Tomography Verification of Treatment Plans

It is possible to verify the treatment plan (i.e., to identify the position of the SOBP) in the case of carbon ions by means of a positron emission tomography (PET) scan. The basis is as follows: When a beam of carbon ions penetrates a thick absorber, a small fraction of the ions will undergo nuclear fragmentation—that is, they will break up. A frequent process is the stripping of one or two neutrons, converting the stable carbon-12 to the positron-emitting isotopes carbon-11 and carbon-10. These isotopes travel with *almost* the same velocity as the main beam and stop in *almost* the same place. They have short half-lives, and as they annihilate, they emit γ -rays that can be detected in a conventional PET

scanner. Consequently, the location of the SOBP, and therefore the high-dose treatment volume, is visualized. This technique can also be used with protons or other ions, but it is much more difficult.

Reasons for the Choice of Carbon Ions

Sufficiently detailed experimentation has not been carried for the statement to be made unequivocally that carbon is the “Optimal Ion.” It remains possible that a slightly lighter or even a slightly heavier ion such as nitrogen or oxygen might be as good or superior. However, carbon ions have a combination of properties that are very attractive. These are summarized in [Table 25.1](#).

Table 25.1 Properties of Carbon Ions for Heavy Ion Beam Therapy

1. The LET stays low in the entrance plateau (normal tissue) allowing repair to take place as with x-rays, whereas the RBE maximum coincides with the Bragg peak (reduced repair, increased cell killing in the tumor).
2. Carbon ions are relatively stable and have a small nuclear fragmentation tail beyond the Bragg peak (see [Fig. 25.8](#)).
3. Compared with protons, carbon ions have less lateral scattering leading to sharper beam edges.
4. Carbon is the simplest ion for PET analysis (to check the position of the SOBP) because the PET spectrum consists of only two isotopes of carbon, namely, carbon-10 and carbon-11. By contrast, nitrogen and oxygen have additional isotopes with different lifetimes.

Based on Weber U, Kraft G. Comparison of carbon ions versus protons. *Cancer J.* 2009;15:325–332.

SUMMARY OF PERTINENT CONCLUSIONS

Hadron Therapy

Particle therapy using beams of neutrons, protons, or heavy ions is sometimes referred to as hadron therapy, that is, therapy with particles that are made of quarks.

Neutrons

Neutrons are indirectly ionizing. In tissue, they give up their energy to produce recoil protons, α -particles, and heavier nuclear fragments.

Biologic properties of neutrons differ from those of x-rays in several ways: reduced OER, little or no repair of sublethal damage or potentially lethal damage, and less variation of sensitivity through the cell cycle.

The rationale for the use of neutrons in radiotherapy has changed over the years. The earlier rationale was the reduced OER to overcome the problem of hypoxic cells. The revised rationale is based on a higher neutron RBE for slowly growing tumors.

A small advantage has been demonstrated in clinical trials for neutrons in the treatment of salivary gland and prostate tumors and soft tissue sarcomas but not for most cancer sites tested. The downside of neutrons is the unacceptable level of normal tissue damage.

A new generation of hospital-based cyclotrons with isocentric mounts and generating neutrons by the $p^+ \rightarrow Be$ reaction became available, but by then, enthusiasm for neutrons had waned.

Boron Neutron Capture Therapy

The principle of BNCT is to deliver a drug-containing boron that localizes only in tumors and then to treat with low-energy thermal neutrons that interact with boron to produce α -particles.

Boron is a suitable substance because it has a large cross section for thermal neutrons and emits short-range, densely ionizing α -particles if bombarded by thermal neutrons. Its chemistry is such that it can be incorporated into a wide range of compounds.

Many attempts have been made to synthesize boron-containing compounds that are selectively localized in tumors relative to normal tissues but with limited success. They fall into two categories:

1. Low-molecular-weight agents that simulate chemical precursors needed for tumor cell proliferation

2. High-molecular-weight agents such as monoclonal antibodies and bispecific antibodies

Thermal neutrons are poorly penetrating in tissue, with a half-value layer of only 1.5 cm.

Epithermal neutrons are somewhat more penetrating. They are degraded to thermal neutrons by collisions with hydrogen atoms in tissue. The peak dose is at 2 to 3 cm, and the high surface dose is avoided.

Results of clinical trials of the efficacy of BNCT are tantalizing but not definitive.

The concept of BNCT is very attractive, but there are formidable practical difficulties in making it a treatment modality even for relatively shallow tumors.

Protons

Protons result in excellent physical dose distributions.

Protons have biologic properties similar to those of x-rays.

There is an established place for protons in the treatment of choroidal melanoma or tumors close to the spinal cord in which a sharp cutoff of dose is important.

Hospital-based high-energy cyclotrons with isocentric mounts are now being used to treat a broader spectrum of cancer patients with protons. Their efficacy has yet to be proved in clinical trials, but they offer the obvious physical advantage of good dose distributions with reduced dose to normal structures.

The clinical proton facilities have agreed to assume an RBE of 1.1 for protons in an SOBP relative to high-energy x-rays.

Carbon Ion Radiotherapy

The use of high-energy carbon ions has experienced a renaissance in Europe and Japan.

For carbon ions, as for protons, the narrow Bragg peak must be spread out to cover a tumor of realistic dimensions by varying the energy of the beam (SOBP).

The main reason for using carbon ions in tumor therapy is that the LET stays

low in the entrance plateau (normal tissue) allowing repair to take place as with x-rays, whereas the RBE maximum coincides with the Bragg peak (reduced repair, more cell killing in the tumor).

Carbon ions are relatively stable and have only a small nuclear fragmentation tail beyond the Bragg peak.

Compared with protons, carbon ions have less lateral scattering leading to sharper beam edges.

Carbon is the simplest ion for PET analysis (to check the position of the SOBP) because the PET spectrum consists of only two isotopes of carbon, namely, carbon-10 and carbon-11.

Hypofractionation with only one or two large-dose fractions is under investigation for carbon ions.

BIBLIOGRAPHY

- Asbury AK, Ojemann RG, Nielsen SL, et al. Neuropathologic study of fourteen cases of malignant brain tumor treated by boron-10 slow neutron capture radiation. *J Neuropathol Exp Neurol.* 1972;31:278–303.
- Barth RF, Soloway AH, Fairchild RG. Boron neutron capture therapy of cancer. *Cancer Res.* 1990;50:1061–1070.
- Batterman JJ. *Clinical Application of Fast Neutrons: The Amsterdam Experience.* Amsterdam, The Netherlands: Rodipi; 1981.
- Blakely EA, Tobias CA, Ngo FQH, et al. Physical and cellular radiobiological properties of heavy ions in relation to cancer therapy applications. In: Pirruccello MD, Tobias CA, eds. *Biological and Medical Research with Accelerated Heavy Ions at the Bevalac, 1977–1980.* Berkeley, CA: Lawrence Berkeley Laboratory; 1980:73–86.
- Brada M, Pijls-Johannesma M, De Ruysscher D. Proton therapy in clinical practice: current clinical evidence. *J Clin Oncol.* 2007;25:965–970.
- Broerse JJ, Barendsen GW, van Kersen GR. Survival of cultured human cells after irradiation with fast neutrons of different energies in hypoxic and oxygenated conditions. *Int J Radiat Biol Relat Stud Phys Chem Med.* 1968;13:559–572.
- Catterall M. Results of neutron therapy: differences, correlations and improvements. *Int J Radiat Oncol Biol Phys.* 1982;8:2141–2144.

- Catterall M, Sutherland L, Bewley DK. First results of a randomized clinical trial of fast neutrons compared with X or gamma rays in treatment of advanced tumours of the head and neck. Report to the Medical Research Council. *Br Med J*. 1975;2:653–656.
- Catterall M, Vonberg DD. Treatment of advanced tumours of head and neck with fast neutrons. *Br Med J*. 1974;3:137–143.
- D'Angio GJ, Aceto M, Nisce LZ, et al. Preliminary clinical observations after extended Bragg peak helium ion irradiation. *Cancer*. 1974;34:6–11.
- Drake CG. Arteriovenous malformations of the brain. The options for management. *N Engl J Med*. 1983;309:308–310.
- Field SB, Hornsey S. RBE values for cyclotron neutrons for effects on normal tissues and tumours as a function of dose and dose fractionation. *Eur J Cancer*. 1971;7:161–169.
- Fowler JF, Morgan RL, Wood CAP. Pre-therapeutic experiments with fast neutron beam from the Medical Research Council cyclotron: I. The biological and physical advantages and problems of neutron therapy. *Br J Radiol*. 1963;36:77–80.
- Goitein M, Cox JD. Should randomized clinical trials be required for proton radiotherapy? *J Clin Oncol*. 2008;26:175–176.
- Gueulette J, Blattmann H, Pedroni E, et al. Relative biological effectiveness determination in mouse intestine for scanning proton beam at Paul Scherrer Institute, Switzerland. Influence of motion. *Int J Radiat Oncol Biol Phys*. 2005;62:838–845.
- Hall EJ. Radiobiology of heavy particle radiation therapy: cellular studies. *Radiology*. 1973;108:119–129.
- Hall EJ, Graves RG, Phillips TL, et al, eds. Particle accelerators in radiation therapy. Proceedings of the CROS/RTOG Part III International Workshop. Houston, Texas. February 10-11, 1982. *Int J Radiat Oncol Biol Phys*. 1982;8:2041–2210.
- Hatanaka H. A revised boron-neutron capture therapy for malignant brain tumors: II. Interim clinical result with the patients excluding previous treatments. *J Neurol*. 1975;209:81–94.
- Hatanaka H, Amano K, Kanemitsu H, et al. Boron uptake by human brain tumors and quality control of boron compounds. In: Hatanaka H, ed. *Boron-*

- Neutron Capture Therapy for Tumors.* Niigata, Japan: Nishimura; 1986;77–106.
- International Commission on Radiation Units and Measurements. *Prescribing, Recording, and Reporting Proton-Beam Therapy.* Oxford, United Kingdom: Oxford University Press; 2007. Report 78.
- Javid M, Brownell GL, Sweet WH. The possible use of neutron-capturing isotopes such as boron-10 in the treatment of neoplasms: II. Computation of the radiation energies and estimates of effects in normal and neoplastic brain. *J Clin Invest.* 1952;31:604–610.
- Kjellberg RN, Hanamura T, Davis KR, et al. Bragg-peak proton-beam therapy for arteriovenous malformations of the brain. *N Engl J Med.* 1983;309:269–274.
- Koehler AM, Preston WM. Protons in radiation therapy. Comparative dose distributions for protons, photons, and electrons. *Radiology.* 1972;104:191–195.
- Kraft G. Tumor therapy with heavy charged particles. *Prog Part Nucl Phys.* 2000;45:S473–S544.
- Laramore GE, Krall JM, Thomas FJ, et al. Fast neutron radiotherapy for locally advanced prostate cancer: results of an RTOG randomized study. *Int J Radiat Oncol Biol Phys.* 1985;11:1621–1627.
- Larsson B. Pre-therapeutic physical experiments with high energy protons. *Br J Radiol.* 1961;34:143–151.
- Locher GL. Biological effects and therapeutic possibilities of neutrons. *AJR.* 1936;36:1–13.
- Parodi K, Bortfeld T, Haberer T. Comparison between in-beam and offline positron emission tomography imaging of proton and carbon ion therapeutic irradiation at synchrotron- and cyclotron-based facilities. *Int J Radiat Oncol Biol Phys.* 2008;71:945–956.
- Particle Therapy Co-Operative Group. Home page 2009. Available at: <http://ptcog.web.psi.ch/>
- Raju MR. *Heavy Particle Radiotherapy.* New York, NY; Academic Press; 1980.
- Schulz-Ertner D, Karger CP, Feuerhake A, et al. Effectiveness of carbon ion radiotherapy in the treatment of skull-base chordomas. *Int J Radiat Oncol Biol Phys.* 2007;68:449–457.

- St. Clair WH, Adams JA, Bues M, et al. Advantage of protons compared to conventional X-ray or IMRT in the treatment of a pediatric patient with medulloblastoma. *Int J Radiat Oncol Biol Phys.* 2004;58:727–734.
- Suit H, DeLaney T, Goldberg S, et al. Proton vs carbon ion beams in the definitive radiation treatment of cancer patients. *Radiother Oncol.* 2010;95:3–22.
- Suit H, Kooy H, Trofimov A, et al. Should positive phase III clinical trial data be required before proton beam therapy is more widely adopted? No. *Radiother Oncol.* 2008;86:148–153.
- Sweet WH. The use of nuclear disintegration in the diagnosis and treatment of brain tumor. *N Engl J Med.* 1951;245:875–878.
- Tsuji H, Kamada T, Baba M, et al. Clinical advantages of carbon-ion radiotherapy. *New J Phys.* 2008;10:075009.
- Weber DC, Trofimov AV, DeLaney TF, et al. A treatment planning comparison of intensity modulated photon and proton therapy for paraspinal sarcomas. *Int J Radiat Oncol Biol Phys.* 2004;58:1596–1606.
- Weber U, Kraft G. Comparison of carbon ions versus protons. *Cancer J.* 2009;15:325–332.
- Wilson RR. Radiological use of fast protons. *Radiology.* 1946;47:487–491.
- Withers HR, Thames HD, Peters LJ. Biological bases for high RBE values for late effects of neutron irradiation. *Int J Radiat Oncol Biol Phys.* 1982;8:2071–2076.

chapter 26

The Biology and Exploitation of Tumor Hypoxia

Hypoxia-Inducible Factor

- Oxygen-Dependent Regulation of Hypoxia-Inducible Factor
- Cancer Mutations that Activate Hypoxia-Inducible Factor
- Important Roles of Hypoxia-Inducible Factor in Tumors
- Hypoxia-Inducible Factor and Radiotherapy

Unfolded Protein Response

Radiosensitizing Hypoxic Cells

- Hyperbaric Oxygen
- Improving the Oxygen Supply to Tumors
- Hypoxic Cell Radiosensitizers
- Overgaard's Meta-analysis of Clinical Trials Addressing the Problem of Hypoxia
- Nicotinamide and Carbogen Breathing

Hypoxic Cytotoxins

- Tirapazamine
- Clinical Trials with Tirapazamine and New Bioreductive Drugs

Targeting Tumor Metabolism to Kill Hypoxic Cells

- Targeting Tumor Metabolism to Enhance the Efficacy of Radiotherapy

Summary of Pertinent Conclusions

- Hypoxia-Inducible Factor
- The Unfolded Protein Response
- Radiosensitizing Hypoxic Cells
- Hypoxic Cytotoxins

Bibliography

oxygen homeostasis is dysregulated in several pathologic settings.

OHypoxia, or low oxygen conditions, exists in virtually all solid tumors. As tumor cells rapidly expand, their growth outpaces the ability of the existing vasculature to supply both nutrients and oxygen, resulting in tumor hypoxia. Cells experiencing hypoxia can cope with the low oxygen tension by either increasing delivery of oxygen or adapting to the low oxygen level.

HYPOXIA-INDUCIBLE FACTOR

Hypoxia-inducible factors (HIFs) are transcription factors that facilitate both oxygen delivery and adaptation to oxygen deprivation by regulating the expression of genes that are involved in many cellular processes including glucose uptake and metabolism, angiogenesis, erythropoiesis, cell proliferation, and apoptosis. HIFs bind to DNA as heterodimers composed of an oxygen-sensitive α -subunit and a constitutively expressed β -subunit, also known as the aryl hydrocarbon receptor nuclear translocator (ARNT). To date, three HIFs (HIF-1, HIF-2, and HIF-3) have been identified that regulate transcriptional programs in response to low oxygen levels.

HIF-1 was the first HIF family member to be characterized. Using DNA affinity purification, HIF-1 was identified as a hypoxic-induced factor that bound an 18-nucleotide fragment of the *erythropoietin* enhancer required for the hypoxic activation of *erythropoietin* in Hep3B cells. Structural analysis of the HIF-1 α protein revealed four distinct domains, including an oxygen-dependent degradation domain (ODD) that regulated HIF-1 α degradation by the ubiquitin-proteasome pathway. HIF-1 has been designated the global regulator of hypoxia-inducible gene expression because it is ubiquitously expressed and induces the expression of most hypoxia-inducible genes.

HIF-2 was the second HIF family member identified and shares approximately 50% sequence homology with HIF-1. HIF-2 α is also sensitive to changes in oxygenation and possesses an ODD. Although HIF-2 α heterodimerizes with ARNT like HIF-1 α , the expression of HIF-2 α is selectively inducible in endothelial cells, glial cells, pneumocytes type II, cardiomyocytes, epithelial cells of the kidney, interstitial cells of the pancreas and duodenum, and hepatocytes.

The third HIF family member, HIF-3 α , also possesses an ODD, can dimerize with ARNT and bind to hypoxia response elements *in vitro*. The role of HIF-3 in the hypoxic regulation of target gene expression *in vivo* is not well understood.

Oxygen-Dependent Regulation of Hypoxia-Inducible Factor

The transcriptional activity of HIF is regulated through changes in protein stability and through the recruitment of transactivation coactivators (Fig. 26.1). In the presence of oxygen, HIF- α is hydroxylated on two highly conserved proline residues: prolines 402 and 564, both found within the ODD. A family of 4-prolyl hydroxylases (PHDs), distinct from the structurally important collagen-4-prolyl hydroxylases, modifies these prolines. These enzymes catalyze a hydroxylation reaction, which uses molecular oxygen and 2-oxoglutarate as substrates and iron and ascorbate as cofactors. Hydroxylation of HIF- α is necessary for binding to the von Hippel-Lindau (VHL) tumor suppressor protein. Under normoxic conditions, HIF- α protein is rapidly turned over because of hydroxylation, binding to VHL, and destruction by the proteasome. Under hypoxic conditions, the 4-prolyl hydroxylases have reduced activity as oxygen is a requisite substrate of the hydroxylation reaction. Decreased hydroxylation of HIF- α allows it to escape recognition by VHL, resulting in protein stabilization. Once stabilized, HIF- α dimerizes with ARNT and binds to a core sequence of 5'-RCGTG-3' in the enhancer elements of target genes to initiate gene transcription.

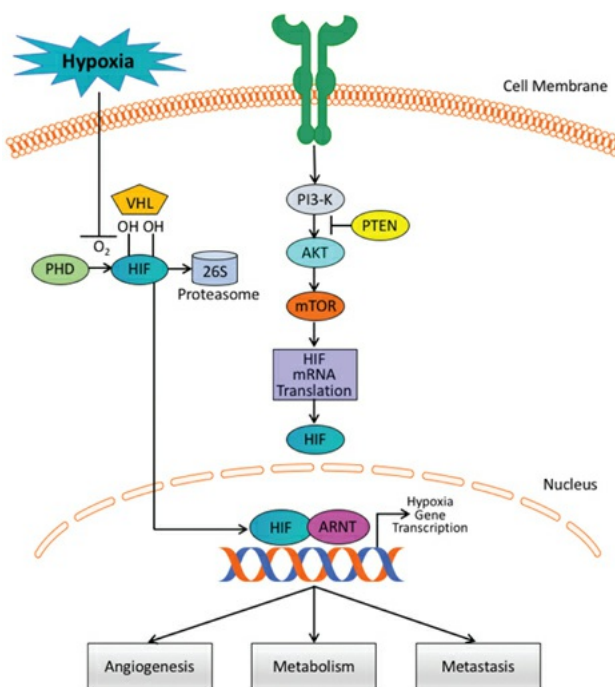


FIGURE 26.1 Critical steps in the regulation of the hypoxia-inducible transcription factor HIF- α . Under normoxic conditions, a group of enzymes called 4-prolyl hydroxylases (PHDs) adds hydroxyl groups (OH) to two proline residues of HIF- α . The hydroxylation of HIF- α by PHDs allows the VHL tumor suppressor gene to bind HIF- α and promote the addition of ubiquitin groups. The addition of ubiquitin groups targets HIF- α for degradation in the

proteasome. Under hypoxic conditions, the PHDs cannot hydroxylate HIF-1 α on proline residues owing to their requirement for molecular oxygen, and HIF-1 α becomes stabilized. It then binds with the HIF-1 β subunit in the nucleus and promotes transcription of target genes that regulate angiogenesis, erythropoiesis, tissue remodeling, and glycolysis. Most of the studies to date have shown that HIF is essential for tumor growth. HIF levels can also be increased under oxic conditions due to the dysregulated expression of the phosphoinositol-3-kinase (PI3-K)/Akt pathway or the loss of tumor suppressor genes such as PTEN. (This diagram is courtesy of Dr. Erinn Rankin, Stanford University.)

An additional layer of HIF regulation occurs at the level of recruitment of coactivators. A third hydroxylation of HIF- α takes place on the C-terminal transactivation domain on asparagine residue 803. This hydroxylation reaction is catalyzed by a separate asparaginyl hydroxylase, factor inhibiting HIF (FIH). Hydroxylation of this residue under normoxic conditions prevents interaction with p300, which, in turn, diminishes gene transcription. These modifications of HIF demonstrate the very stringent regulation of HIF under normoxic conditions.

Cancer Mutations that Activate Hypoxia-Inducible Factor

Tumor hypoxia is only one mechanism of HIF activation in tumors. HIF can also be activated under normoxic conditions through mutations in VHL, which plays a central role in regulating HIF protein stability. Inactivation of VHL results in HIF stabilization and increased target expression irrespective of oxygen concentrations. Germ line mutations in VHL result in a familial tumor syndrome that predisposes patients to the development of highly vascularized neoplasms including hemangioblastomas of the retina and central nervous system, renal cell carcinomas (RCCs), endocrine and exocrine pancreatic tumors, as well as pheochromocytomas. VHL is also found to be inactivated in most sporadic RCC and hemangioblastomas, reinforcing the important role of VHL tumor suppressor activity in HIF regulation and tumor progression. In addition to mutations in VHL, inactivation of the PTEN tumor suppressor gene can also result in phosphoinositol-3-kinase (PI3-K)/Akt increased HIF activity in tumors through the mammalian target of rapamycin (mTOR) signaling pathway.

Important Roles of Hypoxia-Inducible Factor in Tumors

The ability of tumor cells to adapt and survive their growth inhibitory microenvironment is accomplished in part by HIF activation. HIFs have been found to promote key steps in tumor progression, including angiogenesis, metabolism, and metastasis.

Tumor Angiogenesis

The formation of new blood vessels is critical for tumor expansion because the supply of oxygen and nutrients is reduced to tumor cells that are located more than 100 μm away from a blood vessel. Unlike normal tissues where there is a balance between proangiogenic and antiangiogenic factors, tumors tip the balance toward proangiogenic factors. Of all the proangiogenic factors induced by HIF, vascular endothelial growth factor-A (VEGF-A) appears to be the most critical because it has potent proangiogenic properties and is expressed in a large number of human tumors.

Tumor Metabolism

More than 70 years ago, cancer cells were found to shift glucose metabolism from an oxidative to glycolytic pathway. This shift has become known as the Warburg effect and is characterized by decreased mitochondrial respiration and increased lactate production even in the presence of oxygen. Numerous studies have established that HIF-1 regulates the expression of genes involved in glycolytic metabolism including glucose transporters, glycolytic enzymes, lactate production, and pyruvate metabolism (Fig. 26.2).

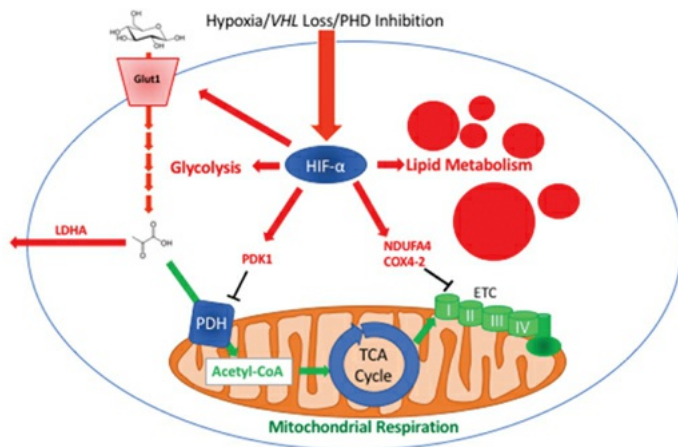


FIGURE 26.2 Hypoxia-inducible factor (HIF) is a pleiotropic regulator of metabolism in tumor cells exposed to hypoxia or which possess cancer mutations that activate HIF and generate a pro-glycolytic phenotype due to decreased mitochondrial respiration and increased lactate production. In fact, glucose transporter 1 (Glut1), all of the glycolytic genes, and lactate dehydrogenase A (LDHA) are HIF targets. The decreased mitochondrial respiration found in aerobic tumor cells is due to HIF inhibiting the conversion of acetyl coenzyme A (CoA) to pyruvate through increasing the expression of pyruvate dehydrogenase (PDH) kinase and increasing inhibitors of the electron transport chain (ETC). In addition to inhibiting mitochondrial function, elevated levels of HIF increase

lipid accumulation. The best example of this is in clear cell renal cancer, which is defined by lipid droplet accumulation. The role of lipid accumulation in tumor cells has not been clearly elucidated as of yet but may act as a radical scavenger. PDK1, pyruvate dehydrogenase kinase 1; TCA, tricarboxylic acid. (This diagram is courtesy of Dr. Edward LaGory, Stanford University.)

Tumor Metastasis

Metastasis is the cause of most human cancer deaths. It occurs in a series of distinct steps that include tumor cell invasion, intravasation, extravasation, and proliferation. HIF activation correlates with metastasis in multiple tumors and promotes metastasis through the transcriptional regulation of key factors such as metalloproteinases (MMPs), lysyl oxidase, and CXCR4 that govern cell adhesion, extracellular matrix formation, and cell migration.

Hypoxia-Inducible Factor and Radiotherapy

It has recently been proposed that HIF-1 plays an important role in determining tumor response to radiotherapy and tumor regrowth. Radiation results in a reoxygenation-dependent increase in HIF-1 activity by two distinct mechanisms. Tumor reoxygenation results in both HIF-1 stabilization and enhanced translation of HIF targets through the release of reactive oxygen species. The effects of HIF on tumor radiosensitivity are twofold. On one hand, HIF-1 stabilization promotes tumor vasculature radioresistance through the release of proangiogenic cytokines such as VEGF. Paradoxically, HIF-1 can also induce tumor radiosensitivity through the induction of apoptosis. Overall, HIF-1 stabilization promotes radioresistance and HIF-1-deficient tumors are more sensitive to radiation compared to wild-type tumors.

Studies by Ahn and Brown have identified an important role for bone marrow (BM)-derived cells in regenerating tumor vasculature following radiotherapy. Tumors grown in previously irradiated tissues exhibit decreased growth caused by insufficient neovascularization that results from radiation-induced injury to the host vasculature and connective tissue. They hypothesized that the vasculature of tumors grown in previously irradiated tissues is derived from cells from the BM. In particular, they demonstrated an important role for tissue MMP-9 and CD11b⁺ myelomonocytic cells from the BM to restore tumor growth in these preirradiated sites. HIF plays an important role in this recruitment of BM-derived cells by regulating several factors such as CXCR4 and SDF-1. Inhibition of HIF results in an inhibition of tumor vascularization. This study implicates vasculogenesis as an important target for adjunct therapy.

to radiotherapy.

UNFOLDED PROTEIN RESPONSE

Prolonged periods of hypoxia can activate non-HIF signaling pathways such as the unfolded protein response (UPR). The UPR is a cellular stress response that is induced by the accumulation of unfolded proteins in the endoplasmic reticulum (ER) in order to deal with the problems associated with the accumulation of misfolded proteins. Activation of the UPR results in a transient inhibition of protein translation to prevent further misfolded proteins from accumulating and through the induction of chaperone proteins that function in the ER to assist in folding, trafficking, and secretion of proteins. The UPR has been well characterized in yeast and, more recently, a greater understanding has been elucidated in humans. The ER stress sensor inositol-requiring enzyme 1 (IRE1) is found both in yeast and in humans. IRE1 becomes activated through homodimerization and trans-autophosphorylation. Biochemically, the endoribonuclease activity of IRE1 splices the pre-messenger ribonucleic acid (mRNA) of the X-box binding protein 1 (XBP1) transcription factor that results in translation of XBP1. The XBP1 transcription factor has many target genes involved in ER protein maturation. Koong et al. have shown that XBP1 could be inhibited by small molecules and that this inhibition resulted in a significant inhibition of tumor growth.

A second ER stress sensor is the protein kinase-like endoplasmic reticulum kinase (PERK). Activation of PERK prevents further translation of proteins. PERK activation occurs rapidly under severe hypoxia on the order of minutes, whereas under milder hypoxic conditions, PERK activation occurs on the order of hours. Through a combination of oligomerization and autophosphorylation, PERK becomes activated and inhibits translation by directly phosphorylating serine 51 of eIF2 α , a key initiator of the mRNA translation machinery. Koumenis and colleagues have shown that activation of PERK is important to survive under hypoxic conditions as PERK-deficient cells undergo apoptosis following hypoxia, resulting in a lower survival rate compared to genetically matched cells that have the PERK pathway intact. These PERK-deficient cells are less tumorigenic, likely in part because of higher apoptosis in the hypoxic regions of the tumor. Thus, one cellular response to chronic conditions of hypoxic stress is to limit the load of misfolded proteins.

RADIOSENSITIZING HYPOXIC CELLS

As described in [Chapter 21](#), a great deal of experimental work through the years had established that at least in transplanted tumors in animals, tumor control by x-rays frequently is limited by the foci of hypoxic cells that are intransigent to killing by x-rays, which may result in tumor regrowth. Among the methods suggested to overcome this problem are treatment in hyperbaric oxygen chambers and the introduction of high-linear energy transfer (LET) radiations, such as neutrons and heavy ions. Chemical sensitizers address the same problem. High-LET radiations are discussed in [Chapter 7](#). This chapter addresses hyperbaric oxygen, chemical radiosensitizers, and hypoxic cytotoxins.

Hyperbaric Oxygen

Following the identification of hypoxia as a possible source of tumor resistance, a major effort was made to solve the problem by the use of hyperbaric oxygen. Patients were sealed in chambers filled with pure oxygen raised to a pressure of three atmospheres. Churchill-Davidson at St. Thomas' Hospital in London pioneered this work, but it was taken up by researchers on both sides of the Atlantic. The clinical trials that were performed involved small numbers of patients and were difficult to interpret because unconventional fractionation schemes were used; that is, a few large fractions were used because of the time and effort involved in the technical procedures. Patient compliance was also a problem because of the feeling of claustrophobia from being sealed in a narrow tube. There was also the serious risk of fire because tissue is highly flammable in pure oxygen (as evidenced by the accident when the crew of a space capsule died in an oxygen fire on the ground), although in practice, an accident of this nature never happened during the treatment of several thousand patients. The largest multicenter trials performed by the Medical Research Council in the United Kingdom showed a significant benefit both in local control and in survival for patients with carcinoma of the uterine cervix and advanced head and neck cancer but not for patients with bladder cancer. The data generated a great deal of debate. An overview of the trials showed a 6.6% improvement in local control, with a suggestion, too, of an increase in late normal tissue damage. Hyperbaric oxygen fell into disuse partly because it is cumbersome and difficult in practice and partly because of the promise of drugs that would achieve the same result by simpler means.

The notion of improving tumor oxygenation by breathing 100% oxygen rather than air has been revived in recent years by experiments involving carbogen. If pure oxygen is breathed, it tends to lead to vasoconstriction, a closing down of some blood vessels, which, of course, defeats the object of the

exercise. This is avoided if 5% carbon dioxide is added to the oxygen, a mixture called *carbogen*. Breathing carbogen at atmospheric pressure, then, is a relatively simple attempt to overcome chronic hypoxia, that is, diffusion-limited hypoxia. The use of carbogen in combination with nicotinamide is described subsequently in this chapter.

Improving the Oxygen Supply to Tumors

A group at the Princess Margaret Hospital in Toronto showed convincingly that a blood transfusion prior to radiotherapy led to a significant improvement in local tumor control probability in patients with carcinoma of the uterine cervix. Several other studies have shown that hemoglobin levels can influence the success of radiation therapy.

Tumor oxygenation also can be improved by the use of artificial blood substances such as *perfluorocarbons*. Because smoking can decrease tumor oxygenation, it is clearly advisable for patients to give up smoking at least during radiotherapy.

Hypoxic Cell Radiosensitizers

Spurred largely by the efforts of radiation chemists (most notably, Adams), a search was under way in the early 1960s for compounds that mimic oxygen in their ability to sensitize biologic materials to the effects of x-rays. Instead of trying to “force” oxygen into tissues by the use of high-pressure tanks, the emphasis shifted to oxygen substitutes that diffuse into poorly vascularized areas of tumors and achieve the desired effect by chemical means. The vital difference between these drugs and oxygen, on which their success depends, is that the sensitizers are not rapidly metabolized by the cells in the tumor through which they diffuse. Because of this, they can penetrate further than oxygen and reach all of the hypoxic cells in the tumor, including those most remote from a blood supply. In the early 1960s, many simple chemical compounds were found to have the ability to sensitize hypoxic microorganisms. These studies were guided by the hypothesis, now known to be correct, that sensitizing efficiency is related directly to the electron affinity of the compounds.

Adams and his colleagues listed properties that would be essential for a clinically useful hypoxic cell sensitizer. First, it has to selectively sensitize hypoxic cells at a concentration that would result in acceptable toxicity to normal tissues. Second, it should be chemically stable and not subject to rapid metabolic breakdown. Third, it must be highly soluble in water or lipids and must be

capable of diffusing a considerable distance through a nonvascularized cell mass to reach the hypoxic cells, which in a tumor may be located as far as 200 μm from the nearest capillary. Fourth, it should be effective at the relatively low daily doses of a few grays used in conventional fractionated radiotherapy. The first candidate compound that appeared to satisfy these criteria was misonidazole.

Misonidazole

Figure 26.3 illustrates the numbering of the basic ring structure of the nitroimidazoles. The side chain determines position 1, and the position of the nitro group (NO_2) leads to the classification of the drug as a 2-nitroimidazole, 4-nitroimidazole, and so on. In general, 2-nitroimidazoles have a higher electron affinity than 5-nitroimidazoles, the class that includes metronidazole, which was briefly tried as a radiosensitizer. Misonidazole is a 2-nitroimidazole; its structure is shown in Figure 26.4.

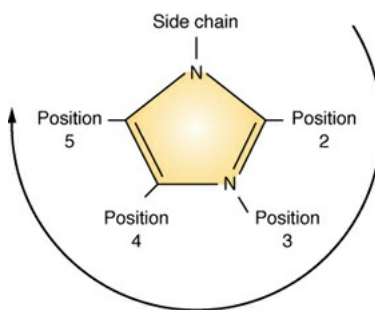


FIGURE 26.3 Method of numbering the basic ring structure of the nitroimidazoles. The side chain determines position 1. If the nitro group (NO_2) is in the second position, the drug is a 2-nitroimidazole. If the NO_2 group is in the fifth position, the drug is a 5-nitroimidazole. In general, 2-nitroimidazoles are more efficient radiosensitizers of hypoxic cells.

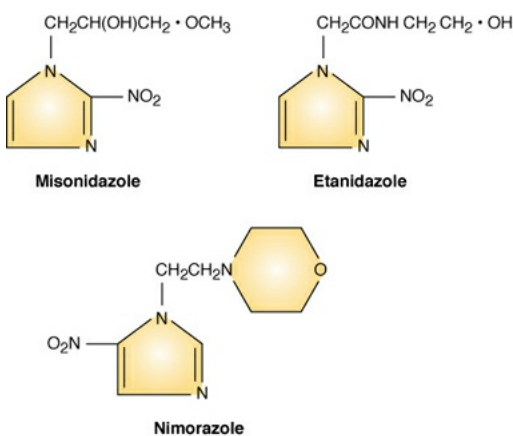


FIGURE 26.4 The structure of misonidazole, etanidazole, and nimorazole, the three compounds most widely used in clinical trials. Misonidazole and

etanidazole are 2-nitroimidazoles; nimorazole is a 5-nitroimidazole. Misonidazole and etanidazole are equally active as radiosensitizers, but etanidazole is less neurotoxic because it has a shorter half-life and is hydrophilic. Nimorazole is less active but very much less toxic than either misonidazole or etanidazole so that larger doses are tolerable.

Misonidazole produces appreciable sensitization with cells in culture (Fig. 26.5). Hypoxic cells in 10 mM of misonidazole have a radiosensitivity approaching that of aerated cells. Misonidazole also has a dramatic effect on tumors in experimental animals. This is illustrated in Figure 26.6, which shows the proportion of mouse mammary tumors controlled as a function of x-ray dose delivered in a single fraction. If x-rays are used alone, the dose required to control half of the tumors is 43.8 Gy. This falls to 24.1 Gy if the radiation is delivered 30 minutes after the administration of misonidazole (1 mg per gram body weight). This corresponds to an enhancement ratio of 1.8. Dramatic results, such as those shown in Figure 26.6 in which an enhancement ratio of 1.8 was obtained, are rather misleading; they represent single-dose treatments, in contrast to the multifraction regimens common in conventional radiotherapy. Most animal tumors reoxygenate to some extent between irradiations, so in a multifraction regimen, the enhancement ratio for a hypoxic cell sensitizer is usually much less than for a single-dose treatment.

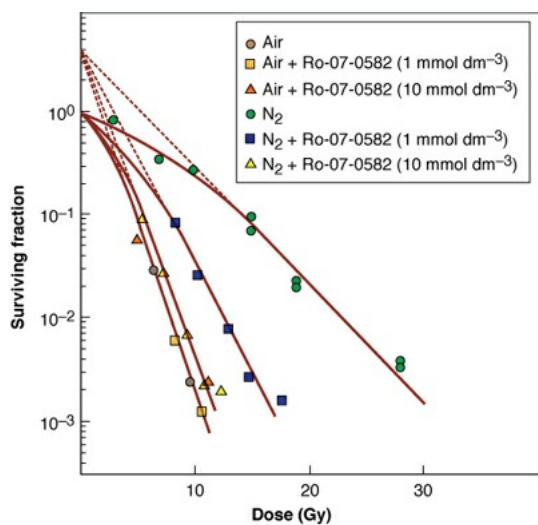


FIGURE 26.5 Survival data for aerated and hypoxic Chinese hamster cells x-irradiated in various concentrations of misonidazole (Ro-07-0582). At a concentration of 10 mM of this drug, the radiosensitivity of hypoxic cells approaches that of aerated cells. The response of aerated cells is not affected by the drug at all. (Adapted from Adams GE, Flockhart IR, Smithen CE, et al. Electron-affinic sensitization. VII. A correlation between structures, one-electron reduction potentials, and efficiencies of nitroimidazoles as hypoxic cell

radiosensitizers. *Radiat Res.* 1976;67:9–20, with permission.)

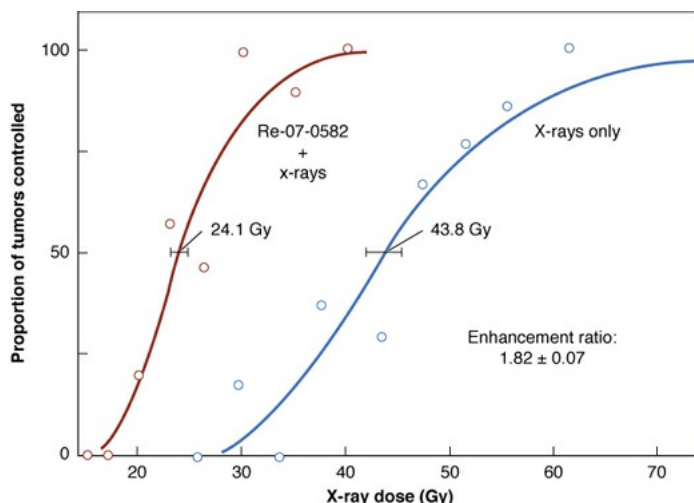


FIGURE 26.6 Proportion of mouse mammary tumors controlled at 150 days as a function of x-ray dose for a single treatment. The *right curve* represents x-rays only; the *left curve* refers to x-rays delivered after the administration of 1 mg per gram body weight of misonidazole (Ro-07-0582). The enhancement ratio is the ratio of x-ray doses in the absence or presence of the drug that results in the control of 50% of the tumors; it has a value of 1.8. (Adapted from Sheldon PW, Foster JL, Fowler JF. Radiosensitization of C3H mouse mammary tumours by a 2-nitroimidazole drug. *Br J Cancer*. 1974;30:560–565, with permission.)

After encouraging results in laboratory studies, misonidazole was introduced into a large number of clinical trials, involving many different types of human tumors, in Europe and the United States. In general, the results have been disappointing. Of the 20 or so randomized prospective controlled clinical trials performed in the United States by the Radiation Therapy Oncology Group (RTOG), none yielded a statistically significant advantage for misonidazole, although a number indicated a slight benefit. The only trial that shows a clear advantage for misonidazole was the head and neck cancer trial performed in Denmark, the largest single trial performed with the sensitizer. If patients of all categories are compared in this trial, the addition of misonidazole to the radiotherapy schedule conferred no significant advantage. If the patients are categorized into several subgroups, however, males with high hemoglobin levels and cancer of the pharynx showed a great benefit from the addition of misonidazole. Tumor control at 3 years was about double in the group receiving the drug compared with those patients receiving radiotherapy alone. This interesting result is shown in Figure 26.7. Other subgroups, including patients with cancer of the larynx, showed no benefit from the addition of the sensitizer.

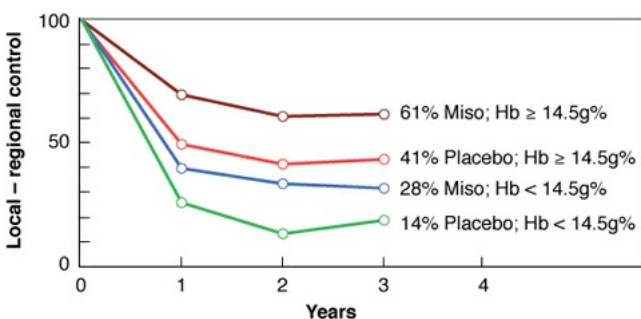


FIGURE 26.7 Some results from the Danish head and neck cancer trial of misonidazole. Misonidazole (Miso) produced a significant improvement of tumor control by radiotherapy only for males with tumors of the pharynx and depended on hemoglobin (Hb) status. (Data from Dr. Jens Overgaard.)

When misonidazole was used in the clinic, the dose-limiting toxicity was found to be peripheral neuropathy that progressed to central nervous system toxicity if drug administration was not stopped. This toxicity prevented use of the drug at adequate dose levels throughout multifraction regimens. The disappointing results obtained with misonidazole in the clinic must be attributed largely to the fact that doses were limited to inadequate levels because of this toxicity.

Etanidazole and Nimorazole

Spurred by the promise of misonidazole in the laboratory compared with its failure in the clinic, efforts were made to find a better drug. The compound chosen for the next series of clinical trials in the United States was etanidazole, a 2-nitroimidazole, the structure of which is also shown in Figure 26.4. This compound equals misonidazole as a sensitizer but is less toxic so that doses could be increased by a factor of 3. The lower neurotoxicity is a function of a shorter half-life *in vivo* plus a lower partition coefficient so that it penetrates poorly into nerve tissue and does not cross the blood–brain barrier. Controlled clinical trials by the RTOG in the United States and a multicenter consortium in Europe showed no benefit when etanidazole was added to conventional radiation therapy.

Nimorazole is a 5-nitroimidazole (structure also shown in Fig. 26.4); it is less effective as a radiosensitizer than either misonidazole or etanidazole, but it is much less toxic so that very large doses could be given. In a Danish head and neck cancer trial, this compound produced a significant improvement in both locoregional control and survival compared with radiotherapy alone in patients with supraglottic and pharyngeal carcinoma. It is surprising that nimorazole has not been used elsewhere.

The development of nitroimidazoles is illustrated by the following:

Metronidazole



Misonidazole: more active, toxic; benefit in subgroups



Etanidazole: less toxic, no benefit



Nimorazole: less active, much less toxic; benefit in head and neck cancer

Overgaard's Meta-analysis of Clinical Trials Addressing the Problem of Hypoxia

For more than three decades, an enormous effort has been expended in an attempt to overcome the perceived problem of hypoxia. Dozens of clinical trials have been performed, most of which have been inconclusive or have shown results with borderline significance. Overgaard and colleagues performed a meta-analysis in which the results of all the trials were combined and analyzed together. They identified 10,602 patients treated in 82 randomized clinical trials involving hyperbaric oxygen, chemical sensitizers, carbogen breathing, or blood transfusions. Tumor sites included the bladder, uterine cervix, central nervous system, head and neck, and lung.

Overall, local tumor control was improved by 4.6%, survival by 2.8%, and the complication rate increased by only 0.6%, which was not statistically significant. The largest number of trials involved head and neck tumors, which also showed the greatest benefit. It was also concluded that the problem of hypoxia may be marginal in most adenocarcinomas and most important in squamous cell carcinomas.

Nicotinamide and Carbogen Breathing

Hypoxic cell radiosensitizers, such as the nitroimidazoles, were designed primarily to overcome chronic hypoxia, that is, diffusion-limited hypoxia resulting from the inability of oxygen to diffuse farther than about $100\ \mu\text{m}$ through respiring tissue. As explained in [Chapter 6](#), however, there is another form of hypoxia known as *acute hypoxia*, in which local regions of hypoxia are caused by the intermittent closing down of blood vessels. Nicotinamide, a vitamin B₃ analogue, prevents these transient fluctuations in tumor blood flow

that lead to the development of acute hypoxia at least in mouse tumors.

A combination of nicotinamide to overcome acute hypoxia and carbogen breathing to overcome chronic hypoxia is the basis of the accelerated radiotherapy, carbogen, and nicotinamide (ARCON) trials under way at several European centers. The trials are also accelerated and hyperfractionated to avoid tumor proliferation and damage to late-responding normal tissues. Here, briefly, is a summary of the ARCON treatment:

Accelerated, to overcome proliferation

Hyperfractionated, to spare late-responding normal tissues

Carbogen breathing, to overcome chronic hypoxia

Nicotinamide, to overcome acute hypoxia

HYPOXIC CYTOTOXINS

An alternative approach to designing drugs that preferentially *radiosensitize* hypoxic cells is to develop drugs that selectively *kill* hypoxic cells. It was pointed out at an early stage that the greater reductive environment of tumors might be exploited by developing drugs that are reduced preferentially to cytotoxic species in the hypoxic regions of tumors. Five classes of agents in this category are known:

- 1.** Quinone antibiotics
- 2.** Nitroaromatic compounds
- 3.** Benzotriazine di-N-oxides
- 4.** Dinitrobenzamide modified nitrogen mustard
- 5.** 2-Nitroimidazole attached to dibromo isophosphoramide

Mitomycin C is an example of the first class and has been used as a chemotherapy agent, active against hypoxic cells, for many years. The aerated–hypoxic differential, however, is relatively small for these compounds. Examples of the second class of compounds include dual-function agents developed previously by Adams and his group at the Medical Research Council Radiobiology Unit in England. Normal tissue toxicity prevented the trial of these compounds in the clinic. The lead compound of the third class, tirapazamine, shows highly selective toxicity toward hypoxic cells both *in vitro* and *in vivo*. The third and fourth members of this class represent a new strategy of modifying a cytotoxic chemotherapy moiety to make it hypoxia activated.

Tirapazamine

Figure 26.8 shows survival curves for Chinese hamster cells treated with graded concentrations of tirapazamine. Note the oxic/hypoxic cytotoxicity ratio of about 100. The oxic/hypoxic cytotoxicity ratio is not as large (about 20) in cell lines of human origin, presumably reflecting a different spectrum, or different levels, of enzymes.

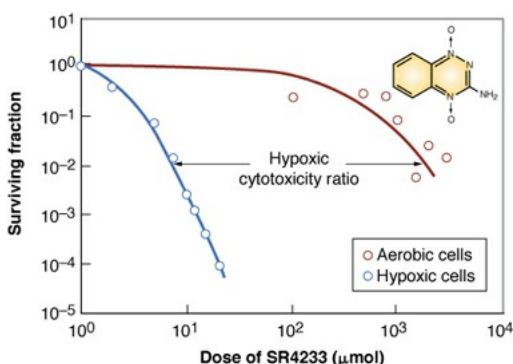


FIGURE 26.8 Dose-response curves for Chinese hamster cells exposed for 1.5 hours to graded concentrations of SR 4233 (tirapazamine) under aerated and hypoxic conditions. Cells deficient in oxygen are killed preferentially. The hypoxic cytotoxicity ratio (defined as the ratio of drug concentrations under aerated and hypoxic conditions required to produce the same cell survival) is variable between different cell lines. For the Chinese hamster cells shown, the ratio is about 100; for cells of human origin, the ratio is somewhat smaller, closer to 20. Tirapazamine is an organic nitroxide synthesized by Stanford Research International. Its structure is shown in the inset. (Courtesy of Dr. J. Martin Brown.)

The effect of x-rays plus tirapazamine is evidently much greater than additive (what would be expected from independent cell killing of the two agents). Experimentally, this was shown by treating tumors with x-rays alone, tirapazamine alone, or a combination of both agents (Fig. 26.9). The radiation schedule consisted of eight 2.5-Gy fractions designed to mimic, as far as possible, a clinical radiation therapy protocol. The combination of drug and radiation is highly effective, with the time sequence of drug before radiation slightly more effective than the reverse. In parallel experiments using the same x-ray and drug protocols, skin reactions were scored, and no radiosensitization or additive cytotoxicity was observed by the addition of the tirapazamine to the radiation treatments. This substantiates the tumor selectivity of the radiation enhancement.

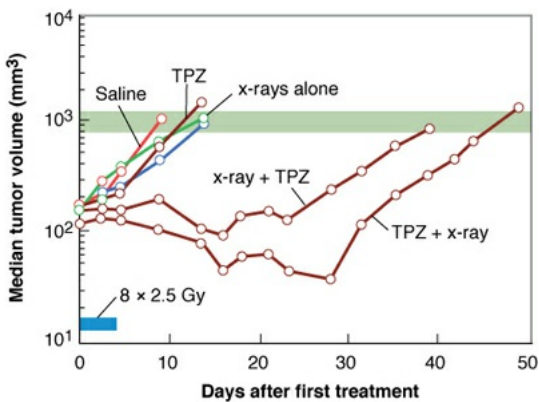


FIGURE 26.9 Tumor volume as a function of time after various treatments of an SCCVII transplantable mouse carcinoma. Tirapazamine (TPZ) or radiation alone had little effect. The combination of tirapazamine and x-rays caused significant growth delay, with radiation following the drug causing a slightly greater effect. (Adapted from Brown JM, Lemmon MJ. Tumor hypoxia can be exploited to preferentially sensitize tumors to fractionated irradiation. *Int J Radiat Oncol Biol Phys.* 1991;20:457–461, with permission.)

Similar results were obtained in four different mouse tumors that differed significantly in their hypoxic fractions. The observed interaction between x-rays and tirapazamine results largely from the selective hypoxic toxicity of the drug. This does not totally explain the observations, however. It appears that tirapazamine can act as an aerobic radiosensitizer of cells exposed to the drug under hypoxic conditions before or after the aerobic irradiation. This latter mechanism would be important for intermittent or acute hypoxia, that is, where a given region of a tumor cycles between aerated and hypoxic conditions.

Clinical Trials with Tirapazamine and New Bioreductive Drugs

Despite the extensive laboratory data *in vitro* and *in vivo* showing the greater-than-additive effect of the combination of x-rays with tirapazamine, little has been done clinically to combine tirapazamine with radiation therapy, except for one RTOG phase II trial. The reason may be the side effects of nausea and severe muscle cramping.

The situation adding tirapazamine to chemotherapy protocols is more advanced. One of the largest phase III trials in head and neck cancer has been completed comparing tirapazamine, cisplatin, and radiation to cisplatin and radiation for advanced squamous cell carcinoma of the head and neck (TROG 02.02, HeadSTART). In this trial, previously untreated stage III or IV squamous cell carcinomas of the head and neck were randomly assigned to receive 70 Gy

of radiotherapy concurrently with cisplatin alone or cisplatin in combination with tirapazamine. A total of 861 patients were enrolled from 89 sites worldwide. The 2-year survival analysis indicated that there was no significant differences in either failure-free survival, time to locoregional progression, or quality of life.

Various explanations have been brought forth to explain this result, including failure to stratify patients based on whether their tumor was hypoxic, poor radiotherapy at some sites, and insufficient levels of hypoxia in head and neck tumors. Hay, Wilson, and Denny in Auckland have developed a series of novel tricyclic triazine-di-N-oxides (TTOs) that are related to tirapazamine but are superior to it in regard to *in vivo* activity. Furthermore, because the same reductase that activates these TTOs is also responsible for activating the hypoxia marker EF5, the potential to combine the two in clinical trials and properly stratify patients could be achieved.

During the last 5 years, several other targeted therapeutics have entered clinical testing: PR-104, a novel hypoxia-activated DNA crosslinking agent, and TH-302, a hypoxia-activated dibromo isophosphoramide mustard. Unfortunately, clinical testing of these molecules has not demonstrated statistically significant efficacy to achieve FDA approval.

TARGETING TUMOR METABOLISM TO KILL HYPOXIC CELLS

Tumor cells exhibit altered metabolism that is highly glycolytic at the expense of oxidative phosphorylation. This shift from the normal oxidative metabolism gives tumor cells a growth advantage *in vivo*. Papandreou et al. have identified the HIF-1–pyruvate dehydrogenase kinase 1 (PDK1) axis as one of the major regulators responsible for this shift. HIF-1 induction of PDK1 results in phosphorylation and inactivation of pyruvate dehydrogenase (PDH), the first committed step for pyruvate entry into the mitochondria. Hypoxic tumors reduce mitochondrial function to conserve oxygen and, as a result, have a compensatory increase in glycolysis. Inhibition of PDK increases tumor hypoxia ([Fig. 26.10](#)).

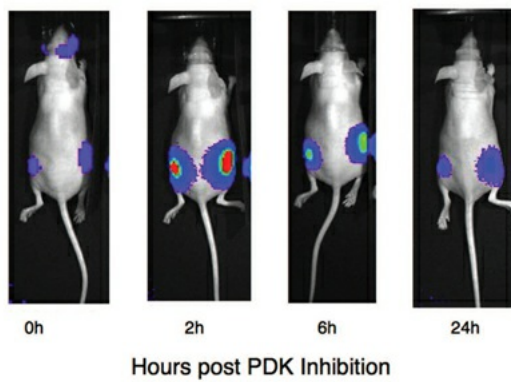


FIGURE 26.10 The effect of inhibiting PDK activity with dichloroacetate (DCA) on tumor hypoxia using a hypoxia-inducible factor (HIF)-driven luciferase reporter gene. Treatment with DCA induces a transient increase in hypoxia as detected by increased luciferase activity. (Adapted from Cairns RA, Papandreou I, Sutphin PD, et al. Metabolic targeting of hypoxia and HIF1 in solid tumors can enhance cytotoxic chemotherapy. *Proc Natl Acad Sci USA*. 2007;104:9445–9450, with permission.)

Dichloroacetate (DCA) was found more than 30 years ago to be a safe inhibitor of PDKs that has been used to treat patients with inborn errors of metabolism. DCA increases mitochondrial metabolism in these patients by inhibiting the activity of PDKs. DCA in preclinical tumor models increases mitochondrial function and “reprograms” tumor metabolism to be more oxidative like normal tissue. At the molecular level, DCA can inhibit PDH phosphorylation, reduce glucose uptake, increase mitochondrial function, and inhibit tumor growth in model tumors grown in nude mice. Figure 26.11 shows that DCA treatment can enhance the efficacy of hypoxic cytotoxins, such as tirapazamine in tumor xenografts, without causing depression of hematologic parameters. Clinical trials investigating the efficacy of DCA to alter tumor metabolism and increase tumor hypoxia have been pursued, using positron emission tomography imaging of radiolabeled fluorodeoxyglucose (^{18}F) (FDG) and EF5 to quantify metabolic changes in the tumor.

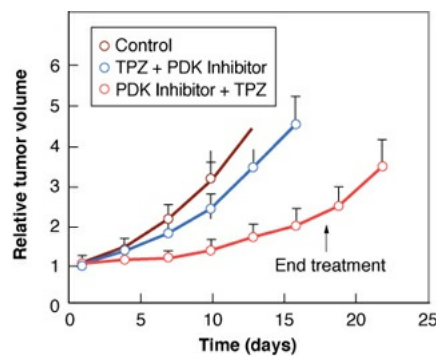


FIGURE 26.11 Demonstration of the increased efficacy of tirapazamine (TPZ) killing in transplanted tumors by inhibiting PDK. The graph shows a tumor growth delay experiment. The *key point* lies in the sequencing of PDK inhibition and tirapazamine. If tirapazamine is administered to the animal first, followed by a PDK inhibitor, little increase in cell killing beyond administering tirapazamine alone is observed. In contrast, if a PDK inhibitor is administered first and then tirapazamine is administered subsequently, a significant increase in tumor growth delay is observed because tumor hypoxia has been increased. (Adapted from Cairns RA, Papandreou I, Sutphin PD, et al. Metabolic targeting of hypoxia and HIF1 in solid tumors can enhance cytotoxic chemotherapy. *Proc Natl Acad Sci USA*. 2007;104:9445–9450, with permission.)

Targeting Tumor Metabolism to Enhance the Efficacy of Radiotherapy

If increasing mitochondrial activity in moderately hypoxic cells results in increased hypoxia through metabolizing oxygen, then decreasing mitochondrial activity in hypoxic cells should result in increased oxygen levels due to less metabolism of oxygen. In looking at the cartoon of the mitochondria in [Figure 26.2](#), the most straightforward means of reducing mitochondrial activity is by targeting the electron transport chain (ETC), which moves electrons from a donor such as NADH or QH₂ to a terminal electron acceptor (O₂) through a series of redox reactions. Specific inhibitors for each of the four complexes which make up the ETC exist and targeting the ETC with these inhibitors in hypoxic cells will result in decreased oxygen consumption and increased radiosensitivity. Thus, the mitochondria is a key target in altering the oxygen consumption of a tumor cell.

SUMMARY OF PERTINENT CONCLUSIONS

Hypoxia-Inducible Factor

At both the molecular and cellular levels, in physiologic and pathologic settings, oxygen homeostasis is controlled primarily through the function of a heterodimeric transcription factor, the HIF-1.

The HIF- α subunits are oxygen regulated through hydroxylation, binding to VHL and degradation in the proteasome.

Loss of certain tumor suppressor genes such as VHL and PTEN can cause HIF to become active under normoxic conditions.

HIF plays various critical roles in tumors, regulating metabolism, angiogenesis, and metastasis.

HIF can also influence the response of tumors to radiotherapy by increasing the resistance of the vasculature through the increased expression of proangiogenic factors and by promoting vasculogenesis through the recruitment of BM-derived cells.

The Unfolded Protein Response

The UPR responds to an accumulation of misfolded proteins by stopping protein translation through the activation of PERK and through the induction of XBP-1 and chaperone proteins that function in the ER to assist in folding, trafficking, and secretion of proteins.

Inhibition of PERK or XBP-1 activities result in decreased tumor growth.

Radiosensitizing Hypoxic Cells

Hypoxic cell radiosensitizers increase the radiosensitivity of hypoxic cells but not aerated cells. The differential effect on tumors is based on the presence of hypoxic cells in tumors but not in normal tissues.

Sensitization is a free radical process. The sensitizer mimics oxygen by “fixing” damage produced by free radicals.

Misonidazole, the first compound used widely, sensitizes cells in culture as well as in both animal and human tumors.

Doses of misonidazole that can be used clinically are limited to suboptimal levels by peripheral neuropathy. Only 1 of 30 or so clinical trials showed an advantage for misonidazole.

Etanidazole is less toxic than misonidazole, and 3 times larger doses are tolerated. However, clinical trials in Europe and the United States showed no advantage of combined radiotherapy and etanidazole over radiotherapy alone.

Nimorazole is less active as a radiosensitizer but so much less toxic than either misonidazole or etanidazole that much larger doses can be given. A benefit was shown for adding nimorazole to conventional radiotherapy for head and neck cancer (Danish head and neck cancer trial).

A meta-analysis of all 82 trials of hyperbaric oxygen and hypoxic cell radiosensitizers showed a 4.6% gain in local tumor control.

Hypoxic Cytotoxins

Bioreductive drugs are compounds that are reduced intracellularly to form cytotoxic agents.

Bioreduction is favored under hypoxia; this is a rationale for selectivity in solid tumors.

Mitomycin C is active against hypoxic cells in a wide range of tumors. The hypoxic/oxic cytotoxicity ratio is quite small.

Tirapazamine is an organic nitroxide. It shows a large hypoxic/oxic cytotoxicity ratio. The compound is active in many animal tumors and has undergone several clinical trials in conjunction with radiation or chemotherapy agents.

The future of targeting hypoxia lies in developing small molecules that target mitochondrial metabolism.

BIBLIOGRAPHY

- Adams GE. Chemical radiosensitization of hypoxic cells. *Br Med Bull.* 1973;29:48–53.
- Adams GE. Failla Memorial Lecture. Redox, radiation, and reductive bioactivation. *Radiat Res.* 1992;132:129–139.
- Adams GE. Hypoxic cell sensitizers for radiotherapy. In: Becker FF, ed. *Cancer.* Vol. 6. New York, NY: Plenum Press; 1977:181–223.
- Adams GE, Clarke ED, Flockhart IR, et al. Structure-activity relationships in the development of hypoxic cell radiosensitizers. I. Sensitization efficiency. *Int J Radiat Biol Relat Stud Phys Chem Med.* 1979;35:133–150.
- Adams GE, Clarke ED, Gray P, et al. Structure-activity relationships in the development of hypoxic cell radiosensitizers. II. Cytotoxicity and therapeutic ratio. *Int J Radiat Biol Relat Stud Phys Chem Med.* 1979;35:151–160.
- Adams GE, Dewey DL. Hydrated electrons and radiobiological sensitization. *Biochem Biophys Res Commun.* 1963;12:473–477.
- Adams GE, Flockhart IR, Smithen CE, et al. Electron-affinic sensitization. VII. A correlation between structures, one-electron reduction potentials, and efficiencies of nitroimidazoles as hypoxic cell radiosensitizers. *Radiat Res.* 1976;67:9–20.

- Adams GE, Stratford IJ, Bremner JC, et al. Nitroheterocyclic compounds as radiosensitizers and bioreductive drugs. *Radiother Oncol.* 1991;20:85–91.
- Ahn GO, Brown JM. Matrix metalloproteinase-9 is required for tumor vasculogenesis but not for angiogenesis: role of bone marrow-derived myelomonocytic cells. *Cancer Cell.* 2008;13:193–205.
- Ahn GO, Brown M. Targeting tumors with hypoxia-activated cytotoxins. *Front Biosci.* 2007;12:3483–3501.
- Alper T. The modification of damage caused by primary ionization of biological targets. *Radiat Res.* 1956;5:573–586.
- Ash DV, Peckham MJ, Steel GG. The quantitative response of human tumours to radiation and misonidazole. *Br J Cancer.* 1979;40:883–889.
- Bagshaw MA, Doggett RL, Smith KC, et al. Intra-arterial 5-bromodeoxyuridine and x-ray therapy. *Am J Roentgenol Radium Ther Nucl Med.* 1967;99:886–894.
- Baker MA, Zeman EM, Hirst VK, et al. Metabolism of SR 4233 by Chinese hamster ovary cells: basis for selective hypoxic cytotoxicity. *Cancer Res.* 1988;48:5947–5952.
- Bi M, Naczki C, Koritzinsky M, et al. ER stress-regulated translation increases tolerance to extreme hypoxia and promotes tumor growth. *EMBO J.* 2005;24:3470–3481.
- Brizel DM, Scully SP, Harrelson JM, et al. Tumor oxygenation predicts for the likelihood of distant metastases in human soft tissue sarcoma. *Cancer Res.* 1996;56:941–943.
- Brown JM. Evidence for acutely hypoxic cells in mouse tumours, and a possible mechanism of reoxygenation. *Br J Radiol.* 1979;52:650–656.
- Brown JM, Giaccia AJ. The unique physiology of solid tumors: opportunities (and problems) for cancer therapy. *Cancer Res.* 1998;58:1408–1416.
- Brown JM, Goffinet DR, Cleaver JE, et al. Preferential radiosensitization of mouse sarcoma relative to normal skin by chronic intra-arterial infusion of halogenated pyrimidine analogs. *J Natl Cancer Inst.* 1971;47:75–89.
- Brown JM, Lemmon MJ. Potentiation by the hypoxic cytotoxin SR 4233 of cell killing produced by fractionated irradiation of mouse tumors. *Cancer Res.* 1990;50:7745–7749.

- Brown JM, Lemmon MJ. Tumor hypoxia can be exploited to preferentially sensitize tumors to fractionated irradiation. *Int J Radiat Oncol Biol Phys.* 1991;20:457–461.
- Brown JM, Siim BG. Hypoxia-specific cytotoxins in cancer therapy. *Semin Radiat Oncol.* 1996;6:22–36.
- Bush RS. The significance of anemia in clinical radiation therapy. *Int J Radiat Oncol Biol Phys.* 1986;12:2047–2050.
- Cairns RA, Papandreou I, Sutphin PD, et al. Metabolic targeting of hypoxia and HIF1 in solid tumors can enhance cytotoxic chemotherapy. *Proc Natl Acad Sci USA.* 2007;104:9445–9450.
- Ceradini DJ, Kulkarni AR, Callaghan MJ, et al. Progenitor cell trafficking is regulated by hypoxic gradients through HIF-1 induction of SDF-1. *Nat Med.* 2004;10:858–864.
- Chan DA, Giaccia AJ. Hypoxia, gene expression, and metastasis. *Cancer Metastasis Rev.* 2007;26:333–339.
- Chan DA, Sutphin PD, Yen SE, et al. Coordinate regulation of the oxygen-dependent degradation domains of hypoxia-inducible factor 1 α. *Mol Cell Biol.* 2005;25:6415–6426.
- Chapman JD, Urtasun RC, Franko AJ, et al. The measurement of oxygenation status of individual tumors. In: *Prediction of Response in Radiation Therapy: The Physical and Biological Basis.* 1989;7:49–60.
- Chapman JD, Whitmore GF. Chemical modifiers of cancer treatment. *Int J Radiat Oncol Biol Phys.* 1984;10:1161–1813.
- Churchill-Davidson I. The oxygen effect in radiotherapy: historical review. *Front Radiat Ther Oncol.* 1968;1:1–15.
- Cole S, Stratford IJ, Bowler J, et al. Oral (po) dosing with RSU 1069 or RB 6145 maintains their potency as hypoxic cell radiosensitizers and cytotoxins but reduces systemic toxicity compared with parenteral (ip) administration in mice. *Int J Radiat Oncol Biol Phys.* 1991;21:387–395.
- Coleman CN. Hypoxia in tumors: a paradigm for the approach to biochemical and physiologic heterogeneity. *J Natl Cancer Inst.* 1988;80:310–317.
- Coleman CN. Hypoxic cell radiosensitizers: expectations and progress in drug development. *Int J Radiat Oncol Biol Phys.* 1985;11:323–329.

- Dische S. Chemical sensitizers for hypoxic cells: a decade of experience in clinical radiotherapy. *Radiother Oncol.* 1985;3:97–115.
- Dische S, Gray AJ, Zanelli GD. Clinical testing of the radiosensitizer Ro-07-0582. II. Radiosensitization of normal and hypoxic skin. *Clin Radiol.* 1976;27:159–166.
- Duan JX, Jiao H, Kaizerman J, et al. Potent and highly selective hypoxia-activated achiral phosphoramidate mustards as anticancer drugs. *J Med Chem.* 2008;51:2412–2420.
- Epstein AC, Gleadle JM, McNeill LA, et al. C. elegans EGL-9 and mammalian homologs define a family of dioxygenases that regulate HIF by prolyl hydroxylation. *Cell.* 2001;107:43–54.
- Erler JT, Bennewith KL, Nicolau M, et al. Lysyl oxidase is essential for hypoxia-induced metastasis. *Nature.* 2006; 440:1222–1226.
- Foster JL, Conroy PJ, Searle AJ, et al. Metronidazole (Flagyl): characterization as a cytotoxic drug specific for hypoxic tumour cells. *Br J Cancer.* 1976;33:485–490.
- Gatenby RA, Kessler HB, Rosenblum JS, et al. Oxygen distribution in squamous cell carcinoma metastases and its relationship to outcome of radiation therapy. *Int J Radiat Oncol Biol Phys.* 1988;14:831–838.
- Grau C, Khalil AA, Nordsmark M, et al. The relationship between carbon monoxide breathing, tumour oxygenation and local tumour control in the C3H mammary carcinoma in vivo. *Br J Cancer.* 1994;69:50–57.
- Gray AJ, Dische S, Adams GE, et al. Clinical testing of the radiosensitiser Ro-07-0582. I. Dose tolerance, serum and tumour concentrations. *Clin Radiol.* 1976;27:151–157.
- Hall EJ, Astor M, Geard C, et al. Cytotoxicity of Ro-07-0582; enhancement by hyperthermia and protection by cysteamine. *Br J Cancer.* 1977;35:809–815.
- Hall EJ, Roizin-Towle L. Hypoxic sensitizers: radiobiological studies at the cellular level. *Radiology.* 1975;117:453–457.
- Hay MP, Hicks KO, Pchalek K, et al. Tricyclic [1,2,4]triazine 1,4-dioxides as hypoxia selective cytotoxins. *J Med Chem.* 2008;51:6853–6865.
- Hicks KO, Myint H, Patterson AV, et al. Oxygen dependence and extravascular transport of hypoxia-activated prodrugs: comparison of the dinitrobenzamide mustard PR-104A and tirapazamine. *Int J Radiat Oncol Biol Phys.*

2007;69:560–571.

Hirst DG. Anemia: a problem or an opportunity in radiotherapy? *Int J Radiat Oncol Biol Phys.* 1986;12:2009–2017.

Hockel M, Schlenger K, Aral B, et al. Association between tumor hypoxia and malignant progression in advanced cancer of the uterine cervix. *Cancer Res.* 1996;56:4509–4515.

Horsman MR. Nicotinamide and other benzamide analogs as agents for overcoming hypoxic cell radiation resistance in tumors. *Acta Oncol.* 1995;34:571–587.

Horsman MR. Nicotinamide and the hypoxia problem. *Radiother Oncol.* 1991;22:79–80.

Horsman MR, Chaplin DJ, Overgaard J. Combination of nicotinamide and hyperthermia to eliminate radioresistant chronically and acutely hypoxic tumor cells. *Cancer Res.* 1990;50:7430–7436.

Horwich A, Holliday SB, Deacon JM, et al. A toxicity and pharmacokinetic study in man of the hypoxic-cell radiosensitizer RSU-1069. *Br J Radiol.* 1986;59:1238–1240.

Ivan M, Kondo K, Yang H, et al. HIF α targeted for VHL-mediated destruction by proline hydroxylation: implications for O₂ sensing. *Science.* 2001;292:464–468.

Jaakkola P, Mole DR, Tian YM, et al. Targeting of HIF- α to the von Hippel-Lindau ubiquitylation complex by O₂-regulated prolyl hydroxylation. *Science.* 2001;292:468–472.

Jameson MB, Rischin D, Pegram M, et al. A phase I trial of PR-104, a nitrogen mustard prodrug activated by both hypoxia and aldo-keto reductase 1C3, in patients with solid tumors. *Cancer Chemother Pharmacol.* 2010;65:791–801.

Jenkins TC, Naylor MA, O'Neill P, et al. Synthesis and evaluation of alpha-[(2-haloethyl)amino]methyl]-2-nitro-1H-imidazole-1-ethanols as prodrugs of alpha-[(1-aziridinyl)methyl]-2-nitro-1H-imidazole-1-ethanol (RSU-1069) and its analogues which are radiosensitizers and bioreductively activated cytotoxins. *J Med Chem.* 1990;33:2603–2610.

Jette DC, Wiebe LI, Flanagan RJ, et al. Iodoazomycin riboside (1-[5'-iodo-5'-deoxyribofuranosyl]-2-nitroimidazole): a hypoxic cell marker. I. Synthesis and in vitro characterization. *Radiat Res.* 1986;105:169–179.

- Jiang BH, Rue E, Wang GL, et al. Dimerization, DNA binding, and transactivation properties of hypoxia-inducible factor 1. *J Biol Chem.* 1996;271:17771–17778.
- Jiang BH, Zheng JZ, Leung SW, et al. Transactivation and inhibitory domains of hypoxia-inducible factor 1 α . Modulation of transcriptional activity by oxygen tension. *J Biol Chem.* 1997;272:19253–19260.
- Jiang D, Niwa M, Koong AC. Targeting the IRE1 α -XBP1 branch of the unfolded protein response in human diseases. *Semin Cancer Biol.* 2015;33:48–56.
- Kinsella T, Mitchell J, Russo A, et al. Continuous intravenous infusions of bromodeoxyuridine as a clinical radiosensitizer. *J Clin Oncol.* 1984;2:1144–1150.
- Kinsella T, Mitchell J, Russo A, et al. The use of halogenated thymidine analogs as clinical radiosensitizers: rationale, current status, and future prospects for non-hypoxic cell sensitizers. *Int J Radiat Oncol Biol Phys.* 1984;10:1399–1406.
- Kinsella T, Russo A, Mitchell J, et al. A phase I study of intravenous iododeoxyuridine as a clinical radiosensitizer. *Int J Radiat Oncol Biol Phys.* 1985;11:1941–1946.
- Kjellen E, Joiner MC, Collier JM, et al. A therapeutic benefit from combining normobaric carbogen or oxygen with nicotinamide in fractionated X-ray treatments. *Radiother Oncol.* 1991;22:81–91.
- Koumenis C, Naczki C, Koritzinsky M, et al. Regulation of protein synthesis by hypoxia via activation of the endoplasmic reticulum kinase PERK and phosphorylation of the translation initiation factor eIF2 α . *Mol Cell Biol.* 2002;22:7405–7416.
- Krishnamachary B, Zagzag D, Nagasawa H, et al. Hypoxia-inducible factor-1-dependent repression of E-cadherin in von Hippel-Lindau tumor suppressor-null renal cell carcinoma mediated by TCF3, ZFHX1A, and ZFHX1B. *Cancer Res.* 2006;66:2725–2731.
- Laderoute K, Wardman P, Rauth AM. Molecular mechanisms for the hypoxia-dependent activation of 3-amino-1,2,4-benzotriazine-1,4-dioxide (SR 4233). *Biochem Pharmacol.* 1988;37:1487–1495.
- Lando D, Peet DJ, Gorman JJ, et al. FIH-1 is an asparaginyl hydroxylase enzyme that regulates the transcriptional activity of hypoxia-inducible factor. *Genes*

Dev. 2002;16:1466–1471.

- Lando D, Peet DJ, Whelan DA, et al. Asparagine hydroxylation of the HIF transactivation domain a hypoxic switch. *Science*. 2002;295:858–861.
- Lin AJ, Cosby LA, Shansky CW, et al. Potential bioreductive alkylating agents. 1. Benzoquinone derivatives. *J Med Chem*. 1972;15:1247–1252.
- Masson N, Willam C, Maxwell PH, et al. Independent function of two destruction domains in hypoxia-inducible factor- α chains activated by prolyl hydroxylation. *EMBO J*. 2001;20:5197–5206.
- Mitchell JB, Kinsella TJ, Russo A, et al. Radiosensitization of hematopoietic precursor cells (CFUc) in glioblastoma patients receiving intermittent intravenous infusions of bromodeoxyuridine (BUDR). *Int J Radiat Oncol Biol Phys*. 1983;9:457–463.
- Mitchell JB, Morstyn G, Russo A, et al. Differing sensitivity to fluorescent light in Chinese hamster cells containing equally incorporated quantities of BUDR versus IUdR. *Int J Radiat Oncol Biol Phys*. 1984;10:1447–1451.
- Mitchell JB, Russo A, Kinsella T, et al. The use of non-hypoxic cell sensitizers in radiobiology and radiotherapy. *Int J Radiat Oncol Biol Phys*. 1986;12:1513–1518.
- Moeller BJ, Cao Y, Li CY, et al. Radiation activates HIF-1 to regulate vascular radiosensitivity in tumors: role of reoxygenation, free radicals, and stress granules. *Cancer Cell*. 2004;5:429–441.
- Moeller BJ, Dreher MR, Rabbani ZN, et al. Pleiotropic effects of HIF-1 blockade on tumor radiosensitivity. *Cancer Cell*. 2005;8:99–110.
- Mohindra JK, Rauth A. Increased cell killing by metronidazole and nitrofurazone of hypoxic compared to aerobic mammalian cells. *Cancer Res*. 1976;36:930–936.
- Morstyn G, Hsu SM, Kinsella T, et al. Bromodeoxyuridine in tumors and chromosomes detected with a monoclonal antibody. *J Clin Invest*. 1983;72:1844–1850.
- Nordsmark M, Overgaard M, Overgaard J. Pretreatment oxygenation predicts radiation response in advanced squamous cell carcinoma of the head and neck. *Radiother Oncol*. 1996;41:31–39.
- Ohh M, Park CW, Ivan M, et al. Ubiquitination of hypoxia-inducible factor requires direct binding to the beta-domain of the von Hippel-Lindau protein.

Nat Cell Biol. 2000;2:423–427.

Overgaard J. Clinical evaluation of nitroimidazoles as modifiers of hypoxia in solid tumors. *Oncol Res.* 1994;6:509–518.

Overgaard J, Horsman MR. Modification of hypoxia-induced radioresistance in tumors by the use of oxygen and sensitizers. *Semin Radiat Oncol.* 1996;6:10–21.

Overgaard J, Sand Hansen H, Andersen AP, et al. Misonidazole combined with split-course radiotherapy in the treatment of invasive carcinoma of larynx and pharynx: report from the DAHANCA 2 study. *Int J Radiat Oncol Biol Phys.* 1989;16:1065–1068.

Overgaard J, Sand Hansen H, Lindeløv B, et al. Nimorazole as a hypoxic radiosensitizer in the treatment of supraglottic larynx and pharynx carcinoma. First report from the Danish Head and Neck Cancer Study (DAHANCA) Protocol 5-85. *Radiother Oncol.* 1991;20:143–149.

Overgaard J, Sand Hansen H, Overgaard M, et al. The Danish Head and Neck Cancer Study Group (DAHANCA) randomized trials with hypoxic radiosensitizers in carcinoma of the larynx and pharynx. In: Dewey WC, Eddington M, Fry RJM, et al., eds. *Radiation Research: A Twentieth-Century Perspective*. Vol. II. New York, NY: Academic Press; 1992:573–577.

Papandreou I, Cairns RA, Fontana L, et al. HIF-1 mediates adaptation to hypoxia by actively downregulating mitochondrial oxygen consumption. *Cell Metab.* 2006;3:187–197.

Parliament MB, Chapman JD, Urtasun RC, et al. Non-invasive assessment of human tumour hypoxia with ^{123}I -iodoazomycin arabinoside: preliminary report of a clinical study. *Br J Cancer.* 1992;65:90–95.

Patterson AV, Ferry DM, Edmunds SJ, et al. Mechanism of action and preclinical antitumor activity of the novel hypoxia-activated DNA cross-linking agent PR-104. *Clin Cancer Res.* 2007;13:3922–3932.

Rankin EB, Giaccia AJ. The role of hypoxia-inducible factors in tumorigenesis. *Cell Death Differ.* 2008;15:678–685.

Rasey JS, Koh WJ, Grierson JR, et al. Radiolabelled fluoromisonidazole as an imaging agent for tumor hypoxia. *Int J Radiat Oncol Biol Phys.* 1989;17:985–991.

Rischin D, Hicks RJ, Fisher R, et al. Prognostic significance of [^{18}F]-

- misonidazole positron emission tomography-detected tumor hypoxia in patients with advanced head and neck cancer randomly assigned to chemoradiation with or without tirapazamine: a substudy of Trans-Tasman Radiation Oncology Group Study 98.02. *J Clin Oncol.* 2006;24:2098–2104.
- Rischin D, Peters LJ, O’Sullivan B, et al. Tirapazamine, cisplatin, and radiation versus cisplatin and radiation for advanced squamous cell carcinoma of the head and neck (TROG 02.02, HeadSTART): a phase III trial of the Trans-Tasman Radiation Oncology Group. *J Clin Oncol.* 2010;28:2989–2995.
- Roizin-Towle LA, Hall EJ, Flynn M, et al. Enhanced cytotoxicity of melphalan by prolonged exposure to nitroimidazoles: the role of endogenous thiols. *Int J Radiat Oncol Biol Phys.* 1982;8:757–760.
- Romero-Ramirez L, Cao H, Nelson D, et al. XBP1 is essential for survival under hypoxic conditions and is required for tumor growth. *Cancer Res.* 2004;64:5943–5947.
- Rose CM, Millar JL, Peacock JH, et al. Differential enhancement of melphalan cytotoxicity in tumour and normal tissue by misonidazole. In: Brady LW, ed. *Radiation Sensitizers*. New York, NY: Masson; 1980:250–257.
- Sheldon PW, Foster JL, Fowler JF. Radiosensitization of C3H mouse mammary tumours by a 2-nitroimidazole drug. *Br J Cancer.* 1974;30:560–565.
- Staller P, Sulitkova J, Lisztwan J, et al. Chemokine receptor CXCR4 downregulated by von Hippel-Lindau tumour suppressor pVHL. *Nature.* 2003;425:307–311.
- Stratford IJ, Adams GE. Effect of hyperthermia on differential cytotoxicity of a hypoxic cell radiosensitizer, Ro-07-0582, on mammalian cells in vitro. *Br J Cancer.* 1977;35:307–313.
- Stratford IJ, Stephens MA. The differential hypoxic cytotoxicity of bioreductive agents determined in vitro by the MTT assay. *Int J Radiat Oncol Biol Phys.* 1989;16:973–976.
- Sutherland RM. Selective chemotherapy of noncycling cells in an in vitro tumor model. *Cancer Res.* 1974;34:3501–3503.
- Thomlinson RH, Dische S, Gray AJ, et al. Clinical testing of the radiosensitizer Ro-07-0582. *III. Response of tumours.* *Clin Radiol.* 1976;27:167–174.
- Urtasun RC, Band P, Chapman JD, et al. Clinical phase I study of the hypoxic cell radiosensitizer RO-07-0582, a 2-nitroimidazole derivative. *Radiology.*

- 1977;122:801–804.
- Urtasun RC, Band P, Chapman JD, et al. Radiation and high-dose metronidazole in supratentorial glioblastomas. *N Engl J Med*. 1976;294:1364–1367.
- Urtasun RC, Chapman JD, Raleigh JA, et al. Binding of 3H-misonidazole to solid human tumors as a measure of tumor hypoxia. *Int J Radiat Oncol Biol Phys*. 1986;12:1263–1267.
- Wong TW, Whitmore GF, Gulyas S. Studies on the toxicity and radiosensitizing ability of misonidazole under conditions of prolonged incubation. *Radiat Res*. 1978;75:541–555.
- Wouters BG, Koritzinsky M. Hypoxia signalling through mTOR and the unfolded protein response in cancer. *Nat Rev Cancer*. 2008;8:851–864.
- Zeman EM, Brown JM, Lemmon MJ, et al. SR-4233: a new bioreductive agent with high selective toxicity for hypoxic mammalian cells. *Int J Radiat Oncol Biol Phys*. 1986;12:1239–1242.
- Zeman EM, Hirst VK, Lemmon MJ, et al. Enhancement of radiation-induced tumor cell killing by the hypoxic cell toxin SR 4233. *Radiother Oncol*. 1988;12:209–218.

chapter 27

Chemotherapeutic Agents from the Perspective of the Radiation Biologist

Biologic Basis of Chemotherapy

Classes of Agents and Their Mode of Action

- Alkylating Agents
- Antibiotics
- Antimetabolites
- Nucleoside Analogues
- Vinca Alkaloids
- Taxanes
- Hormone Targeted Therapies
- Topoisomerase Inhibitors
- Targeted Therapy
- Immune Checkpoint Therapies

Dose–Response Relationships

- Sublethal and Potentially Lethal Damage Repair
- The Oxygen Effect and Chemotherapeutic Agents
- Resistance to Chemotherapy and Hypoxic Cytotoxins
- Drug Resistance and Cancer Stem Cells
- Comparison of Chemotherapeutic Agents with Radiation
- Adjunct Use of Chemotherapeutic Agents with Radiation
- Assays for Sensitivity of Individual Tumors
- Second Malignancies
- Summary of Pertinent Conclusions
- Bibliography

Alice: There's no use trying—one can't believe impossible things.

The Queen: I dare say you haven't had much practice. Why, sometimes I've believed as many as six impossible things before breakfast.

—*Alice in Wonderland*
(Lewis Carroll)

This chapter is included after much thought and some equivocation. It was written in response to numerous requests that chemotherapeutic agents be compared and contrasted with radiation from the perspective of the experimental biologist. Many of the techniques and concepts used in chemotherapy were developed initially by radiation biologists, including quantitative tumor assay systems, the concept of cell cycle, sensitivity changes through the cell cycle, and, particularly, population kinetics. The term **growth fraction**, for example, was coined by a radiation biologist but never assumed the importance in radiotherapy that it has in chemotherapy.

The study of chemotherapeutic agents in the laboratory, as well as in the clinic, is vastly more complicated than the study of ionizing radiation. For example, **dose** is more difficult to define or to measure, and time of drug exposure is a critical parameter. Variations in sensitivity through the cell cycle are more dramatic for chemicals than for radiation, assuming essentially an all-or-nothing effect for some agents; there are many more factors involving the microenvironment that can influence cellular response.

The term **chemotherapy** was coined by Paul Erhlich around the turn of the 20th century to describe the use of chemicals of known composition for the treatment of parasites. Erhlich synthesized an organic arsenic compound that was effective against trypanosome infections and rabbit syphilis. This was the first synthetic chemical effective in the treatment of parasitic disease and was rather optimistically named *salvarsan*, which roughly translates to “the savior of mankind.” The next milestone was the discovery and clinical use of penicillin in the early years of World War II. Alkylating agents had been developed as military weapons by both belligerents in World War I, but it was an explosion in Naples harbor and the exposure of seamen to these agents during World War II that led to the observation that these agents cause marrow and lymphoid hypoplasia. As a result, they were first tested in humans with Hodgkin disease in 1943 at Yale University.

It has long been known beyond doubt that a single chemotherapeutic drug,

used in the appropriate schedule, can cure patients with certain rapidly proliferating cancers. The initial demonstration of this was the use of methotrexate to cure patients with choriocarcinoma and, later, the use of cyclophosphamide for Burkitt lymphoma.

The next major step forward was the use of combination chemotherapy in the treatment of acute lymphocytic leukemia in the early 1960s and, subsequently, in the treatment of Hodgkin disease, diffuse histiocytic lymphoma, and testicular cancer in the mid-1970s. These trials verified that multiple non-cross-resistant drugs with different dose-limiting normal tissue toxicities could be used effectively in combination to cure tumors that were not curable with a single agent. The principle of combination therapy was then extended to combined modality treatment, in which chemotherapy was used in conjunction with surgery or radiotherapy, or both, to cure tumors such as pediatric sarcomas.

Today, various antineoplastic agents are used routinely in clinical oncology. Drug-induced cures are claimed for choriocarcinoma, acute lymphocytic leukemia of childhood, other childhood tumors, Hodgkin disease, certain non-Hodgkin lymphomas, and some germ cell tumors of the testes. Other evidence suggests that chemotherapeutic agents given in an “adjuvant” setting for clinically inapparent micrometastatic disease may prolong disease-free survival and possibly effect cure of breast cancer and osteogenic sarcoma.

There are about 13 types of cancer for which cures are claimed by chemotherapy; this accounts for about 10% of all cancers. For comparison, the proportion of cancer patients cured by radiation therapy often is claimed to be about 12.5%. This comes from the so-called $1/2 \times 1/2 \times 1/2$ rule; that is, one-half of all cancer patients receive radiation therapy, one-half of those treated are treated with intent to cure, and one-half of those treated definitively are cured.

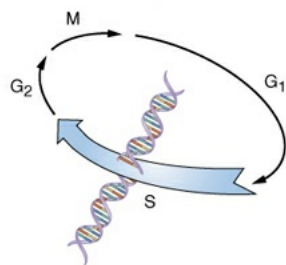
The bad public image of chemotherapy relates in large part from the toxicity to normal tissue resulting from multidrug protocols used to induce remissions and achieve tumor cure. “The dose makes the poison” was the advice of Paracelsus, the 16th-century German-Swiss physician and alchemist who established the role of chemistry in medicine. In other words, anything powerful enough to help also has the power to harm. In the past, the lack of tumor-specific agents carried the burden of damage to self-renewing normal tissues, such as the gut and bone marrow. There is hope that the situation is improving with the development of targeted therapies and the new concept of synthetic lethality (both will be discussed later in this chapter).

BIOLOGIC BASIS OF CHEMOTHERAPY

Most cytotoxic anticancer drugs work by affecting DNA synthesis or function, and they usually do not kill resting cells unless such cells divide soon after exposure to the drug. Consequently, the effectiveness of anticancer drugs is limited by the growth fraction of the tumor—that is, by the fraction of cells in active cycle. Rapidly growing neoplasia with a short cell cycle, a large proportion of cells in S phase, and therefore, a large growth fraction are more responsive to chemotherapy than large tumor masses in which the growth fraction is small. There is a strong tendency for growth fraction to decrease as tumor size increases at least in experimental animal tumors.

Agents that are mainly effective during a particular phase of the cell cycle, such as S phase or M phase, are said to be **cell cycle specific** or **phase specific**. Those whose action is independent of the position of the cell in the cycle are said to be **cell cycle nonspecific** or **phase nonspecific**. Figure 27.1 illustrates two contrasting cell cycle–specific drugs. *Cis*-platinum compounds produce interstrand crosslinks and thus inhibit DNA synthesis; this occurs in S phase. Taxanes bind to microtubules and, by enhancing their stability and preventing disassembly, adversely affect their function. They act as mitotic inhibitors, blocking cells in the G₂/M phase of the cell cycle.

Cis-platinum compounds produce interstrand crosslinks and thus inhibit DNA synthesis. This occurs during the S phase of the cell cycle.



Paclitaxel binds to microtubules and, by enhancing their stability and preventing disassembly, adversely affects their function. It acts as a mitotic inhibitor, blocking cells in the G₂/M phase of the cycle.

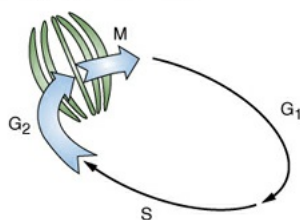


FIGURE 27.1 Two contrasting chemotherapy agents that are both cell cycle specific but produce their effects at quite different phases. **A:** *Cis*-platinum compounds produce DNA interstrand crosslinks that inhibit DNA synthesis; this

occurs in the S phase. **B:** Taxanes bind to microtubules and, by enhancing their stability and preventing disassembly, adversely affect their function. Taxanes act as mitotic inhibitors, blocking cells in the G₂/M phase of the cycle and, if the concentration is sufficient, killing them in this phase.

Agents that are most effective against cells in S phase are relatively ineffective against cell populations that turn over slowly and have large proportions of dormant cells. On the other hand, the action of alkylating agents and other drugs interacting primarily with macromolecular DNA is largely independent of the phase of the cell cycle, and they may be effective against tumors with relatively low proliferative activity.

The other side of the coin is that the selective normal tissue toxicity of anticancer drugs is reflected in cytotoxic effects on stem cells of the intestinal epithelium or hematopoietic stem cells, which have high growth fractions.

Although many clinical oncologists claim that their thinking has been influenced by research on tumor growth kinetics, it is hard to point to clear advances in treatment that may be attributed to anything more than inspired clinical experimentation. The study of growth kinetics in human tumors is not being ardently pursued at the present time.

CLASSES OF AGENTS AND THEIR MODE OF ACTION

Many of the classical chemotherapeutic agents fall into one of three classes: alkylating agents, antibiotics, or antimetabolites. However, many of the newer and most widely used agents do not fall into any of these classes. This includes the platinum compounds, procarbazine, the vinca alkaloids, the taxanes, and the newest of all, the topoisomerase inhibitors and “targeted therapy” agents that target a specific pathway that may be elevated or vulnerable in some tumor cells.

An attempt to summarize the classification of chemotherapeutic drugs is presented in [Table 27.1](#). A few of the most commonly used agents are described briefly, with emphasis on their characteristics and mechanism of action and comments on the extent to which they interact with radiation. A thorough discussion of their clinical usefulness is outside the scope of this book.

Table 27.1 Chemotherapeutic Agents

COMPOUND	CLASS	DISEASES FOR WHICH DRUGS ARE	TARGETED PATHWAY/
----------	-------	------------------------------	-------------------

CHEMOTHERAPEUTIC AGENT	USEFUL (INDICATIONS)	UNIQUE/MAJOR TOXICITY	(MECHANISMS OF ACTION)
ALKYLATING AGENTS Busulfan (Myleran)—BSF	Regular-dose therapy in Myelosuppression chronic myelogenous pulmonary toxicity interstrand crosslinking leukemia (CML) (FDA approved especially with total body irradiation and bone marrow transplant). High-dose therapy in high doses for bone marrow transplant.	DNA alkylating agent; interstrand crosslinking.	DNA alkylating agent; interstrand crosslinking.
Carboplatin (Paraplatin)—Carbo, CBDCA	FDA approved for Myelosuppression, ovarian cancer and used especially extensively in testicular thrombocytopenia, squamous cell cancer; cancers of the head, neck, and cervix; and lung cancer.	is DNA via association with the molecule, leading to strand breakage and replication.	Produces interstrand crosslinking.
Carmustine (BiCNU)—BCNU, Bis-chloronitrosourea	FDA approved for brain tumors, multiple myeloma, Hodgkin disease, and lymphoma. which is slow in onset and cumulative, is dose limiting. Interstitial lung disease, including fibrosis, is rare but can occur with any dose. Weak synergy with radiation therapy (RT).	Penetrates cell cycle crosslinking.	Cell cycle crosslinking.
Chlorambucil (Leukeran)	FDA approved for Myelosuppression is chronic lymphocytic leukemia (CLL) and low-grade lymphomas.	Cell cycle crosslinking may be cumulative.	Cell cycle crosslinking.

	Also used for Waldenström macroglobulinemia, multiple myeloma, hairy cell leukemia, and rarely in some solid tumors.	
Cyclophosphamide (Cytoxan, Neosar)—CTX, CPM, Cy (prototypical alkylator)	FDA approved for many malignancies and used dose limiting, with crosslinking being activated in living cells. Commonly used for most significant. breast carcinoma, non-Hodgkin lymphoma, common with doses ovarian carcinoma, and more than 2 g/m ² . testicular cancer.	Myelosuppression is Cell cycle
Dacarbazine (DTIC-Dome)—DTIC, DIC, imidazole carboxamide	FDA approved for the treatment of malignant melanoma and Hodgkin disease and also used for severe without adult sarcomas and aggressive neuroblastoma. Strong synergy with RT.	Myelosuppression is Methylates g preferentially; vomiting are nonspecific. nausea and vomiting are nonspecific. disease and also used for severe without adult sarcomas and aggressive antiemetic therapy. Strong synergy with RT.
Ifosfamide (Ifex)	FDA approved for the treatment of recurrent hemorrhagic cystitis, alkylating agent for many other tumor types, including adult and childhood cancer, and ovarian cancer. can largely be prevented by coadministration of the uroprotective agent mesna.	Myelosuppression, Nonspecific treatment of recurrent hemorrhagic cystitis, alkylating agent for many other tumor types, including adult and childhood cancer, and ovarian cancer. can largely be prevented by coadministration of the uroprotective agent mesna.

Lomustine CCNU	(CeeNU)—FDA approved for Myelosuppression, primary brain tumors especially and Hodgkin disease. thrombocytopenia, is barrier. Also used in melanoma, dose limiting and multiple myeloma, other tends to be lymphomas, and breast cumulative. cancer.	Cell cycle Penetrates
Mechlorethamine (Mustargen)—nitrogen mustard, HN2	FDA approved for This drug is a Cell cycle various hematologic powerful vesicant, so alkylating age malignancies and solid optimal extravasation tumors, but generally precautions and rapid used less in the last infusion are a must. decade. Still used for Myelosuppression is Hodgkin disease and expected and also topically for cutaneous often dose limiting. T-cell lymphoma. Secondary leukemia.	
Melphalan (Alkeran)—L- Used primarily for Myelosuppression is Cell cycle PAM, L-phenylalanine multiple myeloma but expected and is dose alkylating age mustard, L-sarcolysin also FDA approved for limiting. Recovery ovarian carcinoma. can be prolonged, Could also be useful in and effects can be high-dose cumulative. chemotherapy/transplant Secondary leukemia. settings and in regional perfusion of extremities for melanoma and sarcoma.		
Oxaliplatin (Eloxatin)	FDA approved for Neurotoxicity, in the Cell cycle metastatic colorectal form of a transient intrastrand an cancer in combination neuropathy with each crosslinks with 5- dose and a persistent platinum asso	

	<p>fluorouracil/leucovorin. cumulative typical in the molecular It has been used as a sensory single agent in this polyneuropathy, is disease and is being very common and studied in other dose limiting. malignancies.</p>
Procarbazine (Matulane)— N-methylhydrazine	<p>FDA approved for Myelosuppression is Cell cycle Hodgkin disease and expected and dose Penetrates might also be useful in limiting, but anemia barrier. non-Hodgkin is uncommon. Hives lymphoma, multiple and photosensitivity myeloma, brain tumors, sometimes occur. melanoma, and lung Dietary restrictions. cancer.</p>
Temozolomide (Temozar)	<p>FDA approved for Myelosuppression is Penetrates treatment of recurrent expected and dose barrier. Oral high-grade limiting. Enhances agent. Prodrug astrocytomas. Used radiation response of commonly for other MGMT deficient gliomas and also for glioblastomas. metastatic melanoma.</p>
ATYPICAL ALKYLATING AGENTS Cisplatin (Platinol)— cDDP, DDP, <i>cis</i> -platinum, <i>cis</i> -diamminedichloroplatinum (II)	<p>Used for almost every Nephrotoxicity is Produces interstrand class of solid tumor and dose limiting for an interstrand cross-linking agent. lymphoma. FDA individual dose, DNA via association with the and ovarian cancers and neurotoxicity, molecule, leading to transitional cell especially painful strand break carcinomas. peripheral replication. neuropathy, is dose limiting for cumulative doses. Cumulative ototoxicity is also common. Intermediate synergy</p>

		with RT.
ANTIBIOTICS	FDA approved for germ Pulmonary toxicity, Causes DNA cell tumors, Hodgkin including reversible directly in disease, and squamous and irreversible neoplastic cell cell cancers. Used off- fibrosis, is dose label for melanoma, limiting. Strong ovarian cancer, and synergy with RT. Kaposi sarcoma. Also used as a sclerosing agent for malignant pleural or pericardial effusions.	
Dactinomycin (Cosmegen)—Actinomycin D, ACT-D	FDA approved for Wilms tumor, Ewing moderate vesicant. complexing with sarcoma, Myelosuppression is prevents rhabdomyosarcoma, dose limiting. RNA polymer uterine carcinoma, germ cell tumors, and skin erythema, sarcoma botryoides, and acneiform lesions, also used for other and sarcomas, melanoma, hyperpigmentation acute myeloid leukemia, are common. Strong ovarian cancer, and synergy with RT. trophoblastic neoplasms.	
Doxorubicin (Adriamycin, Rubex)—Adria, Hydroxydaunorubicin	FDA approved for various cancers and potent vesicant, and used for many more. extravasation Most commonly used precautions are a for breast carcinoma, must. adult sarcomas, Myelosuppression is pediatric solid tumors, universal and usually Hodgkin disease, non-dose limiting with Hodgkin lymphomas, each individual cycle. and ovarian cancer. Cardiotoxicity is common and can be	

	<p>dose limiting, although usually subclinical. Chronic, cumulative cardiomyopathy is expected when total dose exceeds 400–500 mg/m². Strong synergy with RT. Recall skin reactions that correspond to prior RT treatment fields may develop and can be severe. Concurrent RT or initiation of RT within 2 weeks of administration of doxorubicin should be avoided.</p>
Mitomycin C (Mutamycin)	<p>FDA approved for Mitomycin C is a Inhibits DNA synthesis. adenocarcinomas of the vesicant; stomach, pancreas, and extravasation anus. Also used precautions are a commonly in breast must. cancer and lung cancer. Myelosuppression is expected and is dose limiting, with a white blood cell nadir at 4 weeks and full recovery at 6–7 weeks. Strong synergy with RT.</p>
ANTIMETABOLITES 5-Fluorouracil (Adrucil, Efudex)—5-FU	<p>FDA approved for GI toxicities, Inhibitor of colon, rectum, gastric, primarily mucositis synthase; pancreas, and breast for bolus injection cycle dependent carcinomas and used for and diarrhea for a wide range of other prolonged infusions,</p>

	<p>neoplasms in are dose limiting. combination regimens. Rare patients with Used for intrahepatic dihydropyrimidine arterial infusion for liver dehydrogenase metastases from deficiency have gastrointestinal (GI) excessive GI toxicity. tumors and also used Dermatitis and other topically for various cutaneous toxicities, cutaneous neoplasms including hand-foot and disorders. syndrome, are common. Intermediate synergy with RT.</p>	
Capecitabine (Xeloda) FDA approved for Myelosuppression (antimetabolite prodrug)	<p>metastatic breast cancer and palmar-plantar and metastatic colorectal erythrodysesthesia cancer. Used also in are dose limiting. head and neck Diarrhea, fatigue, squamous cell cancer. stomatitis, and hyperbilirubinemia are uncommon. Intermediate synergy with RT.</p>	Prodrug of 5-f
Hydroxyurea (Hydrea)— Hydroxycarbamide	<p>FDA approved for Myelosuppression is Inhibitor of r CML; commonly used common and dose reductase, w for other limiting. Other nucleotides myeloproliferative toxicities include deoxyribose disorders and also used rash, headache, fever, DNA synthesis occasionally for and hyperuricemia. dependent. metastatic melanoma, Nausea and vomiting blood-brain b refractory ovarian are uncommon. Liver carcinoma, and toxicity and serious squamous cell neurologic toxicity carcinoma of the cervix are rare. Weak and head and neck. synergy with RT.</p>	r

Methotrexate (Mexate, FDA approved for a Myelosuppression is Interferes with Folex, others)—MTX, wide spectrum of expected and is synthesis by Amethopterin	malignant and usually dose limiting. dihydrofolate nonmalignant diseases. Renal toxicity is cell cycle Most often used for uncommon and Penetrates acute leukemias, usually reversible but barrier at high lymphomas, breast can be severe. doses. cancer, bladder cancer, Encephalopathy is squamous cell cancers, rare with moderate to and sarcomas.	low-dose therapy but is more common with high doses, intrathecal administration, or concomitant CNS radiation. It can be severe and permanent. Drug should be administered prior to rather than concurrently or following brain RT when feasible to lessen risk of leukoencephalopathy. Weak synergy with RT.
---	---	---

NUCLEOSIDE ANALOGUES

Cytarabine (Cytosar-U)—AraC, cytosine arabinoside

Acute myelogenous Myelosuppression, Incorporated leukemia (AML), acute often severe and during replication prolonged, is dose to strand break lymphoma (ALL), and limiting. Neurologic phase specific non-Hodgkin lymphoma toxicity, mostly blood-brain barrier lymphoma. Intrathecal central with ataxia being predominant, is use in acute leukemia. common and usually mild, but it is dose dependent and could leave permanent dysfunction. It is more common with

		intrathecal administration.
Fludarabine (Fludara)—FAMP	FDA approved for the Neurotoxicity, treatment of CLL. Also including cortical DNA polymerase used for low-grade blindness, confusion, partially cell cycle lymphomas and for somnolence, coma, AML. and demyelinating lesions, is dose limiting, but the lower doses conventionally used rarely produce these side effects.	Purine analog
Gemcitabine (Gemzar)	FDA approved for Myelosuppression, advanced pancreatic including anemia, is exhibits S phase adenocarcinoma, non-mild but dose cytotoxicity. In small cell lung cancer limiting. Strong synthesis. (NSCLC), synergy with RT metastatic breast cancer; even at low doses of extensively used in drug. bladder cancer also.	A nucleoside
VINCA ALKALOIDS Vinblastine (Velban, Velsar, others)—VLB, vincristine	FDA approved for Vinblastine is a soft Inhibitor of multiple hematologic tissue vesicant, polymerization and solid neoplasms. requiring mitosis; G ₂ phase. Most often used for extravasation Hodgkin disease, non-precautions during Hodgkin lymphoma, administration. germ cell tumors, and Myelosuppression, breast cancer. especially leukopenia, is expected and dose limiting.	of
Vincristine (Oncovin, FDA approved for Vincristine is a	Inhibitor of	c

Vincasar)—lurocristine, VCR	Hodgkin disease and vesicant and should polymerization other lymphomas, acute be administered with mitosis; G ₂ ph leukemias, extravasation rhabdomyosarcoma, precautions. neuroblastoma, and Neurotoxicity is dose Wilms tumor. Used for limiting in the form many other neoplasms of peripheral neuropathy, which is as well. related to total cumulative dose.
Vinorelbine (Navelbine)—5'-noranhydrovinblastine, NVB	FDA approved for the Vinorelbine is a mild Inhibitor treatment of relapsed vesicant, requiring polymerization metastatic breast cancer extravasation mitosis; G ₂ ph and for NSCLC as a precautions. single agent or Myelosuppression, combined with a mostly leukopenia, is platinating agent. expected and dose limiting. Neurotoxicity in the form of neuropathy is less common and milder than that seen with vincristine. Tumor pain during administration has been reported.
TAXANES Docetaxel (Taxotere)	FDA approved for Myelosuppression is Inhibits the metastatic breast cancer universal and dose apparatus by and first- and second- limiting. Alopecia is tubulin polycline NSCLC. Clinical also universal. Edema to death of mi experience increasing in and fluid ovarian cancer and other accumulation, epithelial neoplasms. including pleural effusions and ascites, are common and can be dose limiting. Fluid accumulation is partially preventable

	<p>with corticosteroid treatment before and after each cycle of docetaxel. Mild sensory or sensorimotor neuropathy is common.</p>
Paclitaxel (Taxol, Onxol)	<p>FDA approved for Paclitaxel is an Inhibits depolarization of tubulin in ovarian cancer and for vesicant breast cancer in both the extravasated metastatic and adjuvant subcutaneous tissue. setting. Used also in Myelosuppression, lung cancer, head and predominantly neck cancers, and neutropenia, is bladder cancer. is expected and is dose limiting. Shorter infusions of the same dose produce less neutropenia. Mucositis is with very common, particularly with longer infusions. Peripheral neuropathy is common, usually mild, and increases with cumulative dose. Acute neuromyopathy is also common and occurs for several days after each dose. Hypersensitivity reactions to paclitaxel, including urticaria, wheezing, chest pain, dyspnea, and hypotension, are</p>

		common but are reduced in frequency and severity by premedication with corticosteroids and H1 and H2 histamine receptor blockers (recommended regimen is dexamethasone 20 mg PO 12 and 6 h prior to paclitaxel and diphenhydramine 50 mg. and cimetidine 300 mg IV 30 min prior to paclitaxel). Weak synergy with RT.
Nab-paclitaxel (Abraxane)	FDA approved for Myelosuppression, treatment of metastatic predominantly breast, lung, and neutropenia. Other pancreatic cancer. toxicities similar to paclitaxel.	An injectable of paclitaxel.
MISCELLANEOUS AGENTS Enzymes I-Asparaginase (Elspar)—Colaspase	FDA approved for ALL; Hypersensitivity can Catalyzes the also used in AML, late- be life-threatening, amino acid stage CML, CLL, and requiring anaphylaxis which is an es non-Hodgkin lymphomas.	precautions and a 2- acid required unit test dose. proliferating Coagulopathy is aspartic acid. common and requires monitoring. Lethargy, somnolence, fatigue, depression, and confusion are seen, as are pancreatitis and fever.

<p>CORTICOSTEROIDS</p> <p>Prednisone (Deltasone, others)</p>	<p>FDA approved for Toxicity is mostly in Same as various malignant and the form of occurring ones nonmalignant constitutional conditions. Used in symptoms, including oncology for lymphoid mood changes malignancies, for (depressive, anxious, palliative care, and for or euphoric), management of side insomnia, effects/toxicities.</p> <p>indigestion, enhanced appetite, weight gain, acne, and cushingoid features. Other side effects may be more serious but are less common.</p> <p>Hyperglycemia and increased stomach acid predisposing to ulceration occur acutely, whereas osteopenia, cataracts, skin atrophy, and adrenal insufficiency occur with prolonged use.</p>
<p>STEROIDAL PROGESTATIONAL AGENTS</p> <p>Megestrol acetate (Megace) —megestrol</p>	<p>FDA approved for Toxicities are similar Little known treatment of breast and to those of other targets. endometrial carcinoma. progestins as noted Also used for renal cell previously. They carcinoma and for include menstrual appetite stimulation in changes, hot flashes, HIV disease and cancer edema, weight gain, patients. fatigue, acne, hirsutism, anxiety, depression, sleep disturbance, and headache. Urinary frequency can also occur. Nausea, vomiting, diarrhea,</p>

		skin rash or allergy, jaundice, and thrombophlebitis are uncommon.
CYTOPROTECTANTS Amifostine (Ethyol)—WR-2721, Ethiofos	FDA approved for Transient pretreatment with hypotension is dose cisplatin. Useful as a limiting. Nausea, bone marrow, kidney, vomiting, and nerve somnolence are cytoprotectant. Useful common. with other alkylators. Also FDA approved as a radiation protectant to reduce xerostomia.	Free radical sc
HORMONE TARGETED THERAPIES Luteinizing hormone-releasing hormone (LHRH) Goserelin acetate (Zoladex)	FDA approved for Toxicity is advanced prostate Endocrine cancer and used also in effects are metastatic breast cancer. prominent include hot flashes, tissues, include diminished libido, cancer and b impotence, gynecomastia, amenorrhea, and breakthrough vaginal bleeding.	mild. Inhibits pitu side axis function most steroid and withdrawal fro include hot flashes, tissues, include diminished libido, cancer and b impotence, gynecomastia, amenorrhea, and breakthrough vaginal bleeding.
Leuprolide acetate (Lupron) —leuprorelin acetate	FDA approved for the treatment of hormone-tolerated, but dependent advanced effects can used for breast cancer including and endometriosis.	Usually well Gonadotropin side hormone age dependent advanced effects can affect shuts down systems, release of g endocrine resulting in (hot flashes, decrease in impotence, estrogens and gynecomastia, breast and growth tenderness, hormone-depe diminished libido, neoplasms.

		amenorrhea, atrophic vaginitis, and increased cholesterol).
Bicalutamide (Casodex)	FDA approved for stage Constitutional D2 prostate cancer, in combination with an LHRH agonist agent.	Androgen receptor antagonist through binding. including hot flashes, decreased libido, depression, weight gain, edema, gynecomastia, early disease-site pain (flare reaction), and constipation.
Tamoxifen (Nolvadex)	FDA approved for the Tamoxifen is usually Cytostatic treatment of breast cancer, generally in postmenopausal patients or those with estrogen receptor-positive tumors. The same dose has been approved for breast cancer in high-risk patients. Higher doses are used for melanoma and pancreatic cancer.	very well tolerated. estrogen-dependent nondependent symptoms are most common. dose limiting. Hot flashes, sweating, mood changes, prevention of weight gain or loss, stomach upset are most common. are used for
Anastrozole (Arimidex)	As adjuvant therapy for breast cancer and for postmenopausal women with breast carcinoma who have progressed on Thrombophlebitis has	The drug is very well tolerated. Asthenia, selectively. treatment of headache, and hot flashes occur in less than 15% of women. Thrombophlebitis has

	tamoxifen therapy.	been reported.	
Abiraterone (Zytiga)	FDA approved for the treatment of metastatic castration-resistant prostate cancer.	Well tolerated. High binding affinity in patients with liver disease, cardiovascular disease, hypokalaemia, and adrenocorticoid insufficiency.	Should be used with AR. Precaution in patients translocation of AR to nucleus and DNA.
Enzalutamide (Xtandi)	FDA approved for the treatment of castration-resistant prostate cancer.	Gynecomastia, pain, CYP17A1 induced fatigue, hot flashes, androgen resistance; sexual dysfunction; inhibitor. 1% of patients develop seizures through inhibition of GABA _A receptors.	
TOPOISOMERASE INHIBITORS	Etoposide (Vespid)—VP-16, epipodophyllotoxin; also available as etoposide phosphate (Etopophos)	FDA approved for germ cell tumors and small cell lung cancer is universal and dose limiting. Nausea and vomiting are common with PO high-dose therapy in the administration setting for rare when the drug is breast cancer, ovarian given IV. Stomatitis and diarrhea are rare with normal doses but common with high doses. Secondary AML has been reported after etoposide.	Myelosuppression, primarily leukopenia, Topoisomerase inhibitors are common with PO high-dose therapy in the administration setting for rare when the drug is breast cancer, ovarian given IV. Stomatitis and diarrhea are rare with normal doses but common with high doses. Secondary AML has been reported after etoposide.

Irinotecan (Camptosar)—CPT-11	<p>Irinotecan is FDA approved for refractory primarily or recurrent metastatic neutropenia, is colon cancer, and it has common and dose limiting. Diarrhea is malignancies, including also common and can lung cancer, ovarian cancer, and lymphoma.</p>	Partly cell cycle Topoisomeras
TARGETED THERAPIES Bevacizumab (Avastin)	<p>FDA approved for first- and second-line of angiogenesis. GI factor. Causes treatment of metastatic perforation is the existing tumor; for colorectal cancer; for major life-threatening side effect. Treatment vessels more carboplatin and can also inhibit supplying paclitaxel; for wound healing and chemotherapy unresectable, locally may prevent surgical new tumor vessels more advanced, recurrent, or incisions to close, metastatic non-small cell lung cancer; and for instances. Bleeding combination with interferon alpha for nose, and vagina. metastatic renal cell cancer. Common side effects are nosebleeds, high blood pressure, headache, and inflammation.</p>	
Cetuximab (Erbitux)	<p>Colorectal cancer, lung cancer, head and neck cancer. Self-limiting sterile, non-suppurative dimerization acne-like skin rash is kinase inhibitor common. Resolves which inhibits with cessation of kinase pathway drug. Patients transduction. exhibiting a grade 2 rash or above have better survival. Strong synergy with</p>	

	RT.	
Crizotinib (Xalkori)	FDA approved for About 50% of Oral selective EML4-ALK fusion or patients develop triphosphate ROS1-positive non- nausea, vomiting, competitive small cell lung cancers. vision, or diarrhea. inhibitor of A More severe and ROS1. toxicities such as hepatotoxicity, interstitial lung disease, QT interval prolongation, or vision loss occur in 2%–5% of patients.	
Erlotinib (Tarceva)	FDA approved for non- Acne-like rash occurs Erlotinib binds small cell lung cancer in majority of irreversible and pancreatic cancer. treatment patients. ATP-binding site Diarrhea, fatigue, hair loss.	
Imatinib mesylate (Gleevec)	FDA approved for There is no definite Specific receptor treatment of CML in the dose-limiting toxicity kinase inhibitor imatinib. selectively in the accelerated phase, and Myelosuppression is tyrosine kinase in blast crisis. It is also significant in CML the bcr-abl, approved for treatment but mild in GI platelet-derived growth factor (PDGF) of recurrent inoperable stromal tumors. Hepatotoxicity is common but usually tumors. mild. Liver function tests should be monitored closely during therapy. Fluid retention is common but usually mild, as are nausea, vomiting, and diarrhea. Rash	

		and fever are uncommon.
Poly adenosine diphosphate-ribose polymerase inhibitors	FDA approved BRCA-mutation-positive ovarian and prostate cancer. Clinical trials for metastatic BRCA-mutation-positive breast cancer, triple negative breast cancer, and non-small cell lung cancer.	Dizziness, nausea, vomiting, diarrhea, and lymphopenia, leading to anemia, and fatigue. In replication generation of strand break possessing mutations can PARP inhibition DNA double-strand break by recombination
Rituximab (Rituxan)	FDA approved for relapsed or refractory low-grade or follicular, CD20-positive, lymphomas. Directed against common surface antigens on B-cell administration, even with premedication with acetaminophen and diphenhydramine. Other infusion-related symptoms include nausea, vomiting, flushing, urticaria, angioedema, hypotension, dyspnea, bronchospasm, fatigue, headache, rhinitis, and pain at disease sites. These symptoms are generally self-limited, improve with slowing of the	Fever, chills, and malaise are common surface antigens on B-cells. These symptoms are generally self-limited, improve with slowing of the

		infusion, and resolve after infusion. Short-lived myelosuppression, abdominal pain, and myalgia are uncommon. Arrhythmias and angina pectoris are rare.
Sunitinib (Sutent)	FDA approved for renal cell carcinoma and imatinib resistant stromal tumor (GIST). cell carcinoma and imatinib resistant GI hypertension, skin including I	FDA approved for renal Fatigue, diarrhea, Sunitinib targets anorexia, receptor tyrosine kinase, and vascular endothelial growth factor (VEGFR) 1, 2, and 3 or 4 toxicities of factor (VEGFR 1, 2, and 3) on the same side and CD117. These effects occur in <10% of patients.
Sorafenib (Nexavar)	cell carcinoma, are diarrhea, rash, molecule in advanced liver cancer, fatigue, pain, nausea, VEGF receptor, and advanced thyroid and cancer.	FDA approved for renal cell carcinoma, are diarrhea, rash, molecule in advanced liver cancer, fatigue, pain, nausea, VEGF receptor, and advanced thyroid and cancer.
Trastuzumab (Herceptin)	overexpressing HER2/neu in metastatic or locally advanced breast cancer; headache. Trastuzumab has shown clinical benefit as a single agent to and in conjunction with paclitaxel-based chemotherapy.	Common side effects include acute fever, chills, nausea, receptor overexpression, vomiting, and many invasive carcinomas; neutropenia, leukopenia, anemia, unknown but may worsen in breast and diarrhea when given with lysis, antibiotic chemotherapy compared with induction of a

	<p>chemotherapy alone. Also, trastuzumab could have uncommon acute cardiotoxicity, which might add to the more common anthracycline-induced cardiotoxicity; therefore, the use of trastuzumab with doxorubicin is not indicated by the FDA.</p>
Vemurafenib (Zelboraf)	FDA approved for Arthralgia, skin rash, Only works treatment of melanoma. and photosensitivity. with BRAF mutations. I Raf/MEK/ERK
IMMUNE CHECKPOINT THERAPIES	
Atezolizumab (Tecentriq)	FDA granted Common side effects Atezolizumab accelerated approval for include nausea, interaction of urothelial carcinoma and fatigue, decreased PD-L1 and non-small cell lung appetite, and inhibitory eff cancer. infections, including on T cells. urinary tract infection.
Ipilimumab (Yervoy)	FDA approved for Grade 3 and 4 Ipilimumab immune effects in CTLA-4, neu 10%–20% of patients inhibitory due to T-cell stimulating T activation especially tumor cells. in GI tract.
Nivolumab (Opdivo)	FDA approved first time Rash, itchy skin, Nivolumab is

	treatment for melanoma infections, with ipilimumab, second fatigue, chest pain, and prevents time for squamous small and shortness of PD-L2 binding cell lung cancer and breath. second line for renal cancer.
Pembrolizumab (Keytruda)	FDA approved for Infusion-related melanoma, non-small cell lung cancer, head and neck cancer, reactions including refractory Hodgkin lymphoma, and mismatch repair deficient tumors. Pembrolizumab binds to PD-1 that prevents PD-1 from binding to its receptor. This leads to increased immune response and inflammation.

+ indicates the degree of synergy with radiation.

FDA, U.S. Food and Drug Administration; PO, ; IV, intravenous; GABA_A, γ -aminobutyric acid type A.

Modified from Christopher Schultz, MD.

The effectiveness of at least some chemotherapeutic agents depends on the presence or absence of molecular oxygen, in much the same way as x-rays. This is not surprising, at least for drugs whose action is mediated by free radicals.

Alkylating Agents

The alkylating agents are highly reactive compounds with the ability to substitute alkyl groups for hydrogen atoms of certain organic compounds, including DNA. There are five classes of alkylating agents:

1. Nitrogen mustard derivatives, such as cyclophosphamide, chlorambucil, and melphalan
2. Ethylenimine derivatives, such as thiotepa
3. Alkyl sulfonates, such as busulfan
4. Triazine derivatives, such as dacarbazine
5. Nitrosoureas, including bischloroethylnitrosourea (BCNU) (carmustine), chloroethyl-cyclohexyl-nitrosourea (CCNU) (lomustine), and methyl CCNU

Most of these drugs contain more than one alkylating group and therefore are considered **polyfunctional alkylating agents**. The nitrosoureas and dacarbazine have mechanisms and cytotoxicity over and above their ability to alkylate nucleic acids. As a class, alkylating agents are considered cell cycle nonspecific.

Nitrogen mustard is the prototype for three other useful alkylating agents: cyclophosphamide, chlorambucil, and melphalan. Nitrogen mustard given intravenously interacts rapidly with cells *in vivo*, producing its primary effect in seconds or minutes. By contrast, cyclophosphamide (Cytoxan) is inert until it undergoes biotransformation in the liver. Disappearance of injected cyclophosphamide from the plasma is biexponential, with an average half-life of 4 to 6.5 hours. Like all useful alkylating agents, cyclophosphamide produces toxicity in rapidly proliferating normal tissues. Chlorambucil (Leukeran) is an aromatic derivative of nitrogen mustard and is the slowest acting alkylating agent in general use. Melphalan (Alkeran, L-PAM) is a phenylalanine derivative of nitrogen mustard.

The nitrosoureas are a group of lipophilic alkylating agents that undergo extensive biotransformation *in vivo*, leading to various biologic effects, including alkylation, carbamylation, and inhibition of DNA repair. The multiple mechanisms of action may explain why the nitrosoureas generally lack cross-resistance with other alkylating agents. These compounds are very lipid soluble and readily cross the blood–brain barrier. They disappear from plasma rapidly, but their metabolites may persist for days.

Procarbazine

Procarbazine is a hydrazine derivative that must undergo biotransformation before it can exert its cytotoxic effects. The precise mechanism of action is not clear because it interferes with various biochemical processes. Procarbazine is well absorbed from the gastrointestinal tract and is cleared from the plasma with a half-life of about 10 minutes. The drug freely crosses the blood–brain barrier. It is used primarily in the treatment of advanced Hodgkin disease.

Cis-Platinum

Structurally, *cis*-platinum (*cis*-dichlorodiammine-platinum) is an inorganic complex formed by an atom of platinum surrounded by chlorine and ammonium ions in the *cis* position of the horizontal plane. *Cis*-platinum bears a resemblance to the bifunctional alkylating agents based on nitrogen mustard. It inhibits DNA synthesis to a greater extent than it does the synthesis of RNA or protein. It binds to DNA, causing both interstrand and intrastrand *crosslinking*.

Cis-platinum is cell cycle nonspecific. Its isomer, *trans*-platinum, is much less cytotoxic presumably because of the different way that it *crosslinks* to DNA. There is some evidence that *cis*-platinum is more toxic to hypoxic than to aerated cells—that it is a hypoxic cell radiosensitizer, although not as powerful in this regard as the nitroimidazoles.

Antibiotics

The clinically useful antibiotics are natural products of various strains of the soil fungus *Streptomyces*. They produce their tumoricidal effects by directly binding to DNA, and so their major inhibiting effects are on DNA and RNA synthesis. As a class, these drugs behave as cell cycle–nonspecific agents. Doxorubicin (Adriamycin) and daunorubicin (also known as daunomycin) are closely related anthracycline antibiotics. After intravenous injection, both drugs undergo extensive bioreduction in the liver to active and inactive metabolites, are bound extensively in tissues, and persist in plasma for prolonged periods. Neither drug crosses the blood–brain barrier to any appreciable extent. Both doxorubicin and daunorubicin are highly toxic drugs, producing various severe reactions; the major limiting toxicity, however, is cardiac damage.

Dactinomycin (actinomycin D) inhibits DNA-primed RNA synthesis by intercalating with the guanine residues of DNA; at higher concentrations, it also inhibits DNA synthesis. The net effect is cell cycle–nonspecific cytotoxicity. Dactinomycin must be administered intravenously. It is important longer plasma half-life is about 36 hours, and the drug is extensively bound to tissues.

Bleomycin sulfate (Blenoxane) affects cells by directly binding to DNA, resulting in reduced synthesis of DNA, RNA, and proteins. It also can lead to single-strand DNA breaks. Drugs acting by intercalation appear to augment the cytotoxic effects of bleomycin, as do x-rays and chemicals that generate superoxide radicals. Bleomycin is considered cell cycle nonspecific. It is more damaging to nonproliferating cells than to most proliferating cells.

Mitomycin C (Mutamycin) is an extremely toxic antitumor antibiotic. Unlike most other antibiotics, it is activated *in vivo* to a bifunctional or trifunctional alkylating agent. It is cell cycle nonspecific and is considerably more toxic to hypoxic than to aerated cells. Mitomycin C is usually administered intravenously; it is cleared rapidly from the plasma, with a half-life of 10 to 15 minutes, primarily by metabolism in the liver. It does not appear to cross the blood–brain barrier. The major toxicity of mitomycin C is myelosuppression.

Antimetabolites

The antimetabolites are analogues of normal metabolites required for cell function and replication. They may interact with enzymes and damage cells by any of these modes of action:

1. *Substituting* for a metabolite normally incorporated into a key molecule
2. *Competing* successfully with a normal metabolite for occupation of the catalytic site of a key enzyme
3. *Competing* with a normal metabolite that acts at an enzyme regulatory site, thereby altering the catalytic rate of the enzyme

Methotrexate is a folic acid antagonist. It works by competing for the folate-binding site of the enzyme dihydrofolate reductase. This results in decreased synthesis of thymidine and purine nucleotides. The cytotoxicity of methotrexate can be reversed by leucovorin, which is converted readily to other forms of reduced folate within the cell and which then can act as methyl donors for various biochemical reactions. The use of high-dose methotrexate with leucovorin rescue is based on the pharmacology of the two drugs, with the possibility of a differential effect between tumors and normal tissues in their ability to transport the two drugs across cell membranes. How true this differential effect turns out to be is another matter.

5-Fluorouracil

5-Fluorouracil (5-FU) is a structural analogue of the DNA precursor thymine. It works primarily as an irreversible inhibitor of the enzyme thymidylate synthetase but only after intracellular conversion to the active metabolite. It is also degraded by the liver and some other tissues. As a single agent, 5-FU is most useful in the treatment of carcinoma of the breast and gastrointestinal tract. The degradative enzymes are found in high concentrations in the gut but not in colonic carcinomas, and it has been suggested that this may explain in part the susceptibility of colon cancer to 5-FU.

Hydroxyurea

Hydroxyurea was first synthesized as long ago as 1869 and was found to be bone marrow suppressive in 1928. It was not used in the treatment of cancer until the 1960s. It acts as an inhibitor of ribonucleotide reductase, an enzyme essential to DNA synthesis, and is consequently specifically cytotoxic to cells in the S phase of the cell cycle. In experimental biology, hydroxyurea is used to synchronize cells because in addition to killing S phase cells, it causes survivors to pile up at

a block at the G₁/S interface. Clinically, hydroxyurea is used primarily in the treatment of chronic myeloid leukemia.

Nucleoside Analogues

Various nucleoside analogues have been synthesized and tested for antineoplastic properties. They are transported readily into rapidly dividing cells and activated by the single metabolic step of phosphorylation. Two analogues of cytosine are useful in cancer chemotherapy.

Cytarabine (cytosine arabinoside) is an analogue of deoxycytidine in which the sugar moiety is altered. The active form of cytarabine is the triphosphate that functions as a competitive inhibitor of DNA polymerase. Cytarabine is cell cycle specific and, in clinical practice, is usually used in combination with other drugs in the treatment of acute myeloid leukemia.

5-Azacytidine contains a single nitrogen substitution in the pyrimidine ring of cytidine. It undergoes a sequence of biotransformations similar to cytarabine, with the ultimate formation of an active triphosphate. The major biochemical effect of 5-azacytidine is believed to be the inhibition of the processing of large molecular weight species of RNA, with less important effects on DNA and protein synthesis. Like cytarabine, it is cell cycle specific.

Vinca Alkaloids

Some of the most useful antineoplastic agents are produced from plants. Vincristine sulfate (Oncovin) and vinblastine sulfate (Velban) are alkaloids produced from the common periwinkle plant. The clinically useful alkaloids are large, complex molecules that exert their major antitumor effect by binding to cellular microtubular proteins and inhibiting microtubule polymerization. Because these are essential compounds of the mitotic spindle of dividing cells, this binding leads to mitotic arrest.

Taxanes

The toxicity of products of the yew tree has been known for thousands of years. For example, essentially every rural village in England has a huge spreading yew tree, dating from medieval times when the archer's weapon, the long bow, was fabricated from the wood of the yew—but the tree is always found in the walled-in church cemetery because the leaves or bark are toxic to browsing livestock. This toxicity is caused by a class of compounds known as taxanes. For those who see chemotherapy for cancer as simply the latest round in the never-ending

battle between plants and animals, taxanes do indeed provide the perfect example.

Paclitaxel is the prototype of a new class of antineoplastic agents, the taxanes that targets the microtubules. It is a natural product, isolated from the bark of the western yew, *Taxus brevifolia*. Docetaxel is a largely synthetic derivative. The newest member of this family is nab-paclitaxel, which represents a formulation of paclitaxel bound to albumin as a delivery vehicle.

Taxanes are potent microtubule-stabilizing agents and promoters of microtubule assembly. This is in contrast to agents such as the vinca alkaloids and colchicine that bind to tubulin, the subunit of microtubules, and inhibit microtubule formation. The taxanes block or prolong the transit time of cells in the G₂/M phase of the cell cycle. The inability of these cells to pass through the G₂ and M phases of the cycle results from the inability of these cells to form a competent mitotic spindle or to disassociate a drug-treated spindle.

In addition to multiple *in vitro* studies from the early 1970s on, human studies have demonstrated the ability of taxanes to increase the mitotic index in various normal tissues *in vivo*, whereas the two taxanes in clinical use, paclitaxel (Taxol) and docetaxel (Taxotere), have demonstrated significant levels of activity in a broad range of human tumors. The taxanes are of particular interest to radiobiologists because of the way in which they interact with radiation (described later).

Hormone Targeted Therapies

Great success has been found in treating both breast and prostate cancer with treatments which target estrogen and androgen signaling. Drugs such as leuprolide acetate (Lupron) which inhibit gonadotropin-releasing hormone and inhibit the pituitary release of gonadotropins result in significantly diminished levels of estrogen and androgens. These diminished levels of estrogens and androgens are effective in inhibiting the growth and viability of hormone responsive breast and prostate cancer cells. However, newer therapies that are effective in blocking estrogen production and activity and which have few side effects have been developed. For example, tamoxifen has been widely given to postmenopausal women with estrogen receptor-positive (ER+) tumors. Tamoxifen itself is a prodrug that requires metabolic conversion to its active form 4-hydroxytamoxifen by cytochrome P450 isoforms. The prodrug tamoxifen has low affinity for binding to ER α or ER β , but the active metabolite 4-hydroxytamoxifen has 2 to 3 times greater affinity than estrogen to bind to the

ER receptors. For those patients who have progressed on tamoxifen, aromatase inhibitors are the treatment of choice and block estrogen production selectively.

Similar to breast cancer, prostate cancer also has several effective therapeutics. For example, the combination of gonadotropin-releasing hormone agonists with antiandrogens such as bicalutamide (Casodex) were highly effective for the treatment of prostate cancer. However, newer more effective therapies have been developed. Abiraterone is a synthetic, steroidal CYP17A1 inhibitor. In addition to inhibiting CYP17A1, abiraterone also inhibits 5α -reductase, a critical enzyme in the production of androgens that converts testosterone to the more potent form dihydrotestosterone. A recent study demonstrates a significant survival benefit of abiraterone if added to long-term hormone therapy for prostate cancer. The development of enzalutamide has also greatly impacted the treatment of prostate cancer. Enzalutamide binds to the androgen receptor, prevents androgen receptor translocation to the nucleus, and binding to DNA resulting in the inhibition of critical androgen-regulated target genes. Unfortunately, like most targeted agents, enzalutamide provides a highly selective pressure for the outgrowth of resistant variants.

Topoisomerase Inhibitors

DNA topoisomerases are nuclear enzymes that reduce twisting and supercoiling that occur in selected regions of DNA as a result of transcription, replication, and repair recombination. Little is known of the actual mechanism by which they kill cells.

Top I inhibitors, thus far consisting primarily of camptothecin analogues, interact with the enzyme–DNA complex and prevent the resealing of DNA strand breaks, leading to cell death in cells actively replicating.

Top II inhibitors prevent religation of DNA cleaved by top II and lead to cell death. Etoposide, a semisynthetic podophyllotoxin derivative, is a prime example.

Targeted Therapy

Achieving tumor response with traditional chemotherapeutic agents, such as the alkylating agents, *cis*-platinum, and 5-FU, for example, inevitably involved substantial toxicity to self-renewal normal tissues, such as the gastrointestinal tract and the blood-forming organs. There is some promise that the situation is much more favorable in the case of the new generation of targeted therapeutic agents that, in combination with radiotherapy, enhance tumor control with little,

if any, increase in normal tissue toxicity. Cetuximab (Erbitux) might be regarded as a model for this class of pathway-targeting agents. Promising but still early results for bevacizumab await further clinical testing.

Cetuximab (Erbitux)

There appears to be a strong correlation between both locoregional control and overall survival and the level of epidermal growth factor receptor (EGFR) expression in advanced head and neck squamous carcinoma. Because high levels of EGFR predict for a poor outcome, EGFR is an attractive target for cancer therapy.

Cetuximab (Erbitux) is a recombinant human/mouse chimeric monoclonal antibody produced in mammalian cell culture. Cetuximab specifically binds to EGFR, blocking phosphorylation and activation of receptor-associated kinases, resulting in inhibition of cell growth, induction of apoptosis, and decreased matrix metalloproteinase and vascular endothelial growth factor (VEGF).

Studies using cetuximab with a xenograft tumor in mice indicate that although the antibody alone produces a modest tumor growth delay, there is a substantial interaction with radiation. These promising preclinical results led to a phase III trial that demonstrated that the addition of cetuximab to high-dose radiotherapy in patients with locoregionally advanced squamous cell carcinoma of the head and neck produced a statistically significant prolongation in overall survival ([Fig. 27.2](#)). Median survival increased from 29 to 49 months. The 5-year overall survival increased from 36.4% to 45.6%. Subgroup analysis showed that patients who developed a grade 2 to 4 acne-like rash have a 2.5 greater overall survival than patients with grade 1 or no rash ([Fig. 27.2B](#)). This is the first phase III clinical trial to show an increased survival benefit when a targeted therapeutic is combined with radiotherapy.

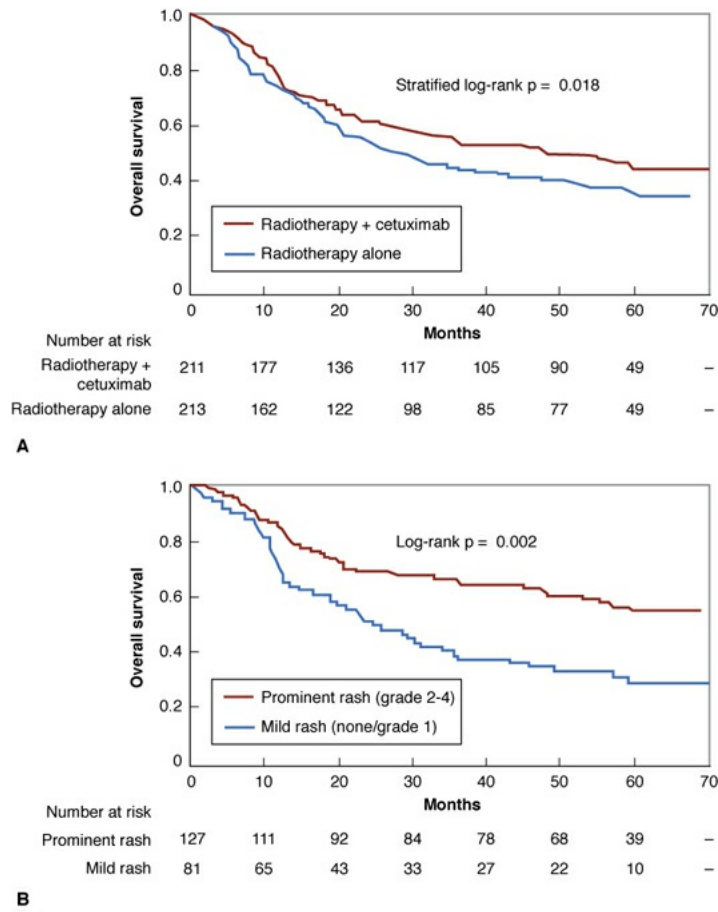


FIGURE 27.2 A: Five-year survival data for locoregionally advanced head and neck cancer patients treated with radiotherapy alone or the combination of radiotherapy and cetuximab. The addition of cetuximab increased survival by 9%. **B:** Five-year survival for locoregionally advanced head and neck cancer based on whether patients had an acne-like rash of grade 2 to 4. Patients with a rash above grade 2 had 2.5 times longer survival than those who had a grade 1 rash or no rash. (Adapted from Bonner JA, Harari PM, Giralt J, et al. Radiotherapy plus cetuximab for locoregionally advanced head and neck cancer: 5-year survival data from a phase 3 randomised trial, and relation between cetuximab-induced rash and survival. *Lancet Oncol.* 2010;11:21–28, with permission.)

Bevacizumab (Avastin)

In 1971, Judah Folkman proposed that the formation of new blood vessels (angiogenesis) was an essential process for tumor growth and metastasis. This concept has been widely confirmed by other investigators and launched the era of “antiangiogenic agents.” The most commercially successful of these agents is bevacizumab, a monoclonal antibody that neutralizes the activity of the proangiogenic mitogen VEGF.

The first clinical trials with bevacizumab in the treatment of recurrent and metastatic breast cancer resulted in failure to demonstrate a survival benefit. The major insight in the use of antiangiogenic agents was found to be in combination with cytotoxic chemotherapy. Currently, bevacizumab is approved with chemotherapy for metastatic colorectal cancer, lung cancer, and renal cancer. The increased survival of patients treated with the combination of antiangiogenic agents and chemotherapy compared to antiangiogenic therapy alone brought about the vascular normalization hypothesis that proposes that agents such as bevacizumab eliminate the malformed and inadequate vessels in a tumor, reducing tumor size and making it better perfused and more responsive to cytotoxic chemotherapy and radiotherapy (Fig. 27.3).

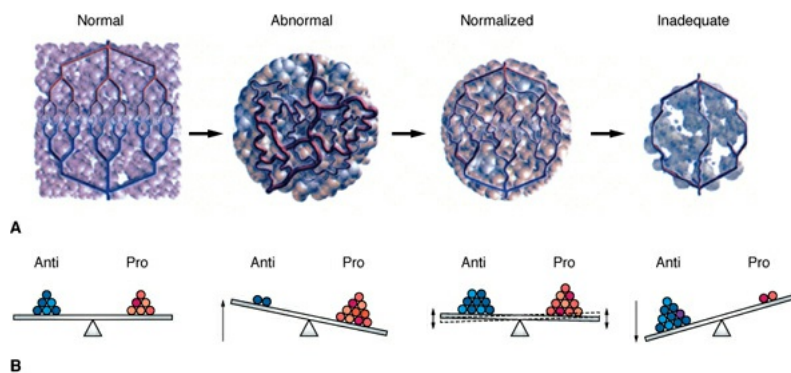


FIGURE 27.3 Cartoon depicting the concept of vascular normalization that occurs after treatment with antiangiogenic agents. **A:** The vasculature of tumors compared to normal tissues is abnormal and inadequate to sufficiently supply the tumor with oxygen and nutrients. Treatment with antiangiogenic agents such as bevacizumab results in inhibition of new vessel formation and pruning of malformed vessels, resulting in a vasculature that resembles normal tissue. However, continuous treatment with antiangiogenic agents will result in damage to even these normalized vessels that will ultimately result in tumor cell shrinkage and reduction. If the tumor is not completely eradicated by treatment with the antiangiogenic therapy, it will regrow and become refractory to antiangiogenic therapy and ultimately develop a new blood supply. **B:** The changes associated with tumor vasculature reflect the dynamic balance between proangiogenic and antiangiogenic factors. Normal tissues have a good balance between the two, whereas tumors are more skewed toward proangiogenic factors. Antiangiogenic therapy restores the balance. However, continuous antiangiogenic treatment will result in tipping the balance that will result in destruction of tumor vasculature. (Panel A from Jain RK. Normalizing tumor vasculature with anti-angiogenic therapy. *Nature Med.* 2001;7:987, with permission. Panel B from Jain RK. Normalization of tumor vasculature: an

emerging concept in antiangiogenic therapy. *Science*. 2005;307:58–62, with permission.)

Willet and his colleagues previously reported the results of some small clinical trials to determine whether inhibition of VEGF is safe and enhances the effect of chemoradiotherapy with locally advanced rectal cancer. The combination of bevacizumab, 5-FU, and external beam irradiation resulted in decreased tumor vasculature density and decreased interstitial fluid pressure. These results are consistent with the inhibition of angiogenesis and a vascular normalizing effect of bevacizumab. In contrast, in the setting of stereotactic body radiotherapy (SBRT), antiangiogenic agents appear to prevent normal tissue recovery and make SBRT-related toxicity more likely.

Poly Adenosine Diphosphate-Ribose Polymerase Inhibitors

The enzyme poly adenosine diphosphate-ribose polymerase 1 (PARP-1) plays an essential role in the base excision repair pathway, in particular, in the recruiting of x-ray cross complementing factor 1 (XRCC1), which acts as a scaffold protein to coordinate the repair of damaged bases (see [Chapter 2](#)). Inhibition of PARP results in decreased based excision repair activity and accumulation of single-strand breaks that will lead to the collapse of replication forks in the S phase of the cell cycle and the generation of DNA double-strand breaks (DSBs) and cell lethality. If tumors are deficient in the repair of DNA DSBs by homologous recombination in the S phase of the cell cycle because of mutations in BRCA1 or BRCA2, then PARP inhibition will result in cell lethality. This so-called synthetic lethal interaction between PARP inhibition and BRCA deficiency has served as the basis for several clinical trials where PARP inhibitors are administered alone or in combination with cytotoxic chemotherapy agents to patients with BRCA mutations in breast, ovarian, or prostate cancer or to patients with triple negative breast cancer. The scientific rationale behind these trials is that inhibition of PARP alone or mutations in BRCA genes alone have little effect on cell viability. However, only when the two are combined do you have cell killing. This type of interaction has been termed *synthetic lethality* because of the requirement that two pathways need to be inhibited that typically are unaffected and lead to very few viable progeny ([Fig. 27.4](#)). Not surprisingly, most studies to date have focused on PARP-1 inhibitors as a monotherapy or administered with some forms of cytotoxic chemotherapy. However, inhibition of PARP renders cells sensitive to radiotherapy and even more so in a BRCA mutation containing tumors. Thus, although PARP inhibitors are quite new, the combination of impressive phase I and II clinical results and potential synergism

with radiotherapy will most probably increase their use with radiotherapy in the future.

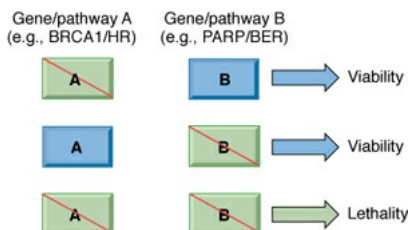


FIGURE 27.4 Schematic representation of the synthetic lethality principle. Synthetic lethality occurs when individual loss of two genes (*A* or *B*) is viable but is lethal when in combination (*A* and *B*). This principle is exemplified with genes involved in DNA repair pathways, poly adenosine diphosphate-ribose polymerase (PARP) (base excision repair [BER]) and BRCA1 (homologous recombination [HR]). (From Hammond EM, Pires I, Giaccia AJ. DNA damage and repair. In: RT Hoppe, TL Phillips, M Roach, eds. *Leibel and Phillips Textbook of Radiation Oncology*. 3rd ed. Philadelphia, PA: Elsevier; 2010:31–39, with permission.)

Immune Checkpoint Therapies

Programmed death receptor-1 (PD-1) is located on the surface of T cells and binds to programmed death ligand 1 or 2 (PD-L1 or PD-L2), resulting in an inactive T cell. PD-L1 and PD-L2 are expressed by many different types of cancer cells. Therefore, inhibiting PD-1, PD-L1, or PD-L2 should inhibit the negative regulation of T cells (T-cell checkpoint) and allow them to attack tumor cells. This fundamental finding on the roles of PD-1 and PD-L1 and PD-L2 molecules is the basis for T-cell checkpoint therapies.

T-cell checkpoint inhibitors have produced noteworthy responses against metastatic disease in several indications, but to date, single-agent responses to PD-1/PD-L1 inhibitors (nivolumab, pembrolizumab, atezolizumab) and CTLA-4 (ipilimumab) antibodies have been limited to 10% to 30% of the treated population. One of the major factors in determining T-cell checkpoint inhibitor activity has been the presence of pretreatment CD8+ T cells within the tumor. In contrast, immune-unresponsive tumors usually have limited numbers of T cells within their tumors and fail to increase their numbers even after the addition of T-cell checkpoint inhibitors. Recent studies have indicated that tumors with the highest number of CD8+ T cells within their tumors (so called inflamed or hot tumors) and which have a high mutational burden have a much greater probability of exhibiting a long-term durable response to T-cell checkpoint

inhibitors. Although there is little question that T-cell checkpoint inhibitors are effective therapeutics, they also come with high levels of normal tissue complications. Most of the complications with the use of these inhibitors are on target side effects such as increased immune-related reactions due to inappropriate T-cell activation such as in the gastrointestinal system. However, even with these complications, there is great interest in expanding the use of these inhibitors, especially in combination therapy. Currently, there are well over 1,000 clinical trials ongoing in combination therapies using T-cell checkpoint inhibitors.

With the knowledge of immune reactions induced by chemotherapy and radiotherapy, there is great interest in combining cytotoxic therapies with T-cell checkpoint therapies. This interest in large part stems from a case report study by Postow and his colleagues at Memorial Sloan Kettering Cancer Center (MSKCC) who reported a dramatic effect on the metastatic disease of a young woman who was given palliative radiotherapy with anti- cytotoxic T-lymphocyte-associated protein-4 (CTLA-4) therapy (ipilimumab). In addition, radiation has been postulated to increase the quantity of neoantigens and therefore increase T-cell activation, making the combination of immunotherapy and radiotherapy even more attractive. However, early results have not demonstrated a great increase in responses or survival, which can be explained by the fact that the addition of radiation does not overcome the problem of T-cell exclusion. For the foreseeable future, combination trials with T-cell checkpoint inhibitors and radiotherapy will be ongoing, but there is a need to better understand the mechanisms of T-cell exclusion and how it can be overcome.

DOSE-RESPONSE RELATIONSHIPS

Dose-response relationships have been produced for a wide range of chemotherapeutic agents using techniques developed initially for radiation, although much less effort has been expended on fitting data to models than has been the case for ionizing radiations. From even a cursory examination of the data, however, it is evident that—with some clear exceptions—the shape of the survival curve is unremarkable and reminiscent of that of survival curves for ionizing radiations. If surviving fraction is plotted on a log scale against drug dose on a linear scale, the dose-response curve has an initial shoulder followed by a region that becomes steeper and straighter ([Fig. 27.5](#)). The antibiotics doxorubicin (Adriamycin), bleomycin, and dactinomycin (actinomycin D) are clear exceptions. For these agents, the dose-response curve appears to have no shoulder, and the curve is concave upward. A dose-response curve with this

shape is usually associated with a variation of sensitivity within the population (i.e., nonuniform sensitivity of cells). This has never been demonstrated experimentally, however. For example, synchronously dividing cells likewise show the same upwardly concave dose-response curve. This shape therefore must remain unexplained at the present time.

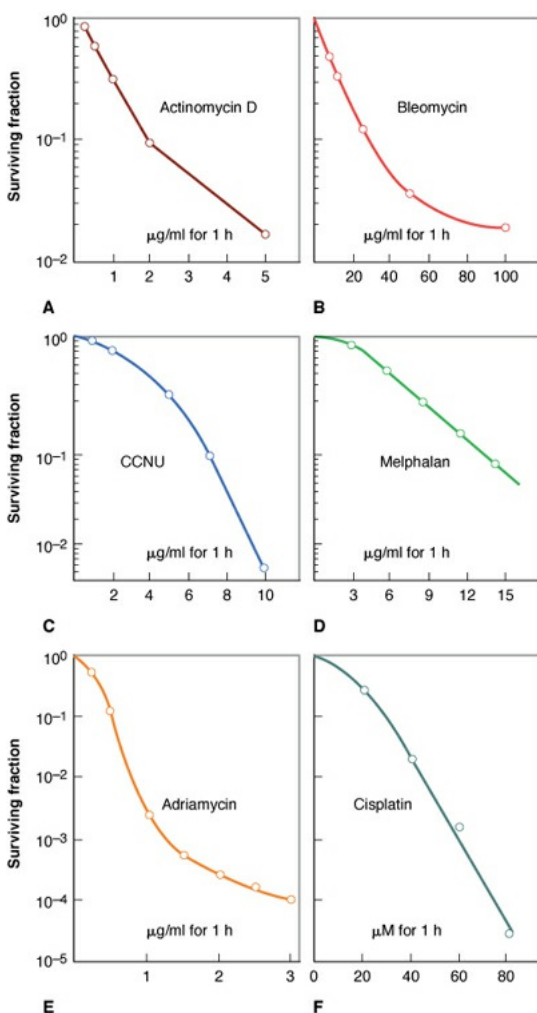


FIGURE 27.5 Dose-response relationships *in vitro* for six commonly used chemotherapeutic agents. Note the diverse shapes. Many have shapes similar to survival curves for x-rays, except that drug concentration replaces absorbed dose. The antibiotics bleomycin (**graph B**), doxorubicin (Adriamycin) (**graph E**), and actinomycin D (**graph A**) have dose-response relationships that are concave upward. **A:** Dose-response relationship for dividing CHO cells treated for 1 hour with graded doses of actinomycin D. (Adapted from Barranco SC, Flournoy DR. Modification of the response to actinomycin-D-induced sublethal damage by simultaneous recovery from potentially lethal damage in mammalian cells. *Cancer Res.* 1976;36:1634–1640, with permission.) **B:** Dose-response relationship for plateau-phase CHO cells treated for 1 hour with graded doses of bleomycin. (Adapted from Barranco SC, Novak JKJ, Humphrey RM. Response

of mammalian cells following treatment with bleomycin and 1,3-bis(2-chloroethyl)-1-nitrosourea during plateau phase. *Cancer Res.* 1973;33:691–694, with permission.) **C:** Dose–response relationship for CHO cells treated for 1 hour with graded doses of chloroethyl-cyclohexyl-nitrosourea (CCNU). (Adapted from Barranco SC. In vitro responses of mammalian cells to drug-induced potentially lethal and sublethal damage. *Cancer Treat Rep.* 1976;60:1799–1810, with permission.) **D:** Dose–response relationship for human lung cancer cells exposed for 1 hour to graded doses of melphalan. (Unpublished data, courtesy of Dr. Laurie Roizin-Towle.) **E:** Dose–response relationship for V79 Chinese hamster cells exposed for 1 hour to graded doses of doxorubicin (Adriamycin). (Adapted from Belli JA, Piro AJ. The interaction between radiation and Adriamycin damage in mammalian cells. *Cancer Res.* 1977;37:1624–1630, with permission.) **F:** Dose–response relationship for V79 Chinese hamster cells exposed for 1 hour to graded doses of *cis*-platinum (cisplatin). (Unpublished data, courtesy of Dr. Laurie Roizin-Towle.)

Dose–response curves indicate that, at best, anticancer drugs kill by first-order kinetics; that is, a given dose of the drug kills a constant fraction of a population of cells, regardless of its size. This assumes, of course, that the growth fraction and the proportion of sensitive to resistant cells remains the same. This leads to the conclusion that the chance of eradicating a cancer is greatest if the population size is small or that there is an inverse relationship between curability and the tumor cell burden at the initiation of chemotherapy. This conclusion has been arrived at from long and bitter clinical experience, but, in fact, it is an inevitable consequence of the shape of the simplest dose–response relationship.

Another characteristic of chemotherapy agents is that the sensitivity to cell killing varies enormously among cell types. Radiosensitivity varies, too, of course, but not to the same extent as chemosensitivity. Dose–response curves for several cell lines exposed to paclitaxel are shown in [Figure 27.6](#), illustrating the wide range of sensitivities.

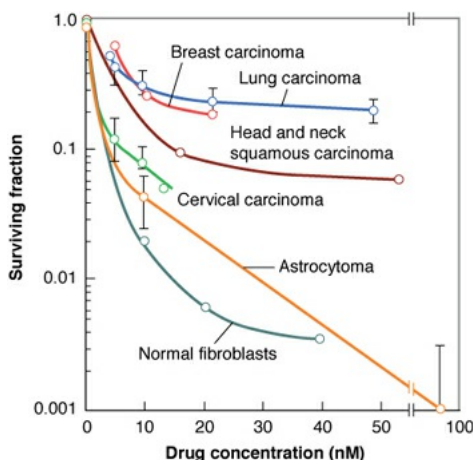


FIGURE 27.6 Illustrating the wide variability in sensitivity to taxanes. All the data refer to cells of human origin exposed for 24 hours. (Data for the cervical carcinoma line and the astrocytoma line from Geard CR, Jones JM, Schiff PB. Taxol and radiation. *J Natl Cancer Inst Monogr.* 1993;15:89–94; data for the head and neck squamous carcinoma line from Leonard CE, Chan DC, Chou TC, et al. Paclitaxel enhances in vitro radiosensitivity of squamous carcinoma cell lines of the head and neck. *Cancer Res.* 1996;56:5198–5204; data for the lung carcinoma line [A545] from Liebmann JE, Hahn SM, Cook JA, et al. Glutathione depletion by L-buthionine sulfoximine antagonizes taxol cytotoxicity. *Cancer Res.* 1993;53:2066–2070; data for the breast carcinoma line [MCF-7] from Liebmann JE, Cook JA, Lipschultz C, et al. Cytotoxic studies of paclitaxel [Taxol] in human tumour cell lines. *Br J Cancer.* 1993;68:1104–1109.)

SUBLETHAL AND POTENTIALLY LETHAL DAMAGE REPAIR

Studies with radiation led to the concepts of sublethal damage repair and potentially lethal damage repair, which are discussed in some detail in [Chapter 5](#). These are still largely operational terms. Sublethal damage repair is demonstrated by an increase in survival if a dose of radiation (or other cytotoxic agent) is divided into two or more fractions separated in time. There is a tendency for the extent of sublethal damage repair to correlate with the shoulder of the acute dose-response curve, but this is not always true. Repair of potentially lethal damage is manifested as an increase in survival if cells are held in a nonproliferative state for some time after treatment.

Similar studies have been performed with various chemotherapeutic agents. The results are not as clear-cut as for radiation, and there is much greater variability between different cell lines.

Potentially lethal damage repair is a significant factor in the antibiotics bleomycin and doxorubicin. Data for bleomycin are shown in Figure 27.7. Potentially, lethal damage repair is also seen after treatment with dactinomycin. Sublethal damage repair is essentially absent with all of these drugs.

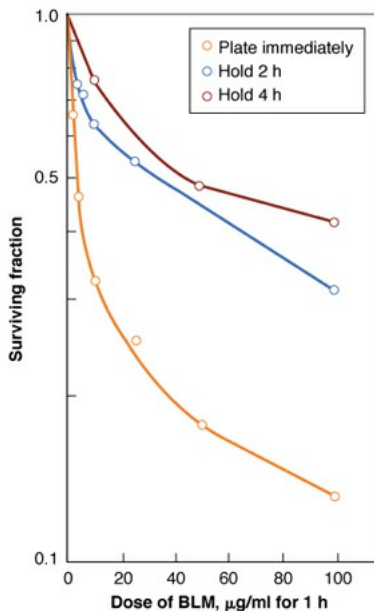


FIGURE 27.7 Potentially lethal damage repair (PLDR) in cultured Chinese hamster cells treated with bleomycin (BLM). An increase in survival is observed, interpreted as PLDR, when cells are held in depleted medium for 2 to 4 hours after the drug treatment. (Adapted from Barranco SC, Humphrey RM. Response of mammalian cells to bleomycin-induced potentially lethal and sublethal damage. *Prog Biochem Pharmacol*. 1976;11:78–92, with permission.)

No potentially lethal or sublethal damage repair is seen with nitrosourea, even though the dose-response curves for single doses have substantial shoulders. The breakdown products of the nitrosoureas are known to inhibit DNA repair, and this may be a contributing factor.

Studies of repair of sublethal damage with drugs are complicated because if a split-dose study is performed, decisions must be made about the equivalence of drug concentration and time. It is frequently assumed that biologic response is determined by an *integral dose* (i.e., the product of concentration and time), but this has not been checked and confirmed in all cases. There appears to be no correlation between the existence of a shoulder on the dose-response curve for single doses and the appearance of sublethal damage repair, as evidenced by an increase in survival in a split-dose experiment. It is possible that a shoulder in a survival curve does not have the same meaning for chemically induced damage as it does for radiation-induced damage. A shoulder on a survival curve for a

chemotherapeutic agent may reflect more about drug concentrations and the time required for entry of the drug into the cells and interaction with a target molecule than it does about the accumulation and repair of sublethal damage.

THE OXYGEN EFFECT AND CHEMOTHERAPEUTIC AGENTS

The importance of the oxygen effect for cell killing by radiation is discussed in [Chapter 6](#). It has been known for more than half a century that the presence or absence of molecular oxygen has a dramatic influence on the proportion of cells surviving a given dose of x-rays. Only in more recent years has the influence of oxygen on the cytotoxicity resulting from chemotherapeutic agents been studied. It is certainly more complicated than for ionizing radiations.

Some agents, such as bleomycin, are more toxic to oxygenated cells than to chronically hypoxic cells. Dose-response curves for cells exposed to graded concentrations of bleomycin in the presence or absence of oxygen are shown in [Figure 27.8](#). At high concentrations of the drug, there is an extra log of cell killing if oxygen is present, compared with hypoxic conditions. Other examples of agents that are more toxic to aerated than to hypoxic cells are procarbazine, dactinomycin, and vincristine. It should come as no surprise to those familiar with x-rays that oxygen is a factor in the response of cells to any chemotherapeutic agent in which the mechanism of cell killing is mediated by free radicals.

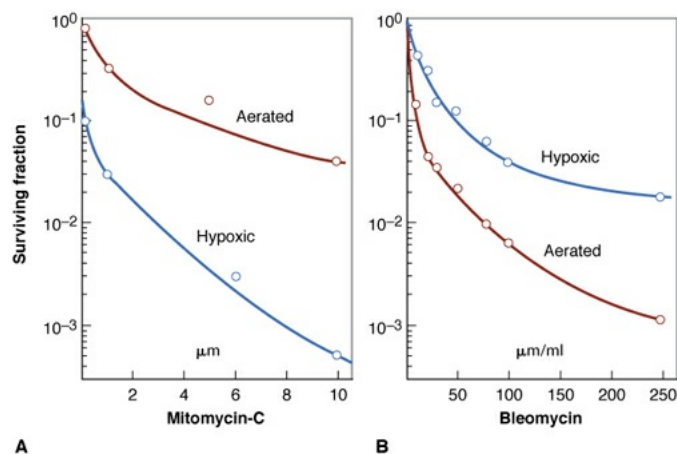


FIGURE 27.8 Molecular oxygen can be either a sensitizer or a protector, depending on the particular chemotherapeutic agent. **A:** Survival curves for EMT6 cells treated for 1 hour with graded doses of mitomycin C under aerated or hypoxic conditions. In the absence of oxygen, the cells are substantially more sensitive. (Data from Teicher BA, Lazo JS, Sartorelli AC. Classification of

antineoplastic agents by their selective toxicities toward oxygenated and hypoxic tumor cells. *Cancer Res.* 1981;41:73–81.) **B:** Survival curves for Chinese hamster cells in culture exposed for 4 hours to graded doses of bleomycin under aerated or hypoxic conditions. In the absence of molecular oxygen, the cells are more resistant. (Adapted from Roizin-Towle L, Hall EJ. Studies with bleomycin and misonidazole on aerated and hypoxic cells. *Br J Cancer*. 1978;37:254–260, with permission.)

By contrast, agents such as mitomycin C are substantially more toxic to hypoxic than to aerated cells (see Fig. 27.8) because the drug undergoes bioreduction in the absence of oxygen. The same is true, of course, of bioreductive drugs, which is discussed in Chapter 26.

A third group of drugs, including 5-FU, methotrexate, *cis*-platinum, and the nitrosoureas, appears to be equally cytotoxic to aerated or hypoxic cells. This oversimplified classification only holds true if the level or duration of the hypoxia is not sufficient to disturb the movement of cells through the cell cycle. Table 27.2 is a summary of the classification of antineoplastic agents based on the effect of the presence or absence of molecular oxygen.

Table 27.2 Classification of Antineoplastic Agents Based on Cellular Oxygenation

PREFERENTIAL TOXICITY TO AEROBIC CELLS	PREFERENTIAL TOXICITY TO HYPOXIC CELLS	MINIMAL OR NO SELECTIVITY BASED ON CELLULAR OXYGENATION
Bleomycin	Mitomycin C	5-Fluorouracil ^a
Procarbazine	Doxorubicin	Methotrexate ^a
Streptonigrin	Metronidazole Tirapazamine	Cisplatin

Dactinomycin

5-Thio-D-glucose, 2-deoxy-D-glucose, BCNU, CCNU

"These conclusions are based on experiments in which hypoxic cells were still capable of DNA synthesis and cellular replication. These agents have cytotoxic effects primarily on cells in the S phase of the cell cycle. Thus, in hypoxic cells that are blocked in their progression through the cell cycle or cycling slowly, agents such as these that act on the S phase of the cell cycle would be expected to be relatively noncytotoxic.

Based on Teicher BA, Lazo JS, Sartorelli AC. Classification of antineoplastic agents by their selective toxicities toward oxygenated and hypoxic tumor cells. *Cancer Res.* 1981;41:73–81, with permission.

RESISTANCE TO CHEMOTHERAPY AND HYPOXIC CYTOTOXINS

Tumor cells protect themselves from changes in the microenvironment resulting from a decrease in both nutrients and oxygen by reducing macromolecular synthesis and inducing genes that promote angiogenesis and tissue remodeling. This is discussed in some detail in [Chapter 26](#). The ability of malignant cells to survive fluctuations in oxygen tension is important in the context of cancer therapy because it is well documented that tumors that are hypoxic are aggressive and respond poorly to all forms of treatment.

The shortage of oxygen in hypoxic cells renders them refractory to killing by ionizing radiations that require oxygen to "fix" the damage produced in DNA by the hydroxyl radicals; it is equally true that cells may be refractory to killing by "radiation-mimetic drugs" that operate via a free radical mechanism. Cessation of cell division and loss of apoptotic potential (cell suicide), however, in hypoxic cells are likely to be more important reasons why hypoxic cells are resistant to chemotherapy. Hypoxic cells located remote from capillaries are least likely to be killed by radiation but most likely to be killed by a hypoxic cytotoxin. This is illustrated in [Figure 27.9](#).

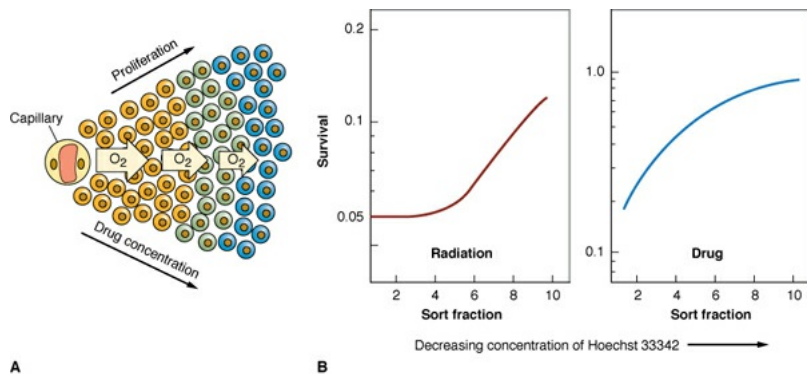


FIGURE 27.9 Illustrating why the microenvironment in a tumor may lead to resistance to chemotherapy agents. **A:** Oxygen diffuses from a capillary, but the concentration falls with distance because of respiration in the mass of tumor cells. This leads to a region of hypoxia and a region of anoxia. Chemotherapeutic agents must also diffuse through a tumor from capillaries. The effect of the agent decreases with distance from the capillary because the drug concentration falls because of metabolism, proliferation decreases with distance from a capillary because of lack of oxygen, and cells that are not dividing are resistant to many chemotherapeutic agents. **B:** The fraction of cells surviving a treatment with radiation or most chemotherapeutic agents rises with distance from a capillary because both are less effective in hypoxic nondividing cells. (Adapted in part from Brown JM, Siim BG. Hypoxia-specific cytotoxins in cancer therapy. *Semin Radiat Oncol*. 1996;6:22–36, with permission.)

The most effective way to partly circumvent the problem introduced by hypoxia in reducing the efficacy of chemotherapy is to introduce a bioreductive drug or hypoxic cytotoxin that is most effective at reduced oxygen concentrations. This is described in more detail in [Chapter 26](#). Mitomycin C and its derivatives have been used for this purpose for many years.

DRUG RESISTANCE AND CANCER STEM CELLS

The biggest single problem in chemotherapy is drug resistance, which either may be evident from the outset or may develop during prolonged exposure to a cytostatic drug. Cells resistant to the drug take over, and the tumor as a whole becomes unresponsive. The development of resistance can be demonstrated readily for cells in culture. [Figure 27.10](#) shows substantial resistance to doxorubicin developing as cells are grown continuously in a low concentration of the drug for a period of weeks.

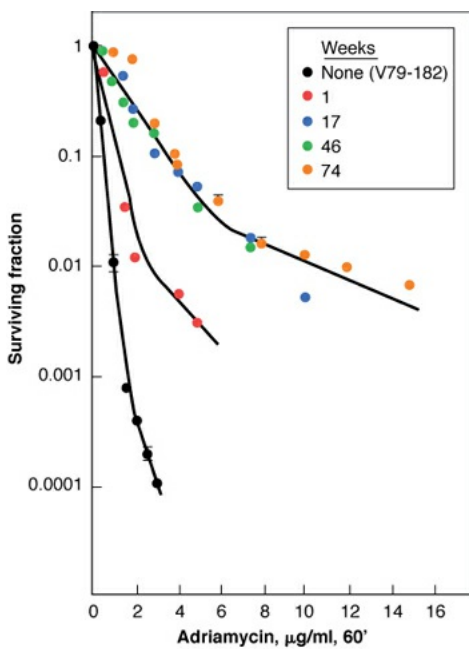


FIGURE 27.10 Change in survival response to doxorubicin (Adriamycin) of Chinese hamster cells grown in culture and exposed continuously to a low concentration of the drug ($0.05 \mu\text{g}/\text{mL}$) for prolonged periods, namely, 1, 17, 46, or 74 weeks. The *closed circles* show the survival response for the parent cell line. A dramatic resistance to the drug develops by 17 weeks; that is, prolonged exposure at a low concentration renders the cells resistant to subsequent high concentrations. (Adapted from Belli JA. Radiation response and Adriamycin resistance in mammalian cells in culture. *Front Radiat Ther Oncol.* 1979;13:9–20, with permission.)

Underlying this problem of drug resistance are genetic changes that can sometimes be seen in chromosome preparations. Figure 27.11 shows two illustrations involving gene amplification or the presence of multiple minute chromosome fragments.

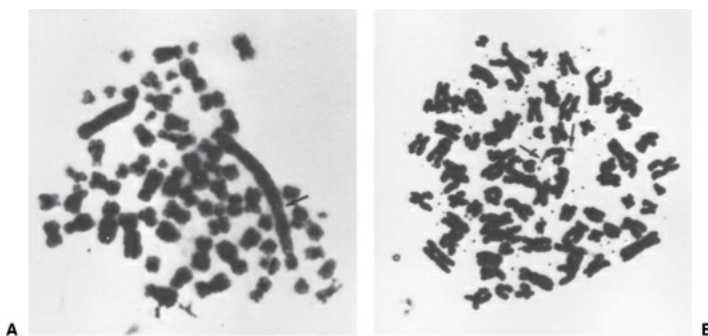


FIGURE 27.11 Most forms of drug resistance probably have a genetic basis. A few extreme examples can be seen in chromosome changes. **A:** The *arrow* indicates an elongated chromosome, which on banding shows the features of an extended homogeneously staining region. This karyotype was observed in the

human breast cancer cell line (MCF-7), which is resistant to methotrexate. (From Cowan KH, Goldsmith ME, Levine RM, et al. Dihydrofolate reductase gene amplification and possible rearrangement in estrogen-responsive methotrexate-resistant human breast cancer cells. *J Biol Chem.* 1982;257:15079–15086, with permission.) **B:** Small-cell lung carcinoma line derived from a patient treated with methotrexate. These cells are very resistant to the drug and contain numerous double minute chromosomes. A pair is indicated by *arrows*. (From Curt GA, Carney DN, Cowan KH, et al. Unstable methotrexate resistance in human small-cell carcinoma associated with double minute chromosomes. *N Engl J Med.* 1983;308:199–202, with permission.)

Drug resistance is an important factor that occurs readily—a phenomenon quite alien to the radiobiologist. Radiation-resistant cells can be produced and isolated, but it is a difficult and time-consuming process. For instance, cells continuously irradiated at low dose rates occasionally do spawn radioresistant clones. By contrast, resistance to chemotherapeutic agents is acquired quickly, uniformly, and inevitably.

If a resistant clone can arise by a chance mutation of a gene responsible for one of the important steps in drug action, then the probability of it occurring would be expected to increase rapidly as the tumor increases in size. The average mutation rate for mammalian genes is about 10^{-5} to 10^{-6} per division, so that in a tumor containing 10^{10} cells that go through many divisions, a mutation is almost certain to occur, especially in the presence of a powerful mutagen, which most chemotherapeutic agents are.

Another contributing factor to chemotherapy resistance is cancer stem cells. The current model of cancer stem cells proposes that although these cells represent only a small subpopulation of the tumor, they are the most important because they possess the potential to give rise to both stem cells and differentiated non-stem cells. Therapeutically, stem cells have been reported to be resistant to ionizing radiation and chemotherapy. Resistance to radiation has been proposed to be mediated through decreased reactive oxygen species that are scavenged before they give rise to DNA strand breaks. In contrast, chemotherapy resistance is thought to be associated with members of the adenosine triphosphate-binding cassette (ABC) transporter that transports drugs across the membrane. High levels of free radical scavengers in cancer stem cells will also make them refractory to certain chemotherapy agents such as bleomycin and doxorubicin. In addition to intrinsic mechanisms of resistance, cancer stem cells may also reside in specialized niches that are hypoxic or

impede chemotherapy activity.

The usual strategy to overcome the problem of induced resistance is to use a battery of different drugs, applied sequentially and cyclically, that produce their cytotoxicity by diverse mechanisms. By this strategy, cells that develop resistance to drug A are killed by drug B, and so on.

The bigger problem is pleiotropic resistance, the phenomenon by which the development of resistance to one drug results in cross-resistance to other drugs, even those with different mechanisms of action. There are four interesting points to be made:

1. Multidrug resistance in tumor cells is caused by extrusion of the drugs; that is, cells pump the drugs out as fast as they get in. This is mediated by increased expression of the product of the multiple drug resistance gene (*mdr*), a p-glycoprotein expressed in the cell membrane. This membrane protein is a polypeptide of 1,280 amino acids composed of two similar domains, each containing six potential transmembrane segments and two putative adenosine triphosphate-binding regions. Its structure is similar to that of various transporters of ions, amino acids, peptides, or proteins in bacterial, yeast, and animal cells. Indeed, it has been reported that the *mdr* gene in human tumor cells shows considerable homology to the gene in yeast that extrudes an attractant that is important in the reproductive cycle. The *mdr* gene has been mapped to human chromosome 7. Resistance by this means can be reversed by calcium channel-blocking drugs, such as verapamil. This has been shown to be an important mechanism of resistance to doxorubicin in Chinese hamster ovary (CHO) cells in culture, and there appears to be expression of this same gene for resistance in cells from some human solid tumors that have acquired resistance.
2. Glutathione is a naturally occurring thiol in all cells. Elevated levels of glutathione have been observed in resistant cells, especially those made resistant by treatment with melphalan. Drugs are available that block the synthesis of glutathione and that can be used to lower the levels of this compound in tumors and normal tissues. The best known example is buthionine sulfoximine. Use of buthionine sulfoximine has been shown to reduce cross-resistance, particularly between melphalan and *cis*-platinum in tumor-bearing mice. The use of buthionine sulfoximine would not be advisable in combination with doxorubicin or *cis*-platinum because an increase in specific normal tissue toxicity (lung or kidney, respectively) would be expected.

3. A marked increase in DNA repair has been noted in some cells resistant to melphalan or *cis*-platinum. In principle, drugs could be used to block repair; aphidicolin has been used in experimental systems, but no suitable drugs are available for clinical use.
4. A debatable issue is whether cells that have acquired resistance to chemotherapeutic agents are also resistant to radiation. The consensus is that they are not. There may be some data from clinical experience to suggest that they are, but the laboratory data show rather clearly that acquiring resistance to a drug does not necessarily result in radioresistance. This is illustrated in [Figure 27.12](#), in which cells that have acquired extreme resistance to melphalan show a normal response to radiation. Radioresistance and chemoresistance may occur together, but radiation rarely induces chemoresistance and vice versa.

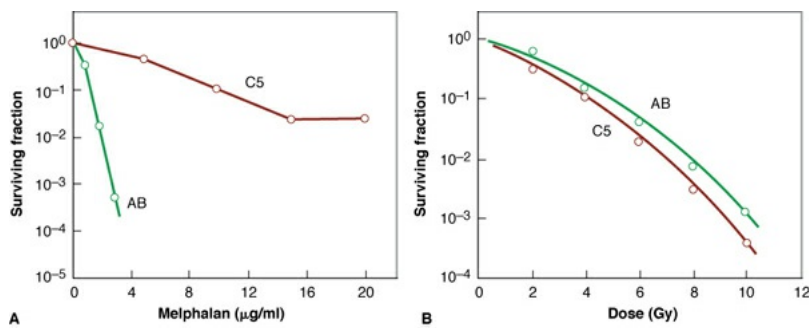


FIGURE 27.12 Chinese hamster pleiotropic multidrug-resistant cells are not necessarily resistant to radiation. The parental ovary cell line is designated *AB*. The multidrug-resistant cell line *C5* was isolated by Dr. Victor Ling by exposing the parental line to the mutagen ethyl methane sulfonate, after which surviving cells were grown for an extended period in increasing concentrations of colchicine. A clone was isolated that is resistant to colchicine and to various chemotherapeutic agents. **A:** *C5* cells are resistant to melphalan, compared with the parental line (*AB*). They are also resistant to other agents, such as daunorubicin. **B:** The radiation responses of the parental and the chemotherapy-resistant cell lines are virtually indistinguishable. (Adapted from Mitchell JB, Gamson J, Russo A, et al. Chinese hamster pleiotropic multidrug-resistant cells are not radioresistant. *NCI Monogr.* 1988;6:187–191, with permission.)

The evolving story of drug resistance has an impact on the development and screening of new drugs. In the past, the initial screening for new agents consisted of fast-growing, highly drug-sensitive mouse tumors. Tests against specific patterns or types of drug resistance were not included. The screening systems, therefore, were weighted heavily in favor of producing more of the same types of

drugs. This has changed, and the screening of new drugs for activity is performed using a battery of cells of human origin cultured *in vitro*.

COMPARISON OF CHEMOTHERAPEUTIC AGENTS WITH RADIATION

The title of this chapter includes the words “from the perspective of the radiation biologist.” This limited and specialized viewpoint must be kept in mind in what follows. Several important differences are evident in the response of cells to chemotherapeutic agents versus ionizing radiation:

1. There is a much greater variation of sensitivity to chemotherapeutic agents than there is to radiation. In the case of x-rays, the variation of D_0 from the most sensitive to the most resistant known mammalian cells may be a factor of about four. By contrast, the response of various cell lines to a given chemotherapeutic agent may differ by orders of magnitude. A particular cell line may be exquisitely sensitive to one drug and extremely resistant to another. A different cell line may have a different order of sensitivity to various drugs as well as a quite different absolute sensitivity. Different clones derived from a common stock may exhibit quite different sensitivity to a given agent. This variability is shown in [Figure 27.13](#), which gives the response of one cell line to nine different cytotoxic agents, and in [Figure 27.14](#), which shows the widely different response to methyl CCNU of three permanent clones derived from a common astrocytoma cell line.

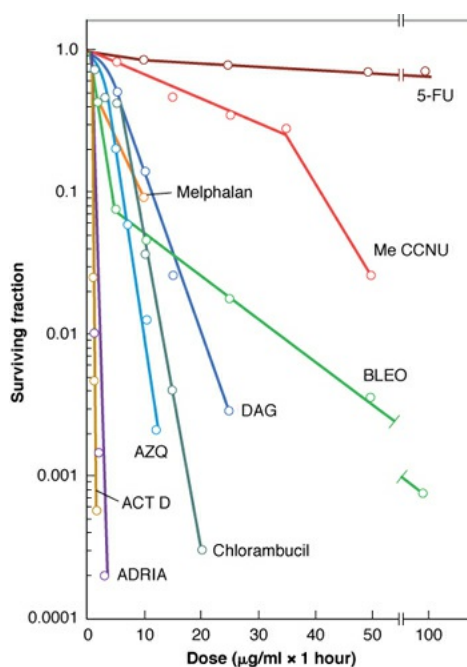


FIGURE 27.13 Comparison of dose–response curves of a stomach cancer cell

line in culture exposed for 1 hour to graded doses of nine anticancer drugs. There is a wide variation in sensitivity and in the shape of the various curves. Me CCNU, methyl chloroethyl-cyclohexyl-nitrosourea; BLEO, bleomycin; DAG, dianhydrogalactitol; AZQ, aziridinylbenzoquinone; ACT D, actinomycin D; ADRIA, Adriamycin. (Adapted from Barranco SC, Townsend CM Jr, Quraishi MA, et al. Heterogeneous responses of an in vitro model of human stomach cancer to anticancer drugs. *Invest New Drugs*. 1983;1[2]:117–127, with permission.)

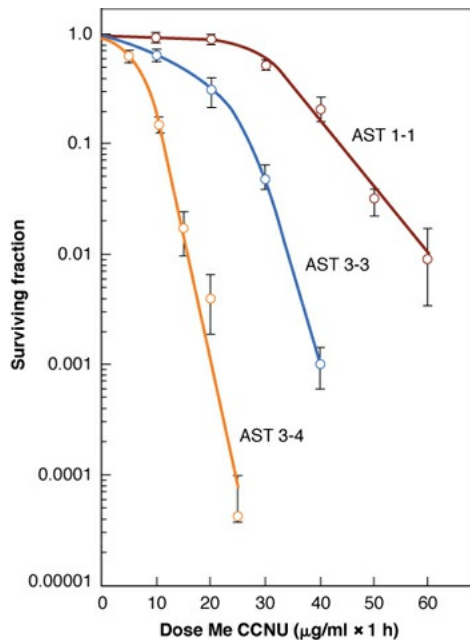


FIGURE 27.14 Dose–response data for three permanent clones derived from a common astrocytoma cell line exposed to the anticancer drug methyl chloroethyl-cyclohexyl-nitrosourea (Me CCNU). Note the great variation in sensitivity. (Adapted from Rubin NH, Casartelli C, Macik BG, et al. In vitro cellular characteristics and survival responses of human astrocytoma clones to chloroethyl-nitrosoureas and dianhydrogalactitol. *Invest New Drugs*. 1983;1:129–137, with permission.)

2. The sensitivity of a given cell line to a given drug may be manipulated to a much greater extent than for radiation.
3. Repair of sublethal and potentially lethal damage is more variable and less predictable for drugs than for radiation.
4. The oxygen effect is more complex for drugs than for ionizing radiations. For radiation, the presence or absence of molecular oxygen has an important influence on the proportion of cells surviving a given dose of low–linear energy transfer (LET) radiation, in which about two-thirds of the damage is

caused by indirect action (i.e., mediated by free radicals). As the LET of the radiation increases and the balance shifts from indirect to direct action, the importance of oxygen decreases. For very high-LET radiations (above about 200 keV/ μ m), the biologic effect for a given dose is independent of the presence or absence of molecular oxygen. Under no circumstances is oxygen protective in the case of ionizing radiations.

For drugs in which the biologic effect involves free radicals, the presence or absence of oxygen is important in the same way as for low-LET ionizing radiations. The new factor in the case of drugs is that there is a whole class of antineoplastic agents that undergo bioreduction in the absence of oxygen so that they are more effective in hypoxic cells. There is no parallel for ionizing radiations.

Other agents do not depend primarily on free radicals for their biologic effects, nor do they undergo bioreduction under hypoxic conditions; consequently, the effect of a given treatment is independent of the presence or absence of molecular oxygen, a property these agents have in common with very densely ionizing radiations.

5. Resistance to drugs develops more quickly and more regularly than it does to radiation. Acquired resistance to drugs does not necessarily involve resistance to x-rays as well.
6. Drug resistance may be caused by changes in thiol levels or by molecular changes observable at the chromosome level that result in the activation of a gene that functions to pump the drug out of the cells.

ADJUNCT USE OF CHEMOTHERAPEUTIC AGENTS WITH RADIATION

The initial rationale for the combination of radiation and chemotherapeutic agents was what is usually known as “spatial cooperation” ([Fig. 27.15](#)). Radiation may be more effective for controlling the localized primary tumor because it can be aimed and large doses are given, but it is difficult to use against disseminated disease. Chemotherapy, on the other hand, may be able to cope with micrometastases, whereas it could not control the larger primary tumor. In other situations, chemotherapy is the primary treatment modality, and radiation is used only to treat “sanctuary” sites not reached by the drug.

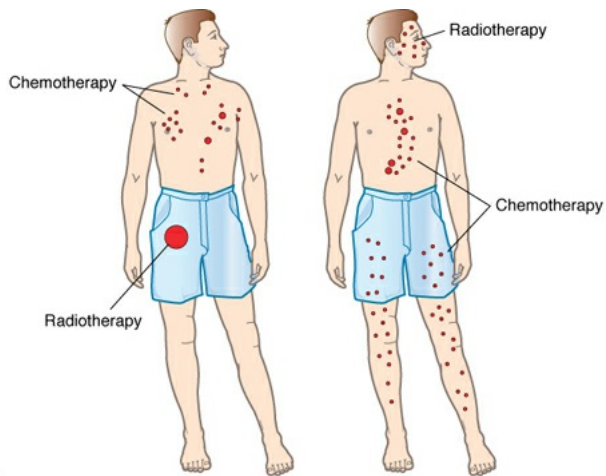


FIGURE 27.15 Spatial cooperation. **A:** In some instances, radiation may be used to treat a large primary tumor, with chemotherapy added to cope with systemic disease in the form of disseminated metastases. **B:** In other situations, chemotherapy may be used as the primary treatment, with radiation added to treat “sanctuary” sites that the cytotoxic drug cannot reach.

Although spatial cooperation was the original rationale, it is no longer the only one. Radiation and chemotherapeutic agents are combined in an attempt to achieve better local control. A specific example is the integrated use of taxanes and x-rays for the treatment of breast cancer. This is based on laboratory experiments *in vitro*. The initial hypothesis for the mechanism of interaction is that cell cycle alterations induced by paclitaxel leave cells in a state in which they are more sensitive to radiation. This is illustrated in Figure 27.16, which shows survival curves for astrocytoma cells of human origin cultured *in vitro* and exposed to graded doses of γ -rays, either alone or following a 24-hour treatment with 10-nM paclitaxel. This drug treatment alone kills about 95% of the cells and accumulates the survivors in the radiosensitive G₂/M phase (see Fig. 27.16, inset).

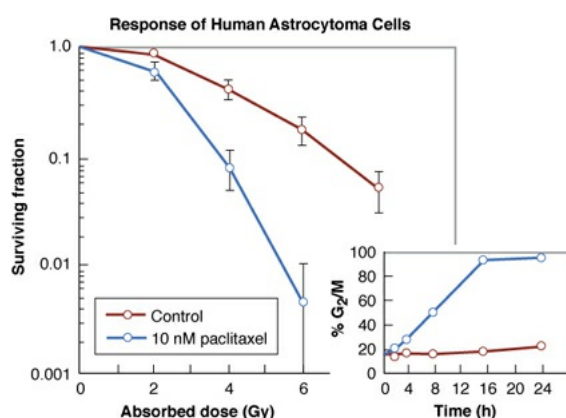


FIGURE 27.16 Survival curves for astrocytoma cells of human origin exposed

to graded doses of γ -rays alone and after a 24-hour treatment with a 10-nM concentration of paclitaxel. This drug concentration killed 95% of the cells and, as indicated by the inset, synchronized the survivors in the radiosensitive phase of the cell cycle. (Data from Tishler RB, Geard CR, Hall EJ, et al. Taxol sensitizes human astrocytoma cells to radiation. *Cancer Res.* 1992;52:3495–3497.)

Inasmuch as the cell killing resulting from the combination of drug and radiation is greater than the sum of the two separately, the interaction may be described as “synergistic.” For this to occur, the drug must accumulate some cells in G₂/M, which is a radiosensitive phase of the cycle, without killing them. Although similar results have been obtained for several cell lines, there are a significant number of reports in the literature in which the interaction between radiation and paclitaxel was shown to be purely additive. Additivity is observed in any cell line in which the G₂/M-arrested cells are doomed to die as a consequence of the drug alone. Even an additive interaction, however, may be therapeutically useful. For example, in animal tumors *in vivo*, the paclitaxel-induced death of G₂/M cells can lead to tumor shrinkage and reoxygenation, which result in an enhanced response to subsequent irradiation.

Although the initial rationale for the combination of taxanes and radiation was based on classic radiobiologic considerations regarding the cell cycle dependence of radiosensitivity, there are other possible explanations for a synergistic effect if the two agents are used together. For example, the contribution of *p53* to paclitaxel-dependent cytotoxicity is in marked contrast with its role for DNA-damaging agents such as radiation. Cells with a mutant *p53* phenotype are more sensitive to paclitaxel treatment than are nontransformed or wild-type *p53* cells. This finding explains the effectiveness of paclitaxel as a cytotoxic agent alone as well as for the efficacy of its combination with radiation. In this theory, paclitaxel and radiation act as non-cross-resistant agents; radiation is more effective against wild-type *p53* cells in a tumor population, and paclitaxel is relatively more cytotoxic to cells with a mutant *p53* phenotype.

In general, a therapeutic gain requires differential effects between tumor and normal tissue. One or more of the following tumor characteristics may be exploited to achieve this difference:

1. Genetic instability of tumor cells
2. Rapid proliferation of some tumor cells

- 3.** Cell age distribution of tumor cell populations
- 4.** Hypoxia (characteristic of larger tumors)
- 5.** pH (often low in tumors)
- 6.** Elevation of specific pathways in tumors (e.g., EGFR)

The goal of combining the two modalities of radiation and cytotoxic drugs is to increase local tumor control, relapse-free survival, and overall survival and to alter the pattern of relapse. Three obvious strategies are (1) to start chemotherapy after the completion of the local treatment (*adjuvant chemotherapy*), (2) to start chemotherapy before the local treatment (*induction chemotherapy*), or (3) to give chemotherapy during local treatment (*concurrent chemotherapy*). Most cytotoxic agents do not provide enough differential sensitization of tumors compared with normal tissues; consequently, the probability of dose-limiting or life-threatening toxicity to critical tissues may be increased.

Integrating surgery, chemotherapy, and radiotherapy has been found to increase materially the cure rate of a dozen or more experimental animal tumors. Emerging principles include the following:

- 1.** The lower the initial body burden of the tumor, the better.
- 2.** A maximally effective drug regimen should begin as soon as possible after surgery, with maximum practicable doses.
- 3.** Concurrent chemotherapy may lead to improved local control but at the price of increased local toxicity.

Improving local control can improve overall survival rates and avoid uncontrolled local growth and the possible need for mutilating surgery. For example, induction chemotherapy prior to radiation therapy has a proven benefit in larynx preservation. For this reason alone, aggressive use of combined modalities to improve local control is warranted.

It has often been said that “you can only kill the sensitive cells once.” There is no point in using a battery of different agents that all target the same subpopulation of sensitive cells. Rather, the *heterogeneity* of the tumor cell population should be acknowledged and exploited. One agent should be effective against cycling cells, another against resting cells, and a third perhaps against hypoxic cells; in other words, the strategy should be to combine agents that specifically attack the different subpopulations in the tumor.

A problem to be avoided is the triggering of “accelerated repopulation.” This

refers to triggering surviving clonogens to divide and repopulate even more rapidly as a tumor shrinks after treatment with a cytotoxic agent. It is a phenomenon described in [Chapter 22](#). It may be one of the reasons why radiotherapy after induction chemotherapy has shown disappointing results.

ASSAYS FOR SENSITIVITY OF INDIVIDUAL TUMORS

A great deal of effort has been expended to develop ways to assess which agents are likely to be effective for a particular tumor. The long-term goal would be to mimic the testing of a bacterial infection for sensitivity to a wide range of antibiotic drugs to select the one most suitable and effective.

One approach is to take biopsy specimens from a tumor in a patient, grow the cells *in vitro*, and subject the cells to a battery of chemotherapeutic agents in the petri dish. This approach has the advantages of not being too expensive to be practical and of providing answers quickly enough to influence the treatment and modify the protocol of the patient from whom the cells were taken. It suffers, of course, from the obvious disadvantages of focusing attention solely on the question of inherent cellular sensitivity and not addressing the questions of drug access, hypoxia, or any of the more complex factors involved as determinants of overall tumor response.

A different approach is to grow cells from human tumors as xenografts in immune-suppressed mice. This is a difficult and limited technique beset with problems, some of which are discussed in [Chapter 21](#). Human tumor cells, however, maintain many characteristics of the clinical response of the donor tumors. Indeed, there is a good correlation between clinical remission in donor patients and growth delay in xenografts established from transplanted cells. The method of establishing xenografts and then performing the necessary growth delay experiments is sufficiently slow and time-consuming that the technique cannot be expected ever to provide realistic input into deciding treatment strategy in individual patients, although it can provide guidance on the sensitivity of broad categories of human tumors to a battery of chemotherapeutic agents.

SECOND MALIGNANCIES

Late effects are the key to the acceptance of combined treatments. The induction of second malignancies is one of the unfortunate late effects of treatment with radiation or cytotoxic drugs. In a large series of 3,000 patients with Hodgkin disease treated with a combination of radiotherapy and chemotherapy, 114 developed second malignancies. The greatest relative risk was leukemia, but the

greatest in number were solid tumors.

Radiation is a relatively weak carcinogen; chemotherapeutic agents vary widely. There is a choice of many chemotherapeutic agents, and the variable potential for producing a second malignancy must be a factor influencing the choice of drug in patients who are likely to be long-term survivors.

Table 27.3 compares radiation, bleomycin, ultraviolet radiation, and benzopyrene in terms of the number of DNA lesions per cell necessary to kill 63% of the cell population, that is, to allow 37% to survive. Radiation is characterized by a relatively small number of DSBs, only about 40 per cell on average, at a dose that allows 37% of the cells to survive. At the other extreme, ultraviolet light produces 1 million dimers, and benzopyrene produces 100,000 lesions for the same level of survival. These interesting figures show that radiation is a weak carcinogen because it is efficient at killing cells; the same is true of bleomycin. By contrast, benzopyrene produces many more DNA lesions for a given level of cell killing and is therefore a powerful carcinogen; ultraviolet light is in the same category.

Table 27.3 Lesions Produced for a Given Level of Cell Killing by Various Cytotoxic Agents

AGENT	D ₃₇	DNA LESION	NUMBER OF LESIONS PER CELL PER D ₃₇
X-rays	1 Gy	SSB	1,000
		DSB	40
Bleomycin	5.5 µg × 1 h	SSB	150
		DSB	30

Ultraviolet light	10 J/m ²	TT dimer	1,000,000
		SSB	100
Benzopyrene	—	Adduct	100,000

SSB, single-strand break; DSB, double-strand break; TT, thymine-thymine.

Courtesy of Dr. John Ward, University of California, San Francisco.

It is an interesting speculation, supported by these data, that the factor that determines whether an agent is a powerful or a weak carcinogen is the number of DNA lesions required, on average, to kill a cell. If the number is small, the agent is an efficient cytotoxic agent but is likely to be a weaker carcinogen. If the number is large, there will be many DNA lesions in cells that are not killed, and some of these lesions may involve the transformation to a neoplastic state.

SUMMARY OF PERTINENT CONCLUSIONS

Single chemotherapeutic agents have been used successfully to cure a few rapidly proliferating tumors.

Combinations of drugs are used routinely for the treatment of various malignancies.

Most anticancer drugs work by affecting DNA synthesis or function.

Inevitably, many traditional anticancer drugs are toxic to stem cells of the intestinal epithelium and hematopoietic stem cells because they have a high growth fraction. Some of the new targeted therapy drugs (e.g., cetuximab) have the potential to increase tumor response with minimal effect on normal tissue toxicity.

Agents that are mainly effective during a particular phase of the cell cycle, such as the S phase or M phase, are said to be cell cycle specific, or phase specific.

Agents whose action is independent of the position of the cell in the cycle are said to be cell cycle nonspecific, or phase nonspecific.

Many classically used chemotherapeutic agents fall into one of several classes:

Alkylating agents, which are highly active, with the ability to substitute alkyl groups for hydrogen atoms in DNA, include nitrogen mustard derivatives, cyclophosphamide, chlorambucil, melphalan, and the nitrosoureas (BCNU and CCNU).

Antibiotics, which bind to DNA and inhibit DNA and RNA synthesis, include dactinomycin, doxorubicin, daunorubicin, and bleomycin.

Antimetabolites, which are analogues of the normal metabolites required for cell function and replication, include methotrexate, 5-FU, cytarabine, and 5-azacytidine.

Many of the newer and widely used drugs do not fall into any of these classes, including the vinca alkaloids, the taxanes, procarbazine, hydroxyurea, platinum complexes, topoisomerase inhibitors, and “targeted therapy” agents that target a specific pathway that may be elevated in some tumors (cetuximab [Erbitux], trastuzumab [Herceptin], imatinib mesylate [Gleevec], and rituximab [Rituxan]).

Dose-response relationships for many chemotherapeutic agents resemble those for radiation, with drug concentration replacing absorbed dose; that is, there is an initial shoulder followed by an exponential relationship between surviving fraction and dose. The exceptions are doxorubicin, bleomycin, dactinomycin, and taxanes, which have dose-response curves that are concave upward.

At best, traditional anticancer drugs kill cells by first-order kinetics; that is, a given dose kills a constant fraction of cells. Consequently, the chance of eradicating a cancer is greatest if the population size is small (i.e., there is an inverse relationship between curability and tumor cell burden) at the initiation of chemotherapy.

Studies of sublethal damage and potentially lethal damage are more confusing and less clear-cut for drugs than for radiation.

Some drugs (e.g., bleomycin) are more toxic to aerated than to hypoxic cells. For these drugs, free radicals are involved in the mechanism of cell killing, as is the case for x-rays.

Some drugs (such as mitomycin C) are more toxic to hypoxic than to aerated cells because they undergo bioreduction. This applies also to tirapazamine, as discussed in [Chapter 26](#).

Other drugs (including 5-FU, methotrexate, *cis*-platinum, and the nitrosoureas)

appear to be equally cytotoxic to aerated and hypoxic cells.

The effectiveness of chemotherapeutic agents decreases with distance from a capillary because the drug concentration falls off because of metabolism and because cells are not proliferating because they are hypoxic.

Drug resistance is the biggest single problem in chemotherapy. For example, cells exposed continuously to low levels of doxorubicin become very resistant to subsequent treatments with this drug.

The usual strategy to overcome resistance to cytotoxic chemotherapy is to use a battery of drugs that produce cytotoxicity by diverse mechanisms.

The strategy to overcome resistance to targeted therapy is to identify the molecular basis of resistance.

Pleiotropic resistance occurs if the development of resistance to one drug results in cross-resistance to other drugs with a different mechanism of action.

Resistance may be associated with the following: decreased drug accumulation and the expression of p-glycoproteins in the cell membrane from gene amplification, elevated levels of glutathione, and marked increase in DNA repair.

Radioresistance and chemoresistance may occur together, but radiation rarely induces chemoresistance and vice versa.

The adjunct use of chemotherapy with radiation may involve sequential or concurrent treatments.

The extent to which chemotherapeutic agents show synergy with radiation varies widely. Some interact strongly (e.g., doxorubicin, gemcitabine), others less so, and some not at all (see [Table 27.1](#).)

Antiangiogenic agents can enhance the efficacy of fractionated radiotherapy but can increase normal tissue toxicity when combined with SBRT.

Some agents penetrate the blood–brain barrier (e.g., BCNU, temozolomide, cytosine arabinoside, hydroxyurea), others only at high intravenous doses (e.g., methotrexate), whereas many do not cross the blood–brain barrier at all (see [Table 27.1](#)).

A therapeutic gain requires a differential between tumor and normal tissue. This may be achieved by exploiting one or more of the following tumor characteristics: genetic instability, rapid proliferation, cell age distribution,

hypoxia, pH, and dysregulated signaling pathways (e.g., EGFR).

Sensitive cells can be killed only once. Tumor heterogeneity should be exploited by using a combination of drugs effective against different cell subpopulations.

Sensitivity of individual tumors to chemotherapeutic agents with or without radiation may be assessed by the following: *in vitro* clonogenic assays, xenografts in nude mice, micronuclei in treated cells.

Synthetic lethality is the basis for using PARP inhibitors to treat patients with defects in the homologous recombination repair (HRR) such as BRCA1.

Targeted therapies such as cetuximab have been demonstrated to work well in combination with radiotherapy in the treatment of head and neck cancer.

PD-1 is located on the surface of a T cell, and if it binds to PD-L1 or PD-L2, the T cell becomes inactive.

T-cell checkpoint therapeutics work by blocking inhibitory signals (PD-L1 or PD-L2 binding to PD-1) that prevent activated T-cells from attacking the cancer.

T-cell checkpoint therapeutics are now being tested in combination with radiotherapy and in some cases have resulted in dramatic responses.

BIBLIOGRAPHY

Barranco SC. In vitro responses of mammalian cells to drug-induced potentially lethal and sublethal damage. *Cancer Treat Rep.* 1976;60:1799–1810.

Barranco SC, Flournoy DR. Modification of the response to actinomycin-D-induced sublethal damage by simultaneous recovery from potentially lethal damage in mammalian cells. *Cancer Res.* 1976;36:1634–1640.

Barranco SC, Humphrey RM. Response of mammalian cells to bleomycin-induced potentially lethal and sublethal damage. *Prog Biochem Pharmacol.* 1976;11:78–92.

Barranco SC, Novak JJJ, Humphrey RM. Response of mammalian cells following treatment with bleomycin and 1,3-bis(2-chloroethyl)-1-nitrosourea during plateau phase. *Cancer Res.* 1973;33:691–694.

Barranco SC, Townsend CM Jr, Quraishi MA, et al. Heterogeneous responses of an *in vitro* model of human stomach cancer to anticancer drugs. *Invest New Drugs.* 1983;1(2):117–127.

- Belli JA. Radiation response and Adriamycin resistance in mammalian cells in culture. *Front Radiat Ther Oncol.* 1979;13:9–20.
- Belli JA, Piro AJ. The interaction between radiation and Adriamycin damage in mammalian cells. *Cancer Res.* 1977;37:1624–1630.
- Bissery MC, Vrignaud P, Lavelle F. Preclinical profile of docetaxel (Taxotere): efficacy as a single agent and in combination. *Semin Oncol.* 1995;22(6 suppl 13):3–16.
- Boice JD Jr, Greene MH, Killen JY Jr, et al. Leukemia and preleukemia after adjuvant treatment of gastrointestinal cancer with semustine (methyl-CCNU). *N Engl J Med.* 1983;309:1079–1084.
- Bonadonna G, Valagussa P. Dose–response effect of CMF in breast cancer. *Proc Am Soc Clin Oncol.* 1980;21:413.
- Bonner JA, Harari PM, Giralt J, et al. Radiotherapy plus cetuximab for locoregionally advanced head and neck cancer: 5-year survival data from a phase 3 randomised trial, and relation between cetuximab-induced rash and survival. *Lancet Oncol.* 2010;11:21–28.
- Bonner JA, Harari PM, Giralt J, et al. Radiotherapy plus cetuximab for squamous-cell carcinoma of the head and neck. *N Engl J Med.* 2006;354:567–578.
- Brown JM, Siim BG. Hypoxia-specific cytotoxins in cancer therapy. *Semin Radiat Oncol.* 1996;6:22–36.
- Carney DN, Winkler CF. In vitro assays of chemotherapeutic sensitivity. *Important Adv Oncol.* 1985;78–103.
- Chabner BA. Karnofsky memorial lecture. The oncologic end game. *J Clin Oncol.* 1986;4:625–638.
- Chabner BA, Sponzo R, Hubbard S, et al. High-dose intermittent intravenous infusion of procarbazine (NSC-77213). *Cancer Chemother Rep.* 1973;57:361–363.
- Chan HS, Haddad G, Thorner PS, et al. P-Glycoprotein expression as a predictor of the outcome of therapy for neuroblastoma. *N Engl J Med.* 1991;325:1608–1614.
- Cowan KH, Goldsmith ME, Levine RM, et al. Dihydrofolate reductase gene amplification and possible rearrangement in estrogen-responsive methotrexate-resistant human breast cancer cells. *J Biol Chem.*

- 1982;257:15079–15086.
- Curt GA, Carney DN, Cowan KH, et al. Unstable methotrexate resistance in human small-cell carcinoma associated with double minute chromosomes. *N Engl J Med.* 1983;308:199–202.
- Debenham PG, Kartner H, Siminovitch L, et al. DNA-mediated transfer of multiple drug resistance and plasma membrane glycoprotein expression. *Mol Cell Biol.* 1982;2:881–889.
- DeVita VT Jr. Cell kinetics and the chemotherapy of cancer. *Cancer Chemother Rep.* 1971;2:23–33.
- DeVita VT Jr. The James Ewing lecture: The relationship between tumor mass and resistance to chemotherapy. Implications for surgical adjuvant treatment of cancer. *Cancer.* 1983;51:1209–1220.
- DeVita VT Jr, Goldin A, Oliverio VT, et al. The drug development program and clinical trials programs of the Division of Cancer Treatment, National Cancer Institute. *Cancer Clin Trials.* 1979;2:195–216.
- DeVita VT Jr, Henney JE, Hubbard SM. Estimation of the numerical and economic impact of chemotherapy in the treatment of cancer. In: Burchenal JH, Oettgen HS, eds. *Cancer—Achievements, Challenges, and Prospects for the 1980s.* New York, NY: Grune & Stratton; 1981:857–880.
- DeVita VT Jr, Henney JE, Stonehill E. Cancer mortality: the good news. In: Jones SE, Salmon SE, eds. *Adjuvant Therapy of Cancer II.* New York, NY: Grune & Stratton; 1979:212–216.
- DeVita VT Jr, Serpick AA, Carbone PP. Combination chemotherapy in the treatment of advanced Hodgkin's disease. *Ann Intern Med.* 1970;73:881–895.
- Duda DG, Jain RK, Willett CG. Antiangiogenics: the potential role of integrating this novel treatment modality with chemoradiation for solid cancers. *J Clin Oncol.* 2007;25:4033–4042.
- Durand RE. The influence of microenvironmental factors during cancer therapy. *In Vivo.* 1994;8:691–702.
- Elkind MM, Kano E, Sutton-Gilbert H. Cell killing by actinomycin D in relation to the growth cycle of Chinese hamster cells. *J Cell Biol.* 1969;42:366–377.
- Endicott JA, Ling V. The biochemistry of P-glycoprotein-mediated drug resistance. *Annu Rev Biochem.* 1989;58:137–171.

- Erlich E, McCall AR, Potkul RK, et al. Paclitaxel is only a weak radiosensitizer of human cervical carcinoma cell lines. *Gynecol Oncol*. 1996;60:251–254.
- Fine RL, Patel J, Allegra CJ, et al. Increased phosphorylation of a 20,000 new protein in pleiotropic drug-resistant MCH-7 human breast cancer lines. *Proc Am Assoc Cancer Res*. 1985;26:345.
- Frei E III. The clinical use of actinomycin. *Cancer Chemother Rep*. 1974;58:49–54.
- Frei E III, Canellos GP. Dose: a critical factor in cancer chemotherapy. *Am J Med*. 1980;69:585–594.
- Frei E III, Freireich EJ, Gehan E, et al. Studies of sequential and combination antimetabolite therapy in acute leukemia: 6-mercaptopurine and methotrexate. *Blood*. 1961;18:431–454.
- Geard CR, Jones JM, Schiff PB. Taxol and radiation. *J Natl Cancer Inst Monogr*. 1993;15:89–94.
- Gottesman MM, Pastan I. The multidrug transporter, a double-edged sword. *J Biol Chem*. 1988;263:12163–12166.
- Gottesman MM, Schoenlien PV, Currier SJ, et al. Biochemical basis for multidrug resistance in cancer. In: Pretlow TG, Pretlow TP, eds. *Biochemical and Molecular Aspects of Selected Cancers*. San Diego, CA: Academic Press; 1991:339–371.
- Graeber TG, Osmanian C, Jacks T, et al. Hypoxia-mediated selection of cells with diminished apoptotic potential in solid tumours. *Nature*. 1996;379:88–91.
- Grandis JR, Melhem MF, Gooding WE, et al. Levels of TGF-alpha and EGFR protein in head and neck squamous cell carcinoma and patient survival. *J Natl Cancer Inst*. 1998;90:824–832.
- Green SL, Giaccia AJ. Tumor hypoxia and the cell cycle: implications for malignant progression and response to therapy. *Cancer J Sci Am*. 1998;4:218–223.
- Hamburger AW, Salmon SE. Primary bioassay of human tumor stem cells. *Science*. 1977;197:461–463.
- Hennequin C, Giocanti N, Favaudon V. Interaction of ionizing radiation with paclitaxel (Taxol) and docetaxel (Taxotere) in HeLa and SQ20B cells. *Cancer Res*. 1996;56:1842–1850.

- Hockel M, Schlenger K, Aral B, et al. Association between tumor hypoxia and malignant progression in advanced cancer of the uterine cervix. *Cancer Res.* 1996;56:4509–4515.
- Hu G, Liu W, Mendelsohn J, et al. Expression of epidermal growth factor receptor and human papillomavirus E6/E7 proteins in cervical carcinoma cells. *J Natl Cancer Inst.* 1997;89:1271–1276.
- Hutchinson DJ. Cross-resistance and collateral sensitivity studies in cancer chemotherapy. In: Haddow A, Weinhouse S, eds. *Advances in Cancer Research*. Vol. 7. New York, NY: Academic Press; 1963:235–350.
- Hyde SC, Emsley P, Hartshorn MJ, et al. Structural model of ATP-binding proteins associated with cystic fibrosis, multidrug resistance and bacterial transport. *Nature*. 1990;346:362–365.
- Iihara K, Shiozaki H, Tahara H, et al. Prognostic significance of transforming growth factor-alpha in human esophageal carcinoma. Implication for the autocrine proliferation. *Cancer*. 1993;71:2902–2909.
- Jain RK. Barriers to drug delivery in solid tumors. *Sci Am.* 1994;271:58–65.
- Jain RK. Normalization of tumor vasculature: an emerging concept in antiangiogenic therapy. *Science*. 2005;307:58–62.
- Juranka PF, Zastawny RL, Ling V. P-Glycoprotein: multidrug-resistance and a superfamily of membrane-associated transport proteins. *FASEB J.* 1989;3:2583–2592.
- Klijn JG, Berns PM, Schmitz PI, et al. The clinical significance of epidermal growth factor receptor (EGF-R) in human breast cancer: a review on 5232 patients. *Endocr Rev.* 1992;13:3–17.
- Lee IP, Dixon RL. Mutagenicity, carcinogenicity, and teratogenicity of procarbazine. *Mutat Res.* 1978;55:1–14.
- Leonard CE, Chan DC, Chou TC, et al. Paclitaxel enhances in vitro radiosensitivity of squamous carcinoma cell lines of the head and neck. *Cancer Res.* 1996;56:5198–5204.
- Liebmann JE, Cook JA, Fisher J, et al. In vitro studies of Taxol as a radiation sensitizer in human tumor cells. *J Natl Cancer Inst.* 1994;86:441–446.
- Liebmann JE, Cook JA, Lipschultz C, et al. Cytotoxic studies of paclitaxel (Taxol) in human tumour cell lines. *Br J Cancer*. 1993;68:1104–1109.

- Liebmann JE, Hahn SM, Cook JA, et al. Glutathione depletion by L-buthionine sulfoximine antagonizes taxol cytotoxicity. *Cancer Res.* 1993;53:2066–2070.
- Ling V, Kartner N, Sudo T, et al. Multidrug-resistance phenotype in Chinese hamster ovary cells. *Cancer Treat Rep.* 1983;67:869–874.
- Ling V, Thompson LH. Reduced permeability in CHO cells as a mechanism of resistance to colchicine. *J Cell Physiol.* 1974;83:103–116.
- Lokeshwar BL, Ferrell SM, Block NL. Enhancement of radiation response of prostatic carcinoma by taxol: therapeutic potential for late-stage malignancy. *Anticancer Res.* 1995;15:93–98.
- Madoc-Jones H, Mauro F. Interphase action of vinblastine and vincristine: differences in their lethal action through the mitotic cycle of cultured mammalian cells. *J Cell Physiol.* 1968;72:185–196.
- Mendelsohn J. Epidermal growth factor receptor inhibition by a monoclonal antibody as anticancer therapy. *Clin Cancer Res.* 1997;3:2703–2707.
- Milas L, Hunter NR, Mason KA, et al. Role of reoxygenation in induction of enhancement of tumor radioresponse by paclitaxel. *Cancer Res.* 1995;55:3564–3568.
- Milas L, Mason K, Hunter N, et al. In vivo enhancement of tumor radioresponse by C225 antiepidermal growth factor receptor antibody. *Clin Cancer Res.* 2000;6:701–708.
- Milas L, Milas MM, Mason KA. Combination of taxanes with radiation: preclinical studies. *Semin Radiat Oncol.* 1999;9(suppl 1):12–26.
- Milross CG, Mason KA, Hunter NR, et al. Relationship of mitotic arrest and apoptosis to antitumor effect of paclitaxel. *J Natl Cancer Inst.* 1996;88:1308–1314.
- Mitchell JB, Gamson J, Russo A, et al. Chinese hamster pleiotropic multidrug-resistant cells are not radioresistant. *NCI Monogr.* 1988;6:187–191.
- Mote PA, Davey MW, Davey RA, et al. Paclitaxel sensitizes multidrug resistant cells to radiation. *Anticancer Drugs.* 1996;7:182–188.
- Piccart MJ, Gore M, Ten Bokkel Huinink W, et al. Docetaxel: an active new drug for treatment of advanced epithelial ovarian cancer. *J Natl Cancer Inst.* 1995;87:676–681.
- Postow MA, Callahan MK, Barker CA, et al. Immunologic correlates of the

- abscopal effect in a patient with melanoma. *N Engl J Med.* 2012;366:925–931.
- Rave-Fränk M, Meden H, Jäschke A, et al. The effect of paclitaxel on the radiosensitivity of gynecological tumor cells. *Strahlenther Onkol.* 1997;173:281–286.
- Roizin-Towle L, Hall EJ. Studies with bleomycin and misonidazole on aerated and hypoxic cells. *Br J Cancer.* 1978;37:254–260.
- Rouleau M, Patel A, Hendzel MJ, et al. PARP inhibition: PARP-1 and beyond. *Nat Rev Cancer.* 2010;10:293–301.
- Rowinsky EK, Donehower RC. Paclitaxel (Taxol). *N Engl J Med.* 1995;332:1004–1014.
- Rubin NH, Casartelli C, Macik BG, et al. In vitro cellular characteristics and survival responses of human astrocytoma clones to chloroethyl-nitrosoureas and dianhydrogalactitol. *Invest New Drugs.* 1983;1:129–137.
- Saito Y, Mitsuhashi N, Takahashi T, et al. Cytotoxic effect of paclitaxel (taxol) either alone or in combination with irradiation in two rat yolk sac tumour cell lines with different radiosensitivities in vitro. *Int J Radiat Biol.* 1998;73:225–231.
- Salmon SE. Application of the human tumor stem cell assay in the development of anticancer therapy. In: Burchenal JF, Oettgen HS, eds. *Cancer—Achievements, Challenges, and Prospects for the 1980s.* New York, NY: Grune & Stratton; 1981.
- Salmon SE, Hamburger AW, Soehnlen BJ, et al. Quantitation of differential sensitivity of human-tumor stem cells to anticancer drugs. *N Engl J Med.* 1978;298:1321–1327.
- Sartorelli AC. Approaches to the combination chemotherapy of transplantable neoplasms. *Prog Exp Tumor Res.* 1965;6:228–288.
- Schiff PB, Fant J, Horwitz SB. Promotion of microtubule assembly in vitro by Taxol. *Nature.* 1979;277:665–667.
- Schiff PB, Horwitz SB. Taxol stabilizes microtubules in mouse fibroblast cells. *Proc Natl Acad Sci USA.* 1980;77:1561–1565.
- Siemann DW, Keng PC. Characterization of radiation resistant hypoxic cell subpopulations in KHT sarcomas. (II). Cell sorting. *Br J Cancer.* 1988;58:296–300.

Skipper HE. Reasons for success and failure in treatment of murine leukemias with drugs now employed in treating human leukemias. In: *Cancer Chemotherapy*. Vol. 1. Ann Arbor, MI: University Microfilms International; 1978:1–166.

Skipper HE, Hutchison DJ, Schabel FM Jr, et al. A quick reference chart on cross-resistance between anticancer agents. *Cancer Chemother Rep.* 1972;56:493–498.

Skipper HE, Schabel FM Jr, Wilcox WS. Experimental evaluation of potential anticancer agents. XIII. On the criteria and kinetics associated with “curability” of experimental leukemia. *Cancer Chemother Rep.* 1964;35:1–111.

Tannock IF. Cell kinetics and chemotherapy: a critical review. *Cancer Treat Rep.* 1978;62:1117–1133.

Tannock IF. The relation between cell proliferation and the vascular system in a transplanted mouse mammary tumour. *Br J Cancer.* 1968;22:258–273.

Teicher BA, Lazo JS, Sartorelli AC. Classification of antineoplastic agents by their selective toxicities toward oxygenated and hypoxic tumor cells. *Cancer Res.* 1981;41:73–81.

Tishler RB, Geard CR, Hall EJ, et al. Taxol sensitizes human astrocytoma cells to radiation. *Cancer Res.* 1992;52:3495–3497.

Tishler RB, Schiff PB, Geard CR, et al. Taxol: a novel radiation sensitizer. *Int J Radiat Oncol Biol Phys.* 1992;22:613–617.

Trent JM, Buick RN, Olson S, et al. Cytologic evidence for gene amplification in methotrexate-resistant cells obtained from a patient with ovarian adenocarcinoma. *J Clin Oncol.* 1984;2:8–15.

Wahl AF, Donaldson KL, Fairchild C, et al. Loss of normal p53 function confers sensitization to Taxol by increasing G₂/M arrest and apoptosis. *Nat Med.* 1996;2:72–79.

Wani MC, Taylor HL, Wall ME, et al. Plant antitumor agents. VI. The isolation and structure of Taxol, a novel antileukemic and antitumor agent from *Taxus brevifolia*. *J Am Chem Soc.* 1971;93:2325–2327.

Weinstein JM, Magin RL, Cysyk RL, et al. Treatment of solid L1210 murine tumors with local hyperthermia and temperature-sensitive liposomes containing methotrexate. *Cancer Res.* 1980;40:1388–1395.

Willett CG, Boucher Y, di Tomaso E, et al. Direct evidence that the VEGF-specific antibody bevacizumab has antivascular effects in human rectal cancer. *Nat Med.* 2004;10:145–147.

chapter 28

Hyperthermia

Historical

Response to Heat at Cytotoxic Temperatures

Dose Response

Sensitivity to Heat as a Function of Cell Age in the Mitotic Cycle

Hypoxia and Hyperthermia

Effect of pH and Nutrient Deficiency on Sensitivity to Heat

Response of Normal Tissues to Heat

Thermotolerance

Heat and Tumor Vasculature

Methods of Heating and the Impact on Clinical Hyperthermia

Methods of Heating in Experimental Systems

Methods of Heating in Patients

Thermal Ablation

Response to Heat at Noncytotoxic Temperatures

Reoxygenation

Immunologic Effects of Hyperthermia

Thermal Enhancement Ratio

Heat and the Therapeutic Gain Factor

Measuring Thermal Dose in Patients

Phase III Clinical Trials Testing Benefits of Hyperthermia for Enhancing Radiation Therapy

Clinical Trials Assessing the Benefit of Hyperthermia in Combination with Chemotherapeutic Agents

Development and Evaluation of “Thermosensitive” Liposomes for Improved Tumor Targeting of Chemotherapy

Methods of Tumor Heating

Magnetic Hyperthermia

Clinical Thermometry

Invasive Thermometry Methods

Progress toward Clinically Achievable Noninvasive Thermometry

Summary of Pertinent Conclusions

Hyperthermia at Cytotoxic Temperatures (42° to 45° C)

Hyperthermia at Modest Temperatures that Can Be Achieved in Human Tumors

Bibliography

HISTORICAL

In Greek mythology, Prometheus, a demigod, stole fire from Olympus and taught humans how to use it. For this act, he was chained to a rock by Zeus, the king of the gods, and a vulture fed daily on his liver.

The use of hyperthermia for the treatment of cancer is certainly not new. The very first medical text known today contains a case study describing a patient with a breast tumor treated with hyperthermia. The case is cited in the Edwin Smith Surgical Papyrus, an Egyptian papyrus roll, which is said to date from more than 3,500 years ago and to be a copy of an even older text. Later, heat was used in all cultures as one of the most prominent medical therapies for almost any disease, including cancer. Thus, Hippocrates (470–377 BC), in one of his aphorisms, states, “Those who cannot be cured by medicine can be cured by surgery. Those who cannot be cured by surgery can be cured by fire [hyperthermia]. Those who cannot be cured by fire, they are indeed incurable.”

The attempt in more recent times to exploit elevated temperatures to treat cancer has a longer history than the use of ionizing radiations. In 1866, 30 years before Röntgen discovered “a new kind of ray,” the German physician W. Busch described a patient with a sarcoma in the face that disappeared after a prolonged infection with erysipelas, an infectious disease normally characterized by high fever. This and similar cases led the New York surgeon William B. Coley to believe that the bacteria causing erysipelas may be effective against cancer. He extracted a toxin (Coley toxin, or mixed bacterial toxin), with which he treated a number of patients.

Although it is difficult to evaluate the direct role of heat in this combined total-body hyperthermia and unspecific immunotherapy, the work by Coley initiated a number of other studies using local hyperthermia applied to patients and to tumors in experimental animals. In 1898, Westermark, a Swedish gynecologist, published a paper describing a marked regression of large

carcinomas of the uterine cervix after local hyperthermia, although the treatments involved were poorly controlled and the cases are largely anecdotal. The use of hyperthermia, either alone or in combination with radiation, has been attempted at irregular intervals over the years but has never found a permanent place in the management of cancer. Historical reviews of the early clinical use of hyperthermia can be found in several excellent articles (e.g., by Dewey and colleagues, 1977, and by Overgaard, 1984).

The modern discipline of thermal therapy emerged from a number of radiation-oriented laboratories in the mid to late 1970s. At this stage, the emphasis was on temperatures that caused cell killing. A brief description of the principal results follows.

RESPONSE TO HEAT AT CYTOTOXIC TEMPERATURES

Dose Response

It was shown that heat kills cells in a predictable and repeatable way. Figure 28.1 shows a series of survival curves for cells exposed for various periods of time to a range of temperatures from 41.5° to 46.5° C. The cell survival curves for heat are similar in shape to those obtained for x-rays (i.e., an initial shoulder followed by an exponential region) except that the time of exposure to the elevated temperature replaces the absorbed dose of x-rays.

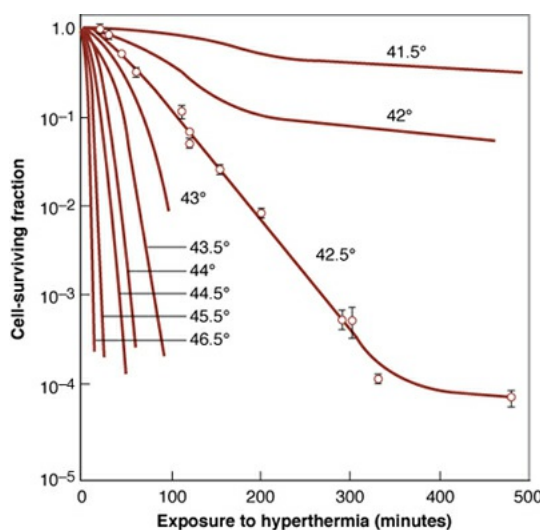


FIGURE 28.1 Survival curves for mammalian cells in culture (Chinese hamster ovary line) heated at different temperatures for varying lengths of time. (Adapted from Dewey WC, Hopwood LE, Sapareto LA, et al. Cellular responses to combinations of hyperthermia and radiation. *Radiology*. 1997;123:463–474, with

permission.)

For lower temperatures, the picture is complicated because the survival curves flatten out after a protracted exposure to hyperthermia, indicating the development of a resistance or tolerance to the elevated temperature. The similarity in the shape of the cell survival curves for heat and x-rays is misleading. It is important, therefore, not to draw conclusions for heat based on the interpretation of radiation dose-response curves because the amount of energy involved in cell inactivation is a thousand times greater for heat than for x-rays. This reflects the different mechanisms involved in cell killing by heat and x-rays.

Families of survival curves similar to those in [Figure 28.1](#) have been obtained for many different cell types, and it is clear that cells differ widely in their sensitivity to hyperthermia. As with ionizing radiations, there is no consistent difference between normal and malignant cells.

Survival data for cells exposed to various levels of hyperthermia (taken from [Fig. 28.1](#)) are replotted in [Figure 28.2](#), with $1/D_0$ on the ordinate and $1/T$ on the abscissa. T is the absolute temperature; D_0 is the reciprocal of the slope of the exponential region of the survival curve (i.e., the time at a given temperature that is necessary to reduce the fraction of surviving cells to 37% of their former value). This type of presentation is known as an **Arrhenius plot**; its slope gives the activation energy of the chemical process involved in the cell killing. The dramatic *change* of slope that occurs at a temperature of about 43° C , which means that the activation energy is different above and below this temperature, may reflect different mechanisms of cell killing (i.e., different targets for cytotoxicity above and below 43° C).

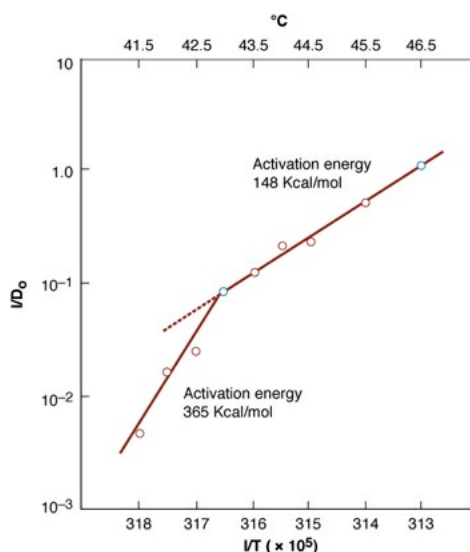


FIGURE 28.2 An Arrhenius plot for heat inactivation of mammalian cells in culture. The reciprocals of the D_0 values obtained for Figure 28.1 are plotted versus the reciprocal of the absolute temperature. (Adapted from Dewey WC, Hopwood LE, Sapareto LA, et al. Cellular responses to combinations of hyperthermia and radiation. *Radiology*. 1997;123:463–474, with permission.)

The similarity of the activation energy for protein denaturation to the activation energy for heat cytotoxicity, calculated from the Arrhenius analysis, led to the hypothesis that the target for heat cell killing may be a **protein**. The structural chromosomal proteins, nuclear matrix and cytoskeleton repair enzymes, and membrane components all have been identified as possible targets that are denatured by hyperthermia.

Sensitivity to Heat as a Function of Cell Age in the Mitotic Cycle

The age-response function for heat complements that for x-rays. The phase of the cycle most *resistant* to x-rays, late in the DNA synthetic phase (late S), is most *sensitive* to hyperthermia treatment. On this basis, cycling tumor cells should be killed selectively by hyperthermia compared with the slowly turning over normal tissues responsible for late effects that are in a G₁ or G₀ state.

Hypoxia and Hyperthermia

The response of hypoxic cells constitutes a vital difference between x-rays and hyperthermia. Hypoxia protects cells from killing by x-rays. By contrast, hypoxic cells are not more resistant than aerobic cells to hyperthermia; indeed, the evidence suggests that under some conditions, they may be slightly more sensitive to hyperthermia.

Effect of pH and Nutrient Deficiency on Sensitivity to Heat

Cells in an acid pH environment appear to be more sensitive to killing by heat. This is certainly true of cells treated with heat soon after their environmental pH is altered by adjusting the buffer. The intracellular pH (pH_i) of cells in an acidic environment is slightly higher than the extracellular pH (pH_e). The pH dependence of cytotoxicity at elevated temperatures, however, is affected by pH history. Cells can adapt to pH changes and avoid the pH_i heat sensitivity shown for low pH.

Cells deficient in nutrients are certainly heat sensitive. This can be

demonstrated with cells in culture, in which sensitivity to heat increases progressively as cells have their energy supply compromised, either by depriving them of glucose or by the use of a drug that uncouples oxidative phosphorylation.

These conclusions about pH and nutrients, obtained under controlled conditions with cells in culture, led to the speculation that cells in tumors that are nutritionally deprived and at acid pH because of their location remote from a blood capillary may be particularly sensitive to heat. Because of their environment, it is likely that these cells are out of cycle and possibly hypoxic also. This conclusion certainly correlates with the observation that large necrotic tumors often shrink dramatically after a heat treatment (HT). In this context, also, heat and x-rays appear to be complementary in their action because the cells that are most resistant to x-rays (out of cycle and hypoxic because of their remoteness from a capillary) show enhanced sensitivity to heat.

Response of Normal Tissues to Heat

Normal tissues respond to heat in a way that is substantially different from their more familiar response to x-rays. The principal difference is that after irradiation, cells die only in attempting the next or a subsequent mitosis (except in very unusual circumstances), whereas heated cells die by apoptosis so that heat damage is expressed early. In addition, heat affects differentiated as well as dividing cells. The familiar delay between exposure to x-rays and the subsequent response of a cell renewal tissue is because moderate doses of x-rays kill the dividing stem cells and leave the differentiated cells functional. The response is delayed for a time that is related to the natural lifetime of the mature differentiated cells and the time it takes for stem cells to progress through the process of differentiation and become functional. This delay is absent in the case of heat because all cells are affected, differentiated or dividing; the damage to the tissue is expressed immediately.

Thermotolerance

The development of a transient and nonhereditary resistance to subsequent heating by an initial HT has been described variously as induced thermal resistance, thermal tolerance, or, most commonly, **thermotolerance**. In 1975, Henle and Leeper and Gerner and Schneider independently showed that the resistance induced in cells by one heat exposure exceeded anything that could be expected from repair of sublethal damage or progression into a resistance phase of the cycle.

If heating at 44° C is interrupted after 1 hour and resumed some 2 hours later, the dose-response curve is much shallower (i.e., the cells have become more resistant) than if heating had been continued. Operationally, there are two ways in which heating can induce thermotolerance. First, at lower temperatures of around 39° to 42° C, thermotolerance is induced during the heating period after an exposure of 2 or 3 hours. This phenomenon is already apparent by the change of slope in the survival curves of [Figure 28.1](#). Second, at temperatures above 43° C, thermotolerance cannot be produced during the heating, and it takes some time to develop after the heating has been stopped. It then decays slowly.

Thermotolerance is a substantial effect; the slope of a survival curve may be altered by a factor of 4 to 10, which translates into a difference in cell killing of several orders of magnitude. It is a factor to be reckoned with in fractionated hyperthermia. For cells in culture, the time taken for cells that have become thermotolerant to revert to their normal sensitivity (i.e., the decay of thermotolerance) may be as long as 160 hours. Groups led by Overgaard and by Urano have shown that thermotolerance can be induced in transplantable mouse tumors and that this thermotolerance also decays very slowly, requiring something on the order of 120 hours before the decay is complete.

There is evidence from the work of Field and Law and their colleagues at Hammersmith Hospital that in normal-tissue systems, such as gut, skin, and cartilage, the appearance of thermotolerance may not reach a maximum until 1 or 2 days after heating, depending on the initiating treatment. It may take as long as 1 or 2 weeks to decay completely.

Thermotolerance is a serious problem in the clinical use of hyperthermia at cytotoxic temperatures because it imposes a limit of one or at most two HTs per week.

Heat and Tumor Vasculature

Tumors in general have a less organized and less efficient vasculature than most normal tissues. All functional capillaries in tumors are open and used to capacity, even under ordinary conditions; in normal tissues, many capillaries are closed under ambient conditions. Consequently, although blood flow may be greater in tumors (particularly those that are small) compared with normal tissues at physiologic temperatures, the capacity of tumor blood flow to increase during heating appears to be rather limited in comparison with normal tissues. It is well documented that in normal tissues, heat induces a prompt increase in blood flow

accompanied by dilation of vessels and an increase in permeability of the vascular wall. As a result, heat dissipation by blood flow is slower in tumors than in normal tissues, and so, it often is found that the temperature within a tumor is higher than in the surrounding normal tissues. In a practical situation, therefore, the difference in intrinsic sensitivity between normal and malignant tissues becomes a moot point because the tumor is often hotter anyway.

METHODS OF HEATING AND THE IMPACT ON CLINICAL HYPERTERMIA

Methods of Heating in Experimental Systems

Essentially all of the work with cells cultured *in vitro*, as well as much of the early animal experimentation, involves heating by hot water baths. The simplest and most reliable way to heat a petri dish or a tumor transplanted into the leg of a mouse is to immerse it totally in a thermostatically controlled bath of water. Water temperature can be controlled within a fraction of a degree and is uniform over the treated area, temperature measurement involves no problem, and cytotoxic temperatures of 45° C are readily available.

Methods of Heating in Patients

However, it is obvious that tumors in patients cannot be heated in this way, and when localized, hyperthermia is achieved by microwaves, radiofrequency-induced currents, or ultrasound, there are serious technical problems and limitations, although significant progress has been made as a result of the clever application of focused arrays. For example, in the case of microwaves, good localization can be achieved at shallow depths, but at greater tumor depths, even if the frequency is lowered to allow deeper penetration, the localization is much poorer and surface heating limits therapy. If ultrasound is used, the presence of bone or air cavities causes distortions of the heating pattern, but adequate penetration and reasonably good temperature distributions can be achieved in soft tissues, particularly with ultrasound in focused arrays. In practice, then, tumors such as recurrent chest wall nodules can be treated adequately with microwaves, and it should theoretically be possible to heat deep-seated tumors below the diaphragm with focused ultrasound, or regional microwave devices, but in neither case is it possible to achieve cytotoxic temperatures or achieve a uniform temperature across the tumor. The best that can be achieved is a heat distribution at a more modest temperature of perhaps 39° to 42° C.

Consequently, unless there is a major breakthrough in the technology of

localized heating in patients, much of the data obtained in the laboratory at cytotoxic temperatures is largely irrelevant to clinical thermal therapy. On the other hand, as we will see later, there is some evidence that hyperthermia combined with radiotherapy (RT) conveys benefits that are somewhat better than RT alone, even when the heating produces a temperature distribution in the range of 39° to 42° C, which would not be expected to result in much cytotoxicity.

Thermal Ablation

Thermal ablation refers to the destruction of tissue by extreme hyperthermia (elevated tissue temperatures) and is a minimally invasive treatment option for cancer. The temperature change is concentrated to a focal zone in and around the tumor. At 50° C, it takes a few minutes to kill cells, at 60° C, it takes only seconds. Ablative heating is produced by needle-type radiofrequency (RF) or microwave applicators, 1.5 mm in diameter, which are inserted into the tumor under computed tomography (CT) or ultrasound imaging guidance.

The most common anatomic site is the liver, which may involve primary or metastatic cancers. It may often be used in patients who, for one reason or another, are not eligible for surgery. Thermal ablation has effectively replaced surgery as the treatment of choice for osteoid osteomas, especially in pediatric patients, as well as a large proportion of primary kidney tumors and inoperable pulmonary nodules. Thermal ablation competes with stereotactic body radiotherapy (SBRT) for treating relatively small tumors in anatomical sites that are difficult to reach surgically, with the advantage that the patient is not exposed to ionizing radiation.

RESPONSE TO HEAT AT NONCYTOTOXIC TEMPERATURES

Reoxygenation

Early studies with transplanted tumors in rodents showed that heat at cytotoxic temperatures caused vascular damage. It was concluded, therefore, that care was needed in combining heat and radiation because the oxygen status of the tumor would be compromised by heating. However, it turns out that tumor vasculature in spontaneous human tumors is considerably more resistant to thermal damage than in transplanted tumors in mice, and in any case, much of the early work with mice utilized thermal doses far in excess of those that can be achieved clinically.

It is now recognized from animal studies that mild hyperthermia (41° to 41.5° C) can actually promote tumor reoxygenation, with the degree of reoxygenation correlating with the level of the radiosensitivity of the tumor. Song reviewed 22 different studies and concluded that mild hyperthermia of animal tumors increases tumor oxygenation, which can last as long as 24 hours. This is illustrated quite dramatically in [Figure 28.3](#).

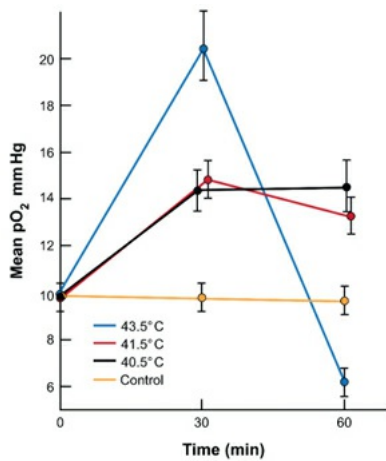


FIGURE 28.3 Illustrating how “mild” hyperthermia at noncytotoxic temperatures of 40.5° to 41.5° C for up to an hour increases the median oxygen concentration in animal tumors, whereas hyperthermia at a cytotoxic temperature (43.5° C) decreases the median oxygen concentration due to vascular damage. (Replotted from the data of Song CW, Shakil A, Osborn JL, et al. Tumour oxygenation is increased by hyperthermia at mild temperatures. *Int J Hyperthermia*. 2009;25[2]:91–95.)

Reoxygenation by mild hyperthermia has also been confirmed in a clinical study of patients with soft tissue sarcomas and breast cancer. Brizel and colleagues showed that one HT led to reoxygenation within 24 to 48 hours, whereas there was no measurable reoxygenation during a week of standard radiation therapy.

Jones and colleagues reported that mild hyperthermia (41° to 41.5° C at 90% of the measured points for 1 hour) significantly increased the pO_2 in hypoxic but not normoxic, human tumors. Such increases in tumor oxygenation significantly improved tumor response to RT, as will be described later.

Immunologic Effects of Hyperthermia

It has been suggested that the thermal stimulation of the antitumor immune response contributes to improved local control and/or long-term survival of patients receiving treatments with hyperthermia. This is based on the report that

cancer patients who experienced the highest fevers following injection with infectious agents (i.e., Coley toxins) in an attempt to treat tumors may have also experienced the longest survival. Although there are major and important differences between hyperthermia and fever, both involve an upward shift in body temperature, a phenomenon that has been strongly correlated with improved survival following infection in multiple species. One possibility that has been suggested is that modest hyperthermia, at temperatures that are not lethal to cells, may trigger some of the same thermally sensitive targets in the immune system that have evolved over millions of years to respond to fever.

Although not yet proven, current evidence that supports this possibility includes (1) enhanced immunogenicity and heat shock protein (HSP) expression seen after tumor cells are heated, (2) thermally enhanced immune effector cell activation and function, and (3) thermally enhanced vascular perfusion and delivery or trafficking of immune effector cells to tumors (Fig. 28.4).

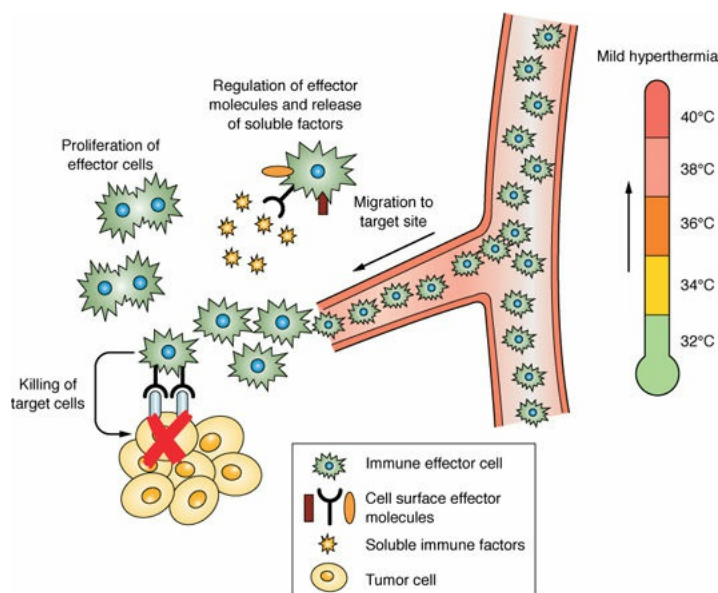


FIGURE 28.4 Mild hyperthermia can affect multiple aspects of the antitumor immune system. (From Peer AJ, Grimm MJ, Zynda ER, et al. Diverse immune mechanisms may contribute to the survival benefit seen in cancer patients receiving hyperthermia. *Immunol Res*. 2010;46:137–154, with permission.)

THERMAL ENHANCEMENT RATIO

The extent of the interaction of heat and radiation can be expressed in terms of the thermal enhancement ratio (TER) defined as the ratio of doses of x-rays required to produce a given level of biologic damage with and without the application of heat. The TER has been measured for various normal tissues, including skin, cartilage, and intestinal epithelium. The data form a consistent

pattern of increasing TER with increasing temperature, up to a value of about 2 for a 1-hour HT at 43° C. The TER is more difficult to measure in transplanted tumors in laboratory animals because the direct cytotoxic effect of the heat tends to dominate. Heat often can control experimental tumors with acceptable damage to normal tissues because cell killing by heat is strongly enhanced by nutritional deprivation and increased acidity, conditions that are typical of the poorly vascularized parts of solid tumors. Thus, a moderate HT, which can be tolerated by well-vascularized normal tissues, destroys a large proportion of the cells of many solid tumors in experimental animals. In those cases in which thermal radiosensitization has been studied, typical TER values are 1.4 at 41° C, 2.7 at 42.5° C, and 4.3 at 43° C, with heat applied for 1 hour. TERs have been developed for canine and human tumors, however, in studies by Gillette et al. and Overgaard et al. These estimates came from retrospective analyses of dose–effect relationships with and without hyperthermia. In canine oral squamous cell carcinomas, it was estimated to be approximately 1.15, when hyperthermia was administered twice a week during a course of fractionated RT. Importantly, the use of hyperthermia increased the slope of the TCD₅₀ curve, such that the doses required to achieve a high level of local tumor control were maintained well below that which caused normal tissue damage (defined here as bone necrosis). TERs have also been estimated to be in the range of 1.5 for several superficial human tumor types.

HEAT AND THE THERAPEUTIC GAIN FACTOR

The therapeutic gain factor can be defined as the ratio of the TER in the tumor to the TER in normal tissues. There is no advantage to using heat plus lower doses of x-rays if there is no therapeutic gain compared with the use of higher doses of x-rays alone. The question of a therapeutic gain factor is complicated in the case of heat because the tumor and normal tissues are not necessarily at the same temperature. If the statement is made that heat preferentially damages tumor cells compared with normal tissue, it is implied that they are both at the same temperature. In a practical situation, however, this is not always the case. For example, if a poorly vascularized tumor is treated with microwaves, it may reach a higher temperature than the surrounding normal tissue because less heat is carried away by the flow of blood. In addition, the overlying skin can be cooled actively by a draft of air or even a cold water pack. In these circumstances, the normal tissues may be at a significantly lower temperature than the tumor, which therefore exaggerates the differential response in a favorable direction.

MEASURING THERMAL DOSE IN PATIENTS

For every form of hyperthermia to be accurately delivered and evaluated in clinical trials, it is essential to achieve optimal quality control of heat delivery and temperature monitoring in patients. As was discussed previously, the temperature-induced cytotoxicity of tumor cells depends on both temperature and time so that some type of time-integrated temperature analysis is considered the best approach to determining thermal dose. However, achieving this information in patients is not straightforward. Patient's tumors differ in fundamental ways, including the ability to be heated, a parameter that may depend not only on physiologic factors such as blood flow but also on body size, tumor positioning, and the power deposition of the heating device. Moreover, temperatures within a given tumors are not uniform, and hotter and cooler regions are seen (probably because of uneven vascular drainage), which limits the goal of reaching a uniform target temperature-time combination for therapy.

A major advance toward development of a tool by which to compare thermal dose among different patients was achieved when Sapareto and Dewey proposed to use the information obtained from the Arrhenius plot (which shows that there is a predictable relationship between the rate of cell killing and temperature) to help solve the problem of how to normalize the time-temperature data, which was seen to vary significantly from patient to patient. Sapareto and Dewey proposed the concept of “cumulative equivalent minutes” (CEM) at 43° C. More specifically, the measure of thermal dose stated as CEM 43° C T₉₀ refers to the number of CEM at 43° C exceeded by 90% of the monitored points within the tumor. For this analysis, 43° C was chosen because it represents the breakpoint temperature for most human cells as judged from the Arrhenius plot. How does this idea work in practice? Because it is generally agreed that the effects of a 1° C rise of temperature is equivalent to a reduction of time by a factor of 2, consequently, above this transition temperature,

$$\frac{t_2}{t_1} = 2^{T_1 - T_2}$$

in which t_1 and t_2 are the heating times at temperatures T_1 and T_2 , respectively, to produce equal biologic effect. For temperatures lower than the transition temperature, an increase in temperature by 1° C requires that time be decreased by a factor of 4 to 6:

$$\frac{t_2}{t_1} = (4 \text{ to } 6)^{T_1 - T_2}$$

The CEM 43° C T₉₀, or the thermal dose, may be calculated from one of the

other of these expressions or a combination of both: That is, the heat dose associated with a changing temperature may be calculated as the sum of equivalent heating times at 43° C for each temperature. Thus,

$$\text{CEM } 43^\circ\text{C} = tR^{(43-T)}$$

where CEM 43° C refers to the CEM at 43° C (the temperature suggested for normalization), t is the time of treatment, T is the average temperature during desired interval of heating, and R is a constant. When above the breakpoint, R is 0.5. When below the breakpoint, R is 0.25. For a complex time-temperature history, the heating profile is broken into short intervals of time “ t ” length (typically 1 to 2 minutes), where the temperature remains relatively constant. CEM 43° C is calculated for each interval and summed to give a final CEM 43° C for the entire HT:

$$\text{CEM } 43^\circ\text{C} = \sum tR^{(43-T_{avg})}$$

CEM 43° C, also known as the “thermal isoeffect dose formulation,” has now been used to retrospectively evaluate heating efficacy in several clinical trials. Moreover, two recent phase III clinical trials by Jones et al. and Thrall et al. used this formulation to prospectively evaluate patient’s tumors to determine whether they were “heatable” prior to randomization. Furthermore, this concept was used to define a thermal dose, which could identify patients who received a higher thermal dose from those who received a lower dose. These trials have been extremely important for showing that not all tumors are heatable to the same degree and the ability to actually control thermal dose delivery can affect the probability for response and duration of local tumor control. Using the concept of CEM 43° C, these trials have clearly established that the actual temperatures achieved in patient’s tumors is less than the target temperature of 43° C for a significant portion of time, over a significant portion of tumor. Nevertheless, a small but significant clinical benefit is obtained.

PHASE III CLINICAL TRIALS TESTING BENEFITS OF HYPERTHERMIA FOR ENHANCING RADIATION THERAPY

There are now at least 10 randomized clinical trials that demonstrate benefits to hyperthermia as an adjuvant to radiation for the treatment of various types of cancers, including superficial and deep tumors, and involving both palliative and potentially curable settings. Moreover, several additional phase III trials provide evidence for combining hyperthermia with chemoradiation or chemotherapy.

Carcinoma of the cervix: A phase III trial conducted in The Netherlands tested the use of radiation alone versus radiation and hyperthermia in patients in locally advanced pelvic tumors (cervical carcinoma as well as bladder and rectal tumors were included). A total of 361 patients were enrolled. In this study, HT was given once weekly for five treatments using technology that was adequate to treat deep-seated tumors. Although improved responses were seen in all tumor types, most of the benefit appeared to occur in patients with cervical cancer. The complete response (CR) rate following RT + HT was 83% compared with 57% after RT alone. Three-year survival was 27% in the RT-alone group of cervix cancer patients, 51% in the RT + HT group ($p = .003$).

Recurrent chest wall breast cancer: Five separate phase III trials of recurrent chest wall breast cancer have been conducted, which were eventually combined as an international collaborative study. In this study, patients were randomized to either RT alone or RT with HT, and a significant improvement in CR rate was seen for patients receiving HT + RT compared with RT alone. It is notable that the greatest effect was observed in patients with lesions in areas that had previously been irradiated, thus limiting the ability of those patients to receive optimal subsequent irradiation.

Superficial malignancies: An important single-institution prospective randomized trial of radiation and hyperthermia for various superficial tumors (most of which were recurrent chest wall breast tumors) was conducted by Jones et al. and included patients who were candidates for local RT for a superficial lesion less than 3 cm in thickness. In this study, the investigators decided to first determine whether a tumor was “heatable” prior to randomization by conducting a test hyperthermia treatment and measuring whether the tumor could be heated to a prescribed temperature ahead of time. All patients whose tumors were judged to be heatable were later randomized to receive radiation alone (with no additional heat) or radiation combined with hyperthermia. The CR rate in the hyperthermia/radiation group was 66% versus 42% in the radiation-alone group. Again, previously irradiated patients had the greatest benefit, enjoying a 68.2% response rate in the hyperthermia/radiation group versus 23.5% in the radiation-alone group (Fig. 28.5). This was the first study to capitalize on the idea that for hyperthermia to act as a radiation sensitizer, the tumor must be able to be heated, and it will surely help to define the need for improved pretreatment identification of the patients most likely to benefit from hyperthermia in the future. Moreover, as discussed previously, this trial provides strong evidence that although heating is designed to bring the tumor to at least 43° C, the resultant CEM 43° C T₉₀ is significantly lower, suggesting that mild hyperthermia can have significant

radiosensitizing effects, which may not be caused by thermal cytotoxicity.

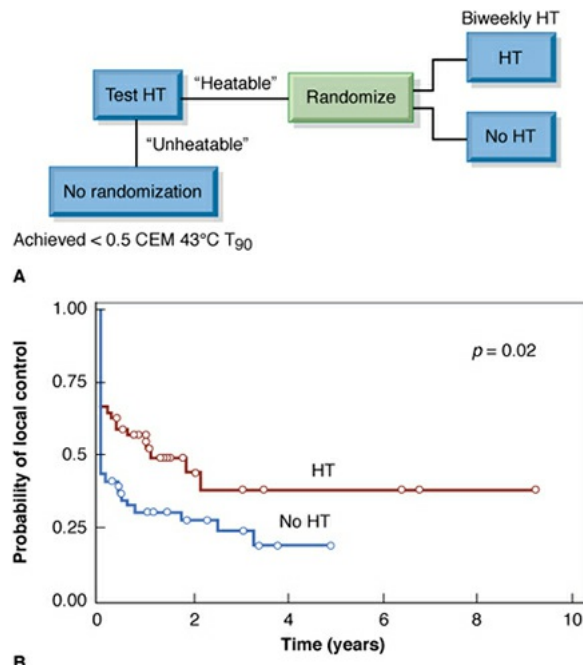


FIGURE 28.5 Results of a randomized phase III trial comparing efficacy of delivering a low versus high cumulative thermal dose in combination with radiotherapy for superficial tumors (primarily chest wall recurrences of breast cancer). **A:** Clinical trial design. **B:** Duration of local control in patients with superficial tumors treated with a low versus high cumulative thermal dose combined with RT. The difference in CR rate was significant as well as duration of local control following administration of a higher cumulative thermal dose. (From Jones EL, Oleson JR, Prosnitz LR, et al. Randomized trial of hyperthermia and radiation for superficial tumors. *J Clin Oncol*. 2005;23:3079–3085, with permission.)

A second phase III trial, which has been completed, that prospectively evaluated heatability prior to randomization is an important canine trial conducted by Thrall et al., conducted on pet dogs with spontaneous soft tissue sarcomas; again, the data from this trial confirm the benefit of the heatability of tumors with respect to clinical benefits.

Head and neck cancer: Head and neck cancers are significantly more likely to respond better if hyperthermia is added to RT. In studies conducted by Valdagni and Amichetti, patients in stage III receiving RT + HT had a 58% CR compared with 20% in the RT group. Similarly, patients with stage IV disease achieved a CR of 38% compared with 7% for those receiving RT alone. Despite the difficulties encountered when trying to heat tumors in the head and neck region, this trial evaluated both the primary site as well as neck nodes. In another

trial by this group in which only metastatic cervical lymph nodes from patients with advanced local regional squamous cell carcinoma were heated, the CR rate was 83% for RT + HT versus 41% for radiation alone. Remarkably, 5-year survival was 0 for RT alone and 53% in the RT + HT group.

Glioblastoma multiforme: Brain tumors may also benefit from hyperthermia. The group of Sneed et al. at the University of California in San Francisco evaluated the combination of interstitial hyperthermia and brachytherapy radiation for patients with glioblastoma multiforme. Patients whose tumors were implantable for brachytherapy following external beam radiation and chemotherapy were randomized to receive brachytherapy alone or combined with hyperthermia. Impressively, even in this rapidly progressing type of cancer, both times to tumor progression and 2-year survival were significantly improved for patients who received hyperthermia compared with those treated with brachytherapy alone (31% vs. 15%). However, toxicity appeared to be slightly greater in patients who received hyperthermia.

CLINICAL TRIALS ASSESSING THE BENEFIT OF HYPERTHERMIA IN COMBINATION WITH CHEMOTHERAPEUTIC AGENTS

In vitro data indicated the potential for enhanced chemosensitization for several chemotherapeutic agents by increased temperature of only 1° to 2° C. Agents that have been shown to synergize with hyperthermia include melphalan, cisplatin and related compounds, anthracyclines, bleomycin, mitomycin C, nitrosoureas, and nitrogen mustards. Moreover, hypoxic cell sensitizers have been shown to synergize with heat. **Table 28.1** lists some drugs that are potentiated by heat and some that are not. There may be several different mechanisms that underlie the interaction of heat with chemotherapeutic drugs *in vivo*. These include (1) increased drug uptake and/or retention in cells, (2) increased DNA damage and inhibition of repair processes, (3) increased oxygen radical formation, and (4) increased vascular delivery and tumor penetration. It is also clear that the extent of hypoxia and the pH of the tumor may affect the interaction between heat and chemotherapy.

Table 28.1 Interaction of Heat and Chemotherapeutic Agents

EFFECT	DRUG

Potentiated by heat	Melphalan
	Cyclophosphamide
	BCNU
	<i>Cis</i> -DDP
	Mitomycin C
	Bleomycin
	Vincristine
Unaffected by heat	Hydroxyurea
	Methotrexate
	Vinblastine
Complex interaction	Doxorubicin

BCNU, bischloroethylnitrosourea; *Cis*-DDP, *cis*-diamminedichloroplatinum.

From Kano E. Hyperthermia and drugs. In: Overgaard J, ed. *Hyperthermic Oncology*. London, United Kingdom: Taylor & Francis; 1985:277–282, with permission.

Esophageal cancer: Two randomized studies by Sugimachi et al. have now demonstrated a significant clinical advantage of adding hyperthermia to CT alone or to chemoradiotherapy during neoadjuvant treatment of squamous cell carcinoma of the esophagus. In one study, patients were randomized to preoperative hyperthermia, RT, and chemotherapy (bleomycin) compared with radiation and chemotherapy alone. Clinical CRs as well as pathologic responses were significantly improved in the trimodality arm. In a follow-up study, patients were treated with CT alone (bleomycin and cisplatin) or combined with hyperthermia (i.e., no RT was given in this trial). A significant improvement in histopathologic response was noted in the group receiving hyperthermia (19% vs. 41%).

High-risk sarcoma: In clinical data reported by Issels and colleagues in a randomized phase III trial involving 341 patients with localized high-risk soft tissue sarcoma (the largest phase III trial for any evaluation of therapy for sarcoma), it was shown that heating the tumor and the surrounding area (i.e., deep regional or part-body heating at a range between 40° and 43° C) during chemotherapy can significantly improve tumor control, including those in the extremities ([Fig. 28.6](#)). Specifically, regional hyperthermia during induction is associated with a 42% reduction in risk of local progression or death compared with chemotherapy alone. Furthermore, there was a 30% improvement in disease-free survival and an improved treatment response rate in the combined heat–chemotherapy group. In this study, patients were randomized to neoadjuvant chemotherapy (etoposide, ifosfamide, and doxorubicin) alone or combined with regional hyperthermia achieved by using RF for 60 minutes on days 1 and 4 of each chemotherapy cycle during induction and postinduction therapy. This trial demonstrates that a nonuniform heating field can be very successful (the temperature across the tumor varied over 1° to 3° C), which should simplify the design of heating equipment for future clinical applications. Although determination of whether there are long-term survival benefits from the addition of hyperthermia must await future analysis, recently completed interim analysis does suggest the possibility of improved long-term survival.

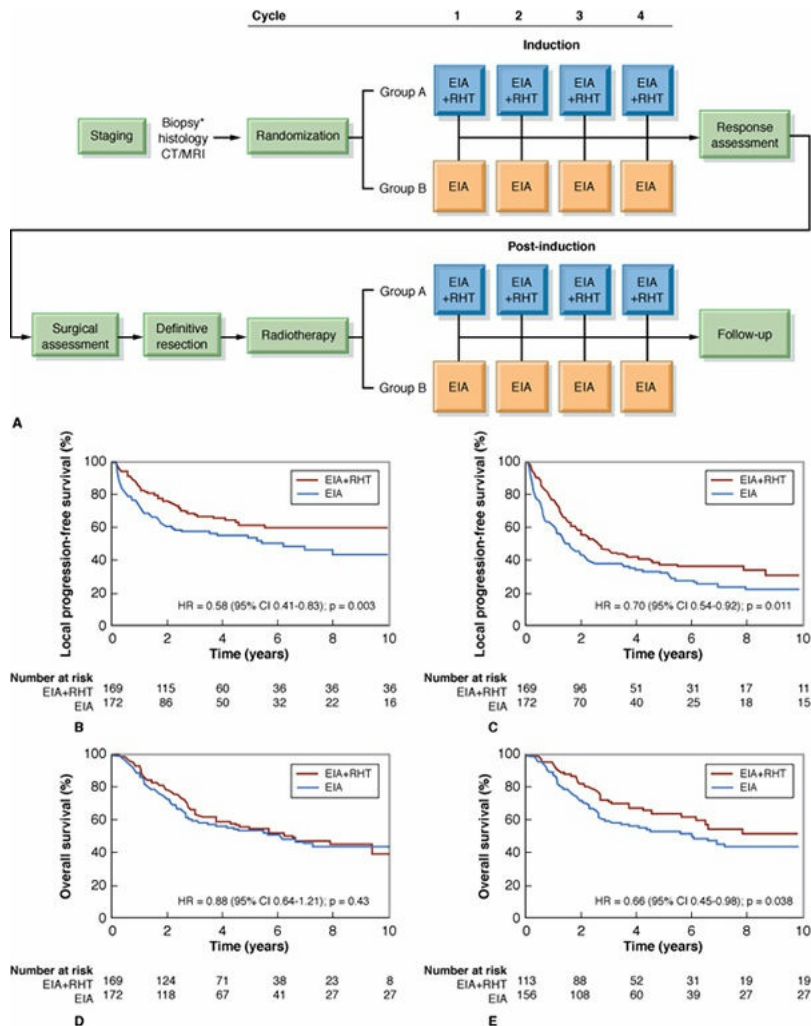


FIGURE 28.6 Results of a phase III trial in patients with high-risk sarcoma. **A:** Schematic of the trial design. Patients with previous surgery were also assigned to receive the complete induction and postinduction therapy for randomization. EIA, etoposide + ifosfamide + doxorubicin; RHT, regional hyperthermia. Kaplan-Meier estimates of local progression-free survival (**B**), disease-free survival (**C**), overall survival in all patients randomly allocated treatment (**D**), and overall survival in the per-protocol-induction population (**E**). (From Issels RD, Lindner LH, Verweij J, et al. Neo-adjuvant chemotherapy alone or with regional hyperthermia for localised high-risk soft tissue sarcoma: a randomised phase 3 multicentre study. *Lancet Oncol.* 2010;11:561–570, with permission.)

Development and Evaluation of “Thermosensitive” Liposomes for Improved Tumor Targeting of Chemotherapy

The addition of local hyperthermia to systemically delivered chemotherapy may have the obvious advantage of “targeting” and localizing the principal effect of the drug, allowing greater tumor cell killing for a given systemic toxicity. This

would help to overcome one of the principal problems and limitations of chemotherapy. This possibility is being realized in exciting new preclinical and clinical research by Dewhirst and colleagues in which hyperthermia is being used to direct the release of chemotherapeutic drugs at the site of tumors through the use of thermosensitive liposomes. Liposomes consist of a lipid membrane that can be filled with a cytotoxic chemotherapeutic agent such as doxorubicin. Long circulating liposomes that are covered with polyethylene glycol reduce recognition by the reticuloendothelial system and can extravasate from tumor blood vessels and accumulate in the extravascular space. This is termed the *enhanced permeability and retention* (EPR) effect. Whereas this effect can passively lead to enhanced drug accumulation in tumors by virtue of the presence of endothelial cell membrane pores, hyperthermia can increase the size of these pores and enhance drug delivery by four- to fivefold over what can be achieved from just the EPR effect. Further enhancement of drug delivery can be achieved by using thermally sensitive liposomes that are engineered to melt at mild temperatures (e.g., 41° to 42° C). These formulations yield further improvement in drug delivery by an additional factor of 4 to 5 versus nonthermally sensitive liposomes. Indeed, these latter formulations have been shown to enhance doxorubicin delivery by 25- to 30-fold, compared with free drug, resulting in impressive antitumor effects in tumors that were completely refractory to free drug. It is speculated that the combination of hyperthermia-enhanced liposomal extravasation and intravascular-triggered drug release results in enhanced delivery to tumor cells and a large therapeutic effect. The mechanism is illustrated in [Figure 28.7](#). More recent studies by this group are helping to establish more details by which liposomally encapsulated doxorubicin may work in combination with hyperthermia. For example, it has been determined that although pH_e or *in vitro* sensitivity to doxorubicin does not appear to predict efficacy *in vivo*, tumor cell doubling time, vascular perfusion, and extent of hypoxia do appear to correlate. Clinical validation of this strategy is now well under way for patients with recurrent chest wall cancers and hepatocellular carcinomas. In the latter setting, thermosensitive liposomes are being combined with high-temperature RF ablation. Here, the strategy is designed to increase the zone of tumor destruction particularly at the tumor margins but capitalizing on the ability of the mild hyperthermia that occurs in this region to release drug from the liposomes.

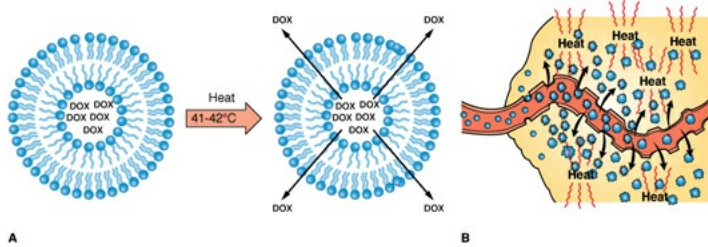


FIGURE 28.7 Characteristics of thermally sensitive liposome. **A:** The liposome contains a mixture of phospholipids including a small percentage of single-chain fatty acid. At body temperature, the liposome is in a frozen or gel state. The single-chain fatty acid tends to concentrate between plates of frozen lipid. When heated, the grain boundaries melt first, the single-chain fatty acids line the grain boundaries, creating pores in the lipid membrane. This permits very rapid release of drug (doxorubicin in this example) from the liposome (<20 s). **B:** In a heated tumor, this feature promotes deposition of high amounts of drug because of intravascular release, which drives the drug far into the interstitial tissue, down its concentration gradient. (Panel B from Kong G, Anyarambhatia G, Petros WP, et al. Efficacy of liposomes and hyperthermia in a human tumor xenograft model: importance of triggered drug release. *Cancer Res.* 2000;60:6950–6957, with permission.)

METHODS OF TUMOR HEATING

Most of the original laboratory research that led to clinical applications of local hyperthermia used cells cultured *in vitro* usually heated by hot water baths. Indeed, the simplest and most reliable way to heat cells in a petri dish, or to heat a tumor grown in the leg of a mouse or rat, is to immerse the target in a thermostatically controlled bath of water because temperature can be controlled within a fraction of a degree, and temperature measurement involves no problem.

However, for localized hyperthermia in human tumors to be achieved by microwaves, RF-induced currents, or ultrasound, there have been some serious technical problems that have had to be overcome. In the case of microwaves, good localization can be achieved at shallow depths, but at greater tumor depths, even if the frequency is lowered to allow deeper penetration, the localization is much poorer and surface heating limits therapy. If ultrasound is used, the presence of bone or air cavities causes distortions of the heating pattern, but adequate penetration and good uniform temperature distributions can be achieved in soft tissues, particularly with ultrasound in focused arrays. In practice, then, superficial tumors such as recurrent chest wall nodules can be

treated adequately with microwaves or plane wave ultrasound, and it should theoretically be possible to heat deep-seated tumors below the diaphragm with focused ultrasound, regional microwave devices, or interstitial techniques.

In all cases, however, methods of heating pose a complex problem, although significant progress has been made as a result of the clever application of focused arrays. For example, the use of multiphased arrays allows uniformity of temperature to the edge of the field. The picture is complicated, and it is unlikely that one simple answer to all the complex problems will be found.

Magnetic Hyperthermia

Magnetic hyperthermia is the name given to an experimental cancer treatment based on the fact that magnetic nanoparticles, when subjected to an alternating magnetic field, generate a great deal of heat. The trick is to get the nanoparticles to localize in the tumor(s), with a lower concentration in normal tissues.

In studies involving transplanted tumors in mice, iron nanoparticles were covered with a biocompatible shell because iron is toxic, injected intravenously, and allowed to circulate in the blood. The nanoparticles, if they are of the appropriate size, tend to accumulate in tumors more than in normal tissues because of the phenomenon of EPR effect. The general explanation of this widely observed effect is that in order for tumors to grow, they must stimulate the production of blood vessels which they depend on for their nutritional and oxygen supply. These newly formed tumor blood vessels are abnormal in form and architecture and tend to leak particles of a particular size. It is claimed that the concentration of iron nanoparticles in mouse tumors was found to be greater than in normal tissues by a factor of 16. When the nanoparticles have accumulated in the tumor, the alternating magnetic field is applied, and it is claimed that temperatures of 60° C have been observed within a few minutes.

In the few human studies that have been reported, utilizing patients with prostate cancer and glioma multiforme, the iron nanoparticles were injected directly into the tumors rather than into circulating blood, and as a result, a much lower concentration of iron nanoparticles was achieved than in the animal experiments. Variable temperatures between 40° and 48° C were reported in prostate patients. This HT was combined with radiation therapy.

This, as yet highly experimental technique, has captured the imagination of the scientific community and may prove to be an ideal way to treat deep-seated tumors that are difficult to heat adequately with conventional methods.

CLINICAL THERMOMETRY

No area in thermal engineering research is more important than the need to accurately assess the resultant temperature of tumors or normal tissues following heating. This is essential for accurate comparison of clinical trial data using different heating equipment or different tumor targets.

Invasive Thermometry Methods

Direct measurement of temperatures during clinical hyperthermia with invasive sensors was for many years, the only method of treatment monitoring, control, and thermal dose calculation. Sensors should be able to measure temperatures to an accuracy and precision of about 0.1° C in a water bath and of about 0.2° C *in vivo* in intense electromagnetic (EM) or ultrasound fields.

There are three basic kinds of invasive thermometers: (1) electrically conducting, (2) minimally conducting, and (3) nonconducting (optical) sensors. Thermistors and thermocouple sensors with metallic leads are examples of the first kind that are not suitable for EM hyperthermia. A commonly used minimally conducting sensor is the high-resistivity thermistor with carbon-impregnated plastic leads. The high-resistivity material allows accurate measurement in strong EM environment. Nonconducting optical sensors use materials at the tip of an optical fiber whose optical properties are a known function of temperature. The second and third kinds of sensors are used in EM hyperthermia.

An important clinical reality is that only a limited number of invasive catheters are desired or feasible, whereas a more complete knowledge of the temperature field in humans during treatment is desirable. This requires noninvasive thermometry methods.

Progress toward Clinically Achievable Noninvasive Thermometry

Several noninvasive thermal measurement approaches are under investigation, including infrared thermography and thermal monitoring sheet fiber-optic arrays (surface distributions only), electrical impedance tomography, microwave tomography, microwave radiometry, ultrasonic temperature estimation techniques, and magnetic resonance thermal imaging (MRTI). The most promising approach to date for monitoring complete three-dimensional tissue temperature distributions during thermal therapy is proton resonance frequency

shift (PRFS)-based MRTI. This method has been used successfully to monitor temperatures during thermal therapy with both EM and ultrasound heating approaches. PRFS-based MRTI has demonstrated an accuracy of about 1° C per 1 cm³ of tissue in multiple slices acquired at least once per minute. Application of this noninvasive technology allows accurate measurement of the volumetric temperature distribution.

SUMMARY OF PERTINENT CONCLUSIONS

Hyperthermia at Cytotoxic Temperatures (42° to 45° C)

Survival curves for heat are similar in shape to those for radiation except that time at the elevated temperature replaces absorbed dose. No consistent difference in inherent sensitivity exists between normal and malignant cells.

The inactivation energy is different above and below a break temperature of about 43° C.

The inactivation energy suggests that the target for heat toxicity may be protein.

The age-response function for heat complements that for x-rays. S phase cells that are resistant to x-rays are sensitive to heat.

Hypoxia does not protect cells from heat as it does from x-rays. Hyperthermia may be very effective at reversing hypoxia through its effects on vascular perfusion. This may be an important mechanism of radiosensitization by hyperthermia.

Cells at low pH and nutritionally deprived (more likely to be in tumors) are more sensitive to heat, although cells can adapt to pH changes and lose their sensitivity to heat.

Thermotolerance is the induced resistance to a second heat exposure by prior heating and may be monitored by the appearance of HSPs.

Heat damage in normal tissues is expressed more rapidly than x-ray damage because heat kills differentiated as well as dividing cells and because cells can die in interphase rather than at the next (or subsequent) mitosis, as is the case for x-rays.

The TER is the ratio of radiation doses with and without heat to produce the same biologic effects. TER values of 2 to 4 can be obtained in tumors and normal tissues in experimental animals.

Hyperthermia at Modest Temperatures that Can Be Achieved in Human Tumors

Hyperthermia at modest temperatures that can be achieved in human tumors results in little cytotoxicity but has been shown to result in reoxygenation in animal and human tumors.

There is some evidence that hyperthermia at temperatures that result in little cytotoxicity can induce an immune response that may account for some of the benefits of combining hyperthermia with radiation. This remains to be proven.

Several phase III randomized trials now demonstrate a clear and significant benefit for the addition of hyperthermia to standard RT and/or chemotherapy. The cancer types tested include cervical cancer, superficial localized breast cancer, recurrent or metastatic malignant melanoma, nodal metastases from head and neck cancer, glioma, esophageal cancer, and high-risk sarcoma.

The TER is the ratio of radiation doses with and without heat to produce the same biologic effects. TER values of between 1.15 and 1.5 have been reported in clinical analyses.

Temperature measurement *in vivo* is difficult but improving. Progress toward noninvasive thermometry includes the use of magnetic resonance imaging.

Novel applications of heat include enhanced targeted delivery of chemotherapy by thermosensitive liposomes.

Thermal ablation refers to the destruction of tissue by extreme hyperthermia (more than 60° C) delivered by needle-type RF or microwave applicators implanted directly into the tumor under CT or ultrasound guidance.

BIBLIOGRAPHY

Adam A, Kenny LM. Interventional oncology in multidisciplinary cancer treatment in the 21st century. *Nat Rev Clin Oncol.* 2015;12:105–113.

Arthur RM, Straube WL, Trobaugh JW, et al. Non-invasive estimation of hyperthermia temperatures with ultrasound. *Int J Hyperthermia.* 2005;21:589–600.

Arunachalam K, Maccarini PF, Craciunescu OI, et al. Thermal characteristics of thermobrachytherapy surface applicators for treating chest wall recurrence. *Phys Med Biol.* 2010;55:1949–1969.

Brace C. Thermal tumor ablation in clinical use. *IEEE Pulse*. 2011;2(5):28–38. doi:10.1109/MPUL.2011.942603.

Bradley WG Jr. MR-guided focused ultrasound: a potentially disruptive technology. *J Am Coll Radiol*. 2009;6:510–513.

Brizel DM, Scully SP, Harrelson JM, et al. Radiation therapy and hyperthermia improve the oxygenation of human soft tissue sarcomas. *Cancer Res*. 1996;56:5347–5350.

Bull JM, Scott GL, Strebel FR, et al. Fever-range whole-body thermal therapy combined with cisplatin, gemcitabine, and daily interferon-alpha: a description of a phase I-II protocol. *Int J Hyperthermia*. 2008;24:649–662.

Calderwood SK, Theriault JR, Gong J. How is the immune response affected by hyperthermia and heat shock proteins? *Int J Hyperthermia*. 2005;21:713–716.

Cheng KS, Dewhirst MW, Stauffer PR, et al. Effective learning strategies for real-time image-guided adaptive control of multiple-source hyperthermia applicators. *Med Phys*. 2010;37:1285–1297.

Corry PM, Armour EP. The heat shock response: role in radiation biology and cancer therapy. *Int J Hypertherm*. 2005;21:769–778.

Craciunescu O, Blackwell E, Jones J, et al. DCE-MRI parameters have potential to predict response of locally advanced breast cancer patients to neoadjuvant chemotherapy and hyperthermia: a pilot study. *Int J Hypertherm*. 2009;25:405–415.

Craciunescu O, Stauffer P, Soher B, et al. Accuracy of real time noninvasive temperature measurements using magnetic resonance thermal imaging in patients treated for high grade extremity soft tissue sarcomas. *Med Phys*. 2009;36:4848–4858.

Das SK, Macfall J, McCauley R, et al. Improved magnetic resonance thermal imaging by combining proton resonance frequency shift (PRFS) and apparent diffusion coefficient (ADC) data. *Int J Hyperthermia*. 2005;21:657–667.

Datta NR, Bose AK, Kapoor HK, et al. Head and neck cancers: results of thermoradiotherapy versus radiotherapy. *Int J Hyperthermia*. 1990;6:479–486.

de Bruijne M, Wielheesen DH, van der Zee J, et al. Benefits of superficial

- hyperthermia treatment planning: five case studies. *Int J Hyperthermia*. 2007;23:417–429.
- Dewey WC, Hopwood LE, Sapareto LA, et al. Cellular responses to combinations of hyperthermia and radiation. *Radiology*. 1977;123:463–474.
- Dewhirst MW, Vujaskovic Z, Jones E, et al. Re-setting the biologic rationale for thermal therapy. *Int J Hyperthermia*. 2005;21:779–790.
- Diederich CJ, Hynnen K. Ultrasound technology for hyperthermia. *Ultrasound Med Biol*. 1999;25:871–887.
- Diederich CJ, Khalil IS, Stauffer PR, et al. Direct-coupled interstitial ultrasound applicators for simultaneous thermobrachytherapy: a feasibility study. *Int J Hyperthermia*. 1996;12:401–419.
- Emami B, Scott C, Perez CA, et al. Phase III study of interstitial thermoradiotherapy compared with interstitial radiotherapy alone in the treatment of recurrent or persistent human tumors. A prospectively controlled randomized study by the Radiation Therapy Group. *Int J Radiat Oncol Biol Phys*. 1996;34:1097–1104.
- Fatehi D, van der Zee J, de Bruijne M, et al. RF-power and temperature data analysis of 444 patients with primary cervical cancer: deep hyperthermia using the Sigma-60 applicator is reproducible. *Int J Hyperthermia*. 2007;23:623–643.
- Field SB, Law MP. The response of skin to fractionated heat and x rays. *Br J Radiol*. 1978;51:221–222.
- Gellermann J, Hildebrandt B, Issels R, et al. Noninvasive magnetic resonance thermography of soft tissue sarcomas during regional hyperthermia: correlation with response and direct thermometry. *Cancer*. 2006;107:1373–1382.
- Gellermann J, Wlodarczyk W, Ganter H, et al. A practical approach to thermography in a hyperthermia/magnetic resonance hybrid system: validation in a heterogeneous phantom. *Int J Radiat Oncol Biol Phys*. 2005;61:267–277.
- Gerner EW, Schneider MJ. Induced thermal resistance in HeLa cells. *Nature*. 1975;256:500–502.
- Gillette EL. Large animal studies of hyperthermia and irradiation. *Cancer Res*. 1979;39:2242–2244.

Gonzalez Gonzalez D, van Dijk JDP, Blank LE, et al. Combined treatment with radiation and hyperthermia in metastatic malignant melanoma. *Radiother Oncol.* 1986;6:105–113.

Grünhagen DJ, de Wilt JH, ten Hagen TL, et al. Technology insight: utility of TNF-alpha-based isolated limb perfusion to avoid amputation of irresectable tumors of the extremities. *Nat Clin Pract Oncol.* 2006;3:94–103.

Haar GT, Coussios C. High intensity focused ultrasound: physical principles and devices. *Int J Hyperthermia.* 2007;23:89–104.

Habash RW, Bansal R, Krewski D, et al. Thermal therapy, part IV: electromagnetic and thermal dosimetry. *Crit Rev Biomed Eng.* 2007;35:123–182.

Hand JW. Heating techniques in hyperthermia. II. Non-ionizing electromagnetic waves. *Br J Radiol.* 1981;54:446–459.

Hehr T, Wust P, Bamberg M, et al. Current and potential role of thermoradiotherapy for solid tumours. *Onkologie.* 2003;26:295–302.

Henle KJ, Leeper DB. Combination of hyperthermia (40 degrees, 45 degrees C) with radiation. *Radiology.* 1976;121:431–454.

Hildebrandt B, Wust P, Ahlers O, et al. The cellular and molecular basis of hyperthermia. *Crit Rev Oncol Hematol.* 2002;43:33–56.

Hiraoka M, Jo S, Dodo Y, et al. Clinical results of radiofrequency hyperthermia combined with radiation in the treatment of radioresistant cancers. *Cancer.* 1984;54:2898–2904.

Hokland SL, Pedersen M, Salomir R, et al. MRI-guided focused ultrasound: methodology and applications. *IEEE Trans Med Imaging.* 2006;25:723–731.

Hornback NB, Shupe RE, Shidnia H, et al. Advanced state IIIB cancer of the cervix treatment by hyperthermia and radiation. *Gynecol Oncol.* 1986;23:160–167.

Huang HS, Hainfeld JF. Intravenous magnetic nanoparticle cancer hyperthermia. *Int J Nanomedicine.* 2013;8:2521–2532.

Hurwitz MD. Today's thermal therapy: not your father's hyperthermia: challenges and opportunities in application of hyperthermia for the 21st century cancer patient. *Am J Clin Oncol.* 2010;33:96–100.

Hynynen K, McDannold N. MRI guided and monitored focused ultrasound

- thermal ablation methods: a review of progress. *Int J Hyperthermia*. 2004;20:725–737.
- Issels RD, Lindner LH, Verweij J, et al. Neo-adjuvant chemotherapy alone or with regional hyperthermia for localised high-risk soft-tissue sarcoma: a randomised phase 3 multicentre study. *Lancet Oncol*. 2010;11:561–570.
- Johannsen M, Gneveckow U, Eckelt L, et al. Clinical hyperthermia of prostate cancer using magnetic nanoparticles: presentation of a new interstitial technique. *Int J Hyperthermia*. 2005;21(7):637–647.
- Jolesz FA. MRI-guided focused ultrasound surgery. *Annu Rev Med*. 2009;60:417–430.
- Jones EL, Oleson JR, Prosnitz LR, et al. Randomized trial of hyperthermia and radiation for superficial tumors. *J Clin Oncol*. 2005;23:3079–3085.
- Jones EL, Prosnitz LR, Dewhirst MW, et al. Thermochemoradiotherapy improves oxygenation in locally advanced breast cancer. *Clin Cancer Res*. 2004;10:4287–4293.
- Kapp DS, Cox RS. Thermal treatment parameters are most predictive of outcome in patients with single tumor nodules per treatment field in recurrent adenocarcinoma of the breast. *Int J Radiat Oncol Biol Phys*. 1995;33:887–899.
- Kong G, Anyarambhatia G, Petros WP, et al. Efficacy of liposomes and hyperthermia in a human tumor xenograft model: importance of triggered drug release. *Cancer Res*. 2000;60:6950–6957.
- Kong G, Braun RD, Dewhirst MW. Characterization of the effect of hyperthermia on nanoparticle extravasation from tumor vasculature. *Cancer Res*. 2001;61:3027–3032.
- Kowalski ME, Jin JM. A temperature-based feedback control system for electromagnetic phased-array hyperthermia: theory and simulation. *Phys Med Biol*. 2003;48:633–651.
- Kroon HM, Thompson JF. Isolated limb infusion: a review. *J Surg Oncol*. 2009;11:169–177.
- Lagendijk JJ. Hyperthermia treatment planning. *Phys Med Biol*. 2000;45:R61–R76.
- Lee RJ, Suh H. Design and characterization of an intracavitary ultrasound hyperthermia applicator for recurrent or residual lesions in the vaginal cuff.

Int J Hyperthermia. 2003;19:563–574.

Leopold KA, Dewhirst M, Samulski T, et al. Relationships among tumor temperature, treatment time, and histopathological outcome using preoperative hyperthermia with radiation in soft tissue sarcomas. *Int J Radiat Oncol Biol Phys*. 1992;22:989–998.

Li GC, Li LG, Liu YK, et al. Thermal response of rat fibroblasts stably transfected with the human 70-kDa heat shock protein-encoding gene. *Proc Natl Acad Sci USA*. 1991;88:1681–1685.

Li GC, Petersen NS, Mitchell HK. Induced thermal tolerance and heat shock protein synthesis in Chinese hamster ovary cells. *Br J Cancer Suppl*. 1982;5:132–136.

Lüdemann L, Włodarczyk W, Nadobny J, et al. Non-invasive magnetic resonance thermography during regional hyperthermia. *Int J Hyperthermia*. 2010;26:273–282.

Maier-Hauff K, Ulrich F, Nestler D, et al. Efficacy and safety of intratumoral thermotherapy using magnetic iron-oxide nanoparticles combined with external beam radiotherapy on patients with recurrent glioblastoma multiforme. *J Neurooncol*. 2011;103(2):317–324.

McDannold N, Tempany CM, Fennessy FM, et al. Uterine leiomyomas: MR imaging-based thermometry and thermal dosimetry during focused ultrasound thermal ablation. *Radiology*. 2006;240:263–272.

Moros EG, Fan X, Straube WL. Ultrasound power deposition model for the chest wall. *Ultrasound Med Biol*. 1999;25:1275–1287.

Moros EG, Roemer RB, Hynynen K. Pre-focal plane high-temperature regions induced by scanning focused ultrasound beams. *Int J Hyperthermia*. 1990;6:351–366.

Oleson JR, Samulski TV, Leopold KA, et al. Sensitivity of hyperthermia trial outcomes to temperature and time: implications for thermal goals of treatment. *Int J Radiat Oncol Biol Phys*. 1993;25:289–297.

Overgaard J. Historical perspectives of hyperthermia. In: Overgaard J, ed. Introduction to Hyperthermic Oncology. Vol. 2. New York, NY: Taylor & Francis; 1984.

Overgaard J. The current and potential role of hyperthermia in radiotherapy. *Int J Radiat Oncol Biol Phys*. 1989;16:535–549.

- Overgaard J, Gonzalez Gonzalez D, Hulshof MC, et al. Hyperthermia as an adjuvant to radiation therapy of recurrent or metastatic malignant melanoma. A multicentre randomized trial by the European Society for Hyperthermic Oncology. *Int J Hyperthermia*. 1996;12:3–20.
- Peer AJ, Grimm MJ, Zynda ER, et al. Diverse immune mechanisms may contribute to the survival benefit seen in cancer patients receiving hyperthermia. *Immunol Res*. 2010;46:137–154.
- Rawnsley RJ, Roemer RB, Dutton AW. The simulation of discrete vessel effects in experimental hyperthermia. *J Biomech Eng*. 1994;116:256–262.
- Rieke V, Butts Pauly K. MR thermometry. *J Magn Reson Imaging*. 2008;27:376–390.
- Robins HI, Longo W. Whole body hyperthermia: simple complexities. *Intensive Care Med*. 1999;25:898–900.
- Sakurai H, Mitsuhashi N, Tamaki Y, et al. Clinical application of low dose-rate brachytherapy combined with simultaneous mild temperature hyperthermia. *Anticancer Res*. 2001;21:679–684.
- Samulski TV, Fessenden P. Thermometry in therapeutic hyperthermia. In: Gautherie M, ed. *Methods of Hyperthermia Control*. Berlin, Germany: Springer-Verlag; 1990:1–34.
- Sapareto SA, Dewey WC. Thermal dose determination in cancer therapy. *Int J Radiat Oncol Biol Phys*. 1984;10:787–800.
- Segal BH, Wang XY, Dennis CG, et al. Heat shock proteins as vaccine adjuvants in infections and cancer. *Drug Discov Today*. 2006;11(11–12):534–540.
- Sherar M, Liu FF, Pintilie M, et al. Relationship between thermal dose and outcome in thermoradiotherapy treatments for superficial recurrences of breast cancer: data from a phase III trial. *Int J Radiat Oncol Biol Phys*. 1997;39:371–380.
- Smith NB, Merrilees NK, Dahleh M, et al. Control system for an MRI compatible intracavitary ultrasound array for thermal treatment of prostate disease. *Int J Hyperthermia*. 2001;17:271–282.
- Sneed PK, Stauffer PR, McDermott MW, et al. Survival benefit of hyperthermia in a prospective randomized trial of brachytherapy boost ± hyperthermia for glioblastoma multiforme. *Int J Radiat Oncol Biol Phys*. 1998;40:287–295.
- Song CW. Effect of local hyperthermia on blood flow and microenvironment: a

- review. *Cancer Res.* 1984;44(10 suppl):4721s–4730s.
- Song CW, Park HJ, Griffin RJ. Improvement of tumor oxygenation by mild hyperthermia. *Radiat Res.* 2001;155:515–528.
- Song CW, Shakil A, Griffin RJ, et al. Improvement of tumor oxygenation status by mild temperature hyperthermia alone or in combination with carbogen. *Semin Oncol.* 1997;24:626–632.
- Song CW, Shakil A, Osborn JL, et al. Tumour oxygenation is increased by hyperthermia at mild temperatures. *Int J Hyperthermia.* 1996;12:367–373.
- Straube WL, Klein EE, Moros EG, et al. Dosimetry and techniques for simultaneous hyperthermia and external beam radiation therapy. *Int J Hyperthermia.* 2001;17:48–62.
- Subjeck JR, Sciandra JJ, Chao CF, et al. Heat shock proteins and biological response to hyperthermia. *Br J Cancer Suppl.* 1982;45:127–131.
- Sugimachi K, Kuwano H, Ide H, et al. Chemotherapy combined with or without hyperthermia for patients with oesophageal carcinoma: a prospective randomized trial. *Int J Hyperthermia.* 1994;10:485–493.
- Thrall DE, LaRue SM, Pruitt AF, et al. Changes in tumor oxygenation during fractionated hyperthermia and radiation therapy in spontaneous canine sarcomas. *Int J Hyperthermia.* 2006;22:365–373.
- Urano M. Kinetics of thermotolerance in normal and tumor tissues. *Cancer Res.* 1986;46:474–482.
- Valdagni R, Amichetti M. Report of long-term follow-up in a randomized trial comparing radiation therapy and radiation therapy plus hyperthermia to metastatic lymph nodes in stage IV head and neck patients. *Int J Radiat Oncol Biol Phys.* 1994;28:163–169.
- Vernon CC, Hand JW, Field SB, et al. Radiotherapy with or without hyperthermia in the treatment of superficial localized breast cancer: results from five randomized controlled trials. International Collaborative Hyperthermia Group. *Int J Radiat Oncol Biol Phys.* 1996;35:731–744.
- Waterman FM. Invasive thermometry techniques in thermoradiotherapy and thermochemotherapy. In: Seegenschmiedt MH, Fessenden P, Vernon CC, eds. *Thermoradiotherapy and Thermochemotherapy: Biology, Physiology and Physics.* Vol. 2. Berlin, Germany: Springer-Verlag; 1995:331–360.
- Wyatt C, Soher B, Maccarini P, et al. Hyperthermia MRI temperature

measurement: evaluation of measurement stabilisation strategies for extremity and breast tumours. *Int J Hyperthermia*. 2009;25:422–433.

Xu Y, Choi J, Hylander BL, et al. Fever-range whole body hyperthermia increases the number of perfused tumor blood vessels and therapeutic efficacy of liposomally encapsulated doxorubicin. *Int J Hyperthermia*. 2007;23:513–527.

Glossary

A: Symbol for mass number.

absolute risk: The risk of an adverse health effect that is independent of other causes of that same health effect.

absorbed dose (D): The energy imparted per unit mass by ionizing radiation to matter at a specific point. The International Standard (SI) unit of absorbed dose is joule per kilogram (J/kg). The special name for this unit is gray (Gy). The previously used special unit of absorbed dose, the rad, was defined to be an energy absorption of 100 erg/g. Thus, 1 Gy = 100 rad.

absorption: Removal of x-rays from a beam.

accelerated fractionation: Reduction in overall treatment time; a schedule in which the average rate of dose delivery exceeds the equivalent of 10 Gy per week in 2-Gy fractions.

accelerated proliferation: Increase in the clonogen proliferation rate after treatment with radiation or chemotherapy, relative to its pretreatment value.

accelerator (linear): A machine, often called a *linac*, that produces high-energy x-rays for the treatment of cancer.

acentric ring: A circular piece of a chromosome lacking a centromere.

acidic fibroblast growth factor (FGF): A mitogen for many types of cells of mesodermal origin, including endothelial cells, chondrocytes, and fibroblasts. In presence of heparin, induces blood vessel growth.

action level: Concentration of radon in a house above which it is recommended that some action be taken to reduce that radon level; currently, the action level is 148 Bq/m³ in the United States.

activation: The process of making a material radioactive by bombardment with neutrons, protons, or other nuclear particles. See **activation analysis**.

activation analysis: Identifying and measuring chemical elements in a sample of material. First, the sample is made radioactive by bombardment with neutrons, charged particles, or γ -rays. Then, the newly formed radioactive atoms in the sample give off characteristic nuclear radiations, such as γ -rays, which tell the types and quantities of atoms present. Activation analysis is usually more sensitive than chemical analysis.

activity: Quantity of a radionuclide that describes the rate at which decays occur in an amount of a radionuclide. The SI unit of radioactivity is the becquerel (Bq), which replaced the old unit, the curie (Ci). One becquerel corresponds to one disintegration of a radionuclide per second.

acute hypoxia: Low oxygen concentration in regions of a tumor associated with changes in blood flow through vessels, for example, by transient closing of vessels. Also called *perfusion-limited hypoxia*.

acute radiation syndrome (ARS): Biologic changes and symptoms, including death, that occur within weeks after a high-intensity total body irradiation.

acyclovir: A nucleoside analogue of guanosine that blocks DNA replication when incorporated into an elongating polynucleotide. Used under the trade name Zovirax as a treatment for herpes.

additive: A situation in which the effect of a combination is the sum of the effects of the separate treatments (i.e., independent cell kill).

adenoma: A benign tumor of epithelial origin, such as a polyp of the colon.

adenovirus: One of a group of viruses responsible for upper respiratory and other infections in humans, other mammals, and birds. Adenoviruses are useful as a vector in gene therapy because they infect both dividing and nondividing cells, but the downside to their use is that they evoke an immune response, which makes their repeated use difficult.

adjuvant therapy: A treatment method used in addition to the primary therapy. Radiation therapy is often used as an adjuvant to surgery or chemotherapy.

agarose gel electrophoresis: Electrophoresis in which a matrix composed of purified agarose is used to separate larger DNA and RNA molecules ranging from 100 to 20,000 nucleotides.

agreement state: Any state with which the Nuclear Regulatory Commission has entered into an effective licensing agreement to enable the state to regulate source, special nuclear, and by-product materials.

alleles: Alternate forms of a gene or DNA sequence on the two homologous chromosomes of a pair.

alopecia: Hair loss.

alpha/beta ratio (α/β ratio): The ratio of the parameters α and β in the linear-quadratic model; used to quantify the fractionation sensitivity of tissues.

alpha fetoprotein (AFP): A 70-kDa glycoprotein synthesized in embryonic development by the yolk sac. High levels of this protein in the amniotic fluid are associated with neural tube defects such as spina bifida. Lower than normal levels may be associated with Down syndrome.

α -particle: A positively charged particle emitted by radioactive materials. It consists of two neutrons and two protons bound together; hence, it is identical with the nucleus of a helium atom. It is the least penetrating of the three common types of radiation— α , β , and γ —and it is stopped by a sheet of paper. It is not dangerous to plants, animals, or humans unless the α -emitting substance has entered the organisms. α -Particles are ejected from a nucleus during the decay of some radioactive elements; for example, an α -particle is emitted if either of the radon progeny polonium-218 or polonium-214 decays.

alpha ray (α -ray): A stream of α -particles. Used loosely as a synonym for α -particles.

Alt-NHEJ: A form of NHEJ that uses 5 to 25 bp homologies to align broken ends before repair occurs.

ALU sequence: An interspersed DNA sequence of approximately 300 bp found in the genome of primates that is cleaved by the restriction enzyme *Alu* I. *Alu* sequences are composed of a head-to-tail dimer, with the first monomer approximately 140 bp and the second approximately 170 bp. In humans, they are dispersed throughout the genome and are present in 300,000 to 600,000 copies, constituting some 3% to 6% of the genome. See [SINES](#).

Ames test: A procedure devised by Bruce Ames to test carcinogenic properties of chemicals by their ability to induce mutations in the bacterium *Salmonella*.

amino acid: Any of the 20 subunit building blocks that are covalently linked to form proteins.

ampicillin: An antibiotic that prevents bacterial growth.

amplify: To increase the number of copies of a DNA sequence by inserting into a cloning vector that replicates within a host cell *in vivo* or *in vitro* by the polymerase chain reaction.

analogue: A chemical compound structurally similar to another but differing by a single functional group (e.g., 5-bromodeoxyuridine is an analogue of thymidine).

anaphase: Stage of cell division in which chromosomes begin moving to opposite poles of the cell.

anaphase bridge: Results from breaks that occur late in the cell cycle (G_2) after chromosomes have replicated. Sticky ends of broken chromatids rejoin correctly to form a sister union. This type of aberration is always lethal.

anemia: Having too few red blood cells. Symptoms of anemia include feeling tired, weak, and short of breath.

aneuploidy: A condition in which the chromosome number is not an exact multiple of the haploid set.

angiogenesis: The process of the formation of new blood vessels.

angiography: The radiographic visualization of blood vessels following introduction of contrast material.

angioplasty: Reconstruction of blood vessels.

angstrom (\AA): A unit of length equal to 10^{-10} m.

anneal: To pair complementary DNA or RNA sequences, via hydrogen bonding, to form a double-stranded polynucleotide.

anode: Positive side of the x-ray tube; contains the target.

anorexia: Poor appetite.

anoxia: The absence of oxygen.

antibiotic: A class of natural and synthetic compounds that inhibit the growth of or kill microorganisms.

antibiotic resistance: The ability of a microorganism to disable an antibiotic or prevent transport of the antibiotic into the cell.

antibody: Protein (immunoglobulin) produced in response to an antigenic stimulus with the capacity to bind specifically to the antigen.

antiemetic: A drug used to control nausea and vomiting.

antigen: Any foreign substance that elicits an immune response by stimulating the production of antibodies.

antiparallel: Describing molecules in parallel alignment but running in opposite directions. Most commonly used to describe the opposite orientations of the two strands of a DNA molecule.

antisense RNA: A complementary RNA sequence that binds to a naturally occurring (sense) mRNA molecule, thus blocking its translation.

apoptosis: A mode of rapid cell death after irradiation in which the cell nucleus displays characteristic densely staining globules and at least some of the DNA is subsequently broken down into internucleosomal units. Sometimes postulated to be a “programmed,” and therefore potentially controllable, process. Plays an important part in embryogenesis and in tissue regeneration following an insult and can eliminate cells whose DNA has been damaged and not repaired with a high fidelity.

ARCON therapy: The use of accelerated radiotherapy in conjunction with carbogen and nicotinamide.

Arrhenius plot: Probably the most common life-stress relationship when the stress is thermal. In hyperthermia research, a plot of $1/D_0$ versus $1/T$, where D_0 is the reciprocal of the slope of the cell survival curve and T is the absolute temperature. Named after the Swedish physical chemist.

as low as reasonably achievable (ALARA): The principle of limiting the radiation dose of exposed persons to levels as low as are reasonably achievable, economic and social factors being taken into account.

asexual reproduction: Production of offspring in the absence of any sexual process.

ataxia-telangiectasia (AT): A rare autosomal recessive disease in which individuals present with progressive cerebellar ataxia caused by increased loss of Purkinje cells in the cerebellum as well as oculocutaneous telangiectasia. AT individuals are often immunodeficient and hypersensitive to ionizing radiation.

ataxia-telangiectasia-like disorder (ATLD): A rare autosomal recessive disease caused by mutations in the MRE11 gene. Individuals are radiosensitive.

ATM: The ATM gene encodes for a kinase that phosphorylates a serine or threonine that is followed by a glutamine motif (S/T-Q) in target proteins. It is rapidly activated by ionizing radiation and found mutated in AT patients.

atomic mass: See [atomic weight](#).

atomic mass unit (amu): One-sixteenth the mass of a neutral atom of the most abundant isotope of oxygen, oxygen-16. See [atomic weight](#); [mass number](#).

atomic number (Z): The number of protons in the nucleus of an atom and also its positive charge.

atomic weight (at. wt.): The mass of an atom relative to other atoms. The present-day basis for the scale of atomic weights is oxygen; the most common

isotope of this element arbitrarily has been assigned an atomic weight of 16. The unit of the scale is 1/16 the weight of the oxygen-16 atom or roughly the mass of one proton or one neutron. The atomic weight of any element is approximately equal to the total number of protons and neutrons in its nucleus. Compare **atomic number**.

autoimmune disease: The production of antibodies that results from an immune response to one's own molecules, cells, or tissues. Such a response results from the inability of the immune system to distinguish self from nonself. Diseases such as arthritis, scleroderma, systemic lupus erythematosus, and perhaps diabetes are considered autoimmune diseases.

autophagy: A cellular mechanism that disassembles through a regulated physiologic process, unnecessary or dysfunctional cellular components. Autophagy allows the orderly degradation and recycling of cellular components.

autoradiography: Use of a photographic emulsion to detect the distribution of a radioactive label in a tissue specimen.

autosomes: Chromosomes other than the sex chromosomes. In humans, there are 22 pairs of autosomes.

B lymphocyte: A white blood cell responsible for production of antibodies involved in the humoral immune response.

background radiation: The radiation in the natural environment, including cosmic rays and radiation from the naturally radioactive elements, both outside and inside the bodies of humans and animals. Also called *natural radiation*. The term also may mean radiation that is unrelated to a specific experiment.

bacterial artificial chromosome: A vector used to clone DNA fragments of up to 300,000 bp, which contains the minimum chromosomal sequences needed to replicate at low copy number in bacteria.

bacteriophage: A virus that infects bacteria. Altered forms are used as vectors for cloning DNA.

bacterium: A single-celled prokaryotic organism.

basal cells: Cells at the base of the wall of the lung airways. These cells divide to replenish the other cells in the lung wall and often are considered the key cells that, if damaged, can lead to lung cancer.

base pair: A pair of complementary nitrogenous bases in a DNA molecule—adenine–thymine and guanine–cytosine. Also, the unit of measurement for DNA

sequences.

basic fibroblast growth factor (FGF): A mitogen for many types of cells of mesodermal or neuroectodermal origin. Has various angiogenic properties.

B-DNA: See [double helix](#).

beam: A stream of particles or electromagnetic radiation moving in a single direction.

becquerel (Bq): Unit of radioactivity, corresponding to one radioactive disintegration per second. See [activity](#).

benign: Describing a slow-growing, not malignant, tumor that does not spread to other parts of the body. If completely removed, benign lesions do not tend to recur. Incompletely removed tumors may recur but do not spread. Although benign, these tumors may cause permanent damage to some structures in the brain.

BER: Base excision repair, a pathway for repairing damage to DNA bases.

beta particle (β -particle): An elementary particle emitted from a nucleus during radioactive decay, with a single electrical charge and a mass equal to 1/1,837 that of a proton. A negatively charged β -particle is identical to an electron. A positively charged β -particle is called a *positron*. β -Radiation may cause skin burns, and β -emitters are harmful if they enter the body. β -Particles, however, are stopped easily by a thin sheet of metal.

BeV: One billion electron volts. Also written as *GeV*.

bilateral: On both sides of the body.

bioassay: A technique used to identify, quantify, and/or specify the location of radionuclides in the body by direct or indirect analysis of tissues or excretions from the body.

biochemistry: Chemical reactions that sustain life.

biologic half-life: See [half-life, biologic](#).

biologic therapy: Treatment to stimulate or restore the ability of the immune system to fight infection and disease. Also called *immunotherapy*.

biologically effective dose (BED): In fractionated radiotherapy, the quantity by which different fractionation regimens are compared.

biopsy: The removal of a small portion of a tumor to allow a pathologist to examine it under a microscope and provide a diagnosis of tumor type.

biotechnology: Commercial or industrial processes that use biologic organisms or products.

blob: A concentration of about 12 ion pairs in a region about 7 nm in diameter.

blood count: The number of red blood cells, white blood cells, and platelets in a sample of blood.

BNCT: Boron neutron capture therapy.

body burden: The amount of radioactive material present in a human or an animal. See **background radiation; whole-body counter**.

bone marrow: Spongy tissue in the cavities of large bones where the body's blood cells are produced.

bone seeker: A radioisotope that tends to accumulate in the bones; for example, the strontium-90 isotope, which behaves chemically like calcium.

brachytherapy: Internal radiation treatment achieved by implanting radioactive material directly into the tumor or very close to it. Sometimes called *internal radiation therapy*.

Bragg peak: Region of maximum dose deposition near to the end of the track of a charged particle, such as a proton or carbon ion. This allows precise spatial definitions of dose distributions for radiotherapy with charged particles.

breeder reactor: A nuclear reactor that produces fissionable fuel as well as consuming it, especially one that creates more than it consumes. The new fissionable material is created by neutron capture in fertile materials. The process by which this occurs is known as *breeding*.

bremsstrahlung x-rays: X-rays resulting from interaction of the projectile electron with a target nucleus; braking radiation.

bronchial epithelium: The surface layer of cells lining the conducting airways of the lung.

by-product material: Any radioactive material (except source material or fissionable material) obtained during the production or the use of source material or fissionable material. By-product material includes fission products and many other radioisotopes produced in nuclear reactors.

bystander effect: Induction of biologic effects in cells that are not directly traversed by a charged particle but are in close proximity to cells that are.

cancer: A general name for more than 100 diseases in which abnormal cells

grow out of control; a malignant tumor.

cancer stem cell: Cells within a tumor that have the capacity to self-renew.

carcinogen: A physical or chemical agent capable of causing cancer, such as radon progeny, cigarette smoke, or asbestos.

carcinogenesis: Process that leads to the formation of a cancer. It involves several stages (resulting from successive alterations of the genome). The first stage is *initiation* (which may, e.g., be caused by the mutation of a proto-oncogene into an oncogene). For a normal cell to be “transformed” (i.e., for it to become preneoplastic), its genome has to undergo several modifications: appearance of an oncogene, inactivation of both copies of a suppressor gene, immortalization (i.e., acquisition of an unlimited capacity to proliferate), changes affecting the apoptosis system, and so on. A transformed cell can give rise to an invasive cancer at the end of the second stage, known as *promotion*, which is associated with the proliferation of the descendants of the initiated cell and the escape of one of them from the control of the normal surrounding cells and of the body.

carcinogenic: Having the potential (as, e.g., tobacco smoke or alcohol) to contribute to the development of cancer (same as oncogenic).

carcinoma: A malignant tumor derived from epithelial tissue, which forms the skin and outer cell layers of internal organs.

cardiac catheterization: Passage of a small catheter through a vessel in an arm, leg, or neck and into the heart, permitting the securing of blood samples, determination of intracardiac pressure, detection of cardiac anomalies, and the injection of contrast media for imaging.

Cas9: CRISPR associated protein 9 is an RNA-guided endonuclease. Cas9 unwinds foreign DNA and searches for sites complementary of the 20 base-pair spacer region of the guide RNA.

caspase: A family of cysteine-dependent protease enzymes that induce ultrastructural changes in cells undergoing apoptosis.

CAT scan: Computerized axial tomography, often called a *CT scan*, which provides three-dimensional x-ray images of some part of the body. It is useful for diagnosing cancer and for planning radiation therapy treatments.

catalyst: A substance that promotes a chemical reaction by lowering the activation energy of a chemical reaction but itself remains unaltered at the end of the reaction.

cataract: An opacification in the normally transparent lens of the eye.

cathode: Negative side of the x-ray tube; contains the filament and focusing cup.

CD11b+: A cell surface glycoprotein found on monocytes, granulocytes, NK cells, and some peripheral blood lymphocytes. Usually CD11b is found as a heterodimer with beta 2 integrin.

Cdc2 (also known as Cdk1): Kinase that associates with cyclin B to regulate entry into mitosis. Complex is activated by Cdc25-mediated dephosphorylation. Also associates with cyclin A during M phase.

Cdc25C: Phosphatase that activates the cyclin B–Cdc2 complex.

Cdk2: Kinase that associates with cyclin E during the G₁/S transition and cyclin A during S phase. Inhibited by *p21* and *p27*.

Cdk4: Kinase that associates with cyclin D₁. Complex can phosphorylate pRb to allow cells to progress through G₁. Inhibited by *p16*, *p21*, and *p27*.

cDNA (complementary DNA): DNA synthesized from an RNA template using reverse transcriptase.

cDNA library: A library composed of complementary copies of cellular mRNAs (i.e., the exons without the introns).

cell cycle: Sum of the phases of growth of an individual cell type; divided into G₁ (gap 1), S (DNA synthesis), G₂ (gap 2), and M (mitosis); the cycle of cellular events from one mitosis to the next.

cell cycle checkpoint: Control mechanism to verify that each phase of the cell cycle has been accurately completed before progression to the next phase.

cell cycle time: The time between one mitosis and the next.

cell loss factor (Φ): The rate of cell loss from a tumor as a proportion of the rate at which cells are being added to the tumor by mitosis.

cells: The body's tiny functioning units, which can be observed under a microscope. Each cell plays a specialized role in the body. Groups of cells are organized together to form tissues. Tissues are organized to form organs in the body.

cellular oncogene (proto-oncogene): A normal gene that if mutated or improperly expressed contributes to the development of cancer.

centimorgan: A unit of distance between genes on chromosomes. One

centimorgan represents a value of 1% crossing over between two genes.

central nervous system (CNS): The brain and spinal cord.

centriole: A cytoplasmic organelle composed of nine groups of microtubules, generally arranged in triplets. Centrioles function in the generation of cilia and flagella and serve as foci for the spindles in cell division.

centromere: The chromosome constriction to which the spindle fiber attaches. The position of the centromere determines whether chromosomes are metacentric (X-shaped; e.g., chromosomes 1, 3, 16, 19, 20) or acrocentric (inverted V-shaped; e.g., chromosomes 13 to 15, 21, 22, Y). During mitosis, the identical chromatids of each chromosome are separated by shortening of the spindle fibers attached to opposite poles of the dividing cell.

ceramide: A family of lipid molecules composed of sphingosine and fatty acids. Ceramide is generated in cells exposed to ionizing radiation and induces a signal transduction cascade that regulates cell viability. Ceramide is formed by sphingomyelinase activity which is antagonized by ATM.

c-Erb-B2 (HER2/neu): A gene closely related to the epidermal growth factor receptor, which is amplified in various cancers, including that of the breast.

cervix: The lower part of the uterus, which projects out into the vagina.

c-fos: An early-response gene induced by mitogenic stimuli. Forms complexes in the nucleus that act as transcription factors. Recognizes AP-1 sites if complexed with c-jun.

chain reaction: A reaction that stimulates its own repetition. In a fission chain reaction, a fissionable nucleus absorbs a neutron and fissions, releasing additional neutrons. These, in turn, can be absorbed by other fissionable nuclei, releasing still more neutrons. A fission chain reaction is self-sustaining if the number of neutrons released in a given time equals or exceeds the number of neutrons lost by absorption in nonfissioning material or by escape from the system.

characteristic x-rays: X-rays produced following ionization of inner shell electrons; characteristic of the target element.

charged particle: An ion; an elementary particle that carries a positive or negative electrical charge.

chemotherapist: A physician who specializes in the use of drugs to treat cancer, now called a *medical oncologist*.

chemotherapy: A treatment for cancers that involves administering chemicals toxic to malignant cells.

ChIP-Seq: A method to analyze protein binding to DNA by combining chromatin immunoprecipitation with massively parallel DNA sequencing.

CHOP chemotherapy regimen: C: Cyclophosphamide, H: Adriamycin (hydroxyl doxorubicin), O: vincristine (Oncovin), P: Prednisone for lymphoma.

chromatid: Each of the two progeny strands of a duplicated chromosome joined at the centromere during mitosis and meiosis.

chromatin: The complex of DNA, RNA, histones, and nonhistone proteins that make up chromosomes.

chromatin immunoprecipitation: The selective purification of transcription factors bound to DNA that provide information on transcriptional regulation.

chromatography: Technique for the separation of a mixture of solubilized molecules by their differential migration over a substrate.

chromosomal aberration: Any change resulting in the duplication, deletion, or rearrangement of chromosomal material.

chromosomal instability: An effect of irradiation in which chromosomal aberrations continue to appear through many cell generations.

chromosomal mutation: See **chromosomal aberration**.

chromosomal polymorphism: Alternate structures or arrangements of a chromosome that are carried by members of a population.

chromosome: In prokaryotes, an intact DNA molecule containing the genome; in eukaryotes, a DNA molecule complexed with RNA and proteins to form a threadlike structure containing genetic information arranged in a linear sequence.

chromosome banding: Technique for the differential staining of mitotic or meiotic chromosomes to produce a characteristic banding pattern or selective staining of certain chromosomal regions such as centromeres, the nucleolus organizer regions, and GC- or AT-rich regions.

chromosome map: A diagram showing the location of genes on chromosomes.

chronic: Persisting for a long time.

chronic hypoxia: Persistent low oxygen concentrations, such as exists in viable tumor cells close to regions of necrosis.

c-jun: An early-response gene induced by mitogenic stimuli and stress responses. Forms complexes in the nucleus that act as transcription factors. Recognizes AP-1 sites if complexed with c-fos.

classical scattering: Scattering of x-rays with no loss of energy.

clinical trials: Medical research studies conducted with volunteers. Each study is designed to answer scientific questions and to find better ways to prevent or treat disease.

clone: Genetically identical cells or organisms all derived from a single ancestor by asexual or parasexual methods; for example, a DNA segment that has been enzymatically inserted into a plasmid or chromosome of a phage or bacterium and replicated to form many copies.

cloned library: A collection of cloned DNA molecules representing all or part of an individual's genome.

clonogenic cells: Cells that have the capacity to produce an expanding family of descendants (usually at least 50). Also called *colony-forming cells* or *clonogens*.

c-myc: An early-response gene induced by mitogenic stimuli as well as TGF- β . Highly overexpressed as a result of translocations in Burkitt lymphomas. Gene is amplified in certain cancers, as is its relative, N-myc.

cobalt-60: A radioactive substance used as a radiation source to treat cancer.

code: See [genetic code](#).

codon: A group of three nucleotides that specifies the addition of one of the 20 amino acids during translation of mRNA into a polypeptide.

colchicine: An alkaloid compound that inhibits spindle formation during cell division. Used in the preparation of karyotypes to collect a large population of cells inhibited at the metaphase stage of mitosis.

collective dose: Usually refers to the collective effective dose obtained by multiplying the average effective dose by the number of persons exposed to that given dose. Expressed in person-sieverts. The old unit was the man-rem.

collective effective dose (person-sievert): The sum of all the individual effective doses in the population of concern.

colon: Large intestine.

colony: A group of identical cells derived from a single ancestor cell.

combination chemotherapy: The use of more than one drug to treat cancer.

committed effective dose: Effective dose due to absorbed doses in the specified organs or tissues integrated over 50 years following an intake of a radionuclide by ingestion, inhalation, or dermal absorption.

complementarity: Chemical affinity between nitrogenous bases as a result of hydrogen bonding. Responsible for the base pairing between the strands of the DNA double helix.

complementary DNA (cDNA): DNA synthesized from an RNA template using reverse transcriptase.

complementary nucleotides: Members of the pairs adenine–thymine, adenine–uracil, and guanine–cytosine, which have the ability to hydrogen-bond to each other.

complementary RNA (cRNA): RNA synthesized from a cDNA template using T7 RNA polymerase for microarray hybridization.

complementation: Identification of whether a (radiosensitive) phenotype in different mutants is caused by the same gene. Studied by means of cell fusion.

complementation test: A genetic test to determine whether two mutations occur within the same gene. If two mutations are introduced into a cell simultaneously and produce a wild-type phenotype (i.e., they complement each other), they are often nonallelic. If a mutant phenotype is produced, the mutations are noncomplementing and are often allelic.

Compton effect: Scattering of x-rays resulting in ionization and loss of energy. The energy lost by the photon is given to the ejected electron as kinetic energy.

concomitant boost: The practice of adding an extra dose to a smaller field on the later days of a fractionated regimen.

concordance: Pairs or groups of individuals identical in their phenotype. In twin studies, a condition in which both twins exhibit or fail to exhibit a trait under investigation.

conduction: Transfer of heat by molecular agitation.

conductor: Material that allows heat or electrical current to flow.

connective tissue: The tissues of the body that bind together and support various structures of the body. Examples are bone, cartilage, and muscle.

consequential late effects: Late effects that develop as a consequence of severe early effects.

contig: A collection of DNA sequences that overlap at portions of their ends.

continuous hyperfractionated accelerated radiotherapy (CHART): Delivering 54 Gy in 36 fractions with 3 fractions on 12 consecutive days.

contrast agent: A chemical used to highlight disease processes on x-ray tests, contrasting them against the background of normal tissues.

control group: A group of people subject to the same conditions as another group under study, except that the control group is not exposed to the specific factor being investigated in the study group.

cosmic rays: Radiation of many sorts but mostly protons and heavier atomic nuclei with very high energies originating outside the earth's atmosphere. Cosmic radiation is part of the natural background radiation. Some cosmic rays are more energetic than any human-made forms of radiation.

cosmid: A vector designed to allow cloning of large segments of foreign DNA (25,000 to 45,000 bp). Cosmids are hybrids composed of the cos sites of lambda inserted into a plasmid. In cloning, the recombinant DNA molecules are packaged into phage protein coats, and after infection of bacterial cells, the recombinant molecule replicates and can be maintained as a plasmid.

covalent bond: A nonionic chemical bond formed by the sharing of electrons.

CRISPR: Clustered regularly interspersed short palindromic repeats.

critical: Capable of sustaining a chain reaction. See **criticality**.

critical assembly: An assembly of sufficient fissionable material and moderator to sustain a fission chain reaction at a very low-power level, permitting study of the assembly's components for various fissionable materials in different geometric arrangements.

critical mass: The smallest mass of fissionable material that supports a self-sustaining chain reaction under stated conditions.

criticality: The state of a nuclear reactor if it is sustaining a chain reaction.

cross section (σ): A measure of the probability that a nuclear reaction will occur. Usually measured in barns, it is the apparent or effective area presented by a target nucleus or particle to an oncoming particle or other nuclear radiation, such as a photon of γ -radiation.

crossing over: The exchange of chromosomal material (parts of chromosomal arms) between homologous chromosomes by breakage and reunion. The

exchange of material between nonsister chromatids during meiosis is the basis of genetic recombination.

CT scan (CAT scan, CT x-ray): A three-dimensional x-ray. *CT* stands for *computerized tomography*.

cure: An outcome of treatment that leaves the patient disease free, with no likelihood of recurrence.

curie (Ci): Old unit of radioactivity, corresponding to 3.7×10^{10} radioactive disintegrations per second. Now replaced by the becquerel.

CXCR4: Receptor for the chemokine stromal derived factor-1 (SDF-1) that is involved in regulating chemotaxis. Plays an important role in vascularization.

cyclic adenosine monophosphate (cAMP): An important regulatory molecule in both prokaryotic and eukaryotic organisms.

cyclin A: Regulatory protein that associates with Cdk2 during the S phase of the cell cycle.

cyclin B: Regulatory protein that associates with Cdc2 to regulate entry into mitosis.

cyclin D₁: One of three cyclin D family members (also D₂, D₃). Associates with Cdk5 or Cdk6 to regulate through the G₁ phase of the cell cycle. Induced by various mitogens.

cyclin E: Protein that associates with Cdk2 during late G₁ phase and is thought to regulate entry into S phase.

cyclin-dependent kinases (Cdks): Proteins that complex with their cyclin regulatory subunits to phosphorylate proteins necessary for progression through the cell cycle.

cyclins: Proteins that complex with Cdks to regulate progression through the cell cycle.

cyst: A cavity, usually filled with a liquid, sometimes associated with benign or malignant tumors.

cytogenetics: Study that relates the appearance and behavior of chromosomes to genetic phenomena.

cytokines: Polypeptides originally defined as being released from lymphocytes and involved in maintenance of the immune system. These factors have

pleiotropic effects not only on hematopoietic cells but also on many other cell types as well.

D₀: A parameter in the multitarget equation: the radiation dose that reduces survival to e^{-1} (i.e., 0.37) of its previous value on the exponential portion of the survival curve.

dalton: A unit of measurement equal to the mass of a hydrogen atom, 1.67×10^{-24} g; 1/Avogadro's number.

daughter: A nuclide formed by the radioactive decay of another nuclide, which in this context is called the *parent*. Replaced by *progeny*.

decay, radioactive: The spontaneous transformation of one nuclide into a different nuclide or into a different energy state of the same nuclide. The process results in a decrease, with time, of the original radioactive atoms in a sample. Radioactive decay involves the emission from the nucleus of α -particles, β -particles (electrons), or γ -rays; the nuclear capture or ejection of orbital electrons; or fission. Also called *radioactive disintegration*. See **half-life**; **radioactive series**.

decay series (decay chain): A series of radioactive atoms, each the progeny of the one before and the parent of the one after; the series ends if any progeny is not radioactive.

deletion: A segment of a chromosome that is missing as a result of two breaks and the loss of the intervening piece.

denature: To induce structural alterations that disrupt the biologic activity of a molecule. Often refers to breaking hydrogen bonds between base pairs in double-stranded nucleic acid molecules to produce single-stranded polynucleotides or altering the secondary and tertiary structure of a protein, destroying its activity.

depleted uranium: Uranium with less than 0.7% of uranium-235.

dermatitis: A skin rash.

deterministic effect: An effect for which the severity of the effect in affected individuals varies with the dose and for which a threshold usually exists.

detriment: See **radiation detriment**.

deuterium (hydrogen-2, D): An isotope of hydrogen whose nucleus contains one neutron and one proton and therefore is about twice as heavy as the nucleus of normal hydrogen, which contains only a single proton. Deuterium often is

referred to as *heavy hydrogen*; it occurs in nature as 1 atom to every 6,500 atoms of normal hydrogen. It is nonradioactive. Compare **tritium**. See **heavy water**.

deuteron: The nucleus of deuterium. It contains one proton and one neutron.

dicentric chromosome: A chromosome having two centromeres.

dideoxynucleotide (ddN): A deoxynucleotide that lacks a 3' hydroxyl group and is thus unable to form a 3' to 5' phosphodiester bond necessary for chain elongation. Dideoxynucleotides are used in DNA sequencing and the treatment of viral diseases.

differential diagnosis: A list of the most likely diagnoses for a particular set of symptoms and x-ray findings. The use of different imaging techniques often narrows the differential diagnosis to the most likely disease present.

differentiation: The process of complex changes by which cells and tissues attain their adult structure and functional capacity.

digest: To cut DNA molecules with one or more restriction endonucleases.

diploid: A condition in which each chromosome exists in pairs; having two of each chromosome.

direct action: Ionization or excitation of atoms within DNA leading to free radicals, as distinct from the reaction with DNA of free radicals formed in nearby water molecules.

disjunction: The separation of chromosomes at the anaphase stage of cell division.

diuretics: Drugs that help the body get rid of excess water and salt.

dizygotic twins: Twins produced from separate fertilization events; two ova fertilized independently. Also known as *fraternal twins*.

DNA damage-induced nuclear foci: The formation of complexes of signaling and repair proteins that localize to sites of DNA breaks in the nucleuse of a cell.

DNA (deoxyribonucleic acid): An organic acid composed of four nitrogenous bases (adenine, thymine, cytosine, and guanine) linked via sugar and phosphate units. DNA is the genetic material of most organisms and usually exists as a double-stranded molecule in which two antiparallel strands are held together by hydrogen bonds between adenine–thymine and cytosine–guanine base pairs.

DNA fingerprint: A unique pattern of DNA fragments identified by Southern hybridization or by polymerase chain reaction.

DNA polymerase: An enzyme that catalyzes the synthesis of DNA from deoxyribonucleotides and a template DNA molecule.

DNA polymorphism: One or two or more alternate forms of a chromosomal locus that differ in nucleotide sequence or have variable numbers of repeated nucleotide units.

DNA sequencing: Procedures for determining the nucleotide sequence of a DNA fragment.

DNA stability genes: A class of genes involved both in monitoring and maintaining the integrity of DNA.

DNase (deoxyribonuclease): An enzyme that degrades or breaks down DNA into fragments or constitutive nucleotides.

dominance: The expression of a trait in the heterozygous condition.

dominant gene: A gene whose phenotype is expressed if it is present in a single copy.

dominant-acting oncogene: A gene that stimulates cell proliferation and contributes to oncogenesis when present in a single copy.

dose: General term for the quantity of radiation. See **absorbed dose; equivalent dose; effective dose; collective dose**.

dose limit: A limit on dose that is applied for exposure of individuals to prevent the occurrence of tissue reactions and to limit the probability of stochastic effects.

dose rate: The radiation dose delivered per unit time and measured, for instance, in grays per hour.

dose-modifying factor (DMF): A ratio indicating the dose without to the dose with the agent for the same level of effect. (Similarly, *dose-reduction factor* or *sensitizer enhancement ratio*.)

dose-rate effect: Decreasing radiation response with decreasing radiation dose rate.

dosimetrist: A person who plans and calculates the proper radiation dose for treatment.

double helix: The model for DNA structure proposed by James Watson and Francis Crick, involving two antiparallel, hydrogen-bonded polynucleotide chains wound into a right-handed helical configuration, with 10 bp per full turn

of the double helix. Often called *B-DNA*.

double minutes: Chromosome fragments that are the result of chromosome duplication and in which oncogenes may be amplified. A common cytologic feature of tumor cells.

double trouble: The situation in which a hot spot within a treatment field receives not only a higher dose but also a higher dose per fraction, which means that the biologic effectiveness of the dose is also greater.

doubling dose: Applied to heritable effects, the dose required to double the spontaneous mutation incidence; put another way, the dose required to produce an incidence of mutations equal to the spontaneous rate.

doubling time: The time it takes for a cell population or tumor volume to double its size.

***Drosophila melanogaster*:** The fruit fly, whose common use in genetic studies was introduced by Thomas Hunt Morgan in the early 1900s.

early response gene: A gene such as *c-fos*, *c-jun*, or *c-myc*, whose mRNA levels are induced dramatically following mitogenic stimuli or stress.

early responses: Radiation-induced normal tissue damage that is expressed in weeks to a few months after exposure. Generally caused by damage to parenchymal cells. The α/β ratio tends to be large.

ED₅₀ (effect dose 50%): Radiation dose that produces a specified effect in the normal tissues of 50% of animals.

edema: Abnormal accumulation of fluid (e.g., pulmonary edema, a buildup of fluid in the lungs).

EF5: This molecule is a fluorinated derivative of the 2-nitroimidazole etanidazole and is used to determine oxygen levels in normal and tumor tissue. It binds rather selectively and irreversibly to cellular macromolecules in hypoxic cells. A radioactive version has been generated for PET imaging is currently undergoing testing.

effective dose: The radiation dose allowing for the fact that some types of radiation are more damaging than others, and some parts of the body are more sensitive to radiation than others. It is defined as the sum over specified tissues of the products of the equivalent dose in a tissue and the tissue weighting factor for that tissue.

eIF2 α : Eukaryotic translation initiation factor 2 alpha is a protein that catalyzes

the formation of the preinitiation complex involved in protein synthesis.

electromagnetic radiation: Radiation consisting of associated and interacting electrical and magnetic waves that travel at the speed of light, such as light, radio waves, γ -rays, and x-rays. All electromagnetic radiation can be transmitted through a vacuum.

electron (e): An elementary particle with a unit negative electrical charge and a mass $1/1,837$ that of the proton. Electrons surround the positively charged nucleus and determine the chemical properties of the atom. Positive electrons, or *positrons*, also exist.

electronvolt (eV): The amount of energy gained by a particle of charge e (-1.6×10^{-19} C) if it is accelerated by a potential difference of 1 V. $1 \text{ eV} \approx 1.6 \times 10^{-19} \text{ J}$.

electrophoresis: The technique of separating charged molecules in a matrix to which an electrical field is applied.

electroporation: A process whereby high-voltage pulses of electricity are used to open pores in the cell membrane, through which foreign DNA can pass.

Ellis formula: The relation between dose, overall time, and number of fractions in radiotherapy (NSD).

endonuclease: An enzyme that cleaves at internal sites in the substrate molecule.

epidermal growth factor (EGF): Protein that promotes growth of epidermal cells and can stimulate or inhibit the proliferation and differentiation of various cells.

epithelium: A thin layer of cells in the skin, mucous membrane, or any duct that replaces worn-out cells by cell division.

Eppendorf probe: An oxygen probe with a fast response time that can be moved quickly through a tumor under computer control to obtain a large number of oxygen measurements. See [oxygen probe](#).

equivalent dose: A quantity used for radiation protection purposes that takes into account the different probability of effects that occur with the same absorbed dose delivered by radiations with different radiation weighting factor values. It is defined as the product of the average absorbed dose in a specified organ or tissue and the radiation weighting factor values. If dose is in grays, equivalent dose is in sieverts.

erb-B (EGFR/HER1): Membrane receptor that binds epidermal growth

hormone.

error-free repair: DNA repair whereby the molecule is reconstituted with a high fidelity (i.e., without loss of information).

erythropoietin: Cytokine that stimulates late erythroid progenitors to form small colonies of erythrocytes.

***Escherichia coli* (*E. coli*):** A bacterium found in the human colon that is used widely as a host for molecular cloning experiments.

ethidium bromide: A fluorescent dye that is used to stain DNA and RNA and that intercalates between nucleotides and fluoresces if exposed to ultraviolet light.

eukaryote: An organism whose cells possess a nucleus and other membrane-bounded vesicles, including all members of the protist, fungi, plant, and animal kingdoms.

evolution: The origin of plants and animals from preexisting types. Descent with modifications.

excision repair: Repair of DNA lesions by removal of a polynucleotide segment and its replacement with a newly synthesized, corrected segment.

exon: DNA segment of a gene that is transcribed and translated into protein.

exonuclease: An enzyme that breaks down nucleic acid molecules by breaking the phosphodiester bonds at the 3' or 5' terminal nucleotides.

exponential growth: Growth according to an exponential equation.

exponential survival curve: A survival curve without a threshold or shoulder region that is a straight line on a semilogarithmic plot.

exposure (X): (Often used in its more general sense and not as the specially defined radiation quantity.) A measure of the quantity of x- or γ -radiation based on its ability to ionize the air through which it passes. The SI unit of exposure is coulomb per kilogram (C/kg). The previously used special unit of exposure was the röntgen (R).

expression library: A library of cDNAs whose encoded proteins are expressed by specialized vectors.

expression vector: A plasmid or phage-carrying promoter region designed to cause expression of cloned DNA sequences.

external radiotherapy: Radiation therapy that uses a machine located outside

the body to aim high-energy rays at cancer cells. Sometimes called *external beam radiotherapy*.

extrapolated total dose (ETD): Calculated isoeffect dose when the dose rate is very low or when fraction size is very small.

extrapolation number: A parameter in the multitarget equation: the point on the survival scale to which the straight part of the curve back-extrapolates.

fallout: The radioactive material falling from the atmosphere to Earth's surface after a nuclear event, such as a weapon's test or accident.

familial breast cancer: Familial breast cancer is due to mutations in breast cancer susceptibility genes (BRCA1 and BRCA2). Clinical characteristics are early age of onset and higher incidence of cancer within an affected family.

familial trait: A trait transmitted through and expressed by members of a family.

FANCD1: Fanconi anemia complementation group D1 is a very rare disorder with individuals highly susceptible to childhood malignancies. The molecular defect is mutations of the BRCA2 gene.

fast neutrons: Neutrons with energy greater than approximately 100,000 eV. Compare **thermal neutrons**.

fibroblast: A precursor cell of connective tissue that is relatively easy to maintain in cell culture.

field: A term used in radiation oncology to describe or define an area through which x-rays are directed toward the tumor.

field-size effect: The dependence of normal tissue damage on the size of the irradiated area; also known as *volume effect*.

film badge: An assembly containing a packet of unexposed photographic film and various filters (absorbers); when the film is developed, the dose and type of radiation to which the wearer was exposed can be estimated.

fingerprint: The pattern of ridges and whorls on the tip of a finger. The pattern obtained by enzymatically cleaving a protein or nucleic acid and subjecting the digest to two-dimensional chromatography or electrophoresis.

FISH (fluorescence *in situ* hybridization): The process whereby fluorescent dyes are attached to specific regions of the genome, thus aiding the identification of chromosomal damage.

fission: The splitting of a heavy nucleus into two approximately equal parts (which are nuclei of lighter elements), accompanied by the release of a relatively large amount of energy and generally one or more neutrons. Fission can occur spontaneously, but usually, it is caused by nuclear absorption of γ -rays, neutrons, or other particles.

fission products: The nuclei (fission fragments) formed by the fission of heavy elements plus the nuclides formed by the fission fragments' radioactive decay.

5-bromodeoxyuridine (BrdU or BrdUrd): A mutagenically active analogue of thymidine in which the methyl group at the 6' position in thymine is replaced by bromine.

flanking region: The DNA sequences extending on either side of a particular locus or gene.

flexible tissues: Nonhierarchical cell populations in which function and proliferation take place in the same cells.

flow cytometry: Analysis of cell suspensions in which a dilute stream of cells is passed through a laser beam. DNA content and other properties are measured by light scattering and fluorescence following staining with dyes or labeled antibodies.

fluoroscopy: A medical x-ray procedure used for observation of the internal features of the body by means of the fluorescence produced on a screen by a continuous field of x-rays transmitted through the body.

founder effect: A form of genetic drift. The establishment of a population by a small number of individuals whose genotypes carry only a fraction of the different kinds of alleles in the parental population.

fractionation: The daily dose of radiation based on the total dose divided into a particular number of daily treatments.

fragile site: A gap or nonstaining region of a chromosome that can be induced to generate chromosome breaks.

frameshift mutation: A mutational event leading to the insertion of one or more base pairs in a gene, shifting the codon reading frame in all codons following the mutational site.

free radical: A fragment of an atom or molecule that contains an unpaired electron, which, therefore, makes it very reactive.

functional imaging: Imaging methods aimed at detecting physiologic changes,

in contrast to structural or anatomical imaging.

functional subunits (FSUs): Many tissues can be thought of as consisting of discrete FSUs. These may be arranged in series as in the spinal cord, or in parallel as in the kidney.

fusion, thermonuclear: The reaction that occurs when two or more light nuclei coalesce to form a heavier nucleus with the release of energy.

fusion gene: A hybrid gene created by joining portions of two different genes (to produce a new protein) or by joining a gene to a different promoter (to alter or regulate gene transcription).

gamete: A specialized reproductive cell with a haploid number of chromosomes.

gamma rays (γ -rays): High-energy, short-wavelength electromagnetic radiation. γ -Radiation frequently accompanies α - and β -emissions and always accompanies fission. γ -Rays are very penetrating and are stopped best or shielded against by dense materials, such as lead or depleted uranium. γ -Rays are indistinguishable from x-rays except for their source: γ -Rays originate inside the nucleus, x-rays from outside.

gastrointestinal (GI): Having to do with the digestive tract, which includes the mouth, esophagus, stomach, and intestines.

gene: The fundamental physical unit of heredity whose existence can be confirmed by allelic variants and that occupies a specific chromosomal locus; a DNA sequence coding for a single polypeptide.

gene amplification: The presence of multiple copies of a gene and one of the mechanisms by which proto-oncogenes are activated to result in neoplasia.

gene expression: The process of producing a protein from its DNA- and mRNA-coding sequences.

gene mutation: See [point mutation](#).

gene pool: The total of all genes possessed by reproductive members of a population.

genetic burden: Average number of recessive lethal genes carried in the heterozygous condition by an individual in a population. Also called *genetic load*.

genetic code: The three-letter code that translates nucleic acid sequence into protein sequence.

genetic counseling: Analysis of risk for genetic defects in a family and the presentation of options available to avoid or ameliorate possible risks.

genetic disease: A disease that has its origin in changes to the genetic material, DNA. Usually refers to diseases that are inherited in a mendelian fashion, although noninherited forms of cancer also result from DNA mutation.

genetic drift: Random variation in gene frequency from generation to generation, most often observed in small populations.

genetic effects of radiation: Radiation effects that can be transferred from parent to offspring; any radiation-caused changes in the genetic material of sex cells. Now called *heritable effects*.

genetic engineering: The manipulation of an organism's genetic endowment by introducing or eliminating specific genes. A broad definition of genetic engineering also includes selective breeding and other means of artificial selection.

genetic polymorphism: The stable coexistence of two or more discontinuous genotypes in a population. If the frequencies of two alleles are carried to equilibrium, the condition is called *balanced polymorphism*.

genetically significant dose: The dose that, if given to every member of a population, should produce the same heritable harm as the actual doses received by the individuals. Expressed in sieverts, this dose takes into account the childbearing potential of those receiving the dose.

genetics: The branch of biology that deals with heredity and the expression of inherited traits.

genome: The genetic complement contained in the chromosomes of a given organism, usually the haploid chromosome state.

genomic instability: The failure to pass an accurate copy of the whole genome from a cell to its progeny cells some generations after radiation. Expressed, for example, by the appearance of chromosome aberrations many generations later.

genomic library: A library composed of fragments of genomic DNA.

genomics: Study of DNA sequence, organization and structure.

genotype: The structure of DNA that determines the expression of a trait (phenotype).

GeV: One billion electronvolts. Also written as BeV.

GI: Gastrointestinal.

giga: A prefix that multiplies a basic unit by 1 billion (10^9).

gonads: The ovaries or testes.

grade: In reference to tumors, the aggressiveness of the cell type, from very low aggressiveness with slow growth pattern to very aggressive with rapid spread. Tumor grading classifications vary according to type of tumor.

graft-versus-host disease (GVHD): In transplants, reaction by immunologically competent cells of the donor against the antigens present on the cells of the host. In human bone marrow transplants, often a fatal condition.

granulocyte colony-stimulating factor (G-CSF): Cytokine that stimulates differentiation of progenitors into granulocytes.

granulocyte-macrophage colony-stimulating factor (GM-CSF): Cytokine that stimulates differentiation of progenitors into granulocytes, macrophages, and eosinophils.

gray (Gy): The special name for the SI unit of absorbed dose, kerma, and specific energy imparted equal to 1 J/kg. The previous unit of absorbed dose, rad, has been replaced by the gray. One gray equals 100 rad.

ground state: The state of a nucleus, an atom, or a molecule at its lowest (normal) energy level.

growth delay: Extra time required for an irradiated tumor to reach a given size, compared with an unirradiated control.

growth factor: A serum protein that stimulates cell division when it binds to its cell surface receptor.

growth factor receptor: A membrane-spanning protein that selectively binds its growth factor and then transduces a signal for cell division to other molecules in the cytoplasm and nucleus.

growth fraction: Proportion of viable cells in active cell division.

growth hormone (GH): Secreted by the anterior pituitary gland, a hormone that acts mainly on the growth of bone and muscles. Can be secreted by lymphocytes in response to phorbol ester treatment and may be involved in lymphocyte growth. Also known as *somatotropin*.

hadron therapy: Radiotherapy using particles that are made of quarks. In practice, this means neutrons, protons carbon ions, or other positive ions.

half-life ($t_{1/2}$): The time taken for the activity of a radionuclide to decay to half its initial value.

half-life, biologic: The time required for a biologic system, such as a human or an animal, to eliminate by natural processes half the amount of a substance, such as a radioactive material, that has entered it.

haploid: Having only one of each type of chromosome, as is usually the case in gametes (oocytes and spermatozoa).

heat shock: A transient response following exposure of cells or organisms to elevated temperatures. The response involves activation of a small number of loci, inactivation of previously active loci, and selective translation of heat-shock mRNA. Appears to be a nearly universal phenomenon, observed in organisms ranging from bacteria to humans.

heavy water (D_2O): Water containing significantly more than the natural proportion (1 in 6,500) of heavy hydrogen (deuterium) atoms to ordinary hydrogen atoms. Heavy water is a moderator in some nuclear reactors because it slows down neutrons effectively and also has a low cross section for absorption of neutrons.

helicase: An enzyme that participates in DNA replication by unwinding the double helix near the replication fork.

hematocrit: The percentage of blood made up of red blood cells.

hematology: The study of blood and its disorders.

hemizygous: Describing a condition in which a gene is present in a single dose. Usually applied to genes on the X chromosome in heterogametic males.

hemoglobin (Hb): An iron-containing, conjugated respiratory protein occurring chiefly in the red blood cells of vertebrates. Carries oxygen to the tissues.

hemophilia: A sex-linked trait in humans associated with defective blood-clotting mechanisms.

herpesvirus: One of a group of viruses causing herpes in man and other primates. These viruses are potentially useful as vectors in gene therapy because they are large and can accommodate a large insert, but they are seldom used in practice because they are potentially more pathogenic and difficult to control.

heterochromatin: The heavily staining, late-replicating regions of chromosomes that are condensed in interphase. Thought to be devoid of structural genes.

heterozygote: An individual with different alleles at one or more loci. Such individuals produce unlike gametes and therefore do not breed true.

hierarchical tissues: Cell populations comprising a lineage of stem cells, proliferating cells, and mature cells. The mature cells do not divide.

high-dose-rate (HDR) remote brachytherapy: A type of internal radiation in which each treatment is given in a few minutes with the radioactive source in place. The source of radioactivity is removed between treatments.

histones: Proteins complexed with DNA in the nucleus. They are rich in the basic amino acids arginine and lysine and function in the coiling of DNA to form nucleosomes.

HLA: Cell surface proteins, produced by histocompatibility loci, that are involved in the acceptance or rejection of tissue and organ grafts and transplants.

homogeneously staining region (HSR): Segment of mammalian chromosomes that stains lightly with Giemsa following exposure of cells to a selective agent. These regions arise in conjunction with gene amplification and are regarded as the structural locus for the amplified gene.

homologous chromosomes: Chromosomes that have the same linear arrangement of genes; a pair of matching chromosomes in a diploid organism.

homologous recombination (HR): DNA repair pathway for double-strand breaks by using as a template an undamaged homologous DNA sequence, usually from the sister chromatid.

homologue: Any member of a set of genes or DNA sequences from different organisms whose nucleotide sequences show a high degree of one-to-one correspondence.

homozygote: An individual with identical alleles at one or more loci. Such individuals produce identical gametes and therefore breed true.

hormesis: The hypothesis that low levels of radiation are beneficial, activating repair mechanisms that protect against disease. Rejected by Biological Effects of Ionizing Radiation (BEIR), UNSCEAR, ICRP, and National Council on Radiation Protection and Measurements (NCRP).

hormones: Factors synthesized in endocrine glands that if released, act to regulate and modulate the functions of multicellular organisms.

Human Genome Project: A project coordinated by the National Institutes of Health and the Department of Energy to determine the entire nucleotide

sequence of the human chromosomes.

hybrid: The offspring of two parents differing in at least one genetic characteristic.

hybridization: The hydrogen bonding of complementary DNA or RNA sequences to form a duplex molecule.

hybridoma: A somatic cell hybrid produced by the fusion of an antibody-producing cell and a cancer cell, specifically a myeloma. The cancer cell contributes the ability to divide indefinitely, and the antibody cell confers the ability to synthesize large amounts of a single antibody.

hydrogen bond: An electrostatic attraction between a hydrogen atom bonded to a strongly electronegative atom such as oxygen or nitrogen and another atom that is electronegative or contains an unshared electron pair.

hyperbaric oxygen (HBO): The use of high oxygen pressures (two or three atmospheres) to enhance oxygen availability in radiotherapy.

hyperdiploid: Additional chromosomes; the modal number is 47 or more.

hyperfractionated radiation: Division of the total dose of radiation into smaller doses usually given more than once a day.

hyperthermia: The use of heat to treat cancer.

hypodiploid: Loss of chromosomes with modal number 45 or less.

hypofractionation: The technique of administering radiotherapy in a large single fraction or in a few dose fractions larger than the conventional level of 2 Gy.

hypopharynx: Part of the lower throat beside and behind the larynx (voice box).

hypoxia: Low oxygen tension; usually the very low levels required to make cells maximally radioresistant. Sometimes used to mean *anoxia* (literally, the complete absence of oxygen).

hypoxia-inducible factor (HIF): A family of transcription factors that respond to low levels of oxygen. There are three family members: HIF-1, HIF-2, and HIF-3. Each family member is composed of an oxygen labile alpha subunit and a constitutively expressed aryl hydrocarbon receptor nuclear translocator (ARNT).

hypoxic cell cytotoxin: Any agent, typically a bioreductive drug, that preferentially kills hypoxic cells.

hypoxic fraction: The fraction of hypoxic cells in a tumor that are resistant to

radiation but still viable.

ICRP: International Commission on Radiological Protection.

identical twins: See [monozygotic twins](#).

IFN α : Cytokine that is produced in response to viral infection and that protects cells from viruses and causes growth arrest of normal and tumor cells.

IFN β : Cytokine that is produced in response to viral infection and that protects cells from viruses and causes growth arrest of normal and tumor cells.

IFN γ : Cytokine that is produced in response to viral infection and that activates macrophages, protects cells from viruses, and causes growth arrest of normal and tumor cells.

IL-1: Cytokine involved in the regulation of immune and inflammatory responses.

IL-2: Cytokine that stimulates growth of T-cells. Also stimulates B cell growth and differentiation, generation of lymphokine-activated killer cells, activation of macrophages, and production of other cytokines.

IL-3: Cytokine that induces the proliferation of hematopoietic cells, particularly erythroid and myeloid cells. Produced by activated T cells and mast cells.

IL-4: Cytokine that has general effects on hematopoietic cells, including the activation, growth, and differentiation of B cells. Also induces growth of mast cells and T cells.

IL-5: Cytokine that induces eosinophil differentiation as well as B cell activation, growth, and differentiation.

IL-6: Cytokine that regulates B cell differentiation, T-cell activation, killer cell induction, and other physiologic responses. Induced by cytokines, ultraviolet irradiation, and other stimuli. Many effects are similar to IL-1 and TNF.

IL-7: Cytokine that promotes the growth of B and T-cell progenitors.

IL-8: One of an extended family of cytokines that act as chemoattractants for neutrophils, T cells, and basophils.

IL-9: Cytokine that stimulates proliferation of T cells and enhances mast cell activity and growth.

IL-10: Cytokine that enhances IL-2 and IL-4 proliferative response of T cells. Also acts to inhibit cytokine production by various different cells.

IL-11: Cytokine that together with other cytokines stimulates the growth of various hematopoietic progenitors.

IL-12: Cytokine that promotes growth of T and natural killer cells and enhances cytotoxic T-cell responses.

immortalization: Term used to describe the change as cells from somatic tissues that are only able to perform a limited number of cell divisions undergo a “crisis” and become capable of unlimited cell divisions.

immortalizing oncogene: A gene that upon transfection enables a primary cell to grow indefinitely in culture.

immune system: The body’s defense system, which protects it from foreign substances, such as bacteria and viruses that are harmful to it.

immunoglobulin: The class of serum proteins having the properties of antibodies.

implant: A quantity of radioactive material placed in or near a cancer.

in situ hybridization: A technique for the cytologic localization of DNA sequences complementary to a given nucleic acid or polynucleotide.

in vitro: Literally, in glass; outside the living organism; occurring in an artificial environment.

in vivo: Literally, in the living; occurring within the living body of an organism.

inbreeding: Mating between closely related organisms.

incomplete repair: Increased damage from fractionated radiotherapy if the time interval between doses is too short to allow complete recovery of sublethal damage.

indirect action: Damage to DNA by free radicals formed through the ionization of nearby water molecules.

inducible response: A response to irradiation that is modified by a small dose of radiation given shortly before.

infusion: Slow or prolonged intravenous delivery of a drug or fluid.

initial slope: The steepness of the initial part of the oxic cell survival curve.

initiating agent: Something that causes initial “latent” damage to the DNA. The cell requires more damage from a second “promoting agent” before the damage is expressed as cancer. Radiation usually is considered an initiating agent.

initiation codon: The mRNA sequence AUG, which codes for methionine and initiates translation.

intensity-modulated radiation therapy (IMRT): A technique using nonuniform radiation beams to achieve high conformality treatment plans.

intercalating agent: A compound that inserts between bases in a DNA molecule, disrupting the alignment and pairing of bases in the complementary strands (e.g., acridine dyes).

interferon: One of a family of proteins that act to inhibit viral replication in higher organisms. Some interferons may have anticancer properties.

interphase: That portion of the cell cycle between divisions.

interphase death: The death of irradiated cells before they reach mitosis.

interstitial implant: The placement of fine tubes in a gridlike pattern through tissues containing a cancer; these tubes are filled later with radioactive sources for brachytherapy.

intracavitary implant: The placement of a small tube within a body cavity, such as the bronchus or vagina; this tube later is filled with radioactive sources for brachytherapy.

intraoperative radiation: A type of radiation used to deliver a large dose of radiation therapy to the tumor bed and surrounding tissue at the time of surgery.

intravenous (IV): Into a vein.

intron: A portion of DNA that is located between coding regions in a gene and which is transcribed but which does not appear in the mRNA product.

inverse square law: A physical law stating that the intensity of x- or γ -radiation from a point source emitting uniformly in all directions is inversely proportional to the square of the distance from the source.

inversion: Two breaks occurring in the same chromosome with rotation of the intervening segment. If both breaks are on the same side of the centromere, it is called a *paracentric* inversion. If they are on opposite sides, it is called a *pericentric* inversion.

ion: An electrically charged atom or group of atoms.

ion pair: A closely associated positive ion and negative ion (usually an electron) having charges of the same magnitude and formed from a neutral atom or molecule by radiation.

ionization: The process of adding one or more electrons to, or removing one or more electrons from, atoms or molecules, thereby creating ions. High temperatures, electrical discharges, or nuclear radiations can cause ionization.

ionization chamber: A device for detection of ionizing radiation or for measurement of radiation dose and dose rate.

ionizing radiation: Any radiation displacing electrons from atoms or molecules, thereby producing ions. Examples of ionizing radiation are α -, β -, and γ -radiation; x-rays; and shortwave ultraviolet light. Ionizing radiation may produce severe skin or tissue damage. See **radiation burn**; **radiation illness**.

ipsilateral: On the same side of the body (opposite of contralateral).

irradiation: Exposure to radiation, as in a nuclear reactor.

isobars: Atoms having the same number of nucleons but different numbers of protons and neutrons.

isochromosome: A chromosome that consists of identical copies of one chromosome arm with loss of the other arm. Thus, an isochromosome for the long arm of chromosome 17 (i[17][q10]) contains two copies of the long arm (separated by the centromere) with loss of the short arm of the chromosome.

isoeffect plots: Graphs of the total dose for a given effect (e.g., ED₅₀) plotted, for instance, against dose per fraction or dose rate.

isomers: Atoms having the same number of protons and neutrons but a different nuclear energy state.

isotopes: Forms of a chemical element that have the same number of protons and electrons but differ in the number of neutrons contained in the atomic nucleus. Unstable isotopes undergo a transition to a more stable form with the release of radioactivity.

isotropic: Having equal intensity in all directions.

Karnofsky score: A measure of the patient's overall physical health following treatment, judged by his or her level of activity.

karyotype: Arrangement of chromosomes from a particular cell according to a well-established system such that the largest chromosomes are first and the smallest ones are last. Normal female karyotype is 46,XX; normal male karyotype is 46,XY.

kerma: The sum of the initial kinetic energies of all the charged ionizing

particles liberated by uncharged ionizing particles per unit mass of a specified material. Kerma is measured in the same unit as absorbed dose. The SI unit of kerma is joule per kilogram, and its special name is gray (Gy). Kerma can be quoted for any specified material at a point in free space or in an absorbing medium.

kilobase (kb): A unit of length consisting of 1,000 nucleotides.

kilovolt (kV): A unit of electrical potential difference equal to 1,000 V.

labeling index (LI): Proportion or percentage of cells in the population (S phase) that take up tritiated thymidine or other precursors, such as bromodeoxyuridine; that is, the proportion synthesizing DNA.

late responses: Radiation-induced normal tissue damage that in humans is expressed months to years after exposure. Generally results from damage to connective tissue cells. The α/β ratio tends to be small (<5 Gy).

latency period: The time between an injury occurring and the effects of the injury expressing themselves as disease.

LD_{50/30}: Radiation dose to produce lethality in 50% of animals by 30 days; similarly, LD_{50/7}, and so on.

leader sequence: That portion of an mRNA molecule from the 5' end to the beginning codon. May contain regulatory or ribosome-binding sites.

leading strand: During DNA replication, the strand synthesized continuously 5' to 3' toward the replication fork.

leakage radiation: All radiation coming from within the source assembly except for the useful beam.

LET: Linear energy transfer.

lethal dose (LD): A dose of ionizing radiation sufficient to cause death. Median lethal dose (MLD, or LD₅₀) is the dose required to kill, within a specified period of time, half the individuals in a large group of organisms similarly exposed. The LD_{50/60} for humans is about 4 Gy.

lethal gene: A gene whose expression results in death.

leucine zipper: A secondary protein structure in which projecting leucine residues on two polypeptide chains interdigitate to form a stable dimer.

leukemia: A malignant cancer of the blood-forming tissues (bone marrow or

lymph nodes), generally characterized by an overproduction of white blood cells.

leukocyte: White blood cell.

lifetime risk: The risk of dying of some particular cause over the whole of a person's life.

Li–Fraumeni syndrome: A rare autosomal, dominantly inherited disease that predisposes individuals to develop a wide spectrum of tumors. Caused by mutations in p53 or Chk2 tumor suppressor genes.

ligase: An enzyme that catalyzes a reaction that links two DNA molecules by the formation of a phosphodiester bond.

ligation: The process of joining two or more DNA fragments.

linear accelerator: A machine creating high-energy radiation to treat cancers. See [accelerator](#).

linear energy transfer (LET): The rate of energy loss along the track of an ionizing particle, usually expressed in keV/ μm .

linear no–threshold (LNT): The hypothesis that cancer risks at low doses can be linearly extrapolated from risks at high doses, with no threshold in dose.

linear-quadratic model: Model in which the effect (E) is a linear-quadratic function of dose (d): $E = \alpha d + \beta d^2$. For cell survival: $S = \exp(-\alpha d - \beta d^2)$.

linkage: Condition in which two or more nonallelic genes tend to be inherited together. Linked genes have their loci along the same chromosome; do not assort independently but can be separated by crossing over.

LNT: See [linear–no threshold](#).

local invasion: The spread of cancer from an original site to the surrounding tissues.

local tumor control: The complete remission of a tumor without later regrowth. This requires that all cancer stem cells are inactivated.

localized tumors: Tumors that are contained in one particular site and have not spread.

locally multiply damaged site: Any of various complex lesions, including base damage as well as double-strand breaks, produced by “spurs” and “blobs” from a high-LET track.

log-phase culture: A cell culture growing exponentially.

long terminal repeat (LTR): Sequence of several hundred base pairs found at the ends of retroviral DNAs.

lymph node: A collection of lymphocytes within a capsule and connected to other lymph nodes by fine lymphatic vessels; a common site for certain cancer cells to grow after traveling along lymphatic vessels.

lymphatic system: A network of fine lymphatic vessels that collects tissue fluids from all over the body and returns these fluids to the blood. Accumulations of lymphocytes, called *lymph nodes*, are situated along the course of lymphatic vessels.

lymphocyte: A type of white blood cell that helps protect the body against invading organisms by producing antibodies and regulating the immune system response.

lymphoma: A type of cancer beginning in an altered lymphocyte. There are two broad categories of lymphomas: Hodgkin disease and non-Hodgkin lymphoma.

lysis: The destruction of the cell membrane.

macrophage: A type of white blood cell assisting in the body's fight against bacteria and infection by engulfing and destroying invading organisms.

macrophage colony-stimulating factor (M-CSF): Cytokine that stimulates formation of macrophages from pluripotent hematopoietic cells.

magnetic resonance imaging (MRI): A method of taking pictures of body tissue using magnetic fields.

mammogram: An x-ray of the breast used to detect cancer, sometimes before it can be detected by palpation. Women older than 50 years are advised to have a mammogram every year; women in their 40s, every 2 years.

mapping: Determining the physical location of a gene or genetic marker on a chromosome.

mass number (A): The sum of the neutrons and protons in a nucleus. It is the nearest whole number to an isotope's atomic weight. For instance, the mass number of the uranium-235 isotope is 235. Compare [atomic number](#).

massively parallel DNA sequencing: A series of approaches to DNA sequencing using the concept of massively parallel processing.

mean: Arithmetic average.

median: The value in a group of numbers below and above which there are an

equal number of data points or measurements.

medical oncologist: A doctor specializing in using chemotherapy to treat cancer.

mega: A prefix that multiplies a basic unit by 1 million (10^6).

meiosis: The process in gametogenesis or sporogenesis during which one replication of the chromosomes is followed by two nuclear divisions to produce four haploid cells.

melanoma: A type of cancer that begins in the pigment-containing cells of a skin mole or the lining of the eye.

mendelian: Referring to diseases that are caused by mutations in single genes located on either the autosomes or the sex chromosomes and that show a simple, predictable pattern of inheritance.

meningioma: A type of brain tumor that is relatively common and usually benign.

messenger RNA (mRNA): The class of RNA molecules that copies the genetic information from DNA in the nucleus and carries it to ribosomes in the cytoplasm and is translated into the amino acid sequence of a polypeptide.

metacentric chromosome: A chromosome with a centrally located centromere, producing chromosome arms of equal lengths.

metaphase: The stage of cell division in which the condensed chromosomes lie in a central plane between the two poles of the cell and in which the chromosomes become attached to the spindle fibers.

metastasis: The ability of cancerous cells to invade surrounding tissues, enter the circulatory system, and establish new malignancies in body tissues distant from the site of the original tumor.

metastatic cancer: An advanced stage of cancer in which cells from the original (primary) site have spread (metastasized) to other organs.

methionine: The amino acid encoded by the sequence AUG.

methylate: The addition of one or more methyl groups (CH_3) to a molecule.

MeV: One million (10^6) electron volts.

micro (μ): A prefix that divides a basic unit by 1 million (10^{-6}).

micro RNA (miRNA): Small (19 to 22 nucleotides) single-stranded noncoding RNAs expressed in cells that can regulate gene expression.

microarray: An array of DNA spots of known sequence, usually on a glass slide, used to quantify amounts of genomic DNA or mRNA (reverse transcribed into cDNA or cRNA) present in cells or tissues. Capable of monitoring expression of all known genes and their variants. Also known as “gene expression microarrays” or “chips.”

microinjection: Introducing DNA into a cell using a fine microcapillary pipette.

micrometer (μm): A unit of length equal to 1×10^{-6} m. Previously called a *micron*.

micron: See **micrometer**.

migration coefficient: An expression of the proportion of migrant genes entering the population per generation.

millimeter (mm): A unit of length equal to one thousandth of a meter.

minimal medium: A medium containing only those nutrients that support the growth and reproduction of wild-type strains of an organism.

mismatch repair (MMR): DNA repair pathway for repairing or replacing mismatched bases in DNA.

misrepair (error-prone repair): Reconstitution with a loss of information (e.g., deletion caused by the loss of a fragment of the molecule or mutation or translocation).

missense mutation: A mutation that alters a codon to that of another amino acid, causing an altered translation product to be made.

mitigator: A drug added some time after irradiation but before symptoms of normal tissue toxicity appear, intended to reduce the severity of the radiation response.

mitochondrion: Found in the cells of eukaryotes, a cytoplasmic, self-reproducing organelle that is the site of ATP synthesis.

mitogen: A substance (e.g., phytohemagglutinin) that stimulates mitosis in nondividing cells.

mitogen-activated protein (MAP) kinase: A family of two protein kinases of 42 and 44 kDa (ERK1 and ERK2) and 38 kDa that act to induce certain early-response genes.

mitosis: The replication of a cell to form two progeny cells with identical sets of chromosomes.

mitotic death: Cell death associated with a postirradiation mitosis.

mitotic delay: Delay of entry into mitosis, or accumulation in G₂, as a result of treatment.

mitotic index (MI): Proportion or percentage of cells in mitosis at any given time.

MMP-9: Matrix metallopeptidase 9 encodes a 92 kDa type IV collagenase. This enzyme is involved in breaking down the extracellular matrix and has been implicated in the metastatic process of tumor cells.

molecular imaging: Medical imaging visualizing the spatial distribution of molecular targets, signaling pathways, or cellular phenotypes. Examples include PET and SPECT.

molecule: A group of atoms held together by chemical forces. The atoms of the molecule may be identical, as in H₂, S₂, and S₈, or different, as in H₂O and CO₂. A molecule is the smallest unit of matter that can exist by itself and retain all its chemical properties.

monoclonal antibodies: Immunoglobulin molecules of single-epitope specificity that are secreted by a clone of B cells.

monosomic: Describing an aneuploid condition in which one member of a chromosome pair is missing; having a chromosome number of 2n – 1.

monozygotic twins: Twins produced from a single fertilization event; the first division of the zygote produces two cells, each of which develops into an embryo. Also known as *identical twins*.

morbidity: Sickness, side effects, and symptoms of a treatment or disease.

mRNA: See [messenger RNA](#).

mtDNA: Mitochondrial DNA.

mucositis: Inflammation of the lining of areas such as the mouth.

multifactorial: Referring to diseases known to have a genetic component but whose transmission patterns cannot be described as simple mendelian.

multitarget model: Model that assumes the presence of a number of critical targets in a cell, all of which require inactivation to kill the cell. Survival is given by $S = 1 - [1 - \exp(D / D_0)]^n$.

mutagen: Any agent that causes an increase in the rate of mutation.

mutant: A cell or organism carrying an altered or mutant gene.

mutation: A relatively stable change in the DNA of the cell nucleus. Mutations in the germ cells of the body (ova and sperm) may lead to inherited effects in the offspring. Mutations in the somatic cells of the body may lead to effects in the individual (e.g., cancer).

mutation component: This allows for the observation that only a proportion of mutations lead to a disease.

mutation rate: The frequency with which mutations take place at a given locus or in a population.

myc: A nuclear oncogene involved in immortalizing cells.

myeloma: A tumor of the cells of the bone marrow.

nano (n): A prefix that divides a basic unit by 1 billion (10^{-9}).

nanometer (nm): A unit of length equal to 1×10^{-9} m.

nasopharynx: Part of the breathing passage behind the nasal cavity.

natural radioactivity: See **background radiation**.

natural selection: Differential reproduction of some members of a species resulting from variable fitness conferred by genotypic differences.

natural uranium: Uranium as found in nature, containing 0.7% of the isotope uranium-235, 99.3% of uranium-238, and a trace of uranium-234.

negligible individual dose: Level of effective dose to an individual per source or practice that may be ignored. Defined by NCRP as 0.01 mSv.

neutrino (ν): An electrically neutral elementary particle with a negligible mass. It interacts very weakly with matter and hence is difficult to detect. It is produced in many nuclear reactions (e.g., in β decay) and has high penetrating power. Neutrinos from the sun usually pass right through the earth.

neutron (n): An uncharged elementary particle that has a mass slightly greater than that of the proton and that is found in the nucleus of every atom heavier than hydrogen. A free neutron is unstable and decays with a half-life of about 13 minutes into an electron, a proton, and a neutrino. Neutrons sustain the fission chain reaction in a nuclear reactor.

Nijmegen breakage syndrome (NBS): A rare autosomal recessive disease leading to genomic instability. Individuals are sensitive to ionizing radiation and

possess mutations in the NBS gene, part of the MREII, RAD50, and NBS (MRN) complex which senses DNA strand breaks.

nimorazole: A 5-nitroimidazole used as a radiosensitizer for head and neck cancer.

nominal standard dose (NSD): Nominal standard dose in the Ellis formula.

nondisjunction: An accident of cell division in which the homologous chromosomes (in meiosis) or the sister chromatids (in mitosis) fail to separate and migrate to opposite poles; responsible for defects such as monosomy and trisomy.

nonhomologous end-joining (NHEJ): A DNA repair pathway for repairing double-strand DNA breaks without using any homologous sequence as a template.

nonsense mutation: A mutation that alters a codon to one that encodes no amino acid; for example, UAG (amber codon), UAA (ochre codon), or UGA (opal codon). Leads to premature termination during the translation of mRNA.

nonstochastic effect: An effect, the severity of which increases with increasing dose, after a threshold region. Now called **tissue reaction**.

normal distribution: A probability function that approximates the distribution of random variables. The normal curve, also known as a *Gaussian* or *bell-shaped curve*, is the graphic display of the normal distribution.

Northern blotting: A procedure in which RNA fragments are transferred from an agarose gel to a nitrocellulose filter from which the RNA is then hybridized to a radioactive probe.

NSG or NOD scid gamma mice: A strain of inbred laboratory mice, which lack T cells, B cells, and natural killer cell.

nuclear fuel cycle: Activities associated with production, utilization, and disposition of fuel for nuclear reactors and related by-products.

nuclear reactor: A structure in which nuclear fission may be sustained in a self-supporting chain reaction. In thermal reactors, the fission is produced by fission neutrons, and in fast reactors, by fast neutrons.

nuclease: An enzyme that breaks bonds in nucleic acid molecules.

nucleic acid: A class of organic acids that play a role in protein synthesis, in the transmission of heritable traits, and in the control of cellular activities.

nucleon: Proton or neutron.

nucleoside: A purine or pyrimidine base covalently linked to a ribose or deoxyribose sugar molecule.

nucleotide: A building block of DNA and RNA, consisting of a nitrogenous base, a five-carbon sugar, and a phosphate group.

nucleotide pair: The pair of nucleotides (A and T or G and C) in opposite strands of the DNA molecule that are hydrogen-bonded to each other.

nucleus (of a cell): The membrane-bounded region of a eukaryotic cell that contains the chromosomes.

nucleus (of an atom): The small, positively charged core of an atom. It is only about 1/10,000 the diameter of the atom but contains nearly all the atom's mass. All nuclei contain both protons and neutrons except the nucleus of ordinary hydrogen, which consists of a single proton.

nuclide: A general term applicable to all atomic forms of the elements. The term is often used incorrectly as a synonym for *isotope*, which properly has a more limited definition. Whereas isotopes are the various forms of a single element (hence are a family of nuclides) and all have the same atomic number and number of protons, nuclides comprise all the isotopic forms of all the elements. Nuclides are distinguished by their atomic number, atomic mass, and energy state.

occupationally exposed: Exposed to radiation as a direct result of occupational duties.

oligonucleotide: A DNA polymer composed of only a few nucleotides.

oncogene: A gene that contributes to cancer formation when mutated or inappropriately expressed.

oncogenic: Having the potential to cause cancer (same as carcinogenic).

oncologist: A physician specializing in the study and treatment of cancer.

oncology: The study of cancer.

1 4-3-3: A protein that interacts with *raf* to promote translocation to the cell membrane, in which *raf*, in turn, interacts with *ras*.

open reading frame: A long DNA sequence, uninterrupted by a stop codon, that encodes part or all of a protein.

organ or tissue weighting factor (W_T): A factor that indicates the ratio of the

risk of stochastic effects attributable to irradiation of a given organ or tissue to the total risk if the whole body is uniformly irradiated. Organs that have a large tissue weighting factor are those susceptible to radiation-induced carcinogenesis (such as the breast or thyroid).

organoid: A model of deriving a three-dimensional normal organ or cancer from a small number of stem cells.

oxidative stress: Formation of reactive oxygen species (ROS) in and outside cells, such as those resulting from the lysis of water molecules induced by ionizing radiation. This stress not only can activate several enzyme systems but also can modify the transcription of genes. These reactions are known collectively as *oxidative stress*.

oxygen enhancement ratio (OER): The ratio of the radiation dose given under anoxic conditions to produce a given effect relative to the radiation dose given under fully oxygenated conditions to produce the same effect.

oxygen probe: An electrode that can be implanted directly into a tumor to measure oxygen concentration by a polarographic technique. See [Eppendorf probe](#).

p15: G₁ inhibitor induced in epithelial cells by TGF- β . Inhibits cyclin D₁-Cdk4 and cyclin D₁-Cdk6 complexes.

p16: G₁ inhibitor of epithelial cells. Inhibits cyclin D₁-Cdk4 and cyclin D₁-Cdk6 complexes. Gene is deleted in familial melanomas and other tumor types.

p21 (WAF1): Inhibitor of Cdc2, Cdk4, and Cdk6. Induced through *p53* pathway.

p27: Cell cycle inhibitor induced in epithelial cells by TGF- β . Inhibits cyclin E-Cdk2 complex.

p53: Considered the guardian of the genome. Mediates cellular responses to DNA-damaging agents such as ionizing radiation at the G₁ checkpoint; induces p21. The gene *p53* on chromosome 17 is mutated in colon, breast, esophageal, and other various human cancers. Binds DNA; can act as transcription factor.

palindrome: A word, number, verse, or sentence that reads the same backward or forward. In nucleic acids, a sequence in which the base pairs read the same on complementary strands (5' → 3'). For example: 5' GAATTC 3', 3' CTTAAG 5'. These often occur as sites for restriction endonuclease recognition and cutting.

palliative care: Treatment to relieve, rather than cure, symptoms caused by cancer. Palliative care can help people live more comfortably.

palpate: To examine by carefully feeling with the fingers.

paracentric inversion: A chromosomal inversion that does not include the centromere.

parent: Radioactive atom that disintegrates to a different atom, its progeny.

particle: A minute constituent of matter, generally one with a measurable mass. The primary particles involved in radioactivity are α -particles, β -particles, neutrons, and protons.

pathologist: A specialist who attempts to describe the nature of a disease by analyzing samples obtained from tissues, organs, or body fluids.

pathology: The study of diseased tissues, both by gross and by microscopic examination of tissues removed during surgery and postmortem.

patient-derived xenograft (PDX): A cancer model based on the direct implantation of a tumor biopsy into a severely immunodeficient mouse.

pedigree: In human genetics, a diagram showing the ancestral relationships of a given genotype manifest in a specific mutant phenotype associated with a trait.

penetrance: The frequency (expressed as a percentage) with which individuals of a given genotype manifest at least some degree of a specific mutant phenotype associated with a trait.

peptide bond: The covalent bond between the amino group of one amino acid and the carboxyl group of another amino acid.

pericentric inversion: A chromosomal inversion that involves both arms of the chromosome and thus involves the centromere.

person-sievert: The unit of collective dose.

phage: See [bacteriophage](#).

pharynx: Medical term for the throat from the nasal and oral cavities above to the larynx and esophagus below.

phosphatase and tensin homolog (PTEN): The gene is commonly found mutated in many different cancers and is classified as a tumor suppressor gene. The gene encodes a phosphatidylinositol-3,4,5-trisphosphate 3-phosphatase that dephosphorylates phosphoinositide substrates and is critical in the regulation of the Akt signaling pathway.

phosphodiester bond: In nucleic acids, the covalent bond between a phosphate group and adjacent nucleotides, extending from the 5' carbon of one pentose

(ribose or deoxyribose) to the 3' carbon of the pentose in the neighboring nucleotide. Phosphodiester bonds form the backbone of nucleic acid molecules.

photodynamic therapy: Cancer treatment using light to activate a photosensitizing agent, thereby releasing cytotoxic free radicals.

photoelectric effect: Absorption of an x-ray by ionization.

photon: The carrier of a quantum of electromagnetic energy. Photons have an effective momentum but no mass or electrical charge.

pico (p): A prefix that divides a basic unit by 1 trillion (10^{-12}). Same as *micromicro*.

picocuries per liter (pCi/L): A unit of measurement of the activity concentration of a radioactive material; measures, for example, how many radioactive disintegrations of radon occur every second in a liter of air.

plaque: A clear spot on a lawn of bacteria or cultured cells on which cells have been lysed by viral infection and replication.

plasmid (p): A circular DNA molecule, capable of autonomous replication, which typically carries one or more genes encoding antibiotic resistance proteins.

plateau-phase cultures: Cell cultures grown to confluence so that proliferation is markedly reduced (also called *stationary phase*).

platelet-derived growth factor (PDGF): A protein that induces growth fibroblasts and is involved in wound healing. Also acts on some epithelial and endothelial cells and on mesenchymal cells.

platelets: Special blood cells that help stop bleeding.

plating efficiency: The proportion or percentage of *in vitro*-plated cells that form colonies.

pleiotropy: Condition in which a single mutation simultaneously affects several characters.

ploidy: Relates to the number of sets of chromosomes in a cell. Diploid cells have two sets of chromosomes, a chromosome complement twice that found in the gametes. Tetraploid cells have four sets of chromosomes.

point mutation: A mutation that can be mapped to a single locus. At the molecular level, a mutation that results in the substitution of one nucleotide for another.

polar body: A cell that is produced at either the first or second meiotic division in females and contains almost no cytoplasm as a result of an unequal cytokinesis.

polyacrylamide gel electrophoresis: Electrophoresis through a matrix composed of a synthetic polymer, used to separate small DNA or RNA molecules (up to 1,000 nucleotides) or proteins.

polyclonal antibodies: A mixture of immunoglobulin molecules secreted against a specific antigen, each recognizing a different epitope.

polymerase: An enzyme that catalyzes the addition of multiple subunits to a substrate molecule.

polymerase chain reaction (PCR): A procedure that enzymatically amplifies a DNA sequence through repeated replication by DNA polymerase.

polymorphism: The existence of two or more discontinuous, segregating phenotypes in a population.

polypeptide: A molecule made up of amino acids joined by covalent peptide bonds. This term is used to denote the amino acid chain before it assumes its functional three-dimensional configuration.

polyploid: A cell or individual having more than two sets of chromosomes.

population: A local group of individuals that belong to the same species and that are actually or potentially interbreeding.

positron (β^+): An elementary particle with the mass of an electron but charged positively. It is the “antielectron.” It is emitted in some radioactive disintegrations and is formed by the interaction of high-energy γ -rays with matter.

positron emission tomography (PET): An imaging technique using radionuclides that emit positrons whose annihilation photons are imaged in coincidence to form tomographic views of the body.

potential doubling time (T_{pot}): Tumor doubling time, taking into account the cell cycle time and the growth fraction but ignoring cell loss.

potentially lethal damage (PLD): Cellular damage that is repaired during the interval between treatment and assay, especially under suboptimal growth conditions.

pRb: A protein of ~110 kDa that regulates cell cycle progression through G₁.

Phosphorylated by cyclin D–Cdk complexes to release G₁ transcription factors. Inactivated in hereditary retinoblastoma and sporadic tumors of the bone, breast, esophagus, and other tissues.

precursor: In a radioactive decay chain, a member of the decay chain that occurs before a particular atom in question.

pre-mRNA: The initial mRNA transcript prior to any mRNA processing.

primary cell: A cell or cell line that is taken directly from a living organism and that is not immortalized.

primary tumor: The place in which a cancer originates, which is referred to regardless of the site of its eventual spread. Thus, prostate cancer that spreads to the bone is still prostate cancer and is not referred to as bone cancer.

primer: A short DNA or RNA fragment annealed to single-stranded DNA.

primordial: Existing at the beginning of the universe or at the beginning of the earth.

prion: An infectious pathogenic agent devoid of nucleic acid and composed mainly of a protein, PrP, with a molecular weight of 27,000 to 30,000 Da. Prions are known to cause scrapie, a degenerative neurologic disease in sheep, and are thought to cause similar diseases in humans, such as kuru and Creutzfeldt–Jakob disease.

probability: Ratio of the frequency of a given event to the frequency of all possible events.

probe: A single-stranded DNA (or RNA) that has been labeled radioactively and is used to identify complementary sequences.

prodromal phase: Signs and symptoms in the first 48 hours following irradiation.

progeny: Formerly called a “daughter” in a radioactive decay chain.

prognosis: The predicted or likely outcome.

programmed cell death: Cell death that occurs as the result of an active process carried out by molecules in the cell, for example, apoptosis.

prokaryotes: Organisms lacking nuclear membranes, meiosis, and mitosis. Bacteria and blue-green algae are examples of prokaryotic organisms.

promoter: A region of DNA extending 150 to 300 bp upstream from the transcription start site that contains binding sites for RNA polymerase and

several proteins that regulate the rate of transcription of the adjacent gene.

promoter site: Region having a regulatory function and to which RNA polymerase binds prior to the initiation of transcription.

promoting agent: Something that acts on earlier cellular damage caused by an initiating agent; can cause the earlier damage to be expressed as cancer. Tobacco smoke usually is considered a promoting agent.

prophylactic: Preventive measure or medication.

prostate: A gland at the base of the bladder in males for the production of seminal fluids. Cancer of this gland is common in elderly men.

protein: A molecule composed of one or more polypeptides, each composed of amino acids covalently linked together.

protein kinase: An enzyme that adds phosphate groups to a protein molecule at serine, threonine, or tyrosine residues.

protein kinase C (PKC): A family of protein kinases involved in mitogenic signaling. Activated by second messengers, including diacylglycerol and Ca^{2+} (some isoforms). Can be activated directly by the phorbol ester class of tumor promoters. Can induce early-response genes through *raf*.

proteomics: Study of the proteins expressed in cells including structure and function.

protocol: A standardized combination of therapies developed specifically for particular tumors.

proton: An elementary particle that is a component of all nuclei and that has a single positive electrical charge and a mass approximately 1,837 times that of the electron. The nucleus of an ordinary or light hydrogen atom. The atomic number of an atom is equal to the number of protons in its nucleus.

proto-oncogene: A gene generally active in the embryo and fetus and during proliferation processes. A mutation can result in the permanent activation of a proto-oncogene, which then becomes an oncogene.

pulsed-field gel electrophoresis (PFGE): Process whereby current is alternated between pairs of electrodes set at angles to one another to separate very large DNA molecules of up to 10 million nucleotides.

purines: Organic bases with carbon and nitrogen atoms in two interlocking rings; components of nucleic acids and other biologically active substances.

pyrimidines: Nitrogenous bases composed of a single ring of carbon and nitrogen atoms; components of nucleic acids.

quality factor: The factor by which absorbed dose is multiplied to obtain a quantity that expresses on a common scale, biologic effects (risks) from exposure to different radiations. Largely replaced by radiation weighting factor.

quantitative real-time PCR: A very sensitive PCR technique to quantify changes in DNA or RNA accurately in a high-throughput manner.

quasithreshold dose (D_q): Point of extrapolation of the exponential portion of a multitarget survival curve to the level of zero survival: $D_q = D_0 \ln(n)$.

rad: The old unit of absorbed dose, equivalent to an energy absorption of 10^{-2} J/kg. Replaced by the gray (Gy). See **absorbed dose**.

radiation: The emission and propagation of energy through matter or space by means of electromagnetic disturbances (x-rays) that display both wavelike and particle-like behavior; in this context, the “particles” are known as *photons*. Also, the energy so propagated. The term has been extended to include streams of fast-moving particles, such as α - and β -particles, free neutrons, and cosmic radiation. Nuclear radiation is that emitted from atomic nuclei in various nuclear reactions, including α -, β -, and γ -radiation and neutrons.

radiation (ionizing): Any electromagnetic or particulate radiation capable of producing ions, directly or indirectly, by interaction with matter. Examples are x-rays, photons, charged atomic particles and other ions, and neutrons.

radiation absorbed dose: See **gray**.

radiation accidents: Accidents resulting in the spread of radioactive material or in the exposure of individuals to radiation.

radiation burn: Radiation damage to the skin. β -Burns result from skin contact with or exposure to emitters of β -particles. See **beta particle**; **ionizing radiation**.

radiation chemistry: The branch of chemistry that is concerned with the chemical effects, including decomposition, of energetic radiation or particles on matter.

radiation detriment: Measure of stochastic effects from exposure to ionizing radiation that takes into account the probability of fatal cancers, probability of heritable effects in future generations, probability of nonfatal cancers weighted by the lethality fraction, and the relative years of life lost per fatal health effect.

radiation dose: The amount of radiation absorbed by an irradiated object. This unit is the gray (Gy), defined to be 1 J/kg.

radiation illness: An acute organic disorder that follows exposure to relatively large doses of ionizing radiation. It is characterized by nausea, vomiting, diarrhea, blood cell changes, and (in later stages) hemorrhage and loss of hair.

radiation oncologist: A physician specializing in the treatment of tumors by radiation therapy.

radiation protection: Legislation and regulations to protect the public and workers against radiation. Also, measures to reduce exposure to radiation.

radiation quality: Relative penetrability of an x-ray beam determined by its average energy; usually measured by half value layer (HVL) or peak kilovoltage (kVp).

radiation shielding: Reduction of radiation by interposing a shield of absorbing material between any radioactive source and a person, laboratory area, or radiation-sensitive device.

radiation sterilization: Using radiation to make a plant or animal sterile. Also, radiation to kill all forms of life, especially bacteria, in food or surgical equipment.

radiation therapy: Treatment of disease with any type of radiation. Often called *radiotherapy*.

radiation warning symbol: An officially prescribed symbol, a magenta trefoil on a yellow background, that should be displayed whenever a radiation hazard exists.

radiation weighted dose: New name proposed by ICRP for equivalent dose.

radiation weighting factor (W_R): A factor used for radiation protection purposes that accounts for differences in biologic effectiveness between different radiations. The radiation weighting factor is independent of the tissue weighting factor.

radioactive decay: See [decay, radioactive](#).

radioactive half-life: Time for a radioisotope to decay to one-half its activity.

radioactive isotope: One of the forms of an element, differing in atomic weight and possessing an unstable nucleus that emits ionizing radiation.

radioactive series: A succession of nuclides, each in turn transforming by

radioactive disintegration into the next nuclide until a stable nuclide is reached. The first member is called the *parent*, the intermediate members are called *progeny*, and the final, stable member is called the *end product*.

radioactive tracer: A small quantity of a radioactive isotope, either with or without a carrier, used to follow biologic, chemical, or other processes by detection, determination, or localization of the radioactivity.

radioactive waste: Unwanted radioactive materials in any form. Often categorized in the nuclear power industry into low-level, intermediate-level, and high-level waste.

radioactivity: A property of all unstable elements that regularly decay to an altered state by releasing energy in the form of photons (γ -rays) or particles (e.g., electrons, α -particles).

radiobiology: The body of knowledge and the study of the principles, mechanisms, and effects of ionizing radiation on living matter.

radiogenic: Of radioactive origin; produced by radioactive transformation.

radiography: The production of images on film or other media by the action of x-rays transmitted through a patient.

radioisotope: A radioactive isotope; an unstable isotope of an element that decays or disintegrates spontaneously, emitting radiation. More than 1,300 natural and artificial radioisotopes have been identified.

radiologist: A physician with special training in reading diagnostic x-rays and performing specialized x-ray procedures.

radiology: The science that investigates all forms of ionizing radiation in the diagnosis and treatment of disease.

radionuclide: A radioactive nuclide.

radioprotector: A chemical compound that reduces the biologic consequences of radiation.

radioresistance: A relative resistance of cells, tissues, organs, or organisms to the harmful action of radiation.

radioresponsiveness: A general term indicating the overall level of clinical response to radiotherapy.

radiosensitivity: (1) A relative susceptibility of cells, tissues, organs, or organisms to the effects of radiation. (2) The radiation dose required to produce a

defined level of cell inactivation, usually indicated by the surviving fraction at 2 Gy (i.e., SF₂) or by the parameters of the linear-quadratic or multitarget equations.

radiosensitizer: In general, any agent that increases the sensitivity of cells to radiation. Most commonly applied to electron-affinic chemicals that mimic oxygen in fixing free radical damage.

radiotherapy: The treatment of disease with ionizing radiation. Often termed *radiation therapy*.

radium (Ra): A radioactive metallic element with atomic number 88. As found in nature, the most common isotope has an atomic weight of 226. It occurs in minute quantities associated with uranium in pitchblende, carnotite, and other minerals. The uranium decays to radium in a series of α - and β -emissions. By virtue of being an α - and γ -emitter, radium is used as a source of luminescence and as a radiation source in medicine and radiography.

radon (Rn): Colorless, odorless, naturally occurring radioactive gas; a radioactive element and the heaviest gas known. Its atomic number is 86 and its atomic weight varies from 200 to 226. Radon-222 is the progeny of radium in the uranium radioactive series.

radon daughter: Any atom that is below radon-222 in the uranium decay chain; often specifically refers to polonium-218 and polonium-214, as these have the most biologic significance; now referred to as *radon progeny*.

raf: A protein kinase that is activated by GTP-bound *ras*. Acts to transduce mitogenic signaling by phosphorylation of MAP kinases.

ras: A family of 21-kDa proteins (H-, K-, and N-*ras*) found to be activated by point mutations at codons 12, 13, and 61 in various tumors. Involved in mitogenic signaling, coupling growth signals from growth factor receptors to *raf* activation, and downstream stimulation of early-response genes. Binds GTP in its activated state. Is found at the inner face of the cell membrane.

RBE: See **relative biologic effectiveness**.

reading frame: A series of triplet codons beginning from a specific nucleotide.

reassortment (redistribution): Return toward a more even cell age distribution, following the selective killing of cells in certain phases of the cell cycle.

recessive: Term describing an allele that is not expressed in the heterozygous condition.

recessive gene: Gene whose phenotype is expressed only when both copies of the gene are mutated or missing.

recessive-acting oncogene (anti-oncogene): A single copy of this gene is sufficient to suppress cell proliferation; the loss of both copies of the gene contributes to cancer formation.

reciprocal translocation: A chromosomal aberration in which nonhomologous chromosomes exchange parts.

recombinant DNA: The process of cutting and recombining DNA fragments as a means to isolate genes or to alter their structure and function.

recovery: An increase in cell survival as a function of time during or after irradiation. See [repair](#).

recurrence: The return of a cancer after all detectable traces had been removed by primary therapy; recurrences may be local (near the primary site) or distant (metastatic).

regression rate: The rate at which the tumor volume shrinks during or after treatment with radiation or a chemotherapy agent.

relapse: Recurrence of a disease following treatment.

relative biologic effectiveness (RBE): A factor used to compare the biologic effectiveness of different types of ionizing radiation. It is the inverse ratio of the amount of absorbed radiation required to produce a given effect to a standard (or reference) radiation required to produce the same effect.

relative risk: Situation in which the risk of a disease resulting from some injury is expressed as some percentage increase of the normal rate of occurrence of that disease; in contrast to an absolute risk in which the risk of a disease resulting from an injury does not depend on the normal rate of occurrence of that disease.

rem: Old unit of equivalent or effective dose. It is the product of absorbed dose (in rad) and the radiation weighting factor. One rem is one hundredth of a sievert.

remediation: Reducing a home's indoor radon level.

remission, complete: Condition in which no cancerous cells can be detected and the patient appears to be free from disease.

remission, partial: Generally means that by all methods used to measure the existence of a tumor, there has been at least a 50% regression of the disease

following treatment.

remote brachytherapy: See [high-dose-rate remote brachytherapy](#).

reoxygenation: The process by which surviving hypoxic clonogenic cells become better oxygenated during the period after irradiation of a tumor.

repair: Restoration of the integrity of damaged macromolecules.

repair saturation: Explanation of the shoulder on cell survival curves on the basis of the reduced effectiveness of repair after high radiation doses.

repopulation: The proliferation of surviving clonogenic tumor cells during a fractionated radiotherapy regime. Also, the regeneration of early responding normal tissues during a protracted treatment, which leads to an increase in tolerance with increasing overall time.

reproductive death: The loss of the proliferative ability of a cell. Commonly restricted to those cells having an indefinite capacity to divide.

reproductive integrity: Ability of cells to divide many times and thus be “clonogenic.”

resection: Surgical removal. In relation to cancer resection, the pathologist often indicates if the outer margins of the resection had no cancer cells present or were “negative.”

restriction endonuclease: Nuclease that recognizes specific nucleotide sequences in a DNA molecule and cleaves or nicks the DNA at that site. Derived from various microorganisms; those enzymes that cleave both strands of the DNA are used in the construction of recombinant DNA molecules.

restriction fragment length polymorphism: Differences in nucleotide sequence between alleles that result in restriction fragments of varying lengths.

retrovirus: A member of a class of RNA viruses that uses the enzyme reverse transcriptase to reverse copy its genome into a DNA intermediate, which integrates into the host cell chromosome. Many naturally occurring cancers of vertebrate animals are caused by retroviruses. They are convenient to work with as a vector in gene therapy but infect only dividing cells, which is a severe limitation.

reverse transcriptase (RNA-dependent DNA polymerase): An enzyme isolated from retrovirus-infected cells that synthesizes a complementary cDNA strand from an RNA template.

reversion: A mutation that restores the wild-type phenotype.

ribosomal RNA: The RNA molecules that are the structural components of the ribosomal subunits. In prokaryotes, these are the 16S, 23S, and 5S molecules; in eukaryotes, they are the 18S, 28S, and 5S molecules.

ring chromosome: Formed by radiation-induced breaks in each arm of a single chromatid in prereplication chromosomes. The sticky ends of the chromatids rejoin and form a ring and a fragment.

RNA (ribonucleic acid): An organic acid composed of repeating nucleotide units of adenine, guanine, cytosine, and uracil, whose ribose components are linked by phosphodiester bonds.

RNA polymerase: An enzyme that catalyzes the formation of an RNA polynucleotide strand using the base sequence of a DNA molecule as a template.

RNA-Seq: A powerful technique using whole transcriptome sequencing for analyzing changes in gene expression levels.

robertsonian translocation: A form of chromosomal aberration that involves the fusion of long arms of acrocentric chromosomes at the centromere.

röntgen (R): A unit of exposure to ionizing radiation named after Wilhelm Röntgen, the German scientist who discovered x-rays in 1895. It is the amount of γ - or x-rays required to produce ions carrying one electrostatic unit of electrical charge (either positive or negative) in 1 cm^3 of dry air under standard conditions.

Saccharomyces cerevisiae: Brewer's yeast.

sarcoma: A type of cancer derived from connective bone or fat tissue. Examples include fibrosarcoma, osteogenic sarcoma, and liposarcoma.

satellite DNA: DNA that forms a minor band if genomic DNA is centrifuged in a cesium salt gradient. This DNA usually consists of a short sequence repeated many times in the genome.

scan: A diagnostic test usually involving the movement or scanning of a detector to produce a picture. Examples include ultrasound, nuclear medicine, computer-assisted tomographic, and magnetic resonance scans.

scattered radiation: Radiation that, during passage through matter, is changed in direction (the change is usually accompanied by a decrease in energy).

SCCVII: Squamous cell carcinoma VII is the name of a rodent tumor. It has been extensively used in preclinical testing of different radiation protocols to

identify biologic modifiers of the radiation response.

SCE: See [sister chromatid exchange](#).

Scheimpflug imaging system: An imaging system that gives an objective and quantitative assessment of the severity of an ocular cataract. Named after the Austrian army officer Theodor Scheimpflug (1865–1911).

SDF-1: The ligand for the chemokine receptor CXCR4. Plays important roles in chemotaxis and vascularization.

secondary cancer: Cancer arising from a primary cancer; metastatic cancer.

Seckel syndrome: A rare autosomal recessive disorder characterized by microcephaly and abnormal development: Seckel cells have reduced activity of the ATR gene.

segregation: The separation of homologous chromosomes into different gametes during meiosis.

selectable marker: A gene whose expression makes it possible to identify cells that have been transformed or transfected with a vector containing the marker gene. It is usually a gene for resistance to an antibiotic.

selection: The force that brings about changes in the frequency of alleles and genotypes in populations through differential reproduction.

semiconservative replication: A model of DNA replication in which a double-stranded molecule replicates in such a way that the progeny molecules are composed of one parental (old) and one newly synthesized strand.

senescence: Permanent arrest of cell division associated with aging, differentiation, or cell damage.

sensitizing agent: A substance that increases the biologic effectiveness of a given dose of radiation.

severe combined immunodeficiency (SCID): Both human and mouse forms result in loss of functional T and B cells. Some human forms are the result of mutations in the Artemis gene. The mouse form is the result of loss of DNA-PK activity.

sex chromosome: A chromosome, such as the X or Y in humans, that is involved in sex determination.

sex linkage: The pattern of inheritance resulting from genes located on the X chromosome.

sexual reproduction: Reproduction through the fusion of gametes, which are the haploid products of meiosis.

SF₂: Surviving fraction at 2 Gy.

short-hairpin RNA (shRNA): A complementary hairpin expressed from a vector that causes target cellular RNA to be degraded.

short-interfering RNA (siRNA): A short inhibitory double-stranded RNA molecule that causes target cellular RNA to be degraded.

sickle cell anemia: A genetic disease in humans caused by an autosomal recessive gene, usually fatal in the homozygous condition. Caused by an alteration in the amino acid sequence of the β chain of globin.

side effects: Symptoms directly related to treatment, such as the side effect of nausea resulting from radiation treatment over the stomach. Side effects are considered acute if they occur during treatment and subside when treatment is complete. Those symptoms persisting over a longer period are considered chronic.

sievert (Sv): Unit of equivalent dose or effective dose. It is equal to the dose in gray multiplied by a weighting factor. One sievert equals 100 rem.

SINES: Short interspersed repetitive sequences found in the genomes of higher organisms, such as the 300-bp *Alu* sequence.

single-cell electrophoresis (comet assay): A sensitive and simple technique to analyze DNA damage in individual cells. The amount of DNA migrating from the nuclear matrix into the agarose is proportional to the amount of DNA damage in the cell. Can be used to access base damage, single, and double DNA strand breaks.

single photon emission computed tomography (SPECT): An imaging technique in which one or more gamma cameras sample a region of the body from several angles, producing tomographic images (slices) of the body.

single strand annealing: A repair process involving homologous recombination between two DNA repeat sequences.

sister chromatid exchange (SCE): A crossing-over event that can occur in meiotic and mitotic cells. Involves the reciprocal exchange of chromosomal material between sister chromatids (joined by a common centromere). Such exchanges can be detected cytologically after BrdUrd incorporation into the replicating chromosomes.

slow repair: Long-term recovery that takes place on a time scale of weeks to months.

solid tumor: A cancer originating in an organ or tissue other than bone marrow or the lymph system.

somatic: Pertaining to the body; pertaining to all cells except the germ cells.

somatic cell: Any cell other than a germ cell that composes the body of an organism and that possesses a set of multiploid chromosomes.

somatic effects of radiation: Effects of radiation limited to the exposed individual, as distinguished from genetic effects, which also affect subsequent, unexposed generations. Large radiation doses can be fatal. Smaller doses may make the individual noticeably ill, may produce temporary changes in blood cell levels detectable only in the laboratory, or may produce no detectable effects.

somatic homozygosity: A process in which one chromosome of a pair is lost and a deletion occurs in remaining chromosome.

somatic mutation: A mutational event occurring in a somatic cell. Such mutations are not heritable.

SOS response: The induction of enzymes to repair damaged DNA in *Escherichia coli*. The response involves activation of an enzyme that cleaves a repressor, activating a series of genes involved in DNA repair.

Southern blotting: A procedure in which DNA restriction fragments are transferred from an agarose gel to a nitrocellulose filter, where the denatured DNA is then hybridized to a radioactive probe.

spatial cooperation: The use of radiotherapy and chemotherapy to treat disease in different anatomic sites.

species: A group of actually or potentially interbreeding individuals isolated reproductively from other such groups.

specific activity: The radioactivity of a radioisotope of an element per unit weight of the element in a sample; the activity per unit mass of a pure radionuclide; the activity per unit weight of any sample of radioactive material.

spheroid: Clump of cells grown together in tissue culture suspension.

spindle fibers: Cytoplasmic fibrils formed during cell division that are involved in the separation of chromatids at anaphase and their movement toward opposite poles in the cell.

split-dose (SLD) recovery: Decrease in radiation effect if a single radiation dose is split into two fractions separated by times up to a few hours. Also called *Elkind recovery* or *recovery from sublethal damage*.

spontaneous mutation: A mutation that is not induced by a mutagenic agent.

spore: A unicellular body or cell that is encased in a protective coat and that is produced by some bacteria, plants, and invertebrates. Capable of survival in unfavorable environmental conditions and can give rise to a new individual upon germination. In plants, spores are the haploid products of meiosis.

spur: A concentration of about three ion pairs in a volume about 4 nm in diameter. See **locally multiply damaged site**.

SSBR: Single-strand break repair. DNA repair pathway for repairing a break in only one of the DNA strands.

stable isotope: An isotope that does not undergo radioactive decay. Compare **radioisotope**.

stage: The anatomic extent of a cancer. Cancer may exist in the organ of origin and extend locally, or it may spread to regional tissues, then to local lymph nodes, and then to distant areas as metastases.

standard deviation: A quantitative measure of the amount of variation in a sample of measurements from a population.

standard error: A quantitative measure of the amount of variation in a sample of measurements from a population.

stathmokinetic method: Study of cell proliferation using agents that block cells in mitosis.

stem cells: Cells capable of self-renewal and of differentiation to produce all the various types of specialized cells in a lineage.

stereotactic ablative radiotherapy (SABR): Refers to tumors outside the brain treated with 1 to 5 dose fractions (essentially the same as SBRT).

stereotactic body radiotherapy (SBRT): Refers to tumors outside the brain treated with 1 to 5 dose fractions (essentially the same as SABR).

stereotactic radiosurgery (SRS): Usually a single dose fraction to the brain.

sterility: The condition of being unable to reproduce; the condition of being free from contaminating microorganisms.

sticky end: A single-stranded nucleotide sequence produced if a restriction

endonuclease cleaves off-center in its recognition sequence.

stochastic effects: Effects, the probability of which, rather than their severity, is a function of radiation dose without threshold. (More generally, *stochastic* means random in nature.)

strain: A group with common ancestry that has physiologic or morphologic characteristics of interest for genetic study or domestication.

stringency: Reaction conditions, such as temperature, salt, and pH, that dictate the annealing of single-stranded DNA/DNA, DNA/RNA, and RNA/RNA hybrids. At high stringency, duplexes form only between strands with perfect one-to-one complementarity; lower stringency allows annealing between strands with less than a perfect match between bases.

sublethal damage (SLD): Nonlethal cellular injury that can be repaired or accumulated with further dose to become lethal.

submetacentric chromosome: A chromosome with the centromere placed so that one arm of the chromosome is slightly longer than the other.

suppressor genes: Genes that oppose the continuous proliferation of cells. Also known as *tumor suppressor genes*.

supra-additivity (synergism): A biologic effect caused by a combination of effects that is greater than would be expected from the addition of the effects of the component agents.

survival curve: Curve obtained by plotting the number or the percentage of organisms surviving against the dose of radiation.

symbiont: An organism coexisting in a mutually beneficial relationship with another organism.

symmetric chromosome translocation: Generated by breaks in two prereplication chromosomes with broken ends being exchanged between the two chromosomes. This type of aberration is usually stable and transmitted for many generations.

syndrome: A group of signs or symptoms that occur together and characterize a disease or abnormality.

synergism: Two or more agents reacting together to produce a result greater than the sum of the individual agents.

synthetic lethality: Arises when a combination of mutations in two or more

genes leads to cell death, whereas a mutation in only one of these genes does not, and by itself is said to be viable.

systemic: Having a widespread effect on the body as a whole rather than just on local tissue.

T cell checkpoint: Molecules used by tumor cells to protect them from T cell-mediated cytotoxicity. Antibodies to CTLA-4 and PD-1 inhibitory molecules are currently used to stimulate T cell activity in tumors alone or in combination with radiotherapy.

Taq polymerase: A heat-stable DNA polymerase isolated from the bacterium *Thermus aquaticus* and used in PCR.

target cell: A stem cell whose death contributes to a reduction in growth or tissue function.

target theory: (1) A theory based on the idea that death of a cell is caused by the inactivation of specific targets within the cell. (2) The idea that the shoulder on cell survival curves is a result of the number of unrepaired lesions per cell.

targeted agents: Small molecules or antibodies that inhibit cellular pathways that are specific to cancer cells or substantially overexpressed in malignant compared with normal cells.

targeted radiotherapy: Treatment of disseminated cancer by means of drugs that localize in tumors and carry therapeutic amounts of radioactivity.

TBI: Total-body irradiation.

TCD₅₀: The radiation dose that results in a 50% probability of tumor control.

TCP: Tumor control probability.

telangiectasia: Pathologically dilated capillaries, observed in tissues as a late effect of radiation.

telocentric chromosome: A chromosome in which the centromere is located at the end of the chromosome.

telomerase: A reverse transcriptase that polymerizes TTAGGG repeats to offset the degradation of chromosome ends that occurs with successive cell divisions.

telomeres: Long arrays of TTAGGG repeats that cap and protect the ends of chromosomes. Each time a normal somatic cell divides, the terminal end of the telomere is lost.

telophase: The stage of cell division in which the progeny chromosomes reach

the opposite poles of the cell and re-form nuclei. Telophase ends with the completion of cytokinesis.

temperature-sensitive mutation: A conditional mutation that produces a mutant phenotype at one temperature range and a wild-type phenotype at another temperature range.

template: An RNA or single-stranded DNA molecule on which a complementary nucleotide strand is synthesized.

teratocarcinoma: Embryonal tumors that arise in the yolk sac or gonads and are able to undergo differentiation into various cell types. These tumors are used to investigate the regulatory mechanisms underlying development.

termination (stop) codon: Any of three mRNA sequences (UGA, UAG, UAA) that do not code for an amino acid and thus signal the end of protein synthesis.

therapeutic gain factor: In hyperthermia, the ratio of the thermal enhancement ratio in the tumor to the thermal enhancement ratio in normal tissue. For high-linear energy transfer radiations, the therapeutic gain factor is the ratio of the relative biologic effectiveness in the tumor to the relative biologic effectiveness in normal tissue.

therapeutic index (therapeutic ratio): Tumor response for a fixed level of normal-tissue damage.

thermal dose: A function of temperature and heating time that is thought to relate well to biologic effect. It is defined to be the cumulative equivalent minutes at 43° C.

thermal enhancement ratio (TER): The ratio of radiation doses, with and without heat, to produce the same biologic effects.

thermal neutrons: Neutrons in thermal equilibrium with their surrounding medium. Thermal neutrons are those that have been slowed down by a moderator to an average speed of about 2,200 m/s at room temperature from the much higher initial speeds that they had when expelled by fission.

thermoluminescent dosimeter (TLD): A dosimeter containing a crystalline solid for measuring radiation dose, plus filters (absorbers) to help characterize the types of radiation encountered. If heated, TLD crystals that have been exposed to ionizing radiation give off light proportional to the energy they received from the radiation.

thermotolerance: The induced resistance to a second heat exposure by prior

heating.

thorium series: Radioactive decay chain starting with thorium-232; one member of the chain is radon-220. This chain is of much less significance than the uranium decay chain containing radon-222.

threshold: A level (e.g., of radiation dose) below which there is no observable effect. There is no threshold for induction of cancer by radiation: All levels of radiation are considered harmful.

threshold dose: The minimum dose of radiation that produces a detectable biologic effect.

thymidine kinase (*tk*): An enzyme that allows a cell to use an alternate metabolic pathway for incorporating thymidine into DNA. Used as a selectable marker to identify transfected eukaryotic cells.

thymine dimer: A pair of adjacent thymine bases in a single polynucleotide strand between which chemical bonds have formed. This lesion, usually the result of damage caused by exposure to ultraviolet light, inhibits DNA replication unless repaired by the appropriate enzyme system.

time-dose relationships: The dependence of isoeffective radiation dose on the duration (and number of fractions) in radiotherapy.

tissue reaction: New ICRP term for what used to be called a *deterministic effect*. Refers to damage due to cells being killed and removed from a tissue or organ as a result of radiation exposure. Characteristics include (1) threshold in dose; (2) severity of the effect increases with dose above the threshold; (3) caused by damage to many cells; and (4) examples include fibrosis, effects on fertility, and lethality due to total body exposure. Ocular cataracts used to be classified as such, but there are now some doubts.

tissue weighting factor (W_T): A factor that indicates the ratio of the risk of stochastic effects attributable to irradiation of a given organ or tissue to the total risk when the whole body is uniformly irradiated.

tolerance dose: The maximum radiation dose or intensity of fractionated radiotherapy that the therapist judges to be acceptable, usually expressed in dose units. Actual values depend on fractionation, field size, concomitant treatments, and so on.

topoisomerase: A class of enzymes that converts DNA from one topologic form to another. During DNA replication, these enzymes facilitate the unwinding of

the double-helical structure of DNA.

totipotent: Referring to the ability of a cell or embryo to give rise to all adult structures. This capacity usually is restricted progressively during development.

trait: Any detectable phenotypic variation of a particular inherited character.

transcription: Transfer of genetic information from DNA by the synthesis of an RNA molecule copied from a DNA template.

transfection: The uptake and expression of foreign DNA by cultured eukaryotic cells.

transformation: In higher eukaryotes, the conversion of cultured cells to a malignant phenotype. In prokaryotes, the natural or induced uptake and expression of a foreign DNA sequence.

transforming growth factor alpha (TGF- α): Functional and structural analogue of epidermal growth factor. Induces the growth of epithelial cells as well as fibroblasts and keratinocytes. May be involved in tumor-associated neovascularization.

transforming growth factor β (TGF- β): A cytokine that regulates many of the biologic processes essential for embryo development and tissue homeostasis and which therefore plays a role in the healing of a tissue and carcinogenesis. The effects of TGF- β may differ, depending on the tissue involved. For instance, TGF- β inhibits the proliferation of epithelial cells but stimulates that of fibroblasts.

transforming oncogene: A gene that upon transfection converts a previously immortalized cell to the malignant phenotype.

transgenic: A vertebrate organism in which a foreign DNA gene (a transgene) is stably incorporated into its genome early in embryonic development. The transgene is present in both somatic and germ cells, is expressed in one or more tissues, and is inherited by offspring in a mendelian fashion.

transient hypoxia: Low oxygen concentrations associated with the transient closing and opening of blood vessels. Sometimes called *acute* or *cyclic hypoxia*.

translation: The process of converting the genetic information of mRNA on ribosomes into polypeptides.

translocation: The movement or reciprocal exchange of large chromosomal segments, typically between two different chromosomes.

transfer RNA (tRNA): A small RNA molecule that contains a three-base segment (anticodon) that recognizes a codon in mRNA, a binding site for a specific amino acid, and recognition sites for interaction with the ribosome and the enzyme that links it to its specific amino acid.

trisomy: The condition in which a cell or organism possesses two copies of each chromosome, except for one, which is present in three copies. The general form for trisomy is therefore $2n + 1$.

tritium ($^3\text{H-TdR}$): A radioactive isotope of hydrogen with two neutrons and one proton in the nucleus. It is human-made and heavier than deuterium (heavy hydrogen). Tritium is used in industrial thickness gauges and as a label in chemical and biologic experiments. Its nucleus is a triton.

tumor: An abnormal growth of cells or tissues. Tumors may be benign (noncancerous) or malignant (cancerous).

tumor bed effect (TBE): Slower rate of tumor growth after irradiation, resulting from stromal injury in the irradiated “vascular bed.”

tumor cord: Sleeve of viable tumor growing around a blood capillary.

tumor necrosis factor (TNF): Two proteins, TNF- α and TNF- β , involved in immune response control and inflammation. Induced by cytokines, ultraviolet radiations, and other agents.

unfolded protein response (UPR): A cellular stress response that is induced by the accumulation of unfolded proteins in the endoplasmic reticulum.

UNSCEAR: United Nations Scientific Committee on the Effects of Atomic Radiation.

uranium (U): A radioactive element with atomic number 92 and, as found in natural ores, an average atomic weight of approximately 238. The two principal natural isotopes are uranium-235 (0.7% of natural uranium), which is fissionable, and uranium-238 (99.3% of natural uranium), which is fertile. Natural uranium also includes a minute amount of uranium-234.

uranium series (sequence): The series of nuclides resulting from the radioactive decay of the uranium isotope uranium-238. The end product of the series is the lead isotope lead-206. The series includes radium and radon.

variance: A statistical measure of the variation of values from a central value, calculated as the square of the standard deviation.

vascular targeted therapies: Treatments designed to specifically target tumor

vasculature, including angiogenesis inhibitors.

vector: An autonomously replicating DNA molecule into which foreign DNA fragments are inserted and then propagated in a host cell.

viability: The measure of the number of individuals in a given phenotypic class that survive, relative to another class (usually wild-type).

viral oncogene: A viral gene that contributes to malignancies in vertebrate hosts.

virulent phage: A bacteriophage that infects and lyses the host bacterial cell.

virus: An infectious particle that is composed of a protein capsule and a nucleic acid core and that is dependent on a host organism for replication.

volume effect: Dependence of radiation damage to normal tissues on the volume of tissue irradiated.

volume-doubling time: Time taken for a tumor to double in volume.

waste, radioactive: Equipment and materials (from nuclear operations) that are radioactive and have no further use. Wastes are generally classified as high level: radioactivity concentrations of hundreds to thousands of curies per gallon or cubic foot, low level: in the range of 1 μCi (microcurie) per gallon or cubic foot, or intermediate: between these extremes.

wavelength: Distance between similar points on a sine wave; length of one cycle.

Western blotting: Similar to a Southern blot (for DNA) or a Northern blot (for RNA), except that protein is used.

white blood cells: The blood cells that fight infection.

whole body counter: A device used to identify and measure the radioactivity in the body (body burden) of humans and animals. It uses heavy shielding (to keep out background radiation), ultrasensitive scintillation detectors, and electronic equipment.

wild type: The most commonly observed phenotype or genotype, designated as the norm or standard.

X chromosome: The female sex chromosome.

xenografts: Transplants between species; usually applied to the transplantation of human tumors into immune-deficient mice and rats.

xerostomia: Dryness of the mouth caused by malfunctioning salivary glands.

X-linkage: See [sex linkage](#).

X-linked disease: A genetic disease caused by a mutation on the X chromosome. In X-linked recessive conditions, a normal female “carrier” passes on the mutated X chromosome to an affected son.

x-ray: A penetrating form of electromagnetic radiation emitted either if the inner orbital electrons of an excited atom return to their normal state (these are characteristic x-rays) or if a metal target is bombarded with high-speed electrons. X-rays are always extranuclear in origin.

x-ray crystallography: A technique to determine the three-dimensional structure of molecules through diffraction patterns produced by x-ray scattering by crystals of the molecule under study.

Y chromosome: Sex chromosome in species in which the male is heterogametic (XY).

yeast artificial chromosome (YAC): A vector that is used to clone DNA fragments of up to 400,000 bp and that contains the minimum chromosomal sequences needed to replicate in yeast.

Z: The symbol for atomic number; the number of protons in the nucleus.

zinc fingers: A structural motif of DNA-binding proteins in which fingerlike loops of amino acids are stabilized by interactions with zinc atoms.

zygote: The diploid cell produced by the fusion of haploid gametic nuclei.

Index

Page numbers followed by *f* indicate figure and page numbers followed by *t* indicate table.

AAV. *See* adeno-associated viruses, as vectors

abdominal CT, 212*t*, 216*t*

abdominal x-rays, 213*t*, 214*t*, 216*t*

abiraterone, 487*t*, 493

abl gene, 300, 301*f*

abscopal effect, 328

absolute risk model, 139

absorbed dose, 103, 211–212, 238–239, 242*t*, 253

absorption

Compton process, 6–8, 7*f*

neutron, 10

photoelectric, 7–8, 7*f*

proton, 10

x-ray, 6–8, 7*f*

accelerated radiotherapy, carbogen, and nicotinamide (ARCON) trials, 467

accelerated repopulation, 423–424, 424*f*, 425*f*, 510

accelerated treatment, 427

acentric fragments, 26, 27*f*, 28*f*

acid sphingomyelinase, 320–321, 321*f*

ACR. *See* American College of Radiology

actinomycin D. *See* dactinomycin

acute (early) effects, 201, 352–353, 352*f*

acute hypoxia, 86, 89, 89*f*, 466–467

acute radiation syndrome (ARS), 111–125

average time to emesis in, 121
bone marrow transplantation for, 121
cerebrovascular syndrome in, 111–112, 113
critical phase of, 119, 120*t*
data sources on, 111
early lethal effects in, 111–112
in females *vs.* males, 116
50% lethal dose (LD₅₀) in, 116–117, 117*t*
first death from, 118, 119
gastrointestinal syndrome in, 111–112, 113–115
hematopoietic syndrome in, 111–112, 115–118
latent period in, 111*f*, 112, 116, 119, 119*t*
lymphocyte count in, 112–113, 119*t*, 120*t*, 121–123
modes of death in, 111–112
prodromal syndrome in, 111, 111*f*, 112–113, 112*t*, 116, 119, 119*t*
pulmonary syndrome in, 118, 118*f*
recent death (assassination) from, 117–118, 117*f*, 202
response/resources in, 123, 203
survivors in United States, 123
symptoms associated with, 119–120, 119*t*, 120*t*
terrorism and, 197–199, 201
time course/stages of, 111, 111*f*
treatment, for doses close to LD_{50/60}, 120–121
triage in, 121–123
Adams, G. E., 463, 464*f*, 467
adenine, 11, 12*f*, 16, 16*f*, 259–260, 259*f*–261*f*
adeno-associated viruses (AAV), as vectors, 266
adenoviruses, as vectors, 266

adjunct chemotherapy, 508–510, 508*f*, 509*f*
adjuvant chemotherapy, 476, 510
adrenal gland, 359*t*
Adriamycin. *See* doxorubicin
Advisory Committee on X-Ray and Radium Protection, 237
agarose gel electrophoresis, 270–271, 271*f*, 290
age at exposure, 139, 143, 148, 149*f*
age-response function, 58–65
 for high-linear energy transfer radiations, 64–65
 hyperthermia and, 518
 mechanisms for, 65
 possible implications in radiotherapy, 65
 and sublethal damage repair, 70–72
 for tissue *in vivo*, 63–64, 64*f*
aging, 25. *See also* senescence, cellular
agreement states, NRC, 238, 239*f*
Ahn, G. O., 461
air travel, 206, 207
ALARA. *See* as low as reasonably achievable
alkaline and neutral filter elution, 13
Alkeran. *See* melphalan
alkyl sulfonates, 477
alkylating agents, 476, 477–491, 478*t*–480*t*
 atypical, 480*t*
 history of, 475
 polyfunctional, 477
alleles, 275, 290
alpha (α) particles, 5, 6, 6*f*

LET values of, 103, 103*t*
oxygen enhancement ratio for, 83, 84*f*
radiation weighting factor of, 239, 239*t*
alternative DNA end-joining (Alt-EJ), 18
alternative modalities, 444–457
 boron neutron capture therapy, 446–447
 carbon ion radiotherapy, 451–455
 fast neutrons, 445–446
 proton therapy, 448–451
altitude, and radiation exposure, 206, 207
ALV. *See* avian leukosis virus
American College of Radiology (ACR), 203
American Society for Therapeutic Radiology and Oncology (ASTRO), 203, 429
americium-241, 78, 78*t*, 199–200, 200*f*
Amichetti, M., 526
amifostine, 128–130, 128*t*, 486*t*
amino acids, 258–262
 coding for, 260, 262*t*
 definition of, 290
aminothiol radioprotectors, 130
ampicillin, 290
ampicillin resistance, 264
amplification
 DNA, 271–273
 gene, 275, 291, 300, 502
 oncogene, 300
 RNA, 279
amplify, definition of, 290

anaphase, 24
anaphase bridge, 26, 27*f*, 30*f*
anastrozole, 487*t*
Andrews, G. A., 122*f*
Andrews, J. R., 385*f*
anemia, 361
angiogenesis, 313–314, 460
 chemotherapy targeting, 494–496, 496*f*
 definition of, 313
 hypoxia-inducible factor in, 460
angiography, 218
angioplasty, 218
ankylosing spondylitis, 138, 140, 142
annealing, 18, 272, 290
annual limit on intake, 253
anthracycline antibiotics, 491
antiandrogens, 493–494
antiangiogenic agents, 494–496, 496*f*
antibiotic(s)
 for acute radiation syndrome, 120–121
 chemotherapeutic, 480*t*–481*t*, 491–492, 498
 definition of, 290
 dose–response relationship for, 498, 499*f*
antibiotic resistance, 59, 264–265, 264*f*–265*f*, 277–278, 278*f*, 290
antibodies
 definition of, 290
 monoclonal, 284, 291
 polyclonal, 284, 292

production of, 284
radiolabeled, 228
antigen, 284, 290
antimetabolites, 481*t*, 492
“antioncogenes,” 301. *See also* tumor suppressor genes
antioxidants, 131–132
aphidicolin, 505
apoptosis, 35, 41–43, 328
 caspases and, 309–310, 309*f*, 310*f*
 cell loss from, 410
 cell type and, 41
 definition of, 35, 41
 diminished, in cancer therapy, 43
 and dose-rate effect, 73–74
 failure, in cancer biology, 295, 296, 309–312, 315
 microenvironment and, 381–382, 381*f*
 in model tumor systems, 380–382, 381*f*
 myc oncogene and, 311, 311*f*
 sequence of morphologic events in, 41
apoptotic bodies, 41
Archambeau, J., 450*f*
ARCON. *See* accelerated radiotherapy, carbogen, and nicotinamide (ARCON) trials
ARNT. *See* aryl hydrocarbon receptor nuclear translocator
aromatase inhibitors, 493
Arrhenius plot, 517–518, 518*f*, 523
ARS. *See* acute radiation syndrome
aryl hydrocarbon receptor nuclear translocator (ARNT), 458–459

as low as reasonably achievable (ALARA), 243, 246, 253

Ascaris, oxygen effect in, 82

ascorbic acid, 132

asparaginase, 485*t*

association, causation *vs.*, 186

ASTRO. *See* American Society for Therapeutic Radiology and Oncology

ataxia-telangiectasia, 48, 48*t*, 316–318, 316*t*

ataxia-telangiectasia mutated (ATM) protein, 15, 18, 19*f*, 21, 48, 304, 400*f*, 401

ataxia-telangiectasia–like disorder (ATLD), 319

atezolizumab, 490*t*, 497–498

Atgs (autophagy-related genes), 43

ATLD. *See* ataxia-telangiectasia–like disorder

ATM. *See* ataxia-telangiectasia mutated (ATM) protein

atomic bomb. *See* Hiroshima, Nagasaki survivors

atomic number, 8

aurora borealis, 5, 207, 207*f*

autochthonous tumor models, 389–390

automated DNA sequencing, 275

autophagosomes, 43, 311

autophagy, 43, 311–312

autophagy-related genes (Atgs), 43

autoradiography, 54–56, 55*f*, 56*f*, 398

 in growth fraction measurement, 409

 in percent-labeled mitoses technique, 402–405, 403*f*

 pulsed flow cytometry *vs.*, 407, 408*f*

autosomal dominant disease, 166–167

autosomal recessive disease, 166–167

Avastin. *See* bevacizumab

avian leukosis virus (ALV), 297
5-azacytidine, 492
azoospermia, 162, 367
B lymphocytes (B cells)
antibody production in, 284, 290
radiosensitivity of, 363
Bacq, Z. M., 126
bacterial artificial chromosomes (BACs), 264, 266, 290
bacteriophages (bacteriophage λ), 264, 265, 265*f*, 290
bacterium, definition of, 290
bait, in protein analysis, 284–285
bar code, molecular, 267
Barendsen, G. W.
on biologically effective dose, 430
on LET and RBE, 105*f*, 106*f*
on linear-quadratic model, 429*f*
on oxygen enhancement ratio, 84*f*, 107, 108*f*, 109*f*
on tumor growth measurements, 382, 383*f*
on *in vivo/in vitro* assays, 387, 387*f*
Barranco, S. C., 499*f*, 500*f*, 507*f*
base(s)
of DNA, 11, 12*f*, 16, 16*f*, 259, 259*f*–261*f*
of RNA, 259–260, 261*f*
base excision repair (BER), 16, 16*f*
base pairs, 11, 12*f*, 16, 16*f*, 259, 259*f*–261*f*, 290
basic fibroblast growth factor, 358
Basic Local Alignment Search Tool (BLAST), 288
BBI. *See* Bowman-Birk inhibitor

- Bcl-2 protein family, 309–310, 382
- BCNU, 477, 478*t*, 502*t*, 526*t*
- bcr* gene, 300, 301*f*
- becquerel (Bq), 253
- Becquerel, A. H., 2, 3*f*
- BED. *See* biologically effective dose
- Bedford, J. S., 41, 42*f*, 74*f*, 77*f*, 407*t*
- BEIR. *See* Biological Effects of Ionizing Radiation (BEIR) Committee
- Bell, A. G., 77
- Belli, J. A., 70*f*, 499*f*, 503*f*
- Bennington, J. L., 412*t*
- benzopyrene, 511, 511*t*
- BER. *See* base excision repair
- Bergonié, J., 352, 414
- Berrington, A., 156*t*, 157*t*
- Berry, R. J., 386*f*, 407*t*
- bevacizumab, 487*t*, 494–496, 496*f*
- Bhatia, S., 151
- Biade, S., 47*f*
- bicalutamide, 486*t*, 493
- Biological Effects of Ionizing Radiation (BEIR) Committee, 139, 238
- on DDREF, 146
 - on doubling dose, 170
 - on embryonic and fetal effects, 185–186
 - on linear no-threshold, 155–156
 - on radon, 209, 248
 - on risk estimates, 147–148
- Biological Effects of Ionizing Radiation (BEIR) VII Report*, 123, 138, 139, 143,

- biologically effective dose (BED)
 - calculations of, 430–433
 - definition of, 430
 - retreatment and, 439
- bioreductive drugs, 468–469, 502
- bischloroethylnitrosourea (BCNU), 477, 478*t*, 502*t*, 526*t*
- Bishop, J. M., 298*f*
- black film badges, 32–33
- bladder. *See* urinary bladder
- Blakely, E. A., 453*f*
- BLAST. *See* Basic Local Alignment Search Tool
- Bleehen, N. M., 94, 95*f*
- Blenoxane. *See* bleomycin
- bleomycin, 480*t*, 491
 - dose–response relationship for, 498, 499*f*, 507*f*
 - hyperthermia combined with, 526–527, 526*t*
 - oxygen effect and, 501, 501*f*, 502*t*
 - potentially lethal damage repair with, 498–500, 500*f*
 - second malignancies from, 511, 511*t*
- blobs, 12–13, 13*f*
- blood cells
 - counts after total body irradiation, 361–362, 362*f*
 - hematopoietic syndrome and, 111–112, 115–118
 - radiation mitigators and, 130–131
- blood transfusions, 463
- blood vessels, 360*t*, 368, 374*t*
- Bloom syndrome, 320

BNCT. *See* boron neutron capture therapy

Boice, J. D., Jr., 142*f*, 149–151

Bond, V., 137*f*

bone, 368–369

bone cancer, 137, 143

bone marrow, 359*t*, 360–363

H-type populations in, 357

hypoxia-inducible factor and, 461

stem cells

dose–response relationships for, 329, 336–339, 338*f*, 339*f*

early response in, 329

bone marrow death, 111–112. *See also* hematopoietic syndrome

bone marrow transplantation, 121

bone metastases, 227–228, 440–441

Bonner, J. A., 495*f*

boron neutron capture therapy (BNCT), 446–447

Bowman-Birk inhibitor (BBI), 132

brachytherapy, 77–78

interstitial, 77, 78

advantages for patient, 78

radionuclides for, 78, 78*t*

intracavitory, 77–78

LDR *vs.* HDR, 77–78

radionuclides for, 77, 78*t*

origin of term, 77

Bragg peak

heavy (carbon) ion, 452–454, 453*f*

proton, 448–450, 448*f*, 449*f*

brain

dose to

in diagnostic radiology, 212*t*

in nuclear medicine, 224*t*

QUANTEC analysis of, 370*t*

radiosensitivity and response of, 359*t*, 366

retreatment of, 439–440

SOMA scoring for, 374*t*

stereotactic procedures for, 427–428

brain tumor

hyperthermia and radiation for, 526

proton *vs.* carbon ion therapy for, 453, 454*f*

Brazil, natural background radiation in, 209

BRCA1 and *BRCA2* genes, 303–304, 496–497, 497*f*

BRCA1 protein, 15, 21

breast, 360*t*, 374*t*

breast cancer, 141, 142*f*

in A-bomb survivors, 141, 142*f*

adjunct chemotherapy with radiation for, 508–509, 509*f*

age at exposure and, 139, 148

ataxia-telangiectasia and, 316, 316*t*

biomarkers in, 15

continuous low dose rate for, 441

familial, 303–304

fluoroscopy in tuberculosis and, 138, 142*f*

genomic analysis in, 273

in Hodgkin disease survivors, 151–152, 153, 153*f*

homologous recombination in, 21, 304

- hormone targeted therapies for, 493
hyperthermia for, 441, 516, 524–525
PARP inhibitors for, 496–497, 497*f*
pulsed dose rate for, 441
radiotherapy for mastitis and, 138, 141, 142*f*
retreatment of, 441
breast mammography, 212, 212*t*, 213*f*, 213*t*, 216*t*
breastfeeding, nuclear medicine and, 231
breathing frequency, radiation damage and, 329, 343, 345*f*
Brenner, D. J., 150*f*, 153, 153*f*, 157, 212*t*
Brent, R. L., 178, 179*f*
Bresciani, F., 412*t*
Brewen, J. G., 28*f*–29*f*, 30*f*
Brizel, D. M., 521
Broerse, J. J., 84*f*, 105*f*, 108*f*, 387*f*
bromodeoxyuridine, for cell labeling, 55–56, 55*f*, 56*f*
bronchial carcinoma, chronic hypoxia in, 86–88, 87*f*, 88*f*
Brown, J. M.
 on cell cycle and tumor kinetics, 407*t*, 409*t*, 410*t*
 on hypoxia, 89, 89*f*
 on hypoxic cytotoxins, 467*f*, 468*f*, 503*f*
 on rodent skin, 344*f*
 on stereotactic procedures, 428, 428*f*
 on tumor angiogenesis, 461
Brummelkamp, T. R., 279*f*
Busch, W., 516
Bush, R. S., 386, 387*f*
busulfan, 477, 478*t*

buthionine sulfoximine, 500*f*, 505
bystander effect, 40–41, 328
Cairns, R. A., 469*f*, 470*f*
calcium-DTPA (ca-DTPA), 131
Canada, cosmic radiation in, 208*f*
“The Canadian Genome Atlas” (TCGA), 273
cancer. *See also* carcinogenesis; *specific types*
 amifostine as protector against, 129–130
 heritable syndromes affecting, 317–320
 HIF activation in, 460
 invasion and metastasis in, 314–315, 314*f*
 proteomics in, 287, 287*f*
 risk estimates for, 123
 stem cells
 chemotherapy/chemoresistance and, 476, 504–505
 intrinsic radiosensitivity and, 48–49
 T cell checkpoint therapy for, 321–322, 322*f*, 497–498
 telomerase and, 25
cancer biology, 295–326
 angiogenesis in, 313–314
 DNA stability genes in, 295, 296, 296*f*, 315–316, 316*t*
 dysregulated proliferation in, 306–307
 escape from senescence in, 312–313, 312*f*
 failure of apoptosis in, 295, 296, 309–312, 315
 failure to respond to growth-restrictive signals in, 307–309
 malignant transformation in, 295–296, 296*f*
 mechanisms of carcinogenesis in, 296
 mismatch repair genes in, 316–317, 317*t*

multistep process in, 305–306, 305*f*, 306*f*
oncogene activation in, 295, 296*f*, 297–301, 298*f*, 299*f*, 301*t*
oncogene discovery in, 296–297
oncogene function in, 306–315
predisposition genes in, 303, 304*t*
tumor suppressor genes in
 function of, 306–315
 gatekeepers and caretakers, 315–316
 mutation or inactivation of, 295, 296*f*, 301–305, 302*f*–303*f*
 somatic homozygosity and, 304–305, 305*f*
two-hit hypothesis in, 302
cancer genome, 273
Cancer Genome Atlas, 288
capecitabine, 481*t*
carbogen, 463, 466–467
carbon ion radiotherapy, 428–429, 451–455
 beam design for clinical use, 453–454, 454*f*
 depth-dose profiles of, 452, 452*f*
 ion properties in, 455*t*
 PET verification of treatment plan, 454
 proton therapy *vs.*, 453, 454*f*
 radiobiologic properties in, 452–453, 453*f*, 454*f*
 reasons for choosing, 455
 scattering and fragmentation in, 453*f*, 454
carboplatin, 478*t*
carcinogenesis, 135–161
 in A-bomb survivors, 144–148 (*See also* Hiroshima, Nagasaki survivors)
 age at exposure and, 139, 143, 148, 149*f*

in children

- after in utero exposure, 156–157, 186–187, 186*t*, 230
- radiosensitivity and, 148, 149*f*, 228
- treated for thyroid cancer, 138
- treated for tinea capitis, 138, 141, 144
- concern over, vs. heritable effects, 173, 173*f*, 250
- diagnostic radiology and, 211
- in dial painters, 143, 144*f*
- dose–response relationship for
 - at high doses, 152–154
 - threshold-sigmoid for, 135, 136*f*
- gender and, 149, 150*f*
- Gray’s bell-shaped curve for, 152–153, 152*f*
- human experience of, 136–138, 136*f*, 137*f*
- latent period in, 139
- linear dose response in, 153–154, 153*f*
- low dose rate and DDREF in, 146
- mammalian cell studies of, 270
- mechanisms of, 296
- multistep process of, 305–306, 305*f*, 306*f*
- in nuclear industry workers, 154–155, 154*f*, 155*f*, 156
- overview of specific cancers in, 140–144
- in radiologists, 138, 143–144, 156, 156*t*, 157*t*
- in radiotherapy-treated ankylosing spondylitis, 138
- risk assessment in, 139
- risk estimates in, 123, 144–148, 145*f*, 146*t*, 147*f*
 - committees concerned with, 139–140
- extrapolating risks from high to low doses, 155–156, 155*f*

highlighting need for protection, 244–245, 244*t*
organ-specific, 147–148, 148*f*
population average per sievert, 147, 147*t*
second malignancies in, 148–152
cervical carcinoma treatment and, 149–151
Hodgkin disease treatment and, 151–152
prostate cancer treatment and, 149, 150*f*
stochastic effects in, 135–136, 136*f*, 201, 211, 230
terrorism and, 198
time since exposure and, 139

carcinoma. *See also specific types*

apoptosis in, 381
cell loss in, 410–411
cardiology, 218–221
nuclear, effective doses from, 222, 223*f*, 225*t*
occupational exposure in, 220, 220*f*, 221*t*
patient doses and effective doses in, 219–220, 220*t*
cardiomyopathy, 368
cardiovascular system, 145*f*, 157, 368, 374*t*
caretakers, 315–316
carmustine, 477, 478*t*
Carpenter, D. M., 156
cartilage, 359*t*, 368–369
Cas (CRISPR-associated genes), 276–277, 277*f*
Cas9 nuclease, 277, 290
Casarett, G. W., 356, 356*t*
Casarett's classification system, 356–357, 356*t*
Casodex. *See* bicalutamide

caspases, 309–310, 309*f*, 310*f*
cataract (cataractogenesis), 191–196
classification of, 193, 193*f*
definition of, 191
dose–response relationship in, 194–195, 195*f*
in experimental animals, 192
in humans, 192–195, 192*f*
interventional radiology and, 220
latent period in, 192, 194
Scheimpflug imaging of, 193–194, 193*f*
stage 1, 193
causation, association *vs.*, 186
CCNU, 477, 479*t*, 499*f*, 502*t*, 506, 507*f*
CDC. *See* Centers for Disease Control and Prevention
Cdk–cyclin complexes, 57–58, 57*f*, 398–400, 399*f*
cDNA. *See* complementary DNA
cell cycle, 54–58, 54*f*, 398, 399*f*
age-response function in, 58–65
for high-linear energy transfer radiations, 64–65
hyperthermia and, 518
mechanisms for, 65
possible implications in radiotherapy, 65
sublethal damage repair and, 70–72
for tissue *in vivo*, 63–64, 64*f*
in cancer biology, 307–309
Cdk–cyclin complexes in, 57–58, 57*f*, 398–400, 399*f*
cell-labeling techniques in, 54–56, 55*f*, 56*f*, 402
checkpoint pathways in, 400–401, 400*f*

chemotherapy and, 475, 476, 477*f*
crosslink repair in, 21
G1 restriction point in, 398–399
homologous recombination in, 18, 20–21
kinetics of, 398–407
molecular checkpoint genes and, 62–63, 63*f*
nonhomologous end-joining in, 18, 18*f*
oxygen effect in, 63, 82
percent-labeled mitoses technique in, 402–405, 403*f*–406*f*, 412–413
phases of, 56–58, 57*f*
pulsed flow cytometry in, 407, 408*f*
quantitative assessment in, 401–402, 402*f*
synchronously dividing cells in, 58–62, 58*f*–62*f*
in vivo/in vitro measurements in, 405–406, 406*f*, 407*f*, 407*t*
in yeast, 267

cell cycle nonspecific, 476

cell cycle specific, 476, 477*f*

cell cycle time (T_c), 54, 405–406, 406*f*, 407*f*, 407*t*

cell death (cell killing), 35, 40–44, 328

apoptotic, 35, 41–42, 328 (*See also* apoptosis)

autophagic, 43, 328

bystander effect in, 40–41, 328

in Casarett’s classification system, 356–357, 356*t*

caspases and, 309–310, 309*f*, 310*f*

chromosomal aberrations and, 41–42, 42*f*

deterministic effects and, 135–136, 136*f*

failure, in cancer biology, 295, 296, 309–312, 315

mechanisms of, 40–44, 328

mitotic, 35, 41–43, 328, 356
in model tumor systems, 380–382, 381*f*
myc oncogene and, 311, 311*f*
necrotic, 328
pathways mediating, 309, 309*f*
programmed type II, 43
reproductive, 35
senescence in, 43–44, 328
survival curve shape and mechanisms of, 45–46
cell division, 23–25, 41–43, 54–58
 radiosensitivity/response in, 351–352, 355
 synchronous, in cultures, 58–62
cell-labeling techniques, 54–56, 55*f*, 56*f*
cell lines, established, 36, 268–270
cell loss, 381, 409–411
 in animal tumors, 410–411, 410*t*
 in human tumors, 413–414
cell-loss factor (ϕ), 410, 410*t*, 413–414
cell survival, definition of, 35
cell survival curves, 35–53
 cytotoxic temperatures and, 517–518, 517*f*
 definition of, 35
 dose-rate effect and, 72–77
 effective, for multifraction regimen, 49, 49*f*
 human and rodent cell, in asynchronous cultures, 45–46, 47*f*
 linear-quadratic model of, 38*f*, 39–40
 mammalian cells in culture, 44–45, 44*f*
 multitarget model of, 38*f*, 39

oxygen effect and, 85–86, 85*f*, 86*f*
paired, for hypoxic cells, 89–90, 91*f*
radiosensitivity in, 45–51
 genetic control of, 47–48
 human syndromes associated with, 48, 48*t*
 intrinsic, and cancer stem cells, 48–49
 mammalian cells compared with microorganisms, 50, 51*f*
 oncogenes and, 46–47
shape of, 38–40, 38*f*, 45–46
sublethal damage repair and, 69–72
tumor cell calculations using, 49–50
in vitro, 35–38, 36*f*, 37*f*, 44–46
x-ray effects on, 59–62, 60*f*, 61*f*

cellular oncogene, 290

CEM. *See* cumulative equivalent minutes

Center for Devices and Radiological Health, 212

Centers for Disease Control and Prevention (CDC), 203

central nervous system, 352, 366–367, 374*t*. *See also* brain; spinal cord

centromere, 24, 290

ceramide pathway, 320–321, 321*f*

cerebrovascular syndrome, 111–112, 113

cervical carcinoma

 hyperthermia and radiation for, 524

 hypoxia markers in, 93–94, 93*f*

 intracavitary brachytherapy for, 77–78

 second malignancies after radiotherapy for, 149–151

cesium-137, 77, 78*t*, 200–202, 200*f*–201*f*

cetuximab, 488*t*, 494, 495*f*

CFP. *See* cyan fluorescent protein

CGH. *See* comparative genomic hybridization

Chaplin, D. J., 89

Chapman, J. D., 47*f*

CHART. *See* continuous hyperfractionated accelerated radiation therapy

checkpoint pathways, 400–401, 400*f*

checkpoint therapies, 321–322, 322*f*, 490*t*, 497–498

chemical repair, radioprotectors and, 127

chemotherapy, 475–515. *See also* specific agents

adjunct use with radiation, 508–510, 508*f*, 509*f*

adjuvant, 476, 510

biologic basis of, 476–477

cardiotoxic, 368

cell cycle-nonspecific, 476

cell cycle-specific, 476, 477*f*

classes and modes of action, 477–498, 478*t*–490*t*

comparison with radiotherapy, 505–508

concurrent, 510

dose of, 475, 500

dose–response relationships for, 498, 499*f*, 505–506, 507*f*

growth fraction in, 475, 476

hematopoietic effects of, 362–363

history of, 475–476

hyperthermia with, 526–528, 526*t*

induction, 510

integration with surgery and radiotherapy, 510

oxygen effect and, 97, 477, 501, 501*f*, 502*t*, 506–508

public image of, 476

resistance to, 97, 502–505, 503*f*
cancer stem cells and, 504–505
genetics of, 502–504, 504*f*
relationship with radioresistance, 505, 506*f*, 508
second malignancies from, 511, 511*t*
sensitivity, 498, 500*f*, 505–506, 507*f*
sensitivity assays for individual tumors, 510
sublethal and potentially lethal damage repair in, 498–500, 506
“thermosensitive” liposomes for, 527, 529*f*
tirapazamine added to, 468–469

Chernobyl disaster
ARS in, 111, 112, 114–115, 116, 120–121
carcinogenesis in, 140
cataractogenesis in, 193–194, 193*f*
collective effective dose in, 212, 242
internal contamination in, 202
radionuclide eliminators used in, 131
terrorism scenario compared to, 198
tissue reactions in, 201
treatment for victims, 120–121

chest wall breast cancer, hyperthermia for, 524–525
chest x-ray, 212, 212*t*, 213*t*, 216*t*
chicken sarcoma, oncogenes in, 296–297
children
of A-bomb survivors (F1 generation)
carcinogenesis in, 144–146, 145*f*, 186–187, 228
heritable effects in, 172–173, 172*t*, 228
cancer in, after in utero exposure, 156–157, 186–187, 186*t*, 230

- CT scanning in, 214
- effective dose in, 228–230, 229*t*
- “Image Gently” campaign for, 214
- nuclear medicine in, 228–230
- radiosensitivity of, 148, 149*f*, 228
- Chinese hamster cells
 - autoradiography of, 56*f*
 - cell cycle in, 56–57, 56*f*, 57*t*
 - chemotherapy resistance in, 505, 506*f*
 - cytotoxic temperatures and, 517–518, 517*f*, 518*f*
 - dose-rate effect in, 74*f*
 - hyperthermia in, 517*f*
 - misonidazole in, 464*f*
 - oxygen effect in, 85, 85*f*, 501*f*
 - proton *vs.* carbon ion therapy in, 453, 454*f*
 - spheroid, 390
 - sublethal damage repair in, 69–70, 69*f*, 72*f*
 - tirapazamine in, 467–468, 467*f*
 - x-ray effects on, 59–62, 60*f*, 61*f*, 62*f*
- ChIP. *See* chromatin immunoprecipitation
- chlorambucil, 477–491, 478*t*
- chloroethylcyclohexyl-nitrosourea. *See* CCNU
- choroidal melanoma, 449–450, 449*f*
- Chow, E., 440–441
- chromatid aberrations, 25–26
- chromatin immunoprecipitation (ChIP), 280–283, 281*f*, 290
- chromatin immunoprecipitation (ChIP) chips, 281–282
- chromatin immunoprecipitation (ChIP)-Seq, 283

chromosomal diseases, 165, 165*t*, 166*t*, 167
chromosome(s), 163–164
 breaking and rejoining, 167
 and cell division, 23–25
 condensation of, 23–24, 24*f*
 heterologous, 164
 homologous, 164
 mitosis and, 54
 telomeres of, 24–25
chromosome aberrations, 23–33, 167. *See also specific types and effects*
 radiation-induced, 25–33
 in acute radiation syndrome, 112–113
 anaphase bridge, 26, 27*f*, 30*f*
 dicentric, 26, 27*f*, 28*f*
 examples of, 26–29, 27*f*–31*f*
 in human lymphocytes, 29–33, 32*f*
 lethal, 26, 41–42, 42*f*
 ring, 26, 27*f*, 29*f*
 small interstitial deletion, 29, 31*f*
 symmetric translocations, 26–29, 31*f*
 unstable *vs.* stable, 33
chromosome painting, 26
chronic hypoxia, 86–89, 87*f*–89*f*, 466
cisplatin, 97, 480*t*, 499*f*, 502*t*, 526–527
cis-platinum agents, 491
 cell-cycle specificity of, 476, 477*f*
 oxygen effect and, 501, 502*t*
 resistance to, 505

CLDR. *See* continuous low dose rate

Clifton, K. H., 329, 339–341, 340*f*

clinical response. *See* normal tissues, clinical response of

clinical thermometry, 530

clonogenic assays, 329

clonogenic end points, dose–response relationships for, 329–341

clonogenic survival, 35, 46

clustered lesion, 13

clustered regularly interspaced short palindromic repeats (CRISPR), 276–277, 277*f*, 290

codons, 260, 262*t*, 290

initiation, 260, 291

termination, 260, 292

Cohen, S., 259

Coley, W. B., 516

collective committed effective dose, 241–242, 242*t*, 253

collective effective dose, 241, 242*t*, 253

 CT and, 217, 217*f*

 definition of, 217

 detriment from, 217–218

 in diagnostic radiology, 212, 214–218

 in interventional radiology, 218

 in nuclear medicine, 222–225, 223*f*

 occupational, 217, 218

 patient, 217–218

 principal contributors to, 231, 232*f*

collective equivalent dose, 240, 253

Collins, V. P., 411–412

colony, 266, 290
lung assay, 380, 386–387, 387*f*
skin, dose–response relationships for, 329–331, 330*f*, 331*f*
colony-stimulating factors, 130–131, 130*f*
Colorado, natural background radiation in, 207, 208
colorectal cancer, 305, 305*f*, 315
comet assay, 13–14, 14*f*
committed effective dose, 240, 242*t*, 253
committed equivalent dose, 240–241, 242*t*, 253
comparative genomic hybridization (CGH), 275–276, 276*f*
complementary base pairing, 11, 12*f*, 16, 16*f*, 259, 259*f*–261*f*
complementary DNA (cDNA), 265, 290
complementary DNA (cDNA) library, 267, 284–285, 290
complementary nucleotides, 259
complementary RNA (cRNA), 279, 290
Compton process, 6–8, 7*f*
computed tomography (CT)
 collective effective dose from, 217, 217*f*
 dose from, 212*t*, 213–214, 213*t*
 effective dose from, 214, 216*t*
 increase in scanners/scanning, 213, 215*f*
 pediatric, 214
concomitant boost, dose calculation for, 431, 432*t*
concurrent chemotherapy, 510
Conference of Radiation Control Program Directors, 212
consequential late effect, 353
contig, 266, 290
contiguous mapping, 274

continuous exposure, limits for, 247

continuous hyperfractionated accelerated radiation therapy (CHART), 427, 431, 432, 432*t*

continuous labeling, 409

continuous low dose rate (CLDR), 441

Cornforth, M. N., 31*f*, 41, 42*f*

coronary angiography/angioplasty, 218

corticosteroids, 485*t*

cosmic radiation, 206–207, 207*f*, 208*f*

Coulomb interactions, 10

Courtenay assay, 48

Cowan, K. H., 504*f*

Crabtree, H. G., 82

Cramer, W., 82

CRI. *See* cutaneous radiation injury

Crick, F., 258, 259

crisis, in senescence, 312, 312*f*

CRISPR/CRISPR-associated genes, 276–277, 277*f*, 290

critical organ, 225

crizotinib, 488*t*

cRNA. *See* complementary RNA

crosslink repair, 21, 22*f*

CT. *See* computed tomography

cumulative equivalent minutes (CEM), 523–524

Curie, I., 136, 136*f*

Curie, M., 2, 136, 136*f*

Curie, P., 2, 3*f*

Curt, G. A., 504*f*

Curutchet, H. P., 412*t*

cutaneous radiation injury (CRI), 119. *See also* skin

cyan fluorescent protein (CFP), 284

cyclin(s), 398–400, 399*f*

cyclin-dependent kinases (Cdks), 57–58, 57*f*, 398–400

cyclophosphamide, 477–491, 478*t*, 526*t*

cyclotron, 222, 223*f*, 225

Hammersmith, 445–446

Harvard, 448–450, 449*f*

Uppsala (Sweden), 448, 450

U.S., 446

cysteamine, 126, 127–128, 128*t*

cysteine, 126, 127

cytarabine, 482*t*, 492

cytoprotectants, 486*t*

cytosine, 11, 12*f*, 16, 16*f*, 259–260, 259*f*–261*f*

cytotoxic temperatures, 517–520. *See also* hyperthermia

cytotoxins, hypoxic, 467–469, 502

Cytoxin. *See* cyclophosphamide

dacarbazine, 477, 478*t*

dactinomycin, 480*t*, 491

dose–response relationship for, 498, 499*f*, 507*f*

oxygen effect and, 501, 502*t*

Danish Head and Neck Cancer (DAHANCA) trials, 424–426, 426*f*, 426*t*, 465, 466*f*

Darby, S. C., 157

databases, genomic, 288

daunorubicin (daunomycin), 491

de minimis dose, 248–249
de Vita, V. T., 412*t*
deep sequencing, 275
Dekaban, A. S., 184
Delaney, T., 451*f*
deletions, 29, 31*f*, 166, 267
Denekamp, J., 409*t*, 410
Denko, N., 14*f*
densely ionizing radiation, 101, 102*f*
density-inhibited stationary-phase cell cultures, 67, 68*f*
dental x-ray, 212, 212*t*, 213*t*
Denver, Colorado, radiation exposure in, 207
deoxyribonucleic acid. *See* DNA
deoxyribose, 11, 259
Department of Energy (DOE), 237, 238, 250
dermis, 357–361, 361*f*
deterministic effects, 135–136, 136*f*, 242–243. *See also* tissue reactions (deterministic effects)
detiment, radiation, 217–218, 249
Dewey, W. C., 517, 517*f*, 518*f*, 523
Dewhirst, M. W., 527
Diagnosis and Treatment of Radiation Injuries, 119–120, 119*t*, 120*t*
diagnostic radiology, 210–218
 absorbed dose in, 211–212
 collective effective dose in, 212, 214–218
 dose in, 210–214
 effective dose in, 211–212, 214, 216*t*
 interventional *vs.*, 210–211

organ doses in, 212–214, 212*t*–214*t*
pediatric, “Image Gently” campaign on, 214
stochastic effects in, 211

dial painters, 143, 144*f*

dicentric, 26, 27*f*, 28*f*, 29–33, 32*f*, 72

dichloroacetate (DCA), 470, 469*f*

dideoxynucleotide chain termination method, 274–275

dietary supplements, 131–132

diethylenetriamine pentaacetic acid (DTPA), 131, 132*f*

differentiating intermitotic cells, 356*t*, 357

differentiation, and radiosensitivity, 351–352, 356*t*, 357

digest, 266, 290

digestive tract, 363–365

Dilution assay technique, 380, 384–386, 385*f*, 386*f*, 393

direct action, 8–9, 8*f*

directly ionizing radiation, 6

“dirty bomb,” 198–199, 198*f*, 199*f*

Disaster Preparedness of Radiology Professionals: Response to Radiological Terrorism (ASTRO), 203

DNA, 11, 163–164

- amplification of, 271–273, 272*f*
- bases of, 11, 12*f*, 16, 16*f*
- chromosomal condensation in, 23–24, 24*f*
- complementary, 265, 290
- definition of, 290
- laddering, in cell survival curves, 45–46, 47*f*
- recombinant, 292 (*See also* recombinant DNA technology)
- replication of, 259, 260*f*

separation into fragments, 270–271, 271*f*
single-strand structure of, 11, 12*f*
structure of, 11, 23, 24*f*, 258, 259, 259*f*
as target for radiation effects, 11, 40
transcription of, 258, 260, 261*f*

DNA damage, 8–9, 8*f*, 11–34
checkpoint pathways for, 400–401, 400*f*
chromosomal aberrations in, 23–33
locally multiply damaged site of, 13, 13*f*
number and type of lesions per cell, 11
repair of (*See* DNA repair)

DNA damage-induced nuclear foci, 13, 14–15, 15*f*

DNA fingerprint, 275, 291

DNA methylation, 173–174

DNA polymerase, 271–272, 291, 399

DNA polymorphisms, 275, 291

DNA repair, 15–22
age-response function and, 65
alternative DNA end-joining, 18
base excision, 16, 16*f*
crosslink, 21, 22*f*
double-strand break, 18–21, 65
homologous recombination, 18, 20–21, 20*f*
mismatch, 21–22, 23*f*
nonhomologous end-joining, 18–20, 18*f*, 19*f*
nucleotide excision, 16–18, 17*f*
single-strand annealing, 18

DNA sequencing, 266–267, 273–276

databases on, 288
definition of, 274, 291

DNA stability genes, 315–316, 316*t*
definition of, 295
loss of activity, 295, 296, 296*f*

DNA strand breaks, 11–15
double, 11–15, 12*f* (*See also* double-strand breaks)
measurement of, 13–15, 14*f*, 15*f*
radiation-induced, 25
single, 11, 12*f*

DNA-mediated gene transfer, 270

docetaxel, 484*t*, 493

DOE. *See* Department of Energy

Doll, R., 156, 157, 186

dominant genes, 164, 165*t*, 166–167

Dorie, M. J., 14*f*, 96*f*

dose, chemotherapy, 475, 500

dose, radiation, 238–239. *See also* specific types and procedures
diagnostic radiology, 210–218
embryonic or fetal effects of, 177, 180, 185–186, 185*t*, 187
equivalent, 108
interventional radiology, 218–221
lymphocyte estimation of, 29–33, 32*f*
maximum permissible, 168, 173, 244, 250, 250*t*
natural background radiation, 206–210
nuclear medicine, 222–225
relationship with cell survival, 35 (*See also* cell survival curves)

dose, thermal, 523–524

dose and dose-rate effectiveness factor (DDREF), 146

dose calculations, radiation

- allowance for proliferation in, 431–432
- for CHART therapy, 431, 432, 432*t*
- choice of α/β in, 430
- for concomitant boost, 431, 432*t*
- for conventional treatment, 430
- for hyperfractionation, 430, 432*t*
- linear-quadratic concept for, 429–433, 429*f*, 430*f*
- model, 430–433
- for one-fraction-a-day control schedule, 431
- pragmatic approach to (Peters), 432–433
- for retreatment, 439

“dose painting,” 93

dose ranges, 250–252, 251*f*

dose reduction factor (DRF), 126, 128, 128*t*

dose-rate effect, 72–77

- classic, 73
- examples *in vitro* and *in vivo*, 73–76
- idealized experiment, 73, 73*f*
- inverse, 76, 76*f*
- magnitude of, cell type and, 73
- summary of, 76–77, 77*f*

dose–response relationships, 327–328, 327*f*

- assays for, 329
- for bone marrow stem cells, 329, 336–339, 338*f*, 339*f*
- for carcinogenesis
 - at high doses, 152–154

threshold-sigmoid for, 135, 136*f*
for cataractogenesis, 194–195, 195*f*
for cells transplanted to another site, 336–341
for chemotherapy, 498, 499*f*, 505–506, 507*f*
for clones regrowing *in situ*, 329–336
for clonogenic end points, 329–341
for early- *vs.* late-responding tissues, 329, 420–422, 421*f*, 422*f*
for functional end points, 329, 341–347
grade (severity) in, 327
incidence in, 327, 327*f*
inferring α/β ratio from multifraction experiments, 329, 347, 348*f*
for jejunal crypt cells in mice, 329, 331–332, 332*f*, 333*f*, 334*f*
for kidney tubules, 329, 336, 337*f*, 338*f*
for lungs in mice, 329, 343, 345*f*
for mammary and thyroid cells, 329, 339–341, 340*f*
for model normal tissues, 327–350
for organ function *vs.* cell survival, 420–421
for pig skin, 329, 341–343, 342*f*, 342*t*, 343*f*
for rodent skin, 329, 343, 344*f*, 344*t*
for skin colonies, 329–331, 330*f*, 331*f*
for spinal cord, 329, 343–347, 345*f*–347*f*
summary of curves for clonogenic assays, 341, 341*f*
for testes stem cells, 329, 332–336, 335*f*, 336*f*
therapeutic ratio (index) in, 327–328, 327*f*, 328*f*
for tissue reactions *vs.* stochastic effects, 243–244, 243*f*
types of cell death in, 328
double helix, of DNA, 11, 23, 24*f*, 259, 259*f*
double minutes, 300

double-strand breaks (DSBs), 11–15, 12*f*
apoptotic, 41
chromosomal aberrations in, 23
homologous recombination of, 18, 20–21, 20*f*
interaction of, 11
measurement of, 13–15, 14*f*, 15*f*
nonhomologous end-joining of, 18–20, 18*f*, 19*f*
optimal LET and, 105–106, 106*f*
radiation-induced, 25
repair of, 18–21
age-response function and, 65
sublethal damage and, 72
types of, 11–12
yield in irradiated cells, 12

doubling dose
definition of, 168
in fruit flies, 168
in mice, 170–171
in risk estimates for humans, 170–173, 171*t*, 172*t*

doubling time, 411–414
data and studies on, 411–412
of human tumors, 412–414, 413*t*
potential (T_{pot}), 409

Douglas, B. G., 329

Down syndrome, 167

doxorubicin, 481*t*, 491
cardiotoxicity of, 368

dose–response relationship for, 498, 499*f*, 507*f*

hyperthermia combined with, 527, 528*f*
oxygen effect and, 502*t*
potentially lethal damage repair with, 498–500
resistance to, 502, 503*f*, 505

DRF. *See* dose reduction factor

Drosophila melanogaster

- dose limits based on, 250
- doubling dose in, 168
- heritable effects in, 168
- maximum permissible dose based on, 168, 173, 244

drug-induced synchrony, 58–59, 58*f*, 59*f*

DSBs. *See* double-strand breaks

DTPA, 131, 132*f*

Dutch famine, post-World War II, 174

ear, 360*t*, 370*t*, 374*t*

- early effects, 201, 352–353, 352*f*
- early radiation lethality, 111–112
- early response genes, 320
- early-responding tissues, 329

- dose–response relationship for, 420–422, 421*f*, 422*f*
- fraction size and overall treatment time in, 423
- fractionation and, 419–423, 419*f*, 420*f*
- retreatment and, 438

earth’s crust, natural radioactivity in, 208, 209*f*

education, exposure limits for, 245*t*, 247

Edwin Smith Surgical Papyrus, 516

effective dose, 240, 242*t*

- in children, 228–230, 229*t*

collective, 212, 240, 242*t*, 253 (*See also* collective effective dose)
collective committed, 241–242, 242*t*, 253
committed, 240, 242*t*, 253
definition of, 211, 240, 253
in diagnostic radiology, 211–212, 214, 216*t*
in interventional radiology, 219–220
in nuclear medicine, 222–225, 223*f*, 224*t*
relevance of, 211
unit of, 211

EGFR. *See* epidermal growth factor receptor

Egypt, natural background radiation in, 209

Eisenbud, M., 249

electrical field, 3

electrodes, oxygen, 92–93

electromagnetic radiation, 3–5

electromagnetic spectrum, 4, 4*f*

electron(s), 5

 Compton process and, 6–7, 7*f*

 ejection (ionization) of, 3

 excitation of, 3

 free, 6

 radiation weighting factor for, 239, 239*t*

electron transport chain (ETC), 470

electrophoresis

 definition of, 291

 gel (*See* gel electrophoresis)

 single-cell, 13–14, 14*f*

 two-dimensional, 288, 293

electroporation, 270, 291

Elkind, M. M., 69*f*, 73*f*, 85*f*, 331–332

Ellis, F., 418, 429

Elsässer, T., 454*f*

Emami, B., 360*t*, 369

embryonic or fetal effects, 210

- “all or nothing” in early stage, 179
- association *vs.* causation, 186
- childhood cancer after in utero exposure, 156–157, 186–187, 186*t*, 230
- dose and, 177, 180, 185–186, 185*t*, 187
- dose rate and, 177
- fetal period, 178, 181
- gestational stage and, 177, 183–184
- growth disturbances/retardation, 177, 180–181, 182, 182*t*
- historical perspective on, 177, 188*t*
- in humans, 181–184
 - in A-bomb survivor in utero cohort, 144–146, 145*f*, 181–184, 186–187
 - comparison with animal data, 184–186, 185*f*, 185*t*
 - after medical exposures, 181, 184
- lethal, 177, 178–179
- malformations, 177, 178–181
- medical care/exposure of women and, 187, 230–231
- mental retardation, 177, 182–184, 183*f*, 210, 230
- microcephaly (head diameter), 182–184, 182*f*, 182*t*, 183*f*, 185, 210, 230
- mouse and rat studies of, 177–181
- MRI findings of, 184
- nuclear medicine and, 230–231, 231*t*
- occupational exposure of women and, 187

organogenesis, 178, 179–181
examples of, 180*f*–181*f*
incidence of, 178*f*–179*f*
overview of, 177
preimplantation, 178–179, 178*f*–180*f*
protection against
dose limits for, 245*t*, 246
risk estimates highlighting need for, 244–245, 244*t*
emergency occupational exposure, 246–247
Emery, E. W., 70*f*
emesis, average time to, 121
EMT. *See* epithelial to mesenchymal transition
endocrine glands, 359*t*
endocurietherapy, 77. *See also* brachytherapy
endoplasmic reticulum, hypoxic response in, 461–462
energy average, 102, 102*f*
enhanced natural sources, 206
enhanced permeability and retention (EPR), 527, 530
Environmental Protection Agency (EPA), 209, 238, 248
enzalutamide, 487*t*, 493–494
EORTC. *See* European Organisation for Research and Treatment of Cancer
EPA. *See* Environmental Protection Agency
epidermal growth factor receptor (EGFR), 494
epidermal reactions, 360
epidermis, 357, 358–361, 361*f*
epigenetics, 173–174
epithelial to mesenchymal transition (EMT), 315
epithermal neutrons, 447

Eppendorf probe, 92

EPR. *See* enhanced permeability and retention

equivalent dose, 108, 240, 242*t*, 253–254

collective, 241, 253

committed, 240–241, 242*t*, 253

Erbitux. *See* cetuximab

Erhlich, P., 475

erlotinib, 488*t*

ERR. *See* excess relative risk

erythema, 351, 358–361. *See also* skin

erythropoietin, 458

Escherichia coli (*E. coli*)

cell survival curve for, 50, 51*f*

definition of, 291

molecular techniques using, 259, 264*f*, 266, 267

esophageal cancer, hyperthermia and radiation for, 526–527

esophagus, 359*t*, 364, 371*t*, 374*t*

established cell lines, 36, 268–270

Estevez, 412*t*

ESTRO. *See* European Society for Therapeutic Radiology and Oncology

etanidazole, 464*f*, 465–466

ETC. *See* electron transport chain

ethidium bromide, 271, 291

ethylenimine derivatives, 477

Ethyol. *See* amifostine

etoposide, 487*t*, 527, 528*f*

European Organisation for Research and Treatment of Cancer (EORTC), 369, 426–427

European Society for Therapeutic Radiology and Oncology (ESTRO), 429
excess relative risk (ERR), 153, 153*f*
excitation, 3
exfoliation, cell loss in, 410
exons, 163, 260, 261*f*, 291
exposure limits. *See* limits, exposure
expression library, 267, 291
external exposure, 201–202
extranuclearly produced radiation, 3
extrapolation number, 39
eyes. *See also* cataract (cataractogenesis)
 protons for melanoma of, 448, 449–450, 449*f*
 radiosensitivity and response of, 359*t*
 SOMA scoring for, 374*t*
F1 generation. *See* children, of A-bomb survivors
Fanconi anemia (FA), 21, 22*f*, 48*t*, 319–320
Far Western blot, 284
Farese, A. M., 130*f*
fast neutrons, 445–446, 445*f*
fatigue, 351
FAZA (fluoroazomycin arabinoside), 226
Fazel, R., 225, 234
FDA. *See* U.S. Food and Drug Administration
FDG (fluorodeoxyglucose), 226, 227*t*
female genitalia, 368
fertility, radiation and, 162, 163*t*, 367–368
fetal effects. *See* embryonic or fetal effects
fetal period, 178, 181

fibroblast growth factor (FGF), 307, 358
fibrosarcoma, mouse
potentially lethal damage repair in, 68*f*
in vivo/in vitro assay in, 387–388
Field, S. B., 519
50% lethal dose (LD₅₀)
in acute radiation syndrome, 116–117
definition of, 116
species differences in, 116–117, 117*t*
treatment for exposures close to, 120–121
filgrastim, 130–131, 130*f*
final slope, in cell survival curve, 38*f*, 39
FISH. *See* fluorescent *in situ* hybridization
fixed postmitotic cells, 356*t*, 357
flanking region, 280, 291
flash-labeled cells, 402
flexible (F)-type populations, 357–358
flow cytometry, 407, 408*f*
FLT (fluorothymidine), 226
fludarabine, 483*t*
fluorescence recovery after photobleaching (FRAP), 284
fluorescence resonance energy transfer (FRET), 284
fluorescent *in situ* hybridization (FISH), 26–29, 31*f*, 33, 300
fluorescent proteins, 280, 284
fluorine-18, 226
fluoroazomycin arabinoside (FAZA), 226
fluorodeoxyglucose (FDG), 226, 227*t*
fluoromisonidazole (FMISO), 226

fluoroscopy

- in interventional radiology, 218–221
- occupational exposure in, 220, 220*f*, 221*t*
- radiation doses from, 213, 213*t*, 214*t*
- skin reactions in, 219, 219*t*
- in tuberculosis, and breast cancer, 138, 141, 142*f*

fluorothymidinie (FLT), 226

5-fluorouracil, 97, 481*t*, 492, 501, 502*t*

FMISO (fluoromisonidazole), 226

Focht, E. F., 193, 193*f*

Folkman, J., 494

four Rs of radiobiology, 70, 417–418

Fowler, J. F.

- on biologically effective dose, 430
- on dose–response relationships, 329, 341–343, 342*f*, 342*t*, 343*f*, 344*t*
- on linear-quadratic model, 429, 429*f*
- on local control in fractionation, 425
- on proliferation, 419*f*, 431–432
- on reoxygenation, 97

fractionated hyperthermia, 519

fractionation, 417–436

- accelerated repopulation in, 423–424, 424*f*, 425*f*

- accelerated treatment in, 427

- basis of, 417–418

- dose calculations in

 - allowance for proliferation in, 431–432

 - for CHART therapy, 431, 432, 432*t*

 - choice of α/β in, 430

for concomitant boost, 431, 432*t*
for conventional treatment, 430
for hyperfractionation, 430, 432*t*
linear-quadratic concept for, 429–433, 429*f*, 430*f*
model, 430–431
for one-fraction-a-day control schedule, 431
pragmatic approach to (Peters), 432–433
dose-rate effect in, 72–77
early- *vs.* late-responding tissues in, 419–423, 419*f*, 420*f*
dose-response relationships for, 420–422, 421*f*, 422*f*
fraction size and treatment time influence on, 423
hematopoietic response in, 362
history of, 417, 417*f*
hyperfractionation in, 426–427, 430, 432*t*
hypofractionation in, 427–429, 428*f*
idealized experiment, 73, 73*f*
inverse dose-rate effect in, 76, 76*f*
and lungs, 345*f*, 346, 346*f*
nominal standard dose in (Ellis), 418, 429
operational classifications of damage in, 67
overall treatment time in, importance of, 424–426, 426*f*, 426*t*
potentially lethal damage repair in, 67–69
proliferation as factor in, 418–420, 419*f*
radiation quality and, 72, 72*f*
relative biologic effectiveness and, 104–105, 104*f*
stereotactic procedures in, 427–429, 427*t*, 428*f*
Strandquist plot of, 418*f*, 418*f*
sublethal damage repair in, 69–77

France, natural background radiation in, 209

FRAP. *See* fluorescence recovery after photobleaching

Fraumeni, J. R., 303*f*

free radicals, 9, 10, 12
chemotherapy and, 477, 502, 506
oxygen effect and, 83–84
radioprotection and scavenging for, 10, 127, 127*f*

French Academy of Sciences, 156

frequency, 4, 4*f*

frequent exposure, limits for, 247

FRET. *See* fluorescence resonance energy transfer

Freund, L., 2

Freyer, G., 272*f*

Frindel, E., 410*t*, 412*t*

Frost, P., 412*t*

fruit flies. *See* *Drosophila melanogaster*

Fry, M., 403*f*

FSUs. *See* functional subunits

F-type populations, 357–358

Fu, K. K., 75*f*

Fukushima accident (Japan), 131, 198

functional cells, 357

functional end points, dose–response relationships for, 329, 341–347

functional subunits (FSUs), 353–355
kidney, 353, 365
liver, 365
lung, 365
minimum number required (TRU), 327, 353

spatial arrangement of, 354–355, 354*f*
spinal cord, 346, 354, 367
structurally defined, 353
structurally undefined, 353
G (gap) phases, in cell cycle, 56–58, 57*f*
G₁ restriction point, 398–399
gain-of-function mutations, in oncogenes, 295, 296*f*
 γ -rays, 3–5, 4*f*
exposure from earth's crust, 208, 209*f*
ionization density of, 101, 102*f*
LET values of, 103, 103*t*
oxygen enhancement ratio for, 82–83, 84*f*
gastrointestinal fluoroscopy, 213, 214*t*
gastrointestinal syndrome, 111–115, 114*f*, 115*f*
gatekeepers, 315–316
G-CSF. *See* granulocyte colony-stimulating factor
Geard, C. R., 27*f*, 55*f*, 56*f*, 500*f*
Geiger counter, 202
gel electrophoresis, 259
agarose, 270–271, 271*f*, 290
polyacrylamide, 283, 288, 292
pulsed-field, 13, 14*f*
two-dimensional, 288, 293
gemcitabine, 483*t*
GenBank, 288
gender, and carcinogenesis, 149, 150*f*
gene(s), 163–164
definition of, 163, 291

dominant and recessive, 164, 165*t*, 166–167
imprinted, 174
locus of, 163
gene amplification, 275, 291, 300, 502
gene editing, CRISPR system of, 276–277, 277*f*
gene expression, 266, 278–283, 291
gene knockout strategies, 276–278, 277*f*, 278*f*
gene mapping, 274
gene transfer
 bacterial artificial chromosomes and, 264, 266
 bacteriophages and, 264, 265, 265*f*
 DNA-mediated, 270
 plasmids and, 259, 264–265, 264*f*, 270
 transfection and, 268, 270
 transformation and, 268–270, 268*f*
 vectors for, 264–266
viruses and, 264, 266
gene-cloning strategies, 273
genetic code, 258, 260, 291
genetic diseases. *See* heritable diseases; heritable effects
genetic information, flow of, 260, 261*f*
genetic reporters, 280, 284
genetically significant dose (GSD), 254
genetics
 environmental factors and, 173–174
 review of, 163–164
genome, 163
cancer, 273

composition of, 163
copying, in cell cycle, 399
databases of, 288
definition of, 291
Human Genome Project, 274
individual heterogeneity in, 273
retroviral, 266
sequencing of, 273–276
genomic analyses, 273–276
Genomic Data Commons, 288
genomic instability, 317–320
genomic library, 266–267, 291
genomics, 273
germ cell production, 162, 163*t*, 332–336, 367–368
germanium-68, 225
Gerner, E. W., 519
GFP. *See* green fluorescent protein
GG-NER. *See* global genome repair
GGR. *See* global genome repair
Ghorson, R. O., 178, 179*f*
glioblastoma multiforme, 526
global genome repair (GGR or GG-NER), 16–18, 17*f*
glucose metabolism, hypoxia and, 460, 461*f*, 469–470, 469*f*, 470*f*
glutathione, in chemoresistance, 505
GM-CSF. *See* granulocyte-macrophage colony-stimulating factor
Goans, R. E., 121
gold-198, 78*t*
Goldstein, L., 177, 184, 188*t*

Gompertz function, 411, 411*f*
goserelin acetate, 486*t*
Gould, D., 45
Gould, M. N., 329, 339–341, 340*f*
granulocyte colony-stimulating factor (G-CSF), 130–131, 130*f*
granulocyte-macrophage colony-stimulating factor (GM-CSF), 130
granulopenia, 361
Grasty, R. L., 208*f*
gray (Gy), 103, 108, 211, 238, 242*t*, 254
Gray, J. W., 408*f*
Gray, L. H., 82, 86–88, 87*f*, 88*f*, 152–153, 152*f*
green fluorescent protein (GFP), 280, 284, 291
growth delay, tumor, 382, 382*f*, 383*f*, 393
growth factors
 in cancer biology, 306–307
 in radiosensitivity and response, 358
growth fraction, 407–409, 409*t*, 413, 475, 476
growth kinetics, tumor, 411–414
 Gompertz function in, 411, 411*f*
 histology and, 412
 in human tumors, 412–414, 412*t*, 413*t*
growth measurements, tumor, 380, 382, 382*f*, 383*f*, 393
growth retardation, intrauterine, 177, 180–182, 182*t*
GSD. *See* genetically significant dose
guanine, 11, 12*f*, 16, 16*f*, 259–260, 259*f*–261*f*
Gutin, P. H., 346*f*, 347*f*
hadron therapy, 444
hair dysplasia, 360

Hall, E. J., 59*f*, 72*f*, 76*f*
Hammersmith Hospital (London), 445–446, 519
Hammond, E. M., 14*f*, 15*f*, 381*f*, 497*f*
hamster cells, Chinese. *See* Chinese hamster cells
hamster embryo cells, transformation in, 268–270, 268*f*, 269*f*
Hap Map, 273
Harms, W., 441
Hartwell, L. H., 398
Harvard cyclotron, 448–450, 449*f*
Hay, M. P., 469
HDR. *See* high dose rate
head and neck cancer
 accelerated repopulation in, 423–424, 425*f*
 cetuximab for, 494, 495*f*
 hyperthermia and radiation for, 526
 intensity-modulated radiation therapy for, 432–433, 440
 misonidazole in, 465, 466*f*
 overall treatment time in, 424–426, 426*f*, 426*t*
 radiosensitivity and response in, 363–365
 retreatment in, 440
 salivary gland regeneration in, 375–376
 tirapazamine added to chemotherapy for, 468–469
head CT, 212*t*, 216*t*
head diameter (microcephaly), 182–184, 182*f*, 182*t*, 183*f*, 185, 210, 230
heart, 145*f*, 157, 352, 359*t*, 368, 371*t*, 374*t*
heat. *See also* hyperthermia
 response of normal tissues to, 519
 response to cytotoxic temperatures, 517–520

response to noncytotoxic temperatures, 521–522, 521*f*, 522*f*
heat radiation, 4, 4*f*
heat shock protein (HSP), 522
heavy charged particles (ions), 5, 6
absorption of, 10
application and use of, 444–445, 451–455
beam design for clinical use, 453–454, 454*f*
Bragg peak, 452–454, 453*f*
carbon ion radiotherapy, 428–429, 451–455
depth-dose profiles of, 452, 452*f*
oxygen enhancement ratio of, 452
proton therapy *vs.*, 453, 454*f*
radiation weighting factor of, 239, 239*t*
radiobiologic properties of, 452–453, 453*f*, 454*f*

HeLa cells

- cell cycle in, 56–57, 57*t*
- dose-rate effect in, 73–74, 74*f*
- inverse dose-rate effect in, 76, 76*f*
- survival curve for, 44–45, 44*f*
- x-ray effects on, 60–62, 61*f*, 62*f*

helium, alpha (α) particles from, 6, 6*f*

hematopoietic syndrome, 111–112, 115–118, 116*f*, 117*t*

hematopoietic system, 352, 357, 360–363, 362*f*

Henle, K. J., 519

Henschke, U. K., 116*f*

hereditary nonpolyposis colon cancer (HNPCC), 316–317

heritable diseases, 164–168. *See also* heritable effects

- baseline frequencies of, 165, 166*t*

definition of, 164
heritable effects, 162–176
 in children of A-bomb survivors, 172–173, 172*t*
 chromosomal, 165, 165*t*, 167
 concern over, *vs.* carcinogenesis, 173, 173*f*, 250
 diagnostic radiology and, 211
 in fruit flies, 168
 in humans, 170–171
 mendelian, 165–167, 165*t*
 in mice, 168–170
 multifactorial, 165, 165*t*, 167–168
 mutant/monster misconception of, 165, 165*f*
 mutation component in, 170
 mutations causing, 164–168
 mutations in, 164–168
 risk estimates of, 171–173, 171*t*, 172*t*
 highlighting need for protection, 244–245, 244*t*
 stochastic effects and, 135–136, 136*f*, 211
Hermens, A. F., 387, 410*t*, 424*f*
heterologous chromosomes, 164
heterozygous, definition of, 164
Hewitt, H. B., 91*f*, 384
hierarchical shotgun sequencing, 273
hierarchical (H)-type populations, 357–358
HIF. *See* hypoxia-inducible factor
high dose rate (HDR), 73–77
 in *in vitro* and *in vivo* experiments, 73–76, 74*f*–75*f*
 in intracavitary brachytherapy, 77–78

Hill, R. P., 386, 387*f*
hind limb paralysis, in rats, 329, 343–347, 345*f*–347*f*
Hippocrates, 516
Hiroshima, Nagasaki survivors
 acute radiation syndrome in, 111
 breast cancer in, 141, 142*f*
 carcinogenesis in
 dose-response relationship for, 152–153, 153*f*
 extrapolating risks from high to low doses, 155–156, 155*f*
 organ-specific, 147–148, 148*f*
 risk estimates of, 123, 144–148, 145*f*, 146*t*, 147*f*
 studies of, 138, 144
 cataractogenesis in, 192, 194, 195*f*
 children of (F1 generation)
 carcinogenesis in, 144–146, 145*f*, 186–187, 228
 heritable effects in, 172–173, 172*t*, 228
 in utero cohort of, 181–184
 carcinogenesis in, 144–146, 145*f*, 186–187
 comparison with animal data, 184–186, 185*f*
 growth retardation in, 182, 182*t*
 mental retardation in, 182–184, 183*f*
 microcephaly in, 182–184, 182*f*, 182*t*, 183*f*
 latent period in, 139
LD_{50/60} for, 117
leukemia in, 140, 144–146, 145*f*
Life Span Study of, 138, 144–146, 145*f*
lung cancer in, 142
noncancer (cardiovascular) effects in, 145*f*, 157

risk assessment in, 139
solid tumors in, 145*f*, 146, 146*t*
thyroid cancer in, 140
tissue reactions in, 201
translocations in, 33
histone modification, 173–174
HNPCC. *See* hereditary nonpolyposis colon cancer
Hodgkin disease
breast cancer after treatment for, 153, 153*f*
cardiomyopathy in, 368
chemotherapy for, 475–476
second malignancies in, 151–152, 511
Holliday junctions, 20*f*, 21
Holthusen, H., 82
homogeneously staining regions (HSR), 300
homologous chromosomes, 164
homologous recombination, 277–278, 278*f*, 304
homologous recombination repair (HRR), 18, 20–21, 20*f*
homozygosity, somatic, 304–305, 305*f*
homozygous, definition of, 164
Hoppe, R. T., 497*f*
hormesis, 155*f*, 156
hormone targeted therapies, 486*t*–487*t*, 493–494
hosts, 267–271
Howard, A., 54, 56, 57, 398
H-ras oncogene, 299–300, 301*t*
HRR. *See* homologous recombination repair
HSP. *See* heat shock protein

HSR. *See* homogeneously staining regions

H-type populations, 357–358

Huebner, R. J., 297

human activity, radiation from, 210, 210*f*

human cells. *See also specific radiobiology*

- in asynchronous cultures, cell survival curves in, 45–46, 47*f*
- dose-rate effect in, 74, 75*f*
- embryo, 268
- foreskin, 268
- skin fibroblasts, 268
- spheroids of, 391–392, 394

Human Genome Project, 274

human tumors. *See also specific radiobiology*

- doubling time of, 412–414, 413*t*
- growth kinetics in, 412–414, 412*t*, 413*t*
- hypoxia in, 92
- organoid models of, 392–393, 394
- xenografts of, 388–389, 389*f*, 393–394

hybridization, 267

- comparative genome, 275–276, 276*f*
- definition of, 291

hydroxyurea

- chemotherapy, 482*t*, 492
- synchrony induced by, 58–59, 58*f*, 59*f*

hyperbaric oxygen, 462–463

hyperfractionation, 426–427

- accelerated treatment in, 427
- continuous accelerated therapy in, 427, 431, 432, 432*t*

dose calculations for, 430, 432*t*
hyperthermia, 516–533
age-response function in, 518
Arrhenius plot in, 517–518, 518*f*, 523
for breast cancer, 441, 516, 524–525
for cervical carcinoma, 524
clinical thermometry in, 530
clinical trials
assessing combination with chemotherapy, 526–528, 526*t*, 528*f*
assessing combination with radiation therapy, 524–526, 525*f*
dose response in, 517–520, 517*f*, 518*f*
for esophageal cancer, 526–527
fractionated, 519
for glioblastoma multiforme, 526
for head and neck cancer, 526
heat response at cytotoxic temperatures, 517–520
heat response at noncytotoxic temperatures, 521–522, 521*f*, 522*f*
heating methods in, 520–521
for high-risk sarcoma, 527, 528*f*
historical perspective on, 516–517
hypoxia and, 518
immunologic effects of, 521–522, 522*f*
magnetic, 529–530
nutrient deficiency and, 519
pH and, 518–519
protein as target of, 518
reoxygenation in, 521, 521*f*
for superficial malignancies, 525–526, 525*f*

therapeutic gain factor in, 523
thermal ablation in, 520–521
thermal dose in, measuring, 523–524
thermal enhancement ratio on, 522–523
thermotolerance and, 519–520
tumor heating methods in, 529–530
tumor vasculature and, 520

hyperthyroidism, radioactive iodine-131 for, 226–227

hypofractionation, 427–429
carbon ion beams in, 428–429
stereotactic procedures in, 427–428, 428*f*, 428*t*

hypoxia, 458–474
acute, 86, 89, 89*f*, 466–467
and chemotherapy, 97, 501, 501*f*, 502*t*
chronic, 86–89, 87*f*–89*f*, 466
in human tumors, evidence of, 92
and hyperthermia, 518
overcoming
 cytotoxins for, 467–469
 radiosensitizing cells for, 462–467

Overgaard’s meta-analysis of, 466

oxygen effect and, 82–100
oxygen enhancement ratio in, 82–83, 83*f*, 84*f*
reoxygenation and, 94–97
techniques for measuring, 92–94
and tumor progression, 97–98
unfolded protein response in, 461–462

hypoxia markers, 93–94, 93*f*

hypoxia-inducible factor (HIF), 93–94, 313, 458–461, 459*f*, 461*f*

hypoxic cell sensitizers, 463–467

cis-platinum as, 491

clinically useful, properties of, 463

etanidazole, 465–466

hyperthermia with, 526

misonidazole, 463–465, 464*f*–466*f*

nimorazole, 465–466

nitroimidazoles, 463–466

hypoxic cells, in tumors

first experimental demonstration of, 89–90, 90*f*

killing

cytotoxins for, 467–469, 502

dichloroacetate for, 470, 470*f*

targeting tumor metabolism for, 469–470, 469*f*, 470*f*

tirapazamine for, 467–469, 467*f*, 468*f*

proportion, in animal tumors, 90–92, 91*f*

radiosensitizing, methods of, 462–467

hyperbaric oxygen, 462–463

improving oxygen supply, 463

radiosensitizers, 463–467

reoxygenation of, 94–97

resistance of, 502

ICR. *See* International Congress of Radiology

ICRP. *See* International Commission on Radiological Protection

ICRU. *See* International Commission on Radiation Units and Measurements

IEF. *See* isoelectric focusing

ifosfamide, 479*t*, 527, 528*f*

“Image Gently” campaign, 214
imatinib mesylate, 488*t*
immortal cells, 25, 269
immune checkpoint therapies, 321–322, 322*f*, 490*t*, 497–498
immune system, 363
immunoprecipitation, 284
chromatin, 280–283, 281*f*, 290
definition of, 291
immunotherapy, 321–322, 322*f*, 497–498
imprinted genes, 174
improvised nuclear device, 197–198, 197*t*, 199
IMRT. *See* intensity-modulated radiation therapy
in utero exposure. *See also* embryonic or fetal effects
A-bomb cohort, 144–146, 145*f*, 186–187
childhood cancer after, 156–157, 186–187, 186*t*, 230
in vivo/in vitro assay
in cell cycle, 405–406, 406*f*, 407*f*
in model tumor systems, 380, 387–388, 387*f*, 393
“inactionable” cancer genomes, 273
incidence, in dose–response relationship, 327, 327*f*
IND. *See* Investigational New Drug
India, natural background radiation in, 209–210
indirect action, 8*f*, 9
indirectly ionizing radiation, 6
induction chemotherapy, 510
infrared (heat) radiation, 4, 4*f*
infrequent exposure, limits for, 247
ingested radiation, 207*f*, 208–209

initial slope, in cell survival curve, 38*f*, 39
initiation codon, 260, 291
integral dose, 500
integrins, 315
intensity-modulated proton therapy, 450, 451*f*
intensity-modulated radiation therapy (IMRT), 93, 432–433, 440
interleukin-1, 358
interleukin-6, 358
internal contamination, 202
internal exposure (ingestion), 207*f*, 208–209
International Atomic Energy Agency, 119–120, 119*t*, 120*t*
International Commission on Radiation Units and Measurements (ICRU), 237–238
International Commission on Radiological Protection (ICRP), 140, 237–238
 on cataractogenesis, 194
 on committed equivalent dose, 240
 on DDREF, 146
 on deterministic and stochastic effects, 135
 on embryonic or fetal effects, 178, 183–184, 246
 on emergency occupational exposure, 246
 on heritable effects, 170–173, 172*t*
 history of current dose limits, 250
 on justification, 244
 on linear no-threshold, 155–156
 NCRP standards vs., 238
 on radiation detriment, 217, 249
 on radiation weighted dose, 240
 on radiation weighting factor, 107–109

on radiopharmaceuticals and breastfeeding, 231
on stochastic effects, 242
on tissue reactions, 242
on tissue weighting factor, 240, 241*t*

International Commission on Radiological Units, 101

International Congress of Radiology (ICR), 140, 237–238

International Nuclear Workers Study (INWORKS), 154–155, 154*f*, 155*f*, 156

International X-Ray and Radium Protection Committee, 237

interphase, 24, 54

interstitial brachytherapy, 77, 78, 78*t*

interventional radiology, 210–211, 218–221
collective effective dose in, 218
definition of, 218
occupational exposure in, 220, 220*f*, 221*t*
patient doses and effective doses in, 219–220, 220*t*
skin reactions in, 219, 219*t*

intestinal epithelium
early response in, 329, 352, 352*f*
H-type populations in, 357
mice jejunal cells of
age-response function in, 63–64, 64*f*
compartments of, 331–332, 332*f*
dose-rate effect in, 74–76, 75*f*
dose–response relationships in, 329, 331–332, 332*f*, 333*f*, 334*f*

intestines, 359*t*, 364–365, 372*t*, 374*t*

intracavitary brachytherapy, 77–78, 78*t*

intranuclearly produced radiation, 3

introns, 163, 260, 261*f*

invasion, cancer, 314–315, 314*f*
inverse dose-rate effect, 76, 76*f*
Investigational New Drug (IND), 130–131
INWORKS. *See* International Nuclear Workers Study
iodine-125, 78, 78*t*
iodine-131, 226–228, 231, 231*t*
ion, 9. *See also* heavy charged particles
ionization, 3
ionization density, 101, 102*f*, 127
ionizing radiation
 chromosome aberrations from, 25–33
 definition of, 3
 directly, 6
 effect on living things, 3 (*See also* radiobiology)
 electromagnetic radiation, 3–5
 energy release in, 3
 indirectly, 6
 vs. nonionizing, 4
 types of, 3–6
ipilimumab, 490*t*, 497–498
iridium-192, 77, 78*t*
irinotecan, 487*t*
isoelectric focusing (IEF), 288
isolation and barrier nursing, 120
isotopes, radioactive, 3
Issels, R. D., 528*f*
Jain, R. K., 496*f*
jejunal (jejunal crypt) cells, in mice

age-response function in, 63–64, 64*f*
compartments of, 331–332, 332*f*
dose-rate effect in, 74–76, 75*f*
dose–response relationships in, 329, 331–332, 332*f*, 333*f*, 334*f*
Job, T. T., 188*t*
Jones, E. L., 521, 524, 525*f*
justification, 243, 244
Kallman, R. F., 91*f*, 94, 95*f*, 96*f*, 387, 389*f*
Kano, E., 526*t*
Kellerer, A., 102*f*
Kember, N. R., 329
Kerala, India, natural background radiation in, 209–210
Keriakes, J., 231*t*
Kerr, J. F., 41
KHT sarcoma, lung colony assay in, 386–387, 387*f*
kidney(s)
 functional subunits of, 353, 365
 late response in, 329, 352, 352*f*
 QUANTEC analysis of, 372*t*
 radiosensitivity and response of, 359*t*, 365
 retreatment and, 438
 volume effect in, 354–355
kidney tubules, 329, 336, 337*f*, 338*f*
kiloelectron volt per micrometer (keV/ μ m), 101
kinetic energy
 in Compton process, 6–7, 7*f*
 in photoelectric absorption, 7–8, 7*f*
 in x-ray production, 3

kinetics, 398–416

cell cycle, 398–407, 399*f*

- checkpoint pathways in, 400–401, 400*f*
- cyclins and kinases in, 398–400, 399*f*
- flash-labeling in, 402
- percent-labeled mitoses technique in, 402–405, 403*f*–406*f*, 412–413
- pulsed flow cytometry in, 407, 408*f*
- quantitative assessment in, 401–402, 402*f*
- in vivo/in vitro* measurements of times, 405–406, 406*f*, 407*f*, 407*t*

tumor, 407–416

- cell loss in, 381, 409–411, 410*t*
- Gompertz function in, 411, 411*f*
- growth fraction in, 407–409, 409*t*, 413, 475, 476
- growth kinetics in, 411–414
- histology and, 412
- in human tumors, 412–414, 412*t*, 413*t*
- potential doubling time in, 409

Kleiman, N., 192*f*

Kneale, G. W., 186–187, 186*t*, 188*t*

knockouts. *See* gene knockout strategies

Knudson, A. G., Jr., 301–302, 302*f*

Koehler, A. M., 449*f*

Kolesnick, R., 321*f*

Kong, G., 529*f*

Koumenis, C., 462

Kraft, G., 452*f*, 453*f*, 455*t*

Kummermehr, J., 96*f*

labeling index (LI), 402

LaGory, E., 461*f*
large intestine, 359*t*, 364–365, 374*t*
Larsson, B., 448*f*
late effects, 201, 352–353, 352*f*, 369–375
Late Effects of Normal Tissue (LENT), 369–375, 374*t*–375*t*
latent period
in acute radiation syndrome, 111*f*, 112, 116, 119, 119*t*
in carcinogenesis, 139
in cataractogenesis, 192, 194
late-responding tissues, 329
dose–response relationship for, 329, 420–422, 421*f*, 422*f*
fraction size and overall treatment time in, 423
fractionation and, 419–423, 419*f*, 420*f*
retreatment and, 438
latitude, and radiation exposure, 207
Law, M. P., 519
Lawrence, E. O., 222, 223*f*, 445
Lawrence, J., 445*f*
Lawrence Berkeley Laboratory, 445, 445*f*
LD₅₀. *See* lethal dose, 50%
LDR. *See* low dose rate
Le, Q., 314*f*
lead, 208
Leeper, D. B., 519
LENT. *See* Late Effects of Normal Tissue
Leonard, C. E., 500*f*
LET. *See* linear energy transfer
lethal chromosome aberrations, 26, 41–42, 42*f*

lethal damage, definition of, 67

lethal dose, 50% (LD₅₀)

- in acute radiation syndrome, 116–117
- definition of, 116
- species differences in, 116–117, 117*t*
- treatment for exposures close to, 120–121

lethal effects, in utero, 177, 178–179

lethality, synthetic, 496–497, 497*f*

leucovorin, 492

leukemia, 140

- in A-bomb survivors, 140, 144–146, 145*f*
- chemotherapy for, 475–476
- in children, after in utero exposure, 157, 186–187
- dilution assay technique in, 384–385
- human history/experience of, 136–138, 136*f*
- latent period in, 139
- lifespan susceptibility to, 148
- in nuclear industry workers, 154, 154*f*
- in radiologists, 138
- in radiotherapy-treated ankylosing spondylitis, 138, 140
- second malignancies in, 153–154, 153*f*
- terrorism and, 198
- translocation in, 300, 301*f*

Leukeran. *See* chlorambucil

Leukine (sargramostim), 130

leuprolide acetate, 486*t*, 493

Leuraud, K., 154*f*

Leydig cells, 367

Lhermitte's sign, 366

LI. *See* labeling index

Li, F. P., 303*f*

libraries

cDNA, 267, 284–285, 290

definition of, 291

expression, 267, 291

genomic, 266–267, 291

Liebmann, J. E., 500*f*

Life Span Study (LSS), 138, 144–146, 145*f*

Li–Fraumeni syndrome, 301, 302–303, 303*f*, 313–314

ligases, 259, 291

ligation, definition of, 291

limitation, principle of, 243

limits, exposure

ALARA, 243, 246

basis for, 244–245

continuous or frequent exposure, 247

de minimis dose, 248–249

education or training, 245*t*, 247

embryonic or fetal, 245*t*, 246

emergency occupational exposure, 246–247

glossary of terms, 253–254

history of current, 250

ICRP vs. NRCP, 238, 249–250

infrequent exposure, 247

negligible individual dose, 245*t*, 249, 254

occupational, 245–246, 245*t*

- public, 245*t*, 247
- linear energy transfer (LET), 8–9, 101–103
average energy in, 101–102, 102*f*
cell age and radiosensitivity in, 64–65
criticism of measure, 102
definition of, 101
heavy (carbon) ion, 452–453, 455*t*
low, genetic risks from, 171, 171*t*
optimal, 105–106, 106*f*
oxygen effect and, 107, 108*f*, 109*f*
RBE as function of, 105, 105*f*, 106*f*
typical values of, 103, 103*t*
- linear no-threshold (LNT) hypothesis, 155–156, 155*f*
- linear-quadratic model, 38*f*, 39–40
in calculating effective doses, 429–433, 429*f*, 430*f*
in carcinogenesis, 140, 153–154, 153*f*
in dose–response relationships, 329, 347, 348*f*
in early- vs. late-responding tissue, 329, 420–422, 421*f*, 422*f*, 422*t*
in stochastic effects, 136*f*
- Ling, V., 506*f*
- liposomes, thermosensitive, 527, 528*f*
- Little, J. B., 40, 67, 68*f*, 115*f*
- Little, M. P., 186–187
- Litvinenko, A., 117–118, 117*f*, 202
- liver
F-type populations in, 357
functional subunits of, 365
late response in, 352

QUANTEC analysis of, 372*t*
radiosensitivity and response of, 359*t*, 365–366
liver tumors, radiation exposure and, 137
LNT. *See* linear no-threshold (LNT) hypothesis
locally multiply damaged site, 13, 13*f*
locus, of gene, 163
Loma Linda proton facility, 450, 450*f*
lomustine. *See* CCNU
long terminal repeat (LTR), 297–299
Los Alamos, accidents at
cerebrovascular syndrome from, 113
first ARS death from, 118, 119
loss of heterozygosity (LOH), 21
loss-of-function mutations, in tumor suppressor genes, 295, 296*f*
low dose rate (LDR), 73–77
DDREF in, 146
genetic risks from, 171, 171*t*
in idealized fractionation experiment, 73, 73*f*
in *in vitro* and *in vivo* experiments, 73–76, 74*f*–75*f*
in intracavitary brachytherapy, 77–78
in inverse dose-rate effect, 76, 76*f*
radiation weighting factor and, 239
L-PAM. *See* melphalan
LSS. *See* Life Span Study
LTR. *See* long terminal repeat
luciferase, splitting in protein analysis, 285–287, 286*f*
Luippold, H. E., 28*f*–30*f*
lumbosacral x-rays, 213*t*, 214*t*

lung(s)

dose to

in diagnostic radiology, 212*t*

in nuclear medicine, 224*t*

dose-response relationships in mice, 329, 343, 345*f*

functional subunits of, 365

late response in, 329, 352

QUANTEC analysis of, 371*t*

radiosensitivity and response of, 359*t*, 365

volume effect in, 354–355

lung cancer, 141–143

history of radiation exposure and, 137

proton beam therapy for, 441

radon exposure and, 6, 137, 142–143, 208–209

retreatment for, 441

stereotactic procedures for, 427–428, 428*f*, 441

lung colony assay, 380, 386–387, 387*f*

Lupron. *See* leuprolide acetate

Lushbaugh, C. C., 121

luteinizing hormone-releasing hormone (LHRH), 486*t*

lymphocyte(s)

B cells

antibody production in, 284, 290

radiosensitivity of, 363

chromosome aberrations in, 29–33, 32*f*

radiosensitivity of, 356, 361–363

T cells

checkpoint therapy, 321–322, 322*f*, 497–498

radiosensitivity of, 363

lymphocyte count, in ARS, 112–113, 119*t*, 120*t*, 121–123

lymphoid tissue, 360*t*, 363

lymphoma

- apoptosis in, 381

Hodgkin

- breast cancer after treatment for, 153, 153*f*
- cardiomyopathy in, 368
- chemotherapy for, 475–476
- second malignancies in, 151–152, 511

radioimmunotherapy for, 228

lymphopenia, 361

lymphosarcoma, mouse, 89–90, 90*f*

Lynch syndrome, 317

Mabuchi, K., 145*f*

MacMahon, B., 157, 186

macrophages, 363

magnetic field, 3

magnetic hyperthermia, 529–530

magnetic resonance thermal imaging (MRTI), 530

Malaise, E. P., 412–413, 412*t*, 415

malignant transformation, 295–296, 296*f*

mammalian cells. *See also specific types*

- cell cycle and cell cycle time in, 56–57, 57*t*
- in culture, survival curves for, 44–45, 44*f*
- monolayer *vs.* spinner culture, 390
- radiosensitivity of, 45–46, 46*f*, 356–357, 356*t*
 - compared with microorganisms, 50, 51*f*

human and rodent, in asynchronous cultures, 45–46, 47*f*
relative biologic effectiveness in, 103–104, 104*f*
transformation studies in, 268–270, 268*f*

mammary cells, dose–response relationships for, 329, 339–341, 340*f*

mammary tumors, mouse
autochthonous and transgenic models, 389–390
misonidazole in, 464–465, 465*f*
reoxygenation in, 94–96, 96*f*, 97
tumor cure assay in, 384, 384*f*
in vivo/in vitro assay in, 387–388

mammography, 212, 212*t*, 213*f*, 213*t*, 216*t*

Management of Terrorist Events Involving Radioactive Material (NCRP), 203

man-sievert (person-sievert), 212, 241, 242*t*

mapping (gene mapping), 274

Marshall Island, atomic fallout in, 111, 140

mass absorption coefficient, 8

mass spectrometry, 288

Massachusetts General Hospital, 450

mastitis, 138, 141, 142*f*

maturing partially differentiated cells, 357

maximum permissible dose, 168, 173, 244, 250, 250*t*

MC. *See* mutation component

McCulloch, E. A., 329, 336–339, 338*f*

McNally, N. J., 387

MD Anderson Hospital, 431, 441, 450

MEA. *See* mercaptoethylamine

mechlorethamine, 479*t*

medical countermeasures, 126–134

classes of, 126
dietary supplements, 131–132
need for developing, 126
radiation mitigators, 126
radiation therapeutics, 126
radionuclide eliminators, 131, 132*f*
radioprotectors, 126–130
supportive care, 131
in terrorism, 126, 128–129, 132, 202–203, 203*t*

Medical Research Council, 445–446, 462, 467

megamouse experiment, 168–171, 169*f*, 170*f*

megestrol acetate, 485*t*

melanoma, choroidal, protons for, 448, 449–450, 449*f*

melphalan, 477–491, 479*t*
dose–response relationship for, 499*f*
hyperthermia combined with, 526, 526*t*
resistance to, 505

Memorial Sloan Kettering Cancer Center, 497–498

mendelian diseases, 165–167, 165*t*
baseline frequency of, 166*t*
definition of, 165
dominant and recessive mutations in, 166–167
X-linked, 166

Mendelsohn, M. L., 409, 409*t*, 410*t*

mental retardation, 177, 182–184, 183*f*, 210, 230, 244–245, 244*t*

mercaptoethylamine (MEA, cysteamine), 126, 127–128, 128*t*

Merriam, G. R., Jr., 191*f*, 193, 193*f*, 194

messenger RNA (mRNA)

definition of, 291
DNA transcription to, 258, 260, 261*f*
translation of, 258, 260, 261*f*

metaphase, 24

metastasis, 314–315, 314*f*
cell loss in, 410
growth rates of, 412
hypoxia-inducible factor in, 460
T cell checkpoint therapy in, 321–322, 322*f*, 497–498

methotrexate, 97, 475, 482*t*, 492, 501, 502*t*

metronidazole, 502*t*

Metting, N., 251*f*

Mettler, F. A., Jr., 214, 216*t*, 219, 220*t*, 223–225, 224*t*

MI. *See* mitotic index

mice
dose–response relationships for
bone marrow stem cells, 336–339, 338*f*, 339*f*
jejunal crypt cells, 329, 331–332, 332*f*, 333*f*, 334*f*
lungs, 329, 343, 345*f*
skin, 329–331, 330*f*, 331*f*, 343, 344*f*, 344*t*
testes stem cells, 329, 332–336, 335*f*, 336*f*
doubling dose in, 170–171
embryonic or fetal effects in, 177–181, 184–186
fractionation and skin of, 419–420, 419*f*, 420*f*
heritable effects in, 168–170
knockout, 278
lens opacification in, 192
maximum permissible dose in, 244

megamouse experiment, 168–171, 169*f*, 170*f*
nude, xenografts in, 388–389, 389*f*
severe combined immunodeficiency in, 319

mice cells

in asynchronous cultures, cell survival curves of, 45–46, 47*f*
jejunal (jejunal crypt)
age-response function in, 63–64, 64*f*
compartments of, 331–332, 332*f*
dose-rate effect in, 74–76, 75*f*
dose-response relationships in, 329, 331–332, 332*f*, 333*f*, 334*f*
skin, dose-response relationships for, 329–331, 330*f*, 331*f*
stem, dose-response relationships in
bone marrow, 336–339, 338*f*, 339*f*
testes, 329, 332–336, 335*f*, 336*f*
sublethal radiation damage repair in, 70–71, 70*f*

mice tumors

cell cycle times in, 405–406, 406*f*
growth kinetics in, 412
hypoxic cells in, 89–90, 90*f*, 91*f*, 92
model systems of
apoptosis in, 381
autochthonous and transgenic, 389–390
dilution assay technique in, 384–386, 385*f*, 386*f*
lung colony assay in, 386–387, 387*f*
patient-derived xenografts, 389
transplantable, 380
tumor cure assay in, 384, 384*f*
in vivo/in vitro assay in, 387–388

xenografts of human tumors, 388–389, 389*f*
potentially lethal damage repair in, 68*f*
reoxygenation in, 94–96, 95*f*, 96*f*, 97
tirapazamine in, 468, 468*f*

Michałowski, A., 357

Michałowski's tissue classification, 357–358

microarray, 275–276, 276*f*, 282–283, 282*f*, 291

microcephaly, 182–184, 182*f*, 182*t*, 183*f*, 185, 210, 230

Micrococcus radiodurans, 50, 51*f*

microinjection, 270, 291

microorganisms, radiosensitivity in, 50, 51*f*

mild hyperthermia, 521–522, 521*f*, 522*f*

Miller, R., 360*t*

miners, 137, 142–143

mismatch repair (MMR), 21–22, 23*f*

mismatch repair genes, 316–317, 317*t*

misonidazole, 463–465, 464*f*, 464*f*–466*f*

Mitchell, J. B., 76*f*, 506*f*

mitochondrial activity, decreasing, 470

mitogens, 306–307

mitomycin C, 467, 481*t*, 491–492

hyperthermia combined with, 526, 526*t*
as hypoxic cytotoxin, 467, 502
oxygen effect and, 501, 501*f*, 502*t*

mitosis, 24, 398

cell cycle kinetics, 398–407

percent-labeled technique in, 402–405, 403*f*–406*f*, 412–413

mitotic cycle, 54–58

age-response function in, 58–65
for high-linear energy transfer radiations, 64–65
mechanisms for, 65
possible implications in radiotherapy, 65
and sublethal damage repair, 70–72
for tissue *in vivo*, 63–64, 64*f*
cell-labeling techniques in, 54–56, 55*f*, 56*f*
definition of, 54
synchronously dividing cells in, 58–62
definition of, 58
hydroxyurea-induced, 58–59, 58*f*, 59*f*
techniques for producing, 58–59
x-ray effects on, 59–62, 60*f*, 61*f*, 62*f*
mitotic cycle time, 54
mitotic death, 35, 41–43, 328, 356
mitotic harvest, 58, 63
mitotic index (MI), 401–402
mitotic inhibitors, 476, 477*f*
MLH repair genes, 22
MMR. *See* mismatch repair
Modan, B., 138
model fractionated dose calculations, 430–431
model normal tissues. *See* normal tissues
model tumor systems, 380–397
apoptosis in, 380–382, 381*f*
assay techniques in, 380
autochthonous and transgenic, 389–390
comparison of, 393–394, 395*f*

dilution assay technique in, 380, 384–386, 385*f*, 386*f*, 393
lung colony assay in, 380, 386–387, 387*f*
misleading results of, 393, 394*f*
organoid, of human tumors, 392–393, 394
patient-derived xenografts, 389, 394
spheroid, 390–392, 391*f*, 392*f*, 394
transplantable, in experimental animals, 380
tumor cure (TCD₅₀) assay in, 380, 382–384, 384*f*
tumor growth measurements in, 380, 382, 382*f*, 383*f*, 393
in vivo/in vitro assay in, 380, 387–388, 387*f*, 393
xenografts of human tumors, 388–389, 389*f*, 393–394

Mohiuddin, M., 440

moisture density gauges, 200, 200*f*
molecular checkpoint genes, 62–63, 63*f*
molecular clock, telomere length as, 25, 313
molecular techniques, 258–294
agarose gel electrophoresis in, 270–271, 271*f*
DNA-mediated gene transfer in, 270
gene expression analysis in, 278–283
gene knockout strategies in, 276–278
gene-cloning strategies in, 273
genomic analyses in, 273–276
glossary of terms, 290–293
historical perspectives on, 258–259
hosts in, 267–271
libraries in, 266–267
polymerase chain reaction in, 271–273, 272*f*
protein analysis in, 283–288

restriction endonucleases in, 262–264, 263*t*, 264*f*
vectors in, 264–266

molybdenum-99, 225

monkeys, ARS in, 116, 116*f*

monoclonal antibodies, 284, 291

monocytes, 363

Mottram, J. C., 82

Moulder, J. E., 91*f*, 92

Mount Vernon Hospital (United Kingdom), 427

mRNA. *See* messenger RNA

MRTI. *See* magnetic resonance thermal imaging

MSH repair genes, 22

mucosa

- oral, radiosensitivity and response of, 359*t*, 363–364
- SOMA scoring for, 374*t*
- volume effect in, 355

mucositis, 364–365

Muggia, F. M., 412*t*

Muirhead, C. R., 147*t*

Mulcahy, R. T., 340*f*

Müller, H. J., 168

multidrug resistance, 505

multifactorial diseases, 165, 165*t*, 167–168

- baseline frequency of, 166*t*
- characteristics of, 168
- definition of, 167

multifraction experiments/regimen

- effective survival curve for, 49, 49*f*

inferring dose-response curve from, 329, 347, 348*f*
ram, 417, 417*f*

multitarget model, 38*f*, 39

murine double minute 2 (Mdm2), 310, 400*f*, 401

Murphy, D. P., 177, 184, 188*t*

muscle, 360*t*

Mut genes, 22

mutation(s), 163–168. *See also specific types and processes*
definition of, 163
doubling dose for, 168, 170–173, 171*t*, 172*t*
fruit fly, 168
gain-of-function, in oncogenes, 295, 296*f*
human, 170–171
loss-of-function, in tumor suppressor genes, 295, 296*f*
mice, 168–170
PCR-mediated creation of, 272–273
point, 166, 275, 292
potential number of, 164
relative risk, 168
somatic, in carcinogenesis, 296
stochastic effects and, 135–136, 136*f*

mutation component (MC), 170

mutator phenotype, in cancer, 305–306, 306*f*, 316

myc oncogene, 300, 301*t*, 311, 311*f*

Nab-paclitaxel, 485*t*

Nagasaki. *See* Hiroshima, Nagasaki survivors

Nagasawa, H., 40

NASA. *See* National Aeronautics and Space Administration

- Nath, R., 78*t*
- National Academy of Sciences (U.S.), 155–156, 238
- National Aeronautics and Space Administration (NASA), 132
- National Bureau of Standards, 103, 237
- National Cancer Institute (NCI), 149, 186, 273
- National Center for Biotechnology, 288
- National Council on Radiation Protection and Measurements (NCRP), 140, 155–156, 187, 194, 203, 217, 237–238
- on collective effective dose, 217, 217*f*
 - on dose to staff during cardiac studies, 221*t*
 - on emergency occupational exposure, 246
 - on exposure limits, 245–250, 245*t*
 - ICRP standards *vs.*, 238
 - on nuclear medicine, 222–223, 223*f*
 - on radiation in pregnancy, 230, 245*t*, 246
- National Human Genome Research Institute (NHGRI), 273
- National Institute for Radiological Sciences (Japan), 131, 132*f*
- Nationwide Evaluation of X-ray Trends (NEXT), 212–214, 212*t*
- natural background radiation, 3, 5, 6, 206–210
 - from cosmic radiation, 206–207, 207*f*, 208*f*
 - from enhanced natural sources, 206
 - high, areas of, 209–210
 - human sources of radiation *vs.*, 210, 210*f*
 - from internal exposure, 207*f*, 208–209
 - from natural sources, 206, 207*f*
- natural sources, of radiation, 206, 207*f*
- nausea, 351, 364
- NBS. *See* Nijmegen breakage syndrome

NCI. *See* National Cancer Institute

NCRP. *See* National Council on Radiation Protection and Measurements

neck. *See* head and neck cancer

necrotic cell death, 328

negative π -mesons, 5, 444–445

Neglia, J. P., 153*f*

negligible individual dose, 245*t*, 249, 254

NER. *See* nucleotide excision repair

Neriishi, K., 195*f*

nervous system. *See also* brain; spinal cord

late response in, 352

radiosensitivity and response in, 366–367

Neulasta (pegfilgrastim), 130–131

Neupogen (filgrastim), 130–131, 130*f*

neutrons, 5, 6

absorption of, 10

application and use of, 444–447

boron neutron capture therapy, 446–447

boron compounds for, 447

challenges in, 446

clinical trials of, 447

neutron sources for, 447

epithermal, 447

fast, 445–446

first use for cancer, 445, 445*f*

Hammersmith experience, 445–446

rationale for, 445

U.S. experience, 446

LET values of, 103, 103*t*
oxygen enhancement ratio for, 83, 84*f*, 444
radiation weighting factor of, 239, 239*t*, 240*f*
RBE of, 444
thermal, 447

NEXT. *See* Nationwide Evaluation of X-ray Trends

next generation sequencing (NGS), 275

NHGRI. *See* National Human Genome Research Institute

nicotinamide, 466–467

Nijmegen breakage syndrome (NBS), 48*t*, 400*f*, 401

nimorazole, 464*f*, 465–466

nitrogen mustard derivatives, 477–491. *See also specific agents*

nitroimidazoles

- as hypoxia markers, 93–94, 93*f*
- as hypoxic cell sensitizers, 463–466
- structure of, 463–464, 463*f*, 464*f*

nitrosoureas, 477–491

- hyperthermia combined with, 526
- oxygen effect and, 501, 502*t*
- repair inhibition with, 500

Niue Island, natural background radiation on, 209

nivolumab, 490*t*, 497–498

nominal standard dose (NSD), 418, 429

nonneoplastic disease, radiation exposure and, 145*f*, 157

nonstochastic effects, 254

normal tissues

- cell categories in, 357
- clinical response of, 351–379

Casarett's classification of, 356–357, 356*t*
cell division and, 351–352, 355
class I organs, 359*t*
class II organs, 359*t*–360*t*
class III, 360*t*
early and late effects in, 352–353, 352*f*
factors governing, 351, 355
growth factors in, 358
LENT/SOMA classification of, 369–375, 374*t*–375*t*
Michałowski's H- and F-type populations in, 357–358
progression of, 352–353
quantitative analysis of, 369, 370*t*–373*t*
radiation pathology in, 355–356
specific tissues and organs, 358–369, 359*t*–361*t*
time interval in, 355–356
volume effect and tissue architecture in, 354–355, 354*f*
dose–response relationships for, 327–350
assays for, 329
for bone marrow stem cells, 329, 336–339, 338*f*, 339*f*
for cells transplanted to another site, 336–341
for clones regrowing *in situ*, 329–336
for clonogenic end points, 329–341
for early- *vs.* late-responding tissues, 329
for functional end points, 329, 341–347
inferring α/β ratio from multifraction experiments, 329, 347, 348*f*
for jejunal crypt cells in mice, 329, 331–332, 332*f*, 333*f*, 334*f*
for kidney tubules, 329, 336, 337*f*, 338*f*
for lungs in mice, 329, 343, 345*f*

for mammary and thyroid cells, 329, 339–341, 340*f*
for pig skin, 329, 341–343, 342*f*, 342*t*, 343*f*
for rodent skin, 329, 343, 344*f*, 344*t*
for skin colonies, 329–331, 330*f*, 331*f*
for spinal cord, 329, 343–347, 345*f*–347*f*
summary of curves for clonogenic assays, 341, 341*f*
for testes stem cells, 329, 332–336, 335*f*, 336*f*
functional subunits in, 353–355
heat response in, 519
stem cells for regeneration of, 375–376

Northern blotting, 278, 283, 291

northern lights, 5, 207, 207*f*

Nowell, P., 300

NRC. *See* Nuclear Regulatory Commission

NSD. *See* nominal standard dose

nuclear device, improvised, 197–198, 197*t*, 199

nuclear industry workers

carcinogenesis in, 154–155, 154*f*, 156
dose limits for, 249–250

nuclear medicine, 222–231

in breastfeeding women, 231
in children, 228–230, 229*t*
critical organ in, 225
definition of, 222
diagnostic *vs.* therapeutic, 222
effective dose and collective effective dose in, 222–225, 223*f*, 224*t*
embryonic/fetal doses in, 231, 231*t*
growth of specialty, 222

historical perspective on, 222
in pregnancy, 230–231
principles in, 225
target organ in, 225
therapeutic use of radionuclides in, 226–228
nuclear power station, as terrorist target, 198
nuclear reactors, 222
Nuclear Regulatory Commission (NRC), 238, 250
nucleoid sedimentation, 13
nucleoli, 24
nucleoside analogues, 482*t*–483*t*, 492
nucleotide, 259, 291
nucleotide excision repair (NER), 16–18, 17*f*
nude mice, xenografts in, 388–389, 389*f*
nutrition, inadequate
and cell loss, 410
and hyperthermia, 519
Oak Ridge Associated Universities, 121
Oak Ridge Institute for Science and Education, 123
Oak Ridge National Laboratory
megamouse experiment, 168–171, 169*f*, 170*f*
Y-12 accident, 121, 122*f*, 123
occupational exposure
diagnostic radiology and, 217, 218
emergency, 246–247
interventional radiology and, 220, 220*f*, 221*t*
limits for, 245–247, 245*t*
nuclear industry workers, 154–155, 154*f*, 156

radiologists

- carcinogenesis in, 138, 143–144, 156
- cataractogenesis in, 192–193, 192*f*, 220
- interventional radiology dose to, 220, 220*f*, 221*t*
- mortality patterns in, 156, 156*t*, 157*t*

women, 187

Occupational Safety and Health Administration (OSHA), 238

ocular lens

- anatomy and physiology of, 191, 191*f*
- cataracts of, 191–196

OER. *See* oxygen enhancement ratio

Okamoto, Y., 441

oligo arrays, 282*f*, 283

oligospermia, 162

oncogenes, 296–301

activation of, 295, 296*f*, 297–301, 298*f*

by amplification, 300

by DNA mutation of regulatory sites, 299–300, 299*f*

by retroviral integration, 297–299, 298*f*

by translocations, 300–301, 301*f*, 301*t*

concept of, 298*f*

definition of, 292

function of, 306–315

mammalian cell studies of, 270

and radioresistance, 46–47

Rous's landmark studies on, 296–297

tumor suppressor genes *vs.*, 301

Oncovin. *See* vincristine

open reading frame, 260, 292
optic nerve/chiasm, 370*t*
oral mucosa, 359*t*, 363–364
organ doses, in diagnostic radiology, 212–214, 212*t*–214*t*
organ or tissue weighting factor (W_T), 240, 241*t*, 254
organogenesis
 definition of, 178
 radiation effects during, 179–181, 230
 comparison of human and animal data, 184–185, 185*f*
 examples of, 180*f*–181*f*
 incidence of, 178*f*, 179*f*
organoid models, of human tumors, 392–393, 394
organ-specific risk estimates, 147–148, 148*f*
OSHA. *See* Occupational Safety and Health Administration
osteonecrosis, 369
Otake, M., 172*t*, 183*f*, 188*t*, 194
ovarian cancer, 496–497, 497*f*
ovaries, 162, 359*t*, 367–368
Overgaard, J., 424–426, 426*f*, 466, 466*f*, 517, 526*t*
oxaliplatin, 479*t*
Oxford Survey of Childhood Cancers (Stewart and Kneale), 186–187, 186*t*
oxygen, hyperbaric, 462–463
oxygen effect, 63, 82–100
 acute hypoxia in, 86, 89, 89*f*, 466–467
 and chemotherapy, 97, 477, 501, 501*f*, 502*t*, 506–508
 chronic hypoxia in, 86–89, 87*f*–89*f*, 466
 history of studies, 82
 and hyperthermia, 521, 521*f*

hypoxic cells in tumors

- first experimental demonstration of, 89–90, 90*f*
 - proportion, in animal tumors, 90–92, 91*f*
 - and linear energy transfer, 107, 108*f*, 109*f*
 - nature of, 82–83, 83*f*
 - oxygen concentration required for, 84–86, 85*f*, 86*f*
 - radioprotectors and, 127
 - reoxygenation and, 94–97
 - timing and mechanism of, 83–84
 - and tumor progression, 97–98
 - variations in cell cycle, 82
- oxygen enhancement ratio (OER), 63, 82–83, 83*f*
- definition of, 82
 - heavy ion, 452
 - and linear energy transfer, 107, 108*f*, 109*f*
 - neutron, 83, 84*f*, 444
 - proton, 448
 - type of radiation and, 83, 84*f*
 - unity, 83, 84*f*
 - variation in cell cycle, 82
- oxygen fixation hypothesis, 84, 85*f*
- oxygen probes, 92–93
- oxygen-15, 226
- p53* tumor suppressor gene, 303, 310–311
- adjunct chemotherapy with radiation and, 509
 - apoptosis and, 381–382, 381*f*
 - cell cycle kinetics and, 401
 - reporter genes and, 280

paclitaxel, 484*t*–485*t*, 493
adjunct use with radiation, 508–509, 509*f*
cell-cycle specificity of, 477*f*
sensitivity to, 500*f*

PAGE. *See* polyacrylamide gel electrophoresis

Paget, S., 314

Palcic, B., 83*f*

palindromic sequence, 263, 276–277

palladium-103, 78*t*

Papandreou, I., 469, 469*f*, 470*f*

Paracelsus, 476

parathyroid scan, 224*t*

PARP inhibitors, 488*t*, 496–497

particulate radiation, 3, 5–6

patient-derived xenografts (PDXs), 389, 394

Patt, H. M., 126

Pauling, L., 258–259

PCR. *See* polymerase chain reaction

PDGF. *See* platelet-derived growth factor

PDK inhibitors, 469–470, 469*f*, 470*f*

PDR. *See* pulsed dose rate

PDXs. *See* patient-derived xenografts

Peckham, M. J., 412*t*

Pedersen, R. A., 179, 180*f*

Peer, A. J., 522*f*

pegfilgrastim, 130–131

pegylated G-CSF, 130–131

Pelc, S. R., 54, 56, 57, 398

pembrolizumab, 490*t*, 497–498
penicillin, 475
penis, 373*t*
percentage of labeled mitoses, 403
percent-labeled mitoses technique, 402–405, 403*f*–406*f*, 412–413
percutaneous transluminal coronary angioplasty, 218
perfluorocarbons, 463
pericarditis, 368
peripheral nerves, 359*t*, 367
PERK. *See* protein kinase-like endoplasmic reticulum kinase
personalized medicine, 273, 287, 287*f*
person-sievert, 212, 241, 242*t*
PET. *See* positron emission tomography
Peter McCallum Cancer Center (Australia), 433, 437
Peters, L. J., 432–434
Petricoin, E., 287*f*
Petry, E., 82
PFGE. *See* pulsed-field gel electrophoresis
pH, and hyperthermia, 518–519
phase nonspecific, 476
phase specific, 476, 477*f*
PHDs. *See* 4-prolyl hydroxylases
phosphate group, covering sulphhydryl compounds with, 127–129, 128*t*
phosphate mining, 206
phosphate-32, 228
photoelectric absorption, 7–8, 7*f*
photons, 4–5
absorption of, 6–8

radiation weighting factor for, 239, 239*t*
size, and biologic effects of radiation, 4–5, 5*f*

Phusion, 272

Pierce, D. A., 147*f*

pig skin, 329, 341–343, 342*f*, 342*t*, 343*f*

pimonidazole, 93–94, 93*f*

Pirruccello, M. D., 453*f*

pitchblende miners, 137

pituitary gland, 359*t*

Planck's constant, 4

plaque, 265, 292

plasmids, 259, 264–265, 264*f*, 270, 277, 280, 292

platelet-derived growth factor (PDGF), 307

platelet-derived growth factor β , 358

plating efficiency, 36, 36*f*

PLD. *See* potentially lethal damage

pleiotropic resistance, 504–505

Plummer, G., 188*t*

pneumonitis, in acute radiation syndrome, 118, 118*f*

point mutations, 166, 275, 292

polarographic technique, 92–93

polonium, discovery of, 2

polonium-210 assassination, 117–118, 117*f*, 202

poly adenosine diphosphate- ribose polymerase (PARP) inhibitors, 488*t*, 496–497

polyacrylamide gel electrophoresis (PAGE), 283, 288, 292

polyclonal antibodies, 284, 292

polycythemia vera, 228

polyfunctional alkylating agents, 477

polymerase, 292

- DNA, 271–272, 291, 399
- RNA, 260, 261*f*, 292

polymerase chain reaction (PCR), 271–273

- definition of, 292
- quantitative real-time, 279–280, 283, 292
- reverse transcription, 278, 279, 283
- site-directed mutagenesis mediated in, 272–273
- technique of, 272*f*

polymerase chain reaction- restriction fragment length polymorphisms (PCR-RFLP), 275

polymorphisms, 275, 291

polypeptides, in proteins, 260–262

positron emission tomography (PET), 222, 225–226

- doses in, 226, 228*t*
- hypoxia imaging in, 93
- principle of, 226
- radiation dose from, 212*t*
- radionuclides used for, 226, 227*t*
- verifying carbon ion plan with, 454

Postow, M. A., 497–498

potassium iodide, 131, 132*f*

potassium-40, 208

potential doubling time (T_{pot}), 409

potentially lethal damage (PLD), 67

potentially lethal damage (PLD) repair, 67–69

- chemotherapy and, 498–500, 500*f*, 506

in density-inhibited stationary-phase cell cultures, 67, 68*f*
importance to clinical radiotherapy, 67–69
relevance to radiotherapy, 67

Potten, C. S., 331

Powell, M., 308*f*

Powers, W. E., 89–90, 90*f*

PR-104, 469

PrC-210 radioprotector, 130

precision radiotherapy, 273

predisposition genes, in cancer, 303, 304*t*

prednisone, 485*t*

pregnancy. *See also* embryonic or fetal effects
care and medical exposure during, 187
exposure limits in, 245*t*, 246
nuclear medicine in, 230–231

preimplantation
“all or nothing” effect in, 179
definition of, 178
radiation effects during, 178–179, 230
comparison of human and animal data, 184, 185*f*
incidence of, 178*f*–179*f*

Preston, D. L., 146*t*

Preston, R. J., 28*f*–30*f*

prey, in protein analysis, 284–285

primer
definition of, 292
in DNA sequence analysis, 274–275
in PCR, 271–272

Princess Margaret Hospital (Toronto), 463
probe, DNA or RNA, 266, 292
probe, oxygen, 92–93
procarbazine, 479*t*, 491, 501, 502*t*
prodromal radiation syndrome, 111, 111*f*, 112–113, 116
 laboratory findings in, 112–113
 signs and symptoms of, 112, 112*t*, 119, 119*t*
programmed cell death. *See* apoptosis
programmed cell death receptor, 497
programmed cell death receptor ligand, 497
programmed type II cell death, 43
progression, tumor, hypoxia and, 97–98
proliferation
 dose allowance for, 431–432
 dysregulated, in cancer, 306–307
 fractionation and, 418–420, 419*f*
4-prolyl hydroxylases (PHDs), 459, 459*f*
Prometheus, 516
promoter(s), 280–281
 in ChIP analysis, 280–281, 281*f*
 in reporter gene expression, 280
promoter bashing, 280, 281*f*
prophase, 24
prostate cancer
 hormone targeted therapies for, 493–494
 hypofractionation in, 427
 PARP inhibitors for, 496–497, 497*f*
 second malignancies after radiotherapy for, 149, 150*f*

protein(s)

- amino acid composition of, 258–259
- fluorescent, 280, 284
- folding of, 262
- as hyperthermia target, 518
- shape of, 262
- synthesis of (translation), 258, 260, 261*f*

protein analysis, 283–288

protein kinase-like endoplasmic reticulum kinase (PERK), 43, 462

protein–DNA interaction arrays, 281–282

proteomics, 287, 287*f*

proton(s), 5

- absorption of, 10
- application and use of, 444–445, 448–451
- Bragg peak, 448–450, 448*f*, 449*f*
- LET values of, 103, 103*t*
- oxygen enhancement ratio of, 448
- radiation weighting factor for, 239, 239*t*
- RBE of, 448
- recoil, 10, 101

proton therapy, 444–445, 448–451

- advantages of, 451
- broad beam, 450
- carbon ion therapy *vs.*, 453, 454*f*
- for choroidal melanoma, 448, 449–450, 449*f*
- depth-dose patterns and Bragg peak in, 448–450, 448*f*, 449*f*
- dose distribution in, 450, 451*f*
- Loma Linda facility, 450, 450*f*

for lung cancer, 441
Massachusetts General Hospital, 450
for retreatment, 438, 441

proto-oncogenes
activation of, 296*f*
definition of, 290, 295
gain-of-function mutation in, 295, 296*f*
retroviral integration of, 297–299, 298*f*

prudent and conservative assumption, 156

Prussian blue capsules, 131, 132*f*, 202

PSM repair genes, 22

public exposure limits, 245*t*, 247

Puck, T. T., 44*f*

pulmonary syndrome, 118, 118*f*

pulsed dose rate (PDR), for breast cancer, 441

pulsed flow cytometry, 407, 408*f*

pulsed-field gel electrophoresis (PFGE), 13, 14*f*

purines, 11, 12*f*, 259–260

pyrimidines, 11, 12*f*, 259–260

pyruvate dehydrogenase kinase (PDK) inhibitors, 469–470, 469*f*, 470*f*

Quantitative Analysis of Normal Tissue Effects in the Clinic (QUANTEC), 369, 370*t*–373*t*

quantitative real-time PCR (qRT-PCR), 279–280, 283, 292

quasithreshold dose, 39, 331

Quastler, H., 407*t*

rad, 238–239, 254

radar, 4

radiation. *See also specific types, effects, and uses*

absorption of, 6–8, 7*f*
biologic effects of, 2–5, 3*f*, 5*f*
direct action of, 8–9, 8*f*
electromagnetic, 3–5
indirect action of, 8*f*, 9
ionizing, 3–6
natural background, 3, 5, 6, 206–210
particulate, 3, 5–6
radiation, fractionated. *See* fractionation
radiation absorbed dose (rad), 238–239, 254
radiation burns, 119
radiation carcinogenesis. *See* carcinogenesis
radiation casualty team, 203
radiation damage. *See also specific types*
operational classifications of, 67
Radiation Effects Research Foundation (RERF), 145*f*, 146–146
Radiation Emergency Assistance Center/Training Site (REAC/TS), 123, 203
Radiation Emergency Medical Management website, 203
radiation exposure. *See also specific doses and effects*
chromosomal aberrations in lymphocytes as biomarker of, 29–33
FISH scoring of, 33
limits on (*See* limits, exposure)
medical countermeasures to, 126–134
real *vs.* suspected, 32–33
radiation exposure device (RED), 199
radiation mitigators, 126, 130–131
radiation protection, 237–255. *See also specific techniques and substances*
ALARA, 243, 246

basis for exposure limits in, 244–245
continuous or frequent exposure, 247
de minimis dose, 248–249
dose ranges in, 250–252, 251*f*
education or training, 245*t*, 247
embryonic or fetal, 245*t*, 246
emergency occupational exposure, 246–247
free radical scavengers in, 10, 127, 127*f*
glossary of terms in, 253–254
history of current limits, 250
ICRP vs. NRCP, 238, 249–250
infrequent exposure, 247
main elements of, 243
negligible individual dose, 245*t*, 249
objectives of, 243
occupational, 245–246, 245*t*
organizations involved in, 139–140, 237–238
origins of, 237
principles of, 243–244
public, 245*t*, 247
quantities and doses in, 238–242, 242*t*
radiation therapeutics, definition of, 126
Radiation Therapy Oncology Group (RTOG), 129, 369, 440, 465, 466, 468
radiation weighted dose, 240, 254
radiation weighting factor (W_R), 107–109, 239, 239*t*, 240*f*, 254
radiation-induced foci assay, 13, 14–15, 15*f*
radiation-mimetic drugs, 502
radio waves, 4, 4*f*

radioactive isotopes, 3

radioactive material

availability of, 199–201, 200*f*, 201*f*

contamination with, 201–202

NRC regulation of, 238

radiobiology. *See also specific processes and effects*

definition of, 3

direct action in, 8–9, 8*f*

DNA as target for biologic effects, 11, 40

first recorded effects of radiation, 2, 3*f*

four Rs of, 70, 417–418

indirect action in, 8*f*, 9

mechanisms of cell killing in, 40–44

photon concept in, 4–5, 5*f*

Radiogardase (Prussian blue capsules), 131, 132*f*, 202

radioimmunotherapy, 228

radiologic dispersal device (RDD), 198–199, 198*f*, 199*f*

radiologic terrorism. *See* terrorism, radiologic

radiologists

carcinogenesis in, 138, 143–144, 156

cataractogenesis in, 192–193, 192*f*, 220

interventional radiology dose to, 220, 220*f*, 221*t*

mortality patterns in, 156, 156*t*, 157*t*

radionuclide(s), 222–231

in breastfeeding women, 231

in children, 228–230, 229*t*

embryonic/fetal doses of, 231, 231*t*

manufacture of, 225

in PET imaging, 226, 227*t*
in pregnancy, 230–231
therapeutic use of, 226–228

radionuclide eliminators, 131, 132*f*

radiopharmaceuticals, 222–231

- in breastfeeding women, 231
- in children, 228–230, 229*t*
- effective dose of, 225
- embryonic/fetal doses of, 231, 231*t*
- in PET imaging, 226, 227*t*
- in pregnancy, 230–231
- production of, 225
- target organ of, 225

radioprotectors, 126–130

- aminothiol, new family of, 130
- definition of, 126
- developing more effective compounds, 127–129, 128*t*
- discovery of, 126
- dose reduction factor of, 126, 128, 128*t*
- key design elements for, 130
- mechanism of action, 126–127, 127*f*

radiation mitigators, 126, 130–131

- against radiation-induced cancer, 129–130
- in radiotherapy, 129

radioresistant cells, 352

radioresistant DNA synthesis, 318

radioresponse, 352. *See also specific cells, organs, and tissues*

radiosensitivity, 352. *See also specific cells, organs, and tissues*

age-response function in, 58–65
for high-linear energy transfer radiations, 64–65
mechanisms for, 65
possible implications in radiotherapy, 65
sublethal damage repair and, 70–72
for tissue *in vivo*, 63–64, 64*f*
apoptosis susceptibility and, 381
cell differentiation and, 351–352
in cell survival curves, 45–51
in children, 148, 149*f*
genetic control of, 47–48
heritable syndromes affecting, 317–320
human and rodent cell, in asynchronous cultures, 45–46, 47*f*
human syndromes associated with, 48, 48*t*
hypoxic cells, methods of sensitizing, 462–467
intrinsic, and cancer stem cells, 48–49
mammalian cell, 45–46, 46*f*, 356–357, 356*t*
mammalian cell compared with microorganisms, 50, 51*f*
normal tissue, 351–379
Casarett’s classification of, 356–357, 356*t*
cell division and, 351–352, 355
early and late effects in, 352–353, 352*f*
factors governing, 351, 355
growth factors in, 358
LENT/SOMA classification of, 369–375, 374*t*–375*t*
Michałowski’s H- and F-type populations in, 357–358
progression of, 352–353
quantitative analysis of, 369, 370*t*–373*t*

radiation pathology in, 355–356
specific tissues and organs, 358–369, 359*t*–360*t*
time interval in, 355–356
volume effect and tissue architecture in, 354–355, 354*f*

oncogenes and, 46–47
oxygen effect and, 63, 82–100
stem cells for organ regeneration in, 375–376

radiosensitizers, hypoxic cell, 463–467
cis-platinum as, 491
hyperthermia with, 526

Radiotherapy Oncology Group (RTOG), amifostine trial of, 129

radium
biologic effects of, 2, 3*f*
decay of, 6, 6*f*
discovery of, 2
ingestion of, 143, 144*f*, 208
for intracavitary brachytherapy, 77

radium-224, 143

radium-226, 143

radium-228, 143

radon, 208–209, 248
and carcinogenesis, 6, 137, 142–143, 208–209
as enhanced natural source, 206
EPA action level for, 209, 248
natural production of, 6, 6*f*

rams, multifraction experiments in, 417, 417*f*

Rankin, E., 459*f*

Ras protein family, 307, 308*f*

rat(s)

cell cycle times in, 405, 406*f*

dose-response relationships in

mammary and thyroid cells, 339–341, 340*f*

spinal cord, 329, 343–347, 345*f*–347*f*

embryonic or fetal effects in, 177–181, 184–186

fractionation and spinal cord of, 419–420, 419*f*, 420*f*

model tumor systems in, transplantable, 380

rhabdomyosarcoma in

accelerated repopulation in, 423, 423*f*

growth measurements of, 382, 383*f*

in vivo/in vitro assay in, 387–388, 387*f*

tumor growth kinetics in, 412

rat embryo cells, 268

RBE. *See* relative biologic effectiveness

RDD. *See* radiologic dispersal device

REAC/TS. *See* Radiation Emergency Assistance Center/Training Site

Read, J., 82

reassortment, 70, 417–418

recessive genes, 164, 165*t*, 166–167

recoil protons, 10, 101

recombinant DNA, definition of, 292

recombinant DNA technology, 258–294

agarose gel electrophoresis in, 270–271, 271*f*

DNA-mediated gene transfer in, 270

gene expression analysis in, 278–283

gene knockout strategies in, 276–278

gene-cloning strategies in, 273

genomic analyses in, 273–276
glossary of terms, 290–293
historical perspectives on, 258–259
hosts in, 267–271
libraries in, 266–267
polymerase chain reaction in, 271–273, 272*f*
protein analysis in, 283–288
restriction endonucleases in, 262–264, 263*t*, 264*f*
vectors in, 264–266

recombination
homologous, 277–278, 278*f*
breast cancer and, 21, 304
repair, 18, 20–21, 20*f*
retroviral integration through, 297–299, 298*f*

RecQ, 320

rectum, 359*t*, 373*t*, 374*t*, 440

RED. *See* radiation exposure device

red fluorescent protein (RFP), 280, 284

regeneration, stem cells for, 375–376

Reiskin, A. B., 410*t*

relative biologic effectiveness (RBE), 103–109
biologic system for measuring, 103
carbon ion, 453–454, 454*f*
in cataractogenesis, 192
definition of, 103, 254
for different cells and tissues, 105
factors determining, 107
for fractionated doses, 104–105, 104*f*

as function of LET, 105, 105*f*, 106*f*
in mammalian cells in culture, 103–104, 104*f*
neutron, 444
oxygen effect and, 107, 108*f*, 109*f*
proton, 448
radiation weighting factor and, 107–109, 239
relative mutation risk, 168
relative risk model, 139
rem, 254
reoxygenation, 70, 94–97, 417–418
 definition of, 94
 in hyperthermia, 521, 521*f*
 importance in radiotherapy, 96–97
 mechanism of, 96
 process of, 94, 95*f*
 time sequence of, 94–96, 95*f*, 96*f*
repair, 70, 417–418. *See also specific mechanisms*
 DNA, 15–22
 potentially lethal damage, 67–69
 sublethal dose, 69–77
replication, DNA, 259, 260*f*
replication protein A (RPA), 15
repopulation, 70, 417–418
 accelerated, 423–424, 424*f*, 425*f*, 510
reporters, genetic, 280, 284
reproductive death, 35
reproductive integrity, 35, 351–352
RERF. *See* Radiation Effects Research Foundation

resistance

to antibiotics

bacteriophages and, 265, 265*f*

definition of, 290

homologous recombination and, 277–278, 278*f*

plasmids and, 259, 264, 264*f*

to chemotherapy, 502–505, 503*f*

cancer stem cells and, 504–505

genetics of, 502–504, 504*f*

hypoxia and, 97, 502

multidrug, 505

pleiotropic, 504–505

relationship with radioresistance, 505, 506*f*, 508

to hyperthermia, 519–520

to radiotherapy, 318, 352

restriction endonucleases, 262–264, 263*t*, 292

action of, 263–264, 264*f*

nomenclature for, 262

type II restriction enzymes as, 262, 263*t*

restriction fragment length polymorphisms, 274, 275, 292

retinoblastoma paradigm, 301–303, 302*f*

retreatment, 437–443

bone metastases, 440–441

brain, 439–440

breast, 441

clinical studies on, 438–441

early- and late-responding tissues in, 438

head and neck, 440

lung, 441
nature of problem, 437–438
preclinical data on, 438
proton beam therapy for, 438
rectum, 440
safety and organ tolerance in, 437–438
spinal cord, 346–347, 439

retroviruses
in cancer biology, 296–299
integration through recombination, 297–299, 298*f*
Rous's landmark studies on, 296–297
definition of, 292, 297
as vector, 266

reverse transcriptase, 279, 292
reverse transcription (RT) polymerase chain reaction, 278, 279, 283
reverting postmitotic cells, 356*t*, 357

RFP. *See* red fluorescent protein

rhabdomyosarcoma, rat
accelerated repopulation in, 423, 423*f*
growth measurements of, 382, 383*f*
in vivo/in vitro assay in, 387–388, 387*f*

rhesus monkeys, ARS in, 116, 116*f*

ribose, 259

Richardson, D. B., 155*f*

Ricks, R., 121

ring, 26, 27*f*, 29*f*
in human lymphocytes, 29–33, 32*f*

RISC. *See* RNA-induced silencing complex

risk assessment, 139

risk estimates

- for carcinogenesis, 144–148, 244–245, 244*t*
 - in A-bomb survivors, 123, 144–148, 145*f*, 146*t*, 147*f*
 - extrapolating risks from high to low doses, 155–156, 155*f*
 - organ-specific, 147–148, 148*f*
 - population average per sievert, 147, 147*t*
- committees concerned with, 139–140
- heritable effects, 171–173, 171*t*, 172*t*, 244–245, 244*t*
- highlighting need for protection, 244–245, 244*t*

rituximab, 489*t*

RNA, 259–260

- amplification of, 279
- bases of, 259–260, 261*f*
- complementary, 279, 290
- definition of, 292
- DNA transcription to, 258, 260, 261*f*
- Northern blot analysis of, 278
- translation of, 258, 260, 261*f*

RNA interference (RNAi), 278–279, 279*f*

RNA polymerase, 260, 261*f*, 292

RNA-induced silencing complex (RISC), 279, 279*f*

RNA-Seq, 283, 285*f*

Robertsonian translocations, 165*t*, 167

Rockwell, S. C., 91*f*, 92, 387, 407*f*

rodents. *See* Chinese hamster cells; hamster embryo cells, transformation in; mice; rat(s)

Röntgen, W. C., 2

Roizin-Towle, L., 499*f*, 501*f*
Ron, E., 141*f*
Rothmund–Thompson syndrome, 320
Rous, P., 296–297
Rous sarcoma virus (RSV), 297
Rowland, R. E., 144*f*
RSV. *See* Rous sarcoma virus
RTOG. *See* Radiation Therapy Oncology Group
rubidium-81, 225
Rubin, N. H., 507*f*
Rubin, P., 356*t*, 360*t*, 374*t*, 375*t*
Rugh, R., 178, 180*f*, 181*f*
Russell, L. B., 168, 178, 178*f*, 188*t*
Russell, W. L., 168, 169*f*, 170*f*, 178, 178*f*, 188*t*
S (synthetic) phase, of cell cycle, 55–58, 57*f*
SABR. *See* stereotactic ablative radiotherapy
Saccharomyces cerevisiae, 267, 284–285, 292
Sachs, R. K., 153, 153*f*
St. Jude Children’s Research Hospital, 153–154, 153*f*
salivary gland(s), 359*t*, 370*t*
salivary gland regeneration, 375–376
salvarsan, 475
samarium-145, 78*t*
sanctuary sites, chemotherapy for, 508, 508*f*
Sanger sequencing, 274–275
Sankila, R., 151
Sapareto, L. A., 523
sarcoma

apoptosis in, 381
cell loss in, 410–411
chicken, oncogenes in, 296–297
high-risk, hyperthermia and chemotherapy for, 527, 528*f*
KHT, lung colony assay in, 386–387, 387*f*
mouse, reoxygenation in, 94, 95*f*
sargramostim, 130
SBRT. *See* stereotactic body radiotherapy
scattered radiation, exposure to, 247
scattering, carbon ion, 453*f*, 454
Scheimpflug imaging, 193–194, 193*f*
Schizosaccharomyces pombe, 267
Schneider, M. J., 519
Schull, W. J., 172*t*, 183*f*, 188*t*, 194
Schultz, C., 490*t*
SCID. *See* severe combined immunodeficiency syndrome (SCID), mouse vs. human
sebaceous glands, 360
Seckel syndrome, 48*t*, 318–319
second malignancies
 chemotherapy and, 511, 511*t*
 radiation-induced, 148–152
 cervical carcinoma treatment and, 149–151
 creditable studies of, criteria for, 148
 Hodgkin disease treatment and, 151–152
 prostate cancer treatment and, 149, 150*f*
 retreatment for, 437
SEER. *See* Surveillance, Epidemiology, and End Results (SEER) program

selectable marker, 270, 292

self-renewal tissue

- acute radiation syndrome and, 112, 114
- early response in, 329
- gastrointestinal epithelium as, 114, 115*f*
- general characteristics of, 114, 114*f*
- radiosensitivity/response of, 355

senescence, cellular, 25, 43–44, 328

- cancer and escape from, 312–313, 312*f*
- crisis in, 312, 312*f*

sensitivity assays, for chemotherapy, 510

Sertoli cells, 367

serum response element (SRE), 320

severe combined immunodeficiency syndrome (SCID), mouse *vs.* human, 319

sex-linked diseases, 165*t*, 166–167

sex-linked traits, 164

SH. *See* sulphhydryl (SH) compounds

Sheldon, P. W., 465*f*

Sherman, F. G., 407*t*

Shimizu, Y., 157

short tracks, 12–13, 13*f*

short-hairpin RNA (shRNA), 278–279, 279*f*, 292

short-interfering RNAs (siRNAs), 278–279, 279*f*, 292

shotgun DNA sequencing, 266, 273, 274*f*

sickle cell anemia, 166

sievert (Sv), 108, 211, 240, 242*t*, 254

- person-sievert, 212, 241, 242*t*

population average cancer risk per, 147, 147*t*

sigmoid, in dose–response relationship, 135, 136*f*, 243, 243*f*, 327, 327*f*
signal transduction
 in cancer, 306–309
 radiation-induced, 320–321
Sinclair, W. K., 59–60, 60*f*, 61*f*
single photon emission computed tomography (SPECT), 93, 225
single-cell electrophoresis, 13–14, 14*f*
single-strand annealing (SSA), 18
single-strand breaks (SSBs), 11, 12*f*
skin
 anatomy of, 358, 361*f*
 dose–response relationships for
 colonies, 329–331, 330*f*, 331*f*
 pig skin, 329, 341–343, 342*f*, 342*t*, 343*f*
 rodent skin, 329, 343, 344*f*, 344*t*
 early response in, 329, 352
 fluoroscopic exposures on, 219, 219*t*
 H- and F-type populations in, 357
 radiation injury to, 119
 radiosensitivity and response of, 358–361
 recovery and retreatment, 438
 volume effect in, 355
skin appendages, 360
skin cancer, 143–144
 in children treated for tinea capitis, 138
 human history/experience of, 137, 138
Slater, J., 450*f*
SLD. *See* sublethal damage

small interstitial deletion, 29, 31*f*
small intestine, 359*t*, 364–365, 372*t*, 374*t*
smoke detectors, radioactive material in, 199–200, 200*f*
smoking, avoidance of, 463
SMR. *See* Standard mortality ratio
Sneed, P. K., 526
Sobhanifar, S., 93*f*
SOBP. *See* spread-out Bragg peak
solid tumors
in A-bomb survivors, 145*f*, 146, 146*t*
kinetics of
cell loss in, 381, 409–411, 410*t*
Gompertz function in, 411, 411*f*
growth fraction in, 407–409, 409*t*, 413, 475, 476
growth kinetics in, 411–414
histology and, 412
in human tumors, 412–414, 412*t*, 413*t*
potential doubling time in, 409
latent period for, 139
model systems of, 380–397
apoptosis in, 380–382, 381*f*
assay techniques in, 380
autochthonous and transgenic, 389–390
comparison of, 393–394, 395*f*
dilution assay technique in, 380, 384–386, 385*f*, 386*f*, 393
lung colony assay in, 380, 386–387, 387*f*
misleading results of, 393, 394*f*
organoid, of human tumors, 392–393, 394

patient-derived xenografts, 389, 394
spheroid, 390–392, 391*f*, 392*f*, 394
transplantable, in experimental animals, 380
tumor cure (TCD₅₀) assay in, 380, 382–384, 384*f*
tumor growth measurements in, 380, 382, 382*f*, 383*f*, 393
in vivo/in vitro assay in, 380, 387–388, 387*f*, 393
xenografts of human tumors, 388–389, 389*f*, 393–394
in nuclear industry workers, 154–155, 155*f*

SOMA classification, 369–375, 374*t*–375*t*

somatic homozygosity, 304–305, 305*f*

somatic mutations, in carcinogenesis, 296

somnolence, 351

Song, C. W., 521*f*

sorafenib, 489*t*

Southern blotting, 275, 278, 292

spallation products, 10

sparsely ionizing radiation, 101, 102*f*

spatial cooperation, 508, 508*f*

Spear, F. G., 45

SPECT. *See* single photon emission computed tomography

sperm, 162, 163*t*, 332–336, 367

spheroids, 390–392, 391*f*
cross section through, 392*f*
of human tumor cells, 391–392, 394
radiosensitivity of cells in, 390–391

sphingomyelin hydrolysis, 320–321, 321*f*

spinal cord
dose–response relationship for, 329, 343–347, 345*f*–347*f*

fractionation/protraction and, 345*f*, 346, 346*f*, 419–420, 419*f*, 420*f*
functional subunits of, 346, 354, 367
late response in, 329, 353, 374*t*
latency in, 346
QUANTEC analysis of, 370*t*
radiosensitivity and response of, 359*t*, 366–367
retreatment of, 346–347, 439
SOMA scoring for, 374*t*
stereotactic body radiotherapy for, 439
volume effects in, 346, 347*f*

spinal cord myelopathy, 343–347, 366–367. *See also* spinal cord

spinner culture, 390

spleen, mouse, dose–response relationship in, 336–339, 338*f*, 339*f*

split luciferase complementation assay, 285–287, 286*f*

split-dose experiments, sublethal damage repair in, 69–72, 69*f*, 71*f*, 72*f*

spotted arrays, 283

spread-out Bragg peak (SOBP), 449, 453, 454, 454*f*

spurs, 12–13, 13*f*

src oncogene, 297, 307

SRE. *See* serum response element

SRS. *See* stereotactic radiosurgery

SSBs. *See* single-strand breaks

Standard mortality ratio (SMR), for radiologists, 156, 156*t*, 157*t*

start codon, 260

Steel, G. G.

on cell cycle and tumor kinetics, 406*f*, 407*f*, 407*t*, 412*t*

on cell loss/cell loss factor, 410, 410*t*, 413–414, 415

on xenografts, 388, 389*f*

stem cells, 357

- acute radiation syndrome and, 112, 114

cancer

- chemotherapy/chemoresistance and, 476, 504–506
- intrinsic radiosensitivity and, 48–49

dose–response relationships for

- bone marrow, 329, 336–339, 338*f*, 339*f*
- testes, 329, 332–336, 335*f*, 336*f*

organ regeneration with, 375–376

radiation-induced chromosome aberrations in, 33

radiosensitivity and response of, 351–352, 356–357, 361

in self-renewal tissue, 112, 114, 114*f*

stereotactic ablative radiotherapy (SABR), 427–428, 427*t*, 428*f*

stereotactic body radiotherapy (SBRT), 427–428, 427*t*, 428*f*, 439, 441, 496

stereotactic radiosurgery (SRS), 427–428, 427*t*

sterility, radiation-induced, 162, 163*t*, 367–368

steroidal progestational agents, 485*t*

Stewart, A., 156–157, 186–187, 186*t*, 188*t*

sticky ends, 25, 263, 264*f*, 292

stochastic effects, 135–136, 136*f*, 230, 242–243

- definition of, 135, 201, 243, 254

diagnostic radiology and, 211

dose–response relationship in, 243–244, 243*f*

limiting, 243

occupational limits for, 245, 245*t*

radiation weighting factor and, 239

terrorism and, 201

stomach, 212*t*, 359*t*, 364, 372*t*, 374*t*

- Stone, R., 445, 445*f*
stop codon, 260, 292
Strandquist, M. A., 418*f*
Strandquist plot, 418, 418*f*
streptonigrin, 502*t*
stress response, in hypoxia, 461–462
structurally defined FSUs, 353
structurally undefined FSUs, 353
sublethal damage (SLD), 67
sublethal damage (SLD) repair, 69–77
 chemotherapy and, 498–500, 506
 dose-rate effect and, 72–77
 in *in vivo* systems in mice, 70–71, 70*f*
 mechanisms of, 72
 processes in, 70
 radiation quality and, 72, 72*f*
 split-dose experiments with, 69–72, 69*f*, 71*f*, 72*f*
sucrose gradient sedimentation, 13
Sugimachi, K., 526
Suit, H. D., 384, 384*f*, 449*f*, 454*f*
“suitcase bombs,” 197–198, 199
sulphydryl (SH) compounds
 covering with phosphate group, 127–129, 128*t*
 mechanism of action, 126–127, 127*f*
 as radioprotectors, 126–130
Sulman, E. P., 440
sunitinib, 489*t*
superficial malignancies, radiation and hyperthermia for, 525–526, 525*f*

supportive care, as countermeasure, 131

Surveillance, Epidemiology, and End Results (SEER) program, 149

Sutherland, R. M., 391*f*, 392*f*

Swift, M., 316, 316*t*

Symington, T., 412*t*

symmetric translocations, 26–29, 31*f*

- frequency, FISH scoring of, 33
- in Hiroshima/Nagasaki survivors, 33
- as stable aberrations, 33

synchrocyclotron (Sweden), 448

synchronously dividing cell cultures, 58–62

- definition of, 58
- hydroxyurea-induced, 58–59, 58*f*, 59*f*
- techniques for producing, 58–59
- x-ray effects on, 59–62, 60*f*, 61*f*, 62*f*

synergistic interaction, chemotherapy and radiation, 509

synthetic lethality, 496–497, 497*f*

T cell checkpoint therapy, 321–322, 322*f*, 497–498

T lymphocytes (T cells), radiosensitivity of, 363

tamoxifen, 486*t*, 493

tandem repeats, 275

Tannock, I. F., 410*t*

Taq polymerase, 271–272, 292

target organ, in nuclear medicine, 225

targeted radiotherapy, hypoxia monitoring for, 93

targeted therapies (chemotherapy), 487*t*–490*t*, 494–496

taxanes, 484*t*–485*t*, 493

- adjunct use with radiation, 508, 509*f*

cell-cycle specificity of, 476, 477*f*
sensitivity to, 500*f*

Taxol. *See* paclitaxel

Taxotere. *See* docetaxel

Taylor, L., 237

T_c. *See* cell cycle time

TCD₅₀. *See* tumor cure (TCD₅₀) assay

TC-NER. *See* transcription-coupled repair

TCP. *See* tumor control probability

TCR. *See* transcription-coupled repair

technetium-99m, 225

Teicher, B. A., 501*f*, 502*t*

teletherapy, 77

telomerase, 25, 312*f*, 357

telomeres, 24–25, 312–313, 312*f*, 357

telophase, 24

temozolomide, 480*t*

temperatures. *See also* hyperthermia

 cytotoxic, 517–520

 noncytotoxic, 521–522, 521*f*, 522*f*

template, DNA, 259, 292

TER. *See* thermal enhancement ratio

Terasima, T., 58, 60–61, 61*f*

termination codons, 260, 292

terrorism, radiologic, 197–205

 availability of radioactive material for, 199–201, 200*f*, 201*f*

 “dirty bomb,” 198–199, 198*f*, 199*f*

 external exposure in, 201–202

health effects in, 201
improvised nuclear device, 197–198, 197*t*, 199
internal contamination in, 202
medical countermeasures in, 126, 128–129, 132, 202–203, 203*t*
nuclear power station attack, 198
patient management priorities in, 203, 203*t*
possible scenarios for, 197–199
radiation exposure device, 199
resources on, 203

Terz, J. J., 412*t*

testes, 359*t*, 367
testes stem cells, 329, 332–336, 335*f*, 336*f*

TGF- β . *See* transforming growth factor β

TH-302, 469

Thames, H. D., 334*f*, 336*f*

therapeutic gain factor, in hyperthermia, 523

therapeutic ratio (index), 327–328, 327*f*
definition of, 327
drug or radiosensitizer and, 327–328, 328*f*

thermal ablation, 520–521

thermal dose, 523–524

thermal enhancement ratio (TER), 522–523

thermal isoeffective dose formulation, 524

thermal neutrons, 447

thermometry
clinical, 530
invasive methods of, 530
noninvasive, progress toward, 530

thermosensitive liposomes, 527, 528*f*
thermotolerance, 519–520
thiotepa, 477
Thomlinson, R. H., 86–88, 87*f*, 88*f*, 96*f*
thorium, 137, 208
Thorotrast, 137
Thrall, D. E., 524, 525–526
threshold dose, 135, 351
threshold-sigmoid, 135, 136*f*, 243, 243*f*
thrombopenia, 361
thrombospondin 1 (TSP-1), 313–314
thymidine, for cell labeling, 54–55, 55*f*
thymine, 11, 12*f*, 16, 16*f*, 259–260, 259*f*–261*f*
thyroid cancer, 140–141, 141*f*
 in A-bomb survivors, 140
 age at exposure and, 148
 in children receiving radiotherapy, 138, 140
 radioactive iodine-131 for, 227
thyroid cells, 329, 339–341, 340*f*
thyroid gland, 357, 359*t*, 374*t*
thyroid scan, 224*t*
tiling arrays, 283
Till, J. E., 329, 336–339, 338*f*
time, treatment. *See* treatment time
time since exposure, 139
time-dependent relative risk model, 139
tin-113, 225
tinea capitis, carcinogenesis in children treated for, 138, 141, 143, 144

TIPS. *See* transjugular intrahepatic portosystemic shunt

tirapazamine, 467–469, 467*f*, 468*f*, 502*t*

Tishler, R. B., 509*f*

tissue, normal. *See* normal tissues

tissue reactions (deterministic effects), 135–136, 136*f*, 242–243

- cataractogenesis as, 194
- definition of, 135, 201, 210, 254
- dose–response relationship in, 243–244, 243*f*
- interventional radiology and, 219–220
- occupational limits for, 245–246, 245*t*
- prevention of, 243
- terrorism and, 201

tissue rescue unit (TRU), 327, 353

tissue weighting factor (W_T), 240, 241*t*, 254

TNF. *See* tumor necrosis factor

Todaro, G. J., 297

Tokaimura accident (Japan), 111, 118

tolerance dose, 244, 354

Tolmach, L. J., 58, 60–61, 61*f*, 89–90, 90*f*

tongue, 363

tonsils, 363

topoisomerase inhibitors, 487*t*, 494

T_{pot} . *See* potential doubling time

track average, 102, 102*f*

Tradescantia paludosa, anaphase bridge in, 26, 30*f*

training, exposure limits for, 245*t*, 247

transcription, 258, 260, 261*f*

ChIP studies of, 280–281, 281*f*

definition of, 292
transcription-coupled repair (TCR or TC-NER), 16–18, 17*f*
transfection, 270
 in cancer biology, 299, 299*f*
 in chromatin immunoprecipitation, 280
 definition of, 293
 in gene transfer, 268, 270
 in knockout strategies, 277, 278*f*, 279*f*
 in promoter bashing, 280, 281*f*
transfer RNA (tRNA), 260, 293
transformation
 in cancer biology, 299–300, 299*f*, 306–307
 definition of, 293
 in mammalian cells, 268–270, 268*f*
transforming growth factor β (TGF- β), 358
transgenic tumor models, 389–390
transjugular intrahepatic portosystemic shunt (TIPS), 218, 219
translation, 258, 260, 261*f*, 293
translocations, 167
 in Hiroshima/Nagasaki survivors, 33
 oncogene activation in, 300–301, 301*f*, 301*t*
 Robertsonian, 165*t*, 167
 symmetric, 26–29, 31*f*, 33
trastuzumab, 489*t*
Travis, E. L., 343, 345*f*
Travis, L. B., 151
treatment time
 influence on early- vs. late-responding tissue, 423

overall, importance of, 424–426, 426*f*
Strandquist plot of, 418, 418*f*
triage, in radiation exposure, 121–123, 203, 203*t*
triazine derivatives, 477
Tribondeau, L., 352, 414
tricyclic triazine-di-N-oxides (TTOs), 469
tRNA. *See* transfer RNA
Trofimov, A. V., 451*f*
TRU. *See* tissue rescue unit
TSP-1. *See* thrombospondin 1
TTOs. *See* tricyclic triazine-di-N-oxides
tuberculosis, fluoroscopy and breast cancer in, 138, 141, 142*f*
Tubiana, M., 412–413, 412*t*, 415
tumor control probability (TCP), 327, 328, 428, 428*f*
tumor cure (TCD₅₀) assay, 380, 382–384, 384*f*
tumor growth measurements, 380, 382, 382*f*, 383*f*, 393
tumor kinetics
 cell loss in, 381, 409–411, 410*t*
 Gompertz function in, 411, 411*f*
 growth fraction in, 407–409, 409*t*, 413, 475, 476
 growth kinetics in, 411–414
 histology and, 412
 in human tumors, 412–414, 412*t*, 413*t*
 potential doubling time in, 409
tumor metabolism
 hypoxia-inducible factor in, 460
targeting
 to enhance radiotherapy, 470

to kill hypoxic cells, 469–470, 469*f*, 470*f*

tumor model systems. *See* model tumor systems

tumor necrosis factor (TNF), 358

tumor suppressor genes

- definition of, 295
- familial breast cancer and, 303–304
- function of, 306–315
- gatekeepers and caretakers, 315–316
- Li–Fraumeni paradigm of, 301, 302–303, 303*f*
- mutation or inactivation of, 295, 296*f*, 301–305
- retinoblastoma paradigm of, 301–303, 302*f*
- somatic homozygosity and, 304–305, 305*f*

two-dimensional electrophoresis, 288, 293

two-hit hypothesis, 302

two-hybrid screening, 284–285, 285*f*

ultraviolet radiation, 4*f*, 511, 511*t*

unfolded protein response (UPR), 461–462

United Kingdom

- CT scanners in, 213, 215*f*
- Hammersmith neutron experience in, 445–446
- sources of radiation exposure in, 210, 211*f*

United Nations Scientific Committee on the Effects of Atomic Radiation (UNSCEAR), 139, 238

- on computed tomography, 213, 215*f*
- on DDREF, 146
- on doubling dose, 170
- on effective dose, 222–223
- on heritable effects, 165, 166*t*, 170–173, 171, 171*t*

on linear no-threshold, 155–156

on nuclear medicine, 222–223

United States

collective effective dose in, 217

cosmic radiation in, 207, 208*f*

CT scanners in, 213, 215*f*

sources of radiation exposure in, 210, 211*f*

unity, in oxygen enhancement ratio, 83, 84*f*

UNSCEAR. *See* United Nations Scientific Committee on the Effects of Atomic Radiation

Uppsala cyclotron (Sweden), 448, 450

UPR. *See* unfolded protein response

uracil, 260, 261*f*

uranium

decay of, 6

in earth's crust, 208

uranium miners, 137, 142–143

ureters, radiosensitivity and response of, 359*t*

urinary bladder

doses from diagnostic radiology, 212*t*

QUANTEC analysis of, 373*t*

radiosensitivity and response of, 359*t*, 366

retreatment and, 438

U.S. Food and Drug Administration (FDA), 129, 202, 212

uterus, 360*t*

vagina, 360*t*, 368

vaginal metastases, recurrent, 441

Valdagni, R., 526

van der Kogel, A. J., 343–347, 345*f*, 346*f*, 347*f*

Van Putten, L. M., 91*f*, 94, 96, 96*f*

Vañó, E., 220*f*

vascular endothelial growth factor (VEGF), 313, 460–461, 494–496

vascular system, 368

vectors, 264–266

- bacterial artificial chromosomes as, 264, 266
- bacteriophages as, 264, 265, 265*f*
- definition of, 264, 293
- plasmids as, 264–265, 264*f*
- viruses as, 264, 266

vegetative intermitotic cells, 356–357, 356*t*

VEGF. *See* vascular endothelial growth factor

Velban. *See* vinblastine

velocity, 3–4, 4*f*

vemurafenib, 490*t*

Vent polymerase, 272

Vernon, C. C., 441

Vicia faba

- oxygen effect in, 82
- synchrony induced in, 59, 59*f*

vinblastine, 483*t*, 492–493

vinca alkaloids, 483*t*, 492–493

vincristine, 483*t*, 492–493

- hyperthermia combined with, 526*t*
- oxygen effect and, 501, 502*t*

vinorelbine, 483*t*

viruses, as vectors, 264, 266

visible light, 4, 4*f*
vitamin E succinate, 132
Vogelstein, B., 305*f*
volume effect, 354–355
 kidney, 354–355
 lung, 354–355
 skin and mucosa, 355
 spinal cord, 346, 347*f*, 354
vomiting, 351, 364
von Hevesy, G., 222, 222*f*
von Hippel-Lindau gene/protein (*VHL/VHL*), 286*f*, 313, 459, 460
von Kölliker, R. A., 2
Vriesendorp, H. M., 117*t*
vulva, 368
Wagner, L. K., 219*t*
Wakeford, R., 157, 186–187
Walter Reed Institute of Research, 127–128
Wang, Z., 285*f*
Warburg effect, 460, 461*f*
Ward, J., 13, 511*t*
Watson, J., 258, 259
wavelengths, 3–4, 4*f*
Weber, D. C., 451*f*
Weber, U., 455*t*
Weichselbaum, R., 46*f*
Weinert, T. A., 398
Weinstein, G. D., 412*t*
Werner syndrome, 320

Westermark, F., 516

Western blotting, 283–284, 288, 293

Weyrather, W. K., 453*f*

WHO. *See* World Health Organization

whole genome shotgun sequencing, 273

Willers, H., 15

Wilson, C. W., 91*f*, 384

Wilson, R. R., 448

Withers, H. R.

- on age-response function, 63–64, 64*f*
- on dose-response in normal tissue, 354*f*
- on dose-response assays, 329–336
- on early- vs. late-responding tissue, 421*f*, 422*f*
- on fractionation, 421*f*, 422*f*, 423, 425, 425*f*
- on jejunal crypt cells, 331–332, 333*f*, 334*f*
- on kidney tubules, 336, 337*f*, 338*f*
- on skin colonies, 329–331, 330*f*, 331*f*
- on testes stem cells, 332–336, 335*f*, 336*f*

women

- medical exposure of, 187
- occupational exposure of, 187
- pregnant (*See also* embryonic or fetal effects)
 - care and medical exposure during, 187
 - exposure limits in, 245*t*, 246
 - nuclear medicine in, 230–231

Worgul, B. V., 192, 193*f*

working level, 254

working level month, 254

World Health Organization (WHO), 119–120, 119*t*, 120*t*
World Trade Center attack (9/11), 132, 197
 W_R . *See* radiation weighting factor
WR-638 (cystaphos), 128, 128*t*
WR-1065 (amifostine metabolite), 129
WR-2721 (amifostine), 128–130, 128*t*. *See also* amifostine
 W_T . *See* tissue weighting factor
X chromosome, 164
xenografts
 chemotherapy assays in, 510
 definition of, 388
 of human tumors, 388–389, 389*f*, 393–394
 patient-derived, 389, 394
xerostomia
 amifostine for prevention of, 129
 salivary gland regeneration for, 375–376
X-linked diseases, 165*t*, 166–167
X-linked traits, 164
x-rays, 3–5, 4*f*
 absorption of, 6–8
 Compton process and, 6–8, 7*f*
 discovery of, 2
 first medical use of, 2
 first publicly taken radiograph, 2, 2*f*
 first therapeutic use of, 2
 ionization density of, 101, 102*f*
 LET values of, 103, 103*t*
 oxygen enhancement ratio for, 82–83, 84*f*

photoelectric process and, 7–8, 7*f*
radiosensitivity effects of, 59–62, 60*f*, 61*f*, 62*f*
Y chromosome, 164
yeast
 cell cycle in, 267
 cell survival curve for, 50, 51*f*
 molecular techniques using, 267, 284–285
yeast artificial chromosome, 266, 293
yellow fluorescent protein (YFP), 284
Young, R. C., 412*t*
ytterbium-169, 78*t*
yttrium-90, 228
Yugoslav scientists, radiation exposure in, 121, 122*f*
Yun, Z., 281*f*
Z (atomic number), 8
zinc DTPA (ZnDTPA), 131